Wireless Communications and Mobile Computing

Artificial Intelligence-Driven Sensing for Wireless Communications in Cyber-Physical Mobile Computing

Lead Guest Editor: Mohamed Elhoseny
Guest Editors: Xiaohui Yuan and Mohammad Hammoudeh

Artificial Intelligence-Driven Sensing for Wireless Communications in Cyber-Physical Mobile Computing

Wireless Communications and Mobile Computing

Artificial Intelligence-Driven Sensing for Wireless Communications in Cyber-Physical Mobile Computing

Lead Guest Editor: Mohamed Elhoseny
Guest Editors: Xiaohui Yuan and Mohammad Hammoudeh

Chief Editor

Associate Editors

Academic Editors

Contents

Contents

Hindawi
Wireless Communications and Mobile Computing
Volume 2023, Article ID 9835251, 1 page
https://doi.org/10.1155/2023/9835251

Retraction

Retracted: Dynamic Data-Driven Modelling of Water Allocation for the Internet of Things

Wireless Communications and Mobile Computing

Received 8 August 2023; Accepted 8 August 2023; Published 9 August 2023

This article has been retracted by Hindawi following an investigation undertaken by the publisher [1]. This investigation has uncovered evidence of one or more of the following indicators of systematic manipulation of the publication process:

(1) Discrepancies in scope
(2) Discrepancies in the description of the research reported
(3) Discrepancies between the availability of data and the research described
(4) Inappropriate citations
(5) Incoherent, meaningless and/or irrelevant content included in the article
(6) Peer-review manipulation

The presence of these indicators undermines our confidence in the integrity of the article's content and we cannot, therefore, vouch for its reliability. Please note that this notice is intended solely to alert readers that the content of this article is unreliable. We have not investigated whether authors were aware of or involved in the systematic manipulation of the publication process.

Wiley and Hindawi regrets that the usual quality checks did not identify these issues before publication and have since put additional measures in place to safeguard research integrity.

We wish to credit our own Research Integrity and Research Publishing teams and anonymous and named external researchers and research integrity experts for contributing to this investigation.

The corresponding author, as the representative of all authors, has been given the opportunity to register their agreement or disagreement to this retraction. We have kept a record of any response received.

References

[1] Z. Du and Z. Dong, "Dynamic Data-Driven Modelling of Water Allocation for the Internet of Things," *Wireless Communications and Mobile Computing*, vol. 2022, Article ID 4581734, 8 pages, 2022.

Hindawi
Wireless Communications and Mobile Computing
Volume 2022, Article ID 2437578, 12 pages
https://doi.org/10.1155/2022/2437578

Research Article

Network Lifetime Enhancement by Elimination of Spatially and Temporally Correlated RFID Surveillance Data in WSNs

Lucy Dash,[1] Binod Kumar Pattanayak,[1] Debabrata Singh,[2] Debabrata Samanta,[3] and Yagyanath Rimal[4]

[1]*Department of Computer Science and Engineering, Siksha 'O' Anusandhan University, Bhubaneswar, India*
[2]*Department of Computer Application, Siksha 'O' Anusandhan University, Bhubaneswar, India*
[3]*Department of Computer Science, CHRIST (Deemed to Be) University, Bengaluru, Karnataka 560029, India*
[4]*Department of Computer Science, Pokhara University, Pokhara 30, Khudi, Kaski, Gandaki, Nepal*

Correspondence should be addressed to Debabrata Singh; debabratasingh@soa.ac.in,
Debabrata Samanta; debabrata.samanta369@gmail.com, and Yagyanath Rimal; rimal.yagya@gmail.com

Received 16 February 2022; Revised 22 July 2022; Accepted 30 July 2022; Published 7 September 2022

Academic Editor: Chuanwen Luo

In wireless sensor networks (WSNs), radio frequency identification (RFID) plays an important role due to its data characteristics which are data simplicity, low cost, simple deployment, and less energy consumption. It consists of a series of tags and readers which collect a huge number of redundant data. It increases system overhead and decreases overall network lifetime. Existing solutions like Time-Distance Bloom Filter (TDBF) algorithm are inapplicable to the large-scale environment. Received Signal Strength (RSS) used in this algorithm is highly dependent on quality of tag and application environment. In this paper, we propose an approach for data redundancy minimization for RFID surveillance data which is a modified version of TDBF. The proposed algorithm is formulated by using the observed time and calculated distance of RFID tags. To overcome these problems, we design our approach to relevantly reduce the spatiotemporal data redundancy in the source level by adding the Received Signal Strength Indicator (RSSI) concept for energy-efficient RFID data communication in wireless sensor network scenario. We introduce in this paper the new improved idea of an existing algorithm which efficiently reduces the rate of data redundancy spatially and temporally. The implemented results overcome the limitations of existing algorithm for data redundancy reduction. Nevertheless, the performance evaluation shows the efficiency of proposed algorithm in terms of time and data accuracy. Furthermore, this algorithm supports multidimensional and large-scale environment suitable for sensor network nowadays.

1. Introduction

In wireless sensor network, electromagnetic signals from sensor nodes are detected by RFID technology which consists of antenna, transceiver, and tags optimized with technical programs. Antennas build the emitted radio signal communication bridge between the tag and the transceiver emitted for tag activation and data encryption-decryption [1]. RFID has a wide range of application in agriculture, military, defence, health care, supply chain management, logistics, access control, IT access tracking, material management, race timing, tool tracking, video surveillance, product tracking, and payment. It is vastly used in passenger identification in airport and postal tracking [2]. A simple example of RFID is NFC (Near Field Communication) tag reader in smartphones. NFC supports reader modes which are having operations as writer or reader, tag identification, and peer-to-peer tracking. For simplified meaning, NFC reader tags used in iPhone can enable devices within the perimeter of few centimetres for wirelessly exchanging information among each other. Applications in iOS (iPhone operating system) mobile operating system can read the scanned data through NFC tag reader attached to the real-environment objects. For example, a working employee from retail sector can scan different products for tracking, or the mobile users can scan their devices attached to tag reader in order to equip their video game feature with any toy [3].

In access monitoring field, RFID technology is used for accurate tag data measurement. Risk assessment due to real-time performance of RFID tags is an influencing factor affecting the loss of tag information, advanced risk detection, and real-time event handling. According to the RFID reader architecture, it collects a huge number of relevant data within the detection range of the reader which eventually leads to the collection of redundant data. Massive gathering of redundant data can lead to system overhead and loss of important information. It leads to storage space scarcity, increased network latency, and decreased quality of service (QoS). So it is important to reduce the number of redundant data for loss-less data communication, efficiency increase of RFID systems, and enhanced overall network lifetime. RFID tags work densely in WSNs and due to high density in the sensor environment; observations are highly correlated in the space domain. The nature of network topology and physical phenomenon constitutes the temporal correlation among tags [4]. These spatial and temporal correlations bring huge number of redundant data for consecutive observations between RFID reader and RFID tag. Communication operation involves huge power consumption, as it is associated with activities like collision of data, overemission of sensing information, overhearing of sensed information, and idle channel listening in absence of communications. These spatially and temporally correlated redundant data need to be filter out for efficient overall system management of RFID technology. In RFID system, most of the data are static which can be filtered out easily as compared to the dynamic data. In this paper, we have proposed a modified version of Time-Distance Bloom Filter (TDBF) proposed by Wang et.al in [5] to eliminate the existing limitations of this algorithm for RFID redundant data elimination and filtering out the irrelevant data. We have renamed it as mTDBF (Modified Time-Distance Bloom Filter). Experimental results show that this approach can efficiently improve the performance of RFID system in real scenario as compared with the existing methods [6]. The rest of the paper is descripted as follows. In Section 2, the RFID system model is described, followed by RFID data and its characteristics in brief in Section 3, followed by data characteristics in Section 4. Section 5 presents the signal characteristics and real-time performance. Section 6 presents the related works. The proposed system model is discussed in Section 7. Section 8 discusses the experimental results, performance evaluation, and comparison. Section 9 presents the conclusion and future work.

2. RFID System Model

RFID technology is an emerging technology which is used for various applications like supply chain management, habitat monitoring, and wild fire detection [7]. It consists of RFID tags, RFID reader (active and passive), and software (middleware) as described in Figure 1.

2.1. RFID Tag. RFID tags associated with the objects are responsible for identification without using line of sight eliminating the limitations of barcode [8]. RFID tags are

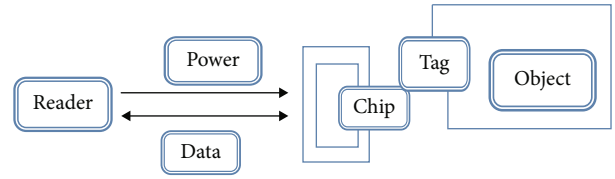

Figure 1: Architecture of RFID tag.

made of three different components: an RFID chip, which is an integrated circuit (IC), an antenna, and a substrate. A tag manufacturer typically does not make all three components in-house. The IC is typically designed and made by a semiconductor manufacturer, while an antenna is usually designed and made by a tag manufacturer. Tags are available in various sizes, designs, and form factors, and they can be customized for a particular application. An electronic circuit, microchip, or chip is designed and manufactured by a semiconductor manufacturer. The IC needs power to operate. This power may come from a battery on the tag (in an active tag), or it may be obtained from the radio energy radiated by the interrogator antenna. The processing logic implements the communication protocol. It also is used to modulate/demodulate signals during the communication between the interrogator and the tag. Making tag ICs more efficient in power usage and requiring less power to operate increases the read range of passive tags.

2.2. RFID Reader. RFID readers are responsible for collaborating relevant information from various tags within the read range. It can also alter the tag information according to need. EPC (Electronic Product Code) Class 1 Gen 2 RFID standard [9] is one of the suitable reader for various applications. Active readers are equipped with battery power supply whereas passive readers are free from a finite source of power supply as shown in Figure 2.

2.3. Middleware. RFID middleware is responsible for collecting and processing the data received from readers and converting it into relevant information as described in Figure 3.

2.4. Workflow of RFID. UHF (ultrahigh frequency) RFID tags are vastly used in many applications of WSNs. It ranges from 433 MHz (megahertz) to 956 MHz; our work is focused on UHF RFID tags as shown in Figure 4.

In RFID system, the reader collects the data from the tags adhered with the objects in the real environment. The middleware processes the data with some actions such as aggregation, filtering, and transforming raw data to information. Then, these processed and filtered data proceed to the application server for next execution of events such as sending theft alarms, fire detection, gas explosion, and earthquake detection [10].

3. RFID Data and Its Characteristics

3.1. Data Description. Basically, a RFID tag storehouse EPC (Electronic Product Code) [11] is a unique identification entity. Tags attached to the reader when comes under the

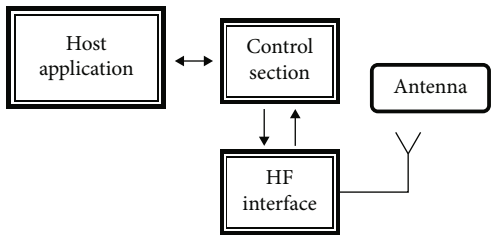

Figure 2: RFID reader architecture.

reading range can generate EPC. Air Interface Protocol is used for reading the tag code. An inbuilt clock synchronises the read tad data along with the time of observation. The time duration is known as epoch time [12]. A number of observations are recorded in epoch time consisting of various time stamps known as epoch duration. These readings are optimized to the middleware depending upon the requirements of the application. Middleware data server receives the information along with location, and time can be represented as

$$(\mathrm{EPC}_i, \mathrm{loc}_i, t_i), \tag{1}$$

where EPC_i is the code of the tag, loc_i is the location of the reader, t_i is the current time, and $t_1, t_2, \cdots, t_i$ is the epoch duration.

3.2. Spatiotemporal RFID Data. In RFID, the timestamp of a tag exhibits the spatial change of a tag in a timestamp due to its space-time functionality. Related events are being identified by tags are influenced by the time-space association of data. Due to multilocational data, a single RFID reader can exhibit multiple same data in the specified time interval [13]. This generates temporally and spatially correlated redundant data for a single reader. RFID readers collecting information of different tagged items form a group. A series of observations of multiple RFID tags exhibits temporal correlation among each read data for a specific timestamp. Data representation groups multiple EPC IDs for different timestamps in a time-interval yield spatial correlation [14]. Exploiting spatial and temporal correlation among different RFID readers with unique $\mathrm{tag}_{\mathrm{ID}}$ can reduce the redundant data by the following ways:

(1) By reducing the false negative rate by minimizing the percentage of epochs in a certain time interval (ρ value) of multiple observations

(2) By reducing the false positive rate by maximizing the ρ value

False negative rate arises when multiple tags are detected simultaneously or a tag is not detected due to radio frequency interference (noise). False positive rate arises when tags read captures the data outside the read range or readers get affected by environment. Getting the nonredundant data as a subset of codes which is a part of larger group can efficiently yield the redundant data [15].

4. Data Characteristics

RFID data has some unique characteristics which make it suitable for large-scale environment and multidimensional application scenario.

4.1. Large Volume of Redundant Data. RFID technology is a unique technology as it generates hundred to thousand times the data volume as compared to existing barcode technique. This large volume of data eventually yields a series of redundant data increasing the overall system overhead. In an ultrahigh frequency, the RFID devices frequently collect the data due to low-cost communication between the readers and the tags [16].

4.2. Unreliable Data. RFID data are very simple in nature. This simplicity attribute of data is represented as ID, loc, and t where ID is the $\mathrm{tag}_{\mathrm{ID}}$, loc is the location, and t is the time. Due to this simplicity nature, the data can be recorded and altered without any extra cost or communication in the data warehouse. Data stream produced by RFID readers is often inaccurate which marks the drawback of using RFID technology. In real-world scenario, the read rate of RFID readers is approximately 70%. Inaccuracy of read data often generates high error rate and important data loss in data warehouse [17].

4.3. Query Processing. Frequent queries are processed as RFID data are collected hugely due to their wide range of applications. In presence of active tags, the generated sensor data get refined by execution of complex queries to meet the emerging challenges. Depending upon the large intensity of data, the queried data are authenticated by frequently updating the $\mathrm{tag}_{\mathrm{id}}$ information. Physical movement of the data leads to its mobility and hence identifies the location of the RFID tag. For nonmobile or static tag, several authentications have been carried out for ensuring its presence in the prescribed location. Increase in volume of data may generate frequent RFID tag polling [18].

4.4. Privacy Concerns. In management systems like supply chain management, ticket countering system, and blockchain management system, the privacy issues of customers who are in association with the objects physically connected to the tag are of paramount significance. In connection to this, the RFID tags go through malicious attacks like Denial of Service (DoS) attack, Man-in-Middle attack, and Distributed Denial of Service (DDoS) attack. However, the attacked tags may replicate it and use necessary information violating the user's copyrights. The unintended user can manipulate the information as RFID generates rich source of information. Thus, data must be made secure generated by RFID tags [19].

5. Signal Characteristics and Real-Time Performance

RFID data are based on electromagnetic radio frequency waves which have different range from low to high. The range of frequencies can be categorized into 4 types which are described as follows in Table 1.

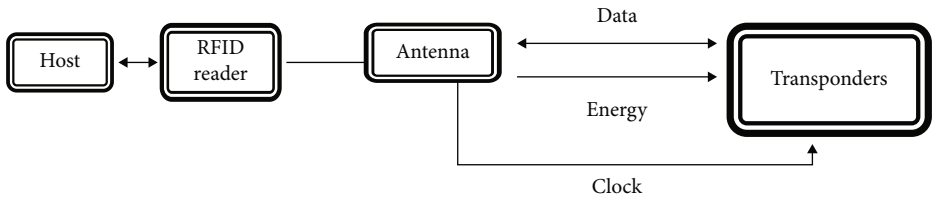

Figure 3: RFID middleware architecture.

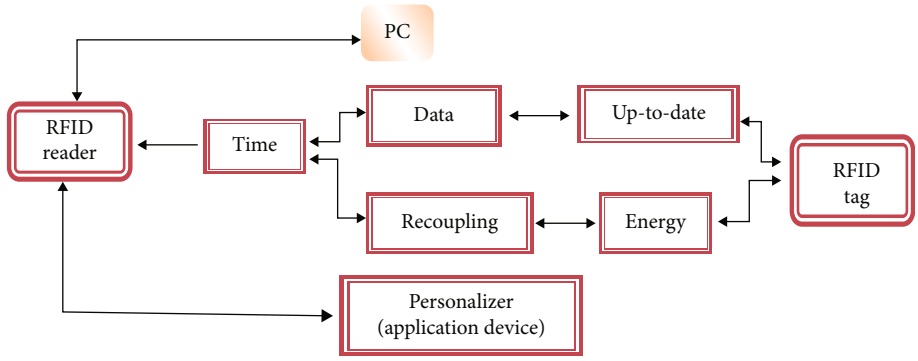

Figure 4: Overall system workflow of RFID.

Table 1: RFID frequency bands and its description.

Frequency band	Range (in hertz)	Data transfer rate (in kilobits)	Detection range (in meters)	Penetrating device	Applications
Low	125 KHz to 134 KHz	1	0.5	Water	Animal identification
High	13.56 MHz	25	1.5	Water	Access and security
Ultrahigh	433 MHz to 956 MHz	100	0.5 to 5	None	Logistics
Micro	2.45 GHz	100	10	None	Mobile vehicle toll

Electromagnetic radio signals read by readers from tags in RFID technology have important characteristics known as Received Signal Strength (RSS) [20]. It is a set of scalars associated with some linear equations. It is inversely proportional to the distance of transmission, i.e., RSS value decreases with the increase in transmission distance and vice versa. RSS gets affected by variation in latency. So it needs to be filtered to efficiently utilise the read rates in short distance [21].

5.1. Clustering Algorithms. In many situations, the data collected by many nodes will be the same. In such cases, redundant data transmission can be eliminated by forming group of nodes called clusters and by electing one node among the nodes in the cluster to be cluster head. All nodes can send data to the cluster head where the aggregation of data can take place. There are two types of clustering techniques. The clustering technique applied in homogeneous sensor networks is called homogeneous clustering schemes, and the clustering technique applied in the heterogeneous sensor networks is referred to as heterogeneous clustering schemes. If we have used fixed node as the cluster head, then it has to collect data from all of its child nodes and has to process the data for all the time period. This leads to faster battery drainage in the fixed cluster head. Even if one cluster head dies, it will affect the working of the network. By choosing dynamic cluster head, this problem can be eliminated. LEACH is an example of clustering protocol for wireless sensor network which considers homogeneous sensor networks where all sensor nodes are designed with the same battery energy. HEED and PEGASIS are some of the other examples of the clustering algorithm.

5.2. LEACH. It stands for low-energy adaptive clustering hierarchy which is the first protocol of hierarchical routing which proposed data fusion, and it is of milestone significance in clustering routing protocol. LEACH minimizes the communication energy that is dissipated by the cluster heads and the cluster members as much as 8 times when compared with direct transmission and minimum transmission energy routing. LEACH incorporates randomized rotation of the high-energy cluster-head position such that it rotates among the sensors in order to avoid draining the battery of any one sensor in the network. In this way, the energy load associated with being a cluster head is evenly distributed among the nodes. Since the cluster-head node knows

all the cluster members, it can create a TDMA schedule that tells each node exactly when to transmit its data. In addition, using a TDMA schedule for data transfer prevents intracluster collisions. The operation of LEACH is divided into rounds. Each round begins with a set-up phase when the clusters are organized, followed by a steady-state phase where several frames of data are transferred from the nodes to the cluster head and onto the base station.

5.3. HEED. It stands for hybrid energy-efficient distributed clustering. HEED is one of the most effective cluster-based routing protocols in WSN. HEED has four primary objectives:

(i) Prolonging network lifetime by distributing energy consumption

(ii) Terminating the clustering process within a constant number of iterations

(iii) Minimizing control overhead (to be linear in the number of nodes)

(iv) Producing well-distributed cluster heads

It is a distributed, energy efficient clustering approach which makes use of two parameters to cluster the network: the sensor residual energy as a primary parameter and intracommunication like node degree and node proximity as a secondary parameter. The HEED operation for clustering is divided into three phases: the initialization phase in which the sensors put their probabilities to become CHs, the main processing phase in which the sensors go through many steps to elect the CHs, and the finalization phase in which each sensor joins the least communication-cost CH or announces itself as a CH. The reclustering in HEED is triggered dynamically at the beginning of each round which is a predefined period of time; the round in HEED can be in the range of seconds, minutes, or even hours depending on the application at hand. The HEED clustering operation is invoked at each node in order to decide if the node will elect to become a cluster head or join a cluster. A cluster head is responsible for two important tasks:

(1) Intracluster coordination, i.e., coordinating among nodes within its cluster

(2) Intercluster communication, i.e., communicating with other cluster heads and/or external observers

The cluster range or radius is determined by the transmission power level used for intracluster announcements and during clustering. We refer to this as the cluster power level. The cluster power level should be set to one of the lower power levels of a node, to increase spatial reuse, and reserve higher power levels for intercluster communication. Selecting cluster heads is based on two parameters: a primary parameter and a secondary one. HEED uses the primary parameter to probabilistically select an initial set of cluster heads and the secondary parameter to "break ties." A tie in this context means that a node falls within the "cluster range" of more than one cluster head. The mechanism of breaking ties according to cost also ensures that the probability of having two cluster heads within the same cluster range is minimized, i.e., cluster heads are well-distributed in the network.

5.4. PEGASIS. System PEGASIS is another hierarchical routing protocol which considered as an improvement over LEACH. PEGASIS stands for power-efficient gathering in sensor information system. In PEGASIS, the primary idea is having each node to receive from and transmit to adjacent neighbours and then each node will take its turn later to be the chain leader. The nodes in PEGASIS are organized to form a chain either by the sensors themselves using a greedy algorithm starting from the randomly chosen node, usually the farthest nodes from the sink, or by having the sink construct the chain and transmits these information to the rest of sensors. In PEGASIS, the data aggregation is performed at every node on the chain except the end nodes in the chain and the network topology is assumed to be known. PEGASIS performs better than LEACH because it reduces the consumed energy in its phases. In its local gathering stage, the summation of distances among transmitting nodes is less than transmitting to a CH in LEACH. Also, the amount of data received by the leader of chain is much less from that in LEACH. Finally, in each round, only there is one node envoys the collected data to the sink node.

6. Related Works

Tremendous works have been done in the field of RFID regarding duplicate data elimination. We discuss here some of the works done so far. Traditionally, the data warehouse stores all the data after redundancy processing algorithm. Then, relevant query processing is done. But due to large volume of data stream in RFID, inaccurate queries are being processed sometimes. So, RFID cube has been evolved as a basic concept of filtering the redundant data according to the tag locations related to the movement and static state of the tags [22]. To eliminate this limitation, sliding window concept was evolved which stores the smaller size of data as compared to the actual size. But it faces problem when flooded data stream encounters smaller window size or a large window size computes the appropriate data with huge time constraint [23]. Depending on the type of RFID data stream, various works are done so far. A data cleaning algorithm (Improved SMRUF) is proposed by Wang et al. which is based on probability which considers the time complexity of sliding window. This adaptive process reduces redundancy for dynamic tags [24]. Luo et al. have proposed another approach for dynamic tags which takes time tolerance into account and sets up a threshold value for it to simplify the data instead of filtering [25]. Sometimes this kind of technique increases the system overhead due to nonfiltering. To eliminate this type of problems, some techniques like Dynamic Bayesian Networks (DBNs) [26] and Finite State Machine [27] are seen into picture. DBNs focus on not recording new data stream as the weight of new data is configured with the observed value of the data. Finite State

Input: RFID Data
x : $x.tid$, x time, $x.RSS$, $x.loc$, $x.RSSI$
Output: x is Redundant or not
Step 1: Begin
Create two events
Event (Hash mapping of arrival tid)
Event-check(for comparison)
for K no. of IDs(1)
$P[i] = Hash_i(x.tid)$[Hash mapping]
Step 2: Initiate proposed algorithm
for K no.of IDs(i)
if $\text{TDBF}_{P[i]}\text{x} \cdot \text{RSSI} \neq 0$ [Already detected that is why RSSI ≠ 0]
Update TDBF(x · RSSI)
else [detected for the first time]
if x · RSS > ω[no need to check time as already checked in RSSI condition above.
Only check the threshold within the range]
Update TDBF (x.time, x.RSS)
else if $x \cdot \text{time-TDBF}_{P[i]}[time] > \tau$ and $x \cdot RSS > \omega$
[x is in range or not decided by RSS and
whether after certain time interval τ checked by first condition]
Update TDBF (x.time, $x.RSS$)
Send x to Event$_c heck$
break
elseifx.timer¿$\text{TDBF}_{\text{P[i]}}$ [time]
and $x.RRS > TDBF_{P[i]}[RSS]$
Update TDBF (x.time, $x.RSS$)
Send x to Event check
break
end if
Identify x by comparing Event and Event check
END

Algorithm 1: Proposed algorithm (m-TDBF).

Machine filters the valid data according to the state machine but it is not suitable for large-scale environment.

To eliminate such kind of inefficiency, Bloom filter concept came into the picture. Bloom filter is a data structure based on probability of existence of an element belonging to the collection or not. If we compare the features of Bloom filter with that of data structure, then the result is very obvious that Bloom filter is more efficient as it is independent of storage capacity based in terms of space and time [28]. In [29], log-log-Bloom-filter concept is taken to estimate the smart grid data processing whereas in [30], Hyper-Log-Log Bloom Filter describes the performance improvement of cardinality estimation of large datasets. In [31], Compare Bloom Filter concept is evolved which is responsible for data filtering in physical space dimension. Approximate Probability Synthesis Bloom Filter (PSBF) concept in [32] filters and removes the overlapped redundant data based on probabilistic occurrences. Time Interval Bloom Filter proposed by Chen et al. in [33] takes into account the total number of timestamps in a total time period to evaluate and filter the redundant data. Time Space Bloom Filter discernments the mobility of the tags of RFID detected by based on time-space features [34]. All these algorithms based on Bloom filter concept are very efficient in terms of exploiting spatial and temporal characteristics of data redundancy but these algorithms fail to do the needful in case of real-world scenario and changing environment conditions. Also, the tag quality of the RFID is a factor which lacks these concepts behind. In order to find out the fittest and efficient algorithm for real-world scenario and to work it out in a certain range, in this paper, we propose the modified version of existing TDBF algorithm. The experimental results and performance evaluation along with comparison yield it to be fit to remove the limitations of TDBF algorithm.

6.1. RFID Redundant Data. RFID redundant data can be defined as invalid data reading which comes after first reading repeatedly. The inbuilt architecture of RFID makes it prone to collect repeated data not only from the nearest tags but also nearby readers adjacent to it. The environmental conditions also affect it. Usually, RFID data are listed as a description of tuple which can be written as $<\text{ID}_{\text{tag}}, \text{loc}, t>$ for capturing the data from the reader. For example, the RFID tags present near any device from the entrance of a shopping mall can read the data from the entrance as well as the readings of data captured from the RFID readers employed near the entrance gate. So the repetitive data can lead to the system overhead decreasing the overall network lifetime. To analyse the data complexity, it is important to note that a single object should be read once by the reader only.

In order to reduce the complexity of data analysis, previous works assume that each object is read once and read

by one reader only. Clearly, this assumption is difficult to enforce, and more importantly, it oversimplifies the reality. Because the RFID readings are of low quality, many applications have to employ nonredundant readers to cover the target area completely in order to improve the localization accuracy [35], which means the objects are read by multiple readers simultaneously. Indeed, in RFID systems, the spatial redundancy is very common. A RFID reader is located at the centre of each zone. Spatial overlapping of reader's detection ranges often leads to duplicate readings carried away by the multiple readers. Temporal overlapping can be formed by the duplicate readings recorded at a particular timestamp [36].

6.2. Bloom Filter. A Bloom filter can be classified as a kind of data structure which evaluates the presence of any element in a set or not. It consists of a fixed sized array and independent hash functions mapping to the elements of the array. Initially, the value is set to be 0, and gradually, it is incremented to 1 according to the mapping of hash function to the different elements of the set. To examine whether an element is present in the set, the numerical value 1 decides the needful as in Bloom filter; this value decides the existing element. When a new element arrives in the set, 0 indicates the newly arrive element in the set [37]. In RFID, the tag IDs are inserted in the set and checked their presence by hash functions for existence of duplicate values present in the set. Changed mapping positions of different tag IDs of RFID tags can be indicated from 0 to 1 depending on the examination of newly arrived tag IDs to the bit array [38]. Bloom filter takes the advantage of independent hash functions by saving all the incoming data in terms of space and time which makes it more efficient as compared to the other data structures. In terms of security and privacy concerns, the traditional Bloom filter does not overload the system by storing all the incoming data which makes it inefficient in terms of data rate loss, increased false negative rates, and decreased false positive rates [39].

6.3. TDBF Data Redundancy Approach. As compared to the traditional Bloom filters, the TDBF (Time-Distance Bloom Filter) algorithm can be extensively used to filter the repetitive data coming from the tags of the RFID readers. It takes into consideration of the parameters like time, distance, and Received Signal Strength (RSS) [40]. RSS is greatly affected by tag quality and environmental situations. It has some fluctuations in reading with the increase and decrease in distance. It has the advantages of limited error rate along with higher performance measures. TDBF algorithm measures the distance uniquely at particular space and time. Starting at a fixed sized array, the algorithm is initialized to a user defined notation where each cell represents the two-dimensional integer arrays consisting of time and RSS, respectively. The recorded timestamps of read tags are presented by the negative values to make the first value of TDBF as 0. The recoded distance value is a user-defined threshold function integer value. Upon arrival of new RFID data, the hash functions

Table 2: Comparison of compression rate of three datasets for TDBF and m-TDBF.

Algorithm	Data 1	Data 2	Data 3
m-TDBF	5.000	5.000	3.330
TDBF	5.000	2.000	2.000

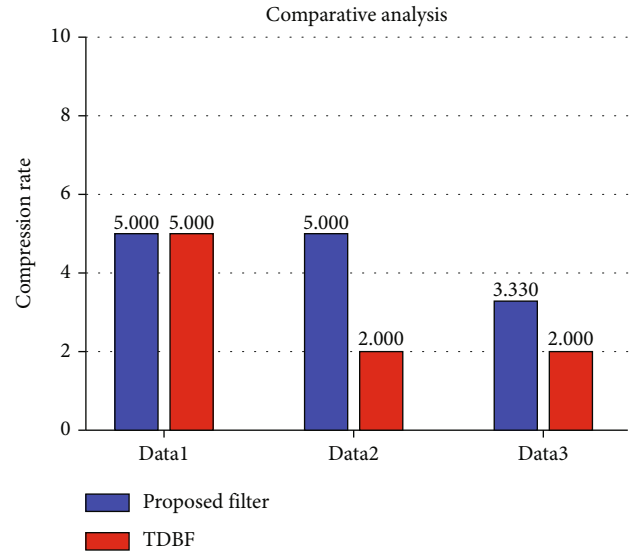

Figure 5: Comparison of 3 datasets in terms of compression ratio.

Table 3: Comparison of space saving of three datasets for TDBF and m-TDBF.

Algorithm	Data 1	Data 2	Data 3
m-TDBF	60.000	80.000	90.000
TDBF	60.000	60.000	70.000

filter the duplicate value on the basis of recorded timestamp and the RSS value of that particular tag. After detection of duplicate data, it deletes the unnecessary stuffs and keeps the useful information. Data compression ratio is considered as an important performance measure to detect the efficiency of filtering the duplicate data. The false negative rate (FNR) [38] and false positive rate (FPR) are also evaluated to measure the efficiency of filtering the data. Whenever the useful information is treated as redundant data, it generates greater FPR, and when the redundant data is mistaken as a nonredundant data, it generates higher FNR. However, excessive filtering is done when the data compression score is high, and it leads to higher rate of loss of useful data. TDBF algorithm is suitable for single-reader architecture and does not work well in large-scale environment.

To overcome such kind of limitations, we have proposed and implemented the modified version of existing TDBF algorithm in this paper which is examined to outperform the existing algorithm.

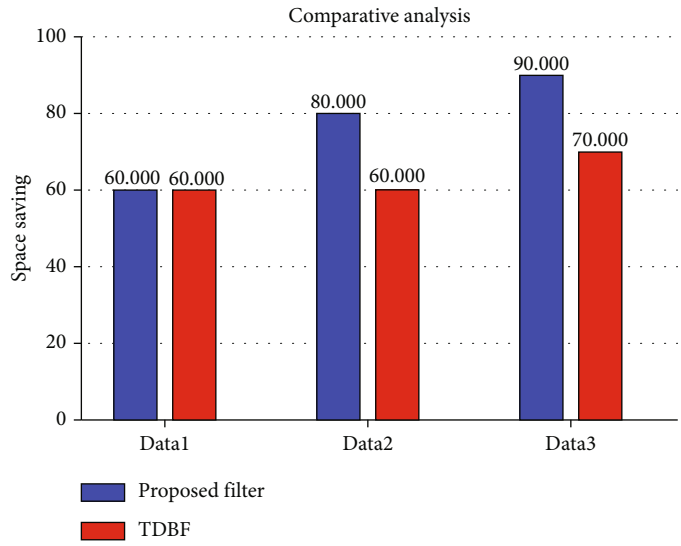

Figure 6: Comparison of 3 datasets in terms of space saving.

7. Proposed System Model

7.1. Data Generation. Let us consider a vehicular wireless sensor network where the tag identification of RFID devices has 5 fields which are

(i) ID (ID of RFID)

(ii) Time (total time)

(iii) RSS (Received Signal Strength)

(iv) loc (location of RFID)

(v) RSSI (Received Signal Strength Indicator)

7.2. Dynamic Environment Experiment. To set up the experiment in dynamic environment, we have considered some readings which are considered as "n." Here we have considered 10 different readings. So here, $n = 10$. To make these 10 readings random, we have used variable "n" that randomly takes "n" values from time, RSS, loc, and RSSI fields. Again to make it dynamic, the time, RSS, loc, and RSSI fields are chosen randomly from its corresponding matrices, e.g., time: l, RSS: r, loc: t, RSSI: i, and threshold: ω.

For the data generation of our proposed algorithm, we have considered a vehicular wireless sensor network where we have taken into consideration of "n" no. of vehicles randomly. The observations are taken on a random basis to check the effectiveness of our algorithm. As discussed earlier, every tag of RFID device is mapped through the hash function. After the hash function has been called, we consider the data generation part. As RFID comes with less no. of real dataset for our experiment, we have used synthetic dataset which is generated randomly by using Cooja Simulator. Now the dataset is ready by assigning alone values to tag IDs. All these values are also randomly developed to make it realise that reading time, RSS, loc, and RSSI are not the same always.

Table 4: Comparison of detection ratio of three datasets for TDBF and m-TDBF.

Algorithm	Data 1	Data 2	Data 3
m-TDBF	5.000	5.000	3.330
TDBF	5.000	2.000	2.000

Data generation file is executed 3 times to make it sure that reading is not repeating, i.e., reading changes as in the case of dynamic network.

Once the dataset is available, we then can generate two events which are

(i) Event (for initial hash mapping)

(ii) Event 1 (for comparing)

Data=tag=stores all tag data.

7.3. m-TDBF Algorithm. So now, we will process all IDs, and we are expecting it should return detected for IDs except last two. Initially, we calculate hash values or index for ID. Then, check corresponding index in m-TDBF matrix, third column (RSSI). If it is zero, then only we will go for time and RSS value checking. Else it is already detected so we assign RSS to it. No need to calculate hash. If it is 0, it is detected for first time and rest algorithms as per paper, i.e., it will calculate hash values and assign it to Event 1.

7.4. m-TDBF vs. TDBF. If we compare the existing TDBF algorithm with our proposed algorithm which is the modified version of TDBF algorithm (m-TDBF), then we can observe the following scenario

Condition 1

Vehicle is read when x.time == 0 that means RSS > ω.

Condition 2

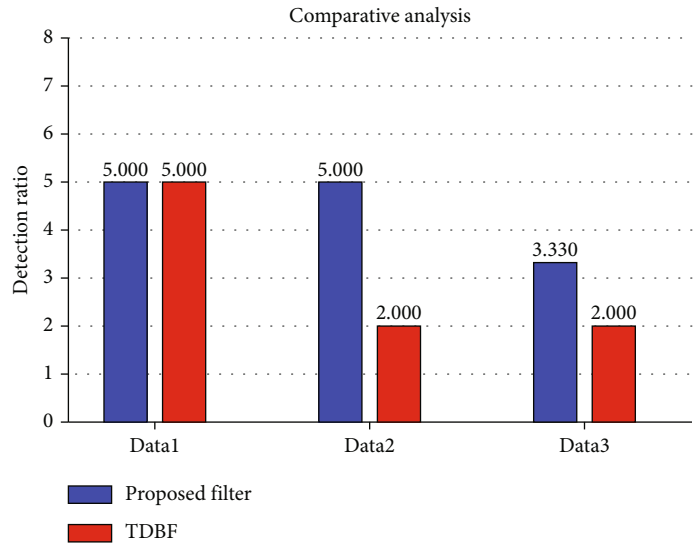

Figure 7: Comparison of 3 datasets in terms of detection ratio.

Next, vehicle will be read by the same tag where x.time $-$ TDBF(time) $> \tau$.

Condition 3

Repetitive reads were done by the same reader reading another vehicle.

In TDBF algorithm, the three above conditions are checked repetitively which enhances the time complexity factor of the algorithm and hence slows down the processor. But in m-TDBF algorithm, if RSSI is detected for the first time, then we can directly go to the third condition without wasting time on checking condition 1 and condition 2. But if the vehicle is already detected, then we can just update RSS which improves the time complexity factor. The same RSSI is repeated; hence, the above three conditions of TDBF will not proceed. This limitation of TDBF has been enhanced in m-TDBF which can be observed by the experimental results of the proposed algorithm.

8. Experimental Results and Performance Evaluation

8.1. Performance Measures. For our experiment, we have considered three datasets of our generated synthetic data to compare different parameters used for it. The performance measures which have been used for this experiment can be coined as follows:

8.2. Compression Ratio. It can be defined as the score of RFID data collected with respect to filtered tags. Error rate is minimized when we have higher compression rate. The comparison of compression ratio of two algorithms for three datasets data 1, data 2, and data 3 is given in Table 2. Equation (2) describes the mathematical formula of compression ratio in terms of data rate which is as follows:

$$\text{Compression ratio} = \frac{\text{uncompressed data rate}}{\text{compressed data rate}}. \quad (2)$$

Figure 5 describes the graphical representation of the comparative analysis of compression ratio.

8.3. Space Saving. Storage space of a Bloom filter relies on the average inaccurate rate. The space saving attribute yields different value for the EPC class of RFID reader. With the increase of false positive and false negative rate, the Bloom filter compresses the data nearly 10 times as compared to the original data. So in our proposed method, the warehouse model is efficient in space saving. Equation (3) formulates the space saving which is as follows:

$$\text{Space saving} = 1 - \left[\frac{\text{compressed size}}{\text{uncompressed size}}\right]. \quad (3)$$

Here we have made a comparative analysis of existing algorithm and proposed algorithm for three datasets which is provided in Table 3, and the bar chart is shown in Figure 6 graphically.

8.4. Detection Ratio. It can be defined as the score of false negative rates with respect to the false positive rate. In Table 4, we have given the comparison of two algorithms for 3 datasets and presented it graphically in Figure 7.

8.5. Time Complexity. The comparison of time difference between two algorithms is observed. Time is taken in seconds with respect to the number of tags. From 0 to 10 seconds, the graph is stagnant for both the algorithms. But after 15 seconds, the proposed algorithm shows a decreasing trend with respect to the number of tags which makes it more efficient than the other. For this experiment, we have used Impinj Revolution series of passive readers and several supporting tags.

8.6. Comparative Analysis. TDBF has always been best observed in closed room scenario as the tag is fluctuated by environment, but here in this paper, we have done the

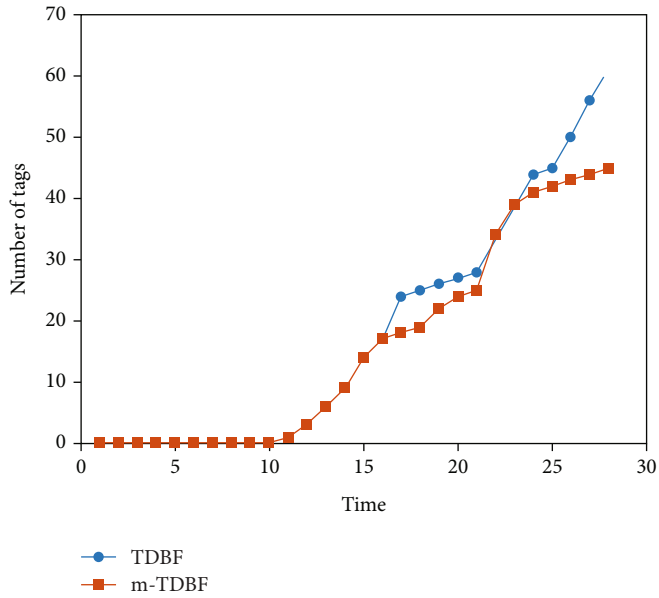

Figure 8: Comparison of time complexity between TDBF and m-TDBF.

experiment for the proposed algorithm in open air environment to taste the best fit practice. We have taken randomly selected 3 datasets, namely, data 1, data 2, and data 3. The tabular representation of three datasets is given below where we have compared TDBF and m-TDBF algorithms in terms of compression ratio, space saving, detection ratio, and time complexity. The obtained results of bar graphs shows a clear picture of consistency of the proposed algorithm. The graph of time complexity shows the efficiency of our proposed algorithm in terms of time management.

8.7. Results. From the above comparative analysis and graphical representation, it is clear that our proposed algorithm (m-TDBF) is more efficient than the existing TDBF in terms of compression ratio, space saving, detection ratio, and time complexity. So the m-TDBF algorithm maintains an increasing trend for all the performance measures as compared to TDBF. Hence, in both static and dynamic environment, m-TDBF can filter out more number of valid data enhancing the system requirements and limiting the loss of useful information. This comparative analysis can be graphically represented which is shown in Figure 8 below:

9. Conclusion and Future Work

In practical scenario the RFID data contains a huge variety of repetitive data which overburdens the system and results in slow processing. Existing data structure cannot enhance the performance due to overloading of huge amount of data streams coming to it. It is eventually difficult to process and filter the data resulting inefficiency in the system. So Bloom filter has come into picture which is considered to be a probabilistic data structure enhancing the system utility by managing the fruitful processing and filtering of huge amount of data streams in RFID. So in this paper, we have introduced the modified version of TDBF algorithm which is proven to be fit for enhancing system efficiency in large-scale application environment. The comparative study of TDBF algorithm with m-TDBF algorithm shows the results that the proposed algorithm is more efficient to reduce the error impact by introducing the RSSI. The fluctuations in RSS value can be handled by RSSI effectively without depending on the quality of tag or environment factors. Here we have compared the compression ratio, space saving, and detection ratio attributes as three important performance measures which gives a clear picture about the efficiency of the proposed algorithm. The proposed algorithm is fit for dynamic scenario in terms of effectively filtering the valid data into the system. To check the effectiveness of our proposed algorithm, by adding more number of parameters will be next step of our research.

Data Availability

The evaluation data used to support the findings of this study are available on request from the corresponding author.

Conflicts of Interest

The authors declare no conflict of interest.

References

[1] H. El Alami, A. Najid, H. El Alami, and A. Najid, "Optimization of energy efficiency in wireless sensor networks and internet of things: a review of related works," *Nature-Inspired Computing Applications in Advanced Communication Networks*, 2020.

[2] H. E. Alami and A. Najid, "EEA: clustering algorithm for energy-efficient adaptive in wireless sensor networks," *International Journal of Wireless Networks and Broadband Technologies (IJWNBT)*, vol. 7, no. 2, pp. 19–37, 2018.

[3] H. E. Alami and A. Najid, "(SET) smart energy management and throughput maximization: a new routing protocol for WSNs," in *Security Management in Mobile Cloud Computing*, pp. 1–28, IGI Global, 2017.

[4] J.-S. Lee and W.-L. Cheng, "Fuzzy-logic-based clustering approach for wireless sensor networks using energy predication," *IEEE Sensors Journal*, vol. 12, no. 9, pp. 2891–2897, 2012.

[5] S. Wang, Z. Cao, Y. Zhang, W. Huang, and J. Jiang, "A temporal and spatial data redundancy processing algorithm for RFID surveillance data," *Wireless Communications and Mobile Computing*, vol. 2020, Article ID 6937912, 12 pages, 2020.

[6] R. Angeles, "RFID technologies: supply-chain applications and implementation issues," *Information Systems Management*, vol. 22, no. 1, pp. 51–65, 2005.

[7] J.-P. Qian, X.-T. Yang, X.-M. Wu, L. Zhao, B.-L. Fan, and B. Xing, "A traceability system incorporating 2D barcode and RFID technology for wheat flour mills," *Computers and Electronics in Agriculture*, vol. 89, pp. 76–85, 2012.

[8] J. Yin, J. Yi, M. K. Law et al., "A system-on-chip EPC Gen-2 passive UHF RFID tag with embedded temperature sensor," *IEEE Journal of Solid-State Circuits*, vol. 45, pp. 2404–2420, 2010.

[9] E. Evizal, T. A. Rahman, and S. K. A. Rahim, "Active RFID technology for asset tracking and management system," *TELKOMNIKA (Telecommunication Computing Electronics and Control)*, vol. 11, no. 1, pp. 137–146, 2013.

[10] P. V. Nikitin, R. Martinez, S. Ramamurthy, H. Leland, G. Spiess, and K. V. S. Rao, "Phase based spatial identification of UHF RFID tags," in *2010 IEEE International Conference on RFID (IEEE RFID 2010)*, pp. 102–109, Orlando, FL, USA, 2010.

[11] F. Thiesse and F. Michahelles, "An overview of EPC technology," *Sensor Review*, vol. 26, no. 2, pp. 101–105, 2006.

[12] J. Kim, S. Kumara, S.-T. Yee, and J. Tew, "Dynamic shipment planning in an automobile shipment yard using real-time radio frequency identification (RFID) information," in *IEEE International Conference on Automation Science and Engineering*, pp. 148–153, Edmonton, AB, Canada, 2005.

[13] B. Nath, F. Reynolds, and R. Want, "RFID technology and applications," *IEEE Pervasive Computing*, vol. 5, no. 1, pp. 22–24, 2006.

[14] H. Chen, W.-S. Ku, H. Wang, and M.-T. Sun, "Leveraging spatio-temporal redundancy for RFID data cleansing," in *Proceedings of the 2010 ACM SIGMOD International Conference on Management of data, SIGMOD'10*, pp. 51–62, Indianapolis, Indiana, USA, 2010.

[15] D. Bleco and Y. Kotidis, "RFID data aggregation," in *Proceedings of the 3rd International Conference on GeoSensor Networks, GSN'09*, pp. 87–101, Oxford, UK, 2009.

[16] C. M. Roberts, "Radio frequency identification (RFID)," *Computers and Security*, vol. 25, no. 1, pp. 18–26, 2006.

[17] A. P. Sample, D. J. Yeager, P. S. Powledge, A. V. Mamishev, and J. R. Smith, "Design of an RFID-based battery-free programmable sensing platform," *IEEE Transactions on Instrumentation and Measurement*, vol. 57, no. 11, pp. 2608–2615, 2008.

[18] A. Juels, "RFID security and privacy: a research survey," *IEEE Journal on Selected Areas in Communications*, vol. 24, no. 2, pp. 381–394, 2006.

[19] M. Feldhofer, S. Dominikus, and J. Wolkerstorfer, "Strong authentication for RFID systems using the AES algorithm," in *Cryptographic Hardware and Embedded Systems-CHES 2004*, M. Joye and J.-J. Quisquater, Eds., pp. 357–370, Springer, Berlin, Heidelberg, 2004.

[20] H. Gonzalez, J. Han, X. Li, and D. Klabjan, "Warehousing and analyzing massive RFID data sets," in *22nd International Conference on Data Engineering (ICDE'06)*, p. 83, Atlanta, GA, USA, 2006.

[21] L. V. Massawe, J. D. M. Kinyua, and H. Vermaak, "Reducing false negative reads in RFID data streams using an adaptive sliding-window approach," *Sensors*, vol. 12, no. 4, pp. 4187–4212, 2012.

[22] K. Hu, L. Li, C. Hu, J. Xie, and Z. Lu, "A dynamic path data cleaning algorithm based on constraints for RFID data cleaning," in *2014 11th International Conference on Fuzzy Systems and Knowledge Discovery (FSKD)*, pp. 537–541, Xiamen, China, 2014.

[23] X. Wu, H. Liu, L. Zhang, M. J. Skibniewski, Q. Deng, and J. Teng, "A dynamic Bayesian network based approach to safety decision support in tunnel construction," *Reliability Engineering and System Safety*, vol. 134, pp. 157–168, 2015.

[24] B. Babagholami-Mohamadabadi, S. Yoon, and V. Pavlovic, "D-MFVI: distributed mean field variational inference using Bregman ADMM," 2015, https://arxiv.org/abs/1507.00824.

[25] L. Luo, D. Guo, R. T. B. Ma, O. Rottenstreich, and X. Luo, "Optimizing Bloom filter: challenges, solutions, and comparisons," *IEEE Communications Surveys Tutorials*, vol. 21, no. 2, pp. 1912–1949, 2019.

[26] Y. Yao, S. Xiong, H. Qi, Y. Liu, L. M. Tolbert, and Q. Cao, "Efficient histogram estimation for smart grid data processing with the loglog-Bloom-filter," *IEEE Transactions on Smart Grid*, vol. 6, no. 1, pp. 199–208, 2015.

[27] Q. Xiao, Y. Zhou, and S. Chen, "Better with fewer bits: Improving the performance of cardinality estimation of large data streams," in *IEEE INFOCOM 2017- IEEE Conference on Computer Communications*, pp. 1–9, Atlanta, GA, USA, 2017.

[28] H. Mahdin and J. Abawajy, "An approach for removing redundant data from RFID data streams," *Sensors*, vol. 11, no. 10, pp. 9863–9877, 2011.

[29] M. S. Mekala, R. Patan, S. H. Islam, D. Samanta, G. A. Mallah, and S. A. Chaudhry, "DAWM: cost-aware asset claim analysis approach on big data analytic computation model for cloud data centre," *Security and Communication Networks*, vol. 2021, Article ID 6688162, 16 pages, 2021.

[30] X. Wang, Y. Ji, and B. Zhao, "An Approximate Duplicate-Elimination in RFID Data Streams Based on d-Left Time Bloom Filter," in *Web Technologies and Applications*, L. Chen, Y. Jia, T. Sellis, and G. Liu, Eds., pp. 413–424, Springer International Publishing, Cham, 2014.

[31] W. Rui, L. Guoqiong, and D. Guoqiang, "Filtering redundant RFID data based on sliding windows," in *2014 International Conference on Management of e-Commerce and e-Government*, pp. 187–191, Shanghai, China, 2014.

[32] S. Ur Rehman, R. Liu, H. Zhang, G. Liang, Y. Fu, and A. Qayoom, "Localization of moving objects based on RFID tag array and laser ranging information," *Electronics*, vol. 8, no. 8, p. 887, 2019.

[33] D. Samanta, A. H. Alahmadi, M. P. Karthikeyan et al., "Cipher block chaining support vector machine for secured decentralized cloud enabled intelligent IoT architecture," *IEEE Access*, vol. 9, pp. 98013–98025.

[34] X. Li, "Collaborative localization with received-signal strength in wireless sensor networks," *IEEE Transactions on Vehicular Technology*, vol. 56, pp. 3807–3817, 2007.

[35] C. Metzger, S. Gershwin, and E. Fleisch, "The impact of false-negative reads on the performance of RFID-based shelf inventory control policies," *Computers and Operations Research*, vol. 40, no. 7, pp. 1864–1873, 2013.

[36] H. Ma, Y. Wang, and K. Wang, "Automatic detection of false positive RFID readings using machine learning algorithms," *Expert Systems with Applications: An International Journal*, vol. 91, pp. 442–451, 2018.

[37] E. Q. Shahra, T. R. Sheltami, and E. M. Shakshuki, "A comparative study of range-free and range-based localization protocols for wireless sensor network," *International Journal of Distributed Systems and Technologies*, vol. 8, no. 1, pp. 1–16, 2017.

[38] M. Maheswari, S. Geetha, S. S. Kumar, M. Karuppiah, D. Samanta, and Y. Park, "PEVRM: probabilistic evolution based version recommendation model for Mobile applications," *IEEE Access*, vol. 9, pp. 20819–20827, 2021.

[39] R. C. Costa and J. R. Sodré, "Compression ratio effects on an ethanol/gasoline fuelled engine performance," *Applied Thermal Engineering*, vol. 31, no. 2-3, pp. 278–283, 2011.

[40] M. Cafaro, M. Pulimeno, I. Epicoco, and G. Aloisio, "Parallel Space Saving on Multi- and Many-Core Processors," *Concurrency and Computation: Practice and Experience*, vol. 30, no. 7, 2018.

Hindawi
Wireless Communications and Mobile Computing
Volume 2022, Article ID 5626764, 13 pages
https://doi.org/10.1155/2022/5626764

Research Article

Autonomous Robots for Deep Mask-Wearing Detection in Educational Settings during Pandemics

Huma Zia[1], **Marah Alhalabi**[1], **Maha Yaghi**[1], **Amer Barhoush**[1], **Omar Farag**[1], **Mohammad Alkhedher**[2], **Adel Khelifi**[3], **Ahmed M. A. Ibrahim**[4] and **Mohammed Ghazal**[1]

[1]*Electrical, Computer and Biomedical Engineering Department, College of Engineering, Abu Dhabi University, Abu Dhabi 59911, UAE*
[2]*Mechanical Engineering Department, College of Engineering, Abu Dhabi University, Abu Dhabi 59911, UAE*
[3]*Computer Science and Information Technology Department, College of Engineering, Abu Dhabi University, Abu Dhabi 59911, UAE*
[4]*Mansoura University, Mansoura, Egypt*

Correspondence should be addressed to Mohammed Ghazal; mohammed.ghazal@adu.ac.ae

Received 3 March 2022; Revised 3 July 2022; Accepted 8 July 2022; Published 27 July 2022

Academic Editor: Xiaohui Yuan

The COVID-19 pandemic has severely impacted various aspects of life, where countries closed their borders, and workplaces and educational institutions shut down their premises in response to lockdowns. This has adversely affected the lives of everyone, including millions of students worldwide, socially, mentally, and physically. Governments and educational authorities worldwide have taken preventive measures, such as social distancing and mask wearing, to control the spread of the virus. This paper proposes an AI-powered autonomous robot for deep mask-wearing detection to enforce proper mask wearing in educational settings. The system includes (1) Simultaneous Localization and Mapping framework to map and navigate the environment (i.e., laboratories and classrooms), (2) a multiclass face mask detection software, and (3) an auditory system to identify and alert improper or no mask wearing. We train our face mask detector using MobileNetV2 architecture and YOLOv2 object detector classification. The results demonstrate that our robot can navigate an educational environment while avoiding obstacles to detect violations. The proposed face mask detection and classification subsystem achieved a 91.4% average precision when tested on students in an engineering laboratory environment.

1. Introduction

The COVID-19 epidemic, which the World Health Organization (WHO) has labelled a global pandemic, has severely impacted people's lives. This highly infectious disease has caused a rapid increase in COVID-19 incidents around the world and triggered the need for immediate countermeasures [1]. Countries enforced strict laws and regulations to reduce the transmission of the virus and prevent its spread [2], especially following the lift of the nationwide lockdown. For instance, some counties have made wearing face masks in public mandatory [3, 4], including the United Arab Emirates (UAE), as it is an efficient way to limit the spread of the virus [5, 6].

The pandemic disrupted teaching and learning in schools and universities. It has been necessary for educators, students, institutions, and parents to adapt, implement measures, and make optimal use of the resources, technologies, and instructional methodologies that are currently accessible [7]. Many universities in the UAE have already implemented alternative educational methods such as online, hybrid, and blended learning, making teaching and learning more adaptable and accessible to students' needs. While blended learning incorporates elements of online course delivery,

alternative approaches include the hybrid model, which combines online course delivery with in-person sessions. Additionally, the hybrid approach in some universities includes the need for students to attend online and other face-to-face lab sessions and assessments while adhering to the COVID-19 guidelines of face mask wearing and social distancing. However, the lack of awareness and failure to comply with such rules allows for the disease's unrestricted spread. Currently, the implementation techniques for mask enforcement are primarily human-monitored, making them challenging to enforce successfully in highly populated venues [8].

Researchers and manufacturers constantly aim to develop systems that can aid in pandemic preventive measures, specifically robotics. With a total market share of 27 billion USD, the prominence of service robots at this day and age is unwavering [9], especially with estimations pointing towards the imminent integration of service robots in our daily lives [10]. Moreover, the pandemic has encouraged the development of systems designed to identify recurring violations relating to social distancing measures such as mask detection or the distance between two individuals. Such systems or robots can also approach the violators and notify them to adhere to the set measures [11]. Furthermore, there is a strong emergence of tracking systems that can track social distancing metrics. Most of these systems are efficient, accurate, and easily applicable to any CCTV surveillance camera in any environment, regardless of visual challenges such as occlusion [12]. In addition to service robots and detection systems, the pandemic has also triggered the development of tracing applications used on smartphones; such applications allow the identification of any person in contact with an infected person prior to them knowing about the infection [13]. Whereas privacy concerns regarding such applications have risen, they remain effective and highly used in countries such as the UAE [14]. Such developments in the field will aid us in developing an automated mask detection monitoring system capable of detecting mask violations and notifying the violator. Various factors make face mask detection algorithms challenging. This includes various mask types, differing degrees of obstruction, varying angles, implementation of detection models on machines with limited computing capabilities, poor-quality images, facial expressions, and lack of real-world image database [4].

Deep learning artificial intelligence approaches are being widely used for face mask detection algorithms. Authors of [15] developed a hybrid model that consists of a feature extraction component using Resnet50 followed by a classification component using Support Vector Machine (SVM). The AI model was trained and tested on three different datasets and achieved a reasonable accuracy. Another implementation based on deep learning face mask detection is presented in [2], where the authors have used the YOLOv3 model along with a novel data augmentation technique to detect face masks. Their data augmentation methodology involves filtering images through greyscale and Gaussian blurring. In [5], the authors utilize YOLOv4 to detect whether pedestrians adhere to the rules of face mask wearing or not, especially at night time. Alok et al. [16] proposed CNN and VGG16 model to detect people not wearing a mask. Their work utilizes data augmentation, normalization, and transfer learning to build the model. They train their model on Google Colab using Tensorflow. For the dataset, the public domain Simulated Masked Face Dataset (SMFD) is used. The dataset included 1315 images, 657 for no mask and 658 with mask, which were included for the training set, 142 for validation, and 194 for testing. Other studies that deploy deep learning-based models for the detection of face masks are presented in [4, 8, 17, 18].

In [19], the authors presented a face mask-wearing condition identification method that addresses a classification problem for three categories based on unconstrained 2D facial pictures by merging image super-resolution and classification networks (SRCNet). They train and test the model using the Medical Masks Dataset, which includes images of people without face masks, people wearing face masks incorrectly, and others wearing them correctly. However, one of the study's limitations is that the dataset utilized is quite limited, limiting the study's ability to cover all postures and situations.

A two-stage real-time face mask detection and classification is proposed in [3]. In the face detection step, the detector filters out nonfaces and divides the facial areas into two groups based on their location on the face. The authors trained and tested both models using benchmark datasets. Thus, the proposed detector performs well and has a good level of accuracy compared to other detectors.

Authors of [20] developed a real-time face mask detection model. They use a Haar cascade classifier and YOLOv3 for face and mask detection, respectively. This system has been built as a safety solution for office entrance. The DL model has been trained on 7000 samples, 5000 training, 1000 validation, and 1000 testing. The algorithm achieved up to 83% precision. This proposed algorithm can work in real time with 30fps, and it uses image enhancement techniques to improve accuracy.

Several approaches proposed in the literature include robots designed to navigate and automate the process of face mask detection autonomously. In [21], a TurtleBot3 robot was used alongside a LiDAR sensor for obstacle detection. The sensor scans and maps the environment using a 3D visualization software available in the ROS environment. Authors of [22] designed and built a robot that will assist authorities in preventing the transmission of COVID-19 and its outbreaks. With biosensors and temperature detectors, the robot can check for the virus. It also deploys a deep learning artificial intelligence-based face mask detection. In [23], the authors built a mobile robot called Thor that classifies people wearing masks from those who are not. This robot is trained using ResNet50 to primarily detect unmasked people and provide them with a mask to limit the virus spread. The model's accuracy was reasonable despite the challenging nature of the dataset.

To the best of our knowledge, none of the existing mask-wearing systems has catered primarily for students' health nor tested in educational settings. This research work proposes an AI-powered self-driving robot to enforce student

mask wearing through automated face mask detection and classification techniques to address these limitations. We design our robot to autonomously navigate an educational environment using Simultaneous Localization and Mapping (SLAM), especially in laboratories and classrooms, while avoiding obstacles. The face mask detection and classification system uses MobileNetV2 and YOLOv2 to detect students with or without face masks and classify them into three categories. The system uses bilingual auditory alerts to notify students who are not wearing their masks or wearing their masks incorrectly. This proposed system aims to limit the spread of the COVID-19 virus in educational institutions, especially in laboratories and classrooms.

The remainder of the paper is structured as follows. The Materials and Methods section presents the methodology of our proposed research work, while the Results and Discussion section discusses the results of our proposed system and subsystems. We conclude our work in the Conclusions section.

2. Materials and Methods

2.1. Proposed System Overview. We propose an AI-powered self-driving robot to enforce student mask wearing that consists of face mask detection and autonomous navigation subsystems as shown in Figure 1. The autonomous navigation subsystem consists of a TurtleBot3 robot and a LiDAR sensor. This subsystem allows the robot to navigate the educational environment autonomously, determining the optimum path, mapping its surroundings, and avoiding obstacles. The face mask detection subsystem simultaneously gets activated while navigating a laboratory or a classroom. We train a machine learning model to detect and classify students into three main categories: wearing masks, not wearing masks, and wearing masks incorrectly. The proposed system deploys auditory alerts to warn students without masks or wearing them incorrectly. Through such preventive measures, our approach ensures that students are wearing their masks correctly at all times, controlling the transmission of the disease.

2.2. Robot Design. Our autonomous robot consists of a Turtlebot3 Burger base with a built-in 360 degree LiDAR for obstacle detection, SLAM and navigation, a gyroscope, and an accelerometer. The robot is equipped with a Raspberry Pi 3, an OpenCR control board to configure and control the sensors and motors, respectively, and a battery. The robot also consists of a camera for real-time video capturing, a Bluetooth speaker for alerts, and an NVIDIA Jetson Xavier for running the face mask detection algorithm. The robot design, including the camera and other components' positions, is illustrated in Figure 2.

2.3. Autonomous Navigation Subsystem. The proposed robot navigates the educational premises autonomously using the ROS framework as illustrated in Figure 3. The robot begins by creating a static map of the surroundings using the SLAM method, fed with 360 LiDAR sensor data. We first use a joystick to drive the robot around manually. The ROS Navigation stack's Gmapping [24] SLAM method is then used to create the map of the environment accordingly, where the map's accuracy depends on the accuracy of the localization. The LiDAR sensor's odometry data and the data from the motor encoders and gyroscope are used for localization. The navigation algorithm then takes the odometry data, the LiDAR sensor stream, and the static map of the surroundings and outputs the velocity commands accordingly to the motor driver, where they are then input to the navigation stack.

While the robot is navigating a laboratory or a classroom, it may encounter various static and dynamic obstacles that may obstruct its path. The robot performs a cautious reset in the first recovery behavior, clearing the barriers identified from the local cost map. If no path can be found because the obstacles have not been cleared, the robot rotates in its current location and checks whether the obstacles have been removed. If it is still obstructed, the cost map is reset entirely by clearing all obstacles. If the robot still cannot discover a way, it will perform one final rotation in its place after clearing the cost map. The robot will then abort the mission if none of the recovery attempts succeed.

2.4. Face Mask Detection and Classification Subsystem. We train the face mask detector to identify students without masks or wearing masks incorrectly and classify them into three categories: correct, incorrect, or no mask. A Logitech C920 camera is mounted on the robot to provide real-time feedback while navigating the laboratory or a classroom setting. We use three face mask detection datasets [25–27] to develop the proposed detection model. These datasets include people wearing face masks properly, improperly, and without masks at all. Conducting many experimental tests to increase accuracy, performance, and generalization has led to 8 different datasets throughout this project. The first dataset (refer to Table 1) collected had 4,400 images. The dataset contained images of people wearing face masks correctly and was not equally distributed. The model trained based on this dataset did not satisfy our requirements, so we have increased the dataset size. The second dataset contained a total of 9,200 images. The model's average precision has improved, but it was not reliable enough. The dataset size continued to increase until we reached a point where the device used for training runs out of memory while training more than 15,200 images. To further improve our model, we increased the number of categories into three categories (correctly, incorrectly worn face masks, and without face masks). We started with a dataset size of 6,600 images (2,200 images per category). Starting with small dataset sizes is critical to test whether the model's average precision will improve after increasing the dataset size and reducing the weight on the detection models since the more trained data used, the slower the detection model will be. The dataset that built the highest precision models contained significant differences than the previous ones. The finalized dataset included more generalized images based on face angles, distances, and mask colors. Each dataset will be used to create a unique face mask detection model. We will evaluate the precision and recall of the models to find the best model

Figure 1: System overview diagram.

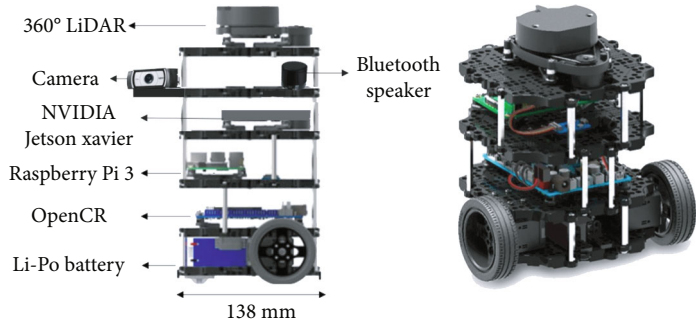

Figure 2: Robot hardware design.

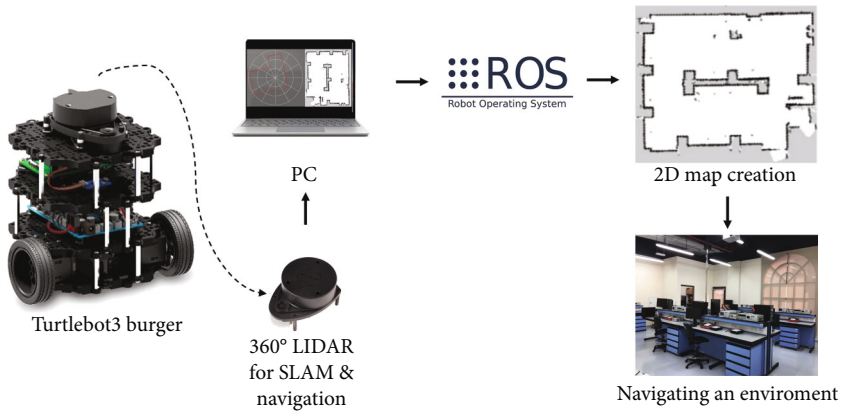

Figure 3: Autonomous navigation subsystem diagram.

performance to be used for this study. The summary of each dataset created can be presented in Table 1.

Due to the limited adequate amount of data available for training the face mask detector AI model, image augmentation is performed. Images are rotated, zoomed in and out, and shifted to generate various versions of each picture and improve accuracy [28].

We use the Caffemodel and prototxt for the implementation for the detection of facial masks. Each frame is input through a pretrained face detector model designed to identify and crop every detected face with a confidence of 70% or higher. The cropped image is then scaled to 224 x 224 pixels, RGB encoded, and inputted into the classifier along with the cropped face's X and Y coordinates. We perform face mask detection using the pretrained MobileNetV2 network, a light-weight deep CNN model, and initialize the networks with the weights of the pretrained models trained on the ImageNet dataset.

Table 1: Datasets created.

Name	Total images	Categories	Models generated
Dataset 1	15,200	Correct, incorrect	Model 1
Dataset 2	9,200	Correct, incorrect	Model 2
Dataset 3	4,400	Correct, incorrect	Model 3
Dataset 4	10,000	Correct, incorrect, without	Model 4
Dataset 5	6,600	Correct, incorrect, without	Model 5
Dataset 6	12,000	Correct, other	Model 6
Dataset 7	12,000	Incorrect, other	Model 7
Dataset 8	12,000	Without, other	Model 8

Table 2: Models created in experiment 1.

Name	Total images trained	No. of epochs	Batch size	Categories
Model 1	15,200	12	32	Correct, incorrect
Model 2	9,200	12	32	Correct, incorrect
Model 3	4,400	12	32	Correct, incorrect

We conduct three main experiments to develop a detector that can detect face masks of students' faces with high accuracy and precision. All detectors in the upcoming experiments were trained using Keras and TensorFlow2. In the first experiment, different dataset sizes with two categories only were used to generate various models for evaluation. The models created in this experiment can be shown in Table 2.

In the second experiment, different dataset sizes with three categories were used to generate models for evaluation. The models created in this experiment can be shown in Table 3.

In the third experiment, one dataset containing three categories was divided to generate three models in which one category is dominant to the other categories within each model. The dominant category contains half the dataset size while the other categories share the other half equally. The models created in this experiment can be shown in Table 4.

The output of the face mask detector includes the location of the bounding boxes for each detected face, a colored label, and the confidence score of those predictions. To further classify the images, we use the You Only Look Once (YOLO) object detector [29], shown in Figure 4 to detect cases where students are wearing a full mask, nose exposed, or chin mask and customize the bilingual alerts provided to the user.

Table 3: Models created in experiment 2.

Name	Images trained	No. of epochs	Batch size	Categories
Model 4	10,000	11	32	Correct, incorrect, without
Model 5	6,600	11	32	Correct, incorrect, without

Table 4: Models created in experiment 3.

Name	Images trained	No. of epochs	Batch size	Categories
Model 6	12,000	14	128	Correct, other
Model 7	12,000	14	128	Incorrect, other
Model 8	12,000	14	128	Without, other

The full subsystem pipeline is illustrated in Figure 5.

3. Results and Discussion

3.1. Autonomous Navigation Results. We tested the AI-powered robot in the engineering labs at Abu Dhabi University, UAE, and in various lab-like and classroom environments. Such settings include workstations, chairs, desks, and other objects. The robot successfully mapped the lab's overall shape and the static objects using the LiDAR sensor, as illustrated in Figure 6. It travelled through the goal points defined on the planner without colliding with any obstacles to arrive at the final destination. The local planner constructs a map once an obstacle appears that takes approximately 30 seconds to get around the obstacle and to the goal point.

3.2. Face Mask Detection and Classification Results

3.2.1. Face Mask Detection Results. The trained models from the face mask detection and classification subsystem were used to generate a total of 6 face mask detectors to be tested in real time. All detectors will then be compared to find the best performance detector for this research work. Table 5 shows the testing results of each trained detector in real time.

From Table 5, Detectors 4 and 6 showed the highest average precision compared to the other detectors. The real-time results of the captured testing images can further support the performance of all detectors. Figure 7 shows the detection accuracy of Detector 6 for a single student captured by the robot, which has the highest precision out of all other detectors.

In Figure 8, the robot captures 2 students in the laboratory environment in two different scenarios.

3.3. Face Mask Detection Model Evaluation 261. In this section, we evaluate the performance of both the baseline

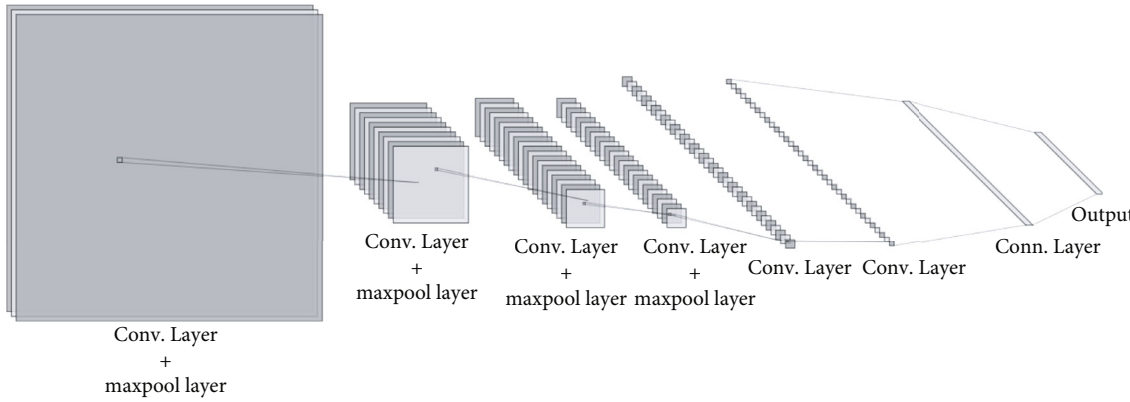

Figure 4: YOLOv2 network architecture.

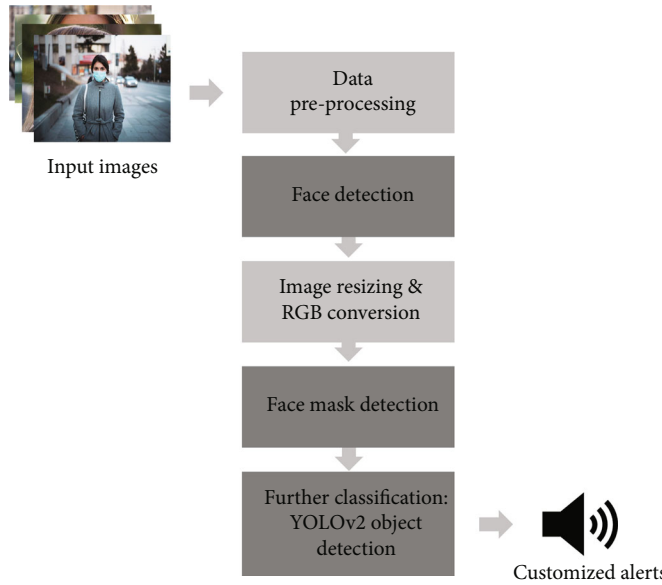

Figure 5: Face mask detection pipeline.

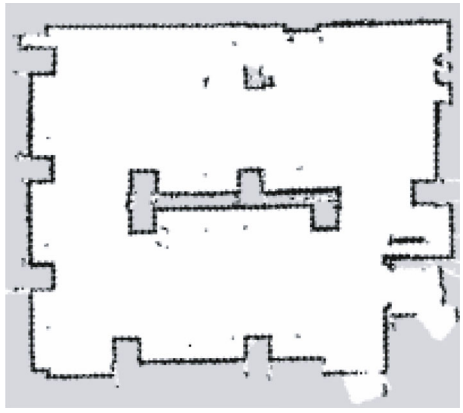

Figure 6: Map generated of the lab environment using the LiDAR sensor.

(*Detector 4*) and improved model detectors (*Detector 6*) and discuss the main differences that led to better precision and performance. To describe the model's performance, we construct a confusion matrix, as shown in Figure 9.

We primarily focus on the model's predictive ability, precision, and recall, instead of the classification time of the model. We elaborate on these two metrics as follows:

(i) *Precision* quantifies how correct the model's positive predictions are, where positives mean correctly worn masks and negatives mean incorrectly worn masks, in our case. This means that the more the model correctly classifies the label "correctly worn masks," the more precise it will be. It can be computed using Equation (1).

$$Precision = \frac{TP}{TP + FP}. \quad (1)$$

(ii) *Recall* is otherwise referred to as *Sensitivity* or *True Positive Rate (TPR)*. This measure refers to how many people wearing their mask correctly did the

Table 5: Performance of the MobileNetV2 detectors.

Name	Models used	Avg. precision	Avg. recall
Detector 1	Model 1	0.692	0.562
Detector 2	Model 2	0.624	0.511
Detector 3	Model 3	0.538	0.445
Detector 4	Model 4	0.775	0.654
Detector 5	Model 5	0.707	0.633
Detector 6	Model 6	0.914	0.654

AI model miss out of all people who wore their face masks correctly. It can be determined using Equation (2).

$$Recall = \frac{TP}{\mathrm{TP} + FN}. \tag{2}$$

Due to the nature of this research work, precision is a significant metric to report. We want to ensure that our AI model can correctly identify students who wear their masks correctly from those who do not. In other words, if the AI model predicts that the student is wearing their face mask correctly while they are not, the chances of spreading the infection increases due to those wearing the face incorrectly but not alerted.

We evaluate the proposed AI models and report on their performance in terms of their precision. We also construct Receiver-Operating Characteristic (ROC) curves using True Positive Rates, TPR, vs. False Positive Rate (FPR). To construct an ROC curve, we need to:

(1) Use the face mask detection model to produce a probability of correctly worn masks (P (correctly worn masks)) in each frame captured from the live stream camera. The total number of test instances (frames) that will be used is 100

(2) Sort the instances in descending order according to the P (correctly worn masks).

(3) Count the number of TP, FP, TN, and FN after applying a threshold to each unique P-value (correctly worn masks).

(4) Calculate the TPR using Equation (2) and FPR using Equation (3).

$$FPR = \frac{FP}{FP + TN}. \tag{3}$$

Following the previous steps, we build a table that will help us construct an ROC curve for the model. We implement the following to improve the performance of the face mask detection model:

(i) Increase the number of augmented images showing students wearing face masks correctly in varying angles

(ii) Use binary classification (one vs. all classification) and repeat the experiment three times. The first time to classify the correctly worn mask images vs. the rest, while the second time to classify the incorrectly worn face mask vs. the rest. The last experiment classifies students without a face mask vs. the rest

We train the improved face mask detection model on 100 frames and construct its ROC curve. We display the first 20 frame instances for the improved face mask detection model along with their respective positive class probabilities and confusion matrix metrics in Table 6.

The constructed ROC curve for the improved model taken from Table 6 along with the ROC curve for the base and default models can be seen in Figure 10.

As can be seen in Figure 10, the AUC for the improved model is greater than the default classifier, which means it is more precise than the base model presented in green. We summarize the major differences between the base model initially used and the improved face mask detection model in Table 7.

We observe that the improved model's detection speed is affected by the dataset size, computing compatibility (GPU), and the camera's quality. A high-quality camera with better shutter speed and exposure will increase the performance significantly. Similarly, deploying the model on a more powerful GPU with high compatibility can improve performance.

3.4. Face Mask Classification Results. We present the outcome of the YOLOv2 face mask classification system. The test images are labelled *Full Mask*, *Nose Exposed*, or *Chin Mask*. Figure 11 demonstrates the effectiveness of our model in detecting and classifying students wearing masks from varying angles regardless of the color of the mask worn.

The system can also accurately classify students wearing their masks incorrectly as can be seen in Figure 12, where the student had his nose exposed in (a) and both his nose and mouth exposed in (b).

3.5. Computational Complexity and Inference Speed. The frames captured using the camera mounted on the robot go through different functions. Each function/process is unique when it comes to complexity. In addition, the more complex the process is, the more time the frame needs to be processed. Frames captured by the camera start their processing journey. At first, the frame gets resized since the models trained are based on 224x224 pixel images. After that, the spatial dimensions of the frame get extracted, and a blob gets constructed. This constructed blob will pass through the pretrained face detector to extract the confidence and face coordinates of the captured frame. Next, the frame with high confidence (face detection probability above 70%) will pass through the face mask detectors (3 in total). Each face mask detector will give a prediction based on the input frame, and the face mask detector with the

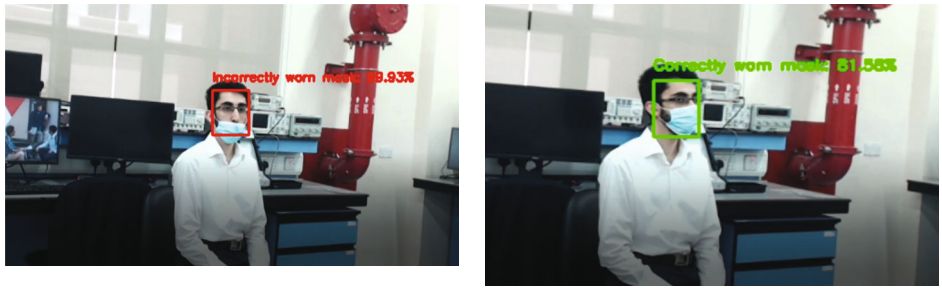

(a) (b)

Figure 7: Face Mask Detector testing accuracy for a student wearing a face mask (a) incorrectly and (b) correctly.

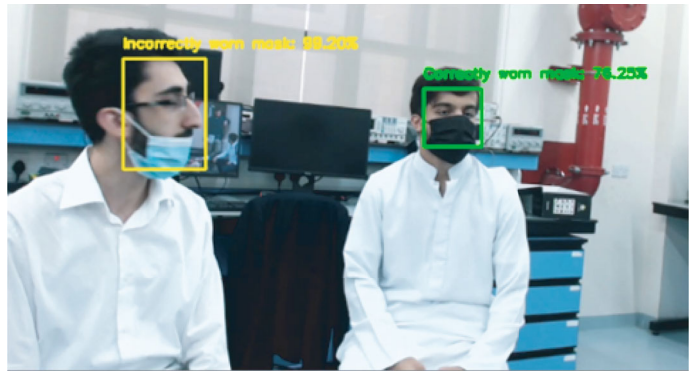

(a)

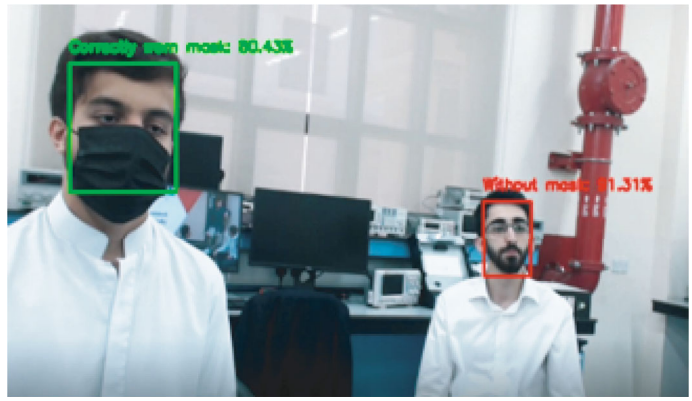

(b)

Figure 8: Face Mask Detector testing accuracy for two students in the lab, where (a) one student is wearing a face mask incorrectly while the other student is wearing it correctly and (b) one student is wearing a face mask correctly while the other one is not wearing a face mask.

		Predicted class	
		Class 1: correct	Class 2: correct
Actual class	Class 1: correct	a (TP)	b (FN)
	Class 2: incorrect	c (FP)	d (TN)

TP: True positive
FN: False negative
FP: False positive
TN: True Negative

Figure 9: Confusion matrix.

highest accuracy will select the most accurate label to label the input frame. Finally, the processed frames will be displayed using OpenCV with the corresponding face boundaries and labels. To compute the complexity of this process, we calculated the frame rate (FPS) before and after the face mask detection process. The frame rate without mask detection using real-time video capturing was 25 frames per second. Once faces and masks are detected, the frame rate drops to 10 frames per second. This means that it takes 2.5 seconds additionally per frame to get processed, detected, and labelled. The device used to obtain such results was a laptop with a 2.4 GHz CPU. Testing on GPU was

Table 6: Testing instances up to 30 frames, probability of correctly worn masks, true class, prediction, TP, FP, TPR, FPR, recall, and precision for the improved face mask detection model.

#	P (+)	True class	Prediction	TP (++)	FP (-+)	TPR (recall)	FPR	Precision
1	99.99	+	+	1	0	0.015	0	1
2	99.97	+	+	2	0	0.290	0	1
3	99.93	+	+	3	0	0.044	0	1
4	99.92	+	+	4	0	0.059	0	1
5	99.92	+	+	5	0	0.074	0	1
6	99.91	+	+	6	0	0.088	0	1
7	99.91	+	+	7	0	0.103	0	0.857
8	99.88	+	+	8	0	0.118	0	0.875
9	99.85	+	+	9	0	0.132	0	0.889
10	99.85	+	+	10	0	0.147	0	0.900
11	99.81	+	+	11	0	0.162	0	0.909
12	99.75	+	+	12	0	0.176	0	0.917
13	99.71	+	+	13	0	0.191	0	0.923
14	99.71	+	+	13	1	0.191	0.031	0.929
15	99.70	+	+	14	1	0.206	0.031	0.933
16	99.70	+	+	15	1	0.221	0.031	0.938
17	99.69	+	+	16	1	0.235	0.031	0.941
18	99.65	+	+	17	1	0.250	0.031	0.944
19	99.63	+	+	18	1	0.265	0.031	0. 947
20	99.62	+	+	19	1	0.279	0.031	0.950
21	99.57	+	+	20	1	0.294	0.031	0.952
22	99.51	+	+	21	1	0.309	0.031	0.955
23	99.36	+	+	22	1	0.324	0.031	0.957
24	99.12	+	+	23	1	0.338	0.031	0.958
25	99.12	+	+	24	1	0.353	0.031	0.960
26	99.08	+	+	25	1	0.368	0.031	0.962
27	99.00	+	+	26	1	0.382	0.031	0.963
28	98.93	+	+	27	1	0.397	0.031	0.964
29	98.91	+	+	28	1	0.412	0.031	0.966
30	98.86	+	+	29	1	0.426	0.031	0.967

inapplicable since the GPU capability was below 3.0. As for the Jetson Xavier NX, the compute capability is 7.2, which can run the detection process in real time with a frame rate of 8 frames per second. The computing device plays a critical role in speeding up the detection process. Additionally, compatible versions of TensorFlow 2, CUDA, and cuDNN can accelerate deep learning significantly. cuDNN provides highly tuned implementations for standard routines such as forward and backward convolution, pooling, normalization, and activation layers. [30]

3.6. Convolutional Neural Network (CNN) Architectures. Inference speed and mean average precision (mAP) are critical in CNNs. Choosing the correct CNN to train object detection models will enhance the model's performance. The depth and types of layers (such as convolution, batch normalization, and rectified linear unit (ReLU) activation) are the main characteristics of CNNs. The deeper the CNN is, the more precise the trained model will be. However, deep CNNs are heavier than CNNs with few layers, which means they will be much slower. Precision comes at a cost, so choosing a CNN that can be both precise and fast is very important. For this project, the model is pretrained on a CNN with enough speed to achieve exact results. Moreover, MobileNetV2 SSD CNN architecture was used to balance precision and speed. To further support our choice, we present in Table 8 a comparison between some of the different pretrained CNNs based on speed and mAP. [31]

3.7. Enhancing the Generalization of the Proposed Model. The generalization of deep learning models using data augmentation helps ensure model optimization. Data augmentation is a technique to increase the number of training samples by modifying the already existing data. In [28], a full-stage data augmentation framework is proposed to improve the accuracy of deep CNN for image classification. Two benchmarks CIFAR-10 and CIFAR-100, based on coarse-grained and fine-grained tiny images dataset, were used in the study. The experimental results for the study on the coarse-grained dataset CIFAR-10 and dataset

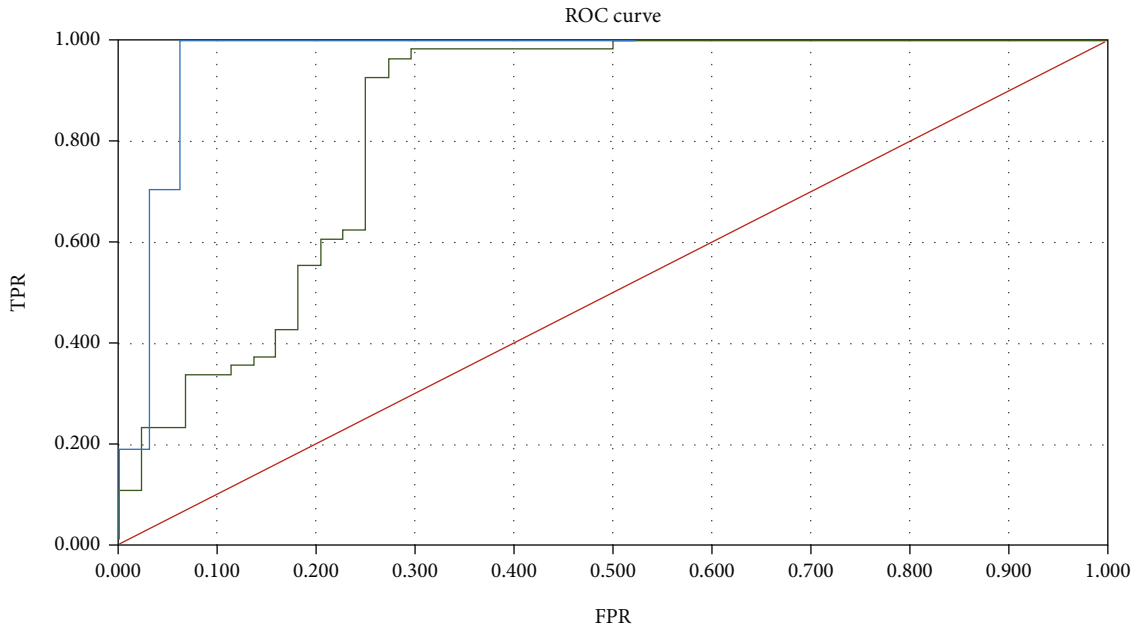

Figure 10: Comparison of the ROC curves of the improved face mask detection performance model shown in blue vs. the baseline model shown in green vs. the default classifier in red.

Table 7: Differences between the base and improved models.

Differences	Base model	Improved model
Number of models	1 model	3 models
Categories	Correct, incorrect, and without	Correct, incorrect, and without
Dataset size	10,000 images	12,000 images
Mask colors	Bright mask colors only	Bright and dark mask colors
Face angles	Facing the camera directly	Face angles between 45 and 90 degrees
Frame rate	12 FPS	10 FPS
Inference time	83 ms	100 ms
Avg. precision	0.775	0.914
Avg. recall	0.654	0.654

CIFAR-100 demonstrated 93.41% and 70.22% accuracy, respectively. In another study [32], deep transfer learning method is used for facial diagnosis from uncontrolled 2D face images of various diseases like beta-thalassemia, hyperthyroidism, Down syndrome, and leprosy with a relatively small dataset of 350 face images. The experiments showed 90% accuracy and demonstrate the effectiveness of CNN for feature extraction of small datasets but emphasize the need for data augmentation to increase the ability of the model to detect more diseases with higher accuracy to perform facial diagnosis. This research [12] proposes real-time AI platform for people detection and social distancing measure, and social distancing classification of individuals using thermal camera. YOLO-v4-Tiny is used for model development, which is a lighter version of YOLO-v4. Two datasets were used of 1000 and 950 images, respectively. The dataset was collected from different sources on the Internet of people sneaking, walking, and running in different body positions. The final algorithm achieved up to 95% accuracy and was deployed in Nvidia Jetson devices.

Based on the literature to better optimize our model, we used utilized data generalization for our developed algorithm. Our model's ability to adapt to new unseen data relies on different factors, such as face angles, distance, and mask color, which are critical in improving the model's generalization ability. Moreover, numerous experimental tests were conducted to enhance the models' generalization ability. In the first few experiments, the detection models struggled to detect face masks at sharp angles between 45 and 90 degrees, so we have improved our dataset by increasing the images of people facing the camera at an angle to reach about 60% of the total dataset. Furthermore, we noticed in our tests that the model's accuracy against masks of dark colors is low. To avoid increasing the number of images containing people wearing a dark face mask (such as black or brown), we have used data augmentation to grayscale a considerable portion

(a) (b)

(c)

Figure 11: Full face mask classification using YOLOv2 object detection for a student wearing (a) blue mask and facing forward, (b) black mask and facing to the left, and (c) white mask and facing to the right.

(a) (b)

Figure 12: (a) Nose exposed and (b) mask worn under the chin incorrectly detected with the proposed model.

of our training dataset. Hence, the model now detects dark and light-colored masks more accurately. In addition, it is well-known that faces become unrecognizable at long distances. Likewise, face masks can be difficult to detect from a distance. The pixel ratio between people's faces and face masks will change significantly. Two steps were taken to

Table 8: Differences between some COCO pretrained models.

Model name	Speed	mAP	Outputs
SSD MobileNet v2 320x320	19	20.2	Boxes
SSD MobileNet V1 FPN 640x640	48	29.1	Boxes
CenterNet HourGlass104 512x512	70	41.9	Boxes
EfficientDet D1 640x640	54	38.4	Boxes
SSD ResNet50 V1 FPN 640x640 (RetinaNet50)	46	34.3	Boxes
Faster R-CNN Inception ResNet V2 640x640	206	37.7	Boxes
SSD ResNet101 V1 FPN 640x640 (RetinaNet101)	57	35.6	Boxes

solve this limitation. In the first step, we included images that contain multiple people shown at different distances while wearing face masks correctly and not. In the second step, we have used data augmentation to apply "zoom-out" on the training data. With these two solutions, we have managed to sort out the distance issue. The model can now detect face masks from distances that can reach 6 meters.

4. Conclusions

In conclusion, we propose an AI-powered self-driving robot to enforce student mask wearing in educational settings during pandemics. We design and build the robot to navigate and map lab and classroom environments autonomously. Simultaneously, the face mask detection and classification system can identify students wearing masks from those wearing masks incorrectly or without a mask at all. Our bilingual and customized auditory system alerts students with no masks or incorrectly wearing their masks. We propose a mask-wearing robot as a solution to prevent the spread of the disease in educational premises, primarily laboratories and classrooms. Our face mask detection system is trained on a dataset based on 3 Kaggle datasets, including various images of people wearing face masks properly with different colors, not wearing face masks properly, and people with no mask. We train the model using MobileNetV2 architecture and classify the face masks correctly, incorrectly, or not wearing a mask. The training process resulted in different face mask detectors for real-time performance and precision testing. We use the YOLO object detector to classify the images into students wearing full masks, nose exposed, or chin masks. The face mask detector with three integrated models showed the highest performance and precision (77.5%) of all other face mask detectors. The improved performance detector had more images of students facing 90-degree angles. In addition, the better performance detector had three models in which each model had a dominant category (Correct, Incorrect, and Without) and achieved a precision of 91.4%. The overall system can operate for 2 hours and be extended using higher-capacity batteries. We tested the proposed approach in the lab and concluded that it efficiently alerts students not wearing a mask or wearing it incorrectly while navigating the environment. The system's limitations include small obstacles that are not in the LiDAR's range of vision, which can be overcome by using ultrasonic sensors. Moreover, to reduce camera blur and jitter and increase the prediction accuracy, we have programmed the robot to stop when detecting a face, capture an image, and continue moving.

Data Availability

The face mask detection datasets used to support the findings of this study are available from the corresponding author upon request.

Conflicts of Interest

The authors declare that there is no conflict of interest regarding the publication of this paper.

Authors' Contributions

Marah Alhalabi, Maha Yaghi, and Amer Barhoush contributed equally to this work.

Acknowledgments

The authors would like to thank Sohrab Setoodeh and Zaid Mohammad for their roles in the implementation and testing. This research was funded by the Office of Research and Sponsored Programs in Abu Dhabi University with a grant number [19300578].

References

[1] R. Salgotra, I. Rahimi, and A. H. Gandomi, "Artificial intelligence for fighting the COVID-19 pandemic," in *Humanity Driven AI*, pp. 165–177, Springer, Cham, 2022.

[2] M. Prusty, V. Tripathi, and A. Dubey, "A novel data augmentation approach for mask detection using deep transfer learning," *Intelligence-Based Medicine*, vol. 5, article 100037, 2021.

[3] M. Putro, D. Nguyen, and K. Jo, "Real-time multi-view face mask detector on edge device for supporting service robots in the COVID-19 pandemic," *Intelligent Information and Database Systems*, vol. 12672, 2021.

[4] E. Mbunge, S. Simelane, S. Fashoto, B. Akinnuwesi, and A. Metfula, "Application of deep learning and machine learning models to detect COVID-19 face masks - a review," *Sustainable Operations and Computers*, vol. 2, pp. 235–245, 2021.

[5] Z. Cao, M. Shao, L. Xu, S. Mu, and H. Qu, "MaskHunter: real-time object detection of face masks during the COVID-19

pandemic," *IET Image Processing*, vol. 14, no. 16, pp. 4359–4367, 2020.

[6] V. Cheng, S. Wong, V. Chuang et al., "The role of community-wide wearing of face mask for control of coronavirus disease 2019 (COVID-19) epidemic due to SARS-CoV-2," *Journal of Infection*, vol. 81, no. 1, pp. 107–114, 2020.

[7] R. Vijayan, "Teaching and learning during the COVID-19 pandemic: a topic modeling study," *Education in Science*, vol. 11, no. 7, p. 347, 2021.

[8] R. Katari, "A comparative analysis of variant deep learning models for COVID-19 protective face mask detection," *Turkish Journal of Computer and Mathematics Education (TURCOMAT)*, vol. 12, no. 6, pp. 2841–2848, 2021.

[9] J. A. Gonzalez-Aguirre, R. Osorio-Oliveros, K. L. Rodríguez-Hernández et al., "Service robots: trends and technology," *Applied Sciences*, vol. 11, no. 22, p. 10702, 2021.

[10] S. H. Shah, O. M. Steinnes, E. G. Gustafsson, and I. A. Hameed, "Multi-agent robot system to monitor and enforce physical distancing constraints in large areas to combat COVID-19 and future pandemics," *Applied Sciences*, vol. 11, no. 16, p. 7200, 2021.

[11] M. Mende, M. Scott, J. van Doorn, D. Grewal, and I. Shanks, "Service robots rising: how humanoid robots influence service experiences and elicit compensatory consumer responses," *Journal of Marketing Research*, vol. 56, no. 4, pp. 535–556, 2019.

[12] S. Saponara, A. Elhanashi, and Q. Zheng, "Developing a real-time social distancing detection system based on YOLOv4-tiny and bird-eye view for COVID-19," *Journal of Real-Time Image Processing*, vol. 19, no. 3, pp. 551–563, 2022.

[13] E. Hernández-Orallo, C. T. Calafate, J. C. Cano, and P. Manzoni, "Evaluating the effectiveness of COVID-19 Bluetooth-based smartphone contact tracing applications," *Applied Sciences*, vol. 10, no. 20, p. 7113, 2020.

[14] D. Storm van Leeuwen, A. Ahmed, C. Watterson, and N. Baghaei, "Contact tracing: ensuring privacy and security," *Applied Sciences*, vol. 11, no. 21, p. 9977, 2021.

[15] M. Loey, G. Manogaran, M. Taha, and N. Khalifa, "A hybrid deep transfer learning model with machine learning methods for face mask detection in the era of the COVID-19 pandemic," *Measurement*, vol. 167, article 108288, 2021.

[16] A. Negi, K. Kumar, P. Chauhan, and R. S. Rajput, "Deep neural architecture for face mask detection on simulated masked face dataset against covid-19 pandemic," in *2021 International Conference on Computing, Communication, and Intelligent Systems (ICCCIS)*, pp. 595–600, Greater Noida, India, 2021.

[17] P. Nagrath, R. Jain, A. Madan, R. Arora, P. Kataria, and J. Hemanth, "SSDMNV2: A real time DNN-based face mask detection system using single shot multibox detector and MobileNetV2," *Sustainable Cities and Society*, vol. 66, article 102692, 2021.

[18] M. Almghraby and A. Elnady, "Face mask detection in real-time using MobileNetv2," *International Journal of Engineering and Advanced Technology*, vol. 10, no. 6, pp. 104–108, 2021.

[19] B. Qin and D. Li, "Identifying facemask-wearing condition using image super-resolution with classification network to prevent COVID-19," *Sensors*, vol. 20, no. 18, p. 5236, 2020.

[20] T. Q. Vinh and N. T. Anh, "Real-time face mask detector using yolov3 algorithm and haar cascade classifier," in *2020 International Conference on Advanced Computing and Applications (ACOMP)*, pp. 146–149, Quy Nhon, Vietnam, 2020.

[21] L. Galtarossa, "Obstacle avoidance algorithms for autonomous navigation system in unstructured indoor areas," October 2018, https://bit.ly/2Sla6AV.

[22] S. Senhaji, S. Faquir, and M. Ouazzani Jamil, "Towards robotics and artificial intelligence for the prevention of Covid 19 pandemic," *E3S Web of Conferences*, vol. 229, p. 01035, 2021.

[23] S. Snyder and G. Husari, "Thor: a deep learning approach for face mask detection to prevent the COVID-19 pandemic," in *SoutheastCon 2021*, Atlanta, GA, USA, 2021.

[24] Base_LOCAL_PLANNER-ROS Wiki, *Wiki.ros.org*, 2021, http://wiki.ros.org/base_local_planner.

[25] Face Mask Detectionhttps://www.kaggle.com/andrewmvd/face-mask-detection.

[26] Face Mask Detection Datasethttps://www.kaggle.com/omkargurav/face-mask-dataset.

[27] Face Mask Detection 12K Images Datasethttps://www.kaggle.com/ashishjangra27/face-mask-12k-imagesdataset.

[28] Q. Zheng, M. Yang, X. Tian, N. Jiang, and D. Wang, "A full stage data augmentation method in deep convolutional neural network for natural image classification," *Discrete Dynamics in Nature and Society*, vol. 2020, 11 pages, 2020.

[29] J. Redmon and A. Farhadi, "YOLO9000: better, faster, stronger," in *2017, IEEE Conference on Computer Vision and Pattern Recognition (CVPR)*, Honolulu, HI, USA, 2017.

[30] S. Srivastava, A. V. Divekar, C. Anilkumar, I. Naik, V. Kulkarni, and V. Pattabiraman, "Comparative analysis of deep learning image detection algorithms," *Journal of Big Data*, vol. 8, no. 1, p. 66, 2021.

[31] A. Teoh, *TensorFlow 2 Detection Model Zoo - CoCO mAP vs Speed*, 2020, https://public.tableau.com/app/profile/aaronteoh/viz/TensorFlow2DetectionModelZoo-CoCOmAPvsSpeed/COCOmAPvsSpeedms.

[32] B. Jin, L. Cruz, and N. Gonçalves, "Deep facial diagnosis: deep transfer learning from face recognition to facial diagnosis," *IEEE Access*, vol. 8, pp. 123649–123661, 2020.

Hindawi
Wireless Communications and Mobile Computing
Volume 2022, Article ID 6519605, 13 pages
https://doi.org/10.1155/2022/6519605

Research Article

Virtual Reality Technology in Landscape Design at the Exit of Rail Transit Using Smart Sensors

Chuan Sun[1] **and Li Dong**[2]

[1]*The School of Arts, Hubei University of Education, Wuhan, 430000 Hubei, China*
[2]*School of Art and Design, Wuhan University of Science and Technology, Wuhan, 430000 Hubei, China*

Correspondence should be addressed to Chuan Sun; sunchuan@hue.edu.cn

Received 14 March 2022; Revised 7 May 2022; Accepted 15 June 2022; Published 25 June 2022

Academic Editor: Mohamed Elhoseny

The artistic thought of traditional garden landscape design has an important influence on garden art, and architectural theory and gardening theory are also inextricably linked. In modern gardens, traditional architecture lacks applicability to the construction of garden painting environment. Based on the background of modern gardens today, this paper studies the landscape design approaches that have the effect of painting in modern gardens, in order to provide references for modern gardens design. Virtual reality technology mainly provides users with a three-dimensional image environment through the use of simulation methods, which can truly reflect the changes and interactions of operating objects, thus forming a virtual world and establishing a relationship between users and the virtual world, interactive virtual 3D interactive interface. Based on the comparison of mainstream engine systems, this paper selects a suitable virtual reality system based on the characteristics of garden landscape design. On this basis, it further studies and researches the functions of the engine system selected by the research institute and explores the virtual reality system that meets the characteristics of creating garden landscape engineering. In the real work process, a three-dimensional virtual environment of the garden landscape is finally selected, so as to lay a solid foundation for applying virtual reality technology to garden landscape design, and strive to gain an advantage in the application field of virtual reality technology in this industry. Traffic congestion and frequent traffic accidents have become a major obstacle to urban development, the use of intelligent transportation systems to solve urban traffic problems has become the consensus of managers, so this paper uses intelligent sensor technology to schedule traffic flow. Experimental results show that virtual reality technology mainly uses simulation methods to give users a personal experience. The density of green space corridors simulated by VR technology can be increased from 1.25 km/km^2 to 2.41 km/km^2, which is more than doubled, which significantly improves the connectivity of green spaces and effectively improves the ecological functions of green spaces. Engineers, owners, and the public can see the final design effect in real time from any angle and can also interact with the flowers and trees in the scene to understand the design concept of landscape architects more comprehensively, thereby enhancing publicity effect, to achieve fast and effective dissemination. It is beneficial for users to really participate in the project design. The application prospect will be very broad.

1. Introduction

Since the 20th century, computer science and technology have developed rapidly, and virtual reality technology is the crystallization of its development. Through simulation, virtual reality technology provides users with a real and interactive three-dimensional simulation environment, thereby establishing a virtual world. Traditional Chinese architecture has a long history. As early as the Southern and Northern Dynasties, thanks to the free thinking and open social background at that time, traditional architecture developed rapidly and various architectural painting theories were born.

In modern garden research, scholars often mention the relationship between architecture and gardens. Sun et al. pointed out that historical art techniques are consistent. Gardens are a comprehensive artwork composed of various elements, and each scenery is like a different picture scroll. Architecture needs to have charm and interest, and garden

construction can also refer to [1]. Othman and Kasim proposed that designers must take people-oriented as the main design idea, based on coordination and sustainable development, to effectively plan the residents' activity space and rural landscape design [2]. Scognamiglio proposed that designers must fully understand the industrial development structure of the region and design some fishing, fruit and vegetable picking, sightseeing experience, and other projects while ensuring that the natural ecology of the region will not be damaged [3]. Hwang et al. proposed that the ultimate goal of the landscape transformation of industrial heritage sites is to show the historical culture of industry, inherit history and talk to the future, and use landscape design to express the cultural characteristics of the landscape [4].

Kurtaslan et al. proposed that the creation of virtual scenes for VR training teaching is based on the actual scenes provided by the school-enterprise cooperative enterprise, focusing on the integration of virtual scenes and real scenes. The creation of virtual scenes requires good experience and interactivity [5]. Facing the challenge of smart landscape, Wu combines advanced technology, landscape teaching construction education reform mode under the background of digital landscape design with science and technology, aiming to solve the current problems in landscape design [6]. Hongtao elaborated on the standards and aesthetic principles of architectural creation. As a representative traditional painting theory, it not only has a theoretical guiding role for flat architectural art but also has positive reference and guiding significance for three-dimensional garden art [7]. Xuepeishan decomposes the operational links and technical points of the actual project, finalizes the virtual animation construction model, develops the software, and constructs the training platform [8].

In this paper, a suitable virtual reality system is selected according to the characteristics of the garden landscape design of the rail transit exit. On this basis, the virtual reality system and various functions selected by the laboratory are studied, and the virtual reality that meets the characteristics of the creation of the garden landscape project is studied. Work flow finally choses the 3D virtual environment of garden landscape. According to the beautification effect of the virtual reality technology on the garden landscape, the construction of the garden landscape at the exit of the rail transit is engineered to enhance the connectivity of the garden landscape and improve the ecological function. It also uses smart sensor technology at rail exits to observe and dispatch traffic flow and alleviate traffic difficulties.

2. Virtual Reality Technology and Garden Landscape Design Theory

2.1. Virtual Reality Technology. The current concept of virtual reality technology is divided into two types: macro and micro. The main concept of the micro is based on the natural way of human-computer interaction. Just like the real world environment. In this way, users can naturally feel the virtual world created by the computer. This virtual world is a digital virtual model beyond the real environment, and it is a simulation of the real environment. This interactive interface composed of virtual graphics allows users to there is an immersive feeling [9]. The main concept of the macro is the simulation of the real world in three-dimensional visualization, with some virtual imagination [10]. His main part is the detailed digital simulation of the inside of the object. This simulation is not only an interactive interface but also a simulation of the real environment. The user can directly experience the virtual environment in the easiest way. Sensory stimulation can interact and communicate with it at the same time, making it more immersive [11]. All in all, the definition of virtual reality technology is a virtual digital environment that integrates vision, touch, and hearing. Its main core is computer digital technology [12]. When carrying out landscaping, it is necessary to foresee the changes of the environment and the state of the surrounding scenery in advance, so it is necessary to have a clear and clear concept of the surrounding environment before the project starts. Designers generally use sand tables, visual 3D renderings, or animation to show the final design effect.

The user communicates and communicates with objects in the virtual environment by using professional equipment, thereby producing a real feeling of being in the environment. Its main characteristics are completeness and immersion [13]. Its main core technology is content-based spatial interaction technology, and at the same time, it can most intuitively show the results of garden landscape design. Secondly, this paper has deeply studied the application of virtual reality technology platform in landscape design and planning [14]. And the application of virtual reality technology to garden landscape design is beneficial to speed up the design [15]. Virtual reality technology mainly provides users with a three-dimensional image environment through the use of simulation methods, which can truly reflect the changes and interactions of operating objects, thus forming a virtual world and establishing a relationship between users and the virtual world. The interactive virtual three-dimensional interactive interface allows users to have a personal experience.

2.2. Technical Composition of Virtual Reality in Garden Landscape Design. In the virtual reality technology (VR) garden landscape simulation system, as a digital unified and innovative cognition of the real garden landscape and related phenomena, it can intuitively and comprehensively provide users with realistic scene phenomena and specific information. At present, the combination of landscape garden design and virtual reality technology is still in its infancy, and the application of virtual reality engine Quest3D in landscape garden design still has a lot of room for development. If you want to perfectly combine landscape garden design with Quest3D engine, there are many technologies have to be broken through. The garden landscape VR simulation system can play a number of technical features such as immersion, imagination, and interactivity [16]. As the research object, the garden landscape VR landscape simulation system in this design often has the characteristics of large-scale, massive, long cycle, and difficult technical realization [17]. For garden landscapes, large-scale terrain data usually generates several gigabytes or more. By using

multilevel structure objects for scene description, multiple models can be used to express. The key is the level of detail expressed by the model, that is, the LOD model. The rendering algorithm can simplify the details of the scene one by one without affecting the rendering effect, reduce the complexity of the effect, and also improve the rendering efficiency and the speed of image generation [18]. In the process of garden landscape terrain modeling, through the use of visualized regional terrain and landforms, according to the modeling algorithm, the continuous topographic changes in the garden landscape area are completed, so as to realize the true reflection of the garden landscape terrain [19]. At present, mathematical elevation models are the most commonly used. DTM is used as a garden 3D planning model. The total information storage of terrain features is completed through the use of digital forms. Most of the terrain surface forms represented are information models, which are combined with the needs of different research fields to achieve the combination of terrain and nonterrain information characteristics [20]. With the rapid development of GIS technology, it has also promoted the rapid development of DTM model products and has provided GIS with operational basis numbers that can realize garden landscape spatial analysis and auxiliary decision-making [21]. In particular, the spatial data infrastructure implemented in recent years has also created room for the development of GIS technology [22].

The application of virtual reality technology in the real estate industry is a new real estate marketing method, which integrates various methods such as film and television animation, multimedia, and network resources. In the interior design industry, virtual reality technology is not only a technical medium but also a design tool. Through the three-dimensional visual space, it can more realistically reflect the designer's design intention and vividly transform it into a virtual object and environment that users can see and feel deeply. In this way, it can get rid of the traditional design mode and upgrade it to the perfect realm of digitalization, which greatly improves the quality and efficiency of the design. The concept of roaming in virtual reality the meaning of roaming is mainly to realize from one place to another [23]. In the real world, roaming is mainly driving, traveling, flying, etc. In the virtual world, roaming mainly refers to finding a way and traveling, and these two parts are independent. Generally speaking, the concept of finding a way is that the user knows where he is, and the concept of traveling is that the user moves within the scope of space or time [24]. Through some prompts, the user roams in the virtual reality environment in a more natural way and observes the objects in the virtual reality world in an all-round way and then produces an immersive real feeling. At the same time, you can also manipulate the objects in it. Finding the way refers to determining where you are and determining the route to the target area. Ways to find the way mainly include maps, roads, landmarks, compasses, and coordinates. Among these, along the road is the simplest method, and traveling along the road in the virtual world is the way to find the way. The most commonly used form of finding a way is a map. The map is put into the virtual world environment by means of virtual control, and the map can be put into the method of traveling at the same time [25].

By means of simulation, virtual reality technology provides users with a real and interactive three-dimensional environment, thereby establishing a virtual world. On this platform, users can communicate and interact with objects in the virtual world, thereby creating an immersive feeling. Its main supporting technology is the interactive technology based on three-dimensional space. Although virtual reality technology has been developed by leaps and bounds in recent years, there is still a big gap in technology and research applications compared with developed countries. In addition, in recent years, more and more virtual reality technology has been applied in the engineering industry, but the application of virtual reality technology in the landscape design industry is still in its infancy and internship stage. At present, as a developing multimedia expression method, virtual reality can be introduced into garden landscape design to fully display gardens, trees, landscapes, and engineering work points, it will more vividly show the concept, style, and effect of landscape design and bring closer there is some interactive space with the construction unit, and the digital model established based on some real data is combined into a virtual environment. It is established by virtual reality technology and established according to the requirements of the project and its design standards more realistic three-dimensional scenes; these all truly present the planning project, and the combined application with landscape design helps designers avoid design risks and complete landscape design tasks more quickly and intuitively.

2.3. Virtual Reality Technology Garden Landscape Design Research Model. The user locates a certain point on the map and then moves to this specific place. The control methods often used in the march are virtual control and physical control. According to different goals, different control methods are selected. When it is necessary to show a certain way of movement, such as entering a vehicle or an aircraft, virtual control is often used with equipment such as a steering wheel:

$$y_{it} = \alpha_0 + \alpha_1 D\max_{it} + \alpha_2 X_{it} + \mu_i + \eta_t + \alpha_{it}. \tag{1}$$

$$U_2 = \begin{cases} s - p_1 - kx_2, \\ x - p_2 - k(1 - x_2). \end{cases} \tag{2}$$

Supposing U is the exit of the critical rail transit, the second-stage opposing solutions can be obtained from equations (1) and (2) as follows:

$$\Delta_{\text{ikjl}}(\varepsilon) = \begin{cases} 0, & x_{ik}(\varepsilon) = \dfrac{N}{A} \quad \text{or} \quad x_{jl}(\varepsilon) = \dfrac{N}{A}, \\ 1, & x_{ik}(\varepsilon) = \dfrac{N}{A} \quad \text{and} \quad x_{jl}(\varepsilon) = \dfrac{N}{A}, \end{cases} \tag{3}$$

$$x_1 = \frac{p_2 - p_1 + k}{2k}. \tag{4}$$

Therefore, it is stored in the virtual reality private chain after verification by the entire network node:

$$p_1{}^* = \frac{2k}{k+1} + \frac{2c_1 + c_2 + 3et + 2et\zeta}{3}. \tag{5}$$

$$\begin{aligned} I &= \frac{n\sum_{i=1}^{n}\sum_{j=1}^{n} w_{ij}(x_i - \bar{x})(xj - \bar{x})}{\sum_{i=1}^{n}\sum_{j=1}^{n} w_{ij}(xi - \bar{x})^2} \\ &= \frac{n\sum_{i=1}^{n}\sum_{i\neq j}^{n} w_{ij}(x_i - \bar{x})(xj - \bar{x})}{S^2\sum_{i=1}^{n}\sum_{j=1}^{n} w_{ij}}. \end{aligned} \tag{6}$$

Let the changes in queue length and speed in equation (9) are, respectively, expressed uniformly and substituted into equation (2), we can get

$$P(d_i, w_j) = P(d_i)P(w_j|d_i)\,; P(w_j|d_i) = \sum_{k=1}^{K} P(w_j|z_k)P(z_k|d_i), \tag{7}$$

$$\begin{aligned} \frac{\partial \pi_B^{LH}}{\partial p_2} &= \frac{1 - p_2 + p_1}{2} - \frac{p_2 - c_2}{2} + \frac{k - p_2 + p_1}{2k} \\ &\quad - \frac{p_2 - c_2}{2k} - et\left[-\frac{1}{2} - \frac{1}{2k}\right] = 0. \end{aligned} \tag{8}$$

In addition, there are proxy control or direct user control. The direct user control is through a substitute in the virtual world, moving along a certain route from a specified location to a new location. In the roaming of the virtual environment, users generally need only some kind of interactive control. The optimal system planning is

$$\begin{aligned} C(k) = [&\zeta_1 c_1(t) + \zeta_2 c_2(k) + \zeta_3 c_3(k) + \zeta_4 c_4(k) \\ &+ \zeta_5 c_5(k) + \zeta_6 w_{ik}], \end{aligned} \tag{9}$$

$$c_1(t) \geq 0, c_2(k) \geq 0, c_3(k) \geq 0, c_4(k) \geq 0, c_5(k) \geq 0, \tag{10}$$

$$\zeta_1 + \zeta_2 + \zeta_3 + \zeta_4 + \zeta_5 + \zeta_6 = 1, \tag{11}$$

$$\begin{aligned} \min w_k(t) = \Bigg[&\omega_1\left(\frac{d_k}{V}\right) + \omega_2\left(\frac{d_k}{V}\right) + \omega_3\left(\frac{T_k}{ND_K}\right) \\ &+ \omega_1(P_K T_K)\Bigg]. \end{aligned} \tag{12}$$

This interaction mode is mainly to control the virtual object and its self-control in the scene. These two interaction modes are realized through external device input. Therefore, the solution of the second stage opposition is still

$$\delta_1 = \frac{p_2 - p_1 + 1}{2}, \tag{13}$$

$$\delta_2 = \frac{p_2 - p_1 + k}{2}. \tag{14}$$

The original complex model was improved and streamlined, and 5% of the original face count was used to create a simple model close to the original effect. The texture is mainly used to express the details, and the normal texture is used reasonably, so that some particle objects in the model can have a sense of unevenness without modeling, so as to obtain the balance of the second stage and the optimal planning of the two garden design clusters are

$$\vartheta = \frac{2k}{k+1} + \frac{2c_1 + c_2 + 3et - 2et\zeta}{3}, \tag{15}$$

$$(\text{In-}\alpha W)y = (\text{In-}\alpha W)X\beta + \varepsilon, \tag{16}$$

$$\wp_\kappa = \frac{2k}{k+1} + \left[\frac{1}{2} + \frac{1}{2k}\right]\left[\frac{c_2 - c_1}{3}\right]^2 + \frac{2(c_2 - c_1)}{3}, \tag{17}$$

$$y = \alpha W y + \beta_1 X - W\beta_2 X + \varepsilon. \tag{18}$$

In view of the project characteristics such as poor biodegradability of incoming water quality, high requirements for wetland water quality, limited wetland construction area, and low-temperature operation period, the available garden design data square matrix is

$$\psi = \sum_{x=1}^{\theta} Vx = \sum_{x=1}^{\vartheta}\left(\frac{Wx}{\sum_1^n W_{\Im}} Sx\right). \tag{19}$$

Among them,

$$\Delta Q_L + \Delta Q_S + \Delta Q_R = \Delta Q, \tag{20}$$

$$w_{ik} = \sum_{a}^{n} \tau_1 X_{ik} + \sum_{b}^{n} \tau_2 U(Y_{ik}) + B_{ik}. \tag{21}$$

2.4. Smart Sensors. In recent years, with the rise of the concept of the Internet of Things, as the peripheral nerves of the Internet of Things, smart sensors have attracted more and more attention in the industry. The rail transit industry, which has higher and higher requirements for automation, networking, and intelligence, is no exception. And sensors, the advanced rail transit represented by high-speed rail, are the first gate to the era of intelligence. Smart sensors are sensors with information processing functions. The intelligent sensor has a microprocessor, which has the ability to collect, process, and exchange information. It is the product of the combination of sensor integration and microprocessor. Smart sensors can collect vast amounts of information from the process to reduce downtime and improve quality. The intelligent transportation system is an intelligent system developed on the basis of traditional transportation system. It combines computer technology, electronic technology, automation technology, and other technical means; it has great advantages in traffic information monitoring, traffic control, and traffic scheduling. As a real-time sensing network, the intelligent sensor network can be applied in many aspects of intelligent transportation. It is decided by the decision-making system to find the best plan and return the plan to the execution system to guide vehicles and dispatch traffic.

3. Garden Landscape at the Exit of Rail Transit

3.1. Garden Design Object. Under the guidance of the principles of landscape classification, the garden landscape green space at the exit of rail transit is divided into 6 categories. With the help of GIS, an interpretation map of the status quo of green space and corresponding databases with both graphics and corresponding data are established; on this basis, the corresponding landscape index is selected according to the research needs, and the landscape data analysis software fragst is used to analyze the green space landscape pattern. Combined with the existing 3D database software, MultigenGreator and 3ds Max technology combined modeling was selected in this system design. Then, in the process of modeling landscape terrain, it can be combined with the spatial distribution characteristics of different geographical objects, and divided into discrete entity features based on trees, roads, buildings, etc.; and the continuity feature of the landscape based on landscape terrain and landform scene. Choose the MultigenGreator modeling tool, first complete the Openflight terrain file production, convert the basic elevation data to form the Cerator digital elevation data format, and combine with the landscape topography, area, and degree of refinement. The interaction of landscape architects can affect virtual reality products. The buttons that can interact with the virtual reality system program are called interfaces. The keyboard and mouse are the most basic common interfaces used by most programs.

3.2. Garden Design Steps

3.2.1. Design Sand Table. The garden landscape renovation design adopts the principle of combining garden landscape planning, construction, and management, creating a green ecological corridor, combining local culture to optimize the garden landscape environment, combining with the principles of low-carbon garden landscape, optimizing the living environment of the people in the garden landscape, and improving the local ecological environment; the principle of combining ecological protection and pollution control, based on the existing green ecological resources, building a diversified ecological green space to form a greenway system; combining the principle of green building energy conservation and environmental protection, using existing resources to create energy-saving and environmentally friendly building form, combined with the principle of cultural promotion, fully demonstrates the cultural charm of the garden landscape, strengthens the protection of industrial cultural resources, and shows the characteristics of industrial culture; adopts the principle of ecological sustainability, pays attention to daily plant maintenance, and adopts localization plants, pay attention to the configuration of seedlings, create creative landscape nodes, integrate the principles of sustainability through landscape design, and improve the surrounding ecological environment, but they cannot give users an immersive experience. The aspect deeply feels the effect, usually only the partial effect can be felt. However, the use of virtual reality technology can effectively overcome this deficiency. The application of virtual reality technology can allow designers, management decision-makers, construction technicians, and the public to experience the environmental effects in all directions, making it easier to understand the designer's design intent.

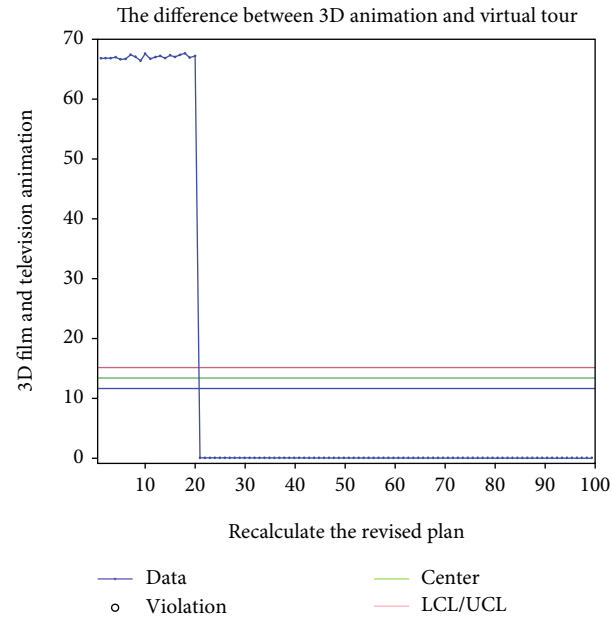

Figure 1: The difference between 3D animation and virtual tour.

Table 1: Application of virtual reality technology is beneficial to avoid design risks.

Independent variable	X value	Standard	3D	VR
Constant	1.5	0.26	2.6	<0.01
Design flaws	0.16	0.06	2.0	0.50
Loss	0.2	0.19	1.5	0.30
Effectiveness	0.9	0.13	1.9	<0.01
Assess quality	0.01	0.04	0.38	0.41

3.2.2. Choose a Garden Design Plan. Using virtual reality technology to be able to compare and modify different design plans. Generally, in the design of landscape gardens, a number of different design plans will be proposed. With the help of modern big data construction, such as the agricultural carnival will be integrated into the VR system, allowing the audience to experience the innermost plant the growth pattern of the worm and the natural secrets that are difficult to observe with the naked eye, such as making the mechanism of photosynthesis into VR material for experience. Continue to enrich popular science products to provide more popular science carriers, adapt to popular science activities in various scenarios, provide more problem solutions for garden design, and develop more home gardening products for citizens. Immersive experience of design effects at different observation points enables users to fully understand the designer's intentions, comprehensively feel and compare the respective characteristics and deficiencies of these multiple design options, which will help decision

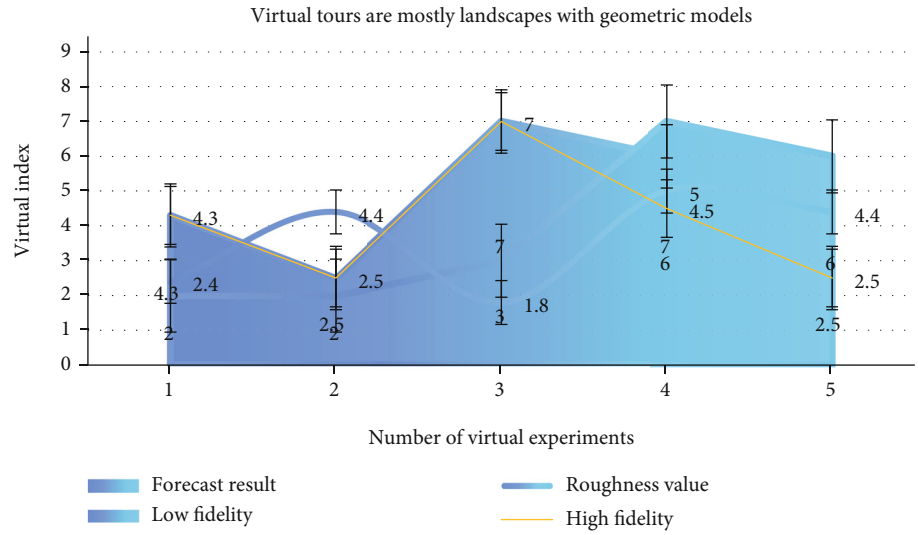

Figure 2: Virtual tours are mostly landscapes with geometric models.

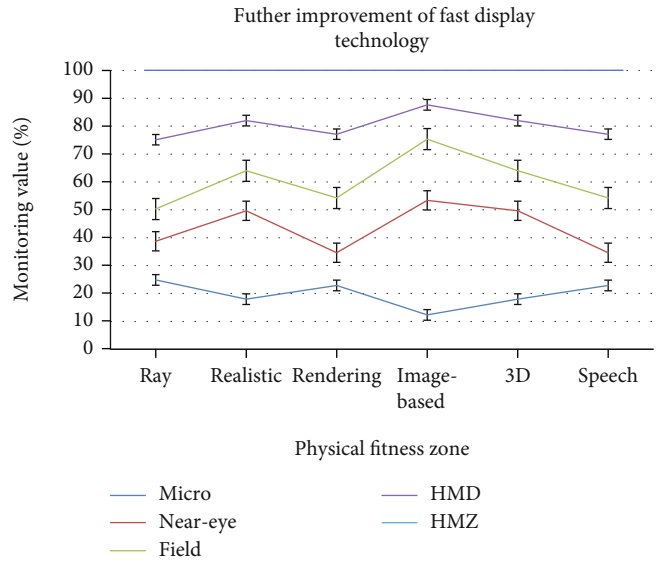

Figure 3: Further improvement of fast display technology.

makers to learn more, make a decision more in line with customer needs.

3.2.3. Effect of VR. Use virtual reality technology to modify in real time, and compare and analyze the difference between the effects before and after modification. The application of virtual reality technology in design can greatly save financial, manpower, and material resources. VR technology is conducive to real-time communication between garden landscape designers and construction units. The network and three-dimensional visual effects allow both parties to see the final effect. Choose the best design plan efficiently.

4. Garden Landscape at the Exit of Rail Transit

4.1. Simulation and Analysis of Virtual Reality Technology. As shown in Figure 1, the difference between three-dimensional animation and virtual roaming although three-dimensional animation has very strong visual expressiveness; it lacks real-time interaction with users. In 3D film and television animation, the viewer is in a passive position and needs to recalculate the modified scheme and changes

Table 2: Model performance index results.

Item	Micro	Near-eye	Field	HMD	HMZ
Ray	6.2	2.4	1.6	3.9	4.3
Realistic	2.5	4.4	2.1	2.5	2.5
Rendering	3.5	3.8	3.3	3.5	3.9
Image-based	4.5	2.8	5.3	4.5	4.3
3D	2.5	4.4	2.4	2.5	2.5
Speech	3.5	1.8	3.6	2.3	3.9

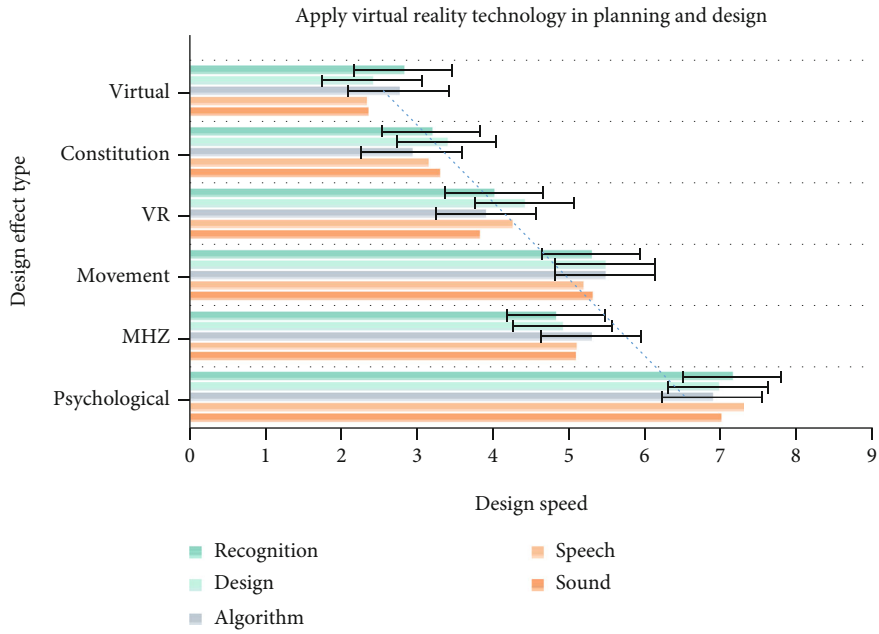

Figure 4: Apply virtual reality technology in planning and design.

in the route. After a period of time, the final result can be seen. Using virtual reality technology in routine data analysis, such as automatic and manual tracking of horizons, characterization of geological bodies, fault analysis and interpretation, etc., can generate and analyze various attributes.

As shown in Table 1, large-scale terrain data usually generates several gigabytes or more bytes for the garden landscape at the exit of rail transit. By using multilayer structure objects for scene description, it can be expressed in multiple models. The key is the level of detail expressed by the model, that is, the LOD model rendering algorithm can simplify the scene details one by one without affecting the rendering effect, reduce the complexity of the effect, and also improve the rendering efficiency and the speed of image generation.

As shown in Figure 2, as a developing multimedia expression means, if virtual reality can be introduced into landscape design to fully display gardens, trees, landscapes, engineering sites, etc., it will more vividly show the concept, style, and effect of the landscape design. The main traffic on the site is divided into three types: main roads, secondary garden roads, and rail trails. The main road consists of four horizontal and vertical roads with a width of 5 m. The east-west main road is the main landscape axis of Hanyang Iron Factory, and the north-south main road is directly connected with the main garden landscape main road. The railway track retains the original train track form, combined with the addition of new paving elements to form a new landscape. The secondary trunk road in the garden is dominated by curved paths, connecting various nodes, with a width of 2.5 to 4.5 m, which serves as a guide for the flow of people.

As shown in Figure 3, some of the original traffic tracks of the site are retained in the design and transformed into a scenic line outside the garden landscape. The garden landscape building adopts a modern and simple style, with a square shape, using wooden materials to build an external frame, while the interior is made of glass to form a closed space to meet the basic viewing functions.

Table 3: Garden virtual reality design structure data.

	Recognition	Design	Algorithm	Speech	Sound
Virtual	2.28	2.36	1.84	1.8	2.43
Constitution	2.83	2.58	2.76	2.72	2.34
VR	3.25	3.19	3.03	3.5	3.08
Movement	4.32	4.29	3.88	4.44	3.91
MHZ	5.39	5	5.16	5.28	5.08
Psychological	5.08	5.17	4.81	5	4.93

As shown in Table 2, in the planning display, the immersion and mutual inductance of the virtual reality system not only give users a great sense of realism and lifelikeness but also make users feel like they are in the environment. In addition, the data set in the virtual environment can be obtained in real time according to the needs of users. In large and complex projects, users can assist in design, bidding, approval, management, and other aspects of project design and program review.

As shown in Figure 4, the application of virtual reality technology in planning and design can increase the speed of design, and it is easy to modify these designs, such as changing the height of the building, the appearance of the building and the material and color of the facade in the architectural design, and the greening, this can speed up the design speed and quality. The virtual reality design structure data of gardens is shown in Table 3.

As shown in Figure 5, in view of the limited construction area of the garden, the existence of low-temperature operation period and other project characteristics; in order to

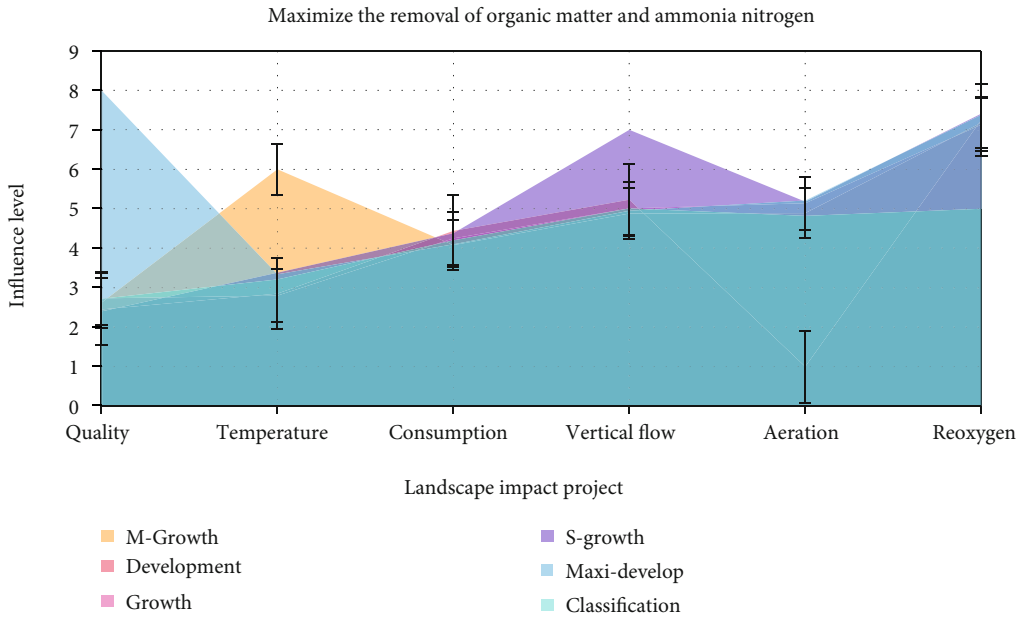

Figure 5: Maximize the removal of organic matter and ammonia nitrogen.

ensure that the garden effluent is stable and meets the standard, the garden is operated with low energy consumption and high efficiency, which is connected with the second phase of the project. Based on the optimization and combination of processes, the addition of aeration and return systems, and comprehensive consideration of various factors, the combined process of vertical underflow garden-oxidation pond-vertical underflow garden in series is finally determined. The two-stage underflow garden can optimize the removal effect and maximize the removal of organic matter and ammonia nitrogen. The addition of oxidation ponds can save head loss, increase the water reoxygenation capacity, and provide space for garden aeration.

As shown in Figure 6, the VR virtual simulation technology can enable people to experience the management and operation technology of the construction site immersively through interactive operations, perform virtual construction operations by completing virtual tasks, and master operating skills and technical points. VR virtual simulation technology can also be used to simulate the entire construction process of each individual project of a certain project, which is conducive to cultivating people's concept of large projects, learning and analyzing the complete construction management system of the project. Create a landscape garden project to lay the foundation for the construction of a VR training system for the wind forest and garden majors.

4.2. Virtual Reality Regression Model of Garden Landscape Design. As shown in Figure 7, from the perspective of ecology, design concept or life, the theme type of garden landscape belongs to the human landscape type and the theme artistic conception type. The sun always symbolizes power and hope, so facing the sun means that we are moving towards hope, symbolizing an upward force. The theme is designed as a combination of a circular sculpture and a fountain. At the same time, red, a color that symbolizes vitality, is used for sculpture creation. The combination of the two not only brings people a sense of visual impact but also makes people feel the positiveness conveyed by it, the power of life, and further shows the rhythm and circulation of life, but also reflects the endless life of life.

As shown in Figure 8, when designing the landscape garden green space landscape, the landscape layout lacks levels, the foreground and the back scenic area are not clear, and the overall design of the garden landscape lacks a sense of hierarchy and sense of order and cannot well highlight the artistic beauty of the garden green space landscape. Reasonable use of the hierarchy method can arrange the front and back of the garden landscape to show the relationship between the front and the back, make the landscape of the garden green space three-dimensional, and better express the artistic conception and meaning of the main theme of the landscape, and attract the attention and interest of tourists.

As shown in Table 4, the minimum distance index of the park green space in the central urban area has increased significantly, indicating that the distribution of park green space has changed from agglomerated to random distribution, which is beneficial to residents' use; unit, residential area green space and road green space the little change indicates that the two types of green space are randomly distributed as before; the minimum distance index for production green space and protective green space is decreasing, indicating that the clustering of the two types of green space distribution has increased. For the garden landscape ecosystem, the primary function of the corridor is its ecological function. As the main channel for the connection between patches, it can promote the protection of garden landscape biodiversity by providing corridors for the migration of animals and plants. Green corridors are mainly composed

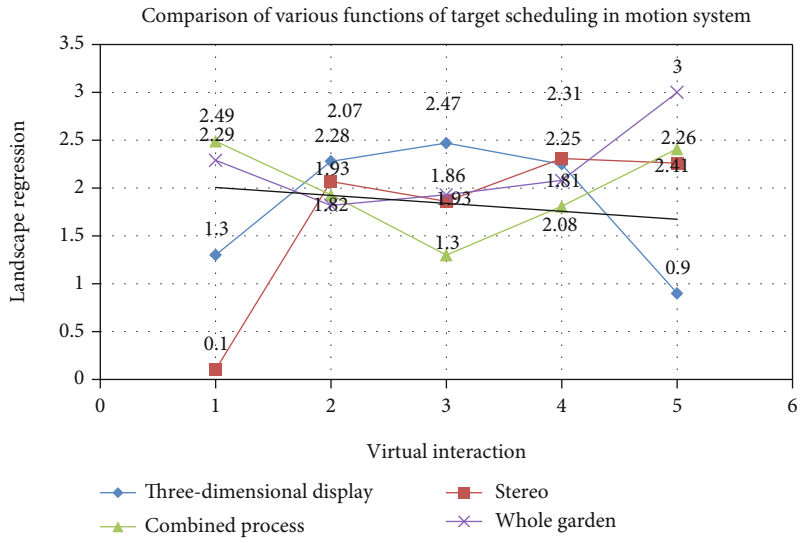

Figure 6: VR virtual simulation technology can be operated interactively.

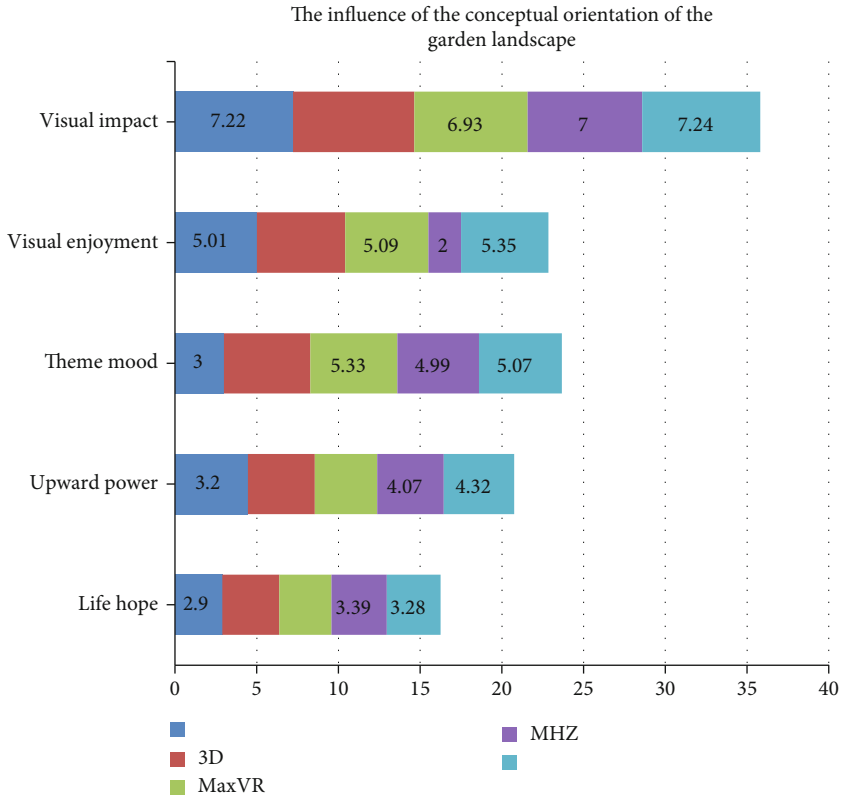

Figure 7: The influence of the conceptual orientation of the garden landscape.

of road green corridors and green corridors. The density of green corridors has increased from 1.25 km/km^2 to 2.41 km/km^2, which is more than doubled, which significantly improves the connectivity of green spaces and effectively improves the green space.

As shown in Figure 9, from the ecological point of view, the theme type belongs to the theme artistic conception type and biological ecology type. Use design techniques such as ingenious reasoning and symbolic metaphor to design themes. Water is the source of life, and the green branches and buds also show the vitality and source of life. The sculpture is built on the edge of the pool, with a leaf standing on the edge of the pool as the shape of the sculpture. Behind the sculpture, there is a huge ginkgo tree that shows the power of life. The combination of the source of life, the young green leaves, and the flourishing tree strongly demonstrates

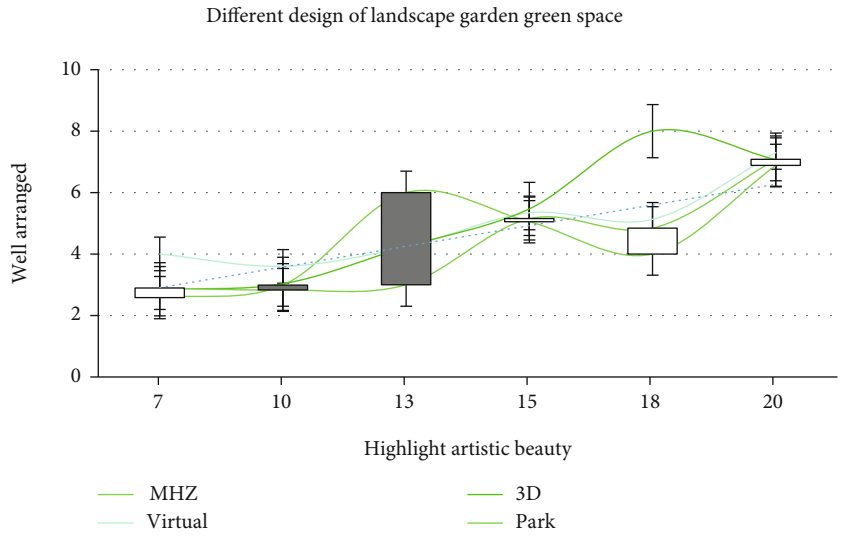

Figure 8: Different designs of landscape garden green space.

Table 4: The minimum distance index of parks and green spaces.

Reunion	Corridor	Matrix type			Linear		
		VR	Virtual	3ds Max	VR	Virtual	3ds Max
Weak	Green space	126.5	172.4	45.66	26.62	63.25	39.55
	Corridor	124.3	171.1	46.89	26.52	61.92	37.46
Strong	Green space	124.5	160.6	34.19	25.59	55.66	30.32
	Corridor	121.6	158.5	36.63	23.63	51.74	28.91

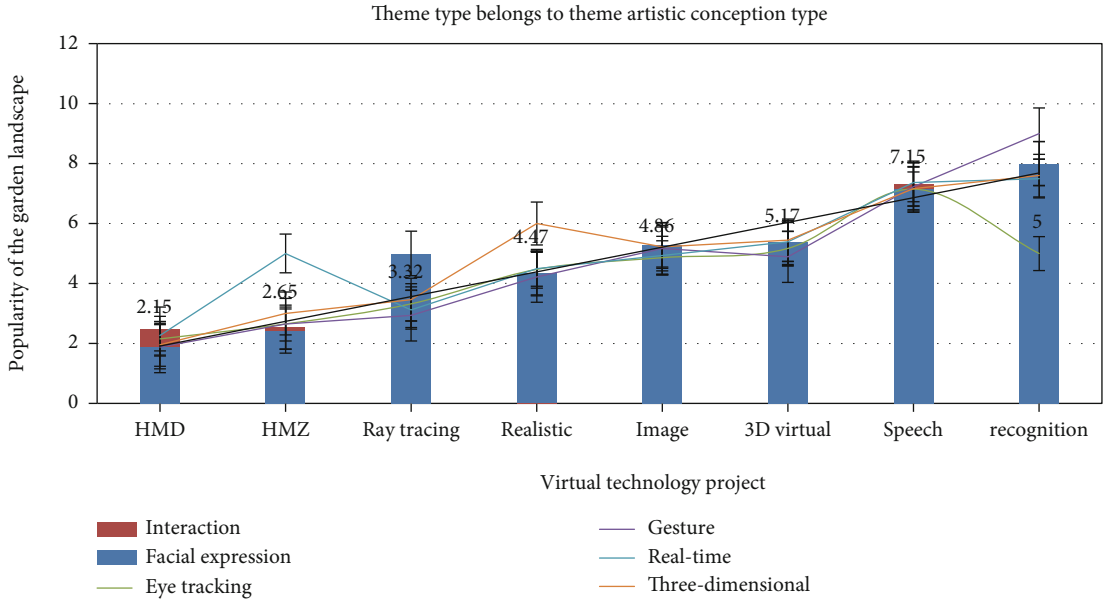

Figure 9: Theme type belongs to theme artistic conception type.

the concept of the source of life. Water and green leaves embody the evergreenness of life, while the big tree embodies the continuation of life, making the meaning of the sculpture more prominent.

As shown in Figure 10, the fragmentation of the garden landscape is the result of being deeply affected by human activities and is closely related to the landscape pattern, function, and process. Further analysis of the data shows

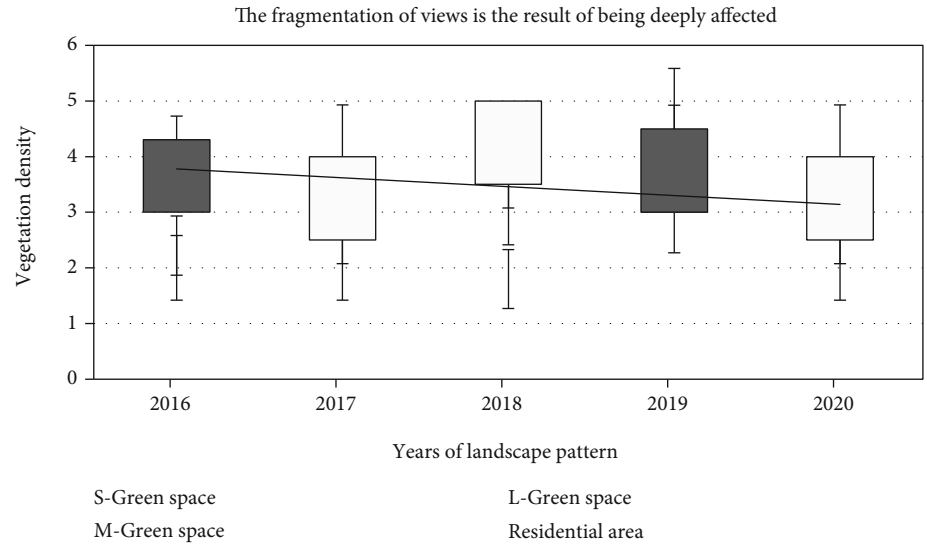

Figure 10: The fragmentation of views is the result of being deeply affected.

Table 5: Comparison of physical shape of garden landscape.

Shape	Flexible	Changeable	Beautiful	Diverse	Match	Meets
Perfect circle	33	32	30	50	30	33
Square	32.5	33	34	38	34	36
Oval	35.6	37	39	45	38	40
Tortuous	40	42	45	50	41	47

that the patch density of urban green space has decreased from 5.97 patches/hm^2 to 2.45 patches/hm^2, indicating that the fragmentation of the landscape has decreased in the past 5 years, and the ecological benefits and biodiversity protection functions have increased accordingly. Among all kinds of green space, the fragmentation degree of other green space and protective green space is low. Although the fragmentation degree of green space in gardens is second only to that of road green space, the vertical contrast has changed greatly, from 22.19/hm^2 to 3.92/hm^2, indicating that the past 5 years the quality of Chinese gardens and green spaces has improved significantly. Although the fragmentation degree of road greenbelt patches has declined, but the decline is not large, and the quality of road greenbelt construction should be improved in the future construction. The absolute elevation of the platform floor at the centerline of the effective platform is 393.709, the absolute elevation of the top of the roof at the centerline of the effective platform is 410.459, the absolute elevation of the rail surface is 392.659, and the absolute elevation of the bottom of the bottom plate is 390.169. The longitudinal gradient of the main body of the station is 2‰, the net height of the platform floor structure is 4.4 m, the floor height of the equipment floor structure is 6 m, and the floor height of the station hall floor structure is 4.5 m. The thickness of the covering soil at the centerline of the effective platform is 3.59 m, the minimum burial depth is 2.45 m, and the maximum burial depth is 4.05 m.

As shown in Table 5, in the landscape garden green space landscape, the main scenery design method of seeking twists and turns is generally to be curved, zigzag, uneven, surface unequal changes in the appearance of the scenery, or change according to the topography of the site. The shapes of pools, flower beds, green spaces, etc. are mostly regular shapes such as a perfect circle, square, oval, etc., and the scenery in the natural garden green space is more flexible and varied than the shape in the regular garden, and it is not restricted to rules. The style of the building, such as the common curved bridges, curved corridors, and other garden buildings or the winding roads that match the landscape. The twists and turns can be seen everywhere in the main landscape layout of the landscape gardens. This design method has a profound influence and important significance to it, but it is not advisable not to twist for the twists and turns.

5. Conclusions

The application research of virtual reality platform in the garden landscape design of rail transit exit, the virtual reality system, is conducive to improving design efficiency. It is not only a multimedia tool for presentation but also a tool for design planning. This is a visual form that uses a subjective perspective to express the designer's design ideas and concepts. Using the virtual reality system, landscape architects can change their observation points in the scene at will to observe the effects of

the design and continue to modify and improve them. The landscape designer, Party A, and the public can see the final effect of the designer's design in real time from all angles and can interact with the flowers and trees in the scene to fully understand the design concept of the landscape designer and achieve the purpose of enhancing the effect of publicity. The application prospects will be very broad.

The main landscape and surface plants at the exit of the rail transit were clearly expressed through virtual reality technology and exceeded the expected effect. Through the key technology of electronic sand table production, the whole picture of Banpo Station after construction was fully demonstrated, the effect was vivid and smooth, and the expected effect was achieved. In the current garden planning process, relevant personnel must advance with the times to establish innovative ideas and people-oriented design ideas, fully understand all aspects of garden planning, and formulate highly scientific and targeted landscape design plans. At the same time, it is necessary to fully understand the historical and cultural connotation of the area and the characteristics of the development of garden landscape, start from different angles, combine the landscape pattern and theme of garden planning, and scientifically introduce some suitable rural landscape elements to make. It can maintain coordination and unity with garden planning. In addition, some advanced design concepts and methods must be introduced in time to comprehensively improve the scientific, standard, contemporary, characteristic, and humanistic nature of rural landscape design, so as to be able to fully develop rural landscape design in the process of garden planning. The intelligent sensing system is adopted at the exit of rail transit to dispatch the traffic flow at the exit and reduce traffic congestion.

The construction of home ecological gardens is an important driving factor for the optimization of the landscape pattern and function of gardens and green spaces. Through ecological restoration, development of green corridors along rivers and roads, and balanced layout of parks and green spaces, the landscape pattern of gardens and green spaces has been continuously optimized. The average area of green patches has increased, the fragmentation of patches has decreased, and the density of corridors has increased. Improve the ecological functions of the garden landscape and green space, and promote the protection of garden landscape biodiversity; the distribution of the park green space is developed to be uniform, which is convenient for residents to use. In the future landscape construction of gardens and landscapes, we should continue to strengthen the construction of parks and greens in weak areas according to requirements, and further improve the uniformity of the distribution of parks and greens; improve the level of road and green construction and the quality of ecological corridors, and further strengthen the connection between green spaces; continue to strengthen ecological restoration and further optimize the landscape structure and pattern of gardens and green spaces.

Data Availability

No data were used to support this study.

Conflicts of Interest

The authors declare that there are no conflicts of interest regarding the publication of this article.

References

[1] S. Sun, P. Ray, and D. De, "Intelligent internet of things enabled edge system for smart healthcare," *National Academy ence Letters*, vol. 40, no. 4, pp. 1–6, 2020.

[2] R. Othman and S. Z. A. Kasim, "Assessment of plant materials carbon sequestration rate for horizontal and vertical landscape design," *International Journal of Environmental ence & Development*, vol. 7, no. 6, pp. 410–414, 2016.

[3] A. Scognamiglio, "Human neuroblastoma cells trigger an immunosuppressive program in monocytes by stimulating soluble HLA-G release," *Cancer Research*, vol. 67, no. 13, pp. 6433–6441, 2016.

[4] Y. H. Hwang, Y. Feng, and P. Y. Tan, "Managing deforestation in a tropical compact city (part B): urban ecological approaches to landscape design," *Smart & Sustainable Built Environment*, vol. 5, no. 1, pp. 73–92, 2016.

[5] B. O. Kurtaslan, O. Demirel, and S. S. K. Konakoglu, "Investigation of Selcuk University campus landscape design in terms of water efficient landscape arrangement," *Journal of Environmental Protection and Ecology*, vol. 20, no. 4, pp. 2130–2140, 2019.

[6] Y. Wu, "Educational reform on landscape design under the background of digital era," *Region-Educational Research and Reviews*, vol. 2, no. 1, pp. 17–19, 2020.

[7] K. Kim, J. S. Jang, C. Keum, and K. S. Chung, "Individual presence-and-preference-based local intelligent service system and mobile edge computing," *Journal of Korean Institute of Communications & Information ences*, vol. 42, no. 2, pp. 523–535, 2017.

[8] C. Xuepeishan, "An analysis of climate impact on landscape design," *Atmospheric and Climate ence*, vol. 6, no. 3, pp. 475–481, 2016.

[9] W. M. El-Bardisy, M. Fahmy, and G. F. El-Gohary, "Climatic sensitive landscape design: towards a better microclimate through plantation in public schools, Cairo, Egypt," *Egypt. Procedia Social & Behavioral Sciences*, vol. 216, no. 4, pp. 206–216, 2016.

[10] L. H. Juang and S. Zhang, "Intelligent service robot vision control using embedded system," *Intelligent Automation And Soft Computing*, vol. 25, no. 3, pp. 451–458, 2019.

[11] N. Mueller and Y. Morimoto, "Landscape design and urban biodiversity," *Landscape & Ecological Engineering*, vol. 12, no. 1, pp. 105-106, 2016.

[12] L. Li, "Landscape design of urban extensive green roofs," *Journal of Landscape Research*, vol. 10, no. 6, pp. 31–33, 2018.

[13] B. Gao, "Research on thematic landscape design," *IOP Conference Series Materials ence and Engineering*, vol. 371, no. 1, pp. 12014–12064, 2018.

[14] M. Xiaodong, "Provisional thoughts on criticism in China's landscape design," *Jola Journal on Landscape Architecture*, vol. 13, no. 3, pp. 21–23, 2018.

[15] F. Chen, X. Zhu, and J. Lin, "Statistical analysis on behavior characteristics of public space users in winter city and landscape design inspirations," *Journal of Xian University of Architecture & Technology*, vol. 49, no. 4, pp. 508–515, 2017.

[16] J. H. Park, "An intelligent service middleware based on sensors in IoT environments," *International Journal of Software Engineering and Knowledge Engineering*, vol. 30, no. 4, pp. 523–536, 2020.

[17] L. Dacan, H. Min, Z. Cailian, Y. Gong, and Y. Zhang, "Construction of 5G intelligent medical service system in novel coronavirus pneumonia prevention and control," *Chinese Journal of Emergency Medicine*, vol. 29, no. 4, pp. 21–28, 2020.

[18] K. Grushevska, T. Notteboom, and A. Shkliar, "Institutional rail reform: the case of Ukrainian railways," *Transport Policy*, vol. 46, no. 2, pp. 7–19, 2016.

[19] B. F. Spencer, J. W. Park, K. A. Mechitov, H. Jo, and G. Agha, "Next generation wireless smart sensors toward sustainable civil infrastructure," *Procedia Engineering*, vol. 171, pp. 5–13, 2017.

[20] X. Cai and F. Gao, "Study on joint regulation and safety supervision of urban rail transit system," *Journal of Physics: Conference Series*, vol. 1437, no. 1, pp. 12037-12038, 2020.

[21] S. Eun and I. N. Sener, "Traffic-related air emissions in Houston: effects of light-rail transit," *Science of the Total Environment*, vol. 651, no. 1, pp. 154–161, 2018.

[22] J. Liu, Y. Zhang, S. Xu et al., "Top-level design study for the integrated disaster reduction intelligent service," *Geomatics and Information ence of Wuhan University*, vol. 43, no. 12, pp. 2250–2258, 2018.

[23] J. Baumgartner, "VR equipment market mixed," *Broadcasting & Cable*, vol. 147, no. 8, pp. 23–23, 2017.

[24] A. Schütze, N. Helwig, and T. Schneider, "Sensors 4.0- smart sensors and measurement technology enable Industry 4.0," *Journal of Sensors and Sensor Systems*, vol. 7, no. 1, pp. 359–371, 2018.

[25] S. Nihtianov, Z. Tan, and B. George, "New trends in smart sensors for industrial applications-part I," *IEEE Transactions on Industrial Electronics*, vol. 64, no. 9, pp. 7281–7283, 2017.

Hindawi
Wireless Communications and Mobile Computing
Volume 2022, Article ID 5719654, 16 pages
https://doi.org/10.1155/2022/5719654

Research Article

Data Fusion Model for Muscle Proteomics in Sports Applications

Chunsheng Xie,[1] **Xian Li**,[2] **and Congying Cui**[3]

[1]*College of Physical Education, University of Sanya, Sanya, 572000 Hainan, China*
[2]*College of PE, Hainan University, Haikou, 570000 Hainan, China*
[3]*Oriental College of International Trade and Foreign Languages, Haikou College of Economics, Haikou, 570000 Hainan, China*

Correspondence should be addressed to Chunsheng Xie; chunshengxie@sanyau.edu.cn

Received 15 February 2022; Revised 8 April 2022; Accepted 19 May 2022; Published 23 June 2022

Academic Editor: Mohamed Elhoseny

Proteome is a cell, tissue, or organism to express all the floorboard of the protein; proteomics is the study of proteomics is an emerging discipline; the research on the law of occurrence of sports fatigue and its mechanism is an important and challenging subject in the field of sports medicine. Exercise-induced fatigue refers to the physiological process in which the body's functional ability or work efficiency declines and cannot be maintained at a specific level during exercise. With the improvement of the modern competitive sports level and the increasingly fierce competition, the athletes have to bear more and more loads in sports training, and the probability of sports fatigue is also higher. Appropriate sports fatigue and reasonable recovery methods can promote the improvement of athletes' functional level; on the contrary, excessive fatigue not only affects the training effect but may also cause various dysfunctions, which may damage the athletes' health. Therefore, understanding the mechanism of sports fatigue is of positive significance for accelerating the elimination of sports fatigue. The purpose of this paper is to study the progress of muscle proteomics in sports. Since each athlete has individual differences, different levels of muscle function corresponding to the left lower limb will produce different EMG signals. Static experiments and random visual stimulation evaluation experiments were performed on the left lower limbs of athletes, and they were coordinated with the right lower limbs, and then the left and right lower limbs were compared with the same muscle-weighted RMS (Recipe Management System) and IEMG (Comprehensive electromyography). Experimental results show that using the statistical method of single-factor variance analysis to the same muscles in two states of RMS was analyzed, respectively, under the two states of differences between muscle electromyography IEMG were analyzed, finally, the muscle integral electrical values on the contribution rate of extent of each muscle under the two states are analyzed. For one-way ANOVA, this study defined the significance level of the difference analysis between groups as $P < 0.05$. $P < 0.05$ is a small probability event, indicating that the possibility of an event occurring is very small, so it is considered that the event is unlikely to occur. A low-probability event is an event that has a low probability of occurring. Then, it is almost impossible to happen in one experiment, but it is bound to happen in many repeated experiments. With the continuous improvement of existing technologies and the emergence of more new technologies, proteomics research will make greater contributions to elucidate the mechanism of exercise on skeletal muscle remodeling and its improvement on health.

1. Introduction

With the development of exercise physiology, the understanding of the mechanism of exercise fatigue at home and abroad has evolved from a simple energy consumption or accumulation of metabolites to a multifactor, multilevel, multilink, and comprehensive understanding. Especially with the development of molecular biology technology, the research of fatigue has been developed to the cellular level and molecular level. In the process of to exercise fatigue, there is a complex network regulation, namely, nerve-endocrine-immune-metabolic regulation networks/networked (chain). In this network regulation, the expression of many proteins (enzymes, receptors, cytokines, membrane transport proteins, etc.) changes. Analyzing the changes in protein expression profile during exercise fatigue, it will be

possible to discover new proteins related to exercise fatigue. After the establishment of DNA double helix structure model, the deciphering of human genome sequence, another important milestone in life science research, marks the beginning of life science research into the postgene era. The postgene era, that is, the genome era after the completion of the human genetic map. In the postgene era, the most important task is to understand the structure and function of all protein products of genes. Although gene plays an unshakable role in the field of life science research, it is only the carrier of genetic information, while the real executor of life activities is the expression product of gene—protein. Proteins can more accurately reflect the dynamic changes of cells, tissues, or organisms, and the research focus of life science has gradually shifted from genes to proteins. Therefore, to understand the body's pathophysiological mechanism more deeply, we must start with proteins, and proteomics is the best method to study the activity of proteins.

With the invention and application of mass spectrometry, protein identification becomes more and more convenient, which makes proteomics research develop rapidly. Mass spectrometry has been widely used in the research and development of new molecular structures in industry and related fields. This method, together with NMR, IR, XRD, UV-Vis, and other technologies, has become an indispensable analytical method in research laboratories in the field of organic chemistry. Mass spectrometry is widely used in drugs (drug design, combinatorial chemistry, pharmacokinetics, drug metabolism, etc.), clinical fields (newborn screening, hemoglobin analysis, drug abuse, and stimulants), environmental protection (water quality and food pollution), geological (it has a wide range of uses in many fields such as petroleum components), and biotechnology (proteins, peptides, and hormones). Common techniques used in proteomics research mainly include gel electrophoresis, immunoassay (western blot, enzyme-linked immunoassay, etc.), PCR, 2D-PAGE, Maldli-TOF-MS, and selDI-TOF-MS, which have been developed in recent years, and among them, PCR technology is relatively used and more important [1]. These technologies provide a good technical platform for proteomics research. Because of a powerful technology platform, proteomic research has been into every field of life science research and clinical medical research fields, such as cardiovascular diseases, especially tumor epidemiology, found closely associated with the disease itself and can be used as biological markers of disease proteomics, to clarify disease pathophysiology mechanisms and clinical prevention and treatment of the disease to provide new ideas and methods. However, in the field of sports medicine, proteomics research is still in its infancy, and there are few relevant studies reported at home and abroad. This paper studies the application progress of proteomics in sports kinematics at home and abroad in recent years, so as to provide reference for subsequent studies [2].

The concept of proteome, first proposed by Williams in 1995, can be defined as the entire protein component of a cell, tissue, or entire organism. Proteomics is the study of all proteins in a cell to gain a comprehensive and holistic understanding of the organism [3]. Farrell and his colleagues used two-dimensional gel electrophoresis to map the proteins of E. coli, mice, and guinea pigs, although they were able to separate the different proteins. However, due to the limitation of technical conditions, the isolated proteins could not be identified [4]. Ren et al. introduced a medical migration prediction model based on medical insurance data. However, existing graph neural networks cannot capture time-series relationships between event-type entities. To this end, Ren et al. propose a prediction model based on graph convolutional network (GCN), namely, event-involved GCN (EGCN). The proposed model aggregates traditional entities based on an attention mechanism and event-type entities based on an LSTM-like gating mechanism. Furthermore, skip connections are deployed to obtain the final node representation. To obtain drug-embedding representations based on external information (drug descriptions), an autoencoder capable of embedding drug descriptions is deployed in the proposed model. Finally, extensive experiments are conducted on a real health insurance dataset. Experimental results show that the predictive ability of our model outperforms the state-of-the-art models [5].

In this paper, proteomics techniques can be used to study the skeletal muscle proteome as a whole. Exercise induces an adaptive response in skeletal muscle, and proteomics adjusts accordingly. Different types, intensity, and duration of exercise and muscle fiber types can cause different changes in skeletal muscle proteome. At present, studies on the proteomics of exercise on skeletal muscle remodeling are being carried out, but there are still some technical difficulties. RMS and IEMG were compared after the right and left lower limb muscles were weighted, respectively. The experimental results showed that for one-way ANOVA, the significance level of the difference analysis between groups was defined in this study as $P < 0.05$.

This paper divides the paper into the introduction, the research progress of muscle proteomics in sports, the muscle proteomics in sports, the discussion of muscle proteomics in sports, and the conclusion.

2. The Research Progress of Muscle Proteomics in Sports

2.1. Proteomics Technology. Proteomics techniques can be used to analyze skeletal muscle-related proteins, which can lead to a deeper understanding of muscle function. However, skeletal muscle includes a variety of functional fiber types, which differ in contraction dynamics, bone fibrin subtypes, metabolic enzymes, and mitochondrial density. Skeletal muscle is a type of striated muscle, a muscle attached to the bone, and skeletal muscle is composed of muscle cells arranged in bundles. The length of each cell is different, the cells are closely arranged, the length is complementary, and the outer surface of each cell is covered with a fine mesh membrane. Complex proteomic analysis of skeletal muscle remains a methodological challenge and is complicated by the different characteristics of individual muscles. Skeletal muscle has a high energy requirement, and many proteomics studies focus on mitochondrial-related proteins. At

the same time, skeletal muscle secretory proteome is also an important research object of proteomics for the purpose of discovering the secreted proteins released by muscle which can act on local or systemic proteins. HP protein is a matrix protein, which is a structural protein connecting the viral envelope and the viral core in virology. It has an affinity for the glycoprotein of the host cell wall, and on the other hand, it has an affinity for a variety of ribonucleic acids, which causes it to form a layer of viral nucleoprotein structure under the cell wall. This structure helps the virus mature to encapsulate the RNA and germinate new viruses. The formula for obtaining the HP matrix of protein is as follows:

$$HP(i,j) = [(B(P(i)),j)] \times [(B(P(i)),j)]', \tag{1}$$

$$Q_i = KQ_0U, \tag{2}$$

$$F_i = L_i \times \frac{N_i}{\eta_1}. \tag{3}$$

The structural information of the high-dimensional space is retained in the low-dimensional space and retained as $BP \in \phi^{p\times q}$:

$$BP(p,q) = L(r,p) \times HP(r,c) \times R(c,q), \tag{4}$$

$$N = H - \frac{G(v)}{2}, \tag{5}$$

$$N_1 = \frac{\exp\left(-M^2\right) - v\sqrt{V}(M)}{2v\sqrt{\pi}} V, \tag{6}$$

$$V = \frac{\cot \varphi_i}{\sqrt{2 \times (\beta_1 + \kappa_1 \cos(2\beta))}}. \tag{7}$$

F_W and F_J have the following formulas:

$$F_W = \sum_{I=1}^{K}\sum_{I=1}^{K} L^T(x-m)RR^T, \tag{8}$$

$$F_J = \sum_{I=1}^{J}\sum_{I=1}^{J} L^T(x-L)RR^T. \tag{9}$$

CWT is continuous wavelet transform, which does not involve discrete wavelet transform and does not involve scaling functions; DWT is the discrete Walsh transform, in which the transformation matrix is simple (only 1 and one 1), occupies less storage space, is easy to generate, and has a fast algorithm. It is widely used in image processing problems that require real-time processing of large amounts of data. The CWT formula for feature extraction can be expressed as follows:

$$\mathrm{CWT}(a,b) = \frac{1}{|a|}\int_{-1}^{+1} A(p(t),1)\beta\left(\frac{t+b}{a+b}\right)dt, \tag{10}$$

$$C(a,b) = \mathrm{CWT}(a,b) \times \mathrm{CWT}(a,b)'. \tag{11}$$

The definition of the DWT function is as follows:

$$\mathrm{DWT}(a,b) = \frac{1}{\sqrt{a}}\int f(t)\psi\left(\frac{t-b}{a}\right)dt, \tag{12}$$

$$B^M(R) = -L\chi M(R) - \nabla\beta(R), \tag{13}$$

$$\vec{E} = -JU\vec{A} - \nabla\phi - \frac{1}{\pi}\nabla \times \lambda_\varepsilon, \tag{14}$$

$$\vec{H} = -ML\vec{A}_\varepsilon - \nabla\varphi_m + \frac{1}{\kappa}\nabla \times \gamma. \tag{15}$$

a means scale parameter, and b means translation parameter. First, normalize the features of the monomodal sample:

$$W(i,j) = \exp\left[-\frac{d^2(x_i,x_j)}{\alpha\phi_{i,j}}\right], \tag{16}$$

$$E(L_i) = \frac{1}{N}\sum_{M=1}^{U_s} L_i^n, \tag{17}$$

$$K(p) = \sum_{i=1}^{C_b} -G_i \log(D_i), \tag{18}$$

$$Q_i = \frac{1}{M_s - 1}\sum_{n=1}^{Ns}\left[K_i^n - E(K_i)\right]^2. \tag{19}$$

a is a hyperparameter.

$$\phi_{i,j} = \frac{\mathrm{mean}(d(x_i,k_i)) + \mathrm{mean}\left(d\left(x_i,k_j\right)\right) + \mathrm{mean}\left(d\left(x_j,k_j\right)\right)}{3}, \tag{20}$$

$$P = \beta\left(Di1 - Gi2 + \kappa\sum_j gij\mathrm{Pr}\right), \tag{21}$$

$$\phi = \beta\left(Yi2 - Gi2 + \kappa\sum_j gij\mathrm{Pr}\right). \tag{22}$$

$\mathrm{mean}(d(x_i,k_i))$ represents the average distance between i and its neighbors. Get the final converged network from the original network:

$$L_{t+1}^{(m)} = S_t^{(m)} \times \frac{\sum L_t^{(m)}}{C-1}. \tag{23}$$

Define the probability propagation matrix as

$$T_{ij} = P_t^{(m)} \times \frac{W_{ij}}{\sum w_{kj}}. \tag{24}$$

2.2. Influence of Muscle Fiber Type on Exercise-Induced Proteomic Remodeling. Muscle fiber types also influence the remodeling of exercise-related proteome. According to the contraction speed and metabolic characteristics of muscle

fibers, they can be divided into fast-shrinking-glycolysis type and slow-shrinking-oxidation type. Skeletal muscle fiber is a kind of multinucleated cell, and the number of nuclei varies with the length of the muscle fiber. Shorter ones have fewer nuclei; older ones have 100 to 200 nuclei, which are located below the sarcolemma. The nuclei are oval, lightly stained, and the nucleoli are clear. The size of the muscle fiber area depends on the diameter of the muscle fiber and is affected by age, training, and muscle fiber type. There were differences in protein expression of the two kinds of fibers related to metabolic processes such as glycolysis, free fatty acid metabolism, citric acid cycle, and oxidative phosphorylation. The six proteins, ATP synthase subunit 5B, mitochondrial creatine kinase, myoglobin, glucose phosphate translocation-1, and WD1 repeat protein, were regulated by exercise. However, only mitochondrial NADH dehydrogenase 1 complex 2 and extension factor Tu were differentially expressed in soleus muscle, and both of them were downregulated. It was found that 19 proteins were differently expressed, and 10 and 17 unique secreted proteins were produced in gastrocnemius muscle and soleus muscle after endurance exercise. The dJ-1 protein is more abundant in the gastrector, while the fatty acid-binding protein fabP-3 (FABP-3) is more abundant in the soleus. The authors believe that DJ-1 protein is related to oxidative stress after muscle contraction, while FABP-3 is related to lipid metabolism [6]. The deep polynomial network is shown in Figure 1.

In conclusion, proteomics techniques can be used to study the skeletal muscle proteome as a whole and in depth. Exercise induces an adaptive response in skeletal muscle, and proteomics adjusts accordingly. Different types, intensity, and duration of exercise and muscle fiber types can cause different changes in skeletal muscle proteome. At present, studies on the proteomics of exercise on skeletal muscle remodeling are being carried out, but there are still some technical difficulties. With the continuous improvement of existing technologies and the emergence of more new technologies, proteomics research will make greater contributions to elucidate the mechanism of exercise on skeletal muscle remodeling and its improvement on health [7].

2.3. Application of Myocardial Proteomics in Sports Research. Long-term exercise training can make the heart adapt to change, so that the heart "pump" function increase and the formation of heart self-protection. The increase of cardiac "pump" function is manifested as physiological hypertrophy of the myocardium to enhance the contraction function of myocardium and increase cardiac output to meet the needs of the body. Proteomics is a science that studies the composition of proteins in cells, tissues, or organisms and their changing laws. That is to say, it includes all proteins expressed by a cell or even an organism. Proteomics essentially refers to the study of the characteristics of proteins on a large scale. In order to compare movement mediated myocardial and normal myocardial hypertrophy of proteomics, the study found that 23 movement mediated hypertrophy heart tissue protein point obviously change, and these changes related to mitochondrial oxidative metabolism of protein, such as A statin, malate dehydrogenase, short chains of acetyl-coa dehydrogenase, triose phosphate isomerase, electron transfer flavoprotein beta subunits, ATP synthase alpha, and isocitrate dehydrogenase subunit. In addition, in addition to the upregulation of statin expression in hypertrophic myocardial tissue, there were also upregulation of scaffold, signaling pathway, and proteins related to oxidative stress response. These changes may be related to the enhancement of mitochondrial oxidative metabolism and ATP synthesis ability. Increasing research in sports training rats and intermittent movement training rats cardiac tissue for two-dimensional gel electrophoresis, the results found that 26 protein point difference, 12 of them increasing protein point are only found in sports training in the rat heart tissue, and western blot method confirmed that heat shock protein HSP -20 clear and continue to exist in experimental rat heart tissue. Moreover, hSP-20 expression was upregulated in the myocardium of exercise rats, and phosphorylation of Serine 16 of HSP-20 was found, which was related to the improvement of myocardial contraction and antiapoptosis self-protection [8]. The protein-coding method is shown in Figure 2.

In addition, endurance training is generally considered to enhance myocardial self-protection against ischemia-reperfusion injury-mediated myocardial damage, while the adaptive changes of mitochondria during endurance training play a crucial role in myocardial self-protection. To study the changes of mitochondrial proteins during exercise training [9]. The oprah-way to (be) rats were divided into experimental group and control group in sports training, at the same time, two groups of myocardial mitochondrial protein membrane were isolated and myocardial mitochondrial protein fiber, they are compared, proteomics results identified 222 heart mitochondrial protein, and follow-up study found that the experimental group compared with control group, there are 11 kinds of myocardial fibers mitochondrial protein (cut) expressed in seven kinds of expression, 4 and 2 kinds of myocardial mitochondrial protein membrane (1 kind of express one kind of expression of proteins of) obvious change, and these proteins belong to different functional groups and cardiac protection regulation factor. The mechanism may be the increased expression of antioxidant enzymes and myocardial antiapoptotic proteins (such as HSP-70) mediated by endurance training in mitochondria. These protective factors play an important role in protecting myocardial function against myocardial damage induced by ischemia-reperfusion during exercise [10].

Domestic scholars, respectively, for the movement of atrial and ventricular muscle of rats and the control group differences in proteomics research, cardiac structure, and function of main protein found myosin subtypes: alpha type myocardial myosin heavy chain (alpha MHC) expression in the exercise group rats myocardial cut, this may be related to long-term movement, and energy consumption increase leads to high ATPase activity of alpha MHC shift towards A low beta MHC TPase activity, which can cause the biggest contraction rate of decline. In the study of the changes of ventricular myproteome in rats after exhaustion exercise, it was found that the expression of tropomyosin-1 chain, as an important regulatory protein during muscle contraction,

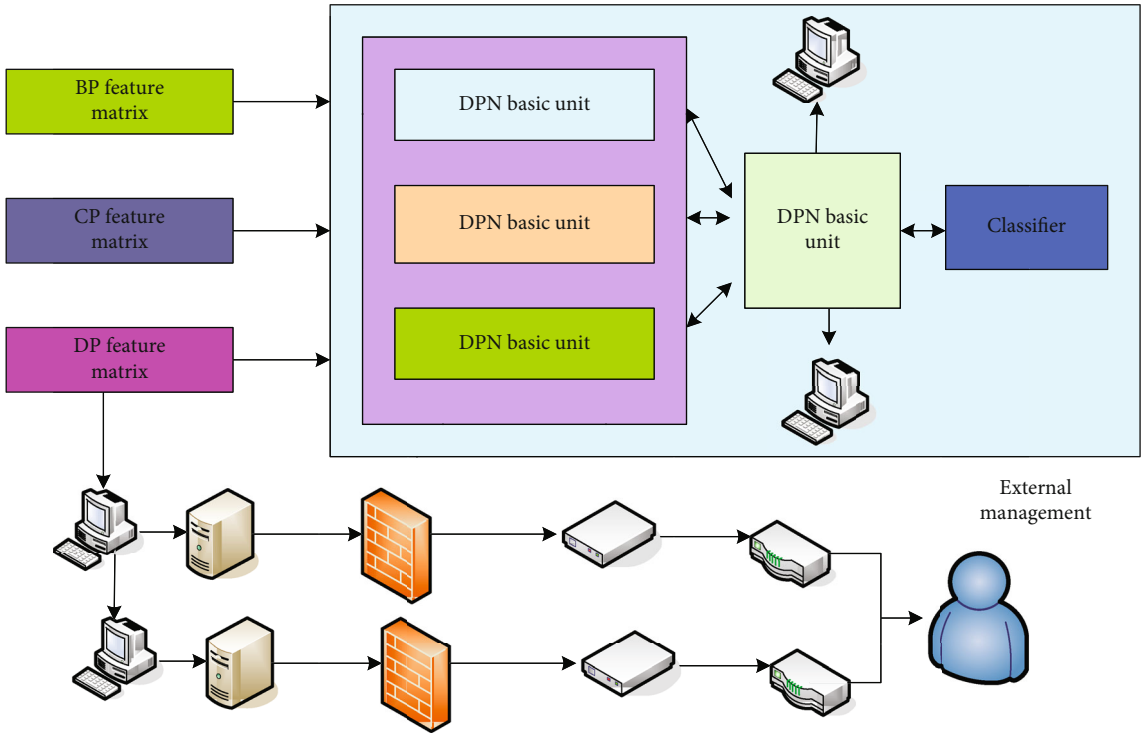

Figure 1: The deep polynomial network.

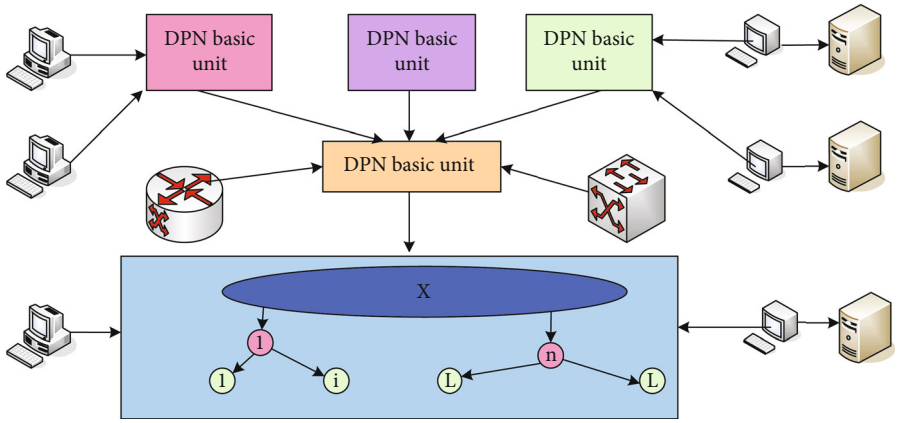

Figure 2: The protein-coding method.

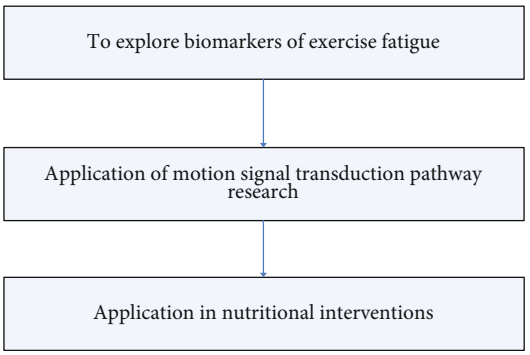

Figure 3: Applied research scope of differential proteomics in sports human science.

Table 1: The isoelectric focusing procedure.

Hydration	50 v	12-16 hours	Active hydration
S1	250 v	30 minutes	Desalination
S2	1000 v	1 hour	Desalination
S3	10000 v	5 hours	Boost
S4	10000 v	60000 volt hours	Focus
S5	500 v	Anytime	Keep

Table 2: The concentration of total RNA and the OD ratio.

Group	1	2	3	4
Sports group	36.2	36.7	90.2	29.5
	1.85	1.81	1.91	1.89
Control group	61.3	53.3	14.1	17.9
	1.89	1.84	1.80	1.86

Table 3: Protein points that disappeared after exercise, and their expression levels were increased by more than twice and decreased to less than below.

SSP number	Mr (KDa) molecular weight	pI isoelectric point	Variation	Fold change range
1251	43	7.93	Up	46.4
1002	66	6.40	Up	13.0
1298	36	8.02	Up	11.7
1025	62	7.27	Up	7.9
1278	39	8.05	Up	7.5

"disappeared" after exhaustion exercise, suggesting that it may be a potential biomarker for the determination of exercise muscle fatigue [11, 12].

2.4. Application of Differential Proteomics in Sports Human Science. Proteins expressed by cells vary in composition and content at specific stages of cell cycle, different stages of differentiation, and different physiological and pathological states. Differential proteomics focuses on such differences, dynamically reflecting the state of the organism, providing accurate molecular description of cells or tissues in a specific state, and more conducive to revealing the essence and laws of life phenomena. Physical exercise changes the physiological environment of human body, such as pH, type and amount of ions, accumulation of metabolic substances, and hormone concentration. Such changes will lead to changes in gene expression and postprocessing modification of protein synthesis, and protein mapping will be different from that under normal physiological conditions [13]. Different exercise mode, exercise intensity, and exercise time have different effects on human physiological function. Different people react differently to the same exercise [14, 15]. Carries on the comparison to the protein mapping between them, we can make a more comprehensive, fully understanding of the different physiological conditions function in the process of life activity metabolism, to reveal the impact of different sports on the body function of biochemical changes in the law, exercise training plan for scientific, medical supervision, and reasonable nutrition intervention to provide theoretical and experimental support, and you can also develop individualized exercise prescription for rehabilitation of patients [16].

(1) Explore the biomarkers of exercise fatigue

In modern sports training theory, without the great physiological load of exercise training, there is no superman, the great physiological load of exercise training inevitably produces exercise fatigue, may even lead to excessive training, cannot be able to eliminate the exercise fatigue again big strength training, and also cannot get good grades, so accurate for diagnosis and effective exercise fatigue of eliminating exercise-induced fatigue is of great significance [17]. Exercise fatigue has always been a practical and challenging topic in the field of sports medicine. The study of exercise fatigue has been going on for a hundred years, ever since digital myography was first used to study the changes in working ability that occur when muscles contract repeatedly. There are many theories about the cause of exercise fatigue, but they all describe one aspect (energy depletion, lactic acid, accumulation of metabolites, etc.). The application of differential proteomics can provide a more comprehensive understanding of the changes of known proteins and some unknown proteins in the process of exercise fatigue. Through comparison, it is possible to find biomarkers that can effectively reflect the generation of exercise fatigue. Thus, it provides a criterion for the diagnosis of the occurrence and development of exercise fatigue. This is of great significance to the development of scientific training plan, effective monitoring of training process, effect evaluation, and prevention of overtraining [18].

(2) Application in the study of motion signal transduction pathways

The changes of body structure and function are realized through a series of motion signal transduction pathways. The signal transduction pathway is composed of a series of proteins. Signal transduction involves protein interactions and posttranslational modifications. At present, in the field of sports medicine, due to the limitations of experimental technology and other factors, the research on the movement signal transduction pathway is still relatively small and shallow. Differential proteomics can identify all proteins that may be involved in signal transduction from the changes of total proteins in cells before and after receptor activation, and start from different protein points to find their upstream and downstream signal transduction molecules. This is a bidirectional or multidirectional method, which can greatly accelerate the research process of signal transduction. By studying the motion signal transduction pathway, we can intervene this process according to different purposes [19, 20].

Table 4: RMS of lower limb muscle surface electromyography in both states.

The experimental project	Shares of rectus muscle	Half tendons	Biceps	Tibialis anterior muscle
Stationary state	4.7 ± 1.8	10.5 ± 5.2	12.8 ± 6.6	4.9 ± 0.9
Random visual excitation	5.2 ± 1.2	31.3 ± 15.2	24.2 ± 10.2	5.6 ± 1.3

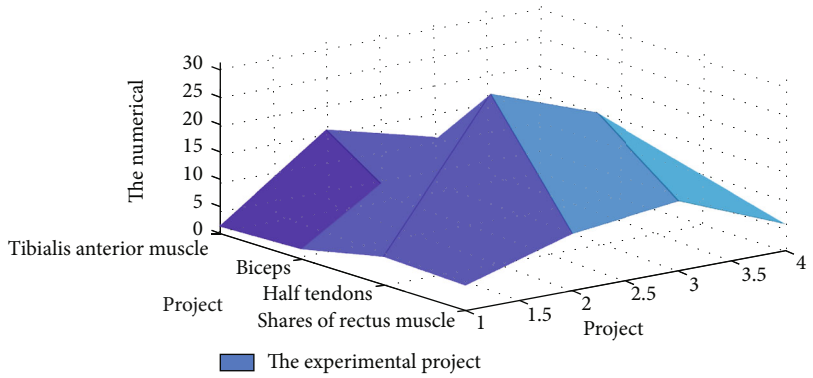

Figure 4: RMS of lower limb muscle surface electromyography in both states.

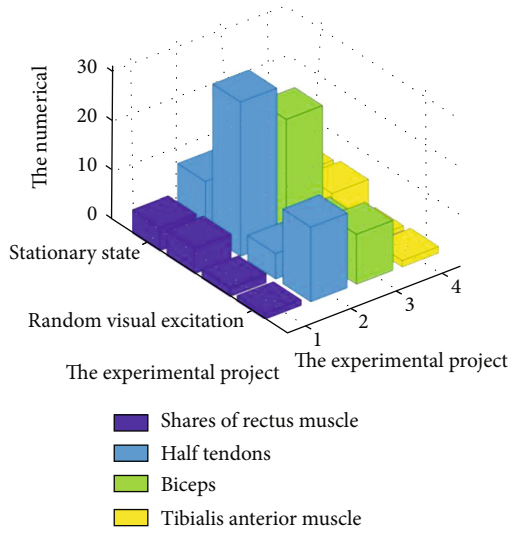

Figure 5: Differences in RMS of the anterior tibia muscle.

(3) Application in nutrition intervention

Lack or excess of nutrients can affect health, physiology, and exercise. Reasonable nutrition supplement for athletes can accelerate the elimination of sports fatigue, enhance immunity, and improve sports ability. Through differential proteomics, new nutritional supplements can be developed, targets of nutritional supplements can be found, mechanism of action and adverse reactions of nutritional supplements can be clarified, and efficacy can be evaluated, so as to improve athletic performance and health. The application and research scopes of differential proteomics in sports human science are shown in Figure 3.

2.5. Development Trend of Proteomics. Proteome research techniques have been applied to various scientific fields, such as cell biology and neurobiology. However, proteome research is still at an early stage of development, and the related technologies and their supporting applications are still very immature. Therefore, the establishment, optimization, and improvement of the technical of proteomics have become one of the main objectives of proteomics research. Proteome technology also has a very attractive prospect in the clinical diagnosis and treatment of major human diseases such as cancer and senile dementia. The focus of future research is to analyze functional proteins and differential proteins. The main technical routes are two-dimensional electrophoresis separation, multidimensional chromatography separation, and mass spectrometry modification analysis of white matter. The main technical routes are enrichment separation and mass spectrometry analysis of modified proteins. Protein complex and protein interaction network analysis are mainly using the existing protein research technology and equipment to carry out the separation and identification of protein complex.

3. Muscle Proteomics Experiments in Sports

3.1. Surface EMG Signal Preprocessing and Feature Extraction. The original EMG signals of the 16 lower limb muscles collected in this paper have not been processed experimentally, and the original signals have a lot of noise, which seriously affects the quality of EMG signals. Therefore, preprocessing and feature extraction of raw EMG signals are required for subsequent muscle activity analysis and nonlinear model of human body dynamic balance. The isoelectric focusing procedure is shown in Table 1.

3.2. Preprocessing of Surface EMG Signals. Based on the nonstationary, nonlinear, amplitude concentration of sEMG signal in 10-10 mV and the main energy concentration in 20-250 Hz frequency, it is extremely easy to be drowned in other noise or interference in the process of signal acquisition. In

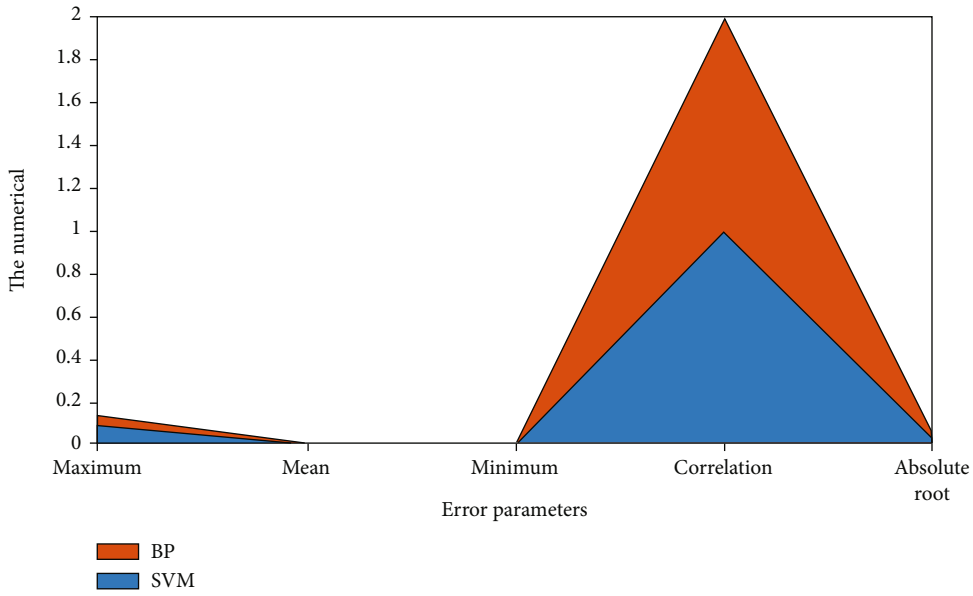

Figure 6: SVM predictive effect data

Table 5: Comparison of BP neural network and SVM prediction results.

Error parameters	BP	SVM
Maximum absolute error	0.0877	0.0467
Mean absolute error	0.00217	0.00182
Minimum absolute error	0.00049	0.00019
Correlation coefficient R	0.9890	0.9922
Absolute root mean square error	0.0275	0.0251

order to reduce the influence of these factors on the subsequent feature extraction and analysis, on the one hand, we should ensure the standard of the experiment during the experiment to overcome some external influences; on the other hand, we should preprocess the signal. In this study, the sEMG signals collected are preprocessed by myoMUSCLE myocle's processing software, and the original EMG signals are filtered by a finite pulse filter at 20-250 Hz. The concentration of total RNA and the OD ratio is shown in Table 2.

3.3. Feature Extraction of Surface EMG Signals. The purpose of this paper is to analyze the activity degree of lower limb EMG signals under stationary state and random visual excitation state and finally use nonlinear identification method to model the nonlinear mapping relationship among surface EMG signals, kinematic data, and dynamic parameters, so as to realize the nonlinear modeling of human dynamic balance. Feature extraction of the task is to determine the activity of muscle data, analyzing the characteristic of the meaningful data as appropriate characteristic parameters extraction is essential to the electromyographic signal analysis, as well as the human body dynamic model of the nonlinear identification provides appropriate input data, on the premise of guarantee of prediction accuracy, keep useful

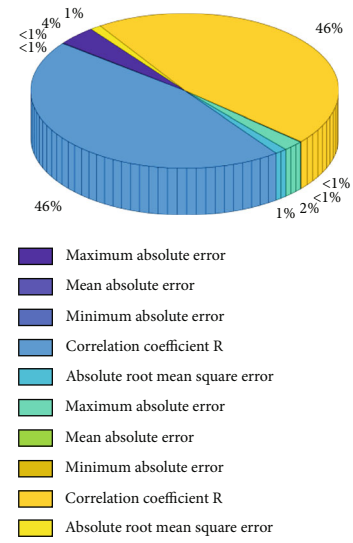

Figure 7: Comparison of BP neural network and SVM prediction results.

information as much as possible, reduce the feature dimension, simplifying the lower limb muscle activity analysis, and speed up the human body dynamic balance of the nonlinear identification process. Table 3 shows the protein points that disappeared after exercise, and their expression levels were increased by more than twice and decreased to less than below.

4. Muscle Proteomics Is Discussed in Sports

4.1. Comparative Analysis of Muscle RMS in the Two States

(1) The experiments using the statistical method of single-factor variance analysis to the same muscles in two states of RMS were analyzed, respectively,

Table 6: Relative net optical density values of the target protein mRNA gel bands in the exercise group and the control group.

Protein name	Changes	Control group ($x \pm s$)	Sports group ($x \pm s$)
Myocardial actin	Upregulate	1.676 ± 0.9683	0.9570 ± 0.6207
Josephin domain protein 1	Upregulate	0.562 ± 0.4207	0.587 ± 0.4338
Adenylate kinase isoenzyme 1	Down	0.859 ± 0.8060	0.714 ± 0.3356
Nucleoside diphosphate kinase B	Down	1.249 ± 0.5923	1.1321 ± 0.3677
Glutathione S-transferase Mu2	Upregulate	0.779 ± 0.3982	0.479 ± 0.1096

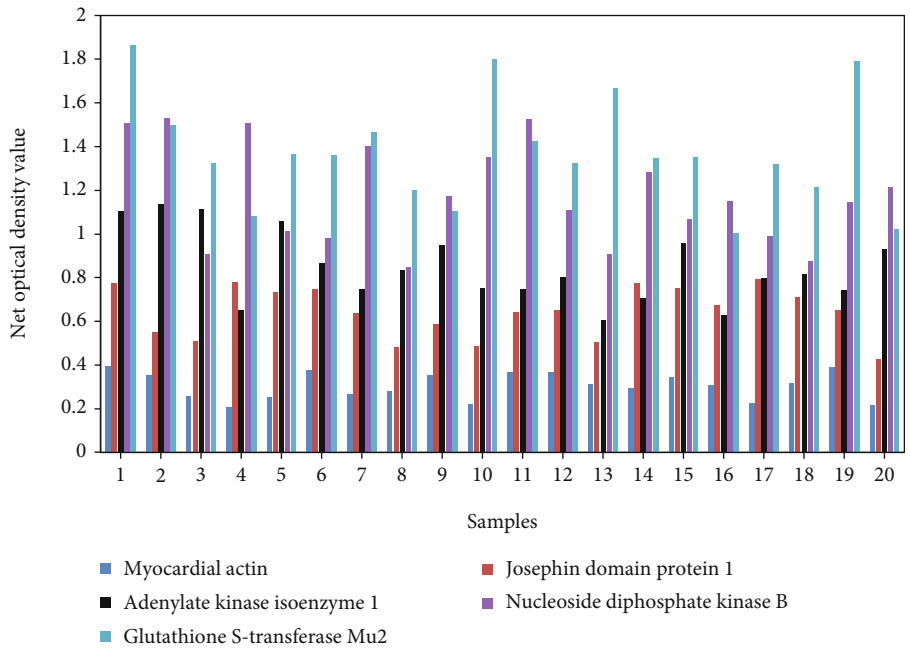

Figure 8: The relative net optical density value of target protein mRNA.

Table 7: The preparation of protein quantification standard curve.

Serial number	Protein content (ug)	Standard solution (5 mg/mlBSA) μL	Double distilled water (μL)	Bradford working fluid (ml)
1	40	8	72	4
2	80	16	64	4
3	120	24	56	4
4	160	32	48	4

under the two states of different between muscle electromyography IEMG were analyzed, finally, the muscle integral electrical values on the contribution rate of extent of each muscle under the two states are analyzed. The protein map basically tells people how to eat, what to eat, and exactly what we need to eat to beat disease. Key levels due to individual differences and two states on the right lower limb corresponding muscles function with the same degree of difference will produce different electromyographic signal, even vary widely, and static experiment and random visual incentive evaluation experiment is done under the left and right side lower limb synergy, and the left and right side lower limb muscles of the same name is adopted, respectively, weighted RMS compared with IEMG later. For one-way ANOVA, this study defined the significance level of the difference analysis between groups as $P < 0.05$. After the stationary experiment and the random visual stimulation experiment, the collected muscles were weighted with the same name, and the statistical results of time-domain eigenvalue-RMS were shown in Table 4 and Figure 4

(2) After one-way ANOVA of RMS of each muscle in the two states, the results showed that the biceps femoris muscle in his half tendons, the lateral gastrocnemius, medial gastrocnemius, long peroneal muscle, and soleus RMS has significant difference ($P < 0.05$), and of the biceps femoris muscle of the lateral sural, soleus RMS difference significantly apparent ($0.01 < P < 0.05$), half tendons, medial gastrocnemius, RMS of long peroneal muscle very significant difference ($P < 0.01$), while rectus, the RMS of the tibialis anterior muscle and no significant

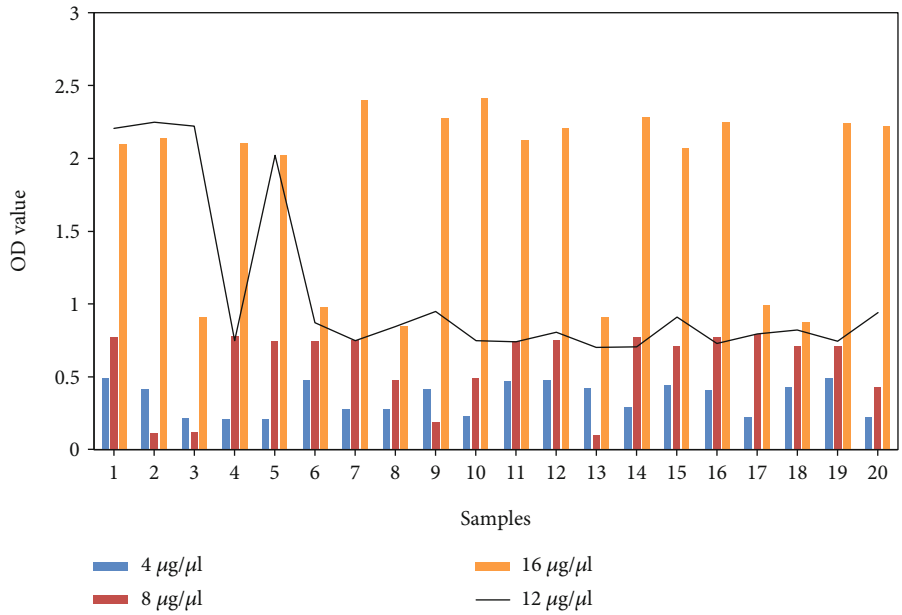

Figure 9: The Bradford quantification standard of atrial muscle extracted protein.

Table 8: The protein spots in the atrial muscle that are upregulated by more than 5 times.

SSP number	Molecular weight (KD)	Isoelectric point (PI)	Increase multiple
1004	20.79	3.89	8.57
1009	21.24	4.62	7.36
1201	30.78	4.92	5.26
1403	38.2	4.56	5.47
2105	55.21	4.77	12.06

Table 9: The protein spots (compared with the control group) that were downregulated by more than 5 times (without the vanishing point) in the atrial muscle.

SSP number	Molecular weight (KD)	Isoelectric point (PI)	Increase multiple
4	22.7	5.48	9.04
201	41.27	4.02	5.52
302	51.51	4.21	0.15
1404	57.05	4.82	9.20
1702	>97	4.68	19.2

Table 10: The protein spots that disappeared in the atrial muscle.

SSP number	Molecular weight (KD)	Isoelectric point (PI)	Increase multiple
4	20.8	3.8	52.8
201	20.77	4.52	202.8
302	55.25	4.86	11.0
1404	>97	5.05	10.4
1702	>97	6.16	17.4

difference ($P > 0.05$), the differences of the RMS of the tibialis anterior muscle as shown in Figure 5

4.2. SVM Prediction Effect

(1) On the basis of previous studies, this study adopts the SVM modeling method to identify the athletes' body dynamic balance nonlinear model. According to the optimized scheme after nonlinear identification, the RMS value of lower limb muscles (lateral gastrocnemius, medial gastrocnemius, peroneus longus, and soleus) and the ankle torque value at the previous moment was input to predict the output value of ankle angle at the next moment. The 5000 sets of data obtained in the experiment were excluded from the data collected at the beginning of discomfort and the data collected when fatigued, and finally 500 sets of data were obtained. The 4500 sets of data in the middle are used for nonlinear recognition of the human dynamics model, the first 4400 sets of data are used as training data, and the last 100 sets ofsamples are used as prediction data. The results show that the SVM predictive output can also approximate the expected output, and the SVM predictive effect is better than that of BP neural network. The SVM predictive effect data are shown in Figure 6

(2) In this paper, a muscle-joint model was established by using SVM, and the predicted output could approach the expected output better. Then compared with the prediction effect of BP neural

Table 11: The differential expression in atrial muscle is predicted.

Serial number	Name	Theoretical molecular weight/isoelectric point	Variety
4	Ferritin light chain 1	(KD/PI)	Down
1009	Tropomyosin beta chain	20.62/5.98	Upregulate
1201	Annexin A5	32. 84/4.66	Upregulate
3102	Glutamine synthetase	35.61/4.93	Down
4506	Transketolase	42.13/6.68	Down

Table 12: The mass spectrometry identification results.

Serial number	Isoelectric point	Points	Variety
1702	5.59	155	Down
1004	4.97	98	Upregulate
6204	6.81	135	Upregulate
2701	5.59	113	Disappear
1705	5.59	132	Down

network, it was found that the correlation between the predicted output of SVM and the expected output was higher than that of BP neural network, and the prediction error was smaller than that of BP neural network. In terms of the prediction effect of athletes' sports dynamic balance, SVM prediction effect was generally superior to BP neural network. The results show that the correlation coefficient between the predicted output and the expected output of SVM is higher than that of BP neural network, and the absolute RMS error between the predicted output and the expected output of SVM model is smaller than that of BP neural network. According to the above analysis, SVM is generally superior to BP neural network in predicting athletes' dynamic balance. The statistical results are shown in Table 5 and Figure 7

Table 6 shows the relative net optical density values of the target protein mRNA gel bands in the exercise group and the control group. As can be seen from the table, the relative net optical density value of cardiac actin mRNA in the control group is 1.676, the exercise group is 0.957, and the exercise group is 0.719 lower than the control group ($P > 0.05$).

Among the 5 target proteins detected, the mRNA expression levels of Josephin domain protein 1, adenylate kinase isoenzyme 1, and nucleoside diphosphate kinase B are consistent with the corresponding protein expression levels. The relative net optical density value of target protein mRNA is shown in Figure 8.

The preparation of protein quantification standard curve is shown in Table 7.

This article carried out three consecutive repetitive electrophoresis and selected a map from the control group and exercise group gel as the reference gel for protein spot matching test, so that the protein spots in each gel correspond to the spots in the reference gel. The Bradford quantification standard of atrial muscle extracted protein is shown in Figure 9.

After exercise, there are 38 protein spots that are reduced by more than 2 times, most of which are concentrated in the molecular weight range of 20-70 KD and the range of 4-8 isoelectric points; among them, 16 protein spots are reduced by more than 5 times (excluding vanishing points) after exercise, and the multiples are reduced. Generally distributed between 5 and 6 times. The protein spots in the atrial muscle that are upregulated by more than 5 times are shown in Table 8.

The protein spots (compared with the control group) that were downregulated by more than 5 times (without the vanishing point) in the atrial muscle are shown in Table 9.

The protein spots that disappeared in the atrial muscle (compared to the control group) are shown in Table 10.

It is inferred that 11 protein spots are differentially expressed more than 5 times after exercise in this study, of which 5 protein spots are upregulated by more than 5 times, and 6 protein spots are downregulated by more than 5 times. The differential expression in atrial muscle is predicted as Table 11 shows.

By comparing the differences in the 2-DE patterns of atrial muscle protein in the exercise group and the control group, the selection prediction is of great significance in sports medicine and clinical medicine. The mass spectrometry identification results are shown in Table 12.

The hydrophobicity of amino acids is one of the factors that affect the stability of protein structure, especially in maintaining and stabilizing protein conformation. The hydrophobicity index of amino acids is shown in Table 13.

Table 13: The hydrophobicity index of amino acids.

Amino acid	A	R	N
Hydrophobicity index	0.61	0.60	0.06
Amino acid	L	K	M
Hydrophobicity index	1.53	1.15	1.18

When $T = 8$, $K = 15$, and $a = 0.4$, the values of ACC, MCC, PE, and SN are 96.71%, 93.61%, 100%, and 93.39%, reaching the peak value. The prediction result of the data set is shown in Figure 10.

One is based on the relative mutation rate of amino acids, using the BLOSUM62 matrix combined with the effective 2DLDA dimensionality reduction method; the other is based on the CWT-based feature extraction of the hydrophobicity of amino acids. The prediction results of the five-fold cross-validation method on the three core data sets are shown in Figure 11.

The average AUC were 97.58%, 95.19%, 95.63%, 97.49%, 96.15%, and 98.43%, and the corresponding standard deviations were 0.28%, 0.73%, 1.02%, 0.46%, 0.24%, and 0.19%. It shows that the average AUC value of the method model TP-

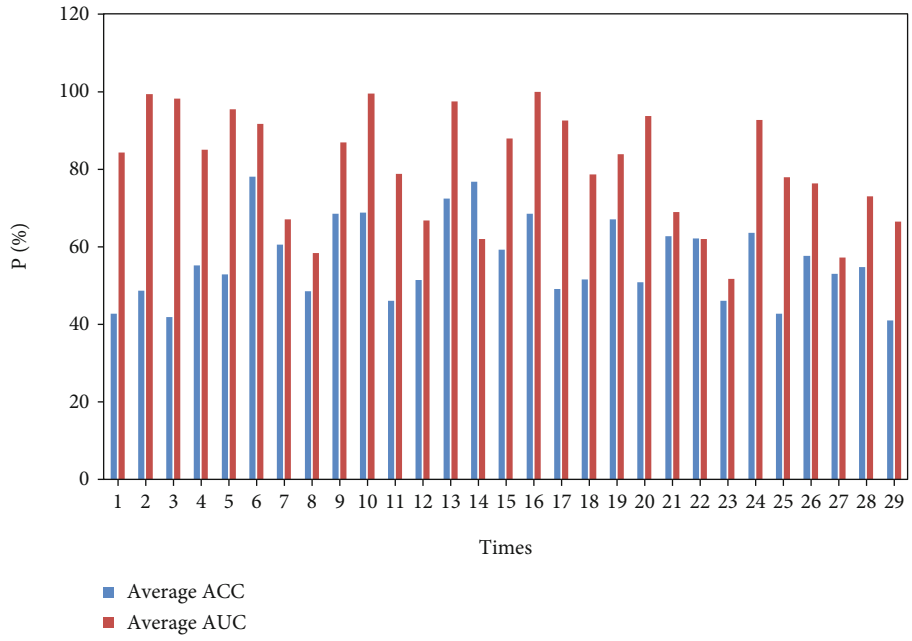

Figure 10: The prediction result of the data set.

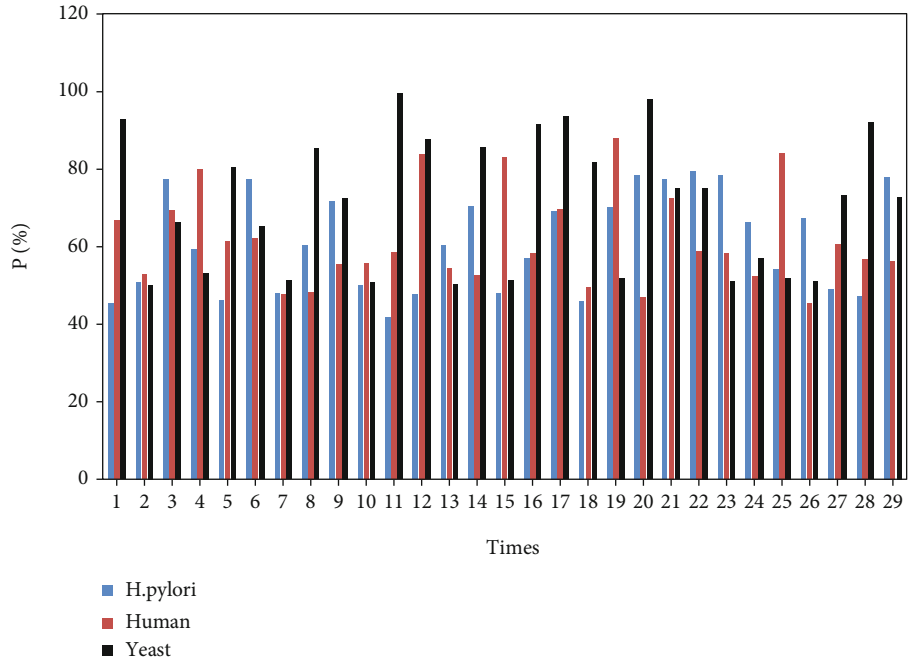

Figure 11: The prediction results of the five-fold cross-validation method on the three core data sets.

SNF-LPA in this paper is increased by at least 0.85%, and the standard deviation is the smallest. The five-fold cross-validation with different other methods on the H. pylori dataset is shown in Figure 12.

The average ACC of the model TP-SNF-LPA in this paper is 94.80%, 97.92%, 94.96%, 97.52%, 98.58% and 99.30%, respectively. The five-fold cross-validation results using other different methods on the Human dataset are shown in Figure 13.

When SVM and LPA are directly used for classification prediction for the same monomodal information, it is obvious that the LPA method has better performance than the

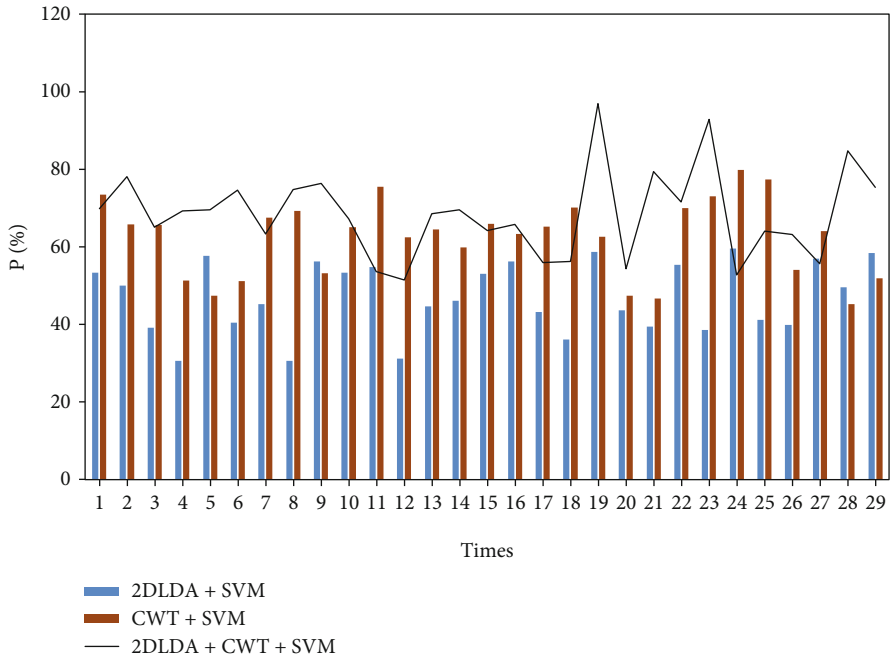

Figure 12: The five-fold cross-validation with different other methods on the H. pylori dataset.

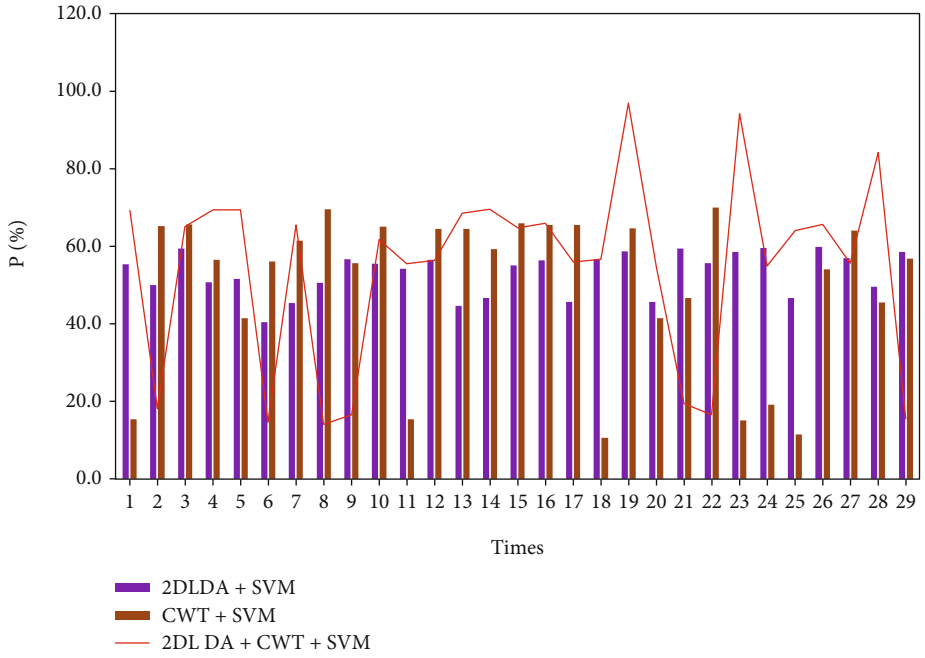

Figure 13: The five-fold cross-validation results with different other methods on the human data set.

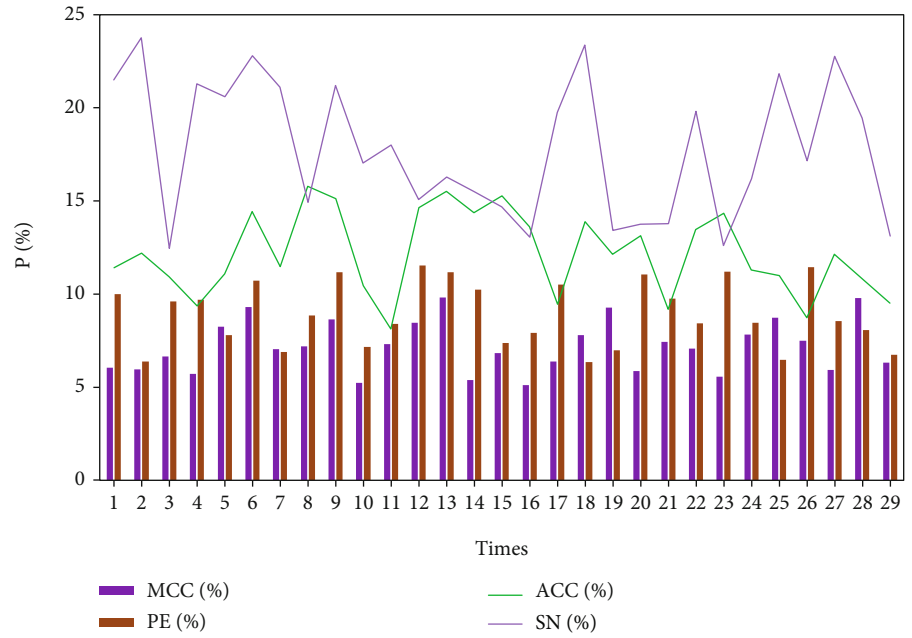

Figure 14: The results of the five-fold cross-validation with different other methods on the yeast dataset.

SVM method. The results of the five-fold cross-validation with different other methods on the yeast dataset are shown in Figure 14.

5. Conclusion

(1) The most direct effect of exercise on the body is to change the shape of skeletal muscles, but the underlying molecular mechanisms are still unknown. Proteomics techniques provide an overview of the molecular pathways that regulate specific stimuli. At present, some progress has been made in the motor mechanism of skeletal muscle remodeling. In this paper, an extensive review and summary analysis of recent proteomics studies on exercise-induced skeletal muscle remodeling is presented. According to the results of this study, protein isolation and protein identification can effectively detect the differentially expressed proteins in skeletal muscles before and after exercise or between exercise and quiet control. Exercise induces an adaptive response in skeletal muscles, so the proteome adjusts accordingly. Different types of exercise, intensity, and duration, and types of muscle fibers lead to different changes in skeletal muscle proteome. With the continuous improvement of existing technologies and the emergence of more and more new technologies, proteomics research will make a great contribution to elucidate skeletal muscle remodeling and improve the movement mechanism of health. Exercise fatigue mainly appears in the early stage-some subjective feelings of discomfort and psychological changes: generally self-feeling tired or even exhausted, poor appetite and sleep, dizziness, dullness, depression, lack of interest and confidence, sensitivity, and irritability wait. Accompanied by the decline in exercise capacity, if the feeling of fatigue develops further without adjustment, there may be slight changes in some objective indicators. Physical functions include weight loss, headache, insomnia, rapid pulse, increased blood pressure, abnormal ECG, decreased hemoglobin, increased white blood cell count, proteinuria, and hematuria. Neurological disorders such as slow response, misjudgment, and inattention. The performance of sports ability is decreased sports quality, fatigue and difficulty in recovery during training, uncoordinated, and inaccurate movements

(2) In sports, muscle proteomics research aimed at understanding sports related to the muscles in the proteome changes, formulate related to sports pathophysiology and molecular mechanism of muscle, to guide and develop scientific and reasonable sports training strategy, and to promote the rapid development of sports undertakings. Although the proteomics research as a whole is still in the preliminary stage, and it is all sorts of deficiencies such as complicated operations, poor experimental requirements, and high sensitivity and accuracy, but as the proteomic technology and the development of genomics and bioinformatics, proteomics will eventually become an optimal approach to study protein expression and functional status. Protein ubiquitously exists in the biological world. It is the material basis of life activities, one of the basic components of organisms, and the most abundant biological macromolecules in organisms. The structure and function of protein are complex, and it is responsible for the tasks of completing various physiological functions in the organism. In terms of material metabolism, body defense, blood coagulation, muscle contraction,

information transmission between cells, individual growth and development, tissue repair, etc., protein plays an irreplaceable role

(3) Muscle tissue is the most abundant tissue in the body of adults. Muscle contraction and relaxation play a very important role in the training of sprinters. The maintenance of various body postures and training movements requires the participation of muscles, which makes the phenomenon of muscle injury become very common. According to the investigation and analysis, muscle injury is a very common training injury among athletes of all ages, which affects the performance and competition ability of athletes, reduces the enthusiasm of athletes to continue to participate in sports training, and may even end their sports career in extremely serious cases. At present, the incidence of muscle injury is increasing year by year, which will affect more athletes and families. Therefore, continuing to study the pathogenesis of muscle injury and exploring more effective treatment methods have become an important research topic in the field of sports medicine. Key levels due to individual differences and two states on the right lower limb corresponding muscles function with the same degree of different will produce different electromyographic signal, even vary widely, and static experiment and random visual incentive evaluation experiment are done under the left and right side lower limb synergy, and the left and right side lower limb muscles of the same name is adopted, respectively, weighted RMS compared with IEMG later. The experimental results showed that for one-way ANOVA, the significance level of the difference analysis between groups was defined in this study as $P < 0.05$

Data Availability

No data were used to support this study.

Conflicts of Interest

The authors state that this article has no conflict of interest.

References

[1] H. Peng, J. Cao, R. Yu, F. Danesh, and Z. Hu, "CKD stimulates muscle protein loss via Rho-associated protein kinase 1 activation," *Journal of the American Society of Nephrology*, vol. 27, no. 2, pp. 509–519, 2016.

[2] P. T. Reidy, M. S. Borack, M. M. Markofski et al., "Post-absorptive muscle protein turnover affects resistance training hypertrophy," *European Journal of Applied Physiology*, vol. 117, no. 5, pp. 853–866, 2017.

[3] L. Williams, "Job satisfaction and organizational commitment as predictors of organizational citizenship behavior and in-role behavior," *Journal of Management*, vol. 17, no. 3, pp. 601–617, 1991.

[4] B. J. Holliday, J. R. Farrell, C. A. Mirkin, K. C. Lam, and A. L. Rheingold, "Metal-directed assembly of triple-layered fluorescent metallocyclophanes," *Journal of the American Chemical Society*, vol. 121, no. 26, pp. 6316-6317, 1999.

[5] Y. Ren, Y. Shi, K. Zhang, Z. Chen, and Z. Yan, "Medical treatment migration prediction based on GCN via medical insurance data," *IEEE Journal of Biomedical and Health Informatics*, vol. 24, no. 9, pp. 2516–2522, 2020.

[6] B. T. Wall, M. L. Dirks, T. Snijders, J. W. V. Dijk, and L. J. C. V. Loon, "Short-term muscle disuse lowers myofibrillar protein synthesis rates and induces anabolic resistance to protein ingestion," *American journal of Physiology Endocrinology & Metabolism*, vol. 310, no. 2, 2016.

[7] S. M. Pasiakos, C. E. Berryman, C. T. Carrigan, A. J. Young, and J. W. Carbone, "Muscle protein turnover and the molecular regulation of muscle mass during hypoxia," *Medicine & Science in Sports & Exercise*, vol. 49, no. 7, pp. 1340–1350, 2017.

[8] L. Henneberger, K. U. Goss, and S. Endo, "Partitioning of organic ions to muscle protein: experimental data, modeling, and implications for in vivo distribution of organic ions," *Environmental ence & Technology*, vol. 50, no. 13, pp. 7029–7036, 2016.

[9] R. Zhang, R. Zhou, W. Pan et al., "Salting-in effect on muscle protein extracted from giant squid (Dosidicus gigas)," *Food Chemistry*, vol. 215, pp. 256–262, 2017.

[10] V. V. Stephan, B. Joseph, M. Isabel, S. Sarah, and B. Nicholas, "Achieving optimal post-exercise muscle protein remodeling in physically active adults through whole food consumption," *Nutrients*, vol. 10, no. 2, p. 224, 2018.

[11] G. Garibotto, A. Sofia, E. L. Parodi, F. Ansaldo, and D. Verzola, "Effects of low-protein, and supplemented very low–protein diets, on muscle protein turnover in patients with CKD," *kidney international reports*, vol. 3, no. 3, pp. 701–710, 2018.

[12] R. Venkatesan, "Intelligent smart dustbin system using internet of things (IoT) for health care," *Journal of Cognitive Human-Computer Interaction*, vol. 1, no. 2, pp. 73–80, 2021.

[13] Z. Jiang, H. Ueda, M. Kitahara, and H. Imaki, "Bark stripping by sika deer on veitch fir related to stand age, bark nutrition, and season in northern Mount Fuji district, Central Japan," *Journal of Forest Research*, vol. 10, no. 5, pp. 359–365, 2017.

[14] C. Kim, H. Huang, Z. Nan, C. C. Lerro, and Y. Zhang, "Use of dietary vitamin supplements and risk of thyroid cancer: a population-based case-control study in Connecticut," *International Journal for Vitamin & Nutrition Research*, vol. 86, no. 3-4, pp. 1–9, 2017.

[15] S. David, K. M. Sagayam, and A. A. Elngar, "Parasitic overview on different key management schemes for protection of Patients Health Records," *Journal of Cybersecurity and Information Management*, vol. 6, no. 2, pp. 96–100, 2020.

[16] M. Ruz, J. Codoceo, J. Inostroza, A. Rebolledo, and K. M. Hambidge, "Zinc absorption from a micronutrient-fortified dried cow's milk used in the Chilean national complementary food program," *Nutrition Research*, vol. 25, no. 12, pp. 1043–1048, 2017.

[17] P. Pinstrupandersen, "Improving human nutrition through agricultural research: overview and objectives," *Food & Nutrition Bulletin*, vol. 21, no. 4, pp. 352–355, 2017.

[18] C. Dubois, M. Tharrey, and N. Darmon, "Identifying foods with good nutritional quality and price for the opticourses intervention research project," *Public Health Nutrition*, vol. 20, no. 17, pp. 3051–3059, 2017.

[19] C. Dubé, C. Aguer, K. Adamo, and S. Bainbridge, "A role for maternally derived myokines to optimize placental function and fetal growth across gestation," *Applied Physiology Nutrition and Metabolism*, vol. 42, no. 5, pp. 459–469, 2017.

[20] P. K. Shukla and P. K. Shukla, "Patient health monitoring using feed forward neural network with cloud based internet of things," *Journal of Intelligent Systems and Internet of Things*, no. 2, pp. 65–77, 2019.

Hindawi
Wireless Communications and Mobile Computing
Volume 2022, Article ID 7876013, 10 pages
https://doi.org/10.1155/2022/7876013

Research Article

Prediction of Building Energy Consumption Based on BP Neural Network

Hailing Sun

School of Architecture and Civil Engineering, West Anhui University, Lu'an 237012, China

Correspondence should be addressed to Hailing Sun; 05000060@wxc.edu.cn

Received 10 February 2022; Revised 28 March 2022; Accepted 13 April 2022; Published 16 May 2022

Academic Editor: Mohamed Elhoseny

In order to solve the energy consumption hypothesis of large buildings, the energy consumption hypothesis based on the BP neural network is proposed. First, to study the system of statistical index of building energy consumption and the system of statistical reporting of energy consumption of civil construction. In addition, to establish reliable consumer authority control to ensure the security and management of the database. Second, based on an analysis of the mechanism by which the BP neural network operates, this article optimizes it and describes the structure of the neural network, which includes the number of network layers, the number of neurons in each layer, and the number of latent neuron layers. hidden neuron layers and hidden neurons. The maximum value method is used to normalize the input sample data; finally, the learning and training process of neural network is determined. Based on BP neural network theory, the energy consumption statistics platform and prediction system are established by using Delphi 6.0. These include functional modules such as basic building information management, building energy consumption information management, building energy consumption summary, energy presampling information management, and building energy consumption forecast; the collection of building energy consumption data is mainly completed by intelligent energy consumption monitoring sensor network system. Finally, the city's building energy consumption information system conducts construction energy audits and analyzes the potential for energy savings. The results show that the hypothesis model determined by the BP neural network algorithm has an average error of 10.6% in predicting the construction energy consumption data, which is better than Matlab's predicted result and the mean error is 12.6%. From this, it can be seen that the BP neural network algorithm can provide better predictions of building energy consumption.

1. Introduction

Energy is the capital of human existence. As the world economy continues to grow, energy issues are becoming more acute in various countries, and energy conservation is a constant topic of discussion around the world. As one of the three largest consumers of social energy, energy consumption in the construction sector accounts for about one-third of society's total energy consumption and is expected to grow steadily. As China's economy grows and urbanization progresses, energy consumption is increasing day by day, and China's energy consumption is a very important part of the world [1]. Relevant data show that energy consumption in the construction sector still accounts for about 1/5 of total social energy consumption, which is significantly lower than in 30-40% of developed countries, but per capita heat consumption does not matter per building area. Energy consumption in construction is one of the most important strategies for the sustainable development of society, as energy consumption in the construction sector is a heavy burden limiting long-term rapid economic growth [2]. As an important index to judge whether the building has low energy consumption, whether the building energy consumption data is objective and comprehensive is very important to the realization of its energy-saving design. Therefore, to achieve real building energy conservation, we need to start from the actual energy consumption data, not simply pursue how many energy-saving technologies are used, but need to

speak with data and scientifically evaluate building energy consumption. The main part of building energy consumption is the use of building energy, such as building heating, ventilation, air conditioning, lighting, household appliances, transportation, energy, cooking, water supply, drainage, and hot water supply. use. At present, China's construction energy consumption accounts for about a quarter of society's total energy consumption. iar reduction. Building energy efficiency is a difficult task, saving 1.1,100 million tons of standard coal energy and reducing emissions. Although China has adopted energy-saving design standards for residential and public buildings, and the energy-efficient work of new buildings has achieved remarkable results, the potential for high-energy construction remains huge [3, 4].

In addition to the influence of its own thermal parameters, the energy consumption level of buildings is closely related to the performance of equipment, operation mode, management level, and energy-saving quality of managers and users. The results of energy consumption statistics give us only a general understanding, and we need to audit the building energy consumption. Energy audit is a process of finding energy efficiency and energy-saving potential through building energy consumption statistics. Some studies have shown that building energy audit without cost or low cost can achieve 6%~30% energy-saving effect. Countries have been successful in establishing a database of energy consumption in construction and have successfully promoted the development of energy efficiency in construction, so China is conducting research to establish a database of energy consumption statistics and establishing energy consumption databases, an effective tool for sorting and analyzing building energy consumption. plays an important role. The building energy audit survey opens up the possibility of building energy savings, which lays the foundation for the implementation of building energy consumption quotas and the establishment of an energy consumption monitoring platform. Estimates of energy consumption of existing buildings can be used for comparative analysis and optimization of building energy consumption schemes for energy-efficient renovations, and can also be used in the design stage to guide whether the actual energy consumption of buildings can achieve the expected purpose after completion, which has important practical significance [5, 6]. Figure 1 shows a zero energy consumption building. This paper proposes a hypothesis of energy consumption in buildings based on the BP neural network. Based on the analysis of the mechanism of action of the BP neural network, optimize it and determine the number of network layers, the number of neurons in each layer, the number of latent neuron layers, and the structure of the neural network. hidden neuron layers and hidden neurons. the maximum value method is used to normalize the input sample data; finally, the learning and training process of neural network is determined. Based on BP neural network theory, using Delphi 6.0 establishes energy consumption statistics platform and prediction system. These include functional modules such as basic building information management, building energy consumption information management, building energy consumption summary, energy presampling information management, and building energy consumption forecast. Finally, the effectiveness of the information system in improving data processing speed, assisting building energy audit, and predicting building energy consumption by BP neural network algorithm is verified by experiments.

2. Related Works

The formulation of energy-saving policies and regulations lacks relevant data guidance; therefore, it is important to find effective models and methods to predict energy consumption. So far, researchers have proposed many effective methods; commonly used are regression analysis, wavelet analysis, and neural network [7]. Yu, W. and others in order to "systematically identify the realities of the process of building energy consumption, creating a heating environment, and saving energy," a study was conducted covering the northern heating zone and various buildings in the middle and lower parts. The Yangtze River aims to understand the relationship between the city's heating environment and building energy efficiency, and to improve energy consumption and building energy-saving policies and plans. This study provides data on energy consumption per unit area of the surveyed city, which provides a solid basis for the development of building energy-saving regulations and policies, and is the first large-scale study of building energy consumption [8]. Wang, Y. and others studied how to use artificial neural network to simulate complex building information system and realize the prediction of energy consumption [9]. Zou, X. and others used artificial neural network instead of time series method, combined artificial neural network and evolutionary algorithm to predict power consumption, and achieved good results [10]. Zhang, Y. and others used artificial neural network to analyze and train the lighting energy consumption of an office building for three consecutive months, and used the trained network to predict the lighting energy consumption of the building [11]. Tao, F. and others combined genetic algorithm and neural network algorithm to construct the prediction model of iron and steel enterprises. It is concluded that the composite model is better than the pure BP network in prediction accuracy and training speed [12]. Wang, W. and others proposed a method of building energy consumption prediction using improved gray model. Based on the traditional gray prediction, this method performs triangular transformation on the existing building energy consumption data [13]. Referring to the meteorological parameters of a city, Liu, C. Y. and others predicted the hourly cooling load of an office building for six consecutive months by using artificial neural network, and the results are very close to those calculated by dynamic simulation method [14]. Xu, H. and others constructed the domestic energy consumption prediction system of civil buildings in Chongqing by using the gray neural network system model, and obtained good results [15]. Deng, Z. and others investigated the current situation of building energy consumption of a large and medium-sized shopping mall, analyzed the characteristics and composition of energy consumption, compared it with the energy consumption of other regions, and analyzed and

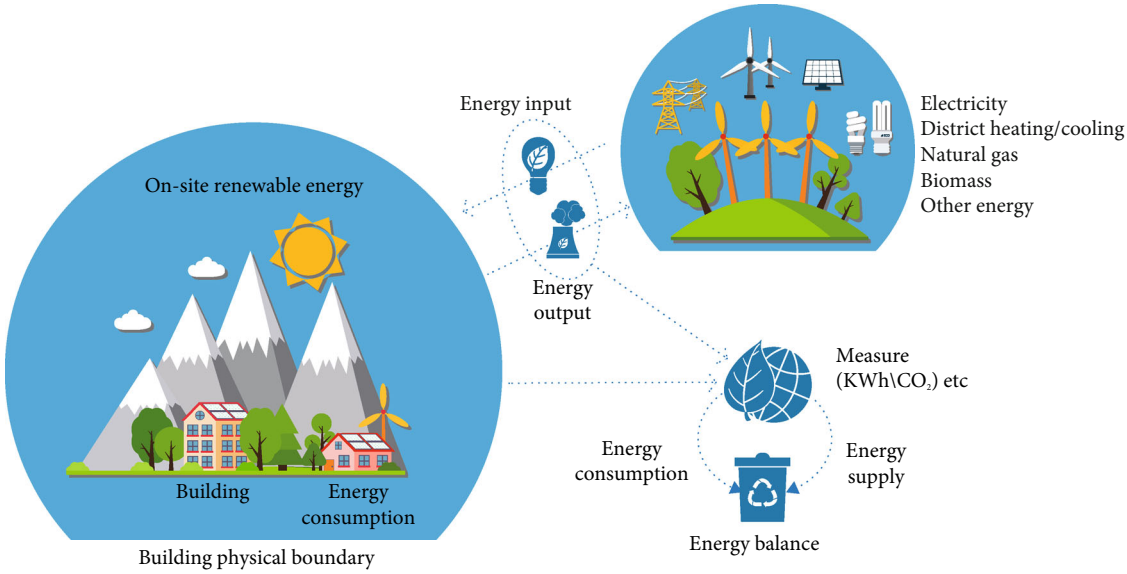

Figure 1: Zero energy consumption building.

evaluated the building energy consumption of shopping mall based on the survey data [16]. Zhang, L. and others building energy consumption database was established, using a spreadsheet to store basic building data and energy consumption data, and MATLAB's own toolbox to predict the energy consumption of buildings and units per building. There are clear differences in the accuracy of the predictions in the energy consumption parameters [17].

3. Research Methods

3.1. Building Energy Consumption Prediction Model

3.1.1. BP Neural Network. Artificial neuron simply and abstractly describes the information transmission process of biological neurons. It is the smallest unit for neural network to control and process information [18]. Many artificial neurons with simple functions are associated through the topological structure to form a neural network. The signal transmission between them realizes the information processing of the neural network, and the repeated correction and adjustment of the connection weight completes the training and learning process of the neural network [19]. Figure 2 shows the simple structure of an artificial neuron model.

It can be seen from Figure 2 that $x_1, x_2, \cdots, x_n$ corresponds to multiple input signals of artificial neurons, but there is only one output signal Y, so the corresponding relationship between $x_1, x_2, \cdots, x_n$ and y can be shown by formula (1):

$$\begin{cases} I = \sum_{j=1}^{n} w_j x_j + \theta \\ y = f(I) \end{cases}. \tag{1}$$

The signal transmission of artificial neurons is simulated by the input signal $x_j (j = 1, 2, \cdots, n)$, the synaptic weight w_j representing the connection strength between neurons, the internal threshold of WJ, the transfer function $f(x)$ simulating the transfer characteristics of biological neurons, and the output signal y. We can customize the transfer function as our desired function, such as log and e^x square root. We can also choose common transfer functions, such as linear transfer function, threshold function, and hyperbolic tangent function. Sometimes, for convenience of expression, $-\theta$ in equation (1) is also regarded as the weight of input x_0. x_0 is equal to 1. The sum of this style (1) can be expressed as equation (2):

$$I = \sum_{j=0}^{n} w_j x_j, \tag{2}$$

where $w_0 = -\theta, x_0 = 1$.

The BP neural network is currently the most widely used neural network, and the transmission function of BP neurons is a nonlinear function. By inserting a known training sample, the first layer calculates the output of each neuron backwards, then the last layer calculates the weight and threshold forward by entering the established network structure, the previous iteration weight, and the threshold. Thus changing the weight and threshold. This is repeated until it merges [20, 21]. The traditional BP algorithm is based on a gradient reduction method, and the merger rate is usually slow. The basic reasons are: the error surface is very flat or steep in the weight space, and the adjustment of the weight will be very small or large, resulting in little or excessive error adjustment effect; the adjustment of the weight of the gradient algorithm may point away from the wrong direction of the gradient algorithm. The main idea of back propagation network (BP network for short) is to transmit the signal forward and the error backward, so as to continuously adjust the weight and threshold of each layer of the network

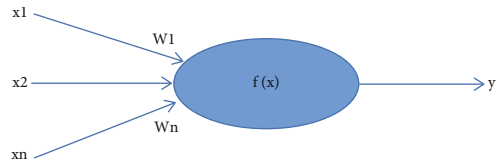

Figure 2: Neuron structure model.

[22]. BP network has the ability of global approximation, and the hidden layer is set so that it can arbitrarily approximate complex nonlinear problems. The BP neural network training process uses gradient search to reduce error step by step, and the transfer function selects a continuous derivative Sigmoid function as shown in Equation (3).

$$f(x) = \frac{1}{1 + \exp(-x)}. \tag{3}$$

If the characteristics of the identified model change in a positive and negative interval, the transfer function of the network can choose hyperbolic function, that is, symmetrical Sigmoid function, see equation (4):

$$f(x) = \text{than}(x) = \frac{1 - \exp(-x)}{1 + \exp(-x)}. \tag{4}$$

3.1.2. BP Neural Network Prediction of Building Energy Consumption. There is a fine nonlinear relationship between energy consumption data and energy consumption impact factor information, which is difficult to be described intuitively and clearly. The neural network algorithm is able to find the hidden relationship between the parameters by studying and training the sample data without knowing in advance the relationship between the sample inputs and outputs, thus determining the mapping between the sample inputs and outputs.

The input vector of the network is equation (5):

$$X = \begin{bmatrix} X_{11} & X_{12} & \cdots & X_{18} \\ X_{21} & X_{22} & \cdots & X_{28} \\ \vdots & \vdots & \vdots & \vdots \\ X_{n1} & X_{n2} & \vdots & X_{n8} \end{bmatrix}. \tag{5}$$

The output vector of the network is equation (6):

$$Y[y_1, y_2, \cdots y_n]^T \tag{6}$$

Among them, X_{ij} represents each influence factor of building energy consumption, $i = 1, 2, \cdots, n$, $j = 1, 2, \cdots, 8$, a line represents a sample, and N represents the number of input samples.

A large number of studies show that in the process of network training, as long as there is a hidden layer, the network can approximate a function arbitrarily. In order to make the network structure as simple and compact as possible, the proposed building energy consumption forecasting model in this document is defined as a three-layer network structure with only one hidden layer. Therefore, the network topology of the building energy consumption training model is shown in Figure 3.

BP network model can be used not only for classification but also for linear approximation. When performing classification processing, the transfer function of the output layer generally selects binary type, such as Sigmoid function. The prediction of building energy consumption is to use the network model to approximately simulate the relationship between energy consumption influence factors and energy consumption values, which belongs to linear approximation. Therefore, the output layer transfer function chooses the linear function. In this paper, the Sigmoid function is selected as an intermediate layer transfer function, and the training strategy is a gradient reduction method [23].

The determination of the number of neurons in the hidden layer is a very important and difficult problem. So far, no scientific method has been found in theory. It is often determined by step-by-step experiments using empirical formulas. If the number of selected hidden layer nodes is too small, network prediction errors will increase, training time will increase, and it will not be possible to accurately represent the corresponding relationship between network inputs and outputs; if the number of hidden layer nodes is too large. There are many factors that affect the number of latent neurons, such as the number of neurons in the input layer, the number of neurons in the output layer, the nature of the data sample, the nature of the transmission functions, and the complexity of the problem to be solved. In this paper, formula (7) is used to select the optimal number of neurons in the latent layer by step-by-step trial and error.

$$b < \sqrt{(m + n)} + a. \tag{7}$$

Of these, a is the constant in the interval [0,10], m is the number of neurons in the input layer, the number of neurons in the output layer, and b is the number of neurons in the latent layer. In this paper,m =8,n =1, and see Table 1 for the results of trial and error.

The above trial and error results represent different network prediction errors caused by the number of neurons in the hidden layer being controlled within the range of [3, 13]. From the data in Table 1, it can be seen that the relative error rate of network prediction will show a trend of first decreasing and then increasing with the increase of the number of neurons in a general range of the number of neurons in the hidden layer. Therefore, the number of neurons in the hidden layer of this paper is determined to be 8 [24].

When selecting the learning rate η of the network, we should consider the stability of the training process. If the selected η is too small, the network training time will be prolonged, the convergence speed will be too slow, and η is too large. In the process of weight adjustment, the change of network connection weight will be too large. Sometimes, the weight may exceed the set error minimum and the algorithm will not converge. Therefore, in order to ensure the stability

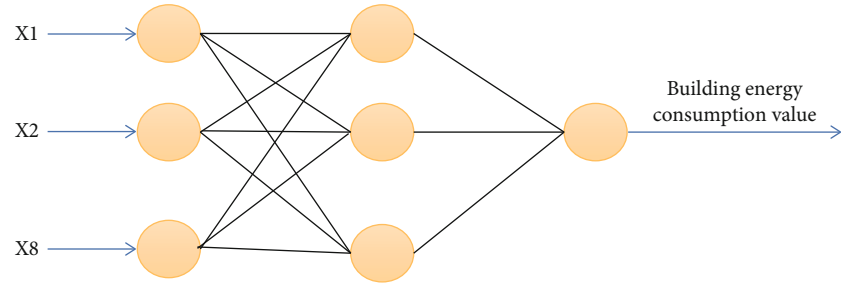

Figure 3: Schematic diagram of building energy consumption network model.

Table 1: The trial and error results that the number of neurons in the hidden layer is controlled within the range of [3, 13].

Number of neurons	Error%	Number of neurons	Error%
3	13.66	8	12.74
4	14.65	9	14.36
5	16.06	10	14.15
6	12.88	11	15.57
7	11.18	12	16.03
8	9.25	—	—

of the system, a smaller value is generally selected as the learning rate, which is usually controlled within the interval of [0.01,0.7]. η selected in this paper is 0.1. There is no rule to follow and no rule to determine the error value of the network. It can be set randomly and determined through continuous testing. In this paper, the maximum training time of the network is 1500, and the network training error target is 0.001. Figure 4 shows the network design training process defined by the building energy consumption sample data.

The following method is used for normalization. In order to avoid the occurrence of 0, a constant a is added to ensure the data volume of the input sample (Equation (8)).

$$y = (x - \min x + a)/(\max x - \min x + a). \tag{8}$$

Using the outputs of each node in the latent layer and the output of each nerve node in the output layer, Equations (9) and (10) are:

$$O_j = f\left(\sum_{i=1}^{n} \omega_{ij} x_i + \theta_j\right), \tag{9}$$

$$Y_k = f\left(\sum_{j=1}^{l} O_j \sigma_{jk} + d_k\right). \tag{10}$$

Using hidden layer error and output layer error, equation (11) is:

$$\delta_j = f'\left(\sum_{i=1}^{n} \omega_{ij} x_i + \theta_j\right) \cdot \sum_k \delta_k \omega_{jk} 及 \delta_k = (H_k - Y_k) \cdot f'\left(\sum_{j=1}^{l} O_j \omega_{jk} + d_k\right). \tag{11}$$

Always adjust the weight. If the global error of network training E is less than the initial minimum error target or the number of learning periods exceeds the initial maximum set R, the algorithm will stop and the algorithm will end [21].

3.2. Building Energy Consumption Statistics and Prediction System

3.2.1. Overall Objective of the System. The hierarchy of building energy consumption is shown in Figure 5:

The energy consumption of the envelope structure has been completed at the design stage. The energy consumption of the envelope structure will not change much after the construction is completed [25, 26]. The power consumption of the equipment will be determined by equipment parameters and equipment maintenance. During the operation of the equipment. Power consumption, system power consumption means the power consumption determined by the system error correction, automatic control, control system design and adjustment, control power consumption normal operation and maintenance. on buildings and consumer energy consumption behavior. Effective management and ways to implement energy consumption, which are determined by improving energy efficiency and improving energy efficiency. The system is divided into six functional modules, as follows:

(1) Comprehensive operation of basic building information, which can be searched according to one or more keywords in building number, building name, building age, and area, so as to carry out accurate retrieval and fuzzy retrieval; you can also enter, modify, and delete data

(2) Comprehensive retrieval of building energy consumption prediction sample data, retrieval according to building number, and data entry, modification, and deletion

(3) Dynamic statistics of building energy consumption data, dynamic statistics of building energy consumption information according to keywords such as month, year, region, and energy type, and produce real-time results. The data results are displayed in various histogram forms

(4) The comprehensive management of the sample data of building energy consumption prediction includes data entry, modification, and division according to

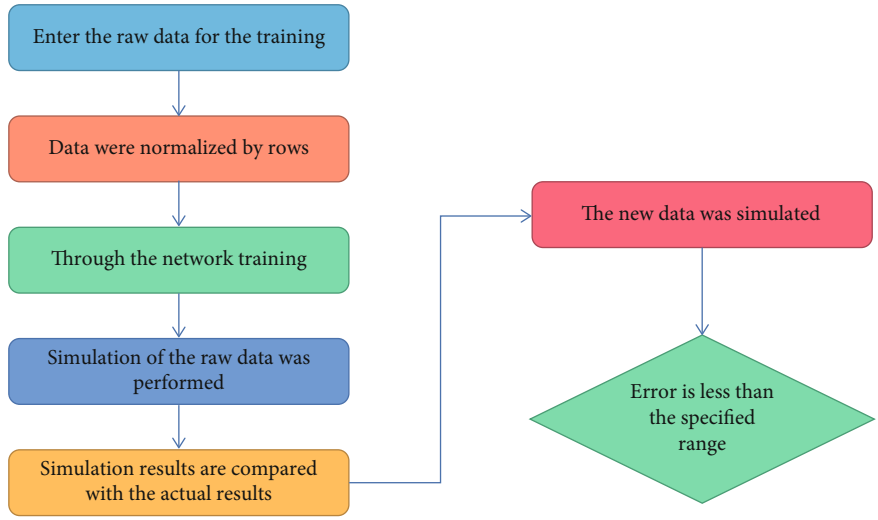

Figure 4: BP neural network flow chart.

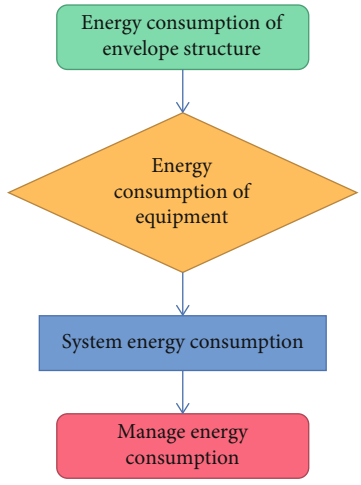

Figure 5: Hierarchy of building energy consumption.

the keyword retrieval. If necessary, it can be imported into the basic information data sheet of building energy consumption

(5) The prediction of future building energy consumption adopts the neural network algorithm. Through the existing energy consumption data in the database, the network can learn and train, find the general law to predict the future energy consumption trend, and provide basis and guidance for the analysis of energy-saving potential

(6) User management, the system creates users according to needs and saves them in the database. Every time a user logs in, they will be authenticated through the database; otherwise, they will not be able to enter the system. The system can dynamically manage user permissions

By using statistical software for historical energy consumption of buildings, it is possible to analyze the energy consumption of buildings in a timely manner, understand the situation of future energy consumption, and develop construction energy saving by forecasting future energy consumption.

3.2.2. Design Principles of Prediction System. This system is used by energy consumption statisticians to perform statistical analysis of data and perform energy consumption forecasts after receiving information in order to implement construction energy-saving work and guide energy consumption decisions in the next stage.

(1) *Accuracy*: the system ensures the accuracy and accuracy of data entry, statistics, and calculation and test results, and provides correct reference materials for relevant personnel

(2) *Reliability*: the system must execute specified functions and instructions without failure within a certain time and under certain conditions. Therefore, the system has been tested for a long time to ensure reliability

(3) *Security*: the information obtained from energy consumption statistics is related to the privacy of residents, companies, and enterprises. In addition, these data must provide an important basis for future scientific decision-making. The system must adopt effective security and confidentiality measures to control the access rights of data information, so as to ensure that the data will not be leaked and tampered with

(4) *Expandability*: the system function module should be expandable. With the change of demand, the system function can be expanded accordingly. The framework of building energy consumption statistical prediction system established in this paper is shown in Figure 6

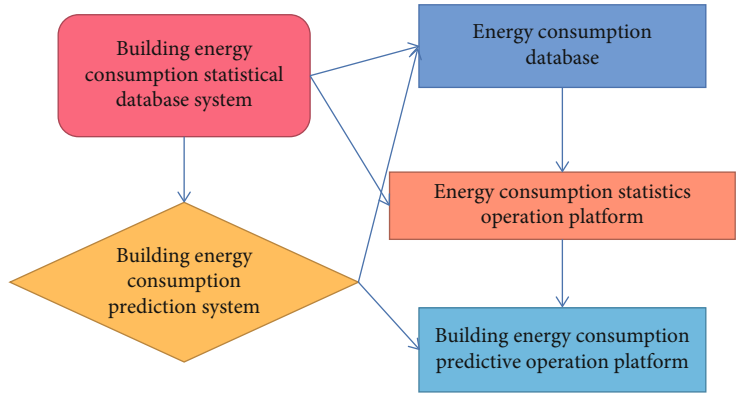

Figure 6: Schematic diagram of building energy consumption system framework.

Table 2: The expected input of forecast 1 adopts the sample data of the annual power consumption index of air conditioners and the forecast error.

	1	2	3	4	5	6	7	8	9
Average heat transfer coefficient of wall	1.51	1.51	1.51	1.54	1.55	1.51	1.51	1.51	1.62
Average thermal inertia index of wall	3.23	3.23	3.21	3.21	3.21	3.23	3.23	3.23	3.27
Roof heat transfer coefficient	0.65	0.65	0.7	0.65	0.65	0.65	0.65	0.65	0.63
Solar radiation absorption coefficient of exterior wall	0.4	0.4	0.4	0.4	0.4	0.4	0.4	0.4	0.64
Window shading coefficient	0.6	0.66	0.7	0.7	0.68	0.66	0.7	0.7	0.45
Comprehensive shading coefficient	0.7	0.68	0.7	0.7	0.68	0.68	0.67	0.7	0.46
Annual power consumption index of air conditioner	58.34	58.4	57.82	65.5	58.1	58.4	63.37	64.83	59.22
Estimate	58.05	58.80	58.14	63.60	58.30	58.81	64.81	64.67	57.15
Error (%)	0.70	0.36	0.28	3.03	0.01	0.38	0.68	1.41	3.10

Table 3: Using MATLAB to predict the second sample, the annual building energy consumption per unit area, and the predicted value.

	1	2	3	4	5	6	7	8	9
Average heat transfer coefficient of wall	1.51	1.51	1.51	1.53	1.55	1.51	1.51	1.51	1.62
Average thermal inertia index of wall	3.23	3.23	3.23	3.21	3.21	3.23	3.23	3.23	3.17
Roof heat transfer coefficient	0.65	0.65	0.70	0.65	0.65	0.65	0.65	0.65	0.63
Solar radiation absorption coefficient of exterior wall	0.4	0.4	0.4	0.4	0.4	0.4	0.4	0.4	0.64
Window shading coefficient	0.6	0.68	0.7	0.7	0.68	0.68	0.7	0.7	0.5
Comprehensive shading coefficient	0.7	0.68	0.7	0.7	0.68	0.68	0.67	0.7	0.0.46
Annual energy consumption per unit building area	8.45	11.30	11.32	11.62	8.51	6.67	10.80	9.58	10.73
Estimate	7.82	9.7	10.60	11.11	9.47	9.65	10.64	11.04	4.81

3.3. Metrics for Evaluating the Regression Model

3.3.1. Mean Squared Error. Mean square error (MSE) is defined as formula (11):

$$\mathrm{MSE} = \frac{1}{n}\sum_{i=1}^{n}(y_i - \hat{y}_i)^2, \in[0,+\infty). \tag{12}$$

3.3.2. Root Mean Square Error. Root mean square error (RMSE) is a typical indicator of the regression model, used to indicate how much error the model will produce in the prediction, with higher weight for larger errors, as shown in formula (13):

$$\mathrm{RMSE} = \sqrt{\frac{1}{n}\sum_{i=1}^{n}(y_i - \hat{y}_i)^2}, \in[0,+\infty), \tag{13}$$

where y is the actual value and $\hat{y}$ is the predicted value; the smaller the RMSE, the better.

4. Result Discussion

4.1. Prediction and Analysis Using MATLAB. The first mock exam is carried out in Matlab (the prediction model of

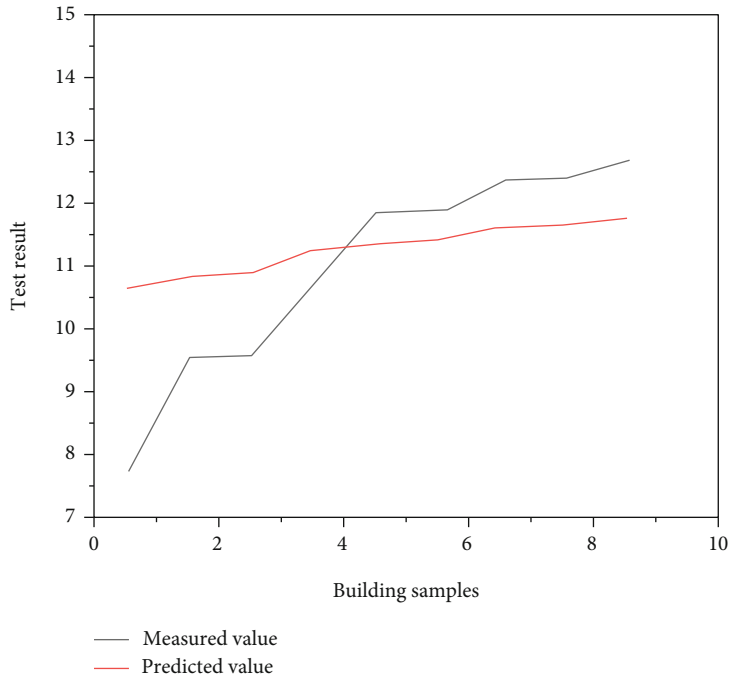

Figure 7: Broken line diagram of predicted value and measured value.

Matlab's self-contained neural network toolbox adopts BP neural network algorithm). The transmission function of neurons in the latent layer of the BP neural network and neurons in the output layer uses the tansig function and the logsig function. The training method adopts "momentum gradient descent back propagation algorithm," which has undergone inverse training), and the network structure and number of hidden neurons are determined. The first one is to use the consumption index of air conditioning year to be expected. The model is obtained by DeST simulation. This model adopts a standard model of residential energy consumption in the standard of energy-efficient design of apartment buildings with hot summers and warm winters, and uses the default values for other parameters. The expected input of prediction 2 adopts the measured value. The sample data and error values of each prediction are shown in Tables 2 and 3.

According to the table, the average error of prediction I is 1.70%. The closer the building parameter value is to the average value of all building parameters, the smaller the prediction error is. Also, if the number of neurons in the latent layer is 5, the error is minimal. The difference between predictions 2 and predictions 1 is based on envelope structural parameters that predict the actual energy consumption of a building. Due to the difficulty of obtaining accurate data on building energy consumption, the forecast includes 9 building samples. There are many human factors that affect energy consumption in predicting real energy consumption, which makes it difficult to predict, so it is necessary to improve the representation of the sample, increase the sample data, and cover it. Try to cover the entire variation range of each parameter. Prediction 2 is a preliminary study that predicts the actual energy consumption of a building based on building cladding parameters. When the number of neurons is 6, the prediction error is minimal.

Comparing the simulated value prediction with the actual value prediction, it is found that the error of predicting the annual energy consumption per unit building area is greater than that of the simulated value prediction, that is, the error of prediction 2 is greater than that of prediction 1. The prediction error of the number 6 of neurons in the optimal hidden layer of prediction 2 is 13.77%, and the prediction error of the prediction value 5 of the number of neurons in the optimal hidden layer of prediction 1 is 1.70%.

4.2. Building Energy Audit, Energy-Saving Potential Analysis, and Energy Consumption Forecast. The building samples in the prediction are 9 buildings, which are predicted by the prediction system in this paper. The prediction method is to use the data of the first eight buildings as the training samples to predict the ninth building, then add the data of the ninth building to the training sample set to replace the eighth building and predict the eighth building, then add the data of the eighth building into the sample set to replace the seventh building, and predict by analogy to obtain the sample and predicted value data table. Arrange the measured value and predicted value in the order from small to large, and then make a broken line diagram, as shown in Figure 7.

The following results can be obtained by analyzing the results:

(1) The test results are all within the range of the maximum and minimum values of the actual values

(2) The average error of the prediction results is 10.6%. According to the broken line chart of predicted value

and measured value, it can be found that the trend of predicted value and measured value is consistent. Although the error is relatively large, the predicted value reflects the change law of energy consumption index

(3) The variation range of the predicted value is obviously smaller than the measured value. In fact, it also proves from the opposite side that under the parameter bar of the sample data, the results of the measured value must be affected by other factors

(4) The magnitude of the error is inversely proportional to the mean of the expected values and is proportional to the difference between the maximum and minimum values of the expected values. The error is significantly higher than in the previous section. To explain this phenomenon, the error index W is defined here, which is determined by the difference between the maximum and minimum values of the desired value and the mean value. The value of the desired value. The formula is as follows (14):

$$W = (\max_{\text{desired value}} - \min_{\text{desired value}})/\text{ave}_{\text{desired value}}. \quad (14)$$

From the above, it can be seen that the higher the error index, the greater the error of the assumed value obtained, so the error of Assumption 3 is much greater than Assumption 1.

5. Conclusion

Energy consumption in the construction sector has always been high, and energy consumption in the construction sector is expected to increase rapidly due to the continuous development of the construction sector and the need to improve people's living conditions. It has become very important to work actively in the energy sector to save energy. It is important to analyze the energy consumption of existing buildings, dig, and create a model of energy consumption forecasts for new buildings to guide the energy consumption forecasts of new buildings during the architectural design phase. In this paper, a building energy consumption database is created by analyzing the building energy consumption statistical reporting system, the energy consumption statistical process, and the building energy consumption forecast index. The actual collection of building energy consumption data is generally completed by the intelligent energy consumption monitoring sensor network system, which can be entered into the database in real time. System prediction software uses neural network algorithms, i.e., neural network algorithms have achieved good results in many aspects of prediction. Using the hypothesis model established by the BP neural network algorithm, the mean error obtained from the hypotheses of the energy consumption data of a particular building is 10.6%, which is better than Matlab's predicted result, and the mean error is 12.6%. It can be seen that the BP neural network algorithm can achieve better results. It is a good result to predict the construction energy consumption. Firstly, the building energy consumption statistical index system and the civil building energy consumption statistical report system are researched, and a database is established based on SQL server 2000, including three major parts: building basic information, building energy consumption information, and building forecasting sample data. Secondly, on the basis of analyzing the working mechanism of BP neural network, this paper optimizes it and determines the neural network structure, including the number of network layers, the number of neurons in each layer, the number of hidden neuron layers, and the number of hidden neurons; the value method normalizes the input sample data and finally determines the learning and training process of the neural network. Finally, based on the statistical data of energy consumption in a city and the building energy consumption data in a city, the system conducts building energy audit and energy-saving potential analysis, and verifies that the information system can improve data processing speed and assist building energy audit and BP neural network algorithm to predict building energy consumption. This paper looks forward to:

(1) The advent of a software requires detailed and scientific testing by professionals. After the completion of the system, due to the limitation of conditions, the test work cannot be done in detail and comprehensively, and it needs to be improved continuously during the use process

(2) At present, the statistical investigation of building energy consumption has just started, and the use of energy consumption data is still in the exploratory stage. With the deepening of the research, the requirements for the functions of the building energy consumption statistical information management system will also increase. System functions need to be further improved.

(3) When BP neural network is used for prediction, if there are enough sample data, and the more comprehensive and accurate the data, the more accurate the prediction result will be. When verifying the prediction part of the system, there is a certain deviation in the prediction accuracy due to too little sample data. In future research, attention should be paid to obtaining better sample data

Data Availability

The data used to support the findings of this study are available from the corresponding author upon request.

Conflicts of Interest

The author declares no conflicts of interest.

Acknowledgments

This work was supported by Anhui Province Federation of Social Sciences Foundation (No.2021CX021) and

Department of Education Anhui Province Foundation (No.2019zyrc097).

References

[1] J. Zhao, C. Zhang, L. Min, N. Li, and Y. Wang, "Surface soil moisture in farmland using multi-source remote sensing data and feature selection with ga-bp neural network," *Nongye Gongcheng Xuebao/Transactions of the Chinese Society of Agricultural Engineering*, vol. 37, no. 11, pp. 112–120, 2021.

[2] Y. A. Du, "Research on the route pricing optimization model of the car-free carrier platform based on the bp neural network algorithm," *Complexity*, vol. 2021, no. 4, Article ID 8204214, 10 pages, 2021.

[3] J. Wang, Z. Zhao, Y. Liu, and Y. Guo, "Research on the role of influencing factors on hotel customer satisfaction based on bp neural network and text mining," *Information*, vol. 12, no. 3, pp. 99–103, 2021.

[4] B. Zhang, J. Liu, Y. Zhong, X. Li, and X. Wang, "A bp neural network method for grade classification of loose damage in semirigid pavement bases," *Advances in Civil Engineering*, vol. 2021, Article ID 6658235, 11 pages, 2021.

[5] Y. Xu, L. Gui, and T. Xie, "Intelligent recognition method of turning tool wear state based on information fusion technology and bp neural network," *Shock and Vibration*, vol. 2021, no. 8, Article ID 7610884, 10 pages, 2021.

[6] Y. Zhang, X. Xiong, X. Wu, Z. Song, and Z. Xue, "Optimization of sofc stack gas distribution structure based on bp neural network and cfd," *E3S Web of Conferences*, vol. 245, no. 7, pp. 03007–03010, 2021.

[7] L. Wu, L. Chen, and X. Hao, "Multi-sensor data fusion algorithm for indoor fire early warning based on bp neural network," *Information*, vol. 12, no. 2, article 03007, pp. 59–63, 2021.

[8] W. Yu, G. Guan, J. Li, Q. Wang, and C. Cui, "Claim amount forecasting and pricing of automobile insurance based on the bp neural network," *Complexity*, vol. 2021, Article ID 6616121, 17 pages, 2021.

[9] Y. Wang and P. Fu, "Integration performance statistics of green suppliers based on fuzzy mathematics and bp neural network," *Journal of Intelligent Fuzzy Systems*, vol. 40, no. 2, pp. 2083–2094, 2021.

[10] X. Zou, "Analysis of consumer online resale behavior measurement based on machine learning and bp neural network," *Journal of Intelligent Fuzzy Systems*, vol. 40, no. 2, pp. 2121–2132, 2021.

[11] Y. Zhang, D. Du, S. Shi, W. Li, and S. Wang, "Effects of the earthquake nonstationary characteristics on the structural dynamic response: base on the bp neural networks modified by the genetic algorithm," *Buildings*, vol. 11, no. 2, pp. 69–74, 2021.

[12] F. Tao, "Performance analysis of real estate management entities based on dea model and bp neural network model," *Journal of Physics Conference Series*, vol. 1744, no. 2, pp. 022025–022029, 2021.

[13] W. Wang, J. Feng, and F. Xu, "Estimating downward shortwave solar radiation on clear-sky days in heterogeneous surface using lm-bp neural network," *Energies*, vol. 14, no. 2, pp. 273–275, 2021.

[14] C. Y. Liu, Y. Wang, X. M. Hu, Y. L. Han, and L. Z. Du, "Application of ga-bp neural network optimized by grey verhulst model around settlement prediction of foundation pit," *Geofluids*, vol. 2021, Article ID 5595277, 16 pages, 2021.

[15] H. Xu, S. Li, S. Fan, M. Chen, and School of Information Science and Engineering, Shandong University, Qingdao 266237, China, "A new inconsistent context fusion algorithm based on bp neural network and modified dst," *Mathematical Biosciences and Engineering*, vol. 18, no. 2, pp. 968–982, 2021.

[16] Z. Deng, M. Yan, and X. Xiao, "An early risk warning of cross-border e-commerce using bp neural network," *Mobile Information Systems*, vol. 2021, no. 1, Article ID 5518424, 8 pages, 2021.

[17] L. Zhang and F. Liang, "Monitoring and analysis of athletes' local body movement status based on bp neural network," *Journal of Intelligent Fuzzy Systems*, vol. 40, no. 2, pp. 2325–2335, 2021.

[18] B. Fan and X. Xing, "Intelligent prediction method of building energy consumption based on deep learning," *Scientific Programming*, vol. 2021, Article ID 3323316, 9 pages, 2021.

[19] H. Cao, L. Liu, B. Wu, Y. Gao, and D. Qu, "Process optimization of high-speed dry milling UD-CF/PEEK laminates using GA- BP neural network," *Composites Part B Engineering*, vol. 221, no. 4, pp. 109034–109038, 2021.

[20] X. Liu and C. Tian, "Design and implementation of large-scale public building energy consumption monitoring platform based on BP neural network," *Security and Communication Networks*, vol. 2021, Article ID 6438909, 9 pages, 2021.

[21] S. S. Roy, R. Roy, and V. E. Balas, "Estimating heating load in buildings using multivariate adaptive regression splines, extreme learning machine, a hybrid model of MARS and ELM," *Renewable and Sustainable Energy Reviews*, vol. 82, pp. 4256–4268, 2018.

[22] Q. Zhang, Y. Guo, and Z. Y. Song, "Dynamic curve fitting and bp neural network with feature extraction for mobile specific emitter identification," *IEEE Access*, vol. 9, no. 99, pp. 33897–33910, 2021.

[23] H. Liu, J. Liu, Y. Wang, Y. Xia, and Z. Guo, "Identification of grouting compactness in bridge bellows based on the bp neural network," *Structure*, vol. 32, no. 5, pp. 817–826, 2021.

[24] J. Zhang, J. Zhang, Y. Zhang, and Y. C. Zhang, "Research on the combined prediction model of residential building energy consumption based on random forest and BP neural network," *Geofluids*, vol. 2021, Article ID 7271383, 12 pages, 2021.

[25] X. Li, Z. Zhang, D. Xu, C. Wu, and Y. Zheng, "A prediction method for animal-derived drug resistance trend using a grey-bp neural network combination model," *Antibiotics*, vol. 10, no. 6, pp. 692–696, 2021.

[26] A. Moradzadeh, B. Mohammadi-Ivatloo, M. Abapour, A. Anvari-Moghaddam, and S. S. Roy, "Heating and cooling loads forecasting for residential buildings based on hybrid machine learning applications: a comprehensive review and comparative analysis," *IEEE Access*, vol. 10, pp. 2196–2215, 2022.

Hindawi
Wireless Communications and Mobile Computing
Volume 2022, Article ID 7732989, 23 pages
https://doi.org/10.1155/2022/7732989

Research Article

A Metaheuristic Algorithm for Coverage Enhancement of Wireless Sensor Networks

Zhigang Wang,[1] **Liqin Tian**,[1,2] **Wenxing Wu**,[2] **Lianhai Lin**,[1] **Zongjin Li**,[1] **and Yinghua Tong**[1]

[1]*School of Computer, Qinghai Normal University, Xining 810000, China*
[2]*School of Computer, North China Institute of Science and Technology, Beijing 101601, China*

Correspondence should be addressed to Liqin Tian; tianliqin@ncist.edu.cn

Received 2 March 2022; Revised 16 April 2022; Accepted 26 April 2022; Published 12 May 2022

Academic Editor: Xiaohui Yuan

When wireless sensors are randomly deployed in natural environments such as ecological monitoring, military monitoring, and disaster monitoring, the initial position of sensors is generally formed through deployment methods such as air-drop, and then, the second deployment is carried out through the existing optimization methods, but these methods will still lead to serious coverage holes. In order to solve this problem, this paper proposes an algorithm to improve the coverage rate for wireless sensor networks based on an improved metaheuristic algorithm. The sensor deployment coverage model was firstly established, and the sensor network coverage problem was transformed into a high-dimensional multimodal function optimization problem. Secondly, the global searching ability and searching range of the algorithm are enhanced by the reverse expansion of the initial populations. Finally, the firefly principle is introduced to reduce the local binding force of sparrows and avoid the local optimization problem of the population in the search process. The experimental results showed that compared with ALO, GWO, BES, RK, and SSA algorithms, the EFSSA algorithm is better than other algorithms in benchmark function tests, especially in the test of high-dimensional multimodal function. In the tests of different monitoring ranges and number of nodes, the coverage of EFSSA algorithm is higher than other algorithms. The result can tell that EFSSA algorithm can effectively enhance the coverage of sensor deployment.

1. Introduction

In the field of sensor monitoring and communication engineering, the development of wireless sensor network (WSN) technology has become the main driving force of the Internet of Things (IoT) technology [1]. With the development of communication and software technology, sensor networks have become a hot spot in essential application fields such as monitoring the ecological environment [2], agricultural production [3], military battlefield [4], and disasters and accidents [5, 6]. Generally, the hardware equipment used for monitoring is composed of multiple sensors with clear functions, low energy, small shape, and portability. The hardware completes the deployment of wireless sensor networks through sensing and communication functions.

In recent years, many new technologies and methods have been adopted to improve the quality of service (QoS) in wireless sensor networks [7]. The coverage effect of the sensor monitoring area is an essential indicator of network quality of service [8], which can measure the perception ability of the sensor to be monitored area under different deployment structures. Usually, the number of sensors is limited and randomly placed in the target monitoring range, and the deployment of sensor nodes is uneven, resulting in the problem of coverage holes, which ultimately affects the network's quality of service. The optimal deployment of sensor nodes is the premise to ensure the data acquisition, transmission, processing, and reliable application of sensor networks. It is an enduring conundrum in sensor networks [9]. For sensor deployment, the main goal is to use limited sensor resources to cover the target area as evenly and widely

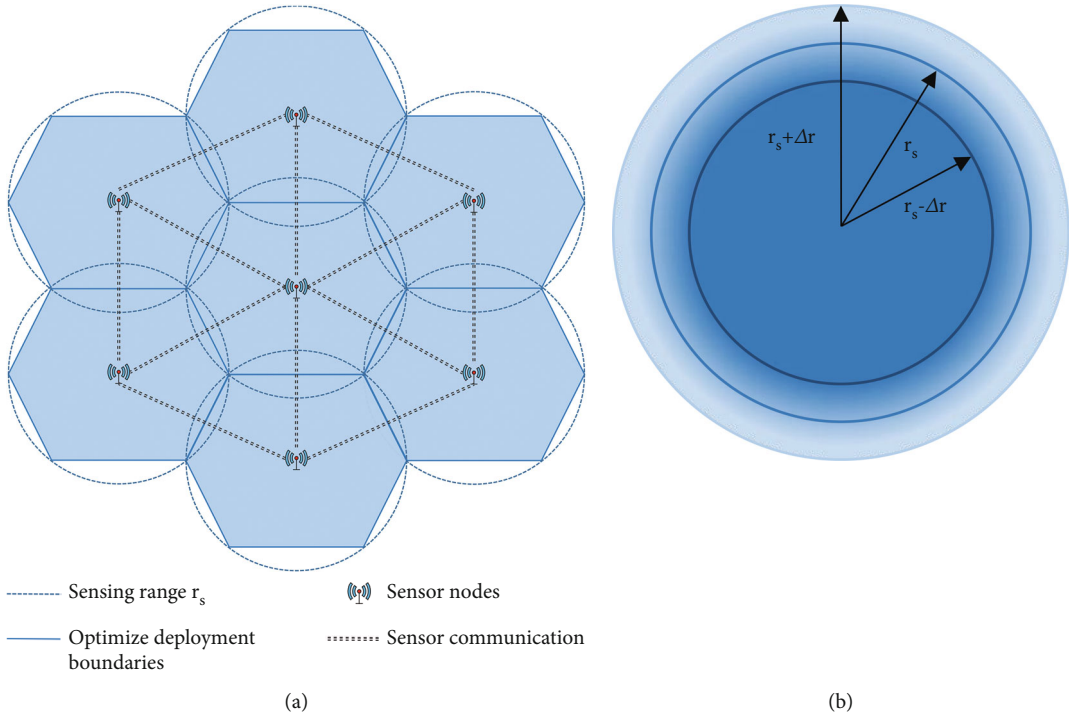

Figure 1: Deployment model. (a) Optimal deployment structure. (b) Probabilistic deployment structure.

/∗Initial the Sparrow Search Population∗/
The Number of Population: n
Maximum Iterations: $I_{\max}$
Initial Finder Number: F_{num}
Initial Detection and Early Warning Ratio: $DE_{\max}$
Initial Warning Value : 0.8
Firefly Parameter: $\alpha = 0.2, \beta_0 = 1, \gamma = 1$
/∗Iterative search∗/
while $(t < I_{\max})$
According to Equation (12) and (13), the elite reverse strategy is implemented for the initial population ($2n$ individuals);
Rank the individuals in the population according to fitness values;
Select the optimal n individuals as the first population;
for $i = 1 : F_{num}$
Based on the results of the last iteration of the finder, update the position according to Equation (8);
end for
for $i = F_{num} + 1 : n$
The position of the joiner is disturbed according to the Equation (10);
end for
for $i = 1 : DE_{\max}$
Based on the results of the last iteration of the detection and early warning, update the position according to equation (11) and (17);
end for
$t = t + 1$;
end while
return the best solution.

Algorithm 1: EFSSA.

as possible [10]. The coverage effect of the area to be monitored can be divided into point coverage, area coverage, and fence coverage [11]. WSN coverage in this paper is based on the method of point coverage. Most studies assume that the points to be monitored are evenly distributed in two-dimensional (2D) or three-dimensional (3D), and these areas are covered by a circular or spherical monitoring range centered on the sensor.

/∗**Initialization**∗/
Initialization EFSSA parameters are consistent with Algorithm 1
Set the number of sensor nodes d
Initialize the sensor node position s_i as population individuals
Set the sensor deployment scope(m^2):
900,2500,4900,8100
/∗**Iterative search**∗/
while ($t < I_{\max}$)
The elite reverse strategy is implemented for the initial sensor position array;
Rank the individuals in the population according to fitness values;
Select the optimal n individuals as the first population;
for $i = 1 : F_{num}$
Update the position of finder;
end for
for $i = F_{num} + 1 : n$
Update the position of joiner;
end for
for $i = 1 : DE_{\max}$
Update the detection and early warning with firefly strategy;
end for
Obtain the current sensor node deployment results by calculating node coverage in Equation (6);
If the new overlay mode is better than the last overlay result, update it;
$t = t + 1$;
end while
return Optimal WSNs deployment results.

Algorithm 2: WSNs deployment based on EFSSA.

The research on sensor deployment is mainly divided into two types: deterministic deployment and random deployment [12, 13]. First of all, the deployment method is primarily used under the conditions of a good geographical environment, such as plains, wheat fields, grasslands, and lakes. In [14], sensors are deployed using a regular lattice model that can be full of space, but the actual monitoring environment cannot be an ideal 2D or 3D space. The environment often has flat terrain and is easy to plan and deploy. Random deployment is mainly used when the sensor nodes are difficult to fix quickly or reach the designated position. The first deployment is formed in a complex or harsh natural environment by aircraft throwing [15]. Obviously, this kind of method will cause a large number of sensor coverage redundancy and coverage holes. It will seriously waste sensor network resources and damage the network's quality of service. In fixed deployment mode, when the sensor does not have mobility, mobile sink can be used to improve the energy consumption and delay of the network [16]. On the other hand, when the sensor is mobile, researchers use the method of moving sensors in a small range to adjust the deployment structure and realize the second deployment of sensors [17]. There are also studies on monitoring target points or target regions by moving sensor nodes with strong mobility [18, 19]. There are also studies that address the deployment reliability of sensors; reference [20] divides sensor coverage methods into centralized and distributed. Wireless sensors are costly to deploy and must be used to maximize coverage for resource-constrained problems [21, 22]. After random deployment of sensor nodes in different scenarios, it is difficult to immediately meet the requirements of network coverage, and it is a hot issue to use the limited mobility of sensors for secondary deployment. However, most methods cannot achieve the expected results, resulting in a waste of resources and energy.

In this paper, we propose a coverage enhancement method for wireless sensor networks based on improved metaheuristic algorithm, which can effectively improve the coverage performance of wireless sensor networks. The main contributions are as follows:

(1) The location model of the area to be monitored and the sensor location model has been established, and the sensor coverage problem was transformed into the solution model of intelligent optimization algorithm

(2) An initial solution construction method is proposed. The quality of the initial solution of the population iteration is improved by an inverse elite solution to further make the location distribution of the random sensors as uniform as possible

(3) According to the fluorescence effect in the firefly intelligent optimization algorithm, the population individual optimization method in order to improve the local binding force during the population iteration and prevent from falling into local optimization is improved

(4) In experimental simulations, on the one hand, a comparison with other metaheuristic algorithms for sensor coverage is made to demonstrate the advantage of the algorithm on high-dimensional

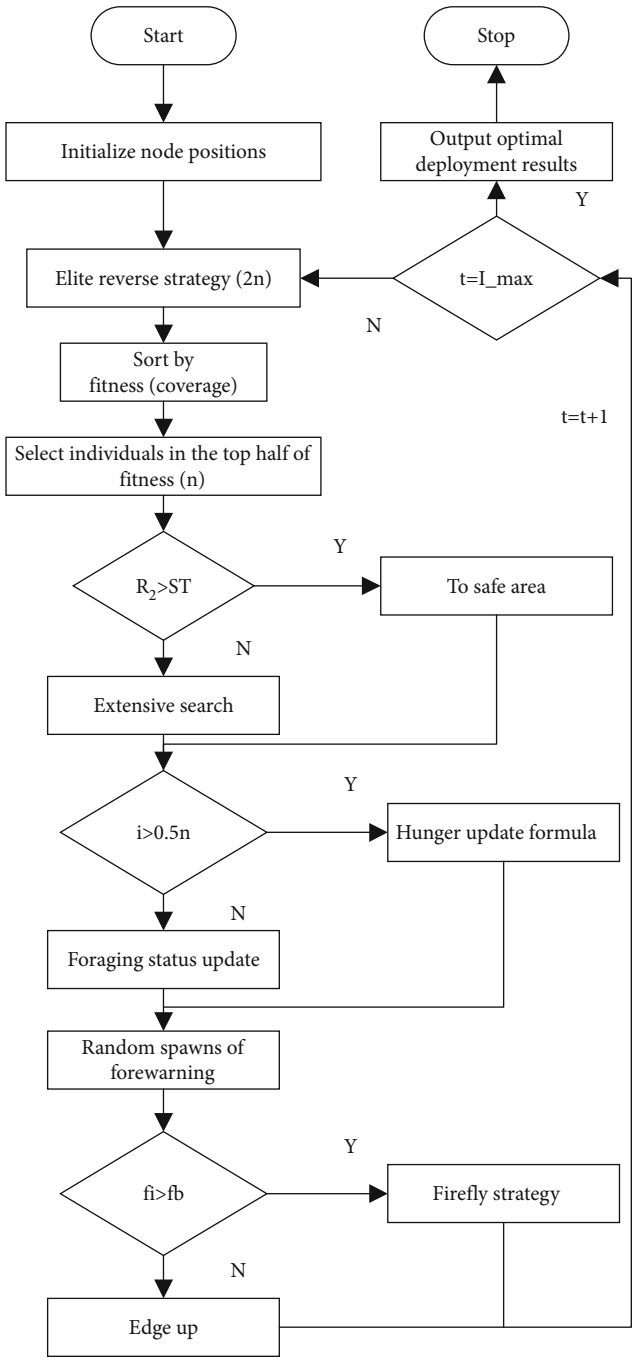

Figure 2: Flowchart for EFSSA wireless sensor network deployment.

multimodal reference functions. On the other hand, it verifies the advantages of deploying coverage in wireless sensor networks

The structure of this paper to enhance the WSN coverage is as follows: Section 2 introduces the current situation of coverage optimization at home and abroad. Section 3 introduces the coverage model in detail. Section 4 discusses the improved sparrow search algorithm. Section 5 presents the performance of the algorithm in the benchmark function and the effect in the application of sensor coverage and analyzes and discusses it. Section 6 gives conclusions and future prospects.

2. Related Work

The approximate solution of the metaheuristic optimization algorithm based on intelligent optimization has strong applicability in practical application compared with an accurate solution, especially in the research of sensor deployment optimization. Intelligent optimization algorithms have become the primary means of research in this direction.

In the deterministic deployment study, when there are few sensor nodes, a grid-based distributed sensor node deployment strategy was used in reference [23] to determine the location of deployed sensor nodes. Xu et al. [24] divided the monitoring area into multiple triangular grids to complete the coverage of the target by adjusting the distance relationship between the nodes and applied it to the underwater sensor network. In reference [25], on the basis of coverage, the connectivity between sensors is considered at the same time, which is able to keep the network connection even if some sensors fail. On the basis of guaranteeing sensor coverage and connectivity, some researchers in the literature [26, 27] further guarantee the connectivity and coverage of deterministic deployment networks by introducing relay nodes. Compared to random deployment, deterministic deployment was aimed at achieving target area coverage mainly with the minimum number of nodes and is closely related to the deployment space structure.

[28] proposed a metaheuristic algorithm based on ant-lion optimization (ALO) for sensor coverage and sensor sensing perception performance. This method transforms coverage into a function maximization problem, which can effectively and quickly achieve reliable deployment of wireless sensors, and proves that the deployment strategy of this algorithm outperforms sensor coverage by genetic algorithm (GA_WSN) and particle swarm optimization (PSO_WSN) algorithm for sensor deployment applications. Reference [29] proposed a sensor random deployment method based on grey wolf optimizer (GWO) to address the problem of low sensor coverage. Liao et al. [30] used the firefly swarm algorithm (FA) [31] to establish two detailed coverage models, central deployment and overlay deployment, for the sensor deployment coverage problem, and compared the coverage efficiency and mobility problems of these two models. These studies are based on the initial random deployment, so before considering the secondary deployment of sensors, the random nodes initially generated are close to the real scene, which is conducive to the implementation of the application. [32] not only generates scientific random deployment nodes of sensor nodes but also proposes the method of generating data packets, which has strong applicability in WSN performance imitation.

In terms of algorithm performance, although the intelligent optimization algorithm has strong optimization ability, few design parameters, and fast running speed, it still has some shortcomings. Compared with other traditional

Table 1: Reference function.

Name	Functions	d	Domain	$f_{\min}$
Sphere	$F_1(x) = \sum_{i=1}^{n} x_i^2$	30	[-100,100]	0
Schwefel-1	$F_2(x) = \sum_{i=1}^{n} \lvert x_i \rvert + \prod_{i=1}^{n} \lvert x_i \rvert$	30	[-10,10]	0
Schwefel-2	$F_3(x) = \sum_{i=1}^{n} \left(\sum_{j=1}^{n} \lvert x_i \rvert \right)^2$	30	[-100,100]	0
Tablet	$F_4(x) = \max \{ \lvert x_i \rvert, -1 \le i \le n \}$	30	[-100,100]	0
Rosenbrock	$F_5(x) = \sum_{i=1}^{n} \left[100 * \left(x_{i+1} - x_i^2 \right)^2 + (x_i - 1)^2 \right]$	30	[-30,30]	0
Step	$F_6(x) = \sum_{i=1}^{n} (\lvert x_i + 0.5 \rvert)^2$	30	[-100,100]	0
Quadric	$F_7(x) = \sum_{i=1}^{n} ix^4 + \text{random}[0, 1)$	30	[-1.28,1.28]	0
Schwefel	$F_8(x) = \sum_{i=1}^{n} -x_i \sin \left(\sqrt{\lvert x_i \rvert} \right)$	30	[-500,500]	0
Rastrigrin	$F_9(x) = \sum_{i=1}^{n} \left[x_i^2 - 10 \cos (2\pi x_i) + 10 \right]$	30	[-5.12,5.12]	0
Ackley	$F_{10}(x) = -20 \exp \left(-0.2 \sqrt{\frac{1}{n} \sum_{i=1}^{n} x_i^2} \right) - \exp \left(\frac{1}{n} \sum_{i=1}^{n} \cos(2\pi x_i) \right) + 20 + e$	30	[-32,32]	0
Griewank	$F_{11}(x) = \sum_{i=1}^{n} \frac{x_i^2}{4000} - \prod_{i=1}^{n} \cos \left(\frac{x_i}{\sqrt{i}} \right) + 1$	30	[-600,600]	0
Penalized	$F_{12}(x) = 4x_1^2 - 2.1x_1^2 + \frac{1}{3} x_1^6 + x_1 x_2 - 4x_2^2 + 4x_2^4$	2	[-5,5]	0
Foxholes	$F_{13}(x) = \left(\frac{1}{500} + \sum_{j=1}^{25} \left(j + \sum_{i=1}^{2} \left(x_i - a_{ij} \right)^6 \right)^{-1} \right)^{-1}$	2	[-65,65]	0
Kowalik	$F_{14}(x) = \sum_{j=1}^{11} \left[a_i - \frac{x_1 \left(b^2 + b_i x_2 \right)}{b_i^2 + b_i x_3 + x_4} \right]^2$	4	[-5,5]	0
Hartman	$F_{15}(x) = -\sum_{j=1}^{4} c_i \exp \left[-\sum_{j=1}^{3} ai_j \left(x_j - p_{ij} \right)^2 \right]$	3	[0,1]	0

algorithms, SSA proposed by Xue and Shen [33] has certain advantages in parameter design and solution accuracy. However, there are still problems of poor population diversity and individual populations easy to fall into local optimization. Sensor network coverage itself is a multidimensional problem. In this paper, the objective function of coverage is established in the high-dimensional mathematical model. Therefore, it is essential to solve poor population diversity and make it easy to fall into local optimization. This paper uses elite reverse strategy and firefly algorithm to solve this problem, and an improved sparrow search algorithm based on firefly (EFSSA) is proposed. [34] studied the optimization ability of population diversity of elite reverse strategy in particle swarm optimization algorithm. Sengathir et al. [35] combined the firefly algorithm with the artificial bee colony algorithm to extend the lifetime of the clustering problem of wireless sensor networks. Some researchers have also used BSA algorithm [36] combined with SSA algorithm to extend the lifetime of wireless sensor networks [37]. For the robot path planning problem, Ref. [38] proposed three different improved methods in SSA. Based on sparrow search, this paper combines elite reverse strategy and firefly so that the intelligent optimization algorithm can have a better performance effect on the problem of sensor coverage.

In recent years, some new evolutionary algorithms have been proposed and have good performance in common test functions. For example, the bald eagle search (BES) algorithm [39] simulates the hunting strategy and intelligent

Table 2: Benchmark function test results.

Test function	Statistical value	ALO	GWO	BES	RK	SSA	EFSSA
F1	Mean	8.050E-05	1.286E-33	1.187E-37	7.230E-201	8.262E-51	6.636E-90
	Std	2.736E-05	1.835E-33	3.498E-37	0.000E+00	2.493E-50	2.003E-89
F2	Mean	3.113E+01	5.521E-20	2.608E-27	1.364E-109	9.793E-47	2.308E-48
	Std	3.903E+01	4.386E-20	3.441E-27	4.081E-109	3.703E-46	7.015E-48
F3	Mean	2.062E+03	1.210E-08	3.702E-05	4.726E-165	7.054E-33	2.650E-80
	Std	7.633E+02	1.384E-08	1.126E-04	0.000E+00	1.496E-32	1.436E-79
F4	Mean	1.542E+01	1.044E-09	2.864E-01	1.707E-34	7.898E-17	1.073E-35
	Std	4.745E+00	2.270E-03	2.460E-01	5.185E-34	1.875E-16	5.879E-35
F5	Mean	9.807E+01	2.658E+01	1.780E+01	2.290E+01	5.913E-04	1.132E-06
	Std	1.228E+02	5.720E-01	4.735E+00	1.034E+00	1.100E-03	2.742E-06
F6	Mean	1.511E-04	4.501E-01	7.296E-29	1.191E-09	2.089E-06	1.483E-11
	Std	1.694E-08	2.843E-01	1.955E-28	4.113E-10	4.154E-06	7.506E-12
F7	Mean	1.514E-01	1.620E-03	1.900E-03	1.278E-04	3.634E-04	1.490E-03
	Std	4.370E-02	8.694E-04	1.350E-03	6.935E-05	3.110E-04	7.961E-04
F8	Mean	-5.519E+03	-6.609E+03	-4.994E+03	-8.222E+03	-1.048E+04	-8.915E+03
	Std	7.357E+02	5.895E+02	4.588E+02	7.791E+02	2.096E+03	1.286E+03
F9	Mean	8.453E+01	7.981E-01	1.344E+01	0.000E+00	0.000E+00	0.000E+00
	Std	1.469E+01	1.644E+00	2.464E+01	0.000E+00	0.000E+00	0.000E+00
F10	Mean	2.179E+00	4.233E-14	4.440E-15	8.880E-16	8.880E-16	8.882E-16
	Std	6.775E-01	1.678E-15	0.000E+00	0.000E+00	0.000E+00	0.000E+00
F11	Mean	2.162E-02	0.000E+00	0.000E+00	0.000E+00	0.000E+00	0.000E+00
	Std	1.270E-02	0.000E+00	0.000E+00	0.000E+00	0.000E+00	0.000E+00
F12	Mean	1.151E+01	2.836E-02	8.881E-26	4.664E-10	3.319E-07	2.184E-13
	Std	3.072E+00	1.233E-02	2.696E-25	1.462E-10	6.935E-07	1.330E-13
F13	Mean	4.504E+00	3.196E-01	3.467E-02	4.310E-03	2.741E-06	4.144E-12
	Std	1.133E+01	1.558E-01	3.895E-02	7.170E-03	3.240E-06	1.397E-12
F14	Mean	1.989E+00	2.562E+00	9.980E-01	1.591E+00	4.220E+00	9.980E-01
	Std	7.847E-01	2.921E+00	1.312E-02	9.286E-01	4.552E+00	1.312E-02
F15	Mean	2.740E-03	2.310E-03	2.340E-03	6.112E-04	3.270E-04	3.073E-04
	Std	5.980E-03	6.120E-03	6.110E-03	4.378E-04	4.029E-05	4.498E-07

information interaction behavior of condor when looking for prey. Ahmadianfar et al. [40] proposed Runge Kutta (RK) optimizer algorithm, which proposed the global optimization search mechanism in the feature space and enhanced solution quality (ESQ) to avoid the local optimization mechanism.

3. Problem Definition

Suppose that the sensor nodes of the wireless sensor networks are distributed in the two-dimensional space of $L \times L(m^2)$, N isomorphic sensors are deployed, and the sensing radius of the sensor is defined as r_s. This study draws on the previous literature [41], an image that divides the space into $N' = m \times n$ pixels, and the coordinates of each point are $p_j = (x_j, y_j), j = 1, 2 \cdots, N$. In addition, assuming that the location set of sensor nodes is expressed as $S = \{s_1, s_2, \cdots, s_N\}$, the location information of each node can be expressed as $s_i = (x_i, y_i)$. To better calculate the coverage of the sensor, therefore, the distance d between node s_i and spatial point p_j in the sensor network is

$$d\left(s_i, p_j\right) = \sqrt{\left(x_i - x_j\right)^2 + \left(y_i - y_j\right)^2}. \quad (1)$$

Assuming that the sensing model is a Boolean model, the sensor node s_i can sense point p_j; according to literature

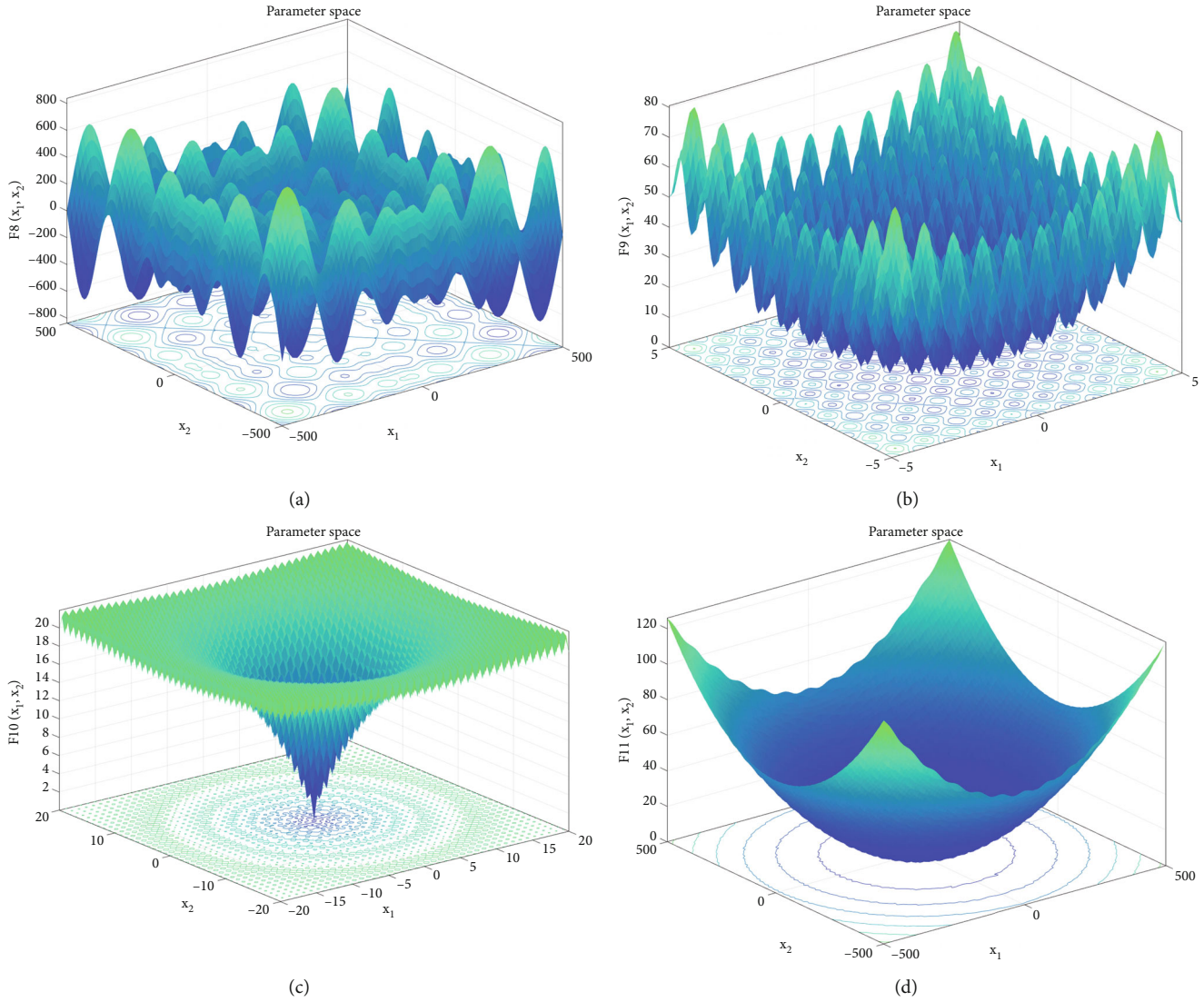

FIGURE 3: High-dimensional multimodal test functions. (a) Schwefel-F8. (b) Rastrigrin-F9. (c) Ackley-F10. (d) Griewank-F11.

[42], the perception probability can be defined as

$$\mathrm{B}\left(s_i, p_j\right) = \begin{cases} 1, & \text{if } d\left(s_i, p_j\right) \le r_s, \\ 0, & \text{others } d\left(s_i, p_j\right) > r_s. \end{cases} \tag{2}$$

In the ideal state, the optimal structure for isomorphic sensor node deployment is the coverage model [43] with the sensor node as the center, the sensing distance as the radius of the circumscribed circle of the positive hexagon, and the tiled area to be monitored (e.g., in Figure 1(a)).The sensor equipment will be disturbed by noise and the physical environment in the actual scene, following a specific regular probability distribution [40]. At this time, the relationship between probability and distance is (see Figure 1(b))

$$P\left(s_i, p_j\right) = \begin{cases} 1, & \text{if } d\left(s_i, p_j\right) \le r_s - \Delta r, \\ \exp\left(-\alpha\lambda^{\beta}\right), & \text{if } \left|d\left(s_i, p_j\right) - r_s\right| \le \Delta r, \\ 0, & \text{others.} \end{cases} \tag{3}$$

In the equation, α and β are related to the physical characteristics of the sensor itself, $\Delta r \epsilon (0, r_s)$ represents the reliable sensing range parameter with sensor coverage change, and λ is an input parameter. Usually, the calculation method of λ is

$$\lambda = d\left(s_i, p_j\right) + \Delta r - r_s. \tag{4}$$

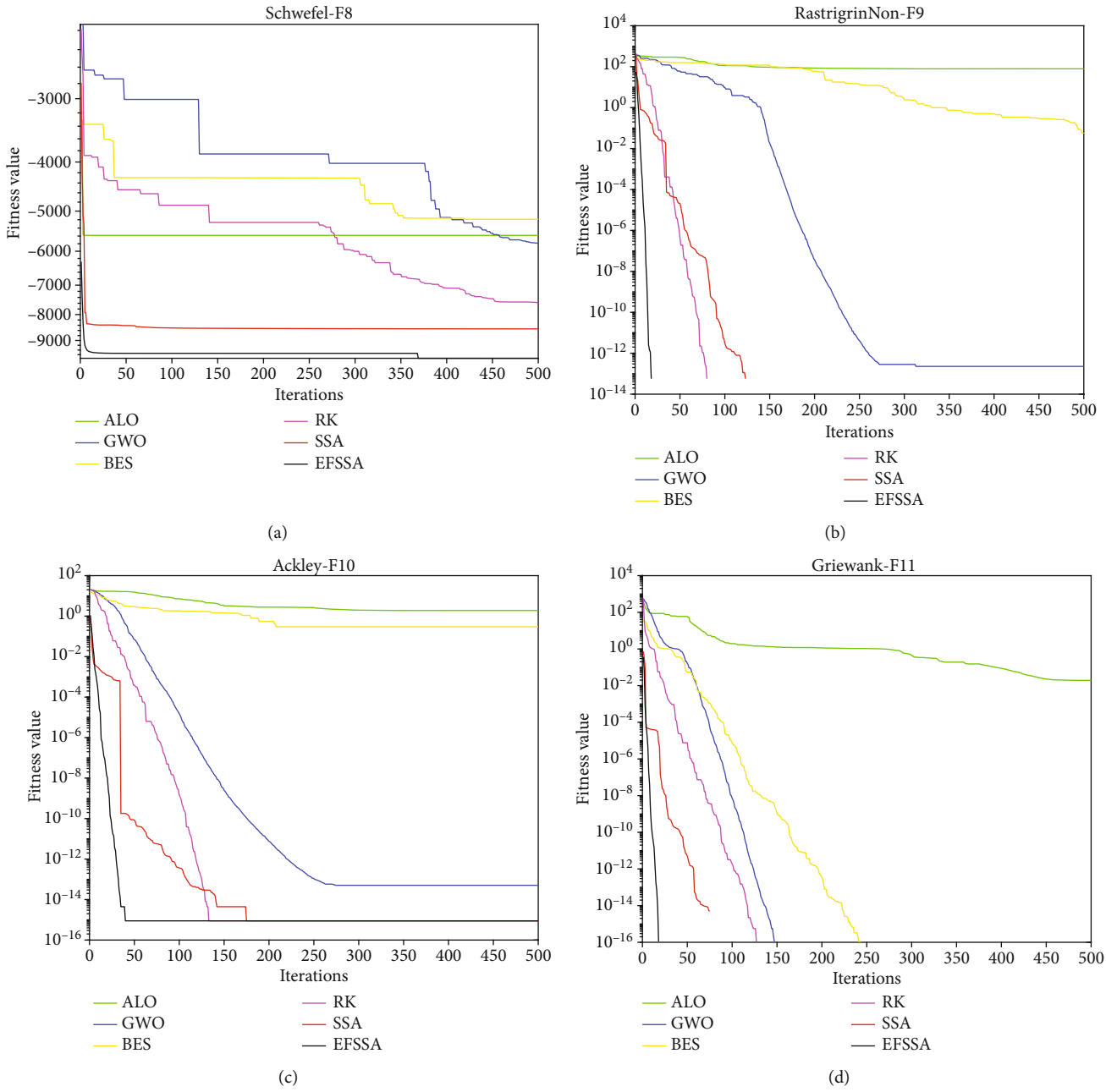

Figure 4: High-dimensional multi-modal test function curve. (a) Schwefel-F8. (b) RastrigrinNon-F9. (c) Ackley-F10. (d) Griewank-F11.

The same point p_j in the area may be sensed by multiple sensors simultaneously because as long as each spatial point is sensed by one sensor, it is considered to cover the area successfully. Then, the perceived probability of a node p_j in the perceived area N' can be further expressed as

$$B_{N'}\left(S, p_j\right) = 1 - \prod_{i=1}^{N}\left(1 - B\left(s_i, p_j\right)\right). \tag{5}$$

Then, the calculation equation for the total coverage R_{cov} of the monitoring area is

$$R_{\text{cov}} = \frac{\sum_{j=1}^{N'} B_{N'}\left(S, p_j\right)}{N'}. \tag{6}$$

At the same time, in order to better reflect the redundancy, utilization, and distribution uniformity of sensor network coverage, the ratio C_e between the monitoring range of real sensor coverage and the total area that all sensors can cover is taken as an evaluation index, and the equation is

Table 3: Simulation parameters.

Parameters	Value
Monitoring area size	30m × 30m 50m × 50m 70m × 70m 90m × 90m
Iterations	500
Perceived radius (r_s)	7m
Probability perception (Δr)	0.5m
Single-step moving distance	1m
The population size	50
Repetitions	30
Finders ratio	0.2
Reconnaissance ratio	0.15
Early warning value	0.8

expressed as

$$C_e = \frac{R_{\text{cov}} \times L \times L}{N \times (\pi \times r_s^2)}. \tag{7}$$

4. Proposed Method

4.1. Overview of Sparrow Search Algorithm. In 2020, a metaheuristic method SSA based on large-scale bird foraging and early warning was proposed [33]. In this algorithm, the whole sparrow group can be abstracted into two groups: entrants and finders, and a reconnaissance and early warning mechanism is added to the search. The finder usually has a high energy reserve. When areas with more food are found, they are able to provide flight directions for the joiners. Joiners always have access to good food sources from the information of the finder. At the same time, in SSA algorithm, the population has the strategy to realize the threat and to adopt antipredatory behavior.

4.1.1. Update Method of the Finder. Firstly, the definition of the population is given. Assuming that each population size is n in SSA, the population matrix $X = [X_1, X_2, \cdots, X_i, \cdots, X_n]^T$ is formed for the d-dimensional coverage problem, where $X_i = [X_{i,1}, X_{i,2}, \cdots, X_{i,j}, \cdots, X_{n,d}]$. All finder is responsible for finding food for the whole population and providing the migration direction of the foraging area for the joiners. Therefore, in SSA, the finder has a large search area. According to the rules, in the iterative process of the algorithm, the location update of the finder is described as follows [33]:

$$X_{i,j}^{t+1} = \begin{cases} X_{i,j}^t \bullet \exp\left(-\dfrac{i}{\alpha \bullet T_{\max}}\right), & \text{if } R_2 < \text{ST}, \\ X_{i,j}^t + Q \bullet L, & \text{if } R_2 \geq \text{ST}, \end{cases} \tag{8}$$

where $T_{\max}$ represents the final number of iterations and $X_{i,j}^t$ denotes the position of the i-th individual at iteration t -th. Both α and Q are random in the range $(0, 1]$. L is a unit matrix of size $1 \times d$. ST indicates a dangerous cut-off value. When $R_2 < ST$, it means that the population is safe; that is, there is no predator around, and the finder can search more widely to find a more suitable foraging place; when $R_2 \geq \text{ST}$, the group found the predator and sounded the alarm. The group immediately stopped foraging, made antipredation behavior, and quickly approached the safety zone.

It should be noted that when the condition $R_2 < \text{ST}$ is satisfied in Equation (1), the critical component of the finder updating the following location around the current location is independently expressed as y (see Figure 1):

$$y = \exp\left(-\frac{i}{\alpha \bullet T_{\max}}\right). \tag{9}$$

In Equation (9), as the search algorithm is computed, the iteration around y of the current node changes in the range of $(0, 1)$. However, the range of population variation becomes smaller in the later iterations. Because the individuals in the population remains unchanged, when iterations increases, the finders are more densely distributed in the smaller y interval than in the larger interval, so the local search ability is stronger. However, the reduction of the search range will also lead to the algorithm not being able to obtain the optimal global solution in complex problems.

4.1.2. Update Method of Joiners. In the sparrow population, after removing the finder, the rest is the joiner, and the joiner will follow the finder. Joiners will also monitor the finders. Once they find a better foraging location, they will abandon their current foraging area and fly to an area with more food based on the information. The equation for updating the position of joiners is expressed as [33]

$$X_{i,j}^{t+1} = \begin{cases} Q \bullet \exp\left(\dfrac{X_{\text{worst}}^t - X_{i,j}^t}{\alpha \bullet T_{\max}}\right), & \text{if } i > \dfrac{n}{2}, \\ X_{\text{best}}^{t+1} + \left|X_{i,j}^t - X_{\text{best}}^{t+1}\right| \bullet A^+ \bullet L, & \text{if } i \leq \dfrac{n}{2}. \end{cases} \tag{10}$$

In Equation (10), X_{worst}^t represents the global worst individual position in the iteration results of the previous generation. Similarly, X_{best}^{t+1} represents the global best position in the current iteration result, that is, the elite solution. A^+ has the same structural dimension as Q above. A is a $d \times d$ matrix composed of 1 or -1. A^+ has the characteristics of $A^+ = A^T(AA^T)^{-1}$. Conditions $i > n/2$ and $i \leq n/2$ in Equation (10) indicate that the sparrow is hungry for foraging and has been in the best foraging position.

4.1.3. Update Methods of Reconnaissance and Early Warning. In the simulation experiment, sparrows with conscious danger signals did not exceed 20% of the total number and their selection was randomized. The update formula for

Table 4: Coverage of different nodes and monitoring areas.

Area	Nodes	Initial	ALO	GWO	BES	RK	SSA	EFSSA
30m × 30m	7	0.52222	0.90667	0.91556	0.88667	0.91222	0.85333	0.92444
	9	0.67889	0.96778	0.99667	0.96556	0.99889	0.91000	1.00000
	11	0.75111	0.99778	1.00000	0.99333	1.00000	0.93444	1.00000
50m × 50m	20	0.58480	0.86080	0.94280	0.84160	0.93640	0.83280	0.96120
	25	0.68280	0.96778	0.98000	0.88600	0.96800	0.84240	0.99600
	30	0.72720	0.97680	0.99640	0.94640	0.99000	0.92800	1.00000
70m × 70m	40	0.64041	0.87490	0.90673	0.79163	0.87551	0.87490	0.95224
	50	0.71429	0.90330	0.80600	0.81050	0.90070	0.80890	0.96920
	60	0.76714	0.95959	0.97755	0.91347	0.98750	0.97000	0.99980
90m × 90m	64	0.65321	0.84543	0.75370	0.76407	0.86753	0.77210	0.92136
	80	0.71568	0.88100	0.79490	0.80500	0.78990	0.80040	0.94460
	96	0.78309	0.96346	0.86185	0.88642	0.94543	0.87099	0.99284

these individuals is as follows [33]:

$$X_{i,j}^{t+1} = \begin{cases} X_{\text{best}}^{t} + \beta \bullet \left| X_{i,j}^{t} - X_{\text{best}}^{t} \right|, & \text{if } f_i > f_b, \\ X_{\text{best}}^{t+1} + K \bullet \dfrac{\left| X_{i,j}^{t} - X_{\text{best}}^{t+1} \right|}{(f_i - f_w) + \varepsilon}, & \text{if } f_i = f_b. \end{cases} \tag{11}$$

Similar to Equation (9), X_{best}^{t+1} originates from the whole population. The function of β is to control the step size, obeying the 0~1 distribution. $K \in (0, 1]$. f represents the fitness; f_i, f_b, and f_w represents the current value, the global best, and the worst value, respectively. The denominator part is by adding ε make sure it is not 0. When $f_i = f_b$, it means that the early warning sparrow is in the middle; it should move immediately to the edge of the population to avoid being attacked. When $f_i > f_b$, another strategy of moving in smaller steps should be adopted.

4.2. Improvement Strategy. In the previous studies, the SSA algorithm has been proved to have good convergence and robustness [33], but there are still some deficiencies. For the convergence speed and local optimum problem of SSA algorithm, this paper will improve the SSA algorithm through elite reverse learning and firefly algorithm and propose a sparrow search algorithm (EFSSA) with elite reverse and firefly crossover. These two strategies are introduced in detail below.

4.2.1. Elite Reverse Strategy. The initial solution of the traditional sparrow search algorithm is initialized in a random way, and the population diversity is poor. Therefore, in this paper, the elite inverse method is added to the position initialization process. The elite individuals are constructed to reverse the sparrow individuals so that the algorithm has a better initial solution. In 2005, Professor Tizhoosh first proposed the concept of reverse learning (OBL) [44]. This paper points out that the initial values of most intelligent algorithms are mainly based on guessing and then finding or close to the optimal solution after many iterations. Randomly generating the initial solution will greatly impact the solution results. Suppose the random value at the beginning of each iteration is far from the optimal solution or even the opposite. In that case, it will greatly impact the algorithm and consume a lot of update time [45].

Therefore, this paper introduces the reverse solution, which can expand the search area of the algorithm. However, the original solution is higher than the reverse solution for those sparrows with high fitness values. If the reverse solution space is searched, it will be a waste of time, and the original domain search should be strengthened. The value of reverse region search is higher for sparrows whose reverse solution is higher than the original solution. The definition of the inverse solution is given below:

(1) Definition of elite solution: suppose $X_i(t) = [X_{i,1}, X_{i,2}, \cdots, X_{i,j}, \cdots, X_{n,d}]$ as solutions for the t-th iteration, and the solution of its reverse learning is $X_i(t)^*$. We calculate the fitness functions $f(X_i(t))$ and $f(X_i(t)^*)$ of the current solution and elite reverse learning solution, respectively. When $f(X_i(t)) \geq f(X_i(t)^*)$, $X_i(t)$ is an ordinary individual in the current iteration. On the contrary, $X_i(t)$ is the elite individual in the current iteration, which is recorded as $E_i(t)$. The elite solution composed of p elite individuals [34]:

$$\left\{E_1(t), E_2(t), \cdots, E_p(t)\right\} \epsilon \left\{X_1(t), X_2(t), \cdots, X_{\text{n}}(t)\right\} \tag{12}$$

(2) Definition of inverse solution: assuming that $X_{i,j}$ is an ordinary individual in $X_i(t)$ and its individual inverse solution is represented by $X_{i,j}(t)^*$, then

$$X_{i,j}(t)^* = k\left(a_j(t) + b_j(t)\right) - X_i(t) \tag{13}$$

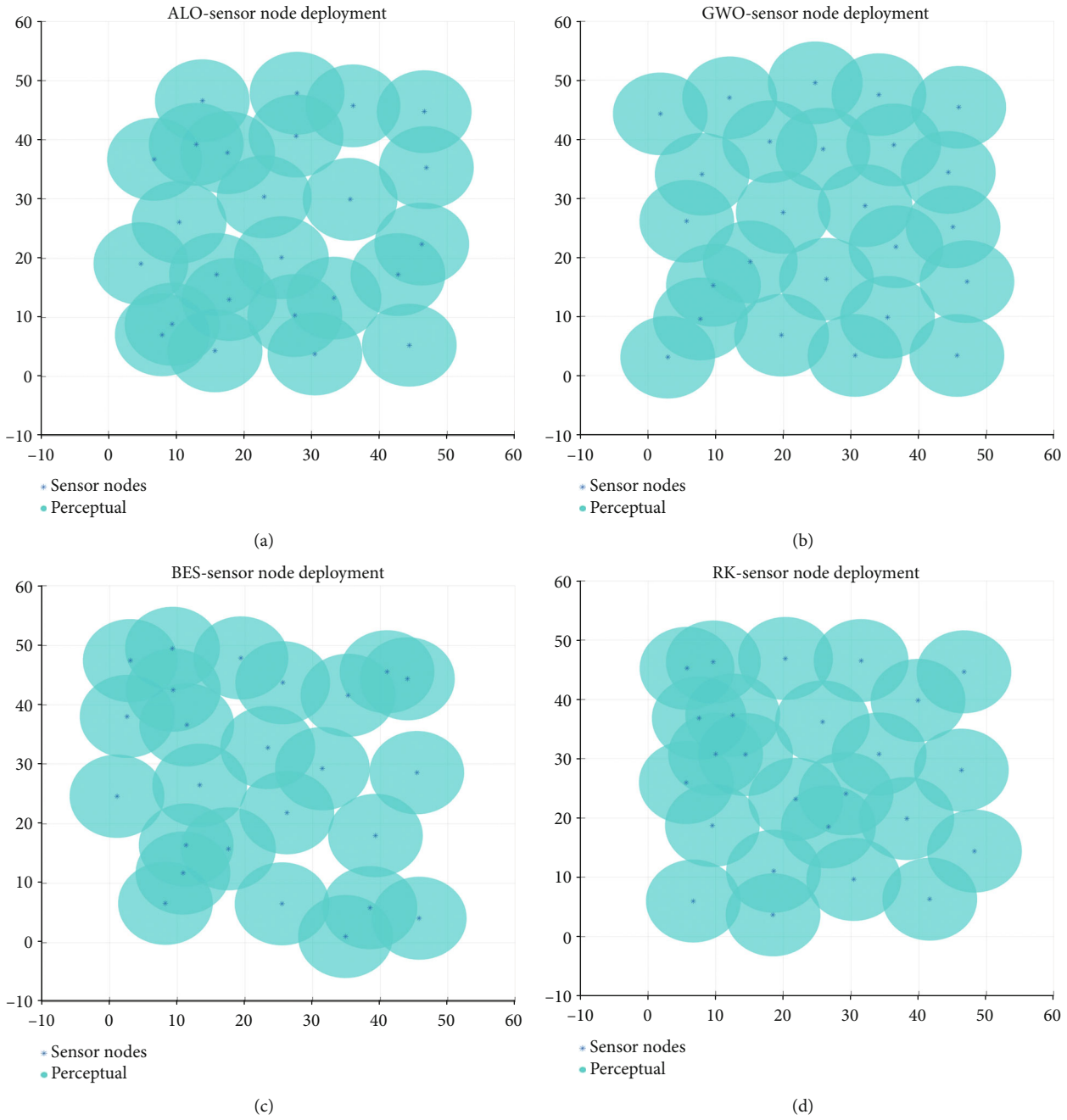

Figure 5: Continued.

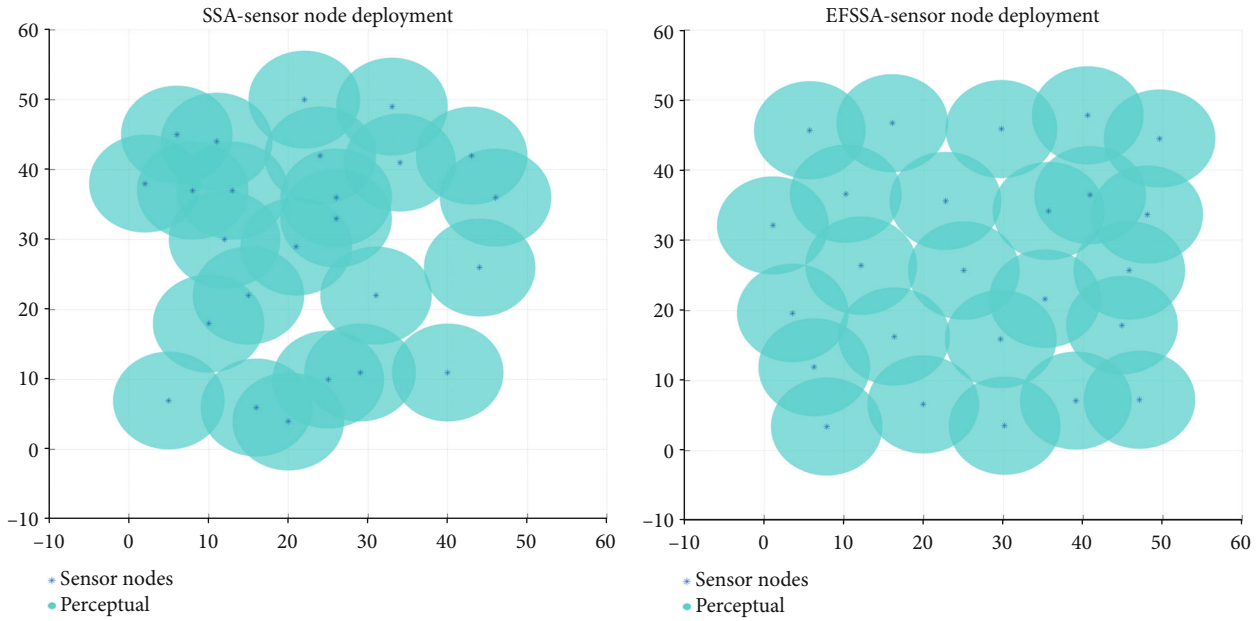

FIGURE 5: Covering effect based on Boolean model. (a) ALO deployment. (b) GWO deployment. (c) BES deployment. (d) RK deployment. (e) SSA deployment. (f) EFSSA deployment.

where $k \in (0,1]$ control step size; the range of the elite group is in interval $[a_j(t), b_j(t)]$, where $a_j(t) = \min\{E_1(t), E_2(t), \cdots, E_p(t)\}$ and $b_j(t) = \max\{E_1(t), E_2(t), \cdots, E_p(t)\}$

4.2.2. Firefly Disturbance Strategy. SSA algorithm is easy to fall into local optimization in the later stage of iteration, which is usually caused by sparrow individuals falling into local optimization in a specific dimension in the calculation process. The firefly algorithm is introduced into the algorithm. All sparrows and the optimal sparrow are disturbed by the algorithm to update the position to improve its search performance. The sparrow after disturbance is compared with the sparrow before disturbance. If it is better, the sparrow position is updated. The main parameters disturbed by the firefly intelligent optimization algorithm include the fluorescence brightness, attraction, and update position of the firefly. The equations are as follows:

Firstly, the expression equation of fluorescence brightness principle based on firefly strategy [35] is

$$I = I_0 \bullet e^{-\gamma r_{i,j}}, \tag{14}$$

where I_0 represents the maximum brightness generated by the firefly population, depending on the function to be optimized. γ is the light intensity absorption coefficient of fireflies. The farther away from the distance, the smaller the coefficient value, and vice versa. $r_{i,j}$ represents the distance between adjacent fireflies. The distance is Cartesian, i.e.,

$$r_{i,j} = \left\| x_i - x_j \right\| = \sqrt{\sum_{k=1}^{d} \left(x_{ik} - x_{jk} \right)^2}. \tag{15}$$

Therefore, in the firefly strategy, the attraction equation of firefly [35] is

$$\beta = \beta_0 \bullet e^{-\gamma r_{i,j}^2}. \tag{16}$$

It can be concluded that the attraction refers to the principle of the fluorescence brightness equation; β_0 indicates the maximum attraction of fireflies.

Suppose the position of firefly i is x_i. When firefly i is attracted by firefly j, it updates its position immediately. The new position calculation equation is

$$X_i^{t+1} = X_i^t + \beta_0 \bullet e^{-\gamma r_{i,j}^2} \bullet \left(x_i - x_j \right) + \alpha \bullet (R - 0.5), \tag{17}$$

where α represents the step size coefficient in the range [0,1] and $R \in [0, 1]$ which is uniformly distributed.

4.2.3. Sensor Deployment Based on Metaheuristic Algorithm. This section gives the flow of EFSSA algorithm (see Algorithm 1 for the specific implementation process).

In Algorithm 1, n individuals are randomly formed in the initial quigroup, and n new individuals are generated in this paper by using elite reverse strategy. Then, the $2n$ individuals are sorted according to the objective function or fitness function, and the first n are selected. The fitness function index R_{cov} of EFSSA applied to WSN in this paper has been given in Equation (6). Next, the location of the finder is updated according to the threshold of the warning value; according to the order of the i-th follower, the joiners are divided into hungry searching individuals and extensive searching individuals. Finally, for the reconnaissance and early warning, whether it is at the population boundary is judged. When the altered individual is

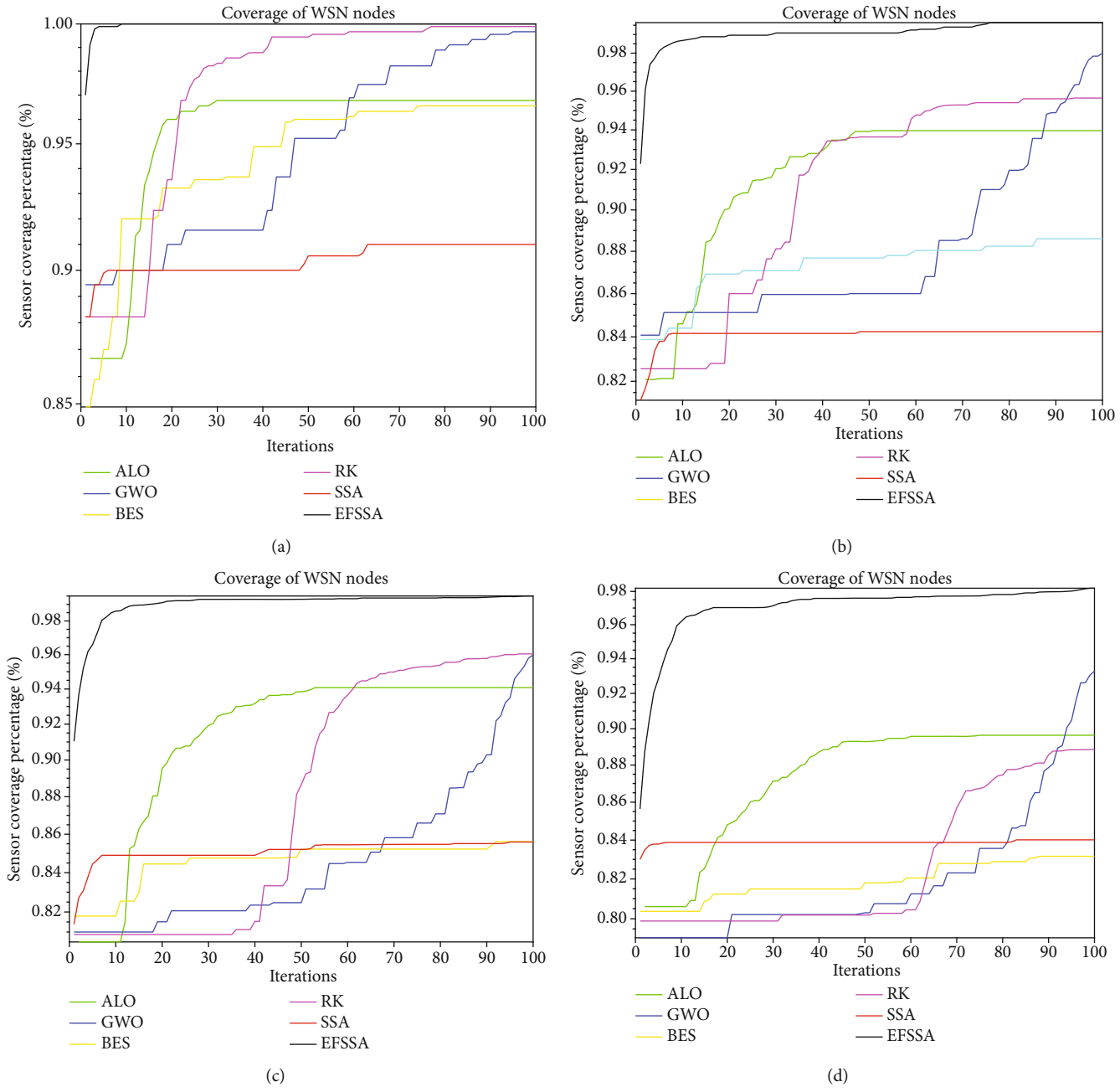

Figure 6: Coverage curve with the number of iterations in balanced deployment mode. (a) 9 nodes are in 30m × 30m. (b) 25 nodes are in 50m × 50m. (c) 50 nodes are in 70m × 70m. (d) 80 nodes are in 90m × 90m.

Table 5: Average rate of increase in coverage of Boolean coverage model.

Nodes	ALO (%)	GWO (%)	BES (%)	RK (%)	SSA (%)	EFSSA (%)
Sparse (-20%)	46.714	48.377	38.571	51.081	40.157	57.782
Balance (9/25/50/80)	33.463	28.561	24.484	31.343	20.625	40.211
Dense (+20%)	28.821	26.910	23.665	29.683	22.422	31.941

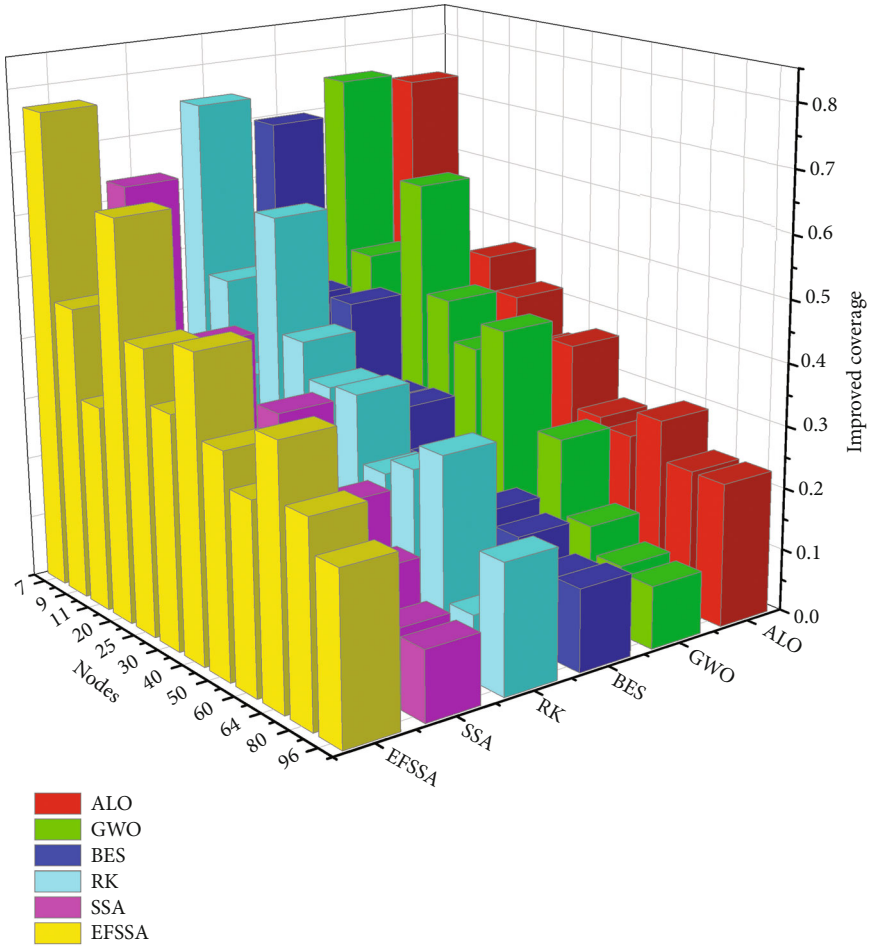

Figure 7: Increased coverage in the Boolean model.

Table 6: Real coverage rate C_e of different nodes and monitoring areas.

Area	Nodes	Initial	ALO	GWO	BES	RK	SSA	EFSSA
30m × 30m	7	0.43617	0.75726	0.76469	0.74056	0.76190	0.71271	0.77211
	9	0.44102	0.62868	0.64745	0.62724	0.64889	0.59115	0.64961
	11	0.39922	0.53032	0.53150	0.52796	0.53150	0.49666	0.53150
50m × 50m	20	0.47487	0.69898	0.76557	0.68339	0.76037	0.67625	0.78051
	25	0.44356	0.62868	0.63662	0.57556	0.62882	0.54723	0.64701
	30	0.39366	0.52878	0.53939	0.51233	0.53593	0.50237	0.54134
70m × 70m	40	0.50962	0.69622	0.72155	0.62996	0.69671	0.69622	0.75777
	50	0.45473	0.57506	0.51312	0.51598	0.57340	0.51496	0.61701
	60	0.40698	0.50908	0.51861	0.48461	0.52389	0.51460	0.53041
90m × 90m	64	0.53705	0.69508	0.61967	0.62819	0.71325	0.63479	0.75751
	80	0.47073	0.57946	0.52283	0.52947	0.51954	0.52645	0.62129
	96	0.42922	0.52808	0.47239	0.48586	0.51820	0.47740	0.54419

at the population boundary, firefly strategy is adopted to move position. Finally, judge whether the maximum number of iterations has been reached I_{max}. If not, continue the iterative calculation; otherwise, output the optimal deployment result.

The optimization performance of SSA algorithm has been proved in literature [33]. This paper will further explore the computational time complexity. Compared with the original SSA algorithm, the time complexity of EFSSA is acceptable. The time complexity of the algorithm is denoted

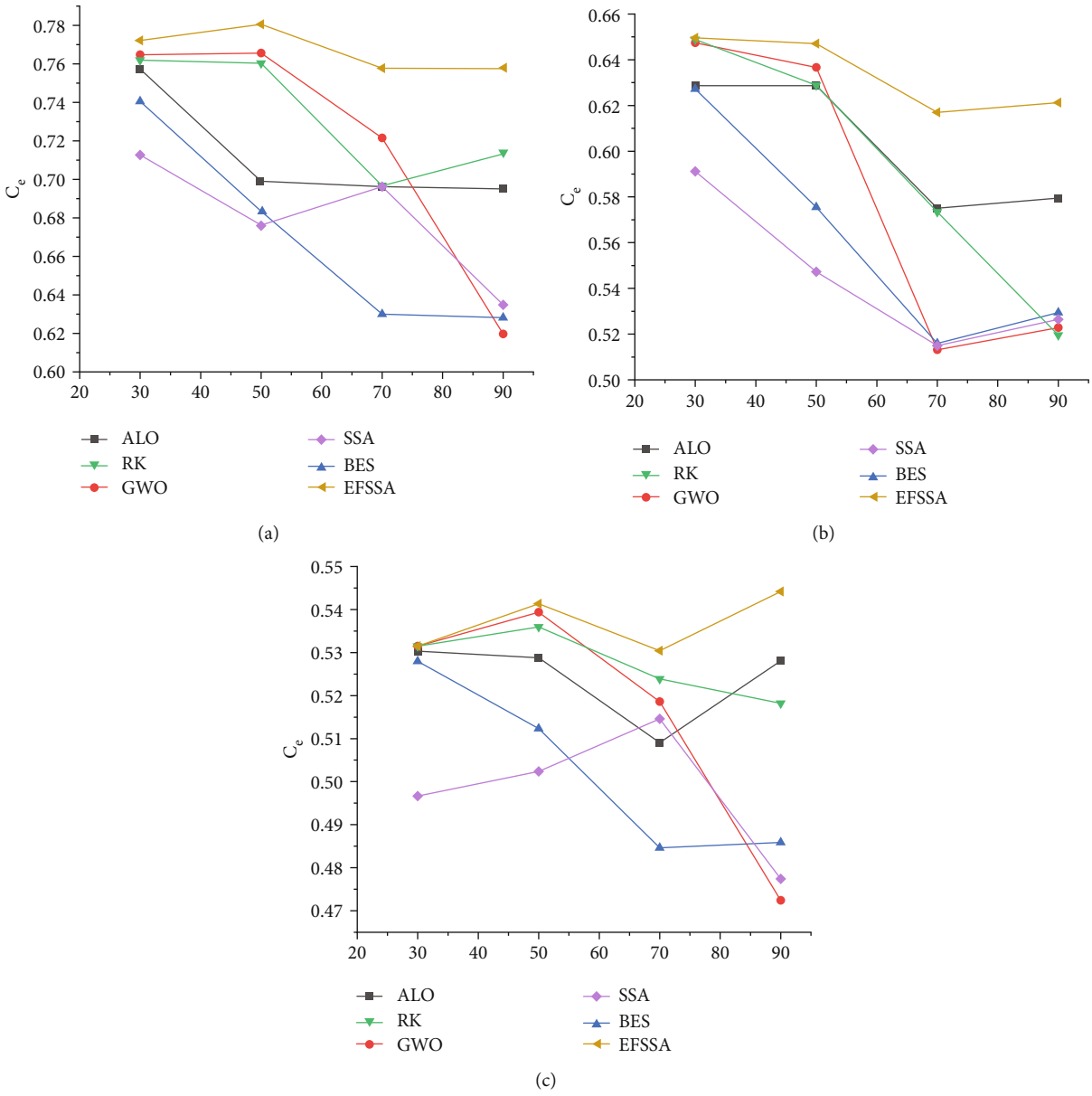

FIGURE 8: Coverage index C_e. (a) Sparse deployment. (b) Balance deployment. (c) Dense deployment.

as $O(\bullet)$, the dimension of individuals in the population is assumed to be m, and the number of populations is n. In the process of population iteration, individuals need to conduct fitness sorting, and the time complexity in the sorting process is $O(n^2)$. Then, the time complexity of finders update is $O(m * F_{\text{num}})$, the time complexity of joiners is $O(m * (n - F_{\text{num}}))$, and the time complexity of detection and early warning is $O(m * n * DE_{\max})$. It can be concluded that the sum of time complexity of finder and follower is $O(mn)$. The proportion of reconnaissance and early warning is 10%~20% [33]. The total time complexity is $O(n * n + mn + mn * DE_{\max})$. The calculation results ignore the constant part, and the time complexity after simplification is $O(n^2 + mn)$.

EFSSA adopts elite reverse strategy, so it increases the size of sorting. When sorting, the time complexity of EFSSA is $O((2n)^2)$. The time complexity of finders and joiners is the same as that of SSA. In the part of reconnaissance and early warning, the algorithm uses firefly strategy for some individuals in order to jump out of local optimal. This strategy also uses the distance between two individuals in Equation (11). Hardly increasing the calculation time, the ratio of this part will not exceed $DE_{\max}$. Therefore, the time complexity is $O(4n * n + mn + mn * DE_{\max})$, and the simplified complexity is still $O(n^2 + mn)$.

Then, the coverage optimization framework is established according to the sensor deployment model (Algorithm 2). Input parameters related to the sparrow search algorithm and coverage are initialized, and the number of sensor nodes and deployment area is set. Then, the coordinates of the sensor nodes are used as the individuals of the population. Under the calculation of the number of

Table 7: Coverage of different nodes and monitoring areas.

Area	Nodes	Initial	ALO	GWO	BES	RK	SSA	EFSSA
30m × 30m	7	0.54471	0.94119	0.95447	0.93452	0.9427	0.86135	0.95785
	9	0.71403	0.98971	0.99860	0.99970	0.99707	0.92022	1.00000
	11	0.77412	0.99986	1.00000	0.99995	0.99995	0.97898	1.00000
50m × 50m	20	0.61927	0.89713	0.95495	0.85740	0.94564	0.86233	0.98819
	25	0.69384	0.98028	0.98480	0.91030	0.99061	0.87222	0.99845
	30	0.78252	0.99571	0.93871	0.95022	0.99581	0.93016	1.00000
70m × 70m	40	0.67723	0.90482	0.92735	0.83029	0.91366	0.80171	0.97860
	50	0.72356	0.94383	0.96897	0.88245	0.95941	0.88160	0.99971
	60	0.79525	0.97713	0.98469	0.94323	0.98750	0.94301	0.99992
90m × 90m	64	0.68236	0.89391	0.79155	0.78534	0.88172	0.81118	0.95985
	80	0.74505	0.94384	0.94525	0.86679	0.94197	0.87512	0.98739
	96	0.80732	0.98012	0.89001	0.92053	0.96962	0.89005	0.99814

iterations I_{max}, the optimal solution with coverage as the objective function is finally solved through the elite reverse strategy and firefly optimization strategy. The algorithm flow is shown in Figure 2.

5. Experimental Analysis

5.1. Benchmark Function Test. In this section, in order to test the optimization performance of EFSSA algorithm, first compare the algorithm with four related evolutionary optimization algorithms on the benchmark function (shown in Table 1), including ALO [28] algorithm, GWO algorithm [29], BES algorithm [39], RK algorithm [40], and SSA algorithm [33]. The experiment was carried out in the test environment of Intel (R) core i7-8750h CPU, 2.20 GHz, 16 GB memory, and windows10 64 bit and was written with MATLAB 2020b software. Table 1 gives the names, equations, dimensions, independent variable ranges, and optimal global values of 15 classical benchmark functions on cec2008, cec2017, and cec2020.

F1~F7 are unimodal high-dimensional test functions, F8~F11 (see Figure 2) are multimodal test functions, and F12~F15 are fixed low-dimensional test functions. In order to avoid errors in the computation of all the given algorithms due to different parameters, the size of the population was set to 50 and all the experiments were repeated 30 times having 500 iterations independently. Through the benchmark function experiment, the optimal value and standard deviation of each algorithm on the same benchmark function are obtained, so as to evaluate their optimization and stability.

As shown in Table 2, the average value of the optimal optimization of the current function is marked in bold in each row of data. The optimization ability of EFSSA algorithm is better than that of other functions in most test functions. Among the 15 test functions, EFSSA algorithm outperforms others in 9 of them. The high-dimensional unimodal test EFSSA has the best optimization effect in F4 and F5 functions. The mean values of F1~F3 and F7 are second only to those of RK algorithm. This is because RK algorithm calls Runge Kutta method for the function to calculate the logic of slope change, so it is better in single-peak function.

Because the F6 function is a concave canyon function with a strong locality, the variation range in the valley is small, and the optimal value is in the only local region, so the effect of the BES algorithm is better. Among the high-dimensional multimodal test functions, EFSSA algorithm has obvious optimization and stability superior to other algorithms. This is because the multimodal function is easy to make the traditional algorithm fall into local solutions and needs a dispersed and uniform population distribution. Here, the applicability of EFSSA algorithm can be obviously reflected. Finally, for low-dimensional functions F12~F15, EFSSA algorithm can basically maintain the superiority of the algorithm, although the performance of F12 is worse than that of BES, it is still superior to other algorithms.

Because functions F8~F11 and sensor network coverage are similar high-dimensional multimodal function problems, we further analyze the testing effect of EFSSA algorithm in this kind of problem. Figures 3 and 4 show the objective function curves and the function graph of benchmark functions Schwefel, Rastrigrin, Ackley, and Griewank with the number of iterations.

As shown from the Figure 4, the EFSSA algorithm has better convergence with the increase of iteration times compared with ALO, GWO, BES, RK, and SSA algorithms. Its optimization performance is also the best. In general, EFSSA performs better than other algorithms in testing functions, especially in high-dimensional multimodal function problems. In the next section, this paper will further verify the effect of EFSSA algorithm in the sensor coverage deployment experiment.

5.2. Simulation Experiment of Sensor Network Coverage. In this section, in order to test the optimization performance of EFSSA algorithm, firstly, the critical parameters of EFSSA algorithm and five related evolutionary optimization algorithms are given. In the experiment, the wireless network perception model uses Boolean model and probability model. Then, the simultaneous interpreting of the two deployment effects of sensors with different monitoring areas and different sensor numbers is compared.

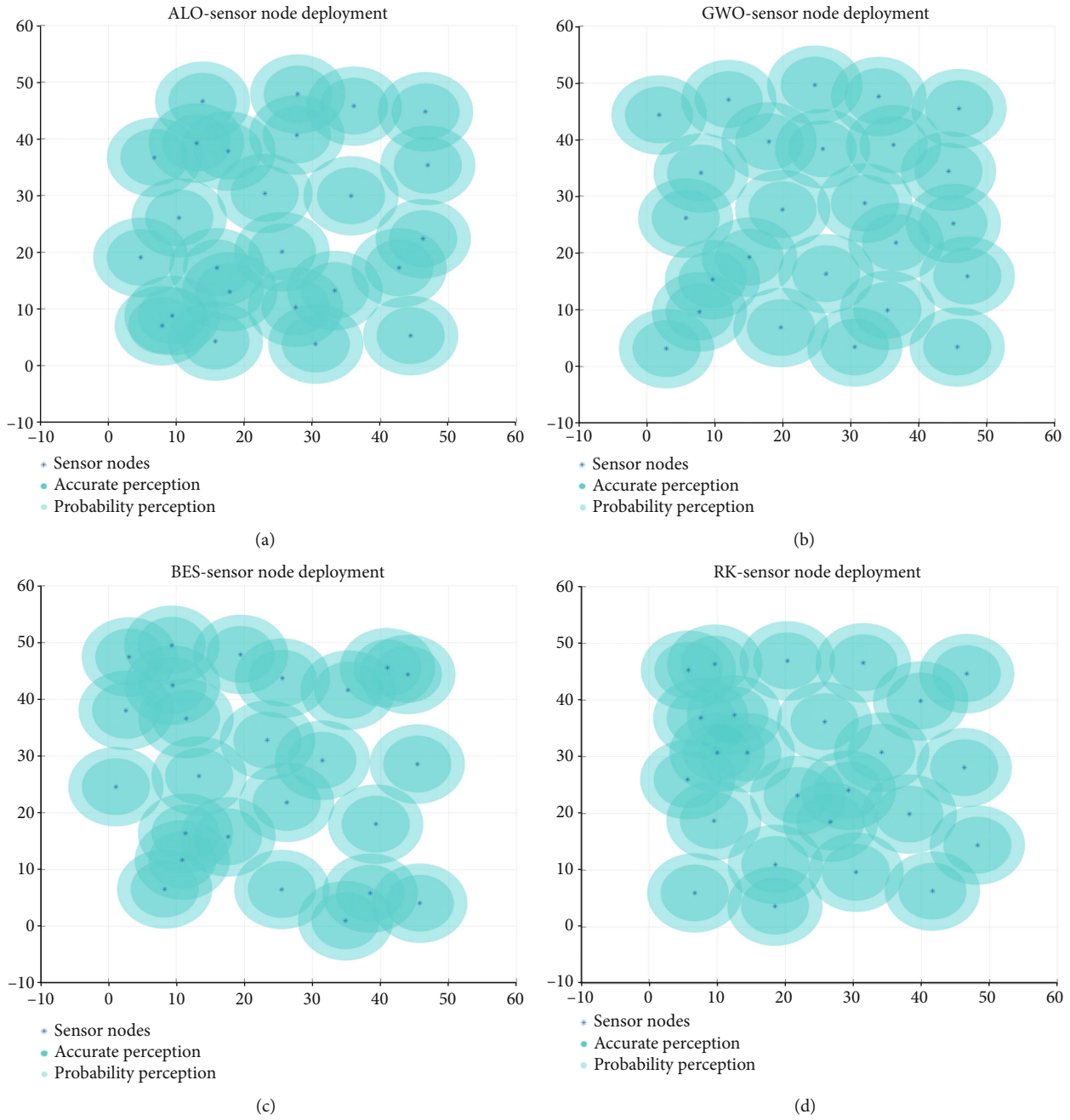

Figure 9: Continued.

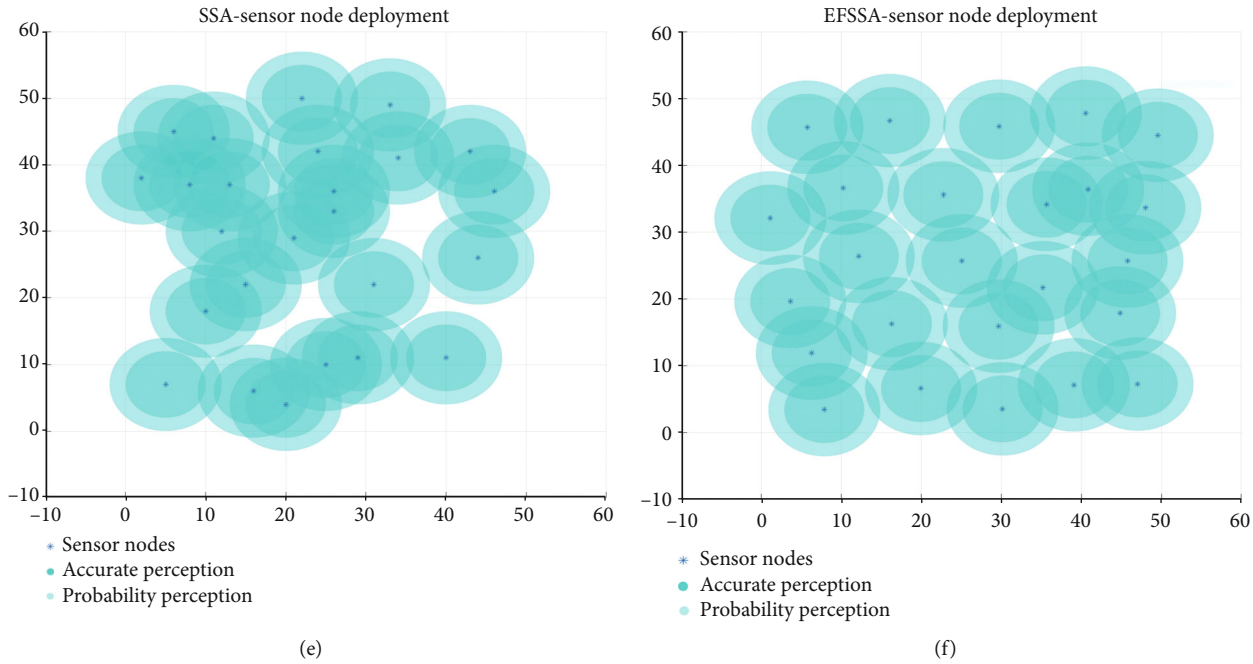

Figure 9: Covering effect based on probability model. (a) ALO deployment. (b) GWO deployment. (c) BES deployment. (d) RK deployment. (e) SSA deployment. (f) EFSSA deployment.

5.2.1. Parameter Setting. In this section, the ability of EFSSA algorithm to solve the coverage problem of wireless sensor networks will be evaluated through a series of simulation experiments. The software and physical platforms tested by the above benchmark algorithm are still used, and the MATLAB experimental environment is used to simulate sensor the coverage effect of sensor deployment. The critical parameters used in the experiment of ALO [28] algorithm, GWO algorithm [29], BES algorithm [39], RK algorithm [40], and SSA algorithm [33] are set by default. For example, the parameters in SSA and FA algorithm come from literature [33, 35]. The parameters of monitoring area parameters and the EFSSA algorithm are shown in Table 3.

The monitoring area for sensor deployment is divided into $900m^2$, $2500m^2, 4900m^2$, and $8100m^2$ two-dimensional monitoring space with three gradient sizes. In all experiments, except for the same monitoring area, the number of iterations of all algorithms is 100, the size of the population is 50, and the number of independent runs of algorithms is 30. Due to the high computational cost of solving practical problems and finding the optimal solution when the number of iterations is small, the number of iterations in literature [33] is set to 50. In order to make the experiment more convincing, this paper increases the number of iterations. In this paper, the finder proportion parameters, detection and early warning parameters, and early warning values of the SSA algorithm and EFSSA algorithm are set to 0.2, 0.15, and 0.8, respectively. In order to study the sensor deployment under different node densities, the experiments of sparse and dense deployment are designed, respectively, on the basis of regular hexagon-balanced node deployment (an approximate integer). The number of sparse and dense nodes is set to 80% and 120% of balanced deployment, respectively.

Table 8: Average rate of increase in coverage of probability coverage model.

Nodes	ALO (%)	GWO (%)	BES (%)	RK (%)	SSA (%)	EFSSA (%)
Sparse	45.566	45.591	36.927	47.474	33.660	55.146
Balance	34.254	35.644	27.376	35.360	23.471	38.661
Dense	25.577	20.754	20.602	25.334	18.784	27.373

5.2.2. Boolean Coverage Experiment. For Boolean coverage model in Equation (2), through the test results of the ALO, GWO, BES, RK, SSA, and EFSSA algorithms, this paper verifies the coverage efficiency of these six different algorithms in a sensor network monitoring environment.

Firstly, the monitoring area is completely covered without considering the boundary effect, and the optimal deployment strategy of a regular hexagon is used to calculate the sensor nodes that need to be evenly deployed within different monitoring area. When all sensor nodes are randomly deployed in a two-dimensional plane, the initial input positions are the same for all algorithms. It can be seen from Table 4 that when 9 nodes are deployed within $30m \times 30m$ monitoring area, the coverage rate (R_{cov}) of EFSSA is 92.444%. Deploying 25 nodes in the $50m \times 50m$ area, the coverage results of algorithms ALO, GWO, BES, RK, and SSA are 96.788%, 98%, 96.8%, and 84.24%, respectively. In

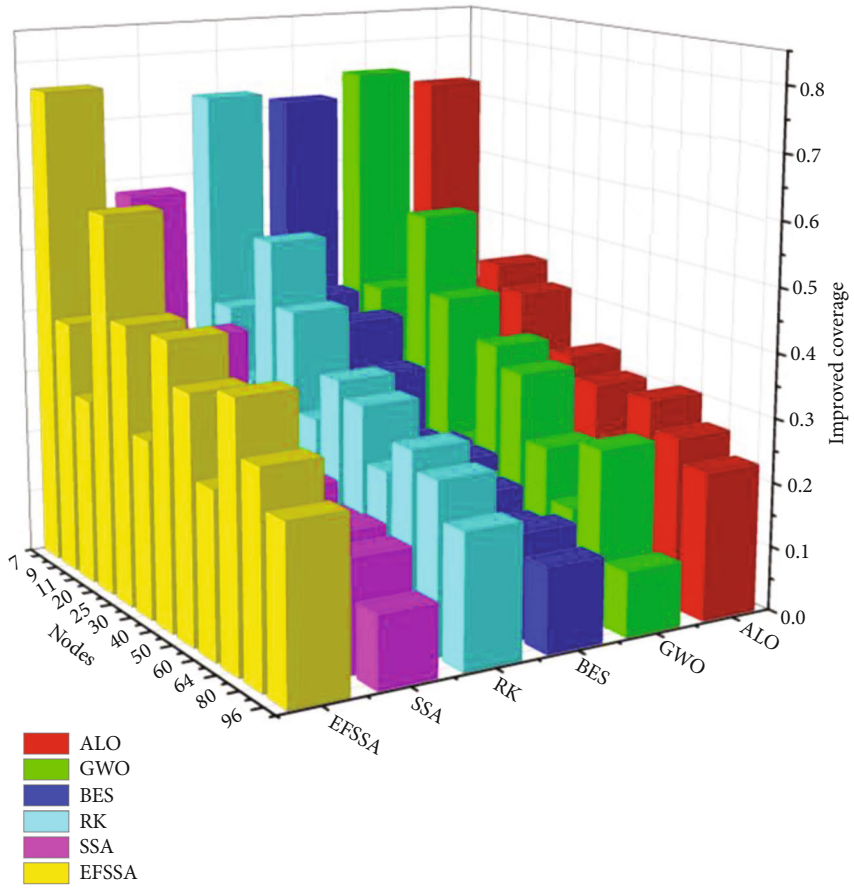

Figure 10: Increased coverage in the probability model.

contrast, the coverage of EFSSA algorithm is 99.6%. In 70 m × 70m area, the number of nodes under the optimal deployment mode is 50. With the second deployment of these sensors, the coverage of EFSSA algorithm reaches 96.92%, which is increased by 6.8%, 16.37%, 16.86%, 16.83%, and 16.54%, respectively, compared with the original coverage, and the coverage of ALO, GWO, BES, RK, and SSA algorithms is 90.33%, 81.05%, 80.58%, 80.6%, and 80.89%, respectively. In 90m × 90m deployment 80 sensor nodes, the coverage of ALO, GWO, BES, RK, SSA, and EFSSA is 88.1%, 79.49%, 80.5%, 78.99%, 80.04%, and 94.46%. In the simulation experiments of wireless sensor deployment optimization under the Boolean model, EFSSA significantly outperforms other algorithms in terms of coverage after secondary deployment of nodes.

In Figure 5, the effect of regional balanced deployment is shown. The uniformity of EFSSA with high coverage is obviously better than that of SSA and BES with low coverage. In Figure 5(f), the EFSSA sensor deployments are nearly universal, but some overlying voids can still be seen. After the optimization of these algorithms for second deployment, which is due to the fact that the experiments in this paper divide the space into two-dimensional pixel points and the noninteger coordinates are not included in the detection area.

In Figure 6, the variation of coverage of different algorithms with the number of iterations in the balanced deployment mode is statistically analyzed. As the monitoring area becomes larger, the convergence speed of each algorithm is affected, because the increase of dimension leads to the difficulty of solving. However, EFSSA algorithm can maintain the superiority of the algorithm and can always be quickly to complete convergence in the case of different monitoring area sizes. Other algorithms, such as GWO algorithm, increase the monitoring range from $900m^2$ to $8100m^2$, the number of iterations approaching the optimal solution increases from 50 to 90 times, and the final coverage is still less than EFSSA algorithm. All SSA algorithms without improved strategy fall into local optimal solution after less than 10 iterations.

This paper analyzes the coverage effect with the number of iterations under these three different monitoring scales (sparse, balanced, and dense). Assuming that the number of sensor nodes is changed, set the sensors to ±20% of the balanced deployment number. When seven nodes are deployed in 30m × 30m region, the coverage of EFSSA can still reach 92.444%, while the deployment effect of SSA algorithm is the worst. When the number of nodes increases to 11, GWO, RK, and EFSSA algorithms almost achieve complete coverage, and only EFSSA can achieve complete

Table 9: Real coverage rate C_e of different nodes and monitoring areas.

Area	Nodes	Initial	ALO	GWO	BES	RK	SSA	EFSSA
30m × 30m	7	0.45495	0.78610	0.79719	0.78053	0.78736	0.71941	0.80001
	9	0.46384	0.64293	0.64870	0.64942	0.64771	0.59779	0.64961
	11	0.41145	0.53143	0.53150	0.53147	0.53147	0.52033	0.53150
50m × 50m	20	0.50286	0.72848	0.77543	0.69622	0.76787	0.70022	0.80243
	25	0.45073	0.63680	0.63974	0.59134	0.64351	0.56660	0.64861
	30	0.42361	0.53902	0.50816	0.51440	0.53908	0.50354	0.54134
70m × 70m	40	0.53892	0.72003	0.73796	0.66072	0.72707	0.63798	0.77875
	50	0.46063	0.60086	0.61687	0.56179	0.61078	0.56124	0.63644
	60	0.42189	0.51838	0.52239	0.50040	0.52389	0.50028	0.53047
90m × 90m	64	0.56101	0.73494	0.65078	0.64568	0.72492	0.66692	0.78916
	80	0.49004	0.62079	0.62172	0.57012	0.61956	0.57559	0.64944
	96	0.44250	0.53721	0.48782	0.50455	0.53146	0.48785	0.54709

coverage among 60 nodes deployed in 50m × 50m. The optimization performance of RK and GWO algorithms proposed by researchers is second only to EFSSA, but their optimization speed is not as fast as EFSSA in sensor deployment problems.

Table 5 shows the percentage of average coverage improvements for these algorithms at different deployment densities. With the increase of node deployment density, the coverage improvement effect of the six algorithms decreases. The reason is the increase in the number of sensor nodes makes the coverage of the initial immediate deployment of sensors larger, so the improvement effect of reoptimization decreases. From another perspective, with the number of sensor nodes increases, the complexity of optimization increases, but the optimization effect decreases. EFSSA algorithm can still maintain a coverage improvement effect of more than 30% in dense mode, which fully demonstrates the applicability of this algorithm. In Figure 7, the data of specific coverage improvement is described, from which we can see the improvement effect of different nodes under different algorithms; EFSSA is superior to other methods.

In terms of node utilization, Table 6 shows the results of performance metrics C_e. In the case of random deployment within the region, 30m × 30m of balanced deployment is close to sparse deployment except for 30 regions. As the number of nodes increases, other regions gradually decrease, indicating that the effective coverage ratio decreases gradually. These optimization algorithms optimize the coverage of the target monitoring area while reducing the real coverage index of the sensor to varying degrees. To further reflect the relationship between sensor coverage cost and coverage, Figure 8 shows different density levels, and the abscissa in the figure represents the length of square deployment area (unit: meter). In the sparse deployment experiment (Figure 8(a)), the real deployment coverage C_e of EFSSA algorithm is higher than other algorithms, resulting in relatively small redundant coverage. In the process of increasing the deployment area, the coverage rate of GWO algorithm is inferior to EFSSA. In the case of 90m × 90m area, C_e of GWO is smaller than other algorithms. In the balanced deployment experiment (Figures 8(b) and 8(c)), the effective coverage C_e of EFSSA algorithm is still superior to other algorithms. RK algorithm and GWO algorithm are generally close to EFSSA, but they have poor performance in large-scale deployment experiments.

5.2.3. Probability Coverage Experiment. According to Equation (3), this section further analyzes the sensor coverage effects of different optimization methods under the probabilistic coverage model (see Table 7).

In the probabilistic perception model structure, the coverage of the sensor edge is strongly influenced by α and β. Here, we take the value of both 0.5. Compared with Table 7, the probability of sensor coverage generally increased because of the coverage edge change from r_s in the original Boolean model to $r_s + \Delta r$ in the probabilistic model, and in this paper, Δr is 0.5 m. In Table 7, the final probabilistic coverage solved by the EFSSA algorithm outperforms all other several algorithms.

In Figure 9, the final distribution result graphs of the six algorithms, ALO, GWO, BES, RK, SSA and EFSSA, are shown when 25 nodes are deployed in a 50m × 50m area, respectively. It is clear from the figure that the coverage effect of EFSSA algorithm is the most uniform. In the probabilistic coverage model, the probabilistic coverage edges are indicated by light colors.

Similar to the Boolean model experiment, the coverage improvement effect of different algorithms under different density deployment under probability model is also given in Table 8. Although the probabilistic perception model is not completely aware of some perception regions, the perception range is increased by 0.5 m. Therefore, the initial random coverage was increased, and the improvement rate of EFSSA algorithm in dense areas was decreased compared with that of Boolean model. In Figure 10, the percentage

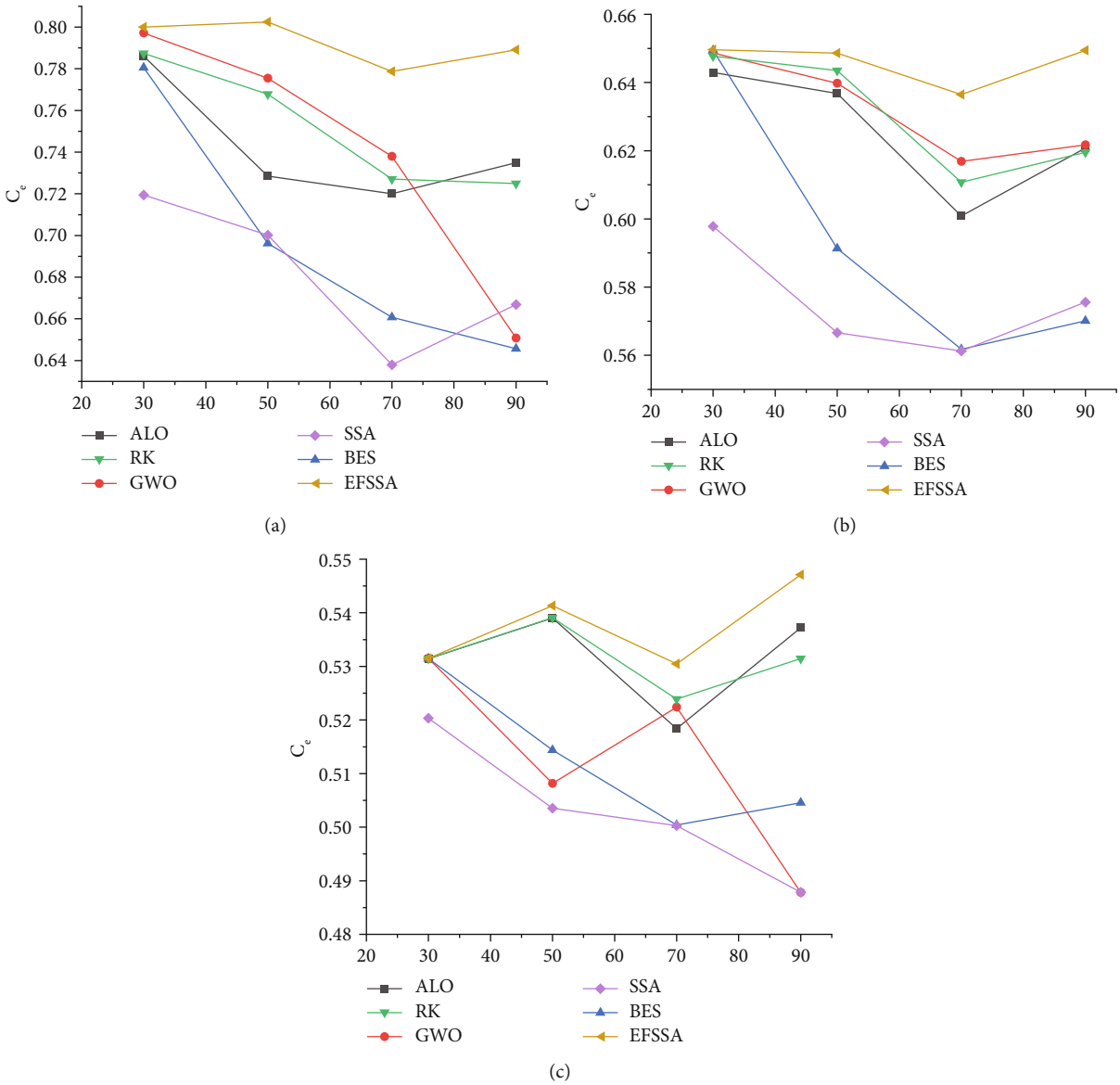

Figure 11: Coverage index C_e. (a) Sparse deployment. (b) Balance deployment. (c) Dense deployment.

improvement of these six algorithms compared to the initial coverage is shown. It can be obtained in the figure that the percentage improvement of the optimization algorithm is relatively high in the region with sparse number of nodes. And EFSSA algorithm has the highest coverage improvement compared to the other five algorithms.

In the probability model experiment, the evaluation index results C_e of real coverage are shown in Table 9. Combined with the results of EFSSA algorithm in Table 7 in deploying 9 nodes and 11 nodes, it can be found that when the sensor achieves full coverage deployment, the increase in the number of nodes will make the value of C_e drop rapidly. With three sensor deployments of different densities (see Figure 11), the C_e of the probabilistic model is generally superior to the Boolean model. The variation trend of the real coverage is almost the same, among which the variation of C_e of SSA algorithm changes greatly. Overall, the C_e of EFSSA is high and stable.

6. Conclusions

An improved metaheuristic algorithm EFSSA has been proposed and successfully applied to solve the node coverage problem of two-dimensional wireless sensor networks. Based on the original sparrow search algorithm, the elite reverse strategy and firefly strategy were combined to improve the generalization ability of the initial population and the global search ability of the population. The original sparrow search algorithm is prone to the stagnation of local optimization in the problem of high-dimensional and multilocal extremum of sensor deployment. The fluorescence effect of the firefly strategy can change the defect that the sparrow algorithm falls into local optimization. Simulation and experimental results show that the EFSSA algorithm can effectively accelerate the convergence speed of solving the optimal coverage and avoid local optima in high-dimensional problems. In Boolean model and probabilistic model experiments, the

EFSSA algorithm is more effective and feasible in applying second sensor deployment than other algorithms.

However, the method proposed in this paper has some limitations. In the experiment of sensor deployment index, the value of C_e will also drop sharply when the increase of the number of nodes almost achieves full coverage ($R_{cov} = 1$). Coverage rate R_{cov} and cost of sensor nodes are contradictory issues, and this paper does not balance this issue. It can be regarded as a multiobjective problem in the future research. In this problem, these two indicators and other possible indicators (such as network connectivity, throughput, and network delay) can be considered to establish a multiobjective model of WSN coverage, solve Pareto frontier, and give an effective scheme. There are still many challenges in the future work of sensor network deployment. For example, more constraints can be introduced, such as terrain constraints, heterogeneous sensor constraints, and deployment dimension constraints. Moreover, the optimization issues of applying EFSSA to IoT-based UAV data collection and edge computing-based sensor data collection also deserve further study.

Data Availability

The data used to support the findings of this study are available from the corresponding author upon request.

Conflicts of Interest

The authors declare no conflict of interest.

Acknowledgments

This research was supported in part by the China National Key Research and Development (No. 2018YFC0808306), Hebei Key Research and Development Program (No. 19270318D), Hebei Internet of Things Engineering and Technology Research Center (No. 3142018055), and Qinghai Internet of Things Key Laboratory (No. 2017-ZJ-Y21).

References

[1] A. Shahraki, A. Taherkordi, Ø. Haugen, and F. Eliassen, "A survey and future directions on clustering: from WSNs to IoT and modern networking paradigms," *IEEE Transactions on Network and Service Management*, vol. 18, no. 2, pp. 2242–2274, 2021.

[2] Z. A. A. Aiziz and S. Y. A. Ameen, "Air pollution monitoring using wireless sensor networks," *Journal of Information Technology and Informatics*, vol. 1, no. 1, pp. 20–25, 2021.

[3] Q. Yu, F. Xiong, and Y. R. Wang, "Integration of wireless sensor network and IoT for smart environment monitoring system," *Journal of Interconnection Networks*, vol. 2021, article 2143010, 2021.

[4] I. Ahmad, K. Shah, and S. Ullah, "Military applications using wireless sensor networks: a survey," *International Journal of Engineering Science and Computing*, vol. 6, no. 6, article 2143010, 2016.

[5] M. Erdelj, M. Król, and E. Natalizio, "Wireless sensor networks and multi-UAV systems for natural disaster management," *Computer Networks*, vol. 124, pp. 72–86, 2017.

[6] G. J. Han, X. Yang, L. Liu, W. B. Zhang, and M. Guizani, "A disaster management-oriented path planning for mobile anchor node-based localization in wireless sensor networks," *IEEE Transactions on Emerging Topics in Computing*, vol. 8, no. 1, pp. 115–125, 2020.

[7] P. K. Donta, T. Amgoth, and C. S. R. Annavarapu, "Machine learning algorithms for wireless sensor networks: a survey," *Information Fusion*, vol. 49, pp. 1–25, 2019.

[8] K. Xu, Z. Zhao, Y. Luo, G. Hui, and L. Hu, "An energy-efficient clustering routing protocol based on a high-QoS node deployment with an inter-cluster routing mechanism in WSNs," *Sensors*, vol. 19, no. 12, p. 2752, 2019.

[9] A. N. Njoya, A. A. A. Ari, M. N. Awa et al., "Hybrid wireless sensors deployment scheme with connectivity and coverage maintaining in wireless sensor networks," *Wireless Personal Communications*, vol. 112, no. 3, pp. 1893–1917, 2020.

[10] R. Priyadarshi, B. Gupta, and A. Anurag, "Deployment techniques in wireless sensor networks: a survey, classification, challenges, and future research issues," *The Journal of Supercomputing*, vol. 76, no. 9, pp. 7333–7373, 2020.

[11] B. Chen, K. Jamieson, H. Balakrishnan, and R. Morris, "Span: an energy-efficient coordination algorithm for topology maintenance in ad hoc wireless networks," *Wireless Networks*, vol. 8, no. 5, pp. 481–494, 2020.

[12] F. Aznoli and N. J. Navimipour, "Deployment strategies in the wireless sensor networks: systematic literature review, classification, and current trends," *Wireless Personal Communications*, vol. 95, no. 2, pp. 819–846, 2017.

[13] M. Rout and R. Rajarshi, "Dynamic deployment of randomly deployed mobile sensor nodes in the presence of obstacles," *Ad Hoc Networks*, vol. 46, pp. 12–22, 2016.

[14] Z. Wang, L. Tian, L. Lin, and Y. Tong, "Lattice-based 3-dimensional wireless sensor deployment," *Journal of Sensors*, vol. 2021, Article ID 2441122, 14 pages, 2021.

[15] M. Kumar and V. Gupta, "A review paper on sensor deployment techniques for target coverage in wireless sensor networks," in *2016 International Conference on Control, Instrumentation, Communication and Computational Technologies (ICCICCT)*, pp. 452–456, Kumaracoil, India, 2016.

[16] P. K. Donta, T. Amgoth, and C. S. R. Annavarapu, "ACO-based mobile sink path determination for wireless sensor networks under non-uniform data constraints," *Applied Soft Computing*, vol. 69, pp. 528–540, 2018.

[17] M. R. Senouci, A. Mellouk, and A. Aissani, "Random deployment of wireless sensor networks: a survey and approach," *International Journal of Ad Hoc and Ubiquitous Computing*, vol. 15, no. 1/2/3, pp. 133–146, 2014.

[18] M. Srinivas, P. K. Donta, and T. Amgoth, "Efficient algorithms for point and area sweep–coverage in wireless sensor networks," in *2021 Sixth International Conference on Wireless Communications, Signal Processing and Networking (WiSPNET)*, pp. 315–320, Chennai, India, 2021.

[19] C. Liu and H. Du, "t,K-Sweep coverage with mobile sensor nodes in wireless sensor networks," *IEEE Internet of Things Journal*, vol. 8, no. 18, pp. 13888–13899, 2021.

[20] D. Kandris, A. Alexandridis, T. Dagiuklas, E. Panaousis, and D. Vergados, "A survey and future directions on clustering: From WSNs to IoT and modern networking paradigms," *Wireless Communications and Mobile Computing*, vol. 2020, Article ID 4652801, 5 pages, 2020.

[21] K. Tarnaris, I. Preka, D. Kandris, and A. Alexandridis, "Coverage and k-coverage optimization in wireless sensor networks using computational intelligence methods: a comparative study," *Electronics*, vol. 9, no. 4, p. 675, 2020.

[22] A. Sangwan and R. P. Singh, "Survey on coverage problems in wireless sensor networks," *Wireless Personal Communications*, vol. 80, no. 4, pp. 1475–1500, 2015.

[23] S. S. Dhillon and K. Chakrabarty, "Sensor placement for effective coverage and surveillance in distributed sensor networks," *Wireless Communications and Networking, WCNC*, vol. 3, pp. 1609–1614, 2003.

[24] K. Xu, G. Takahara, and H. Hassanein, "On the robustness of grid-based deployment in wireless sensor networks,," in *Proceedings of the 2006 international conference on Wireless communications and mobile computings*, pp. 1183–1188, New York, United States, 2006.

[25] S. Miini, S. K. Udgata, and S. L. Sabat, "Sensor deployment and scheduling for target coverage problem in wireless sensor networks," *IEEE Sensors Journal*, vol. 14, no. 3, pp. 636–644, 2014.

[26] N. T. Hanh, P. L. Nguyen, P. T. Tuyen, H. Binh, and Y. Ji, "Node placement for target coverage and network connectivity in WSNs with multiple sinks," in *2018 15th IEEE Annual Consumer Communications & Networking Conference (CCNC)*, pp. 1–6, Flamingo Las Vegas, United States, 2018.

[27] J. Wang, Y. Gao, C. Zhou, R. S. Sherratt, and L. Wang, "Optimal coverage multi-path scheduling scheme with multiple mobile sinks for WSNs," *Materials and Continua*, vol. 62, no. 2, pp. 695–711, 2020.

[28] W. Liu, S. Yang, S. Sun, and S. Wei, "A node deployment optimization method of WSN based on ant-lion optimization algorithm," in *Proceeding of IEEE 4th International Symposium on Wireless Systems within the International Conferences on Intelligent Data Acquisition and Advanced Computing Systems (IDAACSSWS)*, pp. 88–92, Lviv, Ukraine, 2018.

[29] A. Shahraki, A. Taherkordi, Ø. Haugen, and F. Eliassen, "Node coverage optimization algorithm for wireless sensor networks based on improved grey wolf optimizer," *Journal of Algorithms & Computational Technology*, vol. 13, 2019.

[30] W. H. Liao, Y. Kao, and Y. S. Li, "A sensor deployment approach using glowworm swarm optimization algorithm in wireless sensor networks," *Expert Systems with Applications*, vol. 38, no. 10, pp. 12180–12188, 2011.

[31] X. S. Yang, "Firefly algorithms for multimodal optimization," in *International symposium on stochastic algorithms*, Springer, Berlin, Heidelberg, 2009.

[32] D. K. Sah, K. Cengiz, P. K. Donta, V. N. Inukollu, and T. Amgoth, "EDGF: empirical dataset generation framework for wireless sensor networks," *Computer Communications*, vol. 180, pp. 48–56, 2021.

[33] J. K. Xue and B. Shen, "A novel swarm intelligence optimization approach: sparrow search algorithm," *Systems Science & Control Engineering*, vol. 8, no. 1, pp. 22–34, 2020.

[34] H. Zhang and Z. Li, "Energy-aware data gathering mechanism for mobile sink in wireless sensor networks using particle swarm optimization," *IEEE Access*, vol. 8, pp. 177219–177227, 2020.

[35] J. Sengathir, A. Rajesh, G. Dhiman, S. Vimal, C. A. Yogaraja, and W. Viriyasitavat, "A novel cluster head selection using hybrid artificial bee colony and firefly algorithm for network lifetime and stability in WSNs," *Connection Science*, vol. 34, no. 1, pp. 387–408, 2022.

[36] X. Wang, Y. Deng, and H. Duan, "Edge-based target detection for unmanned aerial vehicles using competitive bird swarm algorithm," *Aerospace Science and Technology*, vol. 78, pp. 708–720, 2018.

[37] C. Li, Y. Yue, and Y. Zhang, "A data collection strategy for heterogeneous wireless sensor networks based on energy efficiency and collaborative optimization," *Computational Intelligence and Neuroscience*, vol. 2021, Article ID 9808449, 13 pages, 2021.

[38] C. Ouyang, D. Zhu, and F. Wang, "A learning sparrow search algorithm," *Computational Intelligence and Neuroscience*, vol. 2021, Article ID 3946958, 23 pages, 2021.

[39] K. Kapileswa and P. Phani Kumar, "Energy efficient routing in IOT based UWSN using bald eagle search algorithm," *Transactions on Emerging Telecommunications Technologies*, vol. 33, no. 1, 2022.

[40] I. Ahmadianfar, A. A. Heidari, A. H. Gandomi, X. Chu, and H. Chen, "RUN beyond the metaphor: an efficient optimization algorithm based on Runge Kutta method," *Expert Systems with Applications*, vol. 181, article 115079, 2021.

[41] R. Elhabyan, W. Shi, and M. St-Hilaire, "Coverage protocols for wireless sensor networks: review and future directions," *Journal of Communications and Networks*, vol. 21, no. 1, pp. 45–60, 2019.

[42] H. M. Ammari, "Connected k-coverage in two-dimensional wireless sensor networks using hexagonal slicing and area stretching," *Journal of Parallel and Distributed Computing*, vol. 153, pp. 89–109, 2021.

[43] S. Oktug, A. Khalilov, and H. Tezcan, "3D coverage analysis under heterogeneous deployment strategies in wireless sensor networks," in *In 2008 Fourth Advanced International Conference on Telecommunications*, pp. 119–204, Athens, Greece, 2008.

[44] H. R. Tizhoosh, "A survey and future directions on clustering: from WSNs to IoT and modern networking paradigms," in *International conference on computational intelligence for modelling, control and automation and international conference on intelligent agents, web technologies and internet commerce (CIMCA-IAWTIC'06)*, pp. 675–701, Sydney, Australia, 2006.

[45] X. Wu, X. Shen, J. Zhang, and Y. Zhang, "A wind energy prediction scheme combining Cauchy variation and reverse learning strategy," *Advances in Electrical and Computer Engineering*, vol. 21, no. 4, pp. 3–10, 2021.

Hindawi
Wireless Communications and Mobile Computing
Volume 2022, Article ID 1830201, 12 pages
https://doi.org/10.1155/2022/1830201

Research Article

An Android Malware Detection Leveraging Machine Learning

Ahmed S. Shatnawi,[1] **Aya Jaradat**,[2] **Tuqa Bani Yaseen**,[2] **Eyad Taqieddin**,[2] **Mahmoud Al-Ayyoub**,[3] **and Dheya Mustafa**[4]

[1]*Department of Software Engineering, Jordan University of Science & Technology, Irbid 21110, Jordan*
[2]*Department of Network Engineering and Security, Jordan University of Science & Technology, Irbid 21110, Jordan*
[3]*Department of Computer Science, Jordan University of Science & Technology, Irbid 21110, Jordan*
[4]*Department of Computer Engineering, Faculty of Engineering, The Hashemite University, Zarqa 13133, Jordan*

Correspondence should be addressed to Ahmed S. Shatnawi; ahmedshatnawi@just.edu.jo

Received 4 December 2021; Revised 23 March 2022; Accepted 8 April 2022; Published 6 May 2022

Academic Editor: Mohamed Elhoseny

Android applications have recently witnessed a pronounced progress, making them among the fastest growing technological fields to thrive and advance. However, such level of growth does not evolve without some cost. This particularly involves increased security threats that the underlying applications and their users usually fall prey to. As malware becomes increasingly more capable of penetrating these applications and exploiting them in suspicious actions, the need for active research endeavors to counter these malicious programs becomes imminent. Some of the studies are based on dynamic analysis, and others are based on static analysis, while some are completely dependent on both. In this paper, we studied static, dynamic, and hybrid analyses to identify malicious applications. We leverage machine learning classifiers to detect malware activities as we explain the effectiveness of these classifiers in the classification process. Our results prove the efficiency of permissions and the action repetition feature set and their influential roles in detecting malware in Android applications. Our results show empirically very close accuracy results when using static, dynamic, and hybrid analyses. Thus, we use static analyses due to their lower cost compared to dynamic and hybrid analyses. In other words, we found the best results in terms of accuracy and cost (the trade-off) make us select static analysis over other techniques.

1. Introduction

Cybersecurity has become a primary area of immediate concern to computer scientists and network engineers that satisfactory solutions to many issues are in order. As a result of the rapid evolutions in technology developments and their inherent integrations in all aspects of our lifestyles, a variety of malware applications and their intended targets have become well studied and identified. Among the malware variety that has received attention lately is Android malware which is found to occupy considerable attention in the web world. Android is one of the most common operating systems that dominates the operating system market. In 2020 [1], the Android system accounted for 85% of the total number of smartphones that harness the Android system as the operating system of choice.

In general, an Android system inherently supports a whole host of applications. At the end of April 2020, the number of these applications exceeded the 2.8 million mark [2]. The variety of these applications are commonly found on Google Store, which is home to most Android applications. Moreover, the increasing reliance on this system by application developers and users together with its friendly nature has made it more prone for malware to sneak into these applications [3]. This is by nature of the fact malicious programs execute their functionalities in a seamless manner and are assisted by several key factors. These include, amongst others, calling a third-party code, the environment under which an Android application operates [4], in addition to the level of permissions allowed.

Malware invasive techniques continue to evolve with the aim of evading detection [5], as some malware applications contain more than 50 variables that make detecting them a

great challenge. Therefore, it is necessary to work on finding methods capable of dealing with the continuous evolution of Android malware to detect it, where it happens, and deactivate/remove it effectively [6]. All such challenges did indeed preoccupy researchers in the area and prompted them to do research to discover malware and tackle it in a proper manner [7]. As a result, researchers were able to develop three mechanisms to detect Android malware that fell under static, dynamic, and hybrid analyses techniques. Static analysis is harnessed with the objective of extracting the features that help us identify harmful behavior for an application without a need for actual application deployment. However, this type of analysis was found to suffer from code obfuscation techniques that help malware authors to evade static detection techniques [8]. Dynamic analysis, however, is leveraged to determine the malware behavior of an application during its runtime such as during system calls. Generally, the static analysis feature provides the ability to locate the malware component through the source code, as the dynamic analysis feature provides the ability to identify the malware location through in a runtime environment [4].

In this paper endeavor, we propose a model for Android malware detection based on a combination of static and two dynamic analyses (hybrid analysis) together with machine learning classifiers. In the hybrid analysis part, we set out by conducting experiments through which we would extract those features that can provide the maximum possible amount of important information about the application's behavior by rank selection. After that, we apply different machine learning (ML) algorithms and compare the performance of each to identify the most accurate algorithm. In this, ML is one of the modern technologies currently widely used in many areas, including malware detection, as it is used in the classification process and the selection of features.

The process of selecting and extracting features is one of the most critical steps in an Android malware detection process. The efficiency in feature extraction readily determines the detection quality. Hence, extracting and selecting certain features from the hotspots must be given particular attention in the malware detection process [9–11]. Nonetheless, there are some concerning obstacles that could be encountered in the feature selection process:

(i) The feature extraction process may consume considerable time due to the large size of the Android data file; as the number of features may be in millions, the entire process of extracting features could pose some serious burdens. Furthermore, it is also possible for the malware detection process to become ineffective depending on the choice of some of the features that may have a low impact on the accurate Android malware detection

(ii) As a result of the rapid development and evolution of Android applications, the process of extracting and selecting features is observing continuous improvement due to a large reservoir of different behaviors of the applications and the various forms that have emerged; it is quite possible to reach a feature that had not been met/identified before which ultimately could interject significant bearing towards a more accurate detection process

(iii) It is often that a feature could get selected undercutting the algorithm's ability to skip unnecessary program execution paths, rendering the detection accuracy ineffective for all potential cases. Therefore, one aim of this study would be so to choose the features accurately towards the "best" detection accuracy

Therefore, the main contribution of our paper is to detect malware based on a hybrid analysis scenario, whereby we combine several dynamic and static features together. Here, the permissions represent the static feature that is extracted from the manifest file, which can either be the port and/or the IP address, whereas the action repetition represents the dynamic features that were extracted during the implementation of the application. The action repetition feature is one of the features that is being explored for the first time, including its use with the permissions. In the work presented here, we used four machine learning classifiers with particular abilities to classify correctly when selecting the features appropriately. The results of our evaluation have shown that our system is fairly competitive in terms of the accuracy attained in the malware detection process.

In short, the contribution in this research work fulfills several objectives:

(i) Introduce a new feature, which was never addressed in the literature. This is particularly manifested in the action repetition, whereby actions are monitored and tracked, with the repetition number leading to the detection of a harmful behavior

(ii) Contrive a new, practical and highly effective system capable of detecting malware, leveraging a set of features, the most important of which are action repetition and permissions. The objective, here, entails arriving at experimental results that reflect high accuracy and sufficient efficacy, in an effort to demonstrate the effectiveness of our proposed system

The rest of this paper is organized as follows: Sections 2 and 3 shed some light on related background work. Section 4 describes the methodology proposed in this paper. Sections 5 and 6 discuss the experimental setup used and evaluation of results, respectively. Section 7 arrives at key conclusive remarks of the work addressed in this paper.

2. Background

Malware is a term used to refer to software with inherent malicious objectives. They present illegal activity targeted by attackers towards theft of data or user credentials [12].

Applications form an attack vector through which malware can be delivered on mobile devices. Most users have limited expertise to identify the permissions required by an application nor the exploits that may appear through them. Furthermore, installing the process of selecting and

extracting features is one of the most critical steps in an Android malware detection process.

Many researchers use traditional malware analysis techniques wherein they are restricted between two practical approaches to detect such malware. The Android malware detection analysis-based approaches are static, dynamic, and hybrid. The following subsections introduce these analysis methods, briefly summarizing their employed features. Static-based malware binary classification static analysis involves unpacking the application to analyze the code for any malicious content. By decompiling the files, it is possible to identify critical parts of the code [13]. This may also involve extracting features from the disassembly of the underlying Java code and the AndroidManifest.xml file [13].

This type of analysis does not involve any execution of the application. Accordingly, it does not require large resources and is considered faster in comparison to other approaches [14]. However, with the explosive growth in the number of Android applications, it has become rather challenging to rely solely on such an approach as some malicious applications use repackaging or obfuscation to bypass detection. Meanwhile, dynamic-based malware classification analysis leverages activities associated with an application as the application is being executed. It may involve some interaction from the user or other processes in order to trigger the malicious behavior [15]. Here, the actions of the application are monitored to detect abnormalities in the system call, network activity, processor load, phone calls initiated, or SMS sent in order to extract the dynamic features. Dynamic analysis has an advantage of recording the applications' behavior and detecting any dynamic code being loaded at runtime, which makes it favorably popular for malicious code analysis [16]. However, a major drawback of this form of analysis is the added overhead on the operating system, which makes it harder to implement. Furthermore, it takes a long duration to complete due to the fact that monitoring the activities may not yield useful results without proper triggers.

Hybrid analysis malware classification is a type of analysis that mix of both the static and dynamic analyses to benefit from their combined advantages. It involves analyzing the source files of the application along with monitoring the behavior at runtime. Here, although it achieves higher detection accuracy, it has been found to suffer from the drawbacks of both previous approaches in terms of long duration for detection and consumption of the operating system resources [17].

3. Related Work

Several efforts related to Android malware detection have been addressed in the literature. In the sequel in this section, we present a rundown of the most relevant papers with respect to static, dynamic, and hybrid malware analysis.

The work presented in [18] introduced a static-based malware detection method. There, the authors consider the API call feature by extracting it using correlative analysis. Furthermore, three machine learning algorithms, support vector machine (SVM), random forest (RF), and k-nearest neighbor (KNN), were used to train the feature in order to classify the application as either benign or malicious. The RF classifier produced the best results in terms of accuracy. In [19], Ratyal et al. introduced a model in which they use the features of Android permissions and Android destinations to detect malware. According to the authors, these two features resulted in improved detection. Another approach for static analysis was introduced in [20]. The features were determined based on three steps: graph creation, sensitive node extraction, and method creation. The authors employed four classifiers, of which RF was the best in terms of classification accuracy.

Static analysis was also addressed in [21] by checking open sockets, message digest, and reflection code. The paper develops a process of identifying malware which resulted in 96% accuracy leveraging RF machine learning methodology.

Cai [22] studied the sustainability problem for ML-based app classifiers. He defined sustainability metrics and compared them among five state-of-the-art malware detectors for Android. He also built an infrastructure to mine a mobile software ecosystem with three elements; the mobile platforms, user apps built on the platforms, and users associated with the apps [23]. Fu and Cai investigated the deterioration problem of defense solutions against malware using machine learning classification for four state-of-the-art Android malware detectors [24].

The work in [25] proposes an estimation method that is based on an entropy approach in choosing the best features, thereby averting the need for a standard procedure that chooses all the features to differentiate between benign and harmful malware, particularly that APK files possess many features, making any standard process rather cumbersome and infeasible. The approach in [25] was shown to achieve an accuracy of 96.9% in KNN and SVM machine learning.

Meanwhile, several works in the literature have addressed different approaches of classification harnessing dynamic analysis. In [26], three input generation techniques were used: state-based, random-based, and hybrid techniques. There, the authors use the DroidBot and Monkey tools to extract features from the generated log files. Their results indicate that the best classification results were achieved using RF. The works in [27, 28] also use dynamic analysis to create the permissions then use WEKA to collect the permissions. The main difference between the two papers lies in the number of classifiers used. The former uses five classifiers, with the best results reported were achieved when using the simple logistic (SL), J48, and RF techniques. On the other hand, the work in [28] uses seven classifiers and shows the best classification outcomes when employing RF techniques.

Authors in [29] extract the dynamic analysis features by using the structure, safety, and intercomponent communication dimensions. They found that the features that were extracted using the dimensions of the structure were more important than the other two.

Cai and Jenkins targeted a sustainable Android malware detector that, once trained on a dataset, can continue to effectively detect new malware without retraining [30]. DroidEvolver [31] is an Android malware detection system that can automatically and continually update itself during malware detection without any human involvement.

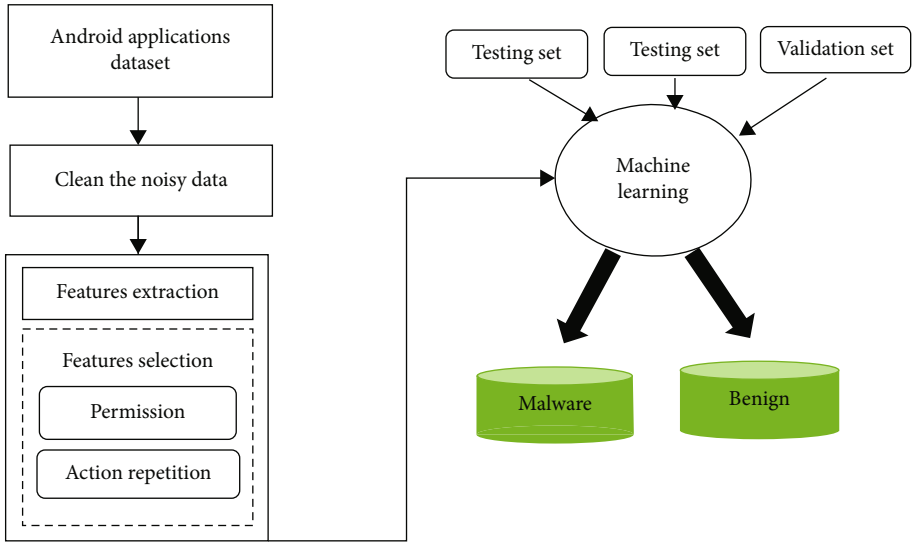

Figure 1: Proposed hybrid analysis approach.

In [16], the authors introduce a malware detection mechanism in which they rely on hybrid analysis features, namely, API calls, permissions, and system calls. They use the tree augmented naive Bayes to capture the interrelation between static and dynamic features. The mechanism used in [29] was shown to achieve a detection accuracy of 97.

The SAMADroid and StormDroid techniques presented in [32, 33],, respectively, offer hybrid analysis tools. The SAMADroid approach combines static and dynamic analysis on both local and remote hosts. The tool uses SVM, RF, and naïve Bayes (NB) and achieves high accuracy in detecting malicious programs. It further adds the advantage of low energy consumption and improved storage efficiency. The StormDroid approach, on the other hand, extracts static and dynamic features from permissions and sensitive API calls by sequencing them directly in the source code.

Another more recent hybrid approach is addressed in [16]; the malware detection model presented is based on a tree augmented naive Bayes (TAN), which uses conditional dependencies against both static and dynamic features such as API permissions and system calls. It then detects malicious behavior by combining the outputs of both of these features as gained from the classifier. Although the model shows 97% accuracy, it does not show the android version or user input generated during dynamic analysis.

In [34], a different hybrid detection system is proposed. The model uses SVM and a linear classifier based on a new open source framework called CuckooDroid. The framework enables Cuckoo Sandbox's features by a misuse detector—"an approach in which attack patterns or unauthorized and suspicious behaviors are learned based on past activities and then the knowledge about the learned patterns is used to detect or predict similar subsequent such patterns in a network.". Misuse detection is commonly adopted to detect well-known malware and classify android malware by combining static and dynamic analysis techniques together. The proposed model benefits from the low false-positive rate of misuse detection and the ability of anomaly detection to detect zero-day malware and is evaluated using 5560 malware and 12000 benign samples. This model was shown to achieve 98.79% accuracy detection rates when classifying 98.32% of the malware samples.

In [35], the authors extract the API and permissions from the source code to access the static analysis features. They also consider the total time needed for the system to extract the dynamic analysis features. The detection accuracy reached based on this came out to be 93.33%. Along the same context, authors in [17] apply the static, dynamic, and hybrid analysis techniques and draw their comparisons. They conclude that the hybrid analysis approach was the one to achieve the better results.

Note, however, that although the hybrid analysis approach was shown to be superior to static or dynamic, the feature selection process remains the most critical factor in determining the detection accuracy.

Several studies investigated Android application permission system. REAPER [36] is a tool that traces the permissions requested by apps in real time and discriminates them from other permissions requested by third-party libraries linked with the app. Fasano et al. [37] proposed a formal method to detect the exact point in the code of an Android application where a permission is invoked at runtime. Dilhara et al. [38] proposed a technique to automatically detect the incompatible permission used in a given app and repairs them when found.

4. Methodology

This section presents our proposed methodology to the classification process. The general methodology of the proposed malware detection Android systems is shown in Figure 1. Commensurate with the figure, the hybrid approach is divided into two stages: (1) static analysis and (2) dynamic analysis. In the first phase of the static analysis stage, APK files are converted from XML to JSON. After that, the process of scanning JSON files begins to extract the permissions

pertinent to the application involved. Once these permissions are made available via static analysis leveraging machine learning, the application is classified as either malicious or suspicious. With this, the static analysis stage terminates, as the dynamic analysis stage commences. The dynamic analysis phase aims to do more checks for any suspicious application. By analyzing the application's runtime behaviors, the application in question is executed to determine the observed dynamic features such as system call, score, intent, and action. The dynamic features obtained are made available for dynamic analysis based on machine learning for final classification. In the process, suspicious applications are classified as either malicious or benign. The applications that get classified as malware are added to the list of malware, as applications that got classified as benign get added to the list of benign applications for future reference.

Each step will, in turn, be separately explained below.

4.1. Dataset. Several studies presented and tested a large-scale datasets of android applications including runtime traces for research community, such as AndroCT [39] and AndroZoo [40]. In this paper, we use a dataset that consists of benign, malware, and Greyware applications. Palo Alto Networks collected these data over a month period back in 2017 [41]. It was derived from a series of mixed Android APK files containing an XML report representing the metadata built during the static and dynamic analyses.

4.2. Extraction of Features. In recent times, it has become common practice to come across datasets containing hundreds of thousands of features. Over time, it became more noticeable that the number of features often converges to the number of observations stored in the database, something that results in attaining a machine learning model that suffers from overfitting [42].To avoid this problem, the tendency is to reduce the number of features by creating a new set of features deduced from the original set, as we create a set of features capable of reducing most of the data's original features. Therefore, in this proposed work, we aim to extract the most prominent features out of dynamic and static analysis while marginalizing the less valued features to create a new set of dynamic and static features.

In reviewing various dataset files emanating from a multitude of applications, it was observed that certain features (over others), both dynamic and static, could particularly impact the classification process altogether. More precisely, we noticed that certain actions were frequently repeated in multiple malware files. We also noticed that three ports were the most that were being used: 443, 80, and 5200. Additionally, we noticed certain IP addresses that were often used, which were sources for further attention and suspicion.

In our database there are two types of analysis:

(1) In the database files subject of our investigation, we conducted two types of analysis: static analysis: the features emanating from this were extracted directly from the source code of the applications. Moreover, among the features that could, also, be extracted from APK applications include the following:

  (i) Permissions: on Android systems, the permission mechanism is relied upon to protect the privacy of users, with the particular objective of requesting permission from the application in order to access data and system features such as calls and camera as most of the time these programs want to request a special set of permissions. Hence, it is good to scrutinize this with care when extracting the anticipated features

  (ii) Intent: usually, some malware families use intent to activate their malicious activity directly after restarting smart devices

  (iii) Suspicious API calls: it is a set of application interfaces that can be used to access sensitive resources and information, as it sometimes leads to harmful behavior without any permission request

  (iv) Restricted API calls: this type of API call aims to achieve roughly the same goal as would suspicious API calls, save for the fact that it is protected by permissions

(2) Dynamic analysis: this type of analysis addresses the features that can be extracted during the implementation of an application under a safe environment where the implementation process is recorded. In our research, there is a number of dynamic features that can be extracted from Android applications. Features that can be extracted during the implementation of the applications include the following:

  (i) DNS query: it is a request which requires information sent from the user to the server. It is considered one of the solutions used to discover and block DNS queries for malicious behavior

  (ii) IP address: there is a number of factors that can make an IP address a suspicious address. Amongst these factors is the sending a lot of spam and linking to devices full of malware and other different suspicious patterns of behavior. Therefore, it is rather essential to be able to differentiate between the IP addresses are they benign or those that arouse suspicion

  (iii) Port: the port feature is a virtual site that establishes connection to the network from the beginning right to the end of the interval of interest, as when sending a package or a group of specific IP address packets. The computer would identify the port to which the packets will be directed commensurate with the components of the application or package

  (iv) Action: this feature refers to an application's activity and is represented in the number of diverse behaviors and activities, which are represented by patterns of access that may be normal or suspicious. Therefore, identifying these

activities is very important because they lead to identify the particular suspicious activity and its source, thereby mitigating any damage caused by such activities

4.3. Feature Selection. After completing the stage of features extraction and identifying new features, we move on to selecting the features stage. The feature selection process is one of the most important steps with which we aim to choose the features from the pool of newly identified features in such a way as to achieve an increase in accuracy, a reduction in complexity, and, in the meantime, avoid any overfitting. Researchers have traditionally applied a number of feature classification approaches to detect malware in applications. In this endeavor, we particularly employ the feature rank approach, as this method leverages certain crucial elements in the arrangement of features due to its ability to choose the appropriate features needed to build the malware detection models.

The feature rank process is based on the random forest [43], as it is one of the ML methods, due to its relatively good accuracy, simplicity, ease of use, and strength. All of these harvested advantages have made it a powerful way to choose features. The random forest (RF) approach consists of a group of decision trees. Each node in the decision tree represents one particular feature, which makes measuring the importance of the feature a fairly simple process. When training a decision tree, we calculate the amount of each feature that reduces impurities in the tree. When applied to the forest, the average impurity reduction for each feature is calculated to arrange the features according to the average number of impurities.

The feature selection process, depending on random forests, can be summarized as follows:

(i) As a first step, we work towards classify each feature separately by implementing a random forest algorithm

(ii) As a second step, we work on classifying features based on minimizing impurities, as the features of less importance are removed, while other features are preserved

(iii) In the third step, we basically reapply the random forest algorithm to the retained features, with the objective of accessing the final essential features

Our dataset contains several features, as we may use all of these features in the process of detecting malware.

After completing the feature selection process based on RF, we obtain the top dynamic and static features:

(1) Dynamic: action repetition

(2) Static: permissions

4.4. Machine Learning Techniques. Machine learning is an integral part of artificial intelligence. It is based on self-learning and development depending on vast amounts of data without clear programming. Machine learning is divided into supervised machine learning, unsupervised machine learning, semisupervised machine learning algorithms, and reinforcement machine learning algorithms. Supervised machine learning algorithms are the most widely used because they depend on the classification of a dataset. This is particularly so due to their ability to analyze the training dataset, and they can classify them into classes according to their characteristics [42].

In this paper, we opted to implement four machine learning algorithms: naïve Bayes (NB) that is based on the principle of maximum likelihood; random forest (RF), which is based on the initiation of packing and the random characteristic for decision making; the decision tree (DT), which is based on the principle of computing all traits and then making the decision; and XGBoost which enhances parallel tree boosting with a fast and accurate mechanism together with gradient boosting. In the sequel, we discuss the features for each algorithm separately, as follows:

(1) The random forest (RF) algorithm: RF is one of the standard algorithms used for the intended purpose; it is based on decision trees, leading to better prediction accuracy. The nomenclature (forest) draws on the fact that it contains a group of decision trees, and it is used with the objective to develop the trees based on independent subsets of the dataset. The algorithm stands out due to its ease of calculation and ability to adapt quickly, and it is considered a stable algorithm

(2) The decision tree (DT) algorithm: DT is one algorithm that leverages the training process to build data structures resembling a tree structure. It is used to make predictions about the test data. The tree that is established as such consists of decision nodes and leaf nodes. This algorithm has gained wide popularity due to its simplicity. Further, its achieves higher accuracy based on fewer decisions taken [44]

(3) XGBoost: this is an algorithm that is considered one of the improved algorithms. It was first derived with the objective to set up an algorithm that achieves high efficiency, portability, and fast calculations. It is now one of the most widely used algorithms in machine learning due to its ability to deal effectively in handling a whole host of problems, be they regression or classification type problems; and it has proven itself well in terms of speed and robustness

(4) The gradient boosting algorithm: the idea behind this algorithm arose from the idea of reinforcement. It functions based on iterative learning, and how many weak learners there exists, in order to obtain a robust model capable of dealing with classification and regression problems. It represents an algorithm capable of improving the cost function [45]

5. Experiment Setup

In this section, we will discuss the steps that were followed in this work to achieve detection of malware in more elaborate detail.

```
1.  Being
2.  Create array of action from apk_ api.
3.  Create array,it have malware permissions which are used by applications.
4.  Read the File dynamic and Static analysis.
5.  For X in range Files
6.  Path File _Dynamic= files [dynamic _json_ file_ path][x]
7.  Path File _Static= files [static _ json_ file_path][x]
8.  open path file_ dynamic
9.  dynamic_feature= load data
10.  open path file_ static
11.  static_feature= load data
12.  Insert [id = dynamic_feature,
13.  port = dynamic_feature,
14.  Ip=dynamic_feature,
15.  If dynamic features.get(action)==action[i]
16.  action =dynamic _features,
17.  If static features.get(permission)==permission[i]
18.  permission=static _feature
19.  end
```

Algorithm 1: Pseudocode of the selection features.

5.1. Data Preparation. At the onset of this research endeavor, we reviewed numerous files for benign and malware-infected applications. Particularly, we had to deal with a total of 195623 applications, consisting of 104747 malware-containing applications and 90876 benign applications. However, the application files would contain some unwanted/unnecessary files that must be removed before pursuing any of the steps prescribed herein as they would not offer adequate pertinent information. Consequently, we ended up having to deal with 166710 files.

With that, we had to split out the static benign files pursuant with their size as the variation in file size ranged from 2.17 KB to 4.12 MB. Files got divided it into two groups; the first group contained files the sizes for which were found to exceed 1 MB; the other group contained data that was less than 1 MB in size. Meanwhile, there was no need to make a similar split for the dynamic benign files. This was not particularly needed as the variations in the file sizes exhibited a smaller range: 498 bytes to 1 MB. Finally, the malware files were split out according to the family labels, which were made up of five families: Trojan, Pup, Adware, Spyware, and Riskware.

5.2. Extract and Select Features. In the next phase, the most important features were extracted and selected based on the classification process prescribed earlier. Algorithm 1 illustrates the feature selection process where we first read all the dynamic and static files within the field. Then, we load the essential features and rely on the following dynamic feature: being action repetition. In the process, we extracted all actions for malware and benign applications with a total number of 176 actions. We also relied on the static permissions feature and extracted the most important permissions that referred to malware applications, where we extracted 668 permissions from a total of 4276 permissions. In the sequel, we will elaborate further on the importance of the permission and the action repetition features. Additionally, we will scrutinize some of the permissions and the action repetitions with the highest bearing on the classification process:

Table 1: Permission for static analysis.

Importance	Features name
0.587484	android.permission.WRIT_EXTERNAL_STORAGE
0.088250	com.google.android.c2dm.permission.RECEIVE
0.049034	android.permission.READ_LOGS
0.033341	android.permission.vending.BILLING
0.018864	android.permission.USE_CREDENTIALS
0.014858	android.permission.GET_PACKET_SIZE
0.013001	android.permission.ACCESS_NETWORK_STATE
0.012275	android.permission.GET_TASKS
0.011658	android.permission.SYSTEM_ALERT_WINDOW
0.010321	android.permission.CAMERA

(1) Permissions: Android permissions are one of the most important security features that can be provided in Android systems as most applications that are downloaded through the Android Play Store are accompanied by a set of permissions that each application requires. Therefore, it is one of the important features that has a great impact on the process of detecting malware. In our experience, a number of permissions were extracted that had the top impact on the classification process, as shown in Table 1

(2) Action repetition: monitoring the actions of Android applications is an important process, as it is one of the features that helps to identify harmful procedures from others, but we have depended on our work on the frequency of these procedures in the

Table 2: Action repetition for dynamic analysis.

Importance	Features name
0.302175	APK file removed the launcher icon
0.197239	File tried to connect to a malicious URL
0.090943	APK file deleted a file
0.080813	APK file displayed a float window
0.026626	APK file uploaded geolocation information to the remote server
0.025072	APK file fetched the information of apps installed on the device
0.023656	File wrote a file on the device
0.021470	APK file tried to connect to the URL
0.020729	File wrote an ELF library file on the device
0.017581	APK file sent out an SMS message

classification process, being that sometimes the procedure may not indicate the presence of malware programs, but repetition may lead to the discovery of these programs. Table 2 shows ten of the top actions relied in classification

5.3. Training of Machine Learning-Based Classifiers. During this stage, we split the dataset into training dataset (70%), testing dataset (15%), and validation dataset (15%). The training dataset is used to build the model. Once the model is established, we use the test dataset to determine whether the model was trained properly in order to provide the most accurate results. The training dataset used consists of 104747 malware applications and 90,876 benign applications. The training process for a machine learning-based static and dynamic analyzer begins by analyzing an Android application into JSON files to extract the permission-related features; the extracted permissions are out of a total of about 668 unique permissions. Furthermore, about 176 actions are collected by the dynamic analyzer. As the training process commences both static and dynamic features are identified concurrently.

Meanwhile, to handle the malware families, we broke them down commensurate with the data split ratios as shown in Table 3.

Table 3: Malware family details.

Family_ Label	Number	Traning (70%)	Testing (15%)	Validating (15%)
Adware	4661	3263	699	699
Riskware	5	3	1	1
Trojan	82425	57697	12364	12364
Spyware	54	38	8	8
Pup	17603	12323	2640	2640

6. Results and Discussion

In this section, we provide the details of the steps that were taken to investigate the results that were obtained. We, also, analyze the performance of the various classifiers used in the study, showing the results for four different machine learning algorithms (RF, DT, XGBoost, and gradient boosting) used in detecting malware with the grid search mechanism being employed for hyperparameter tuning. This is illustrated in Table 4.

We applied classifiers to dynamic and static features, each applied independently to the appropriate type of features involved. Our results have been categorized commensurate with results based on dynamic features without permissions, results based on static features without action repetition, and results based on dynamic and static features.

Equations (1), (2), (3), and (4) show the measures that were taken in the process of testing the performance for each machine learning algorithm. Pursuant with the equations shown, FP (false positive) refers to the number of applications classified as malware when, in reality, they are benign. FN (false negative) refers to the number of applications classified as benign but, in reality, can readily be classified as malware. TP (true positive) indicates the number of applications that are properly classified as malware, while TN (true negative) indicates the amount of applications that are properly classified as benign.

$$\text{Recall} = \frac{\text{TP}}{\text{TP} + \text{FN}}, \tag{1}$$

$$\text{Precision} = \frac{\text{TP}}{\text{TP} + \text{FP}}, \tag{2}$$

$$\text{Accuracy} = \frac{\text{TP} + \text{TN}}{\text{TP} + \text{FP} + \text{TN} + \text{FN}}, \tag{3}$$

$$F1 - \text{Score} = \frac{2 * \text{Precious} * \text{Recall}}{\text{precious} + \text{Recall}}. \tag{4}$$

The static, hybrid, and dynamic models would normally be expected to achieve high F1 score, accuracy, recall, and precision. We trained the analysis tool used on some dataset and used optimized parameters for machine learning. In the proposed mechanism, we firstly do the static analysis part comprising the manifest file, which includes permission. Following this, the mechanism, as prescribed, invokes the dynamic classification model and detects it under a control

Table 4: Grid search setting.

Classifier	Parameter
XGBoost	Permission Only:{'learning rate':0.1,'max_depth':10,'n_estimators':500,'subsample':0.5} Action Only:{'learning rate':0.1,'max_depth':10,'n_estimators':200,'subsample':1.0} Permission & Action:{'learning rate':0.1,'max_depth':5,n_estimators':500,'subsample':0.5}
Gradient boosting	Permission Only: {'learning rate':0.1,'max_depth':10,'n_estimators':500,'subsample':0.5} Action Only:{'learning rate':0.1,'max_depth':10,'n_estimators':200,'subsample':1.0} Permission & Action:{'learning rate":0.1,max_depth':5,'n_estimators':500,'subsample':0.5}
DT	Permission Only:{'criterion':'gini' ,'max_depth':10 ,'max_features':'auto','n_estimators':100}; Action Only:{'criterion': 'gini', 'max*depth*' : 7,' *maxf eatures*' :' *log2*,' *nestimators*' : 10} Permission & Action:{'criterion':'entropy','max_depth":7,'max_features':'auto','n_estimators':10}
RF	Permission Only:{'criterion':'gini','max_depth':10,'max_features':'auto','n_estimators":100} Action Only:{'criterion': 'gini', 'max*depth*' : 7,' *maxf eatures*' :' *log2*,' *nestimators*' : 10} Permission & Action:{'criterion':'entropy','max_depth':7,'max_features':'auto','n_estimators':10}

Table 5: The summary of results of validation file.

Classifier	(a) Static feature result				(b) Dynamic feature result				(c) Hybrid feature result			
	Accuracy	Precision	Recall	F1_ score	Accuracy	Precision	Recall	F1_ score	Accuracy	Precision	Recall	F1_ score
Gradient boosting	0.9954	0.996	0.9967	0.9964	0.993	0.997	0.992	0.994	0.997	0.998	0.996	0.997
XGBoost	0.9956	0.9959	0.9971	0.9965	0.993	0.997	0.992	0.994	0.998	0.999	0.997	0.998
Decision tree	0.9946	0.99501	0.9964	0.9947	0.987	0.991	0.989	0.987	0.996	0.997	0.996	0.996
Random forest	0.962	0.947	0.994	0.970	0.943	0.967	0.941	0.954	0.976	0.994	0.967	0.980

Table 6: The summary of results of test file.

Classifier	(a) Static feature result				(b) Dynamic feature result				(c) Hybrid feature result			
	Accuracy	Precision	Recall	F1_ score	Accuracy	Precision	Recall	F1_ score	Accuracy	Precision	Recall	F1_ score
Gradient boosting	0.995	0.994	0.9969	0.996	0.993	0.997	0.991	0.994	0.997	0.999	0.997	0.998
XGBoost	0.995	0.9946	0.997	0.9958	0.993	0.997	0.991	0.994	0.998	0.997	0.997	0.998
Decision tree	0.9941	0.994	0.9969	0.9942	0.987	0.991	0.988	0.987	0.995	0.997	0.996	0.996
Random forest	0.946	0.951	0.994	0.972	0.943	0.965	0.942	0.953	0.974	0.993	0.966	0.979

environment. Finally, the proposed method would apply the hybrid model. In this way, we would have tested the application against the three different models explained.

The static, hybrid, and dynamic models would normally be expected to achieve high F1 score, accuracy, recall, and precision. We trained the analysis tool used on some dataset and used optimized parameters for machine learning. In the proposed mechanism, we firstly do the static analysis part comprising the manifest file, which includes permission. Following this, the mechanism, as prescribed, invokes the dynamic classification model and detects it under a control environment. Finally, the proposed method would apply the hybrid model. In this way, we would have tested the application against the three different models explained.

Table 5 shows a summary of validation results file. The results show comparable results when XGBoost and gradient boosting are used while reflecting favorably better results than when both DT and RF are implemented. Further, Table 6 shows a summary of the test file results. The results reveal comparable results when both XGBoost and gradient boosting are used and better results than when both DT and RF are applied.

From the results obtained, note that all the classifiers have achieved good results. In our work, we particularly relied on the action repetition feature in which the actions are related to each other. Moreover, the results indicate that we, in fact, have identified a feature which had not been targeted directly, namely, action repetition. Finally, we observe from the our work done on each of the features separately, or when applying the hybrid analysis method, that we have achieve good results in the classification process. Now, in order to analyze the required cost needed in terms of device memory and CPU for every model we evaluated in our experiments, we captured the cost needed for both training and execution using the IPython command which was particularly used to capture these factors:

Table 7: Permission.

Classifier	Train			Test			Validate		
	CPU times		Wall time	CPU times		Wall time	CPU times		Wall time
	User	System		User	System		User	System	
Gradient boosting	9 min 17 s	549 ms	17 min 23 s	1.07 s	20 ms	1.09 s	1.09 s	24 ms	1.1 s
XGBoost	53 min 45 s	1.81 s	2 min 44 s	1.64 s	1 ns	91.8 ms	1.76 s	4.401 ms	142 ms
Decision tree	16.5 s	996 ms	6.33 s	515 ms	36 ms	121 ms	530 ms	20.1 ms	123 ms
Random forest	2.41 s	56 ms	2.49 s	57.7 ms	1 ns	55.6 ms	57 ms	7 Ms	54.9 ms

Table 8: Action.

Classifier	Train			Test			Validate		
	CPU times		Wall time	CPU times		Wall time	CPU times		Wall time
	User	System		User	System		User	System	
Gradient boosting	56 s	696 ms	10 min 40 s	707 ms	64 ms	898 ms	731 ms	68 ms	918 ms
XGBoost	2 min 23 s	292 ms	16.8 s	1.94 s	60 ms	357 ms	1.91 s	64 ms	356 ms
Decision tree	969 ms	852 ms	1.84 s	222 ms	136 ms	385 ms	217 ms	140 ms	385 ms
Random forest	1.77 s	100 ms	1.98 ms	130 ms	64 ms	342 ms	108 ms	104 ms	357 ms

Table 9: Action and permission.

Classifier	Train			Test			Validate		
	CPU times		Wall time	CPU times		Wall time	CPU times		Wall time
	User	System		User	System		User	System	
Gradient boosting	8 min 48 s	792 ms	16 min 4 s	797 ms	116 ms	1.04 s	814 ms	112 ms	1.06 s
XGBoost	38 min 53 s	2.06 s	1 min 58 s	2.86 s	128 ms	414 ms	2.62 s	96 ms	399 ms
Decision tree	1.83 s	1.38 s	2.94 s	309 ms	184 ms	521 ms	326 ms	176 ms	539 ms
Random forest	5.04 s	76 ms	5.25 s	174 ms	120 ms 4	464 ms	177 ms	160 ms	486 ms

(i) %%time: time of the execution for the entire cell. From this command, we were able to get the CPU times for the amount of time the CPU takes for running exclusively the code, the amount of time the CPU takes on system calls, combined user and system times, and the actual time taken by a computer to complete a task (it is the sum of three terms: CPU time, I/O time, and the communication channel delay)

(ii) %memit: measure the memory use of a single statement. From this command, we were able to get the background memory usage from the Python interpreter itself and also the memory needed each line of code affects the total memory needed

According to data revealed in Tables 7–9, the time took for the model to be trained was shown not to exceed a few seconds (3.21 s and 5.12 s) for the random forest and decision tree models and a few minutes (8 min 49 s) for the gradient boosting model. Moreover, for the XGBoost, it was observed that XGBoost consumed longer times due to the formations of trees and parameters involved in the process (38 min 54 s). Meanwhile, however, the time needed in the process is seen as an "optimal" amount of time considering the large number of applications on which models are trained. As for the testing phase, the time observed has been rather short. In particular, when calculated for one application, it was noted that the time needed would not exceed few microsecond (199.26 μs). Furthermore, it was noted that the amount of memory used in the action model is reasonably small commensurate with the number of features used in the model. By running a comparison upon the classifier models, XGBoost was found to consume a significant amount of memory due to the repetition of building the tree, pursuant with what was elaborated earlier(3721.53 MiB).

7. Conclusion

Recent research endeavors across the literature and current technologies deployed that seek to detect malicious programs have lacked a more complete study addressing the collective impact of both action repetition and permissions deployed together to classify Android applications as being malicious or otherwise. In this paper, we investigated the performance of four machine learning classifiers that seek to detect malware depending on the dynamic (action repetition) and static (permissions) features. These features were found to have significant bearing and a key role in the classification process. In particular, we applied the four classifiers in three stages. In the first stage, we leveraged the dynamic features in the dataset. In the second stage, we used the static features involved, while the third stage encompassed a combination of both dynamic and static features.

In the three stages used, the results indicate that classification was done to high accuracy. As we implemented the proposed methodology, we, leveraging the results obtained, have shown that new features, never addressed before, can be extracted in the process. We have also demonstrated that a combination of the permissions and action repetition features has achieved good results in detecting malware in Android applications. Also, the results showed that accuracy achieved from static, dynamic, and hybrid analyses was above 94%, so using static analyses alone should be efficient and less in cost for classification in our case.

As future work, we are planning to investigate and get one step further to develop a novel method based on machine learning to classify malware families rather than binary classification.

Data Availability

The datasets generated during and/or analysed during the current study are available upon request.

Conflicts of Interest

The authors declare that they have no conflicts of interest.

Acknowledgments

This research received partial funding from the Jordan University of Science and Technology.

References

[1] "Smartphonemarket," 2020, https://www.idc.com/promo/smartphone-market-share/os.

[2] "Number of android apps on google play," 2020, https://www.appbrain.com/stats/number-of-android-apps.

[3] G. Suarez-Tangil and G. Stringhini, "Eight years of rider measurement in the android malware ecosystem: evolution and lessons learned," 2018, https://arxiv.org/abs/1801.08115.

[4] K. Liu, S. Xu, G. Xu, M. Zhang, D. Sun, and H. Liu, "A review of android malware detection approaches based on machine learning," *IEEE Access*, vol. 8, pp. 124579–124607, 2020.

[5] H. Cai, F. Xiaoqin, and A. Hamou-Lhadj, "A study of run-time behavioral evolution of benign versus malicious apps in android," *Information and Software Technology*, vol. 122, article 106291, 2020.

[6] H. Cai and B. Ryder, "A longitudinal study of application structure and behaviors in android," *IEEE Transactions on Software Engineering*, vol. 47, no. 12, pp. 2934–2955, 2021.

[7] M. Noman, M. Iqbal, and A. Manzoor, "A survey on detection and prevention of web vulnerabilities," *International Journal of Advanced Computer Science and Applications*, vol. 11, no. 6, pp. 521–540, 2020.

[8] B. Baskaran and A. Ralescu, *A study of android malware detection techniques and machine learning*, In MAICS, 2016.

[9] W. Zhang, H. Wang, H. He, and P. Liu, "DAMBA: detecting android malware by ORGB analysis," *IEEE Transactions on Reliability*, vol. 69, no. 1, pp. 55–69, 2020.

[10] S. Alam, S. A. Alharbi, and S. Yildirim, "Mining nested flow of dominant APIs for detecting android malware," *Computer Networks*, vol. 167, article 107026, 2020.

[11] O. Olukoya, L. Mackenzie, and I. Omoronyia, "Towards using unstructured user input request for malware detection," *Computers & Security*, vol. 93, article 101783, 2020.

[12] P. Ravi Kiran Varma, K. P. Raj, and K. V. S. Raju, "Android mobile security by detecting and classification of malware based on permissions using machine learning algorithms," in *2017 International Conference on I-SMAC (IoT in Social, Mobile, Analytics and Cloud)(I-SMAC)*, pp. 294–299, Palladam, India, 2017.

[13] J. Song, C. Han, K. Wang, J. Zhao, R. Ranjan, and L. Wang, "An integrated static detection and analysis framework for android," *Pervasive and Mobile Computing*, vol. 32, pp. 15–25, 2016.

[14] S. Hahn, M. Protsenko, and T. Müller, "Comparative evaluation of machine learning-based malware detection on android," in *Sicherheit 2016-Sicherheit, Schutz und Zuverlässigkeit*, Gesellschaft für Informatik e.V, 2016.

[15] Q. Fang, X. Yang, and C. Ji, "A hybrid detection method for android malware," in *2019 IEEE 3rd Information Technology, Networking, Electronic and Automation Control Conference (ITNEC)*, pp. 2127–2132, Chengdu, China, 2019.

[16] R. Surendran, T. Thomas, and S. Emmanuel, "A TAN based hybrid model for android malware detection," *Journal of Information Security and Applications*, vol. 54, article 102483, 2020.

[17] W.-C. Kuo, T.-P. Liu, and C.-C. Wang, "Study on android hybrid malware detection based on machine learning," in *2019 IEEE 4th International Conference on Computer and Communication Systems (ICCCS)*, pp. 31–35, Singapore, 2019.

[18] H. Zhang, S. Luo, Y. Zhang, and L. Pan, "An efficient android malware detection system based on method-level behavioral semantic analysis," *IEEE Access*, vol. 7, pp. 69246–69256, 2019.

[19] N. J. Ratyal, M. Khadam, and M. Aleem, "On the evaluation of the machine learning based hybrid approach for android malware detection," in *2019 22nd International Multitopic Conference (INMIC)*, pp. 1–8, Islamabad, Pakistan, 2019.

[20] C. Yang, Z. Xu, G. Gu et al., "Droidminer: automated mining and characterization of fine-grained malicious behaviors in android applications," in *European symposium on research in computer security*, pp. 163–182, Cham, 2014.

[21] H. Fereidooni, M. Conti, D. Yao, and A. Sperduti, "Anastasia: android malware detection using static analysis of applications," in *2016 8th IFIP international conference on new technologies, mobility and security (NTMS)*, pp. 1–5, Larnaca, Cyprus, 2016.

[22] H. Cai, "Assessing and improving malware detection sustainability through app evolution studies," *ACM Transactions on Software Engineering and Methodology (TOSEM)*, vol. 29, no. 2, pp. 1–28, 2020.

[23] H. Cai, "Embracing mobile app evolution via continuous ecosystem mining and characterization," in *Proceedings of the IEEE/ACM 7th International Conference on Mobile Software Engineering and Systems*, pp. 31–35, Seoul, Republic of Korea, 2020.

[24] F. Xiaoqin and H. Cai, "On the deterioration of learning-based malware detectors for android," in *2019 IEEE/ACM 41st International Conference on Software Engineering: Companion Proceedings (ICSE- Companion)*, pp. 272-273, Montreal, QC, Canada, 2019.

[25] L. Cai, Y. Li, and Z. Xiong, "Jowmdroid: android malware detection based on feature weighting with joint optimization of weight-mapping and classifier parameters," *Computers & Security*, vol. 100, article 102086, 2021.

[26] S. Y. Yerima, M. K. Alzaylaee, and S. Sezer, "Machine learning-based dynamic analysis of android apps with improved code coverage," *EURASIP Journal on Information Security*, vol. 2019, Article ID 4, 2019.

[27] A. Mahindru and P. Singh, "Dynamic permissions based android malware detection using machine learning techniques," in *Proceedings of the 10th innovations in software engineering conference*, pp. 202–210, Jaipur, India, 2017.

[28] M. K. Alzaylaee, S. Y. Yerima, and S. Sezer, "Emulator vs real phone: android malware detection using machine learning," in *Proceedings of the 3rd ACM on International Workshop on Security and Privacy Analytics*, pp. 65–72, Jaipur, India, 2017.

[29] H. Cai, N. Meng, B. Ryder, and D. Yao, "Droidcat: effective android malware detection and categorization via app-level profiling," *IEEE Transactions on Information Forensics and Security*, vol. 14, no. 6, pp. 1455–1470, 2019.

[30] H. Cai and J. Jenkins, "Towards sustainable android malware detection," in *Proceedings of the 40th International Conference on Software Engineering: Companion Proceeedings*, pp. 350-351, Gothenburg, Sweden, 2018.

[31] X. Ke, Y. Li, R. Deng, K. Chen, and X. Jiayun, "Droidevolver: self-evolving android malware detection system," in *2019 IEEE European Symposium on Security and Privacy (EuroS&P)*, pp. 47–62, Stockholm, Sweden, 2019.

[32] S. Arshad, M. A. Shah, A. Wahid, A. Mehmood, H. Song, and H. Yu, "SAMADroid: a novel 3-level hybrid malware detection model for android operating system," *Access*, vol. 6, pp. 4321–4339, 2018.

[33] S. Chen, M. Xue, Z. Tang, L. Xu, and H. Zhu, "Stormdroid: a streaminglized machine learning-based system for detecting android malware," in *Proceedings of the 11th ACM on Asia Conference on Computer and Communications Security*, pp. 377–388, Xi'an, China, 2016.

[34] X. Wang, Y. Yang, Y. Zeng, C. Tang, J. Shi, and K. Xu, "A novel hybrid mobile malware detection system integrating anomaly detection with misuse detection," in *Proceedings of the 6th International Workshop on Mobile Cloud Computing and Services*, pp. 15–22, Paris, France, 2015.

[35] Y. Liu, Y. Zhang, H. Li, and X. Chen, "A hybrid malware detecting scheme for mobile android applications," in *2016 IEEE International Conference on Consumer Electronics (ICCE)*, pp. 155-156, Las Vegas, NV, USA, 2016.

[36] M. Diamantaris, E. P. Papadopoulos, E. P. Markatos, S. Ioannidis, and J. Polakis, "Reaper: real-time app analysis for augmenting the android permission system," in *Proceedings of the Ninth ACM Conference on Data and Application Security and Privacy*, pp. 37–48, New York, NY, USA, 2019.

[37] F. Fasano, F. Martinelli, F. Mercaldo, and A. Santone, "Android run-time permission exploitation user awareness by means of formal methods," in *ICISSP*, pp. 804–814, Valletta, Malta, 2020.

[38] M. Dilhara, H. Cai, and J. Jenkins, "Automated detection and repair of incompatible uses of runtime permissions in android apps," in *Proceedings of the 5th International Conference on Mobile Software Engineering and Systems*, pp. 67–71, Gothenburg, Sweden, 2018.

[39] W. Li, F. Xiaoqin, and H. Cai, "Androct: ten years of app call traces in android," in *2021 IEEE/ACM 18th International Conference on Mining Software Repositories (MSR)*, pp. 570–574, Madrid, Spain, 2021.

[40] K. Allix, T. F. Bissyandé, J. Klein, and Y. Le Traon, "Androzoo: collecting millions of android apps for the research community," in *2016 IEEE/ACM 13th Working Conference on Mining Software Repositories (MSR)*, pp. 468–471, Austin, TX, USA, 2016.

[41] I. Amit, J. Matherly, W. Hewlett, Z. Xu, Y. Meshi, and Y. Weinberger, "Machine learning in cyber-security-problems, challenges and data sets," 2018, https://arxiv.org/abs/1812.07858.

[42] "Towards data science," 2019, https://towardsdatascience.com/feature-extraction-techniques-d619b56e31be.

[43] M. S. Rahman, M. K. Rahman, S. Saha, M. Kaykobad, and M. S. Rahman, "Antigenic: an improved prediction model of protective antigens," *Artificial Intelligence in Medicine*, vol. 94, pp. 28–41, 2019.

[44] A. J. Myles, R. N. Feudale, Y. Liu, N. A. Woody, and S. D. Brown, "An introduction to decision tree modeling," *Journal of Chemometrics: A Journal of the Chemometrics Society*, vol. 18, no. 6, pp. 275–285, 2004.

[45] J. H. Friedman, "Greedy function approximation: a gradient boosting machine," *Annals of Statistics*, vol. 29, no. 5, 2001.

Hindawi
Wireless Communications and Mobile Computing
Volume 2022, Article ID 4397610, 14 pages
https://doi.org/10.1155/2022/4397610

Research Article

Sixth-Generation (6G) Mobile Cloud Security and Privacy Risks for AI System Using High-Performance Computing Implementation

Srinivasa Rao Gundu,[1] Panem Charanarur,[2] Kashinath K. Chandelkar,[2] Debabrata Samanta,[3] Ramesh Chandra Poonia,[3] and Partha Chakraborty[4]

[1]*Government Degree College Sithaphalmandi, Hyderabad, Telangana, India*
[2]*School of Cyber Security and Digital Forensic, National Forensic Sciences University, Goa Campus, Goa, India*
[3]*Department of Computer Science, CHRIST (Deemed to Be) University, Bengaluru, Karnataka 560029, India*
[4]*Department of Computer Science and Engineering, Comilla University, Cumilla-3506, Bangladesh*

Correspondence should be addressed to Partha Chakraborty; partha.chak@cou.ac.bd

Received 22 February 2022; Accepted 18 April 2022; Published 5 May 2022

Academic Editor: Mohammed Hammoudeh

The exchange of information from one person to another is called communication. Telecommunication makes it possible with electronic devices and their tools. The scientist Alexander Graham Bell has invented the basic telephone in 1876 in the USA. Telephones now have the new format in the form of mobile phones, which are the primary media for communicating and transmitting data. We are using 5th-generation mobile network standards. Still, there are some requirements for the users that are believed to be solved in the 6th-generation mobile network standards. By 2030, all of the people would be using 6G. The computing model in the cloud is not dependent on either the location or any specific device that would provide the service. It is an on-demand computational service-oriented mechanism. Combining these two technologies as mobile cloud computing provides customized options with more flexible implementations. Artificial intelligence is being used in devices in many fields. AI can be used in mobile network services (MNS) to provide more reliable and customized services to the users, such as network operation monitoring, network operation management, fraud detection, and reduction in mobile transactions and security to the cyber devices. Combining cloud with AI in mobile network services in the 6th generation would improve human beings' lives, such as zero road accidents, advanced level special health care, and zero crime rates in society. However, the most vital needs for sixth-generation standards are the capability to manage large volumes of records and excessive-statistics-fee connectivity in step with gadgets. The sixth-generation mobile network is under development. This generation has many exciting features. Security is the central issue that needs to be sorted out using appropriate forensic mechanisms. There is a need to approach high-performance computing for improved services to the end-user. Considering three-dimensional research methodologies (technical dimension, organizational dimension, and applications hosted on the cloud) in a high-performance computing environment leads to two different cases such as real-time stream processing and remote desktop connection and performance test. By 'narrowing the targeted worldwide audience with a wide range of experiential opportunities,' this paper is aimed at delivering dynamic and varied resource allocation for reliable and justified on-demand services.

1. Introduction

Exchange of information from one person to another is called communication. It is done in many ways. The first form of communication is verbal. It means one speaks, the other one listens, and vice versa. However, if these conversants are located at two different geographical locations and conversation is needed, it is done using some telecommunication approach. Telecommunication is done using some electronic tools that would easily express the required

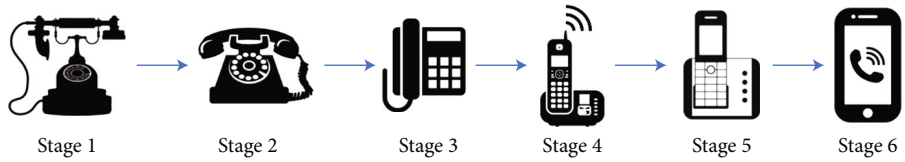

Figure 1: Pictorial representation of telephones.

information or message quickly. The electronic devices transmit the message to a longer distance within a short period. 'Tele' means 'distance'and 'phone'means 'communication' [1]. Therefore, telephone means distant communication. It means communicating with a person who is in a long distance [2]. Alexander Graham Bell is behind all these scientific investigations today about mobile communications. He invented this device in 1876 in the USA. Today, many people might not have seen, but till the early 1990s, rotary dial telephones has dominated almost all areas in public places, government offices, and individual private houses. Figure 1 shows a pictorial representation of telephones.

Later, push-button phones have dominated the market. These are a few examples of landline phones. Later, mobile phones came into existence. Mobile phones are portable phones; they do not have any wires connected to any telephonic links. They run on a wireless network process. These mobile phones will have a simcard which will provide a unique identity to the subscriber. From anywhere on this globe, no other person would have this number. These simcards are removable and insertable into the mobile [3]. All today's mobile phones would have CPUs. But these CPUs will run on lesser electrical or battery power with less memory and more sophisticated work. Today's modern phones will have many features like radio, music, navigational tools, and video games. Mobile phones are the primary media for the communication and transmission of data. Cloud computing is a device-independent and location-independent, on-demand computational service-oriented mechanism. Combining these two technologies as mobile cloud computing provides customized options with more flexible implementations. The recent trends in this field are 'narrowing the targeted global audience with a wide range of experiential opportunities' [4, 5]. Recent times suggest that significant businesses are being carried out using mobile cloud computing. Most companies do not own a cloud and rely on cloud service providers. Lower investments and usage-based billing are the major attraction for major businesses migrating to the cloud [6]. Still, there are unsolved problems in this field, such as the need to improve the GPS with low electricity consumption, screens with higher resolution, and three-dimensional cameras to mobiles. In the 1st-generation mobiles, the network signals used are analog by nature. The 2nd-generation mobiles are digital networks. These networks use approximately 12-15 kbps. In this generation, people have enjoyed text messaging. 3rd generation has increased new frequency bands thereby data transfer rates have increased. 4th generation has given away to the internet accessibility, HD TV, games, and cloud-based services [7, 8]. 5th generation is under development. It is aimed at reducing the latency and increase the efficiency of coverage. Speedwise, the 1st generation has experienced 2 kbps. The speed 200 kbps in 3G and in 5G is aimed at being as fast as 35.46 Gbps [8]. Figure 2 shows analog signal, digital signal, and analog-to-digital signal conversion.

In the earlier days, people used to have lesser transactions on mobiles. They were realistic, and their works have existed in the real world. But today's world is turned much more virtual rather than practical [9]. Perhaps much of the shopping is done on mobiles today. The characteristics of the goods are provided with all minute details and photos on the commercial sites they are being purchased with digital currency. As a result, a considerable amount of data would be generated, and such data need to be used. Hence, there is a need for cloud computing. These cloud services could store a large amount of data related to the customers and the sellers online [10, 11]. Processing these data and the applications would increase the speed enormously. The data is acquired from much more remote locations using a simple internet connection with some simple secured protocols. The cloud space is enough to maintain many volumes of information for many years. A cloud is formed from the collaboration of many data centers to provide a reliable service to customers. This enormous amount of data stored on the servers is not possible; thereby, 3rd party assistance is used in the form of the cloud to support the existing services to the customers [12]. When a user enters some details for his commercial or financial services in his/her mobile needs to connect to a web application, thereby which it should connect to a server that is at a remote location. Inserting noninformation bits into data is known as bit stuffing. Keep in mind that overhead bits and packed bits are two very different things. Bits that do not really contain data but must be sent are known as overhead. It is possible to use bit stuffing to synchronize several channels before multiplexing, to match the rates of two separate channels, and to perform length-limited coding when necessary. Run-length-restricted programming was done in order to restrict the number of consecutive bits of the same value in the data that is to be conveyed. After the maximum allowable number of consecutive bits, a bit of the opposite value is added. Bit suffocation does not guarantee that the data delivered is intact when it reaches its destination. For the most part, this is just a means to guarantee that the transmission begins and stops in the right locations. The delimiting flag sequence in a data connection frame typically consists of six or more consecutive 1 s. A single bit is tucked away in the message to distinguish it from the flag in the event of a similar sequence. At the conclusion of every string of five consecutive 1 s, an additional 0 bit is added for good measure. The stuffed 0 s are removed by the receiver after each five-one sequence. When the message has been unstuffed, it is forwarded up to the

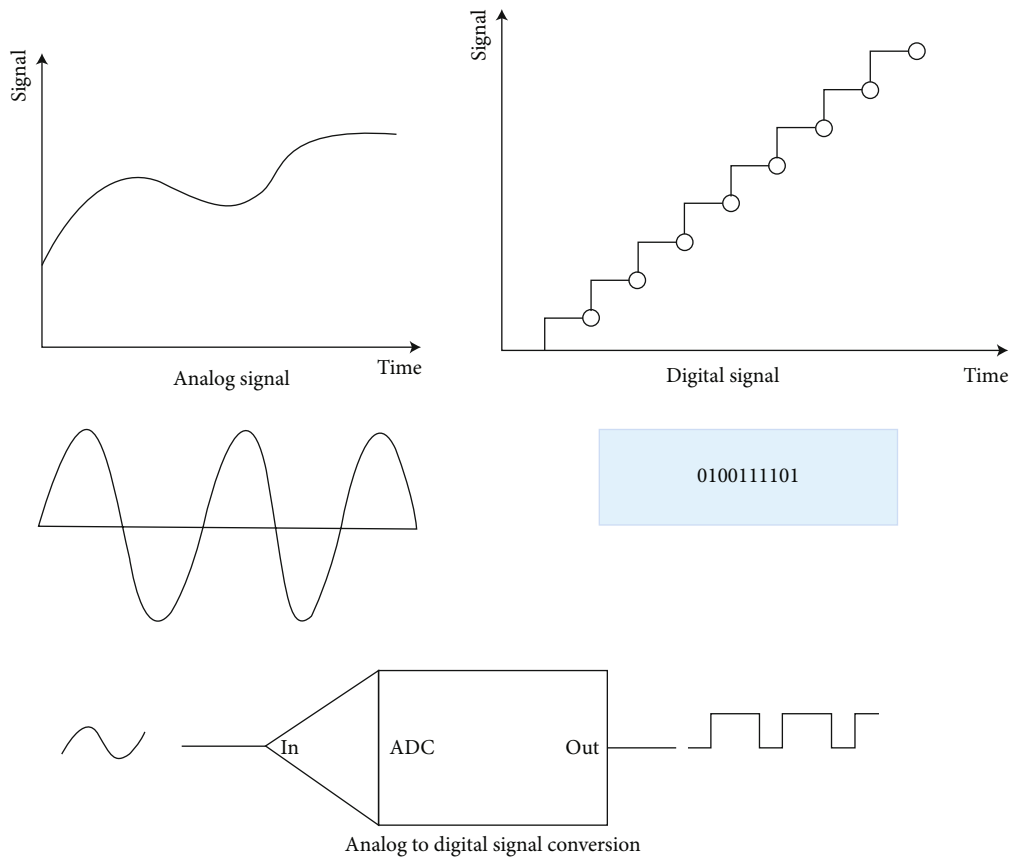

Figure 2: Analog signal, digital signal, and analog-to-digital signal conversion.

higher tiers. As a result of the coding rate instability caused by bit stuffing, it is not always a reliable method of data transmission. All the server services need to be achieved using some web browser that works like a mediator. Generally, Web application service is provided with a blend of added service-oriented architecture. Thereby, it can be known as a sophisticated internet-based application.

1.1. Aim of the Study. The aim of study is by 'narrowing the targeted worldwide audience with a wide range of experiential opportunities,' the goal was to deliver dynamic and varied resource allocation for reliable and justified on-demand services. In fields including manufacturing automation, health care technology, and transportation, the fast growth of the mobile information business has spawned a variety of mobile applications. Mobile devices may not be able to handle the processing demands of these apps, which often need large calculations and severe latency requirements. Mobile edge computing (MEC) is a potential technology for supporting these kinds of applications since it installs edge servers near mobile devices to facilitate computation offloading. MEC has the ability to significantly increase the computational power of mobile devices. There are drawbacks to offloading computations from mobile devices to edge servers, such as increased transmission delay and energy usage. This may lead to nonnegligible compute time due to the limited CPU power available on the edge servers. A cooperative allocation of processing and communication resources is important in MEC systems because their effects are tied together. According to the majority of current research, network slicing and MEC optimization simply takes into account mobile devices' resource slicing, energy scheduling, and power allocation without factoring the operator's income. We cannot have a different network for each application situation since it is not viable. Using network slicing to overcome this problem has been suggested as an option. In network slicing, numerous conceptually distinct networks are operated on top of a shared physical infrastructure, which is the primary characteristic. Network resources may be dynamically and flexibly distributed to logical network slices in response to specific on-demand service needs via the use of network slicing. There has been a shift in network edge service needs due to the fast growth of Internet of Things (IoT) and cyberphysical systems. Existing works, on the other hand, have not been able to keep up with the ever-changing demands of these applications. Therefore, how to enable various apps in a shared physical infrastructure is still an unanswered question. If you are looking for a way to support edge services with special needs, mobile edge computing (MEC) is a potential solution. With MEC, latency and energy usage are lowered since it is closer to the edge of the network than traditional cloud computing systems. In both academics and business, the combination of network slicing with MEC has piqued a lot of interest. Large-scale energy harvesting fog computing networks have been developed with dynamic network slicing design to enhance

resource efficiency and balance workloads across fog nodes. Fog radio access networks were the subject of more study into hierarchical radio resource allocation (F-RAN). Network slicing resource allocation in MEC systems was investigated by most studies, but they did not consider the computing resources. However, the dynamic demand of services has not been addressed in most recent publications on the use of network slicing to MEC systems. Cloud forensics and high-performance computing would offer improvement. However, the authors of this paper suggest considering the fog computing-based dynamic network slicing design would enhance the computational potentialities.

1.2. Motivation for the Study. Since the world has become very gregarious for handling impeccable knowledge to savvy and scrupulous educators, in this era of scientific inventions. Today, it is aimed at gravitating to innovative ideas in the field of science and technologies with human touch. It is the time to tease off and endorse to bring out precocious advancements in the field of science and technologies. Today, all are committed to the creation, dissemination, and acquisition of knowledge through our research and developments. As unprecedented methodologies phase in to create a pathfinder way, new innovative and gravitate ideas are needed. It is needed to focus on thriving technological trends for the prosperity and opportunities for the human endeavor in recent times and in the coming years, too.

2. Review of the Literature

According to Laxman Shankar [13], the Bigonet cloud-based mobile framework was established to meet the requirements of the subsequent standard level in cloud apps. Such following level apps would require parallel processing apart from several connected systems needing to be handled in the distributed environment. They show how the network-based activity analysis in the operating system and robust multipoint to multipoint apps in the distributed switching, highly accessible, scalable infrastructure, and user-friendly interfaces make developing and managing numerous parallel and concurrent processes easier [14]. While network slicing allows on-demand services, many of their apps need multiaccess edge computing (MEC) structural design to be deployed in the 5th-generation distributed system. Originally, edge computing is a key force behind the 5th-generation and 6th-generation mobile standard distributed systems; its role in network slicing remains unknown. The 5th-generation distributed system will use multiaccess edge computing as its structural architecture. As a result of multiaccess edge computing (MEC), traffic and service processing is moved away from the cloud and closer to the end user. The network edge processes, analyzes, and saves data instead of transmitting it all to the cloud. High-bandwidth applications benefit from reduced latency and real-time performance since data is collected and processed closer to the client. In addition, MEC provides a network edge IT service environment and cloud computing capabilities. Distributed data centers at the edge are often used to implement MEC. High bandwidth and low latency are essential for edge applications. Distributed data centers, or distributed clouds, are created by service providers to accomplish this goal. To put it another way, there is no such thing as "the cloud"; it is a collection of resources that can be located in any location, including the customer's location. With the MEC platform, you have the option of employing either a server or CPE for edge computing. It is possible to employ a software-defined access layer as an extension of a cloud. Open source hardware and software, including SDN and NFV, are being used in the majority of edge computing projects. There are a number of popular MEC use cases that may be listed, including data analytics, location tracking services, IoT, and augmented reality. Hosting stuff locally, such as movies, on a server in your area, driving patterns, road conditions, and other vehicle movements may all be monitored by a connected automobile as an example of an Internet of Things (IoT) application. On-time delivery of predictive and prescriptive information is critical. Sensor data must be gathered, processed, and analyzed at the edge in order to deliver low latency insights to the driver. This means that MEC may be used for a broad range of applications requiring immediate reaction time, such as autonomous cars, virtual reality, robots, and other immersive media. Indeed, new technical ideas might bring about a paradigm change from 4G to 5G. An ongoing effort is needed from both academic and industrial sectors to successfully use MEC in 5G networks. MEC technology and its prospective uses and applications are first discussed in this study. This is followed by a summary of the most recent research findings on the integration of MEC with 5G and other emerging technologies. In addition, we provide an overview of edge computing testbeds, experiments, and open source efforts. This section sums up findings from current research and discusses problems and future perspectives for MEC studies. According to Chihani et al. [15], contextual information is used to characterize the conditions of entities (end-users and systems) and their responses. Apps require such data to make adjustments in their processing approach as a response to make change in the context of the end-users. On the other hand, like the machine-to-machine-based communication approach, the cohesiveness of many systems makes keeping the established contextual information extremely challenging. The lack of a scalable and simply customizable solution for efficient context management is a show-stopper in a big and dispersed system. This research presents a scalable cloud-based context management paradigm for dealing with contextual data in large distributed contexts. This framework was developed and proven to allow programs to subscribe to context changes and declare how context data should be handled using an XML-based programming language. Since there is a need of enormous data upload and download in all the time, there is also a need of transmission of data continuously. It is always needed to use extensible markup language- (XML-) based programming language. It is now required for a file format that can store, transport, and reconstruct arbitrary data. Since then, it establishes a set of guidelines for encoding documents in a human- and machine-readable manner. Serialization is

the primary goal of XML. XML is a markup language that labels, categorizes, and arranges information structurally. The data structure is represented by XML tags, which also contain information. The data included within the tags is encoded according to the XML standard. A separate XML schema (XSD) specifies the metadata required for interpreting and validating XML. The canonical schema is another name for this. A well-formed XML document follows basic XML rules, while a valid XML document follows its schema. Characters from the unicode repertoire are used exclusively in XML documents. Except for a tiny number of control characters that are explicitly banned, every unicode character can appear in an XML document's content. The encoding of the unicode characters that make up the document can be identified using XML. Therefore, it is advised to use XML-based programming language for all the needs of 6G. According to Segal et al. [16], heterogeneous computing is a potential approach for high-performance and energy-efficient computing. Till now, the high-performance heterogeneous computing industry was dominated by discrete GPUs, but new options based on APUs and FPGAs have emerged. These innovative concepts have the potential to increase energy efficiency significantly. Heterogeneous computing based on FPGA has a lot of promise since it allows one-of-a-kind hardware for data-centric parallel applications to be designed. Most significant impediment to FPGA acceptance as high-performance computing systems is their programming difficulties. According to El-Araby et al. [17], parallel computers with integrated FPGA chips are high-performance reconfigurable computers. The Cray XT5 h and Cray XD1, the SRC-7 and SRC-6, and the SGI Altix/RASC are examples of such systems. In classic high-performance computers, the single-program multiple data method is used to execute parallel programs on HPRCs (HPCs). FPGAs have previously been used as coprocessors in similar systems. Overall, system resources are typically underutilized because reconfigurable processors are deployed unevenly compared to standard processors.

Because of the asymmetry, the SPMD programming approach cannot be utilized on these devices. In this paper, we describe a resource virtualization technique. Underutilized processors will be able to share reconfigurable processors thanks to this method. According to Ba et al. [18], the message forwarding interface has already become a common communication library for distributed memory computing systems. Since new MPI standard versions are published, several MPI implementations have been made publicly available. In various implementations, different approaches are employed. Communication performance is the key in message passing-based systems, so choosing an appropriate MPI implementation is crucial. According to Kim et al. [19], the TCP/IP protocol suite is the most widely utilized networking computer. They looked on the role of TCP/performance IPs in data sharing under the UNIX operating system once a connection was established in this study. By measuring accurate data for various areas of the protocol implementation, we identify the key bottlenecks and define the maximum performance limitations. They took memory bandwidth requirements into account when processing high-speed TCP/IP. Empirical studies imply that the TCP/IP protocol can process data at up to 85 Mbps under the UNIX operating system when a good data connection layer interface is provided, needing a memory bandwidth of 172 Mbyte/s.

According to Shivabhai and Babu [20], high-performance computing (HPC) is utilized to address vast and difficult computer issues by combining scientific research and industry innovation. The ultimate objective is to connect a high-performance computing cluster to a web-based interface that hides the complexities of high-performance computing. The massive resource broker (MRB) bridges the gap by providing a web-based task submission, administration, and monitoring interface for high-performance computing. Naive users submit jobs, monitor clusters, and produce reports using the MRB portal. Saving time, delivering more productive output, reducing mistakes, and improving consistency are all priorities for large resource brokers. The relevance of MRB, its implementation, and significant elements such as job submission, monitoring, analysis, benefits, and workflow are all discussed in this article. An approach for systematically finding and isolating floating point implementation errors in high-performance multiple CPU computing systems has been devised, according to Ghoshal [21]. A validation suite has been created and put through its paces. The results reveal that the implementation was flawed. Proposed and prototyped guidelines for proper implementation are presented.

2.1. Artificial Intelligence Usage in Mobile Networks. AI is an acronym for artificial intelligence. It is an antonym for natural intelligence. Natural intelligence is an exhibiting nature of natural living beings, and artificial intelligence is done by the devices. These devices are generally called agents [22]. Devices are aimed at achieving their targets more precisely than natural beings. These agents can have the capacity to store in memory, they can learn, and they can make a decision and express appropriately. All these activities simply follow human intelligence thereby possible to deploy in many other fields where human involvement is not possible. AI can be used in mobile network services (MNS) such as to provide more reliable and customized services to the users. Some of them can be (i) network operation monitoring, (ii) network operation management, (iii) fraud detection and reduction in mobile transactions, (iv) security to the cyber devices, (v) customer services, (vi) marketing management, (vii) digital assistance, and (viii) customer relationship management.

2.2. The Sixth-Generation Mobile Network. The fifth-generation network standard would provide new functionalities; along with this, it would also provide improved service quality in contrast with the fourth generation network standard. The fifth-generation network standard would encompass numerous new additional strategies, the latest frequency bands, such as the mmWave and the optical spectra, superior spectrum utilization and control, and the combination of licensed and unlicensed bands. Nevertheless, the fastest boom of the data center-based centric and automated systems can also exceed the competencies of 5G Wi-Fi structures [23].

A few devices, together with virtual reality (VR) devices, would go to head past 5G because they would require not less than 10 Gbps facts charge. The key drivers of sixth generation might be the convergence of past capabilities, including community densification, excessive throughput and reliability at a high level, lesser energy consumption, and higher data for the connectivity. The sixth-generation machine could additionally maintain the traits of the previous generations, which included new offerings with new technology.

As per reliable sources like Cisco, these features include driving and maintenance of different types of vehicles, assigning various tasks and achieving the targets more precisely by robots, running and maintaining other drones in commercial and noncommercial areas, maintenance and safeguarding of home appliances, and supporting them in IOT, supporting many intelligent devices in the fields of constructions, care, and industries [23]. The feature also includes upcoming technologies like augmented reality, extended reality, and virtual reality. Speed of internet access would increase in geometrical proportion. The influence of this technology would bring out some exciting offers to society such as (1) zero road accidents, (2) advanced level special health care, and (3) zero crime rates in community.

2.3. Sixth Generation and Its Challenges. By 2030, all of the people would be using 6G. The upcoming 6G needs more sophisticated services by using 1 TB per second [24]. This means one would have the devices which would receive its signals 8000 GB per second. This prediction is based on a study at Sydney University. It would have decentralized networks. Not based on one single operator, perhaps a collection of operators would cohesively provide the services to the user. Science fiction like communicating with others in space could be easily possible with this 6G. China has already started the 6G development project. Very recently, China has launched 5G. There is going to be a tough challenge for the implementation in 6G. This new wireless communication will require ultrareliable low-latency communication networks. Not only this, the upcoming devices should possess the speed of terabit/second speeds [25]. This requires making much more advancement in the field of electronics.

2.4. Major Demanding Advancements. Some more aspects need to be advanced.

(1) Computational power has to be increased. The present computational power is not sufficient even for 5G. Accommodating present-day computational power for 6G would be unimaginable

(2) The reliability has to be increased. Mission critical tasks in 6G needs a high level of reliability and consistency

(3) The network coverage needs to be widespread. Antennae numbers and density have to rise more

(4) The network speed needs to be much faster. It requires THz of speed

(5) Energy capability needs to be increased. Present-day batteries are not competent enough for 6G

(6) Security has to be increased. There, it should not leave a chance for hackers and crackers

(7) The spectrum share must be focused. There, it should no race but cooperation between the operators

(8) Governing consortium: until now, no formal entity exists that would govern the technology in the coming days

(9) It is needed to be established

3. Service Requirements for 6G

The 6G wireless system will have the following key factors:

(1) Need of security improvement in 6G: 6G is expected to contain sophisticated technology that will provide considerably greater privacy and security to the user's data, such as channel coding and estimation in the physical layer, as well as multiple access in the MAC layer, among other things. It is widely assumed that 6G will employ quantum communication

(2) Mobile broadbands need to increased in 6G: 6G will link devices with extremely low data rates, such as biosensors and IoTs, as well as devices with large data rates, such as HD video streaming in smart cities. As a result, 6G is now supported by mobile broadbands. They ought to be elevated.

(3) Lesser latency communications that are ultrareliable: 6G services should rely on ultrareliable low-latency communications (URLLC) services, which have a latency of less than 1 millisecond and a 99.999 percent reliability, according to the Electronics and Telecommunications Research Institute (ETRI). This URLLC focuses on communications and gives stringent performance guarantees.

(4) Machine type machine communication in 6G: machine type communication, which includes both mission essential and huge connectivity characteristics, is expected to be a crucial cornerstone of 6G development, driven by a desire to supply vertical-specific wireless network solutions [26].

(5) More energy capability need to be increased in 6G: due to their ability to operate in higher-frequency bands than previous generations, 6G gadgets require significantly more energy than previous generations. As a result, energy consumption and efficiency are key concerns that need to be addressed right away

(6) Lesser network access overcrowding in 6G: the key concern is user service delivery. After establishing connectivity, speed, capacity, and latency are used to assess a network's efficiency

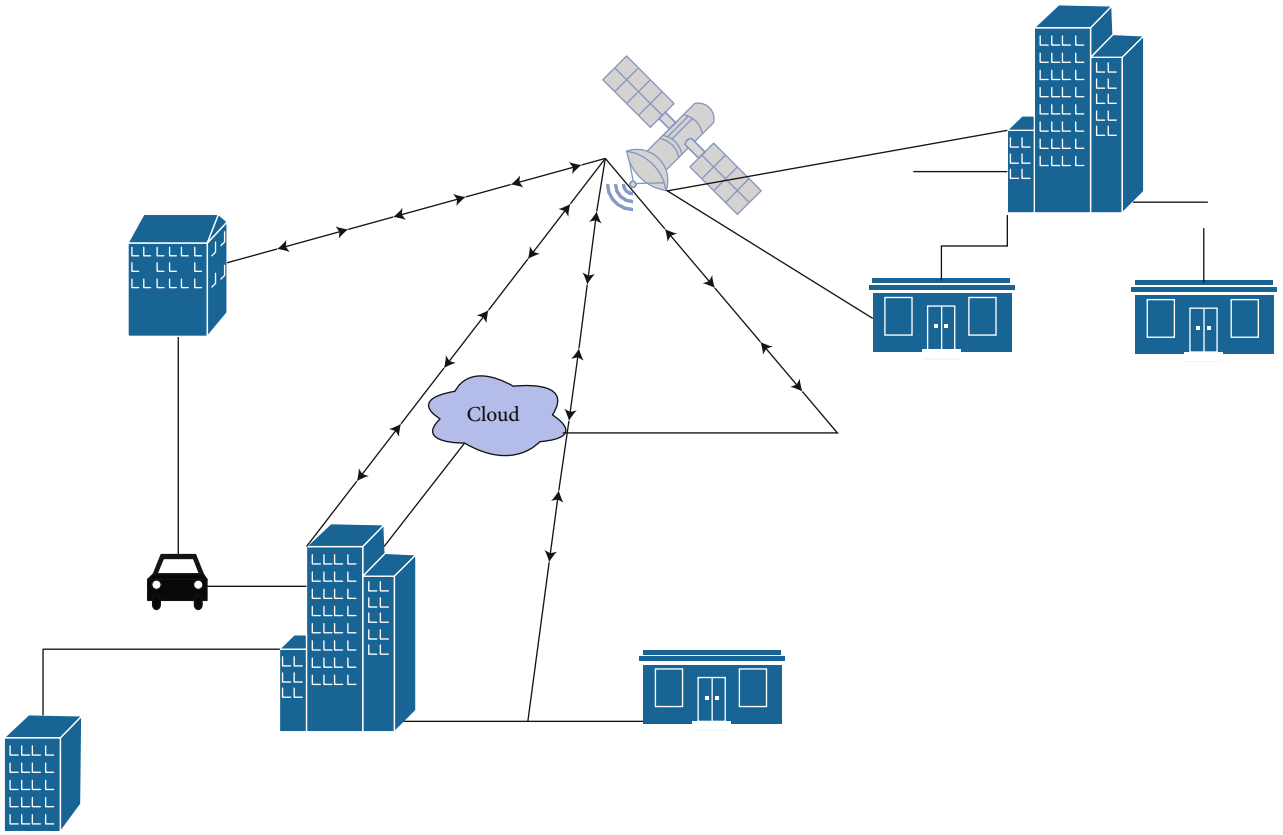

Figure 3: Pictorial representation of sample 6G network usage.

(7) Communication integrated with artificial intelligence: artificial intelligence, automated systems, and 6G mobile communications can all be said to be interconnected. The fundamental technology for automated systems is artificial intelligence. The fundamental driving factor behind automation is a variety of machine learning algorithms and deep learning principles. Real-time learning is a principle that allows an automated system to perform well. When discussing 6G communication technologies, automated systems are important. To get the most out of the potential of 6G communications, many systems must be automated when linked throughout the world.

(8) Lesser backhaul in 6G: mobile backhauling is a physical channel that connects radio controllers and base stations. It is often implemented using optical fibers or microwave radio connections. Backhaul systems today often rely on cost-effective packet-switched technologies (e.g., Wi-Fi and WiMAX).

3.1. Key Performance Indicators in 6G. These below are key performance indicators in upcoming 6G. They are as follows:

(i) System capacity: (a) peak data rate in 1000 Gbps, (b) experienced data rate 1 Gbps, (c) peak spectral efficiency 60 b/s/Hz, (d) experienced spectral efficiency 3 b/s/Hz, (e) maximum channel bandwidth 100 GHz, (f) area traffic capacity 1000 Mbps/m^2, and (g) connection density 107 devices/km^2

(ii) System latency: (a) end-to-end latency 0.1 ms and (b) delay jitter 10^{-3}

(iii) System management: (a) energy efficiency 1 TB/J, (b) reliability 10^{-9} packet error rate, and (c) mobility 1000 km/h.

Figure 3 shows the pictorial representation of sample 6G network usage.

3.2. Key Factor Requirements in Sixth Generation. Essential requirements of the sixth-generation mobile communication standards could be as given below:

(1) High-performance networking: compared with fifth-generation communications, sixth-generation communications would help networking and connect most people. Presently, in highly populated areas, this task may not be easy. Even in the case of less populated regions deep below the water surface, the communication signals are also not possible to connect. Sixth-generation communications will use novel conversation networks to support different data types such as audio and video. This would reach a new kind of experience in touch using virtual networking technology and involvement everywhere

(2) Higher energy efficiency: in sixth-generation mobile network standards, higher energy capability necessities for Wi-Fi gadgets with charging limits would exist. Apart from this, battery for the mobile has become lost for a lesser time. Hence, lengthy battery existence and usage would be the most considerable points for research in this standard communications. Consider the case of unmanned aerial vehicles (UAVs) and electric vehicles (EVs) in the Wi-Fi era. Recently, a new technology called symbiotic radio (SR) was released to overcome power issues for wireless devices [27]. The authors coined the word "unmanned aerial vehicles" with reference to power issue to the upcoming 6th-generation mobile technoloical standard. Unmanned aerial vehicles recently started using symbiotic radio (SR) technology; it is particularly with reference to wireless devices to overcome the power issue. Smart electricity control is every other promising strategy for dynamically optimizing the stability of electricity needs for supply. AI-based solutions for black communication technologies would be critical for optimizing power utilization and power usage scheduling for all Wi-Fi devices in an ever-changing technological environment and more complex optimization goals. For the optimization, available and updated machine learning-based technologies, such as deep reinforcement learning (DRL), could be applied. This would optimize the computing task devolvement in determining the Wi-Fi gadgets and an improved working and suspended time scheduling solution, lowering energy consumption. It integrates passive backscatter devices with a lively transmission device. Ambient backscatter communication is a classic example of SR, which allows network gadgets to use ambient RF indicators to transfer data without requiring vigorous RF transmission, allowing for battery-free communication. Smart electricity control is every other promising strategy for dynamically optimizing the stability of electricity needs for supply

(3) A high-level security and privacy: the available research particularly specialized in network throughput, reliability, and delay in 4G and 5G communications. However, wireless communicational exchange security and privacy issues have been disregarded to some extent in recent years

(4) A high-level intelligence: The sixth generation's high-level intelligence would be useful in providing users with high-quality, tailored, and intelligent services. As shown below, the sixth-generation high-intelligence standard would contain (i) operational intelligence, (ii) application intelligence, and (iii) service intelligence

(i) Traditional network operations entail a slew of resource optimization and multigoal overall performance optimization difficulties. Optimization tactics based on game theory, contract ideas, and many more are widely employed to achieve a high level of network operation. However, those optimization theories will not yield the best results in large-scale time-varying variables and multiobjective scenarios

(ii) Application intelligence: applications connected to fifth-generation networks are becoming increasingly intelligent. Intelligent applications are one of the applicational needs for sixth-generation networks. FL enabled Wi-Fi communication technology, allowing devices to connect to sixth-generation networks and execute a wide range of intelligent applications

(iii) Furthermore, as a human-centric network, the sixth-generation community's excessive intelligence will provide intelligent services satisfaction-oriented and individualized. FL, for example, would provide clients with individualized healthcare and referral services

3.3. Key Factor Requirements in Sixth Generation. In terms of evaluation, respondents in business units are less inclined to transfer power to appropriate IT for picking public clouds (41%), determining/advising on which apps pass to the cloud (45%), and selecting private clouds (40%). Overall, cloud challenges are declining: expertise, security, and spend tie for first place lack of assets/understanding, the top cloud assignment in recent years. Security concerns have also decreased to 25%, down from 29% last year. The most frequently stated venture among seasoned cloud users (24 percentages). Users are focusing on costs resulting from significant waste in cloud spending. The latest trends in this field are server computing and multivendor approach. Here are some predictions for cloud computing for a near future as follows:

(1) Hybrid infrastructure: hybrid infrastructures are now restricted to public and private cloud infrastructures. Hybrid infrastructures will broaden its reach to meet the agencies' demands for efficiency, safety, control, and cost-effectiveness. The services would be improved in terms of performance while also providing dependability and scalability

(2) No. of apps would increase on cloud: cloud computing is the way of the future for businesses, and companies have begun to prepare their programs to be cloud-compatible. Generally, roughly 70% of businesses consider cloud to be a distinguishing factor, and 65% of businesses spend about 10% of their budget on cloud services

4. Research Methodology

There are three dimensions to the research methodology:

(1) Dimensional technical: it is necessary to collect information that is flexible, static, and verifiable. In a remote computing context, such data should be processed using accessible criminal-related logical methods

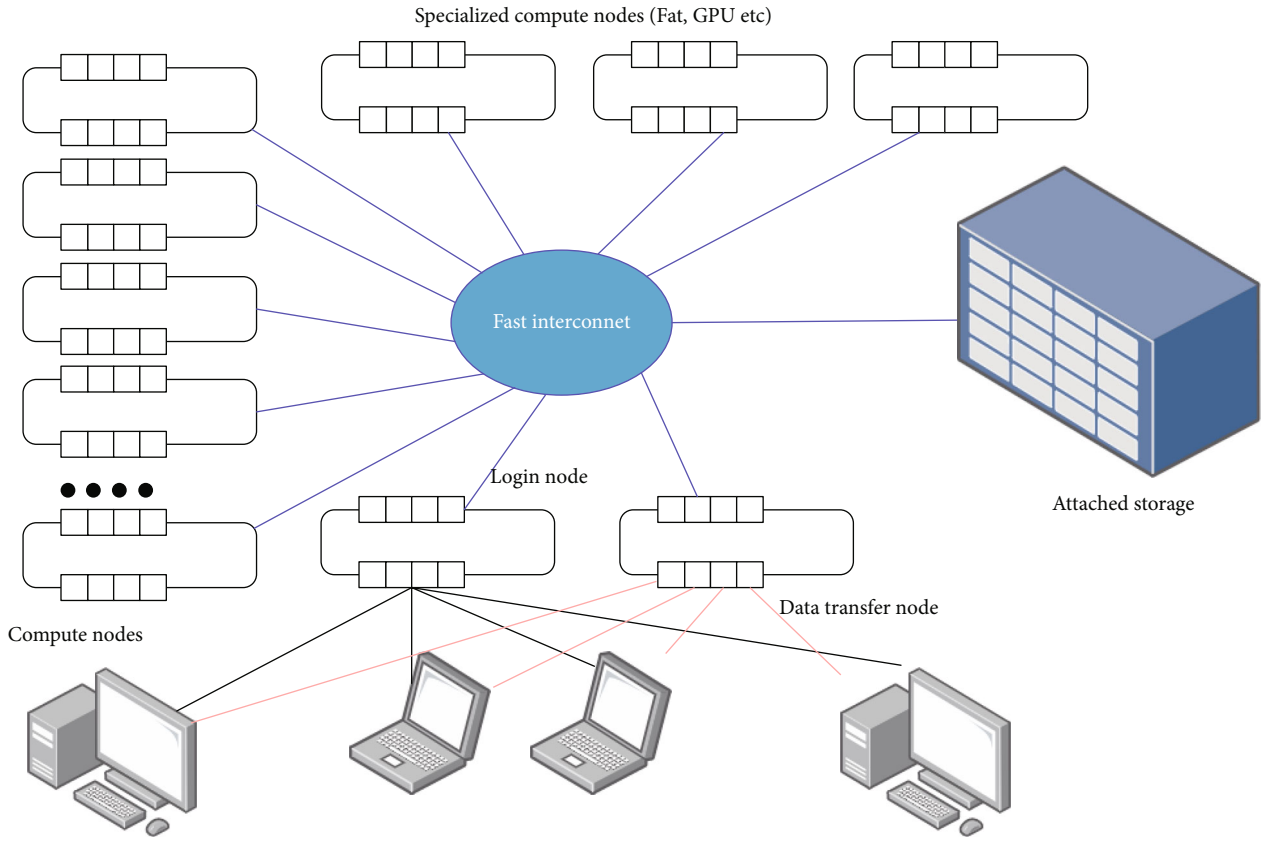

Figure 4: High-performance computing-based scalable 'cloud forensics-as-a-service' readiness framework.

(2) Dimension of organization: it is primarily considered in the context of distributed computing. They are cloud customers and cloud service providers, respectively. The programs are hosted in the cloud

(3) As a result, the services of one cloud service provider are linked to those of other cloud service providers. The inquiry process is complicated by the reliance on multiple parties. As a result, it becomes quite difficult

4.1. Testing Environment Plan. The following are the experimental plans for testing important components of the cloud forensic tools operating mechanism. To verify the viability of the technique's execution, a few tests must be carried out at various stages. Some tests are also designed to set benchmarks for the underlying components. The systems that must be tested before cloud forensics may be implemented are listed in the table below.

There should be an HPC cluster with a large number of nodes. This cluster will need to be hosted on a high-performance computing machine. On the virtualization cluster nodes, virtualization software is installed, allowing one node to function as several nodes. Amazon's Elastic Compute Cloud (EC2) offers cloud computing with elasticity. VMs from one or more physical clusters are put on dispersed servers to form virtual clusters. The goal of employing virtual machines is to integrate multiple functions on a single server. Virtual machines (VMs) can be replicated across many servers to improve distributed parallelism, fault tolerance, and disaster recovery. In order to get started with a typical virtual machine, the administrator must write down or describe the sources of configuration information. Inefficient network configurations almost always lead to overloading or underutilization when additional VMs join a network. EC2 is an excellent example of a web service that delivers scalable computing capacity in a cloud, such as Amazon's EC2. EC2 allows customers to construct virtual machines and manage user accounts throughout their usage. In order to create a virtual cluster, one or more physical clusters must host a virtual machine (VM). The borders of the virtual clusters are shown as different lines. In a virtual cluster, virtual machines (VMs) are dynamically provisioned. Nodes in the virtual cluster might be both real and virtual computers. On a single physical node, many VMs each running a separate operating system may be set up. To operate in a virtual machine, you need a guest operating system, which is typically different from the operating system of your host computer. Consolidating numerous functions on a single server is the goal of virtual machines. This will considerably increase the server's usage and the flexibility of the application. Parallelism, fault tolerance, and disaster recovery may be achieved by colonizing (replicating) VMs over numerous servers. Virtual cluster deployment, monitoring, and administration across huge clusters, as well as resource scheduling, load balancing, server consolidation, and fault tolerance, are all part of this. The ability to efficiently store a large number of virtual

Table 1: Systems needs of cloud forensic tool implementation.

Name	RAM	CPU	Cores	Threads	Disk space
HPC cluster	24 GiB	2 Intel Xeon X5660@2.8 GHz	12	24	100 Mib/s
Virtualization	128 GiB	2E5-2670@2.60 Hz	16	32	1 GiB/s
Cluster work station	SGiB	Intel Core i7- $60@2.8 GHz	4	8	100 Mib/s

Table 2: Data transfer calculations theoretically.

Size of the evidence	100 Mbit/s	10 Gbit/s
100 GiB	02 : 56 : 00	00 : 01 : 43
500 GiB	14 : 45 : 22	00 : 08 : 30
1 TiB	30 : 16 : 32	00 : 16 : 43
5 TiB	153 : 25 : 30	01 : 26 : 43

Table 3: Evidences needed to use in testing processing.

	Ubnistl.gen3.E01	Nps-209-domexusers.E01
Compressed	855 Mib	4.05 GiB
Uncompressed	1.98 GiB	42 GiB

machine images is critical in a virtual cluster system. The nodes in the various virtual clusters are shown in the diagram by the various colors. The most crucial thing to consider when dealing with a big number of virtual machine images is how to store them in the system. Operating systems and user-level programming libraries are among the most popular installs for most users and applications. Preinstalled templates for these software programs are available. Users may create their own software stacks with the help of these templates. The template VM may be used to create new OS instances. These instances allow the installation of user-specific components, such as programming libraries and apps.

This would allow virtualization-based cluster systems to have more nodes, each with 24 gigabytes of RAM. It is necessary to set up task processing from the beginning. These responsibilities will be carried out on the evidences, as well as the possible imaging and encryption of the proof for internet broadcast. This level's testing must be completed entirely on a workstation. Data can be processed quickly, and complex computations can be completed quickly, thanks to high-performance computing. This high-performance computation can be done on any computer with a 3 GHz CPU. This computer is capable of performing over 3 billion operations per second. A supercomputer, on the other hand, has similar powers.

High-performance computers can now do miracles. It advances significantly in a wide range of sectors, including science and technology. It benefits technology such as the Internet of Things, artificial intelligence, and 3D imaging, to name a few. The high-performance computing operating system includes computation, networking, and data storage. A cluster is a group of computers connected together to perform high-speed processing. Workstation clusters are now a viable substitute for supercomputers. In general, these workstation clusters were preferred for all high-performance processing requirements. There are two sorts of parallel hardware and software designs.

4.2. Testing. This test is designed to determine how many nodes each forensic cloud user has. Begin by evenly distributing all nodes over all conditions, starting with one. Increase the number of instances one by one until the processing speed is too slow to bear. Keep track of the number of nodes required to make a scenario operate. The HPC cluster and the workstation performed similarly. It is unable to give it with the same or equal storage device that the virtualization cluster provided due to technological restrictions. If a quicker storage was used, processing performance would improve. Figure 4 shows high-performance computing-based scalable 'cloud forensics-as-a-service' readiness framework. Table 1 shows the system needs of cloud forensic tool implementation.

Simultaneous imaging and upload and encryption are observed. Scenario 1 includes setting up the first processing activities that need be conducted on the evidence, as well as potential imaging and encryption of the evidence for Internet transmission. The data processing should begin at the same time as the imaging procedure. To speed up processing, the client should allow for simultaneous data transmission and picture creation. The client should be run twice: once to just upload the test data to the server, and again to submit the test data while concurrently creating an image of it. This will be used to test if the client can perform both tasks at the same time while maintaining a 120 MB/s upload pace. Each node had 24 Gigabytes of RAM and 12 threads.

4.3. Cloud Security Mechanism in HPC Environment. Once the image has finished uploading, tools that would need the entire image would be run. Because the devices will function in a cluster, the results will be stored in the working directory. The virtual computer's connection will be safeguarded. Only the virtual computer holding the evidence submitted by the cloud forensics expert will be accessible. The virtual machine displays the results of the tools as they are complete on the cluster. They require access to tools that are unable or unwilling to operate on a collection during this virtual machine. They cannot access evidence that belongs to another cloud forensics specialist since virtual machines are separated from one another. The information will be encrypted using the analysis virtual machine for the cloud forensics professional.

5. Results Obtained

To protect the data's secrecy and integrity throughout transmission, encryption must be applied to the evidence being

Table 4: One node for one cluster outputs.

	Parameter-1	Parameter-2	Parameter-3	Parameter-4	Parameter-5	Parameter-6
Factors	HPC	Virtualization	Work station	HPC	Virtualization	Work station
Sec	114.2	43.7	102.1	892.2	559.2	889.9
Mebibyte per second	19.22	46.1	19.06	47.3	71.9	47.2
Mebibyte	2106	2106	2106	42949	42949	42949
Bound	CPU	CPU	CPU	CPU	-None-	CPU
Threads	12	12	8	12	12	8
RAM	24v	24	8	24	24	8

Table 5: Outputs of workstation clusters.

	Ubnist1.gen3.E01				Nps-2009-domexuser.E01			
Factors	Node~1	Node~2	Node~3	Node~4	Node~1	Node~2	Node~3	Node~4
Sec	34.8	43.7	25.8	4.9	459.1	22.8	198.4	44.2
Mebibyte per second	13.9	12.8	19.2	108.4	21.7	51.3	51.7	222.3
Mebibyte	520	520	520	546	10737	10737	10737	10737
Bound	C.P.U.	C.P.U.	C.P.U.	-none-	C.P.U.	C.P.U.	C.P.U.	Input and output

transferred between the client and server. The advanced encryption system (AES) is a well-known symmetric key encryption standard with a proven track record. For data security during network transmission, this is deemed to be sufficient. Table 2 shows data transfer calculations theoretically.

In real-time stream processing: to speed up the analysis process, data must be processed as soon as it becomes available to the server. There are two methods for processing digital evidence. The two possibilities are bulk data analysis and a file-based technique. Data chunks are treated as a whole in bulk data analysis, regardless of their structure. The data must be chunked and supplied to each tool, with suitable nodes assigned. To handle data at the file level, several programs use file-based approaches. By extracting files from a stream in real time, the forensic cloud cluster can perform file-level analysis. Table 3 shows evidences needed to use in testing processing.

In remote desktop connection, performance test, the cloud forensic investigator connects to a distant virtual machine using VDI's built-in remote desktop protocol. There are two protocol alternatives for VMware Horizon View VDI: PCoIP and Microsoft's RDP. As an alternative to Microsoft RDP, the PCoIP protocol for Microsoft RDS is available. For terminal services, the PCoIP protocol is now available for use with PCoIP devices, including low-maintenance, ultrasecure zero clients, for increased performance across any network. Customers of Teradici Arch are able to do the following: by employing the PCoIP protocol to broker and manage both VMware View and RDS session desktops with VMware View Manager, you can provide a rich, interactive experience across any network. The APEX server offload card can protect and ensure a consistent user experience regardless of task or activity level while complying with stringent government and security mandates and being virus-resistant; it can reduce TCO with low-maintenance PCoIP zero clients and eliminate the need for expensive VPN products. Using the latest technology, firms are able to do the following: for both View VDI and RDS published desktops, the PCM facilitates communication between the view connection server (VCS) and end points. Remote access to the PCM may be achieved by implementing the PCM on the corporate network or in a DMZ. PCoIP Security Gateway (PSG) must be configured if the PCM is placed in a firewalled environment (DMZ). The PSG may be added to the PCM as an optional component. VMware View Security Gateway may be replaced with the ova package without the need for a VPN connection, and customers may access their remote workstations from the Internet. The nodes are the clients in this scenario. The files can then be handed to appropriate tools for file-centric processing after they have been made available. Table 4 shows one node for one cluster outputs. More functionalities, such as USB redirection and multimonitor support, are available with PCoIP. The usefulness of the remote desktop protocol will be determined in this test. We connect to the available cloud forensic tools to find out. Table 5 shows outputs of workstation clusters. Table 6 shows outputs of high performance clusters. Table 7 shows outputs based on virtualization cluster.

5.1. Advantages of Present Study. We studied reports and employed forensic tools after making my judgments to verify if the virtual machine was still useful. The virtual machine should react quickly and without any noticeable lag. Before deciding on the optimum processing option for digital data in forensic cloud tools, it is critical to establish a benchmark for how rapidly a forensics workstation can handle digital evidence. When parallelization is employed, both the virtualization and HPC clusters must test the speeds that each tool can achieve.

A variety of forensic cloud workflow components must be studied to identify the particular forensic cloud system.

Table 6: Outputs of high-performance clusters.

	Ubnist1.gen3.E01				Nps-2009-domexuser.E01			
Factors	Node~1	Node~2	Node~3	Node~4	Node~1	Node~2	Node~3	Node~4
Seconds	44.7	63.7	29.2	9.8	479.5	259.3	167.2	54.3
Mebibyte per second	12.4	7.9	14.7.8	48.7	21.8	39.4	64.9	199.8
Mebibyte	520	520	520	546	10737	10737	10737	10737
Bound	CPU	CPU	CPU	-None-	CPU	CPU	CPU	Input and output

Table 7: Outputs based on virtualization cluster.

	Ubnist1.gen3.E01				Nps-2009-domexuser.E01			
Factors	Node-1	Node-2	Node-3	Node-4	Node-1	Node-2	Node-3	Node-4
Sec	19.0	25.8	13.5	5.9	239.2	169.2	164.3	46.8
Mebibyte per second	24.6	18.8	34.8	89.4	43.9	61.6	65.3	224.8
Mebibyte	519	520	520	546	10737	10737	10737	10737
Bound	C.P.U.	C.P.U.	C.P.U.	-none-	C.P.U.	C.P.U.	C.P.U.	Input and output

These tests show discover just how much capacity and processing power a forensic cloud installation can handle.

6. Limitations of Present Study

The advantages of this model are as follows:

(i) The total analyzing time of large volumes of data is reduced by utilizing the capabilities of a high-performance computing environment and modifying current tools to work inside this context

(ii) If a smaller department does not have access to commercial software, it can use it remotely

(iii) Allows for teamwork. Because the data is stored in the cloud, anyone with the right authority from the case owner can access it and perform extra analysis

6.1. Recommendations. The goal of this test is to see if data can be uploaded to a forensic cloud. It uses several data set sizes and uploads and downloads each data set separately from different forensic cloud providers. Keep track of how long it takes for each file to upload. Calculate how long a single user would take to perform the task. This test is used to see if a forensic cloud environment can handle a large number of uploads. Upload and download a 500 GB or larger data collection from two forensic cloud facilities at the same time. Keep track of how long it takes for each file to upload. Increase the number of upload sites by one and reupload the files. Looking at the limitation of this present study, the goal of the nodes per job test is to conclude the optimal node numbers for every task. This test is aimed at examining if data can be uploaded to a forensic cloud environment. It is using various data set sizes, we upload and download each data set and upload and download a data collection with a size of 500 GB or more from two forensic cloud facilities simultaneously. Keep track of how long each file takes to upload. Reupload the files after increasing the number of upload sites by one. Keep track of how long it takes for each file to upload. Continue to add one facility at a time until any user's upload time becomes prohibitive. Therefore, there is a need to search an alternative way to conduct more comprehensive comparison.

7. Conclusions

There is a need of such a congregation of cohesive redressal prognostication which would surely make a solid impression with a comprehensive knowledge on many issues and will increase the knowledge of sharing for a cohesive success due to global technological trends. The world is being embarked on to a greatest reset. This would be an ever-changing innovation and technological advancement. After a detailed study, it is observed that the method of resource management techniques are differed one from the other and one strategy may be useful for real-time interactive application that may not be suitable for some other application area. Therefore, there is a need to find a solution using high-performance computing which would be suitable for mobile cloud computing also. The sixth-generation mobile network is under development. By 2030, all of the people would be using 6G. Combination of mobile networks with cloud computing environment provides customized options with more flexible implementations. AI can be used in mobile network services (MNS) such as to provide more reliable and customized services to the users. However, the most vital needs for sixth-generation standards is the capability of managing large volumes of records and very excessive-statistics-fee connectivity in step with gadgets. Sixth generation has many exciting features. Security is the major issue that needs to be sorted out using appropriate forensic mechanisms. There is a need to approach high-performance computing for the improved services to the end user. This approach would provide dynamic and versatile resource allocation for reliable and warranted on-demand services by narrowing the targeted global audience with a wide range of experiential opportunities.

8. Scope for the Future Work

The combination of 6th-generation mobile network standards with cloud computing along with artificial intelligence, cloud forensics, and high-performance computing would offer improvement in the user experiences; however, for managing the huge volumes of records and very excessive-statistics-fee connectivity in step with gadgets, there is a need to check with machine learning which would automate the analytical model building.

Data Availability

The evaluation data that support the findings of this study are available on request from the corresponding author.

Disclosure

The funder had no role in the design of the study; in the collection, analyses, or interpretation of data, in the writing of the manuscript, or in the decision to publish the results.

Conflicts of Interest

The authors declare no conflict of interest.

Acknowledgments

We wish to thank the late Mr. Panem Nadipi Chennaih for his continued support for the development of this research paper, and it is dedicated to him.

References

[1] V. L. Shirokov, "The basics of methodology for estimation and choosing parameters of multi-service telecommunication systems," *2nd International Conference on Dependability of Computer Systems (DepCoS-RELCOMEX 07)*, vol. 10, pp. 191–197, 2007.

[2] K. Trapezon, T. Gumen, and A. Trapezon, "Basics of using connected me system in the transmission of information signals," in *2018 14th International Conference on Advanced Trends in Radioelecrtronics, Telecommunications and Computer Engineering (TCSET)*, pp. 229–232, Lviv-Slavske, Ukraine, 2018.

[3] T. Minde, S. Bruhn, E. Ekudden, and H. Hermansson, "Requirements on speech coders imposed by speech service solutions in cellular systems," in *1997 IEEE Workshop on Speech Coding for Telecommunications Proceedings. Back to Basics: Attacking Fundamental Problems in Speech Coding*, pp. 89-90, Pocono Manor, PA, USA, 1997.

[4] M. Bahrami, "Cloud computing for emerging mobile cloud apps," in *2015 3rd IEEE International Conference on Mobile Cloud Computing, Services, and Engineering*, pp. 4-5, San Francisco, CA, USA, 2015.

[5] R. Gurunath, A. H. Alahmadi, D. Samanta, M. Z. Khan, and A. Alahmadi, "A novel approach for linguistic steganography evaluation based on artificial neural networks," *IEEE Access*, vol. 9, pp. 120869–120879, 2021.

[6] S. Li and J. Gao, "Moving from mobile databases to mobile cloud data services," in *2015 3rd IEEE International Conference on Mobile Cloud Computing, Services, and Engineering*, pp. 235-236, San Francisco, CA, USA, 2015.

[7] S. Abolfazli, Z. Sanaei, M. Alizadeh, A. Gani, and F. Xia, "An experimental analysis on cloud-based mobile augmentation in mobile cloud computing," *IEEE Transactions on Consumer Electronics*, vol. 60, no. 1, pp. 146–154, 2014.

[8] P. Bondada, D. Samanta, S. A. Chaudhry, Y. B. Zikria, and F. Ishmanov, "Efficient neighbour feedback based trusted multi authenticated node routing model for secure data transmission," *Sustainability*, vol. 13, no. 23, p. 13296, 2021.

[9] J. Y. Zhang, P. Wu, J. Zhu, H. Hu, and F. Bonomi, "Privacy-preserved mobile sensing through hybrid cloud trust framework," in *2013 IEEE Sixth International Conference on Cloud Computing*, pp. 952-953, Santa Clara, CA, USA, 2013.

[10] S. S. Qureshi, T. Ahmad, and K. Rafique, "Mobile cloud computing as future for mobile applications - implementation methods and challenging issues," in *2011 IEEE International Conference on Cloud Computing and Intelligence Systems*, pp. 467–471, Beijing, China, 2011.

[11] H. S. Alqahtani and G. Kouadri-Mostefaou, "Multi-clouds mobile computing for the secure storage of data," in *2014 IEEE/ACM 7th International Conference on Utility and Cloud Computing*, pp. 495-496, London, UK, 2014.

[12] M. M. Fuad and D. Deb, "Cloud-enabled hybrid architecture for in-class interactive learning using mobile device," in *2017 5th IEEE International Conference on Mobile Cloud Computing, Services, and Engineering (MobileCloud)*, pp. 149–152, San Francisco, CA, USA, 2017.

[13] L. Shankar, "Bigonet mobile cloud framework," in *2014 Sixth International Conference on Communication Systems and Networks (COMSNETS)*, pp. 1–3, Bangalore, India, 2014.

[14] S. D. A. Shah, M. A. Gregory, and S. Li, "Cloud-native network slicing using software defined networking based multi-access edge computing: a survey," *IEEE Access*, vol. 9, pp. 10903–10924, 2021.

[15] B. Chihani, E. Bertin, and N. Crespi, "Enhancing M2M communication with cloud-based context management," in *2012 Sixth International Conference on Next Generation Mobile Applications, Services and Technologies*, pp. 36–41, Paris, France, 2012.

[16] O. Segal, N. Nasiri, M. Margala, and W. Vanderbauwhede, "High level programming of FPGAs for HPC and data centric applications," in *2014 IEEE High Performance Extreme Computing Conference (HPEC)*, pp. 1–3, Waltham, MA, USA, 2014.

[17] E. El-Araby, I. Gonzalez, and T. El-Ghazawi, "Virtualizing and sharing reconfigurable resources in highperformance reconfigurable computing systems," in *2008 Second International Workshop on High-Performance Reconfigurable Computing Technology and Applications*, pp. 1–8, Austin, TX, USA, 2008.

[18] Z. Ba, H. Zhou, H. Zhang, and Z. Yang, "Performance evaluation of some MPI implementations on workstation clusters," in *Proceedings Fourth International Conference/Exhibition on High Performance Computing in the Asia- Pacific Region*, pp. 392–394, Mississippi State, MS, USA, 2000.

[19] K. Kim, H. Sung, and H. Lee, "Performance analysis of the TCP/IP protocol under UNIX operating systems for high performance computing and communications," in *Proceedings High Performance Computing on the Information Superhighway. HPC Asia 97*, pp. 499–504, Seoul, Korea (South), 1997.

[20] P. V. Shivabhai and M. R. Babu, "An open source web-based massive resource broker (MRB) for high performance computing (HPC)," in *2016 International Conference on Research Advances in Integrated Navigation Systems (RAINS)*, pp. 1–3, Bangalore, India, 2016.

[21] S. Ghoshal, "A floating-point validation suite for high-performance shared and distributed memory computing systems," in *Proceedings Fourth International Conference on High-Performance Computing*, pp. 88–93, Bangalore, India, 1997.

[22] S.-J. Han and S.-Y. Oh, "Evolutionary algorithm based neural network controller with selective sensor usage for autonomous mobile robot navigation in IJCNN'01," in *International Joint Conference on Neural Networks. Proceedings (Cat. No.01CH37222)*, Washington, DC, USA, 2001.

[23] S. V. Anand and S. P. S. Kumar, "A modular data link layer (M-DALL) for NEXT GEN mobile terminals enabling wireless aware applications: a platform independent software design," in *2010 Global Mobile Congress*, Shanghai, China, 2010.

[24] J. Teng, X. Xuan, and Y. Bai, "A fast Q algorithm based on EPC generation-2 RFID protocol," in *6th International Conference on Wireless Communications Networking and Mobile Computing (WiCOM)*, pp. 1–4, Chengdu, China, 2010.

[25] S. R. Gundu, C. A. Panem, A. Thimmapuram, and R. S. Gad, "Emerging computational challenges in cloud computing and RTEAH algorithm based solution," *Journal of Ambient Intelligence and Humanized Computing*, 2021.

[26] S. R. Gundu, C. A. Panem, and A. Thimmapuram, "Real-time cloud-based load balance algorithms and an analysis," *SN Computer Science*, vol. 1, no. 4, p. 187, 2020.

[27] S. R. Gundu, C. A. Panem, and A. Timmapuram, "Robotic technology-based cloud computing for improved services," *SN Computer Science*, vol. 1, no. 4, p. 190, 2020.

Hindawi
Wireless Communications and Mobile Computing
Volume 2022, Article ID 3632679, 12 pages
https://doi.org/10.1155/2022/3632679

Research Article

Internet Rumor Audience Response Prediction Algorithm Based on Machine Learning in Big Data Environment

Suhong Yang[1], **Shenghui Wang**[2] **and Y. Yiwen**[3]

[1]*Hangzhou Dianzi University Information Engineering College, Hangzhou, 310000 Zhejiang, China*
[2]*Shaanxi Jiatong Electronic Technology Co., LTD, Xi'an, 710075 Shaanxi, China*
[3]*Business School, University of Strathclyde, G1 1XQ, Glasgow, UK*

Correspondence should be addressed to Shenghui Wang; kk743@wfd.edu.ug

Received 20 January 2022; Revised 13 March 2022; Accepted 5 April 2022; Published 30 April 2022

Academic Editor: Mohamed Elhoseny

Rumors are an important factor affecting social stability in some special times. Therefore, the dissemination and prevention and control mechanisms of rumors have always been issues of concern to the academic community and have long been highly valued and widely discussed by experts and scholars. However, in combination with the Internet as a new type of media, although people have begun to pay attention to online rumors, research on it is still relatively fragmented, especially in the cross-domain research specific to the social influence of online rumors, and there is no clear indication of online rumors. The specific definition also did not analyze in detail the internal connection between its influence and group behavior. Therefore, this article will combine actual cases to explore and analyze the spread and influence process of online rumors and show its social influence, hoping to enrich the research of online rumors. Nowadays, the Internet has become the most important carrier to reflect the public grievances. Internet users have expressed their opinions on hot issues such as enterprises, people's livelihood, and government management, which has formed a powerful public opinion pressure, which has far exceeded the traditional media. The hidden dangers of security cannot be ignored. Therefore, how to monitor network public opinion from a large amount of network data is a difficult problem that needs to be solved urgently. Firstly, this consists of four modules: information collection, web page preprocessing, public opinion analysis, and public information report. Secondly, text clustering, the core technology of network public opinion, is optimized, and single-pass algorithm based on double threshold is proposed. Then the dual-threshold single-pass algorithm is optimized based on the MapReduce parallel computing model, and finally a network public opinion collection technology is formed under the background of big data. Simulation results can greatly improve the performance of text clustering and can effectively optimize the design using the parallel computing model based on MapReduce. The average miss rate after optimization is 0.7569 times, the average false alarm rate is 0.5556 times, and C_{det} is 0.5714 times. It proves that the collection technology based on machine learning under the background of big data is effective and has good performance.

1. Introduction

Internet has a positive impact on the economy, politics, culture and people's lives. At the same time, it should be noted that bad and false information still exists on the Internet, which affects the healthy development of society. Rumors caused panic among the people, endangered public safety, and harmed public interests. Due to the convenience and development of the Internet, rumors spread quickly and spread widely, which will cause adverse effects. Rumors disturb people's thinking, psychology, and behavior, destroying the social trust system. In particular, the spread of Internet rumors has become a major social nuisance, severely infringing on citizens' rights and interests, harming public interests, and endangering. The rapid development of Internet technology, on the one hand, is reflected in the Internet technology and, on the other hand, in the development of software and hardware, such as a variety of APP, 3G network upgrade to 4G network. The rapid development of technology has not only facilitated people's lifestyle and enriched people's participation in society, but also profoundly influenced the behavior of each subject in society. By December 2013, the

netizens reached 618 million. In 2013 alone, the netizens reached 53.58 million. The development of network society has expanded the channels for people to participate in society, express their feelings and opinions, and greatly stimulated the people's willingness to express their opinions.

Rumors have existed for a long time, and the limitations of traditional media have determined that traditional rumors are confined in a relatively narrow range, and their influence is far less than today's online rumors. The most direct cause of the spread of rumors is the lack of real information in society. Why is it missing? Because the flow of information is hindered. At the level of public life, because information is relatively more open and transparent and circulates more quickly, people can compare information from all parties, and the space for rumors to survive is much narrower. Content control is the most difficult problem. Anyone can move anything to the Internet. This kind of thing often happens. The Internet poses some rare problems for anyone who wants to clear this trash on the information superhighway. Internet rumors are undoubtedly one of the important issues. When traditional rumors enter the Internet, rumors are like "winged on." They are likely to appear first on the Internet as a "hotbed" and cause rumors to spread. They appear on the silver screen in a radial manner. Either personal curiosity, or hype by a certain person or organization, or simple unintentional action, or purposeful misleading, no matter what mentality, once rumors go through the Internet, it may cause the spread of rumors to increase exponentially. The development of self-media represented by mobile phones has greatly facilitated and speeded up the means by which people express their opinions. By December 2013, the number of mobile phone users has reached 500 million, and the number of users using mobile phones to log on to the Internet has accounted for 73.3% of the new Internet users in China, much more than the proportion using other terminals. This means that the rapid popularization of mobile terminals has promoted the increase of Internet users in China.

The Internet from 2G network to 3G network and from 3G network to 4G network, the combination of massive mobile terminals, followed by the generation of massive data. China produced more than 0.8 ZB (800 million TB) of data in 2013, twice as much as in 2012, equivalent to the total global data in 2009.

It is based on the Internet, with the expression of the people's opinions and the behavior of the government as the manager as the basic content, with the government, netizens, and network media as the three main participants, around the development process of specific events in society, and the process of mutual game. Internet technology, the popularity of mobile terminals and the improvement of people's awareness of participating in hot social events, the traditional channels of expression of public opinion, and the network has gradually become the most important position for people to express their emotions.

In this process of development, due to the rapid spread of the Internet and the combination of online or wireless communication tools such as forums, blogs, Weibo, WeChat, and self-media, the traffic information data has become diversified, and it has become more and more difficult for the government to control and monitor public opinion. In the process of the beginning, fermentation and outbreak of social public opinion, the network plays a great role, as one of the management contents of the government.

Under the background of the big data era, the frequent innovation and application of the emerging network media, especially the popular new media, has created a completely different network public opinion environment, and it has significant characteristics different from any previous period. In such a brand-new network public opinion environment, the era when the dominant power of discourse is in the hands of a certain party or organization has become a history. Every individual member can make his own voice anytime and anywhere by means of the emerging network media or receive and understand the outside world actively and passively. However, it is in such an "open and partially closed" environment that most individual members are at the bottom of the information chain, unable to identify the true and false information, or passively accept a certain point of view, and become "followers" of certain public opinion. It is precisely this reason that exacerbates the uncertainty and uncontrollability of network public opinion, and in reality, people tend to use the network to express all kinds of contradictions and emotions; once become the focus of network hot discussion, it will form a storm of public opinion. If handled improperly, it is likely to form a crisis of network public opinion, which is not only harmful to the stability of social order, but also has a profound impact on the government's social governance and credibility.

Machine learning (ML) is also the core research field of AI. Machine learning is a highly interdisciplinary research field. Machine learning algorithms can be used to solve computer vision, biology, robotics, data analysis, natural language processing, and other fields. Machine learning has been, is, and will bring great impetus to many disciplines. Linear regression is terrible at dealing with nonlinear relationships, inflexible in identifying complex patterns, and extremely tricky and time-consuming to add the correct interaction terms or polynomials.

In short, machine learning is a science that studies, the acquisition of knowledge or skills, and the improvement of performance. ML science first appeared in the 1950s. It is a subject about computer, data construction, model, and simulation of human activities. Its application has covered all aspects of our lives, for example, robotic chess programs, speech recognition, unmanned driving, robots, and other fields. In addition, machine learning theory and methods have also played a huge role in this field. This paper mainly includes the introduction, related work, related methods, experiments discussion, and conclusions.

2. Related Work

It is generally believed that machine learning is a kind of knowledge that studies how computers acquire new knowledge and skills through experience and discover existing knowledge [1–3]. A common definition is to measure the performance of a computer program to accomplish learning

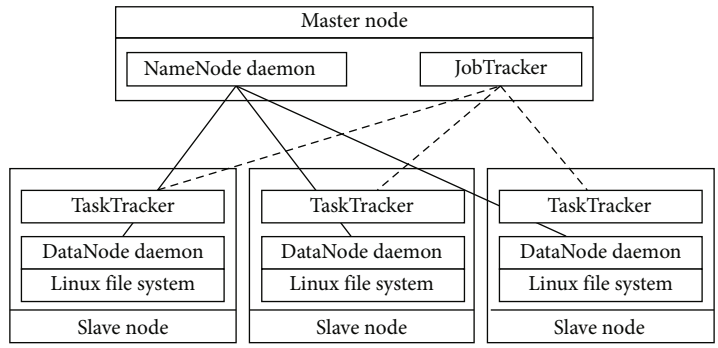

Figure 1: Basic structure of Hadoop.

Table 1: Topic quantity table.

Name	Michel's visit to China	Malaysia airlines plane missing	Poisoning in kindergarten	Balance treasure income	Coal mine accident	Other	In total
Number	178	184	135	88	123	92	800

Table 2: Double-threshold single-pass algorithm for processing result data.

Statistical unit (unit)	Michel's visit to China	Malaysia airlines plane missing	Poisoning in kindergarten	Balance treasure income	Coal mine accident
Correct documentation in cluster	145	148	121	78	109
p_{miss}	0.1713	0.2134	0.0916	0.1063	0.2339
p_{false}	0.0032	0	0.0015	0.0014	0.0029
Mean of p_{miss}			0.1633		
Mean of p_{false}			0.0018		
C_{det}			0.0021		

Table 3: Single-pass algorithm processes result data.

Statistical unit (unit)	Michel's visit to China	Malaysia airlines plane missing	Poisoning in kindergarten	Balance treasure income	Coal mine accident
Correct documentation in cluster	130	128	107	58	83
p_{miss}	0.3122	0.4207	0.2916	0.3211	0.4279
p_{false}	0.0071	0.0069	0.0039	0.0044	0.0042
Mean of p_{miss}			0.3547		
Mean of p_{false}			0.0053		
C_{det}			0.0059		

in experience (E), which requires the program to improve the performance of a tasks (T), and whether the performance of this program can be measured by performance (P).

Since its emergence, machine learning has been entered a bottleneck period. In recent years, there has not been much substantial progress in various branches of AI. It is in this context that machine learning is gradually revalued and has become one of the cores of artificial intelligence. The theory has been put into practice and successfully applied to such fields as pattern recognition, intelligent search, stock market analysis, DNA sequence research, and intelligent robots.

At present, domestic and foreign institutions that use machine learning technology to analyze social networks have achieved more results and are at the forefront level: Stanford University in the United States, IBM (released professional social network analysis software), SAS company, and Microsoft. Researchers from Tsinghua University and other universities and institutions have done more in-depth research in this field in China, according to the

Table 4: Experimental data before and after single-pass improvement.

	Double-threshold single-pass	Classic single-pass	Ratio
Mean of p_{miss}	0.1633	0.3547	0.4604
Mean of p_{false}	0.0018	0.0053	0.3396
C_{det}	0.0021	0.0059	0.3559

learning form and the experience contained in the training data set. Among them, unsupervised learning is inexperienced learning, which can recognize the data without class labels directly and predict the new sample categories using the results of unsupervised algorithms such as clustering.

Based on the advantages machine learning, which can effectively monitor network public opinion from data, the specific contributions of this article are as follows:

(1) This consists of four modules: information collection, web page preprocessing, public opinion analysis, and public information report

(2) The single-pass clustering algorithm in text clustering technology is optimized, and a single-pass algorithm based on double threshold is formed, which makes the public opinion system have more clustering performance. A single (global) threshold that applies to the entire image can be used when the grayscale distribution of object and background pixels is very pronounced. Global thresholding can then be used

(3) The dual-threshold single-pass algorithm is optimized based on the MapReduce parallel computing model so that the algorithm can carry out public opinion analysis in big data environment

However, none of the above studies on big data technology is comprehensive enough and practical enough.

3. Proposed Method

3.1. Framework Design of Public Opinion Analysis System. The public opinion analysis system designed in this paper is divided into four major functional modules, including information acquisition and web page preprocessing. Next, the design of each functional module is explained in detail.

3.1.1. Information Acquisition. The information acquisition module consists of four submodules: crawler module, update module, filter module, black-and-white list management module, and many configuration files, such as entrance address and black-and-white list.

The crawler module interacts directly with the Internet through the initial configuration of the entry address to scrape pages from the Python web crawler. However, because the content on the network is too large, if all pages are crawled, the capacity of the local machine will be a big challenge first, and the huge amount of information crawled is not necessarily the concern of users; at the same time, for the latter, data analysis will also cause a great burden. Therefore, in the design of the system information acquisition module, a filtering module is specially designed. The module filters the crawled web pages through the black-and-white list of URL and the black-and-white list of keywords to determine whether the web page is a page of user concern, thereby reducing the crawling of meaningless web pages.

When the original web pages on the Internet are modified or deleted, if the web crawler does not track their changes and updates in time, there will be a large number of expired pages or invalid links in the local web library. The captured web page is actually a mirror and backup of the Internet content. The Internet changes dynamically, and some content on the Internet has changed. At this time, this part of the captured web page has expired. Updating module is to analyze the pages in the local web database to determine which pages need to be updated. If there is a need to update, it submits an update application to the crawler module, and the data is crawled again by the crawler module.

The entrance address management module and the black-and-white list management module manage the entrance address and the black-and-white list, respectively.

3.1.2. Web Page Preprocessing. Information preprocessing module is mainly to extract the content of the collected web page information, which needs to extract important information such as title, text, links, time, and clicks. In this system, web page information is extracted based on DOM tree.

Web pages are made up of hypertext text markup language (HTML) [4], and document object model (DOM) [5] is a common way to represent and process an HTML or XML document. It can transform semistructured HTML pages into structured DOM tree structure, study the layout structure of web pages through tree structure, and extract the content of web pages. When the DOM parses, it treats the HTML document as a tree, the < HTML > tag as the root of the tree, and other components in the document as nodes in the tree. A node can be a parent node containing child nodes or a brotherhood of the same layer.

In the information preprocessing module, the basic idea of web information extraction based on DOM is to store the web templates of each web site in the form of XML configuration files on the server, where the node content of XML files is the path of nodes in DOM. Then, the paths of each node are obtained by reading these configuration files, and the information is extracted from the DOM nodes according to each path and stored in the database.

3.1.3. Public Opinion Analysis. It can respond to the massive data distributed by the preprocessing module in time. Secondly, it can accurately classify the massive text streams, and then cannot pollute the preprocessed text. Finally, the text orientation analysis aims to analyze the emotional color of each document from the mass of public opinion data

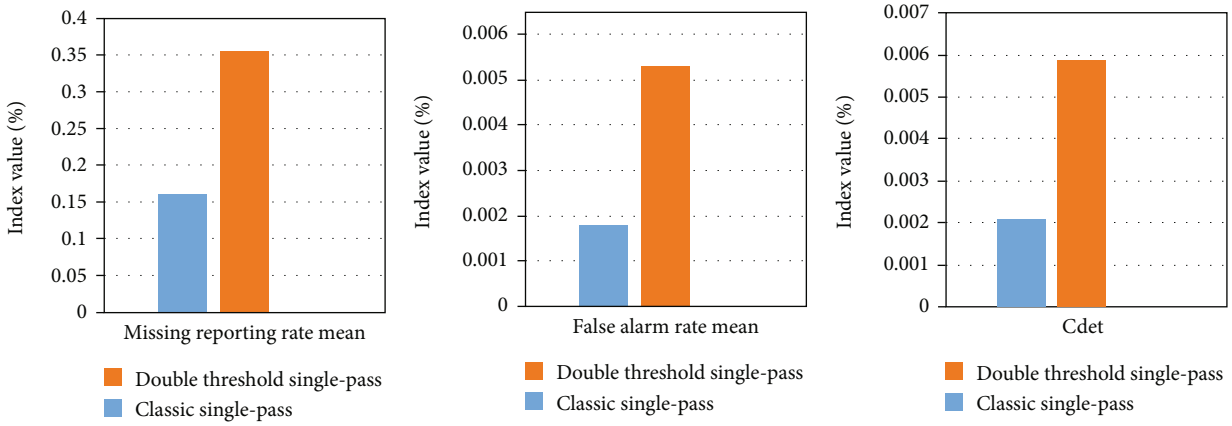

Figure 2: Histogram comparison of experimental data before and after single-pass improvement.

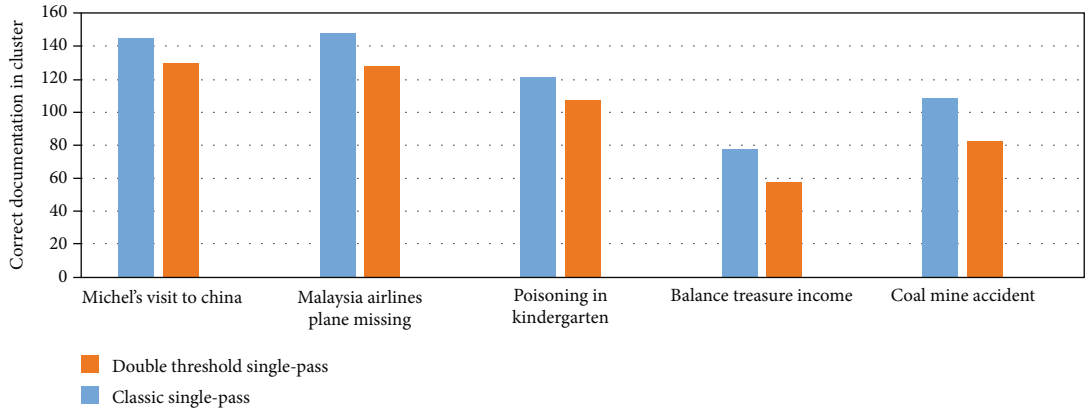

Figure 3: A comparison histogram of correctly identified documents in clusters before and after a single-pass improvement.

Table 5: The result data of double-threshold single-pass algorithm optimized by MapReduce.

Statistical unit (unit)	Michel's visit to China	Malaysia airlines plane missing	Poisoning in kindergarten	Balance treasure income	Coal mine accident
Correct documentation in cluster	156	161	129	83	117
p_{miss}	0.1031	0.1479	0.0876	0.1265	0.1529
p_{false}	0.0032	0	0.0015	0.0014	0.0029
Mean of p_{miss}			0.1236		
Mean of p_{false}			0.0010		
C_{det}			0.0012		

collected so that the users can efficiently browse to the network of emergencies, to understand the direction of public opinion. The core steps of network public opinion analysis are sorted out. According to the characteristics of network public opinion information data, a hybrid word segmentation model based on manual adjustment is proposed to process Chinese texts. The feature extraction technology is integrated into the calculation of the weight of emotional words, and a classification algorithm based on machine learning is proposed. The text sentiment orientation classifier constructed by this algorithm can be used to judge the sentiment orientation of text data. In this paper, a semantic-based text orientation analysis method is used to analyze text orientation systematically, so as to discriminate the emotion of the input document and annotate the emotion category of the document.

3.1.4. Public Opinion Report. The main function of the public opinion reporting module is to push public opinion hotspots. The public opinion hotspot push is mainly used to meet different user needs, automatically push popular public opinion for customers in the near future, provide

Table 6: Simulation data of double-threshold single-pass before and after optimization.

	Double-threshold single-pass optimized by MapReduce	Double-threshold single-pass	Ratio
Mean of p_{miss}	0.1236	0.1633	0.7569
Mean of p_{false}	0.0010	0.0018	0.5556
$C_{\det}$	0.0012	0.0021	0.5714

search keywords for customers, and collect public opinion recently pushed. The public opinion early warning is aimed at the public opinion exceeding the threshold of public opinion early warning, the system through short messages and e-mail and other real-time communication, to achieve automatic alarm, to provide early warning information for customers, and to prevent dangers in the future.

3.2. Optimization Design of Single-Pass Algorithm. Text clustering unsupervised (the number of data classes to be analyzed is unknown) [6]. Its goal is to divide the data into several classes of data clusters so that the data of each class is as different as possible, and the differences within each data cluster are as small as possible. Unsupervised text clustering hopes to discover the laws and patterns of the data itself. Compared with supervised text clustering Q, unsupervised text clustering does not need to label the data. This can save a lot of manpower and material costs. Clustering analysis [7–9] refers to the mathematical method of studying and processing the classification of a given object. Clustering is an important human behavior. A person's growth process is to learn to distinguish things by constantly improving the subconscious clustering pattern. Clustering can help us to discover the implicit association between data and identify the community structure which is closely related.

Single-pass clustering algorithm [10–12] is a simple incremental clustering algorithm, very intuitive, and easy to understand; it is obvious that it uses a greedy strategy; whenever a new document comes in, it will be allocated to a cluster, the order of the document samples has a great impact on the results of this clustering algorithm, and this algorithm is also sensitive to thresholds. The single-pass algorithm is an incremental algorithm, suitable for mining streaming data, and the algorithm has high a time efficiency; the main disadvantage of this method is that the method has the characteristic of input order dependence, that is, for the same clustering object input in different orders, different clustering results will appear.

Algorithm is sensitive to the determination of document order. A double-threshold-based single-pass algorithm is formed:

Step 1: Receive data$t_i$by processing the data features and constructing a space vector model oft_i:

$$M = \frac{1}{T}\sum_{i=1}^{T}\frac{F(H,O)}{F(Y,O)},$$
$$N^* = \ln F(\beta/J), \tag{1}$$
$$G(M,N) = \sum_{x,y} R(M,N)\left[H(X+u, Y+v) + \phi\right]^2.$$

Step 2: Calculate the similarity between the data t_i and all existing topic documents

Step 3: Find the topic of the document with the greatest similarity to the data t_i:

$$H = \sum_{M,N} G(M,N),$$
$$G(K_1, M_2) = \frac{1}{H} e^{-\frac{M^2+N^2}{2N^2}}, \tag{2}$$
$$T = \frac{1}{B} T(M,N).$$

Step 4: Set the threshold T_c. If in the process of allocating the data t_i, the data t_i is assigned to the topic having the greatest similarity. If the similarity is less than the threshold T_c, indicating that the data t_i does not belong to any existing topic, you can use t_i as a document for the new topic and create a new topic category

Step 5: Repeat Steps 2 through 4 until all samples have been assigned to a topic

Aiming at the disadvantage that single-pass algorithm is sensitive to the order of data, in order to improve the clustering effect of single-pass algorithm. The algorithm flow is as follows:

Step 1: Receive data t_i by processing the data features and constructing a space vector model of t_i

Step 2: Determine if there is a topic cluster. If there is no topic cluster, create a topic cluster K_j, and make $t_i \in K_j$, and then go to the eighth step. If there is a topic cluster, go to the third step:

Step 1: Receive data t_i by processing the data features and constructing a space vector model of t_i

$$T_{MIB} = \sqrt{m_x^2 + n_y^2},$$
$$K_{\mathrm{j}} = \sum\left(\frac{q}{t}\right), \tag{3}$$

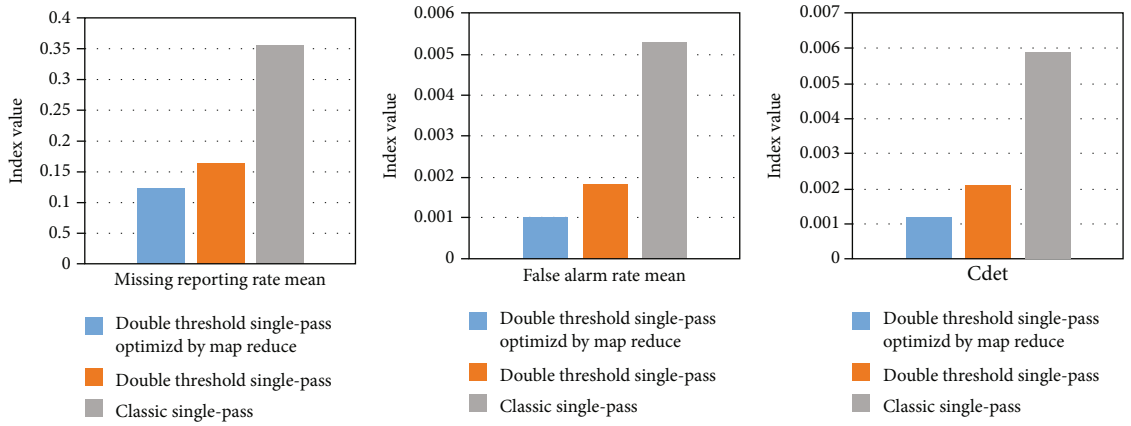

Figure 4: Three algorithms' simulation data contrast histogram.

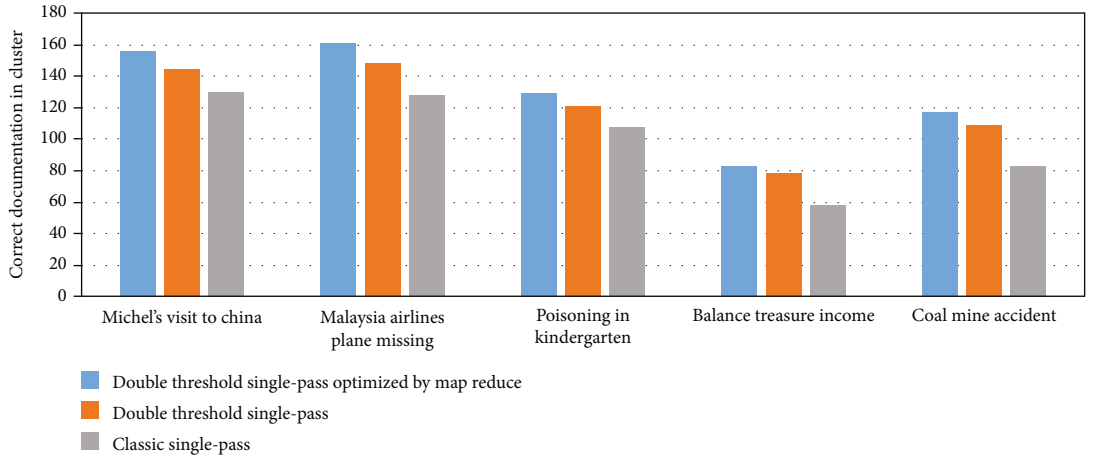

Figure 5: Contrast histogram of correct document in three algorithms' cluster.

$$S_D = S(T|D) = S/(P+Q) \tag{4}$$

Step 3: The data t_i is calculated by similarity with all previous topic documents, and the maximum similarity T is obtained:

$$t_i = \sqrt{y/(x+b)} \tag{5}$$

$$g_1 = n(y|u) = oy/(rm+p) \tag{6}$$

$$t_1 = M(1\text{-}M) \tag{7}$$

Step 4: Unlike the classical single-pass algorithm, this paper uses two thresholds: T_c and T_{mid} (where $T_c > T_{mid} > 0$). If $T > T_c$, the data t_i is merged into the cluster K_j and jumps to the fifth step. If $T_c > T > T_{mid}$, the data t_i is merged into the buffer stack of cluster K_j to wait and jump to the eighth step. If $T < T_{mid}$, the data t_i is separately attributed to create a new cluster, to the eighth step. The global threshold image segmentation region segmentation region growth and split-merge methods are two typical serial region techniques. The processing of the subsequent steps of the segmentation process should be determined according to the results of the previous steps

Step 5: Put the data t_i in the topic cluster K_j, and update the vector model of topic cluster K_j, n++, and determine the relationship between n and N. If $n > N$, then go to the fourth step; if not, turn to the sixth step

Step 6: Update the vector model of topic cluster K_j, and go to the eighth step:

$$\xi_t(I,J) = P\phi \tag{8}$$

$$R_1 = Rm \tag{9}$$

$$\varphi = \lambda \tag{10}$$

Step 7: All the data in the buffer heap of topic K_j are computed and compared with the new central vector after n updates of the central vector of K_j. Let the value of similarity be T. If $T > T_c$, go to cluster K_j, and go to the sixth step. If $T_c > T > T_{mid}$, the data remains unchanged in the buffer area and goes to the eighth step. If $T < T_{mid}$, the data t_i is separately attributed to create a new cluster, to the eighth step

$$t_2 = g[\ln Y(Y)] + g[\ln(\varphi + x(x))], \tag{11}$$

$$f_p(x) = \lambda \prod_{m=1}^{l} \phi_{pm}(\lambda) \tag{12}$$

$$f_1 = v[\|c - x\|] \tag{13}$$

Step 8: End, waiting for new data to arrive

3.3. Improvement of Dual Threshold Single-Pass Algorithm Based on MapReduce. MapReduce [13–15] parallel computing framework is a parallel computing model running on HDFS distributed storage system [16]. It can process large PB-level data in parallel in a high fault-tolerant way and realize the parallel task processing function of Hadoop platform [17, 18]. The core idea of this design is to divide and conquer the problem, not to push the data to the calculation, but to push the calculation to the data, which can greatly reduce the communication overhead.

The MapReduce execution process mainly includes the following five steps [19–21]:

(1) The input large data set slices are decomposed into hundreds of small data sets splits, which are handled by different machines

(2) Each (or several) small data set executes the Map task in parallel by an ordinary computer in the cluster, converting input into an intermediate set of key value pairs

(3) A large number of nodes are sorted and aggregated in the middle form of key value pairs according to the same principle of key value

(4) The value sets with different key values are allocated to different machines for processing, and Reduce computing tasks are performed

(5) Output Reduce calculation results

Double thresholds are improved on the MapReduce parallel framework, which can solve the problem of long iteration time for a large number of data. Based on MapReduce, it divides the improved single-pass clustering algorithm based on double thresholds into three stages: map stage, combine stage, and reduce stage.

Table 7: The analysis dimension and framework of audience response of Internet rumor.

Behavior attitude	Believe	Neutral	Unconvinced
Spread	Disseminator	Witness	Refuting rumor
Not spread	Silent supporters	Silent waiters	Silent doubters

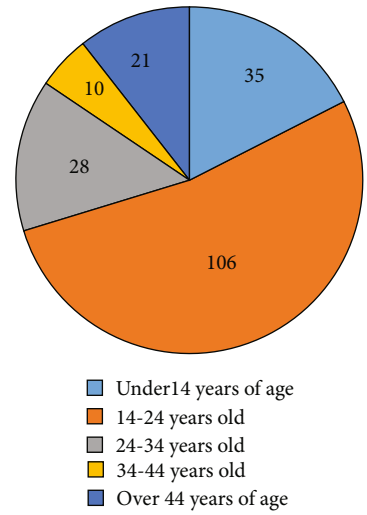

Figure 6: Age pie chart of persuasive communicator.

The specific implementation steps are as follows:

(1) In the cluster client system configuration, start a new task, specify the specific location of input and output content, and configure map and reduce functions to run the required classes, and then commit the new task to execution

(2) The Input Fonnat phase splits the vector value vector of the sample points in the input HDFS distributed file system into 64 MB or 128 MB blocks. Each block is parsed into a key value pair in the URL, and the value represents the vector value obtained from the calculation of the sample points

(3) Map process. The key value pairs in the standard format input at this stage can be expressed as <id, vector>, where id denotes the number of the sample points and vector denotes the vector values formed by the sample points. In this process, the map function is designed to be different from the traditional binary cyclic function. The inner function is mainly used for n updates of the K_j center vector, and the outer function is mainly used for cyclic traversal of the text vector itself

(4) Partitioner process. A hash calculation is performed on the index value, i.e., the value represented by

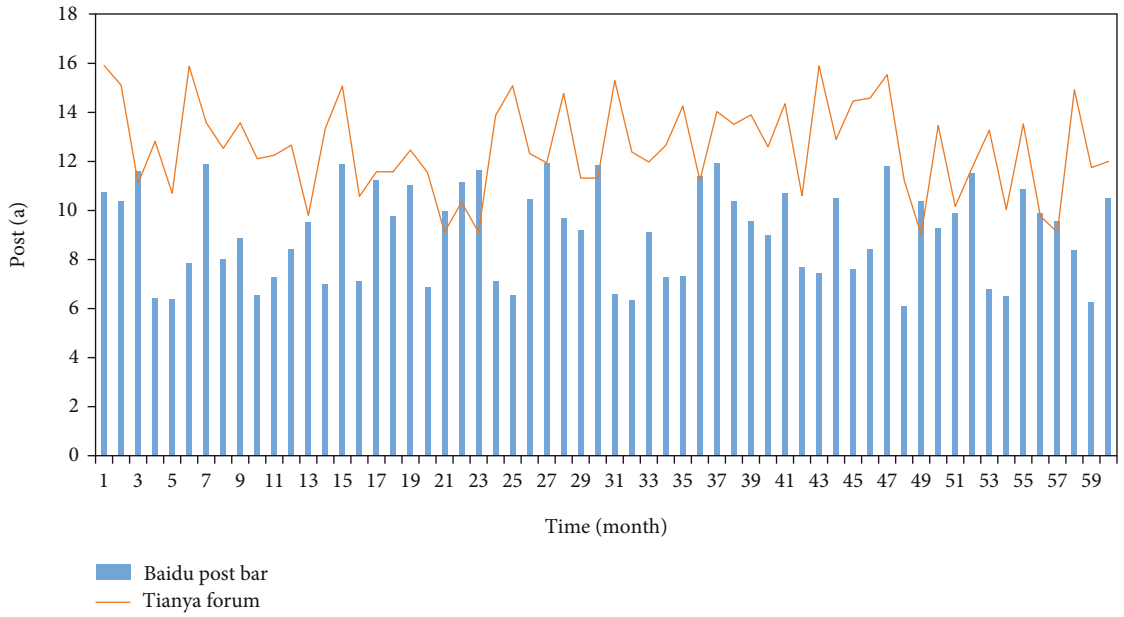

Figure 7: The result of the search.

the key in the key pair. This procedure unifies the sample points with the same index value on the same system node for calculation

(5) Combiner process. The design of this stage is mainly used data output from each map program is normalized locally, and the sample points which are divided into the same category are calculated once their average value

(6) Reduce process. The input of the process is the normalized key value pair with <URL," "> format. The average value obtained from the previous stage is used as the new condensation point or center of mass in the re-classified category

(7) Out format process. This process mainly implements the output of the reduce function. The key is the specific identifier of each class, and the value is the vector writer class used to write content after the final encapsulation of the system. At the same time, the class also stores information about other dimensions of the sample points

4. Experiments

Collection technology machine learning is proposed, in order to adapt to the explosive growth of network collection technology based on machine learning under the background of large data. Among them, the MapReduce parallel computing framework is a parallel computing model running on HDFS distributed storage system. It can process big data at PB level in a high fault-tolerant way and realize the parallel task processing function of Hadoop platform.

The basic structure of Hadoop system is shown in Figure 1. Logically, the basic structure of Hadoop system includes two parts: distributed storage and parallel computing. It uses NameNode as the master node of distributed storage to store and dominate metadata over the entire distributed file system and DataNode as the slave node of large-scale data storage. Each slave node stores real data on its own node based on the underlying Linux system. In parallel computing architecture, Hadoop uses JobTracker as the main control node of MapReduce parallel computing framework to schedule and manage the execution of jobs and TaskTracker.

In order to implement the principle of localized computing in Hadoop system design, data storage node DataNode and computing node TaskTracker will be merged and set up so that each slave node runs simultaneously as DataNode and TaskTracker so that each TaskTracker can process the data stored on the local DataNode as much as possible.

When the cluster is large or the two master nodes are overloaded, they will affect each other.

In this paper, the experimental data is searched through the network search engine, and then the 800 topics are obtained by manually swiping the page. The specific data of the topic are shown in Table 1.

In this paper, the simulation performance indicators are evaluated by TDT2004. The method is mainly through the missed detection rate, false alarm rate, and detection cost [22–25] to evaluate the algorithm designed in this paper.

The missed detection rate is the ratio of the data belonging to a topic to the actual document of the topic in the topic database. The formula is as follows:

$$p_{miss} = \frac{B}{A+B}. \tag{14}$$

The false alarm rate is the ratio of the number of documents on a topic to the number of documents in the topic database that do not describe the topic. The formula is as

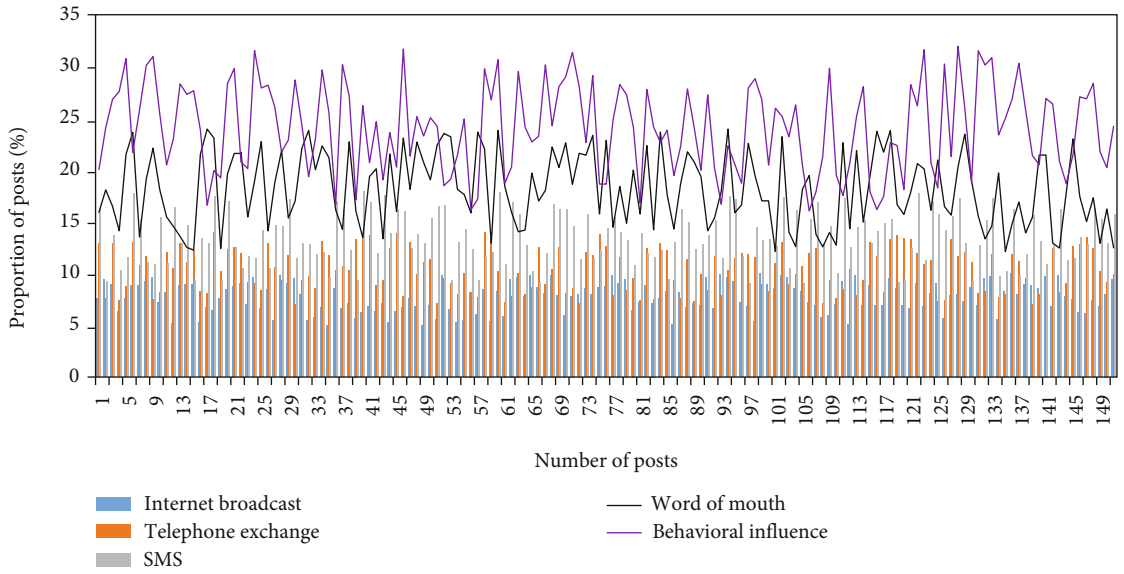

Figure 8: The specific distribution.

follows:

$$p_{false} = \frac{C}{C + D}. \tag{15}$$

A is a document that originally belongs to a topic and is correctly judged as a topic. B is a document that does not belong to a topic and is not correctly classified as a topic. C is a document that does not belong to a topic, but is considered to be a topic. D is a document that does not belong to a topic and is not mistaken for a topic.

In addition, the TDT2004 criterion also provides a test cost. The formula is as follows:

$$C_{\text{det}} = C_{\text{miss}} \cdot p_{miss} \cdot p + C_{false} \cdot p_{false} \cdot (1 - p). \tag{16}$$

Where C_{miss} is the price of missing report, C_{false} is the price of false positives, and p is the possibility of a document appearing in a topic.

5. Discussion

The results of the dual-threshold single-pass algorithm are shown in Table 2, and the data of the single-pass algorithm are shown in Table 3. The relevant experimental parameters are set as follows: $T_c = 0.6$, $T_{mid} = 0.35$, $k = 20$, $C_{miss} = 0.1$, $C_{false} = 1$, and $p = 0.02$.

In the proposed dual-threshold single-pass algorithm, the mean miss rate, the mean false alarm rate, and C_{det} of Table 2 and Table 3 are put into Table 4, and the three performance ratios of the two algorithms are calculated in Table 4. In addition, the column diagram of Table 4 is drawn as shown in Figure 2.

Combining Table 4 and Figure 2, we can see that the double-threshold single-pass algorithm has better performance than the single-pass algorithm in terms of the mean miss rate, the mean false alarm rate, and C_{det}. The average false alarm rate of single-pass algorithm with double thresholds is 0.4604 times of that of the single-pass algorithm, the average false alarm rate is 0.3396 times of that of the single-pass algorithm, and C_{det} is 0.3559 times of that of the single-pass algorithm. Compared with the classical single-pass algorithm, the performance of the proposed single-pass algorithm based on double threshold is better. In addition, Figure 3 shows the contrast histogram of the two clustering algorithms for correctly identifying documents. Similarly, it has better clustering performance than that designed in this paper.

In the big data era of network information explosion, using the big data technology MapReduce to optimize and improve the double-threshold single-pass clustering algorithm can solve the problem of long iteration time. Similarly, the dual-threshold single-pass algorithm optimized by MapReduce is used to simulate the process, and the data is shown in Table 5.

In the same way, the double-threshold single-pass algorithm is put into Table 6 with the mean of miss alarm rate, false alarm rate, and C_{det} before and after the optimization of big data MapReduce, and the three performance ratios of the two algorithms are obtained in Table 6. In addition, the three performance indicators of single-pass algorithm, double-threshold single-pass algorithm, and MapReduce optimized double-threshold single-pass algorithm are drawn as a histogram shown in Figure 4.

Combining Table 6 and Figure 4, it can be seen that the average miss detection rate, the average false alarm rate, and the performance index C_{det} of the dual-threshold single-pass algorithm have been significantly improved after the large data technology MapReduce optimization. The average miss rate after optimization is 0.7569 times, the average false alarm rate is 0.5556 times, and C_{det} is 0.5714 times. It can be seen that it is feasible to use the big data technology MapReduce to optimize the double-threshold single-pass algorithm. And since the MapReduce is a parallel computing

framework, it can improve the iterative efficiency of the double-threshold single-pass algorithm. Therefore, in terms of clustering performance, the double-threshold single-pass algorithm optimized by MapReduce is the best, the algorithm is the second, and the single-pass algorithm is the worst.

In addition, Figure 5 shows the contrast histogram of the three algorithms. It can also be seen that the clustering results of the double-threshold single-pass algorithm optimized by MapReduce are the best, the double-threshold single-pass algorithm takes the second place, and the single-pass algorithm is the worst.

Nowadays, in the network public opinion, the network rumor is more and more harmful; this article divides the network rumor audience from the attitude and the action two dimensions and may subdivide into six kinds of reaction types, such as the rumor propagator, the disclaimer, and the silent supporter, as shown in Table 7.

This paper uses the current hot micro-blogging platform to test the age of the Internet rumor audience. After publishing the topic of Internet public opinion, it analyzes the age of 200 disseminators and gets the disseminator's convincing age pie chart as shown in Figure 6.

From the Figure 6, we can see that the disseminators of online public opinion are mainly concentrated in the 14-26 years old, it is just the adolescent stage of the formation of ideas, and it can be seen that they are easy to form a trend to follow the trend, which will have a very bad impact on their thinking. Therefore, effective extraction of network public opinion information can very well inhibit the spread of network public opinion, so as to correctly guide the network public opinion audience.

Search for related posts in Baidu Tieba and Tianya forums with "earthquake" as the keyword, "in order of relevance." Due to the large number of posts, only the first 20 pages of information are selected from each of the two target websites. The result of the search is shown in Figure 7.

The ways that netizens get information are as follows: Internet communication (QQ, forums, post bars, etc.), phone calls, mobile phone text messages, word of mouth, and behavioral influences (some are learned through multiple channels). The specific distribution is shown in Figure 8.

6. Conclusions

The reason why Internet rumors can influence people is not only related to external factors such as Internet technology, but also the "human" factor, because people choose to believe the content of the rumors. What a rumor is potentially saying is more important than the surface it provides. The stronger the factors that stimulate rumors, the more people will join in the spread of rumors. As mentioned above, in many cases, the truth of the incident also depends on whether the person himself is willing to believe it or not. Therefore, it is necessary to think of ways to refute rumors from the perspective of "people": When online rumors appear, firstly, individuals should maintain rationality and self-discipline, not forward and spread the rumors at will, and secondly actively seek authoritative information and explanations. Nowadays, the network is already a network public opinion information. Aiming at this problem, this paper proposes a machine learning-based network public opinion collection technology in the context of big data, which can effectively extract the network public opinion information in the big data environment. This method is mainly based on the classical single-pass algorithm optimization design. Firstly, it is sensitive to the data processing sequence, based on double thresholds. Secondly, based on double thresholds to big data processing, this paper uses the big data technology MapReduce to optimize it. Simulations show that the proposed double thresholds can effectively reduce the sensitivity of single-pass algorithm to data processing sequence and improve the clustering performance of single-pass algorithm. Moreover, we optimize the dual-threshold single-pass algorithm by using the large data technology MapReduce, which also improves the clustering performance of the algorithm. In addition, because MapReduce is a parallel running framework, it can improve the efficiency of the dual-threshold single-pass algorithm. These simulations show that the network public opinion collection technology is suitable for public opinion information collection in big data environment. Although the single-pass algorithm has excellent performance for topic extraction of network information, the clustering algorithm has a strong dependence on the text input order. For the same data set, different input data may lead to differences in clustering results.

Data Availability

This article does not cover data research. No data were used to support this study.

Conflicts of Interest

The authors declare that they have no conflicts of interest.

Acknowledgments

This research was supported by the Zhejiang Provincial Natural Science Foundation of China under Grant No. LQY20G030001.

References

[1] N. Jean, M. Burke, M. Xie, W. M. Davis, D. B. Lobell, and S. Ermon, "Combining satellite imagery and machine learning to predict poverty," *Science*, vol. 353, no. 6301, pp. 790–794, 2016.

[2] A. L. Buczak, "A survey of data mining and machine learning methods for cyber security intrusion detection," *IEEE Communications Surveys & Tutorials*, vol. 18, no. 2, pp. 1153–1176, 2016.

[3] A. Giusti, J. Guzzi, D. C. Cireşan et al., "A machine learning approach to visual perception of forest trails for mobile robots," *IEEE Robotics & Automation Letters*, vol. 1, no. 2, pp. 661–667, 2016.

[4] Z. Gao, H. Cong, G. Jiang et al., "Computer aided design system for flat-knitted fabric based on hyper text markup language 5," *Journal of Textile Research*, 2017.

[5] H. E. Zhi-lin and L. U. Zhao, "Design and implementation of management platform of comprehensive overload control based on XML document object model," *Journal of Langfang Teachers University*, 2017.

[6] K. K. Bharti and P. K. Singh, "Opposition chaotic fitness mutation based adaptive inertia weight BPSO for feature selection in text clustering," *Applied Soft Computing*, vol. 43, pp. 20–34, 2016.

[7] J. Meng and D. Liu, "A new method for identifying bad data of power system based on spark and clustering analysis," *Power System Protection & Control*, vol. 44, no. 3, pp. 85–91, 2016.

[8] W. Zhang, J. Yang, Y. Fang, H. Chen, Y. Mao, and M. Kumar, "Analytical fuzzy approach to biological data analysis," *Saudi Journal of Biological Sciences*, vol. 24, no. 3, pp. 563–573, 2017.

[9] F. Karaaslan, "Correlation coefficients of single-valued neutrosophic refined soft sets and their applications in clustering analysis," *Neural Computing & Applications*, vol. 28, no. 9, pp. 2781–2793, 2017.

[10] Y. Dang, X. U. Zhiwei, L. Liu, and Y. Wang, "Research on improved single-pass text clustering algorithm in public opinion," *Journal of Inner Mongolia University of Technology*, 2017.

[11] J. Wu, Q. Meng, S. Deng, H. Huang, Y. Wu, and A. Badii, "Generic, network schema agnostic sparse tensor factorization for single-pass clustering of heterogeneous information networks," *PLoS One*, vol. 12, no. 2, article e0172323, 2017.

[12] L. I. Fang, L. L. Dai, Z. Y. Jiang, and S. Li, "The combination of an autoencoder network and single-pass clustering for detection and tracking," *Journal of Beijing university of Chemical Technology*, 2017.

[13] T. R. Sree and S. M. S. Bhanu, "HADM: detection of HTTP GET flooding attacks by using analytical hierarchical process and Dempster–Shafer theory with Map Reduce," *Security & Communication Networks*, vol. 9, no. 17, pp. 4341–4357, 2016.

[14] M. R. Ghazi and D. Gangodkar, "Hadoop, MapReduce and HDFS: a developers perspective," *Procedia Computer Science*, vol. 48, pp. 45–50, 2015.

[15] J. Bai, D. Yanhui, and T. Lu, "Internet rumor reporting system based on the blockchain incentive mechanism," *Mobile Information Systems*, vol. 2021, Article ID 7500639, 7 pages, 2021.

[16] L. Wang and J. Zhai, "Research of distributed storage system based on HDFS," *Intelligent Computer & Applications*, 2016.

[17] C. Wang, H. U. Yuping, and Y. I. Yeqing, "Cross-layer parameter optimization algorithm for Hadoop cloud computing platform," *Journal of Central China Normal University*, 2016.

[18] X. Yang, H. Ma, and M. Wang, "Rumor detection with bidirectional graph attention networks," *Security and Communication Networks*, vol. 2022, Article ID 4840997, 13 pages, 2022.

[19] Q. Chen, C. Liu, and Z. Xiao, "Improving MapReduce performance using smart speculative execution strategy," *IEEE Transactions on Computers*, vol. 63, no. 4, pp. 954–967, 2014.

[20] Q. Liu, D. Jin, X. Liu, and N. Linge, "A survey of speculative execution strategy in MapReduce," in *Cloud Computing and Security*, pp. 296–307, Springer, Cham, 2016.

[21] E. C. Puig, J. A. Interrante, M. D. Osborn, and E. Pool, *Integrating execution of computing analytics within a mapreduce processing environment*, U.S. Patent Application No. 14/317,687, 2016.

[22] A. Ahmed, "Performance analysis of machine learning based Botnet detection and classification models for information security," *Journal of Cybersecurity and Information Management*, no. 1, pp. 44–53, 2019.

[23] F. Amal, "A survey on machine learning techniques for supply chain management," *American Journal of Business and Operations Research*, vol. 2, no. 1, pp. 24–38, 2021.

[24] L. I. Shun, M. O. Nanwen, L. I. Qinyong, and D. O. Orthopedics, "Analysis on curative effect and leakage rate of percutaneous vertebroplasty by different viscosities of bone cement in patients with osteoporotic vertebral compression fractures," *Laboratory Medicine & Clinic*, 2017.

[25] K. Pardee, A. A. Green, M. K. Takahashi et al., "Rapid, low-cost detection of Zika virus using programmable biomolecular components," *Cell*, vol. 165, no. 5, pp. 1255–1266, 2016.

Hindawi
Wireless Communications and Mobile Computing
Volume 2022, Article ID 9327318, 10 pages
https://doi.org/10.1155/2022/9327318

Research Article

An Efficient Energy Management Routing and Scalable Topology in Wireless Sensor Network Using Virtual Backbone

Alanazi Rayan[1], **Ahmed I. Taloba**[1,2], **Nadir O. Hamed**[3], **Heba Y. Zahran**[4,5] **and Emad E. Mahmoud**[6]

[1]*Department of Computer Science, College of Science and Arts in Qurayyat, Jouf University, Sakakah, Saudi Arabia*
[2]*Information Systems Department, Faculty of Computers and Information, Assiut University, Assiut, Egypt*
[3]*Computer Studies Department, Elgraif Sharg Technological College, Sudan Technological University, Khartoum, Sudan*
[4]*Laboratory of Nano-Smart Materials for Science and Technology (LNSMST), Department of Physics, Faculty of Science, King Khalid University, P.O. Box 9004, Abha 61413, Saudi Arabia*
[5]*Nanoscience Laboratory for Environmental and Biomedical Applications (NLEBA), Metallurgical Lab. 1, Department of Physics, Faculty of Education, Ain Shams University, Roxy, Cairo 11757, Egypt*
[6]*Department of Mathematics and Statistics, College of Science, Taif University, P.O. Box 11099, Taif 21944, Saudi Arabia*

Correspondence should be addressed to Nadir O. Hamed; nohamedit@gmail.com

Received 22 January 2022; Revised 18 February 2022; Accepted 2 April 2022; Published 20 April 2022

Academic Editor: Mohamed Elhoseny

The wireless sensor network (WSN) approach is one of the fastest growing approaches in the world of communications and engineering. The primary objective of a WSN is to discover the important information about the environment, depending on the nature of the applications under which it is implemented, and to communicate this information to a single base station (BS) so that appropriate measures can be taken. These sensor nodes communicate via a variety of protocols. The difficulty with the traditional system is that while collecting the observed data, each node transmits its felt information directly to a base station, which quickly exhausts its power. This study suggests a Backbone Energy-Efficient Sleeping (BEES) management strategy with two appealing features: (i) the capacity of backbone is scalable by basic parameters, and (ii) the backbone nodes were distributed equally, implying that the backbone on its own is energy efficient during routine activities. Reliable connections are expected to obtain QoS and routing protocols of such backbone nodes in wireless multihop systems. As a result, present localized routing in virtualized backbone schedule cannot ensure energy-efficient paths. An energy-efficient routing scheme for Virtual Back Bone Nodes (VBS) increases life of node and switches off its radio while in sleep state to spend less power. BEES' performance is evaluated by comparing it to two different topology management techniques. The results show that BEES performs better algorithms. It ensures optimal routing with minimal node power consumption but also implements the essential communication range for backbone networks.

1. Introduction

The primary goal in implementing a wireless sensor network (WSN) is to detect or predict the state of a physically dynamic event from each individual, geographically separated sensor of the network. Each sensor performs a local computation and passes the data or predictions to a synthesis station, which integrates the inputs to create an evaluation of the parameter or process, into a central distributed estimation scheme [1]. Distributed estimate using wireless sensor nodes provides several intriguing issues, including the apparent restrictions of transmission capacity, which contribute to quantization error in addition to a disturbance in the transmitted signal. Another significant limitation is the poor battery power of the detecting nodes themselves [2]. Then, a WSN estimate paradigm that provides adequate efficiency while may be energy efficient is sought to extend the WSN's lifespan.

Because sensors are frequently available sources, their operating period is strictly limited by storage capacity.

Energy-saving procedures must be developed to extend the lifespan of the network [3]. Several energy-efficient solutions for WSNs have indeed planned recently, utilizing numerous levels of the networking protocol load. This study will focus on topological management strategies. Topology management is based on the perception in a realistic WSN with adequate network size; just a limited number of connected devices must be engaged at any given moment to perform the required packet transmission functions [4]. By putting those unnecessary networks to sleep, you may dramatically cut energy use. The Backbone Energy-Efficient Sleeping (BEES) mechanism is proposed in this study as a unique topology management system [5]. BEES have two appealing qualities. Initially, it is typically scalable, with reasonable backbone size restrictions. Furthermore, BEES helps conserve not only by putting numerous detectors to sleep but also by lowering the routing energy consumption of the backbone nodes.

A subset of network nodes is mentioned to as the backbone, and a backbone network is to be connected. Backbone is mostly utilized to improve routing procedures, which boosts high throughput, reduces overall electricity usage, and extends node lifespan [6]. The radio is the most energy-intensive computational operation. Focus on network dynamic loads by building backbone nodes that are engaged whenever the stimulation transmitting procedure occurs and go to sleep by turning off their radios. As a result, it does not affect the quality of communications. Creating a single backbone node, on the other hand, does not provide the greatest node lifespan; so, it is desirable to establish numerous discontinuous Connected Dominated Sets (CDS) that perform effectively and can respond to changes in the network topology [7]. Connected Dominated Sets (CDS) function effectively and can respond to changes in the topology of the network. CDS is divided into several categories: (1) Unit Disk Graph (UDG) and (2) Disk Graphs with Bidirectional Links (DGB). UDG and DGB are both NP-hard. Non-CDS nodes are put into a sleep mode to preserve network energy. Backbone nodes employ the predictable strategy to keep the backbone node small while performing a great amount of computation. As a result, this technique ensures CDS in a network connection [8]. Previously, localized routing consumed more energy than would be optimal. In this work, look at how to maximize the life of a virtual backbone by adopting energy-efficient sequencing. The following are the contributions made:

(i) The network is separated into zones or regions, for each backbone node having a transmission range and being confined to finding neighboring backbone nodes within their broadcasting radius to locate technology which is linked

(ii) A strategy known as the restricted back bone neighbor routine is developed, which ensures effective routing while consuming the least amount of energy. In this case, the backbone nodes choose a neighboring backbone node within the transmitting radius and build the Connected Dominated Set (CDS) of backbones from the sink node [9]. If no node is located within the communication radius, the backbone node expands its transmission radius to identify a next backbone network and establishes a linked dominated collection of backbone networks

(iii) A sink node is located in the center and is always active

(iv) Backbone nodes can be given a lifetime based on the duty ratio assigned to a specific zone or region

Thus, the backbone minimizes network latency, improves bandwidth efficiency, reduces total consumption of energy in the network, and finally covers node life in the WSN.

2. Related Works

The BeeSensor network, which is inspired by bees and is energy-aware, adaptable, and effective, is detailed in [10]. This work makes an important impact by presenting a three-stage protocol strategy plan: first, taking ideas from biological institutions to enhance a sparse, distributed, and simple routing mechanism; then properly designing basic procedures to perform the procedure to gain a diagnostic insight into the behavior; and finally, optimizing the protocol based on the analysis in phase 2. Then, put it through its paces in a sensing simulation environment. The findings of experimentations demonstrate the effectiveness of this three-phase procedure design, which enabled BeeSensor to achieve its strategic objectives while using the least level of collaboration and power processing—two major sources of the energy consumption in a sensor network—when especially in comparison to other SI-based WSN routing algorithms.

Algorithms that take advantage of mobile nodes to enhance system lifetime are explained in [11]. These methods are classified into three types: those that use mobile sinks, those that use mobile sensing redeployment, and those that use mobile relays. Energy is conserved by adopting shorter multihop data delivery channels with mobile sinks, and the collection of sensors situated near a source changes all the time, balancing energy usage across the network. The early installation of mobile sensors can be enhanced by sensor displacement to optimize energy usage and lengthen lifetime of network. Mobile nodes could be employed as a relay, taking over the functions of colocated static devices or carrying information to the base station to decrease the price of long-distance transmission.

Energy efficiency in wireless sensor networks (WSNs) has long been a hot topic that has been researched in [12]. The mechanism of Sleep Scheduling (SS) is an effectual way to control the power of each node and can extend the lifespan of the overall infrastructure. SDN-ECCKN, a Software-defined Networking- (SDN-) based Sleep Schedule technique, is suggested in this study to regulate the network's resources. When implementing a method, use ECCKN as the basic algorithm. Every computation in the planned SDN-ECCKN method is performed in controllers instead of the sensor, so there is no transmission among each pair of nodes, which have been the major aspects of

the existing EC-CKN method. The SDN-ECCKN results demonstrate its benefits in power management, including such network longevity; the findings were presented nodes and the percentage of single nodes within the network.

The main structural goals of routing algorithms for WSN help in lowering final latency and energy effectiveness without overlooking additional design concerns [13]. This assesses routing algorithms that are response time, low energy consumption, and time sensitivity. TEEN (Threshold-sensitivity Energy-Efficient sensor protocols), a responsive network protocol well adapted for time important data electrochemical sensors, is very efficient and effective in energy usage and response time. APTEEN (Adaptive Periodic Threshold-sensitive Energy-Efficient sensor Network protocol), a hybrid model procedure, provides an overall image of the system at regular intervals while using almost no power. SPEED is a unitary, extremely efficient, and scalable sensing network protocol that delivers end-to-end fuzzy real-time communication by preserving a specified delivery performance all transverse systems via a novel combination of control method and nondeterministic geographical routing. RAP is an actual communication system for a large-scale sensor system that utilizes Velocity-Monotonic Scheduling (VMS) to dramatically minimize end-to-end latency. RPAR is an acronym for Real-Time Power Adaptive Routing Algorithm, which promotes energy-efficient actual communication by continuously modifying transmit energy and decisions of routing. Then, it goes over benefits and drawbacks of each routing system.

The energy-efficient design of the linked backbone and unassuming routing stateless over a backbone was demonstrated to attain some goals [14]. This presents an ns2 computational model correlation of data transmission in the WSNs whenever (a) each sensor paths that information of the sensor directly to a drain flat collaborative network and (b) a backbone is placed on the top of both the horizontal routing protocols and only just a few nodes are already in charge of data delivery to the sink's hierarchical organization, here referred to as VBES: Virtual Backbone for Saving Energy. Multiple objects are permitted to roam network of the static sensors. Simulations were run on the networks of density increases, with up to three targets defined and reporting to up to three sinks. The findings show that accessing through such backbone enhances the lifetime of the network by up to seven moments over a plain network organization, under which system capacity is described as (a) the time till the first base station passes away due to depletion of energy, (b) the time mandatory for an assumed proportion of nodes in the network to pass away, and (c) the period needed for the network to just be disengaged.

3. Proposed Methodology

3.1. Constructing Protocol of BEES. Consider an individual sink, interested in establishing a backbone in a disc D of radius R around this specific sink [5]. This can see that D only covers a small portion of this transmission range. The backbone devices should be arranged so that at least one of them is within communication range of every sensor in D. To verify that such backbone has appropriate connectivity characteristics, tend to associate the subnets of backbone devices. The following are the main elements in backbone development protocol:

(i) Phase of tiling

The disc D around the sink is tiled with a series of matching regular geometric shapes, giving the area from around sinks the appearance of a honeycomb.

(ii) Phase selection of backbone

The sensor that is nearest to the center of each hexagon is chosen.

(iii) Phase of clustering

Backbone sensors alert other detectors to their presence and the hexagonal they symbolize. The other sensors use RSS measurements to establish which clusters (hexagon) they belong to.

The disc is tilted. D begins with the sinks: a first hexagon's center aligns with the sink. The diameter of the tiling hexagons' enclosed circle is $t_x/\sqrt{3}$, where t_x is the high propagation distance of a detector [15]. This suggests coordinates for correctly identifying the numerous hexagons as in tiling seen above. The hexagon in column c of row r in sector s, in particular, is individually recognized to use the tuple $\langle s, r, c\rangle$. Although there are numerous routing techniques for hexagonal connections, the coordinate system appears being more suitable for the construction process.

3.2. Backbone Scheduling. This illustrates that backbone scheduling is used to identify efficient routing focused on localized effective backbone routing. The whole modules are explained further below.

(i) Schedule Transition Graph (STG)

The STG method is depicted in the picture below; it is a centralized approximation approach. The time scale is horizontal and is counted in rounds. In each cycle, the possible configurations of the backbone networks are enumerated vertically [16]. The quantity of backbones in each round is equivalent to the total of conceivable states. There's also a one-to-one correspondence among condition and backbone. Energy is consumed in 1 session, which symbolizes the time that elapses during every round when energy is consumed. Whenever a node's condition is depleted, node movement is not permitted as shown in Figure 1.

B is a collection of backbone connection rounds that are used by the backbone routers. All connection is a networking linked subgraph, as well as all nodes become one step away from each point in B_i.

(ii) Energy-efficient localized routing

This section goes into the specifics of the routing idea, which is focused on localized routing. It is a greedy way of

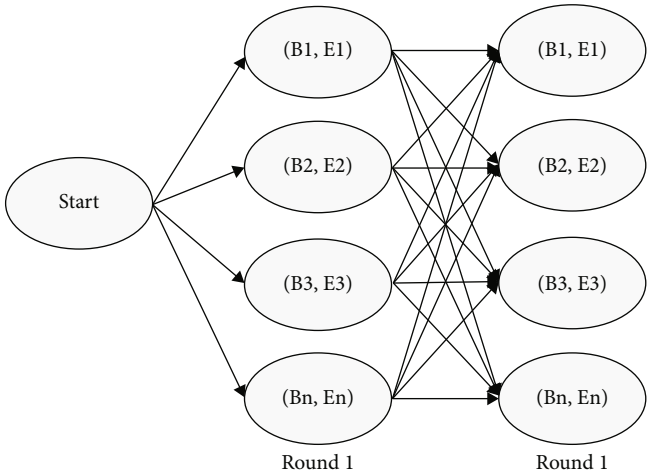

Figure 1: Scheduling of STG.

technique routing. In greedy networking, the router chooses the next-hop neighbor depending on the difference to an objective [17]. As a result, such sequencing may not even be thermally efficient. The transmitting connection must have greater energy efficiency to be more eco-friendly. To utilize less energy, the overall distance traveled should be modest. As a result, a new notion known as a limited zone is established to limit advancing directions.

(i) The backbone nodes with such communication to forwarding locate the neighbor backbone node between several neighbors existing inside the limited area. The greatest neighbor has the most energy efficiency or a stable connection

(ii) When there are no backbone nodes in the closed area, it expands its type of transmission range to select the optimal node

(iii) If there are no nodes in the region or zone, the standard greedy routing is used. Figure 2 depicts the data flow of this process

(iii) Critical transmission radius

In this research, during routing data to a base station, the destination node can delete packets as they arrive at the destination since they are unable to discover a stronger neighbor node. As a result, to discover the better neighbor backbone node and assure productive and effective routing, each backbone network must have a sufficient size broadcasting range.

The critical transmission range is denoted as

$$\rho_x(D_n) = \sqrt{\frac{\beta_X \ln (R.n)}{n\pi}}. \quad (1)$$

ρ_x is a method of generalized routing.
D_n is a number of nodes in the network.

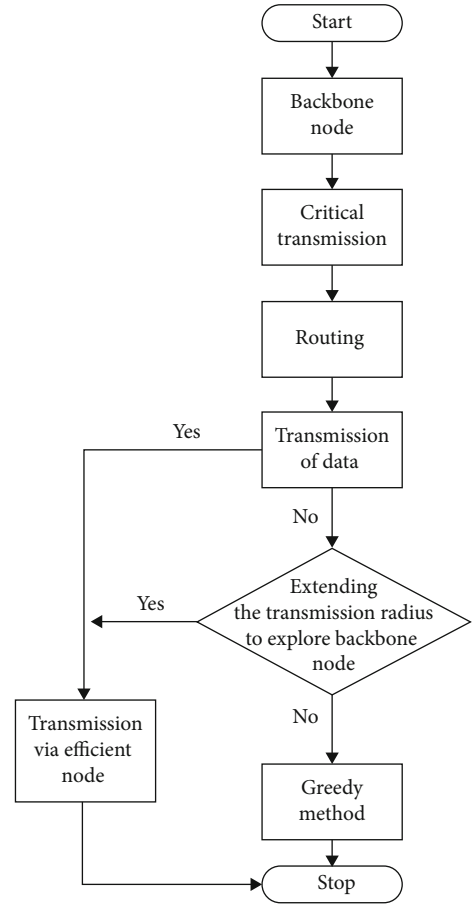

Figure 2: Flow diagram of data.

β_X is a proportion of the center of access point u to the radius r of the transmitting area from which the approximate backbone node u selects its neighbor backbone network w.

3.3. Backbone Establishment

(i) Election of HBN

During the initialization step, all devices have the same amount of energy. HBNs were selected avariciously and in a distributed manner. If a network identifies there is no HBN inside its VND, it declares its desire to become an HBN by transmitting a HEAD communication to the networks through its VND. Any node network that gets the HEAD message will be temporarily labeled as an AFN. If not enough HBNs can be connected to the system, the election system concludes.

(ii) Discovery of ABNs

If the selected HBNs are successful in constructing a linked backbone, the procedure of backbone development is completed. Otherwise, complementary connections are required to connect the individual HBNs. Using the ABN discovery technique, investigate the interconnectivity of

HBNs. The process is initiated by the data center sending out a CHECK notification. Any node that receives the CHECK message should assist in spreading it. The message of CHECK has four critical parameters: LAST ID, LAST TYPE, CURRENT ID, and CURRENT TYPE [3]. Before broadcasting the signal, every node must improve the model. The CURRENT ID and CURRENT TYPE values relate to the ID and type of the input nodes. If the base station can obtain CHECK communications from HBNs, it replaces the variables LAST TYPE and LAST ID again with ID as well as category of last HBN which transmits a message to it; alternatively, unless it can obtain CHECK communications from AFNs, it substitutes the LAST TYPE and LAST ID with both the ID as well as a category during the last AFN which creates the impression to the base station. When an HBN could only accept CHECK signals from AFNs, it knows that it has been disconnected from the Main Backbone Component (MBC) that links it to the cloud server.

3.4. Backbone Maintenance. BEES rotate backbone networks to stability transmitting tasks through all the sensors. The updating procedures for HBNs and ABNs vary, as stated below.

(i) Replacement of HBN

During the initialization phase, all devices have the same amount of energy. HBNs are chosen in a decentralized manner following the -MHP. If a node discovers that there is no HBN in its −ND, it proclaims its intention of becoming an HBN by transmitting a HEAD message to its −ND neighbors. Any node that gets the HEAD packet will be temporarily labeled as an AFN. So that no more HBNs can be connected to the system, the electoral system concludes.

(ii) ABN assignment and withdrawal

Because ABNs are simply nodes that link HBNs, they would be removed whenever the HBNs they belong to are updated. On the other hand, once the HBN is replaced, the current HBN must ensure that the replacement does not disrupt backbone connection. It compares the list of its nearby HBNs to a table of a previous HBN. The connectivity is kept if its list includes all of the elements in the former HBN's. Instead, the new HBN must transmit a discover message for each disconnected HBN in order to find a route to that HBN. If it does not receive a response from the unplugged HBN, new ABNs are required. In its two-hop neighborhood, the incoming HBN will discover some AFNs which will link it to the separated HBN [4]. Whether there are two-hop pathways, this should select the AFNs with the highest power also as ABN. Now, if three-hop pathways are available, it will choose the pairing of AFNs with the highest total power as ABNs. Because there is no such step to ensure, the replacement HBN must designate the outgoing HBN also as ABN. It is significant to mention that such a circumstance occurs with a very small chance, and when it does, the departing HBN would only be in responsible of relaying activities from current HBN to the severed HBN.

4. Analysis of Backbone

In this section, look at the theoretical and experimental elements of BEES' backbone properties. Three crucial aspects are taken into account: HBN connection, distribution of backbone size, and backbone node.

4.1. Connectivity of HBN. The connectivity risk of HBNs is based on the likelihood that HBNs will form a linked backbone in the absence of ABNs. BEES require HBN access for such following purposes. As previously stated, BEES make use of the -MHP principle for routing packets, which makes it easily extensible and cost-efficient. However, the presence of ABNs is a violation of the -MHP notion. The benefits of BEES might well be lost if the ratio of ABNs within the backbone becomes too high [18]. Furthermore, the procedures of ABN assignment and reassignment are far more complex than those of HBN voting and replacements. The presence of ABNs raises the existing system for backbone installation and configuration and also the computational cost. Because ABNs appear only if HBNs fail to form a linked backbone, connectedness of the HBNs affects the percentage of ABNs in a backbone. As a result, the connection of HBNs is closely tied to the actual quality of BEES.

The connection of BEES' HBNs is investigated using simulated results. This takes a square field of $100 \times 100\,\mathrm{m}^2$ with such a network size of $\rho = 0.1/\mathrm{m}^2$. The variable values are transformed from 0 to 1. Each is subjected to $\delta, 10^4$ different random experiments [19], the results of which are used to compute the HBN connection. Node transmission power distances are set to $\mathrm{R} = 15\,\mathrm{m}$ and $R = 30\,\mathrm{m}$, correspondingly. Figure 3 depicts the results. It was found that there is a significant threshold of where the HBNs are coupled with high probability. For example, if 0.5 when $R = 15\,\mathrm{m}$ or 0.8 when $R = 30\,\mathrm{m}$, the connection chance of HBNs is more than 94%.

4.2. Size of Backbone. However, the backbone in BEES is made up of two elements: HBNs and ABNs, the number of ABNs can be quite modest if it is set to a suitable value. As a result, one can determine the backbone size simply by calculating the number of HBNs. To that end, consider the work on the group concentration of the DMAC method, which generated and empirically validated the highest accuracy.

$$P(\mathrm{CN}) = \frac{1}{1 + (E(N)/2)}. \tag{2}$$

$P(\mathrm{CN})$ is the chance that chosen node randomly is a cluster head, i.e., the HBN in this case; and $E\{D\}$ is the anticipated node degrees $P(\mathrm{CN}) = n(\mathrm{HBN})/N$ in the issue, where $n($ HBN$)$ is the amount of HBNs and N is the total number of detectors. Furthermore, the estimated access to smart is provided by $E\{D\} = \rho\pi(\delta V)^2$ in the Poisson point process model. As a result, the approximate size of the backbone is

$$n(\mathrm{BN}) \approx n(\mathrm{HBN}) = \frac{N}{1 + \left(\rho\pi(\delta V)^2\right)/2}. \tag{3}$$

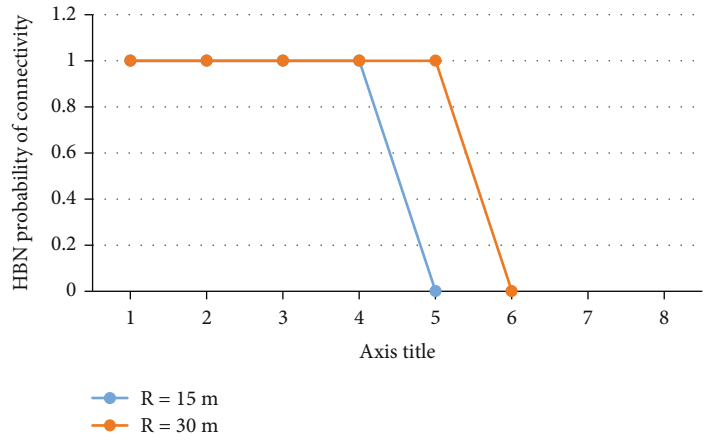

Figure 3: Connectivity of HBNs.

Thus, in simple terms, the frequency of the backbone networks is observed to be

$$\lambda_{\mathrm{BEES}} = \frac{\rho}{1 + \rho\left(\pi(\delta V)^2\right)/2}. \tag{4}$$

Equation (4) is validated through simulation. Figure 4 depicts the results. The lead to improve in (4) matches the outcome extremely well. This means that given characteristic, the backbone diameter in BEES may be accurately calculated by (4). Traditionally, it may control the backbone diameter using the option.

4.3. Distribution of Backbone Node. Another backbone element that interests us is the location of backbone nodes, but it has an intrinsic effect on routing energy usage. This investigates a characteristic from two perspectives: intuitive experience and link speed metrics. In addition to BEES, the findings of two other current sleeping organizations' management, GAF and Naps, are offered for comparison [20]. The arrangement of backbone networks and sleeping networks provides us with a visual representation of the backbone architecture in such three techniques. For the sake of clarity, only plot a $5 \times 5\,\mathrm{m}^2$ zone. In comparison, BEES generates a backbone with more uniformly dispersed nodes than the GAF and Naps.

As previously stated, the minimum backbone connection length in BEES is limited by the δ – MHP notion. However, there is no such restriction in several other sleeping management methods. Study the link structure measures within three components to see this in action [21]. The backbone link distance distribution in GAF and Naps is not constrained, as seen in Figure 5. There are connections with distances ranging from 0 to R, indicating that backbone units are not dispersed uniformly. The backbone link in BEES, on the other hand, is inadequate to a smaller array between δR and R. This link length of limitation decreases the variability of backbone network connections in BEES, allowing it to have a uniform distribution backbone node network.

4.4. Backbone Node Network Lifetime. In this section, the outcome of the suggested methodology is described [22]. The results are exhibited on the ns2 simulator; the notion of VBS and localized routing delivers the best results in locating stable backbone network connections that are region constrained.

4.4.1. Model of Energy. When a node enters sleep mode, it needs energy whenever there is a message transfer and switches off its transmitter [23]. Energy is mostly consumed unless a communication exchange is required to meet the quality of service.

4.4.2. Effective Routing. This demonstrates the efficient routing established by CDS by constructing stable links among the backbone nodes in this study [24–27].

5. Result and Discussion

5.1. Energy Consumption. Because energy is a major issue in WSNs, creating virtual nodes is a great way to reduce energy use while increasing throughput. It is reasonable to measure the amount of power required based on data transmission in an accurate manner [28]. Figure 6 depicts the energy usage of backbone nodes throughout transmitting data, and while in sleep mode, the antennas are turned off to save energy. The graph depicts the number of backbone nodes within a network as well as their energy usage. As a result, the proposed system's energy usage is not more than that of the present scheme. The line graph represents the amount of energy utilized by the backbone nodes in the entire WSN.

5.2. Effective Routing. The overall length of a path identified by LEARN in the routing protocol is always within a continuous optimum. The suggested system is compared to existing localized routing methods and demonstrates that it can ensure energy-efficient pathways from the sender to the receiver. Modern systems are used to performance characteristics of LEARN routing [29]. This demonstrates that the LEARN localized routing method guarantees energy-efficient pathways in a random network with such a high degree of certainty. Figure 7 depicts the backbone nodes that have efficient routing. Throughput numerical simulations are shown as routing protocol.

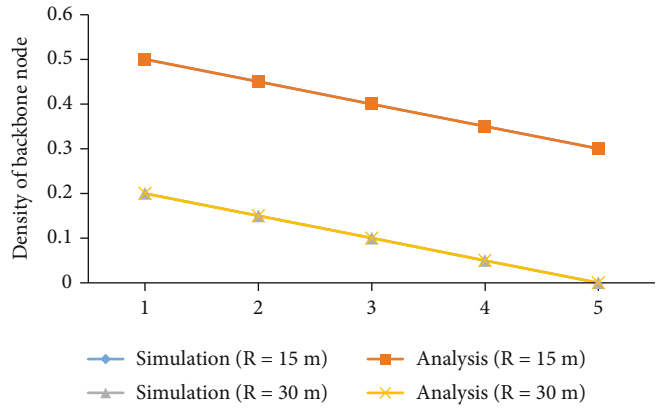

Figure 4: Node density of backbone.

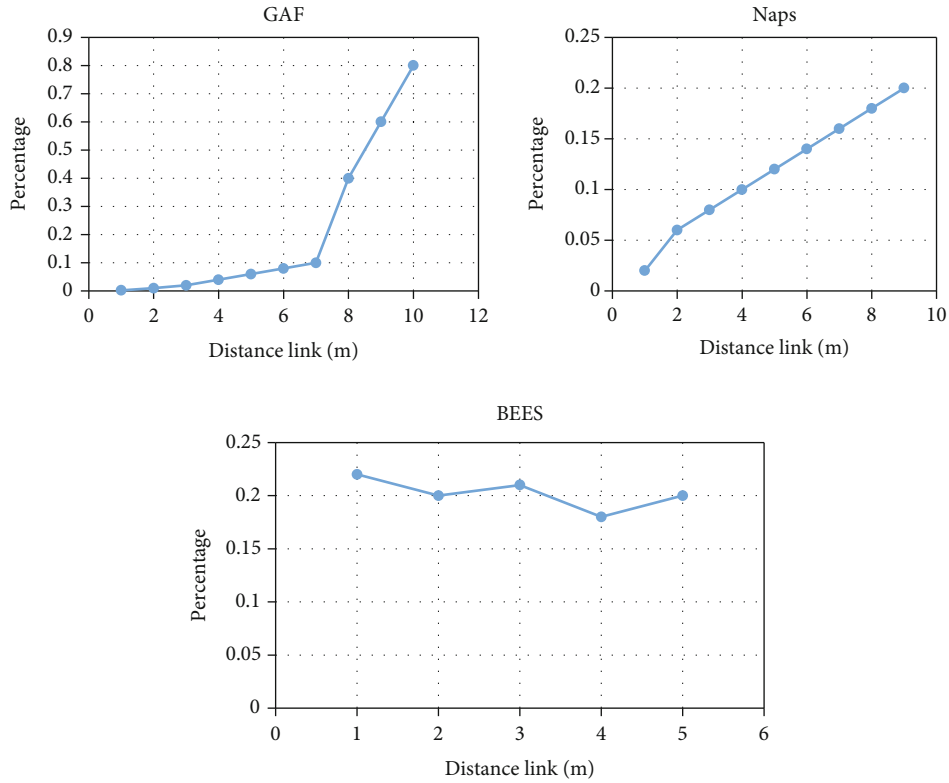

Figure 5: Distance link of statistics.

5.3. Lifetime of Node. Backbone nodes extend network longevity by extending node lifetime. As energy arrangements, accurate reading energy, and unbalanced energies are employed, the communication range is originally fixed; however, the transmission diameter can later be detailed work on the crucial transmission. The obtained network lifespan is depicted in Figure 8, by properly spreading the energy. The blue line represents the lifespan of backbone nodes within the network.

5.4. Delay. This model result reveals that there is less time in determining an effective path and assembling CDS from sensor nodes, as illustrated in Figure 9.

This section compares BEES' effectiveness to two distinct topology processes that require GAF and Naps. Scalability and routing energy efficiency are two performance challenges that are being explored. In the system, all three of these techniques are sustainable. GAF, for example, regulates the number of backbone nodes by adjusting an edge distance r of a synthetic grid. $\lambda_{GAF} = 1/r^2$ is utilized to calculate the density of the backbone nodes. Naps control the size of the backbone by adjusting the neighbor threshold c. The frequency of the backbone nodes is determined by $\lambda_{Naps} = c/\pi R^2$. In BEES, expand the backbone by simply changing the variable and then using it to estimate the density of backbone node. It is important to note that, while a sustainability

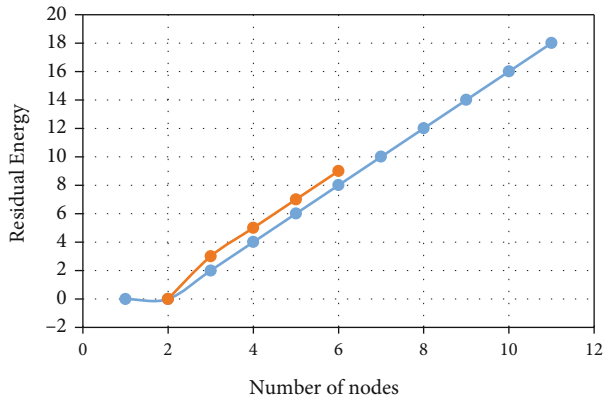

Figure 6: Consumption of energy.

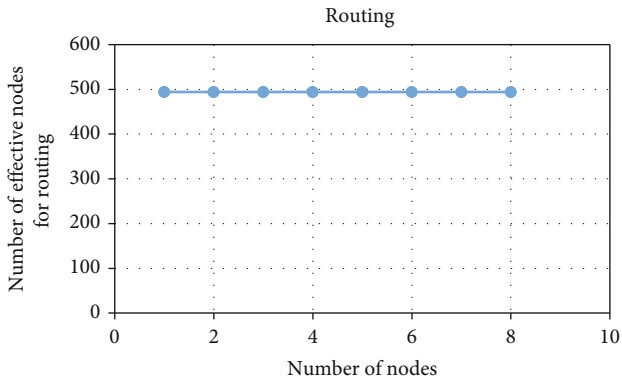

Figure 7: Routing.

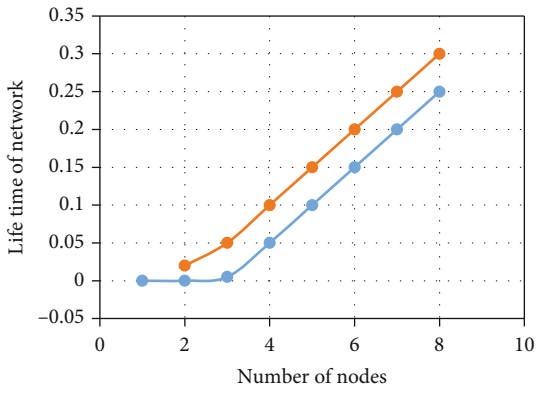

Figure 8: Lifetime of node.

of GAF in is restricted by $r \le R/\sqrt{5}$ to ensure connectivity, see that this restriction can be loosened if the backbone is just mandatory to be linked with a maximum probability. This connection enables the cost of r to be greater than the $R/\sqrt{5}$ in the experiment.

This changes the control settings in the three algorithms to generate backbones with varying node densities. Figure 10 depicts the backbone connection in such three techniques with varying backbone network sizes. According to Figure 10, the backbone scaling range in BEES is substantially wider than in the remaining two algorithms, providing

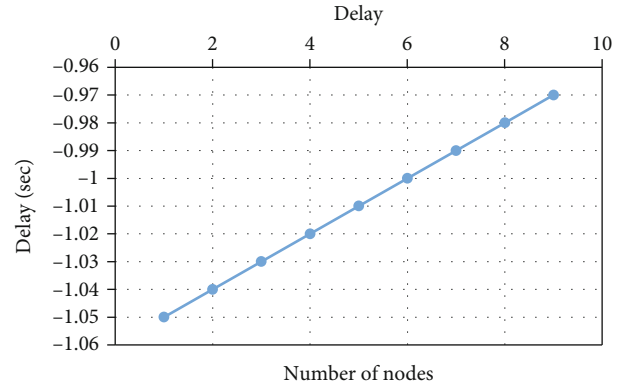

Figure 9: Delay.

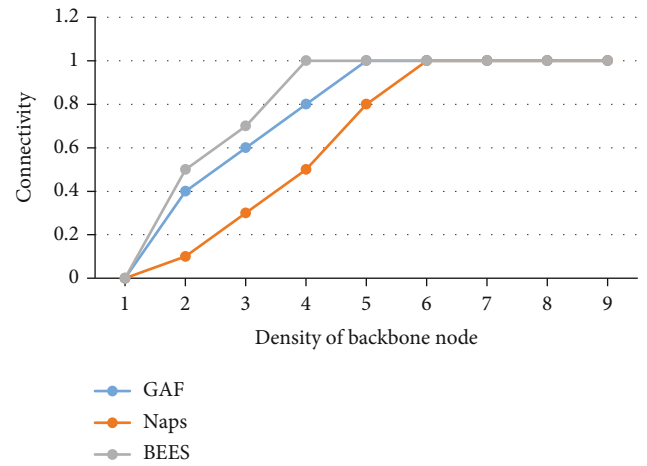

Figure 10: Scalability comparison between Naps, GAF, and BEES.

a connectivity probability. When the interconnectivity probability criterion is set to 90%, the density of backbone node is constrained to $\lambda_{BEES} \ge 0.0158$ in BEES, $\lambda_{GAF} \ge 0.023$ in GAF, and $\lambda_{Naps} \ge 0.024$ in Naps. Because the field size is set at $100 \times 100\ m^2$, the minimal overall amount of backbone connections in 158 BEES, 230 in GAF, and 240 in Naps.

Aside from scalability, evaluate the power consumption of the three backbone routing algorithms. This specifically fixes the placements of the transmitter and the receiver. They are supposed to be 100 metres apart. With varying backbone numbers of units producing requirements, the regular end-to-end energy usage is detected. The energy routing model is as follows: $E_{hop} = ad^{\alpha} + b$, where ad indicates the transmission power consumption, α is the route loss, d is the duration of hop, and b indicates the power consumption only at reception for collecting and on both ends for information processing. For short-range transmissions, use $ad^{\alpha} = 740$ nJ, $b = 570$ nJ, and path loss $\alpha = 4$. Given that the hop frequency is normally $5 \sim 8$ m, set $a = 740/5^4 = 1.18$ nJ/m^4. In addition, the SP-power networking algorithms are used to construct end-to-end connections.

As demonstrated in Figure 11, the end-to-end routing energy usage in BEES is smaller than that in the other two techniques with varying backbone density needs. When it

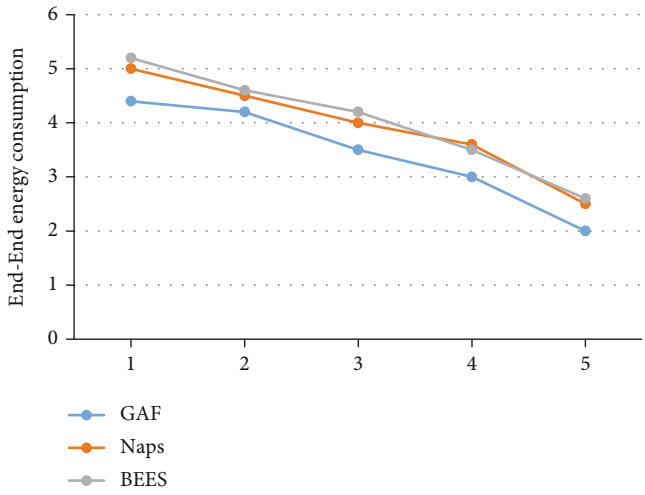

Figure 11: Energy-efficient routing.

remains constant, BEES consumes 85 percent of the energy consumed by GAF and Naps; when it is large, BEES consumes 87 percent of the energy consumed by GAF and Naps. In other terms, BEES uses around 15% less routing energy than GAF and Naps. Because routing energy accounts for the majority of the energy consumed by a backbone, the above detection suggests that a WSN lifetime throughout BEES is approximately $(1/(1-15\%)1-15\%)-1=18\%$ percent extended than in GAF and Naps, assuming that routing activities are well rounded across all detectors in such strategies.

6. Conclusion

This study offers BEES, a scalable topology management approach that consumes less power not only through putting abundant networks to sleep but also by lowering the routing energy usage of backbone networks. Virtual backbone planning is a new scheduling mechanism for WSNs. Power communication is required for WSN to operate for a longer amount of time due to battery resources; thus, network longevity through power-aware network organization is very desirable. To plan the node activities among sleep and active states, an efficient approach based on power-saving planning must be created. One approach is to construct a backbone node and turn off its radios being in sleep state, and the routing must be power saving by extending the lifetime of the network. This results in energy savings while routing jobs. This virtualized backbone scheduling has the potential to conserve and efficiency of wireless sensor networks. BEES offers a wider scaling spectrum and spends around 15% less transit power than existing topological management algorithms, according to simulation results.

Data Availability

The data used to support the findings of this study are included within the article.

Conflicts of Interest

The authors declare that they have no conflicts of interest.

Acknowledgments

The authors express their appreciation to the Research Center for Advanced Materials Science (RCAMS)" at King Khalid University, Saudi Arabia, for funding this work under the grant number KKU/RCAMS/G013-21. The authors extend their appreciation to the Deputyship for Research & Innovation, Ministry of Education, in Saudi Arabia, for funding this research work through the project number IFP-KKU-2020/9and Taif University Researchers Supporting Project number (TURSP-2020/20), Taif University, Taif, Saudi Arabia.

References

[1] N. Roseveare and B. Natarajan, "Distributed tracking with energy management in wireless sensor networks," *IEEE Transactions on Aerospace and Electronic Systems*, vol. 48, no. 4, pp. 3494–3511, 2012.

[2] X. Jiang, J. Taneja, J. Ortiz et al., "An architecture for energy management in wireless sensor networks," *ACM SIGBED Review*, vol. 4, no. 3, pp. 31–36, 2007.

[3] R. Yu, Z. Sun, and S. Mei, "Scalable topology and energy management in wireless sensor networks," in *2007 IEEE Wireless Communications and Networking Conference*, pp. 3448–3453, Hong Kong, China, March 2007.

[4] R. Yu, Y. Zhang, R. Gao, and L. Song, "Sleeping management for scalable topology control in wireless sensor networks," *Wireless Communications and Mobile Computing*, vol. 11, Article ID 876, 1139 pages, 2011.

[5] H. S. AbdelSalam and S. Olariu, "BEES: bioinspired backbone selection in wireless sensor networks," *IEEE Transactions on Parallel and Distributed Systems*, vol. 23, no. 1, pp. 44–51, 2012.

[6] B. N. Umesh and G. Vasanth, "Energy efficient routing of wireless sensor networks using virtual backbone and life time maximization of nodes," *International Journal of Wireless & Mobile Networks*, vol. 5, no. 1, pp. 107–118, 2013.

[7] A. Jawahar and S. Radha, "Energy enhancement using hybrid topology management scheme in wireless sensor networks," in *2009 Annual IEEE India Conference*, pp. 1–4, Ahmedabad, India, Dec 2009.

[8] A. Norouzi and A. Sertbas, "An integrated survey in efficient energy management for WSN using architecture approach," *International Journal of Advanced Networking and Applications*, vol. 3, no. 1, article 968, 2011.

[9] K. M. Alzoubi, P.-J. Wan, and O. Frieder, "Message-optimal connected dominating sets in mobile ad hoc networks," in *Proceedings of the 3rd ACM international symposium on Mobile ad hoc networking & computing*, pp. 157–164, Lausanne, Switzerland, June 2002.

[10] M. Saleem, I. Ullah, and M. Farooq, "BeeSensor: an energy-efficient and scalable routing protocol for wireless sensor networks," *Information Sciences*, vol. 200, pp. 38–56, 2012.

[11] Y. Yang, M. I. Fonoage, and M. Cardei, "Improving network lifetime with mobile wireless sensor networks," *Computer Communications*, vol. 33, no. 4, pp. 409–419, 2010.

[12] Y. Wang, H. Chen, X. Wu, and L. Shu, "An energy-efficient SDN based sleep scheduling algorithm for WSNs," *Journal of Network and Computer Applications*, vol. 59, pp. 39–45, 2016.

[13] D. Baghyalakshmi, J. Ebenezer, and S. A. V. Satyamurty, "Low latency and energy efficient routing protocols for wireless sensor networks," in *2010 International Conference on Wireless Communication and Sensor Computing (ICWCSC)*, pp. 1–6, Chennai, Tamil Nadu, India, Jan 2010.

[14] S. Basagni, M. Elia, and R. Ghosh, "ViBES: virtual backbone for energy saving in wireless sensor networksMilitary communications conference," vol. 3, pp. 1240–1246, 2004.

[15] C. R. Shalini and S. Nirmala, "Virtual backbone scheduling for balancing energy efficiency in wireless sensor networks," *International Journal of Engineering Research*, vol. 2, no. 7, p. 3, 2013.

[16] R. Bolla, R. Bruschi, A. Cianfrani, and M. Listanti, "Enabling backbone networks to sleep," *IEEE Network*, vol. 25, no. 2, pp. 26–31, 2011.

[17] L. Chiaraviglio, A. Cianfrani, E. L. Rouzic, and M. Polverini, "Sleep modes effectiveness in backbone networks with limited configurations," *Computer Networks*, vol. 57, no. 15, pp. 2931–2948, 2013.

[18] X. Di, Z. Zhang, T. Xu, and B. B. Biswal, "Dynamic and stable brain connectivity during movie watching as revealed by functional MRI," 2021.

[19] P. Berman, G. Calinescu, C. Shah, and A. Zelikovsky, "Efficient energy management in sensor networks," *Ad Hoc and Sensor Networks, Wireless Networks and Mobile Computing*, vol. 2, pp. 71–90, 2005.

[20] R. Doverspike, G. Li, K. Oikonomou, K. Ramakrishnan, and D. Wang, "IP backbone design for multimedia distribution: architecture and performance," in *IEEE INFOCOM 2007-26th IEEE International Conference on Computer Communications*, pp. 1523–1531, Anchorage, AK, USA, May 2007.

[21] A. Nasrin Banu, M. Manju, S. Nilofer, S. Mageshwari, A. P. Selvi, and C. Ananth, "Efficient energy management routing in WSN," *International Journal of Advanced Research in Management, Architecture, Technology and Engineering*, vol. 1, pp. 16–19, 2015.

[22] G. K. Pandey and A. Singh, "Recent Advancements in Energy Efficient Routing in Wireless Sensor Networks: A Survey," *Proceedings of Fifth International Conference on Soft Computing for Problem Solving*, M. Pant, K. Deep, J. Bansal, A. Nagar, and K. Das, Eds., Springer, Singapore, 2016.

[23] A. Sharma, K. Shinghal, N. Srivastava, and R. Singh, "Energy management for wireless sensor network nodes," *International Journal of Advances in Engineering & Technology*, vol. 1, no. 1, pp. 7–13, 2011.

[24] R. Al-Mashhadani, G. Alkawsi, Y. Baashar, A. Ahmed Alkahtani, F. Hani Nordin, and W. Hashim, "Deep learning methods for solar fault detection and classification: a review," *Information Sciences Letters*, vol. 10, no. 2, pp. 323–331, 2021.

[25] A. Al-Sammarraee and N. Alshareeda, "The role of artificial intelligence by using automatic accounting information system in supporting the quality of financial statement," *Information Sciences Letters*, vol. 10, no. 2, pp. 223–254, 2021.

[26] I. Atia, M. L. Salem, A. Elkholy, W. Elmashad, and G. A. M. Ali, "In-silico analysis of protein receptors contributing to SARS-COV-2 high infectivity," *Information Sciences Letters*, vol. 10, no. 3, pp. 561–570, 2010.

[27] Y. M. Al-Rawi, W. Subhi Al-Dayyeni, and I. Reda, "COVID-19 impact on education and work in the Kingdom of Bahrain: survey study," *Information Sciences Letters*, vol. 10, no. 3, pp. 427–433, 2021.

[28] I. T. Ahmed and S. S. I. Ismail, "An intelligent hybrid technique of decision tree and genetic algorithm for E-mail spam detection," in *2019 Ninth International Conference on Intelligent Computing and Information Systems (ICICIS)*, pp. 99–104, Cairo, Egypt, Dec 2019.

[29] A. I. Taloba, A. A. Sewisy, and Y. A. Dawood, "Accuracy enhancement scaling factor of Viola- Jones using genetic algorithms," in *2018 14th International Computer Engineering Conference (ICENCO)*, pp. 209–212, Cairo, Egypt, Dec 2018.

Hindawi
Wireless Communications and Mobile Computing
Volume 2022, Article ID 1767295, 11 pages
https://doi.org/10.1155/2022/1767295

Research Article

Research on Wastewater Treatment Monitoring Algorithms Based on Deep Convolutional Neural Networks

Xun Zhang[1,2] **and Yanhui Gu**[2]

[1]*School of Environmental Science & Engineering, Tianjin University, Jinan, Tianjin, 300350, China*
[2]*Jinan Eco-Environmental Monitoring Center of Shandong Province, Jinan, Shandong 250100, China*

Correspondence should be addressed to Xun Zhang; 1218214004@tju.edu.cn

Received 29 December 2021; Revised 17 February 2022; Accepted 28 February 2022; Published 13 April 2022

Academic Editor: Mohamed Elhoseny

Around the problems of data loss, noise, and different temporal and spatial scale features of urban wastewater treatment process data, a method of monitoring and predicting wastewater treatment process data based on deep convolutional neural networks is proposed in the paper. Firstly, to address the problem that urban wastewater treatment process data has multiple spatial and temporal scale characteristics, which makes it difficult for the data to be used effectively, a spatial and temporal data fusion model based on fuzzy neural network (FNN) is proposed. Fuzzy neural networks have strong generalization ability and robustness. Secondly, to enable accurate and real-time monitoring of the content of the monitored components in the effluent of the urban wastewater treatment process, an intelligent prediction model based on SDF-FNN is established for the effluent. Finally, in order to verify the effectiveness of this intelligent prediction model, the model is tested using data collected from actual municipal wastewater treatment plants. The experimental results show that the wastewater treatment intelligent monitoring model is effective and can predict the content of the effluent monitoring index with high accuracy.

1. Introduction

Urban water pollution is a widespread problem, directly endangering the health of the people and the ecological balance, and has become an urgent problem that people are concerned about [1]. The recycling of wastewater, the maximum protection of the water environment, the sustainable use of freshwater resources, and the virtuous cycle, has become a strategic initiative of governments around the world for the comprehensive use of water resources [2]. In recent years, with the construction of municipal wastewater treatment processes (MWTPs) plants and the application of related technology development, the rate of wastewater treatment has been effectively increased. However, the operation of urban wastewater treatment plants is not optimistic, and abnormal conditions have become a major bottleneck in the operation and development of urban wastewater treatment plants [3]. Abnormal conditions are not found and disposed of in a timely manner, and process safety control is not effective, will directly affect the effluent quality, and endanger the operation of the entire wastewater treatment system, and can seriously lead to the collapse of the entire wastewater treatment process. Therefore, there is an urgent need to study effective methods for detecting abnormal working conditions in wastewater treatment, to solve the problem of identifying and suppressing abnormal working conditions and to ensure that the wastewater treatment process operates up to standard. In fact, due to the complexity and lag of the wastewater treatment process, the collected wastewater data is not only delayed but also due to the complex data detection environment of each operation unit such as anaerobic tank, anoxic tank, and aeration tank, which causes unclear data abnormal factors, resulting in abnormal working conditions that are difficult to accurately identify, reject, and compensate, thus preventing effective abnormal working condition location. Therefore, how to design an effective data detection method that can guarantee both the quality of the data detected and the accuracy of the wastewater treatment monitoring is still a challenge for the wastewater treatment process.

In order to make full use of the wastewater treatment process variable data to identify abnormal working conditions online, the researchers analyzed the process data, explored the characteristic variables associated with the abnormal working conditions, established a data-driven process characteristic model to express the abnormal working condition characteristics, and combined with the threshold and parameter settings to determine the occurrence of abnormal working conditions, as shown in Figure 1.

With the increasing demand for recognition of abnormal conditions in terms of level, type and priority, accuracy, stability, and speed have become important indicators for testing abnormal condition recognition methods. In order to meet the recognition requirements and achieve the desired recognition effect, intelligent methods such as neural networks, fuzzy logic, and expert systems have been applied in China and abroad to achieve high quality recognition of wastewater treatment abnormal conditions [(12)].

To further improve the recognition accuracy, Brault et al. applied neural networks to the prediction of filamentous sludge expansion in wastewater treatment, using the key parameters affecting the process as input to the neural network [4]. Lou et al. used a three-layer feedforward neural network to predict the sludge swelling characteristics, using pH, suspended solid concentration, dissolved oxygen dissolution, and other influencing factors as auxiliary variables to predict the occurrence of sludge swelling, thus achieving early warning of sludge swelling [5]. Barnett has developed a rule-based expert system for the identification of abnormal conditions in anaerobic sludge digestion processes. With the help of the process data analysis, sludge concentration, suspended solid concentration, dissolved oxygen concentration, and pH value, which characterize the state in the secondary sedimentation tank, were selected as auxiliary variables, and abnormal conditions were identified as the output [6]. In order to maintain the stability of the abnormal condition identification, Traore et al. used fuzzy rules to identify the sludge height of the secondary sedimentation tank with variables such as sludge concentration, sludge volume, and suspended matter concentration and used the identification results to evaluate the settling performance of the sludge-water mixture in the secondary sedimentation tank to determine whether the abnormal condition occurred [7]. To improve the computability of the model, Han et al. proposed a self-organizing radial basis function (SORBF) method to predict SVI. This method can reduce the computational complexity and ensure the rapidity of SVI prediction while maintaining the computational accuracy [8].

Based on the above analysis, it can be seen that due to the diverse sources of municipal wastewater, the many and mostly unknown water quality components, and the diversity of abnormal conditions, it is difficult for conventional instrumentation to meet a wide range of needs, and the specificity of abnormal conditions requires a high level of real-time accuracy in the identification method. In order to better identify abnormal conditions in the wastewater treatment process, taking into account the operating methods and costs of the wastewater treatment industry, neural network-based intelligent identification technology is currently one of the better options for urban wastewater treatment plants compared to other identification technologies. The main contributions of this paper are as follows: for the problems of data loss, noise, and different spatiotemporal scale features of urban wastewater treatment process data, this paper proposes a method for monitoring and predicting wastewater treatment process data based on deep convolutional neural networks. Firstly, a spatiotemporal data fusion model based on fuzzy neural network (FNN) is proposed to solve the problem that urban wastewater treatment process data has multiple spatiotemporal scale features, which makes it difficult to use the data effectively. Secondly, an intelligent prediction model based on SDF-FNN is established in order to monitor the content of monitored components in the effluent of urban wastewater treatment process accurately and in real time. Finally, in order to verify the effectiveness of this intelligent prediction model, the model was tested using data collected from an actual municipal wastewater treatment plant. The experimental results show that this wastewater treatment intelligent monitoring model is effective and can predict the content of wastewater monitoring indicators with high accuracy.

2. Related Work

In recent years, various tests conducted by the United Nations on water resources have found that one tenth of the world's rivers are polluted to varying degrees, and the pollution of water resources in many countries is alarming. China's total water consumption is 554.8 billion cubic meters, of which a total of 69.3 billion tons of waste water is discharged, most of which is untreated, resulting in a large amount of sewage discharge and low treatment rate, which also makes groundwater and rivers, lakes, and seas seriously polluted. Water pollution not only makes the shortage of freshwater resources more obvious but also puts human health at risk; at the same time, industrial and agricultural production and urban life are inseparable from a stable and reliable water supply, so, under the dual pressure of the quality of the water environment and the energy situation, effective control and optimal operation of the wastewater treatment process to reduce the energy consumed become an urgent need. The characteristics of wastewater treatment process are as follows: multivariable, nonlinear, large lag, and with strong external interference. The main manifestations are as follows: (1) the system is relatively complex, and the reason is that complex biochemical reactions occur in the wastewater treatment process, while complex interactions between substrates and microorganisms; (2) the correlation between elements is low, and although the mathematical model can describe the correlation between substrates and microorganisms, it cannot accurately describe their causal relationships; and (3) the volatile external environment in the system, the treatment process has been in the complex external environment changes, for example, organic matter concentration, flow rate, temperature, and other parameters are always in the change.

Some progress has been made in the existing methods on wastewater testing. In order to predict and identify the

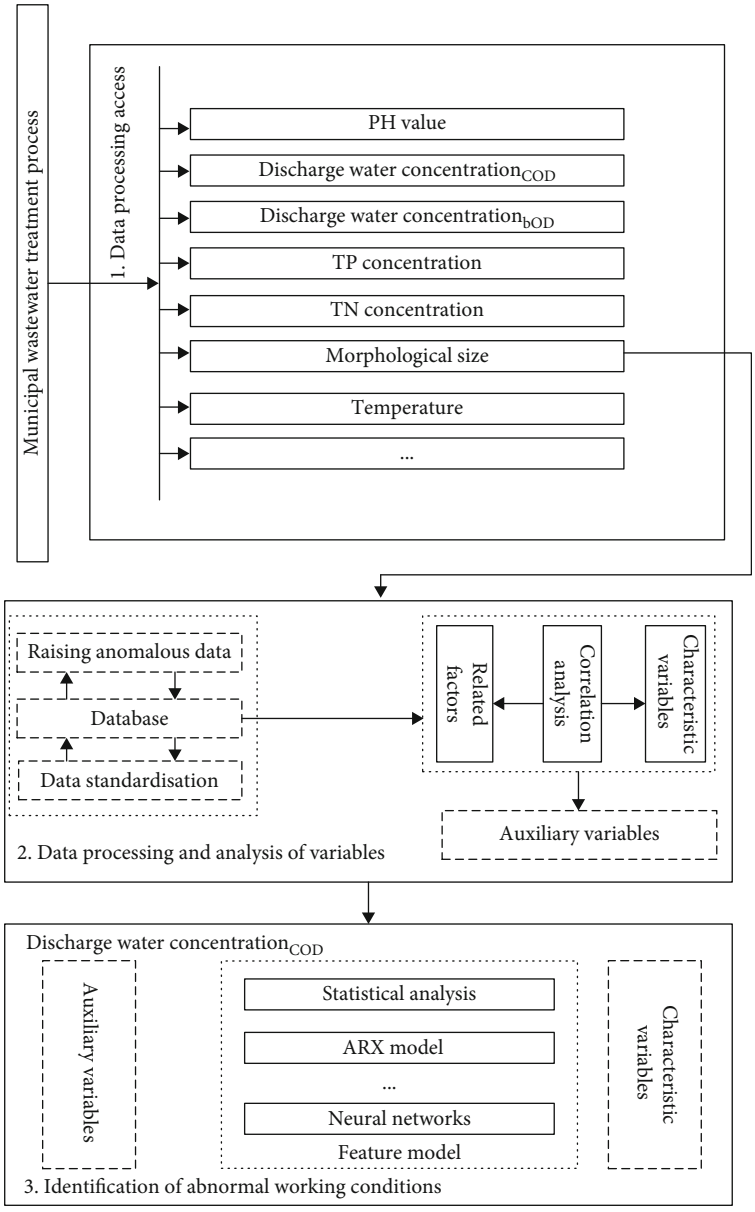

Figure 1: Data-driven identification method for abnormal wastewater treatment conditions.

occurrence of abnormal conditions, Makinia et al. analyzed the formation mechanism of abnormal conditions, analyzed the activated sludge model 3 (ASM3) of wastewater treatment process, established the relationship between sludge substrate concentration removal rate and microbial growth, and identified the microbial growth status by calculating the sludge substrate concentration removal rate online to predict and identify abnormal condition [(4)]. However, this method is usually carried out in a laboratory environment, but the actual wastewater treatment conditions are highly time-varying, it is difficult to adapt the mechanistic model with fixed parameters to the dynamic changes of the process, and the success rate of abnormal conditions identification is low. In order to improve the performance of the model and increase the success rate of anomalous conditions identification, Bansal et al. used the predictive power of Hidden Markov Models for events to find the probability of occurrence of filamentous swelling from historical data and directly implement the prediction of filamentous swelling [9]. However, this approach, which is driven by probabilistic statistics, selects too many variables and ignores the influence of other variables and factors on abnormal conditions.

In addition, the model was poor in identifying and predicting severe disturbance conditions. In order to improve the reliability of the prediction of abnormal conditions, Xavier et al. described four different types of abnormal conditions caused by dissolved oxygen, pH, and sludge loading by empirically summarizing the relationship between abnormal condition characteristics and process variables and also developed a risk assessment model on abnormal conditions to achieve the prediction of abnormal conditions and their types [10]. Mesquita et al. used partial least squares to

Table 1: Contribution of each component.

Ingredients	pH	T	ORP1	ORP2	TSS	DO1	DO2	NH4-N	NO3-N
Contribution rate	0.0602	0.1016	0.2103	0.0165	0.2203	0.3146	0.0421	0.0464	0.0301

analyses the process variables and sludge settling performance, extracted six causal factors for sludge expansion, such as dissolved oxygen, pH, and ammonia nitrogen and established a regression model between the causal factors and the sludge expansion index SVI [11]. Smets et al. developed an autoregressive with extra inputs (ARX) model for the identification of abnormal conditions by combining the relationship between the factors causing abnormal conditions and the characteristics of filamentous bacteria and used the measured data to calibrate the parameters of the ARX model to identify scum, foam failure, toxic effluent, and sludge swelling [12]. The method of identifying abnormal working conditions using causal correlation analysis between the characteristics of the abnormal working conditions and their characteristic variables allows information patterns to be extracted directly from the data. It can be used to identify the signs of abnormal conditions, reducing the reliance on equipment, avoiding the tedious process of observation, measurement, and analysis, and increasing the frequency of identification and prediction, making it easier to apply to the actual wastewater treatment process. However, the method requires a reliable model that can characterize causal associations. Due to the complexity, uncertainty, and high nonlinearity of biochemical reactions in wastewater treatment, models designed using grey model methods [13], parametric evaluation methods [14], and statistical analysis methods [15] are difficult to characterize.

3. Methods

3.1. Selection of Key Water Quality Parameters. Urban wastewater treatment plants are monitored for key water quality parameters to ensure stable operation and compliance with effluent quality standards [16]. The effluent total phosphorus (TP) is a key indicator to ensure that the effluent quality standards are met [17]. Therefore, it is important to monitor it in real time. The process of phosphorus removal relies heavily on microorganisms and therefore, their activity and numbers have a significant impact on the overall effectiveness of phosphorus removal from wastewater. Microbial activity and growth are influenced by various components of the effluent (oxidation reduction potential (ORP), dissolved oxygen (DO) concentration, temperature (T), pH value, etc.). In addition, according to historical data, ammonia (NH4-N), nitrate (NO3-N), and TSS also have an influence on the phosphorus removal process. In summary, seven variables, namely, pH, ORP, DO, T, NH4-N, NO3-N, and TSS, were initially selected as relevant variables for the effluent TP intelligent prediction model.

3.2. Data Preprocessing. In the actual municipal wastewater treatment process, there are inevitably some random errors in the collected data samples due to various factors (e.g., anomalies in the detection instrumentation [18], manual errors, and interference from environmental factors). Therefore, in order to accurately obtain the relevant variables of TP in the water, the collected data samples need to be excluded from the abnormal data. In this paper, the 3σ criterion is used to remove the anomalies, and the algorithm is based on the following steps:

(1) Suppose the collected sample data set is $x_1, x_2, x_3, \cdots, x_n$ and its mean $\bar{x}$. Calculate the deviation v_i as shown in equation (1)

$$v_i = x_i - \bar{x}(i = 1, 2, \cdots, n). \tag{1}$$

(2) Calculate the standard deviation σ for the collected sample data set with the formula shown in equation (2)

$$\sigma = \sqrt{\sum v_i^2/(n-1)}. \tag{2}$$

(3) If the deviation $v_i((1 \le i \le n))$ of the sample data x_i satisfies equation (3), x_i is considered to be anomalous data containing gross errors and should be excluded

$$\left|v_i^2\right| > 3\sigma. \tag{3}$$

The collected data was preprocessed. After removing the abnormal data, 800 sets of sample data were taken. The contribution of each component after dimensionality reduction of the relevant variables using principal component analysis (PCA) is shown in Table 1.

As can be seen from Table 1, the cumulative contribution of DO1, ORP1, TSS, pH, and T was 0.907 (greater than 0.85), starting with the component with the highest contribution, at a fraction of 5. The cumulative contribution of ORP1, TSS, pH, and T is 0.907 (greater than 0.85). Therefore, according to the dimensionality reduction concept of PCA, the variables related to the effluent TP can be reduced from 9 dimensions to 5 dimensions, and the auxiliary variables of the effluent TP intelligent prediction model are determined as follows: aerobic front-end DO concentration, anaerobic end ORP, aerobic end TSS, effluent pH, and T.

3.3. Spatiotemporal Data Fusion Based on Fuzzy Neural Network. The neural network approach is fast; however, its

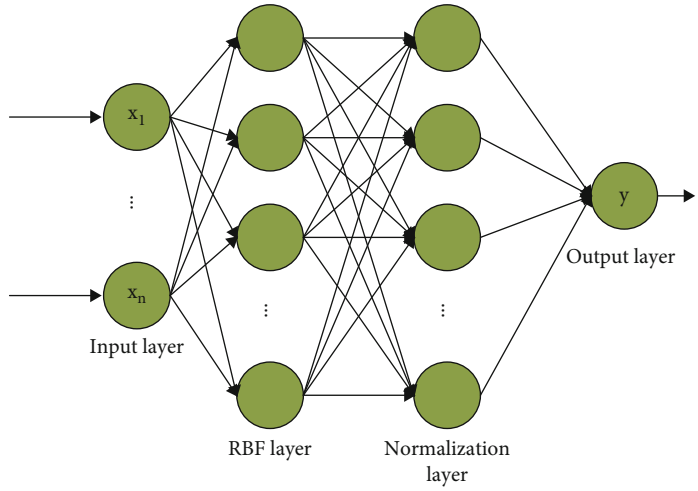

Figure 2: The structure of fuzzy neural network.

dependence on the quality of the data is strong, it is only possible to build a good prediction model if the training data set is sufficient, and the test data set is from the same feature space [19]. When there is data loss, noise, and different temporal and spatial scale features, the prediction results of the neural network method are affected. To this end, we design a Spatiotemporal Data Fusion Based on Fuzzy Neural Network (SDF-FNN) model to fuse multiple spatiotemporal data and improve the accuracy of the model.

3.3.1. Structure of the Model. The fuzzy neural network (FNN) [20] structure used in this paper is shown in Figure 2.

The objective function of the FNN is

$$E(t) = \frac{1}{2}[y(t) - y_d(t)]^2. \tag{4}$$

$y_d(t)$ is the expected output of the nonlinear dynamical system, and $y(t)$ is the output of the FNN.

$$y(t) = \sum_{l=1}^{P} w_l(t) v_l(t), \tag{5}$$

where $w(t) = [w_1(t), w_2(t), w_3(t), \cdots, w_P(t)$ is the weight vector between the FNN normalization layer and the output layer, $w_l(t)$ is the weight between the output layer and the l-th normalized neuron, P is the number of normalized neurons, and $v_l(t)$ is the output of the l-th normalized neuron.

$$v_l(t) = \frac{\varphi_l(t)}{\sum_{j=1}^{P} \varphi_j(t)} = \frac{e^{-\sum_{i=1}^{m} \left(x_i(t) - c_{ij}(t)\right)^2 / 2\sigma_{ij}^2(t)}}{\sum_{j=1}^{P} e^{-\sum_{i=1}^{m} \left(x_i(t) - c_{ij}(t)\right)^2 / 2\sigma_{ij}^2(t)}}, \tag{6}$$

$$\varphi_j(t) = \prod_{i=1}^{m} e^{-\left(x_i(t) - c_{ij}(t)\right)^2 / 2\sigma_{ij}^2(t)} = e^{-\sum_{i=1}^{m} \frac{\left(x_i(t) - c_{ij}(t)\right)^2}{2\sigma_{ij}^2(t)}}, \tag{7}$$

where $c_{ij}(t)$ denotes the center of the j-th RBF neuron at time t for the i-th variable input, and $\sigma_{ij}(t)$ denotes the width of the j-th RBF neuron at time t for the i-th variable input. $x(t) = [x_1(t), x_2(t), \cdots, x_m(t)]$ is the input to the FNN, and $\varphi_j(t)$ is the output of the j-th RBF neuron at time t.

We use gradient descent to learn and optimize each parameter of the FNN. The centering rule for the Gaussian function of the RBF layer [21] is shown in equation (8), and the width adjustment rule is shown in equation (9).

$$c_{ij}(t+1) = c_{ij}(t) + \beta \frac{\partial E(t)}{\partial c_{ij}(t)}, \tag{8}$$

$$\sigma_{ij}(t+1) = \sigma_{ij}(t) + \beta \frac{\partial E(t)}{\partial \sigma_{ij}(t)}. \tag{9}$$

The rules for adjusting the weights between the normalization layer and the output layer are shown in equation (10).

$$w_l(t+1) = w_l(t) + \beta \frac{\partial E(t)}{\partial w_l(t)}, \tag{10}$$

where β is the learning rate, and $w_l(t)$ denotes the weight between the l-th normalized layer neuron and the output neuron of the FNN [22].

3.3.2. SDF-FNN Model Design. The data from the actual application of wastewater treatment and inspection are different in time and space scales, making it difficult for data-driven approaches to utilize them effectively [23]. Therefore, the SDF-FNN model is designed by combining migration learning and FNN with the advantages of FNN [24]. The structure is shown in Figure 3.

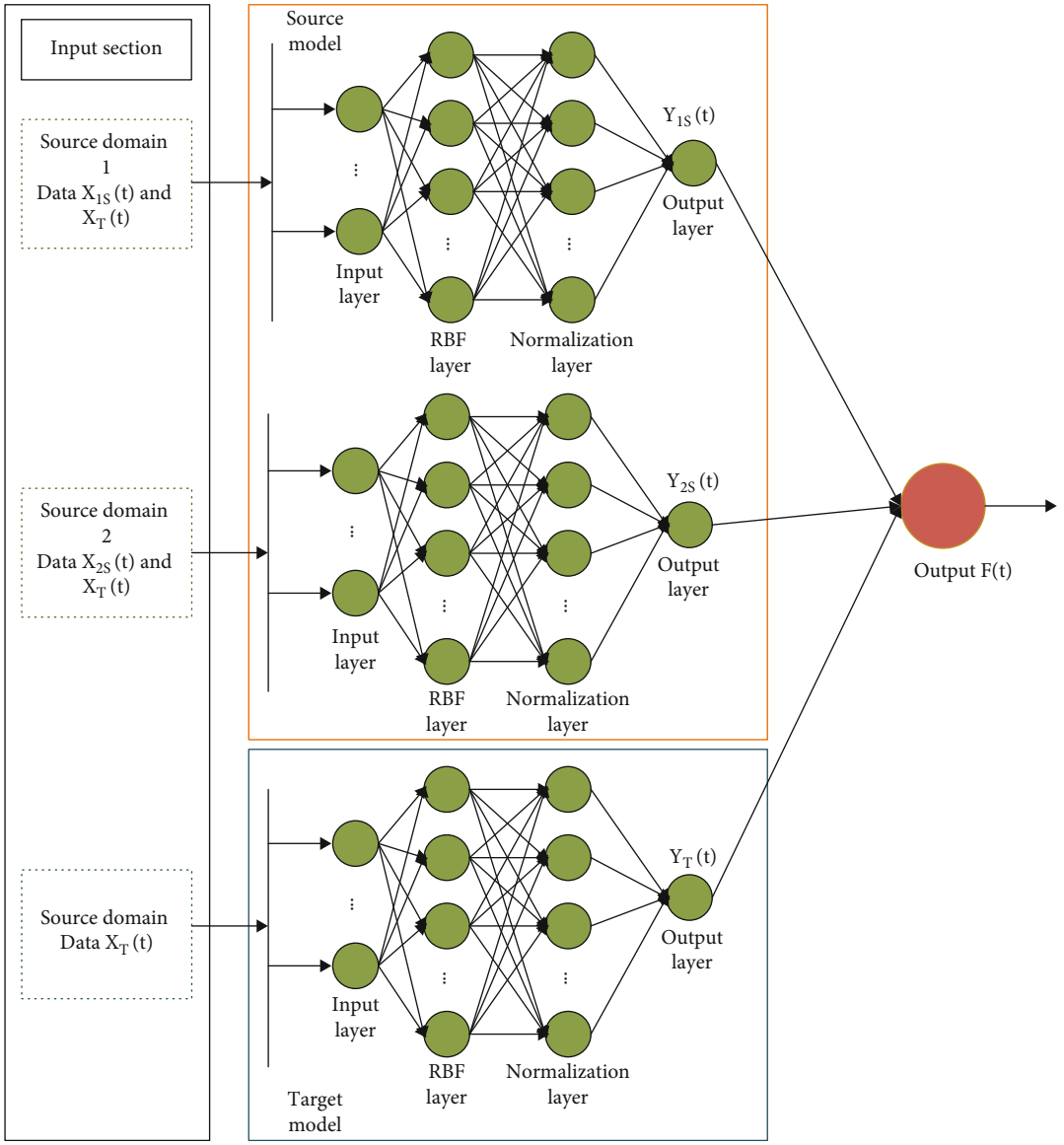

Figure 3: Combining migration learning and FNN to design SDF-FNN model structures.

The source data is defined as shown in equation (11).

$$D_{1S} = \{X_{1S}(\rho), P_{1S}(\rho)\}, \rho = 1, 2, \cdots, N_{1S},$$
$$D_{2S} = \{X_{2S}(\varsigma), p_{2S}(\varsigma)\}, \varsigma = 3, 5, \cdots, 2\rho + 1, \cdots, N_{2S}, \tag{11}$$

where $X_{1S}(\rho) = [x_{1S,1}(\rho), x_{1S,2}(\rho), \cdots, x_{1S,m}(\rho)]$ $X_{2S}(\zeta) = [x_{2S,1}(\zeta), x_{2S,2}(\zeta), \cdots, x_{2S,m}(\zeta)]$, ρ, and ζ represent the time, the natural numbers of $N_{1S} \geq 0$ and $N_{2S} \geq 0$. There are m inputs for each set of data. The target domain data is defined as shown in equation (12).

$$D_T = \{X_T(t), P_T(t)\}, t = 3, 5, \cdots, 2\rho + 1, \cdots, N_T, \tag{12}$$

where $X_T(t) = [x_{Tl}(t), x_{T2}(t), \cdots, x_{Tm}(t)]$, and t represents time, a natural number with $NT \geq 0$. Each set of data has m inputs. From the formula, D_T is different from D_{1S} in terms of time scale; D_T is different from D_{2S} in terms of $P(X_{2S}) \neq P(X_T)$ in terms of domain distribution, but D_T and D_{1S} are similar in terms of spatial distribution.

$$X_T(t) = [x_{Tl}(t), x_{T2}(t), \cdots, x_{Tm}(t)]. \tag{13}$$

In order to improve the prediction accuracy of the model, a source model part and a target model part were designed. The network parameters of the source model are shown in equations (14)–(17).

$$[c_{1s}(t), \sigma_{1s}(t)] = \begin{bmatrix} c_{1s,1}(t), \cdots, c_{1s,j}(t), \cdots, c_{1s,P}(t), \\ \sigma_{1s,1}(t), \cdots, \sigma_{1s,j}(t), \cdots, \sigma_{1s,P}(t) \end{bmatrix}, \tag{14}$$

$$[c_{2S}(t), s_{2S}(t)] = \begin{bmatrix} c_{2S,1}(t), \cdots, c_{2S,j}(t), \cdots, c_{2S,P}(t), \\ s_{2S,1}(t), \cdots, s_{2S,j}(t), \cdots, s_{2S,P}(t) \end{bmatrix}, \quad (15)$$

$$w_{1S}(t) = [w_{1S,1}(t), w_{1S,2}(t), \cdots, w_{1S,P}(t)], \quad (16)$$

$$w_{2S}(t) = [w_{2S,1}(t), w_{2S,2}(t), \cdots, w_{2S,P}(t)], \quad (17)$$

where $c_{1S,j}(t) = [c_{1S,1j}(t), c_{1S,2j}(t), \cdots, c_{1S,mj}(t)]$ $c_{2S,j}(t) = [c_{2S,1j}(t), c_{2S,2j}(t), \cdots, c_{2S,mj}(t)]$ are the centers of the j-th neuron of the RBF layer of the two FNNs of the source model, respectively. $\sigma_{1S,j}(t) = [\sigma_{1S,1j}(t), \sigma_{1S,2j}(t), \cdots, \sigma_{1S,mj}(t)]$ $\sigma_{2S,j}(t) = [\sigma_{IS,1j}(t), \sigma_{2S,2j}(t), \cdots, \sigma_{2S,mj}(t)]$ are the widths of the j-th neuron of the RBF layers of the two FNNs of the source model, respectively [25]. $w_{1S}(t)$ and $w_{2S}(t)$ are the weights between the normalized and output layers of the two FNNs of the source model, respectively.

Target model network parameters are as shown in equations (18) and (19).

$$[c_T(t), \sigma_T(t)] = \begin{bmatrix} c_{T,1}(t), \cdots, c_{Tj}(t), \cdots, c_{TP}(t), \\ \sigma_{T1}(t), \cdots, \sigma_{Tj}(t), \cdots, \sigma_{TP}(t) \end{bmatrix} \quad (18)$$

$$w_T(t) = [w_{T,1}(t), w_{T,2}(t), \cdots, w_{T,P}(t)] \quad (19)$$

where $c_{T,j}(t)$ is the center of the j-th neuron of the target model FNN. $\sigma_{T,j}(t)$ is the width of the j-th neuron of the target model FNN. $w_T(t)$ is the weight between the normalization layer and the output layer of the target model FNN.

Inputting the target domain data into the SDF-FNN, the output of the source model part and the target model part of the FNN network are shown in equations (20)–(22), respectively.

$$y_{1S}(t) = \sum_{l=1}^{P} w_{1S,l}(t) v_{1S,l}(t) = \sum_{l=1}^{P} w_{1S,l}(t) \frac{e^{-\sum_{i=1}^{m} \left(\left(x_i(t) - c_{1S,ij}(t)\right)^2 / 2\sigma_{1,i,j}^2(t)\right)}}{\sum_{j=1}^{P} e^{-\sum_{i=1}^{m} \left(\left(x_i(t) - c_{i,1S,j}(t)\right)^2 / 2\sigma_{1S,j}^2(t)\right)}}, \quad (20)$$

$$y_{2S}(t) = \sum_{l=1}^{P} w_{2S,l}(t) v_{2S,l}(t) = \sum_{l=1}^{P} w_{2S,l}(t) \frac{e^{-\sum_{i=1}^{m} \left(\left(x_i(t) - c_{2S,ij}(t)\right)^2 / 2\sigma_{2S,ij}^2(t)\right)}}{\sum_{j=1}^{P} e^{-\sum_{i=1}^{m} \left(\left(x_i(t) - c_{2S,ij}(t)\right)^2 / 2\sigma_{2S,ij}^2(t)\right)}}, \quad (21)$$

$$y_T(t) = \sum_{l=1}^{P} w_{T,l}(t) v_{T,l}(t) = \sum_{l=1}^{P} w_{T,l}(t) \frac{e^{-\sum_{i=1}^{m} \left(\left(x_i(t) - c_{T,j}(t)\right)^2 / 2\sigma_{T,j}^2(t)\right)}}{\sum_{j=1}^{P} e^{-\sum_{i=1}^{m} \left(\left(x_i(t) - c_{T,j}(t)\right)^2 / 2\sigma_{T,j}^2(t)\right)}}, \quad (22)$$

where $v_{1S,l}(t)$ is the output of the l-th normalized layer neuron in source domain 1, and $v_{2S,l}(t)$ is the output of the l-th normalized layer neuron in source domain 2. $v_{T,l}(t)$ denotes the output of the l-th normalized layer neuron in the target domain. $y_{1S}(t)$ and $y_{2S}(t)$ are the outputs of the source model, and $y_T(t)$ is the output of the target objective model.

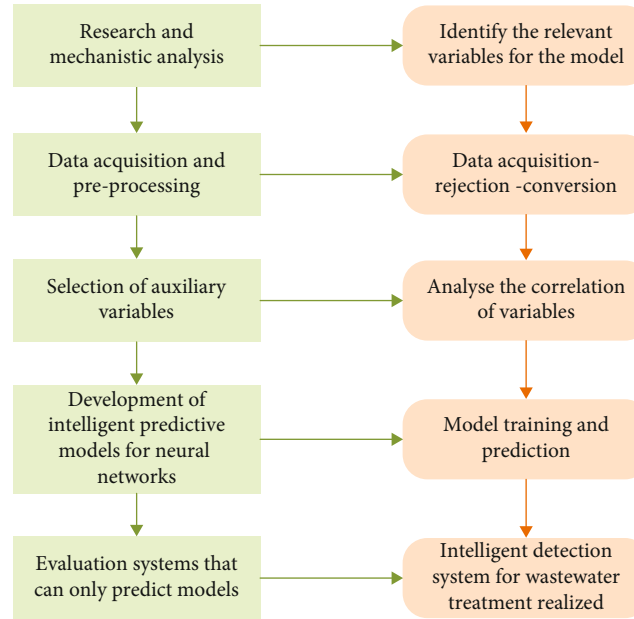

Figure 4: Flow chart of the intelligent prediction model for wastewater treatment effluent TP.

The final output of the network is shown in equation (23).

$$F(t) = \alpha_1(t) \times y_{1S}(t) + \alpha_2(t) \times y_{2S}(t) + \alpha_3(t) \times y_T(t). \quad (23)$$

3.3.3. Spatiotemporal Data Fusion Migration Learning Algorithms. In order to transfer knowledge from the source domain to the target domain, a bridge should exist to connect the source and target domains and to determine how much knowledge needs to be transferred. Therefore, the adaptive correlation parameters $\delta_1(t)$ and $\delta_2(t)$ are introduced to establish the correlation between the source and target domains as shown in equation (24).

$$\begin{aligned} c_{T,ij}(t) &= c_{T,ij}(t-1) + \delta_1(t) c_{1S,ij}(t) + \delta_2(t) c_{2S,ij}(t), \\ \sigma_{T,ij}(t) &= \sigma_{T,ij}(t-1) + \delta_1(t) \sigma_{1S,ij}(t) + \delta_2(t) \sigma_{2S,ij}(t), \\ w_{T,l}(t) &= w_{T,il}(t-1) + \delta_1(t) w_{1S,il}(t) + \delta_2(t) w_{2S,l}(t). \end{aligned} \quad (24)$$

Among them, $c_{T,ij}(t)$ is the center of the j-th RBF neuron of the target model FNN at time t in the target domain with the input of the i-th variable. $\sigma_{T,ij}(t)$ denotes the width of the j-th RBF neuron of the target model FNN at time t in the target domain, when the i-th variable is input. $w_{T,l}(t)$ denotes the weight between the l-th normalized layer neuron and the output neuron of the target model FNN at time t in the target domain. $c_{1S,ij}(t)$ and $c_{2S,ij}(t)$ are the centers of the RBF layer neurons of the two FNNs of the source model at time t, respectively. $\sigma_{1S,ij}(t)$ and $\sigma_{2S,ij}(t)$ are the widths of the RBF layer neurons of the two FNNs of the source model at time t. $w_{1S,il}(t)$ and $w_{2S,l}(t)$ are the weights between the l

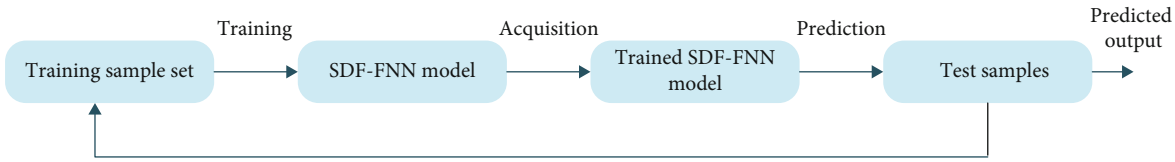

Figure 5: Outflow TP Intelligent predictive model calibration.

Table 2: Experimental data set sources and data volume.

Data sources	Source area 1 (wastewater treatment plant *A*)	Source area 2 (wastewater treatment plant *B*)	Target area (wastewater treatment plant *A*)	
			Training set	Test set
Volume of data	600	600	100	100

-th normalized layer neuron and the output neuron of the two different FNNs at time t, respectively.

4. Experiments and Results

The intelligent prediction of effluent TP after treatment is an attempt to use all the relevant variables that can be easily measured in relation to the effluent TP and intelligent algorithms to measure the effluent TP that is difficult to measure and not easily measured accurately online. The flow chart of the intelligent prediction after treatment is shown in Figure 4.

4.1. Intelligent Monitoring Model. The inputs to the intelligent monitoring model for wastewater treatment are as follows: T, ORP, DO, TSS, and pH. The training of the model is carried out in two parts. (1) Input the source domain data as training samples into the source model and use the FNN algorithm to train and adjust the FNN in the source model to obtain the corresponding parameters; (2) input the target domain data as training samples into both the source and target models and use the gradient descent algorithm to adjust the weight parameters and adaptive parameters of the whole model; finally, use the spatiotemporal data migration learning algorithm to adjust the parameters of the target. Finally, the spatiotemporal data migration learning algorithm is used to adjust the parameters of the target model to ensure the accuracy of the network and complete the training of the intelligent prediction model.

The test samples of the wastewater treatment intelligent monitoring model were used as input to the SDF-FNN model, and when the sample data was entered, the trained SDF-FNNN model was used to predict the effluent TP online for the test sample data.

4.2. Model Parameter Calibration. In the actual urban wastewater treatment process, the reaction process of effluent TP is complex and variable, with nonlinear, time-varying, and strongly coupled characteristics. Before the established effluent TP intelligent monitoring model is put into operation in the actual wastewater treatment plant, it may be disturbed by external factors, which may cause large calculation errors in the model if it is put into use directly. Therefore, in order to ensure the feasibility and validity of the effluent TP intelligent prediction model, the calibration of the intelligent prediction model is an indispensable part of the overall design process. The calibration scheme for the intelligent prediction model for effluent TP is shown in Figure 5.

4.3. Evaluation Indicators. The ability of wastewater treatment monitoring models to predict effluent TP well requires evaluation of the models by means of evaluation metrics. In this paper, two indicators, RMSE and accuracy, are used to evaluate the performance of the SDF-FNN prediction model. The expression for the RMSE is shown in Equation (25).

$$\mathrm{RMSE} = \sqrt{\frac{1}{2P}\sum_{p=1}^{P}\left(\widehat{y}_p(t) - y_d(t)\right)^2}, \tag{25}$$

where P is the total number of sample data. $\widehat{y}_p(t)$ is the actual SDF-FNN output. $y_d(t)$ is the expected SDF-FNN output.

The expression for the evaluation indicator accuracy is shown in Equation (26).

$$\mathrm{accuracy} = \frac{1}{N_T}\sum_{t=1}^{N_T} 1 - \frac{\left|\widehat{y}_p(t) - y_d(t)\right|}{\widehat{y}_p(t)} \times 100\%, \tag{26}$$

where N_T is the total number of experimental samples. The larger the evaluation index accuracy, the better the prediction performance of the SDF-FNN intelligent prediction model for effluent TP.

4.4. Experimental Design and Analysis of Results. This paper collects actual data from two different actual municipal wastewater treatment plants, *A* and *B*. The data sources and data volumes for the experiments are shown in Table 2.

The learning rate η of the intelligent monitoring model for the SDF-FNN effluent TP is 0.015. The weights of the central and width values of the FNN Gaussian function in the source and target models and the weights w between the FNN normalization and output layers are random numbers with [0, 1] distribution. The weights $\alpha_1(t)$, $\alpha_2(t)$, and $\alpha_3(t)$ and the adaptive correlation parameters $\delta_1(t)$ and $\delta_2(t)$ between the source model, the target model, and the final output of the network are also random numbers with [0,1] distribution. Each neural network has 5 input neurons, 1 output neuron, 15 rule layer neurons, and $\lambda_1 = \lambda_2 = 1$. The experimental environment of this article is as follows: the

Table 3: Training set and test set for experimental design.

Experiment title	Training set	Test set
Experiment 1 (FNN)	Training set for municipal wastewater treatment plant *B*	Measurement set of urban wastewater treatment plant *A*
Experiment 2 (FNN1)	Data from urban wastewater treatment plant *A* and training set for municipal wastewater treatment plant *B*	Test set of urban wastewater treatment plant *A*
Experiment 3 (SDF-FNN)	Data from urban wastewater treatment plant *A* and training set for municipal wastewater treatment plant *B*	Test set of urban wastewater treatment plant *A*

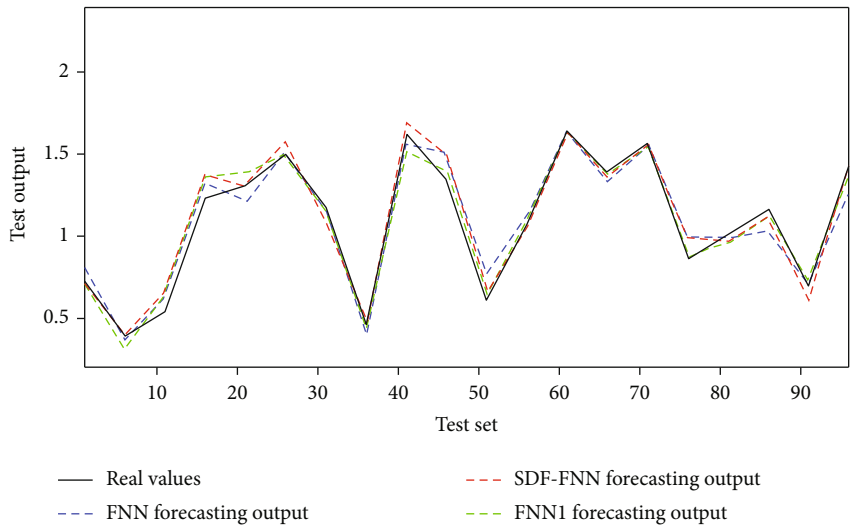

Figure 6: Predicted output of effluent TP test samples.

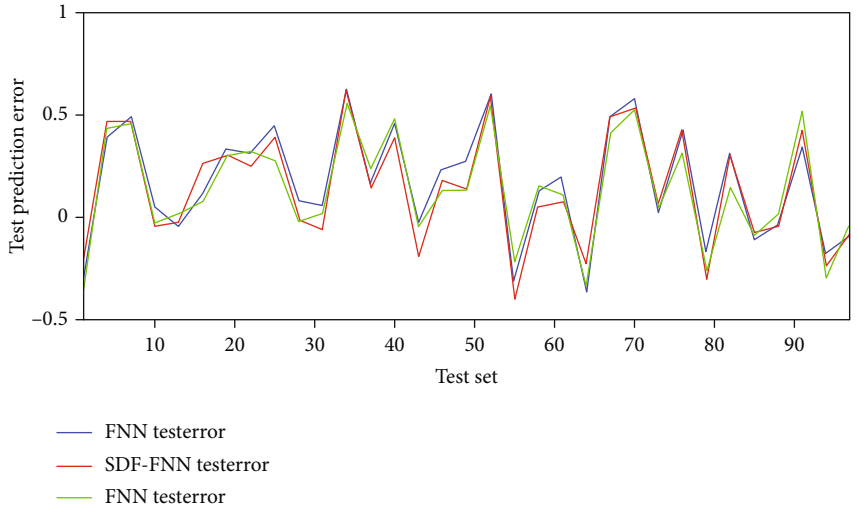

Figure 7: Prediction error for effluent TP test samples.

hardware environment is Linux system, NVIDIA GTX 1080Ti; the software environment is Python3.6, sklearn0.20.1, and other toolkits.

To verify the feasibility of the method, three experiments were designed. The data in the target domain and the data in source domain one is from the same municipal wastewater treatment plant at different time scales. The spatial distribution of the data in the target domain is different from that in the source domain two. The training and test sets for each experiment are shown in Table 3.

The experimental simulation results are shown in Figures 6–8. As can be seen in Figure 6, the proposed SDF-FNN intelligent prediction model for effluent TP is closer to the true value of effluent TP than the FNN. Figure 7 clearly shows that the fluctuation range of the prediction error of the SDF-FNN model for effluent TP is significantly

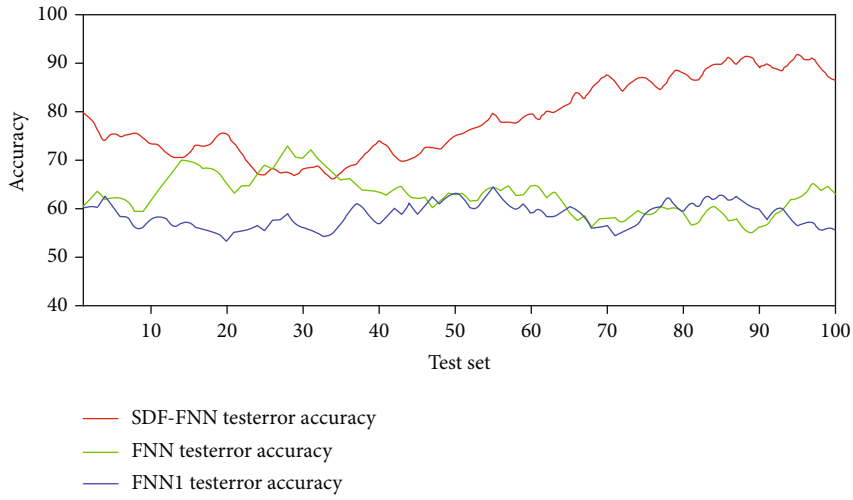

Figure 8: Accuracy values for effluent TP test samples.

Table 4: Effluent TP prediction results.

Algorithms	Testing RMSE	Prediction accuracy (%)
FNN	0.3791	87.86
KL-FNN	0.2394	91.34
SOFNN-AGA	0.2557	92.52
GDFNN	0.2146	92.95
ANFIS	0.2810	90.13
GPFNN	0.3456	89.26
SDF-FNN	0.1943	93.82

smaller than the results of the other two FNNs. In addition, Figure 8 shows that the prediction accuracy of the SDF-FNN is significantly higher than the prediction accuracy of the other two FNNs. By combining the above predicted, actual, and predicted TP values with the accuracy, we can conclude that the proposed intelligent monitoring model for wastewater treatment can predict the TP content of the effluent better.

The purpose is to evaluate the performance of SDF-FNN, and the results were compared with existing methods such as FNN, KL-FNN, SOFNN-AGA, GDFNN, GPFNN, and ANFIS. All methods have the same training and test samples. The details are shown in Table 4 and relate to the following metrics: test RMSE and accuracy. The network models proposed in this paper all achieve optimal results in comparison.

5. Conclusion

Due to the cumbersome operation, low measurement accuracy, and high instrument maintenance costs of existing monitoring methods in actual municipal wastewater treatment plants, it is difficult to achieve real-time online monitoring of effluent indicators. Data-driven methods have been widely used to predict effluent quality parameters. However, the data-driven approach can be affected when there is loss of measurement data, noise, and different temporal and spatial scale characteristics of the urban wastewater treatment process. To enable accurately and real time predict and monitor the TP content in the effluent of urban wastewater treatment processes using different temporal and spatial scale data, an SDF-FNN-based intelligent predictive monitoring model for wastewater treatment effluent TP is proposed in this paper.

The proposed SDF-FNN model is used to develop an intelligent predictive monitoring model based on the FNN effluent TP. The proposed FNN effluent TP model was applied to a real urban wastewater treatment plant, and data from different spatial scales and time scales were selected as the source domain data for the experiments. It is proved that this method is significantly better than other types of neural networks and algorithms in predicting the effluent TP, and the intelligent monitoring model can achieve high accuracy in predicting the effluent TP. In future work, we plan to conduct research on long- and short-term memory networks and attention mechanisms for wastewater testing.

Data Availability

Some or all data, models, or code generated or used during the study are available from the corresponding author by request.

Conflicts of Interest

The authors declare that they have no conflicts of interest.

References

[1] H. Liu, Y. Jia, and C. Niu, ""Sponge city" concept helps solve China's urban water problems," *Environmental Earth Sciences*, vol. 76, no. 14, pp. 1–5, 2017.

[2] A. Y. Hoekstra, J. Buurman, and K. C. H. Van Ginkel, "Urban water security: a review," *Environmental Research Letters*, vol. 13, no. 5, article 053002, 2018.

[3] I. Michael, L. Rizzo, C. S. McArdell et al., "Urban wastewater treatment plants as hotspots for the release of antibiotics in the environment: a review," *Water Research*, vol. 47, no. 3, pp. 957–995, 2013.

[4] J. M. Brault, R. Labib, M. Perrier, and P. Stuart, "Prediction of activated sludge filamentous bulking using ATP data and neural networks," *The Canadian Journal of Chemical Engineering*, vol. 89, no. 4, pp. 901–913, 2011.

[5] I. Lou and Y. Zhao, "Sludge bulking prediction using principle component regression and artificial neural network," *Mathematical Problems in Engineering*, vol. 25, no. 10, pp. 295–308, 2012.

[6] M. W. Barnett, "Knowledge-based expert system applications in waste treatment operation and control," *ISA Transactions*, vol. 31, no. 1, pp. 53–60, 1992.

[7] A. Traoré, S. Grieu, F. Thiery, M. Polit, and J. Colprim, "Control of sludge height in a secondary settler using fuzzy algorithms," *Computers & Chemical Engineering*, vol. 30, no. 8, pp. 1235–1242, 2006.

[8] H. G. Han and J. F. Qiao, "Prediction of activated sludge bulking based on a self-organizing RBF neural network," *Journal of Process Control*, vol. 22, no. 6, pp. 1103–1112, 2012.

[9] N. K. Bansal, X. Feng, W. Zhang, W. Wei, and Y. Zhao, "Modeling temporal pattern and event detection using Hidden Markov Model with application to a sludge bulking data," *Procedia Computer Science*, vol. 12, pp. 218–223, 2012.

[10] X. Flores-Alsina, J. Comas, I. Rodriguez-Roda, K. V. Gernaey, and C. Rosen, "Including the effects of filamentous bulking sludge during the simulation of wastewater treatment plants using a risk assessment model," *Water Research*, vol. 43, no. 18, pp. 4527–4538, 2009.

[11] D. P. Mesquita, A. L. Amaral, and E. C. Ferreira, "Activated sludge characterization through microscopy: a review on quantitative image analysis and chemometric techniques," *Analytica Chimica Acta*, vol. 802, pp. 14–28, 2013.

[12] E. N. Banadda, I. Y. Smets, R. Jenné, and J. F. van Impe, "Dynamic modeling of filamentous bulking in lab-scale activated sludge processes," *IFAC Proceedings Volumes*, vol. 37, no. 9, pp. 383–388, 2004.

[13] C. Zhang and H. Zhang, "Analysis of aerobic granular sludge formation based on grey system theory," *Journal of Environmental Sciences*, vol. 25, no. 4, pp. 710–716, 2013.

[14] W. J. Ng, S. L. Ong, and F. Hossain, "An algorithmic approach for system-specific modelling of activated sludge bulking in an SBR," *Environmental Modelling & Software*, vol. 15, no. 2, pp. 199–210, 2000.

[15] J. Comas, I. Rodríguez-Roda, K. V. Gernaey, C. Rosen, U. Jeppsson, and M. Poch, "Risk assessment modelling of microbiology-related solids separation problems in activated sludge systems," *Environmental Modelling & Software*, vol. 23, no. 10-11, pp. 1250–1261, 2008.

[16] R. Martínez, N. Vela, A. El Aatik, E. Murray, P. Roche, and J. M. Navarro, "On the use of an IoT integrated system for water quality monitoring and management in wastewater treatment plants," *Water*, vol. 12, no. 4, article 1096, 2020.

[17] T. D. Bui, J. Luong-Van, and C. M. Austin, "Impact of shrimp farm effluent on water quality in coastal areas of the world heritage-listed Ha Long Bay," *American Journal of Environmental Sciences*, vol. 8, no. 2, pp. 104–116, 2012.

[18] J. Jiang, M. Chen, and J. A. Fan, "Deep neural networks for the evaluation and design of photonic devices," *Nature Reviews Materials*, vol. 6, no. 8, pp. 679–700, 2021.

[19] J. Liu, T. Li, P. Xie, S. du, F. Teng, and X. Yang, "Urban big data fusion based on deep learning: An overview," *Information Fusion*, vol. 53, pp. 123–133, 2020.

[20] H. K. Kwan and Y. Cai, "A fuzzy neural network and its application to pattern recognition," *IEEE Transactions on Fuzzy Systems*, vol. 2, no. 3, pp. 185–193, 1994.

[21] R. Geirhos, J. H. Jacobsen, C. Michaelis et al., "Shortcut learning in deep neural networks," *Nature Machine Intelligence*, vol. 2, no. 11, pp. 665–673, 2020.

[22] M. Liu, L. Chen, X. Du, L. Jin, and M. Shang, "Activated gradients for deep neural networks," *IEEE Transactions on Neural Networks and Learning Systems*, pp. 1–13, 2021.

[23] V. Sze, Y. H. Chen, T. J. Yang, and J. S. Emer, "Efficient processing of deep neural networks," *Synthesis Lectures on Computer Architecture*, vol. 15, no. 2, pp. 1–341, 2020.

[24] T. Ozturk, M. Talo, E. A. Yildirim, U. B. Baloglu, O. Yildirim, and U. Rajendra Acharya, "Automated detection of COVID-19 cases using deep neural networks with X-ray images," *Computers in Biology and Medicine*, vol. 121, article 103792, 2020.

[25] G. Katz, C. Barrett, D. L. Dill, K. Julian, and M. J. Kochenderfer, "Reluplex: a calculus for reasoning about deep neural networks," *Formal Methods in System Design*, pp. 1–30, 2021.

Hindawi
Wireless Communications and Mobile Computing
Volume 2022, Article ID 5450473, 10 pages
https://doi.org/10.1155/2022/5450473

Research Article

Deep Learning–Based Soft Sensors for Improving the Flexibility for Automation of Industry

Rami Ayadi,[1] **Rasha M. Abd El-Aziz**,[1,2] **Ahmed I. Taloba**,[1,3] **Hanan Aljuaid**,[4] **Nadir O. Hamed**,[5] **and Moaiad A. Khder**[6]

[1]*Department of Computer Science, College of Science and Arts in Qurayyat, Jouf University, Sakakah, Saudi Arabia*
[2]*Computer Science Department, Faculty of Computers and Information, Assiut University, Assiut, Egypt*
[3]*Information System Department, Faculty of Computers and Information, Assiut University, Assiut, Egypt*
[4]*Department of Computer Sciences, College of Computer and Information Sciences, Princess Nourah bint Abdulrahman University, P.O. Box 84428, Riyadh 11671, Saudi Arabia*
[5]*Computer Studies Department, Elgraif Sharg Technological College, Sudan Technological University, Khartoum, Sudan*
[6]*Department of Computer Science, Applied Science University, Bahrain*

Correspondence should be addressed to Nadir O. Hamed; nohamedit@gmail.com

Received 22 January 2022; Accepted 21 March 2022; Published 11 April 2022

Academic Editor: Mohamed Elhoseny

Automation in industries offers the benefits of enhancing quality and productivity while minimizing waste and errors, raising safety and adds stability to the production process. Industrial automation offers high profitability, reliability, and safety. It is beneficial to employ machine learning in the field of industrial automation as it helps in monitoring and performing maintenance on industrial machinery. Rational industrial development is closely associated with efforts for automating industrial techniques in all existing ways. Latest improvements in the automation of industrial systems resulted in decrease in cost of energy consumption and hardware. The proposed system is dealt with deep learning–based soft sensors for automation of industrial processes. The eminent benefits of soft sensors are versatility, flexibility, and low cost. With deep learning, many number of features could be processed. Thus, deep learning–based soft sensor encapsulates the above benefits. Soft sensors offer another way for the measurement of process variables, which are measured offline. Deep learning techniques are famous in the design of soft sensors for tough nonlinear systems due to the robustness and accuracy. The work depicted here designs a soft sensor based on deep learning algorithm for automation of industry. In the proposed system, a soft sensor contemplated on deep learning such as the deep neural network (DNN) is presented. The application of deep learning–based soft sensors in the automation of some industrial processes is also discussed here. The proposed system is tested on automatic control on solar power plants and in the measurement of reactive energy in industries. It was found that the proposed system yielded better results with its application in the automated industrial processes.

1. Introduction

Soft sensor indicates software, which reflects about the output-input connection of a process, contemplated on known parameters of a particular process. These input parameters are referred to as secondary parameters, which are got utilizing physically available sensors [1]. Adding soft sensors are advantageous in various process industries with an objective for operating and maintaining the industrial processes at a stable budget. Soft sensor endeavors are observed in industrial processes like distillation columns and treatment plants, and these advantages are confirmed post addition of these sensors. A soft sensor should offer the correct information regarding the process variable, which any hardware sensor located in the same position for measurement. There are some commonly known reasons for deterioration of soft sensors. They are a variation in the characteristics of the process, which occurs due to deactivation or adhesion in a chemical process, faulty design input or soft sensor updating. For the past decade,

there has been highly rigid trend of usage data-driven methods of artificial intelligence techniques for enhancing products or processes or machines across various domains of industries. This enhancement might fetch various forms from reducing consumption of raw material or energy across better usage machinery or higher automation levels for increasing the output quality [2]. In the current year, optimization of emissions because of stricter regulations of the environment is an eminent driver. But, collecting the essential data for such processes is faced with various challenges, where there exists a longevity of automation of industry. Even the lifetime of official service makes estimation for running depreciation from 6 to 30 years contemplated on industrial sector, machinery type, and country. .Significantly, there is ademand among industrial firms for increased production efficiency, leadingto effective control and measurement policies as a result of governmentlaws imposing severe limits on pollutant emissions and product requirements. On the perception of justifiable development of control of industrial process, the eminence of examining a huge set of processes and parameters with the aid of excess instruments for measurements is found as clear. However, the key challenge for executing a large-scale examining and policy of control is the large cost of online meters [2].

Mathematical techniques, which are contemplated on experimental data with the procedures for systematic identification, could assist greatly in minimizing the requirements for measuring instruments and for developing a strong management policy. The designed mathematical model for the previously mentioned tasks is referred to as soft sensors or virtual analyzers. Soft sensors are employed as a valuable tool in various industries such as industrial pollution monitoring, urban pollution monitoring, nuclear power plants, food processing, paper and pulp industries, power plants, cement kilns, chemical plants, and oil refineries. They are utilized for resolving a greater number of various challenges like backup system measurement, fault diagnosis strategies, sensor testing and installation, and examining with real-time forecasting [3–6].

Challenges are faced by the industries with the option of a suitable production policy that resulted in trade-offs among multiple constraints. Final quality and products of prices are two competing and relevant factors, which estimate the market success of an industry. Soft sensors provide a large number of advantages such as they act as an inexpensive option for hardware devices, which are expensive enabling for various comprehensive examining network; they have a parallel operation with the hardware sensors offering useful information for intervening tasks, thus enabling for more implementation of robust processes; they could be easily implemented on available and restorable hardware like microcontrollers, when there is a change in the settings of the system. They allow for the evaluation of the real-time data, by overcoming the delays in time by slow sensors, thus enhancing the control strategies' effectiveness [7–9].

Deep learning techniques could assist the industrial machines in overcoming their drawbacks by introducing self-learning of a human being with the consistency and speed of a computerized system. Deep learning-based techniques are suitable for industrial processes, which seems complex. Deep learning techniques complement the approaches based on rules, and it minimizes the requirement for deep vision domain of expertise for constructing an efficient inspection. Deep learning converts the logical expressions into a trained system. Hence, the benefits of deep learning techniques and soft sensors are combined in this paper. The proposed system thus encompasses deep learning–based soft sensors for automation of industrial processes. The deep neural network (DNN) is the deep learning technique employed here [10–13].

2. Related Works

Ma et al. proposed a two-stage framework for identifying the subway stations' functional stations. They are made of the smart card data (SCD) and point of interest (POI) data along with online to offline (OTO) data of the e-commerce platform, which is an endeavor that offers the customer with information regarding various businesses such as the comments, the score, and the location. In their paper, such data were combined for analyzing every subway station, taking into consideration, the data diversity, and gaining a feature map of passenger flow of various stations, the POIs and the OTO stores nearby. A two-stage framework was proposed in their paper. The outputs of these two stages were combined with a soft max function, which is utilized for the functional region's final identification. The experimental results of their study indicated a good performance and possessed a reference value within the substation's planning and contribution to the smart city construction. Thus, they employed a soft sensor based on deep learning for detection of functional region in the urban environments [1].

An ensemble deep learning framework for semisupervised-based soft sensor modeling of processes in industries was presented in [2]. Their paper was aimed at high nonlinear and labeled data of soft sensors. .The important features wereidentified with the SAE model for soft sensing. The prediction performance of their soft sensors was improved with an ensemble strategy. Their method eliminated the irrelevant weights and information for highlighting the relevant indications. Thus, the deep information is extracted by their approach. The reliability and performance of the soft sensors were enhanced by the ensemble strategy. The results of their study indicated an improved performance of prediction when compared with the traditional and state-of-the-art methods [2].

In [3], Yuan et al. proposed a novel variable-wise weighted stacked autoencoder (VW-SAE) for hierarchical feature representation related to output for representation of every layer. . With the output variables'correlation analysis, the eminent variables from other variables of the inputlayer in every auto-encoder are identified. Each variable was assigned with variable weights, respectively. Then, the deep networks were designed and ordered by the variable-wise weighted autoencoders. It was found that the proposed system provided a better prediction of performance when compared with SAE and the traditional neural networks.

The possibility of transferring the acquired knowledge in a soft sensor design for a particular purpose of a similar process is investigated [4]. In their study, they proposed two transfer learning methods with the evaluation of their suitability for designing soft sensors contemplated on nonlinear dynamic models. The results of their study indicated that the proposed two transfer learning methods provided suitability in the nonlinear dynamic model design for the industrial systems. Thus, their proposed model examined the dynamical model transferability problem in the development of soft sensors for the industrial endeavors. Their work failed to guarantee the possibility of employing transfer learning and provided an estimation of the expected performance [4].

Sun and Ge carried out a survey on the deep learning techniques based on the soft sensors that are data driven. The significance and necessity of deep learning based on the soft sensor endeavors were initially demonstrated by the analysis of the advantages of deep learning and the industrial processes' trends. Then, the deep learning models of the main stream, toolkits, frameworks, or tricks were summarized in their work, and suggestions were made for assisting the designers for propelling the upcoming progress of the soft sensors. Finally, the available works were analyzed and reviewed for discussing the problems and demands, which would be encountered in the practical endeavors. Finally, the conclusions and outlooks were given in their survey [5].

A soft sensor model, which is contemplated on enhanced Elman Neural Network having preprocessing of variable data and its endeavor, was proposed [6]. They proposed a newer soft sensor model, which is contemplated on variable data preprocessing method and Elman Neural Network to the model based on soft sensor. Feed forward network and local feedback mechanism were employed in the enhanced Elman Neural Network with the context layer for accurately reflecting the soft sensor model's dynamic characteristics that possess the superiority for approximating the delay systems and time varying characteristics adoption. The results of their proposed method indicated that it has excellent robustness and performance of generalization. The model has advanced anti-inference ability and prediction accuracy that are promising and effective.

Shao et al. carried out the soft sensor development for the multimode processes contemplated on semisupervised Gaussian mixture models [7]. For tackling the infrequency of technical or economic limitations, a semisupervised Gaussian mixture model was proposed, where both labeled and unlabeled samples were chosen, and regression coefficients and Gaussian parameters were simultaneously learned contemplated on the maximization-expectation algorithm. Their proposed system proved to be an effective one with the two case studies employed in their system. These case studies were implemented utilizing real-life dataset and simulated dataset gathered from the ammonia synthesis process involving a primary reformer.

The deep learning–based soft sensors for the industrial machinery were developed. They proposed a deep learning contemplated virtual sensor for the estimation of combustion parameters within a large gas engine utilizing the rotational speed as the developed input is then evaluated. The evaluation was contemplated on the data preprocessing influence when compared with the structure and type of network taking into consideration, the quality of estimation. The results of their analysis indicated that the data preprocessing method and the input possessed the most eminent impact on the accuracy of estimation. The output quality of the algorithm was lowered by a fast Fourier transformation, whereas best results were delivered by the rotational speed signal, which was measured. Their study recommends for future research on the data preprocessing effects [8].

In [9], Mahmoud et al. proposed an improved multilayer learning machine (MLLM) for the smart sensor endeavors contemplated on an extreme learning machine (ELM). Deep network based semisupervised autoencoders were utilized for extracting the unsupervised feature with respect to the samples of all process. The extreme learning machine (ELM) is employed during regression with the added quality variable. The simulation results of their proposal made a verification that the prediction accuracy and expectation of their approach showed an enhancement when compared with the existing methods. Also, the deep learning–based soft sensor model for the sour water striping plant was proposed [10]. To overcome the problem of various sampling intervals of quality and process variables, a deep learning–based soft sensor model was proposed. The data scarcity problem was also solved with the deep learning approach. For comparison, identification of traditional methods of MLP was made. The results of the report indicated that the proposed system enhances the neural network performance based on soft sensors.

3. Methodology

Contemplated on the prior research, there is a possibility that estimates the parameters of the signal generated by the deep neural networks (DNN) can be made. The related works all mentioned above vary significantly with their methods. The proposed system is designed for testing three eminent parameters such as neural network structure, neural network type, and the input data preprocessing. Because of the time constraints, the various approaches were examined in determining the first global parameters. Contemplated on the results generated, the promising results of the proposed system were generated for estimating the various parameters. Instead of seeking humans for programming tasks with the help of computer algorithms, the deep learning techniques are employed. Deep learning algorithms are an artificial intelligence subset for gaining prominence with the advancement in technology. With the leveraging of neural networks, the deep learning-based endeavors make spots and collaboration of patterns from huge datasets. With deep learning, a manufacturer identifies the defects in the manufactured products. The deep learning algorithms fetch the archetypes offered by the user and automatically create the clear understanding of the inspected part. Visual defects, scratches, or foreign objects could be identified. The higher the data, the higher will be the observation of faults or defects. While testing the proposed system with the solar

power plant, the measured variables are the geographic location, power, photovoltaic system, and solar power station [11–13].

3.1. Description of Dataset. Here, for the two endeavors mentioned for the testing of the proposed system, the transient simulation of the climate system model was employed for getting dataset of the proposed work. The dataset is created in the environment for MATLAB simulation. The error-free portion is taken as the reference, and the dataset is then created. The proposed system is simulated with ten various conditions with different induced errors for generating the sensors' dataset for our mission. The datasets of the soft sensors are identified as s1, s2, s3, s4…s8. The data of the primary sensors are combined for obtaining the total soft sensor for the climate system model of the solar power plant. The variables, which are mentioned in the dataset, are the geographic location, power, photovoltaic system, and solar power station.

3.2. DLSS Algorithm. The deep learning–based soft sensors (DLSS) are described in this part. Learning with the neural networks forms the imitation of the biological neuron in the system of science and is famous for inducing artificial intelligence in various machines. Figure 1 highlights the basic neuronal representation having no inputs, one output, and bias.

The initiation of theneural network, also called as perceptrons were changed to Widraw-Haff learningrule, which is a back propagation learning rule used for the purpose of shallowlearning and it is executed in diverse and different fields. Additionally, for enhancing the capacity of learning, the deep learning technique is introduced to resemble the human brain and has a high learning capacity. The deep neural network encompasses an output layer and input layer similar to an artificial neural network having two or more than two hidden layers as indicated in the above figure. In the deep neural network, the mathematical representation of a single neuron is given as

$$y^{\wedge} = \sigma\left(\mathrm{W}^{\mathrm{T}}\,\mathrm{X} + \mathrm{b}_{\mathrm{o}}\right), \tag{1}$$

where σ represents the activation function, w^{T} indicates the weight vector, and x indicates the input vector.

The DLSS algorithm, which is employed in the proposed system, is given as follows:

(1) Choose the DNN, which is used for estimating having 10 layers

(2) Configure the weights as w_1, w_2, $\mathrm{w}_3 \ldots \mathrm{w}_{\mathrm{n}}$

(3) Choose the outputs and the inputs

(4) Separate the input data and output data into training data, testing data, and evidence data in the ratio 75 : 10 : 15

(5) Employ the training dataset into the DNN (deep neural network)

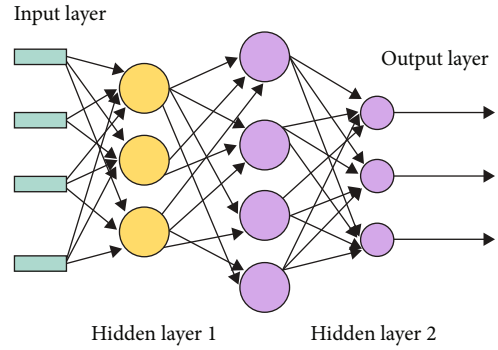

Figure 1: Basic neuron representation in DNN.

(6) Make a repetition of Steps 1 to 5 and an update of the weights until the output values are equal to the known values

(7) The evidence data should be applied

(8) Check for good results with the evidential data

(9) Choose the fault determining the deep neural network having ten layers

(10) The weights should be initialized as w_1, w_2, $\mathrm{w}_3 \ldots \mathrm{w}_{\mathrm{n}}$

(11) Choose the outputs and the inputs

(12) Separate the input and output data into training data, testing data, and evidence data in the ratio 75 : 10 : 15

(13) Employ the training data into the DNN (deep neural network).

(14) The weights must be updated, and Steps 1 until 5 should be repeated until the output becomes equal to the known values of fault classification

(15) The evidence data should be applied

(16) Check whether good results are given by the evidence data

(17) Start the estimated values of the correct data

(18) Assign the default value, which is constant with the faulty data

(19) Choose the testing data as given in Step 4

(20) Check for expected results of the test data

(21) Checks if a fault is detected by the test data in the 2nd DNN (Deep Neural Network)

(22) Examine the faulty data

(23) Make an estimation and replacement of the right data utilizing Step 18

(24) Or else make a repetition of the steps from Step 1 to Step 20

4. The Proposed System

The proposed deep learning contemplated soft sensor (DLSS) system comprises of two deep neural networks having a simultaneous operation. One deep neural network is allotted for the estimation of the soft sensor output, and the other deep neural network is employed for the identification and classification of the faulty data of the inputs of the soft sensor. In addition, an estimator of the correct data is presented for combining the deep neural network that identifies and detects the fault with the deep neural network estimator. This makes an assurance of the update of the soft sensor in accordance with the available correct data got from the other hardware sensors. Figure 2 shows the block diagram of the proposed deep learning–based soft sensor system, which could be employed in the industrial automation.

The method could be summarized as above. The proposed algorithm is indicated in Figure 2 for understanding it easier. From the figure, two deep neural networks are used for representing the two operations with the estimation of the desired value and detection of fault simultaneously. The third block in the figure indicates the estimation of the correct value. The third block functions only when any inequalities or errors or faults are detected by the deep neural network. The simulations of the proposed system were carried out utilizing four citations for obtaining comparative results:

(i) The correct information gathered from all the existing sensors were utilized as sensor inputs for the design of soft sensor

(ii) This correct information is assumed to be gotten from s_1, s_2, s_3, s_5, s_6, and s_7, and the information, which is missing is got from the sensor s_4, were utilized as sensor inputs for the design of soft sensor

(iii) The information from s_4 is gathered as the random information, and correct information is gotten from s_1, s_2, s_3, s_5, s_6, and s_7. These are utilized as inputs for the design of soft sensor

(iv) The information from s_4 is gathered as the estimated information, and correct information is gotten from s_1, s_2, s_3, s_5, s_6 and s_7. These are utilized as inputs for the design of soft sensor

The regression plot and the performance plot compare the outputs of the soft sensor with the above four situations. The regression values and mean square errors are found and are tabulated.

The mean square error (MSE) indicates the variation between the target value (ρ^{ca}) and output value (ρ^{exp}). The ideal value is calculated as zero, and thus the value, which is nearer to zero, represents a good estimated value. The mathematical representation of the mean square error is given as follows:

$$\mathrm{MSE} = \frac{1}{N}\sum_{i=1}^{N} (\rho^{exp} - \rho^{ca})\text{^}2. \tag{2}$$

The values of the mean square error during the testing, evidence, and training phase are indicated in the performance plots, and zero is approached by the three curves for a perfect model of a soft sensor. The regression value represents a correlation between the targets and the outputs. A greater correlation is indicated by an R value near to 1. The relationship between the targets and the outputs is more linear than expected. The mathematical representation of the regression values is given as follows:

$$R^2 = \frac{\sum_{i=1}^{N}\left[\left(\rho i\hat{e}xp - \rho'\right)^2 - (\rho i\hat{e}xp - \rho^{ca})^2\right]}{\sum_{i=1}^{N}\left(\rho i\hat{e}\mathrm{x}p - \rho'\right)}\text{^}2. \tag{3}$$

The network output is related to the regression plot to target values for testing evidence and training. The output of the soft sensor is equal to the target value, when a 45-degree inclination is made by the data plot within the regression plot.

4.1. The Training Based on Deep Learning. The training within a deep neural network–based soft sensor model happens by choosing the best aspects of neurons' weights in between the output layer and the hidden layer and the variable spreads for functioning in the output layer having neurons' bias, center hidden layer, and the hidden layer. Although the deep neural network could be effectively used as a soft sensor model, the entire set of neurons in the DNN hidden layer influence the network complexity, and the ability of generalization of the network, thus is making a decision on the number of neurons hidden layers. When many neurons are used in the hidden layer, under fitting situations might occur. These are resolved with the early shopping regularization and drop-out techniques. The learning algorithm of DNN-based soft sensor model is as shown below:

(i) Initiate with the parameter model values like b for biases and weights, w

(ii) Fetch a set of data samples, and propagate this data to the output layer with the input layer for obtaining the predicted values

(iii) Contemplated on the predicted values, the errors are calculated, and these errors have to be reduced

(iv) For discovering the optimal weights of the neurons, in the soft sensor model, based on deep neural network, the error must be back propagated

(v) The soft sensor model's parameter based on DNN has to be updated utilizing the above algorithm. The above steps are repeated until ideal weights are gained. Figure 3 shows the DNN-based soft sensor model's learning process

The training procedure is carried out on a laptop. The training time is between 20 seconds and one minute. The deep neural network fetches more time when compared with

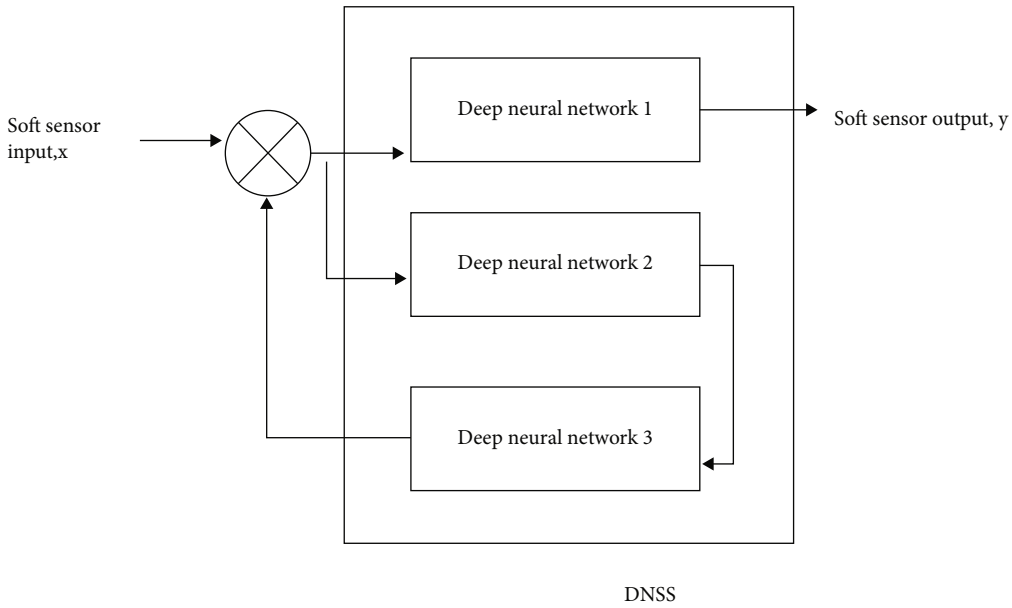

Figure 2: Deep learning contemplated soft sensor system (DLSS).

an ordinary neural network, and additional layers consume more time for computation.

5. Results and Discussion

5.1. Case Study 1

5.1.1. Application to Solar Power Plants. Deep learning–based soft sensors can be utilized in the automatic solar power plant control. In a real solar power plant, there must be a system for data collection and monitoring the performance that offers monitoring parameters, which are eminent to the system. There are various methods, which makes use of classic hardware for collecting and transmitting data. This is very expensive in a large solar power plant because of a huge amount of required sensors, and thus it is impractical for executing. In a solar power plant, the parameters, which could be controlled, are the panel output current, output voltage, output power, and also temperature when employed in a solar tracking system. Such systems have a tough relationship between every parameter, and thus the technique for gathering one or many variables from other measured variable is employed. This is the reason for why soft sensors or virtual sensors are employed for minimizing the need for equipment and also the need for cost. If there exist a suitable number of sensors and equipment within the solar power plant, the control accuracy is enhanced by the soft sensors or the virtual sensors. The real sensors' sampling rate will not be high all times, and thus the controllers' capabilities could not be matched. Thus, by the increase of the data, which is gathered in the controller, it could be enhanced. Every T second, a signal is received from the real sensors by the controllers. Every T/5 second, a signal is received from the soft sensors. Here in the controller, the speed of data processing is "N" times higher than the multirate, which is the sampling period of the actual sensor. Sometimes, real sensors could not gather the relevant information, which could be gathered by the soft sensors. The information on the soft sensors enables the controller for continuing the task of control within the normal level and the impacts of missing information are reduced. Figure 4 shows the deep learning contemplated soft sensor model of a solar power plant, which is a multi-rate technique.

In this model, the real sensor and the DNN-based soft sensor is operated in parallel. Data is received in real-time of the soft sensor, and a signal of control is received additionally from the controller until the actuator. The benefit is the delay, which impacts in the control signal transmission, and the real sensor sampling rate in the real process is considered within the virtual environment offering various reliable information from the DNN- (deep learning network-) based soft sensor. From the figure, the multi-rate controller makes use of the virtual information gathered from the soft sensor contemplated on the process technique for calculating extra control actions transmitted with the actuator. The process of triggering is rigid when compared with the real sensors' actual sampling rate, thus resolving the issue of minimizing the sensors' sampling rate. Here, we propose the execution of the deep learning–based soft sensor model for a solar power plant. One among the eminent aspects of the proposed system is the generated electricity's maximum power. The maximum power point tracking (MPPT) is needed for maximizing the system efficiency utilizing the solar panels. The solar irradiance is linear to the output power. The higher the solar energy, the higher is the system's output power. Thus, it is eminent for receiving timely information on the solar irradiance level for adjusting the solar panel's position. The maximum solar power plant power depends linearly on the performance ratio, which is given by

$$PR = Pi/\mathrm{Pnom} * \mathrm{G\,STC/Gi}. \quad (4)$$

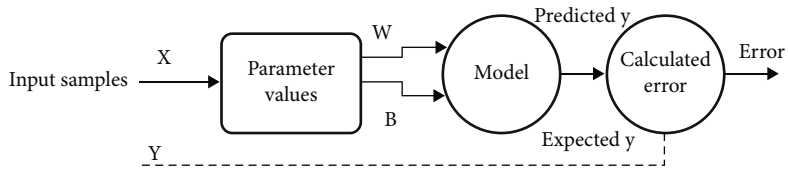

Figure 3: DNN-based soft sensor model's learning process.

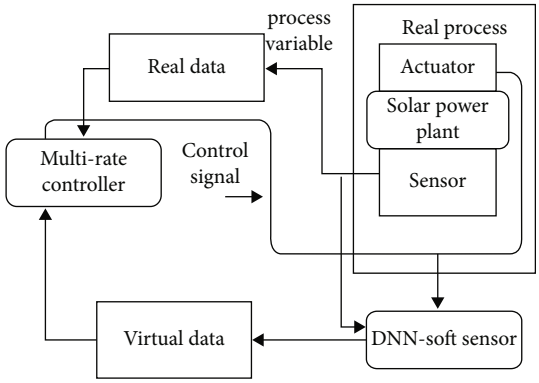

Figure 4: Deep neural network– (DNN–) based soft sensor model of a solar power plant.

Table 1: Forecast errors associated with the prediction of the output power in a solar power plant.

Input data	Data types	MSE (*10^-1)	R (*10^-1)
Correct data	Training data	7.49	9.865
	Evidence data	7.40	9.867
	Testing data	7.36	9.867
Nil	Training data	7.20	9.865
	Evidence data	7.51	9.869
	Testing data	7.30	9.869
Random data	Training data	8.25	9.852
	Evidence data	7.95	9.856
	Testing data	8.15	9.853
Estimated data	Training data	7.48	9.865
	Evidence data	7.30	9.868
	Testing data	7.33	9.868

Table 2: Changes in the R and MSE values of the corrected and faulty inputs in association with the correct input.

Input data	Data types	ΔMSE ($MSE_c - MSE_u$)	ΔR ($R_{c-} R_u$)
Nil	Training data	-0.07	0.002
	Evidence data	0.11	-0.002
	Testing data	-0.28	0.004
Random data	Training data	0.78	-0.013
	Evidence data	0.53	-0.011
	Testing data	0.76	-0.014
Estimated data	Training data	-0.34	0.001
	Evidence data	-0.10	0.002
	Testing data	-0.00	-0.000

Here, P_i shows the instantaneous measured power and P_{nom} measures the solar panel's nominal power.

G_i indicates the solar irradiance actual value, and G_{STC} indicates solar irradiance during normal conditions. The value of performance ratio ranges from 0.6 to 0.8. Thus, the soft sensor would determine the solar radiation, which is needed for increasing the electricity and enhance the solar power plant's efficiency.

In solar power plants, the deep neural network– (DNN–) contemplated soft sensors are utilized for predicting the output power. The performance plots are used here for representing the testing, evidence, and training MSE values with red, green, and blue color used in the plots, respectively, during running of the soft sensor system. When a soft sensor system is chosen, a well-trained soft sensor system should be determined with a test or independent dataset again. The required standard is offered by the test data, which is utilized for evaluating the soft sensor system. The performance evaluation is done with the prediction of the mean square error and regression value. Table 1 shows the forecast errors or MSE (mean square error) associated with the prediction of the output power in a solar power plant.

From the above table, it could be seen that the average regression value lies in the range of 9.86 for all data such as correct data, nil, random data, and estimated data. These data encapsulate all training, evidence, and testing data, which are used for a particular industrial process. Linearity could be observed between the soft sensors' targets and the outputs. The R value and the points of data, which approaches 45°, makes sure the proposed soft sensors' validity. The regression and the mean square observations are compared to the above table, and the changes are observed with the update of the soft sensor with the estimated data on the proposed system, which is indicated in Table 2.

Figure 5 indicates the mean square error (MSE) that got out of the above obtained information.

The following figure indicates the regression values got out of the above obtained information.

Figures 6 and 7 indicate the representation of ΔMSE and ΔR with the above values. The high efficiency is gathered from the training data. The correct values of R and MSE are highlighted by MSE_c and R_c, and the updated values of R and MSE are highlighted by R_u and MSE_u. When the MSE value increases, then it means that the entire system is deteriorating. The proposed system was found to offer only small error values and hence shows stability in the performance of the proposed system.

Regarding the R value, the proposed system either retains a constant value or increases slightly.

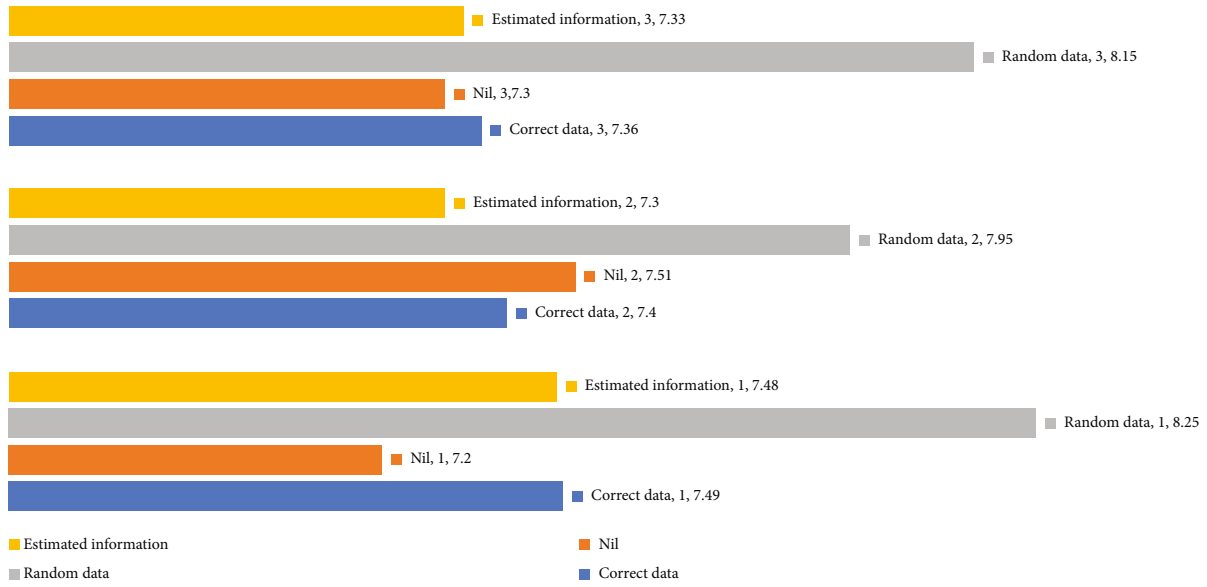

Figure 5: MSE values of the obtained data.

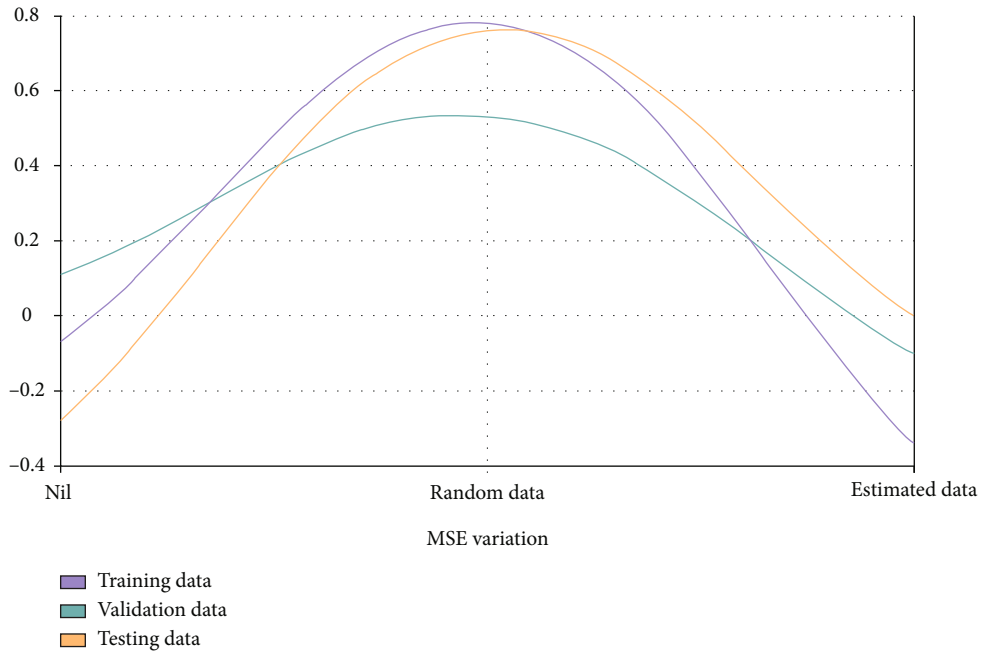

Figure 6: ΔMSE representation.

5.2. **Case:** *Study 2.* Sustainable industrial development is related to increasing needs for the supplied electrical energy quality. Also, the eminent factor is the capability for accurately measuring the flow of power in any network level. This is eminent for both consumers and energy suppliers. With the production increase and quality enhancement of the industries' finished products, there is also a growth in their energy consumption. Alternatively, the need for the power line's capacity of the products is rising. There is a striking surge in the nonstationary and nonlinear loads in the power network, which results in reduced network throughputs because of the flow of reactive capacities observed between them. Here, the problem is related to the high usage of power electronic devices among the electric energy consumers. Variable speed drives, gas discharge lamps, heaters, and induction furnaces are suitable archetypes for these devices. The reactive power growth in these networks builds a high interference amount for the industry and impacts adversely the total distribution network. Along with the industrial power growth in these industries, there are also high losses observed during the transfer of electrical energy transported from one place to another and a

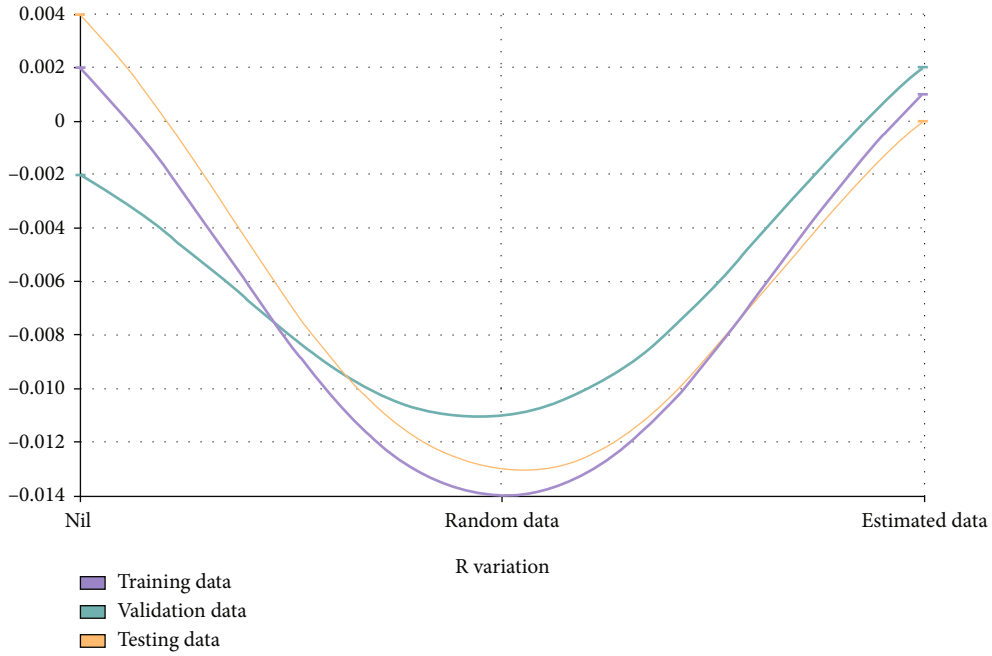

Figure 7: ΔR representation.

Table 3: Statistical data of reactive power consumption in mining and processing plant.

Time, h	Object 1 kvar*h	Object 2 kvar*h	Object 3 kvar*h	Object 4 kvar*h
02 : 00	14347	45	103	973
04 : 00	13217	46	54	913
06 : 00	14648	47	103	913
08 : 00	14470	49	107	793
10 : 00	13770	50	102	81
12 : 00	11533	47	97	805
14 : 00	12791	44	128	1021
16 : 00	13078	47	97	1225
18 : 00	12553	44	97	805
20 : 00	12345	6	118	997
22 : 00	13761	6	95	889
24 : 00	12400	7	96	733

reduction in the consumers' power factor. The measuring and reactive power measurement and control are related to a group of challenges encapsulating the high cost of the system in industries of processing and mining. It is due to the supply of various structural units of power lines and distributed structure. The volumes of reactive power could be calculated from measuring the parameters of the distribution network. In an electrical energy distribution system, which operates linearly in the sinusoidal signal mode, the reactive power is calculated by the following ratio:

$$Q = I \times U \times sin\varphi, \tag{5}$$

where I is the strength of the current in the network; U indicates the value of voltage in the network; and ϕ refers to the variation in phase between the voltage and current. While taking into consideration, the system's operating mode under the nonharmonic signal's influence, the effective current, and voltage values in the electrical network is given as

$$\begin{aligned} U &= \sum_{k=1}^{K} Uksin(2\pi kfot - \theta k), \\ I &= \sum_{k=1}^{K} Iksinsin\,(2\pi kfot - \psi k), \end{aligned} \tag{6}$$

Here, k indicates the harmonic number, f_o indicates the frequency, I_k is the current value of k^{th} harmonic, and θk and ψk are initial signal phases. Here, a large number of quantities have to be measured, which is a complex problem, which is resolved with the use of deep learning–based soft sensors for measuring the reactive power. Let us assume that in a distribution substation, in a processing and mining plant, the reactive power consumption by every structural aspect of the object in the plant impacts the other aspects' consumption. The element having the high reactive power consumption has the highest influence. We consider here the statistical data on the reactive energy consumption in the mining and processing plant. Here, four structural elements are measured by the object. Here, the correlation coefficient is calculated with the existing statistical data for 7 consecutive days.

The results which gotten with the measured correlation coefficients of consumption of reactive power of elements

having the high reactive energy consumption of the objects 2 and 4 for 7 consecutive days are shown in Table 3.

Here, a soft sensor is constructed for estimating the reactive power consumption value for every structural object, which is supplied along with the distribution substation electrical energy contemplated on the reactive power consumption quantity of one of the structural elements.

6. Conclusion

Thus, the research on the deep learning–based soft sensor model employed in the automation of industrial techniques indicates the benefits and versatility of theirs. The use of soft sensors usually acts as a replacement for the hardware due to the operation of the physical sensors in the extreme situations, which are expensive and require frequent change. Soft sensors are advisable to be utilized in conditions or mechanism that has similar conditions. The performance of a mechanism is measured for judging the situation. A different base is exhibited by the soft sensors and is environment friendly. Soft sensors contemplated on deep learning helps in making the automation of industrial processes very easier. The selection of the mathematical model of the soft sensor is contemplated on the specific task and situation. Thus, with the usage of soft sensors, the mechanical equipment amount could be reduced, and the parameters could be measured with the deep learning techniques for industrial automation.

Data Availability

The data that support the findings of this study are available on request from the corresponding author.

Conflicts of Interest

The authors declare that there are no conflicts of interest regarding the publication of this article.

Acknowledgments

This work was supported by the Princess Nourah bint Abdulrahman University Researchers Supporting Project number (PNURSP2022R54), Princess Nourah bint Abdulrahman University, Riyadh, Saudi Arabia.

References

[1] Y. Ma, S. Liu, G. Xue, and D. Gong, "Soft sensor with deep learning for functional region detection in urban environments," *Sensors*, vol. 20, no. 12, p. 3348, 2020.

[2] J. M. M. de Lima and F. M. U. de Araujo, "Ensemble deep relevant learning framework for semi-supervised soft sensor modeling of industrial processes," *Neurocomputing*, vol. 462, pp. 154–168, 2021.

[3] X. Yuan, B. Huang, Y. Wang, C. Yang, and W. Gui, "Deep learning-based feature representation and its application for soft sensor modeling with variable-wise weighted SAE," *IEEE Transactions on Industrial Informatics*, vol. 14, no. 7, pp. 3235–3243, 2018.

[4] F. Curreri, L. Patanè, and M. G. Xibilia, "RNN- and LSTM-based soft sensors transferability for an industrial process," *Sensors*, vol. 21, no. 3, p. 823, 2021.

[5] Q. Sun and Z. Ge, "*A survey on deep learning for data-driven soft sensors*," *IEEE Transactions on Industrial Informatics*, vol. 17, no. 9, pp. 5853–5866, 2021.

[6] H. Zhu and Y. Zhang, "Soft sensor model based on improved Elman neural network with variable data preprocessing and its application," *Journal of Sensors*, vol. 2018, 10 pages, 2018.

[7] W. Shao, Z. Song, and L. Yao, "Soft sensor development for multimode processes based on semisupervised Gaussian mixture models," *IFAC-PapersOnLine*, vol. 51, no. 18, pp. 614–619, 2018.

[8] B. Maschler, S. Ganssloser, A. Hablizel, and M. Weyrich, "Deep learning based soft sensors for industrial machinery," *Procedia CIRP*, vol. 99, pp. 662–667, 2021.

[9] M. S. Mahmoud, A. Al-Nasser, M. M. Hamdan, and S. Arabia, "Multi-layer learning machines and smart sensor applications," *Advances in Artificial Intelligence and Machine Learning*, vol. 1, no. 1, p. 3, 2021.

[10] D. M. Preethichandra, "Design of a smart indoor air quality monitoring wireless sensor network for assisted living," in *2013 IEEE International Instrumentation and Measurement Technology Conference (I2MTC)*, pp. 1306–1310, Minneapolis, MN, USA, 2013.

[11] M. E. Karar, M. F. Al-Rasheed, A. F. Al-Rasheed, and O. Reyad, "IoT and neural network-based water pumping control system for smart irrigation," *Information Sciences Letters*, vol. 9, no. 2, pp. 107–112, 2020.

[12] S. M. E. I. Ammer, "Content analysis of lighting and color in the embodiment of fear concept in horror movies: a semiotic approach," *Information Sciences Letters*, vol. 9, no. 2, pp. 135–142, 2020.

[13] M. E. Karar, F. Alotaibi, A. Al Rasheed, and O. Reyad, "A pilot study of smart agricultural irrigation using unmanned aerial vehicles and IoT-based cloud system," *Information Sciences Letters*, vol. 10, no. 1, pp. 131–140, 2021.

Hindawi
Wireless Communications and Mobile Computing
Volume 2022, Article ID 6254009, 11 pages
https://doi.org/10.1155/2022/6254009

Research Article

Internet of Things Network Topology Discovery Algorithm Based on Wireless Sensors

Hao Sun

College of Engineering and Technology, Xi'an FanYi University, Xi'an, 710105 Shaanxi, China

Correspondence should be addressed to Hao Sun; sharp_syc@126.com

Received 13 January 2022; Revised 23 February 2022; Accepted 8 March 2022; Published 8 April 2022

Academic Editor: Mohamed Elhoseny

Remote sensor network is a multijump self-coordinating organization framework shaped by countless energy-restricted miniature sensor hubs sent in the observing region. Be that as it may, the correspondence conventions of customary organization configuration cannot be straightforwardly applied to remote sensor organizations. The improvement of committed correspondence conventions and estimation techniques has turned into a pressing exploration subject in the field of remote sensor organizations. The research purpose of this paper is to research the Internet of Things network topology discovery algorithm based on wireless sensors. This paper analyzes and mines an adaptive neighbor discovery scheduling algorithm with lower latency, acquires the information of potential neighbor nodes based on existing neighbor nodes, discovers potential neighbor nodes by proactively waking up, and studies the information recommendation mechanism between neighbor nodes and compares. The intimacy between neighbor nodes (such as common neighbor rate) is used to selectively receive recommended information from neighbor nodes, thereby filtering redundant data information, lessening hub energy utilization, and accomplishing the motivation behind broadening the organization life cycle. A geography disclosure calculation in light of versatile specialists is proposed to tackle the geography revelation issue under the various leveled geography structure in remote sensor organizations. The calculation joins the qualities of portable specialist innovation and various leveled Internet of Things network geography and simultaneously further develops the relocation methodology of versatile specialists for information assortment, intermittent undertaking assignment, and organization status observing. Research shows that in the investigation of the effect of hub obligation cycle on framework execution, the energy utilization of the DDC-Group calculation is marginally expanded contrasted and the gathering calculation, and the increase is not more than 1%, but compared to the CNR-Group increase more.

1. Introduction

Remote sensor network incorporates current sensor innovation, microelectronic innovation, correspondence innovation, installed figuring innovation, and appropriated data handling innovation and different disciplines. It is an arising crossresearch field and is applied to military surveillance, natural observing, clinical wellbeing and space investigation, and so forth, overrun all degrees of life, particularly in the fields of public protection and serious debacle occasion checking, which will assume a vital part in the modernization of our country. Topological sort is to sort the nodes on a DAG (Directed Acyclic Graph). Simply put, it is to pull the DAG into a chain without destroying the order of nodes. If you take the technology tree in the game as an example, topological sorting is to find a possible order of the technology tree.

Numerous colleges and research establishments abroad have led a ton of exploration on the examination on the geography revelation calculation of the Internet of Things network in view of remote sensors. For example, Shahzad et al. proposed a topology discovery algorithm based on a mesh network. The method is divided into two steps: one is the diffusion phase, which coordinates the nodes to broadcast the topology request message. After each node receives and rebroadcasts this message, it constructs local neighbor information. Update the corresponding data structure; the second is the collection phase, and all nodes forward the

local neighbor information to the coordinating node [1]. Nesa and Banerjee proposed a distributed topology discovery strategy based on mobile agents. This method cannot provide instantaneous Internet of Things network topology. It takes a long time to find a complete Internet of Things network topology and needs to distribute a lot of messages; so, it is not efficient and consumes bandwidth [2]. Dhanvijay and Patil proposed the ad hoc network management protocol ANMP, which uses a distributed set of nodes to maintain the information of the node and its neighbors, attempts to integrate the characteristics of the SNMP protocol, and uses a layered mechanism to collect topology information. The cluster head node is dynamically selected due to geographic location or connection conditions, and topology information is collected through the MIB in the cluster head [3].

In our country, Wei and Zhou utilizes the hub development model in the sensor organization to foresee the potential neighbor hubs inside the correspondence scope of the hub and progressively changes the obligation pattern of the hub as per the quantity of potential neighbor hubs, so as to find neighbor nodes faster and more. Aiming at the problem of network coverage optimization of the sensor node model with fixed sensing angle and sensing radius used in the past, he proposed a new node model with variable sensing angle and sensing radius [4]. Fu et al. proposed an adaptive RSSI discovery scheme, which improves the accuracy of discovery in the ZigBee network by studying the communication channel state between two nodes, and uses a Markov model to correct the RSSI scale caused by factors such as noise error [5]. Khoufi et al. proposed a distributed discovery algorithm based on MDS-MAP. This algorithm distributes computing tasks to different nodes for distributed computing by defining node classes, reducing the amount of computing tasks and reducing the energy consumption of nodes [6].

The purpose of this paper is to comprehensively, accurately, and quickly perform network topology discovery for IoT network management, fault location, and congestion control. This paper is based on the neighbor discovery algorithm of dynamic duty cycle. Based on the full analysis of Disco, U-Connect, and other algorithms, a neighbor revelation calculation in light of dynamic obligation cycle DDC-Group is proposed for the proper obligation cycle issue of existing neighbor disclosure calculations, and the genuine hub development model is utilized to anticipate potential neighbor hubs, powerfully change the obligation pattern of hubs through the quantity of potential neighbor hubs, and suitably expand the enlivening season of hubs to screen and find neighbor hubs quicker and all the more rapidly, so as to improve the efficiency of neighbor node discovery and reduce discovery delay. Finally, it is compared with Disco, Group, and CNR-Group algorithms through simulation experiments. The neighbor discovery algorithm drives the node to actively discover neighbor nodes when it wakes up, avoiding the long waiting delay of the traditional passive neighbor discovery algorithm, thereby realizing the rapid discovery of neighbor nodes and reducing the delay of neighbor discovery.

2. Internet of Things Network Topology Discovery Algorithm Based on Wireless Sensors

2.1. Overview of the Cluster Routing Algorithm for Wireless Sensor Networks and Mobile Agent Technology

2.1.1. LEACH Cluster Routing Algorithm. Drain mostly haphazardly chooses the group head hub through a roundabout technique to adjust the energy utilization of the whole organization. It characterizes the idea of "round." Each round comprises of three phases: group head determination, bunch development, and stable information transmission [7, 8]. The LEACH (Low Energy Adaptive Clustering Hierarchy) calculation is a versatile bunching geography calculation. Its execution interaction is occasional, and each cycle is isolated into a bunch foundation stage and a steady information correspondence stage.

The group head determination stage is answerable for choosing all bunch head hubs in this round. The primary determination guideline is as follows: every sensor hub produces an irregular number somewhere in the range of 0 and 1. Assuming the irregular number is not exactly the characterized limit $T(n)$, it is chosen as the bunch head and distributes the transmission message that it turns into the group head; if not, it is a part hub.

$$T(n)\begin{cases}\dfrac{p}{\{1-p\times(r \bmod (1/p))} & n\in G\\ 0 & \text{Other}\end{cases}. \tag{1}$$

Among them, p is the level of the quantity of bunch heads in all hubs in the organization, r is the quantity of current determination rounds, and G is the arrangement of hubs that are not group heads in the latest $1/p$ round [9, 10].

2.1.2. GAF Cluster Routing Algorithm. Geological Adaptive Fidelity (GAF) is an energy-effective directing calculation in specially appointed organizations. GAF is a method for saving energy by keeping hubs as off as could really be expected. The node obtains its own "location" in the network through GPS positioning and is thus classified into the corresponding cell. If the "location" of two nodes is the same, they are considered to be equivalent in routing; each cell select a cluster head regularly, only the cluster head remains active, and other nodes go to sleep. The GAF algorithm is mainly divided into two stages:

(1) Divide Cells. Divide the network into several adjacent virtual cells. The maximum distance R between any two points in every two adjacent cells (R is the wireless signal communication radius) and the cell side length r satisfy the following formula condition:

$$r^2+\left(2r^2\right)\le R^2 \longrightarrow r\le \frac{R}{\sqrt{5}}. \tag{2}$$

Condition (2) guarantees that the distance between all hubs between two neighboring cells is not exactly their

remote correspondence distance. Whenever the group head hub replaces any remaining hubs in a similar cell to impart, it can in any case guarantee the availability of the organization [11, 12].

2.1.3. Cluster Head Choice. Every hub has three states: rest, revelation, and dynamic state. At the point when the organization is introduced, all hubs are set to the disclosure state. According to its relative position information and wireless communication radius, each node adopts formula (2) to determine the size and cell number of the cell where it is located.

2.2. Wireless Sensor Network Routing Algorithm Based on Effective Clustering NDEA

2.2.1. Network Model and Related Definitions. To work with research, we make the accompanying suspicions:

(1) A remote sensor network contains a sink hub and a few sensor hubs. These hubs are haphazardly appropriated in a specific region. It is expected that the sensor hubs and sink hubs are static, and the sensor hubs have consistently sent information to the sink hubs

(2) The channel between sensor hubs is a symmetric double channel, or at least, hub A can speak with hub B, and hub B can likewise speak with hub A. Because of the distinction in the sending power and getting responsiveness of the sensor hubs, the presence of a unidirectional connection is not thought of, and the correspondence between the hubs is single-bounce

(3) Definition of energy model

(4) The issue of energy misfortune is the way in to the plan of the bunch directing calculation in remote sensor organizations. The NDEA calculation utilizes a similar energy model as the LEACH calculation. The energy utilization of a sensor hub can be communicated as

$$\begin{aligned} E_i &= E_{Tx} + E_{Rx}, \\ E_{Tx} &= E_{\text{elec}} \times l + \varepsilon_{\text{amp}} \times l \times d^{\lambda}, \\ E_{Rx} &= E_{\text{elec}} \times l, \end{aligned} \tag{3}$$

where E_i is the absolute energy consumed by the sensor hub, E_{Tx} and E_{Rx} are the energy consumed by sending and getting 1-digit information, E_{elec} is the energy consumed by the working of the communicating circuit, $\varepsilon_{\text{amp}}(J/\text{bits}/m^2)$ is the power amplifier energy consumed, l is the length of transmitted information bits, λ is the path loss, and d is the correspondence distance between the beneficiary and the transmitter. As indicated by the distance between the shipper and the beneficiary, the power enhancement misfortune takes on the free space model and the multipath blurring model to decide the worth of λ. While the sending distance is short, the free space model is applied, and λ is 2, while the sending distance is longer. When the multipath blurring model is utilized, λ is 4, and the energy model is displayed in Figure 1 [13, 14].

2.2.2. The Basic Idea of NDEA. In the NDEA calculation, a weight work $W(n)$ is characterized for every hub. The meaning of weight includes two factors, the neighbor hub degree and the excess energy of the hub. The weight work is communicated as

$$W(n) = w_1 f(d_n) + w_2 g(e_n) \tag{4}$$

w_1 and w_2 are weighting parameters, the weighting parameters can be adjusted according to different applications, $f(d_n)$ is a function of node n's neighbor node degree, and $g(e_n)$ is an element of hub n in view of leftover energy, the hub with the littlest weight. It is considered as a competitor hub that can turn into the group head [5, 15].

2.3. Disco Algorithm

2.3.1. Principle of the Disco Algorithm. The process of neighbor discovery is as follows: a node in the network is within the communication range of another node, and at a certain moment, the two nodes are in the awake state at the same time. If one node is broadcasting information by radio, the other node can be awake. After receiving the broadcast information, the two nodes exchange data information, complete neighbor discovery, and become each other's neighbor nodes. The calculation begins from the hub with the biggest degree in the organization, joins neighbor hub search and neighbor hub casting a ballot, grows the hunt from the nearby piece of the organization to the entire, and lastly shapes numerous disjoint networks. The running season of the calculation is near $O(m+n)$.

2.3.2. Network Model Design

(1) Related Definitions. Accepting that there are n sensor hubs in a remote sensor organization, the neighbor disclosure issue includes the development of $\Psi(m,t)$ (where $1 \le m \le n$). The development of $\Psi(m,t)$ should guarantee that any A couple of hubs I and j (where $i \ne j$); at whatever point, they are inside the correspondence scope of one another, and the time they meet surpasses L unit time; they can see as one another. Among them, L represents the delay requirement of neighbor discovery [16, 17]. The neighbor discovery problem is expressed as the following relationship using discovery scheduling $\Psi(m,t)$:

$$\Psi(i,t) = \Psi(j,t) = 1\ (\forall i,j | 1 \le i,j \le n \exists 0 \le t \le L). \tag{5}$$

The simultaneous symmetric neighbor disclosure issue with a postpone prerequisite of L is characterized as a similar revelation timetable and introduction time allocated to n

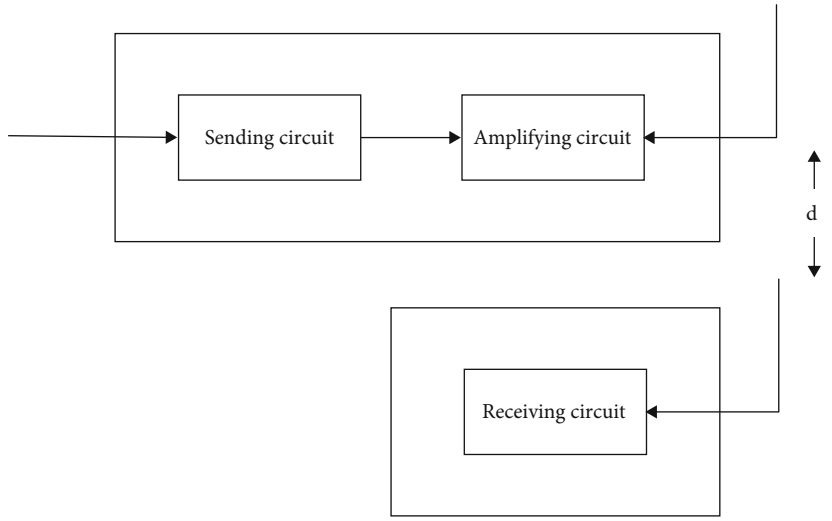

Figure 1: Energy model.

Table 1: Changes in network energy consumption over time in the two algorithms.

Time (s)	0	15	30	45	60	75	90	105	120
LEACH	0	4.65	7.45	15.36	23.16	31.65	35.21	36.72	37.24
NDEA	0	4.71	8.32	13.26	15.72	20.45	26.78	27.85	28.63
Disco	0	4.64	6.45	14.35	17.42	22.15	32.65	32.14	34.24

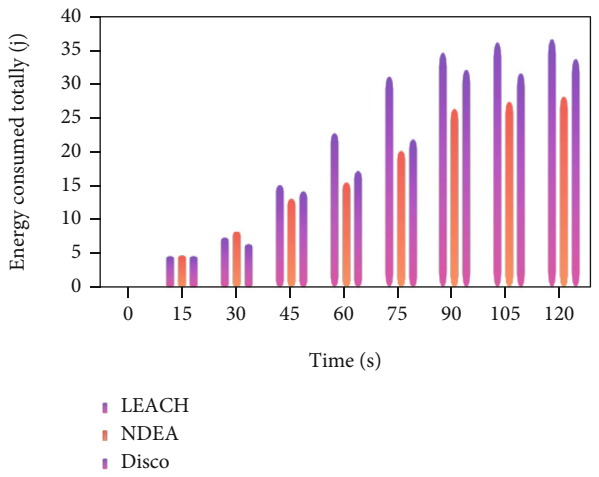

Figure 2: Changes in network energy consumption over time in the two algorithms.

Table 2: Changes in the number of surviving nodes in the three algorithms over time.

Time (s)	0	15	30	45	60	75	90	105	120
LEACH	18	17.86	17.94	17.02	9.24	8.13	6.74	4.24	2.56
NDEA	18	17.59	17.47	16.28	15.36	13.26	11.65	10.64	8.35
Disco	18	17.72	17.62	16.53	12.31	10.43	8.24	7.46	5.32

sensor hubs in the organization, and the accompanying relationship is fulfilled:

$$\Psi(i,t) = \Psi(j,t)\ (\forall t \forall 1 \le i, j \le n). \tag{6}$$

Moreover, the maximum discovery delay in the neighbor discovery process cannot exceed L. The offbeat symmetric neighbor disclosure issue with a defer necessity of L is characterized as a similar revelation timetable and relative stage offset given to n sensor hubs in the organization, and the accompanying relationship is fulfilled:

$$\Psi(i,t) = \Psi\left(j, \phi_{i,j}\right)\ (\forall t \forall 1 \le i, j \le n). \tag{7}$$

Moreover, the maximum discovery delay during the neighbor discovery process cannot exceed L. In formula (7), $\phi_{i,j}$ represents the relative displacement offset of node i and node j at the original time t [18, 19].

(2) Metrics. In order to better evaluate the quality of a neighbor discovery algorithm and whether it has certain practical significance, we will use the energy consumption-delay product M as the evaluation criterion of the neighbor discovery algorithm [20, 21]. To get done with different responsibilities, sensor hubs need to finish the assortment and change of checking information, information the board and handling, reaction to the errand solicitation of the sink hub, and hub control and different assignments. Moving hubs can prompt incoherent work content. For the neighbor discovery scheduling $\Psi(m,t)$ with a period of T, the following relationship is satisfied:

$$\Psi(m,t) = \Psi(m,t+T)(\forall). \tag{8}$$

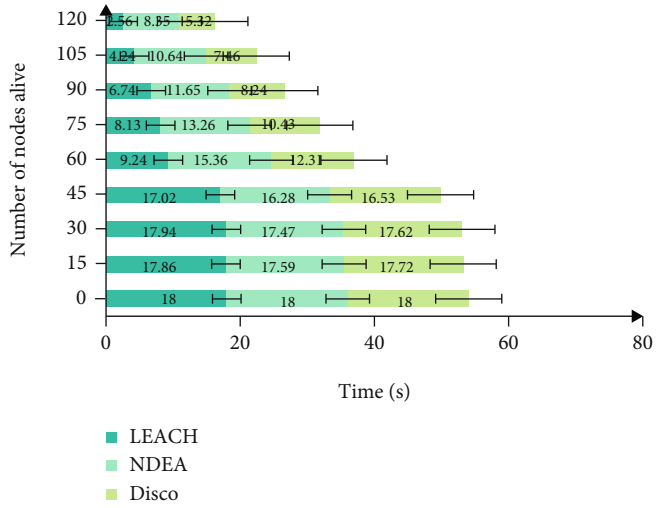

Figure 3: The number of surviving nodes in the three algorithms changes over time.

Table 3: The amount of data received by the sink in the three algorithms.

Time (s)	0	15	30	45	60	75	90	105	120
LEACH	0	36	163	793	1189	1432	2271	3173	3428
NDEA	0	75	139	759	1037	1353	1923	2781	2971
Disco	0	51	148	779	1108	1398	2087	2974	3193

Then, the average energy consumption P in a scheduling period is expressed as

$$P = \frac{1}{T}\int_0^T \Psi(m,t)dt. \tag{9}$$

In this neighbor disclosure booking $\Psi(m,t)$ with a time of T, expecting that the most obviously awful revelation delay among all sets of (hubs give all conceivable relative stage balances) is L, then we will energy-delay. The product M is defined as

$$M = PL = \frac{L}{T}\int_0^T \Psi(m,t)dt. \tag{10}$$

Due to the slot nature of the actual neighbor discovery algorithm, the discovery scheduling is discrete; so, here, we use M to represent the discovery scheduling in the discrete state and the node m with a period of T that meets the delay requirement, L is in the time slot t, the discovery schedule can be expressed as $\xi(m,t)$, and the average energy consumption P in a period is

$$P\frac{1}{T}\sum_{t=0}^{T-1}\xi(m,t)dt. \tag{11}$$

Then, the energy consumption-delay product M is

$$M = PL = \frac{L}{T}\sum_{t=0}^{T-1}\xi(m,t)dt. \tag{12}$$

2.4. Neighbor Discovery Algorithm Based on Dynamic Duty Cycle. On account of a decent obligation cycle, the wake-up time and rest season of the hub are fixed. At the point when the obligation pattern of a hub is in an evolving state, the wake-up time and rest time will change appropriately. The neighbor revelation calculation in light of dynamic obligation cycle is an exhaustive neighbor hub disclosure calculation, which depends on the low-dormancy neighbor disclosure calculation. During the revelation interaction of neighbor hubs, the obligation pattern of the sensor hub is not generally fixed. The hubs in the remote sensor network are occasionally in the wake-up state, and the hubs in this functioning mode can exist together with the hubs in other working modes and help the hubs in other working modes to work.

Whenever a sensor node moves from old position to new position, the duty cycle needs to be adjusted in real time to monitor and discover potential neighbor nodes. Assuming that the communication radius of the sensor node is R, the node's moving speed is v, and the node S reaches S' after time t, the distance the node moves:

$$\text{Distance}_{S\longrightarrow S'} = v * t. \tag{13}$$

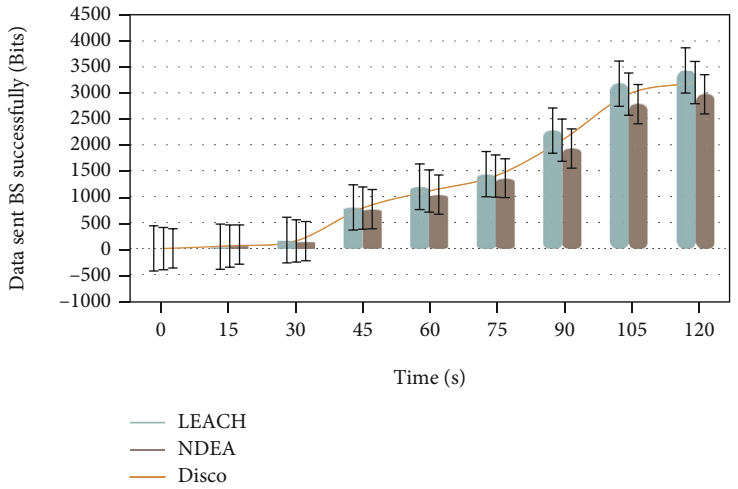

Figure 4: How much information got by the sink in the three calculations.

Table 4: The connection between energy utilization and hub thickness.

Node density	1	3	5	7	9	11	13	15
Disco	17325	37593	98663	127638	184729	348385	416311	458682
Group	15733	36273	75432	132741	196446	372616	438227	483734
CNR-Group	16321	38224	82718	129858	191831	362827	396284	468356
DDC-Group	15914	34213	98375	157324	228368	401722	462826	726357

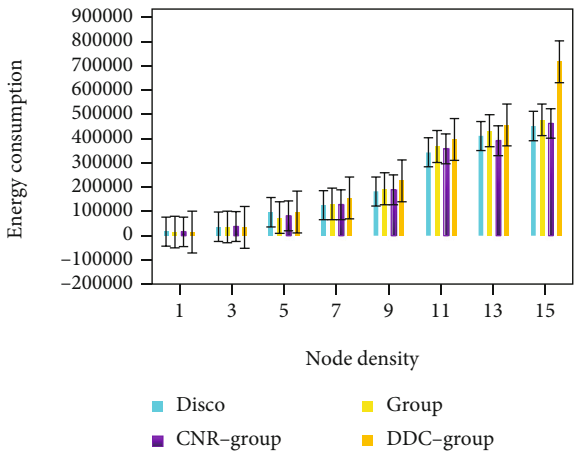

Figure 5: The connection between energy utilization and hub thickness.

Table 5: Discover the relationship between latency and node duty cycle.

Node duty cycle	1%	2%	3%	4%	5%
Disco	38726	34762	33627	29738	32362
Group	33928	31725	31437	28363	27877
CNR-Group	33792	31582	31292	26173	25827
DDC-Group	32673	31382	30183	26381	25383

The area where the communication circles intersect is ΔS , and the area of the newly added area is $\Delta S'$:

$$\Delta S = 2\left(\frac{2\theta}{2} * R^2 - S_{\mathrm{SAB}}\right) = 2\left(\theta * R^2 - S_{\mathrm{SAB}}\right),$$

$$S_{\mathrm{SAB}} = \frac{1}{2} * 2R\sin\theta * \frac{1}{2}\mathrm{Distance}_{S\longrightarrow S'} = \frac{1}{2}R\sin\theta * \mathrm{Distance}_{S\longrightarrow S'},$$

$$\cos\theta = \frac{1/2\mathrm{Distance}_{S\longrightarrow S'}}{R} = \frac{\mathrm{Distance}_{S\longrightarrow S'}}{2R},$$

$$\theta = \arccos\frac{\mathrm{Distance}_{S\longrightarrow S'}}{2R}. \tag{14}$$

From the above formula, the area of the new area can be obtained:

$$\Delta S' = \pi R^2 - \Delta S. \tag{15}$$

Expecting that the dispersion P of sensor hubs in a versatile sensor network complies with the Poisson circulation of λ, or at least, $P \sim P\ (\lambda)$, when the sensor hub moves to another position, the quantity of neighbor hubs found by the CNR-Group calculation in the recently added region is N.

The normal worth of the quantity of neighbor hubs in the recently added correspondence region S' is

$$E\left(S'\right) = \lambda\Delta S'. \tag{16}$$

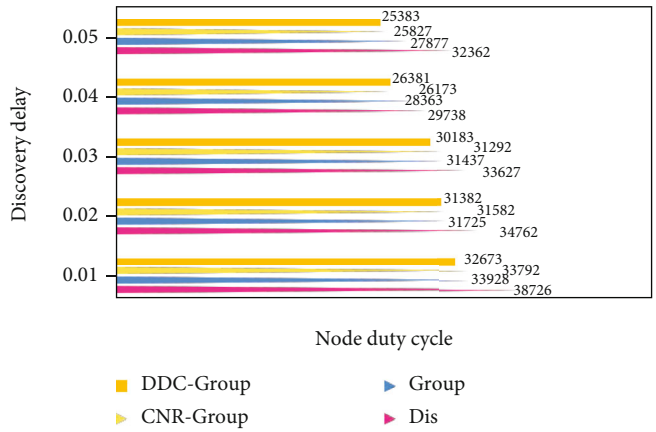

Figure 6: Discover the relationship between latency and node duty cycle.

Table 6: The connection between energy utilization and hub obligation cycle.

Node duty cycle	1%	2%	3%	4%	5%
Disco	103722	217878	312922	437282	581353
Group	173638	343522	413893	538294	685256
CNR-Group	163538	278423	397276	518393	652457
DDC-Group	198373	353281	428648	551837	698362

Then, at that point, the quantity of neighbor hubs not found in the recently added correspondence region is

$$E\left(S'_{\text{no}}\right) = E\left(S'\right) - N = \lambda \Delta S' - N. \tag{17}$$

In recipe (17), λ is the boundary of Poisson dissemination, $\lambda \Delta S'$ addresses the quantity of neighbor hubs in the recently added correspondence region, and N addresses the low-inactivity neighbor revelation calculation CNR-Group has found during hub development the quantity of neighbor hubs.

Assume it is tracked down that the wake-up season of hub DN is T_{active} and the wake-up period is T. Simultaneously, the wake-up time T_{active} is viewed as a container, and the likely $E(S')$ neighbor hubs in the recently added correspondence region are viewed as balls. As indicated by the ball and box model, it should be visible that the likelihood that the expected $E(S'_{\text{no}})$ neighbor hubs not found in the S' area will not awaken inside the wake-up season of the DN hub that is

$$P_{\text{no}}^{\text{active}} = \left(1 - \frac{T_{\text{active}}}{T}\right)^{E\left(S'_{\text{no}}\right)}. \tag{18}$$

In formula (18), T_{active}/T represents the probability of a single node awakening within the DN node wake-up time. The probability P^{active} that there are nodes in the $E(S'_{no})$ nodes in the area S' that wake up within the DN node wake-up time is

$$P^{\text{active}} = 1 - P_{\text{no}}^{\text{active}}. \tag{19}$$

It can be seen from equation (19) that the probability of a node in the area S' awakening within T_{active} time is P^{active}, which means that there are still some nodes that will not wake up within T_{active} time. At this time, it is necessary to adjust the discovery node DN the duty cycle to monitor undiscovered neighbor nodes.

At this time, the wake-up time T_{active} of the discovery node DN is extended to T'_{active}:

$$T'_{\text{active}} = T_{\text{active}} + T_{\text{active}} * P_{\text{no}}^{\text{active}}. \tag{20}$$

Then, it is found that the duty cycle DC of the node DN is adjusted to DC′:

$$DC = \frac{T_{\text{active}} + T_{\text{active}} * P_{\text{no}}^{\text{active}}}{T} * 100\%. \tag{21}$$

Among them, the wake-up period T is the sum of the wake-up time and the sleep time, namely,

$$T = T_{\text{active}} + T_{\text{dormant}}. \tag{22}$$

From the above investigation process, it very well may be seen that the obligation pattern of the hub DN has expanded, that is to say, the time that the hub is in the conscious state increments, and the hub is found to utilize the expanded waking chance to screen and find potential neighbor hubs in the recently added region. The disclosure of the hub the deferral is diminished; however, as the obligation pattern of the hub expands, the energy utilization of the hub should increment.

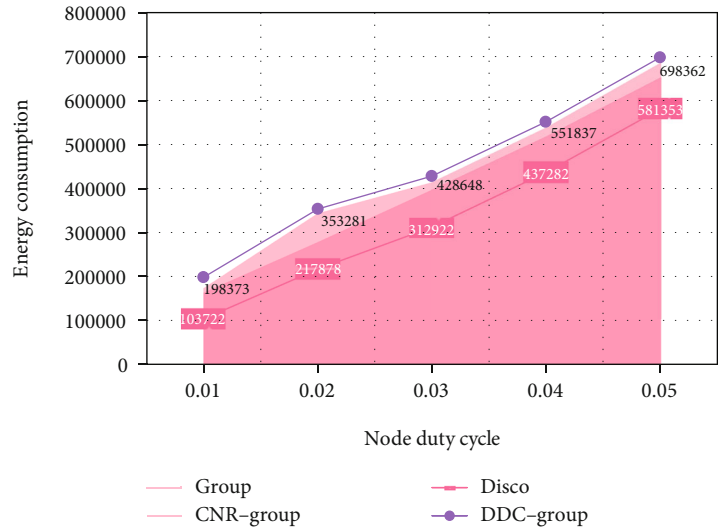

Figure 7: The connection between energy utilization and hub obligation cycle.

Table 7: The connection between energy utilization and hub broadcast inconsistency.

Radio range irregularity	0	20%	40%	60%	80%
Disco	0.76	0.81	0.87	0.91	0.97
Group	0.83	0.93	1.03	1.20	1.38
CNR-Group	0.88	1.11	1.17	1.23	1.43
DDC-Group	0.96	1.62	1.32	1.58	1.79

3. Test Research on the Internet of the Things Network Topology Discovery Algorithm Based on Wireless Sensors

3.1. Simulation Environment. The algorithm simulation environment is Windows XP + cygwin+NS_2.27 and the simulation network parameter setting: 60 wireless sensor nodes are distributed in an area of 100 m × 100 m and are divided into 6 clusters. The mobile agent is randomly generated on the 6 cluster head nodes, where Code_Size is set to 800 bytes; Data_Size is 1000Byte; State_Size is 400 bytes; the time delay factor required for the serialization of unit byte data is $2.3 \times 14 - 9$: the creation of mobile agent. The delay T_c and the processing delay T_p are ignored. The mobile agent sending delay is $T_s + T_p = \text{sizef} \times \text{actor} = 6.25$ ms, and the receiving delay is $T_{\text{wait}} = T_s = 5.34$ ms and $T_{\text{wait}} = 40$ ms.

3.2. Simulation of Mobile Agent Platform. The simulation of the mobile agent platform mainly includes two parts: the mobile agent entity and the execution environment context of the mobile agent. A mobile agent is a software entity that contains code, data, and status.

3.2.1. Simulation of Mobile Agent. The simulation of the mobile agent must have the following modules: the state of the mobile agent, the running module, the event response processing module, and the environment interaction module. The life cycle of a mobile agent entity begins with creation or cloning and then begins execution and enters the active state. During the execution, the mobile agent entity may be dispatched to other nodes, converted to inactive state, or converted from inactive state to active state.

3.2.2. The Execution Environment of the Mobile Agent Context. Context is similar to the data source generator in NS2 (such as FTP and CBR) and is implemented in the application layer of NS2 network simulation. Context includes the following modules: management module, transmission communication module, response processing module, interface module, and execution module. The interface module mainly coordinates and controls other modules and provides basic services such as creation, migration, and message transfer required by the mobile agent; the execution module is responsible for activating the execution of the mobile agent. The node movement model is described as the node first randomly selects a position in the entire moving area as the initial position and randomly selects the size and direction of the movement speed and the moving distance.

3.3. Algorithm Design and Data Collection. During the discovery process of neighbor nodes, the duty cycle of sensor nodes is no longer fixed. During the movement of nodes, sensor nodes dynamically adjust their duty cycle in real time according to the status of surrounding nodes. In a mobile sensor network, the position of a sensor node changes in real time. When a node is found to move from its original position to a new position, at this time, during the time when the node is found to be awake, some of the nodes are still in a dormant state, and the node cannot be found.

In a sensor network with n sensor hubs, take hubs *a*, *b*, and *c* as specific illustrations, where hub an is the hub that needs to find other neighbor hubs, that is, the discovery node, and the three nodes are each scheduled according to their own work arrangements. In the process of node neighbor discovery and movement, the duty ratio of the node is

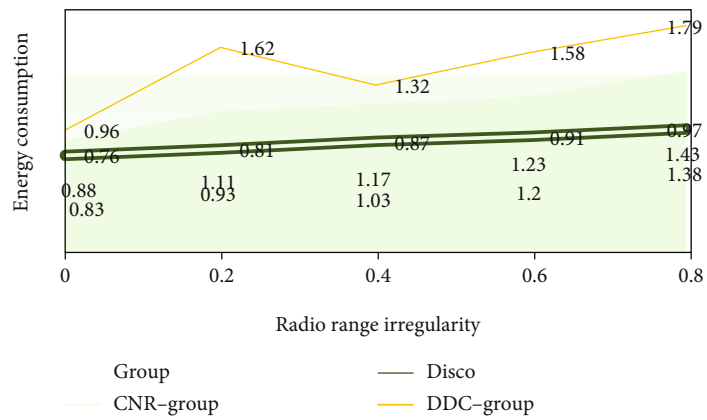

Figure 8: The connection between energy utilization and hub broadcast abnormality.

dynamically adjusted to monitor and discover potential undiscovered neighbor nodes in the newly added area after the node moves, thereby reducing the discovery delay.

4. Test Research and Analysis of the Internet of the Things Network Topology Discovery Algorithm Based on Wireless Sensors

4.1. Data Transfer Volume. To investigate the exhibition of the calculation, this article reenacts under full burden; that is to say, every hub has information shipped off the sink whenever. This article compares and analyzes the NDEA algorithm, LEACH, and Disco algorithm, and the experimental research from the aspect of data transmission is shown in Table 1.

Figure 2 shows the comparison between the improved NDEA algorithm, the original LEACH algorithm, and the sink receiving data volume of the Disco algorithm. In the simulation process, the data sent by the node to other nodes is actually its own ID number; so, the information got before the group head sends information to the sink is the rundown of IDs of the hubs that send information to itself, and the bunch head ships off the sink. This is the ID list; lastly, sink counts the quantity of information sent by every hub in light of the got information.

4.2. NDEA Algorithm and LEACH Algorithm Life Cycle Experiment Analysis. In the simulation process, the simulation data is collected regularly. The reenactment information chiefly incorporates the quantity of hubs right now making due in the organization, the aggregate sum of energy presently consumed by the organization, and how much information as of now gotten by the sink hub. This paper contrasts and breaks down the NDEA calculation and the LEACH calculation and the Disco calculation, and behaviors test research from the organization life cycle. The outcomes are displayed in Table 2.

Figure 3 shows the comparison of the number of surviving nodes in the improved NDEA algorithm and the original LEACH algorithm over time. Since NDEA needs to collect network information during network initialization, which consumes more energy than LEACH, the death of the first node occurs in NDEA at 45 s, before LEACH. Then, the overall network life cycle is about 1.6 times that of LEACH, which is better than LEACH. The curve comparison in the figure shows that NDEA can save energy consumption and make energy loss more evenly distributed to all nodes, extending the life cycle of the network.

4.3. Data Transmission Volume. Table 3 shows the comparison of the sink receiving data volume between the improved NDEA algorithm and the original LEACH algorithm.

As displayed in Figure 4, in the reenactment interaction, the information sent by a hub to different hubs is really its own ID number; so, the information got before the bunch head sends information to the sink is the ID of the hub that sent information to itself list, and the group head sends this ID rundown to the sink; lastly, the sink counts the quantity of information sent by every hub in view of the got information. This article shows the examination of the factual data of the information sent by the hubs under the two calculations. Since the organization lifetime of the NDEA calculation is fundamentally longer than that of the LEACH calculation, the information transmission volume should likewise be higher than that of LEACH.

4.4. Influence of Node Density on System Performance. This gathering of examinations concentrates on the effect of the thickness of sensor hubs in remote sensor networks on framework execution. The presentation boundaries of the framework incorporate the disclosure postponement and energy loss of the sensor organization. The trial results are displayed in Table 4.

The outcomes in Figure 5 show that when the thickness of hubs expands, the energy utilization of the four calculations keeps on expanding. According to the pattern perspective, the energy utilization of the DDC-Group calculation expands the most.

4.5. Effect of Node Duty Cycle on System Performance. The following investigation in this paper is to concentrate on the impact of the hub's obligation cycle on framework execution, including the revelation of postponement and energy utilization. The test results are displayed in Table 5.

The outcomes in Figure 6 show that when the obligation pattern of the hub builds, any of the four calculations, the framework's disclosure defer diminishes; yet, the level of effect is unique. It very well may be seen from the figure that the revelation postponement of the Disco calculation is altogether more noteworthy than the group, CNR-Group, and DDC-Group calculations under various obligation cycles, and the DDC-Group calculation is superior to the group and CNR-Group calculations.

The following examination is the connection between energy utilization and hub broadcast abnormality. The exploratory outcomes are displayed in Table 6.

Figure 7 shows that as the obligation pattern of the hub builds, the energy utilization of the hubs under the four calculations increments, which is close to a linear relationship. However, the energy consumption of the Group, CNR-Group, and DDC-Group algorithms changes more than the Disco algorithm increases more; compared with the group algorithm, the energy consumption of the DDC-Group algorithm is slightly increased, and the increase is not more than 2%, but it increases more than the CNR-Group.

4.6. Impact of Node Broadcast Irregularity on System Performance. This experiment studies the impact of node broadcast irregularity on system performance. In this group of experiments, the irregularity of node broadcasting varies from 0 to 85%. The experimental results are shown in Table 7.

It very well may be seen from Figure 8 that as the abnormality of hubs builds, the disclosure postponement of the four calculations increments to changing degrees. The Group, CNR-Group, and DDC-Group calculations are altogether better compared to the Disco calculation, and the DDC-Group calculation is the most excellent; the postponement is viewed as the least; as far as energy utilization, the DDC-Group calculation consumes the most energy.

5. Conclusions

This paper adopts the demand-wakeup mechanism of active awakening. According to the information of potential neighbor nodes obtained by existing neighbor nodes, potential neighbor nodes are discovered through active awakening, and on this basis, the recommendation mechanism of neighbor node information is studied. High-rate neighbor recommendation mechanism. Through this recommendation mechanism, the CNR-Group algorithm reduces latency and energy consumption, improves network performance, and extends network life cycle.

This paper proposes a geography disclosure calculation in light of versatile specialist. This calculation joins the attributes of versatile specialist innovation and grouping geography. The CNR-Group calculation actually beats the issues of the geography calculation, like enormous link length and establishment responsibility, significant weight on the focal hub, and low appropriated handling limit of each site. In each group, the bunch head is liable for gathering important data of the hubs in the group, including the present status and remaining energy. The mobile agent between clusters is responsible for discovering the cluster heads. Link information improves the migration strategy of mobile agents. Compared with other topology discovery algorithms based on mobile agents, this algorithm has improved globality and convergence speed, effectively reducing redundant data transmission, reducing communication consumption.

In this paper, the genuine hub development model is utilized to anticipate potential neighbor hubs, and the obligation pattern of the hub is powerfully changed through the quantity of potential neighbor hubs, to work on the productivity of neighbor hub revelation and diminish the disclosure delay. Actively waking up according to the exchanged node scheduling information can realize the discovery of neighbor nodes.

Data Availability

The data underlying the results presented in the study are available within the manuscript.

Conflicts of Interest

The authors declared no potential competing interests in our paper.

Authors' Contributions

All authors have seen the manuscript and approved to submit to your journal.

Acknowledgments

This work was supported by the school-level research team: "Artificial Intelligence Technology Application Research" in Xi'an FanYi University in 2021. Project Number: XFU21KYTDB02.

References

[1] F. Shahzad, T. R. Sheltami, and E. M. Shakshuki, "Effect of network topology on localization algorithm's performance," *Journal of Ambient Intelligence and Humanized Computing*, vol. 7, no. 3, pp. 445–454, 2016.

[2] N. Nesa and I. Banerjee, "Sensor rank: an energy efficient sensor activation algorithm for sensor data fusion in wireless networks," *IEEE Internet of Things Journal*, vol. 6, no. 2, pp. 2532–2539, 2019.

[3] M. M. Dhanvijay and S. C. Patil, "Internet of things: a survey of enabling Technologies in Healthcare and its applications," *Computer Networks*, vol. 153, pp. 113–131, 2019.

[4] P. Wei and Z. Zhou, "Research on security of information sharing in Internet of Things based on key algorithm," *Future Generation Computer Systems*, vol. 88, pp. 599–605, 2018.

[5] W. B. Fu, J. Zhang, and Y. L. Chen, "Network Topology Discovery Algorithm against Routing Spoofing Attack in Internet of Things," *Journal of Jilin University (Engineering and Technology Edition)*, vol. 48, no. 4, pp. 1231–1236, 2018.

[6] I. Khoufi, P. Minet, A. Laouiti, and S. Mahfoudh, "Survey of deployment algorithms in wireless sensor networks: coverage and connectivity issues and challenges," *International Journal*

of Autonomous & Adaptive Communications Systems, vol. 1, no. 4, pp. 341–390, 2017.

[7] M. Muhammad and G. A. Safdar, "Survey on existing authentication issues for cellular-assisted V2X communication," *Vehicular Communications*, vol. 12, pp. 50–65, 2018.

[8] C. Del-Valle-Soto, C. Mex-Perera, R. Monroy, and J. A. Nolazco-Flores, "On the routing protocol influence on the resilience of wireless sensor networks to jamming attacks," *Sensors*, vol. 15, no. 4, pp. 7619–7649, 2015.

[9] F. Tong, S. He, and J. Pan, "Modeling and analysis for data collection in duty-cycled linear sensor networks with pipelined-forwarding feature," *IEEE Internet of Things Journal*, vol. 6, no. 6, pp. 9489–9502, 2019.

[10] W. Osamy, A. M. Khedr, and A. Salim, "ADSDA: adaptive distributed service discovery algorithm for internet of things based mobile wireless sensor networks," *IEEE Sensors Journal*, vol. 19, no. 22, pp. 10869–10880, 2019.

[11] L.-D. Chou, C.-C. Liu, M.-S. Lai et al., "Behavior anomaly detection in SDN control plane: a case study of topology discovery attacks," *Wireless Communications and Mobile Computing*, vol. 2020, Article ID 8898949, 16 pages, 2020.

[12] Z. Donglan, "Research on secure network coding in wireless sensor networks based on web of things service," *The Open Automation and Control Systems Journal*, vol. 7, no. 1, pp. 816–820, 2015.

[13] E. Borgia, D. G. Gomes, B. Lagesse, R. J. Lea, and D. Puccinelli, "Editorial special issue on Internet of Things: research challenges solutions," *Computer Communications*, vol. 89, 2016.

[14] Y. Yan and W. Zai, "Research of memetic algorithm based on DSC problem in wireless sensor networks," *Chinese Journal of Sensors and Actuators*, vol. 28, no. 3, pp. 430–436, 2015.

[15] B. Hao and D. S. Kang, "Research on pedestrian detection using CNN-based faster-RCNN algorithm," *Journal of Computational and Theoretical Nanoence*, vol. 24, no. 3, pp. 2156–2159, 2018.

[16] R. Diamant, R. Francescon, and M. Zorzi, "Topology-efficient discovery: A topology discovery algorithm for underwater acoustic networks," *IEEE Journal of Oceanic Engineering*, vol. 43, no. 4, pp. 1200–1214, 2018.

[17] D. P. Mersch, "The social mirror for division of labor: what network topology and dynamics can teach us about organization of work in insect societies," *Behavioral Ecology & Sociobiology*, vol. 70, no. 7, pp. 1–13, 2016.

[18] J. Li and J. Huo, "Uneven clustering routing algorithm based on optimal clustering for wireless sensor networks," *Journal of Communications*, vol. 11, no. 2, pp. 132–142, 2016.

[19] Z. Ying, L. Peisong, and M. Lin, "Research on improved low-energy adaptive clustering hierarchy protocol in wireless sensor networks," *Journal of Shanghai Jiaotong University*, vol. 23, no. 5, pp. 23–29, 2018.

[20] P. Li and J. Cai, "Research on image recognition from wireless sensor data based on deep learning," *CE Ca*, vol. 42, no. 6, pp. 2607–2612, 2017.

[21] J. Zheng, "Research on a cluster system for binary data frames of wireless sensor network," *Cluster Computing*, vol. 19, no. 2, pp. 1–9, 2016.

Hindawi
Wireless Communications and Mobile Computing
Volume 2022, Article ID 8154573, 19 pages
https://doi.org/10.1155/2022/8154573

Research Article

An Effective Data-Collection Scheme with AUV Path Planning in Underwater Wireless Sensor Networks

Wahab Khan,[1] Wang Hua,[1] Muhammad Shahid Anwar,[1] Abdullah Alharbi,[2] Muhammad Imran,[3] and Javed Ali Khan [4]

[1]*School of Information and Electronics, Beijing Institute of Technology, Beijing 100081, China*
[2]*Department of Computer Science, Community College, King Saud University, P.O. Box 28095, Riyadh 11437, Saudi Arabia*
[3]*School of Engineering, Information Technology and Physical Sciences, Federation University, Brisbane 4000, Australia*
[4]*Department of Software Engineering, University of Science and Technology Bannu, Pakistan*

Correspondence should be addressed to Javed Ali Khan; javed_ali@ustb.edu.pk

Received 28 January 2022; Revised 6 March 2022; Accepted 17 March 2022; Published 8 April 2022

Academic Editor: Mohamed Elhoseny

Data collection in underwater wireless sensor networks (UWSNs) using autonomous underwater vehicles (AUVs) is a more robust solution than traditional approaches, instead of transmitting data from each node to a destination node. However, the design of delay-aware and energy-efficient path planning for AUVs is one of the most crucial problems in collecting data for UWSNs. To reduce network delay and increase network lifetime, we proposed a novel reliable AUV-based data-collection routing protocol for UWSNs. The proposed protocol employs a route planning mechanism to collect data using AUVs. The sink node directs AUVs for data collection from sensor nodes to reduce energy consumption. First, sensor nodes are organized into clusters for better scalability, and then, these clusters are arranged into groups to assign an AUV to each group. Second, the traveling path for each AUV is crafted based on the Markov decision process (MDP) for the reliable collection of data. The simulation results affirm the effectiveness and efficiency of the proposed technique in terms of throughput, energy efficiency, delay, and reliability.

1. Introduction

In the last decade, most systems have been investigated for dynamic environment. Probably, the most popular system in this area is the underwater wireless sensor network, which refers to the organized interconnection between various sensor nodes and other devices such as autonomous underwater vehicles (AUVs), which are situated in an observing domain to offer explicit applications, e.g., data collection without the intervention of humans [1–4]. Recent developments in various hardware and software technologies have provided underwater sensor nodes with identifying, sensing, processing, computing, and networking capabilities. Therefore, the UWSN vision includes many applications such as navigation, object localization, detection of mines, and environmental pollution monitoring [5–8]. AUVs are widely employed for these applications in gathering data from UWSNs. An AUV that acts as a mobile sink may efficiently minimize sensor node transmission energy; the AUV could travel to the monitoring area for data gathering from the sensor node using a specified path plan. The AUV would travel, gather, and return to the surface sink to upload the collected data effectively. Figure 1 shows the UWSN [9].

In UWSNs, energy-efficient reliable data collection and aggregation is one of the most critical challenges to meet the requirements of quality of service (QoS), including transmission delay, a priority of data, reliability, and energy consumption [10]. Aggregation of data is an intelligent technique that aggregates data from many UWSN sensor nodes compressed by an aggregation feature to reduce the amount of inserted data traffic in the network [11, 12]. The prime objective of data aggregation is to execute an algorithm at sensor nodes to reduce redundant packet transmission to the sink through AUVs, reduce data transmission

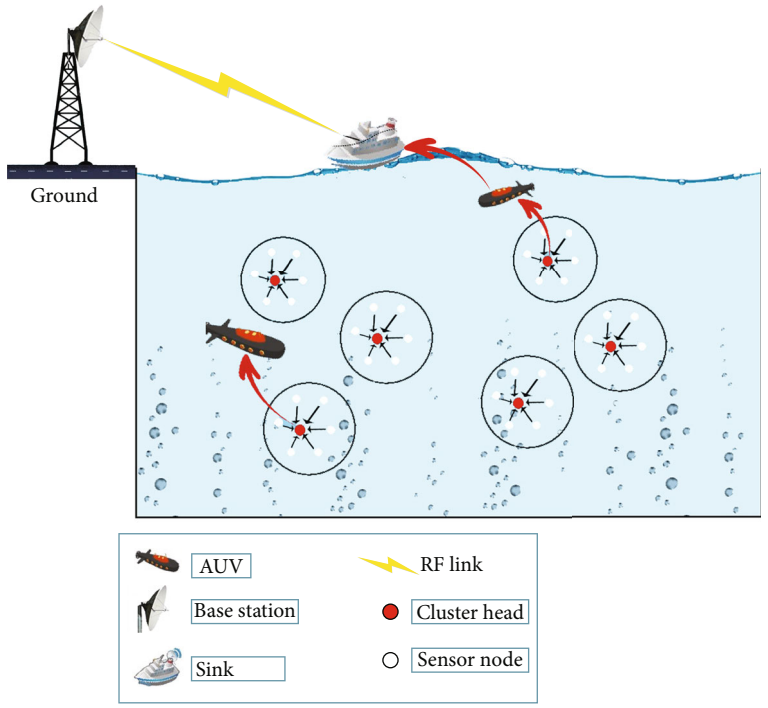

Figure 1: Diagrammatic representation of AUV-based UWSN.

delay, and improve energy use, ultimately enhancing network lifetime. This method gives UWSNs three advantages: (1) in the network, the injected data size is decreased; (2) the delay will be substantially decreased; (3) the transfer of fewer data will help nodes consume less energy, thus maximizing the lifetime of UWSNs.

Limited battery capacity affects sensor node lifespan and decreases system efficiency [13]. Therefore, it is essential to use an effective and energy-efficient data collection method for effective and sustainable UWSN efficiency. As wireless communications generate substantial amounts of energy during data aggregation in UWSNs [14, 15], achieving an efficient link between nodes and effective path planning of AUVs for data collection is a significant challenge.

Most of the existing data-collection approaches in UWSN can be categorized into hop-by-hop, cluster-based, and AUV-assisted [16–18]. In hop-by-hop, data packets are transmitted from the source sensor to the destination in a hop-by-hop manner. However, redundant packets are still a challenging issue in such approaches; therefore, we introduced a clustering technique in the proposed scheme to control the retransmission of packets. The cluster-based strategies organize UWSN into clusters in which each cluster head (CH) is designated to collect data from member sensor nodes and forward it to the sink/AUV. Improved network communication, well-organized topology management, and energy efficiency are the advantages of the clustering method. However, CH selection is a critical problem because CH uses more energy to collect and aggregate data before delivering it to its destination. The introduction of AUV is a promising method to save the wasted energy of sensor nodes during clustering. In AUV-based approaches, the sensor nodes/CHs connect with an AUV to conduct the collection process, and the AUV then transfers the collected data to the sink node. Due to regular AUV position changes, the transmission of control packets to maintain connections between all the sensor nodes, and the AUV results in a substantial amount of energy dissipation, which reduces the network lifetime. Furthermore, the sensor nodes located closer to the AUV use energy rapidly because of the repeated single-hop packet transmission. On the other hand, the sensor nodes far from the AUV sending data directly to the AUV will also consume substantial energy. Therefore, a cluster-based routing design can help minimize transmission energy use.

Although the above methods minimize the energy consumption and improve the life cycle of the UWSNs to some extent, they face additional challenges, including data priority and transmission delay [19–21]. Collection of data has different preferences, since underwater sensor nodes are being installed at diverse locations in the surveillance environment. Few sensor nodes can sense vital information that needs to be collected faster; therefore, the demise of sensor nodes with high priority data would have a larger effect on network stability as compared to other nodes. In UWSN, transmission delay can be specified as the time required to receive all sensor node-generated packets to the sink. In addition, in most of the current approaches in the literature, the sensor nodes near the sink node die earlier than the other sensor nodes, which are far from the sink node, making the whole network useless [22]. Therefore, deploying multiple AUVs is more efficient for resolving data priority problems in UWSNs, transmission delay, energy restriction, and heterogeneity [23, 24]. To use these AUVs effectively, the path planning of each AUV is an essential task, and it also affects network performance [25].

In AUV-based UWSN, the data-collection path taken by AUV could not be neglected. The parameters that rely on the AUV path are energy consumption, network dispersion, data-collection latency, and network lifetime. Fixing the AUV traversal path does not ensure the best and optimal path. To establish the optimal collecting path, we used the traveling salesman problem (TSP) to design the AUV traversal path from the sink to CHs. Many heuristic approaches, such as simulated annealing, greedy method, and genetic algorithm, have been employed to solve the TSP efficiently. In our situation, MDP was used to solve TSP by determining the optimum route to make it possible for the AUV to reach the CHs and then return to the surface sink. We also focused on the energy and data priority parameters of CHs when proposing a traveling path.

Recently, research has been carried out on the AUV-based data collection in UWSNs, such as the greedy and adaptive AUV pathfinding (GAAP) protocol presented by Gjanci et al. [26]. GAAP derives the AUV path to gather the sensed information from nodes and transmits this information to the sink node with the maximum value of information (VoI). GAAP imitates the best routes and obtains the volume of the data provided. Although it is ideal for AUV to tour all the sensor nodes, its prolonged tour time might cause delays in emergencies. Additionally, if AUV travels to all the sensor nodes, AUV must wait until all information is collected from each node before going into the next sensor node. It is possible to conserve transmission energy in UWSNs using AUVs to reach every sensor node and collect data from them. However, this method creates significant collection delays and limited throughput because of low AUV velocity. Thus, AUV-based UWSNs need to optimize network throughput and energy consumption. To encounter these problems, we are driven not only to design a path for an AUV to enhance network throughput and decrease its traveling time but also to establish a network in such a way that decreases energy consumption.

This article suggests an efficient data-collection protocol for UWSN with AUV path planning based on the MDP (APP-MDP). The following are the main steps of our approach: to decrease AUV traveling time and increase energy efficiency, we employ a clustering approach. Each CH collects data from its member node and transfers it to the AUV. After clustering, CHs will be selected based on holding time, and then, the division of clusters into small groups is the means of an angle-based approach. After grouping, the sink node determines the MDP parameters for each AUV. It then calculates the optimal policy using a value-iteration process. This step helps with efficient path planning for each AUV visiting their particular group of CHs. The AUV transfers the collected data of CHs to the sink node. The simulation results verify the efficiency of our proposed scheme in optimizing energy consumption, reliability, and data transfer relative to recent UWSN data-collection approaches.

The main contributions of this article are summarized as follows: (1) the development of an energy-efficient method in UWSNs for the collection of data using AUVs; (2) the clustering of sensor nodes, applying angle-based grouping strategy to arrange CHs in nonoverlapping and energy-efficient groups for providing an AUV; and (3) the development of a novel efficient method of path planning for AUVs using MDP to collect the data from CH groups.

The rest of the paper is arranged in the following manner: Section 2 describes the related work. Section 3 describes the network model and channel model. Section 4 describes the proposed mechanism, and Section 5 describes the simulation results and analysis.

2. Related Work

Data-gathering schemes are designed based on routing algorithms. Earlier studies have proposed many data-gathering schemes where the transmission of data is accumulated using clustering schemes or data gathering using hop-by-hop methods. In these methods, sensed information is sent hop-by-hop alongside the routing tracks. In this way, routing schemes assume an essential role in these methodologies. UWSN is unique concerning terrestrial wireless sensor networks (TWSN) because the sensor nodes drift with water streams automatically underwater. The intended protocol for TWSNs could not be functional for UWSNs straightforwardly. In this manner, the research focuses on structuring an AUV-based reliable and energy-proficient routing protocol. We divide the related work into the following subsections.

2.1. Multihop Techniques. In multihop techniques, the source node uses a relay node to direct the sensed data towards the sink nodes, positioned on the water's surface using routing mechanisms like the shortest-distance strategy and greedy approach. In HH-VBF [27], the direction of a virtual pipeline between the forwarding node and destination node was established. Every time at the next hop, the path of the virtual channel is adjusted to select the most favorable forwarding node. Additionally, the packets are transmitted through that vector, which was established in this plan, because adaptive adjustment of the virtual pipeline on hops will increase end-to-end delay, and much energy will also be consumed.

To overcome the problem of end-to-end delay, the authors in [28] anticipated a routing protocol layer-by-layer angle-based flooding (L2-ABF). This is deployed in layers and measures the sensor node depth. This method uses the multihop technique where all sensor nodes convey data to the destination node by calculating the flooding angle. The appropriate next forwarding node is nominated through the remaining energy. This paper attained a higher packet delivery ratio, and the energy consumption is also low. However, in any case, the decision of flooding angle is a troublesome assignment, particularly in sparse regions. If the flooding angle is not suitable, the possibility of transferring data may cause failure, so it was not appropriate in the sparse areas. Yu et al. presented the AHH-VBF [29] protocol for sparse regions. In this protocol, the radius of the virtual pipeline is adaptively accommodated for packet broadcasting. This protocol changes transmission power dynamically according to the next forwarder to compute holding times

from the source to destination nodes and reduce redundant transmissions to diminish energy consumption. However, each transmission of data through selected nodes will cause the node to die earlier, determined each time for data forwarding. Therefore, the network void hole problem occurs due to higher energy consumption.

To overcome the void hole problem, 2hop-AHH-VBF [30] considered various parameters such as the distance between receiver and sender, residual energy of next appropriate node, a threshold value for the number of nodes in the vector, and from a virtual vector, the distance of the chosen node. The purpose is to avoid consecutively choosing the same node. Well-organized battery dissipation is guaranteed using appropriate node recommendations. Energy calculation is performed at every hop to oblige any adjustments in the capacity for proper node determination as a next forwarder to obtain better results regarding network performance.

2.2. Clustering Approaches. For the reduction of end-to-end delay and better energy efficiency, clustering is the most capable method when planning the routing protocol for UWSNs. In UWSNs, because of the sparse deployment of sensors and harsh environments, clustering is not the same as terrestrial networks. The clustering technique is incorporated to manage the restricted energy constraints in UWSNs. A definitive goal of clustering is to separate the system into tiny areas and make a group of nodes. Each cluster elects one CH considering different parameters. CH totals the detected information and transfers it to the target node (sink node). Propagation distance between sensor nodes is reduced using clustering because only the CHs send the information, and these CHs have a small distance with each other.

Furthermore, this limits the consumption of energy by evading excess information packets. For communication among different clusters, a reasonable topology ought to be chosen. This determination relies upon the cluster size and separation among the sink node and CH [31]. The ideal number of clusters also influences UWSN execution. If the clusters are fewer, this implies that the size of the cluster will be bigger. In bigger estimated clusters, sensors beyond CH desire additional energy to direct the information towards CH. However, if the size of clusters is small, this will cause communication overhead. Therefore, the size of the cluster ought to be kept ideal, neither small nor huge. The perfect number of groups will eventually lessen energy use and improve system lifetime.

ACH2 is introduced in [32]. The primary factor of this scheme is that it is a localization-free process where the nodes are allied with CHs. This plan avoids back transmission and reduces propagation distance. This reduces energy use and results in an improved system lifetime. In this approach, first, based on a threshold value, CHs are chosen. The ideal number of cluster heads is determined based on the perfect distance; due to this method, the loads are adjusted among different clusters. The authors in this article have accomplished improved system lifetime and attained maximum packet delivery ratio (PDR) for UWSNs. However, a high communication delay occurred in this plan. In homogeneous networks, this strategy can be useful, but any dynamicity or unbalance in WSNs might cause intensive run-time issues, such as chronic energy consumption in specific CHs.

Clustering techniques are implemented in [33] for routing in UWSNs to improve network lifetime. Cluster-based routing protocols comprise the CH selection process and data communication process. First, the CH node is selected based on sensor nodes' residual energy and position information. All the cluster members forward data to their respective CH in its range in the data communication process. The CH node then compresses aggregated data and sends a composite compressed data packet to sink through multihop communication. Moreover, a collision occurs in data packet transmission, which is avoided using the time division multiple access (TDMA) technique. Due to the algorithm's centralised nature, it caused high communication overheads.

2.3. AUV and Mobile Agent-Based Approaches. The authors in [34] used the MDP paradigm to formulate the data-collection problem in mobile wireless sensor networks. The ideal movement routes for mobile agents collecting sensor node readings are defined. The mobile agent's location determined the states. The monitoring region is divided into a sector, and each mobile agent directs towards a predefined sector to collect data. The reward function indicates the node energy use and the number of readings gathered. The simulation results indicate that the approach presented surpasses traditional approaches, such as TSP-based approaches. However, the author did not consider the importance of data and residual energy parameters while formulating the MDP parameters. Due to less residual energy, some nodes need importance to collect data, which is why in our approach, we also include the importance of data parameters during MDP parameter formulation.

A mobile geocast routing protocol (3-D ZOR) [35] has been proposed for UWSNs, in which the network is distributed in 3-D ZOR areas. AUV is introduced to gather data from nodes in its vicinity, and the geographic zone where the AUV resides is called 3-D ZOR. At a predefined trajectory, the AUV moves and gathers sensed information from different 3-D ZORs. Sleep–awake mode is used by nodes for data forwarding. The operation of the routing protocol depends on two stages. First is collecting information from sensor nodes inside the 3-D ZOR areas and in the other phase wakes up those nodes to forward data to the AUV in the next 3-D ZOR. Only nodes in the 3-D ZOR forward data to the AUV to save the node power consumption. However, the authors did not consider that much nodes inside the coverage region should be employed to deliver the packet which is a key issue for this approach.

An AUV-based routing protocol in [36] has been proposed for UWSNs. The authors assumed random deployment of identical sensor nodes in the network. The sensor nodes then perform the clustering technique and mutually elect a CH node in each cluster. Each CH node further divides the clusters into subclusters and distinguishes a key

data-collection node called the PN node. To achieve energy conservation, AUV is introduced to gather data from PN. Thus, data collection from PN is done instead of CH as in conventional schemes. Therefore, using AUV for PN data collection achieves efficient sensor node transmission. This scheme enhances the data gain and diminishes the node's energy consumption. However, it experiences severe gathering delay when contrasted with multihop transfer strategies.

In addition, Javaid et al. [37] proposed an AUV-based routing protocol for UWSNs (AEDG) to maximize data reliability in the network. In AEDG, sensor nodes are associated with special nodes (called gateway nodes) using the shortest path selection algorithm (SPA) to improve the network lifetime. All other nodes are associated with special nodes to forward their sensed data. The special nodes accumulate data from member nodes and then forward it to the AUV, which consumes energy efficiently and ensures reliability. Thus, the least number of normal nodes (member nodes) is associated with special nodes to reduce overloading. The AUV traveling ways are not ideal, and the coordinated effort of AUVs between various GNs was an exceptionally troublesome assignment. The plan decreased the delay and member node's energy consumption; however, it might practice the problem of a hot zone.

Cheng and Li anticipated a data-gathering plan that underlined the significance of data [19]. The high load of data forwarding from deep underwater nodes to sink depletes their energy rapidly. The imbalanced energy expenditure of underwater nodes because of multihop transmission in deep water is efficiently mitigated by announcing AUVs to collect data from deep underwater nodes. It identifies the importance level of data and then gathers data in a distributed manner. A mechanism to swap layers is introduced to effectively solve long time delay and imbalance energy consumption problems by introducing AUVs for data collection, improving network performance, and achieving better network lifespan. Due to the extent of significant data, the impact of delay and energy consumption is unsatisfactory for the entire system.

For the most part, fewer researchers take hop-by-hop transmission or clustering for data gathering alone; a large portion of them have started to merge these two methods to deal with configuring better data accumulation schemes. In the future, when structuring novel methodologies, it is essential to know strategies for individual points of advantages and drawbacks. This article uses the benefits of different transmission modes of underwater wireless networks to show the interconnection between other sectors, which empowers efficient and distributed data-collection schemes from underwater nodes to the nodes at the water's surface. The ratio of data delivery underwater is meager, and the BER is very high due to UWSN harsh environment. Delivery ratio, energy consumption, and the bit error rate can be enhanced using decent-quality links. Therefore, better path planning with decent-quality links is a significant problem.

Clustering-based routing schemes extend the efficiency of the network to some extent, such as network lifetime and energy consumption. However, the challenges not considered during planning data aggregation schemes include the delay of data transmission and the priority of data. Moreover, it is already discussed in the above literature that nodes near the sink consume energy faster than other sensor nodes that are far from sink nodes. Therefore, it is crucial to exploit the abilities of AUVs for the collection of data from underwater sensor nodes.

3. Network Model

In this article, the UWSN is shown as $M = (N, L)$, in which N is the number of sensor nodes and L is the links among sensor nodes. The networking area is considered to be $A \times A \times A$, and the sink node is placed at the surface in the center. The sensor nodes are homogeneous and have the same transmission capabilities. Sensor nodes are equally distributed around the networking area using a pressure gauge [38]. Each node determines its position using existing localization algorithms [39, 40], and the sink node knows the location of nodes. A sensor node Si has the following properties:

(i) Dij: Dij presents the Euclidean distance between the sensor node Si and sensor node Sj, a fundamental factor in ensuring effective path planning for data collection through AUVs on UWSN

(ii) Dis: Dis is the Euclidean distance between sensor node Si and the destination node, a sink node that plays a vital part in recommending well-organized path planning for AUVs in UWSNs. In this proposed process, it is considered that the surface sink nodes remain fixed at the surface of the networking area, and the AUVs are repeatedly approaching or retreating from it

(iii) REi: REi represents sensor node (Si) residual energy. During the initialization of the network, each sensor node has specific initial energy, which is dissipated by packets sending/receiving and processing tasks by the AUVs. The sink node energy is considered to be unlimited

(iv) ßi: sensor node (Si) priority of data is demonstrated by ßi. As various sensor nodes are deployed at different monitoring areas, UWSN data collection has varying preferences. A sensor node provides critical data that needs to be collected early. Specifically, if a sensor node with high priority dies, the system's stability is diminished when a sensor node with low priority fails

(v) Tr: this is the sensor node transmission radius

The suggested environment has k AUVs for the collection of data from CHs. Each AUV overall memory size is presumed to be P, while it has a space of memory represented by QP during data collection. The sensor nodes of the network are divided into clusters. Each sensor node in the network transmits its sensed information to its CH,

which provides enough memory to buffer the data obtained from cluster members. Additionally, the selected CHs are supposed to be clustered into R groups. After defining cluster head groups, for collection of data, sink node assigns AUV for every group. Thus, the CH groups and AUVs are equal in number, and this is represented by R. Table 1 lists all the notations.

3.1. Channel Model. The UWSN channel is a challenging communication medium due to poor communication quality and restricted bandwidth. The channel's time-varying and high-frequency selective aspects also make it challenging to develop an effective communications strategy. Different parameters influence the function of acoustic channels, such as water depth, temperature, and salinity. Figure 2 [41]] demonstrates the relationship between water depth and acoustic speed using thermoclines. Equation (1) [42] shows the acoustic signal speed:

$$\begin{aligned} S = 1555.85 + 3.481T - 4.204 \times 10^{-2} \\ T^{-2} + 3.26310^{-2}T^{-3} + 1.230(Y - 25) + 1.53 \times \\ 10^{-1}D + 1.565 \times 10^{-6}D^2 - 1.035 \times \\ 10^{-2}T(S - 25) - 6.129 \times 10^{-14}TD^3, \end{aligned} \tag{1}$$

where S demonstrates the acoustic signal speed, T represents the temperature (0-28 degrees Celsius), Y reflects salinity (30-40 parts per thousand), and D represents the water depth (0-6000 meters). In UWSN, the acoustic channel attenuation is described [24].

$$A(d, fk) = d^{\rho}\alpha(fk)^d, \tag{2}$$

where ρ is the fixed spreading factor 1.5 and d in meters. $\alpha(fk)$ represents the absorption coefficient, which could be shown by the empirical formula of Thorpe [24]:

$$10 \log \alpha(fk) = \frac{0.1f^2k}{1 + f^2k} + \frac{40f^2k}{4400 + f^2k} + \frac{2.75f^2k}{10^4} + 0.0003. \tag{3}$$

Equation (3) is ideal for high frequencies and equation (4) for lower frequencies.

$$10 \log \alpha(fk) = \frac{0.1f^2k}{1 + f^2k} + .01f^2k + .002. \tag{4}$$

The noise of underwater can be stated as [42]

$$N(f) = \mathrm{Nth}(f) + \mathrm{Nw}(f) + \mathrm{Nt}(f) + \mathrm{Ns}(f), \tag{5}$$

where $Nth(f)$, $Nw(f)$, $Nt(f)$, and $Ns(f)$ specify thermal, waves, turbulence, and shipping noise. Mathematically, the level of noise frequency is low, and the attenuation frequency is high. The signal-to-noise ratio can be expressed as

$$\mathrm{SNR}(f, d) = P(f) - N(f) - A(d, f), \tag{6}$$

where $P(f)$ states transmission power, $N(f)$ specifies noise, and $A(d, f)$ represents attenuation.

In contrast to the aforementioned parameters, acoustic modems are an essential component of acoustic channels and influence communication. They are classified as acoustic modems for research and commercial acoustic modems. The properties of commercially available acoustic modems are summarized in Table 2 [43].

4. Mechanism of the Proposed Scheme

In Figure 3, the proposed scheme is shown. This method consists of two main steps.

(1) First of all, sensor nodes are organized into clusters for better scalability. We employ the K-mean algorithm [44–46] as a clustering mechanism as it is pretty adaptive, resistant to outliers, and is shown to be efficient for clustering. After clustering, CHs are defined in each cluster, which is grouped using the angle-based [46] method into the same size sectors based on available AUVs. In the first stage, each group includes at least one CH near the sink to obtain the AUV and send back the AUV to the sink after collecting all CH group's data. Reliable, accurate, and nonoverlapping CH groups for AUV placement are the outcomes of this step

(2) The second step was aimed at giving an effective path planning for each AUV employing the MDP to each CH group separately. The MDP is regarded for its effectiveness in maximizing uncertain decision-making [47–49]. Sensor nodes are prone to failures due to malfunctioning of various components such as hardware, software, and power, resulting in uncertainty and instability. MDP uses sophisticated decision-making techniques based on artificial intelligence to successfully trade off reliability, energy consumption, data priority, and delay. Using the value-iteration process [47], the optimal strategy (the best series of UWSNs nodes that each AUV can visit) is obtained until the parameters of the MDP are determined. In the cases where only the initial state is known [50], the approach is an appropriate forward induction. The value-iteration approach is the best option in our proposed model because only the AUV's first destination is defined

When each AUV path planning is established at the sink node, the sink node directs AUVs to collect data from groups of CH. The sink node determined the final condition to end or continue the mechanism. The overall mechanism is shown in Figure 4.

Figure 4 shows the flowchart of the proposed scheme. The scheme consists of two main phases. In the first phase, we have done clustering of sensor nodes and then grouping CHs to assign an AUV. In the second phase, the scheme exploits MDP parameters to model AUV path planning. After calculating MDP parameters, a method called value iteration is used to determine the best order of CHs, which the AUV should go to.

Table 1: Notations.

Notations	Definition
N	Number of sensor nodes
L	Links of communication between sensor nodes
Dis	The Euclidean distance among sensor node Si and the destination node
REi	REi represents sensor node (Si) residual energy
β_i	Sensor node (Si) priority of data
Tr	Sensor node transmission radius
Dij	The Euclidean distance among the sensor node Si and sensor node Sj
P	AUV overall memory size
QP	Empty memory of an AUV
R	CH groups
A	Monitoring area
ρ	Fixed spreading factor
$\alpha(fk)$	Absorption coefficient
D_{bs}	Distance between the sensor nodes and sink
T	Time period
$\varepsilon_{\text{edtr}}$	Dissipated energy for transmitting and receiving of single bit data
G	State space
Ni	Corresponds to CH Si transmission radius
Rij	Corresponds to distance among CHi and CHj
M	A set in which recent visited CHs data is stored
ϱ^1 Re (zi, yj)	Revenue to select a CH which have a reduced amount of residual energy
Rej(i	CHj initial energy
Rej(t	Corresponds to CHj residual energy at a time t
$\varrho^2\rho(zi, yj)$	Corresponds to priority of data of CHs
$\forall$	Risk region
$\varrho^1, \varrho^2, \varrho^3$, and ϱ^4	Reward compensation coefficients

4.1. Clustering and Grouping of CHs. The cluster center will be measured first to decide the cluster's final number. Suppose the network's initial cluster center number is R, and the total node number is N. Given the average case, each group would have N/R nodes. Assume CHs forward data directly to the sink. Consider the network area is $A * A * A$. The ideal number of clusters according to [45] would be

$$R = \sqrt{\frac{\text{NA}}{\pi D_{bs}}}. \tag{7}$$

D_{bs} is the distance between the sensor nodes and sink.

After the initial R cluster centers are obtained, we use the K-mean algorithm to cluster the network. Distance represents the proximity of nodes, and as a consequence, the usual measuring function is equivalent to the total of the square distances among the cluster center and nodes:

$$L = \sum_{i=1}^{R} \sum_{x \in Ci} D(Ci, x)^2. \tag{8}$$

The assortment of CHs will begin after clustering is done. The sink node will use the following equation to measure each node's holding time (Ht) in each cluster. Each node has its own Ht which is different from other sensor nodes.

$$\text{Ht} = T + \rho \times \frac{\text{Er}}{E0}, \tag{9}$$

where T is the period time and ρ [1, 0.5] is any conflict avoiding value if nodes have equivalent residual energy. From equation (9), we can determine that if the residual energy of a node is high, thus the node will have a lower holding time than other nodes. It will have a better opportunity to choose as CH. When the holding time of a node expires, the node will be selected as CH, which has a lower holding time in the cluster. If multiple nodes have the same holding time (Ht), the node with a high probability will be selected as CH. The probability can be determined using the following equation [22].

$$p = \frac{1}{e^n + 1}. \tag{10}$$

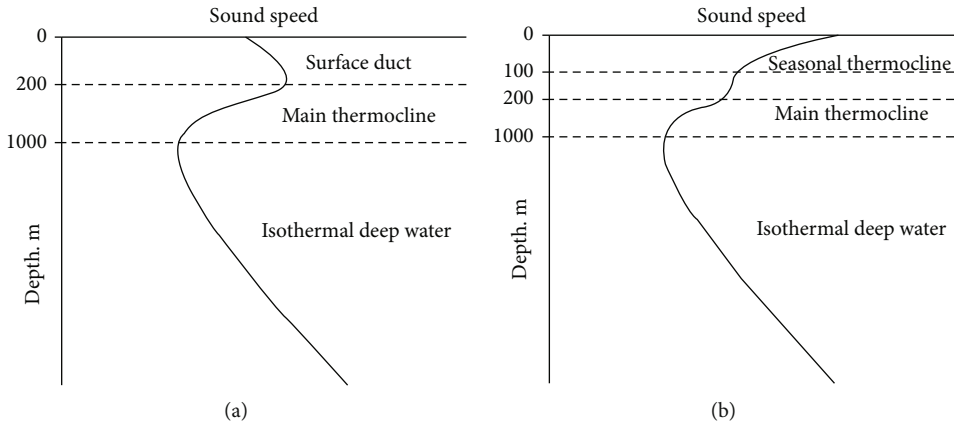

FIGURE 2: Relationship between water depth and acoustic speed using thermoclines for both winter (a) and summer (b) with depth of 200 m.

At this stage, to group CHs, the AAP-MDP system uses an angle-based method [46] to allocate one AUV to each influential and nonoverlapping group. The whole area is categorized into sectors having an equal size, depending on the expected quantity of AUVs. To find adequate AUVs (CH groups), we apply the following equation [46].

$$Y = \sqrt{\frac{A\varepsilon_{\text{edtr}} \mid N \mid}{\varepsilon_{\text{edtr}}(A/6) - E}}, \tag{11}$$

where A is the monitoring area sides and $\varepsilon_{\text{edtr}}$ determines the dissipated energy for transmitting and receiving of single-bit-data.

In cluster head grouping, every group must first cover a CH near the surface sink and then a predetermined threshold value to obtain the AUV and send back to the surface sink after gathering all group data. The threshold value is calculated for UWSN based on its sensor node's transmission range. To group the CHs, if we implement traditional clustering approaches like the K-mean algorithm, certain clusters would be created at locations far away from the surface sink so no group member can share the AUV and collect data with the surface sink. While if the procedure of angle-based grouping is used, in the first step, each group covers at least one CH, which is placed closer to the surface sink to obtain the AUV for data collection. Therefore, using the angle-based method generates stable CH groups to assign an AUV. Generally, suppose the CHs grouping is not performed. In that case, several AUVs may be allocated to a single CH that raises the inserted traffic through the network and challenges the network delay-aware mechanism and energy efficiency.

4.2. Formulation of MDP. This section explains how the MDP model could be used for path planning of an AUV in a UWSN for CH groups. MDP is a statistical optimization framework for making a decision in unpredictable situations [34, 51, 52]. The model assumes that the UWSN is in a given state at any decision and selects one of the possible actions in that state. In addition, after that, due to the transition probability, UWSN is shifted to a new state, and a reward is obtained. The MDP shall be established by a tuple $(S, A, P(y, z), R(y, z), \beta)$, in which S corresponds to a finite set of states, A corresponds to a finite set of actions, $P(y, z)$ corresponds to the distribution of the transfer probability over the group of states when action z is chosen in the state y, and $R(y, z)$ is the reward function for performing action z at state y. The solution of a MDP is a policy that determines the action to be taken once a specific state occurs. The quality of a procedure is the expected sum of future rewards. A discount factor β discounts future rewards to ensure that the expected sum of rewards converges to a finite value. Among many potential policies, the optimal reward-optimizing policy $(\pi *)$ is the main aim.

In the proposed method, MDP collaborates among sensor nodes, such as decision-making for AUV's next destination. The MDP parameters are explained for AUV path planning. The parameters of the MDP method are described below for modeling the path of an AUV:

4.2.1. State Space [G]. In our method, we analyze the CH group as a state in the UWSN network when an AUV travels to a particular sensor node/CH. The group state is indicated by a CH identifier on which AUV has been deployed. For path planning of an AUV, the state space is $Z = [x1, x2.\cdots x n]$, where $x1$ corresponds to the AUV installed at a specific group.

4.2.2. Action [A]. In every group state, decision-making focused on action. In the proposed scheme, the action is a decision regarding the next CH towards which AUV travels. Consequently, some action would be taken if more CHs are available in the current CH transmission radius. In a CH group, for AUV path planning, the actions are measured as $A = [y1, y2.\cdots yn]$, where $y1$ action demonstrates that the AUV moves towards CH Si, and this is the AUV destination over the next phase. Therefore, under any conditions when the $y1$ action is chosen, the UWSN's next state would be xi. Any action selected in either state would impact the chance of a change to another state over the next step.

Table 2: Acoustic modem properties.

Modem	Modulation scheme	Range (m)	Depth (m) (typical-max)	Data rate (bps)	C.F (kHz)	Bit error rate	BW (kHz)	Power consumption (W) (TX)	Power consumption (W) (RX)	Temperature (°C) (min-max)
S2CM HS	S2C	300	200-200	62500	160	10-Oct	80	3.5	0.8	0-60
S2CM 48/78	S2C	1000	200-2000	31200	63	10-Oct	30	18	0.8	0-60
S2CM 42/65	S2C	1000	200-2000	31200	53.5	10-Oct	23	18	0.8	0-60
S2CM 18/34	S2C	3500	200-2000	13900	26	10-Oct	16	35	0.8	0-60
S2CR 48/78	S2C	1000	200-2000	31200	63	10-Oct	30	18	1.1	0-60
UWM2000	BASS	1500	2000-4000	17800	35.7	10-Sep	17.9	2	0.8	(-5) to 45

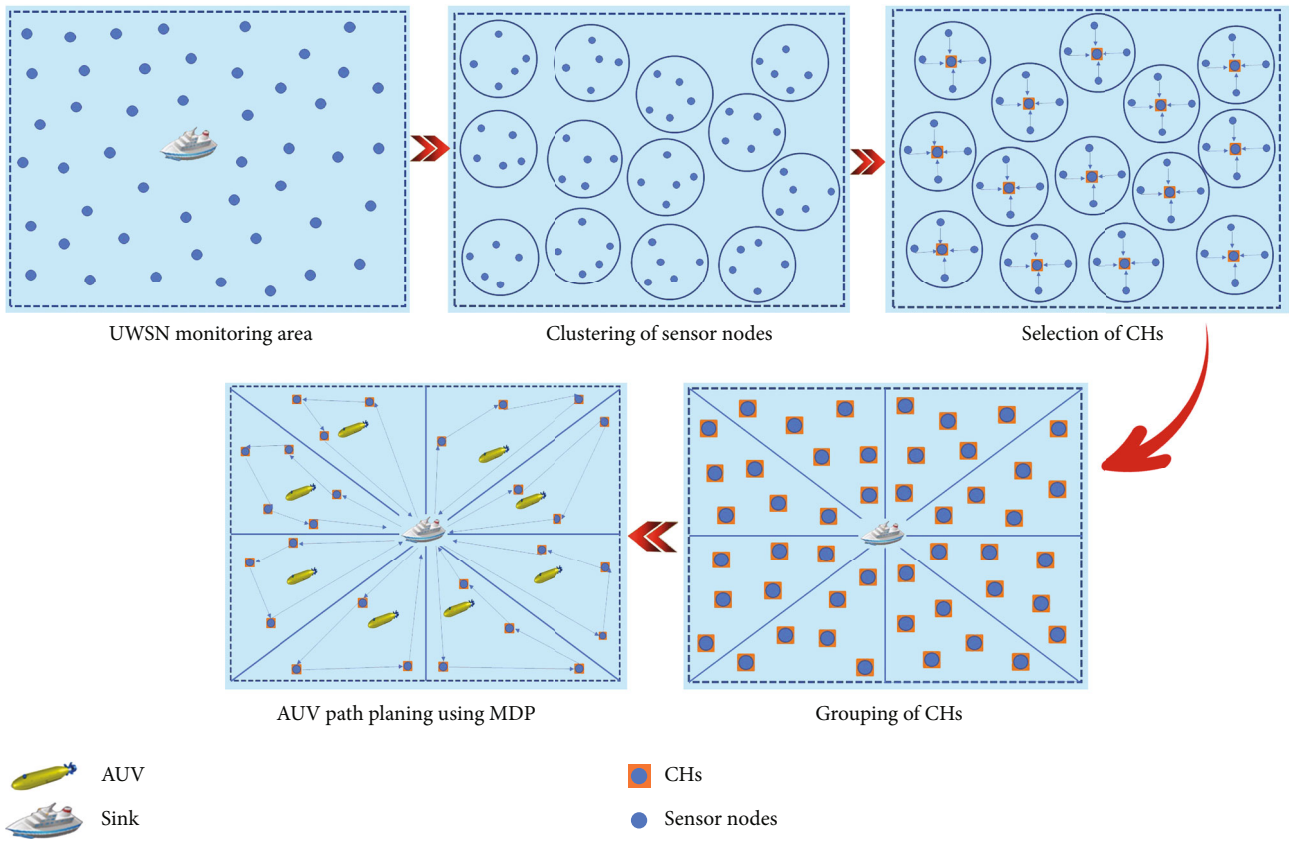

Figure 3: Proposed scheme.

4.2.3. Transition Probabilities. While taking action, in the following two modes, the transition probabilities would be considered to be null.

(i) If the CH Sj location is outside the CH Si (AUV present location) transmission radius, CH Si will not transfer AUV towards CH Sj. Thus, the transition probability will be zero in this mode by choosing action Yj

(ii) If an AUV has obtained CH Sj data in the current phase, Si could not be picked further before the phase is finished. Therefore, choosing the action Yj the transition probability will be zero

In other cases, the transition probability of choosing the Yj action is marked among the CH Euclidean distance. So, at either state of the UWSN system, the transition probability would be determined as follows:

$$P(\text{yi}, \text{yz}) = \begin{cases} 0, & \text{Rij} > \text{Ni}, \\ 0, & j \in M, \\ \text{PR}(\text{yi}, \text{yz}), & \text{otherwise}. \end{cases} \quad (12)$$

In the above equation, Ni corresponds to CH Si transmission radius, Rij corresponds to distance among CHi and CHj. M is a set in which recent visited CH data is stored in the current phase. At first, when the UWSN starts, M is zero. Thus, the AUV collects information from each CH attached to the M list. The key goal of state $j \in M$ is for the AUV only to visit a CH once. At each round, the CHs visited by the AUV would have no chance to acquire the AUV again. The function j also means the list of any CH and can be expressed as [1,2,3....n]. At last, $PR(yi, yz)$ could be found using the following formula:

$$\text{PR}(\text{yi}, \text{yz}) = \text{CDF}(\text{Rij}), \quad (13)$$

where Rij corresponds to cumulative distribution function.

4.2.4. Reward Function ($R(y, z)$). This function uses penalties and revenue to measure the model's outcome when the yj action is chosen at the zi state. The reward function is determined as follows:

$$R(\text{zi}, \text{yj}) = \varrho 1\ \text{Re}\ (\text{zi}, \text{yj}) + \varrho 2\rho(\text{zi}, \text{yj}) + \varrho 3G(\text{zi}, \text{yj}) - \varrho 4\text{Pe}(\text{zi}, \text{yj}), \quad (14)$$

where ϱ1 Re (zi, yj) specifies revenue to select a CH with a reduced amount of residual energy, using this revenue is to collect information from CHs that die quicker than the others to improve UWSNs efficiency.

To fulfill these limitations:

(i) If the CHj residual energy is below the threshold value, the AUV cannot be received, and the data is sent to the other CH or sink. In this scenario, the selection of CHj as the next destination for AUV will be considered null

(ii) Alternatively, AUV will select the CH as the next destination with less residual energy

It is important to note that the threshold value for CHj is the total energy desirable to accept the AUV and transfer it to the subsequent CH or sink node.

$$\tau = \text{Ej}(A) + \text{Ej}(T). \quad (15)$$

Re (zi, yj) could be calculated such as

$$\text{Re}\ (\text{zi}, \text{yj}) = \text{Rej}(i) - \text{Rej}(t), \quad (16)$$

where $Rej(i)$ is the CHj initial energy while $Rej(t)$ corresponds to CHj residual energy at a time t.

$\varrho 2\rho(\text{zi}, \text{yj})$ corresponds to the priority of data of CHs. The AUV prefers to collect the data of those CHs that prioritize more than other CHs. The goal is to manage high-value

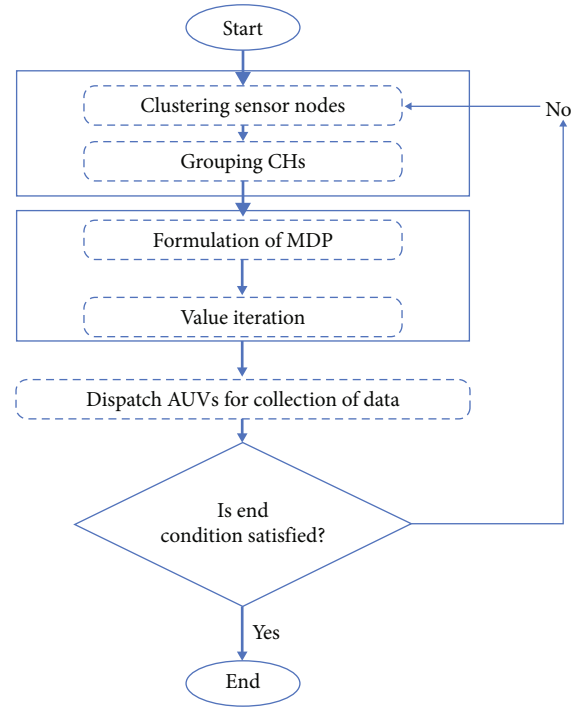

Figure 4: Flow chart of the proposed mechanism.

data in advance to avoid data loss if the AUV data memory is full. $\varrho 2\rho(\text{zi}, \text{yj})$ could be determined as

$$\varrho 2\rho(zi, yj) = \begin{cases} \beta 1, & \text{Low}, \\ \beta 2, & \text{Medium}, \\ \beta 3, & \text{High}. \end{cases} \quad (17)$$

In which $\beta 1$, $\beta 2$, and $\beta 3$ are revenue that takes data priorities into account. It must be considered that data priority parameters can require various values based on the specifications of the different UWSN applications.

$G(\text{zi}, \text{yj}))$ is to select CHs as the AUV next destination near the sink than the ones not yet reached to sink. Since the amount of valuable data in AUV memory expands when accessing each CH, AUV tends to reach the sink progressively to reduce injected network traffic; therefore, the energy usage of the CHs and the lifespan of the sensor nodes as a whole will be improved.

$$G(zi, yj) = \begin{cases} \partial, & \text{djs} < \text{dms}, \\ 0, & \text{Else}. \end{cases} \quad (18)$$

$\partial$is revenue and assumed to be the next destination of the AUV to choose the closest CH to the sink, wheredjscorresponds to Euclidean distance among the sink node and AUV selected CH as the next destination and$dms$is the smallest Euclidean distance among sink and unmet CHs. In different applications, this parameter may have changed values.

At last, $P(zi, yj)$ is the penalty for choosing the CHs arriving in the area of risk. The AUV is less interested in

1: Input: initial energy of all sensor nodes, set of Pi (data priority), sink and sensor node location
2: Output: optimal policies $\pi *$
3: **Begin**
4: **While** Compute Dij
5: Compute Dis
6: Calculate R
7: Cluster sensor nodes via k-medoids method
8: Group the CHs
9: **For** every AUV
10: Compute P (y, z) and Compute M (y, z)
11: Obtain optimal policy via value-iteration process
12: **End for**
13: Transfer AUV with path plan $\pi *$ to all CH groups
14: Sink receive AUV data and revive its memory
15: **End while**
16: **End**

Algorithm 1: AUV path planning using MDP.

choosing the CHs on the boundaries of the monitoring area as their next location.

$$P(\text{zi, yj}) = \begin{cases} \text{dj}, & \text{rm}-\forall<\text{djs} < \text{rm}, \\ 0, & \text{Else}, \end{cases} \quad (19)$$

where $\forall$ is the risk region and *rm* is the monitoring area radius. At last, it should be remembered that $\varrho 1, \varrho 2, \varrho 3,$ and $\varrho 4$ are the reward compensation coefficients.

4.3. Path Planning for AUV and Collection of Data from CHs Using AUV. This segment proposes a path planning framework for AUVs in CH groups, which exploits the value-iteration method [34, 52, 53]. This process utilizes the transition probabilities for future states, and then, the cumulative compensation or value $V(y, z)$ is determined for the action y taken in the state z. For any state, the optimum action is the action that gives a full reward. Indeed, the Q values are determined depending on an optimal strategy for a given step.

(i) Initialize $V(y, z) = 0$

(ii) Repeat $V(y, z) = R(y, z) + \max \sum_z P(y, z, y^*) V(y^*, z^*)$

This procedure will be continued and repeated before the last cycle occurs. Methods of forwarding induction, like the value-iteration method, must be ideal for situations where only the initial condition is specified (the sensor node's initial data is specified in our prescribed system). Algorithm 1 demonstrates the ultimate mechanism operation.

As shown in Algorithm 1, the initial energy of sensor nodes, residual energy, the priority of data, and the location of sensor nodes are considered inputs of the suggested model. When the framework starts to work, all the sensor nodes broadcast their properties across the entire network. Therefore, it can be stated that the sink knows the sensor node's features in the beginning. It determines all sensor nodes' total energy. If each cluster member has the energy to transmit information to the CH, and, respectively, if CH has the required energy to obtain and send back the AUV to the subsequent location, the sink node will measure the sensor node Euclidean distance and also measures the Euclidean distance between the sensor node and sink. First of all, the K-mean algorithm is used to cluster the network. After clustering, CH is determined in each cluster using equation (7). The sink node divided CHs into groups using the angle-based method for assigning AUV to each group.

Next, the sink node determines MDP parameters for each AUV. It then calculates the optimal policy through the value-iteration process (the optimal path of the sensor nodes that any AUV can visit); this stage helps in efficient path planning for each AUV visiting their particular group of CHs. The sink collects AUV data, and after receiving its data, the sink node replenishes the data memory of AUV. After that, the overall energy of sensor nodes is rechecked; if the nodes have much power to send data to CHs and CHs have much energy to receive AUV and dispatch that to other locations, then the process will be repeated; otherwise, it will end.

Table 3: Simulation parameters.

Parameters	Value
Monitoring area	1km * 1km* 1km
Sensor nodes	1000
Initial energy of AUV	15KJ
Initial energy of sensor nodes	5kJ
Sensor nodes transmission range	200 m
Speed of AUV	6 m/s
Channel bandwidth	10 kHz
Transmission power	0.303 watt
Receiving power	.022 watt
Speed of acoustic signal	1.5 km/sec

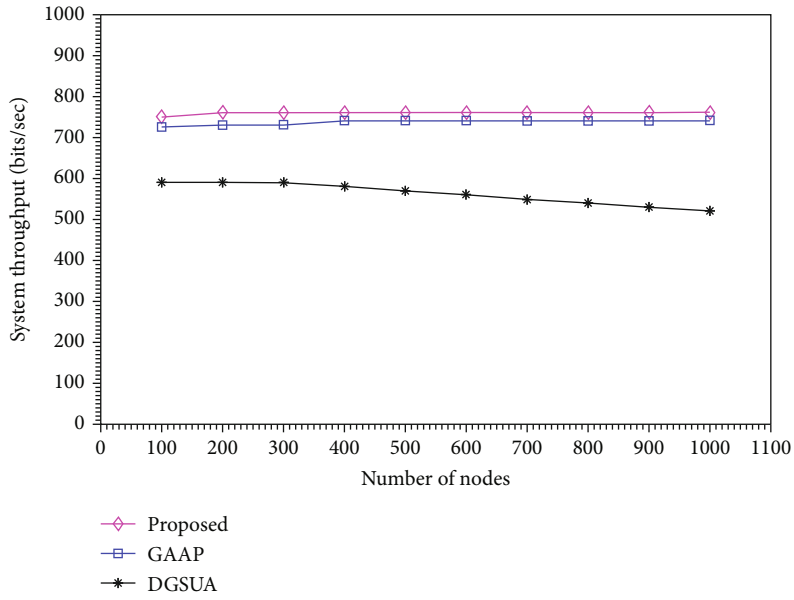

Figure 5: System throughput.

5. Simulation Results and Analysis

5.1. Simulation Setup. Extensive simulations were carried out for the assessment of the proposed method. Since the physical layer of UWSNs varies between acoustic modems, we determined these characteristics using Evologics acoustic modems; they are commercially available products with varying features. We used the S2CR18/34 modem, and the parameters are described in Table 3. In addition, the network parameters are set as follows, a 1 km ∗ 1 km ∗ 1 km deep-sea UWSN was developed where the data-collection sink drifts at the surface. Sensor nodes are installed uniformly at different locations, and multiple AUVs are used for data collection in this simulation. The AUV manages emergencies at the fastest speed. In this analysis, the AUV unit consumption rate is 7 J/m [9]. On land, the SenCar consumption rate is 5 J/m [54], and the AUV's energy consumption increases due to water resistance. It is assumed that the AUV can collect 2048 bits of the system data. We exploit the IEEE 802.15.4 [55] performance dataset, in which 1000 sensor nodes from the dataset are highlighted that are suitable for UWSN applications. Further simulation parameters are described in Table??. For evaluating the MDP-based optimal policy, we use a MATLAB MDP toolbox [56] to apply our policy iteration algorithm. We choose the parameters of the node based on intense Motes (XSM) [57]. The XSM motes contain acoustic, magnetic, temperature, and infrared sensors.

We compare the performance of our proposed scheme with a data-gathering scheme using AUVs (DGSUA) [58] and the greedy and adaptive AUV pathfinding (GAAP) [26] approach. GAAP derives the AUV route from gathering the sensed information from nodes and transmitting this information to the sink node with maximum value of information (VoI). DGSUA designs several AUV movement and coordination processes in data processing. These schemes aim to fix the issues of route planning and task assignments of AUV to enhance the reliability of the UWSN. To analyze possible solutions equally and accurately, we follow the same cluster number and network topology. These algorithms' output is measured in throughput, energy efficiency, collection delay, and reliability. A better approach is intended to minimize collection delay, reduce energy consumption, increase throughput, and boost reliability.

5.2. System Throughput. The throughput of a system refers to the rate at which data packets are received at the sink. Figure 5 shows the system's throughput; since the strategy of multi-AUV in DGSUA performs the collection of data quickly, but the time required for the collection of data is too scattered, not focused on higher-data packet clusters and nodes. The GAAP algorithm takes a long time to perform data collection, preferably selecting sensor nodes with more data packets to maintain maximum throughput. The proposed approach combines the above two frameworks and decreases the cumulative time to gather data, thus preserving a high throughput.

5.3. Energy Efficiency. The ratio of total packets received to total energy consumed by the network to deliver these packets is called energy efficiency. Figure 6 indicates the energy efficiency levels obtained for the three methods. The multi-AUV navigation direction is mechanical and fixed in DGSUA; therefore, DGSUA energy efficiency is comparatively poor, especially when the number of nodes is limited in the network. This paper's suggested algorithm logically organizes the AUV path depending on actual circumstances. Navigation of path planning using MDP decreases high energy consumption compared to other schemes. The figure shows that our suggested method has higher energy efficiency than the other two methods.

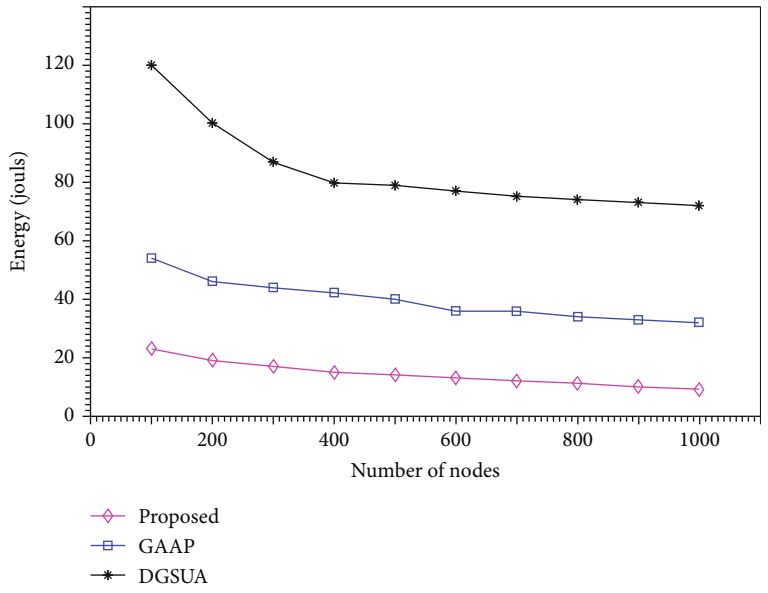

Figure 6: Energy efficiency.

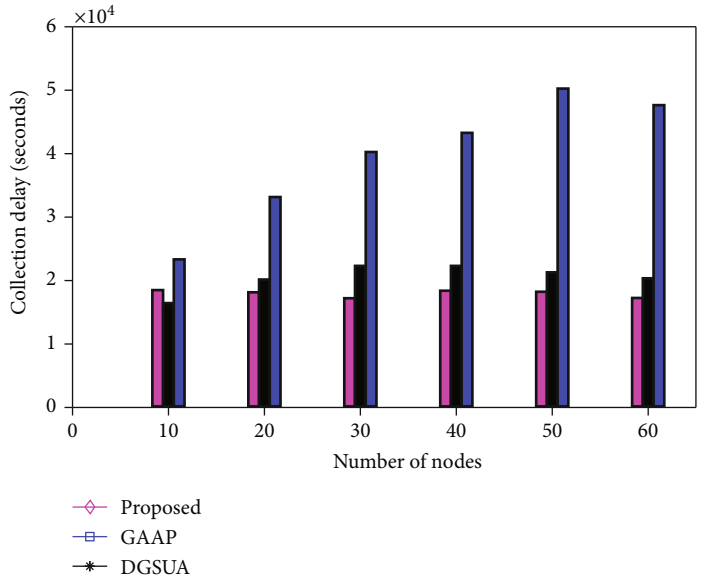

Figure 7: Collection delay.

5.4. Collection Delay. Figure 7 shows that as the number of nodes increases, DGSUA and APP-MDP collection delay remains relatively constant, while GAAP collection delay increases. APP-MDP has the shortest collection delay as compared to others. DGSUA has a minor collection delay as compared to the GAAP algorithm. The reason is that, in the GAAP algorithm, the AUV must visit each node for the collection of data which in turn increases the collection delay. In contrast, in other algorithms, the AUV only visits the selected CHs to collect data. That is why its collection delay is more minor. Furthermore, as DGSUA does not produce the optimum results of CH groups relative to APP-MDP, the distance can be longer among CHs. Therefore, the DGSUA collection delay might be higher as compared to APP-MDP. Comparatively, the proposed scheme has a minor collection delay due to the algorithm's appropriate path planning for AUV.

5.5. Execution Time of AUVs and Their Itinerary Length. Figure 8 indicates AUVs' execution time visiting all CHs and how long they will return to sink. It contrasts our methodology with other current protocols (DGSUA, GAAP). As shown, the time of execution of routing protocols increases with the increasing number of sensor nodes. Among other routing protocols, GAAP has the maximum execution time, due to its poor plan to move sensor nodes closer to the sink.

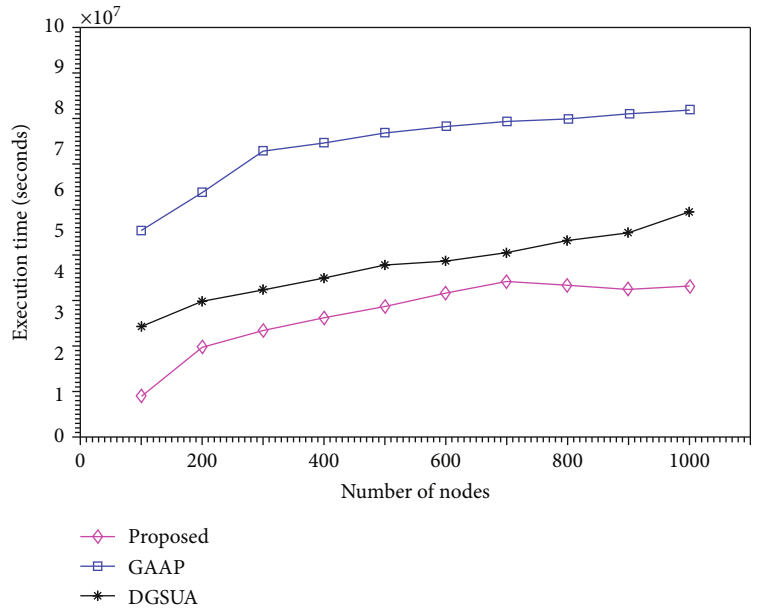

Figure 8: AUVs' execution time.

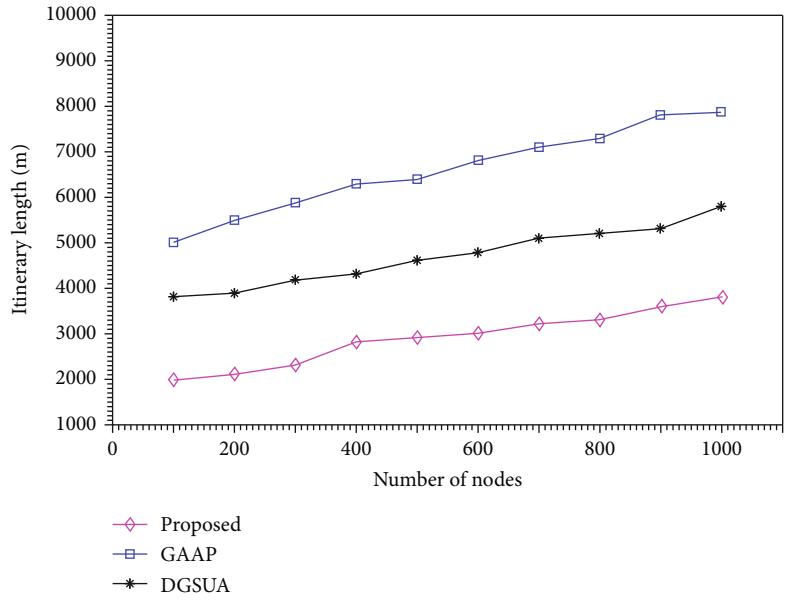

Figure 9: Itinerary lengths of AUVs.

DGSUA has less execution time as compared to the GAAP algorithm. Our proposed approach has the lowest execution time compared to all other routing protocols due to using multiple AUVs and collecting data spending less time on each CH using optimal route planning.

Figure 9 indicates the itinerary length of AUVs for different routing protocols. The size of our suggested protocol is short as compared to other protocols. This is because planning an optimal route for AUVs using MDP and the strategy to plan AUV routes between CHs only, not among all sensor nodes. GAAP has the longest route due to its poor plan to select the closest sensor node as its destination and scheduling AUV routes for all sensor nodes, not only for CHs. DGSUA has a short itinerary length compared to GAAP because of multi-AUVs.

5.6. Energy Consumption Fairness. The network lifespan is linked to the fairness of energy consumption. This metric shows the energy consumption levels of all sensor nodes during the network operating time. Thus, when the fairness of energy consumption is less, it will increase the network's lifespan and produce more live sensor nodes over a period. Figure 10 shows the standard deviation (SD) chart of energy consumed by active sensor nodes. SD is a metric to evaluate

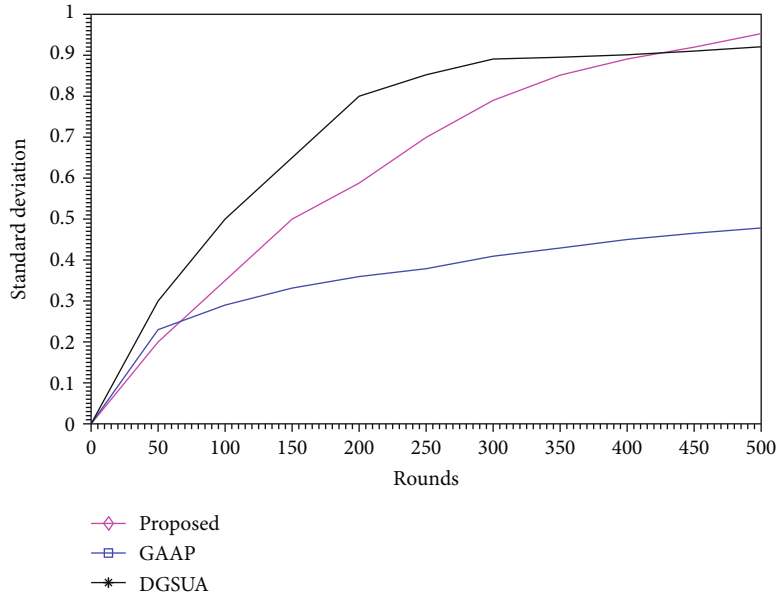

Figure 10: SD of consumed energy.

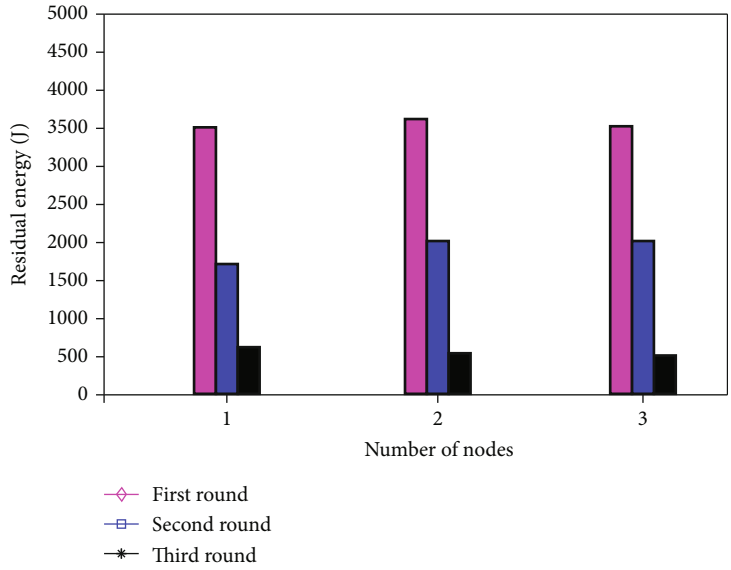

Figure 11: Different AUVs' residual energy.

the amount of energy consumption dispersion by sensor nodes per cycle. Small SD reveals that energy consumption values tend towards the mean, although a huge SD specifies that the values of energy consumption are distributed across a broad range.

As seen in Figure 10, in the first 50 rounds, our method SD is 25.95% smaller than the DGSUA SD. The low value of SD indicates that the energy consumption of all sensor nodes is near the average in our proposed system, which indicates a fair allocation of the network workload across the sensor nodes. In this case, the sensor nodes allocated to some network portions do not expire earlier. The framework would also perform well to meet the requirements of critical applications, like tsunami warnings and pollution monitoring.

Moreover, in the first 450 rounds, our method SD is 50.95% smaller than the GAAP SD. As the rounds progress, our proposed mechanism has a higher SD than the other two techniques. This is because the active sensor nodes are reduced in GAAP and DGSUA techniques after a specified time, and a rapid reduction in their SD is also reasonable because of the reduced alive sensor nodes.

5.7. Reliability. UWSN's reliability is evaluated in this section, which is the critical factor in determining the system's ability to execute its defined tasks under specified conditions.

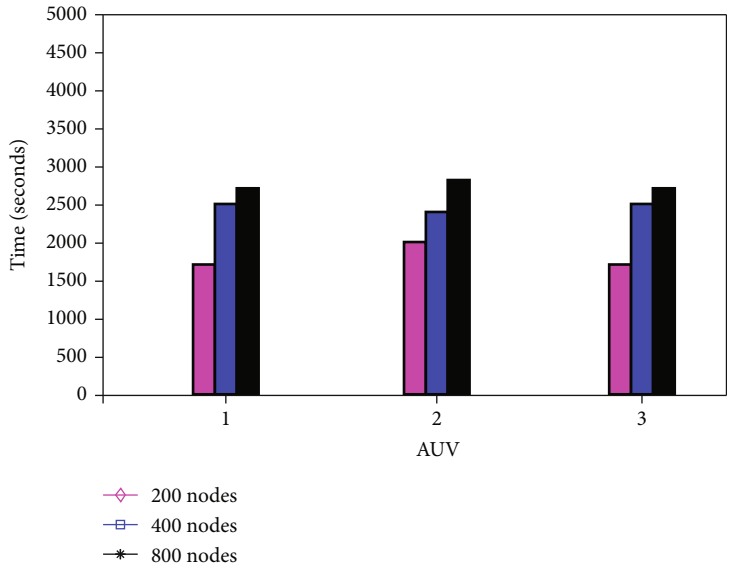

Figure 12: Different AUVs' accomplish time.

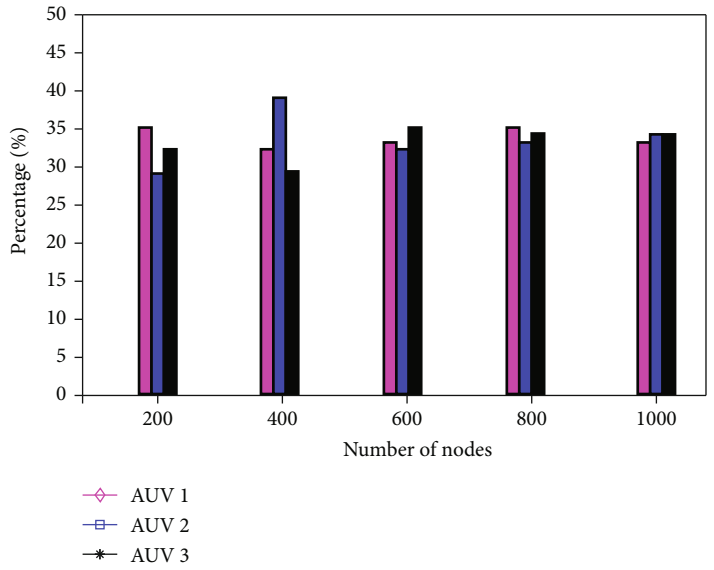

Figure 13: AUVs' load balancing.

Table 4: Reliability.

APP – MDP	DGSUA	GAAP
0.02564	0.01832	0.01875

To avoid the loss of sensitive data, the AUVs tend to collect high priority data if an AUV data memory is being filled. So, system reliability is described as the data priority, which could be calculated as

$$R = \frac{\mathrm{LP} + 2\mathrm{MP} + 3\mathrm{HP}}{\mathrm{LG} + 2\mathrm{MG} + 3\mathrm{HG}}. \quad (20)$$

LP, *MP*, and *HP* are low, medium, and high priority data numbers and have been reached to the sink. *LG*, *MG*, and *HG* provide low priority, medium priority, and high priority data that some sensor nodes generate. As described in Table 4, the APP-MDP mechanism improves system reliability by 1.39 to 1.36 times in contrast with other methods.

5.8. Single AUV Performance. Multi-AUV is often used for data processing in the underwater sensor network. Route planning and task assignment for AUV are essential; both are related to network lifetime and AUV load balancing. Therefore, the system's efficiency of a single AUV is given substantial consideration during the simulation. The amount of AUVs is typically calculated upon network size

and data priority requirements. For the simulation, we considered only three AUVs and separately numbered them.

Figure 11 indicates each AUV's residual energy when the execution rounds increase. The AUVs' initial energy is considered by one-third of the total energy, and for others, it is regarded as the same. After each data gathering round, the energy needed by the AUV stays the same to prevent a single AUV executes more activities and absorbing faster energy.

Figure 12 shows the time each AUV spends executing its task; this is significantly varying due to different route sizes in the region assigned to it. This influences the whole task's completion period. Figure 13 demonstrates the AUV's load balancing, particularly as the number of nodes increases. The supremacy of the geographic division of CHs in groups and route planning using MDP is thoroughly expressed.

In short, the efficiency of several AUVs is essentially the same without considering the impact of specific conditions such as AUV failures and data importance. This flexibility is beneficial to the system's stability in achieving the task.

6. Conclusions

A data-collection protocol for UWSNs based on AUV path planning has been developed in this work. The collection of data is one of UWSN's primary concerns. Using multiple AUVs with efficient and reliable path planning for data collection from sensor nodes significantly decreases the total network energy consumption. It fulfilled QoS criteria, such as data priority, reliability, and delay. The APP-MDP method is proposed in this article. It provides efficient and reliable path planning for AUVs to collect the data from sensor nodes. We divided this method into two steps. The first step is the clustering of sensor nodes using the k-medoids algorithm. After clustering, CHs are specified in each cluster, which is grouped employing angle-based technique into same size sectors for providing of AUVs. In the second step, APP-MDP takes advantage of the MDP using many factors, such as sensor node residual energy and its priority of data, and Euclidean distance between the sink and sensor nodes to deliver efficient and reliable path planning for AUVs in CH groups. Finally, the value-iteration method determines the best route after UWSN modeling. The simulation results affirm that the proposed technique has increased throughput and reduced energy consumption compared to other techniques. Our proposed technique enhances network reliability. The findings show that our proposed approach is better than all the other existing approaches; it takes less execution time and has the shortest itinerary length than others.

In the future, using the APP-MDP as a basis, we intend to research real-world environments. In UWSNs, data gathering based on AUV is a fascinating approach from a practical research perspective. There is still a lot of work to be done on how to maneuver around in real situations under the effects of obstacles, drifting of water, and wind, so we will keep working on that.

Data Availability

Data will be provided upon request.

Conflicts of Interest

The authors declare that they have no conflicts of interest.

Acknowledgments

The authors would like to extend their sincere appreciation to the Research Supporting Project number (RSP2022R444), King Saud University, Riyadh, Saudi Arabia.

References

[1] A. Darehshoorzadeh and A. Boukerche, "Underwater sensor networks: a new challenge for opportunistic routing protocols," *IEEE Communications Magazine*, vol. 53, no. 11, pp. 98–107, 2015.

[2] E. Felemban, F. K. Shaikh, U. M. Qureshi, A. A. Sheikh, and S. B. Qaisar, "Underwater sensor network applications: a comprehensive survey," *International Journal of Distributed Sensor Networks*, vol. 11, no. 11, Article ID 896832, 2015.

[3] Z. Wadud, K. Ullah, S. Hussain, X. Yang, and A. Qazi, "DOW-PR Dolphin and whale pods routing protocol for underwater wireless sensor networks (UWSNs)," *Sensors*, vol. 18, no. 5, p. 1529, 2018.

[4] S. Yoon, A. K. Azad, H. Oh, and S. Kim, "AURP: an AUV-aided underwater routing protocol for underwater acoustic sensor networks," *Sensors*, vol. 12, no. 2, pp. 1827–1845, 2012.

[5] Q. Mao, F. Hu, and Q. Hao, "Deep learning for intelligent wireless networks: a comprehensive survey," *IEEE Communications Surveys & Tutorials*, vol. 20, no. 4, pp. 2595–2621, 2018.

[6] M. Jouhari, K. Ibrahimi, H. Tembine, and J. Ben-Othman, "Underwater wireless sensor networks: a survey on enabling technologies, localization protocols, and Internet of Underwater Things," *Access*, vol. 7, pp. 96879–96899, 2019.

[7] T. Hu and Y. Fei, "QELAR: a machine-learning-based adaptive routing protocol for energy-efficient and lifetime-extended underwater sensor networks," *IEEE Transactions on Mobile Computing*, vol. 9, no. 6, pp. 796–809, 2010.

[8] S. Basagni, V. Di Valerio, P. Gjanci, and C. Petrioli, "MARLIN-Q: multi-modal communications for reliable and low-latency underwater data delivery," *Ad Hoc Networks*, vol. 82, pp. 134–145, 2019.

[9] G. Han, A. Gong, H. Wang, M. Martinez-Garcia, and Y. Peng, "Multi-AUV collaborative data collection algorithm based on Q-learning in underwater acoustic sensor networks," *IEEE Transactions on Vehicular Technology*, vol. 70, no. 9, pp. 9294–9305, 2021.

[10] M. T. Khan, S. H. Ahmed, Y. Z. Jembre, and D. Kim, "An energy-efficient data collection protocol with AUV path planning in the Internet of Underwater Things," *Journal of Network and Computer Applications*, vol. 135, pp. 20–31, 2019.

[11] X. Zhuo, F. Qu, H. Yang, Y. Wei, Y. Wu, and J. Li, "Delay and queue aware adaptive scheduling-based MAC protocol for underwater acoustic sensor networks," *IEEE Access*, vol. 7, pp. 56263–56275, 2019.

[12] G. Han, X. Long, C. Zhu, M. Guizani, and W. Zhang, "A high-availability data collection scheme based on multi-AUVs for underwater sensor networks," *IEEE Transactions on Mobile Computing*, vol. 19, no. 5, pp. 1010–1022, 2020.

[13] A. Khan, M. Khan, S. Ahmed, M. A. Abd Rahman, and M. Khan, "Energy harvesting based routing protocol for underwater sensor networks," *PLoS One*, vol. 14, no. 7, article e0219459, 2019.

[14] N. Goyal, M. Dave, and A. K. Verma, "Data aggregation in underwater wireless sensor network: recent approaches and issues," *Journal of King Saud University-Computer and Information Sciences*, vol. 31, no. 3, pp. 275–286, 2019.

[15] N. Saeed, A. Celik, T. Y. al-Naffouri, and M.-S. Alouini, "Energy harvesting hybrid acoustic-optical underwater wireless sensor networks localization," *Sensors*, vol. 18, no. 1, p. 51, 2018.

[16] I. U. Khan, M. Islam, M. Ismail et al., "Adaptive hop-by-hop cone vector-based forwarding protocol for underwater wireless sensor networks," *International Journal of Distributed Sensor Networks*, vol. 16, no. 9, 2020.

[17] D. Sandeep and V. Kumar, "Review on clustering, coverage and connectivity in underwater wireless sensor networks: a communication techniques perspective," *IEEE Access*, vol. 5, pp. 11176–11199, 2017.

[18] X. Zhuo, M. Liu, Y. Wei, G. Yu, F. Qu, and R. Sun, "AUV-aided energy-efficient data collection in underwater acoustic sensor networks," *IEEE Internet of Things Journal*, vol. 7, no. 10, pp. 10010–10022, 2020.

[19] C.-F. Cheng and L.-H. Li, "Data gathering problem with the data importance consideration in underwater wireless sensor networks," *Journal of Network and Computer Applications*, vol. 78, pp. 300–312, 2017.

[20] C. Lin, G. Han, M. Guizani, Y. Bi, and J. du, "A scheme for delay-sensitive spatiotemporal routing in SDN-enabled underwater acoustic sensor networks," *IEEE Transactions on Vehicular Technology*, vol. 68, no. 9, pp. 9280–9292, 2019.

[21] Z. Hong, X. Pan, P. Chen, X. Su, N. Wang, and W. Lu, "A topology control with energy balance in underwater wireless sensor networks for IoT-based application," *Sensors*, vol. 18, no. 7, p. 2306, 2018.

[22] W. Khan, H. Wang, M. S. Anwar, M. Ayaz, S. Ahmad, and I. Ullah, "A multi-layer cluster based energy efficient routing scheme for UWSNs," *Access*, vol. 7, pp. 77398–77410, 2019.

[23] G. Han, S. Shen, H. Wang, J. Jiang, and M. Guizani, "Prediction-based delay optimization data collection algorithm for underwater acoustic sensor networks," *IEEE Transactions on Vehicular Technology*, vol. 68, no. 7, pp. 6926–6936, 2019.

[24] R. Duan, J. du, C. Jiang, and Y. Ren, "Value-based hierarchical information collection for AUV-enabled Internet of underwater things," *IEEE Internet of Things Journal*, vol. 7, no. 10, pp. 9870–9883, 2020.

[25] S. Chen, Y. Chen, J. Zhu, and X. Xu, "Path-planning analysis of AUV-aided mobile data collection in UWA cooperative sensor networks," in *IEEE International Conference on Signal Processing, Communications and Computing (ICSPCC)*, Macau, China, 2020.

[26] P. Gjanci, C. Petrioli, S. Basagni, C. A. Phillips, L. Bölöni, and D. Turgut, "Path finding for maximum value of information in multi-modal underwater wireless sensor networks," *IEEE Transactions on Mobile Computing.*, vol. 17, no. 2, pp. 404–418, 2018.

[27] P. Xie, Z. Zhou, N. Nicolaou, A. See, J. H. Cui, and Z. Shi, "Efficient vector-based forwarding for underwater sensor networks," *EURASIP Journal on Wireless Communications and Networking*, vol. 2010, Article ID 195910, 2010.

[28] T. Ali, T. J. Low, and A. Sadia, "Flooding control by using angle based cone for UWSNs," in *Proceedings of the 2012 International Symposium on Telecommunication Technologies*, Kuala Lumpur, Malaysia, November 2012.

[29] H. Yu, Y. Nianmin, and L. Jun, "An adaptive routing protocol in underwater sparse acoustic sensor networks," *Ad Hoc Networks*, vol. 34, pp. 121–143, 2015.

[30] N. Javaid, F. Ahmed, Z. Wadud, N. Alrajeh, M. Alabed, and M. Ilahi, "Two hop adaptive vector-based quality forwarding for void hole avoidance in underwater WSNs," *Sensors*, vol. 17, no. 8, p. 1762, 2017.

[31] R. Kumar and N. Singh, "A survey on data aggregation and clustering schemes in underwater sensor networks," *International Journal of Grid and Distributed Computing*, vol. 7, no. 6, pp. 29–52, 2014.

[32] A. Ahmad, N. Javaid, Z. A. Khan, U. Qasim, and T. A. Alghamdi, "$(ACH)^2$ routing scheme to maximize lifetime and throughput of wireless sensor networks," *IEEE Sensors Journal*, vol. 14, pp. 3516–3532, 2014.

[33] G. Yang, D. Lie, and L. Yan, "A secure and energy balanced clustering protocol for underwater wireless sensor networks," in *Proceedings of the 2018 International Conference on Security, Pattern Analysis, and Cybernetics (SPAC)*, Jinan, China, December 2018.

[34] X. Fei, B. Azzedine, and Y. Richard, "An efficient Markov decision process based mobile data gathering protocol for wireless sensor networks," in *Proceedings of the 2011 IEEE wireless communications and networking conference*, Cancun, Mexico, March 2011.

[35] Y.-S. Chen and L. Yun-Wei, "Mobicast routing protocol for underwater sensor networks," *IEEE Sensors Journal*, vol. 13, pp. 737–749, 2012.

[36] J. U. Khan and H. S. Cho, "A data gathering protocol using AUV in underwater sensor networks," in *Proceedings of the OCEANS 2014-TAIPEI*, Taipei, China, April 2014.

[37] N. Javaid, N. Ilyas, A. Ahmad et al., "An efficient data-gathering routing protocol for underwater wireless sensor networks," *Sensors*, vol. 15, no. 11, pp. 29149–29181, 2015.

[38] Y. Noh, U. Lee, P. Wang, B. S. C. Choi, and M. Gerla, "VAPR: void-aware pressure routing for underwater sensor networks," *IEEE Transactions on Mobile Computing*, vol. 12, no. 5, pp. 895–908, 2013.

[39] G. Han, C. Zhang, L. Shu, and J. Rodrigues, "Impacts of deployment strategies on localization performance in underwater acoustic sensor networks," *IEEE Transactions on Industrial Electronics*, vol. 62, no. 3, pp. 1725–1733, 2015.

[40] G. Han, L. Liu, J. Jiang, L. Shu, and J. Rodrigues, "A collaborative secure localization algorithm based on trust model in underwater wireless sensor networks," *Sensors*, vol. 16, no. 2, p. 229, 2016.

[41] L. Bjørnø and M. J. Buckingham, "General characteristics of the underwater environment," in *Applied Underwater Acoustics*, pp. 1–84, Elsevier, Amsterdam, The Netherlands, 2017.

[42] S. Climent, A. Sanchez, J. V. Capella, N. Meratnia, and J. Serrano, "Underwater acoustic wireless sensor networks: advances and future trends in physical, MAC and routing layers," *Sensors*, vol. 14, no. 1, pp. 795–833, 2014.

[43] M. Y. I. Zia, J. Poncela, and P. Otero, "State-of-the-art underwater acoustic communication modems: classifications, analyses and design challenges," *Wireless Personal Communications*, vol. 116, no. 2, pp. 1325–1360, 2021.

[44] Y. Zhang, H. Sun, and J. Yu, "Clustered routing protocol based on improved K-means algorithm for underwater wireless sensor networks," in *Proceedings of the 2015 IEEE International Conference on Cyber Technology in Automation, Control, and Intelligent Systems (CYBER)*, pp. 1304–1309, Shenyang, China, June 2015.

[45] X. Liu, M. Jia, and H. Ding, "Uplink resource allocation for multicarrier grouping cognitive internet of things based on K-means learning," *Ad Hoc Networks*, vol. 96, article 102002, 2020.

[46] P. Arora, S. V. Deepali, and S. Varshney, "Analysis of K-means and K-medoids algorithm for big data," *Procedia Computer Science*, vol. 78, pp. 507–512, 2016.

[47] S. Yousefi, F. Derakhshan, and A. Bokani, "Mobile agents for route planning in internet of things using Markov decision process," in *Proceedings of the 2018 IEEE International Conference On Smart Energy Grid Engineering (SEGE)*, Oshawa, ON, Canada, August 2018.

[48] J. Jagannath, N. Polosky, A. Jagannath, F. Restuccia, and T. Melodia, "Machine learning for wireless communications in the Internet of Things: a comprehensive survey," *Ad Hoc Networks*, vol. 93, article 101913, 2019.

[49] M. Abu Alsheikh, D. T. Hoang, D. Niyato, H.-P. Tan, and S. Lin, "Markov decision processes with applications in wireless sensor networks: a survey," *IEEE Communications Surveys & Tutorials*, vol. 17, no. 3, pp. 1239–1267, 2015.

[50] V. Di Valerio, F. L. Presti, C. Petrioli, L. Picari, D. Spaccini, and S. Basagni, "CARMA: channel-aware reinforcement learning-based multi-path adaptive routing for underwater wireless sensor networks," *IEEE Journal on Selected Areas in Communications*, vol. 37, no. 11, pp. 2634–2647, 2019.

[51] Y. Rizk, M. Awad, and E. W. Tunstel, "Decision making in multiagent systems: a survey," *IEEE Transactions on Cognitive and Developmental Systems*, vol. 10, no. 3, pp. 514–529, 2018.

[52] S. Yousefi, F. Derakhshan, H. Karimipour, and H. S. Aghdasi, "An efficient route planning model for mobile agents on the Internet of Things using Markov decision process," *Ad Hoc Networks*, vol. 98, article 102053, 2020.

[53] M. A. Alsheikh, S. Lin, D. Niyato, and H. P. Tan, "Machine learning in wireless sensor networks: Algorithms, strategies, and applications," *IEEE Communications Surveys & Tutorials*, vol. 16, no. 4, pp. 1996–2018, 2014.

[54] G. Han, H. Guan, J. Wu, S. Chan, L. Shu, and W. Zhang, "An uneven cluster-based mobile charging algorithm for wireless rechargeable sensor networks," *IEEE Systems Journal*, vol. 13, no. 4, pp. 3747–3758, 2019.

[55] R.-H. Hwang, W. Chih-Chiang, and W. Wu-Bin, "A distributed scheduling algorithm for IEEE 802.15.4e wireless sensor networks," *Computer Standards & Interfaces*, vol. 52, pp. 63–70, 2017.

[56] June, 2021, https://www.mathworks.com/matlabcentral/fileexchange/25786-markov-decision-processes-mdp-toolbox.

[57] A. Munir and G.-R. Ann, "An MDP-based dynamic optimization methodology for wireless sensor networks," *IEEE Transactions on Parallel and Distributed Systems*, vol. 23, no. 4, pp. 616–625, 2012.

[58] J. U. Khan and C. Ho-Shin, "A distributed data-gathering protocol using AUV in underwater sensor networks," *Sensors*, vol. 15, no. 8, pp. 19331–19350, 2015.

Hindawi
Wireless Communications and Mobile Computing
Volume 2022, Article ID 7503017, 13 pages
https://doi.org/10.1155/2022/7503017

Research Article

Blockchain-Based Model for Intelligent Supply Chain Production and Distribution

Shurui Gu,[1,2] **Weihwa Pan**,[1] **Tsungting Chung**,[1] **and Xuening Huang**[3]

[1]*Department of Business Administration, National Yunlin University of Science and Technology, Yunlin, 640301 Taiwan, China*
[2]*School of Economics, Guangzhou City University of Technology, Guangzhou, 510800 Guangdong, China*
[3]*Lizhi Inc., Guangzhou, 510630 Guangdong, China*

Correspondence should be addressed to Shurui Gu; gusr@gcu.edu.cn

Received 12 January 2022; Revised 15 February 2022; Accepted 28 February 2022; Published 30 March 2022

Academic Editor: Mohamed Elhoseny

Blockchain is a term in the field of information technology. In essence, it is a shared database, and the data or information stored in it has the characteristics of "unforgeable," "full traces," "traceable," "open and transparent," and "collective maintenance." Based on these characteristics, blockchain technology has laid a solid "trust" foundation, created a reliable "cooperation" mechanism, and has broad application prospects. This paper is aimed at studying a method in view of the integrate of system analysis and system simulation to solve the problems in the production and distribution (P&D) system in the supply chain, proposing a more realistic optimization plan, and then promoting it to various enterprises. This article proposes the idea of using supply chain management, through system analysis, system simulation, case analysis, and comparative research methods, starting from the strategic level, tactical level, and operation level of supply chain management to optimize the P&D system. Pay attention to the P&D system issues in the supply chain environment, and apply the method of system analysis and system simulation to get a better P&D plan. The experimental results of this paper show that the total cost of the supplier selection strategy is 5.204 million yuan, and the delayed delivery rate is 30%. The new reconstruction strategy makes the total cost as low as 3,809,700 yuan, and the total delayed delivery rate is as low as 7%.

1. Introduction

1.1. Background. With the speeded-up of IT transform, Sundry market competition improved global resource reorganization, optimized allocation, and increased uncertainty in supply chain demand forecasts, and the bullwhip effect has been amplified. In addition, the phenomenon of information islands in the supply chain increases the inventory backlog and the difficulty of supply chain system management. In the face of increased randomness of customer demand, reduced delivery lead time, competitive pressure from customer service levels, high-quality product requirements, and improved product supply efficiency, the supply chain urgently needs to adopt a rapid response mechanism to reduce corporate costs and increase economic benefit purpose. Supply chain management is a new management strategy; it integrates different enterprises to increase the efficiency of the whole supply chain, focusing on the cooperation between enterprises. At the same time, scholars have discovered through research that increasing the degree of information sharing between supply chains can effectively suppress the amplification of demand information, the bullwhip effect. This can reduce excess inventory in the supply chain, avoid insufficient production capacity of upstream companies, and optimize operating costs. Manufacturers and distributors make decisions from different angles and can consider problems from various aspects to achieve the best effect of supply chain management.

1.2. Significance. Apply block technology (BT) to optimize supply chain inventory models, explore new supply chain management models, and raise decision makers' cognition of the importance of information sharing and supply chain conformity. Therefore, it is of great practical significance to study how to reduce inventory costs, restrain the time lag of the supply chain, and improve the level of customer

service. It provides a reference for enterprises under supply chain management to make P&D plans, making them a unique competitive advantage in fierce competition and promoting faster and better development of Chinese enterprises in the market economy.

1.3. Related Work. In this dynamic business environment, manufacturers are primarily focused on winning orders by offering performance and competitive prices. Surajit's research shows that manufacturers using flexible procurement systems (FPS) in this uncertain environment are critical to business sustainability. His research goal is to determine the elements of FPS and to simulate the relationships between them and the end to know how FPS is related to supply chain sustainability. In addition to a brief conceptual review of FPS, his research primarily shows the use of an innovative multicriteria decision-making method, named Total Interpretive Structure Modeling (TISM). This overall model based on explanatory structural modeling evaluates causality and explains the elements with relational interpretation and shows that the underlying elements are essential to the sustainability of FPS and risk avoidance [1]. The purpose of Hendalianpour et al.'s research is to assign orders to suppliers in an agile and flexible way suitable for the automotive industry. Parts supplied from a single source are not included in the part collection. Best and worst method of fuzzy rough number by mathematical modeling and interval value (IVFRN-BWM), they try to obtain results that can meet the requirements of the proposed model by introducing new models and provide ideal results. By considering five objective functions, some new aspects of the subject are solved and a robust result is obtained. These functions are included: minimize the production line interruption caused by the supplier's performance, minimize the production line's complaints about the supplied parts, minimize the defective parts (PPM) received from the supplier, and maximize on schedule delivery services. It is also optimized to minimize the total cost of parts supply [2]. In the digital world, everything and products are designed and used with the help of advanced technology. Agriculture is no exception. Wal-Mart has begun to solve food safety issues by using BT in the supply chain. Sharma et al.'s research found that because agriculture is one of the most influential sectors of the world economy, it also has a great impact on people's lives. With the development of the agricultural industry on a global scale, it is difficult to issues to be attached great importance to management information for the entire food supply chain. Therefore, food digitization that can increase transparency, food safety, and customer satisfaction is a top priority. In the context of the Indian economy, there is very little research on the use of BT to solve farmers' problems. Their research will help to solve the main problems of traceability, transparency, quality, and trust in the hybridization of food supply chain management and agriculture through the use of BT [3].

1.4. Innovation. (1) The method of system analysis and system simulation is combined together. Through the organic combination of the two, they can make up for their respective shortcomings and better reflect the actual situation. (2) Using the method of comparative analysis, the data results obtained by the production system and the distribution system are analyzed and compared. The P&D plan obtained through a mixed method is more suitable. It can better reflect the actual situation. (3) Flexible supply chain is more flexible and intelligent, which can save time and cost. At the same time, it is more intelligent to deal with the corresponding supply chain problems and find the unreasonable part of the supply chain immediately.

2. BT-Related Algorithms

2.1. Feasible Byzantine Fault-Tolerant Algorithm. The Feasible Byzantine Fault Tolerant Algorithm (FBFT) is to solve the disorder problem of Byzantine algorithm by introducing master node [4, 5].

Suppose a node belongs to group A, the community key ring $R_A = (pk_1, pk_2, \cdots, pk_n)$, and m is a message to be encrypted, x_i is the secret key, and the community key $pk_i = x_i G$ [5, 6]. The approach of correlative ring cachets is as follows:

Assume the corresponding function, $H_1 : \{0,1\}^* \longrightarrow Z_q$,$H_2 : \{0,1\}^* \longrightarrow G$, and calculate the public key mirror y' as formula (1):

$$y' = x_i H_2(R_A). \tag{1}$$

Generate a random number $\delta \in Z_q$, calculated according to formula (1):

$$c_{i+1} = H_1\left(R_A, y', m, \partial \mathrm{G}, \partial y'\right). \tag{2}$$

In $j = i+1, \cdots, n, 1, \cdots, i-1$, assemble a stochastic number $s_i \in Z_q$, and count c_{j+1} as above (2) can be the following:

$$c_{j+1} = H_1\left(R_A, y', m, s_j G + c_j pk_j, s_j H_2(R_A) + c_j y'\right). \tag{3}$$

Calculate s_i according to formula (3):

$$s_i = \partial - x_i c_i \mod q. \tag{4}$$

Generate signature $\delta_{RG}(m)$ according to formula (4):

$$\delta_{RG}(m) = \left(c_1, s_1, \cdots, s_n, y'\right). \tag{5}$$

The node broadcasts a PREPARE message to the main region node when the ring signature is processed: << PREPARE, v, n, d, $G>$,$\delta_{RG}(m)$, $R_G>$ [7]. When G is the group, if the node is from the A group, it means $G = A$, R_G represents the community key ring of the members of the G group, and $\delta_{RG}(m)$ represents the node's ring signature of the message [8, 9].

2.2. Signature Core Algorithm. In BT systems, signing algorithms are primarily used to verify the legitimacy of a

transaction and the identity information of the transaction sender [10, 11].

A item is flood with n inputs and m outputs and has $\sum_{i=1}^{n} \text{in}_i = \sum_{j=1}^{m} \text{out}_j$. For any i and j, $1 \le i \le n, 1 \le j \le m$, for the purpose of hiding in and out [11, 12]. This article uses an elliptic curve algorithm as protection [12, 13]. Choose G as the generator of F_p, and the transaction forms of in_i and out_j are $I_j = \text{in}_j \cdot G$ and $O_j = \text{out}_j \cdot G$. In line with the calculation rules of elliptic curve, we will know the following [14, 15]:

$$\sum_{i=1}^{n} \text{in}_i \cdot G = \sum_{i=1}^{n} I_i = \left(\sum_{i=1}^{n} \text{in}_i \right) \cdot G, \tag{6}$$

$$\sum_{j=1}^{m} \text{out}_j \cdot G = \sum_{j=1}^{m} O_j = \left(\sum_{j=1}^{m} \text{out}_j \right) \cdot G \tag{7}$$

Through Equations (3) and (4), there is $\sum_{i=1}^{n} I_i = \sum_{j=1}^{m} O_j$, which can verify $\sum_{i=1}^{n} \text{in}_i = \sum_{j=1}^{m} \text{out}_j$, because I_i and O_j are through in_i and out_j [16, 17]. The characteristics and defects of homomorphism in the signature scheme are as follows [18].

In view of the development of quantum computing, homomorphism is an important feature for evaluating the security of algorithms. It can be proved the additive homomorphism of the basic scheme given in formula (7) [19, 20]. Proof: For each i, $1 \le i \le n$, and through the algorithm of elliptic curve, we can get the following:

$$\sum_{i=1}^{n} \text{in}_i \cdot G = \left(\sum_{i=1}^{n} \text{in}_i \right) \cdot G, \tag{8}$$

$$\left(\sum_{i=1}^{n} \text{in}_i \right) \cdot G = \sum_{i=1}^{n} \text{in}_i \cdot G. \tag{9}$$

Further, you can get the following:

$$\left(\sum_{i=1}^{n} \text{in}_i \right) \cdot G = \sum_{i=1}^{n} (\text{in}_i \cdot G). \tag{10}$$

In this article, Equation (10) means that the addition operation is performed first, and then, the encryption operation is performed, and the right side of the equation is the encryption operation first, and then, the addition operation is performed. Express. Therefore, it can be proved that the basic signature format is homomorphic. Because the flexible supply chain model of production and distribution is a single-line model rather than a block model to some extent, only a combination of multiple flexible supply chain models of production and distribution can apply the block chain-related algorithm, so the block chain-related algorithm cannot be used.

3. Establishment of P&D Decision-Making Model under Supply Chain Environment

The systems in the supply chain environment are interconnected and restrict each other. For this reason, in view of the difference between P&D evaluation, it is necessary to establish a fair performance evaluation index system suitable for each field to promote the coordination and connection of P&D in the supply chain. The model only considers the P&D decision-making problem. By establishing this model, the P&D planning problem of the general P&D system can be solved. In a distributed network of flexible supply chains based on BT for P&D, each resource manages its own access strategy only under the control of its owner, resulting in a "decentralized, autonomous organization network" as shown in Figure 1.

3.1. The P&D Decision Model under the Supply Chain Environment

3.1.1. Determination of Variables and Goals of the Decision Model. Production planning and control are mainly the control and process design of the entire manufacturing process, such as material control, scheduling, and inventory control. Distribution and logistics are mainly how to retrieve and deliver products from factories or warehouses to customers. P&D planning is an important factor in the overall optimization of the supply chain, and this problem should be solved under the structure of the overall planning. In order to achieve the overall optimization of the supply chain in the operation process, a supply chain model has been established with deterministic and random methods. However, for the model, it only describes some important factors to be considered in any company and does not propose a specific model to manage the supply chain. The four-tier coordination framework model of the supply chain is shown in Figure 2.

It can be seen from Figure 2 that the supply chain is a complex network formed by the interaction between the nodes of each link. Each link node in the supply chain can be regarded as a separate task agent, such as the management and production, planning, purchase and sale of inadequacy products, and final products by manufacturers. Then, the interaction between elements in the supply chain can be described as autonomous operations between agents. In the agent-based supply chain model, the supply chain can be regarded as a network constituted by a multiagent system. Each agent has certain attributes of research work on the operation mechanism of the four-tier coordination framework of the supply chain based on BT and coevolution and can collaborate with other agents.

3.1.2. Conditional Assumptions of the Decision Model. Input various variables into the model for training, and then, reinput data according to the original data can operate independently, and each part has corresponding tasks to complete. Combining the factors mentioned above, the variables to be considered when establishing the supply chain P&D integration model in this article can be divided into the strategic

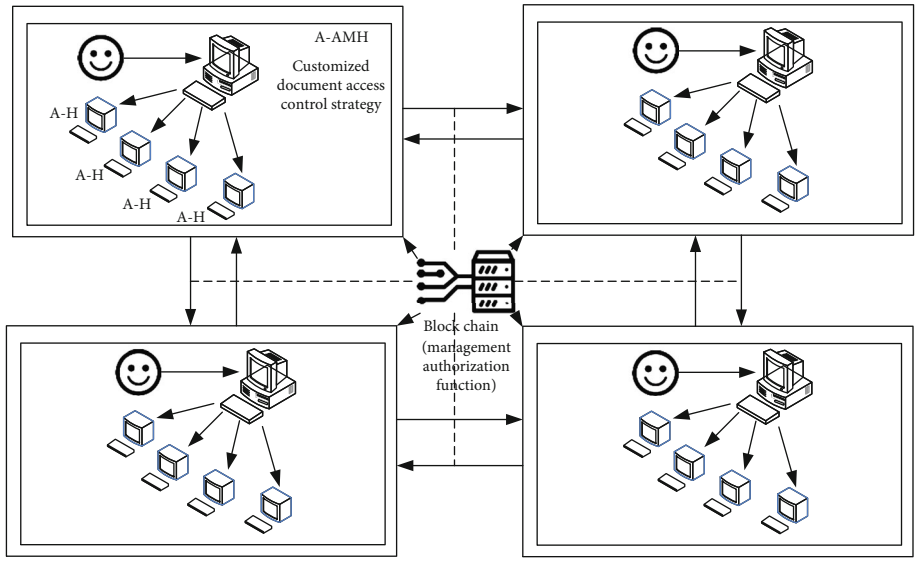

Figure 1: Decentralized supply chain network based on BT P&D flexibility.

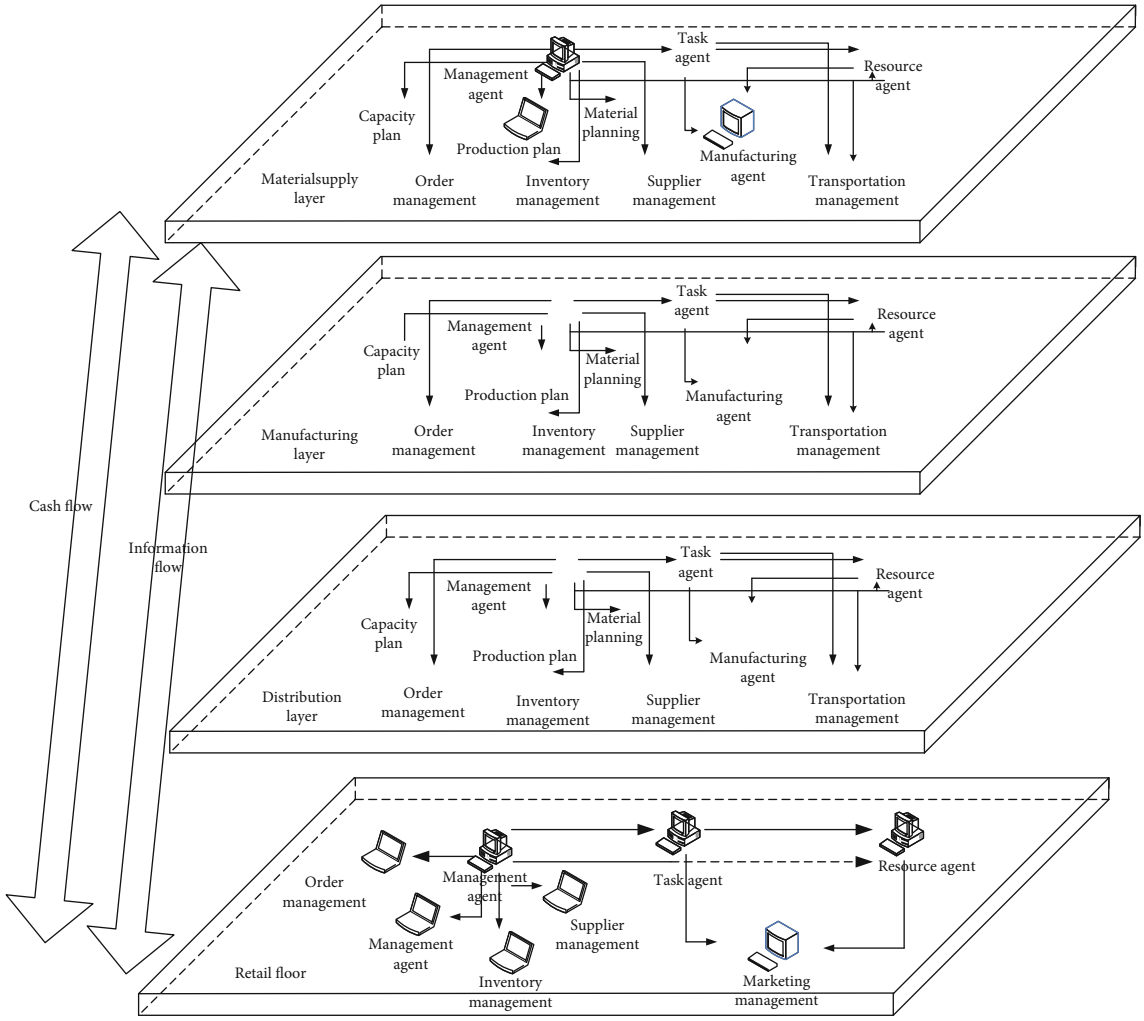

Figure 2: The four-tier coordination framework model of the supply chain.

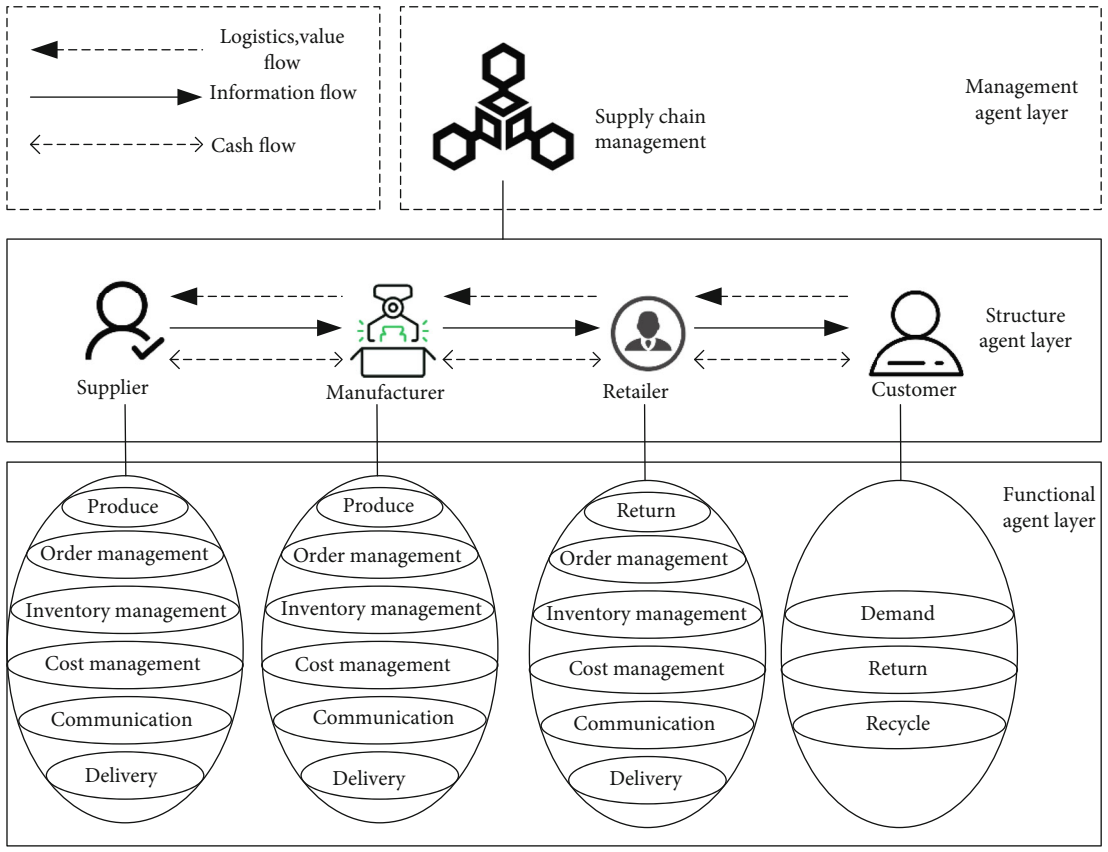

Figure 3: Agent interaction mechanism of each main body of the supply chain.

level and the operational level. The integration and optimization of P&D are to solve strategic optimization problems. The decision variables of the decision model are as follows: the number of raw materials consumed by the production parts and products, the number of final products, the number of finished products at each distribution point, and the factory to each distribution point, each distribution point to each retail, and the total product volume of the supplier. The implementation of the strategic optimization plan requires a detailed operational plan to determine the specific tasks that each member of the supply chain should perform. Only when each member executes the business that should be completed in accordance with the system goal first can the supply chain integration decision played out advantages of the program. Therefore, using the data in the strategy-level decision-making plan can be further applied to the P&D submodels to obtain the specific product order batches, batches, and minimum annual inventory costs of manufacturers and distributors. The detailed plan from the whole to the individual is obtained in this way, and the different subsystems under each entity constitute the functional agent layer. The agent interaction mechanism of each main body of the supply chain is shown in Figure 3.

It can be seen from Figure 3 that each entity agent is composed of the above three types of agents, which are divided according to the working rights of the agents, management agent>task agent>resource agent. The choice of target is the starting point for establishing the model and the key to reflecting the effectiveness of the model. As an important part of the supply chain system, the P&D subsystem has an important function in the actual submission. Its operation status determines the overall target realization status of the supply chain. From a strategic point of view, cost, flexibility, quality, and distribution are not mutually offset but should be optimized at the same time. This is also required by fierce market competition. Just optimizing one of them and sacrificing others will not be conducive to the formation of competitive advantage. Therefore, all factors that affect the decision-making goals must be taken into account. In the entire P&D model studied in this article, cost is also the ultimate goal of optimization. Determine the optimal P&D plan through the optimization of the total cost.

3.1.3. Decision Model Design. According to the previous decision-making parameter selection and model assumptions, the following specific model is established, and the method of system analysis is applied to analyze the model. The system includes two main models: the production system and the distribution system. The objective function is the sum of the P&D system costs of the entire supply chain in the entire cycle. Through the equation description, we can see that the decision-making goal is to decrease the money of P&D. The factors influencing the decision model include the number, location, capacity and type of manufacturing plants and warehouses, supplier selection, and transport channels.

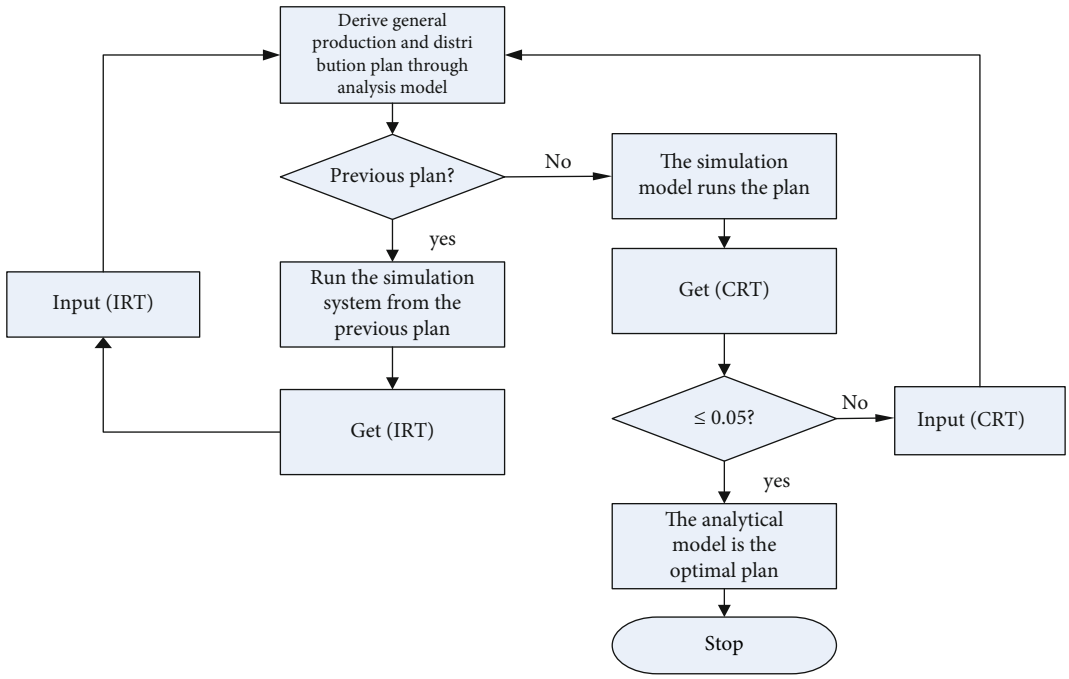

Figure 4: Processing flow based on the hybrid method.

In the production system, the various costs include part i in period t are represented by Equation (11).

$$\sum_{i=1}^{N}\left(ci_{it}X_{it} + hi_{it}li_{it}^{+} + \pi i_{it}li_{it}^{-}\right). \tag{11}$$

Also in the production system, the cost of product j in period t includes production cost, inventory cost, and out-of-stock cost. Due to the product's demand for raw material k, it also includes the purchase cost, inventory cost, and out-of-stock cost of raw material k. The cost is represented by Equation (12).

$$\sum_{j=1}^{M}\left(cj_{jt}Y_{jt} + hj_{jt}li_{it}^{+} + \pi hj_{jt}Ij_{jt}^{-}\right)\sum_{k=1}^{K}\left(ck_{kt}E_{kt} + hk_{kt}Ik_{kt}^{+} + \pi k_{kt}Ik_{kt}^{-}\right). \tag{12}$$

Equation (13) represents the demand cost, inventory cost and out-of-stock cost of raw material r, and the total cost of product j in the distribution system.

$$\sum_{r=1}^{R}\left(cr_{rt}F_{rt} + hr_{rt}Ir_{rt}^{-} + \pi hr_{rt}Ir_{rt}^{-}\right)\sum_{j=1}^{M}\left(SL_{jt}L_{jt}^{+} + SLL_{jt}L_{jt}^{-}\right). \tag{13}$$

Equation (14) represents the sum of the inventory cost and the out-of-stock cost of product j in the distribution system and product j in warehouse q.

Table 1: Product demand plan.

Prt(j)	Cyl(t)			
	a	b	c	d
A	80	80	60	0
B	60	70	60	0

$$\sum_{j}^{M}\sum_{p}^{P}\left(SP_{jpt}P_{jpt}^{+} + SPP_{jpt}P_{jpt}^{-}\right) \tag{14}$$

The sum of the total inventory cost and out-of-stock cost of retailer j in the distribution system is represented by Equation (15).

$$\sum_{j}^{M}\sum_{q}^{Q}\left(SQ_{jqt}Q_{jqt}^{+} + SQQ_{jqt}Q_{jqt}^{-}\right). \tag{15}$$

After the product manufacturer comes out, it is transported to the warehouse by means of transportation. There is a buffer area in between, from which the product can be directly delivered to the retailer. Equation (16) expresses the total transportation cost of the product from the buffer area to the warehouse.

$$\sum_{j}^{M}\sum_{p}^{P}LPC_{p}LP_{jpt}. \tag{16}$$

Table 2: Production route.

Cpt(i) Workshop 1	Ord			Product(j)	Ord Workshop 2		
A	WD1-1	WD2-1	WD3-1	A	WD1-2	WD2-2	WD3-2
B	WD1-1	WD2-1	WD3-1	B	WD1-2	WD2-2	WD3-2

Table 3: Production process time (minutes).

Components(i)	Machine center(u)			Components(i)	Machine center(v)		
	1	2	3		1	2	3
1	1	1	1	1	3	6	4
2	1	1	1	2	4	7	5

Equation (17) expresses the total transportation cost of the product from the buffer area to the retailer.

$$\sum_{j}^{M}\sum_{q}^{Q} LQC_q LQ_{jqt}. \tag{17}$$

Equation (18) represents the total cost of transportation.

$$\sum_{j}^{M}\sum_{p}^{P}\sum_{q}^{Q} PQC_{pq} PQ_{jpqt}. \tag{18}$$

3.2. Solution Method of Decision Model. The model established in this article is a very typical linear programming model, which can be calculated in the linear programming model software. The product production quantity obtained by the optimal solution integration optimization is used as the input variable of the operation-level supplier, manufacturer, and distributor model. The result of the integration and optimization is the quantity of raw materials provided by the supplier to the manufacturer, the quantity of products produced by the manufacturer and the quantity of product inventory, and the quantity of products demanded by the retailer. The transportation volume of the product, the retailer's setting, and the retailer's service to the user area will be the input variables of the distributor level, which restricts the optimization result of the distributor level. These results are substituted into the model formula for calculation. The P&D model is already similar to the decision model for determining the economic order quantity, and the corresponding results can be obtained by the same method. Thereby, the decision result of the whole system in the least cost situation is finally determined. Specific in-depth analysis of the results can be aimed at specific instance data, which is helpful to discover deeper information. Specific examples will be analyzed and verified in the next chapter. Production resources need to be provided by suppliers. In the supply chain, various suppliers need to take detailed resource consideration in order to achieve maximum benefits.

4. Simulation Analysis of Supply Chain P&D Decision Model

The mixed research method of analysis and simulation is a combination of independent analysis models and simulation models to get their own solutions, and finally, the combined solutions are combined to meet the needs of the problem. In this article, first select a rough analysis model, and use it to obtain the output variables of the plan as input variables of the simulation model. The processing flow of the hybrid method is shown in Figure 4.

It can be seen from Figure 4 that the operating time in the simulation model will be used as the running time of the system simulation. It will run through the entire simulation process. It is also the time it takes to produce all products and distribute these products in the analysis model. We will use the running time in the simulation model for operating time in the analysis model. Thence, the operating time in the analysis model is the result of the simulation system, and the analysis model derives a new P&D plan based on this time. And this model also includes the function of predicting production and distribution decisions to promote the balance of supply and marketing. Supply chain is a network line, and the combination of multiple supply chains is a network structure. This process will end when the previous simulation run time (preceding simulation runtime) is close enough to the current simulation run time (current simulation runtime). If they are close enough, we believe that the real situation can be learned through analytical models and simulation experiments, so we can obtain the optimal P&D plan that can well reflect the reality through the analysis model.

4.1. Case Analysis. In the context of supply chain, manufacturers are producing products and distribution is carried out through logistics and express delivery industry. Therefore, supply chain management model can better promote the optimization of production and distribution routes and processes. The purpose of the abovementioned joint research method based on analysis and simulation is to be applied to the P&D system under supply chain management, so as to minimize the cost of the entire P&D system. The distribution system consists of a buffer area, two warehouses, and

Table 4: The number of parts and raw materials required and the number of parts required for raw materials.

Components(i)	Product(j)		Raw materials(k)	Components(i)		Raw materials(k)	Product(j)	
	1	2		1	2		1	2
1	4	4	1	5	7	1	4	5
2	6	6	2	6	4	2	4	3

three retailers. The products are transported to the retailer by a set of transportation vehicles according to the route. In the initial stage, each cycle of the system is 4300 units of time. This time is calculated by the P&D of a certain batch of products. Under the constraints of production capacity and inventory balance, this plan minimizes the sum of production costs, distribution costs, inventory costs, and out-of-stock costs. The following table will give some data required by the production system. The product demand plan is shown in Table 1, and the production route is shown in Table 2.

In the following analysis process of this article, the idea of supply chain management is applied. The production system and the distribution system are considered as a whole. They are both interrelated and affect each other. The decision of any system will affect the decision of the whole system.

First, the simulation model under fixed variables will be analyzed, that is, the damage and maintenance of machines and transportation tools will not be considered.

Secondly, the simulation model under random variables will be analyzed. Through the setting of the functional variables of the machine and the means of transportation, it will obey the normal and exponential distributions.

The traditional supply chain is unable to flexibly rotate the supply route of products, which requires a lot of time cost and transportation cost, while the flexible supply chain is more flexible and intelligent and can operate autonomously to a certain extent. In the model, we assume that there is no quality problem with raw materials. At the same time, we also assume that the inventory capacity in the buffer area is sufficient. Retailers can get products from the buffer area at any time. Retailers are satisfied with the quality of the products. The production process time is shown in Table 3, and the required quantity of parts and raw materials and the required quantity of parts for raw materials are shown in Table 4.

The data required for the model is listed in the chart. In the distribution system, the retailer's demand for products and the distribution time and inventory cost data according to the route will be given in the following four tables. We assume that the inventory capacity of warehouses and retailers is sufficient, and similarly, the inventory capacity in the buffer area is also sufficient. Retailers' demand for products is shown in Table 5, and the transportation time requirements of products in the distribution system are shown in Table 6, and the inventory and out-of-stock costs of products in the distribution system are shown in Table 7.

According to the analysis method, the simulation model concludes that the P&D plan runs in a given period to meet customer needs. The running time of the simulation will be used as the actual operating time in the analysis model for further research.

4.2. Simulation Model Research of Fixed Variables. In the first computer simulation experiment, this article carried out a simulation model without random variables. In other words, the simulation model fails to reflect the random situation in reality, such as random machine failure or repair time. The operating time is used as a fixed variable. The detailed description process is shown in Figures 5 and 6.

Table 5: Retailers' demand for products.

Cyl(t)		A		B		C	
Prt(j)		a	b	a	b	a	b
Retailer	1	30	30	20	25	20	30
	2	25	15	30	25	20	15
	3	20	15	30	20	20	15

Table 6: Transportation time requirements of products in the distribution system (minutes).

Warehouse	1	2	Retailer	1	2	3	Retailer	1	2	3
Buffer	15	20	Buffer	40	35	50	Warehouse	25	30	25

Table 7: Inventory and out-of-stock costs of products in the distribution system.

Cyl(t)		A		B		C	
Prt(j)		a	b	a	b	a	b
Buffer		3 (5)	2 (6)	2 (7)	3 (8)	3 (5)	2 (6)
Whs	1	3 (8)	4 (6)	4 (8)	3 (7)	3 (6)	3 (8)
	2	5 (9)	5 (9)	4 (8)	5 (7)	4 (6)	4 (8)
Rtler	1	2 (8)	4 (7)	2 (5)	4 (6)	3 (8)	4 (6)
	2	3 (8)	3 (7)	4 (7)	5 (7)	4 (6)	4 (7)
	3	4 (9)	2 (5)	3 (8)	2 (5)	4 (5)	5 (5)

As shown in Figure 5, we will find that the operating time of each cycle fluctuates up and down, but we will also find that the amplitude of the fluctuations gradually becomes smaller as the cycle repeats. It shows that as the simulation model runs multiple times, and the operating time gradually tends to a fixed value.

As shown in Figure 6, the different rate of operation time is gradually decreasing as the cycle repeats. Moreover, from Figure 6, we will also find that the difference rate is less than or equal to 5% after the 12th repeat point. At the same time, we will accept the production distribution plan with the 12th repeat point as the operating time as the optimal production plan.

4.3. Simulation Model Research of Random Variables. The combination of supply chain management and model parameter selection is to optimize the route of supply chain. The best optimal distribution scheme can be found in the distribution of goods in the supply chain. The above simulation model does not take into account the random damage and repair time of machines and vehicles. The next model will add these random variables. For the random use of machines and vehicles, we assume that the obey period of machines and vehicles is the exponential distribution of 500 hours, while the maintenance time obeys the normal distribution of 20 hours and 2 hours.

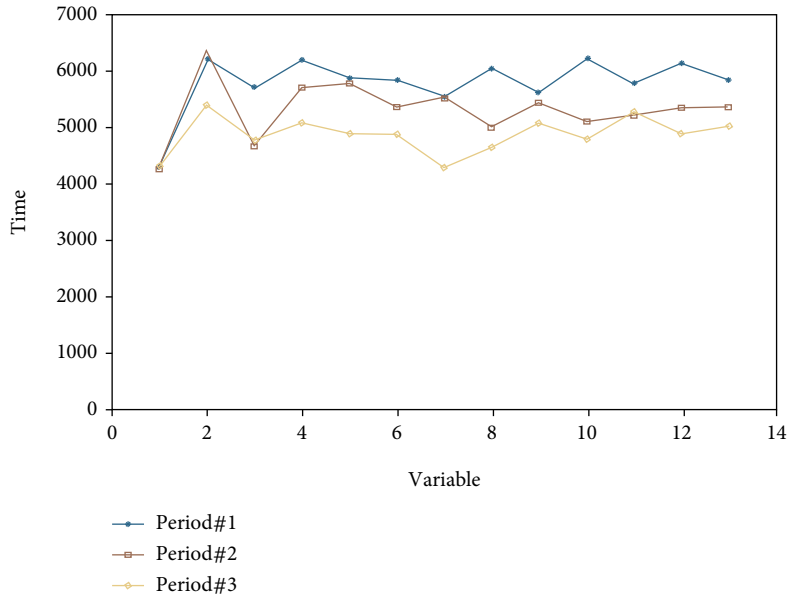

Figure 5: Operating time of each cycle based on the fixed variable simulation model.

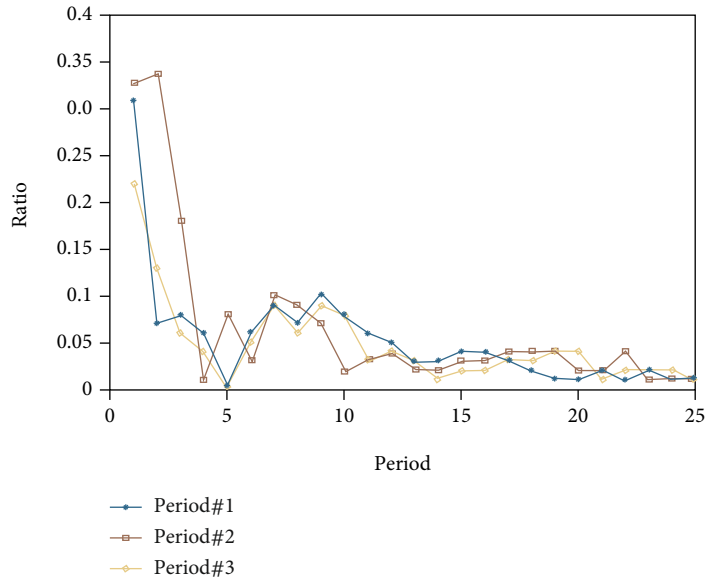

Figure 6: The different rates of operating time in each cycle based on the fixed variable simulation model.

When we think that random phenomena fail in the model, we will run the model more times in order to get the running time. In the research of this article, the average operating time is obtained by running the model multiple times. Although it cannot be guaranteed to be very accurate, it can be guaranteed that the obtained operating time is within the normal range of values under repeated operation. The specific process description is shown in Figures 7 and 8.

From Figures 7 and 8, we can see that the production system under random conditions and the production system under fixed conditions have not changed much. Also in the different rates of operating time, the simulation model under random conditions is not significantly different from the simulation model under fixed conditions. From the figure, we will find that the difference rate is less than 5% after the 22nd repeat point, so we will accept the 22nd repeat point as the operating time as the time point for formulating the optimal production plan in the analysis model. Through the analysis model, we can get the production, inventory, and distribution of products in the P&D system. The integration of production and sales is a vertical sales system that combines production enterprises and selected sales enterprises in the form of joint operation.

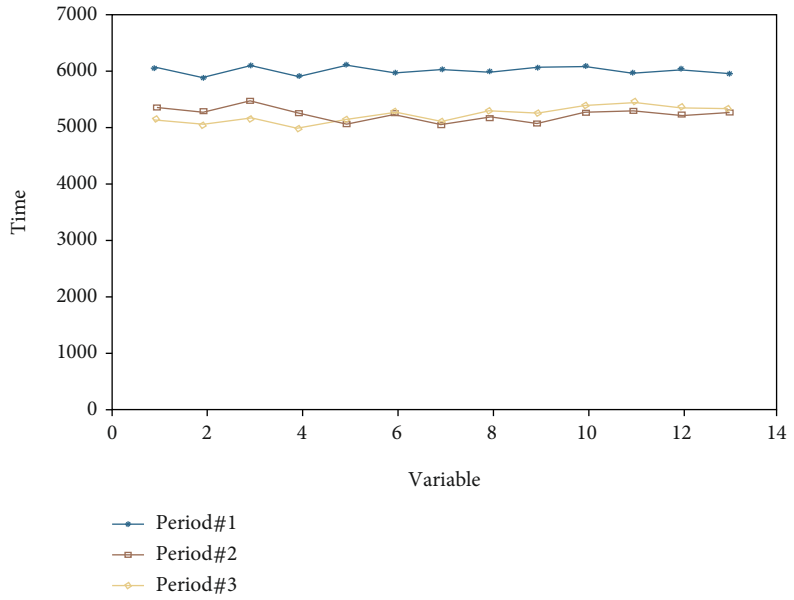

Figure 7: Operating time of each cycle based on random variable simulation model.

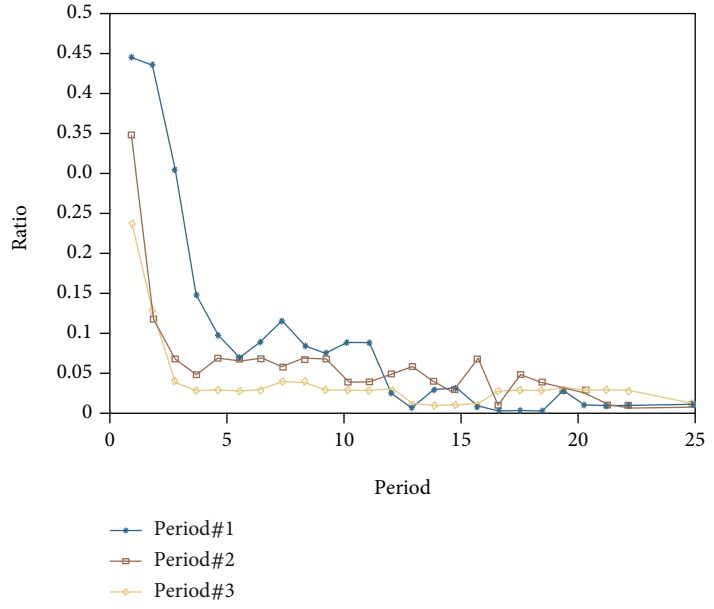

Figure 8: The different rates of operating time in each cycle of the simulation model based on random variables.

5. Conclusions

The thesis mainly applies the management ideas of supply chain. First, it analyzes the P&D system in the supply chain environment through the method of system analysis, and through the further study of the model, it is found that the system analysis method does not reflect the reality well, and the operation time is total. It appears as a fixed value, and system simulation can make up for this shortcoming. Therefore, this paper proposes a combined analysis method of system analysis and system simulation. The data obtained through system simulation is applied to the analysis model, and then, the system analysis method is used to study the P&D system. The following conclusions are obtained: The comprehensive idea of supply chain management can reflect the relationship between overall efficiency and local efficiency and reflect the interdependence and interaction between overall efficiency and local efficiency. Although the independent decision-making of the parties can achieve the optimal, the overall decision-making is more effective.

It is not only a simple summation of the system, but also the utility of the mutual cooperation. In establishing the supply of chain management, in order to benefit the research of this article, this article puts forward some assumptions, so in the decision-making model, the operation time is always regarded as a fixed variable. Therefore, it cannot effectively reflect the actual dynamic characteristics, including machine damage and vehicle damage. Therefore, the P&D plan obtained only by the system analysis method cannot reflect the actual situation well; based on the problems of the system analysis method, the system simulation method can well reflect the dynamic and randomness of the system, and it just makes up for the system analysis method. For the shortcomings, this paper proposes a combined method of system analysis and system simulation to study the P&D system. Apply system simulation for simulation operation, and compare actual operation time through a large amount of data and graph comparison. Reuse the system analysis method to get the optimal P&D plan. However, the researcher in this paper cannot take many uncertain factors into account, so it is hoped that future research can take these uncertain factors into account.

The problems faced by artificial intelligence cannot be solved by traditional technologies. It may be a wise choice to turn to blockchain, which is also an emerging technology. Under the premise of data centralization, there is also a lack of transparency in how data is used. When data providers cannot effectively manage their own data, many people choose not to share data. And blockchain can solve this problem. On the chain, the uploader, usage flow, and results of each piece of data can be traced. Users have ownership and autonomous right to use the data. The data uploader will also receive the digital cryptocurrency provided by the user as compensation. When the user can realize the data generated by himself and control the flow of the data, it is believed that more people will be willing to provide relevant data. For AI, secure data sharing means more data, then better models, better actions, better results, and better new data. Faced with the high cost of computing power, the AI industry may be helpless, but the most important thing in blockchain is probably computing power. Mining is an extremely difficult task that requires a lot of electricity and money to lay out computing power to complete. Redundant computing power can completely save costs for AI. In turn, AI has been proven to be an effective means of optimizing power consumption, providing similar solutions for application in blockchain. This may lead to lower investment in mining hardware. Blockchain can bring bright prospects for the artificial intelligence industry, and artificial intelligence can in turn cheer the blockchain.

Data Availability

No data were used to support this study.

Conflicts of Interest

The authors declare that they have no conflicts of interest.

References

[1] B. Surajit, "Flexible procurement systems is key to supply chain sustainability : original research," *Journal of Transport & Supply Chain Management*, vol. 10, no. 1, pp. 1–9, 2016.

[2] A. Hendalianpour, M. Fakhrabadi, X. Zhang et al., "Hybrid model of IVFRN-BWM and robust goal programming in agile and flexible supply chain, a case study: automobile industry," *IEEE Access*, vol. 7, no. 99, pp. 71481–71492, 2019.

[3] A. Sharma, D. Jhamb, and A. Mittal, "Food supply chain traceability by using BT," *Journal of Computational and Theoretical Nanoscience*, vol. 17, no. 6, pp. 2630–2636, 2020.

[4] A. Shireesh, Nikolai, and Petrovsky, "Will BT revolutionize excipient supply chain management?," *Journal of Excipients and Food Chemicals*, vol. 7, no. 3, pp. 76–78, 2016.

[5] Y. S. Chin, H. V. Seow, S. L. Lai, and R. K. Rajkumar, "Fuzzy mathematical model for solving supply chain problem," *Journal of Computer & Communications*, vol. 6, no. 9, pp. 73–105, 2018.

[6] L. Huang, J. S. Song, and J. Tong, "Supply chain planning for random demand surges: reactive capacity and safety stock," *Operations Research*, vol. 57, no. 5-6, pp. 445–447, 2017.

[7] M. Matsui, "A management game model: economic traffic, leadtime and pricing setting," *Journal of Japan Industrial Management Association*, vol. 53, no. 1, pp. 1–9, 2017.

[8] I. Kazemian and S. Aref, "Multi-echelon supply chain flexibility enhancement through detecting bottlenecks," *Global Journal of Flexible Systems Management*, vol. 17, no. 4, pp. 357–372, 2016.

[9] L. Hatani, H. Bua, D. Sidu, and L. O. Geo, "Development model of cacao agro-industry with sectoral competitive advantage based in Southeast Sulawesi, Indonesia," *Global Journal of Flexible Systems Management*, vol. 17, no. 2, pp. 229–246, 2016.

[10] K. Kume and T. Fujiwara, "Production flexibility of real options in daily supply chain," *Global Journal of Flexible Systems Management*, vol. 17, no. 3, pp. 249–264, 2016.

[11] L. Jardim, S. Pranto, P. Ruivo, and T. Oliveira, "What are the main drivers of block chain adoption within supply chain? – an exploratory research," *Procedia Computer Science*, vol. 181, no. 2, pp. 495–502, 2021.

[12] K. Sato and N. Takezawa, "Dynamic inventory control model with flexible supply network," *Journal of the Operations Research Society of Japan*, vol. 61, no. 2, pp. 217–235, 2018.

[13] K. Pant, A. R. Singh, U. Pandey, and R. Purohit, "A multi echelon mixed integer linear programming model of a close loop supply chain network design," *Materials today: proceedings*, vol. 5, no. 2, pp. 4838–4846, 2018.

[14] X. Bai and Y. Liu, "Robust optimization of supply chain network design in fuzzy decision system," *Journal of Intelligent Manufacturing*, vol. 27, no. 6, pp. 1131–1149, 2016.

[15] Y. N. Huddar, P. P. Kumatagi, and M. R. Latte, "Digital supply chain management- a review," *IARJSET*, vol. 4, no. 1, pp. 34–37, 2017.

[16] M. Sherafati and M. Bashiri, "Closed loop supply chain network design with fuzzy tactical decisions," *Journal of Industrial Engineering International*, vol. 12, no. 3, pp. 255–269, 2016.

[17] Y. Wang, "Research on supply chain financial risk assessment based on block chain and fuzzy neural networks," *Wireless Communications and Mobile Computing*, vol. 2021, 8 pages, 2021.

[18] J. Li, N. Yu, Z. Liu, and L. Shu, "Optimal rebate strategies in a two-echelon supply chain with nonlinear and linear multiplicative demands," *Journal of industrial and management optimization*, vol. 12, no. 4, pp. 1587–1611, 2016.

[19] T. Rodrigues, "BTaplicado a supply chain / BTapplied to supply chain," *Brazilian Journal of Development*, vol. 7, no. 3, pp. 28166–28178, 2021.

[20] L. Al, "The application of block chain in supply chain industry," *Turkish Journal of Computer and Mathematics Education (TURCOMAT)*, vol. 12, no. 3, pp. 1400–1408, 2021.

Hindawi
Wireless Communications and Mobile Computing
Volume 2023, Article ID 9835251, 1 page
https://doi.org/10.1155/2023/9835251

Retraction

Retracted: Dynamic Data-Driven Modelling of Water Allocation for the Internet of Things

Wireless Communications and Mobile Computing

Received 8 August 2023; Accepted 8 August 2023; Published 9 August 2023

This article has been retracted by Hindawi following an investigation undertaken by the publisher [1]. This investigation has uncovered evidence of one or more of the following indicators of systematic manipulation of the publication process:

(1) Discrepancies in scope
(2) Discrepancies in the description of the research reported
(3) Discrepancies between the availability of data and the research described
(4) Inappropriate citations
(5) Incoherent, meaningless and/or irrelevant content included in the article
(6) Peer-review manipulation

The presence of these indicators undermines our confidence in the integrity of the article's content and we cannot, therefore, vouch for its reliability. Please note that this notice is intended solely to alert readers that the content of this article is unreliable. We have not investigated whether authors were aware of or involved in the systematic manipulation of the publication process.

Wiley and Hindawi regrets that the usual quality checks did not identify these issues before publication and have since put additional measures in place to safeguard research integrity.

We wish to credit our own Research Integrity and Research Publishing teams and anonymous and named external researchers and research integrity experts for contributing to this investigation.

The corresponding author, as the representative of all authors, has been given the opportunity to register their agreement or disagreement to this retraction. We have kept a record of any response received.

References

[1] Z. Du and Z. Dong, "Dynamic Data-Driven Modelling of Water Allocation for the Internet of Things," *Wireless Communications and Mobile Computing*, vol. 2022, Article ID 4581734, 8 pages, 2022.

Hindawi
Wireless Communications and Mobile Computing
Volume 2022, Article ID 4581734, 8 pages
https://doi.org/10.1155/2022/4581734

Research Article

Dynamic Data-Driven Modelling of Water Allocation for the Internet of Things

Zhong Du[1,2] **and Zengchuan Dong**[1]

[1]*College of Hydrology and Water Resources, Hohai University, Nanjing, China*
[2]*Hydrology and Water Resources Survey Bureau of Liaoning Province, Shenyang, China*

Correspondence should be addressed to Zhong Du; duzhongvip@hhu.edu.cn

Received 11 January 2022; Revised 25 February 2022; Accepted 5 March 2022; Published 27 March 2022

Academic Editor: Mohamed Elhoseny

The allocation of water resources is an important aspect of maintaining public security, but there are still many problems in water resources management. The application of IoT technology in water resources management mainly focuses on water quality detection and water flow monitoring. For the allocation of water resources, the application of the Internet of things technology is not deep and sufficient, and the advantages of the Internet of things technology in water resources management are not fully utilized. In view of the above problems in the current situation, this paper proposes solutions for smart water resources. Smart water resources combine geographic information technology and Internet of things technology to visualize a map of water resources and realize the whole process management from the source to the end user and automatic data collection and analysis. Therefore, an intelligent system with remote control function is constructed, which can be applied to the practice of water resources allocation and realize the full utilization of water resources.

1. Introduction

Water resources allocation is an important aspect of people's livelihood projects and is the basis for the rapid development of the regional economy and an important guarantee. At present, there are many problems in China's water resources, mainly in the following aspects: firstly, the lack of urban water resources and the lack of township water resources carrying capacity; secondly, the safety of water quality is not fully guaranteed; thirdly, the informatization construction level of water conservancy enterprises is low, and the practicability is low; and finally, water conservancy enterprises have complex business and large amount of data. [1]. Most of the existing digital management systems for water resources equipment focus on the real-time monitoring of water resources equipment and the establishment of a supervisory control and data acquisition (SCADA) system for water resources, but the real-time monitoring system does not combine with geographic information technology and cannot be visualized on a map [2]. The existing SCADA systems are not integrated with geoinformation technology and cannot visualize the location of water resources facilities and networks on a map [3]. In addition, the existing SCADA system does not provide early warning, analysis, remote control, and other functions, and cannot achieve the level of intelligence, which leads to inefficient management of water resources in companies [4].

Information silos is a common phenomenon in the current process of implementation in various industries. To break the dilemma of information isolation without sharing, the project team proposed a set of effective sharing mechanisms for water resources data based on theories and methods related to the digital transformation of government in the literature [5]. On this basis, a water resources data resource sharing process is constructed. Data sharing within the industry should follow the relevant requirements of the Ministry of Water Resources for data resources management. A unified catalogue of water resources should be established, updated in a timely manner at a predetermined frequency, and data sharing at different levels within the industry should be achieved using the system docking, online querying, online browsing, or calling online services.

At the operational level, the provincial water resources information technology departments should build a water resources data warehouse in the government cloud, including business thematic data warehouses and public data warehouses, while developing a data sharing and exchange platform [6].

Sort out and exchange data related to water resources management departments according to the requirements of water resources management departments. If the data has been integrated, it can be shared through the data sharing platform [7]. If the data has not been summarized, the demand can be submitted through the data sharing platform, and then, the submitted water resources data can be reviewed. In the process of data review, the data processing department confirms the integrity and standardization of data items and relevant elements and associates them with the corresponding directory in the water resources data sharing platform to form a database and to realize data collection, classification, and sharing [8]. Data sharing outside the industry should follow the national and provincial government public data management rules and rely on the public data sharing and exchange platform built at the provincial level. High-frequency data that are used by all departments should be collected, and a unified data sharing mechanism should be established to achieve data reuse [9].

The application of Internet of things technology in water resources management mainly focuses on the detection of water quality and the monitoring of water flow. For the allocation of water resources, the application of Internet of things technology is not deep and full, and it does not give full play to the advantages of Internet of things technology in water resources management.

Based on the above problems in the current situation, this paper proposes a solution for smart water resources. Intelligent water resources combines geographic information technology and Internet of things technology, water resources visualization a map to achieve the whole process management from the source to the end user, and the automatic collection and analysis of data; so as to build intelligent systems with remote control functions, it can be applied to the allocation practice of water resources to realize the full utilization of water resources [10].

The structure of this paper is as follows: In Section 2, the basic techniques will be introduced. In Section 3, the intelligent water resources allocation system is illustrated. In Section 4, an optimal configuration model is introduced. In Section 5, this work will explain the system performance validation. In Section 6, the conclusion is given.

2. Basic Techniques

2.1. Real-Time Sensing for IoT. IoT is an inevitable product of the development of Internet technology and sensing technology into the modern era [11]. The massive amount of data collected by manpower in the past is a huge workload and has low collection frequency, and IoT sensing in real time can solve these problems. In the whole process of water resources, the types of sensors mainly include water quality monitoring sensors in reservoirs, water wells, river water sources, water level monitoring sensors, water flow, and pipeline pressure sensors installed on the transmission pipeline, as well as pressure, flow, and water quality sensors in water plants and booster stations [12]. These sensing devices can replace the manual collection of the status of important points on the entire water resources loop in real time to ensure water resources pressure and water quality safety [13].

2.2. Geographic Information Support. The introduction of geoinformation technology has changed the original management mindset of the water resources industry. Managers entering the system are able to see all water resources related information (water sources, water resources equipment, booster pumping stations, transmission pipelines, and water plants [14]) on a map and manage them by means of a map, while real-time monitoring data is also easily and quickly displayed on the map. The system's statistical analysis functions provide auxiliary decision support for the relevant work and can be used in conjunction with the work for scheduling and file management [15].

2.3. Multiple Data Fusion. The unified storage and management of basic spatial data, attribute data, and operation and management data of various types of water resources facilities require the establishment of a unified database management system. The comprehensive database of water resources network is an important support for the whole digital system and is the basis for storing, managing, and sharing various types of data [16].

The data content of the water resources pipeline database includes images, topography and other basic geographic information data, key urban address data, and water resources facilities and pipeline network data [17]. The topographic data mainly includes basic geographic data related to or adjacent to the pipeline (survey control points, independent features, topography, roads and water systems and other ancillary facilities, fences, and the above elements and notes); water resources facilities and pipeline data refer to graphical data of water resources pipelines and related facilities information, mainly obtained through pipeline detection and survey, mainly including X, Y, material, ancillary materials, ground elevation, bottom elevation, top elevation, burial method, pipe diameter, depth of burial, construction date, ownership unit, connection direction, and other attributes [18].

2.4. Big Data Analytics to Support Decision-Making. The system database covers the geographical information data of a city or even a province, but also the water resources business, water resources pipeline network, and facilities' distribution data of the whole region, as well as the attribute data of various types of basic equipment and facilities. In the water resources management system, through the application of Internet technology, the sensor can receive important information such as water quantity, pressure, and water quality in real time, and the video data will not be interrupted. On the server side, the use of cloud storage and cloud computing model can realize large-scale data management and data

mining analysis, which provides decision support for water resources allocation management [19].

Big data analysis focuses on visual analysis of big data, optimization of data mining algorithms, data inspection, and data management, to improve the speed of data access while safeguarding the quality of data and data presentability [20].

3. Intelligent Water Resources Management and Allocation System Construction

3.1. Overall Design. The core of intelligent water resources allocation and management is to integrate existing resources and improve the comprehensive benefits of water resources allocation and management. In terms of the realization of the overall function, it meets the requirements of water resources monitoring, water resources prediction, water resources allocation, water supply prediction, water demand prediction, and water balance analysis. At the specific application level, realize water quality monitoring, tank farm water resource dispatching, domestic water dispatching, and optimal allocation of water resources. In order to build an intelligent water resources allocation and management system, it is also necessary to configure basic water conservancy facilities and relevant technical support. The overall framework is shown in Figure 1.

3.2. Design and Implementation of System Functions. The management of urban water resources pipelines is one of the most important aspects of urban infrastructure management [21]. The intelligent water resources management and allocation platform are a comprehensive system integrating a large database, complex professional models, and advanced software and hardware systems, mainly including the construction of a comprehensive database, application support platform, application software development, and the construction of related hardware platforms [22].

The GIS system of water resources network inputs all pipelines, equipment (pumps, valves, etc.), and structures (ponds, water towers, etc.) in the water resources system into the system; records static information (buried depth, material, age, diameter, connection, and purpose); provides graphic display and query positioning functions; and provides basic support for pipe network modeling, water resources dispatching, equipment maintenance, pipeline rupture treatment, engineering construction, and water quality management. The GIS system is equipped with global positioning system (GPS) interfaces and equipment to quickly measure and locate all pipelines and equipment in the water resources system [23].

The inspection and maintenance system are shown in Figure 2.

The water resources network inspection subsystem provides a full process, refined, and standardized management model. The inspection is carried out using a combination of handheld devices and the web, which allow for timely communication between the site inspectors and the monitoring center. In the inspection process, field personnel log in to the system via handheld devices, obtain the inspection route of the pipe network, make a record of the inspection for the day according to the agreed route, and combine with the GPS navigation function; the inspection personnel can quickly and easily find the equipment to be inspected, check the usage status of the equipment in real time, and upload it to the monitoring center in a timely manner, while the management personnel of the monitoring center can query and audit the inspection details and statistics by logging in to the web system. The management of the monitoring center can query and audit inspection details and statistics by logging into the web system, and can also send out urgent tasks, which can be quickly handled by the on-site inspectors upon receipt. The intelligent water resources management and allocation system improve the efficiency of water resources management and allocation with perfect functions and convenient operation.

4. Construction of an Optimal Configuration Model

Based on the water resources situation and the national economic and social development plan of the city, the minimum regional water shortage indicates the optimal social benefits, and the maximum regional net benefits indicate the optimal economic benefits.

The optimal social benefit objective function is calculated as

$$\min f_1(X) = \min \left\{ \sum_{k=1}^{K} \sum_{j=1}^{J(k)} \left[\varphi_j^k - \sum_{i=1}^{I(k)} X_{ij}^k \right] \right\}, \quad (1)$$

where J is the number of water sectors; φ_j^k is the water demand of user j in subregion k source i to user j in subregion k. Optimal economic efficiency objective function is calculated as

$$\max f_2(X) = \max \left\{ \sum_{k=1}^{K} \sum_{j=1}^{J(k)} \left[\left(b_{kj} - c_{kj} \right) \sum_{i=1}^{I(k)} X_{ij}^k \alpha_i^k \lambda_j^k \right] \right\}, \quad (2)$$

where $f_2(X)$ is the net benefit for user j in subzone k; c_{kj} is the water cost for user j in subzone k; α_i^k is the water sequencing factor from source i to subzone k; and λ_j^k is the priority water factor for user j in subzone k.

Based on the regional planning annual water supply and demand forecasts and development plans, and taking into account the total water use control and efficiency red lines, the main constraints of the model were determined in a comprehensive manner as follows, in addition to the variable nonnegative constraints.

The water resource carrying capacity constraint is calculated as

$$\sum_{j=1}^{J(k)} X_{ij}^k \le p_i^k, \quad (3)$$

where p_i^k is the volume of water from source i to subzone k (million m^3).

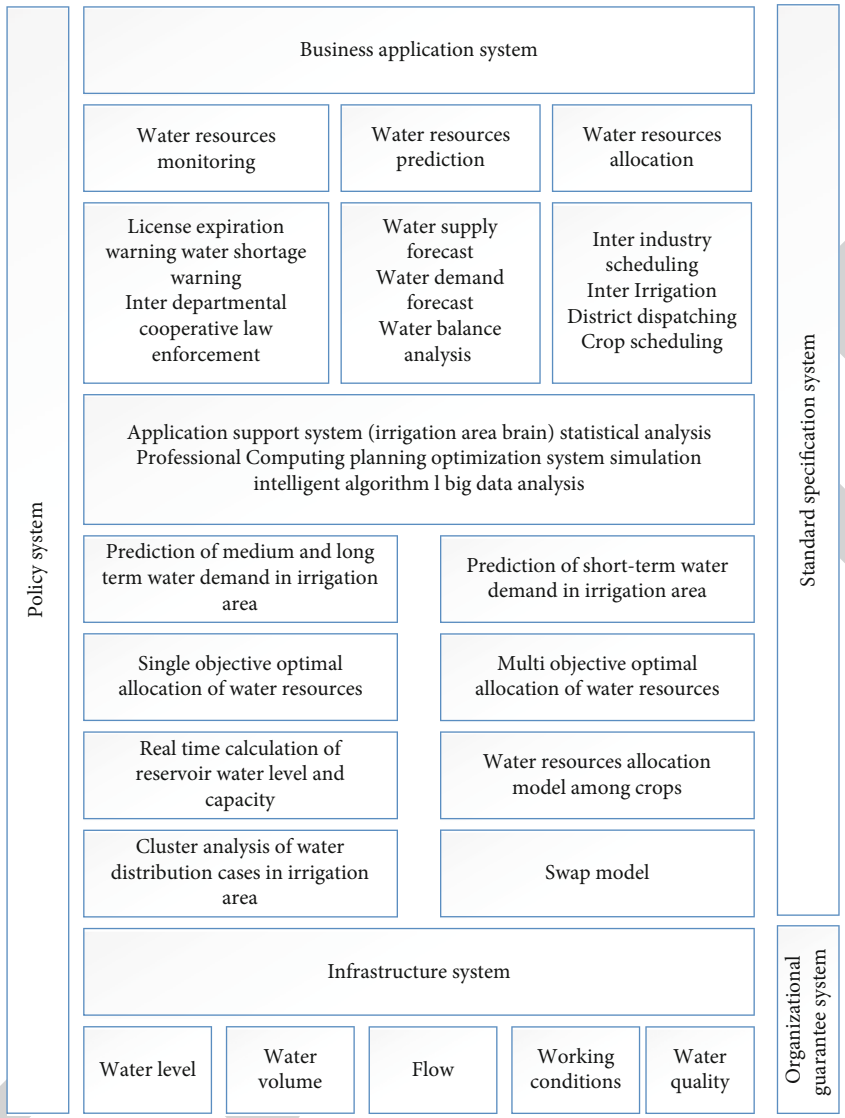

Figure 1: General architecture.

The water demand constraint is calculated as

$$D_{j\,\min}^{k} \le \sum_{i=1}^{I(k)} X_{ij}^{k} \le D_{j\,\max}^{k}, \tag{4}$$

where $D_{j\,\min}^{k}$ and $D_{j\,\max}^{k}$ denote the minimum and maximum water demand (million m^3) for user j in subzone k, respectively, and the water demand quotas for each sector are within the range of the Hebei Provincial Local Standard "Water Quotas", reflecting the implicit constraints on water use efficiency [24, 25].

Total water use control is calculated as

$$\sum_{i=1}^{I(k)} p_i^k \le W, \tag{5}$$

where W is the total water use control target (million m^3).

The water transmission capacity constraint is calculated as

$$X_{ij}^{k} \le Q_i^k, \tag{6}$$

where Q_i^k is the maximum water transfer capacity of source i to subzone k (million m^3).

5. System Performance Validation

Through online data for each water abstraction monitoring point, the cumulative water abstraction of each water abstractor in a certain period of time is calculated, and timely reminders are given for abstraction that is too slow or too fast. By monitoring water quality data, abnormal warnings are given to polluted and highly mineralized water sources [26]; by comparing water quotas and cumulative water consumption, excess water consumption is monitored;

Figure 2: Inspection and maintenance system.

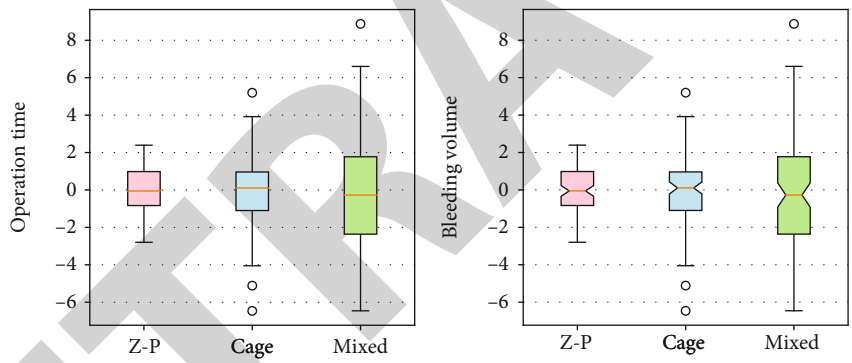

Figure 3: Effect of different water allocations.

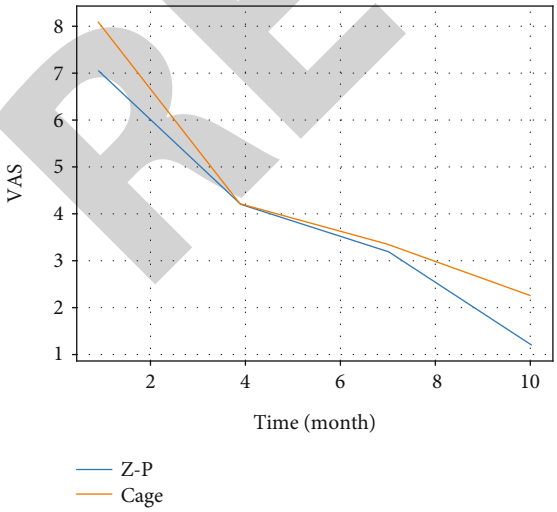

Figure 4: Water storage at different times.

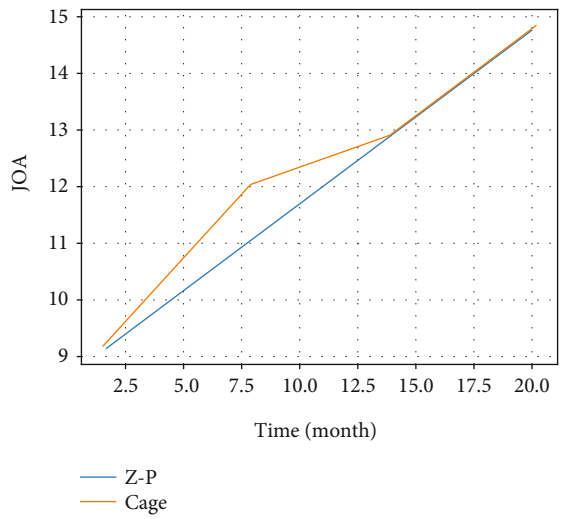

Figure 5: Effectiveness of water measures.

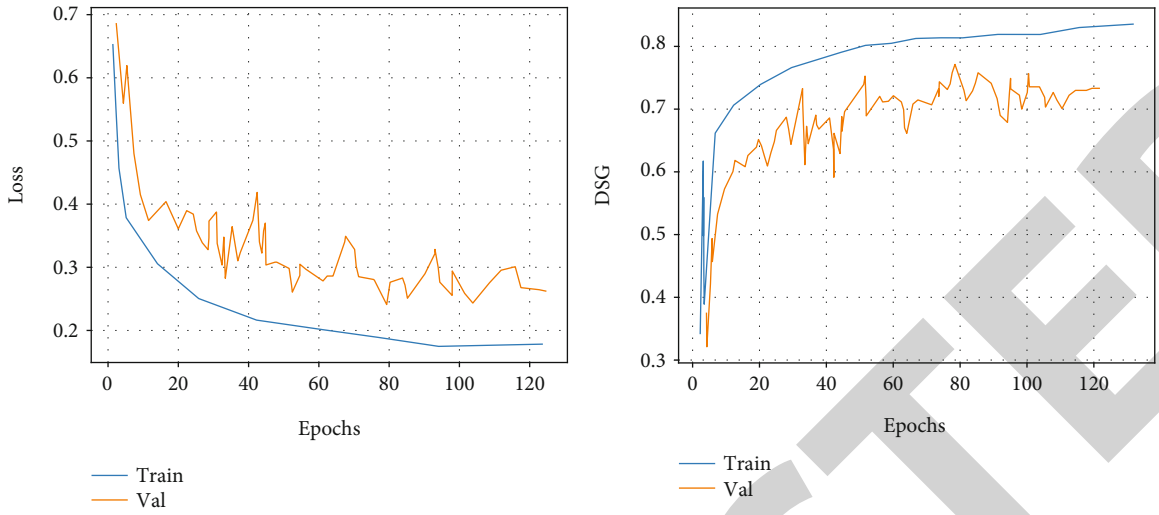

Figure 6: Accuracy of system validation.

and data results characterizing irregularities in water extraction are directly pushed to relevant law enforcement departments to achieve business collaboration, as shown in Figure 3.

Effective prediction of water resources and water demand is the basis for optimal allocation of water resources. The typical application scenario of water resources prediction is based on the water resources data of the current year, predict the rainfall, runoff, runoff yield coefficient, and other factors of water resources in a year, as well as the correlation between water resources, so as to predict the total amount of available water resources [27]. As shown in Figure 4, based on the data of the current year, analyze the impact of different water storage, and analyze the socio-economic influencing factors of water resources in a year, such as population, GDP, water price, water quota, crop planting structure, and irrigation area, so as to realize the accurate prediction of water demand. Based on the forecast of water resources and water demand at a certain time of the year for a given level of development of water resources, the relationship between water resources and water demand balance in each sector is analyzed.

Water-saving water resources evaluation is an important part of water resources allocation. Water-saving water resources evaluation is carried out based on water resources thematic data warehouses [28–30], with as little manual filling as possible; water resources-related planning and construction projects are evaluated for water saving, to prove the necessity and feasibility of water extraction, to analyze the advancedness of water-saving indicators, and to assess the effectiveness of water-saving measures. The effectiveness of water-saving measures is shown in Figure 5.

By analyzing the reporting rate, integrity, and timeliness of the monitoring data of the intelligent allocation and management system of water resources, an intelligent alarm will be issued in case of abnormal data report or poor data report quality [13]. By monitoring the parameters such as electricity and power, alerts are made for abnormal situations where the solar panel power supply facilities are aging and cause insufficient power supply; the gate opening and closing status are monitored, and abnormal opening degrees are investigated. Figure 6 shows the accuracy of the system verification.

6. Conclusions

Using IoT technology in water resources management primarily focuses on the detection and monitoring of water quality and water flow. We are not using the Internet of things technology to its full potential when it comes to water allocation. As a result of the issues raised above and the current state of affairs, this article makes recommendations for more intelligent use of water resources. GIS and the Internet of things combine to create a map of water resources that may be used to manage the entire water cycle, from the source to the end user, as well as automatically collecting and analyzing data. An intelligent system that may be used to allocate water resources and achieve full use of water resources has thus been developed. As part of a larger effort to improve and make full use of water resources, this article outlines the design aims, construction objectives, and construction content of intelligent water resources management and allocation system. Smart water resources management and allocation system can be built with the help of this guide, which gives construction ideas and serves as a model for similar intelligent water resources allocation and management project. A particular implementation plan has yet to be drawn up for this link, and further research is required.

Data Availability

The data used to support the findings of this study are available from the corresponding author upon request.

Conflicts of Interest

The authors declare no conflicts of interest.

References

[1] S. Yadav, S. Luthra, and D. Garg, "Modelling internet of things (IoT)-driven global sustainability in multi-tier agri-food supply chain under natural epidemic outbreaks," *Environmental Science and Pollution Research*, vol. 28, no. 13, pp. 16633–16654, 2021.

[2] M. Yi, Q. K. Chen, and Z. Gang, "Multistage dynamic packet access mechanism of internet of things," *Mobile Information Systems*, vol. 2018, Article ID 3601604, 16 pages, 2018.

[3] S. Y. Hashemi and F. S. Aliee, "Why dynamic security for the internet of things?," *Journal of Computing Science and Engineering*, vol. 12, no. 1, pp. 12–23, 2018.

[4] Y. J. Zhao, B. Du, and B. K. Liu, "Smart environmental protection: the new pathway for the application of the internet of things in environmental management," *Applied Mechanics & Materials*, vol. 411-414, pp. 2245–2250, 2013.

[5] N. Khelifi, E. Nataf, S. Oteafy, and H. Youssef, "Rescue-Sink: Dynamic sink augmentation for RPL in the Internet of Things," *Transactions on Emerging Telecommunications Technologies*, vol. 29, no. 2, 2018.

[6] S. P. A. Datta, "Dynamic socio-economic disequilibrium catalyzed by the internet of things," *Journal of Innovation Management*, vol. 3, no. 3, pp. 4–9, 2015.

[7] N. A. Zhukova, A. M. Thaw, and E. L. Evnevich, "Model of data collection control in the internet of things on the basis of social network technologies," *Journal of Physics Conference Series*, vol. 2021, no. 1, p. 012093, 2021.

[8] X. Tian, W. Huang, Z. Yu, and X. Wang, "Data driven resource allocation for NFV-Based internet of things," *IEEE Internet of Things Journal*, vol. 6, no. 5, pp. 8310–8322, 2019.

[9] M. Ghahramani, Y. Qiao, M. C. Zhou, A. O Hagan, and J. Sweeney, "AI-based modeling and data-driven evaluation for smart manufacturing processes," *IEEE/CAA Journal of Automatica Sinica*, vol. 7, no. 4, pp. 1026–1037, 2020.

[10] L. Gou, X. Zeng, Z. Wang, G. Han, C. Lin, and X. Cheng, "A linearization model of turbofan engine for intelligent analysis towards industrial internet of things," *IEEE Access*, vol. 7, pp. 145313–145323, 2019.

[11] D. Kiritsis, "Closed-loop PLM for intelligent products in the era of the Internet of things," *Computer-Aided Design*, vol. 43, no. 5, pp. 479–501, 2011.

[12] J. Tian and L. Gao, "Using data monitoring algorithms to physiological indicators in motion based on internet of things in smart city," *Sustainable Cities and Society*, vol. 67, no. 4, p. 102727, 2021.

[13] H. Yang, W.-D. Zhong, C. Chen, A. Alphones, and X. Xie, "Deep-reinforcement-learning-based energy-efficient resource management for social and cognitive internet of things," *IEEE Internet of Things Journal*, vol. 7, no. 6, pp. 5677–5689, 2020.

[14] M. Younan, E. H. Houssein, M. Elhoseny, and A. A. Ali, "Challenges and recommended technologies for the industrial internet of things: a comprehensive review," *Measurement*, vol. 151, p. 107198, 2020.

[15] Z. Zhi, "A dynamic management method of domestic internet of things based on cloud computing architecture," *Journal of Computational and Theoretical Nanoscience*, vol. 13, no. 12, pp. 9963–9967, 2016.

[16] V. Borella, G. Queiroz, T. S. Araujo et al., "P.1.h.039 time-course of changes in lipid peroxidation after acute exposure to GBR 12909 in brain areas of mice," *European Neuropsychopharmacology*, vol. 24, pp. S292–S292, 2014.

[17] Y. Chen, N. Zhang, Y. Zhang, and X. Chen, "Dynamic computation offloading in edge computing for internet of things," *IEEE Internet of Things Journal*, vol. 6, no. 3, pp. 4242–4251, 2019.

[18] S. Bohez, T. Verbelen, P. Simoens, and B. Dhoedt, "Discrete-event simulation for efficient and stable resource allocation in collaborative mobile cloudlets," *Simulation Modelling Practice and Theory*, vol. 50, pp. 109–129, 2015.

[19] S. Sicari, A. Rizzardi, D. Miorandi, and A. Coen-Porisini, "Dynamic policies in internet of things: enforcement and synchronization," *IEEE Internet of Things Journal*, vol. 4, 2017.

[20] X. Wang, F. Lin, L. Zhou, X. Zhang, J. Hu, and D. Shen, "Research on intelligent monitoring technology of grouting based on dielectric characteristics," *IOP Conference Series: Earth and Environmental Science*, vol. 861, no. 7, article 072110, 2021(8pp).

[21] X. Wang, Y. Zhang, R. Shen, Y. Xu, and F. C. Zheng, "DRL-based energy-efficient resource allocation frameworks for uplink NOMA systems," *IEEE Internet of Things Journal*, vol. 7, no. 8, pp. 7279–7294, 2020.

[22] O. S. Guma'A, Q. M. Hussein, and Z. T. M. Al-Ta'I, "Dynamic keys generation for internet of things," *TELKOMNIKA Indonesian Journal of Electrical Engineering*, vol. 18, no. 2, pp. 4897–4909, 2019.

[23] E. Bertino, "ACM Press the 2017 Workshop-Dallas, Texas, USA (2017.10.30-2017. 10.30)," in *Proceedings of the 2017 Workshop on Women in Cyber Security-Cyber W \"17- Keynote: Research Challenges and Opportunities in IoT Security*, p. 5, 2017.

[24] X. Xu, R. Mo, F. Dai, W. Lin, S. Wan, and W. Dou, "Dynamic resource provisioning with fault tolerance for data-intensive meteorological workflows in cloud," *IEEE Transactions on Industrial Informatics*, vol. 16, no. 9, pp. 6172–6181, 2020.

[25] Z. Hemel, D. M. Groenewegen, L. C. L. Kats, and E. Visser, "Static consistency checking of web applications with Web DSL," *Journal of Symbolic Computation*, vol. 46, no. 2, pp. 150–182, 2011.

[26] L. Wang, C. Zhang, Q. Chen et al., "A communication strategy of proactive nodes based on loop theorem in wireless sensor networks," in *2018 Ninth international conference on intelligent control and information processing (ICICIP)*, pp. 160–167, IEEE, 2018.

[27] H. Li, D. Zeng, L. Chen, Q. Chen, M. Wang, and C. Zhang, "Immune multipath reliable transmission with fault tolerance in wireless sensor networks," in *International Conference on Bio-Inspired Computing: Theories and Applications*, pp. 513–517, Springer, Singapore, 2016.

[28] C. H. Cao, Y. N. Tang, D. Y. Huang, G. WeiMin, and Z. Chunjiong, "IIBE: an improved identity-based encryption algorithm for wsn security," *Security and Communication Networks*, vol. 2021, Article ID 8527068, 8 pages, 2021.

Hindawi
Wireless Communications and Mobile Computing
Volume 2022, Article ID 6797243, 13 pages
https://doi.org/10.1155/2022/6797243

Research Article

Artificial Intelligence-Driven Model for Production Innovation of Sports News Dissemination

Mengge Wang

School of Art and Design, Guangzhou College of Commerce, Guangzhou, 510000 Guangdong, China

Correspondence should be addressed to Mengge Wang; 20131026@gcc.edu.cn

Received 8 January 2022; Revised 30 January 2022; Accepted 1 March 2022; Published 25 March 2022

Academic Editor: Mohamed Elhoseny

At present, the media's application of artificial intelligence news production is still only at the preliminary exploration and practice stage, and some intelligent applications still have a long way to go from the technical idea to the real realization. This article proposes how to conduct research on the production innovation model of sports news communication based on the era of wireless network communication and artificial intelligence. This article is aimed at studying algorithms based on wireless network communication and artificial intelligence era and analyzes the effects of the two on the production innovation mode of sports news dissemination through neural network algorithms. People's attention to sports has increased year by year, and the dissemination of sports news is constantly innovating in order to keep up with the pace of the times; so, it is also very important to develop new ways of disseminating sports news. With the development of artificial intelligence and wireless communications, more and more news dissemination methods have been developed, and traditional methods can no longer meet the needs of consumers. Therefore, the development of a new innovative production model for sports news dissemination by playing the role of wireless network communication and artificial intelligence is a problem currently attracting attention from scholars, and it is also a practical problem that needs to be solved.

1. Introduction

The advancement of network technology laid a good foundation for the dissemination and development of online sports news. With the continuous development of artificial intelligence, the characteristics and functions of traditional media and new media are gradually being brought into play. The innovation in wireless communication technology has enabled the development of wireless communication across industries and at the same time has promoted the continuous reform and improvement of wireless communication technology. Wireless communication technology plays an extremely important role in different fields. Under the increasingly powerful influence of this new technology product, a broad audience is constantly changing their way of obtaining news.

Artificial intelligence technology is advancing the reform of the news release industry in all directions. This change will not only rebuild the order of news release but will also have a huge impact on the development of the media's news production mechanism and the audience's information environment. In this context, building a sound media platform responsibility, platform algorithm ethics, and user media literacy is indispensable conditions for building a new order of intelligent news production, and they all have positive response significance.

In recent years, wireless communication and artificial intelligence have had a huge impact on society. Rongpeng et al. found that 5G cellular networks are considered to be a key enabler and infrastructure provider in the ICT industry by providing various services with different needs. The standardization of 5G cellular networks is accelerating, which

also means that more candidate technologies will be adopted. Therefore, it is worthwhile to understand the candidate technology as a whole and check the design concept behind it. Rongpeng et al. tried to emphasize one of the most basic characteristics of the revolutionary technology in the 5G era; that is, initial intelligence has appeared in almost every important aspect of the cellular network, including radio resource management, mobility management, and service supply management. However, in the face of increasingly complex configuration issues and emerging new business needs, 5G cellular networks are still not enough without complete artificial intelligence functions. Therefore, Rongpeng et al. further introduced the basic concepts in artificial intelligence and discussed the relationship between artificial intelligence and candidate technologies in 5G cellular networks [1]. Boltaboyev found that mathematical statistics methods are used in the organization of sports activities, the management of various administrative activities, planning, the formulation of decrees and orders, and economic management. And this new approach records management, including creativity, work, patriotism, and other qualities, including the activities of leaders, teachers, scientists, social activists, athletes, and school teachers. This is enough to prove the importance of sports. Although the scholar found that physical activity was important, there were no practical examples [2]. Makridakis found that the industrial and digital revolutions have had a significant impact on human society and life, as well as enterprises. The upcoming artificial intelligence revolution has similar far-reaching effects. By studying similar inventions in the industrial, digital, and artificial intelligence revolutions, Makridakis claims that the latter is targeted, and artificial intelligence will bring about extensive changes and will also affect all aspects of human society and life. In addition, the impact of artificial intelligence on enterprises and employment will be considerable. People will be able to use the Internet to buy goods and obtain services from anywhere in the world and take advantage of the unlimited additional benefits brought about by the widespread use of artificial intelligence inventions. Those who use artificial intelligence extensively and are willing to take risks to reverse the situation will continue to gain a significant competitive advantage [3]. Liu et al. found that artificial intelligence is of great significance to the reliability and safety of modern industrial systems. As an emerging field of industrial applications and an effective solution for fault identification, artificial intelligence technology has attracted more and more attention from academia and industry. However, under different actual operating conditions, artificial intelligence methods are facing huge challenges. He tried to conduct a comprehensive review of artificial intelligence algorithms in mechanical fault diagnosis from the perspective of theoretical background and industrial applications. First, briefly introduce different artificial intelligence algorithms, including the following methods: support vector machines, artificial neural networks, and deep learning. Then, an extensive literature survey of these artificial intelligence algorithms in industrial applications is given. Finally, the advantages, limitations, and practical significance of different artificial intelligence algorithms are discussed, as well as some new research trends [4]. Bennis et al. found that ensuring ultrareliable and low-latency communications for 5G wireless networks and other networks is critical and is currently receiving great attention from academia and industry. The core requirement deviates from the network design method based on expected utility. In this method, relying on the average number is no longer an option, but a necessity. Instead, after providing definitions of latency and reliability, Bennis et al. carefully studied the various enabling factors of URLLC and their inherent trade-offs. Subsequently, Bennis et al. focused his attention on various technologies and methods related to URLLC requirements and their application through selected use cases [5]. Burton et al. found that the recent surge in interest in artificial intelligence may make many educators wonder how to solve moral, ethical, and philosophical issues in their artificial intelligence courses. Burton et al. hopes to develop courses that not only enable students to become artificial intelligence practitioners but also understand the moral, ethical, and philosophical impact that artificial intelligence will have on society. Burton et al. provide practical case studies and resource links that can be used by artificial intelligence educators. Burton et al. also made specific suggestions on how to integrate artificial intelligence ethics into general artificial intelligence courses and how to teach independent artificial intelligence ethics courses [6]. Price and Flach found that the most advanced tools from machine learning and artificial intelligence are automating part of the peer review process. However, there are still many opportunities for further improvement. Analyzing, matching, and opening up, experts find that it is a key task that can be solved using feature-based representations commonly used in machine learning. Such simplified tools also provide insights into how the peer review process might proceed. In particular, analytical ideas will naturally lead to peer review perspectives aimed at finding the best publishing location for submitted papers. In Price and Flach's view, the series established through the profile of continuous reviewers and authors are the key to a stronger and less random peer review process [7]. Polina et al. found that the increase in data availability and the latest advances in artificial intelligence have brought unprecedented opportunities to the healthcare sector, as well as significant challenges for patients, developers, suppliers, and regulators. Novel deep learning and transfer learning technologies are turning any data about people into medical data and turning simple facial pictures and videos into powerful data sources for predictive analysis. Polina et al. outline the next generation of artificial intelligence and blockchain technology, propose innovative solutions that can be used to accelerate biomedical research, enable patients to use new tools to control and profit from their personal data, and provide incentives to accept continuous health monitoring. Polina et al. introduced a new concept of evaluating and evaluating personal records, including the combined value, time value, and relationship value of data [8]. Through the experiments and analysis of scholars, we can know that artificial intelligence is widely used in modern life. Whether it is daily life or business management, it is inseparable from the convenience brought by artificial intelligence. People cannot

do without wireless communication. Based on the era of wireless network communication and artificial intelligence, it is essential to study the production innovation mode of sports news dissemination, but the experiments of scholars also have certain shortcomings: the experiment did not use the latest artificial intelligence and wireless communication methods, and the experiment method was too traditional.

The innovations of this article are as follows: (1) introduce the relevant theoretical knowledge of wireless network communication and artificial intelligence era and use neural network algorithms to analyze how to promote the production and innovation model research of sports news dissemination in the artificial intelligence era. (2) Based on the neural network algorithm and wireless sensor network algorithm to carry out the experiment and analysis of the research on the production innovation mode of sports news dissemination, through investigation and analysis, it is discovered that the era of wireless network communication and artificial intelligence can promote the development of innovative production models for sports news dissemination.

2. Neural Network Algorithm Based on Artificial Intelligence and Wireless Sensor Network Method Based on Wireless Communication

Wireless communication refers to the long-distance transmission communication between multiple nodes without propagation through conductors or cables, and wireless communication can be carried out by radio, wireless, etc. Wireless communication includes a variety of fixed, mobile, and portable applications, such as two-way radios, mobile phones, personal digital assistants, and wireless networks. With the rapid development of information technology, a new generation of information technology, Internet of Things, mobile cloud computing, etc. has gradually matured and begun to be applied to all aspects of society, economy, and life. Mobile cloud computing technology is a fusion of mobile technology and cloud computing technology, and its versatility and efficiency have brought revolutionary changes to today's social life [9]. The artificial intelligence network service is that the smart terminal connects to the cloud computing server through mobile wireless network technology and Internet technology, loads the calculation, processing, and storage of the mobile application program to the cloud computing server for execution, and then feedbacks the execution result to the mobile smart terminal. In this context, this article applies wireless communication and artificial intelligence technology to the dissemination of sports news [10].

2.1. Neural Network Algorithm Based on Artificial Intelligence. Neural network is a kind of computing model, which is composed of a large number of nodes (or neurons) connected to each other. Each node represents a specific output function, called the excitation function. Each connection between two nodes represents a weighted value of the signal passing through the connection, which is called weight, which is equivalent to the memory of artificial neural network. The output of the network is different depending on the connection mode of the network, the weight value, and the activation function.

2.1.1. Neuron Model Algorithm. A neuron is a special type of cell with a cell body and protrusions. Its main structure includes three parts: cell body, dendrites, and axons. The cell body is composed of nucleus, cytoplasm, and cell membrane. The term artificial neural network is derived from biomedical neural network. A neuron can establish contact with multiple surrounding neurons through dendrites and axons to realize the reception, processing, and transmission of information [11]. The complex nervous system of the human body is built on hundreds of millions of neurons. Therefore, simulating the biological nervous system to build a neural network can help understand and obtain the information hidden in the data. The neuron model is shown in Figure 1.

As shown in Figure 1, the unique composition and calculation methods of neural networks have become an important research method in the field of artificial intelligence. The output of the previous neuron is used as the input of the next neuron and then input to the next neuron after the weighted integration of the neuron [12]. The forward transmission of neuron information is as formula (1):

$$x = f(w_i y_i + b). \tag{1}$$

Among them, y_i represents the input signal, w_i represents the weight, b represents the bias part, and x represents the signal output.

The sigmoid function and the tanh function are two activation functions that were widely used in the early research, and both are sigmoid saturation functions. When the input value of the sigmoid function tends to positive infinity or negative infinity, the gradient will approach zero, resulting in gradient dispersion. The output of the sigmoid function is always positive, not zero-centered. The commonly used activation function is the sigmoid function as in formula (2):

$$f(y) = \frac{1}{1 + \exp(y)}. \tag{2}$$

The unique composition and calculation method of neural network have become an important research method in the field of artificial intelligence. After the learning goal is given, the approximation of any function can be achieved, and the internal connection that is difficult to achieve with mathematical formulas can be established [13]. Therefore, it has important applications in many fields such as pattern recognition, prediction, intelligent control, and expert systems. The neuron model is shown in Figure 2.

As shown in Figure 2, the basic structure of a single neuron is very similar to that of a linear perceptron, except that a nonlinear unit is added on the basis of linearity in order to make the model more complex. The nonlinear unit here refers to the activation function. According to different model structures and implementation principles, neural

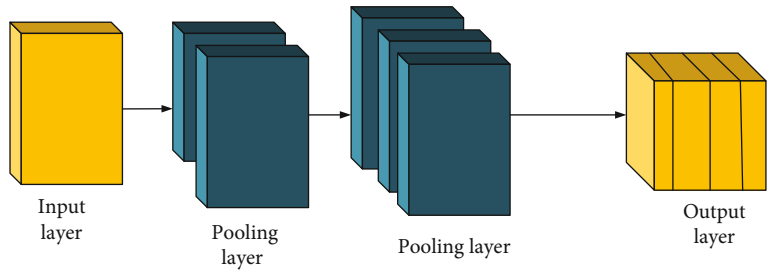

Figure 1: Neural network model.

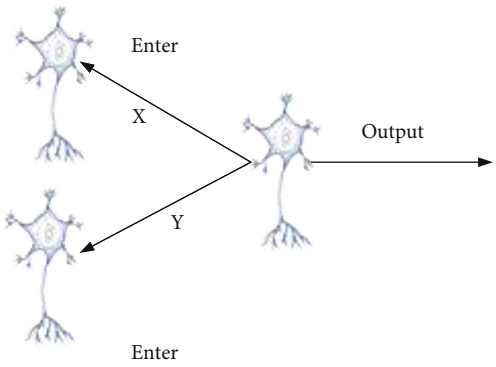

Figure 2: Single neuron model.

networks can classify the following common types: back propagation neural network, radial basis function neural network, wavelet neural network, perceptron neural network, linear neural network, etc. [14]. The BP neural network back-propagates the sensitivity during the adjustment of the model parameters. The sensitivity value of the previous layer is calculated from the sensitivity value of the latter layer, which is the process of propagation from back to front. Perceptron neural network is a single-layer neural network, mainly used for classification [15]. The linear neural network model structure is relatively simple, with only one or a few neurons, and uses a linear transfer function.

In order to obtain an accurate prediction model, the output sequence is compared with the target sequence to adjust the weight parameter E and the bias vector X of the model. Usually, the optimization goal can be set as the error as in formula (3):

$$E(y) = \frac{1}{2}\sum_{i=1}^{n} \|x_i(y_i) - y_i(x_i)\|^2. \tag{3}$$

Among them, $x_i(y_i)$ represents the output data, $y_i(x_i)$ represents the target data, and N represents the number of data. In previous studies, in order to obtain a better prediction model, neural networks are often used in combination with other optimization algorithms (artificial intelligence algorithms) for traffic prediction and data transmission in terms of traffic prediction. Its globality and fast convergence can solve the problem of BP network falling into local optimum [16].

Neurons can not only adjust their own connection weights but also have a certain impact on the value of the connection weight vectors of surrounding neurons. The network uses the neighborhood function to determine the size of adjacent units. The commonly used neighborhood function is shown in Figure 3.

As shown in Figure 3, the adjustment ratio of the neuron connection weight in the winning neighborhood is closely related to the distance to the winning neuron. The closer the distance to the winning neuron, the greater the adjustment of the connection weight. The size of the winning neighborhood is variable. Generally, the range is larger in the initial stage of the algorithm, and it is continuously reduced during the network training process [17].

2.1.2. Support Vector Machine Algorithm. Support vector machine, also known as "support vector network," is a discriminative machine learning classification algorithm. It uses a decision boundary (hyperplane in this case) to divide data points into two categories at a time (this does not mean that it is just a binary classifier, which only divides data points into two categories at a time). The main goal of the support vector classifier is to find the best separation hyperplane (decision boundary). The support vector machine algorithm was originally developed to solve the problem of linear separability. It was developed on the basis of statistical theory and then gradually extended to the case of nonlinearity [18]. In nonlinear classification, the mapping from the input feature space to the W-dimensional space is as formula (4):

$$W(a, b) = \left(a^t b + 1\right)^q, q > 0, \tag{4}$$

but it is realized by the inner product operation of the kernel function. The kernel function is understood as the extension of the concept of matrix and inner product, the properties of the kernel function corresponding to the properties of the matrix are obtained, and the kernel function can be used to solve certain problems like the concept of inner product. The nonlinear mapping can still be classified by a hyperplane, and the optimal hyperplane can be calculated as formula (5):

$$g(a) = w^t a + w_0 = \sum_{i=1}^{n} \lambda_i a_i b_i + w_0. \tag{5}$$

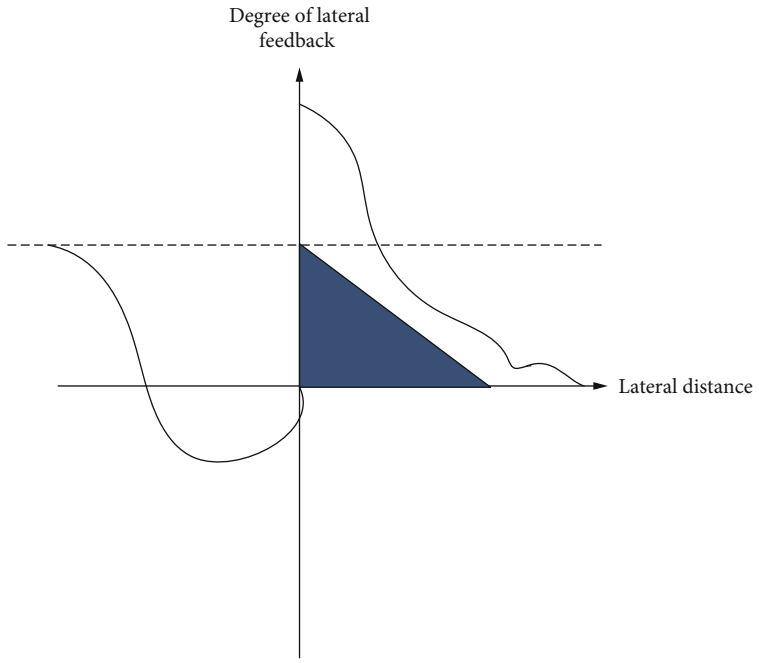

Figure 3: Neighborhood function.

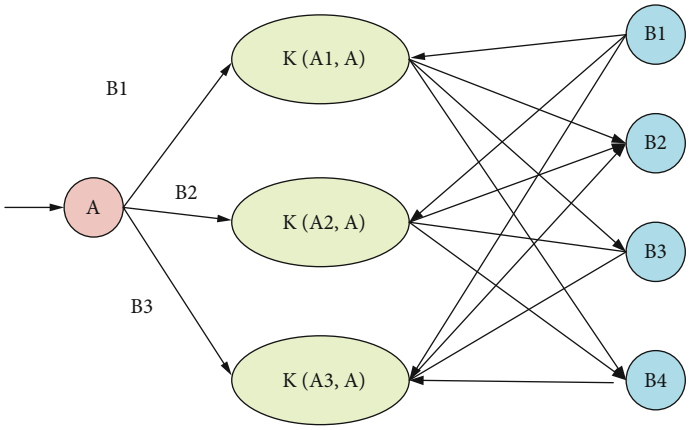

Figure 4: Nonlinear SVM architecture.

Among them, λ_i represents the number of support vectors. The number of nodes is determined by the number of support vectors. The nonlinear SVM architecture is shown in Figure 4.

As shown in Figure 4, the SVM algorithm has a greater advantage when dealing with small sample sizes. When the scale of the problem design is large, or when dealing with multi-category problems, it is difficult to realize due to the complicated solving process and large amount of calculation. As a kind of machine learning algorithm, SVM is often used in image processing, text classification, handwritten digit recognition, and some prediction-related aspects [19].

2.1.3. Autoregressive Moving Average Model. The autoregressive moving average model is a common method for studying time series problems. It consists of two parts: autoregressive and moving average model. It has more superior spectral estimation characteristics and excellent resolution performance [20]. The expression of the model is as formula (6):

$$A_t = \eta + \varphi A_{t-1} + \varphi A_{t-2} + \cdots + \varphi A_{t-p} + \varepsilon_t. \tag{6}$$

This formula expresses the relationship between the current value A_t and its past value A_{t-p}. Among them, φ p is the autoregressive coefficient, and ε_t is the noise disturbance. When $\eta = 0$, it means that the mean is 0.

The MA model is proposed under the inspiration of the autoregressive model, and the expression is formula (7):

$$A_t = \eta + A_t + \theta_1 A_{t-1} + \varphi_2 A_{t-2} + \cdots \varphi_q A_{t-q}. \tag{7}$$

Table 1: Performance comparison of prediction algorithms.

Algorithm	AG-SAEs			BP		
	MAE	MRE/%	RMSE	MAE	MRE/%	RMSE
1	2.45	7.31	3.76	5.52	12.43	6.32
2	2.35	7.02	3.68	5.30	12.01	6.28
3	2.67	7.68	3.21	5.01	10.52	6.16

In the model, the value of A_t is not only related to its historical value but also related to the disturbance of historical moments. Before using the model for parameter estimation, the stationarity test of the time series is first necessary, then using the autocorrelation function$t$and partial autocorrelation function$\varepsilon_t$of the time series to determine the order p and q of the model. After the structure of the model is determined, the sequence can be estimated, and the sequence in a later period of time can be predicted.

Next, there is a comparison of the performance of prediction algorithms, as shown in Table 1.

As shown in Table 1, the other three methods will have some performance fluctuations, but the volatility is not very large. The reason is that the three predictions in this article are only due to the difference in step size. That is, the k data before the prediction point are considered, and the size of the data value itself has not changed. Therefore, the prediction results in the three cases are relatively stable.

2.2. Wireless Sensor Network Algorithm Based on Wireless Communication. Wireless sensor networks have many application scenarios. For different application scenarios, the requirements for network coverage are usually different, as shown in Figure 5:

As shown in Figure 5, in single-objective optimization, a global optimal solution can be determined according to the objective value of the objective function. In multiobjective optimization problems, there are multiple objective functions, and it is difficult to rank feasible solutions according to a single criterion. The goal of noninferior solutions is to find a set of suboptimal solutions that can achieve better values for each goal under certain constraints. The multiobjective optimization problem model is used to solve the problem, and the mathematical expression is formula (8):

$$\max Q = f(a) = \left[f_1(a), f_2(a), \cdots, f_p(a)\right]. \tag{8}$$

The set of solutions is Q, and for any solution $a_i \prec a$, the condition for it to be a noninferior solution is formula (9):

$$R_i^l = \sum_{i=1}^{k} a_1, \log_2\left(1 + \frac{a_1}{1 + a_i}\right). \tag{9}$$

Among them, a_1 and $\log_2(1 + (a_1/1 + a_i))$, respectively, represent the transmission power of the transmitting end of the first pair of users who perform data transmission on the i-th and the downlink transmission power of the base station for communicating with the user. Since wireless communication is only a supplement to traditional cellular network communication, its transmission rate must meet the following conditions as formula (10):

$$R_i^l = \sum_{l=1}^{L} a_1, \log_2\left(1 + \frac{a_1}{1 + a_i}\right) \geq R_c. \tag{10}$$

Among them, R_c represents the user's minimum data transmission rate requirement.

Its optimization goal is to maximize the energy efficiency of all users under the premise of ensuring each user and meeting the maximum transmission power limit of the base station and users. This energy efficiency is defined as the ratio of the sum of the transmission rates of all users in the network to the sum of the power consumption, and its modeling is shown in formula (11):

$$\max \eta_{ee} = \frac{\sum_{l=1}^{l} a_1, \log_2(1 + (a_1/a_i))}{2p}. \tag{11}$$

Among them, $2p$ represents the power consumption of the transmitter and receiver circuits in the user. The inequality constraint is used to ensure that the user does not exceed the maximum transmission power limit when transmitting data and to ensure that the base station does not exceed its maximum transmission power budget when communicating with the user.

Since the objective function in the optimization problem is in fractional form, the optimization problem is a nonconvex optimization problem. In addition, the optimization problem becomes more complicated and difficult to solve directly. In order to make the optimization problem into a form that can be solved, first, based on the nature of the optimization objective function and the user's constraints, the optimization problem is equivalently transformed, as shown in formula (12):

$$P_i \geq \frac{\delta_c(1 + P_i)}{h_i}. \tag{12}$$

From the objective function of the optimization problem, it can be seen that for a given P_i, the value of the optimization objective h_i decreases as the value of P_i increases.

Therefore, combining inequality 12 can get the following conclusion: if you want to get the best solution, it should take the minimum value as in formula (13):

$$\sum_{l=1}^{L} a_i \leq 1. \tag{13}$$

The life cycle of a wireless sensor network is also an important indicator to measure the quality of the network. Under the premise of ensuring a certain coverage rate, reduce the number of working nodes, close the communication modules that make some redundant nodes, and reduce energy consumption as much as possible, as shown in formula (14):

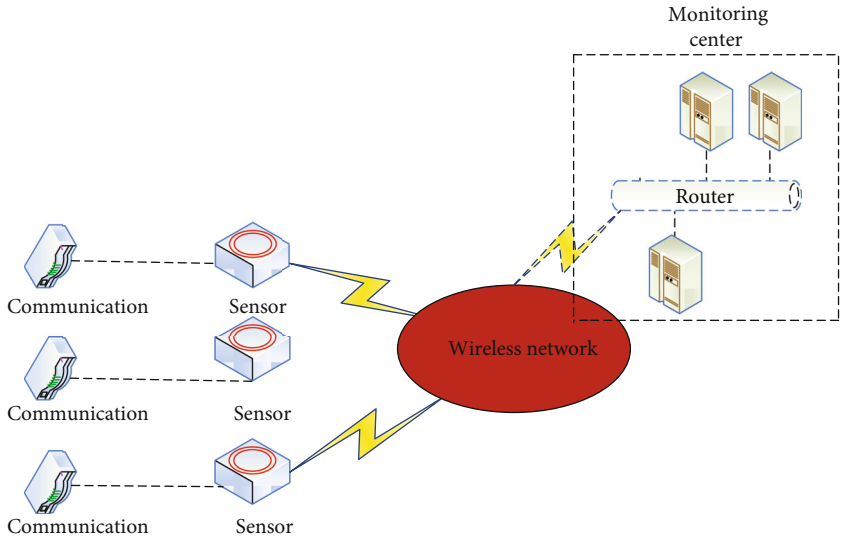

Figure 5: Wireless sensor network transmission diagram.

$$\gamma = \frac{|P|}{M \times N}. \tag{14}$$

Among them, $|P|$ is the number of sensor nodes in working state.

The difference between the remaining energy in the cell and the average remaining energy in the cell is compared to the difference between the maximum and minimum values of the remaining energy in the cell to represent the energy distribution state of the network cell, as shown in formula (15):

$$W_C(T) = \frac{|W_i - W_{\text{avg}}|}{W_{\max} - W_{\min}}. \tag{15}$$

Among them, W_i is the remaining energy of all nodes in the i-th virtual cell, W_{avg} is the average value of the remaining energy in the cell, and $W_{\max}$ and $W_{\min}$ are the maximum and minimum values of the remaining energy in the cell, respectively. W_C reflects the degree of energy difference between cells in the network. The smaller the value, the smaller the energy difference in the network.

To increase the length of the network life cycle, it is necessary to use as few nodes as possible to reduce energy consumption, and to ensure that nodes with higher remaining energy are selected first, so the objective function can be expressed as formula (16):

$$G_2(T) = \min\left(\alpha * \gamma + \beta * E_c(T)\right). \tag{16}$$

Among them, α is the node utilization weight, β is the energy balance weight, and $\alpha + \beta = 1$.

The coverage optimization problem of wireless sensor networks is a multiobjective optimization problem. Network coverage and network life cycle become two optimization subobjectives. The most important feature of wireless sensor network is that the battery energy carried by the node cannot be supplemented. This is the "bottleneck" problem and the focus of research in the application of wireless sensor network. Optimal coverage is a basic problem for wireless sensor network applications. According to the above definitions of network coverage and energy consumption, the mathematical expression of the network coverage multiobjective optimization problem is as formula (17):

$$P = \begin{cases} \max F_1(T) \\ \max 1 - F_2(T) \end{cases}. \tag{17}$$

The sink node adjusts the weights of all nodes in the winning neighborhood by updating the weight vector of the node, as shown in formula (18):

$$H_j(t+1) = H_j(t) + \Delta H_j. \tag{18}$$

After each connection weight adjustment, the sink node will readjust the learning factor and the range of the winning neighborhood and renormalize the connection weight, as shown in formula (19):

$$\alpha(n) = \alpha(n) \times \left(1 - \frac{t}{T}\right). \tag{19}$$

The above process finally establishes each node as in formula (20):

$$\text{Cost}(j, i) = \eta \times \frac{H_0 - H_{CH}}{H_j} \times \sum d^2(j, i). \tag{20}$$

Among them, H_{CH} is the remaining energy of the node, H_0 is the initial energy of the node, H_j is the

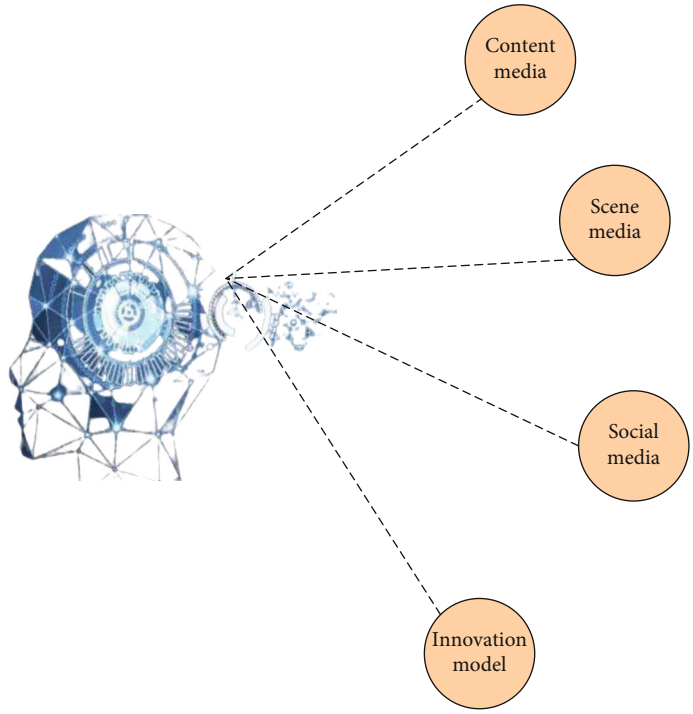

Figure 6: News production innovation model in the era of artificial intelligence.

remaining energy of the node, η is the joint coefficient of energy and distance, and $\text{Cost}(j, i)$ is the distance from node j to node i.

2.3. News Dissemination Methods Relying on Artificial Intelligence. With the changes of the times, the traditional 4C (consumer, cost, convenience, communication) law has emerged some deficiencies. Combined with the actual situation, the new 4C rule is more practical and feasible. Guided by the "New 4C Law," an innovative model of news production in the era of artificial intelligence can be constructed as shown in Figure 6.

As shown in Figure 6, in this model, the content of smart media partially relies on algorithms, big data, and cloud computing to output high-quality segmented news content. Attracting customer communities and advertising, this is the most basic strategic link in the entire value. The social part completes the matching and docking between content and users and can share and discuss content among multiple target user groups through a complete interactive communication mechanism through vertical and accurate information transmission.

Artificial intelligence should be the primary productive force now, and its future development direction, and now it seems that artificial intelligence technology has greatly accelerated the optimization and innovation of the specific links of news gathering and production. The modes of sensor news, robot writing, content information recognition, text-to-speech conversion, and user portraits have become quite professional. The embedding of VR technology makes the content performance more realistic and authentic.

Overall, compared with traditional artificial news reports, artificial intelligence writing does have incomparable advantages.

3. The Experiment of the Questionnaire Survey on the Dissemination of Sports News

In the contemporary society with rapid development of information, people have more and more channels to obtain sports information, and they are becoming more and more convenient. With the development of network technology and the rapid innovation of mobile terminal functions, emerging media have risen rapidly, which has had a great impact on traditional sports media. While everyone is still studying the networked expression of traditional media, the voice of artificial intelligence has sounded.

3.1. Experiments of the Questionnaire Survey. The network not only quickly won a large number of audiences but also used its unique communication advantages to attract audiences while at the same time, it began to have a huge social influence. In recent years, various news release methods have attracted people's attention. This article has conducted a survey of sports attention in recent years, as shown in Figure 7.

As shown in Figure 7, people's attention to sports has been on the rise in 2017; from 25% to 40% at the beginning, it has risen by 15%; in 2018, people's attention to sports has increased more smoothly, from 30% at the beginning to 42%. Regarding the release of online sports news, major international sports events such as the Olympic Games and the Football World Cup have received great attention from

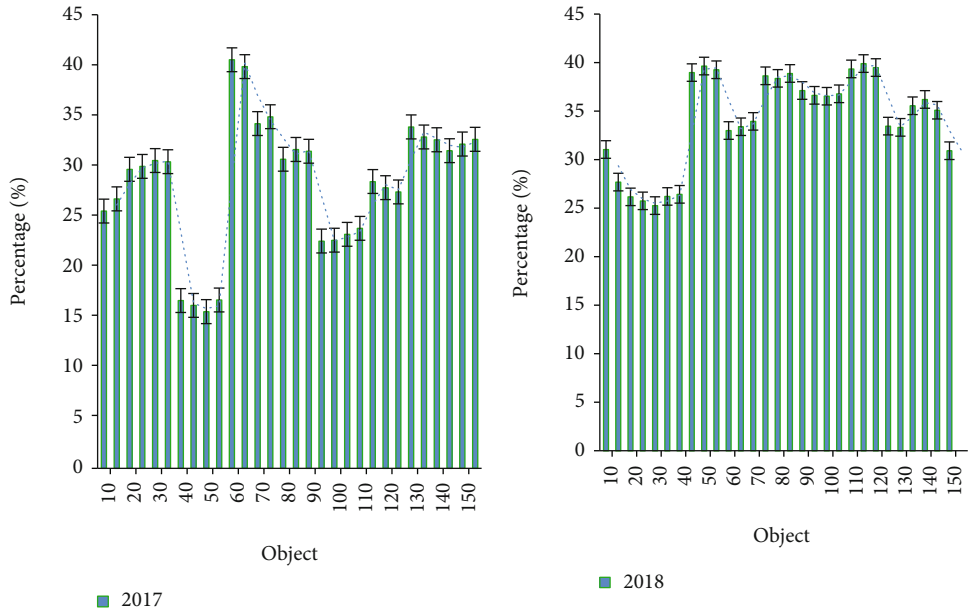

(a) Attention to sports since 2017 (b) Attention to sports since 2018

Figure 7: Attention to sports from 2017 to 2018.

Table 2: Channels for viewers who love to watch sports news to obtain sports information in recent years.

	Number of people	Percentage	Effective percentage	Cumulative percentage
Weibo	87	41%	41%	82%
Television	58	33%	33%	66%
Other channels	30	12%	12%	24%
Newspaper	2	0.5%	0.5%	1%
Baidu	12	6.5%	6.5%	13%
WeChat	15	7%	7%	14%

mainstream people. In addition, many viewers' requests have also stimulated the fierce competition of online media to popularize sports news. In order to gain a more advantageous position in the competition, they continue to use self-renewal methods to meet the audience's demand for sports news.

This article investigates the channels through which viewers who love to watch sports news obtain sports information in recent years, as shown in Table 2.

As shown in Table 2, there are mainly the following channels for viewers who love to watch sports news to obtain sports information: Weibo, TV, other channels, newspapers, Baidu News, and WeChat. Among them, 87 people follow sports news through Weibo, accounting for 41%, ranking first. There are 58 people who follow sports news through TV, accounting for 33%, ranking second, and the least following sports news are through newspapers, with only 2 people, accounting for 0.5%, ranking last. Therefore, it can be seen that Weibo is the most popular way of news dissemination.

This article investigates the development trend of sports news information dissemination from 2014 to 2019, as shown in Figure 8.

As shown in Figure 8, from 2014 to 2019, the proportion of sports news obtained through Weibo increased from 5% in 2014 to 32% in 2019, and the proportion of sports news obtained through newspapers dropped from 18% in 2014 to 4%. Due to the openness, platform, and social nature of the Internet, more and more people obtain, participate, and share sports information through mobile terminals. However, as a form of media, Weibo deserves detailed analysis and research from the viewpoints of the popularization form, characteristics, and development trend of sports information. On this basis, the main role of microblog in the popularization of sports news and the main existing problems and research conclusions and suggestions are put forward.

This article also investigates the factors that influence sports news consumers' choice of news styles, as shown in Table 3.

As shown in Table 3, factors that affect sports news consumers' choice of news methods include information consumer experience, cost and service value-added, accurate push to users, and effective interaction and convenient communication. Among them, 55 people experience information consumers, accounting for 25%; cost and service value-added 40 people, accounting for 20%; 29 people accurately pushing users, accounting for 9%; and there are 90 people for effective interaction and convenient communication, accounting for 46%. It can be seen that the factors that users care most about are effective interaction and convenient

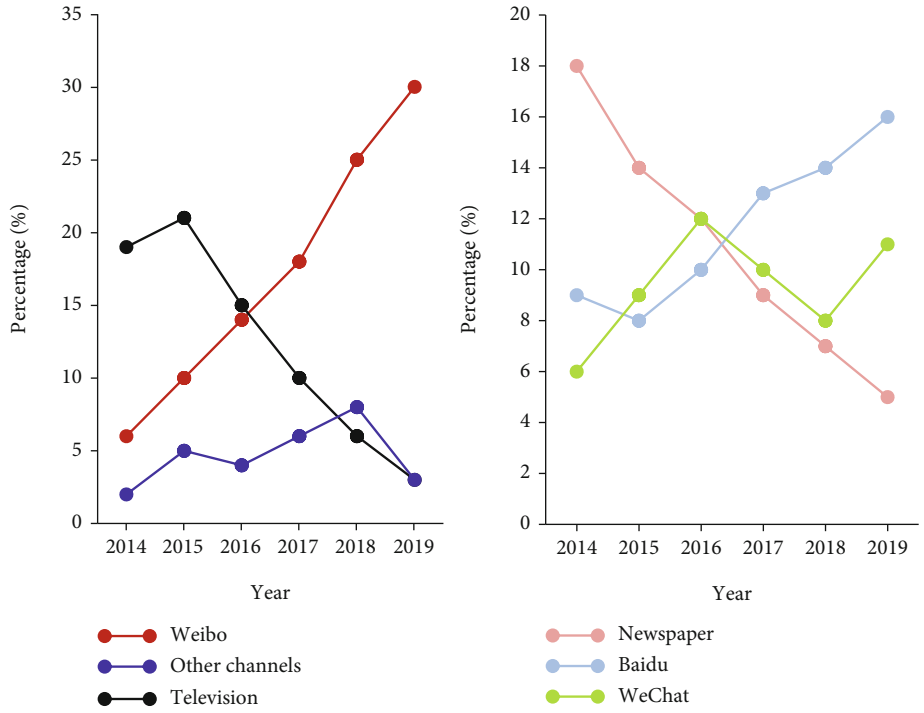

Figure 8: Channels of sports news information dissemination from 2014 to 2019.

Table 3: Factors influencing sports news consumers to choose news styles.

	Number of people	Percentage	Effective percentage	Cumulative percentage
Consumer experience	55	25%	25%	50%
Cost	40	20%	20%	40%
Service	29	9%	9%	18%
Interactive	90	46%	46%	92%

Table 4: Types of online sports news dissemination channels.

	Number of people	Percentage	Effective percentage	Cumulative percentage
Personal website	102	31%	31%	62%
Search engine	46	13%	13%	26%
Forum	89	22%	22%	44%
Instant messaging	120	35%	35%	70%
Blog	87	6%	6%	12%
Online video podcast website	56	14%	14%	28%

communication. Therefore, strengthening effective interaction and convenient communication will help promote the dissemination of sports news.

Sports news shows massive features on the Internet, but if do not summarize and integrate online news topics, it will be difficult for sports news events to be presented to netizens in a comprehensive way. Therefore, the existence of online sports news special reports will effectively overcome the shortcomings of the network in the process of news dissemination.

This article investigates the types of online sports news dissemination channels, as shown in Table 4.

As shown in Table 4, there are the following types of online sports news dissemination channels: personal websites and official websites of institutions, search engines, forums, instant messaging, blogs, and microblogs. Among them, 102 people follow sports news through personal websites and official websites of institutions, accounting for 31%; 46 people follow sports news through search engines, accounting for 13%; 89 people follow sports news through forums, accounting for 22%; 120 people follow sports news through instant messaging, accounting for 35%. It can be seen that the way users follow sports news through Weibo is the most extensive.

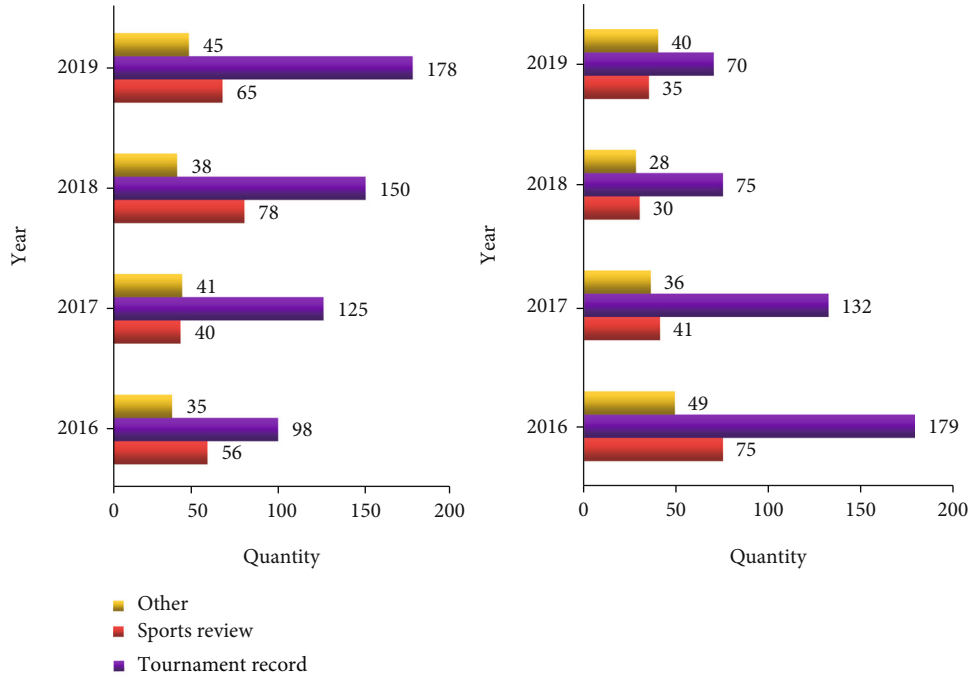

Figure 9: Topic selection of sports news reports on Sina Weibo and WeChat.

The two aspects of sports competitions and tidbits are the content of Sina Sports Weibo reports. Sports competition information mainly includes event documentary reports and sports commentary reports. This article conducted a survey on the topic of Sina Weibo and WeChat sports news reports, as shown in Figure 9.

As shown in Figure 9, since the network is an open large platform, it allows everyone to use this platform to publish and disseminate information. Therefore, relevant individuals and organizations can also use the method of creating a website to carry out news dissemination activities. In the field of online sports news, many individuals and organizations have their own official websites, where they act as witnesses to sports events and events. They use the first-person way to publish news, so that their behavior will not be in aphasia position in the process of network dissemination, but also have a high degree of authority and credibility.

3.2. How to Innovate Sports News Dissemination Methods

3.2.1. Pay Attention to the Information Consumer Experience. The so-called emphasis on information consumer experience is simply a kind of beautiful emotion that users feel. This kind of beautiful feeling is a kind of human nature, and it has unique attributes such as nonmateriality, interaction, irreplaceability, and branding.

3.2.2. Cost Reduction and Service Value Added. The cost here not only includes the user's money expenditure but also includes the user's time and energy. How to provide users with high-quality services while reducing costs is a point that the media should consider.

3.2.3. Accurately Push Users. Convenience here specifically refers to the timely push of news information and accurate push to users. The Tencent News client has a powerful push function, which accurately pushes users based on a large amount of data such as a large number of users' social relationships. Native ads on WeChat use the company's subscription account or service account to regularly push interesting articles to following users for brand promotion. At the same time, it can also reach the gathering effect from hot topics and then transform it into the long-tail distribution of news information, so as to construct user tags. In this regard, the media should also make good use of various big data platforms and big data technologies to carry out targeted operations.

3.2.4. Effective Interaction and Convenient Communication. After entering the mobile Internet, especially with WeChat, the information dissemination of network media is no longer difficult. Because relying on the Internet, people can communicate and connect with each other, forming an intersecting network of relationships. The audience is no longer just a point in the link of information reception, but also a point in the link of information dissemination. The audience can also interact and feedback, and the media's agenda setting function is weakened. Everyone can express their own opinions on hot topics and interact with other users.

4. Discussion

This article analyzes how to research on the production innovation model of sports news dissemination in the era of wireless network communication and artificial intelligence, explains the related concepts of the wireless network communication and artificial intelligence era, researches the related theories based on the wireless network

communication and artificial intelligence era, and explores the research methods of the production innovation mode of sports news dissemination and through the questionnaire survey method case to discuss the importance of wireless network communication and artificial intelligence era to the production innovation mode of sports news dissemination. Finally, take the era of wireless network communication and artificial intelligence integrated into the production innovation model of sports news dissemination as an example to explore the correlation between the two.

This article also makes reasonable use of neural network algorithms based on artificial intelligence. As the scope of application of neural network algorithms has become larger and larger, and its importance has also increased, many scholars have begun to apply neural network algorithms to all aspects of life. The neural network algorithm is a kind of mathematical operation. According to the calculation, the research on the production innovation model of sports news communication based on the era of wireless network communication and artificial intelligence is indispensable for the artificial intelligence era.

Through the questionnaire survey method, this article shows that in the era of artificial intelligence, traditional sports news dissemination methods can no longer satisfy consumers. Therefore, combining the characteristics of wireless network communication and artificial intelligence to find a new innovative production model for sports news dissemination will have a huge impact on sports news dissemination.

5. Conclusions

This article mainly studies how to create a new innovative mode of sports news dissemination based on the era of wireless network communication and artificial intelligence. Through the experimental analysis of the questionnaire survey, this article found that throughout the development of news media, humans can engage in coexisting production, communication, and other social activities through a certain medium. Therefore, from the perspective of the long process of human social development, the truly meaningful and valuable information is not the communication content of each era, but the nature of the communication tools used in this era. Artificial intelligence news will not only change the production mode of news but also change the cultural life of the entire human society. However, in the big wave of artificial intelligence news production and media integration, how to realize the docking and transformation of traditional media is a very realistic and meaningful problem. In this regard, traditional media should proceed from three aspects: ideology, technology, and talents. Therefore, it is of great research significance to create a new production innovation mode of sports news dissemination based on the era of wireless network communication and artificial intelligence.

Data Availability

Data sharing is not applicable to this article as no new data were created or analyzed in this study.

Conflicts of Interest

The author states that this article has no conflict of interest.

References

[1] R. Li, Z. Zhao, X. Zhou et al., "intelligent 5G: when cellular networks meet artificial intelligence," *IEEE Wireless Communications*, vol. 24, no. 5, pp. 175–183, 2017.

[2] K. Boltaboyev, "Meaning of the usage of administrative methods at the organization of PE and sports organizations activity," *Scientific Bulletin of Namangan State University*, vol. 1, no. 2, pp. 322–330, 2019.

[3] S. Makridakis, "The forthcoming artificial intelligence (AI) revolution: its impact on society and firms," *Futures*, vol. 90, pp. 46–60, 2017.

[4] R. Liu, B. Yang, E. Zio, and X. Chen, "Artificial intelligence for fault diagnosis of rotating machinery: a review," *Mechanical Systems & Signal Processing*, vol. 108, pp. 33–47, 2018.

[5] M. Bennis, M. Debbah, and H. V. Poor, "Ultrareliable and low-latency wireless communication: tail, risk, and scale," *Proceedings of the IEEE*, vol. 106, no. 10, pp. 1834–1853, 2018.

[6] E. Burton, J. Goldsmith, S. Koenig, B. Kuipers, N. Mattei, and T. Walsh, "Ethical considerations in artificial intelligence courses," *AI Magazine*, vol. 38, no. 2, pp. 22–34, 2017.

[7] S. Price and P. A. Flach, "Computational support for academic peer review," *Communications of the ACM*, vol. 60, no. 3, pp. 70–79, 2017.

[8] P. Mamoshina, L. Ojomoko, Y. Yanovich et al., "Converging blockchain and next-generation artificial intelligence technologies to decentralize and accelerate biomedical research and healthcare," *Oncotarget*, vol. 9, no. 5, pp. 5665–5690, 2018.

[9] C. Modongo, J. G. Pasipanodya, B. T. Magazi et al., "Artificial intelligence and amikacin exposures predictive of outcomes in multidrug-resistant tuberculosis patients," *Antimicrobial Agents and Chemotherapy*, vol. 60, no. 10, pp. 5928–5932, 2016.

[10] J. Lemley, S. Bazrafkan, and P. Corcoran, "Deep learning for consumer devices and services: pushing the limits for machine learning, artificial intelligence, and computer vision," *IEEE Consumer Electronics Magazine*, vol. 6, no. 2, pp. 48–56, 2017.

[11] D. T. Bui, Q.-T. Bui, Q.-P. Nguyen, B. Pradhan, H. Nampak, and P. T. Trinh, "A hybrid artificial intelligence approach using GIS-based neural-fuzzy inference system and particle swarm optimization for forest fire susceptibility modeling at a tropical area," *Agricultural and Forest Meteorology*, vol. 233, pp. 32–44, 2017.

[12] M. Hutson, "Artificial intelligence faces reproducibility crisis," *Science*, vol. 359, no. 6377, pp. 725-726, 2018.

[13] C. Cath, S. Wachter, B. Mittelstadt, M. Taddeo, and L. Floridi, "Artificial intelligence and the 'Good Society': the US, EU, and UK approach," *Science and Engineering Ethics*, vol. 24, 2018.

[14] D. Endalie and G. Haile, "Automated Amharic news categorization using deep learning models," *Computational Intelligence and Neuroscience*, vol. 2021, Article ID 3774607, 9 pages, 2021.

[15] L. Caviglione, M. Gaggero, J. F. Lalande, W. Mazurczyk, and M. Urbanski, "Seeing the unseen: revealing mobile malware hidden communications via energy consumption and artificial intelligence," *IEEE Transactions on Information Forensics and Security*, vol. 11, no. 4, pp. 799–810, 2016.

[16] M. Seyedmahmoudian, B. Horan, T. K. Soon et al., "State of the art artificial intelligence-based MPPT techniques for mitigating partial shading effects on PV systems - a review," *Renewable & Sustainable Energy Reviews*, vol. 64, pp. 435–455, 2016.

[17] P. Glauner, J. A. Meira, P. Valtchev, R. State, and F. Bettinger, "The challenge of non-technical loss detection using artificial intelligence: a survey," *International Journal of Computational Intelligence Systems*, vol. 10, no. 1, pp. 760–775, 2017.

[18] J. H. Thrall, X. Li, Q. Li et al., "Artificial intelligence and machine learning in radiology: opportunities, challenges, pitfalls, and criteria for success," *Journal of the American College of Radiology*, vol. 15, no. 3, pp. 504–508, 2018.

[19] K. W. Kow, Y. W. Wong, R. K. Rajkumar, and R. K. Rajkumar, "A review on performance of artificial intelligence and conventional method in mitigating PV grid-tied related power quality events," *Renewable & Sustainable Energy Reviews*, vol. 56, pp. 334–346, 2016.

[20] Z. Wang and Z. Dong, "Sports monitoring method of national sports events based on wireless sensor network," *Wireless Communications and Mobile Computing*, vol. 2021, Article ID 5739049, 13 pages, 2021.

Hindawi
Wireless Communications and Mobile Computing
Volume 2022, Article ID 7008467, 10 pages
https://doi.org/10.1155/2022/7008467

Research Article

Intelligent Target Detection and Tracking Algorithm for Martial Arts Applications

Zhiyun Tang

College of Leisure and Health, Guilin College of Tourism, Guilin, 541006 Guilin, China

Correspondence should be addressed to Zhiyun Tang; tzy@gltu.edu.cn

Received 16 November 2021; Revised 24 January 2022; Accepted 24 February 2022; Published 23 March 2022

Academic Editor: Mohamed Elhoseny

Moving object detection and tracking is the basis and key technology for intelligent video surveillance, human-computer interaction, mobile robot and vehicle visual navigation, industrial robot system, and other applications. It has important applications in intelligent monitoring, human-computer interaction, visual navigation, and so on. Intelligent technology can greatly facilitate the monitoring of countless targets. This paper adopts the random motion model to describe the motion state of the target. Based on wireless communication and information security, this paper studies the communication and information security of the intelligent system of martial arts target detection and tracking algorithm, and the basic idea of mean-shift tracking algorithm is to use gradient climbing of probability density to find local optimal. This paper uses the background subtraction method based on the vibe algorithm to obtain the binary image of the foreground object; the shadow detection algorithm is used to remove the shadow of the foreground image; the haar-like (Haar) feature is selected as the feature of motion detection, and the feature value of the rectangular area is quickly calculated to describe the adjacent image area. The difference between the features, the final result image, and then the intelligent system for analysis. Experimental data shows that the time consumed by the tracking algorithm is less than 20 ms, which can meet the real-time requirements of ordinary target tracking systems. The average processing time of the hybrid modeling method is 62.8 ms, and the detection rate is 15.92 frames/SEC. The results show that the algorithm improves the utilization of particles, greatly reduces the complexity, and reduces the degradation of the particle filter.

1. Introduction

Because the generation of intelligent technology needs to collect the track of motion, and then implant it into the system to produce intelligence, so moving target tracking recognition and moving target detection are the basis of intelligent technology, so target detection is a very important step. In video surveillance images, moving target detection is also very important and is the basis of image understanding. With the continuous development of computer video technology, the in-depth research of target detection and tracking technology is driven. Through continuous research on moving target detection and tracking technology in video surveillance, it is widely used in video analysis conferences and based on mobile target recognition, system navigation, security surveillance, traffic dispatch and weather analysis, and other fields. How to apply wireless communication and communication security to martial arts target detection and tracking algorithms is a question worth pondering.

Target detection and tracking are mainly to analyze and process each frame of the video sequence. Target detection is to separate the background image from the image to obtain the foreground target, so that it can carry out tracking, recognition, and other middle-level and high-level instructions. Target tracking is to extract color, texture, scale, shape, edge, and other information from the continuous frame images of the video sequence and then perform feature matching. But in the video, the moving target will be affected by other interference, such as partial occlusion and multitarget interference. External interference can cause temporary disappearance or deformation of the target. The target detection and recognition algorithms we need have strong robustness. The so-called robustness is the ability of the system to survive under abnormal and dangerous conditions.

The detection and tracking of moving targets is an important subject in the field of intelligent systems. Hu et al. discuss how to strike a balance between the quality and life cycle of target detection in wireless sensor networks and puts forward two target monitoring schemes. Although his research idea is correct, it lacks specific experimental content [1]. Hu and Liu believe that in the case of moving target detection, it is very difficult to replace or charge the battery of the sensor node. Due to the inherent resource-constrained characteristics, the value of the parameter will seriously affect energy efficiency and testing quality. He proposed a novel moving target detection method, called the node part with complete duty cycle (PNFDC), to improve the detection quality and energy efficiency of wireless sensor networks (WSN). Each sensor node adopts the best duty cycle according to the network load, which can guarantee the detection quality. In addition, PNFDC sets a certain percentage of nodes to full duty cycle (FDC) based on their energy abundance to further improve the quality of detection. His research lacks experimental data [2]. Shi et al. believe that distributed radar network system has many unique functions. In practice, the networked radar in radar network should maximize its transmitting power to obtain better detection performance, which may be in contradiction with low interception probability (LPI). Therefore, he studies the adaptive power allocation of radar network in the framework of cooperative game theory, which can improve the LPI performance. Considering the emission power constraints and the minimum signal-to-noise ratio (SINR) requirements of each radar, he developed a cooperative Nash bargaining power allocation game (NBPAG) based on LPI. First, he defines a novel SINR based network utility function and uses it as a measure to evaluate power allocation. Then, he proved the existence and uniqueness of Nash bargaining solution (NBS) through the well-designed network utility function. Although his research is relatively comprehensive, the research direction is relatively vague [3]. Yu et al. proposed a new constant false alarm rate (CFAR) target detection algorithm based on superpixels for high-resolution synthetic aperture radar (SAR) images. The detection algorithm includes three stages, namely, segmentation, detection, and clustering. In the segmentation stage, he uses the super pixel generation algorithm to segment the SAR image. In the detection stage, based on the generated superpixels, even in the case of multiple targets, the clutter distribution parameters of each pixel can be estimated adaptively. Then, he uses the two-parameter CFAR test statistic for testing. In the clustering stage, he uses hierarchical clustering to cluster the detected superpixels to obtain candidate targets. He used miniSAR data to prove the effectiveness of the algorithm. His research is not accurate enough [4]. Liu and Zhang based on the fusion of target detection network YOLO V4 and detection based multitarget tracking algorithm DeepSORT, an automatic vehicle detection and tracking method based on deep learning in urban environment was designed. Simulation results show that the proposed algorithm can realize automatic vehicle detection and tracking in urban environment [5, 26].

This paper studies the mean-shift tracking algorithm for the influence of the target partial occlusion on the mean-shift tracking algorithm. The algorithm uses only a few particles to describe the target state completely and can well characterize the target characteristics, improve the utilization of particles, and reduce the time complexity of the algorithm. In this paper, the VIBE algorithm is used to update the martial arts background model, which is beneficial to the research and development of the recognition of a variety of different sports actions, and improves the scalability of the sports training system. And through the experiment to verify the martial arts sports target tracking monitoring research on the development of intelligent technology has a role in promoting.

In this paper, the method of target tracking track is described in detail, the moving target is discussed in depth, the process of image processing is described, and the tracking and detection of martial arts target is verified through experiments.

2. Moving Target Detection and Tracking

2.1. Moving Target Detection. Moving target detection can be used in gait recognition, face detection and tracking, traffic statistics, and intelligent video monitoring, which can provide information about the speed and size of the target. The object of moving target detection is generally passers-by and vehicle. Background modeling is the key to moving target detection. A good background model not only can detect foreground targets well but also adapt to the changes of background itself, such as sudden illumination and periodic motion objects in the scene, so as to prevent them from being mistaken as foreground targets [6]. The Euclidean distance is generally used to calculate the distance between the pixel point and the background model, and the Euclidean distance of two points $p_1(x_1, y_1)$ and $p_2(x_2, y_2)$ is calculated by the following formula.

$$\operatorname{dist}(p_1, p_2) = \sqrt{(x_1 - x_2)^2 + (y_1 - y_2)^2}. \tag{1}$$

In a foreground detection algorithm based on background update vibe, the pixel value is used in the background model, and for a pixel point is the three-dimensional vector $p(R, G, B)$, where R, G, and B are the pixel values of the image RGB space [7]. In order to improve the efficiency of calculation, the distance between pixels is calculated by the following formula in the VIBE model.

$$\operatorname{dist}(p_1, p_2) = |r_1 - r_2| + |g_1 - g_2| + |b_1 - b_2|. \tag{2}$$

The principle of Vibe algorithm is to establish a sample set of pixels by extracting the pixel values around the pixel (x, y) and previous pixel values and then compare the pixel values at another frame (x, y) with the pixel values in the sample set. If the distance between the pixel value and the pixel value in the sample set is greater than the set threshold, the pixel is the front scenic spot; otherwise, it is the background point [8]. Assuming that the current set of previous

scenic spots is $\psi_f = \{Z_1, Z_2, \cdots, Z_m\}$, the distribution of the previous scenic spots in the feature space is

$$p\left(X \mid \psi_f\right) = \alpha\gamma + (1-\alpha)\frac{1}{m}\sum_{i=1}^{m}\phi_H(X - Z_i). \quad (3)$$

The Vibe algorithm is not sensitive to changes in light conditions and is suitable for target detection under dynamic background. But in actual application, the detection effect of Vibe algorithm is very dependent on the time interval when the frame difference is made. If the speed of the moving target in the background is faster, you must choose a two-frame image sequence with a short interval, otherwise, it is easy to detect a false moving target; if the moving target moves slowly, you should choose two frames with a longer time interval, otherwise, the two frames before and after are almost overlapped, and it is difficult to detect the object [8]. In addition, the Vibe algorithm detects that objects are prone to voids. Morphological processing and connectivity analysis of digital images are required for moving objects. If a foreground object is detected in a certain frame, then in the next frame, the probability of the same color value appearing in its adjacent position will increase, which is the use of time constraints. In the end, all the detected spots will be used to update the foreground model, and in order to allow foreground objects to become part of the background, all pixels of the current frame will be used to update the background model. The intensity of the background should be invariable when the light changes and some dynamic textures of the background are removed. Therefore, the background pictures are linearly related to each other, thus, forming a low-rank matrix [9].

In motion detection, the characteristics of moving objects and shadows are very important. According to many research algorithms, the existing methods are mainly divided into two categories, one is based on the shape characteristics of the target, and the other is based on the shadow characteristics. The shadow detection methods can be divided into two categories: light-based direction detection and image feature-based detection. The two-dimensional image feature extraction is based on two-dimensional image feature extraction or texture analysis. The detection based on image features, such as color, texture, and edge features, is divided into spatial feature-based methods, which are pixel-based and region-based methods, respectively [10].

2.2. Moving Target Tracking. Moving target tracking requires accurate and effective tracking of different moving targets under various complex backgrounds. These complex backgrounds include the background of global illumination changes, such as the background of local disturbances such as branches and bushes shaking in the wind [11]. The mean-shift tracking algorithm can converge to the pixel with the maximum local probability density, but the pixels in the image are evenly distributed. In order to reflect the probability of moving objects in the target model, histogram back projection is used to process the next frame image. Because the movement of the tracked target is continuous and regular, it is necessary to expand the target search area appropriately and set the back projection value of other areas to 0 when carrying out back projection, which will help to speed up the convergence of the algorithm and improve the accuracy of the algorithm [12, 13]. Then use the kernel density estimation algorithm to determine the probability density function corresponding to the sample point, and its expression is as follows.

$$f_h(x) = \frac{1}{nh^d}\sum_{i=1}^{n} k\left(\left\|\frac{x - x_i}{h}\right\|^2\right). \quad (4)$$

The core of the algorithm of matching-based moving target tracking is to find the best match with the feature template in the target area. The algorithm first selects all regions to be matched in the current frame through the scan window, then maps these region images to the template feature space, calculates the similarity or distance function with the target template, and finally selects the optimal region center as the target spatial position [14]. The general matching-based moving target tracking process is shown in Figure 1.

The template matching method based on the characteristics of the target region divides the target into different parts and improves the stability of the algorithm against local geometric deformation by matching the template of each part. Such algorithms usually weight the similarity matching results of each part and adjust the contribution of different part templates to the overall matching by assigning weights. This kind of algorithm overcomes the possible rigid deformation of the moving target to a certain extent, but it cannot overcome the influence of target occlusion or scale change on the tracking result. The frequency-domain template matching transforms the image into the frequency domain, and the image matching is realized by calculating the similarity between the phase and amplitude of the target image transform coefficient and the template [15, 16].

2.3. Image Processing. In the process of image transmission, it is always affected by external environmental conditions, and a certain amount of noise is generated. Image smoothing is a method to reduce or even remove the influence of noise. By defining a mathematical model and performing matrix operations, it can effectively denoise and make the image smoother. Common image smoothing methods mainly include neighborhood average method, median filter method, and Gaussian filter method. When the video sequence is collected and transmitted, interference from the scene environment and equipment conditions will produce noise. Noise is an irregular random signal, which will cause false interference to the understanding and analysis of image information. In the process of image sequence input, acquisition, and processing, the focus is to suppress the noise in the acquisition and transmission process. If the noise in the input is large, it will have a negative impact on the processing and output process. So in the image processing system, the first task is to suppress noise [17].

The purpose of video image enhancement is to emphasize some unclear or valuable features of the source image,

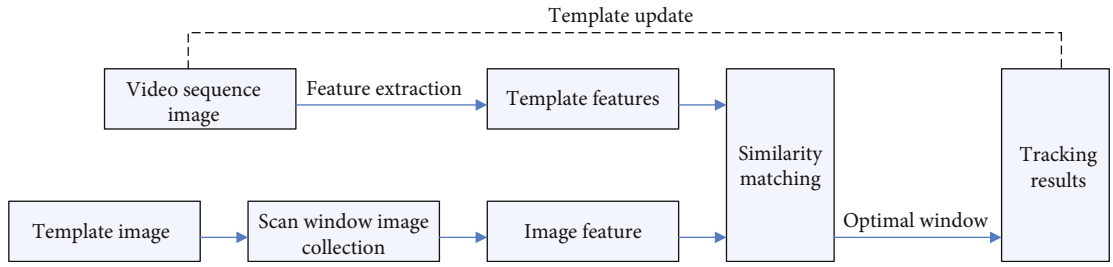

Figure 1: Moving target tracking process.

so that the target area has a better visual effect, and the image processing makes it more suitable for specific application scenarios. However, due to the instability of the external environment and the defects of the shooting instrument itself, there are inevitably various problems in the quality of the collected images. For some special purposes, occasionally more demanding requirements are put forward on the image quality [18]. Therefore, for special needs, the source image must be technically processed and improved to meet the requirements of the machine vision recognition system for image processing. This technology is called image enhancement. Its effect can play a very important role in both human visual effects and computer visualization image analysis. Of course, the enhancement technology can only highlight the characteristic information of the image, but cannot increase the valuable information contained in the image data itself. Only some scenes with blurred edges, texture characteristics, or poor contrast in the image can be enhanced [19].

3. Martial Arts Movement Detection and Tracking Experiment

3.1. Experimental Platform. First, carry out experimental tests on the hardware platform and the drivers of each module to verify whether the basic image acquisition, storage, and real-time display functions are normal. The hardware platform designed in this paper works normally. Images can be collected and stored through the OV7725 camera to achieve real-time display of images with a resolution of 640∗480@60 Hz, which can meet the real-time requirements of the target detection and tracking system [20]. The device resources occupied by basic functions such as image acquisition, storage, and display are shown in Table 1. The basic hardware driver occupies less processor resources, leaving enough resource margin for the realization of moving target detection and tracking algorithms. In addition, this paper integrates the functional modules of the system into a circuit board, no need to design interfaces, high integration, and small size [21].

3.2. Martial Arts Sports Model. When the mean shift tracking algorithm is used to track moving objects, first, a certain motion model is established to describe the state change of particles. Generally speaking, the closer the model is to the actual model, the better the detection effect is. An accurate motion model usually needs a lot of prior information to build. If the movement law of the target changes greatly, it is often difficult to establish an accurate model. In this paper, the random walk model is used to describe the moving state of the target [22, 23].

Table 1: Device resources occupied by basic functions.

	Available resources	Take up resources	Usage rate
LEs	15408	1153	7%
IOs	166	91	55%
Memory bits	516.1 K	24.6 K	5%

3.3. Moving Target Detection

(1) Local Feature Selection. Build an observation window, and move the window at each pixel point in the image. If the gray value in the observation window is different before and after sliding, and the moving in any direction will cause great change in the gray value, we can determine that there are corners in the observation window. Excellent corner features should have the characteristics of fast detection speed, rotation invariance, and insensitive to illumination changes [24]

(2) *Corner Detection*. The improvement of Harris corner detection is to detect the gray changes in all directions, so it has rotation invariance and stability to some affine transformations

(3) *Edge Detection*. First, the Gaussian smoothing filter is used to convolute the original image, and then the first-order partial derivative finite difference is used to calculate the maximum value and direction of gradient, and nonmaximum suppression is applied. At the same time, high and low thresholds are used to realize edge detection and connection [25]

3.4. Moving Target Tracking

Step 1. Input the video frame, perform the background subtraction method modeled by the improved Vibe algorithm, and obtain the binary image of the foreground target.

Step 2. Use the shadow detection algorithm in this article to remove the shadow of the foreground image.

Step 3. Through morphological processing, discard small targets and fill holes to make the detection results more accurate.

Step 4. Start from the top left of the image to find the target contour, and determine the minimum circumscribed rectangle of the moving target according to the target contour. If the area of the circumscribed rectangle is greater than the set value, the circumscribed rectangle is considered to be valid.

Step 5. Determine the center of mass position of the obtained circumscribed rectangle of the moving target, and use the circumscribed rectangle as the initial target tracking frame of the KCF algorithm to execute KCF.

Step 6. Perform feature sampling on the initial target, build a sample set, and train the target detector.

Step 7. Detect whether there is a target in the next frame prediction area, and if there is, update the training sample set with the new target. If the target does not exist and the centroid position of the tracking box does not move for several consecutive frames, then the target detection algorithm based on Vibe is reinvoked to obtain the target region and go to Step 2.

3.5. Target Classification Test

(1) *Sample Acquisition and Preprocessing*. The positive samples of martial arts actions select images with different distances, orientations, colors, and sizes and then normalize them to 24×24 pixel size; the negative samples of actions select the background images without Wushu actions. Here, 2316 martial arts action sample sets and 7708 nonmartial arts action sample sets are selected from the image data set

(2) *Sample Feature Extraction*. Haar feature is selected as the feature of action detection, and the characteristic value of rectangular region is quickly calculated by integral graph method to describe the feature difference of adjacent image regions

(3) *Training Results*. The trained cascade classifier consists of 18 strong classifiers. Each strong classifier has a different number of weak classifiers. Each weak classifier is composed of a Haar feature, a threshold, and an indication of the direction of unequal sign. The larger the number of classifiers, the more weak classifiers are contained in the strong classifier, and the more Haar features are

4. Target Detection and Tracking Results

4.1. Moving Target Detection Effect. The key of moving object detection method is to establish a model describing the target according to its own characteristics and then detect the moving target according to the model. In practical application scenarios, due to the interference of illumination conditions, moving object occlusion, and complex background, there are many difficulties in moving object detection. Moving object detection mainly focuses on the recognition and analysis of moving objects in video image sequences. In real application scenarios, there are multiple moving objects. Scene motion pattern can grasp the temporal and spatial distribution of motion behavior as a whole and obtain high-level semantic knowledge of scene motion. The comprehensive analysis of the scene motion mode can study and grasp the individual's movement intention and movement state change on a higher level of understanding, so as to select and adjust the operation strategy of intelligent video monitoring algorithm, alleviate the adaptive contradiction between the monitoring scene and visual application algorithm, and enhance the accuracy and robustness of various algorithms. The classical hybrid modeling method and the improved hybrid modeling method combined with K-means are used to detect the target of 500 frames in a video initialization stage. The real-time detection results are shown in Figure 2. It can be seen from the figure that the detection performance of the classical hybrid modeling method is higher than that of the improved hybrid modeling method combined with k-means. The peak time of classical algorithm is 43.16 s, while the peak of the improved algorithm is 38.75 s.

The characteristic of the hybrid model is to use multiple Gaussian distributions to describe the pixel value distribution of a point, which is more in line with the multipeak distribution of pixel values in the complex background. For example, if the current scene object stays in the background for a long time, the foreground target will be mistaken for the object in the background image sequence. At this time, the advantages of the multi-Gaussian distribution model are reflected. The Gaussian distribution previously established is still in the Gaussian mixture distribution model, but the weight is reduced correspondingly. If the foreground object suddenly moves again, because the Gaussian distribution describing the background still exists, as long as its weight is increased, the previous background can be quickly segmented.

The real-time comparison before and after the algorithm improvement is shown in Table 2. It can be seen from the table that the average processing time per frame of the hybrid modeling method is 62.8 milliseconds, and the detection rate is 15.92 frames/sec. Combined with k-means improved hybrid modeling method, the average processing time per frame is 41.8 milliseconds, and the detection rate reaches 23.89 frames/sec. Experiments show that the improved hybrid modeling method combined with k-means can effectively improve the real-time detection in the initialization phase. The particles in the particle filter algorithm will degenerate due to traditional resampling. As the number of iterations of the algorithm increases, a large number of high-weight particles are retained, while low-weight particles are deleted, causing serious particle exhaustion. Aiming at the problem of particle degradation caused by traditional resampling in the particle filter algorithm, the improved algorithm improves on the traditional resampling algorithm. First, calculate the normalized cumulative

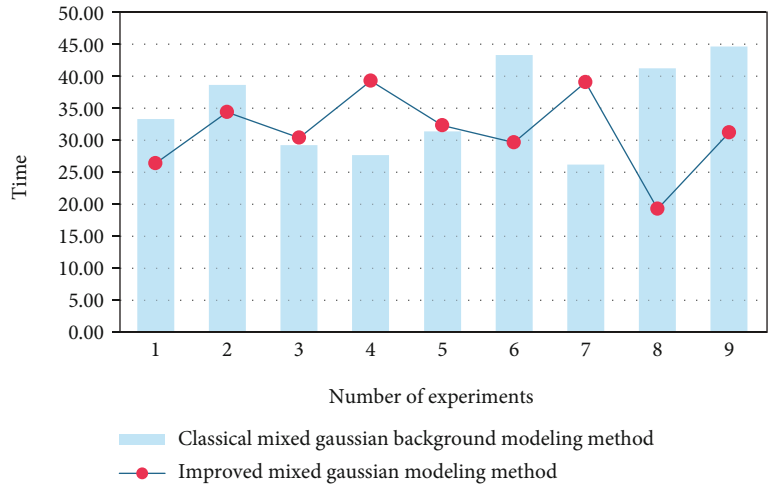

Figure 2: Real-time detection results.

Table 2: Real-time comparison before and after algorithm improvement.

Algorithm	Average processing time per frame	Detection rate
Classic GMM algorithm	62.8	15.92
Improved GMM algorithm	41.8	23.89

Table 3: Single reconnaissance tracking operation time.

Experiment	Basic Camshift	Multifeature fusion Camshift	Method of this article
Test video tracking	13.7 ms	26.8 ms	17.4 ms
Moving target tracking	14.3 ms	29.5 ms	19.1 ms

probability of the weight of the particle set, and then select the smallest particle with the index number that satisfies the weight normalized cumulative probability greater than the random number to add to the new particle set for resampling. Results are shown in Table 2.

4.2. Target Tracking Algorithm. The operation time of single detection and tracking is shown in Table 3. The traditional tracking algorithm consumes the shortest time, mainly because its target model is relatively simple and the amount of data operation is relatively small; the tracking algorithm of multifeature fusion consumes the longest time, mainly because the method needs to constantly calculate the color, texture, and edge features of the image, which greatly increases the amount of data calculation. For the algorithm in this paper, only the process of statistical background histogram is added to the traditional algorithm, and no other auxiliary features are extracted. The target model obtained by this method increases the time consumption, but the increased consumption time is not very large. As can be seen from the table, for single frame image target tracking, the tracking algorithm in this paper consumes less than 20 ms, which can meet the real-time requirements of common target tracking system.

In the field of computer vision, moving object detection technology is a very important technology. In fact, we use a certain detection method to separate the moving object from the background and then extract the unique features which can represent the moving object. Then, we can track the moving object by searching and matching in the subsequent video images. It can also be said that moving target detection is the basis of moving target tracking. If the result of moving target detection is not ideal, the follow-up tracking effect of moving target will also have certain error, which may lead to serious consequences such as the loss of moving target tracking. Therefore, we must select the most appropriate target detection method for moving target detection before target tracking. In this way, the impact on the follow-up tracking can be minimized to the greatest extent. Results are shown in Table 3.

First, the texture feature statistics of the image are complex and time consuming. For example, when the LBP feature is counted, the value of 8 neighboring points around the image should be calculated for each pixel point. Compared with the color feature, the calculation amount of texture feature increases by 8 times when the histogram information of the region is counted; second, the feature information of the inner edge is relatively small. The effect of using edge feature information of image to detect target is not ideal; finally, the correlation between RGB color channels is strong, but the correlation of HSV color space is relatively weak. So when extracting images, RGB color vector is usually converted to HSV color vector, and the conversion process is relatively simple, so the processing time is not increased. The tracking process of the target establishes the relationship between the front and rear frame images, so the error of detection results of a few frame images will not affect the overall tracking effect of the system.

Morphological processing and connected domain labeling were performed to obtain the extraction results, and the extraction results of shadows and bright spots were

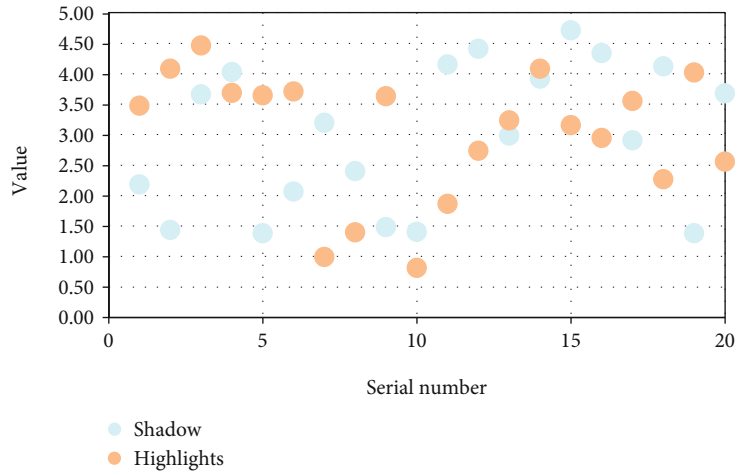

Figure 3: Extraction results of shadows and highlights.

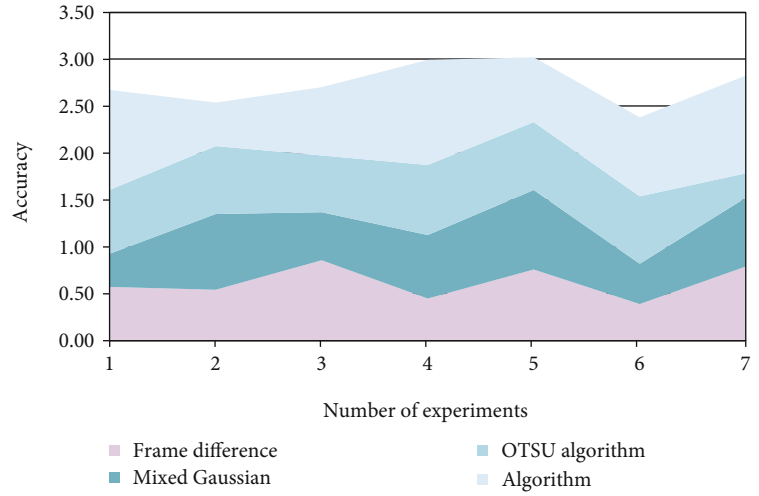

Figure 4: Comparison of algorithm accuracy.

combined and displayed as shown in Figure 3. It can be seen from the figure that in the processed image, the pixel value of the bright spot reaches more than 250, which is convenient for extraction. For the extraction of shadows, when the moving target is close in the scene, the spread of the moving target's shadow in the distance will cause the pixel value between the two targets to also decrease, and the histogram equalization cannot significantly widen this part of the gap. The grayscale piecewise linear stretching method can change the grayscale distribution of a specific pixel interval and highlight the details of the image. However, it can reduce the missed detection rate due to background extraction and image registration errors. For target tracking, especially for maneuvering targets, missed detection increases the probability of occurrence of false follow-up and follow-up time, and the impact on tracking accuracy is greater than the increase in a small amount of false alarms is shown in Figure 3.

4.3. Algorithm Performance. The accuracy comparison of the algorithm is shown in Figure 4. As can be seen from the figure, the accuracy of the algorithm in this paper is the highest, while the accuracy of the frame difference method is the lowest. Because the frame difference method is more sensitive to the disturbance in the background, there is interference in the detected target, which makes the *FP* value larger, which reduces the accuracy of the algorithm. Although the target detected by the Gaussian mixture method also has interference, compared with the frame difference method, the integrity of the target detected by the Gaussian mixture method is higher than that of the frame difference method, which makes the TP value of the algorithm larger than that of the frame difference method. Therefore, the accuracy rate of Gaussian mixture is higher than that of frame difference method; the target integrity detected by OTSU algorithm is higher than that obtained by Gaussian mixture method, and the accuracy rate of OTSU algorithm is higher than that of Gaussian mixture method when the number of interference points is not much different; the integrity degree of target detected by this algorithm is almost the same as that of OTSU algorithm. At the same time, the processing effect of the algorithm is better than the other three algorithms, so

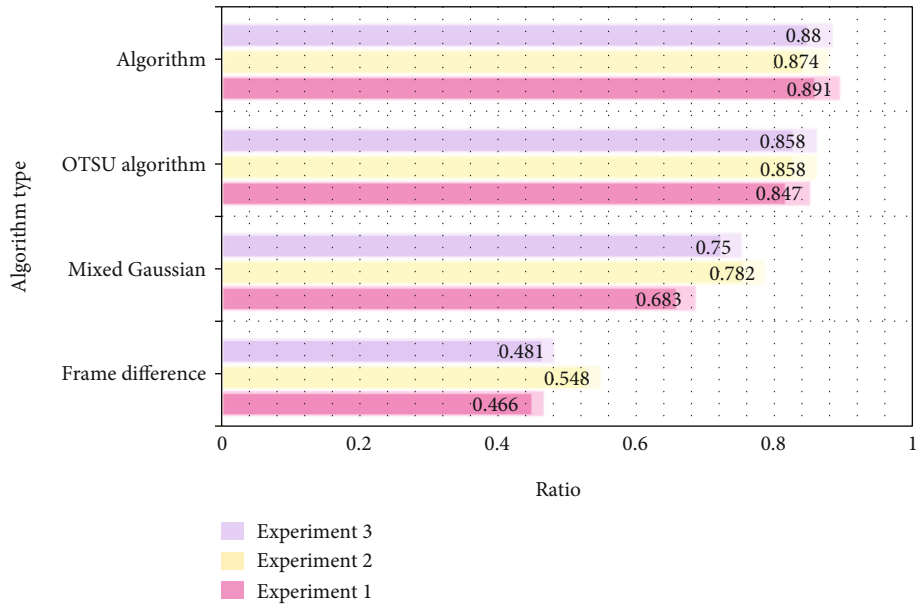

Figure 5: Comprehensive performance comparison of algorithms.

the *TP* value of the algorithm is the largest, the *FP* value is the smallest, and the accuracy of the algorithm is the highest.

Particle filter algorithm includes two steps: prediction and update. First, the motion state of the target in the previous frame is analyzed as information, and the result of the analysis is used to predict the current frame. The motion state of the target in the current frame is obtained by prediction and observation as the posterior information. After the above iterative process, the target motion state is predicted and tracked. But with the extension of tracking time, particle filter algorithm will inevitably lead to the weight of most particles is very low, and a small number of particles are very high, which is called particle degradation. In this case, a large amount of time may be spent on the particles with low weight, and the calculation results of these particles have little effect on the posterior information, and the reliability of the final results is very low. Therefore, we need to use resampling method to remove the particles with small weight and retain and copy the particles with heavy weight to replace the particles with small weight results are shown in Figure 4.

The whole process of moving target detection is that the image collected by the camera is grayed first, and then the moving target is detected by three frame difference method. Then, after filtering and denoising, the gray image is closed by morphology. Finally, the moving object is selected by frame, and the moving target area is obtained in the image. It can be seen from the above detection results that the detection results of moving targets are better. However, the detected moving area is larger than the target, which is because after the image operation, part of the background is covered by the foreground after dilation operation, and the shadow caused by the occlusion of light in the image is mistaken for the moving target. The comprehensive performance comparison of the algorithm is shown in Figure 5. The accuracy and recall rate of frame difference method are the lowest, so its comprehensive index is the lowest among the four algorithms; the comprehensive performance index of Gaussian mixture method in three groups of experiments is higher than that of frame difference method, but it is still lower than OTSU algorithm and the algorithm in this paper, especially in experiment 1, the integrity of the detected target is poor and the recall rate is low. Compared with OTSU algorithm, its comprehensive index is 16.4% lower than that of OTSU algorithm and 20.8% lower than that of this algorithm. Compared with OTSU algorithm, the comprehensive index of this algorithm is higher than that of OTSU algorithm, which is 4.4% higher in experiment 1, 1.6% higher in experiment 2, and 2.2% higher in experiment 3, so the comprehensive performance of this algorithm is the best. Results are shown in Figure 5.

5. Conclusions

This paper mainly studies the martial arts moving target detection and tracking algorithm in intelligent system. Moving target detection and tracking a moving target is a process of two closely linked, detection is the basis of tracking, and tracking is to get the target movement information, such as target position, motion parameters such as speed, direction, these information for subsequent movement behavior, behavior understanding, semantic analysis of high-level applications, and context-sensitive reviews of structurally correct source programs provide unnecessary data for high-level compilation processes. The image is processed according to the grayscale and edge features, and the moving target and background are segmented by appropriate threshold to obtain the moving target. When tracking the moving target, we take the detected moving target as our initial template, extract the key features according to the template, and then select the appropriate tracking algorithm to find the moving target.

The key of the moving target detection method is to establish a model describing the target according to the characteristics of the target itself and then detect the moving target according to the model. Vibe algorithm is a background modeling method proposed in recent years. It is a moving target detection method based on pixel level, using random clustering of samples, and quickly and effectively performing background modeling. In the dynamic background interference environment, the Vibe modeling method does not have a very good foreground and background segmentation effect. According to the variance of the sample set of the current pixel, the fixed radius threshold R is changed to an adaptive threshold. Through experimental comparison and quantitative analysis, under the dynamic background of the algorithm in this paper, the recall rate RE increased by 0.2, and the comprehensive index $F1$ increased by 0.09.

This paper analyzes the importance of background modeling to the background subtraction method and combines the improved background subtraction method and frame difference method to carry out detection experiments. A large number of experiments have proved that the method can accurately extract the target, the influence of background interference on the moving target is suppressed, and the accurate detection of the moving target is realized. For the severe occlusion of the target, this paper uses the mean-shift tracking algorithm to track the occluded target on the basis of using the filter to estimate the target. Through experiments, the algorithm can track the moving target in real-time and realize the accurate tracking of the moving object when it is completely occluded. Of course, there are still many shortcomings in this study for tracking and detection of countless movements. It is hoped that future studies can be more complete and more academic.

Data Availability

No data were used to support this study.

Conflicts of Interest

The author states that this article has no conflict of interest.

Acknowledgments

This study was funded by 2020 Guangxi Philosophy and Social Science planning research topic: Guangxi ethnic minority sports culture inheritance and national fitness integration path research under the Healthy China strategy (20 FTY011).

References

[1] Y. Hu, M. Dong, K. Ota, A. Liu, and M. Guo, "Mobile target detection in wireless sensor networks with adjustable sensing frequency," *IEEE Systems Journal*, vol. 10, no. 3, pp. 1160–1171, 2016.

[2] Y. Hu and A. Liu, "Improvement the quality of mobile target detection through portion of node with fully duty cycle in WSNs," *Computer Systems ence and Engineering*, vol. 31, no. 1, pp. 5–17, 2016.

[3] C. Shi, S. Salous, F. Wang, and J. Zhou, "Power allocation for target detection in radar networks based on low probability of intercept: a cooperative game theoretical strategy," *Radio ence*, vol. 52, no. 8, pp. 1030–1045, 2017.

[4] W. Yu, Y. Wang, H. Liu, and J. He, "Superpixel-based CFAR target detection for high-resolution SAR images," *IEEE Geoscience and Remote Sensing Letters*, vol. 13, no. 5, pp. 730–734, 2016.

[5] X. Liu and Z. Zhang, "A vision-based target detection, tracking, and positioning algorithm for unmanned aerial vehicle," *Wireless Communications and Mobile Computing*, vol. 2021, 12 pages, 2021.

[6] H. Deng, X. Sun, M. Liu, C. Ye, and X. Zhou, "Infrared small-target detection using multiscale gray difference weighted image entropy," *IEEE Transactions on Aerospace & Electronic Systems*, vol. 52, no. 1, pp. 60–72, 2016.

[7] J. Zheng, T. Su, H. Liu, G. Liao, Z. Liu, and Q. H. Liu, "Radar high-speed target detection based on the frequency-domain deramp-keystone transform," *IEEE Journal of Selected Topics in Applied Earth Observations & Remote Sensing*, vol. 9, no. 1, pp. 285–294, 2016.

[8] X. Jingwei, G. Liao, and L. Huang, "Robust adaptive beamforming for fast-moving target detection with FDA-STAP radar," *IEEE Transactions on Signal Processing*, vol. 65, no. 4, pp. 973–984, 2017.

[9] Y. Li, J. Pan, and J. Long, "Multimodal BCIs: target detection, multidimensional control, and awareness evaluation in patients with disorder of consciousness," *Proceedings of the IEEE*, vol. 104, no. 2, pp. 332–352, 2016.

[10] J. Xu, X. Zhou, L. C. Qian, X. I. A. N. G. G. E. N. Xia, and T. Long, "Hybrid integration for highly maneuvering radar target detection based on generalized radon-fourier transform," *IEEE TRANSACTIONS ON AEROSPACE AND ELECTRONIC SYSTEMS AES*, vol. 52, no. 5, pp. 2554–2561, 2016.

[11] Y. Ji, J. Zhang, Y. Wang, and X. Chu, "Vessel target detection based on fusion range-Doppler image for dual-frequency high-frequency surface wave radar," *IET Radar Sonar ? Navigation*, vol. 10, no. 2, pp. 333–340, 2016.

[12] G. Papa, P. Braca, S. Horn, S. Marano, V. Matta, and P. Willett, "Multisensor adaptive bayesian tracking under time-varying target detection probability," *IEEE Transactions on Aerospace Electronic Systems*, vol. 52, no. 5, pp. 2193–2209, 2016.

[13] D. Xiang, T. Tang, Y. Ban, and Y. Su, "Man-made target detection from polarimetric SAR data via nonstationarity and asymmetry," *IEEE Journal of Selected Topics in Applied Earth Observations and Remote Sensing*, vol. 9, no. 4, pp. 1459–1469, 2016.

[14] D. H. Lee, J. W. Shin, D. W. Do, S. M. Choi, and H. N. Kim, "Robust LFM target detection in wideband sonar systems," *IEEE Transactions on Aerospace & Electronic Systems*, vol. 53, no. 5, pp. 2399–2412, 2017.

[15] M. Akcakaya, S. Sen, and A. Nehorai, "A novel data-driven learning method for radar target detection in nonstationary environments," *IEEE Signal Processing Letters*, vol. 23, no. 5, pp. 762–766, 2016.

[16] P. L. Shui, M. Liu, and S. W. Xu, "Shape-parameter-dependent coherent radar target detection in K-distributed clutter," *IEEE Transactions on Aerospace & Electronic Systems*, vol. 52, no. 1, pp. 451–465, 2016.

[17] G. Gassier, G. Chabriel, and J. Barrère, "A unifying approach for disturbance cancellation and target detection in passive

radar using OFDM," *IEEE Transactions on Signal Processing*, vol. 64, no. 22, pp. 5959–5971, 2016.

[18] H. Yang, Z. Cao, and Y. Pi, "Target detection in high-resolution SAR images via searching for part models," *IEEE Geoence and Remote Sensing Letters*, vol. 14, no. 5, pp. 664–668, 2017.

[19] I. Rahman, C. Hollitt, and M. Zhang, "Contextual-based top-down saliency feature weighting for target detection," *Machine Vision & Applications*, vol. 27, no. 6, pp. 893–914, 2016.

[20] S. Tu and Y. Su, "Fast and accurate target detection based on multiscale saliency and active contour model for high-resolution SAR images," *IEEE Transactions on Geoence & Remote Sensing*, vol. 54, no. 10, pp. 5729–5744, 2016.

[21] N. Shi, M. Li, Y. Deng et al., "Experimental demonstration of a multi-target detection technique using an X-band optically steered phased array radar," *Optics Express*, vol. 24, no. 13, pp. 14438–14450, 2016.

[22] Z. Niu, J. Zheng, T. Su, and J. Zhang, "Fast implementation of scaled inverse Fourier transform for high-speed radar target detection," *Electronics Letters*, vol. 53, no. 16, pp. 1142–1144, 2017.

[23] S. Althunibat, A. Antonopoulos, E. Kartsakli, F. Granelli, and C. Verikoukis, "Countering intelligent-dependent malicious nodes in target detection wireless sensor networks," *IEEE Sensors Journal*, vol. 16, no. 23, pp. 1–8639, 2016.

[24] J. Tan, J. Zhang, and Y. Zhang, "Target detection for polarized hyperspectral images based on tensor decomposition," *IEEE Geoence and Remote Sensing Letters*, vol. 14, no. 5, pp. 674–678, 2017.

[25] Q. Hu, H. Su, S. Zhou, Z. Liu, and J. Liu, "Target detection in distributed MIMO radar with registration errors," *IEEE Transactions on Aerospace & Electronic Systems*, vol. 52, no. 1, pp. 438–450, 2016.

[26] Y. Dong, B. Du, and L. Zhang, "Target detection based on random forest metric learning," *IEEE Journal of Selected Topics in Applied Earth Observations & Remote Sensing*, vol. 8, no. 4, pp. 1830–1838, 2015.

Hindawi
Wireless Communications and Mobile Computing
Volume 2022, Article ID 8286371, 12 pages
https://doi.org/10.1155/2022/8286371

Research Article

Application of Multiagent Technology in Intelligent Distributed Sports Training Simulation System

Dongfang Nie[1] **and Jiannan Liu**[2]

[1]*Ministry of Sports, Chongqing University of Science and Technology, 401331 Chongqing, China*
[2]*Ministry of Sports, Chongqing Jiaotong University, 400074 Chongqing, China*

Correspondence should be addressed to Jiannan Liu; 980200900013@cqjtu.edu.cn

Received 22 December 2021; Revised 25 February 2022; Accepted 10 March 2022; Published 23 March 2022

Academic Editor: Mohamed Elhoseny

Multiagent technology, as a conceptual model commonly used in intelligent systems, has now had a lot of related research, and it is also widely used in sports training simulation systems. This paper mainly studies the development of the sports training simulation system based on agent technology. This paper proposes the motion perception system of multiagent technology in sports training. In the research, this paper introduces the related concepts and methods of agent in detail. In order to better simulate the changes of human joints during exercise with the system, this article uses a variety of comparison methods. Among them, the experiment of the imaging analysis module is carried out through the simulation of the simulation system. The experimental results show that the role of multiagent in the simulation system is huge. In linear motion, the accuracy of joint extraction has reached more than 95%. The extraction of joints in the curve movement reached more than 80%, indicating that it can not only complete the relevant processing adaptively but also predict and correct the exercise process of the trainer. Therefore, in the research of sports training simulation system, more attention should be paid to the research of curve motion.

1. Introduction

1.1. Background. Modern competitive sports are rapidly developing towards high, difficult, and sophisticated, and the role of science and technology in promoting the development of competitive sports has become increasingly apparent. At present, competitive sports have developed to a fairly high level. In training simulation of competitive sports, the research hotspot of system simulation in recent years is the object-oriented simulation method. At present, there is no complete sports video analysis software and computer analysis software for human body motion in China. In addition, it does not have the ability to handle multiple input devices. With the continuous advancement of related technologies, virtual reality technology will be popularized. It provides effective and brand-new training methods of athletes through virtual training venues, intelligent interface technology, physiology, and multisensor technology. It should be pointed out that sports training simulation research has just started, providing an effective platform for technical communication and exchanges with athletes and coaches and also providing application space for the expansion of information science. The multiagent system is distributed and autonomous, which can save the energy consumption of the entire system while completing the adaptation to the environment. In the early days, the multiagent system replaced the traditional distributed control system with intelligent control and solved unstructured problems that were difficult to solve by conventional methods by imitating human behavior and thought. It can also accomplish larger and more complex tasks through collaboration. Although intelligent control methods such as fuzzy control were also introduced to/into the later period, most of the research on the application of agent technology to simulation systems stayed in the theoretical research stage.

1.2. Significance. Physical training is vital to the role of athletes. With the development of technology, the sports

training simulation system has also been continuously developed, which is very useful for the training of athletes. In developed countries such as the United States and Canada, they started early, and their use of the sports training simulation system has brought obvious effects. For example, in diving, although the strength of the national team is top, the lack of unified standards such as a simulation system makes it difficult to achieve the purpose of passing on excellent training experience and skills. The simulation system can store motion data. Good standards can be used as template training, and errors can be found in time. Now, related technologies have become mature, so it is meaningful to carry out research on sports training simulation systems.

1.3. Related Work. Although there are not many previous studies on the sports training simulation system, there are still some studies on the realization of some functions, such as video acquisition system and motion analysis system. Higher, faster, and stronger is the purpose of the Olympic Games and the goal of sports. In order to achieve this goal, many related researches and applications for sports training have spontaneously emerged. Hui believes that in the swimming training process, coaches mostly use traditional methods to train students, and the training effect is not good [1]. Rhodes et al. examined the speed curves of elite wheelchair rugby (WCR) players in game simulation training exercises with different player numbers and batting time rules. Use an RF-based indoor tracking system for monitoring during the 5-month training period. Experiments have proved that by reducing the number of players on the field and the hitting time to 15 seconds, the coach can significantly improve the speed curve of WCR elite players in match simulation training [2]. In order to improve the safety control ability of dragon boat sports physical training, Yin and Wang used the advantages of machine learning in data analysis and feature mining in dragon boat sports training and proposed a machine learning-based dragon boat sports physical training safety mode control model [3]. Gokeler et al. were immersed in a virtual reality environment to evaluate the impact of ACL reconstruction (ACLR) on the biomechanics of the patient's knee joint. After ACLR, the patient was immersed in a virtual reality environment and showed knee biomechanics similar to CTRL [4]. When Kłodowski et al. evaluated sports training methods, first, they performed a motion analysis of the object. Based on experimental motion data (motion analysis and multibody simulation), it created two models: rotation control model and torque control model. For comparison, it created a model with motion input from the literature [5]. Zhang and others created an autonomous karate team player (KaraKter) based on the simulation system. This role can be used for VR-based training and research of karate team players. For real-time interaction with KaraKter, human athletes are tracked in a virtual environment. Evaluation shows that all experts consider the system to be very useful in the training of karate players [6]. In terms of multiagent technology, Laatabi and others believe that with the development of powerful computers and the availability of massive data, the use of agent-based models to model and simulate the world is one of the key disciplines emerging in the field of computing today [7]. Mahalaxmi and Esther proposed an improved ant colony optimization routing algorithm for IoT based on multiagent technology. The experimental results show that the network simulator NS-2 is used to evaluate the performance of the proposed algorithm program [8]. In general, the research on sports training simulation systems is more on the opposite of image processing, and there is no simulation training for sports systems, which is urgently needed for trainers.

1.4. Innovation. In this paper, a motion perception system based on multiagent technology in motion training is proposed, and the system has a good effect on joint extraction of linear motion, and the system can help motion simulation training. This paper discusses the application research of multiagent technology in intelligent distributed sports training simulation system. Although there are not many predecessors of sports training simulation system, there are many excellent researches. This article is based on previous research and made some innovations: (1) the system design emphasizes the role of multiagent technology, which is easy to find in the article. This article uses a lot of pen and ink to describe the application of agent technology in the simulation system. (2) For the link of the simulation system to simulate the motion engine, an intelligent distributed pressure sensor is specially added. This is of great significance for complementing the data in the simulation system and better simulating the joint points of motion. (3) Principal component analysis is used in data analysis, and all components are analyzed in the algorithm of traditional simulation system. Principal component analysis is proposed in this article, which will greatly reduce the amount of data for system analysis.

2. Agent Technology and Simulation Method

2.1. Multiagent Technology. The original concept of agent technology is derived from the field of artificial intelligence. Its concept involves a wide range. Generally speaking, the definition of its authority is divided into weak definition and strong definition [9]. In the weak definition, to include the characteristics of autonomy, social ability, etc., the specific program that can complete the given work is the agent. In a strong definition, it is a computing unit with a control problem solving mechanism [10], an individual with knowledge and ability to solve practical problems. It can be a robot, an expert system, a process, a calculation module, or a solution unit [11]. Agent technology is a hot spot in the current recommendation system industry [12].

As an agent model, it can have the following characteristics:

(i) Autonomous ability: it adopts multithreaded realization method, realizes its own functions through continuous actions, and has self-control ability. It can regulate its own behavior and state without the direct intervention of humans or related agents [13]. It can transfer from this place to other places on the same network while ensuring its internal state remains unchanged

(ii) Social ability: it solves problems through information exchange and communication with users, resources, or other agents. And it uses agent communication language and message mode for information exchange and behavioral collaboration [14]. It can find a more reasonable reasoning method to solve its current problems based on the knowledge and experience existing in its current database

(iii) Response ability: agent will automatically recognize changes in the environment, be able to perceive the environment, and take corresponding actions according to the changes, so as to achieve the ability to respond to the environment. When it thinks it can solve the problem it wants to solve, it always tries its best to accomplish this intention [15]

(iv) Proactiveness: controlling action and behavior planning through changes in the state of the mind, which regulates the environment and behavior [16]. It can be actively target-driven according to its own and global knowledge and finally can adapt to the new environment by changing its will

It is precisely because of the relevant capabilities of the agent that it can play an important role in analysis in the system, and it is also because of the multiagent technology composed of each single agent that the functions of the simulation system can be realized.

In application, multiagent technology is generally used. Because of the characteristics of a single agent, when forming a multiagent structure, all submodules can communicate and collaborate to complete a series of complex problems. It is similar to simulating the human way of thinking and the nature of human social collaboration, so it is also more suitable for an open and dynamic social environment to deal with similar problems that require automatic evolution [17]. Multiagent generally has the following structures.

(1) Reactive agent

The reactive type does not have any internal state and does not include symbolic world models and complex reasoning. It is analyzed by the reasoner and planner with the support of the knowledge base. When the external environment changes, it cannot be obtained directly through perception. This is because it does not have any learning ability, but it executes prespecified conditions-action rules. Although its structure is simple, the function is single, and the response speed is fast [18]. The structure is shown in Figure 1.

(2) Deliberate agent

The deliberate agent is a kind of consciousness system. This structure determines that the intelligence of this type of agent is relatively high, but it requires a lot of time and accuracy. The external environment is complex, the internal state symbolization is complicated, and it cannot solve the situation of limited resources [19]. This greatly affects the system efficiency [20]. Based on the deliberate agent, the BDI theoretical model is the most widely used. It adds three different factors to make the model more considerate, so it can handle many complex problems. However, there are not many applications for it, so this article will not describe it too much [21]. The structure is shown in Figure 2.

(3) Hybrid agent

Neither the purely single structure nor the best structure mode of the agent. This structure combines the deliberate and reactive architectures and combines the nonclassical and classic technologies of artificial intelligence technology. It is currently a more popular one [22, 23]. It has both the ability to deal with complex environments in a deliberate manner and the advantages of high reactive efficiency, which makes people gradually agree with the hybrid agent structure [24]. The structure is shown in Figure 3.

2.2. Sports Training Simulation System. Computer simulation technology is based on a variety of disciplines and theories, and the application of simulation technology in Chinese sports has developed relatively quickly. The sports video image analysis system can collect and analyze the actual movement of the human body to construct a realistic training virtual environment, and then, the computer drives the virtual person on the screen according to the recorded data [25–28]. The real-time processing part of the system mainly uses background separation technology to obtain the foreground part of the video, but the operation is complicated, and it is difficult to learn. It requires us to emphasize the practicality of the simulation system [29]. However, due to its high computational complexity or the need to manually set cumbersome parameters, it is difficult to meet actual needs. It is difficult to develop a sports training simulation system, and less than 50% of them have good practicality. For example, parameters such as the physical characteristics of the human body can be selected interactively, and technical actions can be realistically simulated, designed, and analyzed in a three-dimensional manner. Compared with developed countries, application is still relatively backward [30].

There are a large number of applications of virtual reality technology in training simulation, of which the two most critical parts are the modeling of the motion of the simulation object and the construction of the virtual environment. The main goal of virtual human research is to truly reflect the geometry of human beings, while motion modeling needs to be based on the dynamics of the simulated object. Through the establishment of a certain process and a certain system model, a series of experiments are carried out to understand the behavior of the system based on the model or the different operating strategies of the system. In order to make a breakthrough from the traditional theory based on reductionism and linear thinking, the comprehensive application and perfection of training simulation needs further research, and it is currently in the stage of theoretical maturity and social practice. National and international computer networks have emerged one after another. The

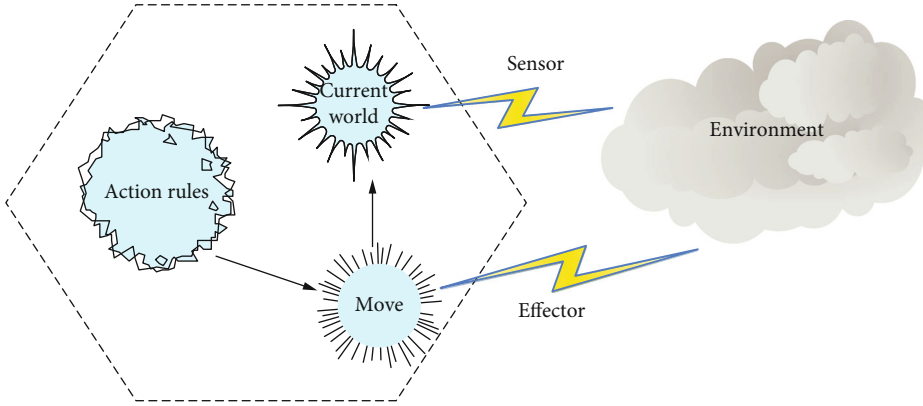

Figure 1: Reactive agent.

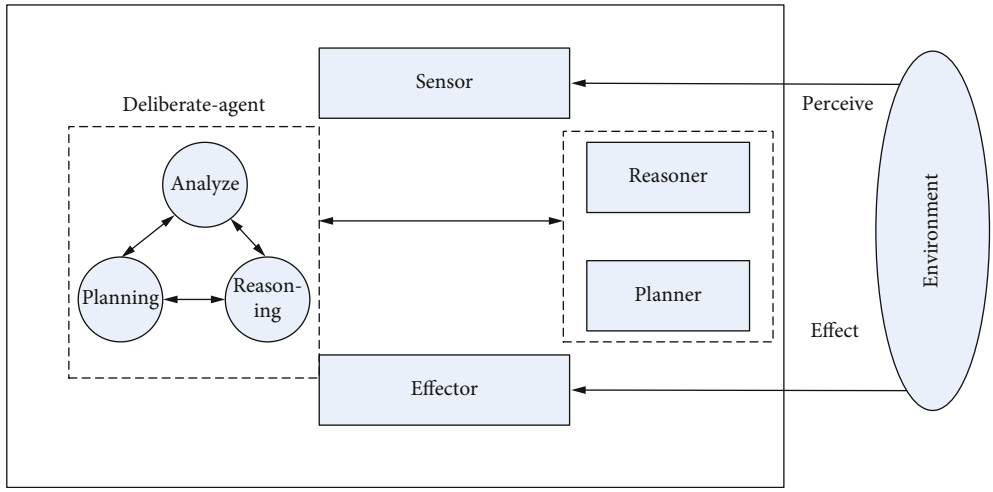

Figure 2: Deliberate agent

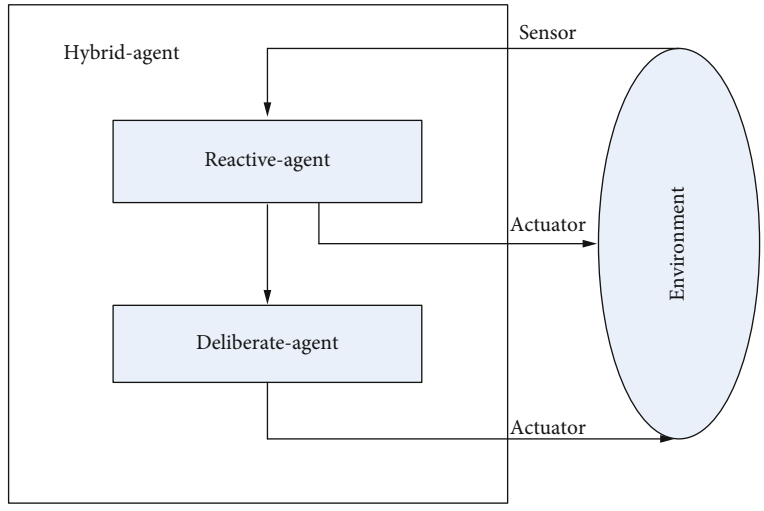

Figure 3: Hybrid agent.

communication standards between the subjects and the behavior design of the subjects have become more mature, and the relationship between the running time and the number of subjects has increased exponentially [31]. In exploring an efficient operation mode, the sports industry environment is taking shape. It needs the support of the network

to facilitate the transmission of sports information and the analysis of sports data. This process achieves the prediction and analysis of the sports system.

3. Construction of Sports Training Simulation System

3.1. Related Technology. In the construction of the training simulation system, an important link is the extraction of moving objects. This article introduces the use of motion camera images to extract the joints of moving objects, including image preprocessing and data analysis.

T_i is the pixel of the extraction target, and I_i is the original pixel. There is a big difference between the gray value of the moving target in the foreground of the moving target and the gray value of the background, and the gray value of the moving object itself will not have a big difference, as in Equation (1), where a represents the grayscale of the moving target and b represents the grayscale value.

$$T_i(a,b) = \begin{cases} 260, & I_i(a,b) - I_{i+1}(a,b) \geq D, \\ 0, & I_i(a,b) - I_{i+1}(a,b) > D. \end{cases} \tag{1}$$

Compare the pixels of the binarized image with the pixels of the original image to achieve the return of the pixel value, as shown in

$$I_i(a,b) = \begin{cases} 0, & \text{if}(T_i(a,b) = 0), \\ I_i(a,b), & \text{else}. \end{cases} \tag{2}$$

A more effective method is adopted, that is, the images of adjacent frames are sequentially superimposed to form the bottom plate E_p, as shown in

$$E_p(a,b) = (S_0(a,b), H_0(a,b), C_0(a,b))^T. \tag{3}$$

For the pixels that have been assigned on the original base plate, the algorithms of formula (4) and formula (5) are used:

$$E_p(a,b)' = \frac{\left(E_p(a,b) + E_k(a,b)\right)}{2}, \tag{4}$$

$$E_p(a,b)' = \left(\frac{\left(S_p(a,b) + S_k(a,b)\right)}{2}, \frac{\left(H_p(a,b) + H_k(a,b)\right)}{2}, \left(C_p(a,b)\right)\right)^T. \tag{5}$$

Among them, $E(a,b)$ represents the adoption of pixels, and its product represents the expectation of the formula.

Figure 4 shows a schematic diagram of the algorithm extracting joints. When analyzing sports data, it is impossible for the computer to extract all the information. Therefore, it mainly extracts important data of its arm and knee joint. In Figure 4, the trainer's side view is recorded, which is also the position of the computer. Because one of its arms will be blocked, it needs to be simulated by algorithms. After categorizing the elbow joint data, it is combined with the motion data for analysis. Knee joints are subjected to fluctuation analysis, and the integrated motion data is saved and entered into the system for retention.

3.2. Design of Virtual Human Walking Engine Based upon ICA. Autocorrelation (ICA) technology can propose outliers in the data and make the simulator more stable. We use autocorrelation(ICA) technology to extract independent motion components from motion data, which correspond to meaningful motion features. And these motion characteristics can describe complex human motion. Similar to the partial autocorrelation (PCA) method, the design idea of the ICA-based virtual human walking engine is by modifying the independent motion components in the ICA domain, that is, operating the basis vectors representing the motion feature space, various types of motion can be generated.

(1) For certain data

Assume that the motion data $\phi(t)$ of the three-dimensional human body is represented as shown in

$$\phi(t) = \phi_1(t), \phi_2(t), \cdots, \phi_n(t)^T. \tag{6}$$

In the ICA model, the mean value of the motion data must be zero, as shown in

$$\overline{\phi}(t) = \phi(t) - E(\phi(t)). \tag{7}$$

Applying the ICA algorithm, it can be represented by a series of independent components as shown in

$$\overline{\phi}(t) = As(t). \tag{8}$$

The purpose of ICA is to find a matrix B, expressed as

$$n(t) = B\overline{\phi}(t). \tag{9}$$

In order to simplify the calculation, as in

$$m(t) = V\overline{\phi}(t). \tag{10}$$

After applying the PCA algorithm, Equation (9) is rewritten as

$$n(t) = W^T m(t). \tag{11}$$

Therefore, the independent component $y(t)$ can be expressed as

$$n(t) = W^T m(t) = W^T V\overline{\phi}(t) = W^T V(\phi(t) - E(\phi(t))). \tag{12}$$

The independent components of the exercise data correspond to different styles of exercise, as in

$$v_{1,2} = v_1 e^1 + v_2 e^2. \tag{13}$$

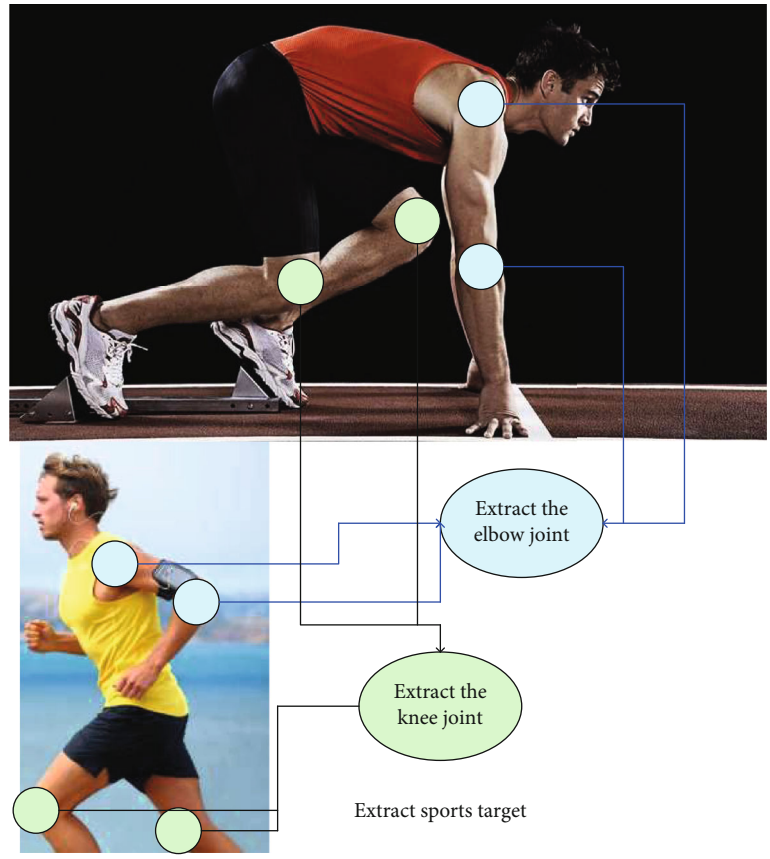

Figure 4: Schematic diagram of extracting joints.

Table 1: Different style selection table.

PCA	a	b	c	n
Style 1	0	1	1	0
Style 2	1	0	1	1
Style	1	1	1	1

Among them, v_1 and v_2 represent two different styles, and the selection is judged by the decision-making agent.

As shown in Table 1, the choices of different styles are represented by binary codes, so that the algorithm will be more convenient.

After the transfer operation of the independent components, the formula becomes

$$v_2' = v_1 + \left(v_2^s - v_1^s\right)^T e^s. \tag{14}$$

Then, simulate the collected data, as shown in Figure 5.

Figure 5 shows the analysis and processing of exercise data. For data with objects, the goal is clear. Taking into account the agent's ability to adapt to the external environment, its generating walking engine is reliable. When performing PCA analysis in Figure 5, two different divisions were selected. For style 1, it is the data when walking, and for style 2, it is the data when running. The system distinguishes according to the algorithm and enters the data into the corresponding data set.

(2) For data without objects

When there is no movement data of object x in the movement database, but a small amount of movement data of object x is collected in advance, calculate the Mahalanobis distance first, because there is no strong connection in the nonobject data, so the Euclidean distance is not considered, as shown in

$$d_n(\phi_1, \phi_2) = \sqrt{\frac{\sum_i \lambda_1^2 \left(\alpha_i^n - \alpha_i^p\right)^2}{\sum_i \lambda_1^2}}. \tag{15}$$

Calculate the correlation coefficient between object x and object i, as shown in

$$\gamma^{x,p} = \frac{\left[d_n(\phi_1, \phi_2)\right]^{-1}}{\sum_{q=1}\left[d_n(\phi_1, \phi_2)\right]^{-1}}, \quad q = 1, 2, 3, \cdots, i, \tag{16}$$

$$\gamma^{x,p} = \sum_{i=1}^{k} \frac{\omega^{x,p,x_i}}{k}, \quad q = 1, 2, 3, \cdots, i. \tag{17}$$

Calculate the PCA coefficient of object x according to the PCA coefficient of object $1 \sim i$ and the PCA coefficient of attribute s, as shown in

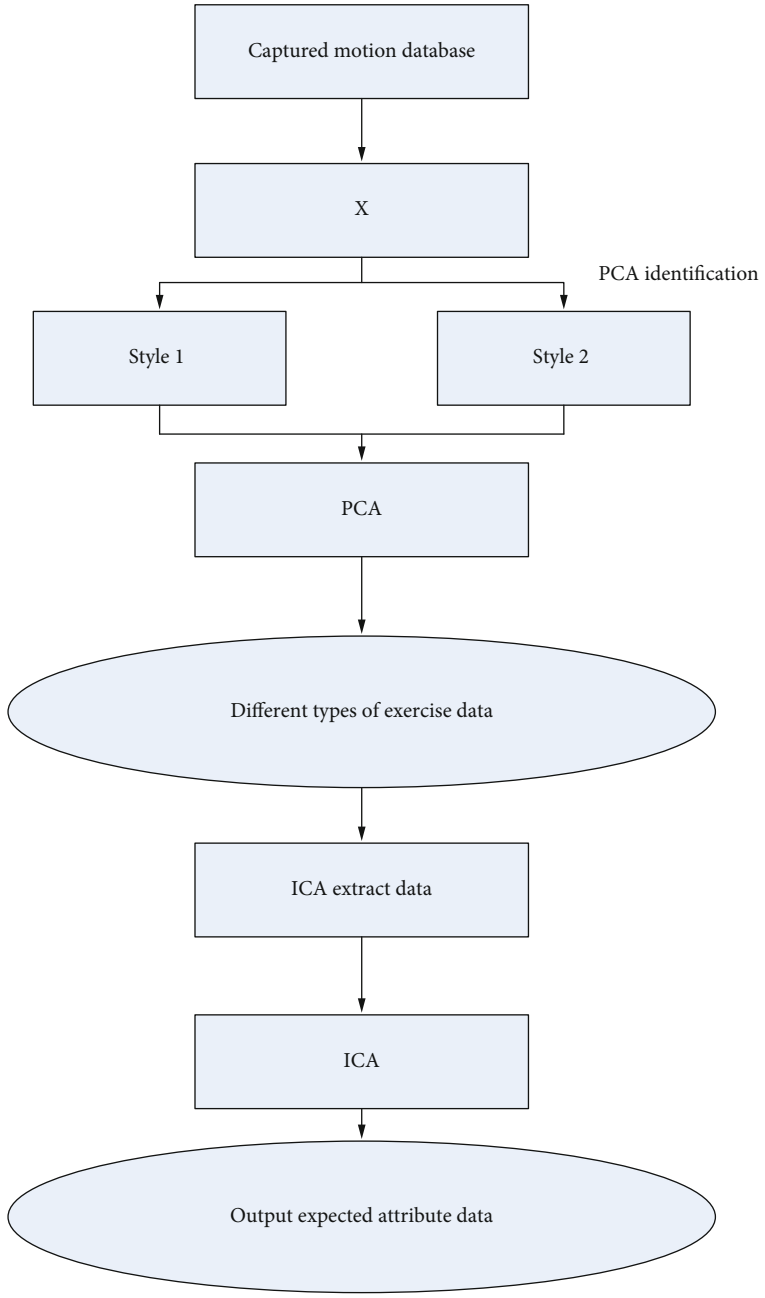

Figure 5: The generation of the walking engine with the motion data of object x in the motion database.

$$\alpha_i^{x,s} = \sum_{i=1}^{k} \gamma^{x,p} \alpha_i^{p,s}. \tag{18}$$

The whole process is shown in Figure 6.

Figure 6 is the processing of motion data without objects. Compared with data processing with objects, it adds the step of creating objects. It can be seen from Figure 6 that because the data is objectless, each object of i is established in the first step. In order to have the correct assignment, in the early stage, there is one data for one object. When i objects are reached, the data is filtered into the previously generated objects, and the objects are directly assigned automatically.

Table 2 shows more reflection terms used in the construction of the agent system, which are listed here.

3.3. Platform Construction. After the introduction of 2.1, we know that the multiagent system has good learning ability, and a human-like social relationship can be formed between a single agent, harmonious, and mutual assistance. Then, this part of the content will design the overall system, through the cooperation of various parts of the agent, to achieve the desired effect of simulated sports training.

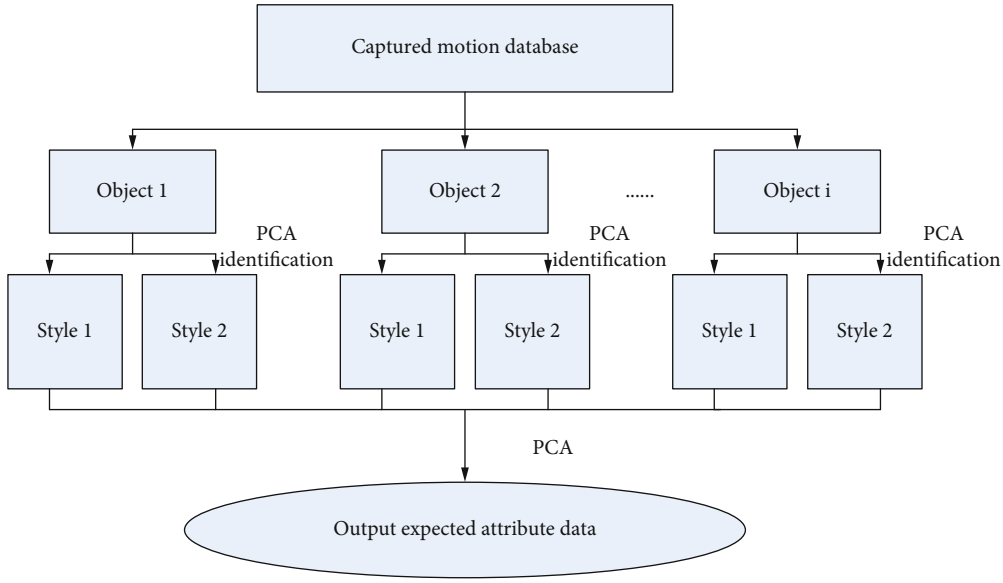

Figure 6: The generation of the walking engine without the motion data of object x in the motion database.

Table 2: Description of main parameters.

Parameter	Illustrate
Inform	Notify other agents that the statement in the message is correct
Agree	Agent accepts the request and agrees to do a certain job
Failure	Notify other agents that a certain task has been executed, and the execution result is a failure
Query	Ask for the correctness of the message

Table 3: Comparison table of main responsibilities of decision-makers and executives.

Decision-maker	Executor
Create and publish a task book	Receiving the task book
Receive and evaluate bids from performers	According to ability to judge whether to accept the task
Pick the right bidder	Send tender notice and create tender
Establish a contract with the winning bidder	If you win the bid, enter into a contract with the manager
Supervise the execution of tasks and check the execution results	Perform tasks and report results as required by managers

(1) Interface agent

Interface agent, as a human-computer interaction interface, accepts the planner's task, then passes it to the functional agent, and requires the planner to input necessary physical and test information. After the plan is made, inform the planner of the plan and make a scientific explanation according to the needs of users. According to the characteristics of problem handling and human-computer interaction components, there must be a corresponding explanation mechanism inside the interface agent.

(2) Blackboard control agent

Since the blackboard control agent is the core of the entire multiagent system, the functional agent and decision-making agent are both regarded as the knowledge source in the blackboard system. It can determine the type of problem according to user needs and play a role in the central nervous system. It does a good job of uploading and distributing, passing the decision-making information to the decision-making machine and the processing information to the processor.

(3) Functional agent

The functional agent categorizes the tasks passed from the blackboard, divides them into multiple small tasks according to actual needs, and assigns them to the corresponding one or more decision-making agents for execution. As a functional agent, it also has other deployment functions. The functional agent also monitors the blackboard and also provides queries on the execution of the system at any time.

(4) Decision agent

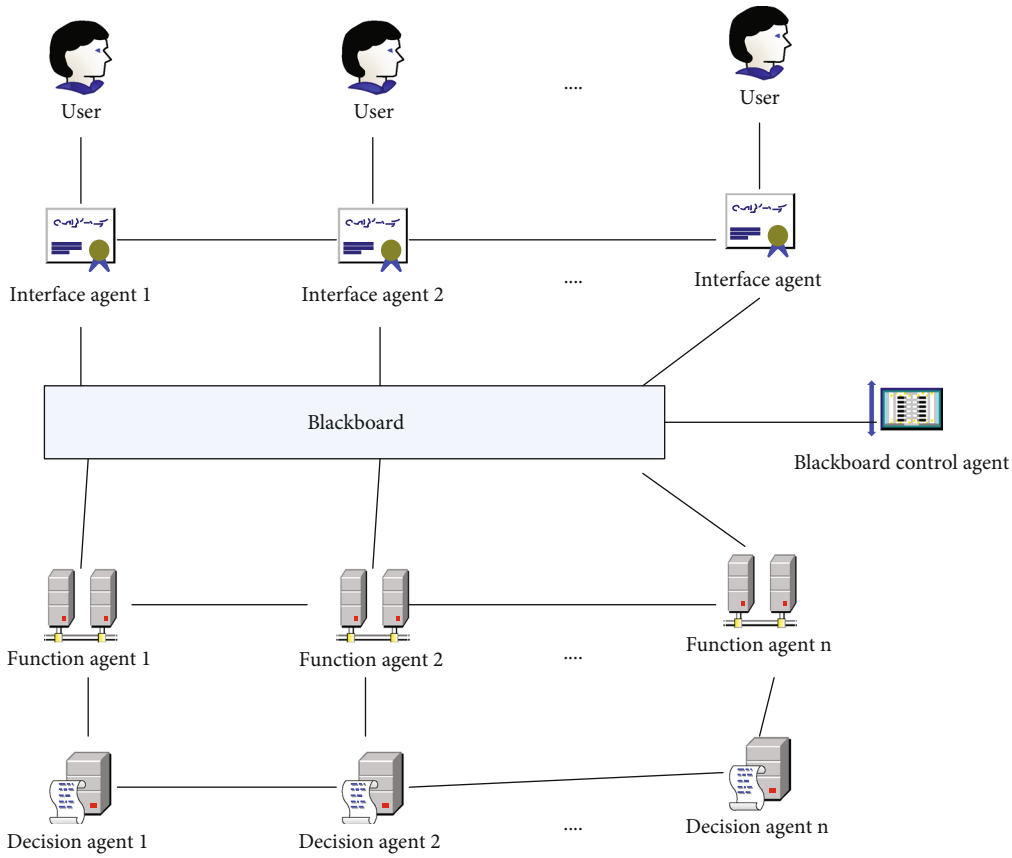

Figure 7: The functional structure diagram of the system.

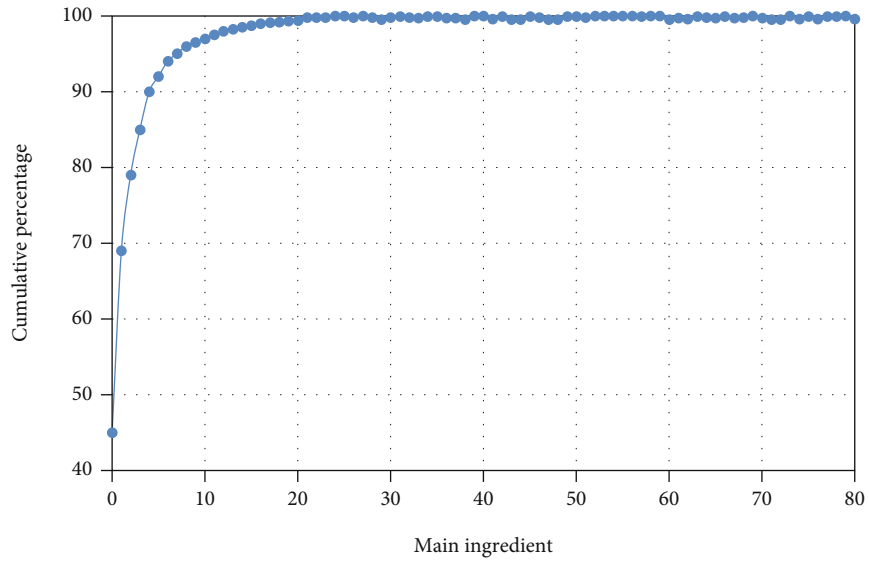

Figure 8: Proportion of principal components in data information.

The decision-making agent class uses a computer and uses a series of algorithms such as a decision tree to give the decision to assign to the task. For some repetitive and simple tasks, it will simply handle it by itself. It can be said that the task of decision-making agent is the highest, and it plays an indispensable role in the system.

Table 3 is a comparison table of the responsibilities of decision-makers and executors. It can be found that decision-makers play more of the role of judgment and assignment.

Figure 7 shows the functional structure of the design system. This is a system structure that is deeply designed based on the user's use, and the interface agent is directly facing

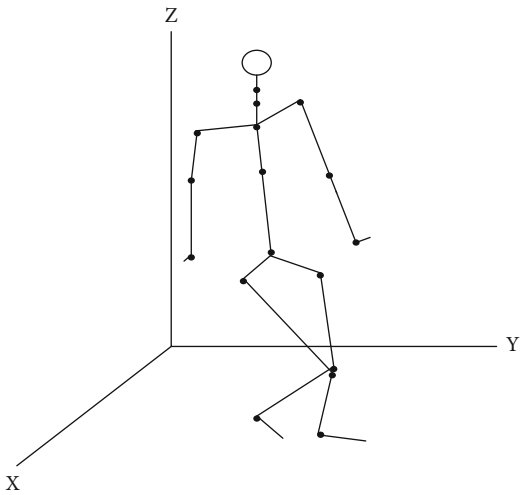

Figure 9: Collection of walking data of a sample.

the user. It handles simple functions through its own feedback and displays the main page to the user as the interface display of the system. The time blackboard in the middle was also mentioned in the introduction to the blackboard agent. As the core of the system, the blackboard plays an important role in uploading and distributing. As can be seen from the structure diagram in Figure 7, all agents must be assembled on the blackboard. It can be seen as central nervous system, which performs the functions of distribution and processing. It is the functional agent, which cooperates with the decision-making agent at the bottom to do various tasks on the blackboard. They can even learn from each other, help each other, and jointly complete some adaptive tasks.

4. System Effect Analysis

4.1. PCA-Based Motion Attribute Changes. The simulation system is to project the captured joint data to the fitting person. Real-time feedback and simulation after data collection are carried out through the multiagent technology, and the height and data of the simulated person can be corrected to produce different effects. Judging from the experimental results, although the system simulation engine is in different data simulating humans, the simulated actions are somewhat distorted, and the results achieved are not like real humans. But in terms of the overall effect, the designed model has a relatively high degree of capture for the simulant in different scenes, and the flow of the movement can be regarded as a comparative flow, and the control of the system can also achieve better results. The main problem is that it cannot perform a good simulation of objects moving in a curve. When the object moves in a curved line, the motion of the simulated human is often greatly distorted to an unrecognizable level, so it is very difficult to change from a curve to a straight one. Therefore, the simulation system can play a greater role in linear motion, but not in curved motion. As shown in Figure 8, generally 2 to 4 principal components are required. This is because in the collected

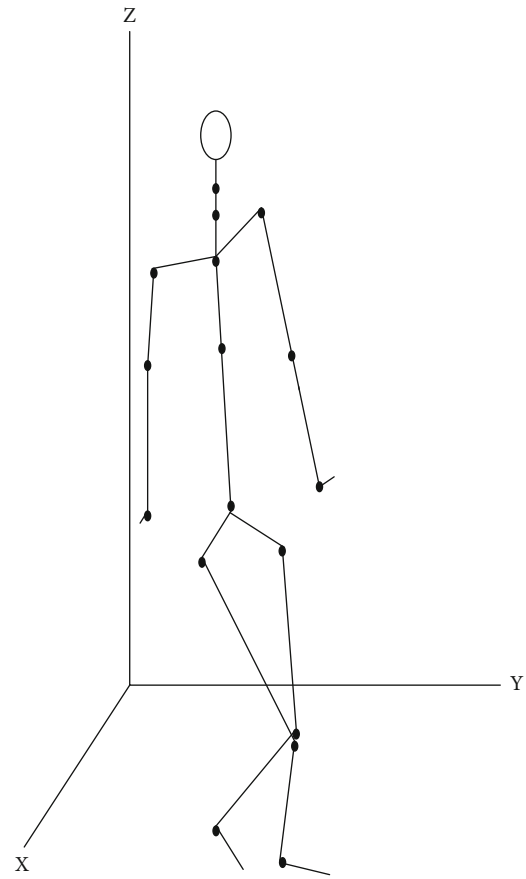

Figure 10: Data used after exercise.

data, more information is obtained from the principal components. The speed of movement can be obtained through changes in the movement of the knee joint. It does not need other data, so we can analyze the principal components, so as to achieve the purpose of improving the calculation efficiency.

In Figure 9, the representation of each joint in the system is unique; some of the movement details are not described. It can be seen that the handling of the arms is still relatively stiff. This is a virtual human supplemented by the system because part of the joints are blocked. In this virtual person, most of the details have already been described, especially the lower body. For the upper body, there are many content nodes, which makes the processing inappropriate.

In Figure 10, the recording is data collection in motion, the frequency is adjusted to 30 frames, and the principal component is used for analysis, so the processing effect will be much better. Although it still cannot analyze the curve movement, the capture of the linear movement is very smooth. In the record of the curve, because the direction vector of the sampling point is always changing, the main joint points are easily occluded. The processing capacity of the decision-making agent and the functional agent will increase, and if they cannot handle it, they will be obfuscated, resulting in a series of constant data points. It leads to little change in the movement range or extremely exaggerated movements.

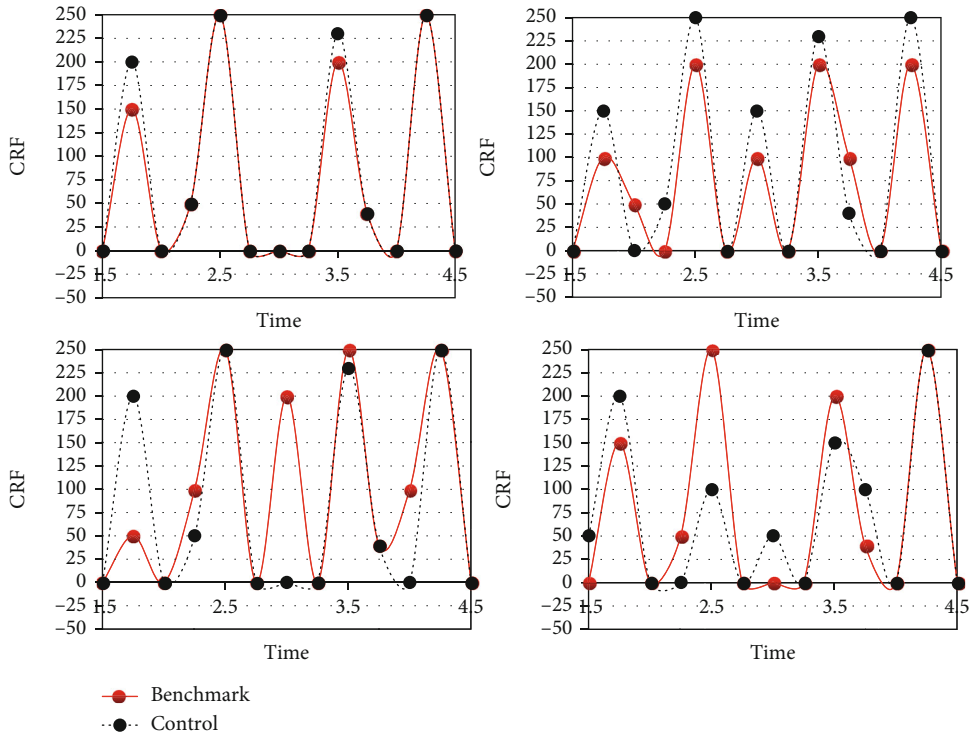

Figure 11: Joint force diagram.

4.2. Joint Force Analysis. The force analysis of the joints is collected by the sensors of the intelligent distributed system, and the force analysis is made on the left and right elbow joints and the left and right knee joints, respectively. The purpose is to obtain the force on the joints of the human body during movement, so as to supplement the data of the occluded part of the imaging system. In the experiment, two sets of data were tested. They were the control group when walking and the experimental group when running.

In Figure 11, the joint force is roughly the same when running and walking, but it is clearly found that the upper limit of the force when running is higher. The force data can be used to measure a state during exercise, which can then be provided to the system as a data supplement. In this way, with the support of data, there will be traces for the processing of the decision-making agent.

5. Conclusions

Nowadays, both virtual technology and computer computing system have made great progress. It is now fully qualified for the design of sports training simulation systems, but the domestic emphasis on related technologies is not particularly enough, and there are technical gaps in some key places, such as video presentation technology. This is actually detrimental to the development of domestic simulation systems. This article starts with the introduction of agent technology. Multiagent technology is very important for the design of the system in this article. It emphatically uses the characteristics of the agent, and uses the agent to complete the corresponding functions. Therefore, the focus has been devoted to describing the principle of agent, and then, the trainer's exercise simulation system is used for running. Human body joints during walking are extracted and simulated for data. After experimentation, although the system can simulate a linear motion engine well, the analysis effect of curved motion is not particularly good. However, because of the intelligent distributed sensor system, it can provide the simulation system with missing data by sensing the joint pressure. This kind of curve movement can also have a good simulation effect. The content of this article is limited by space and knowledge, the research on simulation system is relatively simple, and only part of the content can be realized. However, it is hoped that it can be strengthened in the follow-up research, and it will also provide some reference for the latecomers.

Data Availability

Data sharing is not applicable to this article as no new data were created or analyzed in this study.

Conflicts of Interest

The author state that this article has no conflict of interest.

References

[1] H. Qian, "Optimization of intelligent management and monitoring system of sports training hall based on Internet of Things," *Wireless Communications and Mobile Computing*, vol. 2021, Article ID 1465748, 11 pages, 2021.

[2] J. M. Rhodes, B. S. Mason, T. A. Paulson, and V. L. Goosey-Tolfrey, "Altering the speed profiles of wheelchair rugby players with game-simulation drill design," *International Journal of Sports Physiology and Performance*, vol. 13, no. 1, pp. 37–43, 2018.

[3] J. Yin and X. Q. Wang, "Study on safety mode of dragon boat sports physical fitness training based on machine learning - ScienceDirect," *Safety Science*, vol. 120, pp. 1–5, 2019.

[4] A. Gokeler, M. Bisschop, G. D. Myer et al., "Immersive virtual reality improves movement patterns in patients after ACL reconstruction: implications for enhanced criteria-based return-to-sport rehabilitation," *Knee Surgery Sports Traumatology Arthroscopy*, vol. 24, no. 7, pp. 2280–2286, 2016.

[5] A. Kłodowski, M. E. Mononen, J. P. Kulmala et al., "Merge of motion analysis, multibody dynamics and finite element method for the subject-specific analysis of cartilage loading patterns during gait: differences between rotation and moment-driven models of human knee joint," *Multibody System Dynamics*, vol. 37, no. 3, pp. 271–290, 2016.

[6] L. Zhang, G. Brunnett, K. Petri et al., "Kara Kter: an autonomously interacting karate kumite character for VR-based training and research," *Computers & Graphics*, vol. 72, pp. 59–69, 2018.

[7] A. Laatabi, N. Marilleau, T. Nguyen-Huu, H. Hbid, and M. A. Babram, "Formalizing data to agent model mapping using MOF: application to a model of residential mobility in Marrakesh," in *Agent and Multi-Agent Systems: Technology and Applications*, pp. 107–117, Springer, Cham, 2016.

[8] G. Mahalaxmi and R. K. Esther, "Multi-agent technology to improve the internet of things routing algorithm using ant colony optimization," *Indian Journal of Science & Technology*, vol. 10, no. 31, pp. 1–8, 2017.

[9] W. Zhou, H. Wang, G. Tang, and S. Guo, "Inverse simulation system for manual-controlled rendezvous and docking based on artificial neural network," *Advances in Space Research*, vol. 58, no. 6, pp. 938–949, 2016.

[10] M. Yu, X. Tang, Y. Lin, and X. Wang, "Diesel engine modeling based on recurrent neural networks for a hardware-in-the-loop simulation system of diesel generator sets," *Neurocomputing*, vol. 283, no. 29, pp. 9–19, 2018.

[11] J. Wang and H. A. Rakha, "Longitudinal train dynamics model for a rail transit simulation system," *Transportation Research Part C Emerging Technologies*, vol. 86, pp. 111–123, 2018.

[12] S. Farsoni, L. Astolfi, M. Bonfè, S. Spadaro, and C. A. Volta, "A versatile ultrasound simulation system for education and training in high-fidelity emergency scenarios," *IEEE Journal of Translational Engineering in Health & Medicine*, vol. 5, no. 1, pp. 1–9, 2017.

[13] X. Zhang, J. Wang, C. Jiang et al., "Hardware-in-the-loop simulation system for space information networks," *Journal of Communications & Information Networks*, vol. 2, no. 4, pp. 131–141, 2017.

[14] J. Guo, G. Hug, and O. K. Tonguz, "Intelligent partitioning in distributed optimization of electric power systems," *IEEE Transactions on Smart Grid*, vol. 7, no. 3, pp. 1249–1258, 2016.

[15] M. Semerci, A. T. Cemgil, and B. Sankur, "An intelligent cyber security system against DDoS attacks in SIP networks," *Computer Networks*, vol. 136, pp. 137–154, 2018.

[16] L. Cassettari, I. Bendato, M. Mosca, and R. Mosca, "Energy resources intelligent management using on line real-time simulation: a decision support tool for sustainable manufacturing," *Applied Energy*, vol. 190, pp. 841–851, 2017.

[17] S. U. Jung, J. Zhu, and T. S. Gruca, "A meta-analysis of correlations between market share and other brand performance metrics in FMCG markets," *Journal of Business Research*, vol. 69, no. 12, pp. 5901–5908, 2016.

[18] L. Li, C. F. Lange, Z. Xu, P. Jiang, and Y. Ma, "Feature-based intelligent system for steam simulation using computational fluid dynamics," *Advanced Engineering Informatics*, vol. 38, pp. 357–369, 2018.

[19] S. Wang, J. Wan, D. Zhang, D. Li, and C. Zhang, "Towards smart factory for industry 4.0: a self-organized multi-agent system with big data based feedback and coordination," *Computer Networks*, vol. 101, pp. 158–168, 2016.

[20] Y. Yang, J. M. Zhang, G. Q. Xu, S. Wang, and F. Wang, "Application research on speed negative feedback in mechanical resonance suppression in servo system," *Transactions of China Electrotechnical Society*, vol. 33, no. 23, pp. 5459–5469, 2018.

[21] F. Demir, V. Bajaj, M. C. Ince, S. Taran, and A. Şengür, "Surface EMG signals and deep transfer learning-based physical action classification," *Neural Computing and Applications*, vol. 31, pp. 8455–8462, 2019.

[22] B. Yuan, M. M. Kamruzzaman, and S. Shan, "Application of motion sensor based on neural network in basketball technology and physical fitness evaluation system," *Wireless Communications and Mobile Computing*, vol. 2021, Article ID 5562954, 11 pages, 2021.

[23] H. P. Santiago, L. H. Leite, P. M. A. Lima, G. V. Rodovalho, R. E. Szawka, and C. C. Coimbra, "The improvement of exercise performance by physical training is related to increased hypothalamic neuronal activation," *Clinical & Experimental Pharmacology & Physiology*, vol. 43, no. 1, pp. 116–124, 2016.

[24] L. C. Campos, F. A. Campos, T. A. Bezerra, and Í. L. Pellegrinotti, "Effects of 12 weeks of physical training on body composition and physical fitness in military recruits," *International Journal of Exercise Science*, vol. 10, no. 4, pp. 560–567, 2017.

[25] M. Andrzejczakkarbowska and R. Irzmański, "The impact of the dosing, a 12-week physical training on the concentration of NT-pro BNP and D-dimer in patients with heart failure and impaired functional capacity in VII-X decade of life," *Polski Merkuriusz Lekarski*, vol. 41, no. 241, pp. 11–15, 2016.

[26] X. Zhang, J. Lu, and D. Li, "Confidential information protection method of commercial information physical system based on edge computing," *Neural Computing and Applications*, vol. 33, pp. 897–907, 2021.

[27] P. Shan, "Image segmentation method based on K-mean algorithm," *EURASIP Journal on Image and Video Processing*, vol. 2018, 9 pages, 2018.

[28] S. Sun, M. Kadoch, L. Gong, and B. Rong, "Integrating network function virtualization with SDR and SDN for 4G/5G networks," *IEEE Network*, vol. 29, no. 3, pp. 54–59, 2015.

[29] S. Shibata, H. Kawano, and K. Maemura, "Effects of long-term physical training on the bearers of a float during the Nagasaki Kunchi festival," *Internal Medicine*, vol. 56, no. 1, pp. 11–16, 2017.

[30] T. Hong, W. Zhao, R. Liu, and M. Kadoch, "Space-air-ground IoT network and related key technologies," *IEEE Wireless Communications*, vol. 27, no. 2, pp. 96–104, 2019.

[31] S. Namasudra and P. Roy, "Popularity based access control model for cloud computing," *Journal of Organizational and End User Computing*, vol. 30, no. 4, pp. 14–31, 2018.

Hindawi
Wireless Communications and Mobile Computing
Volume 2022, Article ID 1697531, 12 pages
https://doi.org/10.1155/2022/1697531

Research Article

Data Fusion Model for High-Tech Products Marketing

Weidong Dai[1] and Tiexin Li[2]

[1]*School of Management, Shenyang University of Technology, Shenyang 110000, Liaoning, China*
[2]*Bensheng International College, Shenyang University of Technology, Shenyang 110000, Liaoning, China*

Correspondence should be addressed to Tiexin Li; li123sp@163.com

Received 6 November 2021; Revised 11 January 2022; Accepted 28 January 2022; Published 23 March 2022

Academic Editor: Mohamed Elhoseny

Product differentiation is one of the highlights of the success of today's increasingly competitive marketing. This article aims to study the construction of differentiated marketing strategies for high-tech products. This paper proposes to investigate and study customers, high-tech industry workers and leaders, etc., through the analysis of massive data, introduce the concept of data fusion and the weighting algorithm for data fusion, introduce DS evidence theory to judge the accuracy of the data on this basis, make the data more real and clean up abnormal data, perform relevant data processing on the determined data, and calculate and analyze the data differences of relevant groups. It also proposes to refer to the characteristics of high-tech products, understand the characteristics and implementation directions of differentiated marketing, draw differences between different groups, summarize customer characteristics and marketing directions, so as to trace the needs of customer groups, find customer pain points and difficulties, pinpoint product positioning, and achieve the goal of differentiated marketing. The experimental results of this paper show that big data fusion analysis can find customers in a targeted manner and polish the highlights of high-tech products. Compared with previous results, the performance is improved by more than 30%. Consumer satisfaction increased by more than 20%.

1. Introduction

High-tech enterprises are an important force in a country's national economy and a necessary and powerful pillar that cannot be ignored. High-tech companies not only provide the society with advanced products and high-quality services, but also promote technological changes and the upgrading of traditional enterprises, and provide society with a large number of employment opportunities.

With the in-depth development of the era of knowledge economy, some underdeveloped countries and regions are increasingly feeling the impact of the development of high-tech enterprises. The competitive advantages and market power of traditional enterprises and industries no longer have advantages, while the vitality and competitiveness of high-tech enterprises are becoming more prominent. Therefore, more experts and researchers are attracted to shift their research focus to the production and business models of high-tech companies and study their future development trends based on this. At the beginning of this century, under the leadership of the State Council, a "disconnected" and "transformed" movement promoted popularization in more than 200 scientific research institutes across the country. A large number of national and local scientific research institutions gradually got rid of their institutional identity and reorganized into joint-stock companies. They quickly registered successfully in the capital market. In recent years, high-tech companies have performed well in the capital market. Many private funds have chosen to develop technology or cooperate with scientific research institutions and have joined high-tech enterprises one after another, and the domestic high-tech enterprise team has grown rapidly. From the perspective of development trends, high-tech enterprises have performed well, which to a large extent promoted the rapid development of the national economy. It also brought tremendous changes to commercial production and people's lives. However, due to the short period of birth, these domestic high-tech companies generally have strong research

potential and many technological achievements, but the potential for transforming products and technologies is very weak, and the transformation of results is very small. At the same time, to a certain extent, policies, capital, and human resources are all concentrated on research and development, and there is a lack of attention to marketing. Therefore, these companies have advanced technology, high-quality R&D talents, and high-quality results and scientific research products, but they are always accompanied by weaknesses in poor marketing capabilities.

At present, many domestic companies and experts and scholars in related fields have paid enough attention to product marketing. They have studied high-tech product marketing data acquisition, risk management, and marketing strategy formulation from different directions. Byrne et al. analyzed the relationship between high-tech products and prices, and the article elaborated that high-tech products have a profound impact on the economic growth model [1]. In fact, the speed of innovation in the science and technology sector is faster than that inferred from official statistics (not so fast outside of the high-tech field). These results will deepen the productivity problem. Sheng and He analyzed and summarized the advantages and disadvantages of export competitiveness of high-tech products. By comparing data, it is concluded that the key to the export competitiveness of my country's high-tech products lies in research and development, innovation, financing, and exports. Based on China's relevant policies, Sheng and He provided some suggestions for enterprises to reduce costs [2]. Yang and Gabrielsson's research explored the marketing decision-making process of entrepreneurs who conduct entrepreneurial marketing in International New Ventures (INV) that operate in the high-tech business-to-business market. They developed a dynamic model that showed the alternation between effective and causal processes, as well as the feedback loop of entrepreneurial marketing. This research provides enlightenment for the management of organizations operating under uncertainty, how the decision-making process of these organizations optimizes entrepreneurial marketing, how to create new markets, and how to reduce the perceived uncertainty in the industrial market [3]. Dhebar studied six dangers that marketers face: major market uncertainty, major technical uncertainty, product compatibility issues in complex multi-component systems, coordination of self-enhanced network effects, and response to the complexity of the ecosystem and competition challenges, as well as the inherent risks of making difficult choices among multiple product market options with significant path dependence. He discussed these dangers and suggested steps that marketers can and should take to reduce the risk of entering the market [4]. Lin and Narasimhan started with consumer preferences and studied the different ways in which vertically differentiated market persuasive advertising may affect consumer utility [5]. It was concluded that persuasive advertising can simply increase consumers' booking prices for product categories, persuasive advertising can enhance consumers' perception of the quality of products provided by advertising companies, and persuasive advertising can increase consumers willingness to pay for quality and value-added. Kim took enterprises as the research object to study whether the relationship between corporate social responsibility and consumer response is symmetrical [6]. The Harrington et al.'s study aimed to examine product differences in the minds of customers and non-customers, and to solve the problem of using absolute measures, by integrating the competitive environment and the views of customers and non-customers, to better understand the marketing strategy and its impact on customer value [7]. Liao et al. reported the results related to data fusion, aiming to find a more suitable way to solve the problem through data fusion [8]. These studies have their own unique aspects, but for the marketing of high-tech products, they have never hit the point. In order to achieve the best effect in commercial marketing, it is nothing more to achieve the realm of "others don not have it, I have it, others have it but mine is better." The key lies in the difference of products.

This article starts with the basic business logic and adopts differentiated marketing plans for the relevant characteristics of high-tech products. Its advantages are as follows: (1) The survey is comprehensive. The survey is not only for users and manufacturers. We include the evaluation of enterprise employees, and the data is richer and more reliable. (2) The pertinence of marketing. Marketing is not only a change in sales, but also a comprehensive differentiation of technology, thought, service, and brand. (3) Visualization of data. Through user survey data, analysis, and processing, it ensures the authenticity and observability of the number.

2. Marketing Methods under Data Fusion

2.1. Data Fusion. Data fusion, also known as information fusion, is a cutting-edge technology of multidisciplinary cross-linking, which brings together the development results of computer systems, communications, and microelectronics technology and includes almost all new research fields today [9]. Based on this, it is difficult to give a unified and acceptable definition of data fusion in all fields. At present, a broad overview of data fusion is the integrated process of using computers to process, control, and make decisions on various information sources [10]. Among them, the fusion system provides hardware support, and the data analysis is handled by the fusion method. For different fusion processes, the fusion systems can be the same or similar, but data analysis will vary greatly due to different fusion processes. Therefore, data analysis and fusion methods have become the key to the data fusion process.

2.1.1. Principles of Data Fusion. Data fusion is a common basic function in humans and other logical systems [11]. In daily life, we can collect all the information around us with our audiovisual, smell, touch, and other body sensors and analyze, process, and make decisions about it, so that we can solve all the affairs around us at will. In human integrated information processing, data aggregation simulates the human body's behavioral pattern of processing data. The principle is to integrate multiple sensor resources, analyze and process data information, and determine the target

environment and conflict information according to specific rules. This combination optimization realizes consistent interpretation or description of the measured object and correct judgment of the objective function. Through the sensor system control, the fusion processing system significantly improves the accuracy and stability [12].

2.1.2. Data Fusion Level. In a multi-sensor system, the information represented by each sensor has different characteristics: real-time or non-real-time, fuzzy or deterministic, reliable or unreliable, supportive or complementary, etc. This requires that, in the process of data fusion, the data should be processed step by step and hierarchically based on the data characteristics and application requirements. According to the different operating levels of sensor data, data fusion can be divided into three levels: data layer, feature layer, and decision-making layer.

2.1.3. Main Algorithms of Data Fusion. Multi-sensor information at different fusion levels is redundant or complementary. In order to eliminate redundant information and enhance the complementary relationship between data, a corresponding fusion algorithm is needed to process the data [13]. The division structure is shown in Figure 1.

The least square method (also known as the least square method) is a mathematical optimization technique. It finds the best function match of the data by minimizing the sum of squares of the error. The least squares method can be used to easily obtain unknown data and minimize the sum of squares of errors between the obtained data and the actual data. The least square method can also be used for curve fitting, and some other optimization problems can also be expressed by the least square method by minimizing energy or maximizing entropy. Kalman filtering is an algorithm that uses linear system state equations to optimally estimate system state through system input and output observation data. Since the observation data includes the influence of noise and interference in the system, the optimal estimation can also be regarded as a filtering process. Bayesian inference is a method of inference statistics. This method uses Bayes' theorem to update the probability of a particular hypothesis when there is more evidence and information.

2.1.4. Data Layer Fusion Algorithm. Data layer fusion algorithms mainly include weighted average algorithm, Bayes algorithm, Kalman filter method, etc., which are all classic data processing algorithms. However, they have exposed two problems in practical applications. One is that most algorithms presuppose that the data obey a normal distribution. However, a large number of experiments have shown that most of the meter measurement data does not conform to the normal distribution, but is between uniform and positive. The second is that the algorithm may not be able to eliminate individual outliers. In order to solve the above problems, a fusion algorithm based on the support matrix is proposed here, which only uses the information contained in the data itself, avoids the assumption of normal distribution, and can accurately fuse the data.

First introduce the concept of data support. For any set of measurement data $Z_1, Z_2, Z_3, \ldots, Z_n$, from the perspective of Z_x, it is more likely that Z_y is the real data. Under the concept of support, the authenticity of the data is only determined by itself; that is, the higher the authenticity of Z_x, the higher the degree of support by the rest of the data. On this basis, define the relative distance between the data:

$$S_{xy} = \left|Z_x - Z_y\right|, \quad x, y = 1, 2, 3, \ldots, m. \tag{1}$$

Redefine the support function:

$$a_{x,y} = 1 - \frac{S_{x,y}}{\max\left\{S_{x,y}\right\}}, \quad S_{x,y} \geq 0. \tag{2}$$

Here, $\max\left\{S_{x,y}\right\}$ is the maximum value of the relative distance between data. It can be seen from formula (2) that the degree of support $a_{x,y}$ increases with the relative.

As the distance $S_{x,y}$ increases, it decreases. This shows that the difference between the data is inversely proportional to the degree of mutual support, which is obviously in line with common sense. For data fusion problems, establish a support matrix:

$$A = \begin{bmatrix} a_{11} & \ldots & a_{1m} \\ \vdots & \ddots & \vdots \\ a_{m1} & \ldots & a_{mm} \end{bmatrix}. \tag{3}$$

The degree to which the m-th data is comprehensively supported by other data must be obtained from the support matrix E_m, that is, to determine its own weight coefficient A in the overall data. According to the principle of information sharing, $\sum_{m=1}^{n} E_m = 1$, because E_m should synthesize the overall information of $a_{m1}, a_{m2}, a_{m3}, \ldots, a_{mn}$, and from the theory of probability source merging, there must be a set of non-negative real numbers $t_1, t_2, t_3, \ldots, t_n$, such that

$$E_m = t_1 a_{m1} + t_2 a_{m2} + \ldots + t_n a_{mn}. \tag{4}$$

We have the following:

$$\begin{aligned} E &= \left[E_1, E_2, \ldots, E_n\right]^i, \\ K &= \left[K_1, K_2, \ldots, K_n\right]^i. \end{aligned} \tag{5}$$

Formula (4) is expressed as a matrix form:

$$E = AK. \tag{6}$$

Since the support matrix A is a non-negative matrix, there must be a non-negative maximum eigenvalue $\gamma_{\max}$, which can be expressed as

$$\gamma_{\max} K = AK. \tag{7}$$

The eigenvector $\gamma_{\max}$ corresponding to the largest eigenvalue $K = [k_1, k_2, \ldots, k_n]^i$can be obtained; then, the weight of the l-th data Z_l itself is E_l.

$$E_l = \frac{k_l}{k_1 + k_2 + \ldots + k_n}. \tag{8}$$

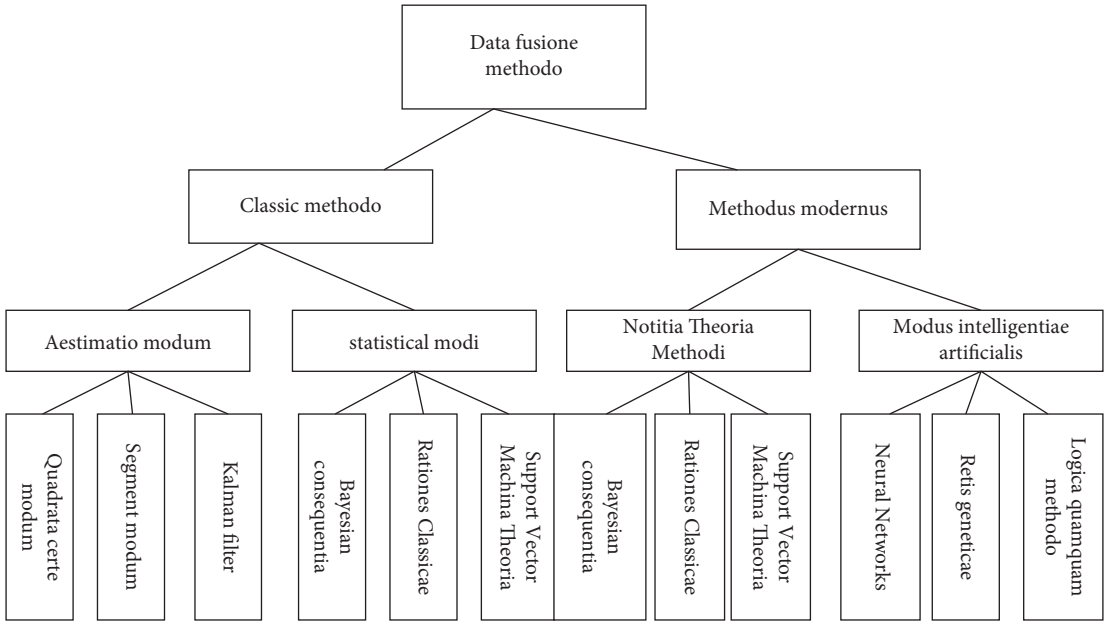

Figure 1: Data fusion method.

Then, the final fusion result of this group of data of $Z_1, Z_2, \ldots, Z_n$ is

$$Z = E_1 Z_1 + E_2 Z_2 + \ldots + E_n Z_n. \tag{9}$$

This is the fusion of intermediate levels. In this method, each sensor observes the target, extracts representative features from the observation data, obtains feature vectors, then fuses these feature vectors, and makes an attribute description based on joint feature vectors. Feature layer fusion is to extract features from the original data provided by sensors. Therefore, a certain amount of data compression is achieved before fusion, which is conducive to real-time processing, but its accuracy is reduced due to the loss of data.

2.1.5. Decision-Level Fusion Algorithm Based on D-S Evidence Theory. D-S evidence theory is short for Dempster-Shafer theory. It was first formally proposed by Harvard University mathematician A.P. Dempster in 1967 and then supplemented and developed by his student G. Shafer, and it has now become a classic theory of uncertain reasoning. Compared with other data fusion algorithms, the outstanding advantage of DS evidence theory lies in its ability to directly express "uncertain" and "unknown," which can make up for the limitations of Bayes algorithm when the prior probability is unknown, and it is mature in the field of uncertainty [14]. DS evidence theory believes that probability is the specific quantification of the target event, which needs to be measured from the perspective of subjective and objective combination. The interval value $[0, 1]$ should be used to judge the result to reflect the degree to which the event is close to right or wrong (or true or false), rather than generally simply classify the result as either true or false (or right or wrong).

(1) Identification Framework. The recognition framework is a collection of all possible results of the target event under certain conditions, and these results are mutually exclusive and mutually exclusive, usually represented by β. For example, for the event of a dice roll, the result of a dice roll can only be one of 1, 2, 3, 4, 5, and 6, and they meet the requirements of being unrelated and mutually exclusive, so the recognition framework of the event of rolling a dice can be expressed as

$$\beta = \{1, 2, 3, 4, 5, 6\}. \tag{10}$$

(2) Basic Probability Distribution. For the recognition framework β, all results in the problem domain should be included in the set function,

$$h\colon 2^{\beta} \longrightarrow [0, 1], \tag{11}$$

and meet

$$h(\beta) = 0, \tag{12}$$

$$\sum_{B \subset \beta} h(B) = 1. \tag{13}$$

Then, h is the basic probability distribution function on the recognition framework β, also known as the BPA function.

$H(B)$ represents the basic probability distribution of result B, that is, the degree of support for the occurrence of result B. Take the event of rolling a dice as an example; if the basic probability distribution of a piece of evidence is $h(\{1\}) = 0.3, h(\{2, 4\}) = 0.6, h(\{5\}) = 0.1$, it shows that this piece of evidence supports $1, \{2, 4\}, 5$, and the degrees of support for them are 0.3, 0.6, 0.1.

(3) Trust Function. D-S evidence theory expresses the support for any hypothesis by defining an interval. The lower limit of this interval is called the trust function, also known as the reliability function. In the recognition framework β can be defined as

$$Bel(B) = \sum_{B \subseteq A} h(B). \tag{14}$$

In particular, when the recognition framework β has only a subset, namely,

$$h(B) = \begin{cases} 1, & B = \beta, \\ 0, & B \neq \beta. \end{cases} \tag{15}$$

Then, there are

$$Bel(B) = \begin{cases} 1, & B = \beta, \\ 0, & B \neq \beta. \end{cases} \tag{16}$$

(4) Likelihood Function. The upper limit of the interval corresponding to the trust function is called the likelihood function. In the recognition framework β can be defined as

$$pl(B) = \sum_{B \cap A \neq \beta} h(B). \tag{17}$$

(5) The Relationship between Trust Function and Likelihood Function. For a certain result B on the recognition framework β, the trust function $Bel(B)$ and the likelihood function $pl(B)$ of the result B are calculated according to the probability distribution of the evidence, and then the trust interval $[Bel(B), pl(B)]$ is determined to indicate the confirmation of the result B degree. The relationship between the two is shown in Figure 2.

$$\begin{aligned} &pl(B) \geq Bel(B), \\ &pl(B) = 1 - Bel(\overline{B}). \end{aligned} \tag{18}$$

(6) Composition Rules. Under the recognition framework β, there are multiple evidences for an event at the same time, and each evidence has a corresponding basic probability distribution. At this time, it is necessary to synthesize multiple pieces of evidence information through the synthesis rules of DS evidence theory and finally obtain a comprehensive basic Probability distribution.

Taking two pieces of evidence as an example, the composite rule can be expressed as

$$h(B) = h_1 \oplus h_2 = \begin{cases} 0, & Q_a \cap W_c = \beta, \\ \dfrac{\sum_{Q_a \cap W_c = B, \forall Q_a, W_c \subseteq \beta} h_1(Q_a) \bullet h_2(W_c)}{1 - f}, & Q_a \cap W_c \neq \beta. \end{cases} \tag{19}$$

Here, $\oplus$ represents the direct sum, $h(B)$ is the basic probability distribution after the result B is synthesized, Q_a and W_c, respectively, represent the subset elements in the first evidence and the second evidence, h_1, Q_a, h_2, W_c is the basic probability distribution, and f is the inconsistency factor; f can be expressed as

$$f = \sum_{Q_a \cap W_c = \beta} h_1(Q_a) \bullet h_2(W_c). \tag{20}$$

When there are multiple evidences, the synthesis rule can be expressed as

$$h(B) = (((h_1 \oplus h_2) \oplus h_3) \oplus \cdots) \oplus h_n. \tag{21}$$

The combination rule between the two pieces of evidence is the same as formula (21), and the final combination result has nothing to do with the combination order of each piece of evidence.

2.2. Differentiated Marketing. Differentiated marketing is based on market segmentation; based on its own advantages, the company produces better quality and more efficient products that surpass others, or in terms of product sales, through specific promotional activities, flexible sales methods and unique after-sales service; the company has established a good independent image in the minds of consumers. Michael Porter proposed a non-traditional strategy, that is, a diversification strategy. It believes that differentiation refers to the differentiation of the company's products or services from the company to form its own unique things in the industry [15]. Philip Kotler put forward the concept of marketing diversification, including image diversification, service diversification, personnel diversification, and product diversification. It believes that this element can help the company create a globally differentiated marketing strategy portfolio, differentiate from competitors, create differentiation, and ultimately gain a competitive advantage. Therefore, the essence of differentiated marketing is the differentiated competitive tool provided by the market.

With the rapid economic growth, product classification has become more and more streamlined and more specialized. At the same time, product marketing models are constantly changing, and the impact of differentiated marketing has become more prominent. The innovation of differentiated marketing is not limited to improving the level of marketing, but more importantly, focusing on image innovation, product concepts, and services. The key to differentiated marketing is to do a good job of market

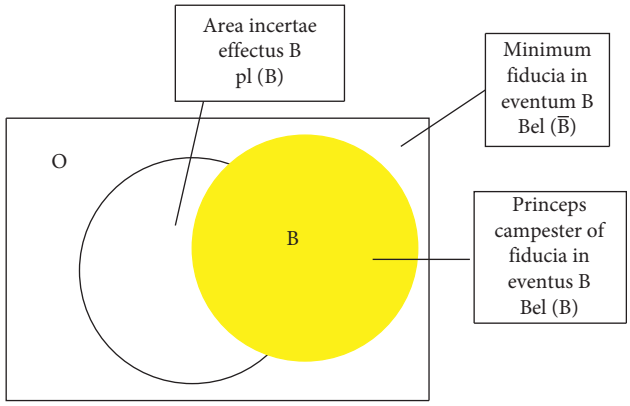

Figure 2: Relationship between trust function and likelihood function.

segmentation, touch different points of attraction, and then use differentiated services to meet the needs of users. Differentiation is a systematic concept, and the key lies in sales innovation.

The so-called "differentiated marketing" does not refer to innovation around a certain marketing method or a certain level of marketing, but through the integration of product value, product design, product concept, marketing methods, marketing promotion methods, and other aspects. To achieve diversified marketing innovation, in addition, it should be used as a basis to subdivide the market so that the product can get more social attention, thereby establishing an advantage in the fierce market competition. The current research on differentiated marketing strategies mainly focuses on products, services, and brands [16].

2.2.1. Product Diversification. Product diversification means that enterprises use their own technological advantages to differentiate their products from competitive products in terms of function, design, flexibility, reliability, and stability. Product diversification marketing is an inevitable trend for enterprises in market competition. Although it seems that companies are selling the same products to different consumers, in fact, consumers will choose to buy different things. Product diversification can help companies significantly increase profitability. Product diversification can enable enterprises to not only form market power, but also form market segments, achieve the effect of creating target markets, and avoid wasting resources. Product diversification not only enhances the competitive advantage of nonprice enterprises, but also enables enterprises to occupy a dominant position and form an industry monopoly to seize market share. Product diversification is an important part of diversified marketing and a necessary condition for improving product competitiveness. Product diversification includes two aspects: vertical product differentiation and horizontal product differentiation. Vertical differentiation refers to the production of products that are better than competitors; horizontal differentiation refers to the production of products with different characteristics from competitors. For example, domestic washing machines firstly have differences in laundry capacity, secondly, there are differences between pulsators and rollers, and finally, there are differences in frequency conversion to meet the diverse needs of customers.

2.2.2. Diversified Services. The service diversification strategy refers to the exclusion of other competitors from companies providing high-quality services to consumers. When product differentiation is not obvious, service quality becomes a very critical factor for business success. Using differentiated marketing, companies can concentrate limited resources on higher-profit users at a certain speed and ultimately maximize profits. The diversification of services enables companies to conform to the characteristics of user needs and the rules of real-time evolution and build a diversified service content, method, concept, and culture, and ultimately form their own competitive advantage. In the process of distinguishing services, companies must adapt to market changes and go beyond traditional forms of information and service provision. The difference in services is reflected in whether to provide after-sales service, whether to be polite and warm to customers, whether to customize sales plans for customer needs, etc.

2.2.3. Differentiation of the Brand Image. Regarding brand differentiation strategy, first of all, on how to build a brand, we can look at it from this perspective: a brand can be a symbol, a name, a mark, a design, or a combination of the above elements. The purpose of brand setting is that it can effectively distinguish the products or services sold and can effectively show the differences between competitors. Diversification strategies can help companies play an important role in shaping and promoting brands. As the final result of differentiation, the emergence of the brand also helps the company to generate its own personality characteristics. Therefore, there is an extremely subtle connection between brand and diversification. A brand can be used as a business symbol for a company, or it can be used as a brand to help companies create differences. Just like what some experts mentioned in "Brand 22 Laws," if you want to create a more successful brand, you must give it based on the company's unique characteristics. Customers left a deep impression, and it is an advantage that other competitors do not have. Brand differentiation is to distinguish competitors in brand concept and character when the market cannot accept excessive segmentation. Brand differentiation is to differentiate competitors in terms of brand concept and character when the market cannot accept excessive segmentation. For example, Pepsi's choice of a new generation to differentiate Coca-Cola is an example of brand differentiation. Brand differentiation requires enterprises to make necessary strategic transformation from terminal strategy to media strategy. This involves a concept of "giving up," which is the key to the success or failure of a business. In order to establish a brand, it is necessary to have the massive delivery of resources, and the enterprise only has the experience of terminal competition at this time. With limited resources, the point input direction must be chosen accordingly.

2.3. Introduction to the SWOT Analysis Method. SWOT analysis method is also called situation analysis method, which is an analysis method with a wide audience. This method was proposed at the end of the last century, and it can visually display the company's current operating conditions, namely, advantages, disadvantages, opportunities, and risks in four aspects [17]. The SWOT analysis method usually starts from the corporate structure, analyzes the overall environment of the company and the company's own strengths and weaknesses, and understands the opportunities and challenges of the company. This method is often widely used in strategic business research. Through the above analysis, this business can put more energy and resources into places with more opportunities, while adjusting existing strategies to achieve expected business goals. If a company can formulate a high-level marketing strategy, it will be very beneficial to the company's long-term development, and it will encourage the company to use its own advantages to make up for its shortcomings, seize opportunities, and counter threats. Its structure is shown in Figure 3:

Strengths: internal factors of the organization, for example, a good brand image; diversified sales channels; good economic conditions; advanced industry technology; excellent product quality; obvious competitive advantages.

Disadvantages: refers to the relative disadvantage of competition, which is also an internal factor of the organization, for example, outdated facilities or equipment; rapid turnover of personnel; complicated internal procedures and nonstandard operating manuals; lack of technical advantages; insufficient funds; excessive inventory products.

Opportunities: external factors of the organization, for example, the launch of new products, the development of new markets, changes in national policies, and the crisis of competitors.

Threats: external factors of the organization, such as the emergence of new competitors, leakage of company secrets, market tightening, and changes in relevant national policies and regulations.

3. Experimental Design and Analysis

3.1. High-Tech Product Survey Questionnaire. In order to better grasp the specific marketing situation of high-tech enterprises, this paper adopts a questionnaire survey method to carefully design the content of the questionnaire on the specific situation of high-tech product marketing and conduct surveys on customers and enterprises. The focus of the questionnaire survey is mainly reflected in the high-tech enterprise product marketing, service strategy, supplier strategy, product strategy, and other issues. The design of the questionnaire mainly covers two main areas. The first piece is the basic information of the survey object, including age, gender, income level, education level, etc., and the second piece is the specific information of the survey, mainly centering on the marketing of high-tech enterprises.

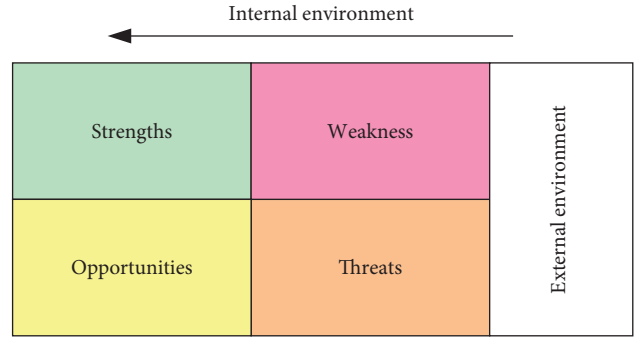

Figure 3: SWOT structure diagram.

This questionnaire is collected on-site. In this questionnaire survey, we randomly selected 65 customers, 45 employees of high-tech enterprises, and 10 executives of high-tech enterprises to conduct the survey, and a total of 95 valid questionnaires were collected. The design of the questionnaire is reasonable. Executives are not the recipients of high-tech products, and customers are the center of our sales. Selecting certain executives and employees also enriches data. Too much data is useless and cannot reflect the value of the marketing department. The questionnaire under this ratio is the best. The survey results of 95 questionnaires were objective, fair, and reliable. The specific data are as follows.

It can be seen from Table 1 that most of the people who use high-tech products are young people with at least high school education. They have good contact with high-tech products, and their satisfaction and sense of use are not low. But for product marketing, most of them are a little plain, and they do not feel much surprise. In this regard, when differentiated marketing, products can be subdivided, targeting people of different age groups, researching their needs, and designing products suitable for them. At the same time, they regularly return visits to investigate their experience of use and suggestions for improvement, thereby enhancing user satisfaction and brand trust.

It can be seen from Table 2 that users are more price-sensitive, and their perception of brands and channels is not obvious. They have a high degree of acceptance and recognition of various marketing plans, and they are willing to listen to brand stories and improve their experience. Based on this, the company can strengthen brand promotion, tell a good brand story, and increase user brand identity and brand value. At the same time, differentiated price marketing strategies can be designed to meet user needs.

It can be seen from Figure 4 that most users have low evaluations of current high-tech products, and they have higher expectations for the appearance, performance, battery life, and supporting equipment of high-tech products. For high-tech enterprises, more attention can be paid to the appearance and supporting facilities, positioning of different groups, differentiated marketing, and meeting the requirements of different groups to achieve the maximum effect. For the improvement of hardware equipment such as performance and battery life, it can be gradually improved and continuously upgraded and optimized.

Table 1: User feeling questionnaire.

	Audience	Education	Product marketing degree (%)	Sense of use (%)	Satisfaction (%)
18–25	55	High school and above	60	75	65
25–40	30	Bachelor's degree and above	65	80	60
Above 40	10	Bachelor's degree and above	70	83	80

Table 2: Survey on user differentiated marketing experience.

	Product differentiation (%)	Price differentiation (%)	Channel differentiation (%)
Sensitivity	70	90	80
Satisfaction	75	88	83
Propaganda perception	85	95	80
Recognition	88	93	82

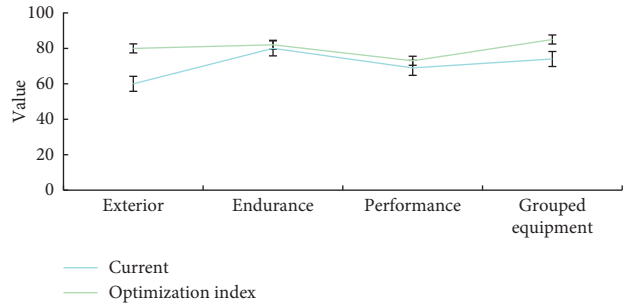

Figure 4: Users expect the value of high-tech products to improve.

3.2. Introduction to the Characteristics of High-Tech Products. High-tech products are products that are based on high technology or original ideas and have a monopoly on the market. This is an inevitable result of high-tech industrialization. High-tech products have gone through various transitional stages of R&D, testing, and commercialization. Finally, they must conform to the market and integrate into market growth trends. High-tech products have the following characteristics:

(1) *High Investment*. The prerequisite for the establishment of high-tech enterprises is that high-tech enterprises must have their own technological advantages. From technology to products, there are many links in the middle, and the investment volume is huge. If it is a self-developed high-tech enterprise, the investment is even greater. Generally speaking, compared with high-tech enterprises, the input cost of traditional enterprises is less than one-thousandth of it. In addition, high-tech enterprises are also facing a huge demand for high-tech talents.

(2) *High Risk*. High-tech products also face multiple risks in the entire industry chain, such as the break of the capital chain, low market return, redundant management systems, and difficulty in upgrading technology. The possibility of failure is extremely high.

(3) *High Returns*. The high-tech content of the products of high-tech enterprises can bring the greatest value to customers, and their high degree of innovation can also easily realize the formation of technological monopoly and high returns.

(4) *High Level of Competition*. In the process of fierce market competition, no company can avoid competition with other companies. The competition among high-tech companies is more intense, because high-tech products often have a certain monopoly in the market, and because of this nature, it can generate greater profits. Therefore, more and more companies choose high-tech industries. This has increased the pressure of competition among enterprises to some extent [18].

(5) *High-Level Knowledge and Technology*. High technology is the product of mutual penetration and integration of many industries. It needs talents with knowledge in multiple fields to integrate multiple knowledge and carry out creative work.

3.3. SWOT Analysis of High-Tech Products. As shown in Figure 5, the advantages of high-tech products are reflected in the high market demand for high-tech products and a wide range of users. With the continuous development of science and technology, people's living standards are improving, and people have more time and experience to enjoy life and chase high-tech products. At the same time, high-tech products generally contain technological achievements, are strong competitors, and can easily form a sex price monopoly and obtain high returns.

As shown in Figure 6, the disadvantages of high-tech products are reflected in the high R&D costs of high-tech products and long R&D time, requiring companies to bear high risks. At the same time, there is uncertainty in the rate of return of high-tech products. It is possible that the hard-working products are not actually welcomed by the market, and the risk of failure is high. High-tech products have strong exclusivity, serious homogeneity, and fierce competition among enterprises.

As shown in Table 3, the opportunities for high-tech products are reflected in the state supports the development of high-tech products and promotes the development of high-tech industries. It has formulated a series of incentive policies to encourage the development of high-tech

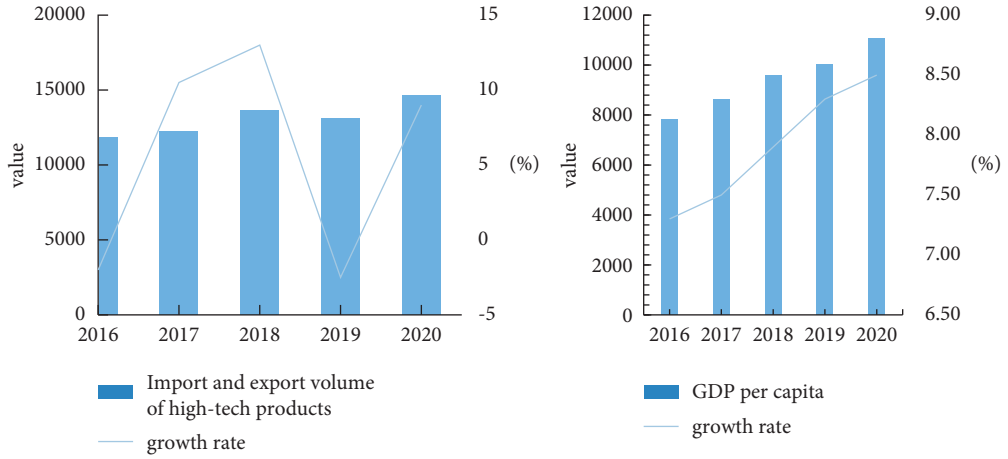

Figure 5: Advantages of high-tech products.

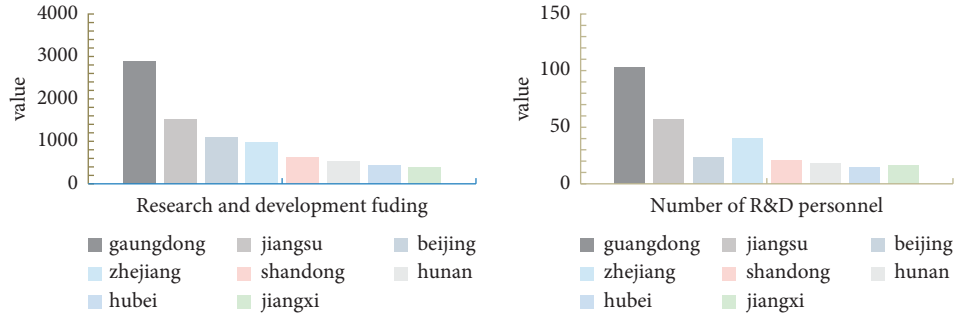

Figure 6: Disadvantages of high-tech products.

industries and at the same time introduced tax reduction and exemption policies and related park benefits. In addition, the government has also issued a talent recruitment conference to attract talents from home and abroad to participate in the development of high-tech industries. The future of high-tech products has a bright future.

As shown in Figure 7, the threat of high-tech products is reflected in the fierce market competition, with external capital participating in the competition before, and high-tech enterprises without core competitiveness and increasing internal friction. Insufficient capital supply for high-tech enterprises has led to slow development of enterprises. While squeezing the development of traditional enterprises, high-tech enterprises will inevitably face resistance from traditional industries, which will bring certain obstacles to the development of high-tech industries.

3.4. Difficulties in High-Tech Product Marketing. More demanding service management and channel management are required. High-tech products have high technical level and complex structure. Some technologies are unprecedented, and users are often unfamiliar with their performance and usage. In addition, high-tech products are often new to the market soon, and the technical performance needs to be further improved. In response to this situation, only relying on printing and distributing product manuals and user manuals, most users have bad senses, and a high-quality service system should be established. Customers can feel the power of service throughout the product sales process. Let users feel the company's strong sense of responsibility, and further encourage users to rely on high-tech products to create future demand. In this regard, the key to achieving service improvement lies in the cultivation of employee service awareness. This requires companies to change their business philosophy, increase channel information input, talk to users at close range, listen to user needs, and feedback and resolve user conflicts, thereby enhancing user service experience and improving corporate reputation [19].

Stronger market pressure leads to more tolerant business vision. On the one hand, due to the characteristics of high technology, the cost of research and development of high-tech enterprises is very high, coupled with the complexity and cutting-edge of technology; it is often not enough to rely on only one enterprise. In contrast to efficiency, even if a company can develop a new product, it may have been abandoned by the market, and the market has been taken over by the company that originally developed it. In addition, high-tech products often rely on the development of interdisciplinary subjects, such as the relationship between sensors and receivers. On the other hand, high-tech products are also facing competitive pressure from traditional enterprises [20, 21]. While traditional industries hyped up high-tech to squeeze employment space, while optimizing and upgrading traditional industries, squeezing the market for high-tech products, as a result, competition in the high-tech

Table 3: National policy to support high-tech industries.

Preferential policy	Tax rate	Talent subsidy	Office land	Share offer transfer
Amount	25%–40%	160–320W	500–600W	180W

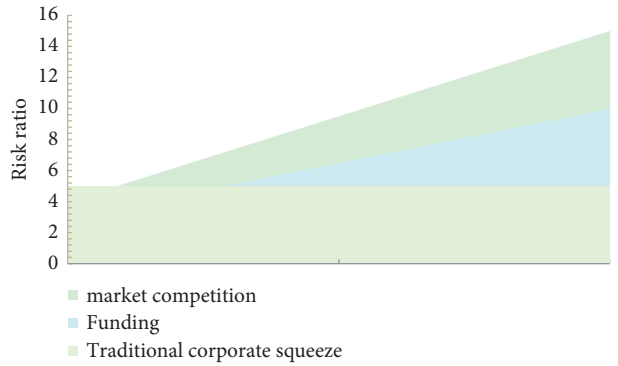

Figure 7: Threats to the development of high-tech products.

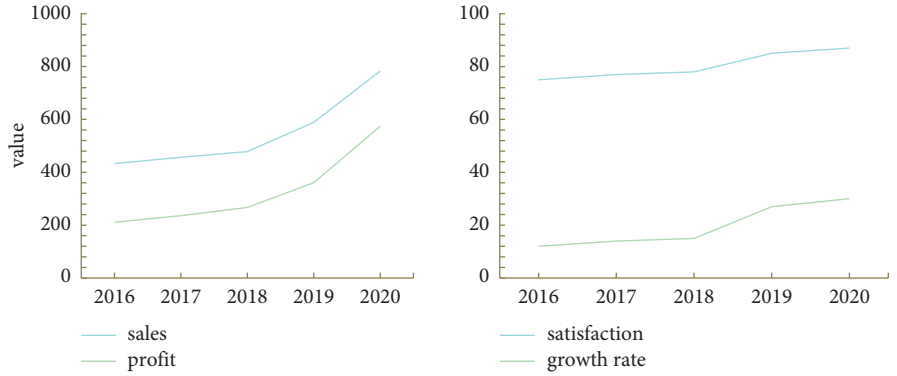

Figure 8: Differential marketing effect chart.

market is fierce. Therefore, high-tech companies need to open their horizons to seek cooperation opportunities. They can cooperate with other companies in complementary ways, and they can also establish alliances or mergers, so as to reduce R&D costs and jointly develop the market.

Broader market tasks. The competition among high-tech companies is more involved in the development of new markets, rather than market share. High-tech products have inherent scalability in technology; that is, mature technology can cover many industries and many countries. In addition, if a technology does not develop a new market and only stays in a smaller market, it will leave room for the development of other high-tech brands, so better companies will soon dominate the market [22]. In every high-tech field, only a few successful companies will survive. Therefore, in addition to continuously improving the performance of products, high-tech companies are also facing the huge task of rapidly developing the market.

4. Discussion

We investigate the marketing effects of relevant high-tech enterprises in accordance with the needs of users and the relevant characteristics of the products. According to random survey and visit data analysis, it can be found that the differentiated marketing details are more eye-catching and in line with the user experience. As shown in Figure 8, compared with the past marketing performance, differentiated marketing has achieved a 30% increase in sales revenue and an 18% increase in profit compared to the previous one, which has achieved good results.

We further analyze the data, and users pay more attention to product quality and related service optimization than prices. Moreover, users' trust in high-tech products is not low, and brand loyalty is better. In the future, high-tech products should pay more attention to product optimization and follow-up service guarantee. If necessary, appropriate price marketing can be carried out during the new product period to achieve the effect of increasing the purchase volume.

During the investigation, we comprehensively compared the high-tech companies and found that their marketing strategies are similar, and the differences are not obvious. However, high-tech products are facing the reality of technological upgrades and short market life cycles. Differentiated marketing has undoubtedly become the key to solving the problem:

(1) Strengthen its leading position in technology. Most of the differentiated advantages of high-tech products lie in the technological leadership of surpassing. Therefore, in order to occupy a leading position, it is necessary to strengthen technological innovation and make good use of patent protection policies. Technological breakthroughs are fundamental to the marketing of high-tech products, not only great breakthroughs, but also minor breakthroughs. For example, the pixels of the mobile phone are improved, the appearance is better, and the storage is larger. These are small breakthroughs that will have a great impact on life.

(2) Increase the cost of product conversion. By increasing the cost of converting existing customers into competing (substitution) products, thereby maintaining high product premiums, the advantages of diversification of existing products can be improved to a certain extent.

(3) Maintain various competitive advantages. Generally speaking, the more advantages of high-tech enterprises, the greater the competitiveness of their products. If the production, sales, and after-sales of products have their competitive advantages, it will be difficult for competitors to imitate, and high-tech products will occupy the leading position.

(4) Create sustainable value. In other words, it can be promoted in multiple channels such as Weibo and WeChat through videos, graphics, and other channels to create product value and tell brand stories. If customers touch this value, the product will undoubtedly be used by more groups. Therefore, we must continue to pay attention to customer needs.

5. Summary

Through the analysis of the characteristics of high-tech products and marketing characteristics, this paper discusses the "marketing myopia" and its manifestations that may occur in the production and operation of domestic high-tech enterprises, as well as the selection of high-tech products in the marketing strategy. Finally, it is pointed out that if high-tech enterprises want to continue to maintain their competitive advantages, they should attach great importance to marketing and draw the following conclusions: the formulation of marketing strategies should focus on the core competitiveness of the enterprise and maximize the display of products in order to achieve technological innovation sustainable development. To attach importance to marketing and improve the strategic position of the marketing department, the key is to ensure that the company's marketing strategy is truly and effectively implemented. If a company wants to ensure sustainable development, it must continue to increase its investment in high-tech research and development and the transformation of results. In order to ensure the ultimate effect of the marketing strategy, strategic control must be strengthened, and control and evaluation measures must be established and improved to monitor the implementation process of the strategy in real time.

Data Availability

No data were used to support this study.

Conflicts of Interest

The authors declare no conflicts of interest.

References

[1] D. M. Byrne, S. D. Oliner, and D. E. Sichel, "Prices of high-tech products, mismeasurement, and pace of innovation," *Business Economics*, vol. 52, no. 2, pp. 1–11, 2017.

[2] W. Sheng and M. He, "Research on tax policies to improve Chinese export competitiveness of high-tech products," *Journal of Tongling University*, vol. 16, no. 4, pp. 31–35, 2017.

[3] M. Yang and P. Gabrielsson, "Entrepreneurial marketing of international high-tech business-to-business new ventures: a decision-making process perspective," *Industrial Marketing Management*, vol. 64, pp. 147–160, 2017.

[4] A. Dhebar, "Bringing new high-technology products to market: six perils awaiting marketers," *Business Horizons*, vol. 59, no. 6, pp. 713–722, 2016.

[5] Y. Lin and C. Narasimhan, "Persuasive advertising in a vertically differentiated competitive marketplace," *Review of Marketing Science*, vol. 18, no. 1, pp. 145–177, 2020.

[6] J. I. Kim, "In asymmetric effects of CSR types on corporate attitude: differentiated implications on resource investment and marketing communication of the bank," *Journal of Korean Marketing Association*, vol. 31, no. 2, pp. 55–72, 2016.

[7] R. J. Harrington, M. C. Ottenbacher, and S. Fauser, "QSR brand value," *International Journal of Contemporary Hospitality Management*, vol. 29, no. 1, pp. 551–570, 2017.

[8] W. Liao, X. Huang, and F. V. Coillie, "Processing of multiresolution thermal hyperspectral and digital color data: outcome of the 2014 IEEE GRSS data fusion contest," *IEEE Journal of Selected Topics in Applied Earth Observations and Remote Sensing*, vol. 8, no. 6, pp. 2984–2996, 2017.

[9] M. Tanabandeh, S. Salajegheh, and M. Pourkiani, "A systematic mapping study on risk management in the export development of high-tech products," *Journal of Science and Technology Policy Management*, vol. 10, no. 3, pp. 834–855, 2019.

[10] X. Liu, "Quiet differentiated marketing strategy based on two-dimensional electricity market segmentation model," *Power Demand Side Management*, vol. 18, no. 3, pp. 46–49, 2016.

[11] X. Gong, H. Wang, and J. Zhu, "Research on the optimal value model of differential marketing of high-speed railway—taking hubao high-speed railway as an example," *Friends of Accounting*, vol. 12, pp. 13–18, 2017.

[12] W. Xie, "Analysis of the differentiated marketing strategy of Hunan embroidery," *Chinese Market*, vol. 4, pp. 144-145, 2016.

[13] Y. Zhang, "Thoughts on the application of enterprise marketing innovation and differentiated marketing concepts—taking coal enterprises as an example," *China Business Forum*, vol. 7, pp. 25-26, 2017.

[14] Z. Peng, "Analysis of differentiated marketing strategies and applications," *Building Materials and Decoration*, vol. 29, no. 682, pp. 190-191, 2017.

[15] L. Han, J. Wang, and W. Wang, "Differential marketing of publishing WeChat official accounts based on "4V

theory"—taking peking university press as an example," *China Publishing*, vol. 15, pp. 9–12, 2018.
[16] N. Liu, "On the construction of the evaluation index system of marketing competitiveness," *Taxation*, vol. 8, p. 193, 2018.
[17] W. Xu, "Comparative research on marketing strategies," *Economics*, vol. 7, p. 181, 2016.
[18] J. Lu and H. Zhao, "Research on the export trade problems and countermeasures of high-tech products in Jiangsu Province," *Market Modernization*, vol. 2, pp. 32-33, 2018.
[19] X. Qi, "Network security situation assessment model based on information fusion," *Science and Technology Innovation and Application*, vol. 30, pp. 190-191, 2017.
[20] X. Yang, J. Sun, and C. Niu, "Research on the application of data fusion in the fire monitoring system of the Internet of Things," *Electronic Measurement Technology*, vol. 39, no. 3, pp. 100–105, 2016.
[21] Z. Wen, Z. Chen, and J. Tang, "Quantitative assessment method of network security situation based on information fusion," *Journal of Beijing University of Aeronautics and Astronautics*, vol. 42, no. 8, pp. 1593–1602, 2016.
[22] J. Esteban, A. Starr, R. Willetts, P. Hannah, and P. Bryanston-Cross, "A review of data fusion models and architectures: towards engineering guidelines," *Neural Computing & Applications*, vol. 14, no. 4, pp. 273–281, 2005.

Hindawi
Wireless Communications and Mobile Computing
Volume 2022, Article ID 2292321, 16 pages
https://doi.org/10.1155/2022/2292321

Research Article

Hybrid IoT and Data Fusion Model for e-Commerce Big Data Analysis

Bing Li[1,2] **and Qi Lei**[3]

[1]*School of Software, Jiangxi Normal University, Nanchang, 330022 Jiangxi, China*
[2]*Research Centre for Management Science and Engineering, Jiangxi Normal University, Nanchang, 330022 Jiangxi, China*
[3]*Department of Nephrology, Dayuan Hospital Affiliated to Jiangxi Academy of Medical Sciences, Nanchang, 330022 Jiangxi, China*

Correspondence should be addressed to Bing Li; 004970@jxnu.edu.cn

Received 25 November 2021; Accepted 21 February 2022; Published 17 March 2022

Academic Editor: Mohamed Elhoseny

This article is aimed at studying the e-commerce big data recommendation model based on data fusion and the Internet of Things. This article chooses an embedded system for the construction of an e-commerce platform and uses data fusion technology to collect, transmit, and filter useful information from various information sources. Then, the collected information and data are analyzed and integrated, and visualization algorithms are used to better present data analysis, and association rules and structural similarity methods for electronic comparison are uses. This article uses the B/S architecture to design the overall framework of the data access layer, business logic layer, and user presentation layer; collects, organizes, stores, and presents the acquired consumer information; and finally analyzes the e-commerce background, platform performance, and supply and demand analysis. The experimental results show that the average clustering coefficient of the platform (0.7559) is smaller than the average clustering coefficient value of 8 items in the store (0.811) and smaller than the average network diameter and average path length of the online store (3.86, 7.7). Store products are better than store products, and the diameter and length of the product should be larger (2.71, 5.75). The recall rate of the e-commerce big data platform and model matching review method designed in this paper is 5% higher than that of the word matching model method and has a better expected effect in terms of user supply and demand.

1. Introduction

For the integration of virtual technology and real economy, e-commerce has been popularized. e-Commerce provides a network platform for corporate transactions, reduces unnecessary processes in business activities, reduces the operation time of business activities, and greatly enhances operational strength. As long as all users connected to the Internet can conduct e-commerce transactions, the scope of e-commerce users will increase and costs will be reduced. For general users, e-commerce can increase the user's choice space, enhance the user's initiative in consumption, and reduce the user's capital investment and time.

e-Commerce has produced a large amount of data. How to use these data reasonably, and how to store and analyze the data has become very important, and it is also an urgent problem for major enterprises to solve. In e-commerce website data, there is a large amount of unstructured data, such as text, image, audio, and video. The indoor play is formed based on the combination of computer and traditional network technology. It includes utility computing, parallel computing, and distributed computing. It has the characteristics of network storage, virtualization, and load balancing. It represents future data management technology development direction. It can manage large amounts of data with less cost and can handle different data classifications and has good scalability.

The innovations of this article are as follows: (1) fully excavate the characteristics and shortcomings of e-commerce, propose specific improvement methods on its shortcomings,

and combine them with the Internet of Things technology according to its characteristics, so as to allow e-commerce to develop better. (2) In the process of building an e-commerce data platform, we use embedded systems in the Internet of Things, break the traditional platform design, better play the role of big data analysis, and provide better analysis results for merchants.

2. Related Work

e-Commerce has become more and more popular with the development of the Internet, so there are more and more researches on it. In Mero J e-retailing, competitors only need to click once, and prices are easy to compare. Providing high-quality customer service and mutual communication through the company's website is an important aspect of attracting and retaining customers. An increasingly popular solution for improving customer service is the "live chat" interface, which allows consumers to have real-time online conversations with customer service agents. Since the literature on the impact of real-time communication through real-time chat is currently very limited, his research has developed and tested a model that proves that the chat service has two-way communication (that is, the core element of perceiving website interactivity) and customer satisfaction and trust degree and repurchase and word-of-mouth (WOM) intentions. The data for this study was collected through an online survey ($N = 6783$). The subjects of the survey were existing customers of five e-retailers that actively use real-time chat as a customer service tool. The research results show that consumers have a low level of awareness of e-commerce. However, in his research, the user's frequency of using e-commerce is low, so it is difficult to better meet the experimental requirements [1]. In order for Maxim et al. to utilize the massive and diverse data captured and stored by the ubiquitous Internet of Things services, forensic investigators need to use evidence acquisition methods and technologies in all areas of digital forensics and may create new Internet-specific investigation processes. Although his research has developed many conceptual process models to solve the unique characteristics of the Internet of Things, many challenges remain unsolved [2]. In order to solve the reliability problem of e-commerce and record any individual business website, they recommend designing a personal business website that is used to purchase books and enable access to the domain by purchasing from the digital ocean cloud, and then, in it, install the server domain; then, they connect it to the website's digital certificate (encrypt it) and then add some software to the client (certbot, root) server assistant program in it, and they have connected the server and the server through Linux instructions and codes. The certifications are linked together, and the commercial website (PHP3.PHP) has been tested in the SSL laboratory. The result is that the service sites are divided into three categories: the current latest, the worst and the current worst, and the detailed information of the classification. However, they did not solve the reliability problem well [3].

3. Method of Constructing an e-Commerce Big Data Analysis Platform Based on Data Fusion and Internet of Things Technology

3.1. Internet of Things Technology

3.1.1. Concept of Internet of Things. The Internet of Things is referred to as IoT (Internet of Things), which is the inheritance and development of the Internet. The concept of the Internet of Things can be analyzed from two aspects. On the one hand, it is a connected network; on the other hand, it is a network that can connect objects to objects and objects to people [4, 5]. This article is mainly to connect the Internet of Things technology and e-commerce to build a big data analysis platform, which is to collect detailed information of goods through infinite sensor devices and then use the embedded system to store and transmit data to realize the analysis and analysis of e-commerce platform data application.

3.1.2. IoT Technology System. The Internet of Things is one of the industries with the most potential for development. It can promote the transformation and upgrading of other industries and make traditional enterprises more innovative. However, with the continuous development of the Internet of Things, my country has been lacking major technologies and related technological innovations, leading to the problem that product quality is average, but the price cost has not been reduced [6, 7]. Technical backwardness restricts development, and the lack of basic technologies such as RFID also strictly restricts the development of the Internet of Things in my country. Therefore, the focus of IoT is mainly on sensors, RFID, and cloud computing. Internet technology is applicable to many industries. In various industries, there are various requirements and technical forms. However, among these various technical systems, the Internet of Things technology is mainly composed of four systems. The four main systems are perception systems, network systems, computer systems, and service and management support systems [8, 9].

(1) Perception recognition technology is the most basic part of the Internet of Things technology, and it is also the foundation of the Internet of Things technology. The detection technology is mainly composed of carbon dioxide sensors, temperature sensors, humidity sensors, optical sensors, and other sensors. The identification technology mainly includes two-dimensional code tags, RFID, and GPS. Perception technology is similar to animals that use ears, eyes, nose, nose, and nerve endings to collect information and determine the source of various objects. The main function of perception technology is to collect relevant data, while the main function of recognition technology is to mark personal traces

(2) The network layer of the network system is composed of various networks. The network layer is equivalent to the computer CPU used to calculate, analyze, and process the sent information. The

network layer must ensure the safe and reliable transmission of information [10, 11]

(3) Computer systems and service systems will send a lot of sensory information. Internet technology is to calculate, process, and display data in a more intuitive form, and perform operator reports and analysis. The ultimate value of this information is used to analyze and report deeper values. Both services and applications are the main methods to realize the value of information [12, 13]

(4) With the continuous development of big data, computing cloud, and other technologies, the Internet of Things technology has also expanded the scope of services supported by these new technologies and can basically assume more areas of enterprise management and control. Promoting the further development of technology is precisely due to the management and support functions of the Internet of Things. Management and support technologies are the key to ensuring the high performance of the Internet of Things, including measurement analysis, network security, and security

3.2. Data Fusion Technology. Data fusion refers to the process of using computer technology to process information under specific standards. This process can automatically analyze, optimize, and integrate the sensor observation results that require sufficient time to complete the required decision-making and evaluation tasks, and the collection, transmission, synthesis, filtering, correlation, and synthesis of useful information from various information sources. Data fusion is also called information fusion or multisensor fusion. The process of using computer technology to process information under certain conditions is used. This process can automatically analyze, optimize, and synthesize time series multisensor observations to complete the required set of decision-making and evaluation tasks. With the continuous development of science and technology, the data environment in life will become more complex in the future, and the amount of data will increase exponentially. At the same time, there is still a lot of uncertain and false information. In this case, the continuous development of data fusion technology will significantly improve the efficiency of information processing and provide accurate, timely, and effective information support for data decision-making.

3.3. e-Commerce

3.3.1. Definition of e-Commerce. The term e-commerce comes from the English electronic commerce, which is usually translated into e-commerce or e-business (electronic business) in China. Since e-commerce was proposed in 1995, e-commerce as a new business model has been recognized by the society, but there is no scientific and complete definition up to now. Governments, scholars, research institutions, companies, etc. have explained e-commerce from different perspectives. It can be summarized as that e-commerce is based on the network and realizes the whole process from product sales, market planning to information management [14, 15].

3.3.2. e-Commerce Model. The e-commerce model refers to a method for companies to provide customers with better and more affordable value and benefit from it in the context of e-commerce. With the rapid development of e-commerce, there are more and more business models. At present, the most conventional classification is based on e-commerce transaction objects, mainly B2B (business to business), B2C (business to consumer), B2G (business to government), C2B (consumer to business), C2C (consumer to consumer), C2G (consumer to government), G2B (government to business), G2C (government to consumer), G2G (government to government), and other nine categories [16, 17], as shown in Table 1.

(1) Business-to-business e-commerce, referred to as B2B, refers to the integration of commodity resources between enterprises and manufacturers on the Internet platform. B2B is the most popular e-commerce development model for enterprises. The integration of the supply chain is realized through the concentration of supply, the automatic realization of procurement, and the high efficiency of the supply and distribution system. Typical representatives of the B2B model include Alibaba, Made-in-China, and Huicong

(2) Business-to-consumer e-commerce, referred to as B2C, is the most intense e-commerce model in the market competition. Enterprises provide consumers with an online trading platform through the Internet, which not only saves consumers' time but also brings huge profits to enterprises, which can be described as a win-win situation. Typical representatives of the B2C model are Amazon, Tmall, Jumei Youpin, etc. [18, 19]

(3) Consumer-to-consumer e-commerce is abbreviated as C2C, which is a business activity in which individuals conduct transactions with the help of a network platform. The C2C platform builds a bridge for both parties to the transaction and provides a series of supporting services to ensure the smooth progress of the transaction. Typical representatives of the C2C model include Taobao, Paipai, and eBay

(4) Consumer-to-business e-commerce, referred to as C2B, is a new e-commerce model that is based on consumer needs and conducts reverse transmission in the business chain. Consumers can apply actively participate in the design, production and pricing of customized products. With the help of the flourishing Internet, Internet of Things, cloud computing and big data, and other information technology, the individual needs of consumers are better and better met. Typical representatives of the C2B model include group buying websites such as Juhuasuan, Baidu Nuomi, and Meituan

Table 1: e-Commerce model.

Object	Government G	Enterprise B	Consumer C
Government G	Information exchange and coordination G2G	Information provision G2B	Information provision G2C
Enterprise B	e-Procurement B2G	Alibaba, HC network B2B	Amazon, JD B2C
Consumer C	e-Tax C2G	Baidu Nuomi, Meituan C2B	Taobao C2C

In the e-commerce model, the four most common types are B2B, B2C, C2C, and C2B, and the other five types will also be applied. In addition, there is the O2O model, which realizes the perfect interaction between online and offline, and connects physical stores with online stores to meet the dual experience of consumers; the B2R model is a new model of transactions between enterprises and retailers, a typical representative is Yiwu Shopping.

3.4. Big Data

3.4.1. The Era of Big Data. As the material foundation of the cloud era, big data has attracted more and more attention. From the point of view of enterprises, some people think that big data is the total amount of data produced or exchanged in the operation of enterprises. These data are huge in quantity and have different structures. It is not yet possible to perform simple classification, calculation, and other operations on the data. The concepts of big data and cloud computing are often confused [20, 21]. In fact, big data refers to the collection of data, and cloud computing refers to the calculation method, but this calculation method is only for big data. The calculation method of big data cannot be calculated by the commonly used standalone computer. No matter how good the performance is, the host cannot receive the data processing and analysis of the supermass set. A distributed processing system must be used to measure and measure to meet the era of big data challenge.

In the era of big data, diversification of data collection methods is a major feature of e-commerce websites. Generally speaking, the data sources of e-commerce platforms can be divided into four types: (1) Platform internal data: these data include users' browsing, search, purchase, evaluation, and transaction data within the platform, as well as merchants' information on the sale of goods. Attribute definition and description, of course, as well as user-business interaction and evaluation data. These data can objectively and comprehensively reflect the psychological factors of both parties to the transaction, and these factors represent the key to the success or failure of the transaction and have high analytical value [22, 23]. (2) Platform external guiding data: mainly through the introduction of web advertisements, the display ranking data of the search platform, service links, and related application recommendations, etc. (3) Direct access to the data: this part of the data mainly comes from browser visits and direct visits to various types of e-commerce websites. These data can reflect the user's preferences and habits, and more often reflect the user's needs. (4) Wireless data: With the rapid increase in the number of mobile electronic devices, the amount of data transmitted wirelessly is also soaring. All e-commerce platforms have opened application interfaces for mobile electronic devices, allowing users to conduct e-commerce activities anytime, anywhere. Wireless devices, like wired devices, generate a large amount of data. Due to the particularity of wireless devices, these data tend to reflect the characteristics of users, and it will be more meaningful and valuable for data analysis and utilization.

3.4.2. Big Data Analysis. The analysis of big data needs to analyze and process the data through standardized processes and tools, which can ensure that the analysis results can achieve better results. Because the diversity of unstructured data brings new challenges to data analysis, a series of tools are needed to parse, extract, and analyze data, and data visualization is the most basic requirement of data analysis tools. Predictive analysis with big data allows data analysts to make predictions on the development trend of data based on visual analysis reports and indirect data information and analyze the natural and social impacts brought about by this.

3.4.3. Big Data Processing. The collection of big data uses databases as data carriers, and these databases receive the data sent by the client. Users can perform data query and other operations in the database. In the era of big data, e-commerce will still consider the timeliness of transactions, using traditional relational databases SQL Server, MySQL, and Oracle to store and process each transaction data. In addition, some nonrelational databases. It is also commonly used for data collection, such as Redis, MongoDB, and HBase. The collection of big data has its main characteristics, which are large throughput and high concurrency. For example, ticketing websites and e-commerce websites are both business-oriented websites, so they have to face huge concurrent visits. If you want to receive and process such a huge amount of data at the same time, you need to rely on big data processing technology to ensure the integrity of the data. And considering the overall performance of the database and the utilization of resources, it needs to be load balanced.

In order to meet the needs of data analysis, statistics and analysis mainly use distributed processing systems or distributed databases to classify and process the massive data stored in them. In this regard, some real-time requirements will use the MPP system adopted by EMC's newly acquired GreenPlum, MySQL-based columnar storage Infobright, and Oracle's Exadata. These systems have certain advantages in decision support and data mining. Facing the statistical analysis of large amounts of data, it has brought severe challenges to system resource utilization and network resource occupancy.

3.5. Research Methods

3.5.1. Reconstruction of the Original Data Distribution. The purpose of reconstructing the distribution of the original data is to make the modified and reconstructed data still is able to perform data mining and obtain more accurate results. Reconstructing the original distribution is to reconstruct the distribution of the original data, not to rewrite the original data in the record.

Suppose the original data $x_1, x_2, \cdots, x_n$ are the sample values of independent and identically distributed random variables $X_1, X_2, \cdots, X_n$. In order to hide the original value, we introduce independent and identically distributed random variables $Y_1, Y_2, \cdots, Y_n$. According to the distribution function Fy of $x_1 + y_1, x_2 + y_2, \cdots, x_n + y_n$ and Y, the cumulative distribution function Fx of X is estimated.

We estimate the posterior distribution function according to Bayes' rule, such as

$$F'_{x_1}(\varepsilon) = \frac{\int_{-\infty}^{\varepsilon} g_Y(q_i - z) g_X(z) dz}{\int_{-\infty}^{\infty} g_Y(q_i - z) g_X(z) dz}. \tag{1}$$

We calculate the average value for it:

$$F'_X(\varepsilon) = \frac{1}{n}\sum_{i=1}^{n} F'_{X_i} = \frac{1}{n}\sum_{i=1}^{n} \frac{\int_{-\infty}^{\varepsilon} g_Y(q_1 - z) g_X(z) dz}{\int_{-\infty}^{\infty} g_Y(q_1 - z) g_X(z) dz}. \tag{2}$$

In the same way, calculating the posterior density function can be obtained by differentiating the above value:

$$f'_X(\varepsilon) = \frac{1}{n}\sum_{i=1}^{n} \frac{g_Y(q_i - \varepsilon) g_X(\varepsilon)}{\int_{-\infty}^{\infty} g_Y(q_i - z) g_X(z) dz}. \tag{3}$$

If the calculable sample size is large enough, the $f'x$ obtained by the above formula (3) is closer to the true value f_X. At this time, f_Y can be made public, but f_X is hidden. Therefore, the joint distribution can be used as the initial estimated value, and the above formula (3) can be repeatedly modified to finally obtain f_X.

3.5.2. Visualization Algorithm. After we can automatically analyze e-commerce big data, we need to choose a visualization tool to present it to the public. According to the visualization algorithm, suppose the value of the ith time point in the sequence is t_i and the value of the uth time point is t_u, any other data between these two data is marked as t_x. The relationship that should be satisfied between them is as follows:

$$t_u < t_x + (t_i - t_x) * \frac{(x - u)}{(x - i)}, i < t < u, \tag{4}$$

$$\frac{(t_x - t_u)}{(x - u)} < \frac{(t_x - t_i)}{(x - i)}. \tag{5}$$

If all the intermediate points between t_i and t_u do not cut off the straight line connecting them, then t_i and t_u have a connecting edge. Using visualization algorithms, time series data can be mapped to form a complex network diagram.

The power-law distribution allows us to better understand the economic meaning of e-commerce, and it can also be called a discrete Pareto distribution. The expression is as follows:

$$p(l) = \frac{l^{-\Gamma}}{\vartheta(\Gamma)}. \tag{6}$$

Among them, l is a positive integer that usually represents a variable of interest, $p(l)$ represents the probability of occurrence of l, and Γ represents a constant power exponent, generally between 1 and 3.

The formula of Pareto cumulative distribution is

$$P(x_j \geq x_i) = \frac{\sum_{j=1}^{N} t(x_j)}{N}. \tag{7}$$

The advantage of the cumulative occurrence probability is that it not only avoids the mediocrity in the distribution description but also does not reduce the amount of data, and each data after accumulation generally contains a lot of original data, so it will minimize statistical fluctuations.

3.5.3. Calculation Method of Structural Similarity. Based on the simple and intuitive graph theory model $H = (B, R)$, Jeh and Widom et al. proposed the SimRank algorithm, where B represents the node in the graph and R represents the connecting edge between the nodes. The similarity between two objects depends on their structural relationship in the graph. The theoretical assumption based on the SimRank algorithm is as follows: two objects are similar if they are related to other similar objects. This assumption is similar to the assumption based on the SimFusion algorithm.

The algorithm first represents the data object in the relational data as a node in the graph theory model, and the relationship between the objects is represented as the directed connecting edge between the nodes. The similarity between the nodes can be obtained by the SimRank calculation formula:

$$S(b, c) = \frac{D}{|U(b)||U(c)|} \sum_{i=1}^{|U(b)|} \sum_{j=1}^{|U(c)|} S_{\text{link}}\left[U_i(b), U_j(c)\right], (b \neq c). \tag{8}$$

It can be seen from the formula that, generally speaking, the similarity between b and c is the average of the similarity between the in-degree neighbor nodes of b and the in-degree neighbor nodes of c. The similarity score between the node pairs calculated by SimRank is symmetric, that is, $S(b, c) = S(c, b)$. The formula can calculate the structural similarity score between any node pair b and c until it converges.

Cluster analysis is a method that automatically divides samples into several groups based on the measurement criteria of the correlation between samples and makes the

samples in the same group similar and different samples in different groups. In this paper, the numerical attributes and category attributes are referred to in the cluster analysis. The calculation formula for calculating the attribute similarity between objects is

$$\mathrm{Sim}_B\left(x_{ij}, x_{il}\right) = e^{-\left\|\left(x_{ij}\cdot B - x_{il}\cdot B\right)\right\|}. \tag{9}$$

The sum of the differences of each attribute of the object is

$$\left\|x_{ij}\cdot B - x_{il}\cdot B\right\| = \sum_{r=1}^{q}\left|x_{ij}B - x_{il}B\right| + \nu\sum_{r=q+1}^{N}\theta\left(x_{ij}B_r, x_{il}B_r\right). \tag{10}$$

The Attribute-SimRank method can calculate the similarity score and use SASimRank to express it; comprehensively considering the attribute similarity and structural similarity, the formula is expressed as follows:

$$T_{\mathrm{ASimRank}}(b,c) = (1-\beta)\cdot T_{\mathrm{attr}}(b,c) + \beta\cdot T_{\mathrm{link}}(b,c). \tag{11}$$

Among them,

$$T_{\mathrm{attr}}(b,c) = e^{-\sum_{r=1}^{n}\theta\left(x_aB_r, x_cB_r\right)}, \tag{12}$$

$$T_{\mathrm{link}}(b,c) = \frac{D}{\left|U(b)U(c)\right|}\sum_{i=1}^{|U(b)|}\sum_{j=1}^{|U(c)|}T_{\mathrm{link}}\left[U_i(b), U_j(c)\right]. \tag{13}$$

For any pair of nodes in H, there will be a SASimRank similarity score. For example, if the number of nodes of a certain type in H is N, there will be a similarity score of $N * N$ pairs of nodes. Similarly, the SASimRank score is symmetric. That is $S_{\mathrm{ASimRank}(a,b)} = S_{\mathrm{ASimRank}(a,b)}$.

We use Attribute-SimRank to calculate the authenticity and reliability of the similarity, and then, we use clustering objective evaluation indicators to verify the effectiveness of the clustering results, the formula is as follows:

$$C_g = \frac{\sum_{i=1}^{l}\sum_{x\in C_i}s(x, a_i)}{\sum_{1\le i\le j\le l}s\left(a_i, a_j\right)}, \tag{14}$$

$$s\left(a_i, a_j\right) = 1 - T_{\mathrm{ASimRank}}\left(a_i, a_j\right). \tag{15}$$

The above formula is defined as the ratio of compactness within clusters to isolation between clusters. A better clustering result is generally that the tightness within the cluster is manifested by the small distance between objects in the cluster, and the greater isolation between clusters is manifested by the greater distance between the centers of each cluster. The value of C_g is the smaller, the better the clustering quality.

3.5.4. Measurement Indicators of Association Rules. The degree of support in the database refers to the ratio of the number of transactions that can be included in a transaction to the number of all transactions at the same time, denoted as

$$\mathrm{Sup}(X => Y) = \sup\left(X\cup Y\right). \tag{16}$$

Confidence degree can be used to measure the credibility of association rules, denoted as

$$\mathrm{Con}(X => Y) = \frac{\mathrm{Sup}(X\cup Y)}{\sup\left(X\right)}. \tag{17}$$

4. System Construction of e-Commerce Big Data Analysis Platform Based on Embedded System

4.1. Demand Analysis. The target user group of this system is the relevant staff involved in e-commerce marketing activities in the enterprise, including the customer department personnel needing to understand the situation of the customer's company store/product and show the outstanding results of the company through cases and data when communicating with customers; operations staff needing to understand the operating platform through data reports such as daily, weekly, and monthly reports and adjust and optimize operations, maintenance, and updates through data reports; and planners needing to understand excellent cases to promote inspiration, and at the same time, when insights are obtained, there must be data support to complete the planning plan more accurately; designers daily needing to check various past cases and materials; understand the layout of excellent case designs, etc., through the feedback of data reports, and can better form design output; and data analysts frequently obtaining data, performing statistics and analysis, completing various types of reports, and better assisting or guiding the output of the program through data reports. In daily work, the target user is not entirely one person responsible for a project alone and often require multiple types of personnel to be responsible for multiple customers, multiple platform/store operations, and multiple activities at the same time. The planning of product inner pages, the design of multiple design drafts, and the output of multiple data reports, so it is necessary to use or obtain data/cases/materials with high frequency and frequency.

In the design of e-commerce big data analysis platform, based on past experience, the following factors will be considered: (1) data security, customers generally only disclose the user name and password of the store to a very small number of people within the enterprise, avoiding data to a certain extent of leaks. This has led to the fact that most of the personnel responsible for the actual work in the company do not have the authority to view the data. Even if this part of the data is completely open to the outside world, generally, it can only be obtained and shared by relevant personnel with the authority, and it is shared in many cases. The information is not necessarily what other people want to

obtain. This leads to the lag and inconsistency of information acquisition. (2) Each store corresponds to a user name and password, and the data of the corresponding store can be viewed and obtained by logging in. This leads to the need to log in to different accounts when viewing the data of different stores on different platforms or the same store on different platforms, which causes a certain degree of cumbersomeness under the condition of ensuring security, and they cannot be done between platforms and stores. (3) The third-party data applications on most platforms, such as Taobao's "Business Staff," have only relevant indicator data, which is relatively shallow data, and it is impossible to directly obtain reports that are more closely related to the business of the enterprise in the application. As a result, no more supplementary or instructive content can be drawn. (4) Third-party data applications on most platforms, such as Taobao's "Business Staff," whose data is provided to all digital marketing companies, are universal and have not been expanded in terms of the business characteristics of different companies and customization.

In response to the above problems, this paper designs and implements an e-commerce big data analysis platform based on the Internet of Things technology. The establishment of the system platform involves the customer department personnel, operation personnel, planners, designers, and data analysis personnel in the enterprise, to provide these users with a data management and analysis platform that is different from the third-party applications currently used, to be closer to the business of the enterprise, and to enable users to obtain more valuable information more conveniently.

4.2. Overall Framework of the System. The data analysis system based on the e-commerce platform adopts the B/S architecture and is designed according to the three-tier architecture, including the data access layer, business logic layer and user presentation layer. (1) Data access layer: the access operation layer to the underlying data, which realizes the reading, adding, modifying, and deleting of data. The access interface of the underlying data for the last business logic layer was provided. In this system, data reading and adding are the main operations, while data modification and deletion operations are relatively few. (2) Business logic layer: for the realization of specific functions, the data is processed according to business logic and the results are returned to the presentation layer. In this system, business logic mainly includes four parts: data acquisition, data processing, storage, and data presentation. (3) User presentation layer: this is responsible for interacting with users. In this system, the user presentation layer is responsible for receiving user output, sending requests to the server, and displaying back to the front-end page.

4.3. Overall Function Module Design of the System

4.3.1. Data acquisition. The data source of the system is composed of three parts. Data is obtained from Taobao's third-party application "Business Staff"; the crawler program crawls the basic information, material information, and buyer comments of the product; the data increase function of the system; increase the product name, links, and terminals; increase the location of monitoring materials; and increase the focus of buyers to search for keywords.

(1) Use data fusion technology to obtain data from Taobao third-party applications. It is mainly based on numerical index data, which is mainly used for the call data of four front-end modules of business details, product sales, traffic sources, and marketing effects. Detailed data includes but are not limited to date, shop, terminal, page views, number of visitors, number of old visitors, per capita page views, number of old buyers, number of products paid, and number of buyers paid, payment amount, payment conversion rate, customer unit price, average length of stay per capita, average daily bounce rate, etc.

(2) The crawler program obtains the data. The data that web crawlers need to crawl from the e-commerce platform is divided into three categories, the crawling of basic product information, the crawling of material information, and the crawling of buyer comments. The basic commodity information includes date and terminal, which is used to call data from the front-end module of commodity analysis. The material information includes two types, full page and point position, which are used to call data by the buyer's attention point data processing module

(3) Add data to the systems' own functions. The system itself has designed the function of adding data, which is mainly used to provide users with personalized and customized monitored products, points, and keywords for buyers to search for. With the expansion of business, users can add corresponding information through the system. The background crawler program crawls data based on the added content, adds new data content to the database, and uses it to add functions to the three modules of product analysis, material analysis, and buyer focus. The commodity analysis module adds commodity names, links, and terminal information. The material analysis module adds the link where the monitored material is located. Buyer focus increases buyer focus search keywords

4.3.2. Data processing. Integrate and process the collected data through data fusion technology. Data processing is divided into 9 parts: (1) Raw data processing: the original data obtained from Taobao's third-party data application has accumulated data from 2015 to 2019 and is stored in multiple tables separately according to the year. Since it is unprocessed source data, there will be attribute columns, abnormal record rows, and blank row records that are not related to this system. Therefore, according to the database design of this system, the original data is reprocessed and stored in the database data. (2) Personalized labeling of a single product: the basic product information crawled by

the crawler program is limited to the data displayed on the product detail page. In order to provide users with a better monitoring product search experience, it is necessary to add personalized labels to the products, including the category, brand, and commodity features. (3) Personalized labeling of material pictures: the material crawled by the crawler program is limited to the image and its title. In order to provide users with a better monitoring product search experience, it is necessary to add personalized tags to the material, including the category, brand, and design features of the material. (4) The construction of special dictionaries in the review field: due to the particularity of the field, the reviews will contain a large number of terms such as category, brand, product name, and special words in the review. Therefore, by obtaining all the categories and brand words on the platform, and Tmall's word segmentation information on the title, a review field is constructed. Dedicated dictionary, auxiliary comment word segmentation improves the accuracy of word segmentation. (5) The construction of buyer focus model: the buyer attention model is used to vote and classify the attention points of buyers' comments. Since the comments are published by buyers, there are many expressions of words. It is necessary to use words for the attention points that appear in the comments. Only by classification can you vote on the buyer's concerns in the comments. This system uses the accumulated review corpus, after word segmentation, manually classifies the word segmentation, and builds a general buyer focus model. (6) Word segmentation and labeling: the purpose of word segmentation is to segment comments in sentence units into comments in word units, which can improve the efficiency of the algorithm. This system combines the well-structured special dictionary for the review field, the Chinese Academy of Sciences NLPIR word segmentation tool, and the common word method based on statistics for word segmentation and labeling. (7) Extraction of candidate feature words: we use the labeling information to extract the content words in each comment to construct the vector representation of the comment. This method reduces the number of words that need to be processed and further improves the efficiency. (8) Identification and statistics of buyers' concerns: the purpose of voting for buyer concerns is to identify the distribution of different concerns in buyer comments. Combining the feature words extracted after word segmentation, the buyer focus model, and the voting classification algorithm, all buyer comments in this category are processed one by one, and the frequency of each focus category is counted, the number of valid comments in the entire category, and finally calculate the proportion of each category of concern. (9) Check the legality, repeatability and completeness of the data added by the system: due to the added functions of the system, users can add product names, links, and terminal information in the product analysis module; add links to monitor material in the material analysis module; and increase buyer focus search keywords in the buyer focus. After adding information, the web crawler will crawling the corresponding information, so the data needs to be checked before entering the database, including whether the input content is legal content, whether it is duplicated with the existing data in the database, and whether it is used as the primary key the information is not empty.

4.3.3. Data storage. The storage method of system data is divided into two parts. The first is stored in the Sql Server database, including all numeric and text data. The image material is stored in the address of the image server, and the second is stored in the image server., The pictures (.jpg, .png) crawled by the crawler program need to store the picture files in the hard disk of the picture server. Calling a picture is to mobilize the picture corresponding to the address in the picture server by obtaining the picture address in the Sql Server database.

4.3.4. Data presentation. The data presentation is divided into two parts: the presentation of the data graph (line graph and bar graph) and the presentation of the detailed table of data content. The development and design mode adopted by this system is B/S (Browser/Server, browser/server) mode. Under this structure, the user interface is realized directly through the client browser. The client sends a service request to the server, including the data request for the database. The server responds to the client request and transmits the response result to the client browser.

The system front-end module is divided into 7 functional modules, which are business details, product sales, traffic sources, marketing effects, product analysis, material analysis, and buyer concerns. There are 4 modules that contain discount graph display: business details, product sales, traffic sources, and marketing effects; modules that contain bar graph display are buyers' concerns; those that contain detailed data table display. There are 6 modules-business details, product sales, traffic sources, marketing effects, product analysis, and material analysis. Figure 1 shows the platform structure of e-commerce big data system.

5. Application Research Analysis of e-Commerce Big Data Platform Based on Data Fusion Technology and Internet of Things Technology

5.1. Background Analysis of e-Commerce. As shown in Table 2, the e-commerce market continues to increase in 2019, and the penetration rate of global online shopping users is high (the penetration rate of online shopping users refers to the ratio of the number of online shopping users to the number of Internet users in a certain period of time). At present, the penetration rate of online shopping users in China is 56%, ranking 4th in the world; and due to China's large population base, online shopping users have reached 374 million, ranking first in the world. Combining the penetration rate of online shopping and the number of netizens, China's e-commerce market still has a lot of room for development.

Judging from the ranking of e-commerce platforms in Figure 2, the top three e-commerce platforms are Taobao, JD, and Tmall. From the ranking status in recent years, it can be concluded that China's e-commerce industry has entered a "duopoly." In the era, the two major forces of Ali

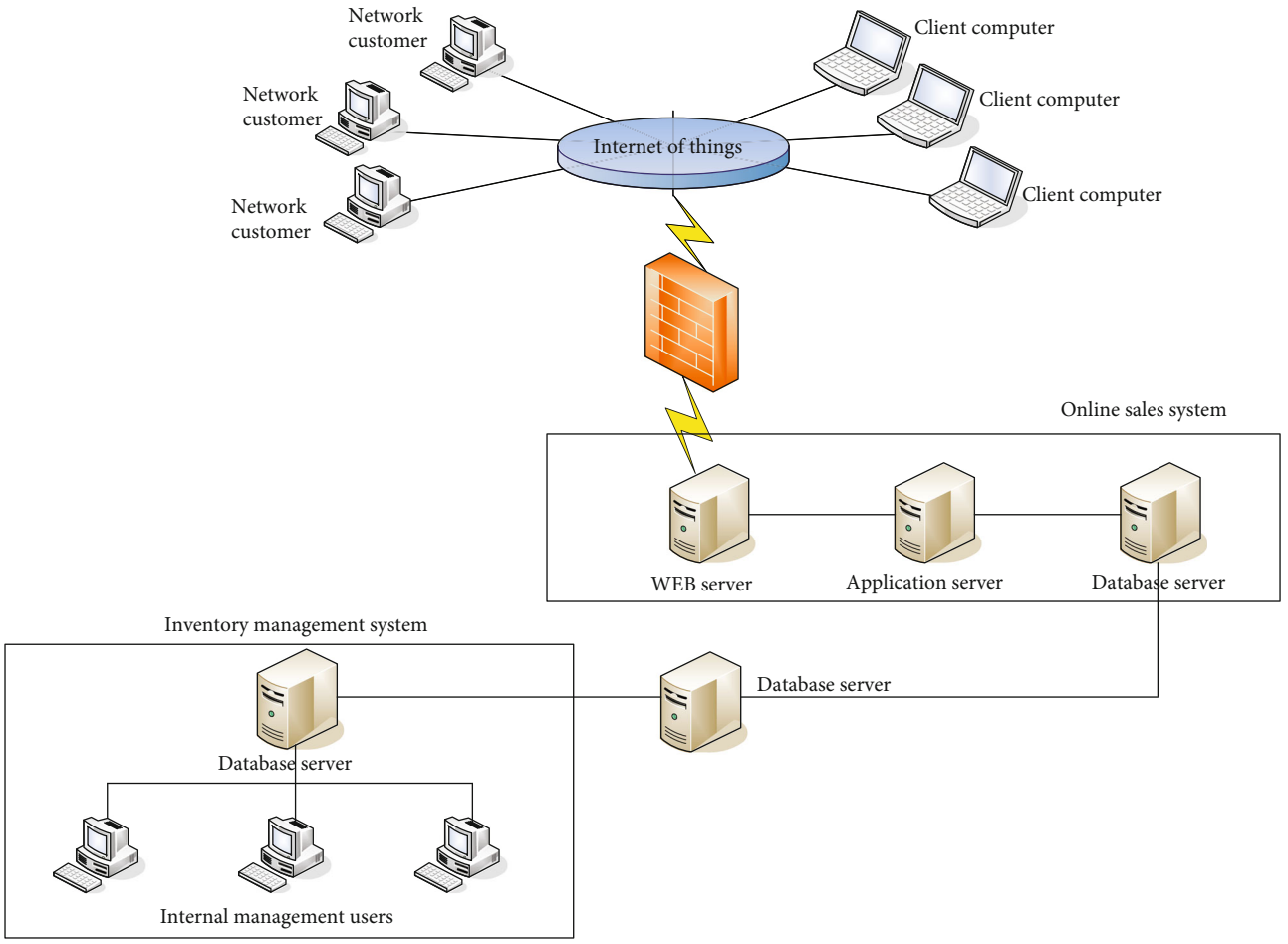

Figure 1: e-Commerce big data system platform.

Table 2: The size of Internet users in various countries and their penetration rate distribution.

Country	Online shopping penetration rate	Online shopping user scale
China	3.75	56.01
United Kingdom	0.45	92.54
Russia	0.88	61.34
United States	1.79	71.68
Japan	0.66	45.58
Germany	1.48	55.42
France	0.72	56.28
Korea	1.69	42.29
Canada	0.88	43.88

(Taobao + Tmall) and http://JD.com divided the market. In the platform model, e-commerce platforms can be divided into B2C platforms, independent shopping malls, C2C platforms, O2O platforms, etc., among which B2C platforms account for the largest proportion. On the one hand, most companies choose the B2C platform as their first choice for online marketing platforms, and because there are so many B2C platforms on the market, in order to expand their market share, companies generally deploy their online marketing business to multiple platforms. On the other hand, the number of users who use mobile clients for online shopping is increasing, and there is even a trend to catch up with the PC side. Therefore, companies also take into account the business of the PC side and the mobile side.

The biggest advantage of e-commerce over traditional retail is that all sales can be controlled and changed through data. Operators check the quantified marketing situation through indicator data, including page views, number of visitors, transaction amount, transaction conversion rate, bounce rate, and number of shopping carts, through the user's shopping list, favorite list, and shopping cart list, and so on, to analyze the user profile of the target user; buyer's rating and comment data, and get the buyer's feedback on the product. By monitoring data changes and further analyzing the data, you can effectively understand the marketing status of stores, products, and activities and analyze the concept of data, overall sales, user portraits, and the results of activities. Others improved valuable conclusions and help operators improve store operations and increase profits. Therefore, through the use of e-commerce to provide services to consumers and traders, we obtain data and use data to further provide services to consumers and

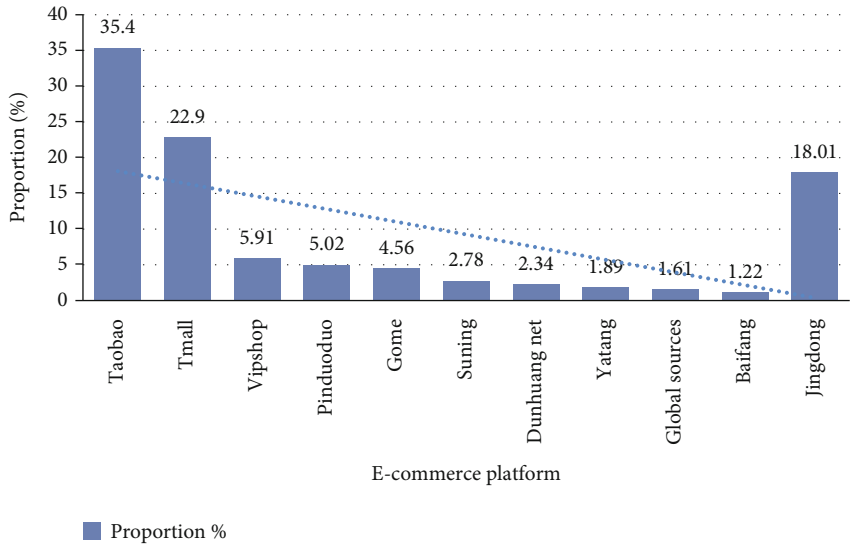

Figure 2: 2019 e-commerce platform rankings.

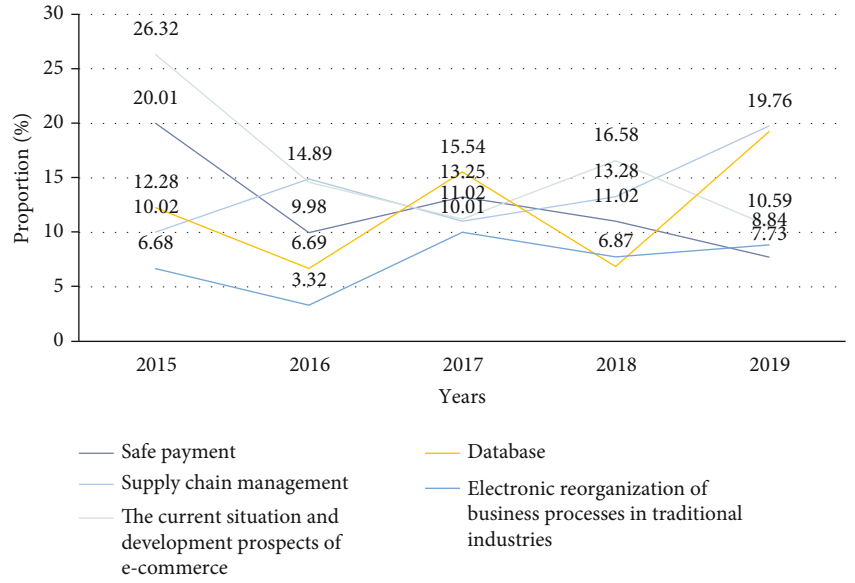

Figure 3: Changes in e-commerce research hotspots.

Table 3: Detection performance under the influence of different impurities.

Performance Testing	All traffic	Detect event Number of cycles = 40, impurity influence = 0.05	Detect event Number of cycles = 40, impurity influence = 0.01	Detect event Number of cycles = 40, impurity influence = 0.001
Number of events	7648823926	1382485298	949241947	680325591
BOT events	2394884311	1139873281	714024972	461692487
Number of events for logged-in users	4057881285	27319423	17423987	15145264
Number of new detection events	—	242612018	235226976	218634104
Login rate	—	2.01%	1.81%	2.20%
New detection rate	—	10.11%	9.82%	9.10%

Table 4: Number of old and new rules detected.

Quantity	Number of events	BOT events	Number of events for logged-in users
All traffic	7648823926	2394884311	4057881285
Number of old rules detected	479534246	301234764	15677342
Number of existing rule detections	1382485298	1139874281	27319423
Increase the number of detections	902951055	838638527	11643082
Add detection ratio	—	279%	—

Table 5: System performance test results.

The amount of data	Days Rows	1 day 2916238268	5 days 16514201586	10 days 34766769874
Data extraction	Real time	10′39	47′13	53′03
	CPU time	7d2h	30d23h	62d19h
Data cleaning	Real time	21′45	1h27′34	3 h3′16
	CPU time	14d2h	68d4h	117d11h
Supply and demand analysis	Real time	15′23	18′54	20′10
	CPU time	1d17h	2d4h	2d13h
Total time	Real time	37′47	2 h33′1	4 h14′29
	CPU time	22d21h	101d5h	182d19h

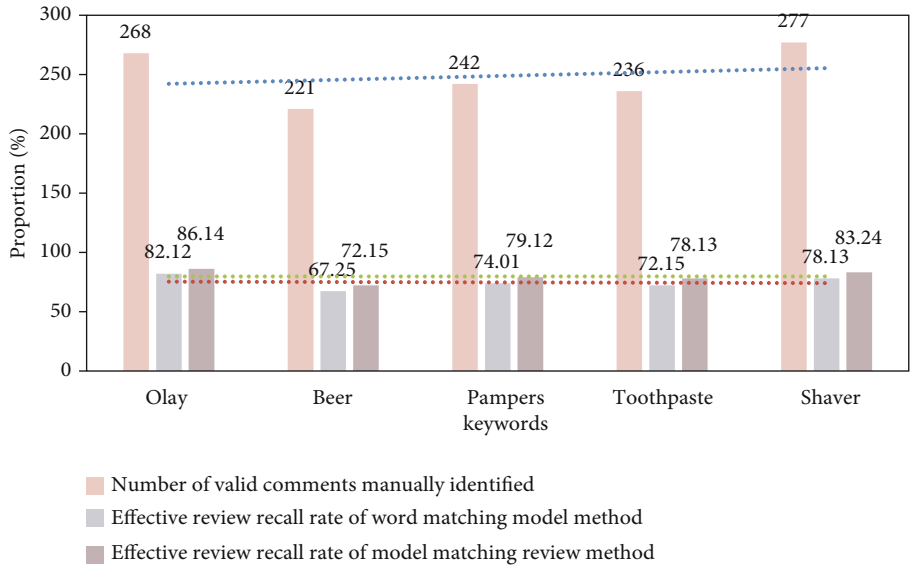

Figure 4: Experimental results of the two methods.

traders in this cycle. Data analysis in the field of e-commerce has become particularly important.

It can be seen from Figure 3 that the research hotspots on e-commerce have been in the process of change. In the past, there was some concern about payment security performance. The attention rate reached 20.01% in 2015. However, with the development of science and technology, security with the improvement of technical means, the attention to safe payment has dropped to 7.73%; however, the attention to the database has not decreased but has increased. In the past, everyone did not understand the role of the database, but now everyone has a better understanding of the database. The database can well grasp the consumer's consumption habits and consumption psychology and analyze the consumption data required by the merchants. Therefore, it has also increased the attention to the database. In 2019, it reached 19.24% of the attention. Therefore, it is necessary and realistic for the research of e-commerce big data analysis platform.

5.2. Performance Analysis of e-Commerce Big Data Platform. We divided the detection events into different impurity situations and then analyzed the e-commerce big data analysis platform system. The results are shown in Table 3. It can

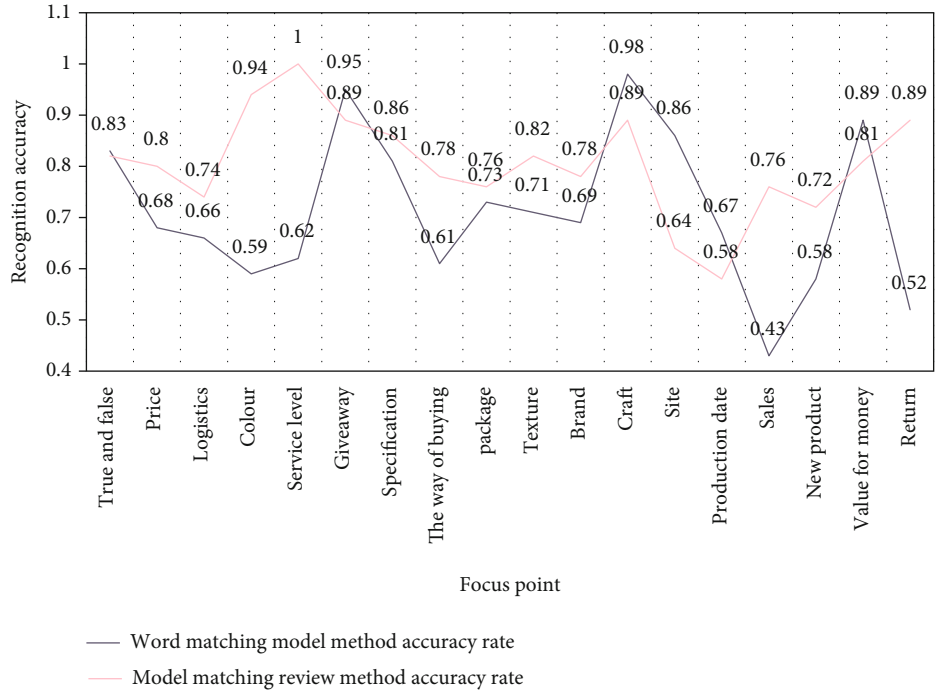

Figure 5: Comparison of the accuracy of each classification of the two identification methods of buyers' concerns.

be seen from the table that the lowest false alarm rate and the highest BOT event detection rate can be achieved after the thresholds of various combinations of parameters are combined.

Table 4 shows the comparison of the number of detections under the new and old rules. When the number of cycles = 40, the impact of impurities = 0.05, and the cycle length = 5, the experimental results are obtained by comparing the old rules with the current rules. It can be seen that the total number of BOT events for all traffic has increased, and the detection ratio has increased by 279%.

The system performance test data is actual user behavior data, and the data volume of 1 day, 5 days, and 10 days are used for testing. As shown in Table 5, the amount of data in 1 day is about 2.9 billion rows, about 16.5 billion rows in 5 days, and 34.7 billion rows. The system performance tests of data extraction, data cleaning, supply and demand analysis and mining are performed on these data, and the results are the test results are shown in Table 5. The results are divided into actual time and CPU time. Actual time refers to the actual time used by the test result, and CPU time refers to the CPU time consumed by the system.

It can be seen from Figure 4 that the effective review recall rate of the word matching model method is more than 67%, and the effective review recall rate of the model matching review method is more than 72%. Among the two methods, "beer" has the worst recall rate, while "Olay" has the best recall rate. In terms of overall performance, the method in this article has a higher recall rate than previous research methods, with an average of 5% higher.

The results of the recognition accuracy of buyers' attention points from each category review are shown in Figure 5. Overall, the trend of the recognition accuracy of the two

Table 6: Comparison of user search and demand analysis.

User raw search data	Demand analysis results
Cybershot Sony DSC-F707 charger	Sony battery charger
15 204 Mercedes man united kit	Mercedes kit
Weather york ambient mercury	Air sensor
Yamaha 50 00 mm ttr	Yamaha piston ttr
Flex iPhone 5s case	iPhone 5s case
Aquarium filter pharmaceuticeal	Aquarium filter
Calor trocador	Exchanger heat
Dome e30 light	bmw light
Eay62810801	Lg power supply
Kei yoki	African violet leaf

methods in each category remains the same, but there are also some categories with large fluctuations, including Budweiser's "gift/trial/reward/benefits," "smell," "appearance," "expiration date/generation date," "return," Pampers's "color,", "origin/manufacturer"; gum care toothpaste, the "purchase channel," "manufacturer/origin," and "new product/style" of the shaver's "specification/content/concentration/capacity/area/weight/quantity."

As shown in Figure 5, the recognition accuracy of each category of the "Olay" two methods is above 45%. The top 5 of the categories with the best performance of the word matching model method are texture, expiration date/production date, taste, manufacturer/origin, and true and false; the TOP5 of the categories that perform best in the model matching comment methods are texture, expiration date, taste, manufacturer, and true and false.

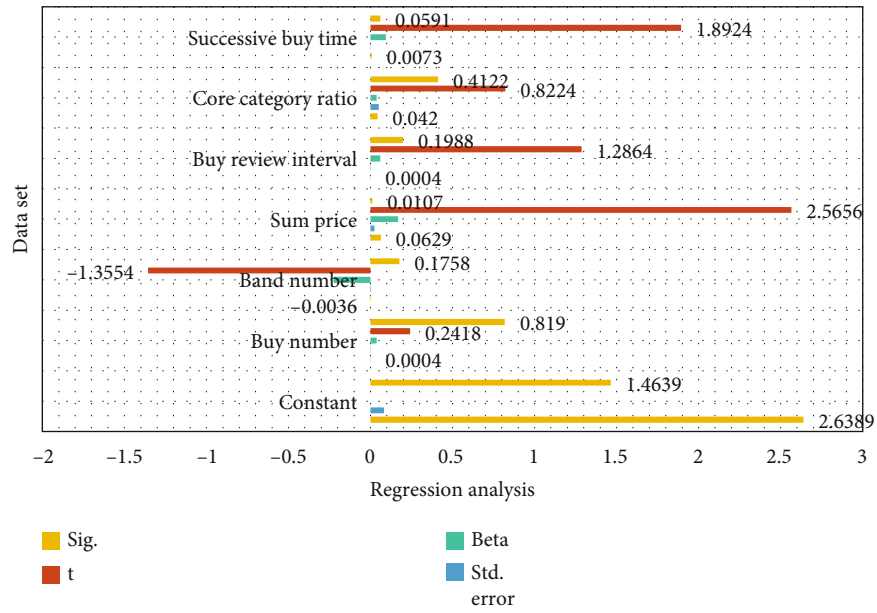

Figure 6: Memory data set-regression coefficient analysis.

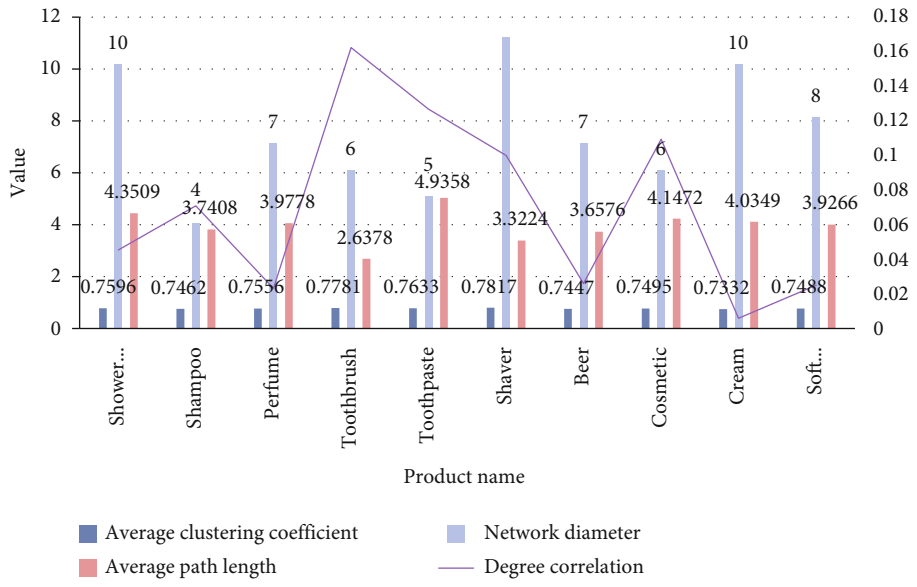

Figure 7: Online statistical value of 10 products in online store.

5.3. e-Commerce Supply and Demand Analysis. The results of the demand analysis are tested by sampling, and the mining of user search data meets the expected results. The results of random extraction are shown in Table 6. It can be seen that through the mining of user search behaviors, the supply and demand analysis module can draw conclusions that are conducive to merging and understanding result.

5.4. Sales Distribution and Similarity Distribution. The regression coefficient beta means that when the other variables remain unchanged, for each additional unit of the independent variable, the dependent variable "increases" by b units on average. When $b > 0$, it means that the dependent variable and the independent variable are positively correlated. When $b < 0$, it means that the dependent variable and the independent variable are negatively correlated. The absolute value of b describes the degree of correlation.

Figure 6 lists the coefficient values of each variable when the linear regression model is applied to the memory stick data set. For buyers who purchase new memory products, the cumulative consumption amount has the greatest impact on the purchase of different grades of products by new product buyers. The correlation coefficient value is 0.0619133. Based on this, we know that the more customers who

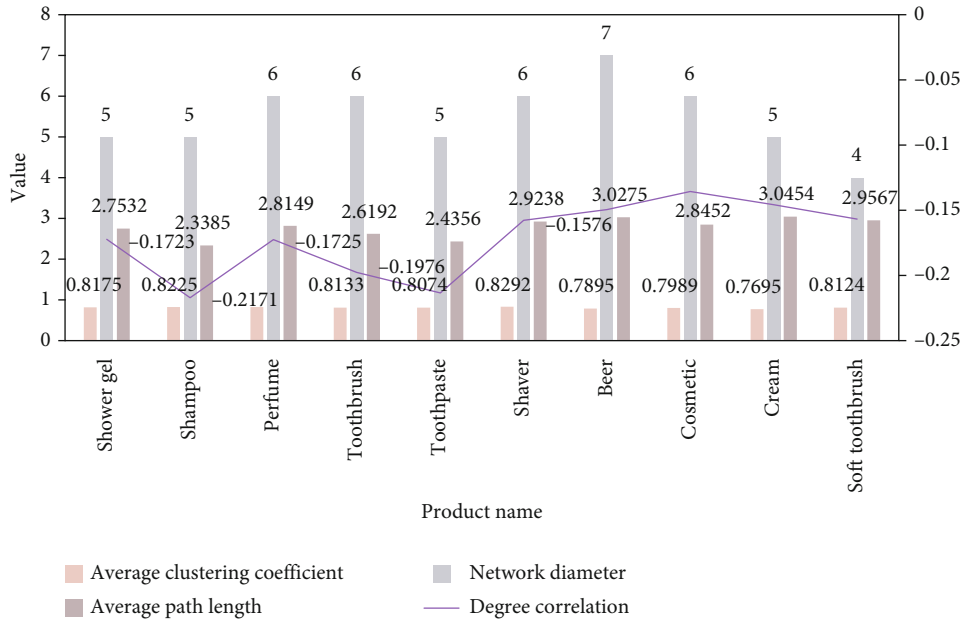

Figure 8: Network statistics of 10 commodities in store and supermarket.

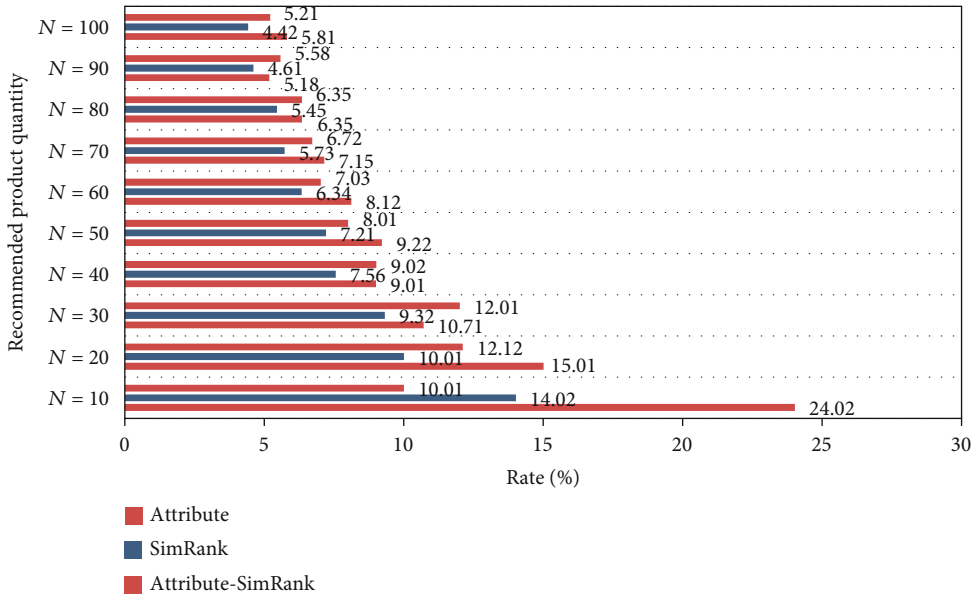

Figure 9: The average hit rate when recommending products to users in the cluster center under the three similarity methods.

purchase new memory products have historically spent on the website, the higher the price of their memory purchases, that is, the higher the grade.

From the numbers shown in Figures 7 and 8, the clustering coefficients of each network are relatively large and between 0.7 and 0.8. It can be seen that the visualization graph constructed by the time series of commodity sales has a higher clustering coefficient. On the whole, the average clustering coefficient (0.75593) of the 10 products in the online store is smaller than the average clustering coefficient of the 8 products in the store (0.811). From the average network diameter and average path length in the figure, the network diameter is between 5 and 7, and the average path length is also relatively small. However, the average network diameter and average path length (3.86, 7.7) of online store products are larger than those of the store product network (2.71, 5.75).

In summary, it can be inferred that the network constructed by the time series of merchandise sales in online stores has a smaller world effect than the network constructed by the time series of merchandise sales in stores. From the network degree correlation column in the figure, we can see that the Pearson correlation coefficient r value of the store product network is less than 0, and the correlation coefficient value of the online store product network is positive or negative. From this, it can be inferred that the

network constructed by the time series of merchandise sales in stores is negatively correlated, and nodes with large degrees in the network tend to be connected with nodes with small degrees. The degree correlation of the network constructed by the time series of online store product sales is related to the specific product, and the degree correlation is not consistent.

It can be seen from Figure 9 that when user similarity calculation adopts the method Attribute-SimRank in this paper, the average hit rate of product recommendation for cluster center users is in most cases higher than that of SimRank and Attribute methods. When the value of N changes from 10 to 100, only when $N = 30$ and $N = 90$, the Avg_HitRate (10.7% and 5.08%) corresponding to the Attribute-SimRank method is slightly lower than the Avg_HitRate (12% and 12%) corresponding to the Attribute method. 5.56%). In general, Attribute-SimRank increased the average hit rate of SimRank by about 2.6 percentage points, and Attribute-SimRank increased the average hit rate of Attribute by about 1.85 percentage points. Therefore, the results of this experiment further indirectly and effectively evaluate the similarity calculation method proposed in this paper. Because in the recommendation application, if the target user's similar interest user acquisition is more accurate, the recommendation result is more meaningful, and the accuracy of finding users with similar interests depends on whether the similarity acquisition between similar users is accurate.

6. Conclusion

This paper mainly studies the construction and application research of e-commerce big data analysis platform based on data fusion technology and Internet of Things technology. This article uses an embedded system to build an e-commerce data analysis platform, solves the current problems of e-commerce from the management and technical level, and processes massive amounts of data reasonably to provide reliable, fast and convenient analysis conclusions. The innovation of this article is the use of a combination of quantitative analysis and qualitative analysis, and a combination of theoretical analysis and empirical research to build a better e-commerce data analysis platform. The shortcomings of this article are that the selection of experimental standards and experimental objects is random and not representative, and the experimental results need to be viewed more comprehensively. With the development of the Internet of Things in the future, e-commerce companies must have more powerful data computing and processing capabilities to better meet the needs of users and provide users with high-quality and high-level services and experience.

Data Availability

No data were used to support this study.

Conflicts of Interest

The authors declare that they have no potential conflict of interest in this study.

Acknowledgments

This work was supported by the National Natural Science Foundation of China (72161020), Jiangxi Social Science Foundation Project (21GL44), and Youth Fund Project of Humanities and Social Sciences in Colleges and Universities of Jiangxi Province (GL19223).

References

[1] J. Mero, "The effects of two-way communication and chat service usage on consumer attitudes in the e-commerce retailing sector," *Electronic Markets*, vol. 28, no. 2, pp. 205–217, 2018.

[2] C. Maxim, Z. Sherali, and B. Zubair, "Internet of Things forensics: the need, process models, and open issues," *IT Professional*, vol. 20, no. 3, pp. 40–49, 2018.

[3] M. A. Sayal, M. H. Alameady, and S. A. Albermany, "The use of SSL and TLS protocols in providing a secure environment for e-commerce sites," *Webology*, vol. 17, no. 2, pp. 503–523, 2020.

[4] M. A. Ziadat, M. Al-Majali, and A. A. Muala, "Factors affecting university student's attitudes toward E-commerce: case of Mu'tah University," *International Journal of Marketing Studies*, vol. 5, no. 5, pp. 88–93, 2018.

[5] B. Palese and A. Usai, "The relative importance of service quality dimensions in E-commerce experiences," *International Journal of Information Management*, vol. 40, no. JUN., pp. 132–140, 2018.

[6] L. Vanneschi, D. M. Horn, M. Castelli, and A. Popovič, "An artificial intelligence system for predicting customer default in e-commerce," *Expert Systems with Applications*, vol. 104, no. aug., pp. 1–21, 2018.

[7] Y. Qi and P. Tapio, "Weak signals and wild cards leading to transformative disruption: a consumer Delphi study on the future of e-commerce in China," *World Futures Review*, vol. 10, no. 1, pp. 54–82, 2018.

[8] F. Arnold, I. Cardenas, K. Sörensen, and W. Dewulf, "Simulation of B2C e-commerce distribution in Antwerp using cargo bikes and delivery points," *European Transport Research Review*, vol. 10, no. 1, pp. 1–13, 2018.

[9] L. Jia, G. Xue, Y. Fu, and L. Xu, "Factors affecting consumers' acceptance of e-commerce consumer credit service," *International Journal of Information Management*, vol. 40, no. JUN., pp. 103–110, 2018.

[10] J. Nan, J. Tao, and J. Du, "Personalized recommendation based on customer preference mining and sentiment assessment from a Chinese e-commerce website," *Electronic Commerce Research*, vol. 18, no. 1, pp. 1–21, 2018.

[11] S. Karim and E. Gide, "Barriers to adopting E-commerce with small to mid-sized enterprises-SMEs in developed countries: an exploratory study in Australia," *Global Journal of Information Technology Emerging Technologies*, vol. 8, no. 2, pp. 43–54, 2018.

[12] M. Chen, D. Wang, and Z. Hu, "Considerations of constructing quality, health and safety management system for agricultural products sold via e-commerce," *International Journal of Agricultural & Biological Engineering*, vol. 11, no. 1, pp. 31–39, 2018.

[13] A. J. Lin, E. Y. Li, and S. Y. Lee, "Dysfunctional customer behavior in cross-border E-commerce: a justice-affect-

behavior model," *Journal of Electronic Commerce Research*, vol. 19, no. 1, pp. 36–54, 2018.

[14] S. Ackermann, I. Adams, and N. Gindele, "The role of e-commerce in the purchase of agricultural input materials," *Landtechnik*, vol. 73, no. 1, pp. 10–19, 2018.

[15] L. F. Chen, "Green certification, e-commerce, and low-carbon economy for international tourist hotels," *Environmental Science and Pollution Research*, vol. 26, no. 18, pp. 17965–17973, 2019.

[16] F. A. Nantembelele and S. Gopal, "Assessing the challenges to e-commerce adoption in Tanzania," *Global Business & Organizational Excellence*, vol. 37, no. 3, pp. 43–50, 2018.

[17] K. Kardoyo, N. Farliana, and M. Feriady, "Pelatihan Pemasaran Hasil Pertanian dan Perkebunan Lembaga Permasyarakatan Terbuka Kendal Melalui E-commerce Berbasis web content management system," *E-Dimas Jurnal Pengabdian kepada Masyarakat*, vol. 12, no. 1, pp. 81–89, 2021.

[18] D. T. L. Jahalia and L. Nafiati, "Niat Menggunakan E-commerce Dengan technology acceptance model (TAM) Pada UMKM," *Jurnal Bisnis dan Kewirausahaan*, vol. 17, no. 1, pp. 24–31, 2021.

[19] A. Lorenc and A. Burinskiene, "Improve the orders picking in e-commerce by using WMS data and big data analysis," *FME Transactions*, vol. 49, no. 1, pp. 233–243, 2021.

[20] D. Santi, E. Magnani, M. Michelangeli et al., "Seasonal variation of semen parameters correlates with environmental temperature and air pollution: a big data analysis over 6 years," *Environmental Pollution*, vol. 235, no. apr., pp. 806–813, 2018.

[21] J. H. Bae and E. A. Burm, "Understanding of rehabilitation nursing based on academic big data analysis," *The Korean Journal of Rehabilitation Nursing*, vol. 23, no. 2, pp. 105–111, 2020.

[22] P. Shukla and B. Radadiya, "Study of artificial intelligence techniques to permit the automated big data analysis in egovernance projects to promote digitalization," *International Journal of Scientific Research*, vol. 8, no. 4, pp. 1–3, 2019.

[23] R. Massobrio, S. Nesmachnow, A. Tchernykh, A. Avetisyan, and G. Radchenko, "Towards a cloud computing paradigm for big data analysis in smart cities," *Programming and Computer Software*, vol. 44, no. 3, pp. 181–189, 2018.

Hindawi
Wireless Communications and Mobile Computing
Volume 2022, Article ID 2472988, 10 pages
https://doi.org/10.1155/2022/2472988

Research Article

High-Reliability Business Management Strategy Analysis Based on GPRS Wireless Communication

Gang Cai and Chunmei Ni

Business School, Shandong Women's University, Jinan, 250300 Shandong, China

Correspondence should be addressed to Chunmei Ni; tracyni0407@163.com

Received 7 December 2021; Revised 15 February 2022; Accepted 21 February 2022; Published 16 March 2022

Academic Editor: Mohamed Elhoseny

Enterprise is an indispensable factor of production in the country's economic and social development, and the operation of the enterprise is indispensable. The development of strategic operation of the enterprise is facing many problems, and the survival of the enterprise is facing serious threats. The purpose of this article is to study the method of establishing a reliable enterprise strategic management system based on GPRS wireless communication and neural network. Let the company continue to grow in a sustainable and healthy way. This article puts forward the importance of corporate strategic management under GPRS wireless communication. Strategic business management can improve the foresight and initiative of enterprises, overcome short-term behaviour, and provide a clear direction for the development of the enterprise. In the experimental data of this article, it can be seen from 2016 that the demand for talent management by enterprises is lower than that in 2019. By 2019, enterprises will have the demand is as high as 85.3%, so enterprise management development needs should be taken seriously. The error between the actual output of the network and the expected output is controlled within 5%, which shows that the established neural network has a good evaluation effect and can be used to evaluate the talents of business operators. This also shows that the established BP neural network can fully absorb the judgment experience of experts and the actual employment of enterprises. The results show that the evaluation results obtained according to the evaluation network model have certain guiding significance for the selection and assessment of employers and the self-evaluation of management talents.

1. Introduction

While adapting to mobile Internet life, the requirements for the transmission quality and transmission speed of the wireless communication system are also increasing. From the wired network to the wireless network, the difference is not only the physical connection method but also changes the way people use the network and behavior habits. The era of a phone line or a network cable has gradually passed, and wireless Internet access anytime, anywhere has become an inevitable trend. The essence of operation is to optimize the allocation of corporate resources and ultimately achieve the functional activities of the organization's goals. The ultimate goal of operation is to maximize the benefits of the enterprise. The development of an enterprise depends on effective operation, and the realization of operation depends on excellent operation to realize the added value of the enterprise. Therefore, it is more important to study the construction method of the enterprise management talent evaluation system according to the actual situation of the enterprise. This article's research on the evaluation of corporate management talents will optimize the current talent evaluation methods and evaluation processes and balance the impact of expert experience and corporate employment tendencies on the results of talent evaluation. Achieve consistent talent evaluation results based on actual business conditions.

By strengthening the management of the development strategy, it will help companies establish a more scientific and appropriate development strategy plan to ensure the development of the company. Especially with regard to risk countermeasures capabilities, companies still have big shortcomings. Therefore, the group's risk management system should be based on a strategic development plan to track

risks in the implementation of the strategy in order to address them. In order to improve the response to various business risks and improve the company's management level and risk countermeasure capabilities, companies need to establish a more complete development strategy management mechanism.

Bennism proposed that 5 g wireless network is very important and has attracted great attention from academia and industry. Fundamentally speaking, the network design method is the most effective. On the contrary, there is still a lack of a reliable process to make decisions. In order to realize this vision, after providing the definition of delay and reliability, we carefully studied the various contributing factors of URLLC and its inherent trade-offs. Then, focus on the various technologies and methods related to URLLC requirements, and their application through selected use cases [1]. Zhang Z pointed out that the main challenge encountered at present is that some interference and signal differences are encountered when implementing FD wireless devices. In this paper, their advantages and disadvantages are listed and which device is better compared [2]. In order to adapt to the field, Ganini introduced a new method of learning. In this method, the architecture of the trained neural network is prominent. This method is influenced by the adaptive theory. As the training progresses, this method promotes the emergence of the following functions: (i) the main learning tasks of the source domain can be distinguished, and (ii) the conversion between domains cannot be distinguished. According to experiments, by expanding with several standard layers and new gradient reversal layers, this kind of adaptive action can be realized by almost all feed forward models. [3]. Classification is the classification method that Jinnianlei has been paying attention to in data resources in recent years. This is one of the data mining methods. On this basis, the neural network method is proposed, but the research found that it is not suitable for data mining method. This method can be used. Accurately extract simple symbol companies from the neural network. In order to meet the requirements, the network must be trained. Then use the network to analyze the activation value [4]. In this paper, Jaderberg proposes a text recognition system, that is, text location, recognition in natural scene images, and text-based image retrieval. Then the convolution neural network is trained to recognize the words in the whole proposal area at the same time, which is different from the previous system based on character classifier. It shows the best advantages of this method, and strict experiments are carried out. [5]. Alnoukari proposed that the integration of business intelligence and corporate strategic management has a direct impact on modern and flexible organizations. This integration helps decision-makers implement their corporate strategy, easily adapt to changes in the environment, and gain a competitive advantage. A BSC-BI framework is proposed, which promotes the integration of business intelligence and balanced scorecard methods. Case studies in the field of telecommunications demonstrate the implementation of the BSC-BI framework [6]. The purpose of VitollaF is to fill the gaps in the existing literature. These documents not only involve the application of social-oriented philosophy to the theme of strategic corporate social responsibility (CSR) integration but also the systematic analysis of the strategic CSR management process, and the creation of a social management philosophy and foundation. The link between the CSR integration dynamic approach of the strategic management process. What is the most important strategic management process for integrating corporate social responsibility according to the concept of social management [7]. Liston-Heyes proposed a planned corporate environmental behavior model, which emphasizes the values and attitudes of managers to the environment, environmental intentions, and the background in which these intentions are formed and transformed into actual performance. The mentality shared by those who give the country the responsibility to protect the environment. A series of hypotheses are generated and tested in the context of a unique data set using structural equation models [8]. Through the research experiments of scholars, we know that there is no advanced and complete mechanism for corporate strategic management, and companies are facing management problems. Therefore, strengthening corporate strategic management and developing a good management system are the top priorities.

The innovations of this article are as follows: (1) the research on the evaluation of enterprise management talents theoretically enriches and expands the scope of use and evaluation content of talent evaluation. From the perspective of research methods, it is introduced in the process of enterprise management talent evaluation. (2) Introduce the theoretical knowledge and related practice of GPRS and develop a set of highly reliable, complete, and true system based on GPRS wireless communication for corporate strategic management.

2. Signal Detection Algorithm of 1 MIMO System Based on GPRS

2.1. GPRS. GPRS is the abbreviation of General Packet Radio Service, and it is a mobile data service available to GSM mobile phone users [9]. GPRS sends and receives data in the form of frames, and the charging method has also changed from the traditional on-time charging to flow-based charging. In the long run, this approach can greatly reduce the user's cost of use [10]. As long as no data is being transferred, you do not have to pay even if you are always "online." To use a "phone call" analogy, when using a GSM+WAP mobile phone to access the Internet, it is like a phone call that starts to be billed as soon as it is connected, whereas with GPRS+WAP it is much more reasonable, like a phone call that is not charged as soon as it is connected, but only when the conversation is calculated. In short, it truly embodies the principle of pay less for less use and pay more for more use. The system structure diagram of GPRS is shown in Figure 1.

2.1.1. 1 MIMO System. 1 MIMO system (multiple-input multiple-output, MIMO) is a technology that uses multiple antennas for wireless transmission and reception of data. By using this technology, the data transmission speed can be doubled [11]. The system model is shown in Figure 2.

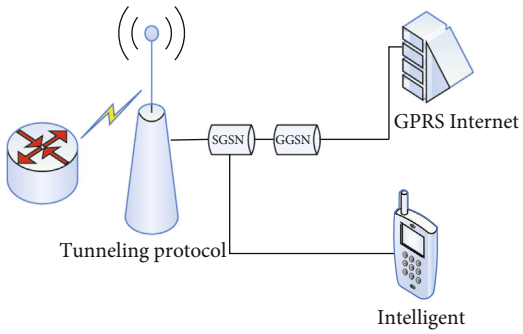

Figure 1: GPRS system structure diagram.

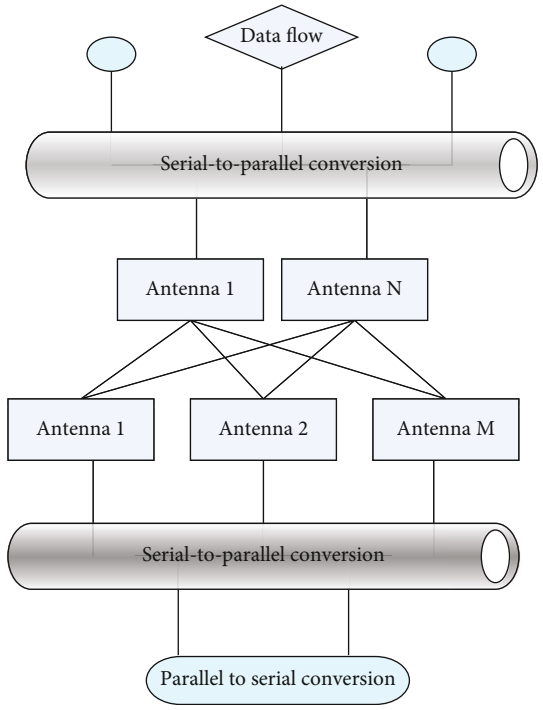

Figure 2: MIMO system block diagram.

Figure 2 shows a V-BLAST MIMO system model with N transmitting antennas and M $(M \geq N)$ receiving antennas [12] as shown in Formula (1):

$$k_t = \left[k^1{}_t, k^2{}_t, \cdots k^N{}_t\right]^T. \tag{1}$$

The corresponding received signal vector is expressed as Formula (2):

$$q_t = \left[q^1{}_t, q^2{}_t, \cdots q^M{}_t\right]^T. \tag{2}$$

The multipath effect caused by the multiantenna transmission signal makes the symbol information transmitted in the MIMO system superimpose on each antenna at the receiving end, as Formula (3):

$$q_K = \sum_{I=1}^{N} (h_{k,i} \cdot x_i) + n_k. \tag{3}$$

2.1.2. MIMO Channel Capacity Analysis. According to different input and output antenna arrangements, the multiantenna system can be divided into three types: single-input multiple-output SIMO system, multiple-input single-output MISO system, and multiple-input multiple-output MIMO system [13]. SVD is performed on the channel matrix H through singular value decomposition. Operation can get formula (4):

$$H = UDV^H. \tag{4}$$

Among them, U and V are both Emirates matrices and satisfy $UU^H = 1$, $VV^H = 1$,; D is a diagonal matrix, and the elements on the diagonal are the singular values of matrix H, that is, the arithmetic square root of the eigenvalues of $HH^H = 1$, which brings the above formula into the MIMO system vector model get Formula (5):

$$Q = UDV_t^H + n \tag{5}$$

Formula (5) is obtained by multiplying U^H to the left of Formula (6):

$$U_q^H = DV_t^H + U_n^H. \tag{6}$$

Since D is a diagonal matrix, if $\begin{cases} \sqrt{\lambda_i} \cdot \tilde{t}_i + \tilde{n}_i (i = 1 \cdots, N) \\ \tilde{n}_i (i = 1 \cdots, M) \end{cases}$ is used to represent the singular value of matrix H, then there is Formula (7):

$$\begin{cases} \sqrt{\lambda_i} \cdot \tilde{t}_i + \tilde{n}_i (i = 1 \cdots, N) \\ \tilde{n}_i (i = 1 \cdots, M) \end{cases}. \tag{7}$$

It can be seen from the above Formula (7) that the equivalent receiving element $\tilde{y}_i$ (when $i > N$) is independent of the transmitted symbol, which is equivalent to thinking that the channel gain is 0 to obtain Formula (8):

$$P_i = B \log_2 \left(1 + \frac{S_i}{\sigma^2}\right), \tag{8}$$

σ^2 is the noise power; $S_i$represents the received power of the i-th antenna at the receiving end. Since the channel state information at the transmitting end is unknown, the method of equal distribution of all antennas is often used when power allocation is performed. Assuming that the total transmit power is S, then the total MIMO channel capacity is Formula (9):

$$P = \sum_{i=1}^{N} P_i = B \sum_{i=1}^{N} \left[\log_2 \left(1 + \sqrt{\lambda_i} \cdot \frac{S}{\sigma^2 N}\right)\right]. \tag{9}$$

Formula (10) can be obtained by derivation:

$$P = B\ \log_2\left[\det\left(I_M + \frac{SNR}{N}HH^H\right)\right]. \tag{10}$$

The experimental analysis surface usually assumes that the bandwidth is large enough. Because the channel state has certain randomness, the expected capacity is usually taken as Formula (11) in the experiment:

$$\bar{P} = E\left(\frac{P}{B}\right) = E\left\{\log_2\left[\det\left(I_M + \frac{SNR}{N}HH^H\right)\right]\right\}. \tag{11}$$

Formula (11) carries out the channel capacity test of the MIMO system with the number of antennas [1], [2], [4], [8], [14], where the number of antennas is [1] The SISO system can be regarded as a special case of MIMO system.

2.2. Signal Detection Algorithm of MIMO System. MIMO signal detection is based on the known receiving end signal vector $T = [t_1, t_2 \cdots t_m]$, and the channel state information (ISI) matrix H obtained through channel estimation, and the environmental noise subject to the Gaussian distribution with a mean value of 0 and a variance of σ^2. A process of estimating the value of [15]. Signal detection technology is the key to the smooth application of MIMO wireless communication technology. The research of detection algorithms with good performance and relatively lower complexity is one of the hot topics in the field of MIMO wireless communication [16].

2.2.1. Maximum Likelihood Detection Algorithm. The maximum likelihood detection algorithm is abbreviated as the ML algorithm [17]. $\max_x S(a|b)$ and since the system model is formula (12):

$$\mathrm{a} = H_b + n \Rightarrow n = a - H_a. \tag{12}$$

The maximum likelihood algorithm needs to search and calculate all possible combinations of the signal vector b (these combinations are called candidate solutions) one by one, Formula (13):

$$n \sim N\left(0, \sigma^2\right) \tag{13}$$

is a known parameter, the conditional probability distribution mentioned earlier is equivalent to the following Gaussian distribution, which is Formula (14):

$$S(a|b) = \frac{1}{\sqrt{2\pi\sigma}} e^{-|a-H_b|^2/2\sigma^2}. \tag{14}$$

Maximizing the conditional probability $S(a|b)$ is equivalent to $\min_b \|a - H_b\|^2$, so the maximum likelihood detection algorithm can be expressed by Formula (15):

$$\tilde{x}_{ML} = \arg\min \|a - H_b\|^2. \tag{15}$$

Its physical meaning is to represent the energy of the signal, $A = A_1 \times A_2 \cdots \times A_n$ represents the signal space, which represents the value space of the i-th element a_i of the signal vector [18]. In order to obtain the optimal solution b_{ML} that satisfies the conditions, so the ML algorithm is a kind of all possible symbols for the sender. Combining the ergodic search algorithm, the best detection performance can be achieved by finding the signal point where the cost function can be minimized as the best emission vector [19]. Because of its traversal search characteristics, ML algorithm has become the best detection algorithm in MIMO system. It can not only make the detection error rate reach the lowest but also can obtain all the hierarchical gains of the system.

2.3. Interference Cancellation Detection Algorithm. Serial interference cancellation detection algorithm was first proposed by scholars. Its basic principle is improved on the basis of wireless communication [20]. It detects each symbol in turn, eliminates the influence of detection symbols, and improves the purpose of detection. The basic flow and steps are as follows: the SiC detection algorithm based on wireless communication is the detection algorithm.

Zero forcing detection of a single symbol: use the detection algorithm to detect the first element of the transmission vector, as shown in Formula (16):

$$\tilde{y} = W^{(1)} \cdot X^{(1)}. \tag{16}$$

Interference cancellation: after the detection in the previous step, the first symbol has been recovered, namely $Y_1 = \Omega_S|\ Y^{\sim}\ |$, and the $x^{(2)}n$ the detected Y_1 is subtracted from the received signal to obtain a new signal model to be detected, the form of which is shown in Formula (17):

$$x^{(2)} = x^{(1)} - h_1 y_1 + z, \tag{17}$$

h_1 is the first column of the channel matrix H, and is the equivalent received signal vector obtained after eliminating the signal component y_1. Through the continuous iterative calculation of the above two steps, all the transmitted symbols can be finally detected and recovered NS. From the previous algorithm analysis, it can be seen that if the first detected signal has an error, and it will interfere with the detection of the following symbols. Therefore, the SIC algorithm has an error propagation phenomenon. In order to reduce the impact of this phenomenon, increase the detection accuracy. Because even the linear detection algorithm can obtain more accurate detection results under the condition of large signal-to-noise ratio, the priority is to detect the symbols with large received signal-to-noise ratio, and to detect the symbols of each layer in order of the signal-to-noise ratio can effectively reduce the error propagation. The impact of this will improve the detection accuracy of the system [21]. The detection signal-to-noise of the i-th layer is shown in Formula (18):

$$SNR_I = \frac{E\left\lfloor |y_i|^2 \right\rfloor}{\sigma_n^2 \|W_i\|^2} = \frac{\sigma_s^2}{\sigma_n^2 \|W_i\|^2}. \tag{18}$$

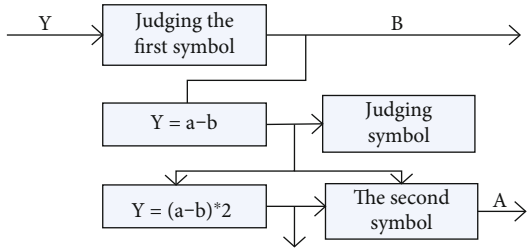

Figure 3: SIC/OSIC algorithm detection step diagram.

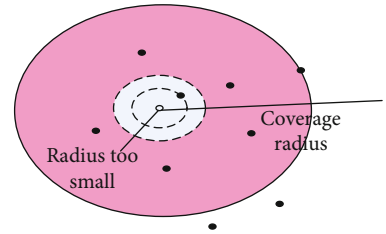

Figure 4: Covering radius.

Compared with the SIC detection algorithm, OSIC detection algorithm adds a sorting step, so the OSIC algorithm can be summarized as: sorting-zeroing-interference cancellation three parts. Taking the zero-forcing sequencing serial interference cancellation algorithm as an example, the specific algorithm flow chart is shown in Figure 3:

As shown in Figure 3, compared with the SIC detection algorithm OSIC detection algorithm adds a sorting step, so the OSIC algorithm can be summarized as sorting-zeroing-interference cancellation three parts. Take the zero-forcing sequencing serial interference cancellation algorithm as an example. In the algorithm, the row with the smallest second norm in the filter matrix is obtained by calculation. This process is equivalent to obtaining the layer with the largest signal-to-noise ratio as the current layer to be detected. The largest layer is the current detection layer.

2.4. SD Sphere Detection Algorithm. The algorithm is based on the maximum likelihood criterion like the ML algorithm. The basic idea is to restrict or narrow the search range by determining a multidimensional sphere with a vector y as the center and a radius r to reduce the number of candidate solutions that need to be searched. Thereby, the computational complexity of the maximum likelihood algorithm is reduced, the operation speed is improved, and the detection accuracy is ensured [22]. The realization of this algorithm needs to solve two main problems: how to determine the appropriate search radius r, and how to determine the search grid points are within the range of the sphere. As shown in Figure 4:

Usually it is very difficult to select a very ideal radius. The radius cannot be selected too small, otherwise there may be no optimal solution or even no grid points in the range of the sphere, and the radius selection is too large, and it cannot reduce the calculation complexity. In order to determine whether the point is in the circle or not, you only need to determine whether its coordinate range meets the conditions one by one. Since R' is an upper triangular square matrix, searching upwards from the Nth layer by layer can finally determine whether the point is within the search range.

When $i = N$, as shown in Formula (19):

$$\sum_{\mathrm{I=N}}^{\mathrm{N}} \left\| \mathrm{x}_{\mathrm{i}}' - \sum_{j=i}^{N} R_{ij}' y_j \right\|^2 = \left\| \mathrm{x}_{\mathrm{N}}' - R_{nn}' y_j \right\|^2 \le r^2. \tag{19}$$

From this, the upper and lower limits of y_Y can be determined as Formula (20):

$$\left| \frac{1}{R_{NN}'} \left(x'_N - r' \right) \right| \le y_N \le \left| \frac{1}{R_{NN}'} \left(x'_N + r' \right) \right|. \tag{20}$$

2.5. Neural Network Method. This paper applies the constructed enterprise management talent evaluation model to the evaluation of enterprise management talents, uses the weights determined by the entropy method to calculate the evaluation results of the research objects, and uses the trained network as an evaluation tool. Use the same sample other than the training sample set [23] for evaluation. The BP network uses a continuous differential possible function with specific threshold characteristics as the activation function of the neuron. Of course, other similar nonlinear functions can also be used. If we combine neural network and enterprise talent management model, we can get the result which shown in Figure 5:

3. Experiment and Analysis

3.1. Entropy Method Experiment and Analysis. Part of the learning sample set of this study is selected from the entropy method used in the previous research to determine the index weight data, and the other part of the learning sample comes from the evaluation data of the investigation of talents who cannot be managed by the same department in different enterprises [24]. Although the data sets are from different sources, the meaning embodied in the data gives a good indication of the differences between the topics, and therefore no comparative data are involved in this paper. Since the value definition of different management talents by the human resources department of the enterprise also has certain learning significance, the combination of the two parts of learning samples can finally train a neural network that not only conforms to the evaluation results of the expert system but also combines the actual situation of the enterprise. The input indicators of the learning sample and the weights of each indicator are shown in Table 1:

From Table 1, it can be seen that the feasibility of using salary level as an output variable in this paper is first demonstrated theoretically. In order to make the final analysis result more scientific, the salary of management talents of the same level in different companies may vary greatly. This is mainly reflected in the fact that different industries have different practices, different management philosophies and

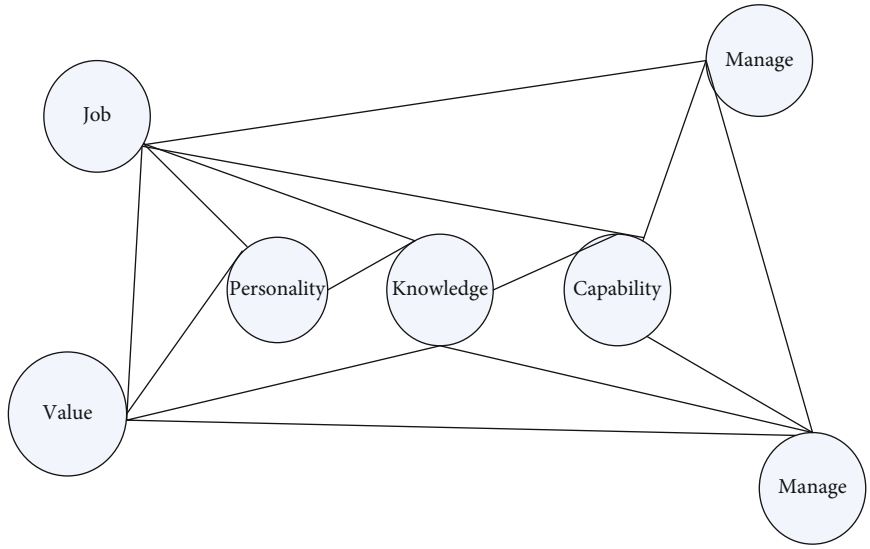

Figure 5: The model diagram of the quality structure of enterprise management talents.

Table 1: The input indicators of the learning sample and the weight of each indicator.

	Company A	Company B	Company C	Company D
Teamwork	0.6	0.4	0.9	0.8
Interpersonal skills	0.6467	0.4657	0.8764	0.5685
Moral character	0.986	0.865	0.754	0.684
Cohesion	0.456	0.564	0.546	0.574
Style of working	0.764	0.657	0.7657	0.784
Knowledge level	0.536	0.364	0.657	0.435
Work efficiency	0.875	0.871	0.685	0.757
Learning ability	0.575	0.466	0.766	0.768

remuneration strategies, different geographical locations of different companies, different levels of value or contribution to the company, and the length of time the incumbent has been in the position. Normalization it is also more difficult, so by consulting the information, this article uses the logarithmic function to reduce the salary level data difference. After the data difference is reduced, then learn from the previous normalization method to directly divide the output value of the original data by the maximum value of the data set value and get the output data after normalization. According to the commonality of management talents pointed out in the previous study, management talents actually create value for the enterprise, and the amount of value created has the same measurement standard in the same enterprise, and the amount of value created corresponds to the salary level of the position. Pay structure design is the process of establishing a linear or nonlinear link between the relative value of each job position in an organisation and the corresponding out-of-pocket pay. It allows the level of pay for each job position to correspond to its relative value. There is an inevitable connection between them. In this sense, it is reasonable to use the salary level corresponding to the position as the output of the comprehensive evaluation of management talents. The trend chart of a company's demand for talent management in 2016 and 2019 is shown in Figure 6:

It can be seen from Figure 6 that in 2016, it can be seen that the demand for talent management by enterprises is lower than that in 2019. By 2019, the demand for talent management by enterprises is as high as 85.3%, so the demand for enterprise management development should be taken seriously. The manager's management activities are to maximize the benefits and the purpose of the enterprise's management activities. Behavioral science theory believes that the essence of management is to improve work efficiency. On the surface, the two seem to be different, but in general, the direct purpose of management is to improve work efficiency, and the improvement of work efficiency ultimately serves to increase profits, so the essence of management In fact, it is to realize the maximization of profits, which is the process of turning limited input into maximizing output.

Finally, through comprehensive evaluation and data statistics, the learning sample set required for neural network modeling is obtained as shown in Table 2:

It can be seen from Table 2, the final evaluation object, for the score of the indicator, part of it comes from the comprehensive evaluation process of experts, combined with the

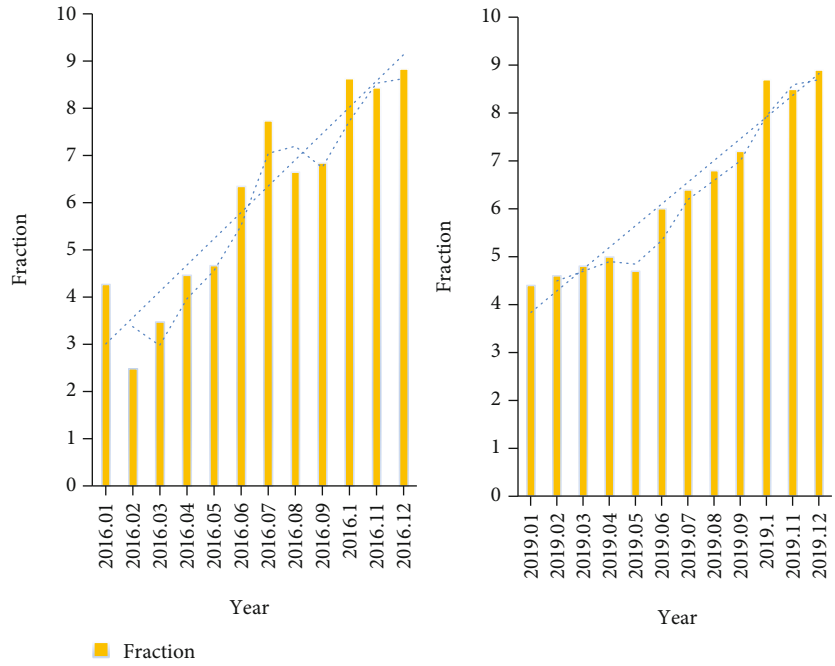

Figure 6: Trend chart of talent management needs.

Table 2: Learning sample set.

Entropy method							Output value	Normalized output
8	7	7	3	8	8	8	4.75434	0.657678
7	9	8	7	6	9	5	4.89643	0.643677
8	6	5	8	3	5	9	5.86465	0.985468
9	7	6	5	7	8	6	6.35673	0.467534
5	4	3	6	8	7	8	5.57644	0.675366
6	8	9	9	5	3	7	7.45778	0.875864
4	6	8	8	9	6	3	7.35675	0.368535

weight obtained by the value entropy method, as the input of the learning sample, the comprehensive evaluation score of each sample can be obtained. And normalized processing, so that the output of the learning sample is obtained, and the other part of the learning sample selects the salary level corresponding to the survey sample as the output [25].

3.2. Experiment and Analysis of BP Neural Network. Entropy is a measure of uncertainty. The greater the amount of information, the smaller the uncertainty and the smaller the entropy; the smaller the amount of information, the greater the uncertainty and the larger the entropy. According to the properties of entropy, we can calculate the entropy value to judge the randomness and disorder of an event, and we can also use the entropy value to judge the degree of dispersion of a certain indicator, the greater the degree of dispersion of the indicator, the greater the influence of the indicator on the comprehensive evaluation. It is hoped that the network model can absorb the evaluation experience of experts, and at the same time, it will test the samples are judged with high precision. NeruoSolutions, a very useful software at present, has a visual operation interface, which can directly perform network creation and network testing, and can also directly manipulate excel files to complete the learning process. As shown in Figure 7.

Figure 7 selects the standardized worksheet interface, clicks the train option under the menu TrainNetwork to set the number of iterations to 6000, trains the network, and then clicks the test option in TestNetwork to test the data. Through network learning and testing, you can select testing in the main interface NeruoSolutions to get the desired and the actual output, this is the output and expected output of the network after training.

It can be seen from Figure 8 that the network input value after network training is very close to the expected output result, indicating that the trained BP network has achieved a good learning effect. After the BP neural network training is completed, the test sample set is started. The data is tested on the network, the comprehensive evaluation results of the enterprise management talents are obtained, and the test results in the following Table 3 are obtained. Finally compare the plan with the actual, and the network output curve in Figure 9 is obtained.

It can be seen from Table 3 that the neural network must also integrate the actual employment of the enterprise, and the enterprise has a maximum expectation of 96% of talent management capabilities. The importance of enterprise talent management is obvious. Therefore, the learning sample set must not only include comprehensive evaluation data as output but also reflect the actual evaluation tendency of enterprise talents. According to the actual value contribution of management talents to the enterprise and the salary feedback of the enterprise to management talents, it must satisfy a certain positive relationship. Therefore, in order to obtain output data that is more representative of different companies' employing tendencies and is easy to obtain, this paper

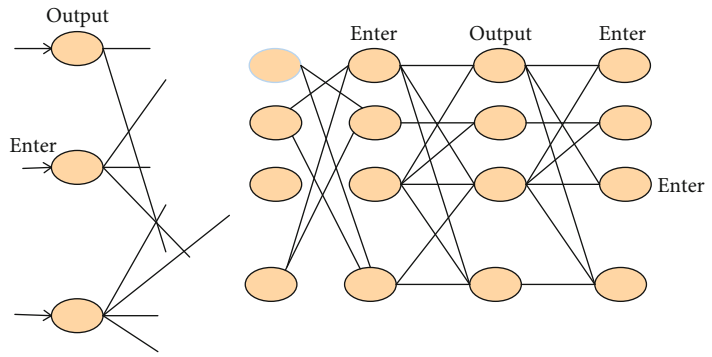

Figure 7: Multilayer forward BP network.

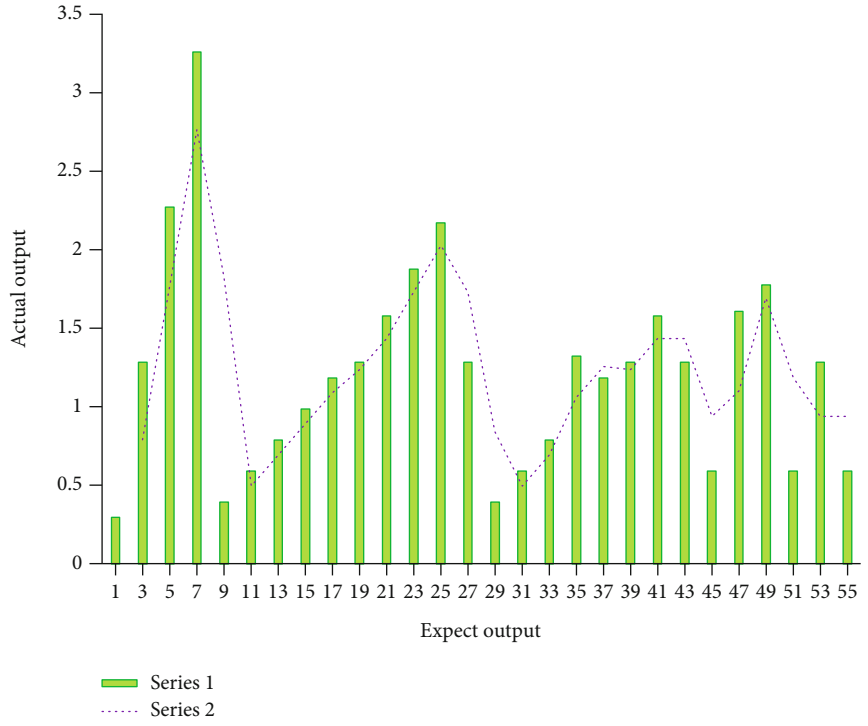

Figure 8: Output and expected output diagram.

Table 3: Expected output and actual output value table.

Serial number	Expected value	Actual value	Error
1	0.76474	0.78545	1.53
2	0.75876	0.78654	0.32
3	0.86856	0.56895	0.53
4	0.85795	0.96433	1.43
5	0.96477	0.54674	1.75
6	0.65781	0.75433	0.84
7	0.85832	0.63678	0.97
8	0.57684	0.74333	0.42
9	0.64746	0.74328	0.53

selects the salary level corresponding to enterprise management talents to represent the actual results of the company's evaluation of talents and regards the salary level as the actual output of the network.

As shown in Figure 9, the neural network should be combined with the talent management of the enterprise. The highest expectation of the enterprise for talent management ability is 96%. It shows that enterprise talent management is very important. Therefore, the learning sample set should not only include the comprehensive score but also reflect the actual score of enterprise management talents. According to the actual value contribution of management talents to the enterprise, it is necessary to make more scientific judgments on the data about their value contribution tested. At the same time, based on the empirical evidence, it further confirms the use of the BP neural network to

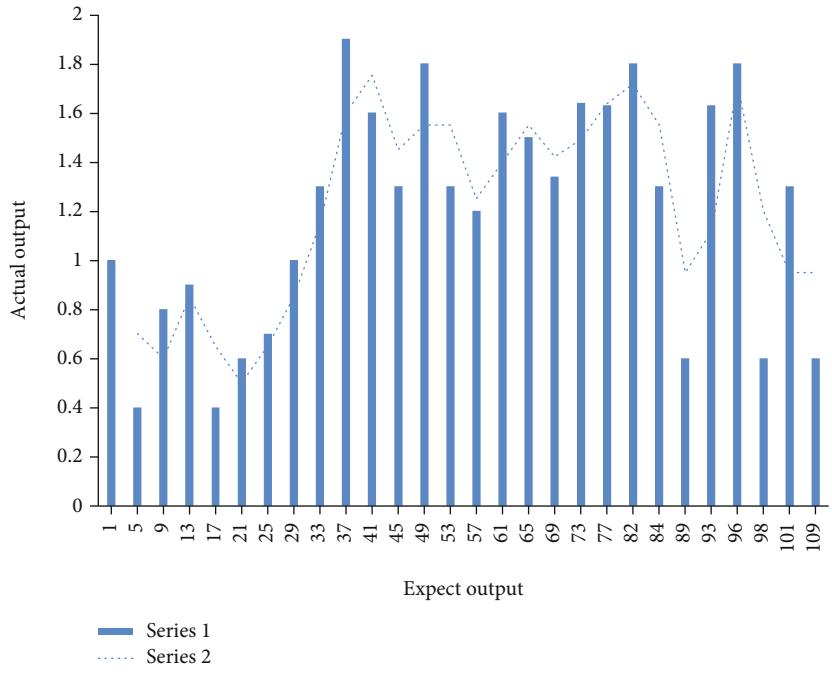

Figure 9: Network output curve.

evaluate the business ability of the enterprise, scientificity, and feasibility. The experimental results show that applying the entropy method and BP neural network to the evaluation process of enterprise management talents can obtain better evaluation results, providing a new way of thinking for the evaluation of enterprise management talents, and the evaluation process is faster and more accurate. According to the evaluation network model, the evaluation results have certain guiding significance for the selection and assessment of employers and the self-evaluation of management talents.

4. Discussion

This article analyzes how to develop a set of highly reliable, complete, and true system for corporate strategic management based on GPRS wireless communication. Strengthen development strategy management, help companies establish more scientific and appropriate development strategy planning, so as to ensure the company's development. The theoretical knowledge of GPRS wireless communication and neural network is explained. Due to the development of digital communication technology and the pursuit of high-quality wireless communication by users, after the end of the century, the wireless communication system has developed into a second-generation wireless communication system represented by digital communication technology. These systems use more advanced systems. Digital technology hopes to use the various advantages of wireless networks to design a reliable enterprise strategic management mechanism that can be accepted by the public. This paper makes reasonable use of the signal detection algorithm of the 1 MIMO system. The ML algorithm has become the detection algorithm with the best performance in the MIMO system because of its traversal search characteristics. The basic idea of establishing a neural network in the experimental analysis of this paper is to briefly analyze the number of network layers, the number of neurons in each layer, the learning rate of neurons, and the activation function, and then use Neruo-Solutions software. Train and test the BP network model and analyze the experimental results. Through the analysis of the experimental results, we can see that the network model has a good evaluation effect. The next step is to look at the technical or other improvements that can be made to the network to make it more widely used.

5. Conclusions

This article mainly starts from the theoretical knowledge of GPRS wireless communication and neural network and discusses how to establish a set of highly reliable business management strategy development model based on GPRS wireless communication and neural network. Based on the signal detection algorithm and neural network model of the 1 MIMO system, it can be seen that the BP neural network is used in the process of evaluating enterprise management talents, and it can obtain better evaluation results and providing a new idea for the evaluation of enterprise management talents and the evaluation process. Faster and more accurate, the evaluation results obtained according to the evaluation network model have certain guiding significance for the selection and assessment of employers and the self-evaluation of management talents. For example, the network model can be used in large companies where the actual situation of a person cannot be determined based on information about that person, but where a conclusion is urgently needed, so that a relatively reasonable assessment can be made. Based on the wide range of related scientific fields involved in the GPRS Wireless Communication Application

Research Institute, the concept of enterprise management has always been disputed, and the author's knowledge has not yet reached the perfect state. The author's academic theory and business capabilities are relatively weak, and there are still many deficiencies. At the same time, the author is constantly discovering and solving problems, striving to be the best.

Data Availability

No data were used to support this study.

Conflicts of Interest

The author states that this article has no conflict of interest.

Acknowledgments

This work was supported by Social Science Planning Project of Shandong Province (Research on the realization path of inclusive finance in Shandong Province based on ecosystem perspective; Project No:(19CJRJ05).

References

[1] M. Bennis, M. Debbah, and H. V. Poor, "Ultrareliable and low-latency wireless communication: tail, risk, and scale," *Proceedings of the IEEE*, vol. 106, no. 10, pp. 1834–1853, 2018.

[2] Z. Zhang, K. Long, A. V. Vasilakos, and L. Hanzo, "Full-duplex wireless communications: challenges, solutions, and future research directions," *Proceedings of the IEEE*, vol. 104, no. 7, pp. 1369–1409, 2016.

[3] Y. Ganin, E. Ustinova, H. Ajakan et al., "Domain-adversarial training of neural networks," *Journal of Machine Learning Research*, vol. 17, no. 1, pp. 2096–2130, 2017.

[4] H. Lu, R. Setiono, and H. Liu, "Effective data mining using neural networks," *Knowledge & Data Engineering IEEE Transactions on*, vol. 8, no. 6, pp. 957–961, 1996.

[5] M. Jaderberg, K. Simonyan, A. Vedaldi, and A. Zisserman, "Reading text in the wild with convolutional neural networks," *International Journal of Computer Vision*, vol. 116, no. 1, pp. 1–20, 2016.

[6] M. Alnoukari and A. Hanano, "Integration of business intelligence with corporate strategic management," *Journal of Intelligence Studies in Business*, vol. 7, no. 2, pp. 5–16, 2017.

[7] F. Vitolla, M. Rubino, and A. Garzoni, "The integration of CSR into strategic management: a dynamic approach based on social management philosophy," *Corporate Governance International Journal of Business in Society*, vol. 17, no. 1, pp. 89–116, 2017.

[8] C. Liston-Heyes and D. V. Brust, "Environmental protection in environmentally reactive firms: lessons from corporate Argentina," *Journal of Business Ethics*, vol. 135, no. 2, pp. 361–379, 2016.

[9] M. A. Izmailova, V. T. Grishina, G. M. Alimusaev, E. A. Kameneva, and V. I. Morgunov, "Contemporary approach to strategic management of logistics processes in integrated corporate structures," *International Journal of Civil Engineering and Technology*, vol. 9, no. 13, pp. 11–27, 2018.

[10] M. Naumenko, "Development of strategic management models of integrated corporate structures," *ScienceRise*, vol. 3, no. 1, pp. 25–28, 2017.

[11] A. Y. Alanis, "Electricity prices forecasting using artificial neural networks," *IEEE Latin America Transactions*, vol. 16, no. 1, pp. 105–111, 2018.

[12] Z. Zeng, T. Huang, and W. X. Zheng, "Multistability of recurrent neural networks with time-varying delays and the piecewise linear activation function," *Neurocomputing*, vol. 21, no. 8, pp. 1371–1377, 2010.

[13] G. Carleo and M. Troyer, "Solving the quantum many-body problem with artificial neural networks," *Science*, vol. 355, no. 6325, pp. 602–606, 2017.

[14] H. R. Roth, L. Lu, J. Liu et al., "Improving computer-aided detection using convolutional neural networks and random view aggregation," *IEEE Transactions on Medical Imaging*, vol. 35, no. 5, pp. 1170–1181, 2016.

[15] J. Salamon and J. P. Bello, "Deep convolutional neural networks and data augmentation for environmental sound classification," *IEEE Signal Processing Letters*, vol. 24, no. 3, pp. 279–283, 2017.

[16] Y. Chen, H. Jiang, C. Li, X. Jia, and P. Ghamisi, "Deep feature extraction and classification of hyperspectral images based on convolutional neural networks," *IEEE Transactions on Geoscience & Remote Sensing*, vol. 54, no. 10, pp. 6232–6251, 2016.

[17] M. Gong, J. Zhao, J. Liu, Q. Miao, and L. Jiao, "Change detection in synthetic aperture radar images based on deep neural networks," *IEEE Transactions on Neural Networks & Learning Systems*, vol. 27, no. 1, pp. 125–138, 2016.

[18] N. Tajbakhsh, J. Y. Shin, S. R. Gurudu et al., "Convolutional neural networks for medical image analysis: full training or fine tuning?," *IEEE Transactions on Medical Imaging*, vol. 35, no. 5, pp. 1299–1312, 2016.

[19] E. Gourdin, D. Medhi, and A. Pattavina, "Design of reliable communication networks," *Annals of Telecommunications*, vol. 73, no. 1-2, pp. 1–3, 2018.

[20] N. Farsad, H. B. Yilmaz, A. Eckford, C. B. Chae, and W. Guo, "A comprehensive survey of recent advancements in molecular communication," *IEEE Communications Surveys & Tutorials*, vol. 18, no. 3, pp. 1887–1919, 2016.

[21] L. Lamport, "On interprocess communication. Part I: Basic Formalism," *Distributed Computing*, vol. 1, no. 2, pp. 77–85, 2016.

[22] Y. Mao, C. You, J. Zhang, K. Huang, and K. B. Letaief, "A survey on mobile edge computing: the communication perspective," *IEEE Communications Surveys & Tutorials*, vol. 19, no. 4, pp. 2322–2358, 2017.

[23] M. Tkach and C. Théry, "Communication by extracellular vesicles: where we are and where we need to go," *Cell*, vol. 164, no. 6, pp. 1226–1232, 2016.

[24] T. Postmes and R. Spears, "LeM.Breaching or building social boundaries: SIDE-effects of computer-mediated communication," *Communication Research*, vol. 25, no. 6, pp. 689–715, 1998.

[25] P. W. Lau, E. Y. Lau, D. P. Wong, and L. Ransdell, "A systematic review of information and communication technology–based interventions for promoting physical activity behavior change in children and adolescents," *Journal of Medical Internet Research*, vol. 13, no. 3, pp. e48–e49, 2011.

Hindawi
Wireless Communications and Mobile Computing
Volume 2022, Article ID 1394946, 12 pages
https://doi.org/10.1155/2022/1394946

Research Article

Maritime Intelligent Monitoring System Based on Wireless Sensor Network and Construction of Shipping Legal System

Hong Fang

School of Law, Shanghai Maritime University, Pudong, 201306 Shanghai, China

Correspondence should be addressed to Hong Fang; 202040910003@stu.shmtu.edu.cn

Received 29 November 2021; Revised 13 January 2022; Accepted 5 February 2022; Published 14 March 2022

Academic Editor: Mohammed Hammoudeh

With the continuous advancement of the rule of law in society, the pace of global integration is accelerating, and all countries are actively expanding the development of sea areas. The previous maritime navigation management model cannot meet the conditions for active ocean development in the new era. The state must manage ships. My country has established a series of legal systems for ship management, including ship inspection systems, ship registration systems, and ship safety inspection systems. New management models, new service concepts, and prospects have gradually become the focus of attention of domestic and foreign waterway managers. With the continuous advancement of the rule of law in our country, the law enforcement requirements of maritime navigation management are also getting higher and higher. It is very important to create a good legal environment. This article is aimed at studying how to play the role of wireless local area network in maritime navigation management and how to establish a relatively complete legal system. This paper proposes a gray fuzzy comprehensive algorithm. If the fuzzy subset method is used to determine the membership matrix in the fuzzy comprehensive evaluation, then there will be a sudden drop in the degree of membership due to a slight change in the critical value of the index level. Based on this algorithm, a set of preliminary models of maritime channel management is established. The experimental data in this article mentions that in 2017-2020, the percentage of a certain maritime management's attention to the legal system has clearly shown an upward trend. In 2020, the attention to the legal system is even as high as 69%. It can be seen that supervision improving the legal system is an effective measure. From the data, we can see that the rule of law score in 2018 was about 1.5 points lower than that in 2019, and the rule of law score in 2019 was 7.5 points. The results show that administration according to law puts forward higher requirements on the ability and service level of administrative agencies and their administrative law enforcement personnel, especially in the process of law enforcement, dealing with affairs related to administrative counterparts. Therefore, it is very necessary to establish a complete legal system.

1. Introduction

After the 1990s, wireless communication has achieved rapid development all over the world. Whether it is military communications or civil communications, many new systems and modes are appearing on different frequency bands, providing people with a variety of services. The development of general maritime affairs is still in the "initial stage." The development and development of general aviation require the guarantee and support of national and local laws, regulations, policies, and operating environment. Sound laws and regulations are an important guarantee for the orderly development of my country's ordinary maritime affairs. Improving the maritime management law to ensure the order, rapid, and sustainable development of maritime affairs can be described as urgent issues and need to be urgently resolved. Therefore, legislative research is of broad importance to the development of the entire maritime channel management. Mainly devoted to personnel training, research, and construction of maritime management disciplines, researched and put forward the concept of maritime management and theoretical models of causes of water traffic accidents, and initially constructed the research object and content system of maritime management.

In recent years, rapid progress has been made in the construction of informatization in the fields of navigation and

maritime affairs. The information networks of all levels of government systems are interconnected, and the transmission of official documents on the Internet has been successful. Various large-scale organizations, water transportation enterprises, and organizations have established computer networks, each established an office automation system, continuously established e-government websites, and each established several business management systems.

With the progress of the times, more and more researches on wireless local area network are carried out. Wang et al. found that in recent years, with the rapid development of the blue economy, broadband maritime communications have attracted much attention. In addition to the traditional MF/HF/VHF frequency bands, people are paying more and more attention to the use of higher frequency bands to provide broadband data services to the sea. To design an efficient maritime communication system, the first and most basic requirement is to develop a framework to understand wireless channels. In an integrated air-ground-sea communication network, there are two main types of channels to study, namely, air-to-sea channels (such as for communication links from aircraft-based base stations or relays) and maritime channels (such as for land-based communication links, ship/ship-to-land, or ship-to-ship communication) links. Due to the unique characteristics of the maritime propagation environment, such as sparse scattering, ocean wave motion, and the pipe effect on the sea surface, the modeling of these maritime channel links is different from traditional terrestrial wireless channels in many aspects [1]. Lionis et al. found that free space optical communication (FSO) uses visible light and infrared spectra for data transmission, which has significant advantages, such as very high data rates, security and immunity, low installation costs, and ease of use, without any licensing restrictions. However, a major challenge faced by FSO systems is its inherent limitations due to environmental conditions, especially atmospheric turbulence. This paper focuses on the experimental performance analysis of the real FSO system in the marine environment. We propose a new model that allows FSO link performance estimation at sea and depends on point measurement of environmental parameters. F has measured the received signal strength index (RSSI) and used regression modeling to construct a second-order polynomial to quantify its relationship with the macroenvironmental parameters collected by the weather station [2]. Jansen et al. presented new experimental evidence to prove the effectiveness of using scene motion information to analyze scene structure in maritime imaging applications. The data captured by the new airborne multichannel SAR (MSAR) system is analyzed, which is particularly suitable for sampling the velocity profile of scatterers in the marine environment. Although previous work has demonstrated a practical MSAR system for correcting blur artifacts caused by scene motion, it has shown for the first time how the information provided by the MSAR system systematically classifies maritime scenes into different perception categories. The provided method is superior to traditional classification techniques based purely on the spatial structure of the image. In addition, the simplicity of the feature space involved and the proven classification performance of the images captured by the airborne MSAR system emphasize the advantages of this method [3]. Araki et al. clarified the structure, applicability, and goals of current Japanese privacy information protection and research ethics legislation and checked the provisions of relevant laws/regulations for academic research purposes. Methodological research design is based on the descriptive research of the system. Using the "e-Gov" database, the laws/regulations concerning private information protection and research ethics applicable to medical research and human genome/gene analysis research involving human subjects are included in the research. The Pharmaceutical Law (Law No. 145 of 1960) and related GCP/GPSP regulations and laws/regulations related to administrative organization, management, and procedures are excluded. In addition, the guidelines and Q&A related to these laws/regulations and all 47 county regulations on the protection of private information are selected from relevant ministries, government organizations, and county websites [4, 5]. The newspaper registration system has always been the basic framework of the Korean publishing industry. In 2016, Park proposed that the Korean Constitutional Court ruled that part of the registration requirements of online newspapers was unconstitutional. Therefore, the registration system needs to be reviewed. Since the "Newspaper Law" imposes penalties on publishers who fail to apply for formal registration with government agencies, the registration system is a constraint for newspaper publishers. In addition, it is questionable whether this registration system can continue to operate effectively in the Internet age. With the increase of single-person media, the registration requirements for Internet newspapers may be unreasonable. In addition, this registration system treats Internet Service Providers (ISPs) unfairly and discriminatorily. This research examines the current newspaper registration system and reviews how the system has evolved historically and legally [6, 7]. Anderson and Gupta combine the company's maritime channel management legal system literature flow to study whether the maritime channel management performance can be improved when its governance structure reflects the requirements of maritime channel management and legal systems. Using a sample of 1736 maritime waterway management companies representing 22 countries, Anderson and Gupta found that the joint effect of a country's maritime waterway management legal system is indeed important when explaining the relationship between the performance of a specific country and the overall level of corporate governance. The results also show that companies operating in market/combined countries tend to obtain higher market valuations than companies with comparable levels of corporate governance [8]. Haller et al. proposed that the interface between mental health and law has expanded rapidly in the past few years because the courts heard more and more cases and passed new laws. Although court decisions and laws may be regarded as infringements by psychiatrists who deal with children with mood disorders, Haller et al. suggests that the effect is to provide professionals with new options to help patients. Haller et al. introduced many situations where the legal system can be used [9]. For

battery-powered wireless stations, energy saving is one of the important issues of IEEE802.11 wireless local area network (WLAN). Recently, Lei and Nilsson studied the power saving mode in IEEE802.11 infrastructure mode through M/G/1 queue with batch service. They obtained the upper and lower bounds for the average packet delay and the average percentage of time the station stays in the doze state (PTD). In this article, the power saving mode is further studied; the simple derivation of the average and variance of the packet delay and the precise value of PTD are obtained. The numerical results show that our analysis results of PTD are in good agreement with the simulation results. Using our performance analysis, we can find the maximum listening interval, while meeting the average quality of service (QoS) and packet delay variance, while minimizing the power consumption of the site [10]. Through the research of scholars, we know that with the rapid development of WLAN technology, more and more people pay attention to the security of wireless local area network. Among the marine infrastructure, the maritime administration department provides the most basic services. Therefore, how to play the role of wireless local area network in maritime management and improve the legal system has become a major problem.

The innovations of this paper are (1) the experiment based on wireless local area network completed the software design of wireless mobile terminal of wireless local area network, realized the basic wireless access function, and made maritime channel management more effective. (2) Use gray fuzzy comprehensive method and risk assessment method to resolve the ambiguity between risk factors. This makes the legal system of maritime management more complete. With the development of wireless communication technology and digital signal processing technology, a new generation of mobile multimedia communication terminals can process multimedia information such as images, sounds, and video streams. And because it can be used in video surveillance systems, personal multimedia data terminals, video phones, network transmission and wireless multimedia communications, and other fields, it has a wide range of applications.

2. Gray Fuzzy Comprehensive Evaluation Method

2.1. Fuzzy Algorithm Based on Local Area Network. This paper mainly proposes the gray fuzzy comprehensive method based on wireless sensor network. At the beginning, the importance of maritime law enforcement is described, and then in the method part, the gray fuzzy comprehensive method is introduced in detail, and it is extended to the fuzzy algorithm based on local area network. WLAN is the abbreviation of wireless local area network, which refers to the application of wireless communication technology to interconnect computer equipment to form a network system that can communicate with each other and realize resource sharing. The essential feature of a wireless local area network is that it no longer uses a communication cable to connect the computer to the network, but connects it wirelessly, which makes the construction of the network and the movement of the terminal more flexible. Cellular network, also known as mobile network, is a mobile communication hardware architecture, divided into analog cellular network and digital cellular network. Because the signal coverage of the communication base stations that constitute the network coverage is hexagonal, the entire network is named like a honeycomb. Wireless network technology based on cellular technology and office area network (WLAN) was widely adopted. The wireless local area network in the Chinese market is mainly used for public services, corporate intranets, campus networks, and governments with special geographic areas [11]. Figure 1 shows the basic structure of a general wireless local area network.

Fuzzy algorithms are intelligent algorithms. When we do not have a deep understanding of the model of the system, or objective reasons make it impossible to conduct in-depth research on the control model of the system, the intelligent algorithm can often play a small role; fuzzy algorithm is used. Gray-fuzzy comprehensive evaluation is an evaluation method established based on fuzzy mathematics and related theories of gray systems on the basis of the definite imperfect information of the evaluation object [12]. The gray fuzzy comprehensive evaluation method is a comprehensive judgment method for the evaluation object, which comprehensively considers a variety of risk factors, and has a good effect on processing gray fuzzy information [13]. The specific modeling steps of the gray fuzzy comprehensive evaluation method are as follows.

The establishment of the evaluation factor set is shown in the following formula:

$$f_i^h(y) = \frac{y - y_i^h(1)}{y_i^h(2) - y_i^h(1)}. \tag{1}$$

Suppose $Y = (y_1, y_2, \cdots y_m)$ is the m types of influencing factors of the assessed object, and the number of influencing factors is determined by the characteristics of the studied object, as shown in the following formula:

$$f_i^h(y) = \frac{y_i^h(4) - y}{y_i^k(4) - y_i^k(3)}. \tag{2}$$

After the establishment of the evaluation index system, a reasonable determination of the index weight is the basis of the evaluation work. The accuracy of the weight of each evaluation index and the objectivity of the evaluation index system directly affect the authenticity and accuracy of the selection results. Suppose $Y = (y_1, y_2, \cdots y_m)$ is the level of the evaluated object, which is generally divided into $3 \sim 5$ levels, mainly to determine the degree of evaluation level to which the evaluated object belongs. The evaluation risk level can be taken as $X = \{\text{high, high, medium, low, very low}\}$.

Determine the gray level and the white component function used to evaluate the gray level. The gray level is determined based on the analysis of the actual evaluation object. Generally speaking, the gray level of the gray level is determined according to the number of inspections, the gray level the number of gray levels corresponding to each index is

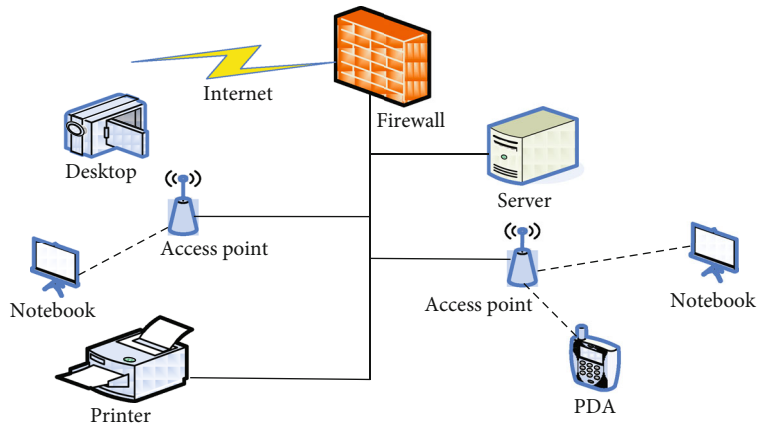

Figure 1: Basic structure diagram of wireless local area network.

determined, and the whitening weighting function to be used is determined according to this [14]. Suppose there are S gray classes, namely, $h \in \{1, 2, \cdots, n\}$, and use f_i^h to indicate that the index I belongs to the whitening weight function of gray class h. The key to system evaluation is to determine the whitening weight function. There are two commonly used whitening weight functions: typical whitening weight function and lower limit measure whitening weight Functions, as shown in Figures 2 and 3.

As shown in Figure 2, the evaluation model is to combine the evaluation index value and the weight of the evaluation index into an overall comprehensive evaluation value through certain mathematical methods and means. The use of mathematical evaluation models to quantitatively analyze maritime law enforcement risks in general navigation management can provide an intuitive basis for maritime risk prevention. In the process of assessing maritime law enforcement risks in general navigation management, the gray whitening weight function is first used to determine the gray statistical value of each index, then the gray weight matrix is obtained, the hierarchical analysis method is used to determine the weight of each index, and finally, the fuzzy evaluation is used to make comprehensive judgment to determine the degree of maritime law enforcement risk in general navigation management [15, 16].

Figure 3 shows that, in general maritime management, the risk factors of implementing maritime law are ambiguous and gray. Therefore, this article combines the fuzzy comprehensive evaluation method and the gray system called the Grifati comprehensive evaluation method [17]. The gray fuzzy comprehensive evaluation method is based on gray fuzzy mathematics and adopts the principle of fuzzy relationship synthesis. Quantification is not an easy task, but based on specific evaluation criteria to quantify several unclearly defined factors. The object belongs to judgment method. The gray fuzzy comprehensive evaluation method uses fuzzy transformation form to make comprehensive evaluation, by establishing a set of risk factors, a set of comments, and determining a set of weights for comprehensive evaluation, making the evaluation process more reasonable [18].

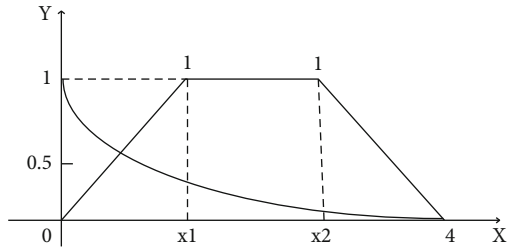

Figure 2: Typical whitening weight function graph.

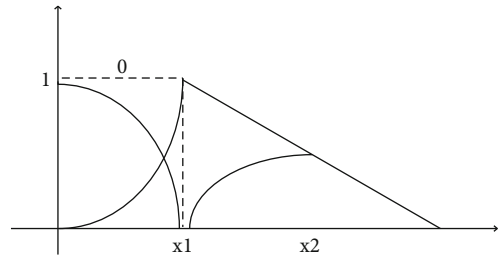

Figure 3: Whitening weight function graph of lower limit measure.

2.1.1. Unary Linear Prediction Model. Univariate linear predictive analysis is a model that deals with the relationship between independent variable a and dependent variable b. The survey object is the linear relationship between these two variables [19]. The mathematical model takes the factors that affect the prediction as independent variables or explanatory variables, and the prediction objects are dependent variables or explanatory variables. The following relationship is shown in the following formula:

$$y_i = a + bx_i + u_i. \tag{3}$$

U is a random variable called a random term, two constants are called a random term, and a and b are two constants.

The number is called the regression coefficient (parameter).

2.1.2. Build a Model. For the regression equation, there are n sets of sample observations, and the difference between the estimated value y_i and y corresponding to $y_i = a + bx_i$ is called the estimation error. Obviously, the error size is an important indicator to measure the quality of the estimator, so the least square sum of the error is used as the minimum measurement on the basis of the total error [20]. Estimation of the parameters: using the least square method to determine the model parameters as shown in the following formula:

$$\widehat{a} = \begin{pmatrix} a \\ u \end{pmatrix} = \left(Q^T Q\right)^{-1} Q^T Y_N. \tag{4}$$

Establish a prediction model, find the cumulative sequence, and derive the cumulative sequence, as shown in formula (5):

$$x^{(1)}(t+1) = \left[x^{(0)}(1) - \frac{u}{a}\right] e^{-at}, \tag{5}$$

$$\tilde{x}(t+1) = (-a) \times \left[x^{0}(1) - \frac{u}{a}\right] e^{-at}. \tag{6}$$

Equation (6) uses the residual analysis method in model testing. After passing the model test, the predicted value of the sequence will be cumulatively generated and restored using accumulation and subtraction to obtain the predicted value of the original sequence Yin.

2.2. Fourier Transform Method. For N-point finite length $X(N)$, the discrete Fourier transform formula is [21] the following formula:

$$Y(k) = IDFT[Y(k)] = \frac{1}{N} \sum_{N=0}^{N-1} Y(k) W^{-nk}. \tag{7}$$

According to the important properties of the discrete Fourier transform, for a statistically decreasing finite-length sequence $Y(n)$, the imaginary part obtained by the Fourier transform will always be negative [22], that is, the following formula:

$$Y(k) = -\sum_{N=0}^{N-1} Y \sin\left(\frac{2\pi nk}{N}\right). \tag{8}$$

If it is a statistically increasing signal strength sequence, $Y(1)$ is greater than 0, and the same formula is used to calculate the attenuation speed of the sequence $Y(n)$ in the following formulas:

$$Y(1) = -\sum_{N=0}^{N-1} Y(n) \sin\left(\frac{2\pi n}{N}\right) \prec 0, \tag{9}$$

$$E[(Y(1))] = E\left\{\sum_{N=0}^{N-1} Y(n) \sin\left(-\frac{2\pi n}{N}\right)\right\} \prec 0. \tag{10}$$

Equations (9) and (10) show that the signal strength change estimation algorithm based on fast Fourier transform can not only detect the current signal strength attenuation in real time but also estimate the moving speed of the mobile terminal. From the previous analysis, it can be seen that in the process of moving wireless LAN devices, in addition to the distance between the wireless access points, the moving speed is also an important factor affecting the trend of the signal strength. The faster the moving speed, the signal strength changes. The magnitude of the change is also more drastic, and the following formula is obtained:

$$E[(Y(1))] = E\left[\sum_{N=0}^{2^{N-T}} \left(y(n) - y\left(\frac{n}{2} + n\right)\right)\right] \prec 0. \tag{11}$$

A new LMS prediction algorithm based on a new variable step size is proposed. On the other hand, according to the fast Fourier transform signal intensity change estimation algorithm used to predict the current moving speed of the mobile terminal MS, in order to avoid the limitation of the moving speed factor when the scanning threshold is fixed, the algorithm is used to dynamically adjust the scanning threshold threshold. On the one hand, based on the new variable step size prediction algorithm, using the real-time detected signal strength sequence as the basic data, predict the signal strength value of the mobile terminal in the next time period to obtain the following formula:

$$V = \frac{|X(1)/N|}{\lambda}. \tag{12}$$

Through actual measurement, it is known that in an indoor environment without interference, the coverage of D-LIN is a circular area with a radius of about 70 meters [23], when the moving speed of the MS is calculated by the signal intensity change estimation algorithm of the fast Fourier transform knowing the situation, according to the corresponding relationship between the change of signal strength in the WLAN and the moving speed of the mobile terminal, the prediction algorithm of the scanning threshold closing value LMS per unit time is shown in the following formula:

$$e(n) = \frac{Y(1)}{N} - \frac{y(1)}{(n-1)}. \tag{13}$$

In the formula, $e(n)$ is the current error, and $e(n-1)$ is the last error. When $e(n)$ increases, the adjustment value of the corresponding step size increases, otherwise, $e(n)$ decreases, and the adjustment value of the corresponding step size decreases. The change is controlled by adjusting parameter Y fast or slow, and finally, control the speed of change of the step size, and get the following formula:

$$\beta(n) = \exp\left(-\left|\frac{e(n-1)}{e(n)}\right|^k\right). \tag{14}$$

Based on the signal strength of the new variable step size

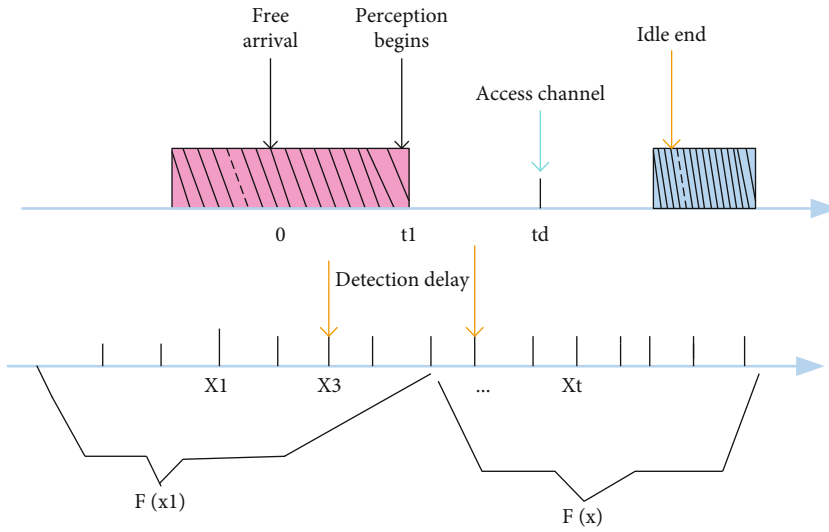

Figure 4: Channel model.

LMS prediction algorithm and formula (15), the mobile terminal can adaptively adjust the scanning threshold according to the moving speed in real time, so that the MS can reduce the signal strength to the switching threshold before the signal strength drops to the switching threshold. There is sufficient time to scan and provide the necessary AP information for the next handover, so that when the MS moves too fast, it can still successfully complete the next target network without increasing the handover delay. The handover work has achieved the purpose of improving the robustness of the handover algorithm and optimizing the handover performance [24], as shown in the following formula:

$$q(n+1) = q(n) - \mu(n)q(n)\{(y(1)-1)\}. \tag{15}$$

The purpose of the second user decision is to achieve a specific optimal operating effect during the entire system operation, that is, to select the most suitable strategy for the development of the control system.

2.3. Channel Model Algorithm. The Y user detects the observed value of the channel. Obviously, in the detection process $t = 0$, the observations obtained by the secondary user before and after the detection channel are distributed according to different distributions [25]: $\{Y_1, Y_2, \cdots, Y_{T_0}\}$ is an independent and identically distributed process with a probability density of $f_0(y)$, and $\{Y_1, Y_2, \cdots, Y_{T_0}\}$ is a process with a probability density of $f_0(y)$ $\{Y_1, Y_2, \cdots, Y_{T_0}\}$ is an independent identically distributed process with a probability density of $f_0(y)$. The time unit in Figure 4 is the detection time interval.

Continue to check the channel to obtain other observations Y_{T+1}. This requires rules that assist users in continuing to detect or access the channel. Assuming $t = T_0$, the user "confirms" that the channel is empty and then visits the channel to start sending. Next, the problem of high-speed access is how to determine the end rule of the user's torque acquisition. Of course, the user's goal is to minimize the time delay from the start of $\{Y_1, Y_2, \cdots, Y_{T_0}\}$ detection to the final access, and at the same time, it is also necessary to reduce the probability of conflict during access. Therefore, there are the following objective functions and restriction in the following formula:

$$\min E[(T_d - T_0)^+]. \tag{16}$$

Among them, $(T_d - T_0)^+$ represents the average value of the aforementioned detection delays. Because the secondary user may access the unfinished channel of the main user due to channel error determination, in expression (16), the restriction condition refers to T_d. The user occupies the channel. In fact, in order to ensure performance, the probability of erroneously accessing the channel is a certain threshold ζ that must be guaranteed to be lower than this, such as the following formula:

$$P_R[T_0 = k] = p(1-p)^{k-1}(1-\lambda_0). \tag{17}$$

Equation (17) is as follows. The geometric distribution refers to the probability of obtaining the first success in the Nth Berunui test. In other words, the N Bernoulli test failed $N-1$ times for the first time, and the Nth Bernoulli test failed. Just success, $1-P$ represents the probability of failure (occupation), and P is the probability of final success (idle). You can also know from the following formula. Observation of the idle probability at the beginning of the following formula:

$$\lambda_0 = \Pr\left[T_0 \le t | Y_1, Y_{2\ldots}, Y_N|\right]. \tag{18}$$

$T \le t$, then the user accesses the channel, and the posterior probability λ is the following equation:

$$T_d = \inf\{t : \lambda_t \ge \eta_d\}. \tag{19}$$

2.3.1. State Space. When analyzing the channel model of the primary user, the secondary user has three basic states 0, 1, and Δ. Among them, 0 and 1, respectively, represent the current channel state (occupied and idle) of the secondary user. Δ represents the decision of the user who accesses the channel. This indicates the end of the access process, so the absorption status is as follows, as shown in Figure 5.

Decision theory refers to the channel switching and channel access strategies adopted by the secondary users under the above optimization problems. When a user accesses a channel, the decision theory is the only basis for selecting a new channel to determine the access, and it is also the basis for determining the state transition of the model. Figure 5 is a state transition diagram. From Figure 5, the state transition and transition probability of the decision theory can be obtained.

2.3.2. Sufficient Statistics. In decision theory, users obtain switching and access strategies under the minimum cost condition, as shown in the following equation:

$$\lambda_t = T(\lambda_0 | y), a(t-1) = S. \tag{20}$$

By analyzing equation (20), we can know that the physical meaning of λ_t is, at the moment, the posterior idle probability of the channel when the user observes the $Y_t = y$ condition.

2.4. Conducive to Wireless Local Area Network to Form an Integrated Access Control Model in Collaborative Office. The security of "username and password" is very low, and the password is easy to be stolen and cause the loss of the enterprise. Therefore, new solutions have been formulated, such as the use of symmetric encryption technology, and the integrated access control strategy of the collaborative office platform to use user management components and role management components. And resource management components, by setting the organization management module, user management module, role management module, and authority management module to manage the access strategy, strengthen security guarantee. The rights management module is mainly the management of system resources [26]. Authorities mainly include two parts of operations and objects. The object is the resource operation in the access control system. The flow chart of the integrated access control to the object resource is shown in Figure 6.

Figure 6 shows that integrated access control mainly involves users, roles, and resources, and the figure shows the relationship between their database table structures. By deleting user information that is no longer a system user and the corresponding permissions that they have in time, it can prevent these users from still using the original permissions to access system resources and cause information leakage, thereby avoiding unnecessary losses and improving system security performance.

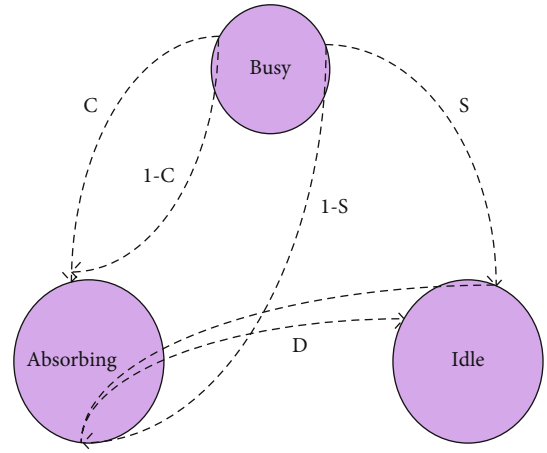

Figure 5: POMDP state transition diagram.

3. Experimental Analysis of Risk Assessment Index System for Maritime Law Enforcement

3.1. Comprehensive Analysis of Examples. Comprehensive evaluation is a complex problem composed of evaluation object set, evaluation index set, evaluation method set, and evaluator set [27]. The selection of various element sets will ultimately affect the result of comprehensive evaluation. This article invites 8 law enforcement officers engaged in navigation management, that is, maritime law enforcement officers responsible for navigation police (announcement), ship traffic management, water and underwater operations or activities, maritime cruises, etc., these maritime law enforcement officers are familiar with the business they are engaged in, with rich experience and representativeness, ask them to rate the maritime law enforcement risks of a certain maritime administration in the general navigation management according to the risk level standard. The expert scores are shown in Table 1.

It can be seen from Table 1 that among the eight law enforcement officers in general navigation management, their legal professional quality is relatively high, with an average of about 6.5, but the score of the legal system is low, about 3, so it can be learned that the law of maritime management. The system needs to be strengthened and improved in order to make maritime management better, so we can take the following measures:

(1) In the navigation management to improve the level of law enforcement equipment, law enforcement equipment is the basis for maintaining shipping safety and ensuring water traffic safety. While improving the quality of maritime law enforcement personnel, in order to increase investment in law enforcement machinery and improve the integrity of law enforcement machinery, maritime agencies need to invest in more law enforcement vehicles and patrol boats as well as transportation and inspection tools in other major sea areas

(2) Improve legal awareness. The legal knowledge of the maritime law enforcement officials determines the

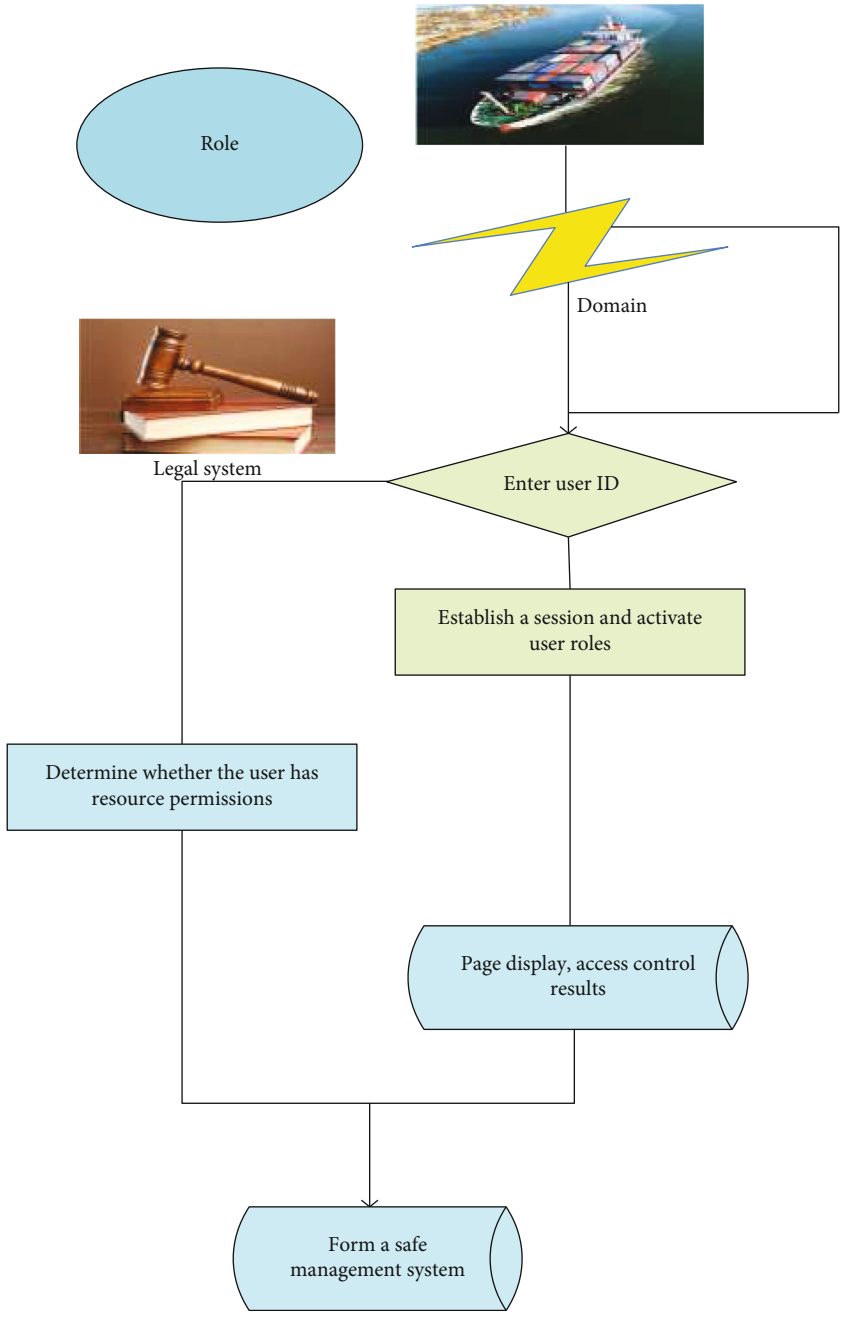

Figure 6: Flow chart of resource integrated access control.

correctness of the maritime law enforcement personnel's understanding of maritime law and regulations and determines the legality of law enforcement measures in the law enforcement process. The law enforcement work of maritime law executives is a complex task that requires purposeful, appropriate, and conscious training

(3) Improving the law enforcement supervision mechanism and strengthening supervision can improve the law enforcement capacity and efficiency of maritime agencies. The Maritime Safety Administration should positively evaluate political trends, thoroughly interview port companies, shipping companies, industry groups, etc., and accept comments. At the same time, the Maritime Safety Administration also needs to expand monitoring channels, increase social participation, and implement monitoring through WeChat, e-government's electronic evaluation system, and other forms of network monitoring

According to the results of the risk assessment of maritime law enforcement in general navigation management, the level of maritime law enforcement risk in the general navigation management of the Maritime Safety

Table 1: Scorers' scores on maritime law enforcement risk factors in general navigation management.

	The scorer's scoring value for maritime law enforcement risk factors in general navigation management					
	Professional quality of law enforcement personnel	Law enforcement personnel's interest view read	Law enforcement equipment	Legal system	Supervision system	Legal awareness
Expert rating	6	7	5	2.8	5.4	2.8
	7	8	4.4	2.5	3.5	5.2
	5	6	6.5	4.3	4.3	3.5
	8	7	6.8	4.8	4.5	3.9
	6	9	6.4	3.9	4.1	4.5
	6	7	7.8	5.4	3.9	4.3
	8	8	6	2.4	5.1	4.8
	7	8	5.3	3.1	5	4.5

4.6.

Administration is moderate, so the Maritime Safety Administration should take reduction measures. From multiple aspects of law enforcement risks, first select 4 out of 8 managers to compare the scores of professional knowledge, law enforcement equipment, and legal system in 2017 and 2018, as shown in Figure 7.

It can be seen from the comparison chart in Figure 7 that the legal expertise of law enforcement officers in 2017 was higher than that of legal awareness and law enforcement equipment, with an average score of about 7.3, while the average score of law enforcement equipment was only about 3. Therefore, the perfection of the legal system is not high. After some measures in 2018, the legal management of the four law enforcement officers has been improved, and the score has increased to about 6. Therefore, a complete maritime management legal system must be improved by improving law enforcement equipment and legal awareness and improving legal system. Improve the law enforcement system for maritime management. After improvement, look at the situation of the four law enforcement officers in 2019 and get Figure 8.

As shown in Figure 8, after improvement, the situation of the four law enforcement officers in 2019 has been significantly improved. The score of law enforcement equipment is as high as about 8.1, and the score of the legal system is as high as about 7.5, which is an increase of about 1.5 from 2018. Therefore, the maritime agency, we must focus on improving the overall quality of maritime law enforcement personnel and establish a maritime law enforcement team that is familiar with maritime laws and regulations, has high ethics and high-level law enforcement capabilities, and has high professional quality.

3.2. RSA/ECC Performance Analysis. The data of the navigation system and the maritime system are not heterogeneous at one level, but are different at multiple levels. The goal of heterogeneous data merging is to realize the combination and sharing of data resources, information resources, hardware equipment resources, and data of different structures including human resources. One of the core points is to establish integrated data for navigation systems and maritime systems through various tools and processing logic based on scattered data and partial data. Build a data warehouse oriented to the maritime field.

At present, the bottleneck problem in the construction of shipping and maritime informatization is the disadvantages of large and scattered information in various business departments. Solve the integrated management of provincial-level navigation and maritime business integration, in order to achieve collaborative management between various business departments, administrative departments, decision-making departments, and other departments. The security analysis of ECC, RSA, and DSA is shown in Table 2.

It can be concluded from Table 2 that the ECC password has many advantages. (1) safe and reliable: as shown in Table 1, the unit security strength of ECC ciphers is higher than that of RSA and DSA, which has its aggressiveness. There are absolute advantages. For example, 160-bit ECC has the same security as 1024-bit RSA and DSA, and a 210-bit ECC cipher has the same security as 2048-bit RSA and DSA. The key length required for ECC ciphers is much shorter than that of RSA ciphers. This will effectively solve the problem that the engineering is difficult to achieve, because the key length needs to be extended to improve the security strength. Efficient implementation: RSA can increase the speed of public key processing by choosing a smaller public key (3). In other words, increase the speed of encryption and signature verification to verify the speed of encryption and signature. Same as ECC, but in terms of processing speed of secret keys (decryption and signature), ECC is much faster than RSA and DSA. Therefore, the overall speed of ECC is much faster than RSA and DSA. Under the same security strength, if a 160-bit ECC cipher is used for encryption, decryption, or digital signature, it is about 5-8 times faster than 1024-bit RSA and DSA (see Table 2). Table 3 is the implementation of ECC cipher and RSA encryption software speed comparison.

It can be seen from Table 3 that the installation cost is low. With the same security strength, the key size and system parameters of the ECC password are much smaller than the RSA password, so the storage space required by the ECC is required. The password is much smaller, and the transmission bandwidth requirement is low. The hardware needs to implement the logic circuit of the ECC password. The

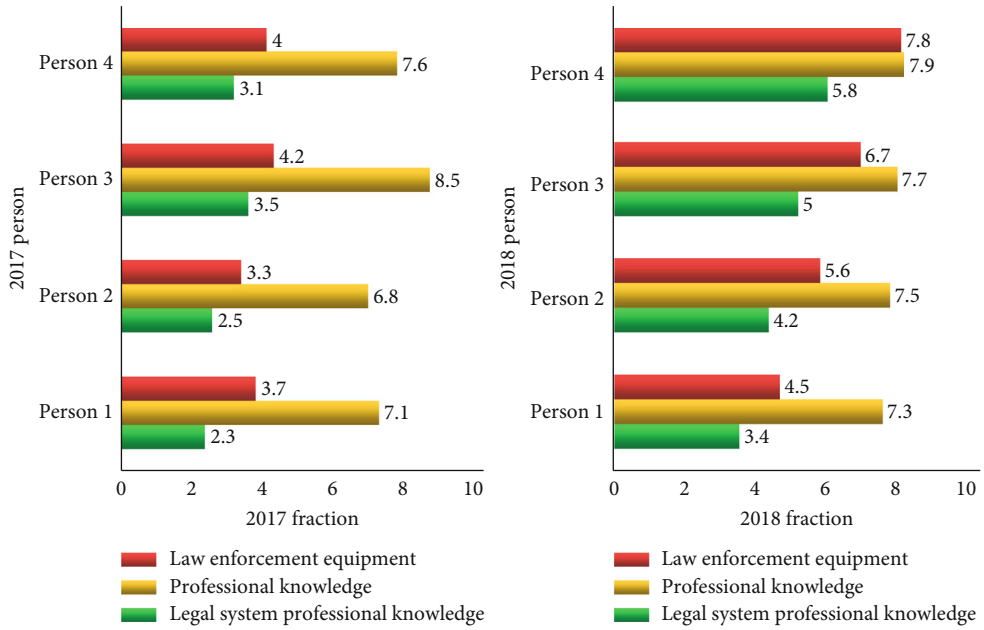

Figure 7: Comparison of law enforcement equipment and legal systems.

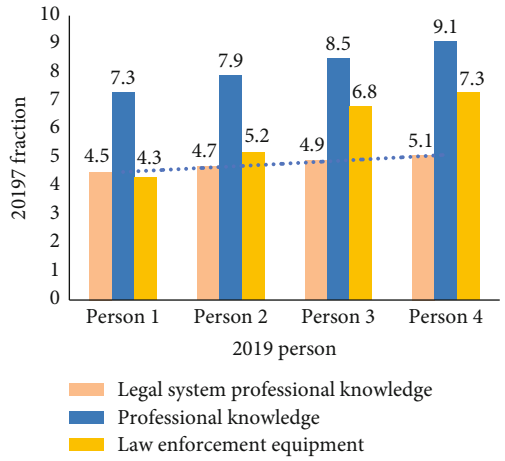

Figure 8: 2019 law enforcement equipment and legal system trends.

Table 2: Security analysis of ECC, RSA, and DSA.

Time required to decipher	RSA/DSA (key length)	RSA/ECC (key length)	ECC (key length)
9^3	535	153	5 : 1
9^7	647	163	7 : 1
9^{11}	748	198	8 : 1
9^{19}	984	216	9 : 1
9^{28}	1073	279	10 : 1

number of logic gates is much less than that of the RSA password, and it consumes less power. Due to all these advantages, ECC ciphers can be implemented in many environments where RSA ciphers cannot be implemented.

Table 3: RSA and ECC speed comparison.

Function	Security builder 1.2 ECC (ms)	BSAFE 5 RSA (ms)
Key pair generation	2.9	3743.5
Sign	1.9 (ECNRA)	198.6
Sign	4.0 (ECDSA)	198.6
Verify	7.8 (ECNRA)	13.8
Verify	9.6 (ECDSA)	13.8
Diffie-Hellman key exchange	7.6	1563.0
Time required to decipher	8	130
RSA/DSA (key length)	65	98

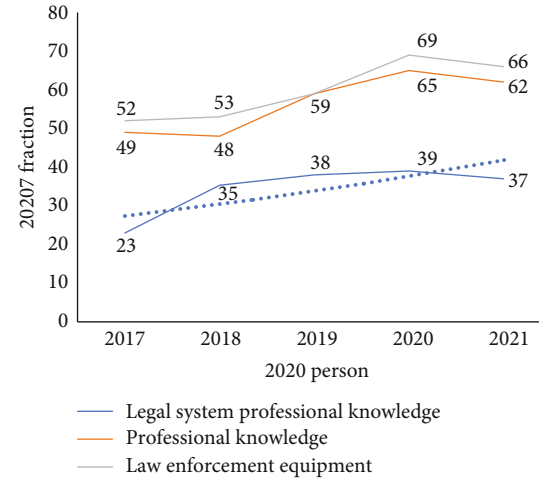

Figure 9: 2017-2021 trend map of the legal system of a maritime department.

The supervision system is not perfect. The maritime agency will have weak supervision, weak supervision, and insufficient supervision, which affects the image of the maritime law enforcement agency to a certain extent. Therefore, the maritime agency should correct its attitude and actively accept supervision [28]. This article continues to collect data from a certain maritime administration department from 2017 to 2021 after the supervision system has been improved, as shown in Figure 9.

Figure 9 shows that from 2017 to 2021, the percentage of a certain maritime management's emphasis on the legal system has clearly shown an upward trend [29], and the emphasis on the legal system in 2020 is even as high as 69%. This shows that the supervision and improvement of the law system is an effective measure and should be maintained [30].

4. Discuss

Based on the introduction of general navigation management related knowledge and based on wireless local area networks, this article studies what role wireless network domains can play in maritime channel management and how to identify maritime law enforcement risks, establish maritime channel management, and establish a sound legal system for law enforcement and risk assessment index system.

This paper also uses the gray fuzzy comprehensive assessment method to establish a risk assessment model for maritime law enforcement in general navigation management. Combining that the maritime law enforcement risk factors are vague and gray, by establishing a gray fuzzy comprehensive evaluation model, not only the overall maritime law enforcement risk situation can be obtained but also which risk factor has the greatest impact on the maritime law enforcement risk.

This paper also verifies the practicability and reliability of the experimental methods selected in this paper through case demonstration and RSA/ECC performance analysis, proposes corresponding preventive measures based on the evaluation results of maritime law enforcement in general navigation management, and establishes a complete legal system.

5. Conclusions

Based on the analysis of the risk factors of maritime law enforcement personnel in the law enforcement process and based on the role of wireless local area network, this paper establishes an index system for maritime law enforcement risk assessment in general maritime management. Through the selection of various evaluation methods, a comprehensive evaluation method combining gray fuzzy comprehensive evaluation and gray system theory is selected, and various algorithms are used to determine the weight of each risk factor of maritime law enforcement, and a mathematical model for maritime navigation management in navigation management is constructed. The public's legal awareness and awareness of rights protection have also increased. Finally, it can be learned that the level of service provided by law enforcement personnel in maritime waterway management is becoming higher and higher. Through the improvement of law enforcement equipment and supervision system, effective and better management can be achieved. Therefore, it is very important to establish a complete legal system. Due to the author's limited research level and ability, this article still has certain deficiencies in the content, and further research is needed.

Data Availability

No data were used to support this study.

Conflicts of Interest

There are no potential competing interests in our paper.

Authors' Contributions

And all authors have seen the manuscript and approved to submit to your journal.

References

[1] J. Wang, H. Zhou, Y. Li et al., "Wireless channel models for maritime communications," *IEEE Access*, vol. 6, pp. 68070–68088, 2018.

[2] A. Lionis, K. Peppas, H. E. Nistazakis, A. D. Tsigopoulos, and K. Cohn, "Experimental performance analysis of an optical communication channel over maritime environment," *Electronics*, vol. 9, no. 7, p. 1109, 2020.

[3] R. W. Jansen, M. A. Sletten, T. L. Ainsworth, and R. G. Raj, "Multi-channel synthetic aperture radar based classification of maritime scenes," *IEEE Access*, vol. 8, pp. 127440–127449, 2020.

[4] K. Araki, Y. Masuzawa, Y. Takahashi, and T. Nakayama, "The Japanese legal system and the applicability of laws and regulations on private information protection and research ethics relating to medical research," *Nihon koshu eisei zasshi Japanese journal of public health*, vol. 65, no. 12, pp. 730–743, 2018.

[5] R. Lou, W. Wang, X. Li, Y. Zheng, and Z. Lv, "Prediction of ocean wave height suitable for ship autopilot," *IEEE Transactions on Intelligent Transportation Systems*, pp. 1–10, 2021.

[6] A. Park, "Legal research on registration system of newspapers and journals," *Journal of Media Law, Ethics and Policy Research*, vol. 15, no. 3, pp. 131–162, 2016.

[7] R. Lou, Z. Lv, S. Dang, T. Su, and X. Li, "Application of machine learning in ocean data," *Multimedia Systems*, pp. 1–10, 2021.

[8] A. Anderson and P. P. Gupta, "A cross-country comparison of corporate governance and firm performance: do financial structure and the legal system matter?," *Journal of Contemporary Accounting & Economics*, vol. 5, no. 2, pp. 61–79, 2009.

[9] L. H. Haller, L. A. Dubin, and M. Buxton, "The use of the legal system as a mental health service for children," *The Journal of Psychiatry & Law*, vol. 7, no. 1, pp. 7–48, 1979.

[10] S. Baek and B. D. Choi, "Performance analysis of power save mode in IEEE 802.11 infrastructure wireless local area network," *Journal of Industrial and Management Optimization*, vol. 5, no. 3, pp. 481–492, 2009.

[11] M. Ji, G. Caire, and A. F. Molisch, "Fundamental limits of caching in wireless D2D networks," *IEEE Transactions on Information Theory*, vol. 62, no. 2, pp. 849–869, 2016.

[12] M. Agiwal, A. Roy, and N. Saxena, "Next generation 5G wireless networks: a comprehensive survey," *IEEE Communications Surveys & Tutorials*, vol. 18, no. 3, pp. 1617–1655, 2016.

[13] Z. Yong, Z. Rui, and J. L. Teng, "Wireless communications with unmanned aerial vehicles: opportunities and challenges," *IEEE Communications Magazine*, vol. 54, no. 5, pp. 36–42, 2016.

[14] W. Hong, S. He, H. Wang et al., "An overview of China millimeter-wave multiple gigabit wireless local area network system," *IEICE Transactions on Communications*, vol. E101. B, no. 2, pp. 262–276, 2018.

[15] K. Murugan and M. Usha, "Time orient flow estimation based data mining approach for intrusion detection in wireless local area networks using delay averaging scheme," *Middle East Journal of Scientific Research*, vol. 24, no. 1, pp. 97–102, 2016.

[16] S. Wan, *Topology Hiding Routing Based on Learning with Errors*, Concurrency and Computation: Practice and Experience, 2020.

[17] B. Bellalta, L. Bononi, R. Bruno, and A. Kassler, "Next generation IEEE 802.11 wireless local area networks: current status, future directions and open challenges," *Computer Communications*, vol. 75, p. 1, 2016.

[18] F. Heidari, F. Dabiri, and M. Heidari, "Legal system governing on water pollution in Iran," *Journal of Geoscience and Environment Protection*, vol. 5, no. 9, pp. 36–59, 2017.

[19] K. Aranovskiy and S. Knyazev, "Constitutional foundations of the execution of the Ecthr judgments in the legal system of the Russian Federation," *Law Enforcement Review*, vol. 1, no. 1, pp. 139–150, 2017.

[20] F. F. Russo, "Informality: the doorstep of the legal system," *SSRN Electronic Journal*, vol. 1, no. 1, pp. 49–70, 2018.

[21] D. T. Johnson, "Juries in the Japanese legal system: the continuing struggle for citizen participation and democracy," *Social Science Japan Journal*, vol. 19, no. 1, pp. 116–119, 2016.

[22] A. Kuersten, "China's changing legal system: lawyers and judges on civil and criminal Law. CHUAN FENG , LEYTON P. NELSON and THOMAS W. SIMON . Basingstoke, UK Palgrave Macmillan, 2016. xv + 264 pp. $110.00; £68.00. ISBN 978-1-137-45205-4," *China Quarterly*, vol. 227, no. 227, pp. 820–822, 2016.

[23] B. Francis, I. Hasan, and L. Li, "A cross-country study of legal-system strength and real earnings management," *Journal of Accounting & Public Policy*, vol. 35, no. 5, pp. 477–512, 2016.

[24] G. L. Wells and A. Quigley-Mcbride, "Applying eyewitness identification research to the legal system: a glance at where we have been and where we could go," *Journal of Applied Research in Memory and Cognition*, vol. 5, no. 3, pp. 290–294, 2016.

[25] F. Perez-Fontan, V. Pastoriza-Santos, F. Machado, F. Poza, N. Witternigg, and R. Lesjak, "A wideband satellite maritime channel model simulator," *IEEE Transactions on Antennas and Propagation*, vol. PP(99):1-1, p. 1, 2021.

[26] X. Zhang, "Fault intelligent processing method for data transmission channel of maritime communication," *Journal of Coastal Research*, vol. 93, no. sp1, pp. 699–699, 2019.

[27] M. Abdullah Al, M. D. Alam, A. Akhtar et al., "Annual pattern of zooplankton communities and their environmental response in a subtropical maritime channel system in the northern Bay of Bengal, Bangladesh," *Acta Oceanologica Sinica*, vol. 37, no. 8, pp. 65–73, 2017.

[28] F. Wang, W. Wu, Q. Peng, E. H. Zhao, and X. X. He, "Maritime wireless channel environment at VHF/UHF bands and its space-time frequency selectivity," *Acta Electronica Sinica*, vol. 45, no. 6, pp. 1523–1529, 2017.

[29] J. Xiao, C. Li, and J. Zhou, "Minimization of energy consumption for routing in high-density wireless sensor networks based on adaptive elite ant colony optimization," *Journal of Sensors*, vol. 2021, no. 3, 12 pages, 2021.

[30] J. Mabrouki, M. Azrour, D. Dhiba, Y. Farhaoui, and S. E. Hajjaji, "IoT-based data logger for weather monitoring using Arduino-based wireless sensor networks with remote graphical application and alerts," *Big Data Mining and Analytics*, vol. 4, no. 1, pp. 25–32, 2021.

Hindawi
Wireless Communications and Mobile Computing
Volume 2022, Article ID 6144744, 10 pages
https://doi.org/10.1155/2022/6144744

Research Article

Multisensor Data Fusion System for Wushu Sanda Teaching in Higher Education Institutions

Zheng Wang,[1] Yihe Liu,[2] and Shuang Zhang[2]

[1]*College of Sport, Neijiang Normal University, Neijiang, 641100 Sichuan, China*
[2]*School of Artificial Intelligence, Neijiang Normal University, Neijiang, 641100 Sichuan, China*

Correspondence should be addressed to Shuang Zhang; zhang.s@njtc.edu.cn

Received 15 December 2021; Revised 26 January 2022; Accepted 1 March 2022; Published 12 March 2022

Academic Editor: Mohamed Elhoseny

Classical data fusion methods can be roughly divided into two categories: one is based on random methods, such as weighted average, least squares, Kalman filtering, Bayesian estimation, DS evidence inference, and production rules; the other is based on artificial intelligence. Intelligent methods include fuzzy logic reasoning, artificial neural networks, and support vector machine methods. This paper introduces, analyzes, and summarizes the advantages and disadvantages of the above methods, as well as the level of use of these methods, and then introduces the current trend of data fusion technology toward the mixed development of multiple methods. This article is aimed at carrying out a research on the innovation of Wushu Sanda teaching mode in colleges and universities based on multisensor data fusion technology. This article puts forward the innovative theory of youth sports training in Sanda in the new era, combined with the current status of physical education in Chinese colleges and universities, and analyzes the practicality of the theory and the effect of system integration. This article accelerates reforms and collects data from four aspects: the policy system at the macro level, the integrated governance system at the meso level, the teacher service system at the micro level, and the digital industry system at the functional innovation level, and proposes innovative strategies for youth sports training and teaching in the new era. The results of the study show that people with 5.99 are more interested in the World Cup, accounting for the largest proportion, while the number of people who are interested in martial arts is the least, only 1.63. The innovative theory of youth sports training in Sanda in the new era improves the training effect of students by 60% compared with ordinary college Sanda training. It can to a large extent protect students from reluctant exercises that do not receive physical education in traditional teaching. Physiologically, it has unique advantages for the development of students. The teaching innovation model of this article can effectively solve the problems of physical education organization difficulty.

1. Introduction

The comprehensive development of the body and mind in College Wushu Sanda Teaching is still lagging behind; the main reason is that the connection between colleges and market economy is not close enough. Although some high-tech means have been used in college sports and fitness, the way is relatively single, the equipment is aging, and the degree of intelligence is not high. Most sports still adopt the traditional teaching mode and competition mode and lack the innovation of teaching mode in teaching and training.

Theint et al. believe that the foundation of youth sports training industry is dynamic and the management of human resources is insufficient. Although the development of youth sports training industry in China is still in the primary stage, there is a contradiction between the demand for large-scale youth sports training and the mechanism of government support, stadium facilities, teaching staff, political and social cooperation, or government enterprise cooperation; moreover, the basic systems such as hardware and software are highly dynamic, and it is difficult to form a relatively stable compound, high-quality, hierarchical technical personnel, or management team due to the lack of mandatory or

supportive mechanisms [1]. Seriţan et al.'s research shows that China lacks preferential policies on venues and facilities for organizations engaged in youth sports training industry, and its idle and wasted resources or high fees make it difficult for teenagers to enjoy sports facilities [2]. Munteanu et al. pointed out that the resources of youth sports training industry are scattered and there is lack of governance capacity building. Under the background of increasing awareness of youth sports to promote health, youth sports training institutions mainly focus on off-campus sports skills training, sports event organization, and sports cultural exchange services [3]. Orique et al. believe that with the diversified development of youth sports reserve talent training, youth sports training institutions will gradually assume the social responsibility of discovering and transporting youth sports reserve talents in the form of cooperating with the government and social organizations or directly entering schools to provide services [4]. Fizeshi believes that pedagogy is the history of the formation of a science, and the current educational trend is still the content of teaching subjects in higher normal colleges; the characteristics of the educational process should follow the laws and principles, methods, and organizational forms [5].

Zou et al. pointed out that at present, there are few technical endowment contents in youth sports training industry, such as homogenization of skill training, strong replicability of curriculum contents, low industry access threshold, and lack of industry certification standards [6]. Shin et al. pointed out that as the service object of youth groups, the lack of policy system and leadership willingness of youth sports training institutions established by their schools hindered the purchase of sports public services and the development of extracurricular sports characteristic services [7]. Lan et al. believe that the resources of ordinary schools and public sports venues are not oriented to the youth sports training industry, and it is difficult for youth sports training institutions to get the support of the government and the market in terms of capital operation and investment system [8]. Zhang et al. pointed out that the discretization of resources leads to the phenomenon of "lack of competition with other industries" or "vicious competition within the industry" in the youth sports training industry [9]. The above research is based on the improvement of physical education curriculum itself. However, for a long time, it is affected by many factors, such as the low status of school physical education in the education system, the relatively closed competitive sports reserve talent system, and the booming sports industry. Therefore, the above research results have great practical obstacles for the application in colleges and universities.

This paper puts forward the new era of youth sports Sanda training teaching innovation theory, combined with the current situation of physical education in colleges and universities in China, and analyzes the practicability of the theory and the effect of system integration. In this paper, from the macro level of the policy system, meso level of the integrated governance system, micro level of the teacher service system, and function innovation level of the digital industry system, four aspects to speed up the reform of data collection, put forward the new era of a youth sports Sanda training teaching innovation strategy. This paper proposes a new and improved Kalman filter data fusion based on covariance fusion estimation and self-correcting-weighted observation Kalman filter method. Based on the problem that the coefficient is difficult to determine in the data fusion of this new improved Kalman filter, it is found that the determination of the coefficient is an optimization problem of finding the minimum value, and this coefficient is relatively small but due to the particle swarm algorithm and quantum particle swarm optimization is relatively easy to fall into the local minimum when solving optimization problems. This paper proposes a new improved quantum particle swarm optimization based on a quantum cross gate. Combined with practical problems, the traditional method of data fusion and the improved method in this paper are used to carry out simulation experiments.

2. Innovative Research Method of the College Wushu Sanda Sports Teaching Model Based on Multisensor Data Fusion Technology

2.1. Multisensor Data Fusion Technology. Data fusion technology is to organically fuse the data from multiple sensors to one or more targets according to certain criteria and filter the fused data in order to obtain reliable information of the target. Data fusion can be regarded as the comprehensive perception and processing of information by the human brain. The function of each sensor is like the human ear, nose, eye, and other organs to judge external information. Then, the information is transmitted to the fusion center in order to better distinguish and process external information. In the process of data processing, it is necessary to divide multiangle and multilevel data processing to improve the comprehensive utilization of information. Data fusion methods usually have two levels of division, namely, high-level data and low-level data fusion. High-level data fusion includes situation assessment and threat estimation, while low-level data fusion includes target detection, target tracking, and identity estimation. Figure 1 shows the information processing model based on data sensors.

Among them, data association is one of the key technologies in the multisensor data fusion tracking system. Before data fusion, it is necessary to judge whether the observation information of each sensor comes from the same target. If it comes from the same target, data fusion is performed, and data association can also complete the target identification of multisensor observation information. Therefore, the performance of the data fusion system is closely related to the data association process. Because of its high availability and effectiveness, the distributed fusion structure has been widely used in many fields. The research on data association in this paper is also carried out on the basis of the distributed fusion structure. When the number of targets is small, there is no interference and clutter; the data association problem is relatively simple. When there are many targets, cross positions, clutter, and interference, the problem is more complicated. There are two main algorithms for distributed data

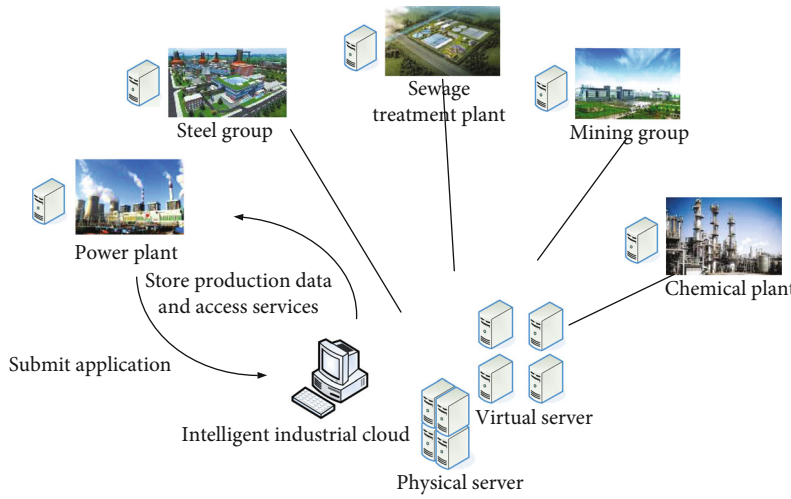

Figure 1: Information processing model based on data sensors.

association. One is an algorithm based on statistical theory, including the weighting method, correction method, sequential method, related double-threshold method, nearest neighbor method, and K-nearest neighbor method. The second is an algorithm based on fuzzy mathematics. There are track correlation algorithms based on fuzzy comprehensive functions, fuzzy track correlation algorithms, gray track correlation algorithms, etc. This method is suitable for intersections or bifurcations in dense target environments. Figure 2 shows the multisensor transmission mode.

2.2. Problems in Sanda Teaching. The unreasonable structure of physical education and the low development efficiency of sports service industry have become the urgent problems to be solved. It is of great theoretical and practical significance to effectively promote the relevant research progress for the development of sports industry. Based on the contradiction between supply and demand of sports service industry, under the background of closely focusing on the upgrading of sports teaching mode, how to promote the development of sports service industry is discussed. From the perspective of internal governance, the dynamic mechanism, operation mechanism, and path mechanism of the development of sports service industry are discussed [10, 11]. On the basis of clarifying that the dynamic mechanism is the source factor of promoting the development of sports service industry, the operational mechanism is the process factor of promoting the development of sports service industry, and the path mechanism is the strategic factor of promoting the development of sports service industry, we should firmly grasp the logical relationship that the dynamic mechanism is the premise of the operational mechanism and the path mechanism is the guarantee and booster of the operational mechanism [12, 13]. Around the two aspects of sports teaching mode policy and sports teaching mode demand, this paper explores the dynamic factors of sports service industry development, explores the operation mechanism of sports service industry development from the interaction, integration, and innovation level of sports service industry and related industries, and explores the path mechanism of sports service industry development from policy guidance, technical support, and demand stimulation, so as to provide reference for the innovative development of sports service industry and provide important ideas [14].

Under the influence of the new crown pneumonia epidemic, people's physical education model concepts have gradually changed, and the awareness of the physical education model of sports services has been significantly increased. This is an important part of the development of the sports service industry [15, 16]. Based on this, under the favorable background of upgrading the physical education model, it is particularly necessary to clarify the dynamic mechanism for promoting the development of the sports service industry. In order to promote the development of the sports service industry, the government has issued a series of related policies to encourage the development of the industry and promote the supply of the industry to meet the people's sports teaching service needs. The formulation and implementation of related sports teaching policies have provided impetus for the effective development of the sports service industry, promoted the development of the sports teaching industry, and thus stimulated the vitality of the sports teaching area [17, 18]. The continuous formation of new sports service industries such as ice and snow resorts and various leisure and sports towns has further stimulated the expansion of training demand and also promoted the formulation and implementation of related policies [12, 19].

2.3. Sanda Training Competition Promotion Model. In terms of the development of fitness and leisure industry, in order to enrich the amateur life of athletes, all kinds of sports towns and leisure resorts have been built one after another, so that the diversified needs of athletes such as vacation, tourism, and health care have been met. In order to encourage and stimulate the masses to participate in sports training and formulate relevant preferential policies, it provides economic support for the development of sports service industry. In addition, we should give full play to the role of government financial support, build a platform for the development of sports service industry, and provide support

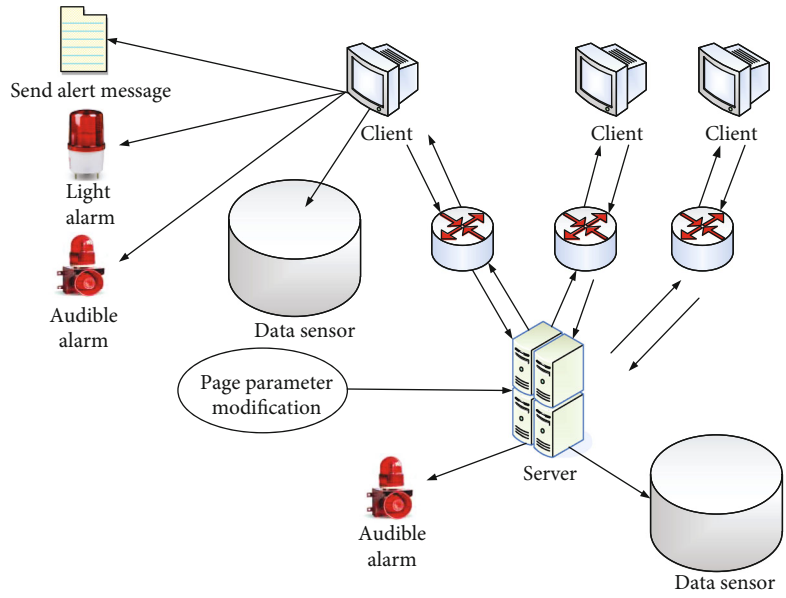

Figure 2: Sensor data transmission method.

for the development of sports service industry by taking preferential measures and security policies [20]. Through the interpretation of the above policies, it is found that the effective formulation and implementation of policies can not only promote the growth of sports training but also provide power and guarantee for the sustainable development of sports service industry. In view of the current situation of policy formulation and implementation, this paper constructs a model that the formulation and implementation of relevant sports training policies are promoting China's sports training and sports service industry into a high-speed development stage:

$$\varpi_i = \begin{cases} \varpi_l, & v_i \le v_l, \\ \varpi_h + \dfrac{v_i - v_h}{v_l - v_h}(\varpi_l - \varpi_h), & v_l \le v_i \le v_h, \\ \varpi_h, & v_i \ge v_h. \end{cases} \tag{1}$$

A physical education teaching area is the basis of the development of sports industry and also an important driving force for the development of sports service industry. The development of sports industry is inseparable from the continuous development and innovation of the sports teaching area. To promote the rapid development of sports industry, we need to further stimulate the vitality of the sports teaching area. In recent years, China's sports market has been constantly updated and enriched, and the form of residents' participation in sports training is no longer single. It tends to be service-oriented training and experience-oriented training, which expands the development space of the sports teaching area. In addition, this model can stimulate the growth of athletes' demand and further stimulate the vitality of regional development of physical education:

$$I_A = E_w + E_{nb} + E_t - Ic. \tag{2}$$

With the continuous improvement of sports marketization and commercialization, the sports teaching area is increasingly showing a standardized and orderly state. In terms of leisure and fitness industry, the leisure and fitness market is booming, which widens the leisure and fitness sports teaching area. In addition, the leisure and fitness industry relies on natural and human resources to develop characteristic sports and promote the regional innovation of physical education. In terms of venue service industry, according to the actual needs of athletes, provide high-quality sports services and products:

$$\psi = \sum_{x=1}^{\theta} Vx = \sum_{x=1}^{\vartheta} \left(\frac{Wx}{\sum_1^n W_{\Im}} Sx \right), \tag{3}$$

$$\mathrm{E}_t = \sum_{v}^{k} \sum_{h=1}^{j-1} G_{jh} \left(p_j s_h + p_h s_j \right) D_{jh} \left(1 - D_{jh} \right). \tag{4}$$

In terms of the utilization rate of facilities, this model greatly improves the utilization rate of sports fitness facilities. Gymnasiums should regularly carry out fitness activities and provide sports guidance services to meet the sports service training needs of athletes. In the competition and performance industry, we should vigorously develop diversified sports events and actively create influential and high-quality brand professional events:

$$M = \frac{d_{jh} - P_{jh}}{d_{jh} + P_{jh}}. \tag{5}$$

In addition, enhance the communication of the event, and promote the event communication through the use of new media technology, in order to enhance the audience's experience effect. The development and innovation of the

sports teaching area have provided a strong driving force for the development of sports service industry and achieved remarkable results in various fields such as leisure and fitness, venue service, and competition performance. However, compared with western developed countries, China's sports service industry has the problems of insufficient training power and unbalanced industrial structure:

$$\theta(p,q) = \arctan\left(\frac{L(p,q+1) - L(p,q-1)}{L(p+1,q) - L(p-1,q)}\right). \tag{6}$$

The final value of the objective function is determined by the average result of K replicates, which is used as the output of the simulation model:

$$f(x) = \frac{1}{Nh}\sum_{i=1}^{N} k\left(\frac{X_i - x}{h}\right). \tag{7}$$

The output of the simulation (i.e., the fitness values of all members of the subpopulation) is sent back to the master node to perform evolutionary operations (i.e., selection, crossover, and mutation) and finally select the regression value of the first generation:

$$P = \sigma t = \frac{\sqrt{1/n\sum_{i=1}^{n}(FI_{it} - FI_{it})^2}}{FI_{it}}, \tag{8}$$

$$h_t = \tanh\left(w_c x_t + u_c r({}_t\Theta h_{t-1}) + b_c\right). \tag{9}$$

In the venue service industry, with the increasing demand for a better life, people will devote more leisure time to physical exercise. In the process of sports participation, people's demand for the content and quality of venue services continues to upgrade. For example, with the gradual improvement of people's awareness of sports, people begin to change from fitness path mode to gym mode and from self-participation to seeking personal coach guidance. Therefore, the upgrading of training demand is an important driving force for the development of venue service industry.

2.4. Preprocessing Process of Multisensor Data Fusion Technology. When using ultrasonic sensors for robot navigation, there is often such a problem: because the sensor data is noisy, that is, the sensor was 3 meters away from the obstacle during the first measurement, but it was 2.9 meters away from the obstacle during the second measurement. It is obviously unreasonable to mark the positions of 2.9 meters and 3 meters with obstacles. In order to better solve this problem, we introduce the method of occupying the grid map.

For a place on a large-scale map, it either has obstacles or no obstacles, so we use $f(x=1)$ to indicate that there is no obstacle and $f(x=0)$ to indicate that there is an obstacle. Obviously, $f(x=0) + f(x=1) = 1$. At the same time, in order to describe the state of the point more conveniently, we introduce the ratio of the two:

$$\text{odd}(x) = \frac{f(x=1)}{f(x=0)} \tag{10}$$

Assuming that a new point is measured at this time, we need to update the original state:

$$\text{odd}(x|g) = \frac{f(x=1g)}{f(x=0|g)}. \tag{11}$$

According to the Bayesian formula,

$$f(x=0g) = \frac{f(y|x=0)f(x=0)}{f(g)}, \tag{12}$$

$$f(x=1|g) = \frac{f(y|x=1)f(x=1)}{f(g)}. \tag{13}$$

Bring in the original formula to get

$$\text{odd}(xg) = \frac{f(y|x=1)f(x=1)/f(g)}{f(y|x=0)f(x=0)/f(g)} = \frac{f(y|x=1)}{f(y|x=0)}\text{odd}(x). \tag{14}$$

In order to simplify the calculation, the logarithm of the above formula can be obtained:

$$\log\ \text{odd}(x|g) = \log\frac{f(y|x=1)}{f(y|x=0)} + \log\ \text{odd}(x). \tag{15}$$

At this time, we have established a model $\log f(g=0|x=1)/f(g=0|x=0)$ of the measured value, which is denoted as state. The model contains two situations:

$$\begin{aligned}\text{free} &= \log\frac{f(g=0|x=1)}{f(g=0|x=0)},\\ \text{free} &= \log\frac{f(g=1|x=1)}{f(g=1|x=0)}.\end{aligned} \tag{16}$$

At this time, the state of position x is $\log\ \text{odd}(x)$, denoted as X, and the rule for updating the state is simplified as follows:

$$X^+ = X^- + \text{state}. \tag{17}$$

In the above formula, X^+ and X^-, respectively, represent the state of X before and after the measurement value is updated.

When there is no measurement, the initial state of point x is

$$X_{\text{init}} = \log\ \text{odd}(x) = \log\frac{f(x=1)}{f(x=0)} = \log\frac{0.5}{0.5} = 0. \tag{18}$$

After the measurement value is updated, if the status value of a point is larger, the point is easier to be judged as

an obstacle, so a status grid map is established. Through appropriate scheduling and application of each sense and their measurement information, the redundant and complementary information of each sense in time and space is appropriately combined according to comprehensive judgment, so as to obtain a consistent reflection of the observed object or state or judgment.

Outliers are referred to as outliers for short, which refer to a small number of numerical points that seriously deviate from the trend of most values in a combination of observed values. Outliers have a huge impact on data analysis. In actual engineering applications, if they cannot be effectively detected and removed, they will have a huge impact on the judgment result and waste valuable frequency band resources. Therefore, before performing multisensor fusion, first eliminate the outliers in the above-mentioned sensors. Figure 3 shows the research of multisensor data fusion technology. This paper introduces the method of covariance fusion estimation and the method of self-correction-weighted observation Kalman filter fusion and then analyzes this filter fusion method to obtain a modified Kalman filter data fusion method based on covariance. And this method has been verified by simulation experiments.

3. Innovative Design of Sanda Teaching Mode

3.1. Innovative Mode of Physical Education. This paper puts forward the new era of youth sports Sanda training teaching innovation theory, combined with the current situation of physical education in colleges and universities in China, and analyzes the practicability of the theory and the effect of system integration.

3.2. Steps. In this paper, from the macro level of the policy system, meso level of the integrated governance system, micro level of the teacher service system, and function innovation level of the digital industry system, four aspects to speed up the reform of data collection, put forward the new era of the youth sports Sanda training teaching innovation strategy.

In the face of the new era of industrial economic transformation, national sports strategy, social awareness and physical and mental development needs, and other policy opportunities, this paper believes that China's youth sports training industry in industrial integration and innovation, organizational systematization, service industrialization, and participation diversification shows good development momentum. However, for a long time, influenced by many factors, such as the low status of school physical education in the education system, the relatively closed reserve talent system of competitive sports, and the booming sports industry, there are a series of problems in China's youth sports training industry, such as the imbalance between supply and demand, the shortage of venues and facility resources, the lack of professional guidance team, the lack of market supervision and management, and the lack of an industry access mechanism. Moreover, due to the fact that the macro policy of service economy and related policies of sports service industry are gradually implemented during the 13th Five-Year Plan period, coupled with the strong technicality of youth sports training, the slow standardization construction, and the lagging of value-added mining in culture and other industries, the industrial advantages, industrial clusters, and industrial chain of youth sports training have not yet been formed. The demand for sports training is the motivation for people to participate in sports training, and the upgrading of sports training is an important performance of the development of sports industry. Under the influence of novel coronavirus pneumonia, people's sports training needs are constantly upgraded, training concepts are gradually updated, and from the satisfaction of weight injection 5to the pursuit of quality improvement, they gradually tend to individualized and diversified service-oriented training. Specifically speaking, the high correlation and interaction of the industry are the prerequisites for the integrated development of sports service industry and related industries.

This paper puts forward the new era of young people's sports Sanda training teaching innovation theory for young people's sports training industry to play a role in promoting physical and mental health, cultivating reserve talents and supporting industrial development.

4. Innovative Model of Wushu Sanda Teaching Based on Multisensor Data Fusion Technology

As shown in Figure 4, according to the survey of the National Youth Sports winter and summer camp in 2020, 71.37% of the event organizers obtain the venue facility resources in the form of leasing or cooperation ($P < 0.05$), the data result is statistically significant. It can be seen that the hardware facilities of most of the youth sports training industrial organizations in China are not fixed assets, which leads to high operating costs and strong organizational liquidity.

As shown in Table 1, the marginalization of physical education and other factors, as well as the lack of compulsory measures such as test baton, make young people's willingness to participate in sports training, competitions, cultural exchanges, and other activities outside school more casual, bring difficulties to the survival of young people's sports training industry organizations, and also cause serious difficulties to their operators in terms of continuing education and training, basic security benefits, career development space, etc.

As shown in Figure 5, under the background of training upgrading, the sports training awareness and training needs of Chinese athletes are constantly upgrading, gradually changing from "physical-type" training to "experience-type" training. In terms of leisure fitness industry, with the promotion of leisure fitness industry, people's concept of leisure fitness training has gradually changed from a single sports training mode to a "sports +tourism" training mode and gradually changed from participating in fitness running, cycling, and other leisure sports to extreme sports, water sports, and other recreational and experiential sports.

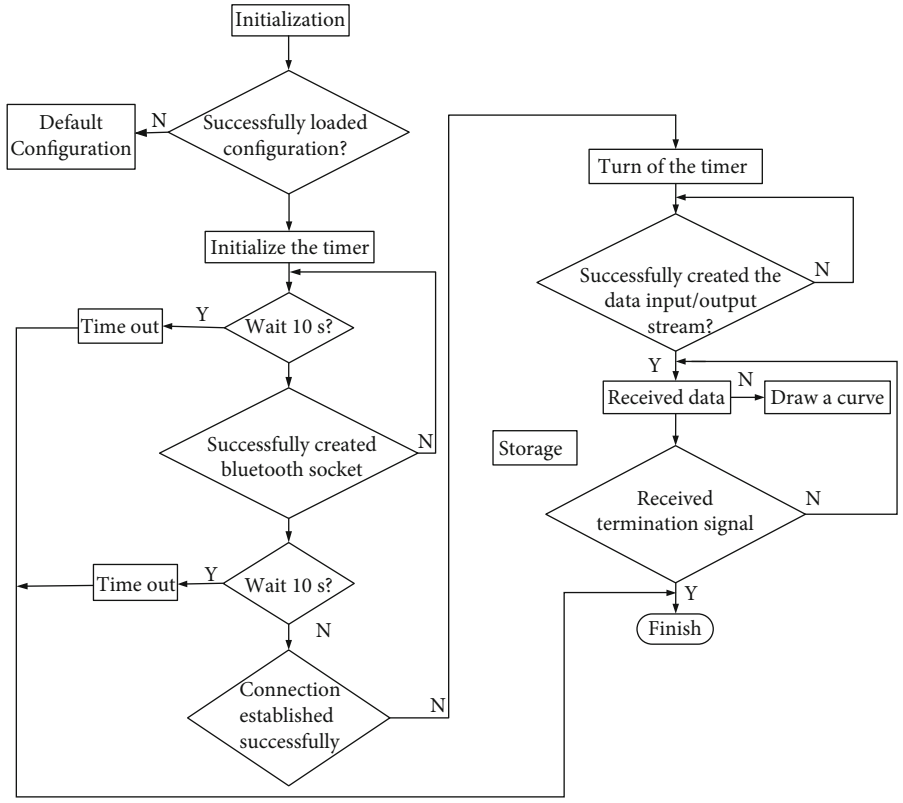

Figure 3: Research on multisensor data fusion technology.

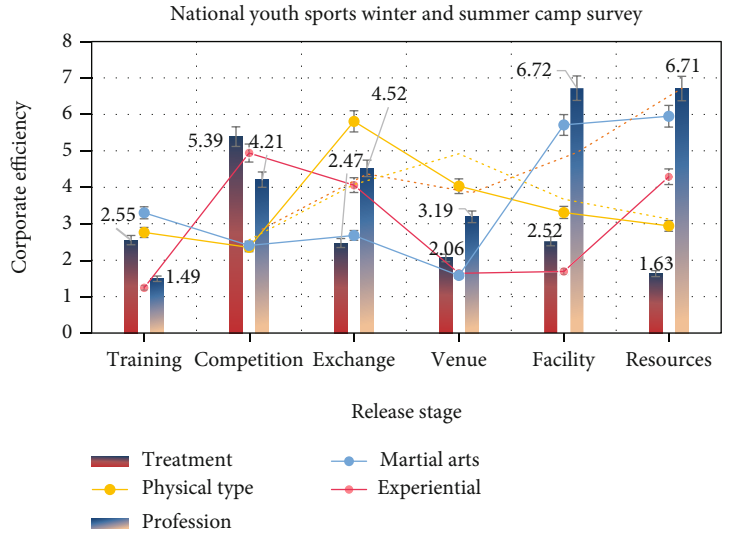

Figure 4: National Youth Sports winter and summer camp survey.

As shown in Table 2, the output results of the Sanda training competition promotion model show that the innovative teaching theory of youth sports Sanda training in the new era improves the training effect of students by 60% compared with the ordinary college Sanda course training, which can to a large extent help the traditional teaching students not accept the physical education and has unique advantages in psychological and physiological development of students. For some athletes, in the process of sports training, regional natural, human, and other resource factors have an important impact on the demand of sports service training, especially in minority areas; athletes tend to choose Wushu and other traditional sports. In the competition and performance industry, with the continuous acceleration of competition supply and the gradual rise of diversified sports events, people's training mode for sports events has

Table 1: Factors such as marginalization of physical education and lack of examination command.

Item	Treatment	Profession	Experiential	Physical type	Martial arts
Training	2.55	1.49	1.24	2.76	3.3
Competition	5.39	4.21	4.94	2.35	2.4
Cultural exchange	2.47	4.52	4.06	5.81	2.68
Venue	2.06	3.19	1.64	4.03	1.58
Facility	2.52	6.72	1.69	3.31	5.71
Resources	1.63	6.71	4.29	2.94	5.95

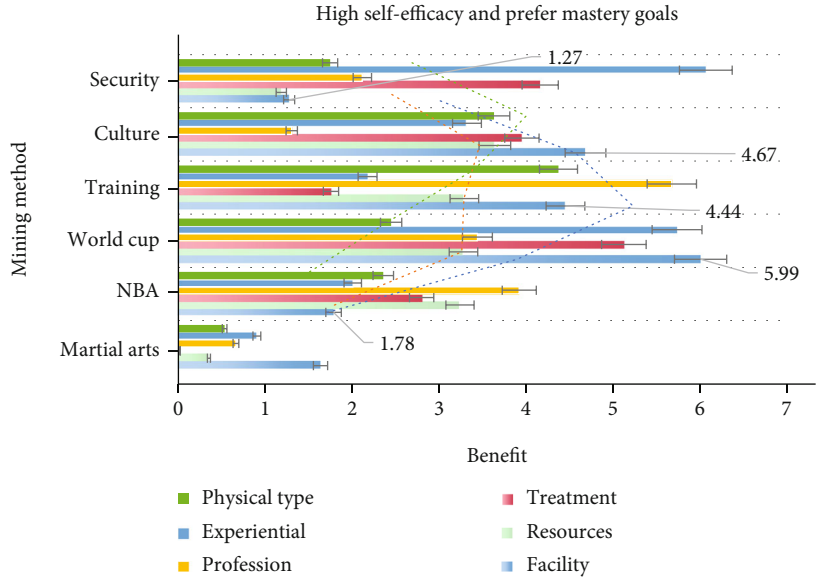

Figure 5: High self-efficacy and preferred mastery goals.

Table 2: Sanda training event promotion model.

Item	Facility	Resources	Treatment	Profession	Experiential	Physical type
Martial arts	1.63	0.35	0.02	0.66	0.9	0.53
NBA	1.78	3.23	2.79	3.91	2	2.35
World Cup	5.99	3.27	5.11	3.43	5.72	2.44
Training	4.44	3.28	1.75	5.66	2.17	4.36
Culture	4.67	3.63	3.94	1.3	3.31	3.62

gradually changed from "watching experience" mode to "participating experience" mode. With the upgrading of people's demand for experience training, people gradually tend to choose the training of NBA, World Cup, and other brand sports events.

As shown in Figure 6, with the continuous upgrading of training mode, people's demand for leisure and entertainment, social interaction, and other aspects is rising, which has led to the development of sports tourism; with the gradual increase in the number of the domestic elderly population, some elderly people's demand for physical fitness, self-cultivation, and other aspects is rising, which has led to the development of sports and health industry. In addition, the integration trend of sports service industry and high-tech, education and training, culture, security services, and other industries is gradually accelerating. As the above industries are highly related to sports service industry, they continuously realize the interaction and sharing of resources with sports service industry in terms of platform, market, and carrier, so as to improve the mutual utilization efficiency of resources. For the sports industry, the strong pull of diversified and compound market demands, the large-scale intervention of capital inside and outside the industry, and the strong penetration of information technology all herald the arrival of an era of integration of the sports industry in a modern sense: social, cultural, environmental, and other fields of high compatibility and benign interaction.

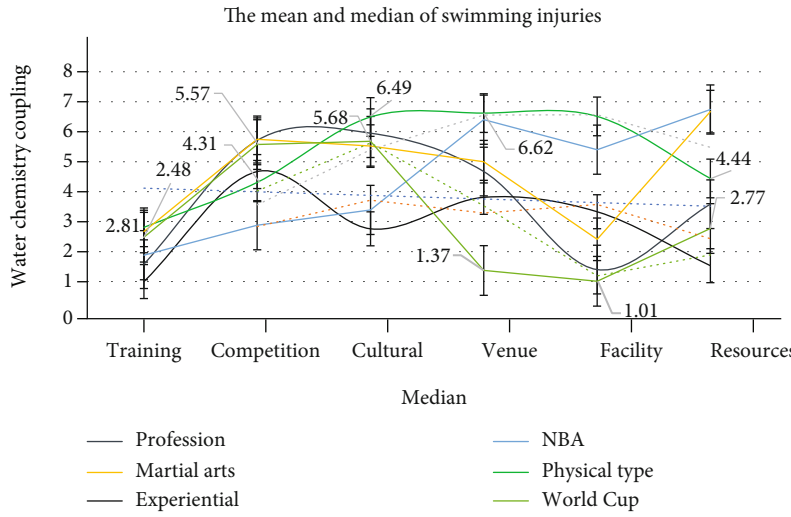

Figure 6: The mean and median of swimming injuries.

5. Conclusions

Since entering the new era, China's youth sports training industry has developed rapidly under the development situation of government guidance, market guidance, and extensive social participation and has become a breakthrough for the transformation of national sports industry from sports goods manufacturing industry to sports service industry. From the perspective of service industry, China's youth sports training industry presents a diversified development trend of organization construction and market demand and forms an integrated industrial chain of organization, venue, curriculum, service, and equipment, which highlights the development characteristics of sports service industry integrating health, education, and culture. However, there are also some practical problems, such as the lack of governance policies caused by the diversification of industrial organizations, the lack of governance human resources caused by the dynamic industrial foundation, and the lack of governance capacity building caused by the scattered industrial resources.

In this paper, from the new era of youth sports Sanda training teaching innovation level, put forward a systematic, linkage, feasible governance strategy, to promote China's youth sports training industry format innovation, coordinated governance, healthy development, regional opening, and resource sharing. From the perspective of youth sports, we need to construct the supply side reform of youth sports with multiple subjects of government, society, and market under the guidance of school and focus on the construction of different types of youth sports organizations, different types of sports, different levels of youth sports activities, etc., so as to build a modern sports governance system with youth physical and mental health as the main body.

The new era of youth sports Sanda training and teaching innovation theory to promote the development of youth sports club policy formed to deepen the integration of sports and education reform, break the bottleneck of school support to create youth sports club, build a diversified youth sports events, especially through the participation of social forces to make up for the lack of government supply, and to consolidate the foundation of various types of youth sports organizations. In order to meet the diversified needs of teenagers, the government should take basic physical education and public services as the main body of teenagers' sports activities. Although the improved quantum particle swarm optimization algorithm proposed in this paper can better avoid falling into the local optimum problem, the number of iterations is obviously more than that of the classical swarm intelligence algorithm. That is to say, the article sacrifices the efficiency of the algorithm to achieve a better optimization effect. There are already many improvement methods based on swarm intelligence algorithms. The next step is to combine other methods to find a skill that avoids effectively falling into the local optimum and has high efficiency.

Data Availability

No data were used to support this study.

Conflicts of Interest

The authors declare that there are no conflicts of interest regarding the publication of this article.

Acknowledgments

This work was supported by the Foundation of Ph.D. Scientific Research of Neijiang Normal University under Grant 18B19 and the Sichuan Applied Psychology Research Center of Chengdu Medical College Funded Projects under Grant CSXL-21103.

References

[1] Z. Theint, Z. T. T. Hlaing, M. P. Phyu, and S. Kyaw, "The effect of changes in teaching/learning schedule pattern in physiology subjects among 2nd MBBS from University of Medicine

Magway," *European Journal of Medical and Health Sciences*, vol. 2, no. 5, pp. 1–4, 2020.

[2] G.-C. Seriţan, B. A. Enache, S. D. Grigorescu et al., "Improvement of teaching activities in higher education: a case study," *Revue Roumaine des Sciences Techniques - Serie Électrotechnique et Énergétique*, vol. 64, no. 2, pp. 169–172, 2019.

[3] S. Munteanu, A. M. Cpraru, and S. Pdureu, "The challenges of designing a course in Romanian for specific purposes," *Bulletin of the Transilvania University of Brasov*, vol. 12, no. 61, pp. 41–52, 2019.

[4] S. B. Orique, L. Despins, B. J. Wakefield, S. Erdelez, and A. Vogelsmeier, "Perception of clinical deterioration cues among medical-surgical nurses," *Journal of Advanced Nursing*, vol. 75, no. 11, pp. 2627–2637, 2019.

[5] O. Fizeshi, "The peculiarities of preparation of masters for teaching of the pedagogical disciplines in the institutions of higher pedagogical education," *Revista Romaneasca pentru Educatie Multidimensionala*, vol. 12, no. 4, pp. 103–117, 2020.

[6] L. Zou, Y. Zhang, L. Yang et al., "Are mindful exercises safe and beneficial for treating chronic lower back pain? A systematic review and meta-analysis of randomized controlled trials," *Journal of Clinical Medicine*, vol. 8, no. 5, pp. 628-629, 2019.

[7] J. H. Shin, Y. Lee, S. G. Kim, B. Y. Choi, H. S. Lee, and S. Y. Bang, "The beneficial effects of tai chi exercise on endothelial function and arterial stiffness in elderly women with rheumatoid arthritis," *Arthritis Research & Therapy*, vol. 17, no. 1, pp. 1–10, 2015.

[8] C. Lan, S. Y. Chen, M. K. Wong, and J. S. Lai, "Tai chi chuan exercise for patients with cardiovascular disease," *Evidence-Based Complementray and Alternative Medicine*, vol. 13, no. 5, article 983208, pp. 983–1008, 2013.

[9] Y. Zhang, Y. Chai, X. Pan, H. Shen, X. Wei, and Y. Xie, "Tai chi for treating osteopenia and primary osteoporosis: a meta-analysis and trial sequential analysis," *Clinical Interventions in Aging*, vol. 14, no. 14, pp. 91–104, 2019.

[10] M. F. Love, A. Sharrief, A. Chaoul, S. Savitz, and J. E. S. Beauchamp, "Mind-body interventions, psychological stressors, and quality of life in stroke survivors," *Stroke*, vol. 50, no. 2, pp. 434–440, 2019.

[11] J. Bowen, "The American with Disabilities Act and its application to sport," *Journal of the Philosophy of Sport*, vol. 54, no. 29, pp. 66–74, 2020.

[12] S. Giblin, D. Collins, and C. Button, "Physical literacy:importance, assessment and future directions," *Sports Medicine*, vol. 44, no. 9, pp. 1177–1184, 2014.

[13] C. L. Ogden, M. D. Carroll, L. R. Curtin, M. M. Lamb, and K. M. Flegal, "Prevalence of highbody mass index in us children and adolescents 2007-2008," *Journal of the AmericanMedical Association*, vol. 303, no. 3, pp. 242–249, 2010.

[14] M. Terry, "An education in politics: the origin and evolution of no child left behind," *Political Science Quarterly*, vol. 129, no. 2, pp. 333–336, 2014.

[15] E. Bayle and L. Robinson, "A framework for understanding the performance of national governing bodies of sport," *European SportManagement Quarterly*, vol. 5, no. 3, pp. 249–268, 2007.

[16] I. M. Vuori, C. J. Lavie, and S. N. Blair, "Physical activity promotion in the health care system," *Mayo Clinic Proceedings*, vol. 88, no. 12, pp. 1446–1461, 2013.

[17] L. T. Labert, "The new physical education," *Educational Leader-ship*, vol. 57, no. 6, pp. 34–39, 2020.

[18] R. J. Skiba, A. B. Simmons, S. Ritter et al., "Achieving equity in special education: history status and current challenges," *Exceptional Children*, vol. 74, no. 3, pp. 264–288, 2008.

[19] C. L. Ogden, M. D. Carroll, L. R. Curtin, M. M. Lamb, and K. M. Flegal, "Prevalence of high body mass index in us children and adolescents, 2007-2008," *Journal of the American Medical Association*, vol. 303, no. 3, pp. 242–249, 2010.

[20] S. Yuma, "The construction of club mode teaching methods in Wushu Sanda teaching in colleges and universities," *Contemporary Sports Science & Technology*, vol. 9, no. 1, pp. 107-108, 2019.

Hindawi
Wireless Communications and Mobile Computing
Volume 2022, Article ID 1581054, 8 pages
https://doi.org/10.1155/2022/1581054

Research Article

Research on NTP Nonlinear Reflection Attack Identification Based on AHP Multidimensional Matrix in Global COVID-19 Environment

Xian Wang[1,2] **and Xiaoyao Xie**[2]

[1]*School of Computer Science and Technology, Guizhou University, Guiyang 550025, China*
[2]*Key Laboratory of Information and Computing Science Guizhou Province, Guizhou Normal University, Guiyang 550001, China*

Correspondence should be addressed to Xiaoyao Xie; xyx@gznu.edu.cn

Received 24 December 2021; Revised 4 February 2022; Accepted 12 February 2022; Published 11 March 2022

Academic Editor: Mohammed Hammoudeh

Under the influence of the global epidemic, various businesses have moved online one after another. With the rise of emerging industries such as online medical treatment, online education, and online conference, the proportion of attacks in the network service industry has increased year by year. UDP-FLOOD is still the primary scenario of DDoS attacks. Among them, with a large number of attack resources and most of them are high configuration servers, NTP (Network Time Protocol) reflection has become the most common UDP reflection attack method, accounting for 59% of the overall distribution. Therefore, establishing an efficient NTP attack detection system is a very important content to prevent network malicious attacks. At present, NTP-attacking based defensed methods mainly include IP filtering, hop mapping, and response packet detection, but they all have obvious weaknesses. Among them, the IP detection scheme can only detect historical attack IP, the implementation of hop mapping scheme is complex, and the resource overhead of response packet detection scheme is too large. Therefore, this paper proposes a nonlinear detection algorithm based on AHP multidimensional matrix quad information entropy. Through simulation experiments, the change of quad information entropy of attack intensity from 10% to 100% is counted. The detection rate based on the traditional target IP and target port algorithm is only 50% and 60%, which is significantly lower than this algorithm. Experiments show that the detection rate of this algorithm is higher.

1. Introduction

In the form of global epidemic, due to the need to reduce personnel contact and more and more businesses migrate online, it is extremely urgent to protect these businesses from DDoS attacks. According to the "global DDoS threat report for the first half of 2021" [1] jointly released by Lvmeng technology and Tencent, the number of large traffic attacks above 100 g in the first half of 2021 reached 2544, an increase of more than half compared with H1 in the same year, and udp-flow is still the primary scenario of DDoS attacks. In the udp-flood attack, an attacker can send a large number of fake source IP addresses for unconnected UDP packages and can quickly fill the target resources, so that they cannot work properly. Among them, because there are a large number of attack resources and most of them are high configuration servers, NTP reflection has become the most common UDP reflection attack method, accounting for 59% of the overall distribution, as shown in Figure 1.

NTP (Network Time Protocol) is a network protocol that synchronizes the clocks of two computers through switching packets. The latest version is NTPv4, and the latest stable version is NTPv4.2.8p15. NTP attack is different from the general DDoS attack, and it uses the serving NTP server as the reflection point to send response packets to the victims [2, 3]. When a large number of response packets flow

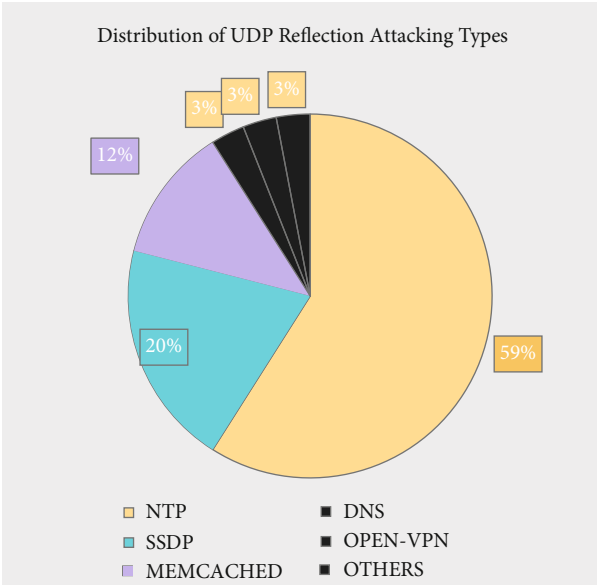

Figure 1: UDP reflection attack type distribution.

to the attack target, the target resources will be exhausted, resulting in denial of service attack [4]. The attacker can forge NTP server to attack by taking advantage of the hidden dangers in key management and can also take advantage of the buffer overflow and other vulnerabilities in NTP to control the server permissions to attack [5]. Therefore, the establishment of an efficient NTP attack detection system is a very important content to defend against network malicious attacks.

2. Related Work

At present, there are many researches on NTP-related UDP reflection attacks. Generally speaking, they can be divided into three categories: IP filtering, hop mapping, and response packet detection. Peng et al. [6] proposed a filtering scheme based on IP address; in this scheme, many reflection monitors are set in the network. After detecting the attack, the monitor sends an attack message to other monitors. But the application area is relatively small, and the attack behavior of existing IP address cannot be detected. Jin et al. [7] proposed a filtering scheme based on packet hop mapping, this scheme clusters the hops of IP packets and establishes a hop mapping table to detect forged attack packets, but it is not easy to operate. Ohta and Yamamoto [8] proposed a response packet detection model, and the author of this article believes that the data packets reflecting DDoS attacks are limited. This scheme only detects limited sessions and confirms the validity of data packets based on the relationship between request and response, so as to identify attacks, but it takes too much resources. In this paper, a nonlinear detection algorithm based on AHP multidimensional matrix quad information entropy is proposed. First, the real attack environment is simulated, and the attack intensity is from 0% to 100%. The entropy values of network quads (source IP address, target IP address, source port, and target port) under different attack intensities are calculated, respectively, Then, the four tuple entropy is normalized based on the judgment matrix, and the comparison shows that this method is more effective than the traditional entropy algorithm: the traditional detection algorithm based on target IP address or target port number is more effective.

Table 1: Quad initial value.

Element	Symbol	Initial value
Source IP address	h_1	3
Destination IP address	h_2	7
Source port	h_3	9
Destination port	h_4	1

Table 2: Weight value of each element of quad.

Element	Value
Source IP address	0.05
Destination IP address	0.35
Source port	0.15
Destination port	0.45

3. Algorithm Design

3.1. Multidimensional Entropy Algorithm Based on Network Quad. Information entropy is a concept created by Shannon, which is used to reflect the degree of data dispersion in the set. In essence, it is a measure of the uncertainty of random events; on the contrary, the smaller the randomness, the greater the certainty, and the smaller the entropy [9]. Entropy is generally expressed in H. Let system m be composed of $M = \{M_1, M_2, \cdots, M_i, \cdots, M_n\}$ n different sets of elements, and the probability of each variable M_i is $(P_1, P_2, P_3, \cdots, P_n)$, expressed as

$$P_i = \frac{Mi}{\sum_{i=1}^{n} Mi}. \tag{1}$$

The formula of information entropy is defined as

$$H(x) = -\sum_{i=1}^{n} p_i \log_2 p_i. \tag{2}$$

In this paper, an entropy algorithm based on network quadruple is proposed. First, we define network packet quadruple (source IP address, destination IP address, source port, and destination port) as a flow table: $F = <\text{Sip, Dip, Sport, Dport}>$, its entropy per unit time $\triangle t$ is $H_1(x), H_2(x), H_3(x), H_4(x)$, then, according to the different sensitivity of entropy to attack, the four tuple entropy is given a certain weight by using the judgment matrix K_1, K_2, K_3, K_4, finally,

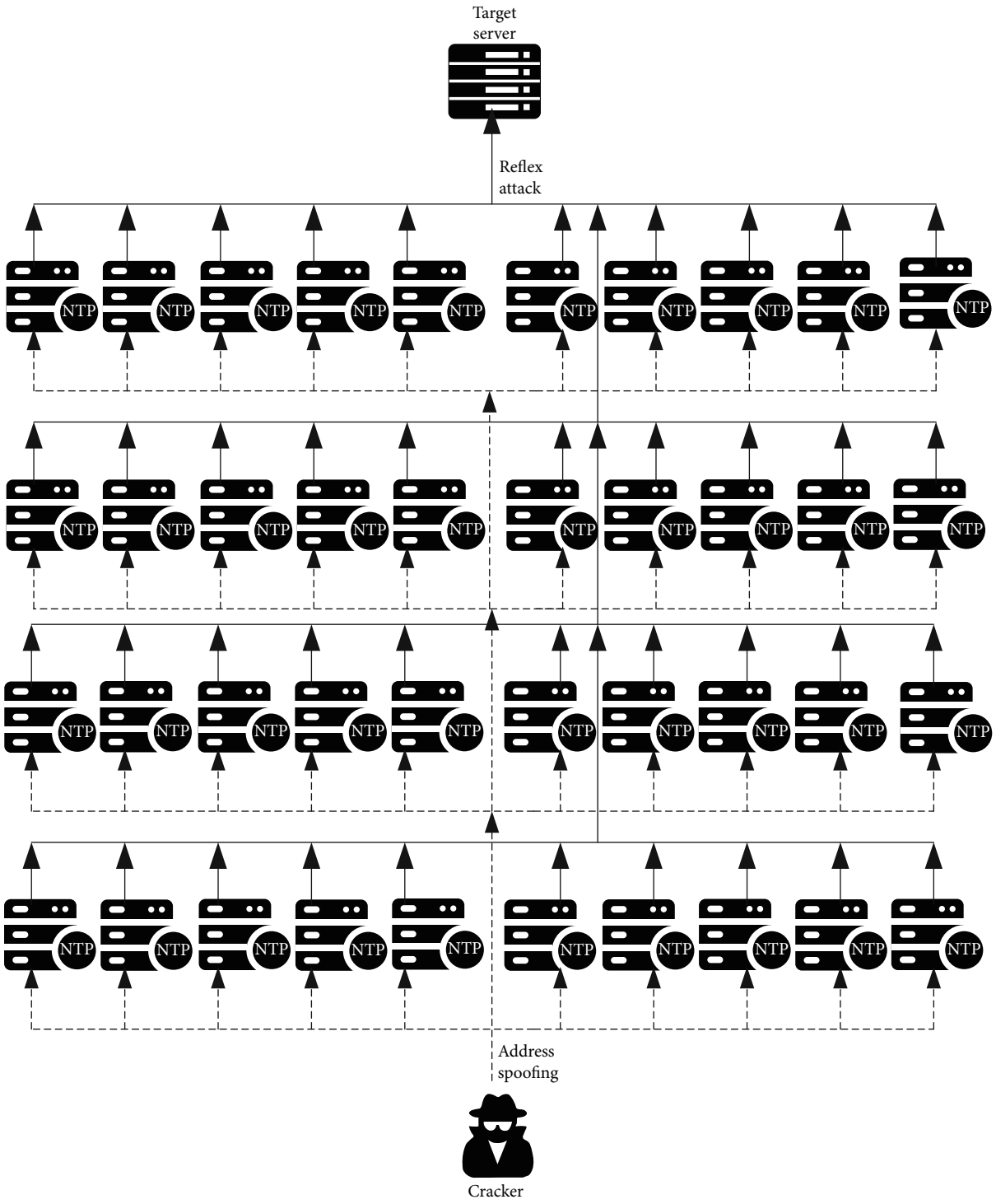

Figure 2: Simulation experiment network topology.

Table 3: Entropy of network quadrutuple elements at different attack strengths.

Iterm Intensities	SIP	DIP	Sport	Dport
0%	5.321928095	4.979470571	7.321928095	6.241446071
10%	5.319552023	4.926273424	7.357552005	6.303423201
20%	5.317811376	4.87314068	7.392317423	6.363286924
30%	5.31665992	4.820265429	7.426264755	6.421165198
40%	5.316055227	4.767795485	7.459431619	6.477175233
50%	5.315958306	4.715844097	7.491853096	6.531424631
60%	5.316333281	4.664497779	7.523561956	6.58401237
70%	5.317147094	4.613822149	7.554588852	6.635029683
80%	5.318369254	4.56386634	7.584962501	6.684560814
90%	5.3199716	4.514666392	7.614709844	6.732683702
100%	5.321928095	4.466247897	7.64385619	6.779470571

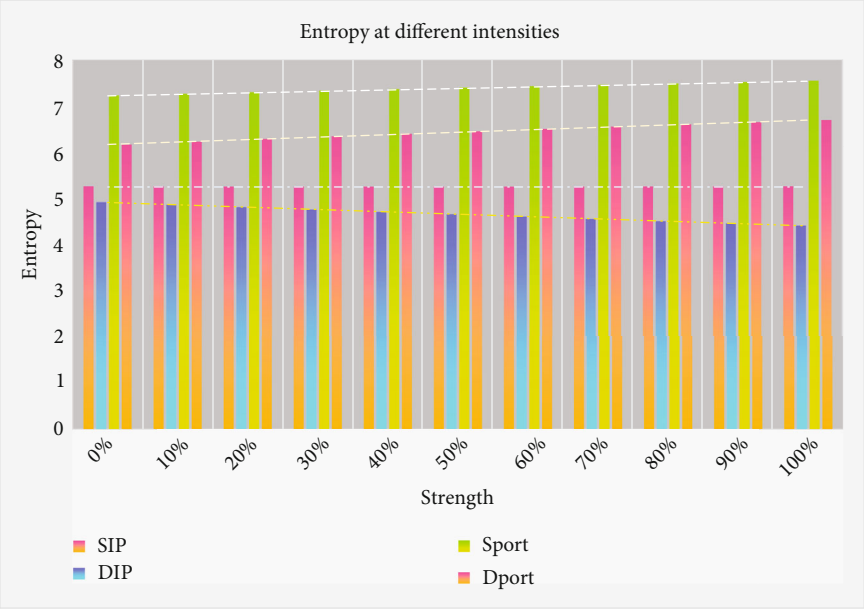

Figure 3: Information entropy change trend of each element of the network quaterniple.

Table 4: Rate of entropy change of each element.

Iterm Growth rate	SIP	DIP	Sport	Dport
0%	0.000000%	0.000000%	0.000000%	0.000000%
10%	0.044647%	1.068329%	0.486537%	0.992993%
20%	0.032722%	1.078559%	0.472513%	0.949702%
30%	0.021653%	1.085034%	0.459224%	0.909566%
40%	0.011374%	1.088528%	0.446616%	0.872272%
50%	0.001823%	1.089631%	0.434637%	0.837547%
60%	0.007054%	1.088804%	0.423245%	0.805150%
70%	0.015308%	1.086411%	0.412396%	0.774867%
80%	0.022985%	1.082742%	0.402056%	0.746510%
90%	0.030129%	1.078032%	0.392188%	0.719911%
100%	0.036776%	1.072471%	0.382764%	0.694922%
Geometric average	0.016812%	1.081832%	0.429955%	0.824970%

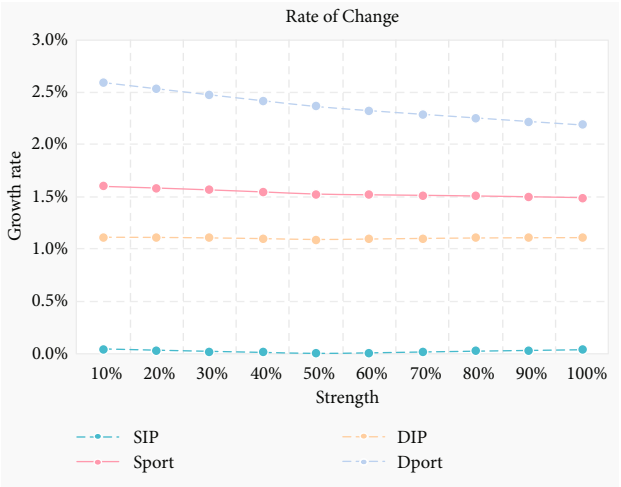

Figure 4: The entropy change trend of each element.

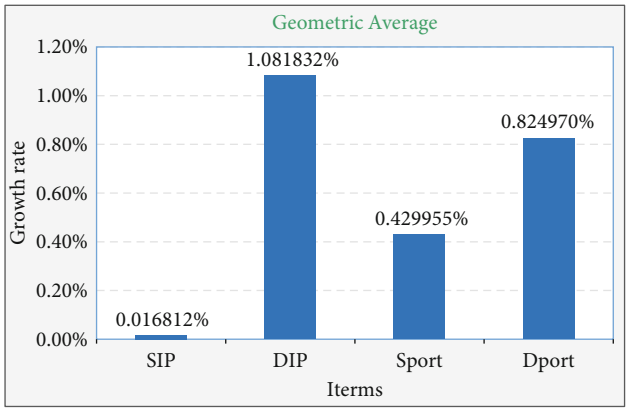

Figure 5: Geometric rate of entropy of each element.

Table 5: Judges the network tetriple information entropy after matrix accumulation.

Iterms Strength	SIP	DIP	Sport	Dport
0%	0.266096	1.742815	1.098289	2.808651
10%	0.265978	1.724196	1.103633	2.836540
20%	0.265891	1.705599	1.108848	2.863479
30%	0.265833	1.687093	1.113940	2.889524
40%	0.265803	1.668728	1.118915	2.914729
50%	0.265798	1.650545	1.123778	2.939141
60%	0.265817	1.632574	1.128534	2.962806
70%	0.265857	1.614838	1.133188	2.985763
80%	0.265918	1.597353	1.137744	3.008052
90%	0.265999	1.580133	1.142206	3.029708
100%	0.266096	1.563187	1.146578	3.050762

the weighted entropy of the data stream is comprehensively calculated, and the formula is defined as

$$H(x) = \sum_{j=1}^{k}\left(-\sum_{i=1}^{n} pi \log 2pi\right). \tag{3}$$

3.2. Evaluation of NTP Attack Packet Value Based on Judgment Matrix Analytic Hierarchy Process

3.2.1. AHP. Analytic Hierarchy Process, AHP [10], is proposed by Saaty, an American operational research scientist. It combines subjective and objective evaluation to simplify the problem and draw the final conclusion. AHP is divided into two steps. The first step is to compare the influencing factors to form a judgment matrix. The second step is to solve the matrix eigenvector to obtain the priority weight and finally calculate the final weight.

3.2.2. Construct Judgment Matrix. The idea of the model is to substitute the network quadruple into the analytic hierarchy process, determine the importance of each element according to the impact of each element on the target attack, and then calculate the value relative relationship of various messages [11]. Based on this, the importance of the network quadruple value evaluation is compared in pairs. Measured on the scale of $1 \sim 9$, the importance of the quadruple is shown in Table 1.

According to the above table, the judgment matrix is obtained:

$$H = \begin{bmatrix} h & h1 & h2 & h3 & h4 \\ h1 & 1 & \frac{3}{7} & \frac{1}{3} & 3 \\ h2 & \frac{7}{3} & 1 & \frac{7}{9} & 7 \\ h3 & 3 & \frac{9}{7} & 1 & 9 \\ h4 & \frac{1}{3} & \frac{1}{7} & \frac{1}{9} & 1 \end{bmatrix}, \tag{4}$$

$$Mi = \prod_{j=1}^{4} bij, \tag{5}$$

$$\varpi i = \sqrt[4]{Mi}, \tag{6}$$

$$\omega i = \frac{\varpi_i}{\sum_{j=1}^{4} \varpi j}. \tag{7}$$

According to formulas (5), (6), and (7):

$$M = \begin{bmatrix} 0.4286 \\ 12.7037 \\ 34.7143 \\ 0.0053 \end{bmatrix}, \varpi_i = \begin{bmatrix} 0.8091 \\ 1.8879 \\ 2.4273 \\ 0.2698 \end{bmatrix}, \omega_i = \begin{bmatrix} 0.15 \\ 0.35 \\ 0.45 \\ 0.05 \end{bmatrix}. \tag{8}$$

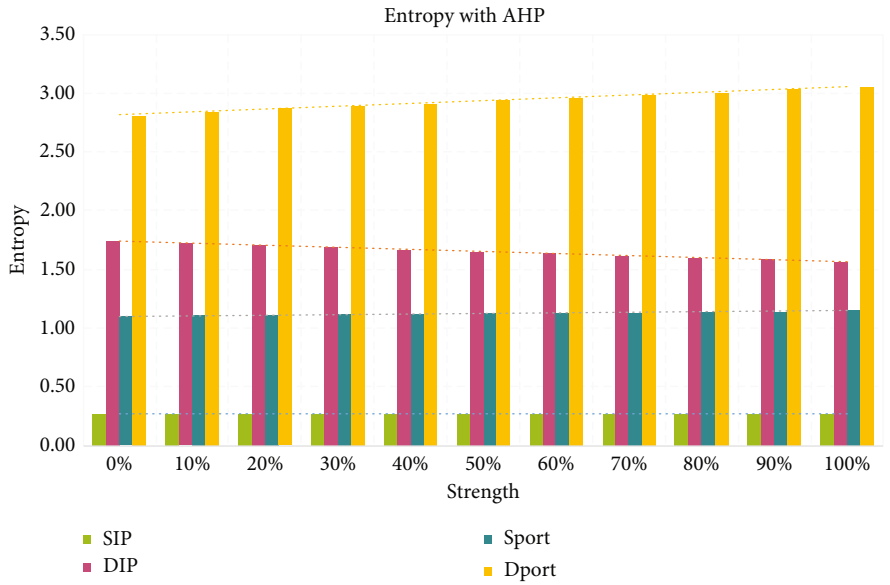

Figure 6: Entropy change diagram after judging the product within the matrix.

Table 6: Comparison plot of the percentage of difference values.

Iterm Strength	DIP	Dport	With AHP
10%	5.319715%	6.197713%	5.197110%
20%	5.313274%	5.986372%	5.083698%
30%	5.287525%	5.787827%	4.970123%
40%	5.246994%	5.601004%	4.857426%
50%	5.195139%	5.424940%	4.746328%
60%	5.134632%	5.258774%	4.641077%
70%	5.067563%	5.101731%	4.538899%
80%	4.995581%	4.953113%	4.439070%
90%	4.919995%	4.812289%	4.341750%
100%	4.841850%	4.678687%	4.247034%

Verification:

$$\sum_{i=1}^{4} \omega_i = 1. \tag{9}$$

Calculate the maximum eigenvalue of the judgment matrix and normalize the fourth-order matrix:

$$kj = \sum_{i=1}^{4} H(i,j), j = 1,2,3,4. \tag{10}$$

Constructing a fourth-order matrix K:

$$K(i,j) = \frac{H(i,j)}{hj}, \tag{11}$$

$$K = \begin{bmatrix} 0.15 & 0.15 & 0.15 & 0.15 \\ 0.35 & 0.35 & 0.35 & 0.35 \\ 0.45 & 0.45 & 0.45 & 0.45 \\ 0.05 & 0.05 & 0.05 & 0.05 \end{bmatrix}. \tag{12}$$

Construct normalized matrix ω:

$$\omega(j,1) = \sum_{j=1}^{4} B(1,j), \tag{13}$$

$$\omega = \begin{bmatrix} 0.15 \\ 0.35 \\ 0.45 \\ 0.05 \end{bmatrix}, A\omega = \begin{bmatrix} 0.6 \\ 1.4 \\ 1.8 \\ 0.2 \end{bmatrix}, \tag{14}$$

$$\lambda = \frac{1}{4} \times \left(\frac{0.6}{0.15} + \frac{1.4}{0.35} + \frac{1.8}{0.45} + \frac{0.2}{0.05} \right) = 4. \tag{15}$$

Calculate Cr and verify consistency:

$$\mathrm{CI} = \frac{\lambda - n}{n-1} = \frac{4-4}{4-1} = 0, \text{Fourth order matrix } RI = 0.9, \tag{16}$$

$$\mathrm{CR} = \frac{\mathrm{CI}}{\mathrm{RI}} = 0. \tag{17}$$

Because CR < 1, the constructed matrix meets the consistency verification, and the weight of each criterion is

$$\omega = (\omega 1, \omega 2, \omega 3, \omega 4) = (0.05, 0.35, 0.15, 0.45). \tag{18}$$

As shown in Table 2.

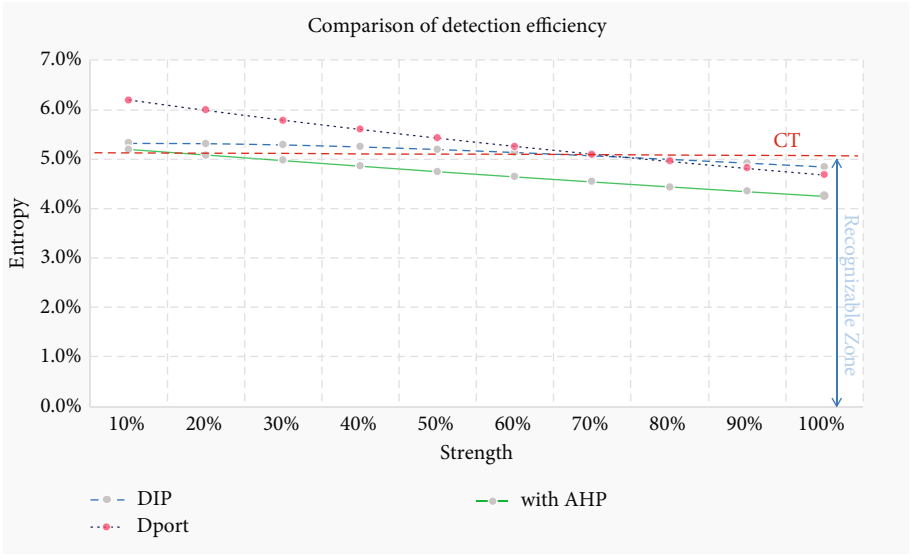

Figure 7: Detection of efficiency comparison.

3.2.3. Network Quad Message Value Calculation. According to Table 2, the normalized quadruple information entropy score can be obtained:

$$Y = [\text{SIP}, \text{DIP}, \text{SPORT}, \text{DPORT}]. \tag{19}$$

Compare s with the evaluation weight calculated in the table ω. The final value of data message can be calculated by inner product and accumulation:

$$V = \sum_{i=1}^{4} si * \omega i = \sum[\text{SIP}, \text{DIP}, \text{SPORT}, \text{DPORT}] \times (0.05, 0.35, 0.15, 0.45). \tag{20}$$

4. Simulation Experiment

4.1. Experimental Environment. The simulated experimental environment is carried on the server Intel(R) Core(TM) i7-7700HQ, RAM 48 G, UBUNTU16.04 operating system device, because Mininet [12, 13] is a very reliable tool, it is a process virtualization network simulation tool developed by Stanford University based on Linux container architecture. It can create a virtual network including host, switch, controller, and link, we installed this tool to simulate the attack environment. The network topology is shown in Figure 2.

Among them, one server is attacked and NTP service is enabled, and 40 PCs are reflective attack devices, which can also generate normal network traffic under different attack intensities.

4.2. Sensitivity of Quantitative Analysis. In the simulation experiment, the attack intensity increased from 0% to 100%, by 10% per $\triangle t$, using wireshark to calculate the network quaterniple flow table F < source IP address (Sip), destination IP address (Dip), source port (Sport), destination port (Dport) > entropy value at different attack intensities, as shown in Table 3.

As can be seen from the table, the information entropy of the nonlinear increase of the attack intensity, as shown in Figure 3.

We used geometric rates of change to quantitatively describe the magnitude of variable variation in unit time, with the formula defined as

$$G = \sqrt[n]{\prod_{n=0\%}^{100\%} (|f(\phi n + \Delta\phi)/f(\phi n)|)}. \tag{21}$$

Each element entropy varies at different nonlinear attack intensities, as shown in Table 4.

From the calculated data, we can quantitatively see the trend of each element change rate, as shown in Figure 4.

The geometric change rate of each element is calculated from formula (21) and Table 4, as shown in Figure 5.

4.3. The Information Entropy under the Judgment Matrix. Bring Table 1 into formula (19), and the calculation is shown in Table 5.

It can be seen from the table that, after the weight assignment of the judgment matrix, the entropy trend of the network quaternel information changes significantly under different nonlinear attack intensities, as shown in Figure 6.

4.4. Calculate the Threshold. The threshold can be obtained by comparing the entropy change rate of the quaternel network without attack to the entropy rate of the unacceptable attack strength network. Defines the entropy rate of change threshold:

$$\text{CTE} = \max\left(\sum_{\beta=1}^{4} (|C\alpha\beta\text{-}C\alpha(\beta - 1)|)\right). \tag{22}$$

$\alpha = 1, 2, \cdots \cdots, 10$, it indicates the attack intensity of 10% to 100% of the attack, represents the network quaterniple

elements, C indicates the entropy change rate, and the calculated CTE represents the value with the largest entropy change rate of all attack intensities.

4.5. Attack Recognition Algorithm Comparison. Currently, based on source IP and target IP are the two most common methods to identify NTP attacks, their percentage difference computed absolute values from the method presented here are shown in Table 6.

Put the results of Table 6 into the formula (17):

$$\mathrm{CTE} = 5.083698\%. \tag{23}$$

Judging from the above table:

(i) Based on the detection rate of the target IP method, both from 10% to 60% are higher than the CTE of 5.197110%, that is, if the attack intensity is 60% and below, the method cannot detect the presence of an NTP attack, with a detection rate of 40%

(ii) Based on the detection rate of the target port method, both from 10% to 70% are above the CTE of 5.197110%, that is, if the attack intensity is 70% or below, the method cannot detect the presence of an NTP attack, and the detection rate is 30%

(iii) The detection rate based on the judgment matrix quaterniple method, at 10% above the 5.083698% CTE, and the detection rate of 90%

As shown in Figure 7.

5. Conclusion

This paper presents a NTP nonlinear attack detection method to judge the information entropy of matrix hierarchical analysis. Through simulation experiments, we find the change rules of the entropy of the quartet under different attack strengths, then use the judgment matrix hierarchical analysis method, and then calculate the CTE under the NTP nonlinear attack. Finally, the experimental conclusion is obtained through data comparison, and the proposed method has the highest detection rate. The detection rate of proposed method is 90%, and it has the highest detection rate. In the next step, applying this algorithm to other types of UDP-FLOOD attacks in the context of global outbreaks is the direction of future research.

Data Availability

The data that support the findings of this study are available from the corresponding author upon reasonable request.

Conflicts of Interest

The authors declare that they have no conflicts of interest.

References

[1] *Global DDoS Threat Report in the First Half of 2021*https://view.inews.qq.com/a/20210907A0DQJE00.

[2] Z. H. A. N. G. Xu-bo, H. U. A. N. G. He, and L. I. A. O. Zhang-liang, "Vulnerability analysis of NTP protocol," *Communications Technology*, vol. 53, no. 11, pp. 2806–2810, 2020.

[3] P. Wang, Z. Cai, D. Kim, and W. Li, "Detection mechanisms of one-pixel attack," *Wireless Communications and Mobile Computing*, vol. 2021, Article ID 8891204, 8 pages, 2021.

[4] X. Bao and C. Z. Honghai, *King of destruction DDoS attack and prevention in-depth analysis*, Machinery Industry Press House, Beijing, 2014.

[5] D. I. A. O. Zao-xiang, Z. H. A. N. G. Xiao-ning, and W. A. N. G. Shu-jun, "The vulnerability of NTP under forged server attack," *Electronic Information Warfare Technology*, vol. 11, no. 6, pp. 67-68, 2016.

[6] T. PENG, C. LECKIE, and K. RAMAMOHANARAO, "Detecting reflector attacks by sharing beliefs," in *GLOBECOM '03. IEEE Global Telecommunications Conference (IEEE Cat. No.03CH37489)*, pp. 1358–1362, San Francisco, CA, USA, 2004.

[7] C. JIN, H. WANG, and K. SHIN, "An effective defense against spoofedtraffic," in *ACM International Conference on Computer and Communications Conference Security*, pp. 30–41, Washington D.C., 2003.

[8] K. OHTA and A. YAMAMOTO, "Detecting DRDoS attacks by a simple response packet confirmation mechanism," *Computer Communications*, vol. 31, no. 14, pp. 3299–3306, 2008.

[9] M. H. Bhuyan, D. K. Bhattacharyya, and J. K. Kalita, "An empirical evaluation of information metrics for low-rate and high-rate DDoS attack detection," *Pattern Recognition Letters*, vol. 51, pp. 1–7, 2015.

[10] T. Saaty, "How to make a decision: the analytic hierarchy process," *European Journal of Operational Research*, vol. 48, no. 1, pp. 9–26, 1990.

[11] Y. U. E. Qiaoli, L. V. Wanbo, H. U. Weihong, and Z. H. A. N. G. Haikuo, "Mitigating DDoS attack based on DNS response value assessment," *Netinfo Security*, vol. 19, no. 9, pp. 56–60, 2019.

[12] N. Dayal, P. Maity, S. Srivastava, and R. Khondoker, "Research trends in security and DDoS in SDN," *Security & Communication Networks*, vol. 9, no. 26, pp. 6386–6411, 2016.

[13] Z.-M. Wang, J.-Y. Tian, J. Qin, H. Fang, and L.-M. Chen, "A few-shot learning-based Siamese capsule network for intrusion detection with imbalanced training data," *Computational ntelligence and Neuroscience*, vol. 2021, article 7126913, 17 pages, 2021.

Hindawi
Wireless Communications and Mobile Computing
Volume 2022, Article ID 2142745, 12 pages
https://doi.org/10.1155/2022/2142745

Research Article

Digital Technology Boosting Agricultural Supply-Side Constitutive Revolution in Poor Areas Based on the Intelligent Environment of the Internet of Things

Hong Wang,[1] Chengying Yang ,[2,3] and Xuetao Li[1]

[1]*School of Economics and Management, Hubei University of Automotive Technology, Shiyan, 442000 Hubei, China*
[2]*School of Management, Universiti Sains Malaysia, Penang 11800, Malaysia*
[3]*School of Science, Hubei University of Automotive Technology, Shiyan, 442002 Hubei, China*

Correspondence should be addressed to Chengying Yang; yangchengying@student.usm.my

Received 27 December 2021; Revised 9 February 2022; Accepted 24 February 2022; Published 11 March 2022

Academic Editor: Mohamed Elhoseny

China is a big agricultural country, and China's agricultural development is related to the development of the country. Especially in poor rural areas, the development of agriculture still stays at low-level manual farming. Therefore, with the help of the developed Internet of Things technology, it is necessary for digital technology to develop and reform the rural areas in poverty-stricken areas. This paper aims to promote the supply-side structural revolution of agriculture in poverty-stricken areas by digital technology based on intelligent environment of Internet of Things. Firstly, the KNN intelligent algorithm is improved to improve the accuracy and reduce the time complexity. Then, based on the data support of Internet of Things technology, a prediction model is built, and the parameters are optimized by particle swarm optimization, and finally the best prediction model with high prediction accuracy, good stability and reduced prediction time complexity is obtained. Taking the source area of the Danjiang River in the South-to-North Water Transfer Project as the research object, the total grain output and soybean production demand in this area from 2010 to 2018 were selected, and the change trend of soybean production and demand in this area from 2019 to 2021 was predicted. The experimental data show that the soybean output in this region has increased year by year, with a cumulative increase of 6,985.4 tons from 2010 to 2018. Soybean output sometimes exceeds demand, and sometimes it is less than demand. There will be an oversupply situation in 2019 and 2021, and an oversupply situation in 2020. Therefore, the prediction model of Internet of Things can effectively predict the supply and demand situation of soybean with an accuracy rate of over 90%, which can provide data support for the decision-making of structural change of agricultural supply side in poverty-stricken areas.

1. Introduction

The transformation of agricultural development mode is also an important measure to break the plight of agricultural development and promote agricultural development [1]. It can promote the sustainable development of agriculture, improve the quality and market competitiveness of agricultural products, and accelerate the process of agricultural modernization [2]. In a smart environment of the IoT, the continuous development of digital technology has brought a huge impact on agricultural development. This kind of influence has advantages and disadvantages. Studying how to transform this influence into a driving force for revolution is of great significance for promoting agricultural development and accelerating agricultural modernization.

In order to promote the constitutive revolution of the agricultural supply side, improve the level of agricultural development and farmers' living standards, and create a sustainable, stable and healthy development path for modern agriculture, this article takes the Danjiang water source area of the South-to-North Water Diversion Project as the research object and conducts research based on digital technology in the intelligent environment of the IoT. The innovation points are as follows: (1) Improve the classic KNN

algorithm to make it have higher accuracy and lower time complexity. (2) Based on the big data technology and the IoT technology, an improved KNN algorithm is used to establish a forecasting model for the supply and demand of agricultural products, which has a good fitting result. (3) Use the model created in this study to successfully predict soybean yield and demand in a certain area and make policy recommendations for supply and demand.

Firstly, this paper introduces the agricultural supply side, and briefly introduces the Internet of Things, and then improves the KNN intelligent algorithm, which improves the accuracy and reduces the time complexity. Then, the digital technology and its algorithm are described in detail, and the realization of the algorithm is represented by formulas and flow charts. Finally, through the algorithm optimization parameters, taking the source area of the Danjiang River in the South-to-North Water Transfer Project as the research object, the total grain output and soybean production demand in this area from 2010 to 2018 are selected, and the change trend of soybean production and demand in this area from 2019 to 2021 is predicted.

2. Related Work

Poverty alleviation through agricultural policies in poor areas has always been the focus of domestic research in related fields. Li Y conducted a nationwide survey of 2,075 households in 22 poverty-stricken counties in 13 provinces, provided rich statistical data and evidence for his thesis, and used the literature to review the history of poverty alleviation in China's agricultural areas [3]. The year of Gan X research data is too early, and it is of little significance to refer to the rapid development of science and technology. The emergence of big data technology and IoT technology has given new ideas for agricultural research [4]. Ruan J combines granulation technology with genetic algorithm (GA) and support vector machine (SVM) to propose a granular GA-SVM. In the comprehensive predictor, three granular methods are introduced. He decomposed the big data in the agricultural network physical system into small granularity and used genetic algorithm to find the optimal value of SVM penalty parameter and kernel parameter from the reduced particles [5, 6]. Their researches are very important for reference, but the influencing factors considered in the simulation experiments are not comprehensive enough.

3. Digital Technology and Agricultural Supply-Side Constitutive Revolution

3.1. Agricultural Supply-Side Constitutive Revolution

3.1.1. The Need for Revolution. The constitutive revolution of the agricultural supply side is to solve the constitutive imbalance in the agricultural sector. Agricultural constitutive problems and contradictions have become increasingly prominent, and the upgrading of the consumption structure has led to changes in the supply and demand relationship of agricultural products [7]. Some agricultural products are in oversupply, but high-quality green agricultural products are in short supply. Effective supply cannot meet the ever-increasing demand, and the grain production structure has changed. The output of products with high demand is reduced, while the output of products with low demand is increasing. Agricultural costs remain high, and the domestic prices of most agricultural products are higher than international levels. And a large amount of surplus of agricultural products will lead to increased financial pressure on the country. Therefore, constitutive revolutions on the agricultural supply side must be implemented.

The constitutive revolution of the agricultural supply side conforms to the laws of agricultural development at this stage. The internal and external structures and characteristics of agricultural development at each stage are different. When there are contradictions and conflicts between the internal and external structures and characteristics, the development of agriculture will be stagnant or even crisis. At the current stage, the original backward development mode of agriculture must be changed, so it is necessary to promote the constitutive revolution of the agricultural supply side. Pursue an efficient, safe and green modern agricultural production method, adapt the internal structure of agriculture to the new requirements of development, and promote the self-repair and adaptation of agriculture [8, 9]. Persist in constitutive revolutions on the agricultural supply side and cultivate new types of agriculture.

3.1.2. Basic Content of Revolution. The constitutive revolution of the agricultural supply side is not only the adjustment of the economic structure and the transformation of the development mode but also a revolution that combines the characteristics of the agricultural field. Carry out production around consumer demand, improve the adaptability of the supply structure of the agricultural product market, and optimize the allocation of resources [10–12].

The primary task of the constitutive revolution on the agricultural supply side is to solve the problem of food supply, which is a necessary foundation for economic development. Not only to meet consumer demand but also to ensure food security. On the premise of ensuring food security and effective supply, according to regional characteristics, adjust the structure of agricultural products according to local conditions to achieve the maximum benefit of resource allocation [13]. When adjusting the supply and demand structure, we must follow the objective laws of economic development to achieve sustainable agricultural development.

Constitutive revolutions on the agricultural supply side need to improve the quality of agricultural products, strengthen the safety and quality supervision of agricultural products, and use modern technology to strengthen the supervision of all links from production to sales of agricultural products to ensure their safety. At the same time, we must eliminate low-end products, provide more green organic foods, adapt to the transformation and upgrading of agricultural structure, and create high-quality agricultural products brands.

The constitutive revolution of the agricultural supply side should also promote the integration of primary,

secondary, and tertiary industries in rural areas and coordinate their development [14]. Promote the upgrading and construction of processing links and circulation facilities for agricultural products. Develop the tertiary industry in the rural areas, extend the industrial chain, improve the mechanism for linking farmers' interests, and generate income for farmers.

3.1.3. Ways to Realize Revolution. The constitutive revolution of the agricultural supply side is not simply to adjust the types and quantities of agricultural products but to better meet the high-level needs of consumers and improve the competitiveness of agricultural products. Therefore, constitutive revolutions on the supply side must be carried out from multiple perspectives to achieve the goal [15].

Stimulate the vitality of agricultural and rural development and continue to deepen various rural revolutions. Deepen the revolution of the rural collective property rights system, ensure the rights of farmers, and clarify the ownership of rural collective assets. Accelerate the establishment of a complete new management system and cultivate new agricultural management and service entities. Improve the agricultural support and protection system, improve the mechanism for continuous growth of agricultural investment, guide financial investment, and implement an agricultural insurance system. Promote the overall development of urban and rural areas, make up for shortcomings in rural development, and achieve a balanced allocation of urban and rural resources. Strengthen and innovate rural social governance, improve the level of rural grassroots management, build a service-oriented government, and improve the level of villager autonomy.

Promote the green development of agriculture and promote the construction of modern ecological circular agriculture pilot projects. Do a good job in the prevention and control of agricultural pollution, reduce agricultural water waste and fertilizer pollution, and increase the utilization rate of agricultural waste. Increase the treatment of existing problems in the agricultural ecological environment and repair the damaged agricultural ecology. Promote the conversion of farmland to forests and grassland, and implement a system of cropland rotation and fallow. At the same time, according to the actual situation in different regions, starting from environmental issues, we will build modern ecological agriculture development models in different regions.

Ensure the quality and safety of food and carry out the construction of a national agricultural product quality and safety demonstration zone. Improve the level of supervision and improve relevant laws and regulations on agricultural security. Develop a green and sustainable agricultural economy, realize energy conservation and emission reduction, and promote the standardization of agricultural production. Strengthen law enforcement and improve market access and risk control management systems. Strengthen the construction of organizational leadership system and strengthen policy support.

3.2. Targeted Poverty Alleviation in the Context of Agricultural Supply-Side Constitutive Revolutions

3.2.1. The Link between the Agricultural Supply Side and Targeted Poverty Alleviation. This measure of targeted poverty alleviation meets the requirements of agricultural supply-side constitutive revolutions. The poverty alleviation work involves improving people's livelihood and developing the economy, and it also coincides with the strategy of supply-side revolution. Insufficient effective supply is the main constitutive problem in the economic system. The important goal of advancing supply-side revolution is to make up for the shortcomings of development and improve people's living standards [16]. The issue of agriculture, rural areas, and farmers is the shortcoming of economic development. The consumption power of poor areas is low, but the consumption margin of poor people is relatively high. More energy must be devoted to improving rural infrastructure, improving the level of regional public services, adjusting the rural industrial structure, and increasing employment opportunities. From the perspective of supply and demand, doing a good job in targeted poverty alleviation can effectively promote constitutive revolutions on the agricultural supply side.

Targeted poverty alleviation requires constitutive revolutions on the agricultural supply side. The utilization rate of poverty alleviation funds in rural areas is not high, because some areas have failed to reasonably study the poverty status in order to obtain quotas in poor areas and cannot accurately implement specific poverty alleviation projects [17]. The supply-side constitutive revolution should optimize the supply pattern of poverty alleviation when adjusting the structure, increase effective supply and improve the quality of supply, and increase the utilization rate of targeted poverty alleviation funds. When carrying out industrial poverty alleviation, it is necessary to guarantee the funds provided for poverty alleviation and ensure that the funds are used in place. Therefore, the constitutive revolution of the agricultural supply side can solve the problem of the imbalance between supply and demand for poverty alleviation solved by precision poverty alleviation and play a supporting role.

Construct a capital supply end focusing on policy loans. Because there are many targets for poverty alleviation and the government is under greater financial pressure, it is possible to appropriately introduce capital from policy banks to provide funds for targeted poverty alleviation. Policy capital can first inflow capital into poverty-stricken areas that require investment in order to improve the economic and social development of the poverty-stricken areas, without first considering whether it is profitable. These policy capitals can guide social funds to flow to poor areas.

Build a funding supply end focusing on poverty alleviation projects. We are currently in the stage of comprehensive poverty alleviation. In this stage, poverty alleviation is very complicated. An important part of poverty alleviation is various poverty alleviation projects. Joint policy banks and government departments to contact poverty alleviation projects and poor households. The government and policy banks use

funds to support poverty alleviation projects, activate poverty alleviation projects, and increase income for poor households.

3.2.2. Implementation Methods of Precision Poverty Alleviation. Improve the rural financial organization system and enhance the supply capacity. Speed up the development of rural service finance and effectively supply poverty alleviation funds for agricultural production. Carry out diversified poverty alleviation, integrate multiple financial capital into the rural poverty alleviation capital market, and create multiple channels for rural poverty alleviation. Strengthen rural mortgage loans and integrate into the coordination of the insurance industry.

Improve the rural financial risk protection mechanism. Improve credit protection in rural areas and expand information sharing in rural credit. Promote related product evaluation activities to encourage farmers' credit level. Establish and improve the structure of risk compensation, issue more loan lines to Mingmin, and establish a loan disposal system involving multiple financial institutions. Strengthen coordination with the insurance industry to reduce the harm of risk accidents.

Change service concepts and innovate rural financial service products and service methods. Promoting the rapid development of rural financial services on the Internet can reduce the cost of agricultural development and solve the problem of high financing costs in rural areas. Promoting rural information exchange and mobile platform information sharing can ensure the healthy and stable growth of agriculture-related industries.

Improve the overall quality and cultural level of agricultural subjects. Farmers have insufficient financial awareness, insufficient awareness of risk resistance, and lack of initiative to participate in rural finance [18, 19]. Therefore, it is necessary to improve the training mechanism to improve farmers' understanding of financial knowledge. Strengthen the financial management education of village cadres and guide farmers to effectively distinguish illegal and fraudulent activities. Carry out relevant knowledge lectures to enable farmers to master more financial knowledge and enhance their credit awareness. Establish a monitoring system and feedback system with a high degree of participation of farmers, and maintain a good rural financial environment.

3.3. Digital Technology

3.3.1. Agricultural Big Data. Agricultural big data takes the agricultural field as the core and integrates data under the macroeconomic background, including data on production, import and export, and prices. From a geographical point of view, agricultural big data takes domestic data as the core and international agricultural data as a reference. Domestic data is even more detailed to provincial and municipal data, providing reference for precise regional research [20]. In addition to statistically accurate data, it also includes information on agricultural economic entities, investment information, and mass media information. The realization of agricultural big data must first construct and integrate professional data resources in the agricultural field, and then make an orderly plan for the professional sub-field data resources.

The application of agricultural big data is very wide, mainly in agricultural situation monitoring, agricultural product monitoring and early warning, agricultural decision-making, and the establishment of rural integrated information service system [21, 22]. Agricultural situation monitoring is to monitor changes in the farmland environment, crop yields, and natural disasters, and to predict changes in the natural environment such as climate one step in advance. By analyzing and collecting weather-related data, combining elements such as weather simulation and land analysis, the accuracy of natural disaster prediction is enhanced. A combination of remote sensing technology and crop simulation technology is used to monitor the growth of crops and estimate their yields.

Agricultural big data provides data support for agricultural product market monitoring and early warning, and related technologies are also conducive to the comprehensive collection of agricultural product information, which makes agricultural product quality monitoring more accurate. Big data processing technology has real-time nature. Once a problem occurs in agricultural products, it can be controlled in time to prevent its scope of influence from expanding and improve the efficiency of the early warning mechanism [23]. Faster data acquisition can speed up the flow of agricultural product market information and reduce the risk of asynchrony of information.

3.3.2. Agricultural IoT. The emergence of the agricultural IoT has promoted the development process of agricultural informatization and modernization and promoted the application of precision agriculture. The structure of the agricultural IoT is generally divided into the perception layer, the transmission layer and the application layer [24]. The sensing layer is distributed with a large number of sensing devices, such as sensors and video collectors, which can accurately collect relevant information of farmland. The transmission layer uses a variety of information transmission methods such as wireless sensor networks for data transmission to promote the diversified transmission of agricultural information. The application layer gathers a large amount of data, processes it, and uses artificial intelligence operation terminals to accurately manage and regulate agricultural production.

When the agricultural IoT works normally, both the transmission layer and the perception layer need to use spectrum. The sensor node collects data and then transmits it at a low rate. Commonly used communication technologies include ZigBee technology and Wi-Fi technology [11]. Real-time monitoring of high-definition cameras requires high-speed communication. Commonly used communication technologies include WiMax technology and ultra-wideband technology.

The function of the transport layer is to transmit data information and command information of the IoT. The wireless communication technologies commonly used at present include cellular mobile communication technology

and broadband wireless access technology. When the number of working nodes in the perception layer is small, the spectrum resources used by the communication technology can meet the requirements for correct data transmission. If the number of working nodes in the sensing layer increases, the available spectrum resources will be tight, and the failure rate in transmission will increase, resulting in the inability to obtain work information in time. IoT agriculture is shown in Figure 1.

3.3.3. KNN Algorithm. The changes in the supply and demand of agricultural products have obvious characteristics of time series. Time series are natural sorting sequences. The IoT prediction model established based on this format can predict future values through existing observations [25]. Generally, linear graphs are often used to visually analyze time series. There are many IoT prediction models for time series, and neural network algorithms, support vector machines, Bayesian algorithms, and nearest neighbor algorithms are often used [26].

The nearest neighbor algorithm (KNN) performs predictive analysis by comparing the similarity between the prediction tuple and the training tuple. The training tuple is described by n attributes and has a known classification label. Each training tuple is a function of n-dimensional space, as shown in Formula (1):

$$f(Y) = f(y_1, y_2, \cdots, y_n). \tag{1}$$

Among them, $f(Y)$ is the classification label, and $y_1, y_2, \cdots y_n$ represents the attribute value. In this way, all training tuples are stored in the n-dimensional pattern space. When predicting a certain prediction tuple, because the prediction tuple has the same format as the training tuple. The KNN algorithm will find the k training tuples that are closest to the unknown tuple in the pattern space. These k tuples are the position tuple and the k nearest neighbors. The similarity is calculated using the Euclidean distance formula, as shown in Formula (2):

$$dist(Y_1, Y_2) = \sqrt{\sum_{i=1}^{n} (y_{1i} - y_{2i})^2} \tag{2}$$

Calculating the two tuples $Y_1 = (y_{11}, y_{12}, \cdots, y_{1n})$ and $Y_2 = (y_{21}, y_{22}, \cdots, y_{2n})$, the smaller the calculated similarity measure, the higher the similarity.

Although the KNN algorithm is a classic predictive model algorithm, it also has some problems. The Euclidean distance formula is used to measure similarity. Each attribute value is assigned the same weight. Therefore, once there is noisy data or different attribute values have different values, it will seriously affect the prediction accuracy. When selecting the value of k, it needs to be determined experimentally. The prediction error of the training tuple is evaluated from $k = 1$. With the continuous change of the value of k, the value of k with the smallest training error is selected to construct the IoT prediction model. It is highly complex, time-consuming, and requires user guidance. Therefore, the KNN algorithm needs to be improved in this research.

3.3.4. Deep Learning Algorithm. Machine learning is to learn through algorithms, so that the machine can draw rules from a large amount of historical data, so as to intelligently identify and automatically judge new samples. In 2003, Bengio et al. proposed the word vector method, using neural networks to build language models. Subsequently, many researchers proposed different word vector training models on this basis. In 2008, the American researchers Collobert and Weston of NEC Lab began to adopt the structure of word vector and multilayer one-dimensional convolution for four typical natural language processing: part-of-speech tagging, sentence segmentation, named entity recognition, and semantic role tagging. Domain issues. They used the same model for different tasks and achieved results comparable to classic algorithms in terms of accuracy (Collobert and Weston 2008). In 2009, the SemanticHashing method proposed by Salakhutdinov et al. applies deep learning to the field of text understanding and analysis. This method implicitly obtains the semantic connection between words in the large-scale text reconstruction training process, so that the feature mapping more reasonable. With the rise of deep neural networks in recent years, people have begun to try to use deep learning methods to solve the problem of text classification. Since Word2Vec in 2013, deep learning has developed rapidly in the field of natural language processing. At present, most of the natural language processing tasks that have achieved important results are in the category of text understanding, such as text classification, machine translation, document summarization, and reading comprehension. The network structure of the convolutional neural network is shown in Figure 2.

The most widely used application of deep learning is convolutional neural networks. Convolutional neural network is a multilayer neural network, each layer in the network is a transformation, commonly used convolution transformation and pooling transformation, each transformation is another feature expression of the input feature; each layer is composed of multiplelayer. It consists of a two-dimensional plane, which is composed of five parts: input layer, convolution layer, downsampling layer, fully connected layer, and output layer.

(1) Input layer: as shown in Figure 2, the input layer of the convolutional neural network is a word vector file, in which the figure shows a part of the screenshot of the matrix in which all words in the data set are arranged in sequence (from top to bottom), if the matrix is $n \times k$, it means that there are n words in the file, and the dimension of the vector is k

(2) Convolutional layer: the input layer obtains several feature images through the convolution operation of the convolutional layer. If the size of the convolution window is $h \times k$, then h represents the number of vertical words, and k represents the dimension of the word vector number. Through a certain size

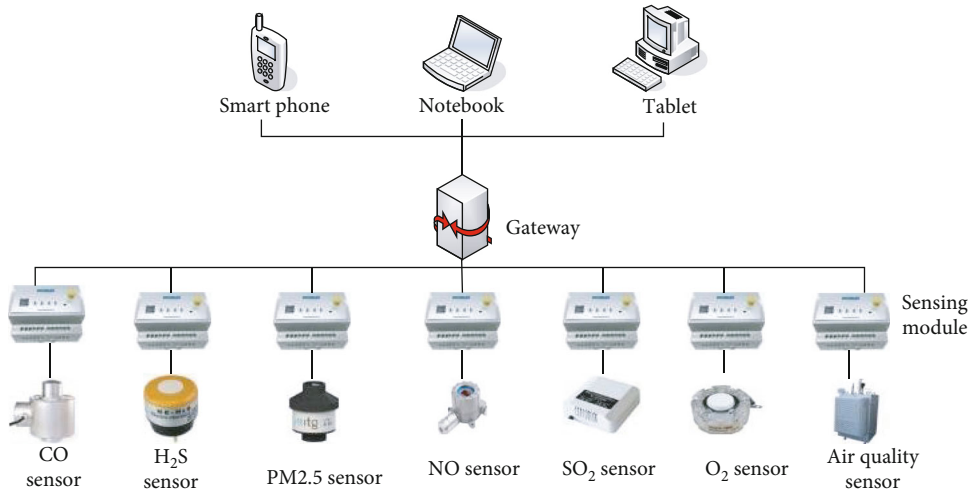

Figure 1: IoT agriculture.

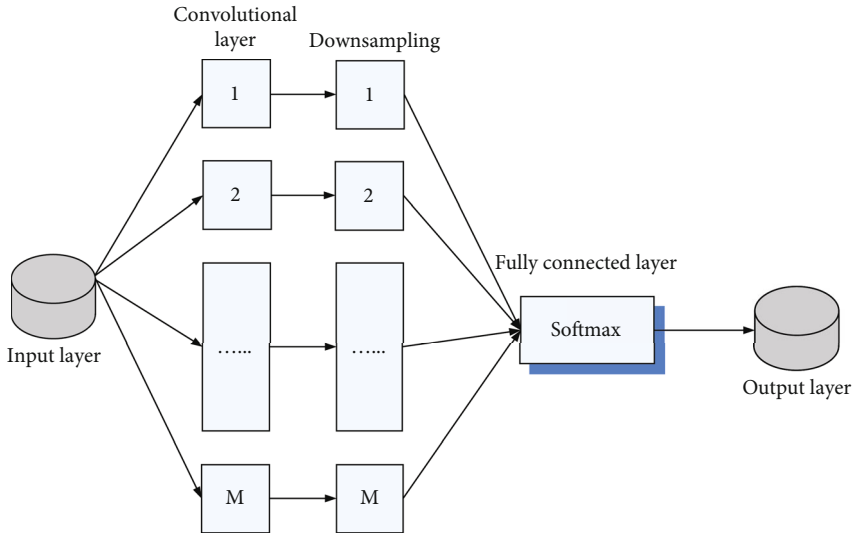

Figure 2: Network structure of convolutional neural network.

of the convolution window, a number of feature images with a column number of 1 will be obtained

(3) Downsampling layer: next is the downsampling layer. The output of the final downsampling layer is the maximum value of each feature image, that is, a one-dimensional vector

(4) Fully connected layer: the output of the one-dimensional vector of the downsampling layer is connected to a Softmax layer in a fully connected way

(5) Output layer: output classification probability

4. Experiments on Algorithm Improvement and Prediction Model Establishment

4.1. KNN Algorithm Improvement. In order to improve the accuracy of prediction, reduce time complexity, solve the problem of weight distribution, and the selection of k value, the KNN algorithm is improved. The supply and demand of agricultural products have the characteristics of time series. Therefore, when forecasting, the role of attribute values is increasing but not linearly. We regard the attribute value of the prediction sequence as the value of the abscissa of the binomial function, and the weight value as the value of the ordinate, and obtain the Euclidean distance formula of the binomial function, as shown in Formula (3):

$$dist(Y_1, Y_2) = \sqrt{\sum_{i=1}^{n} (ai^2 + bi + c)(y_{1i} - y_{2i})^2}. \quad (3)$$

Among them, a, b, c are all binomial coefficients, and i is the attribute value dimension of the prediction sequence. By combining the Euclidean distance formula and the binomial function, the weight distribution problem of attribute values can be solved.

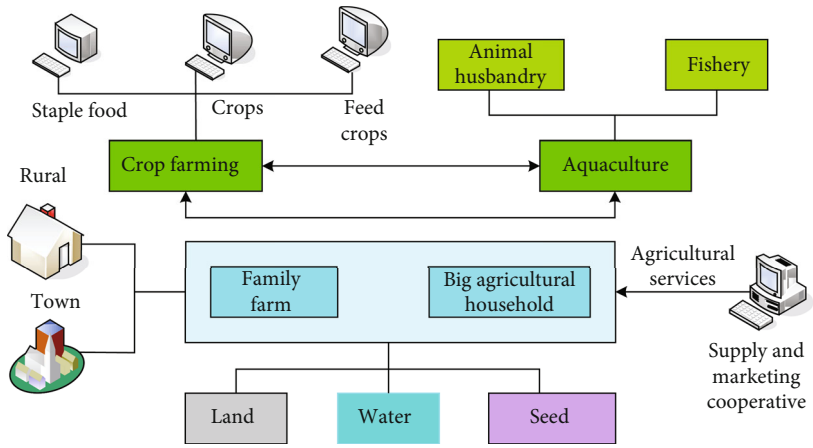

Figure 3: Revolution of the agricultural supply side of the IoT.

4.2. Models for Forecasting the Supply and Demand of Agricultural Products

4.2.1. Data Collection. Take the Danjiang water source area of the South-to-North Water Diversion Project as an example. Soybean production and demand in this area from 2010 to 2018 can be obtained from the agricultural and sideline product database in this area. The amount of data in the database is very large, and the accuracy of the data is also very high. Therefore, it is very conducive to the application of data mining and can provide strong data support for the establishment of the agricultural product supply and demand IoT prediction model for this study.

Due to the large amount of data in the database, the relevant data needs to be imported into the local SQL Server database, and then it can be put into use through further processing and analysis.

4.2.2. Data Preprocessing. There may be omissions in the data collection of the database, such as failure to collect in time during legal holidays. When users perform operations, there may also be improper operations, resulting in data duplication, errors, and missing fields. In order to correct these errors, the data needs to be cleaned up to ensure the practicality and accuracy of the final model. Use a programming language to eliminate duplicate data and deal with errors and missing data. Figure 3 shows the revolution of the agricultural supply side of the IoT. In the greenhouse control system, the temperature sensor, humidity sensor, pH sensor, illumination sensor, CO2 sensor, and other devices of the Internet of Things system are used to detect physical parameters such as temperature, relative humidity, pH value, illumination intensity, soil nutrients, and CO2 concentration in the environment, so as to ensure that crops have a good and suitable growing environment. The realization of remote control enables technicians to monitor and control the environment of several greenhouses in the office. Wireless network is used to measure the best conditions for crop growth.

At the same time, in order to be more intuitive and clear in the analysis, this study uses data cube technology for data integration. The data cube can analyze the collected data from multiple angles, divide it according to the attributes of the supply and demand data of agricultural products, and select the four-dimensional matrix, which are agricultural product output, agricultural product type, time, and demand.

Due to the inconsistent quantification range of the collected data, the output and demand of different types of agricultural products at different times vary greatly. In order to enhance the scalability of the IoT prediction model and accelerate the convergence of the KNN algorithm in this paper, a unified quantization mapping between [0,1] is performed on the data, and the normalization formula is shown in Formula (4):

$$f(e) = \frac{e}{e_{\max} + a}. \tag{4}$$

Among them, e is the demand for the product, $e_{\max}$ is the highest historical demand for the current product collected, and a is a self-defined variable, generally a small value. The value of a in this study is 0.2.

The standardized matrix is

$$S = (S_{ij}) n \times p. \tag{5}$$

Calculate the pairwise correlation matrix P.

$$P = (P_{ij})_{p \times p} = \frac{X^T \times X}{n-1}, (i, j = 1, 2, \cdots, p), \tag{6}$$

Among them

$$P_{ij} = \frac{1}{N-1} \sum_{i=1}^{N} (Y_{ti} - Y_{tj}). \tag{7}$$

4.2.3. Model Establishment. Firstly, we must optimize the parameters of the IoT prediction model, use the improved KNN algorithm in this research to construct the IoT prediction model, and then use the PSO algorithm to optimize the

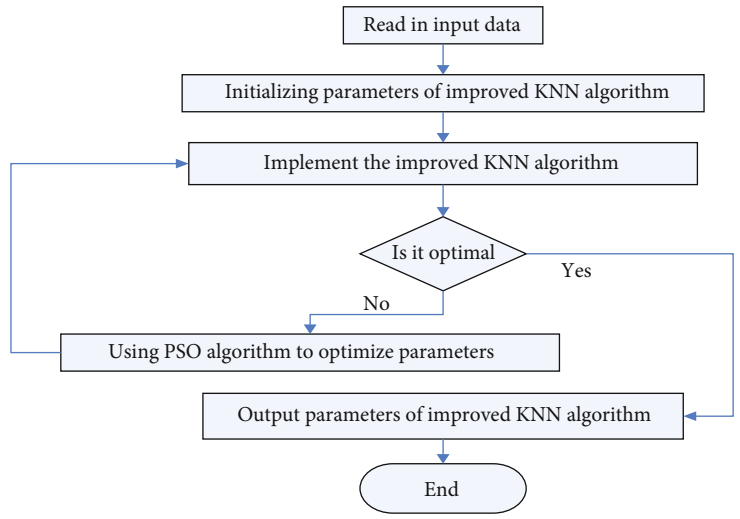

Figure 4: Flow chart of the optimization process of predictive model parameters.

parameters, because it is a random search algorithm based on group cooperation developed by simulating the foraging behavior of birds. It can play a very good role in optimizing parameters, and it plays a significant role in the model and finally get the best IoT prediction model with high accuracy, stability, and reduced prediction time complexity. The process of parameter optimization is as follows:

As shown in Figure 4, optimization is performed according to the process, and the parameters that minimize the training error are selected to establish a forecast model of agricultural product supply and demand based on the KNN algorithm to obtain the predicted value.

5. Discussion on Model Prediction Results

5.1. Improved Algorithm Fitting. In the parameter optimization process, we selected the parameters with the largest training error. After establishing the IoT prediction model, we tested the fitting results of the algorithm. In the experiment, we selected a variety of algorithms to optimize, among which PSO, ant colony algorithm, genetic algorithm, and other common optimization algorithms were compared and analyzed, and finally the best ones were selected for display. The fitting results in an experiment are as follows:

As shown in Figure 5, the improved KNN algorithm has been optimized for parameters, which greatly reduces the time complexity and improves the accuracy of the algorithm compared with the traditional KNN algorithm. It can be seen that the sequence in the figure is very stable. After training and parameter optimization, all the effective information of the time series is retained, which can achieve the optimization effect. Compared with the traditional KNN algorithm, it has more advantages in predicting the supply and demand of agricultural products. Good fitting effect.

5.2. Forecast of Soybean Supply and Demand. This paper selects the data from 2010 to 2018,and selects the data of Danjiangyuan water source of South-to-North Water Transfer Project, so as to reduce the errors of soybean output, soybean trading volume and other data. Narrow the scope to facilitate data tracking, so that the solution is more reliable. However, due to geographical limitations, the forecast results cannot be used as national results. And the data source of the article is the website of regional statistics bureau.

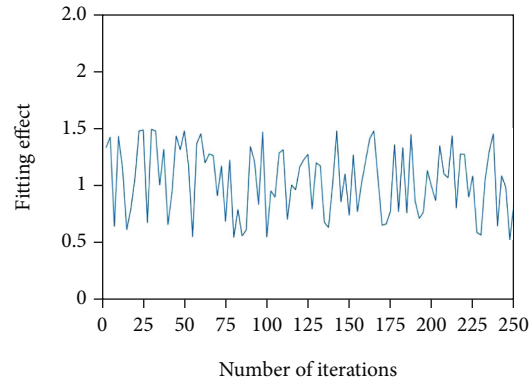

Figure 5: The fitting results of the improved KNN algorithm.

Table 1: Total grain production and soybean production and demand from 2010 to 2018.

Year	Total grain output (ton)	Total yield of soybean(ton)	Soybean trading volume(ton)
2010	46152.4	10174.1	9784.5
2011	45287.3	10818.5	9883.2
2012	47242.7	11402.4	12085.3
2013	49801.4	12133.7	13705.4
2014	50398.8	13584.9	11248.7
2015	52871.5	14705.3	11967.1
2016	54661.7	15412.6	15490.4
2017	57113.9	16591.4	12907.5
2018	60107.7	17159.5	13817.4

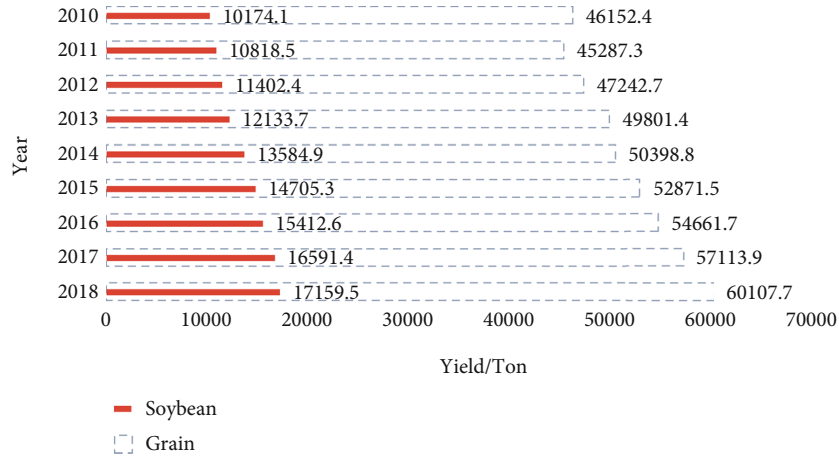

Figure 6: Soybean production and total grain production.

5.2.1. Supply and Demand of Soybeans. Core data of this paper: global soybean output, global soybean import, global soybean export, global soybean crush, and global soybean stock. Taking the Danjiang water source area of the South-to-North Water Diversion Project as the research object, select the total grain output, soybean output, and demand in the region from 2010 to 2018 to predict and analyze the change trend of agricultural product output and trading volume. The total grain output, soybean output, and demand are shown in Table 1.

As shown in Table 1, the total grain output in the region has shown a general trend of continuous growth. Taking the Danjiang water source area of the South-to-North Water Diversion Project as the research object, only in 2011 was a slight decrease of 865.1 tons compared with 2010, and it continued to increase in other years. Soybean production in the region is also increasing year by year, with a cumulative increase of 6985.4 tons from 2010 to 2018. The demand for soybeans does not show a trend of increasing year by year. The demand for soybeans does not show an increasing trend year by year, sometimes the supply exceeds demand, and sometimes the supply is less than demand.

Soybean is the main food crop in this area. The relationship between soybean output and total grain output is as follows.

As shown in Figure 6, taking the Danjiang water source area of the South-to-North Water Diversion Project as the research object, the overall change trend of the total grain output in the region from 2010 to 2018 is increasing, and soybean production has increased year by year. It can be said that with the increase in soybean production, grain production is also increasing, because soybean is the main crop in the region, the proportion of soybean output to grain output in this region is between 23% and 29%, and the proportion is increasing every year, and its output directly affects the total amount of food in the entire region. Water quality change trend is show in Table 2.

Pay more attention to moderate scale operation. Focusing on solving the problem of "who will farm the land," various policy objectives are focused on the development of moderate scale operations, focusing on supporting new business entities such as farmer cooperatives, family farms, and leading enterprises. The number of new business entities is showing an explosive growth trend. The changes of operating entities are shown in Table 3.

Table 2: Water quality change trend.

Water quality index	Rank correlation coefficient	Trend
pH	–0.25	Decline
DO	0.097	Rise
COD	0.824	Rise
NH3-N	0.582	Rise

Table 3: The changes of operating entities.

Subject name	2017	2018	2019	2020
Leading agricultural enterprise	91 09	9220	9100	9000
Farmer cooperatives	98869	13 1554	150000	17000
Family farms	30000	38000	41000	49000

In order to compare the changes in supply and demand per year more intuitively and clearly, the soybean production and demand are plotted as a bar graph for comparison. The results are as follows.

As shown in Figure 7, taking the Danjiang water source area of the South-to-North Water Diversion Project as the research object, in 2010, 2011, 2014, 2015, 2017, and 2018, soybean production exceeded demand, indicating that supply exceeded demand. In 2012, 2013 and 2016, the output of soybeans was less than the demand, showing that the supply exceeded demand. The improved KNN algorithm is used to predict and estimate the data from 2010 to 2018, which is similar to the actual demand, indicating that the agricultural product supply and demand prediction model established by the improved KNN algorithm has a good fitting effect, and the improved KNN algorithm can be used for agricultural products in the next few years. Supply and demand forecast.

5.2.2. Forecast Results. Therefore, it is necessary to make a reasonable forecast of soybean production and demand so

Figure 7: Comparison of soybean production and demand.

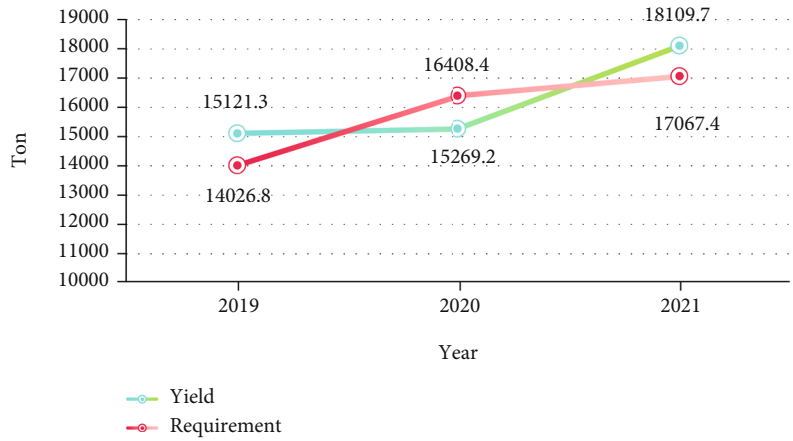

Figure 8: Forecast of soybean production and demand.

that the government can make targeted adjustments to avoid the decrease in farmers' income caused by the decline in soybean prices caused by oversupply. It also circumvents the soaring soybean price that occurs when supply exceeds demand and protects consumer rights. Using the agricultural product supply and demand forecasting model based on the improved KNN algorithm in this study, the supply and demand of soybeans from 2019 to 2021 are predicted. The forecast results are as follows.

As shown in Figure 8, forecast of agricultural product supply and demand forecast model established by improved KNN algorithm. As can be seen from Figure 8, the predicted soybean output is generally on the rise, but it will decrease slightly in 2020, which may be due to the sudden change of data caused by the epidemic situation, while the demand for soybeans has been on the rise. Taking the Danjiang water source area of the South-to-North Water Diversion Project as the research object, there will be an oversupply situation in 2019 and 2021 and there will be an oversupply situation in 2020. Therefore, in 2019 and 2021, the government can appropriately intervene in the demand for soybeans in the market and purchase some soybeans to avoid oversupply of soybeans and low prices. In 2020, we will release stocks of soybeans appropriately to increase the supply of soybeans on the market and avoid too little supply of soybeans and high prices.

5.3. Government Policy Recommendations. In response to the above experimental results, we can also use fiscal policies to support agriculture to promote the supply-side constitutive revolution of agriculture, increase agricultural output value, and improve people's living standards in poor areas.

To properly handle the relationship between the government and the market, the market plays a decisive role, and the invisible hand of the government has to play a macro control role. Give full play to the constitutive guiding role of finance, guide the flow of resources, and increase fiscal support for agriculture. At the same time, increase investment in agricultural science and technology to improve the quality of agricultural products and the efficiency of agricultural production. These measures are all benefited from the successful prediction of soybean yield and demand by the improved KNN algorithm. With these predicted data, we can make policy recommendations for supply and demand.

Increase investment in the education of agricultural producers, improve the cultural level and labor skills of agricultural producers, and carry out relevant training courses through the establishment of relevant training schools. Not only training skills but also a reasonable transmission of national financial support policies, so that agricultural producers understand the direction of national policies.

6. Conclusions

Taking the Danjiang water source area of the South-to-North Water Diversion Project as the research object, the constitutive revolution of the agricultural supply side is not only the adjustment of the economic structure and the transformation of the development mode but also a revolution that combines the characteristics of the agricultural field. The primary task of the constitutive revolution of the agricultural supply side is to solve the problem of food supply, which is a necessary foundation for economic development. Under the premise of ensuring food security and effective supply, realize the maximum benefit of resource allocation. When adjusting the supply and demand structure, we must follow the objective laws of economic development and realize the sustainable development of agriculture. The constitutive revolution of the agricultural supply side should improve the quality of agricultural products and strengthen the safety and quality supervision of agricultural products. The constitutive revolution of the agricultural supply side also needs to promote the integration of primary, secondary, and tertiary industries in rural areas, develop the tertiary industry, extend the industrial chain, improve the mechanism for linking farmers' interests, and generate income for farmers.

Accurately predict the supply and demand of agricultural products through predictive models and provide data support for government decision-making. The government can appropriately intervene in the market and conduct macro control. Purchase some agricultural products when the supply exceeds demand and avoid oversupply leading to too low prices, and farmers' income cannot be guaranteed. When the supply is short of demand, it will appropriately release the stock of agricultural products to increase the supply on the market, so as to avoid too little supply and cause the price to soar, damage the interests of consumers, and cause chaos in the market.

Due to limited time and knowledge, this article takes the Danjiang water source area of the South-to-North Water Diversion Project as the research object and does not consider many factors that affect the supply and demand of agricultural products in the forecast. The supply and demand of agricultural products is not only an interinfluencing relationship but also the adjustment of other factors. Therefore, the IoT prediction model created in this article can only predict data from a small area and cannot predict national data.

Data Availability

No data were used to support this study.

Conflicts of Interest

The authors declare that there is no conflict of interest with any financial organizations regarding the material reported in this manuscript.

Acknowledgments

This work was supported by the MOE Layout Foundation of Humanities and Social Sciences (No.17YJAZH101).

References

[1] L. Bartova, R. M'Barek, and H. van Meijl, "Impact analysis of the CAP revolution on main agricultural commodities. Report I AGMEMOD–Summary report," *Annales de Biologie Clinique*, vol. 23, no. 5, pp. 643–658, 2017.

[2] H. R. Darani, M. R. Kohansal, M. Ghorbani, and M. A. Saboohi, "An integrated hydro-economic modeling to evaluate marketing revolution policies of agricultural products," *Bulgarian Journal of Agricultural Science*, vol. 23, no. 2, pp. 189–197, 2017.

[3] Y. Li, B. Su, and Y. Liu, "Realizing targeted poverty alleviation in China: people's voices, implementation challenges and policy implications," *China Agricultural Economic Review*, vol. 8, no. 3, pp. 443–454, 2016.

[4] X. Gan and L. I. Yong, "Application of big data in agricultural Informationization in Shandong Province under the background of "internet +"," *Asian Agricultural Research*, vol. 11, no. 4, pp. 5–7, 2019.

[5] J. Ruan, H. Jiang, X. Li, Y. Shi, F. T. S. Chan, and W. Rao, "A granular GA-SVM predictor for big data in agricultural cyber-physical systems," *IEEE Transactions on Industrial Informatics*, vol. 15, no. 12, pp. 6510–6521, 2019.

[6] J. A. Rosenheim and C. Gratton, "Ecoinformatics (big data) for agricultural entomology: pitfalls, Progress, and promise," *Annual Review of Entomology*, vol. 62, no. 1, pp. 399–417, 2017.

[7] H. Zhou, L. I. Ruiqi, and D. Ding, ""Revolution of agricultural land transfer of different types of farmers" willingness," *Asian Agricultural Research*, vol. 11, no. 1, pp. 40-41, 2019.

[8] H. Hill, "Comment on "Political Economy of Agricultural Reform in Japan under Abe's Administration"," *Asian Economic Policy Review*, vol. 13, no. 1, pp. 145-146, 2018.

[9] M. Honma and M. A. George, "Political economy of agricultural reform in Japan under Abe's administration," *Asian Economic Policy Review*, vol. 13, no. 1, pp. 128–144, 2018.

[10] S. Wan and S. Goudos, "Faster R-CNN for multi-class fruit detection using a robotic vision system," *Computer Networks*, vol. 168, p. 107036, 2020.

[11] I. Kitouni, D. Benmerzoug, and F. Lezzar, "Smart agricultural enterprise system based on integration of Internet of Things and agent technology," *Journal of Organizational and End User Computing*, vol. 30, no. 4, pp. 64–82, 2018.

[12] M. Adil, M. K. Khan, M. Jamjoom, and A. Farouk, "MHADBOR: AI-enabled administrative distance based opportunistic load balancing scheme for an agriculture Internet of Things network," *IEEE Micro*, vol. 22, 2022.

[13] M. Drechsler, J. Touza, P. C. L. White, and G. Jones, "Agricultural landscape structure and invasive species: the cost-

effective level of crop field clustering," *Food Security*, vol. 8, no. 1, pp. 111–121, 2016.

[14] Y. H. Gong, "The reform and exploration of agricultural practice teaching based on the goal of cultivating innovative applied talents," *Creative Education Studies*, vol. 8, no. 3, pp. 417–421, 2020.

[15] J. Y. Park and B. Huwe, "Effect of pH and soil structure on transport of sulfonamide antibiotics in agricultural soils," *Environmental Pollution*, vol. 213, pp. 561–570, 2016.

[16] X. Dai, L. Wang, and Y. Ren, "The effects of China's targeted poverty alleviation policy on the health and health equity of rural poor residents: evidence from Shaanxi Province," *Health*, vol. 8, no. 3, pp. 256–256, 2020.

[17] Y. Wang, "How does targeted poverty alleviation policy influence residents' perceptions of rural living conditions? A study of 16 villages in Gansu Province, Northwest China," *Sustainability*, vol. 11, no. 24, pp. 6944–6944, 2019.

[18] H. X. Li, "Research on the path of public libraries serving vulnerable groups under the policy of targeted poverty alleviation," *Advances in Social Sciences*, vol. 8, no. 2, pp. 276–281, 2019.

[19] Z. Guangying, L. I. Meixiu, and L. Cuisheng, "An empirical study on targeted poverty alleviation of Chixi Village and Xiadang Village in Ningde City of Fujian Province," *Landscape Studies: English version*, vol. 11, no. 4, pp. 108–112, 2019.

[20] B. Gjelvold, B. R. Chrcanovic, E. K. Korduner, I. Collin-Bagewitz, and J. Kisch, "Intraoral digital impression technique compared to conventional impression technique. A randomized clinical trial," *Journal of Prosthodontics*, vol. 25, no. 4, pp. 282–287, 2016.

[21] J. Lee and D. Kwon, "A digital technique for diagnosing interconnect degradation by using digital signal characteristics," *Microelectronics Journal*, vol. 60, pp. 87–93, 2017.

[22] J. Woodard, "Big data and Ag-analytics," *Agricultural Finance Review*, vol. 76, no. 1, pp. 15–26, 2016.

[23] Z. Yang, Y. Ding, K. Hao, and X. Cai, "An adaptive immune algorithm for service-oriented agricultural Internet of Things," *Neurocomputing*, vol. 344, pp. 3–12, 2019.

[24] S. Navulur, S. Navulur, and A. S. Chandra Sekhara Sastry, "Agricultural management through wireless sensors and IoT," *International Journal of Electrical & Computer Engineering*, vol. 7, no. 6, pp. 3492–3499, 2017.

[25] A. Ortiz-Tapia, "Attention recognition in EEG-based affective learning research using CFS+KNN algorithm," *Computing Reviews*, vol. 59, no. 11, pp. 621–621, 2018.

[26] C. Y. He, M. R. Zhou, and P. C. Yan, "Application of the identification of mine water inrush with LIF spectrometry and KNN algorithm combined with PCA," *Spectroscopy and Spectral Analysis*, vol. 36, no. 7, pp. 2234–2237, 2016.

Hindawi
Wireless Communications and Mobile Computing
Volume 2022, Article ID 9880519, 11 pages
https://doi.org/10.1155/2022/9880519

Research Article

Application of Cluster Analysis Algorithm in the Online Intelligent Teaching Art Resource Platform

Tiankuo Yu

School of Business Administration, Heilongjiang Polytechnic, Harbin, 153000 Heilongjiang, China

Correspondence should be addressed to Tiankuo Yu; xxhzx@hljp.edu.cn

Received 9 December 2021; Revised 14 January 2022; Accepted 10 February 2022; Published 10 March 2022

Academic Editor: Mohamed Elhoseny

With the explosion of knowledge and the high-speed dissemination of information, people's desire for knowledge and information is getting stronger and stronger. At the same time, the updating of knowledge and information is going on at an unprecedented speed. The traditional teaching mode is affected by time and space. Its limitations have become more and more prominent; the traditional classroom teaching has been unable to meet the existing teaching needs. At present, there are many methods for the analysis of network user behavior, such as statistical methods, association analysis methods, and clustering algorithms. Among them, clustering algorithms are more widely used in network user behavior analysis, which is closely related to the unsupervised and high efficiency of clustering algorithms. This paper combines the advantages of clustering algorithm in network user behavior analysis and, on the basis of the existing clustering algorithm research, proposes an improved algorithm for the analysis of online intelligent teaching art resources, so as to obtain the law of online behavior of student users in campus network. Provide some help for students' Internet management and network optimization. Finally, summarize and put forward the concept of intelligent teaching and design and implement an online intelligent teaching art resource platform based on cluster analysis algorithm. Studies have shown that the average number of transactions processed by the platform per second is 65.21, which can well simulate real information query use cases. The transaction processing time of the platform will eventually stabilize between 30 s and meet the performance requirements.

1. Introduction

Since the rapid development of information technology, it has continuously affected all aspects of social life [1, 2]. In recent years, the application of information technology in education and teaching has led to changes in the teaching process that have attracted the attention of experts, scholars, managers, and front-line teachers, whether from the national level, industry level, or front-line education and teaching management departments. At present, there are many cases of teaching resource platform construction, but most of them are modified from the early resource management system. The single system has strong coupling, and the functions of resource collection, processing, retrieval, sharing, and reuse are insufficient [3, 4]. The application support ability of the business system is weak. At the same time, with the rapid development of multimedia and network technology and the popularization of Internet, remote online teaching has become a new generation of education combining computer network and multimedia technology because of its long-distance real-time interactive function and the characteristics of separation of time and space between teaching and learning. Technology: especially at the end of the twentieth century, the development and research of network-based teaching systems have quickly become an important subject for research in various countries.

Foreign research text classification is relatively early, and obvious academic research results have been obtained [5]. In the late 1950s, it was the first to apply statistical theory to text classification; IBM in the United States also carried out groundbreaking research in the field of text classification; Huang et al. first proposed to apply word frequency statistics to automatic text classification [6]; in the early 1960s, Lee and Chung published the first paper in the field of automatic

text classification [7]; subsequently, Kuo and many other scholars proposed to use factor analysis to study document classification [8]. Fang believes that online teaching quality evaluation refers to the process of using effective technical means to comprehensively collect, organize, and analyze teaching conditions and make value judgments to improve teaching activities and improve teaching quality [9]. However, it is not common to explore the application of text classification in intelligent teaching systems, and the research of text classification in this field is still immature. Compared with foreign countries, the domestic research on automatic text classification started late, and it mainly went through three stages of feasibility study, auxiliary classification system, and automatic classification system [10].

This paper attempts to design and implement an open online intelligent teaching art resource platform under the cluster analysis algorithm, realize the storage of basic resource data, meet the resource application support for other business systems, and provide the collection, processing, and retrieval of teaching resources, sharing, multiplexing, and other application functions [11]. This article analyzes the current situation of regional education resources; sorts out the needs of the service object, service content, and basic structure of the regional science art resource service cloud platform; formulates the overall goal of construction; and plans the hardware support infrastructure, application system structure, data business logic, and system deployment plan. Remote online teaching is a new generation of educational technology that combines computer network technology and multimedia technology. Using remote online teaching, the majority of educated people can break through the limitations of traditional education in educational resources and educational methods and can achieve excellence without the constraints of time and space. With the sharing of educational resources and educational methods, the educated can arrange their own learning plans and learning progress according to their own level and time situation, so as to realize the "autonomous choice education" that cannot be achieved by traditional education. Finally, the system test results of the online intelligent teaching art resource platform are given [12]. The clustering results are very satisfactory; at the same time, the individual characteristics belonging to different classes are also obtained. The system realizes targeted and differentiated personalized teaching according to the individual characteristics. The personalized intelligent learning system well implements "individualized" and "intelligent" learning services and can greatly improve the learning efficiency of students and enhance the intelligence of the embedded online intelligent teaching platform. It is used in theoretical research and practical applications. Both are of great significance. The article innovatively applies the improved clustering analysis algorithm to the embedded online intelligent teaching platform and realizes the personalized intelligent learning system of the embedded online intelligent teaching platform. The system integrates learning, testing, and guidance, which well embodies the concept of personalized and intelligent teaching, greatly enhances the intelligence of the embedded online intelligent teaching platform, and provides students with good personalized learning resources and adaptive guidance, and the application of the system also proves the effectiveness and practicability of the algorithm.

2. Clustering Analysis Algorithm of Online Intelligent Teaching Art Resource Platform

2.1. Online Intelligent Teaching Art Resource Platform Based on Cluster Analysis Algorithm

(i) The service objects of the online intelligent teaching art resource platform

Compared with the previous teaching resource service platform, the teaching network intelligent teaching art resource platform designed in this article emphasizes the openness of the system and the convenience of application. Application openness is to achieve resource support for other teaching-related business systems on the basis of meeting the national education resource standards, and convenience is to improve the application effect of users when using the teaching resource system. Specific service objects can be divided into two categories:

(1) Business applications

The business application system includes the user operation interface functions (including browsing, searching, uploading, downloading, and quoting functions) provided by its own resource system, teaching preparation, teaching research, teacher training, etc.

(2) Functional user class

The user design includes resource platform management users, ordinary teachers, ordinary students, ordinary parents, and education administrators. Provide teachers, students, and parents with the basic functions of retrieval, browsing, uploading, downloading, sharing, and quoting of teaching resources and, at the same time, push preferred teaching resources to users based on related algorithms; provide education managers with resource construction, use, and use of resource platforms. Cobuild and share data analysis; provide management functions such as system configuration, resource screening, and elimination for management users [13–15].

The "learning" mode of distance network teaching is mainly defined for the educated. The modes provided by general education websites can be divided into individual learning modes, discussion learning modes, and multiperson cooperation learning modes:

(1) Students can obtain knowledge through individual learning by consulting teachers or using teaching software

(2) A teaching mode in which multiple students learn through discussion with the help of the discussion support system

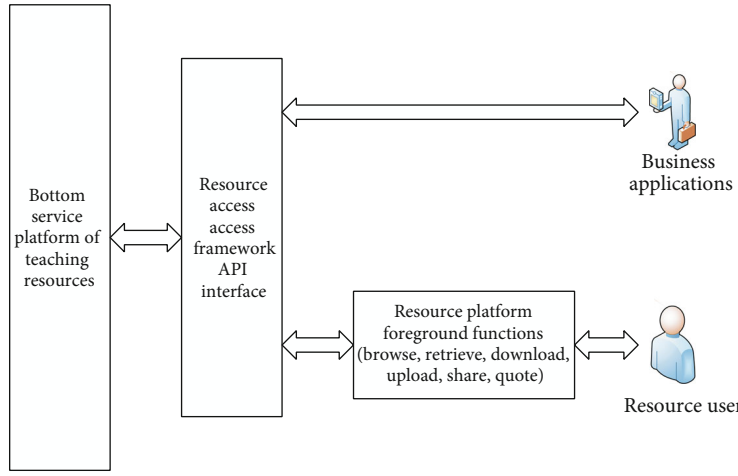

Figure 1: Schematic diagram of the service content of the online intelligent teaching art resource platform.

(3) Using the Internet, multiple students interact and cooperate with each other for the same learning content to complete learning tasks together

(ii) The service content of the online intelligent teaching art resource platform

The online intelligent teaching art resource platform provides services for two types of service objects, provides access to the framework API interface for business application systems, and provides different user operation function interfaces for resource users, as shown in Figure 1.

(iii) The infrastructure requirements of the online intelligent teaching art resource platform

In order to meet the design requirements of the service object and service content of the smart teaching resource service cloud platform, the infrastructure of the entire platform must be different from the previous teaching resource platform, mainly including the following aspects:

(1) Constructed in the cloud computing mode, configure computing resources, and storage resources to achieve elastic expansion of basic hardware resources

(2) Both computing and storage adopt cluster architecture to achieve high availability of application and data access

(3) Open architecture, compatible with national education data standards, to achieve good access to business systems and resource data exchange

2.2. Design Goal of the Online Intelligent Teaching Art Resource Platform. The design goal of the online intelligent teaching art resource platform is based on the support of the underlying hardware structure of the clustering analysis algorithm, adopts an open structure design, is compatible with national education resource standards and specifications, and realizes the separation of the underlying resources, basic services, access frameworks, and upper-level functional application interfaces. Layer design to meet the access requirements of other business application systems related to teaching resources in the region, as well as the retrieval, operations of ordinary users to the teaching resources themselves, and finally, realize as a regional education cloud. The platform provides part of teaching resource management and services [16, 17].

Implement the "three chains and two platforms" regulations by building a regional education cloud service platform to accelerate the efficient development of regional education informatization [18].

2.3. Hardware Support Environment of the Online Intelligent Teaching Art Resource Platform. The design of the online intelligent teaching art resource platform consists of two parts, namely, the hardware support environment and the software application service system.

The hardware support environment of the online intelligent teaching art resource platform based on the clustering analysis algorithm is based on the clustering analysis algorithm data center, structured storage, unstructured storage, and resource underlying services composed of high-performance computing servers and high-performance storage devices, and resource service open access framework; the second part is the front-end business cluster supported by the virtual computing platform to provide users with access to the operation interface [19–22]. Follow the principles of completeness, clarity, understanding, query ability, and ease of operation. Provide students with retrieval mechanism, information network structure diagram, online help manual, preset or preview learning path, record learning path, and allow backtracking, use electronic bookmarks, etc.

Each node of the low-level high-performance computing server is equipped with 4 channels of 12-core CPUs, and 256 GB of memory can provide the resource service platform with powerful resource data processing capabilities. The high-performance storage using 8 G optical fiber connection provides the resource bottom platform with a high speed of over 800 MB/S. Reading and writing capabilities ensure the throughput of resource data. The 200 TB∗2 storage

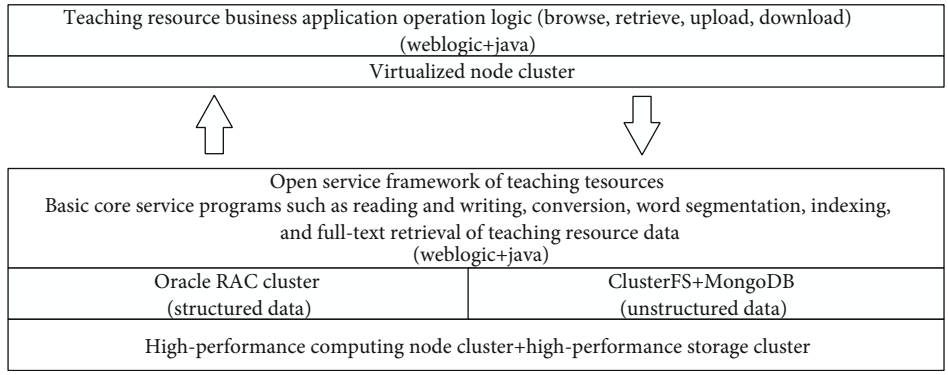

Figure 2: Schematic diagram of software deployment structure for intelligent teaching resource service cloud platform.

configuration provides a large storage space for resource data, which can meet the collection of high-quality resource data for a large number of users within a certain period of time. Virtualized computing provides multinode clusters for resource application front-end services, ensuring high availability while ensuring horizontal resource expansion under extreme pressure conditions [23, 24].

2.4. Software Service System of Online Intelligent Teaching Art Resource Platform

(1) The composition of the software service system of the online intelligent teaching art resource platform based on the clustering analysis algorithm

The intelligent teaching resource platform software service system is composed of two main parts as described above: one is the basic layer service of teaching resources; the second is the application layer of teaching resources.

The business application layer of teaching resources provides access and operation function interfaces for multiple users, including resource browsing, retrieval, uploading, downloading, sharing, quoting, optimization, elimination, resource evaluation activities, resource points, and resource management, to meet users' needs for resources the routine application operation [6, 25, 26].

(2) Data application logic of online intelligent teaching art resource platform software service system

The intelligent teaching resource platform software service system is based on the design structure. The basic layer of teaching resources serves as the data collection and distribution center of teaching resources. Based on structured data storage and unstructured data storage software, it constructs resource data collection, processing, storage, access, and core functions such as indexing, word segmentation, and full-text retrieval, provides an open service framework for teaching resources to realize the operation of resource data at the business application layer of teaching resources, and at the same time, meets the resource data operation needs of other business applications under security control.

Teaching resource base layer services, provide structured storage of resource data, unstructured storage, resource collection, processing, access, indexing, word separation, full-text search, data security control, resource open framework API, etc.

The teaching resource business application layer is mainly used to implement user interaction, complete resource collection, display, and application-related resource logic, and provide users with a convenient and clear operation platform. It is an important source of teaching resource data and data export.

(3) Software deployment structure of online intelligent teaching art resource platform

The online intelligent teaching art resource platform software service system based on the clustering analysis algorithm is designed according to the hierarchical design, and the software deployment is also divided into two levels, the teaching resource basic layer and the teaching resource business application layer, as shown in Figure 2.

The basic layer of teaching resources is deployed in the basic environment of high-performance computing clusters and high-performance storage. File system and MongoDB are combined to realize unstructured data storage, Oracle database cluster mode provides structured data storage, Weblogic middleware is the platform, and JAVA language is used to construct the basic core of teaching resource data such as reading and writing, conversion, word segmentation, indexing, and full-text retrieval. The service program realizes the open service framework of teaching resources and provides support for the upper application system and data interaction [27]. The teaching resource business application layer is deployed on the computing node cluster provided by the cloud computing center virtualization platform.2.5 Cluster Analysis Algorithm.

(1) Cluster analysis algorithm

Clustering analysis is an important task in data mining. Clustering is one of the most common techniques in the field of data mining. It is used to discover unknown object classes in the database. The basis for this classification of object classes is "things are clustered together," that is, to examine the similarity between individuals or data objects and divide individuals or data objects that meet

similar conditions into a group. Individuals or data objects that do not meet the similarity conditions are divided into groups. There are different groups, each group formed by the clustering process is called a cluster.

The goal of cluster analysis is to collect data on the basis of similarity to classify, measure the similarity between different data sources, and classify data sources into different clusters. The specific algorithm is as follows:

$$\begin{aligned} G_1 \cup G_2 \cup \cdots \cup G_k &= X, \\ G_i \cap G_j &= \varnothing, i \neq j. \end{aligned} \tag{1}$$

The nodes in the clustering tree graphically represent a class or use the logical expression of sample attributes to represent the class [28].

(2) Data types

(i) Data matrix of calling object and variable structure

With the quantitative representation of data, the results can be sorted and analyzed more accurately. It uses p variables (also called metrics or attributes) to represent n objects. The relationship is:

$$\begin{bmatrix} x_{11} & \cdots & x_{1f} & \cdots & x_{1p} \\ \vdots & \vdots & \vdots & \vdots & \vdots \\ x_{i1} & \cdots & x_{\mathrm{if}} & \cdots & x_{ip} \\ \vdots & \vdots & \vdots & \vdots & \vdots \\ x_{n1} & \cdots & \mathrm{x}_{nf} & \cdots & x_{np} \end{bmatrix}. \tag{2}$$

(ii) Dissimilarity matrix (or object-object structure): stores the similarity between n objects in the form of an $n \times n$ matrix

$$\begin{bmatrix} 0 & & & & \\ d(2,1) & 0 & & & \\ d(3,1) & d(3,2) & 0 & & \\ \vdots & \vdots & \vdots & 0 & \\ d(n,1) & d(n,2) & \cdots & \cdots & 0 \end{bmatrix}. \tag{3}$$

(3) Similarity measure

The similarity measure can be expressed as:

$$\forall x', x \subset X \forall x', x \in X. \tag{4}$$

Generally speaking, the similarity metrics of clustering algorithms can be standardized as:

$$0 \leq s\left(x, x' \leq 1\right) \forall x', x \in X. \tag{5}$$

However, it is common to use a measure of dissimilarity rather than a measure of similarity as a standard. The measure of dissimilarity is expressed as:

$$d\left(x, x'\right), \forall x', x \in X. \tag{6}$$

Generally, we discuss that the variable describing the object is a continuous interval, and the degree of dissimilarity is usually called the distance. When x and x' are similar, the distance $d(x, x')$ is small. If x and x' are not similar, $d(x, x')$ is very large [29, 30].

Here, we only introduce the distance definition of the data object when the description attributes of the data object are all interval scaled metric attributes. The commonly used distance definitions are as follows:

(1) Manhattan (Manhattan) distance

$$d(i,j) = \left|x_{i1} - y_{j1}\right| + \left|x_{i2} - y_{j2}\right| + \cdots + \left|x_{im} - y_{jm}\right|. \tag{7}$$

(2) Euclidean distance

$$d(i,j) = \sqrt{\left|x_{i1} - y_{j1}\right|^2 + \left|x_{i2} - y_{j2}\right|^2 + \cdots + \left|x_{im} - y_{jm}\right|^2}. \tag{8}$$

(3) Minkowski distance

$$d(i,j) = \left(\left|x_{i1} - y_{j1}\right|^q + \left|x_{i2} - y_{j2}\right|^q + \cdots + \left|x_{im} - y_{jm}\right|^q\right)^{1/q}, \tag{9}$$

where q is a positive integer. When $q = 1$, Minkowski distance is Manhattan distance; when $q = 2$, Minkowski distance is Euclidean distance.

2.5. K-Means Clustering and Grid Clustering

(1) K-means clustering

K-means is an iterative clustering algorithm. In the process of iteration, the members of the cluster are constantly moved until the ideal cluster is obtained. Using the clusters obtained by the K-means algorithm, the calculation of the similarity between the members of the cluster is represented

by the mean value of the objects in the cluster (which is regarded as the centroid of the cluster).

Given cluster $k_1 = \{t_{i1}, t_{i2}, \cdots, t_{im}\}$, its mean value is defined as:

$$M_i = \frac{1}{m}\sum_{j=1}^{m} t_{ij}, \tag{10}$$

where M_i is the average value of the ith cluster, m is the number of objects in the cluster, and t_{ij} is the distance from the jth object to the centroid of the ith cluster.

(2) Grid clustering

The grid-based grouping method uses a multiresolution grid data structure to quantify the space in a limited number of cells. These cells form a grid structure, and all cluster operations are performed in the continuation of the grid operations [31].

2.6. GBKM. The algorithm has achieved impressive results by using iris and other data for testing and applying it to actual systems, satisfactory results [32].

Let $A = (D_1, D_2, \cdots, D_n)$ be n-bounded domains, then $S = D_1 \times D_2 \times \cdots \times D_n$ is an n-dimensional space. We regard $D_1, D_2, \cdots, D_n$ as the dimensions of S. The input of the algorithm is a point set in n-dimensional space, set as $V = \{v_1, v_2, \cdots, v_n\}$, where $v_1 = \{v_{i1}, v_{i2}, \cdots, v_{\text{in}}\}$ represents the ith point, $v_{ij} \in D_j$, which means the component of the jth dimension of the ith point.

(1) Grid unit

Suppose the value on the ith dimension is in the interval $[l_i, h_j)$, $i = 1, 2, \cdots, n$. The length of the grid cell in the ith dimension is

$$\delta_i = \frac{(hi - li)}{p}. \tag{11}$$

The jth interval on the ith dimension can be obtained by:

$$I_{ij} = [l_i + (j-1)\delta_i, l_i + j\delta_i], j = 1, 2, \cdots, p. \tag{12}$$

(2) Clustering center of gravity

Given cluster $K_i = \{t_{i1}, t_{i2}, \cdots, t_{\text{in}}\}$, its mean value, the cluster center of gravity, is defined as:

$$Z_i = \left(\frac{1}{n}\right)\sum_{x,y \in K_i} (x, y)^2. \tag{13}$$

(3) Grid cluster analysis

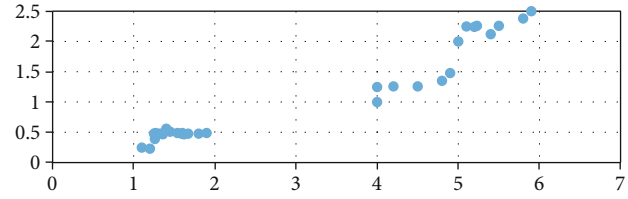

Figure 3: GB clustering results.

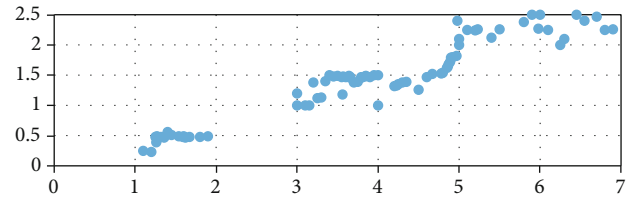

Figure 4: GBKM clustering results.

For the determination of the density threshold in the GBKM algorithm, a new algorithm is proposed:

$$\text{Minpts} = \frac{\left[\sum_{i=1}^{N} \text{Den}(C_i)^2\right]^{1/2}}{N}. \tag{14}$$

Among them, $\text{Den}(C_i)$, $i = 1, 2, \cdots, N$ is the density value of the N dense cells with the highest density. The value of N depends on the specific data. Generally, $\text{Den}(C_i)$ is arranged in descending order. If $\text{Den}(C_i)$ and $\text{Den}(C_{i+1})$ show obvious changes in density, then $N = i$.

3. Application Experiment of Cluster Analysis Algorithm in the Online Intelligent Teaching Art Resource Platform

3.1. Lab Environment. Based on the .NET digital art education information system, there is only one server, which can make the system maintenance more convenient [8, 33]. The system does not use a dedicated server server, only a dual-purpose database [10]. However, because the system has to deal with all kinds of complex and complicated things, it will reduce the slow system speed and allocate some work to its customers. Based on the above reasons, this system uses C/S and B/S two operating modes to combine the system architecture. In this way, it not only utilizes the characteristics of B/S structure maintenance and simple operation but also uses the characteristics of C/S structure safety and high processing efficiency. Use ASP.NET Web database middleware technology to develop Web pages, and use ADO.NET (ActiveX Data Object.NET) technology and OLEDB to connect and access the database. The design, development, debugging, and deployment of the system share the same working environment, which improves the continuity and efficiency of system development.

The back-end database adopts SQLServer2019, while using JavaBean to realize database connection and data

Table 1: GBKM clustering results.

	Intermediate clustering	Postclustering	Final clustering
Class 0	6.733333333	6.840543	6.83
	3.266666667	3.178546	3.04514
	5.479999966	5.685412	5.54154
	2.249999974	2.213351	2.04131
Class 1	4.981818189	5.004151	5.001
	3.486363647	3.41	3.417
	1.475999997	1.495211	1.454
	0.29545455	0.275413	0.215
Class 2	6.37333327	6.542154	6.324
	2.65333356	2.754318	2.651
	4.62333355	4.431541	4.55146
	1.43666665	1.425641	1.43354

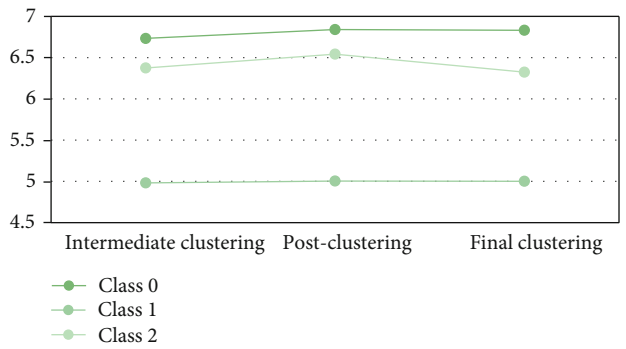

Figure 5: The initial cluster centers of GBKM.

Table 2: Comparing of purity.

	K-means	Grid-based	GBKM
1	0.865	0.654	0.874
2	0.884	0.947	0.875
3	0.894	0.887	0.901
4	0.901	0.887	0.895
5	0.884	0.894	0.901
6	0.654	0.927	0.921
7	0.654	0.654	0.894
8	0.849	0.921	0.924
9	0.849	0.891	0.927
10	0.654	0.654	0.875

query and update operations, and adopts advanced B/S (Browser/Server) architecture, and the page design adopts the current international popular webpage authoring tool Dreamweaver2017; both EditPlus are used for editing; the script language uses Java Script, and the page image processing uses Photoshop CS and Flash5.0.

3.2. Development Model. This system is a system composed of people and computers for information collection, storage, knowledge transfer, and use.

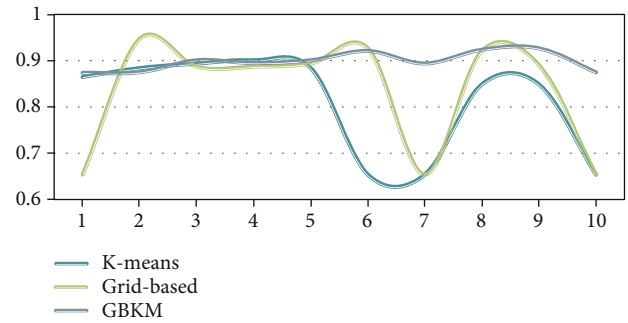

Figure 6: Purity comparison results.

Table 3: Comparing of cohesion.

	K-means	GBKM
1	124.8514	97.325554
2	122.5415	97.541236
3	121.4874	97.845166
4	123.5425	97.541364
5	123.6829	97.514725
6	122.5874	97.142586
7	121.6842	97.584136
8	122.5247	97.541236

Table 4: Comparing of separation.

	K-means	GBKM
1	268.154	272.5412
2	268.5415	273.3541
3	267.5412	271.4514
4	269.5115	273.0041
5	270.9847	272.87
6	269.5417	273.3647
7	268.5987	271.0084
8	269.8741	273.9471

Model design can be said to be the most important core of MVC. Control (controller) can be understood as receiving requests from users, matching the model with the view, and completing user's request together without any data processing.

4. Application Experiment Analysis of Cluster Analysis Algorithm in the Online Intelligent Teaching Art Resource Platform

4.1. Performance Verification of GBKM Clustering Algorithm. This experiment uses Intel(R) Pentium(R) 4 CPU 2.80 GHz processor, 512 memory, Windows XP Professional (5.1, Build 2600) operating system. The code is written in java language.

Table 5: The clustering of GBKM.

Category	Member of class
0	35, 37, 41, 43, 46, 48, 61, 65, 69, 74
1	8, 26, 30, 31, 32, 33, 34, 37, 38, 44, 46, 47, 49, 50, 51, 52, 54, 55, 56, 59, 60, 62, 64, 66, 69, 70, 71, 72
2	48, 75, 76, 77, 78, 79, 80, 82
3	16, 17, 18, 19, 53, 63, 73, 83, 93
4	7, 9, 10, 11, 12, 13, 14, 15, 20, 21, 22, 23, 24, 25, 27, 28, 29, 39, 40, 41, 57, 68

The sample data for the experiment uses the famous Iris dataset. Ins dataset, also known as dataset, dataset or dataset, is a collection of data. Dataset (or dataset) is a collection of data, usually in the form of a table. Each column represents a specific variable. Each row corresponds to a question of a member's dataset. It lists the values as a random number for each variable, such as height and weight of an object or value. Each value is called a data sheet. Corresponding to the number of rows, the data of the dataset may include one or more members. The dataset includes 4 characteristics of 3 types of flowers: sepal width, sepal length, petal width, and petal length, with a total of 150 records.

First, compare the clustering results of GBKM algorithm and grid clustering algorithm. Use the GB algorithm to cluster the data, and the result is shown in Figure 3.

From Figure 3, we can see that the result of grid clustering is missing many points, and the clustering result is not satisfactory. The low-density area of the grid cluster is discarded, and only the high-density area is processed, resulting in the loss of the cluster. However, the result obtained by using GBKM clustering is much better than the result of grid clustering, and the distribution is shown in Figure 4.

On the horizontal axis, the value in the range from 1 to 2 is setosa type, the grid line with value 5 is the watershed, the left is the versicolor type, and the right is the virginica type. The experiment proves that most of the points can be well clustered.

Next, compare the clustering results of the GBKM clustering algorithm with the clustering results of the K-means clustering algorithm. Using the GBKM clustering algorithm for many experiments, the clustering process has gone through intermediate clustering, postclustering, and clustering after one iteration, and the analysis results are quickly obtained. A total of 3 categories are obtained, and the value of the initial center of each category at each clustering stage is shown in Table 1.

Figure 5 shows the line chart of the clustering center changes during this clustering process. The clustering centers of each class in the figure do not change much at each stage, and they converge quickly. This shows that the GBKM clustering algorithm which obtains the dense unit of the dataset simulates the distribution of the dense area in the dataset, quickly determines the K initial clustering center points, then uses the K-means clustering to recluster the free data, and finally, completes it quickly and effectively.

However, the results of multiple experiments on Iris data using K-means clustering vary greatly from the initial cluster center to the final cluster center. In this clustering process,

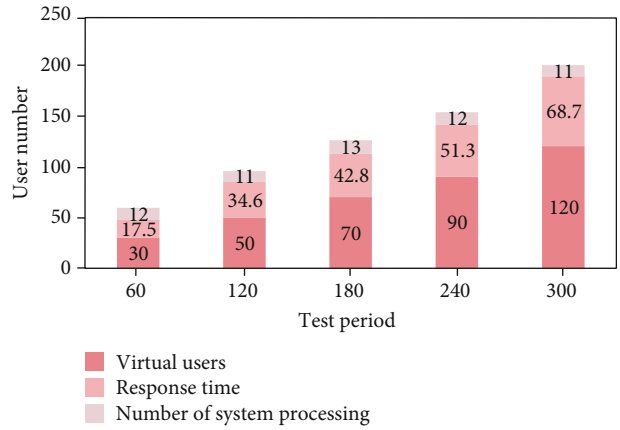

Figure 7: Stress test statistics.

the K-means algorithm randomly selected 3 points as the initial clustering center, and it could not capture the center of natural clustering well. The algorithm continued to find a better initial clustering center. It is the constantly changing clustering center that makes the algorithm unable to converge quickly, and the number of iterations of the algorithm has also increased significantly to 11 or more.

4.2. Purity Comparison. Using the Iris dataset, several experiments were performed, and the result values of the purity of the clusters obtained by the three different algorithms are shown in Table 2.

In order to see the difference between the three more intuitively, Figure 6 shows the purity comparison line chart.

Obviously, the GBKM algorithm is significantly better than other algorithms in terms of purity, and the polyline of the GBKM clustering shown in Figure 5 is more stable than the other two algorithms. Therefore, the GBKM algorithm is more stable and can reconstruct free data compared to other algorithms and finally complete clustering quickly and effectively.

4.3. Evaluation of Cohesion Degree and Separation Degree. After clustering, the data in the clusters should be as compact as possible, and the data gap between the clusters should be as large as possible, the aggregation degree should be as small as possible, and the separation degree should be as large as possible.

The Iris dataset is still used this time, and the K-means clustering and GBKM clustering algorithms are used for repeated experiments. The results obtained are shown in Table 3 and Table 4.

Table 6: Corresponding time for querying physical objects.

Elapsed scenario time mm/ss	0:00	01:00	02:00	03:00	04:00	05:00	06:00	07:00	08:00	09:00	10:00
Average response time	0	30	62	112	163	146	42	31	30	31	30

It can be seen from Table 3 that in the comparison of the aggregation degree of the 8 pairs of clustering results, the aggregation degree obtained by the GBKM clustering is much smaller than the aggregation degree obtained by the K-means clustering. The smaller the degree of aggregation, the tighter the objects in the cluster, and the better the clustering result. At the same time, it can be seen from Table 4 that in the comparison of the degree of separation of the 8 pairs of clustering results, the degree of separation obtained by the GBKM clustering is greater than the degree of separation obtained by the K-means clustering. The greater the degree of separation, the greater the object difference between clusters, and the better the clustering results. The maximum difference reached 270.9847.

4.4. Evaluation of Online Intelligent Teaching Art Resource Platform. In this online intelligent art education resource platform, GBKM generation was used as the basic performance analysis algorithm of the application, and the corresponding content in the database was successfully read, and the GBKM clusters other than the formed clusters were quickly and effectively analyzed. After analyzing and displaying the analysis results on the browser page, save the analysis results in the corresponding test history database table, and update the entries in the database table.

The clustering results are shown in Table 5.

Comparing the characteristics of each class, we can see that the members between the classes are very similar, and the differences between the classes are very large, and the cluster center of each class can represent the characteristics of each class. In the figure, it can be seen that the members belonging to category 0 have high scores in each chapter, especially the relatively low scores of chapter 3, so in the future learning, we must maintain the advantages of chapter 0 and strengthen the study of chapter 3.

4.5. Stress Test. The system was subjected to stress testing, and in the actual application process, an online intelligent teaching art resource platform based on cluster analysis algorithm was selected. Observe the performance of the system, and use the test sample of the full-text search of the survey information as the performance test.

As shown in Figure 7, analyze the results of the stress test, and the response time will increase or decrease with the number of visits. In the high-stress test, it can also maintain good performance and response time to meet the demand.

4.6. Platform Processing Performance. The system transaction performance of the platform is tested, and the results are shown in Table 6.

It can be seen from Figure 8 that the number of transactions processed by the platform per second is 65.21, which can well simulate real information query use cases. The platform transaction processing time will eventually stabilize between 30 s, which can well meet the performance requirements.

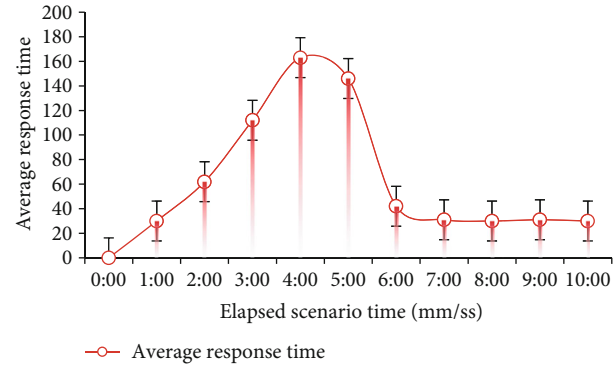

Figure 8: Response time of system transaction processing.

5. Conclusion

In recent years, with the rapid development of the Internet, the Internet has penetrated into all aspects of social life and has become an important part of human life. While the Internet is widely used, along with the explosive growth of network data, information that is of great significance to people's lives and human development is hidden in the huge network data. How to capture hidden campus network behavior information from these data? It has become a hot spot and focus of current research. The application of clustering algorithm in campus user behavior analysis is quite mature and has achieved certain results. However, due to the diversity, dynamics, and relevance of network user behaviors, resulting in complex data structures, there is still no algorithm that can be universally applied to reveal the structural characteristics of various multidimensional network user behavior data. Therefore, by analyzing the advantages and disadvantages of different clustering algorithms, combining the advantages of the algorithm itself in different data structures to propose suitable improved algorithms is still the focus of clustering technology in the application of research. How to apply the GBKM algorithm to the embedded online intelligent teaching platform more widely is the subject of the next research, such as how to tap the learning habits of the majority of students, discover the habits of the majority of students to browse the web, and how to discover the laws and potentials of the students' learning courseware demand. Due to the limited data, the results of the experiment are relatively one-sided and cannot represent the conclusion of all the data, but it can also reflect the problem from a certain aspect. First of all, although the article improves the traditional clustering analysis algorithm, proposes the GBKM clustering analysis algorithm, and has

achieved good results, the algorithm still has shortcomings, such as how to better choose the density threshold, which will affect the performance of the algorithm, and this is also the place that needs to be studied and improved in the future. Secondly, how to apply the GBKM algorithm to the embedded online intelligent teaching platform more widely is the subject of the next research, such as how to mine the study habits of the students, the habits of browsing the web, and the rules of the students learning courseware and potential needs.

Data Availability

The data that support the findings of this study are available from the corresponding author upon reasonable request.

Conflicts of Interest

The author declared no potential conflicts of interest with respect to the research, authorship, and/or publication of this article.

References

[1] A. M. Al-Momani, M. A. Mahmoud, and M. S. Ahmad, "Factors that influence the acceptance of internet of things services by customers of telecommunication companies in Jordan," *Journal of Organizational and End User Computing*, vol. 30, no. 4, pp. 51–63, 2018.

[2] G. Khatwani and P. R. Srivastava, "Impact of information technology on information search channel selection for consumers," *Journal of Organizational and End User Computing*, vol. 30, no. 3, pp. 63–80, 2018.

[3] A. K. Singh, X. Liu, H. Wang, and H. Ko, "Recent advances in multimedia security and information hiding," *Transactions on Emerging Telecommunications*, vol. 32, no. 2, 2021.

[4] Z. Lv and H. Song, "Trust mechanism of feedback trust weight in multimedia network," *ACM Transactions on Multimedia Computing, Communications, and Applications*, vol. 17, no. 4, pp. 1–26, 2021.

[5] L. Zhang and F. Wen, "A novel MIMO radar orthogonal waveform design algorithm based on intelligent ions motion," *Remote Sensing*, vol. 13, no. 10, p. 1968, 2021.

[6] W. Huang, J. Ren, T. Yang, and Y. Huang, "Research on urban modern architectural art based on artificial intelligence and GIS image recognition system," *Arabian Journal of Geosciences*, vol. 14, no. 10, pp. 1–13, 2021.

[7] M. Lee and G. Chung, "Cluster analysis of snowfall observatory using K-means algorithm," *Korean Society of Hazard Mitigation*, vol. 18, no. 2, pp. 55–62, 2018.

[8] R. J. Kuo, J. Y. Lin, and T. Nguyen, "An application of sine cosine algorithm-based fuzzy possibilistic c-ordered means algorithm to cluster analysis," *Soft Computing*, vol. 25, no. 5, pp. 3469–3484, 2021.

[9] C. Fang, "Intelligent online teaching system based on SVM algorithm and complex network," *Journal of Intelligent and Fuzzy Systems*, vol. 40, no. 5, pp. 1–11, 2020.

[10] J. Wang, D. K. Schreiber, N. Bailey, P. Hosemann, and M. B. Toloczko, "The application of the OPTICS algorithm to cluster analysis in atom probe tomography data," *Microscopy and Microanalysis*, vol. 25, no. 2, pp. 338–348, 2019.

[11] U. Srilakshmi, N. Veeraiah, Y. Alotaibi, S. Alghamdi, O. I. Khalaf, and B. V. Subbayamma, "An improved hybrid secure multipath routing protocol for MANET," *Access*, vol. 9, pp. 163043–163053, 2021.

[12] P. Yu, F. Zhou, X. Zhang, X. Qiu, M. Kadoch, and M. Cheriet, "Deep learning-based resource allocation for 5G broadband TV service," *IEEE Transactions on Broadcasting*, vol. 66, no. 4, pp. 800–813, 2020.

[13] J. Jang and D. B. Hitchcock, "Model-based cluster analysis of democracies," *Journal of Data Science*, vol. 10, no. 2, pp. 297–319, 2012.

[14] N. Chen, B. Rong, X. Zhang, and M. Kadoch, "Scalable and flexible massive MIMO precoding for 5G H-CRAN," *IEEE Wireless Communications*, vol. 24, no. 1, pp. 46–52, 2017.

[15] L. Pan, X. Qin, and S. Luo, "DSP-TMM: a robust cluster analysis method based on diversity self-paced T-mixture model," *Journal of Beijing Institute of Technology*, vol. 29, no. 106, pp. 100–112, 2020.

[16] C. Pang, "Simulation of student classroom behavior recognition based on cluster analysis and random forest algorithm," *Journal of Intelligent and Fuzzy Systems*, vol. 40, no. 2, pp. 2421–2431, 2021.

[17] K. Thiyagarajan, M. Jayaraman, V. Vijayan, and R. Ramkumar, "Cluster analysis of lost foam casted Al-Zn-Mg-Cu alloy with K-mean algorithm," *Journal of New Materials for Electrochemical Systems*, vol. 23, no. 1, pp. 45–51, 2020.

[18] C. Xu, L. Xu, Y. Lu, H. Xu, and Z. Zhu, "E-government recommendation algorithm based on probabilistic semantic cluster analysis in combination of improved collaborative filtering in big-data environment of government affairs," *Personal and Ubiquitous Computing*, vol. 23, no. 3-4, pp. 475–485, 2019.

[19] V. Tai and N. Ledai, "A new fuzzy time series model based on cluster analysis problem," *International Journal of Fuzzy Systems*, vol. 21, no. 3, pp. 852–864, 2019.

[20] F. Zhu, C. Zhang, Z. Zheng, and A. Farouk, "Practical network coding technologies and softwarization in wireless networks," *IEEE Internet of Things Journal*, vol. 8, no. 7, pp. 5211–5218, 2021.

[21] M. Adil, M. A. Jan, S. Mastorakis et al., "Hash-MAC-DSDV: mutual authentication for intelligent IoT-based cyber-physical systems," *IEEE Internet of Things Journal*, 2021.

[22] M. Adil, H. Song, J. Ali et al., "EnhancedAODV: a robust three phase priority-based traffic load balancing scheme for internet of things," *IEEE Internet of Things Journal.*, 2021.

[23] Y. R. Yu, X. Fan, L. Chen et al., "Mass spectrometric evaluation of the soluble species of Shengli lignite using cluster analysis methods," *Fuel*, vol. 236, pp. 1037–1042, 2019.

[24] A. Farouk, M. Zakaria, A. Megahed, and F. A. Omara, "A generalized architecture of quantum secure direct communication for N disjointed users with authentication," *Scientific Reports*, vol. 5, no. 1, pp. 1–17, 2015.

[25] A. M. Farid, "Measures of reconfigurability and its key characteristics in intelligent manufacturing systems," *Journal of Intelligent Manufacturing*, vol. 28, no. 2, pp. 353–369, 2017.

[26] Y. Rao, J. Zhang, Y. Zou, Y. Sun, X. Chen, and S. Xu, "An advanced operating environment for mathematics education resources," *SCIENCE CHINA Information Sciences*, vol. 61, no. 9, pp. 1–3, 2018.

[27] H. Abulkasim, A. Farouk, S. Hamad, A. Mashatan, and S. Ghose, "Secure dynamic multiparty quantum private comparison," *Scientific Reports*, vol. 9, no. 1, pp. 1–16, 2019.

[28] A. Farouk, A. Alahmadi, S. Ghose, and A. Mashatan, "Blockchain platform for industrial healthcare: vision and future opportunities," *Computer Communications*, vol. 154, pp. 223–235, 2020.

[29] C. Feng, "An intelligent virtual reality technology in the teaching of art creation and design in colleges and universities," *Journal of Intelligent and Fuzzy Systems*, vol. 40, no. 2, 2021.

[30] X. Xuewen, "Fast search of art culture resources based on big data and cuckoo algorithm," *Personal and Ubiquitous Computing*, vol. 24, no. 1, pp. 127–138, 2020.

[31] M. Huard, "Don't be afraid of religious art: thinking through and resources for art educators," *Art Education*, vol. 73, no. 1, pp. 24–30, 2020.

[32] L. Wen, L. Huang, and F. Yan, "Cluster analysis of CO2 emissions by the Chinese power industry," *Polish Journal of Environmental Studies*, vol. 28, no. 2, pp. 913–921, 2019.

[33] V. I. Zimovets, S. V. Shamatrin, D. E. Olada, and N. I. Kalashnykova, "Functional diagnostic system for multichannel mine lifting machine working in factor cluster analysis mode," *Journal of Engineering Sciences*, vol. 7, no. 1, pp. E20–E27, 2020.

Hindawi
Wireless Communications and Mobile Computing
Volume 2022, Article ID 1940432, 11 pages
https://doi.org/10.1155/2022/1940432

Research Article

Multimedia Wireless-Network-Based Model for Smart Interactive Translation Teaching

Fei Huang

School of Foreign Language, Jiaying University, Meizhou 514015, Guangdong, China

Correspondence should be addressed to Fei Huang; huangfei@jouredu.cn

Received 24 December 2021; Revised 7 February 2022; Accepted 8 February 2022; Published 9 March 2022

Academic Editor: Mohamed Elhoseny

With the acceleration of the internationalization process, the demand for English-speaking talents in all walks of life in China is also increasing. However, the current students' translation ability is weak and cannot meet the demand for talents. This article combines interactive translation teaching mode with multimedia teaching theory to provide an interactive translation teaching method for English translation teaching. This article studies the impact of multimedia-centered interactive translation teaching methods on college students' English learning ability from five dimensions: classroom interaction, learning motivation, learning autonomy, language skills application, and English performance. From the results of the previous test, the English translation ability of the students in the two classes is almost at the same level before the experiment. However, after adopting the interactive method based on multimedia wireless network in one semester, the English translation scores of the two classes differed greatly. Most students can actively practice English translation in their spare time. As a result of collecting information and reading materials on the Internet and preparing daily speeches in their spare time, students gradually accumulate enough written materials, which can alleviate the anxiety caused by insufficient content. In addition, students also actively communicate with their classmates after completing the translation to improve their composition level. Studies have shown that the number of students who complete translation tasks only after class has dropped from 75% to 31%.

1. Introduction

Owing to the widespread use of English, people from different countries tend to use English as a tool for communicating with each other. English plays an increasingly important role in the communication between domestic and foreign countries. At the same time, social development has also led to the increasing demand for international talents in various jobs, and the requirements for talents are also getting higher and higher. In the face of changes in the international society, how colleges and universities can train students who can communicate proficiently in English, and how to improve college students' English communication skills through English teaching practices have become the goals and motivations of colleges and universities.

Traditional English translation teaching focuses on translation technology or a combination of translation theory and translation technology, focusing on the teaching of knowledge, rather than training students' translation ability [1]. Qiang [2] explores the purpose and communicative and cross-cultural features of interactive translation teaching in English majors based on teleology and lays a solid foundation for their professional development [3, 4]. Knowles et al. [5] introduced the results of an empirical study on the translation efficiency of interactive translation prediction (ITP). Compared with postediting (PE), more than half of professional translators use a neural-based machine translation system (NITP) for faster translation [6]. Yang [7] and Andrabi and Wahid [8] used interactive reading theory as a teaching method to design the corresponding teaching process. The traditional teaching model is teacher-centered and mainly focuses on the transmission of basic translation knowledge and technology, which cannot meet the teaching needs, while scientific translation teaching requires new teaching methods to meet the needs of development [9, 10]. Deng [11] suggests to propose five dimensions in different directions to help students develop

translation skills. They are the dimensions of language, culture, literature, politics or thought, functionalism, and digitalization [12]. In the context of the current rapid and continuous development of global communications and professional discourse, it is necessary to design methods to ensure that high-quality professional translations and successful translation training become real challenges. Natalie et al. [13] introduced a translation teaching framework specifically designed for this type of environment. Margrethe [14] tried to test the quality of translation. In particular, the question to consider is whether it is possible to ensure quality of translation. If so, what are the implications of translation theory, translation practice, and translation education?

This article combines multimedia wireless network teaching method with interactive translation theory to provide an interactive translation teaching method for English translation teaching. This article also studies the impact of multimedia-centered interactive translation teaching methods on college students' English-learning ability from five dimensions: classroom interaction, learning motivation, learning autonomy, language skills, and English performance. From the results of the previous test, the English translation ability of the students in the two classes is almost at the same level before the experiment. However, after adopting the interactive method based on multimedia wireless network in one semester, the English translation scores of the two classes differed greatly. Research shows that most students can actively practice English translation in their spare time, reduce anxiety caused by insufficient content, and actively communicate with classmates after completing the translation.

2. Related Work

Wu et al. [15] proposed an interactive teaching system based on MOOC. Chang-Xian et al. [16] used interactive teaching methods to stimulate students' learning enthusiasm and improve the teaching effect of zoonotic diseases. The results show that the interactive teaching method is effective for the teaching of animal infectious diseases and can significantly improve the teaching quality of animal infectious diseases. Wadson [17] and Kim and Xing [18] studied the impact of an interactive teaching method on the learning performance and prevention, relief, preparation, and response abilities of nursing students. It is worth noting that theoretical teaching through comprehensive teaching methods can improve students' perception and motivation to learn disaster response measures. Cai et al. [19] took traditional Chinese clothing as an example and proposed a virtual reality interactive teaching mode for clothing design education. In medicine, interactive tutorials can provide students with the benefits of reading brain CT scans, while e-learning and interactive tutorials can also provide students with different learning advantages in radiology.

2.1. Interactive Translation Teaching Method Based on the Multimedia Wireless Network

2.1.1. Interactive Translation Teaching Theory Based on the Multimedia Wireless Network. Multimedia teaching platform is a kind of comprehensive processing of information and knowledge in the form of text, graphics, images, animation and sound to make courseware, and integrated control through software and hardware such as computers. A technical platform for a series of interactive operations. Compared with other theories in the field of second language acquisition, interactive teaching method is a new method of English teaching and a new research field. It is considered an indispensable part of the field of second language teaching, and its popularity is increasing. The interactive teaching method based on multimedia wireless network regards teaching activities as a multidimensional communication and dynamic interaction process in an information technology environment. In classroom teaching, there are a variety of interactive English translation teaching modes between teachers and students, students and students, and students and computers, as shown in Figure 1:

(1) Teachers, as the main body of teaching design, carry out task design and participate in student knowledge construction based on the analysis of students and teaching resources according to specific teaching goals. The so-called wireless network refers to the network that can realize the interconnection of various communication devices without wiring. Wireless networking technologies cover a wide range of global voice and data networks that allow users to establish wireless connections over long distances, to infrared and radio frequency technologies optimized for short-range wireless connections.

(2) Students interact with teachers, other students, and learning resources in a multidimensional environment such as classrooms, extracurricular activities, and multimedia. Teachers make necessary adjustments to the teaching design according to the actual situation of the activity.

(3) Students focus on the teacher's teaching design, teaching requirements, and teaching tasks and use English as a tool to achieve meaningful construction through personal efforts or group cooperation. Translate the acquired language knowledge into specific learning outcomes, such as improving English proficiency in English translation. Multimedia teaching means that in the teaching process, according to the characteristics of teaching objectives and teaching objects, through teaching design, rational selection, and use of modern teaching media, and organic combination with traditional teaching methods, to participate in the whole process of teaching together, with the role of a variety of media information. For students, form a reasonable teaching process structure to achieve the optimal teaching effect.

(4) Teachers, students, and other learning partners should evaluate the aforementioned learning achievements and tasks in a timely manner and give feedback to the aforementioned steps to improve teaching quality and prepare for a new round of teaching process. Its main operation is shown in Figure 2.

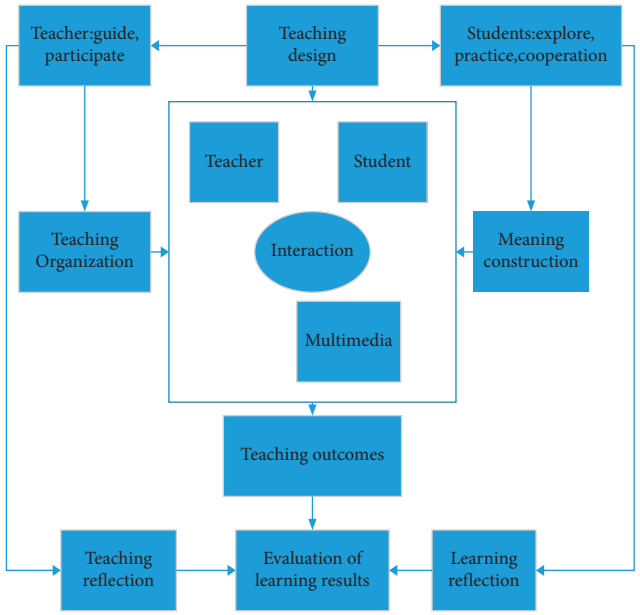

Figure 1: Interactive teaching mode based on multimedia of high school English.

2.1.2. Features of Interactive Translation Teaching Based on the Multimedia Wireless Network. The interactive teaching method based on multimedia is different from the traditional English teaching method. Generally speaking, there are two main functions: one is about changes in the teaching environment, and the other is about changes in the roles of teachers and students. The most important thing is to consider the individual differences of students. As we all know, there are individual differences in learners' personalities and learning methods. This difference is more prominent in foreign language learning. It uses computer technology, network technology, communication technology, and scientific and standardized management to integrate and fully digitize all information resources related to learning, teaching, scientific research, management, and life services to form unified user management and unified resources. Management and unified access control. It focuses on that students can access the campus network and the Internet through Wifi at any time, so that they can easily obtain learning resources. Teachers can use the wireless network to check students' learning status, complete lesson preparation and conduct scientific research anytime and anywhere. Its core lies in the implementation of paperless teaching and the extension of wireless network in campus. According to psychological findings, some people are good at logical thinking, while others are good at image thinking. Figure 3 is a schematic diagram of the multimedia network teaching system.

2.1.3. Wireless Network Technology. A wireless network refers to any type of radio computer network, which is generally combined with a telecommunication network and can be connected between nodes without cables. With the continuous advancement of science and technology, wireless network technology has also been developed. It can play different roles when combined with specific fields. Linear model is a general term for a class of statistical models. The production method is to use a certain process to connect various links, including linear regression models and variance analysis models, which are used in biology, medicine, economy, and management. The linear model is composed of multiple linear weights and is predictive. The specific function expression is as follows:

$$\begin{aligned} t(a) &= \alpha_1 q_1 + \alpha_2 q_2 + \cdots + \alpha_i q_i + k, \\ t(a) &= \alpha^y q + k, \end{aligned} \tag{1}$$

where q represents the attribute value, and the entire model can be determined only after the values of α and k are determined.

$$t(a_h) = \alpha_h q_h + k, \tag{2}$$

where $t(a_h)$ represents the linear regression equation, using this method can reduce the error.

$$\begin{aligned} (\alpha, k) &= \arg\min \sum_h^l \left(t(a_h) - g_h\right)^{5/3}, \\ (\alpha, k) &= \arg\min \sum_h^l \left(g_h - \alpha a_h - k\right)^{5/3}. \end{aligned} \tag{3}$$

The most simplified equation can be obtained by solving α and k.

$$W_{(\alpha,K)} = \sum_h^l \left(g_h - \alpha a_h - k\right)^{5/3}. \tag{4}$$

Derivation of the other program can get

$$\begin{aligned} \frac{\beta W_{(\alpha,k)}}{\beta \alpha} &= 0.5\left(\alpha \sum_h^l a_h^2 - \sum_h^l (g_h - k) a_h\right), \\ \frac{\beta W_{(\alpha,k)}}{\beta \alpha} &= 0.5\left(dk - \sum_h^l (g_h - \alpha a_h)\right). \end{aligned} \tag{5}$$

After we set formula (5) to zero, we can get the optimal solution:

$$\begin{aligned} \alpha &= \frac{\sum_h^l g_h (a_h - \overline{a})}{\sum_h^l a_h^2 - (3/d)\left(\sum_h^l a_h^2\right)^{5/3}}, \\ k &= \frac{3}{d} \sum_h^l (g_h - \alpha a_h). \end{aligned} \tag{6}$$

h is the corresponding coefficient. Where $\overline{a} = (3/d) \sum_h^l a_h^2$ represents the average value of a.

$$\widehat{\alpha} = \arg\min (g - A\widehat{\alpha})^q (g - A\widehat{\alpha}). \tag{7}$$

If you derive the formula, you can get

$$\frac{\beta W}{\beta \widehat{\alpha}} = 2A^q (A\widehat{\alpha} - g). \tag{8}$$

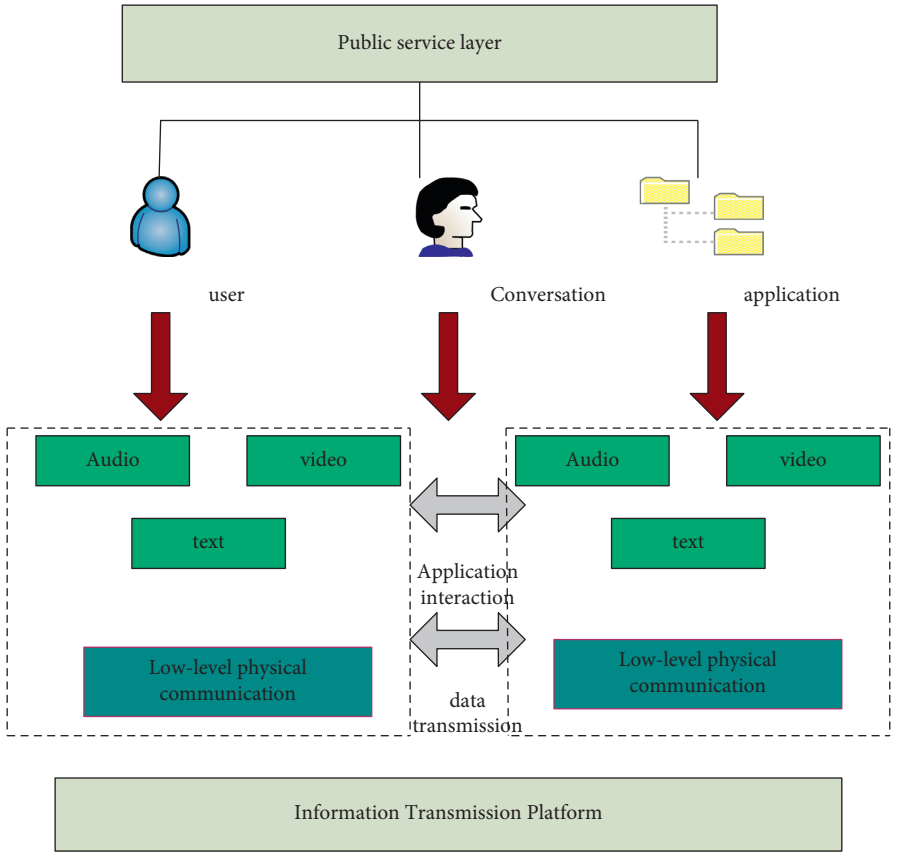

Figure 2: Interactive platform operating model.

If the value of the aforementioned formula is zero, then linear regression parameters can be obtained.

$$U(s) = \frac{3}{2}\sum_{h}^{l}\left(g\left(a_h, s\right) - f_h\right)^{(3/2)},$$
$$\overline{U}(S) = \frac{3}{2}\sum_{h}^{l}\left(g\left(a_h, s\right) - f_h\right)^{(3/2)} + \frac{\partial}{2}\|s\|^{(3/2)}, \tag{9}$$

where ∂ represents the importance of the error term.

$$Y_x(W) = \sum_{w}^{|w|} g_w j_w(W) + X|W|, \tag{10}$$

where $|W|$ represents the number of nodes and w is the node of W.

$$J_x(W) = -\sum_{D}\frac{g_{wd}}{g_w}\log\frac{g_{wd}}{g_w}, \tag{11}$$

where g_{wd} represents the number of samples in category k.

$$Y(X) = \sum_{x=1}^{|x|} g_w j_w(X) = -\sum_{x=1}^{|x|}\sum_{x=1}^{d} g_{wd}\log\frac{g_{wd}}{g_w}. \tag{12}$$

At this time,

$$Y(X) = Y_H(X) + \beta|X|, \tag{13}$$

where $|X|$ represents the complexity of the model.

$$g_s(a) = \sum_{h}^{l} F\left(a, \Theta_s\right), \tag{14}$$

where Θ_s represents the parameter and s represents the total quantity.

$$g_0(a) = \arg\min\sum_{j=1}^{j} S\left(b_j, m\right), \tag{15}$$

where $g_0(a)$ represents the initialization model.

$$h = -\left(\frac{\chi Q\left(d_j, g\left(a_j\right)\right)}{\chi g\left(a_j\right)}\right), \tag{16}$$

where r represents the regression equation of the label $g(a)$ vector fitting.

$$d = \arg\min\sum_{r} Q\left(d_j, g\left(a_j\right) + l\right),$$
$$g(a) = g_i(a) + \sum_{s=1}^{s} \mathrm{d}T. \tag{17}$$

$g(a)$ tends for update model expression.

$$\widehat{g}(a) = g_i(a) = \sum_{s=1}^{s}\sum_{x=1}^{x} \mathrm{d}T, \tag{18}$$

where $\widehat{g}(a)$ represents the gradient boosting regression tree.

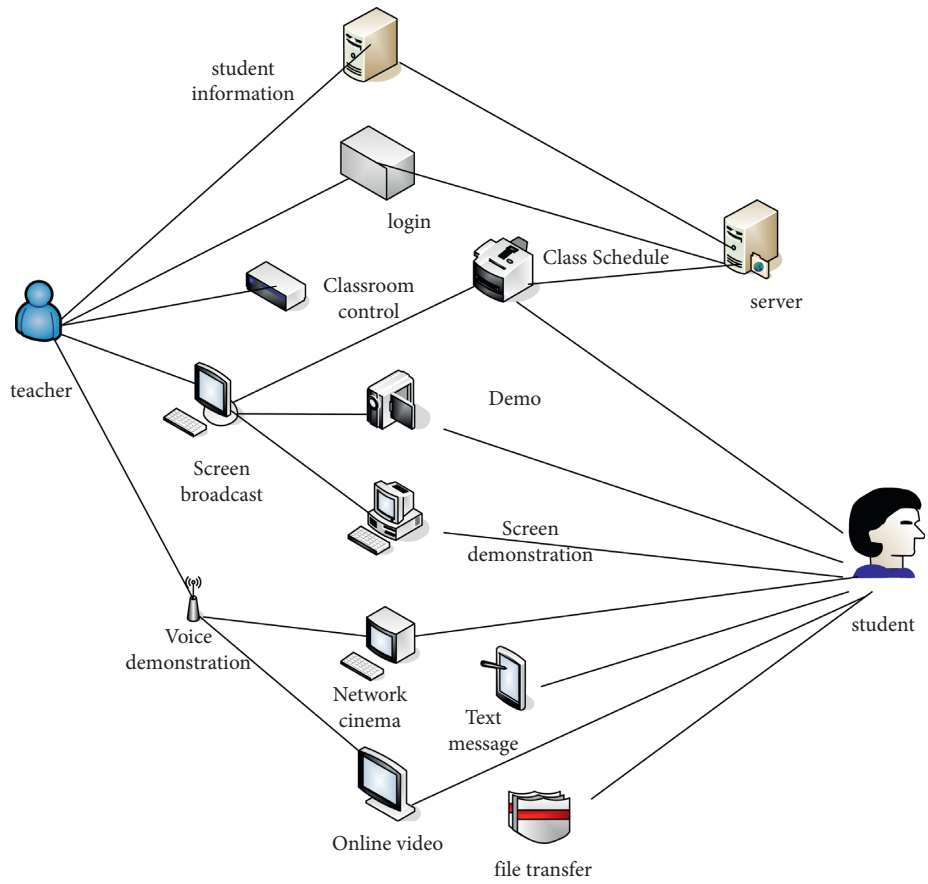

Figure 3: Multimedia network teaching system.

2.1.4. Wireless Network Multimedia Technology. The wireless network covers a very wide range, including wireless voice communication and can also provide users with communication system services. According to the different coverage, it can be divided into wireless personal area network, wireless wide area network, and so on. The main transmission is shown in Figure 4.

The combination of wireless network and multimedia will inject new vitality into the classroom, but to achieve this effect, the network condition must be stable. If the network is unstable, the effect may be somewhat different from the expected. Figure 5 shows the transmission diagram under different network conditions.

Based on the theoretical basis of multimedia wireless networks, we have the following.

(1) Multimedia Classroom Teaching Theory. The difference between traditional classroom and multimedia classroom is reflected in the status and role of students and teachers. Since the establishment of the school, the traditional classroom teaching of teacher teaching and student learning has been carried forward to the present. It has affected today's education to a certain extent, and stifled students' curiosity and thirst for knowledge. Students act as "listeners" in the classroom, and teachers act as "masters" in the classroom. As the masters in the classroom, students actively explore knowledge and communicate with their classmates and teachers. Teachers become student guides, facilitators of learning, help students complete learning tasks, and conduct summary evaluations. The multimedia classroom teaching mode is shown in Figure 6.

(2) Individualized Learning Theory. Personalized learning is mainly reflected in the following aspects. Learners learn through multimedia platforms. In the process of human-computer interaction, teachers can view the learning situation of learners through the background, track learners in real time, and provide personalized guidance. Learner autonomous learning is the main form of personalized learning. In the interactive test process, learners perform their own exercises according to their learning content, and the system will give corresponding scores to help students understand their own shortcomings more truly and make learning more targeted. The implementation process of personalized education is carried out from the stimulation of learning motivation (mindset, concept, and belief), the improvement of learning ability (thinking ability, learning ability, and innovation) to the mastery of knowledge and skills and the acquisition of experience. Education should focus on personality education first, ability education second, knowledge and skills education last, and individualized education is a truly human-oriented education. At the same time, individualized education is the education of balanced development of knowledge and skills education, comprehensive ability education and personality education.

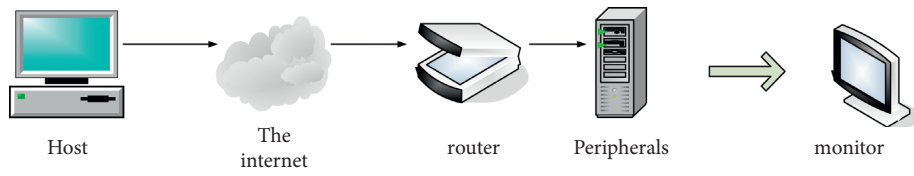

Figure 4: Transmission path.

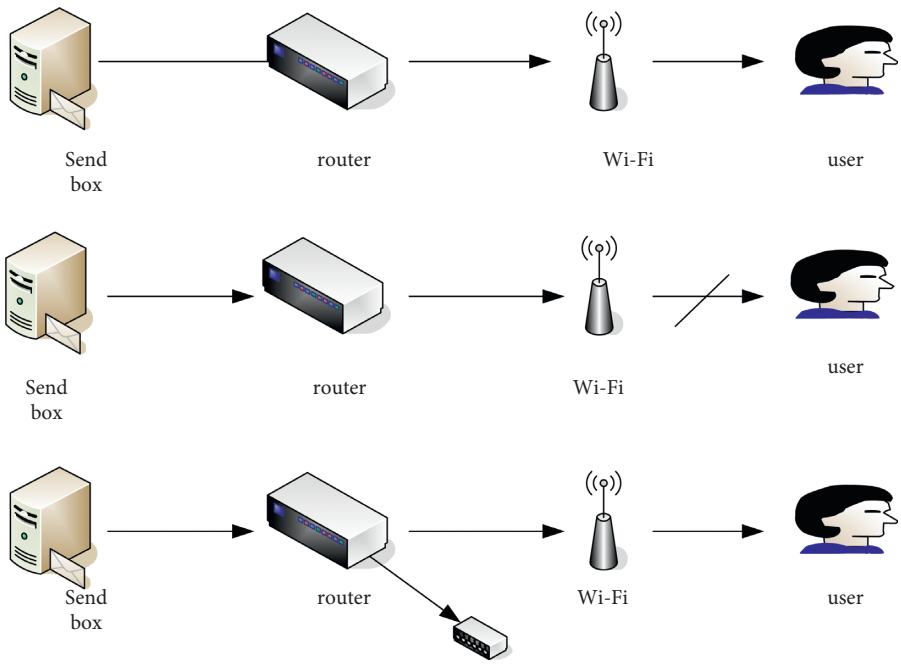

Figure 5: Transmission diagram under different network conditions.

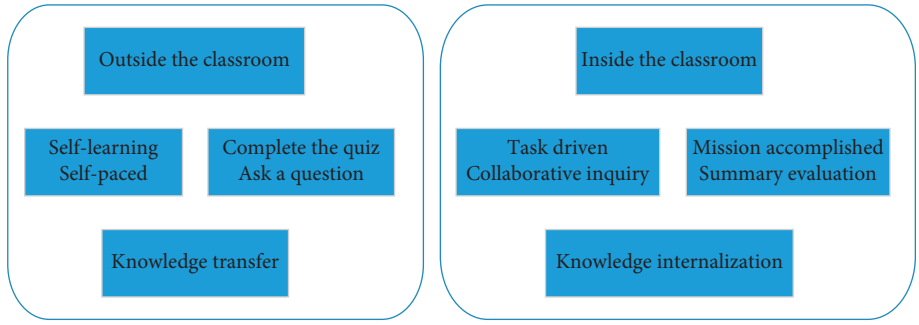

Figure 6: Multimedia classroom teaching mode.

(3) Ubiquitous Learning Theory. Ubiquitous learning refers to a learning method in which learners are not limited by location and time and focus their main energy on learning. In addition to using computers, ubiquitous learning uses wireless networks to connect to devices, which can be in schools, buses, libraries, and wherever you want to study. Ubiquitous learning mainly has the following characteristics: the demand for learning is ubiquitous, and the occurrence of learning is also ubiquitous. Learners can learn at anytime and anywhere according to their needs. Diversified communication methods and high-performance communication enable learners to find suitable learning methods and tools.

3. Design and Implementation of Survey Research Plan

3.1. Research Object. This article takes 86 freshmen, sophomores, and juniors from XX University in XX Province as the research objects. There are 45 students in 5 classes and 41

students in 6 classes. This article analyzes the entrance examination results of these two classes and finds that the average scores of these two classes are relatively close, and the average scores of English translation are also similar. In order to make the experiment more effective, this article immediately organized a comprehensive inspection at the beginning of the semester. After the test, this article collected the English translation results of the two classes. Through independent sample T test, it is found that the English translation level of the two classes is very similar. On this basis, the author can effectively compare multimedia-based interactive translation teaching methods with traditional methods. The researchers used 45 students in 5 classes as the control group (CC) and 41 students in 6 classes as the experimental group (EC).

3.2. Questionnaire Design. In this experiment, a questionnaire is issued after the teaching experiment. The questionnaire is divided into two parts, examining four dimensions in addition to English performance: classroom interaction, learning motivation, learning autonomy, and language skills application.

The first part of the questionnaire is an operability test of the teaching experiment from the perspective of classroom interaction. There are 5 questions in the questionnaire, including the main activities in the classroom, the form of activities, the time of group activities, the role of teachers, and the feelings of students. These 5 questions are used to verify the effectiveness of the experimental operation and ensure that there is a significant difference in the form of classroom interaction between the control group and the experimental group in experimental teaching. Tables 1 and 2 are the specific conditions of the experimental subjects.

The second part is about the scale design of students' learning status. The postexperiment scale has a total of 17 questions, which are composed of completely disagree, disagree, general, agree, and completely agree. The score is 1 to 5. A high score indicates a high degree of agreement on the question. Combined with the research purpose, the scale analyzes the students' English learning situation from the three dimensions of students' learning motivation, learning autonomy, and language skills.

The power consumption of the system during the experiment is represented by the current meter, and the specific conditions are shown in Table 3.

3.3. Interactive Translation Teaching Plan Based on the Multimedia Wireless Network. The interactive teaching method proposes that the ratio of teacher's speech time to effective multimedia activities is 3:7, that is, the teacher's speech time in the classroom is controlled within 30%, and the rest of the time is allocated to students for multimedia activities. However, in the actual teaching process, it is not easy to arrange teaching activities in accordance with the ratio of 30% and 70%. In the teaching method based on group interaction and cooperation implemented in this experiment, the 37 ratio is not a quantitative indicator, but a reference item for class time allocation. The implementation process of the activities based on the multimedia wireless network is shown in Figure 7.

Table 1: Gender situation.

Category		Number of people	Proportion (%)
Sex	Male	15	33.3
	Female	30	66.7
Total people		45	100

Table 2: Age situation.

		Number of people	Proportion (%)
Age	Less than 18	3	6
	18–28	20	44
	Greater than 28	22	50
Total people		45	100

Table 4 shows the performance of different genders in translation classes.

3.4. Reliability and Validity Testing. Before analyzing the results of the questionnaire, generally the reliability test and validity test of the sample data should be performed first to ensure the reliability of the questionnaire. Reliability testing refers to the degree of consistency of the results obtained using the same testing method to repeatedly measure the same test object. Cronbach's alpha reliability coefficient is currently the most common reliability coefficient.

The reliability analysis of the scale was carried out through SPSS21.0, as shown in Table 5. The reliability coefficient alpha = 0.850, which is greater than 0.8, which belongs to high reliability. It shows that the questionnaire has high reliability and meets the reliability requirements of the experiment.

Validity test is a test of the validity of the questionnaire. It is the degree to which the measurement tool can accurately reflect the required measurement purpose. In other words, whether the results of the survey can truly reflect the intent of the measurement. In this study, KMO and Bartlett sphericity test were used to test the validity of the questionnaire. Generally, KMO needs to be greater than 0.6, and the chi-square statistic of Bartlett sphere detection needs to be <0.001.

KMO sampling appropriateness test and Bartlett sphericity test were performed on the questionnaire, as shown in Table 6. The KMO in the article is greater than 0.6, and the chi-square statistic of Bartlett sphere detection also meets the requirements.

4. Results and Discussion

4.1. Analysis about Overall Scores of the Pretest in CC and EC. At the beginning of this semester, both CC and EC conducted pretests to ensure that the translation level of the two courses is the same before applying multimedia-based interactive translation teaching. This article uses SPSS19.0 data analysis software to conduct an independent sample T test on the overall test results of EC and CC. The specific experimental results before the experiment are shown in

Table 3: Network structure current meter.

Category	"Point-to-point" structure	"Star" structure	"Tree" structure
Node idle state	0.65	0.71	0.71
Intermediate node receiving	*	30	28
Intermediate node sends	*	23	23
End node receiving	31	30	30

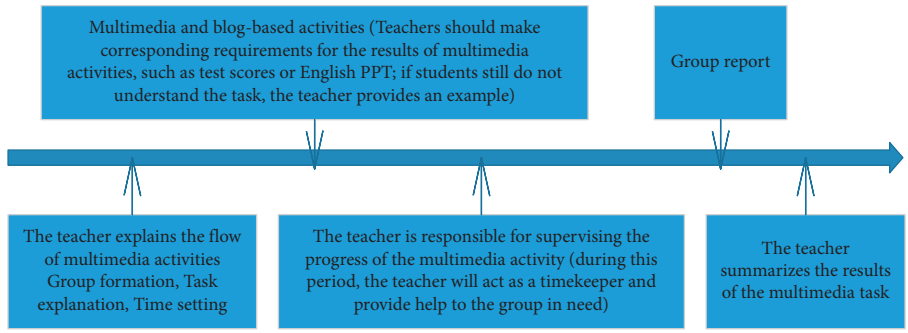

Figure 7: Implementation process of multimedia wireless network activities.

Table 4: Gender differences.

Category	P value	Boys' mean	Average girls
Cooperate	0	2.03	2.87
Access data	0	2.36	3.52
Revision	0	3	4.2

Table 5: Reliability test results.

Cronbach's alpha	Cronbach's alpha based on standardized terms	Number of items
0.850	0.859	18

Table 6: Validity test results.

Kaiser–Meyer–Olkin measure of sampling adequacy		0.913
Bartlett's sphericity test	Approximate chi-square	1964.342
	df	153
	Sig.	0.000

Figure 8. Table 7 and Figure 9 show the predictions of CC and EC. It can be seen from Table 7 that the CC deviation is 19 and the EC deviation is 21. The difference between the two in terms of error is 0.4. The parameters in Figure 9 decrease as a whole.

According to Figure 8, there is no significant difference between the average value of EC and the average value of EC. The average value of EC is 18.3659, while the average value of CC is 18.6444. These data show that the translation level of the first two categories of EC is equivalent this semester. Therefore, it can be concluded that the English translation performance of CC and EC students is roughly the same.

In addition, Table 8 shows that its significance is 0.699, which is higher than 0.05. Through Levene's test for equal variances, it can be seen that the variances of CC and EC are equal. The standard deviations of EC and CC are 1.54525 and 1.49477, respectively. In addition, Sig. (2-tailed) is $0.399 > 0.05$, which also shows that the English translation ability of EC and CC students is at the same level before the test. In addition, the upper and lower scores of the 95% confidence interval for the difference both contain zero. Therefore, it is scientific to choose these two categories as parallel categories in the research. From this, we can also speculate that if there is a significant difference in the English translation performance of the two classes after the experiment, it may be affected by different translation teaching methods.

4.2. Analysis about Overall Scores of the Posttest in CC and EC. In order to verify whether there is a difference in English translation performance between the experimental class and the control group after the experiment, after the end of the semester, the two classes were posttested. The specific experimental results are shown in Figure 5.

From Figure 10, it can be clearly seen that the average score of CC is 19.3556, the average score of EC is 20.4878, and the difference between the average score of EC and CC after the test is 1.1322. The results show that there is a big difference between EC and CC after the experiment, and the average score of EC students is significantly higher than that of CC.

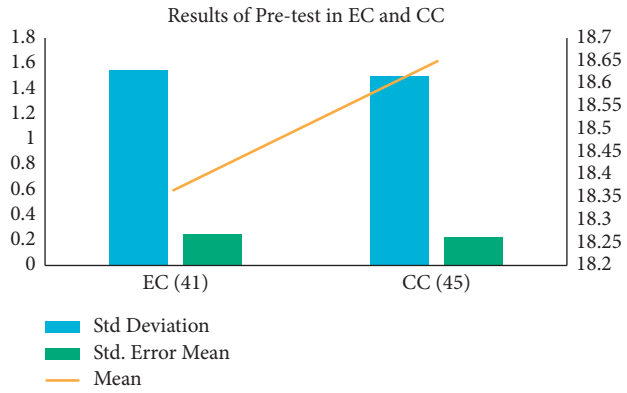

Figure 8: Results of pretest in EC and CC.

Table 7: Forecast data statistics set.

	Statistics			
	Class	Deviation	Error	Standard
Predict	CC	19	3.3	55
	EC	21	2.9	54

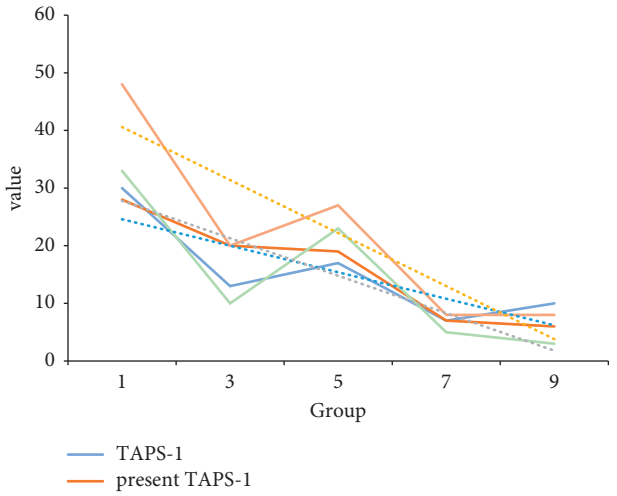

Figure 9: English-Chinese and Chinese-English translation.

According to Table 9, the value of sig is 0.042 lower than 0.05, which indicates that the two assumed variances are not equal. In addition, the data of Sig. (2-tailed) is $0.007 < 0.05$, so there is a huge difference between EC and CC. In other words, according to this method, EC has made greater progress than CC ($20.4878 > 19.3556$). In addition, in the 95% confidence interval of the difference, it is obvious that zero is not included in the upper and lower limits. Therefore, the average scores of these two categories differ greatly. As the English translation teaching methods of the two classes in the experiment are different, the improvement of students' English proficiency is more significant. It can be concluded that the interactive translation teaching method based on multimedia wireless network used in the experimental class is better than the traditional English translation teaching method.

4.3. Analysis about Overall Scores of the Pretest and Posttest in CC and EC. In order to further prove the impact of this new method on improving students' English translation performance, the researchers applied paired sample T-tests to compare and analyze the two tests in CC and EC.

In Figure 11, compared with the average score before the test of CC (18.6444), the improvement of the average score after the test of CC (19.3556) is not obvious. The average score of EC was 18.3659 before the test and 20.4878 after the test, but the result after the test was 2.1 higher than the previous result. At the same time, EC's Sig. (2-tailed) is $0.000 < 0.05$, and there is a big difference between before and after the exam, indicating that the students' translation level has been greatly improved. The Sig. (2-tailed) of CC is $0.187 > 0.05$, and there is no significant difference between the pretest and the posttest, which indicates that the translation performance of CC students has improved slightly. Based on the aforementioned data, we can conclude that EC students have made greater progress in translation performance than CC students. It clearly shows that the correlation coefficient is 0.820, that is, the Sig. value of CC is $0.032 < 0.05$. The data show that there is a relationship between these two variables, so a paired sample t-test can be performed in CC.

4.4. Analysis about Analytical Scores of the Pretest and Posttest in CC and EC. This article conducts a detailed study on the influence of the interactive translation teaching method of multimedia wireless network on students' translation accuracy. Including the use of vocabulary, grammar, sentence patterns, and coherence, this article uses this method to prove whether this method can improve the accuracy of EC class students' English translation. The pre- and post-CC test results are shown in Figure 12.

According to the data in Figure 12, the P value of the control group students in terms of translation vocabulary, grammar, sentence pattern, and coherence are all less than 0.05 ($0.008 < 0.05$, $0.013 < 0.05$, $0.015 < 0.05$, and $0.009 < 0.05$). This shows that the pretest and posttest scores of these four items are statistically significantly different. Through the mean difference, it is found that the average student's vocabulary usage increased by 0.29, grammar usage increased by 0.09, sentence pattern usage increased by 0.04, and coherence usage increased by 0.27. It can be clearly seen that the use of sentence patterns and coherence has been further improved in the control category, followed by grammar. The standard deviation of grammar decreased by 0.092, coherence decreased by 0.144, vocabulary usage increased by 0.31, and text structure increased by 0.008. All in all, the grammatical and coherence results of the control group continued to improve, and the internal gap was narrowing. Students' achievements in these two areas are more concentrated. However, although the scores for sentence patterns and vocabulary use have improved, the internal gap has increased.

Table 8: Independent samples test.

	Sig.	t	df	Sig. (2-tailed)	Mean difference	Std. error difference
Equal variances assumed	0.699	−0.849	84	0.398	−0.27859	0.32796
Equal variances no assumed		−0.848	82.659	0.399	−0.27859	0.32847

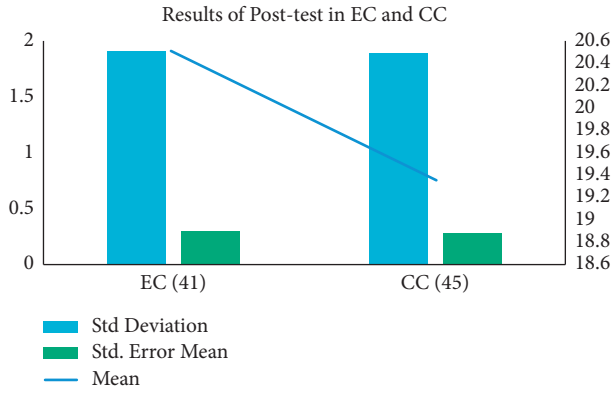

Figure 10: Results of posttest in EC and CC.

Table 9: Independent samples test.

	Sig.	t	df	Sig. (2-tailed)	Mean difference	Std. error difference
Equal variances assumed	0.042	2.772	84	0.007	1.13225	0.40839
Equal variances no assumed		2.772	83.140	0.007	1.13225	0.40835

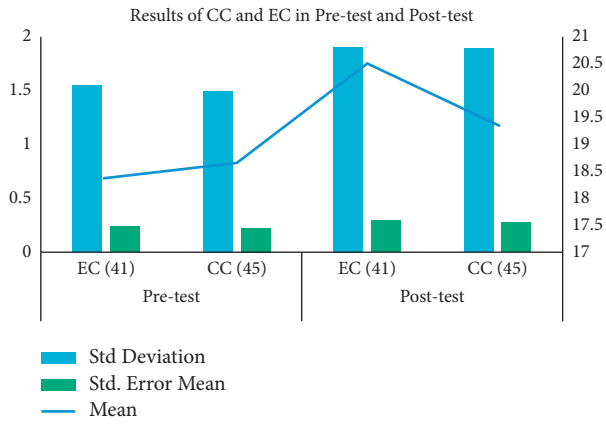

Figure 11: Results of CC and EC in pretest and posttest.

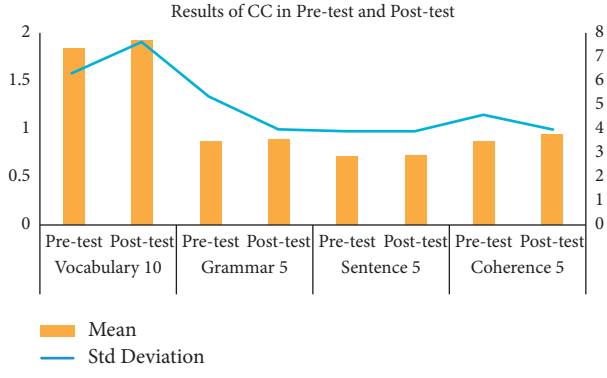

Figure 12: Results of CC in pretest and posttest.

5. Conclusion

After 4 months of experiments, based on the quantitative analysis of the pretest and posttest data, the English translation experimental class has significantly improved its performance. From the results of the pretest, the English translation ability of the students in the two classes is almost at the same level before the experiment. However, after applying the interactive method based on multimedia wireless network in one semester, the English translation scores of the two classes differed greatly.

The accuracy of English translation includes the application of vocabulary, correct grammar, sentence patterns, and coherence of text structure. After a semester of experiments, the students of the experimental class have made greater progress in improving the accuracy of translation than the control class. In terms of average performance, after using the interactive translation teaching method of multimedia wireless network in English translation, the accuracy of the experimental class has a greater improvement than the control group. As students have to edit in groups in translation classes, the application of vocabulary, grammar, and sentence patterns is becoming more and more accurate. Research shows that the number of students who complete translation tasks only after class has dropped from 75% to 31%. Most students can actively practice English translation in their spare time. Owing to the collection of information and reading materials on the Internet and preparation of daily presentations in their spare time, students gradually accumulate enough written materials, which can alleviate the anxiety of lack of content.

Data Availability

No data were used to support this study.

Conflicts of Interest

The author declares no conflicts of interest.

References

[1] Z. Lin-Ying, "Training of students' translation ability under interactive translation teaching model," *Journal of North China University of Science and Technology (Social Science Edition)*, vol. 17, no. 1, pp. 114–118, 2017.

[2] D. Qiang, "Study on interactive translation teaching of English majors based on skopos theory in applied undergraduate universities," *Journal of Hlongjiang College of Education*, vol. 37, no. 7, pp. 133–135, 2018.

[3] W. Lin, "On the strategies of graduation thesis writing teaching of translation major undergraduates based on eco-translatology," *English Language Teaching*, vol. 10, no. 8, pp. 63–68, 2017.

[4] W. Lin, "On interactive teching model of translation course based on wechat," *English Language Teaching*, vol. 10, no. 3, pp. 21–25, 2017.

[5] R. Knowles, M. Sanchez-T, and P. Koehn, "A user study of neural interactive translation prediction," *Machine Translation*, vol. 33, no. 1-2, pp. 135–154, 2019.

[6] D. A. Russell, "Interactive (adjustable) plots and animations as teaching and learning tools," *Acoustical Society of America Journal*, vol. 33, no. 1, Article ID 025001, 2018.

[7] Y. Yang, "An English translation teaching model based on interactive reading theory," *International Journal of Emerging Technologies in Learning (iJET)*, vol. 13, no. 08, pp. 146–158, 2018.

[8] S. A. B. Andrabi and A. Wahid, "Machine translation system using deep learning for English to Urdu," *Computational Intelligence and Neuroscience*, vol. 2022, Article ID 7873012, 11 pages, 2022.

[9] W. Yidan, X. Wentao, and J. I. Xue, "An empirical study of the translation workshop in sci-tech translation teaching," *Journal of Dongguan University of Technology*, vol. 24, no. 2, pp. 107–112, 2017.

[10] Y. Liu and L. Dong, "Research on English translation based on functional equivalence theory and genetic algorithm," *Wireless Communications and Mobile Computing*, vol. 2021, Article ID 6672773, 7 pages, 2021.

[11] W. Deng, "Teaching translation: a house with windows facing different directions," *Theory and Practice in Language Studies*, vol. 10, no. 1, p. 55, 2019.

[12] M. Alkhatnai, "Teaching translation using project-based-learning: saudi translation students perspectives," *Arab World English Journal For Translation and Literary Studies*, vol. 1, no. 4, pp. 83–94, 2017.

[13] K. Natalie, A. Mestivier, and M. Pecman, "Teaching specialised translation through corpus linguistics: translation quality assessment and methodology evaluation and enhancement by experimental approach," *Meta*, vol. 63, no. 3, p. 807, 2018.

[14] P. Margrethe, "Translation and quality management: some implications for the theory, practice and teaching of translation," *Philosophical Explorations*, vol. 9, no. 16, p. 201, 2017.

[15] Y. F. Wu, M. H. Yuan, and Z. C. Peng, "Research on the cultivation of students' autonomous learning ability based on mooc-based network interactive teaching," *International Journal of Continuing Engineering Education and Life-Long Learning*, vol. 29, no. 1/2, pp. 72–86, 2019.

[16] W. Chang-Xian, W. Yan, and Z. Da-Peng, "Exploration and practice of interactive teaching form in the course of evaluation on the soil plant and fertilizer," *Journal of Anhui Agricultural Sciences*, vol. 45, no. 13, pp. 248-249, 2017.

[17] K. Wadson, "Collaborative and interactive teaching approaches have a positive impact on information literacy instruction supporting evidence based practice in work placements," *Evidence Based Library and Information Practice*, vol. 14, no. 1, pp. 62–64, 2019.

[18] M. S. Kim and X. Xing, "Appropriation of affordances of multiliteracies for Chinese literacy teaching in Canada," *Research and Practice in Technology Enhanced Learning*, vol. 14, no. 1, p. 1, 2019.

[19] J.-Y. Cai, P.-P. Zhang, and X. Tan, "A novel physical education environment platform using Internet of things and multimedia technology," *International Journal of Electrical Engineering Education*, 2019.

Hindawi
Wireless Communications and Mobile Computing
Volume 2022, Article ID 9670311, 16 pages
https://doi.org/10.1155/2022/9670311

Research Article

Fine Geological Modeling of Complex Fault Block Reservoir Based on Deep Learning

Zhe Liu,[1] **Wenke Li**,[2] **Lei Zhang**,[3] **and Jiajing Li**[1,4]

[1]*School of Petroleum Engineering, Guangdong University of Petrochemical Technology, Maoming, 525000 Guangdong, China*
[2]*The Research Institute of Petroleum Exploration and Development, Beijing 100083, China*
[3]*School of Petroleum Engineering, Chongqing University of Science & Technology, Chongqing 401331, China*
[4]*School of Earth Sciences, Northeast Petroleum University, Daqing, 163000 Heilongjiang, China*

Correspondence should be addressed to Zhe Liu; liuzhe@gdupt.edu.cn

Received 2 December 2021; Revised 17 January 2022; Accepted 26 February 2022; Published 9 March 2022

Academic Editor: Xiaohui Yuan

Nowadays, people's demand for underground mineral resources is increasing, and geological disasters have occurred frequently in recent years. Geological disasters refer to geological effects or geological phenomena that are formed under the action of natural or man-made factors, causing loss of human life and property, and damage to the environment; such as landslides, collapses, mudslides, and ground subsidence. Under such a background, people must accelerate the exploration of complex geological structures. This paper is aimed at using the methods and concepts of deep reinforcement learning. Deep learning is to learn the inherent laws and representation levels of sample data. The information obtained during these learning processes is of great help to the interpretation of data such as text and images. In this way, the fine geology of complex fault-block reservoirs is modeled and studied. Geological structures and phenomena are discussed through convolutional neural network models and computer techniques. At the same time, the multitask bird recognition network is used to extract and classify geological images, so as to construct geological model maps with different spatial structures. Finally, the quality of the fault reconstruction model, the calculation of reservoir geological simulation reserves, and the evaluation of the water injection development effect of complex fault blocks are analyzed. In the evaluation of the development effect of water injection in complex fault blocks, comparing the relationship curve between the actual comprehensive water content and the oil recovery factor with the standard curve, the comprehensive water content of the initial block increased rapidly. Through timely and dynamic water allocation and comprehensive management, the water cut rising speed is controlled. The current comprehensive water cut of the reservoir is between 60% and 80%, the actual curve is between 25% and 35%, and the estimated waterflooding recovery is about 30%.

1. Introduction

The geological model of complex fault-block reservoirs should take the fine interpretation of faults as a breakthrough point. Reasonable combination of fault points, calculation of fault distance, and division of fault blocks are the basis for understanding complex fault block reservoirs and establishing 3D geological models. The complex fault block reservoir is one of many types of reservoirs. The characteristics of this type of reservoir are it not only exhibits strong reservoir heterogeneity (including affecting the integrity of injection and production between wells) but also the complexity of the nature of the boundary (including the adaptability of the well pattern) and the complexity of the oil-water system. The characteristics of fault-block reservoirs lead to large differences between complex fault-block reservoirs and ordinary reservoirs in terms of water injection development and water flooding effect evaluation.

Due to its geological structural characteristics and a series of special structures, the injection-production well pattern is imperfect, which affects the rapid energy consumption of the reservoir over a period of time, which is faster than the productivity decline of ordinary oil reservoirs. On the other hand, the lower water flooding the degree of

control affects the macroscopic swept volume, leading to a faster rate of water cut. Second, the complex fault block reservoir contains dense natural fractures, which is difficult for water injection development, so it has the characteristics of low recovery. Therefore, modeling research on fine geology of complex fault-block reservoirs is becoming more and more important.

Geological modeling of complex fault block reservoirs has always been a hot and difficult research topic. Chen et al.'s classification is one of the hot issues in hyperspectral remote sensing research. In the past two decades, a large number of methods have been proposed to deal with the classification of hyperspectral data. He introduced the concept of deep learning to the classification of hyperspectral data for the first time. First, they verify the applicability of stacked autoencoders in accordance with the classic classification method based on spectral information. Second, a classification method based on spatial dominant information is proposed. Then, a new deep learning framework is proposed to fuse these two features to obtain the highest classification accuracy. The framework is a mixture of principal component analysis (PCA), deep learning architecture, and logistic regression. Specifically, as a deep learning architecture, stacked autoencoders are designed to obtain useful advanced functions. The experimental results of widely used hyperspectral data show that the classifier constructed under this deep learning-based framework has a good classification effect. However, most algorithms do not extract deep features hierarchically [1]. Xue et al.'s research object is a complex fault block reservoir provided by the China Petroleum Engineering Design Competition. Reservoir characteristics are recorded, including stratigraphic characteristics, vertical changes, and profile characteristics (thickness, sand percentage, and combined percentage). Through the comprehensive analysis of the structural pattern and reservoir characteristics, three-dimensional quantitative modeling of the reservoir was carried out on 69 regional scales × 97 × with the application of geostatistics as the theoretical guide. Then, combining layering, structure, physics, and borehole trajectory data, a high-resolution layered reservoir model of the oilfield was established. The established 3D geological model integrates all well and structural information and provides a basic model for subsequent sedimentary microfacies modeling and physical property modeling. Finally, a series of cross-sections were established in sequence, namely, three-dimensional fence diagrams, connected well section cross-section diagrams, and well group section diagrams. However, its various complex geological construction maps need to be further studied [2]. In the field of X Tan 3D geological modeling, researchers often pay attention to modeling methods and workflow, but ignore the quantitative evaluation of the model. If the evaluation scope is narrowed to the same reservoir type, the comparability and practicality of quantitative evaluation will become apparent. The evaluation system should include three parts: data verification, geological understanding, and process inspection. Data verification is mainly to use actual data to test the accuracy of local predictions, and geological understanding is to test whether the global estimation of the model conforms to geological principles and prior insights. They are quantitative verification from different angles, complement each other, and are the key to quantitative evaluation. Process inspection is also a necessary condition to avoid contingency. Taking complex fault-block sandstone reservoirs as an example, based on feedback from experts in the petroleum industry, a multiparameter three-dimensional geological model quantitative evaluation criterion was established. However, the practical scope of these standards remains to be discussed and discussed [3]. Cui et al. propose a new advanced coupled multistable stochastic resonance method with two first-order multistable stochastic resonance systems, namely, CMSR, to detect motor bearing faults. The comparison with MSR shows that CMSR can achieve higher output signal-to-noise ratio. It is more beneficial to extract weak signal features and realize fault detection. At the same time, the method also has practical application value for engineering rotating machinery [4]. Zhang et al. proposed a three-partition state alphabet-based sequential pattern (Tri-SASP) for MTS. Experimental results on four real-world datasets show that (1) the discovered Tri-SASP and temporal rules can enrich human cognition. (2) Two three-partition strategies can bring us very meaningful and diverse Tri-SASP. (3) Both algorithms are efficient and scalable [5]. Mahmood et al.'s study discussed the effect of five different sizes of sand on the ultimate stress (MPa) of polymer-modified hand cement grouting sand using two different test standards (ASTM and BS). Based on dispersion index (SI), objective function (OBJ) evaluation, and training and testing datasets, the compressive strength of cement grouting sand can be well predicted using NLR and ANN models. The compressive strength tested using the BS standard is 71% higher than the compressive strength of the same mixture tested using the ASTM standard [6]. Firebaugh developed a platform for precise two-dimensional particle manipulation via acoustic forces from Chladni patterns and resonant microscale membranes. The project consists of two distinct phases: (i) macroscale manipulation in air using Chlarney plates; (ii) microscale manipulation in liquid using microscale membranes. The results show that the control method developed at the macroscale can be implemented and used with good precision and accuracy at the microscale [7].

The innovations of this paper are (1) through the methods and concepts of deep reinforcement learning, deep learning is to learn the inherent laws and representation levels of sample data, and the information obtained in these learning processes is of great help to the interpretation of data such as text, images, and sounds. Modeling and research on the fine geology of complex fault-block reservoirs. (2) Geological structures and phenomena are discussed through the convolutional neural network model and computer technology. (3) The multitask bird recognition network is used to extract and classify geological images to construct geological model maps with different spatial structures. (4) The quality of the fault reconstruction model, the calculation of reservoir geological simulation reserves, and the evaluation of the water injection development effect of complex fault blocks are analyzed.

2. Research Method for Fine Geological Modeling of Complex Fault Block Reservoirs Based on Deep Learning

2.1. Deep Learning. In recent years, driven by the rapid development of GPU-based parallel computing technology and the promotion of large-scale data sets, the method represented by deep learning has gradually made huge breakthroughs in multiple application fields of computers, especially in the field of computer vision and nature language processing field. In the field of computer vision, convolutional neural network (CNN) can well aim at the data characteristics of image modalities, establish the relationship between pixels, gradually extract the semantic information in the image, and finally realize the image content. For text sequence data, the method based on long short-term memory network (LSTM) is good at capturing the relationship between sequential data and extracting the inner meaning of the text sequence. Based on the above two mainstream modeling methods, a series of research on multimodal data has gradually become a research hotspot. Convolutional neural network (CNN) was first proposed by LeCun in 1998 and was successfully applied to handwritten digit recognition tasks on checks. Its network structure LeNet is shown in Figure 1.

As shown in Figure 1, the LeNet network contains basic elements such as convolution, downsampling, and nonlinear activation. The original image is convolutional operation to model the pixel relationship in the spatial neighborhood; the spatial resolution of the image is reduced through continuous downsampling operation, while the semantic information of the image is gradually abstracted; and under the action of the nonlinear activation function, the original image features are mapped to other feature spaces to enhance the expressive ability of the network [8]. The original image is input into the LeNet network, and through the abovementioned convolution, downsampling, and nonlinear operations, the recognition result of handwritten digits can be output finally. Although LeNet has a simple structure, it already contains the basic elements of convolutional neural networks, laying a solid foundation for the subsequent development of convolutional neural networks. Although LeNet has been used in handwritten digit recognition tasks in 1998, convolutional neural networks have not been applied on a large scale due to the development of computing power and the scale of image databases. It was not until the emergence of AlexNet in 2012 that the abovementioned status quo was changed [9, 10].

On the one hand, the emergence of AlexNet benefited from the substantial development of parallel computing capabilities supported by GPU hardware, which accelerated the training process of convolutional neural networks; on the other hand, the millions of large-scale image databases represented by ImageNet were used as volumes. The training of the product neural network provides a large amount of data, which promotes the network to be adequately trained, increases the feature expression ability of the network, and avoids the network from falling into an overfitting state due to the small data size [11].

Compared to LeNet, AlexNet has made the following improvements to the basic elements of convolutional neural networks. First of all, on the convolutional elements, AlexNet correspondingly increases the depth of the convolutional network and the number of channels of the convolutional layer [12]. This change has brought a huge improvement to the performance of the convolutional neural network, which is conducive to the convolutional neural network to learn more complex and expressive high-dimensional image features. Second, the maximum pooling operation (max pooling) is introduced on the downsampling method, which retains the maximum activation value of the image feature in the spatial neighborhood [13]. Finally, in the selection of the activation function, a linear rectification unit (ReLU) is used to replace the traditional sigmoid function, which avoids the phenomenon of gradient disappearance and reduces the corresponding amount of calculations and optimizes the problems in the training process as a whole.

And with the increase in the depth and complexity of the AlexNet network, a training strategy to deal with network overfitting is also proposed for the first time and provides a reference for the later training of deep convolutional neural networks [14, 15]. On the one hand, by introducing the data augmentation method (data augmentation), the original image is flipped, random cropping, and color dithering, which enriches the different manifestations of the same image; on the other hand, it proposes the dropout method, which is used in training. During this period, some neurons are randomly selected and cut out, and the value of the neuron is set to zero. The above training strategy can avoid the deep convolutional neural network from falling into an overfitting state due to too many parameters when the amount of data is limited [16, 17].

So far, AlexNet has opened the era of large-scale use of deep convolutional neural networks to model image data, and it has attracted the attention of a large number of researchers. How to better and more effectively express the inherent characteristics of images through sophisticated network structure design has become a research hotspot.

2.2. Complex Fault Block Reservoir. Complicated fault block reservoir is one of many types of reservoirs. It refers to the accumulation of oil and gas resources, etc., which are accumulated in the traps formed by complex and chaotic faults and surrounding rock structures. The characteristics of this type of oil reservoir are it not only exhibits strong reservoir heterogeneity, including affecting the integrity of injection and production between wells, but also exhibits complex boundary properties, including affecting the adaptability of well patterns and oil and water the complexity of the system [18]. Due to the wide existence of this type of reservoir, it is of great significance for the development of fault-block reservoirs, focusing on the characteristics of "small, broken, lean, scattered, and narrow" reservoirs and the difference between water injection development rules and development

dynamic characteristics [19]. It is not difficult to investigate the differences in water injection development rules and development dynamic characteristics of large and medium-sized reservoirs in complex fault-block reservoirs. It is not difficult to conclude that the fluid flow rules, water injection development theory, microscopic water drive oil mechanism, and water drive efficiency under the same conditions are consistent. Second, there may be complex oil-water systems and strong heterogeneity of the reservoir, which will affect the adaptability of the injection-production well pattern [20, 21].

(1) Geological characteristics of complex fault block reservoirs

Complex fault blocks have a certain degree of heterogeneity in terms of geological characteristics. In terms of structural characteristics, due to the cutting and extension of fault blocks, the process of forming oil reservoir traps in the block has the characteristics of fine fragmentation, which is limited by boundary cutting and the scale of sand bodies. A series of factors affect [22, 23], and fault cutting has a great impact on the sand body distribution and sedimentary phase changes of the oil layer. It is difficult to form a complete fault block reservoir, and a certain degree of injection-production system makes the well pattern control not high, which affects the macroscopic swept volume, and thus it affects the recovery efficiency of fault-block reservoirs. Therefore, for complex fault-block reservoirs, the difference in geological factors represented by strong heterogeneity is the influence of fault-block reservoirs the main factors of development [24].

(2) Evaluation of water injection development effect

The current development of the block has entered a higher water-cut stage. The oilfield is facing development difficulties such as increasing difficulty in mining, high dispersion of remaining oil in fault blocks, relatively limited remaining recoverable reserves, deteriorating geological conditions, and accelerating production decline. Flooding has highlighted the contradictions in the development of the oilfield strata, the potential tapping effect has become poor, and the injection-production relationship has become complex. Therefore, how to control the growth of water cut, effectively develop the oilfield, and maintain a stable annual oil production has become a concern for the effect of water injection development. The evaluation of development effects includes evaluations for water injection development, such as water cut and water retention, as well as evaluations for changes in fluid production. It is not only for the entire region, but for the characteristics of fault block oil layer cutting and fine fragmentation, but also for different well groups. To evaluate the effect of water injection development [25, 26]. To develop oilfields by water flooding, it is necessary to continuously evaluate the development effect at different stages of development in order to put forward effective adjustment opinions. During the evaluation process, due to changes in mining conditions, well pattern planning, and different development stages, development indicators are also different [27].

Analyzing the change law of water cut during reservoir development is of great significance for evaluating the effect of oilfield development. The current methods for analyzing water content include water content gray GM (1,1) model, logistic cycle model, generalized usher model, and five models that characterize the relationship between water content and recovery degree (concave type, concave-S transition type, S type, S-convex transition type, and convex type). The main controlling factors affecting the rise of water cut are reservoir heterogeneity and the difference in water absorption status of water wells [28]. The main factors affecting the change law of water cut in low permeability oilfields are fluid properties (oil-water viscosity ratio) and reservoir physical properties (permeability, starting pressure). The lower the permeability, the greater the starting pressure gradient, the faster the relative permeability of the oil phase decreases, and the slower the increase of the water phase permeability [29].

Reasonable reservoir production pressure difference affects oil and fluid production capacity of oil wells. The indexes describing the production capacity of oil wells include oil production index, fluid production index, dimensionless oil production, fluid production index, rice oil production index, etc. The fluid production index is the ratio of the fluid production volume to the production pressure difference [30]. The dimensionless fluid production index refers to the ratio of the fluid production index at a certain stage of development to the fluid production index at the initial stage of oilfield development (under the condition of irreducible water saturation). Through the oil-water two-phase seepage law, we can deduce the dimensionless oil production and fluid production index at different water-bearing stages [31]. The change law of conventional oil reservoirs is with the increase of water cut, the dimensionless oil production and fluid production index all have an upward trend, which indicates that with development the low fluid recovery index is unfavorable to the stable production of oil reservoirs, and the effective driving effect of injected water is reduced [32].

Reservoir recovery factor is an important basis for formulating development plans, and it is of great significance to predict the recovery factor based on the actual situation of the reservoir. Before the oilfield was put into development, it mainly relied on less exploration data, core experiments, or analogy to the same type of reservoir, through analogy to the type of reservoir, reservoir fluid viscosity, porosity, permeability, well pattern density and permeability variation coefficient, etc. Parameters select appropriate values, and the empirical formula method is usually derived from the regression of the production materials in the study area, with a small scope of application and low reliability; in the middle and late stages of development, when the mine data is rich, it can pass type A, B, C, and D. The water drive law curve predicts the recovery factor. This method is widely applicable to water drive sandstone reservoirs. When the

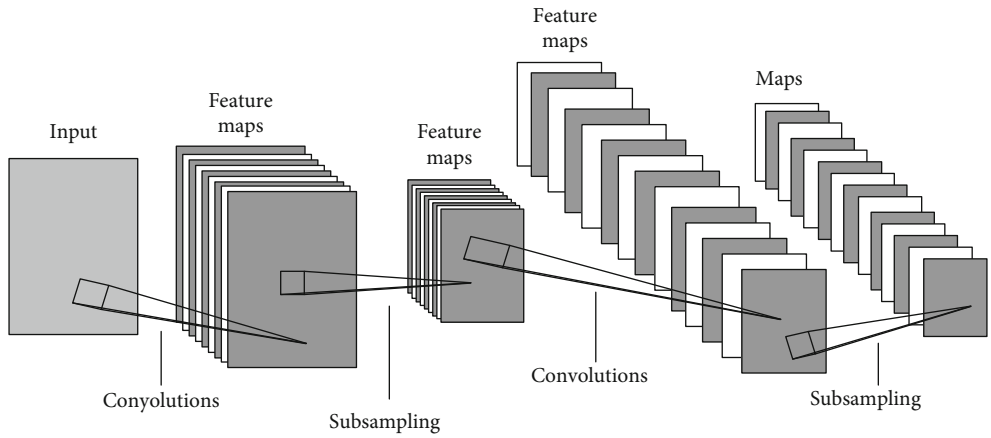

Figure 1: LeNet network structure diagram.

output of the oil field is in the decline stage in the later stage of development, the decline curve (exponential decline, hyperbolic decline, and harmonic decline) can also be used to predict the recovery rate. Tong's chart method can also be applied to oil recovery prediction in the later stage of development. In addition, based on the establishment of a fine geological model of the study area, numerical simulation software is used to predict the recovery factor under the current mining conditions when the history matching meets the accuracy requirements. This method comprehensively considers the geological structure fluctuations, development factors, and reservoirs. The effect of physical properties and fluid properties, the prediction results are more accurate and reliable.

2.3. Multitask Bird Recognition Network (MTBN). Multitask bird network (MTBN) is the joint learning of image recognition and image caption. On the one hand, the improvement of the quality of the underlying image features is conducive to simultaneously improving the accuracy of the image recognition task and the quality of the word generation in the picture-viewing task. On the other hand, the constraints of the joint learning of the top-level multitask can in turn continuously promote the underlying image features learning. And in the image caption task, we also considered the existence of individual text descriptions (individual text descriptions) and shared text descriptions (shared text descriptions). The specific description of the individual description text encourages each image to pay more attention to the learning of its own detailed features, making the image features more refined; and sharing the content of the description text allows the deep convolutional neural network to pay more attention to the confusing image pair. The differences between the details make the image features more distinguishable. Under the joint guidance of these two texts, the learned image features have strong detailed information and discriminative information at the same time, which is beneficial to promote the performance of image recognition tasks.

Convolutional neural networks need to learn from a large amount of data in order to extract key features more efficiently. Therefore, when training a convolutional neural network, it is necessary to learn from the implicit training data as much as possible, and the obtained accuracy rate is more convincing. It is the many advantages of convolutional neural network that make it widely used. We first operate on the image data through a deep convolutional neural network (CNN) to extract image features; then send the image features directly to the classifier module (classifier) to determine the category of the image. At the same time, for each picture, we send its image characteristics and the corresponding individual description text to the individual text processing module. For each pair of images in a confusing category, we send the pair of image features and the corresponding shared description text into the shared text processing module. These three modules will generate corresponding loss functions, then jointly constrain the learning process of the entire network, and jointly promote and improve the underlying image features. Below, we will describe the specific expansion of the abovementioned modules.

In the deep convolutional neural network (CNN) module, we use classic neural networks to extract image features. Convolutional network is composed of common convolution layer (convolution layer), batch normalization layer (batch normalization layer), pooling layer (pooling layer), rectification linear unit (Relu layer), and other basic units combined. The original image I is sent to the deep convolutional network, and the semantic feature a of the image is gradually extracted through the function of the above basic unit, where a $\in \mathrm{RH} \times W \times D$, H, W, and D represent the length and width of the image feature, respectively, and high.

In the classifier module, we apply the global average pooling (GAP) operation to the image feature b to remove the spatial relationship in the image feature and obtain the feature y, $y \in$ with high-level semantic information. RD as shown in the following formula:

$$y = \frac{1}{G * M} \sum_{i=1}^{G} \sum_{j=1}^{M} b(i, j). \tag{1}$$

Among them, $b(i, j)$ represents the value in the i-th row and j-th column of the image feature b. The semantic feature

y obtained by the above operation is sent to the subsequent classification, and the predicted probability q of image recognition is obtained, where $q \in RC$, C represents the number of image categories. Specific as shown in the following formula:

$$q = g_{\text{classifier}}(y), \tag{2}$$

where g represents the image classifier. Calculate the cross-entropy loss function value from the label predicted by the classifier and the real label of the image, as shown in the following formula:

$$K_{\text{classifier}} = \sum_{i=1}^{c} x_i \log q_i. \tag{3}$$

Among them, x_i represents whether the image belongs to the i-th type of image, and the value is 0 or 1, and q_i represents the probability that the image is predicted to be the i-th type of image. In the individual text description module, we input the image feature b into the long short-term memory network (LSTM) as the start of the sequence, output the predicted words of the network in turn, and finally form a description of the image content.

Suppose the input image feature a, and the output word sequence x, where

$$x = \{x_1, x_2, \cdots, x_U\}, x_u \in R^l. \tag{4}$$

T represents the length of the generated word sequence, yt represents the generated t-th word, and K represents the size of the vocabulary. At the same time, we decompose the image feature b into the following form:

$$b = \{b_1, b_2, \cdots, b_K\}, b_k \in R^T. \tag{5}$$

At time t, it is necessary to predict and calculate the weight coefficient αt at that time, the original image feature a is weighted by this weight, and the degree of contribution of the image feature to the predicted word of the LSTM module at different times is changed, as shown in the following formula:

$$e_{tu} = g_{at}(b_i, g_{i-1}), \tag{6}$$

$$\beta_{ti} = \frac{\exp(e_{tu})}{\sum_{k=1}^{L} \exp(e_{tu})}. \tag{7}$$

Among them, e and β, respectively, represent the weight coefficients before and after normalization, and β is obtained by normalizing e by the softmax function. Where formula (6) represents that at time t, the previous LSTM module hidden layer output $ht - 1$ and the vector ai of the image feature at position i are input, and the fat module is transformed, and the output at the spatial position i at time t weight eti. We need to integrate the normalization layer into the current faster RCNN architecture. In our implementation, we follow ParseNet's layer definition. There are also two ROI pooling layers to extract features from the third and fourth convolutional feature maps. The two ROI pooling layers, together with the original ROI pooling layer from the last, the fifth convolutional feature map, then independently pass the data through the normalization layer. Therefore, at time t, the original image feature b is weighted by the above weight coefficient β to obtain the corresponding context feature vector zt, as shown in the following equation:

$$v_t = \sum_{i=1}^{G} \beta_{ti} a_i. \tag{8}$$

Among them, vt indicates that the image features ai of different spatial positions i have different contributions to word prediction at time t. With the aforementioned context feature vector zt, the hidden layer output ht corresponding to the LSTM module at time t and the word yt predicted at that time can be predicted, as shown in the following formula:

$$g_t = g_{lstm}(h_{t-1}, z_t), \tag{9}$$

$$y_t = g_{\text{predict}}(h_t). \tag{10}$$

Through the above operations, we can predict the corresponding word at each moment, compare it with the real word, and calculate the corresponding loss function $K_{\text{individual}}$, as shown in the following formula:

$$K_{\text{individual}} = -\log[q(x|a)] + \gamma \sum_{i}^{K} \left(1 - \sum_{i}^{I} \beta_{ii}\right)^2. \tag{11}$$

Among them, the first item in $K_{\text{individual}}$ is the cross-entropy loss value calculated by comparing the predicted words at all moments with the real words. The second term is the constraint term. The weight value of the network at all moments in space position i is as close to 1 as possible. With the constraints of the $K_{\text{individual}}$ loss function, it can promote the continuous improvement of the quality of the underlying image features, so that the semantic content expressed by the image features can correspond to the individual description text, and the detailed information of the image features can be enhanced. In the shared text description module, we weighted the image features $aj, j \in \{1, 2\}$ of the easily confusing category, respectively, and spliced them into a context vector z and used the spliced context vector z to guide the generation of the shared text sequence. Under the supervision of the shared description text, it helps the network distinguish the differences in the image features of the easily confusing categories. At time t, the weight coefficients ejt and αjt corresponding to the image feature aj are calculated, respectively, $j \in \{1, 2\}$, as shown in the following formula:

$$e_{tu}^{j} = G_{at}\left(b_i^j, g_{t-1}\right), \tag{12}$$

$$\beta_{tu}^{j} = \frac{\exp\left(e_{tu}^{j}\right)}{\sum_{l=1}^{K}\exp\left(e_{tu}^{j}\right)}. \tag{13}$$

Among them, αj is the weight coefficient normalized by the softmax function corresponding to the image feature aj. Among them, $aj, j \in \{1, 2\}$, share the fat module. After calculating the weight coefficient βj of the corresponding image feature, the corresponding context feature zt at time t can be calculated, as shown in the following equation:

$$R_t = G_{\text{concate}}\left(\sum_{i=1}^{K}\beta_{tu}^{1}b_t^1, \sum_{i=1}^{L}\beta_{tu}^{2}b_i^2\right). \tag{14}$$

Among them, G_{concate} means joining the weighted features of $a1$ and $a2$ to form the context feature zt. With the context feature zt at time t, the output ht of the hidden layer of the LSTM module at time t and the predicted word yt can be obtained, and finally, the corresponding loss function value is calculated, as shown in the following equation:

$$\begin{aligned} K_{\text{shared}} = &-\log\left(Q\left(y\middle|b^1, b^2\right)\right) + \phi_1\sum_{i}^{k}\left(1 - \sum_{t}^{T}\beta_{tu}^{1}\right)^2 \\ &+ \phi_2\sum_{i}^{k}\left(1 - \sum_{t}^{T}\beta_{tu}^{2}\right)^2. \end{aligned} \tag{15}$$

The image features are extracted through the underlying deep convolutional neural network, and the image features are sent to the classifier module, the individual description text module, and the shared description text module, respectively; under the joint drive of these three task-driven tasks, improvement from top to bottom. The quality of image features, thereby ultimately improving the accuracy of image recognition. Optimizing the loss function of the entire framework can finally be jointly optimized through the loss function described by the following equation.

$$K_{\text{total}} = K_{\text{classifier}} + \chi K_{\text{individual}} + \eta K_{\text{shared}}. \tag{16}$$

3. Fine Geological Construction Model of Complex Fault Block Reservoir Based on Deep Learning

3.1. Fine Structural Modeling of Complex Fault Block Reservoirs

3.1.1. Structural Modeling Ideas. The essence of 3D geological modeling is to reconstruct, reproduce, and abstract the geological bodies, geological phenomena, and geological processes in the natural world. To achieve this goal, 3D visualization technology must be used. With the essence of 3D geological modeling, it can be seen that the 3D model of geological body should retain the structural characteristics of geological body. These features include the spatial form, location, and distribution of geological body. It should also have complete topological relations and geological semantics. The theory and methods of 3D geological modeling mainly include five aspects, namely, standardization of geological source data, 3D visualization data model of geological bodies, structural model methods of geological bodies, management of geological attribute data, and visualization of geological graphics.

3.1.2. Basic Process. In order to get a better modeling effect, the 3D attribute data volume line can be preprocessed before the isosurface is extracted. The main way of preprocessing is to perform interpolation processing. The purpose of interpolation preprocessing is to obtain more data points with attribute values and coordinate values in the three-dimensional space. Based on the above research, the modeling process is as follows:

(1) Obtain the profile contour line. This paper mainly studies the construction of complex geological bodies based on the contour line method, so the input of the algorithm is a series of profile contour lines. (2) Construct a four-dimensional function. A four-dimensional function is constructed for each point on the plane where the profile contour line is located, and the coordinates (x, y, z) of each point and its attribute value p are obtained. (3) Calculate the attribute value. The calculation of the attribute value is mainly to obtain the symbol of the attribute value by judging the position relationship between the point and the contour line and calculate the distance from the point to the contour line to obtain the value of the attribute value. (4) Generate the attribute data body. Calculate the attribute value for the points of a certain plane contour line to obtain a two-dimensional attribute data body, and calculate the attribute value for all the plane contour points, then, the two-dimensional attribute data body is raised to three-dimensional, and a three-dimensional attribute data body is obtained. (5) Interpolation preprocessing. Not all points in the three-dimensional attribute data body have attributes. In order to get a better modeling effect, the attribute data volume needs to be interpolated. Commonly used interpolation algorithms include inverse distance weighted interpolation, B-spline interpolation, kriging interpolation, and so on. (6) Extract the isosurface. Extract the isosurface from the attribute data volume, and use CGAL to complete the extraction of the isosurface. The drawing of isosurface should first find the intermediate primitives, then triangulate the intermediate primitives to generate a series of triangles, and connect the triangles to generate the isosurface. (7) Generate geological blocks. The extracted isosurface constitutes the geological block model, completing the structure of the complex body model.

3.2. Construction of Four-Dimensional Function. For each point on the plane where the profile contour line is, an attribute value needs to be given to generate the attribute data body. The attribute value of each point is mainly generated by constructing a four-dimensional function, that is, for each point, the coordinate value (x, y, z) of the point and the attribute value p of the point should be obtained. For each point (x, y) on the plane where the profile contour line is located, a field function $f(x, y)$ is defined.

The attribute value p of each point on the plane where the contour line is located is the value of the field function $f(x, y)$. It can be seen from the definition of the field function that if the point is above a certain contour line, the attribute of the point. The value is 0; if the point is within a certain contour line, the attribute value of the point is less than 0; if the point is outside all contour lines, the attribute value of the point is greater than 0.

3.3. Determination of Attribute Value. After constructing the four-dimensional function, it is necessary to determine its attribute value for each point on the plane where the profile contour line is located. In this paper, the distance function is used to construct a four-dimensional function, so the determination of the attribute value of each point is transformed into the calculation of the distance function $\text{dist}(x, y)$. According to the definition of the distance function, the attribute value inside the contour is less than 0, the attribute value outside the contour is greater than 0, and the attribute value above the contour is equal to 0. Therefore, to determine the attribute value of a point, you should first determine the relationship between the point and the contour line and then calculate the distance from the point to the contour line.

3.4. Generate Attribute Body Data. In this paper, the key to the complex closed geological body structure based on attribute volume data is the generation of attribute volume data. The generation effect of volume data directly affects the modeling effect of the geological block after the final isosurface extraction. In this article, the generation of attribute volume data is only achieved by constructing four-dimensional functions.

After constructing a four-dimensional function with a given distance function, it is necessary to obtain the attribute value of the point by calculating the distance function. Among them, by judging the relationship between the point and the contour line, the sign of the attribute value of the point is judged; by calculating the distance between the point and the contour line, the value of the attribute value of the contour line is obtained. Judge the positional relationship between the point and the contour line and calculate the distance between the point and the contour line. Then, the coordinate value and attribute value of the point on the plane where the profile contour line is located are determined, and the attribute volume data is successfully generated. Starting from 3D geological modeling, the geological body modeling of complex fault block reservoirs has been studied in depth, and through the constructed method of contour surface extraction of attribute body data, the problem of multiple bifurcations existing between contours can be exploited to achieve better modeling results.

4. Fine Geological Modeling of Complex Fault Block Reservoirs Based on Deep Learning

4.1. Quality of Fault Reconstruction Model. In the research on the reconstruction of 3D geological bodies, the construction of simple layered geological bodies is relatively mature, but due to the multiple value problems that may exist in complex geological interfaces and the sparse original data of geological modeling, it is impossible to directly use general point cloud weights. The geological interface method requires different reconstruction methods according to different geological conditions. The existing three-dimensional fracture geological model construction methods mainly include "local interpolation method" and "global interpolation method."

As shown in Figure 2, the overall method is used to regrid the inverse fault test model. First, the three-dimensional uniform sampling points as shown in the figure are calculated, and these sampling points are directly triangulated (Figure a) and interpolated. (Figure b). In the result image, it can be observed that there are more obvious intersections and sharp grids at the locations where the elevation values on both sides of the fault are significantly different, and the regriding effect is not ideal.

4.2. Reserve Calculation of Reservoir Geological Modeling. Through the abovementioned reservoir modeling process, different simulation realizations can be performed to obtain the reservoir attribute parameter models realized by different simulations of the Sanjianfang Formation in the Ling 2 District of the Qiuling Oilfield, the effective reservoirs can be screened, and the geological construction of the research block can be calculated separately. The reserves of each layer under different simulation models are shown in Figure 3. It can be seen that the average crude oil reserves calculated by each model are relatively close, and the error is small.

4.3. Evaluation of the Effect of Water Injection Development in Complex Fault Blocks. The influence of crude oil underground viscosity: according to the methods and methods of water injection development at home and abroad, when the viscosity of local crude oil is greater than 5 mPa·s, it will have an impact on conventional water injection development. If it is greater than 70 mPa·s, there will be great difficulties in water injection development. By comparing the successful experience of waterflooding development at home and abroad, it is believed that if the reservoir chooses waterflooding development for perfection, its underground crude oil viscosity should not exceed 190 mPa.s.

As shown in Figure 4, under the same interfacial tension condition, when the viscosity of crude oil increases, the corresponding oil displacement efficiency during the production process also decreases; the oil displacement efficiency is inversely proportional to the oil-water viscosity ratio, and the residual oil displacement efficiency is inversely proportional to the oil-water viscosity ratio. The oil saturation can be seen from the figure showing an upward trend. The increase in residual oil saturation and the decrease in oil displacement efficiency are relatively sudden before the oil-water viscosity ratio is 345, and the oil-water viscosity ratio shows a gentle decline and an upward trend between 345-1600. When the oil-water viscosity ratio is greater than 1500, the oil displacement efficiency and residual oil saturation can be seen to be very small, it looks like a straight line

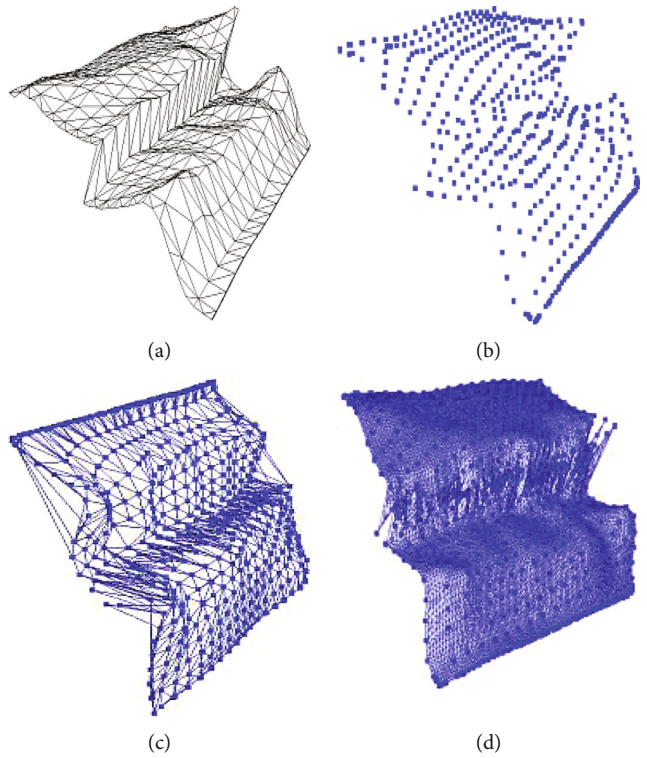

Figure 2: Reverse fault test model (picture from Baidu Gallery).

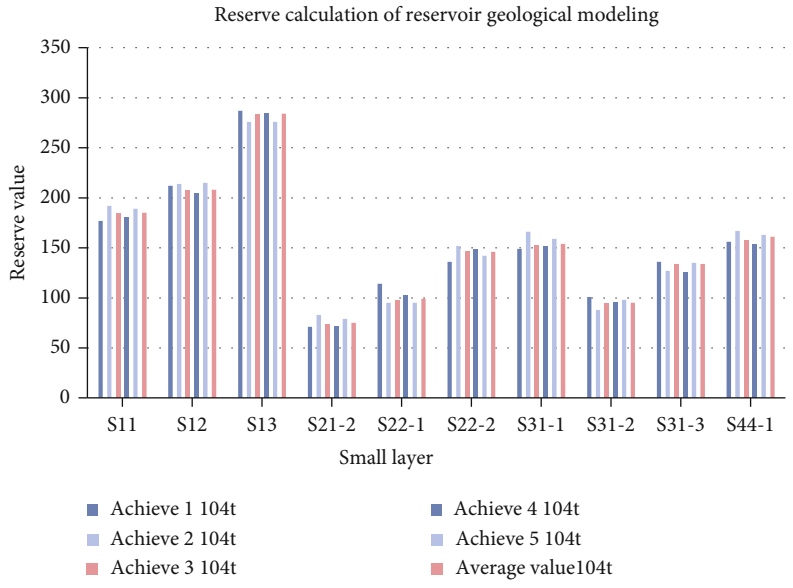

Figure 3: Reserve calculation of reservoir geological modeling.

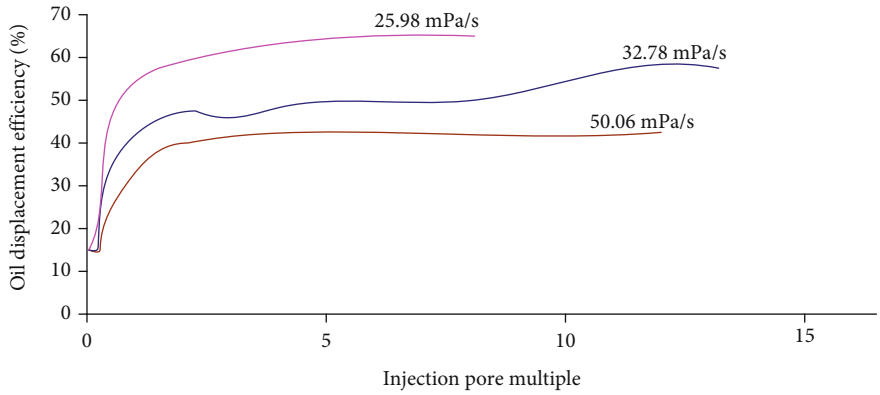

Figure 4: Relation curve of oil displacement efficiency and injection pore multiple.

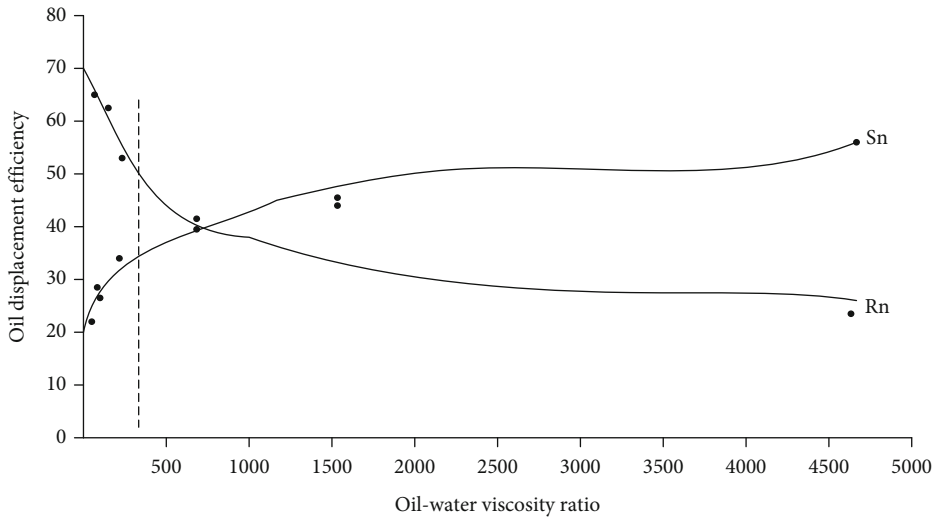

Figure 5: Relation curve of oil displacement efficiency and oil-water viscosity ratio.

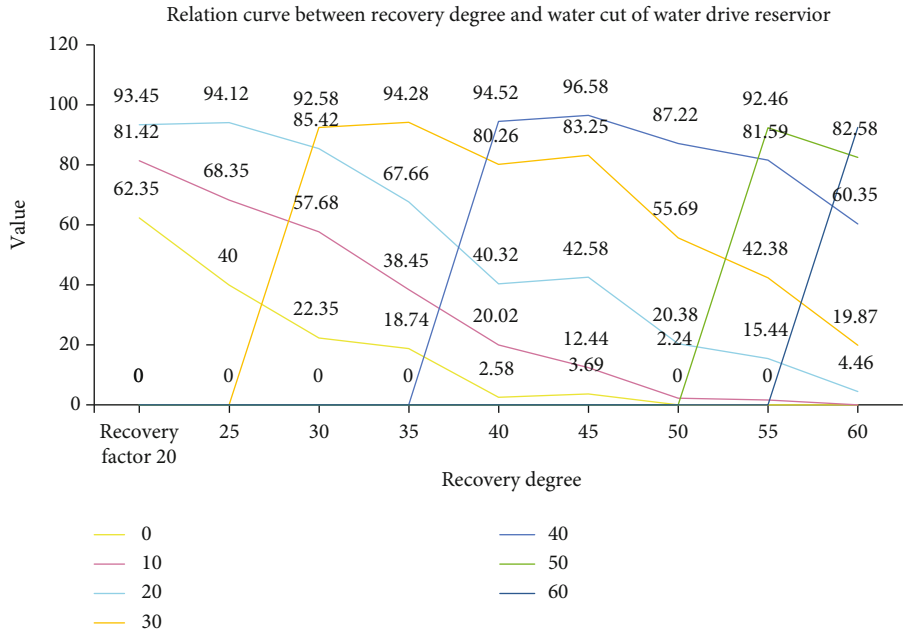

Figure 6: Relation curve between recovery degree and water cut of water drive reservoir.

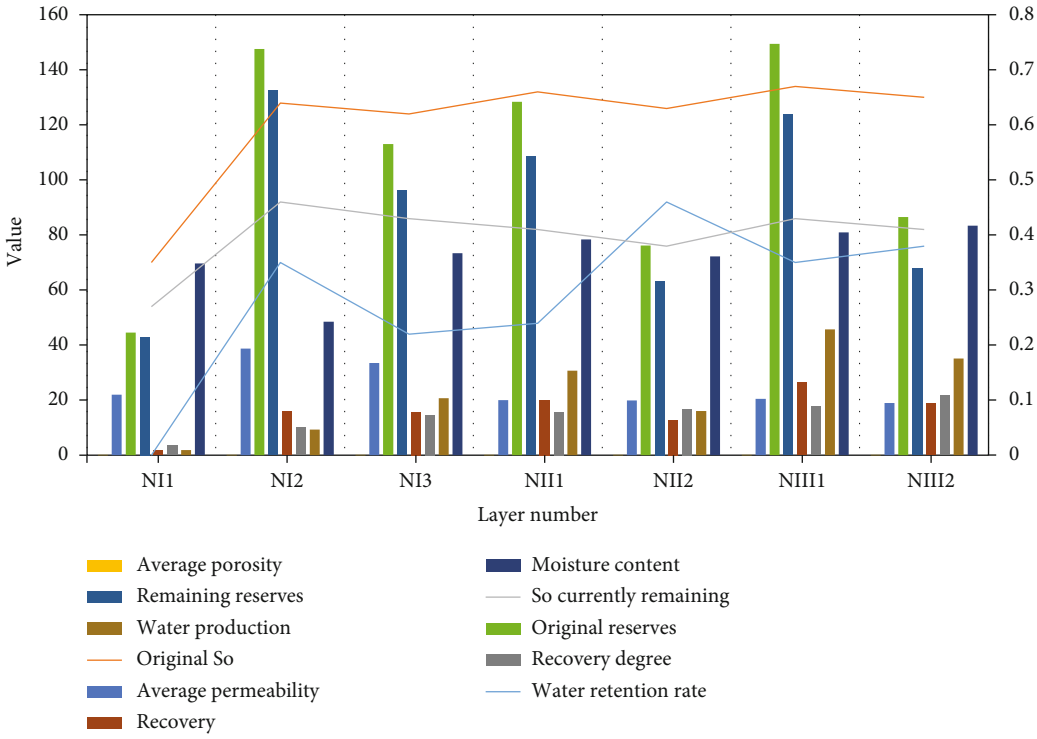

Figure 7: Statistics of development indicators at each small level at this stage.

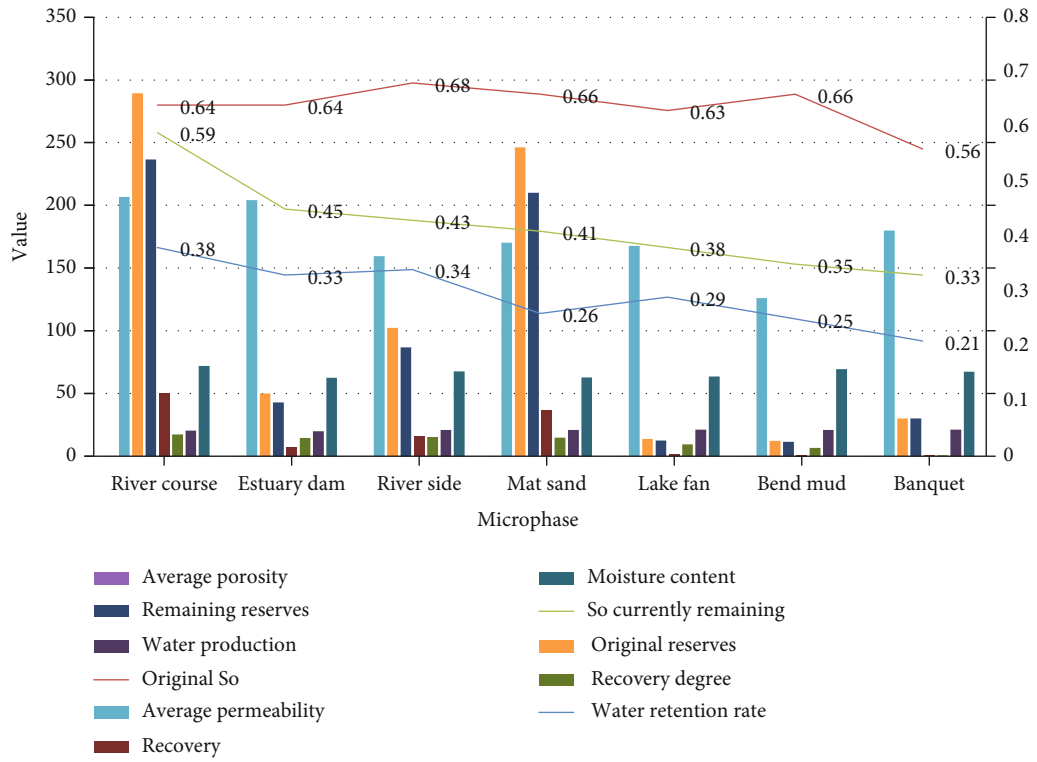

Figure 8: Statistics of development indicators of various sedimentary facies at this stage.

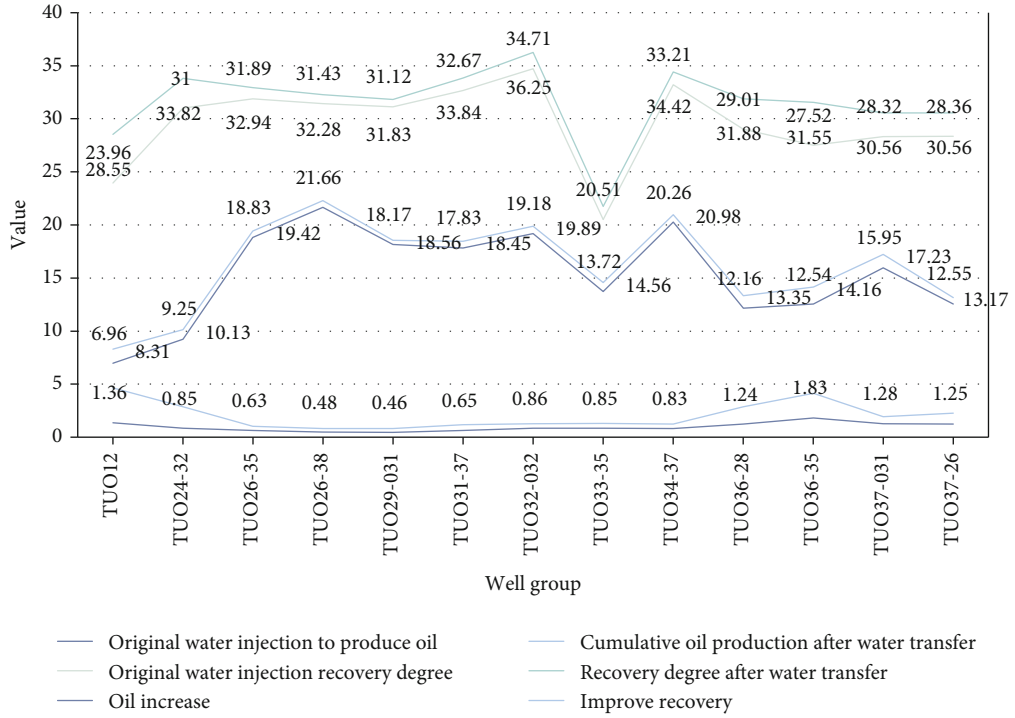

Figure 9: Results of water injection measures for optimal well groups in the whole region.

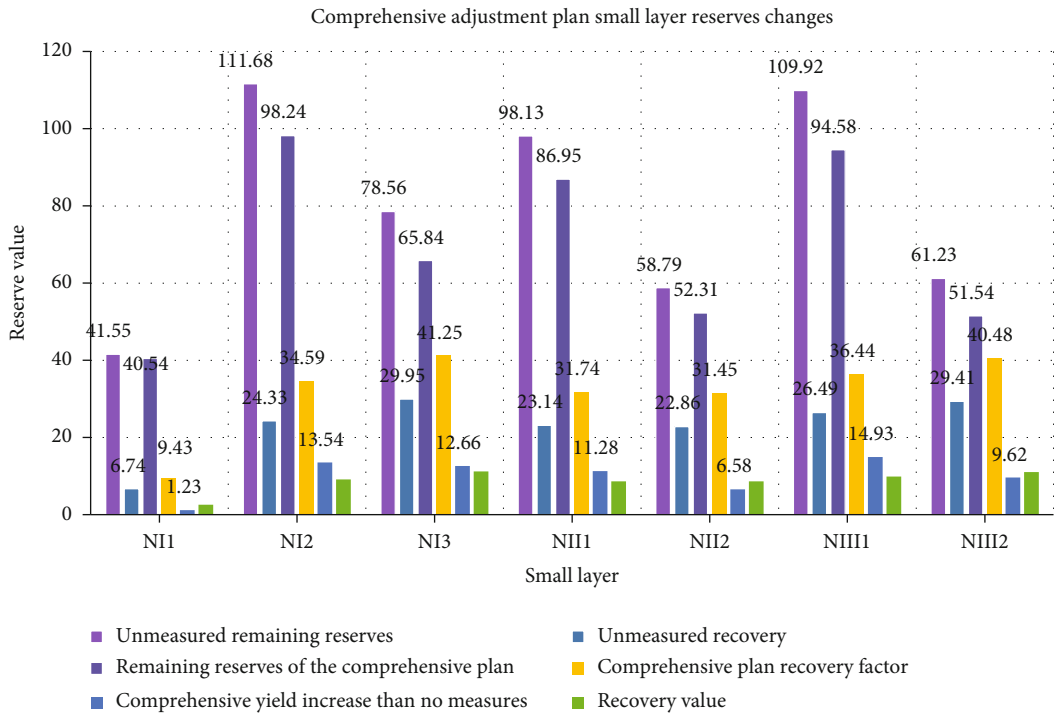

Figure 10: Comprehensive adjustment plan small layer reserves changes.

Table 1: Regrid parallel acceleration comparison.

Number of vertices	CPU	CPU-GPU	Speedup ratio
431	0.5113	0.3725	1.3761
1405	1.8034	0.6643	2.7153
2576	3.8655	0.8942	4.3232

on the whole, and the water injection development effect is not obvious, as shown in Figure 5.

It can be seen from Figure 5 that the crude oil viscosity of this research block is 76.3 mPa.s, which is more suitable for water injection development from the perspective of viscosity. The formation water viscosity is 0.5 mPa.s, its oil-water viscosity ratio is 152.6, its oil displacement efficiency is better, the residual oil saturation is lower than normal, and the study area is more suitable for water injection development.

The water cut of the Niuxintuo oil layer increases sharply with the increase of the oil reservoir's recovery. At present, the Niuxintuo oil layer has a recovery rate of 15.01%, and the water cut has reached 72.4%. Due to the low degree of oil production, the later period of the curve is not obvious, and it can still be seen from the curve shape that the development effect of this block is not good. In the initial stage of water injection development, as the water cut increases, the rate of water cut rises. In the later stage, the oil wells are controlled by water to stabilize the oil. Through water transfer and layer replenishment measures, the current curve gradually moves closer to the theoretical curve, indicating the current overall development deviation of the reservoir. But there is a trend of gradually getting better in the later period, and the rising rate of water content shows a downward trend.

Comparing the relationship curve between the actual comprehensive water cut and the recovery degree of the reservoir with the standard curve, the result is shown in Figure 6. The comprehensive water cut of the initial block rises faster. Through timely and dynamic water allocation and comprehensive management, the rate of water cut rise is controlled., It can be seen from the curve that the current comprehensive water cut of the reservoir is between 60% and 80%, the actual curve is between 25% and 35%, and the estimated waterflooding recovery rate is about 30%.

Through the statistics of each small layer from the early stage of development to the present, the oil produced by each small layer in the entire water injection development process, the changes in the degree of production, and the changes in the original oil saturation and the current remaining oil saturation are shown in Figure 7, and the statistics of water injection are shown in Figure 7. The oil production of each small layer has been developed to date. The water injection effect of each small layer is evaluated by the changes in the reserves, production level, water production, and water content of each small layer from the early stage of development to the present, and it can be seen that the NIII1 included in the NIII layer, NIII2 has a larger oil content, a large amount of production, and a greater degree of recovery than NI and NII, indicating that the water injection development effect of NII2, NIII1, and NIII2 layers is better than that of NI2 and NI3 layers..

As shown in Figure 8, the development status of each microphase at this stage: through statistics of each microphase from the initial stage of development to the present, the oil produced by each microphase in the entire water injection development process, the change in the degree of production, and the original oil saturation and the current remaining. The change in oil saturation, the comparison of the oil production of each microphase from the development of water injection to the present, through the changes in the reserves, recovery, water production, and water content of each microphase from the initial stage of development to the present, the water injection effect of each microphase is carried out. Evaluation, it can be seen that the cumulative oil production and production degree of the channel microfacies are the largest, and it can be judged that the microfacies has the best water injection effect, followed by the side of the channel, the estuary dam, and the sheet sand.

Water injection adjustment measures for optimal well groups in the whole area: for complex fault block oil layers, adjustments are not only made to well groups in finely divided fault blocks, on the other hand, for the whole area, the well groups should also be selected from a macroscopic perspective to be used. The effect of some well groups affects the development effect of other well groups. Adjust the stratification of the above water wells, adjust the water injection volume of each layer, and apply the blocking method to the selected 19 well groups (Figure 9), and the cumulative production before and after the water transfer is obtained. The oil and production levels change, and the 19 well groups are optimized to adjust the water injection volume, adjust the stratification situation and the blocking measures according to their characteristics. After the adjustment, the cumulative oil production increase is obvious, and the cumulative oil production is 193,400 tons increased by 2.6%.

4.4. Comprehensive Plan Index Evaluation Forecast. As shown in Figure 10, by comparing the remaining oil volume of each small layer predicted 20 years after no measures and the comprehensive plan, it is concluded that after the comprehensive plan measures, the oil increase of the NI2-NII1 small layer is obvious, and the cumulative oil increase of each layer is 69.46×104 t.

Due to the uniform method used in the remeshing process, the calculation of the three-dimensional mesh vertices is independent and data-free, and each CUDA thread can process the vertices of a region. The main process can be divided into six steps: area division, data reading, data encapsulation, GRID construction, area remeshing, and output. Regional vertex division is the basis of the parallel process. The large-scale grid 3D vertex data is divided into discrete unit regions according to the resolution requirements, and there is no data overlap between adjacent units; the scheduler allocates multiple divided task units on the CPU side. Threads perform coarse-grained parallel processing, and the regrid calculation of each task area is mapped to the corresponding thread block. The regrid calculation

Table 2: Table of calculation results of artificial fractures in fault blocks.

Calculated interval	$\sigma(H)$ MPa	$\sigma(h)$ MPa	T (MPa)			$\sigma(h)+T$ (MPa)		θ	
			The smallest	Maximum	Average	The smallest	Maximum	T smallest	T maximum
1	30.58	23.45	5	10	7.5	28.42	33.45	63	—
2	33.42	28.13	5	10	7.5	33.24	38.24	77	—
1	34.61	27.24	5	10	7.5	32.25	37.22	61	—
2	37.61	31.25	5	10	7.5	36.21	41.23	64	—
1	28.52	23.15	5	10	7.5	28.13	33.25	75	—
1	37.95	30.16	5	10	7.5	35.12	40.15	58	—
2	34.61	26.21	5	10	7.5	31.22	36.25	56	—
3	36.82	28.81	5	10	7.5	33.81	38.89	52	—
4	34.63	28.26	5	10	7.5	33.24	38.25	64	—
5	33.24	26.31	5	10	7.5	31.25	36.23	63	—

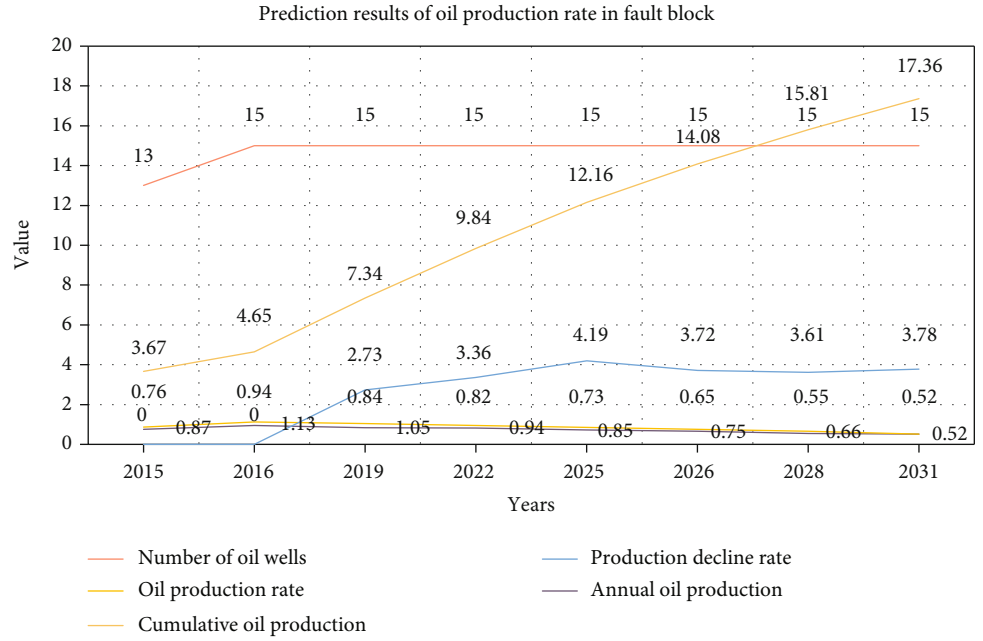

Figure 11: Prediction results of oil production rate in fault block.

process of each vertex is assigned to the threads on the GPU in an atomic task for fine-grained parallelism. The experimental platform: Microsoft Visual Studio 2010, GPU side graphics card is nVIDIAGeForceGT720, CUDAC4.1, CPU is CoreI5-6500, RAM 8 G. Experimental data: local river model A, B, C in a certain area of Nanjing, the number of vertices is 1405, 1939, 2576, and the running time of GPU-CPU coordinated operation and CPU is compared. It can be seen from Table 1 that as the number of model triangle vertices increases, GPU parallel resources are effectively used, and the acceleration effect is more obvious.

As shown in Table 2, the in situ stress data of the fault block mainly refers to the microresistivity scanning imaging and interactive multilevel subarray acoustic logging data in the southern part of the new station. The rock tensile strength T refers to the test data of the Hailar Oilfield, which is 5 ~ 10 MPa between. After calculating $\sigma < \sigma h + T$, the artificial fracture first opens along the direction of the natural fracture. On this basis, the calculation of the limit angle of other wells with data is carried out, and the angle is above 48°.

The oil production rate is predicted by the reservoir numerical simulation data, and the predicted oil production rate of the D165 block is counted. It can be seen from the prediction result in Figure 11 that the annual oil production rate of this block is relatively low and has been declining.

Figure 12 shows the probability distribution histogram between the reservoir porosity and permeability model simulation parameter data of the Ling 2 block of the fault oil field in the study area, the coarsening data at the well point, and the original well data. Compare these two probabilities. From the distribution histogram, it can be seen that their distribution laws are similar, that is, the probability distribution trend of the simulated data volume and the original data

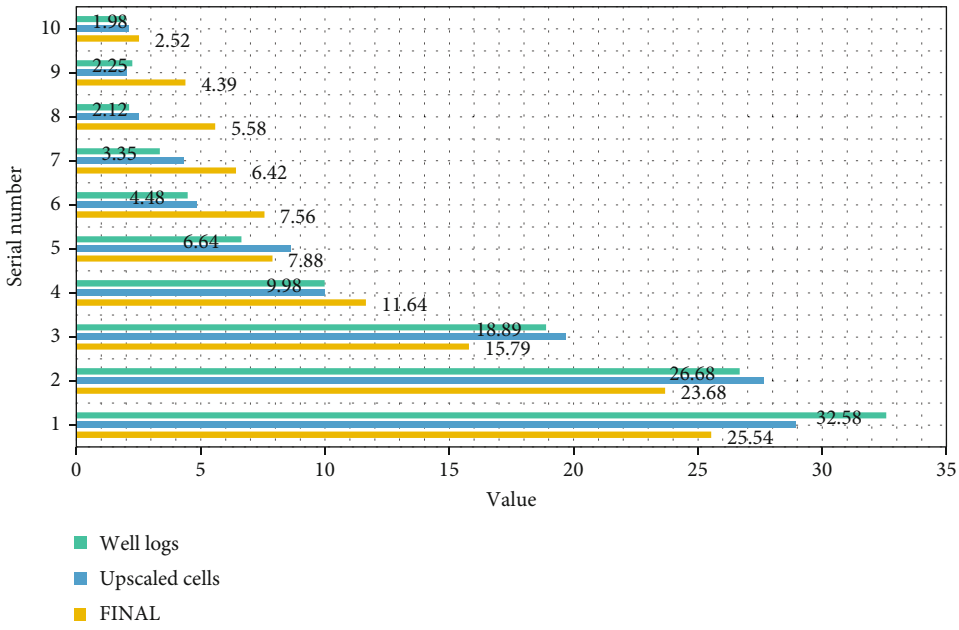

Figure 12: Permeability simulation value, coarsening at the merging point, and frequency distribution diagram of the original permeability value.

is the same, which indicates that the simulation accuracy of the built reservoir parameter model is better, and the simulated value of the model is faithful to the original attributes. Value data are reflecting the changing law of reservoir attribute parameters.

5. Conclusion

This article mainly focuses on the study of fine geological modeling of complex fault block reservoirs based on deep learning. Starting from the 3D geological modeling, this paper conducts an in-depth study on the modeling of complex fault block reservoir geological bodies. Through the isosurface extraction method of attribute volume data constructed in this paper, the existence of multiple bifurcation problems between contour lines can be used. Achieve better modeling results. In addition, this paper also analyzes the relationship between water cut and recovery degree of complex fault block reservoir geology. We need to control water cut rising speed reasonably and improve recovery rate through timely and dynamic water allocation and comprehensive management. At the same time, it is obtained by comparing and analyzing the relationship curve between the actual comprehensive water content and the oil recovery factor and the standard curve. The current comprehensive water cut of the reservoir is between 60% and 80%, the actual curve is between 25% and 35%, and the estimated waterflooding recovery factor is about 30%. The innovation of this article lies in the application of deep learning to geological modeling, and the use of convolutional neural networks for multilevel analysis to meet the completeness standards and requirements of modeling. There are still shortcomings in this paper. More factors are not considered in the selection of complex fault block reservoirs. The representativeness is poor, and further improvement is needed. It is hoped that the research in this article can provide some theoretical support and help for the geological modeling research of complex fault blocks.

Data Availability

The data that support the findings of this study are available from the corresponding author upon reasonable request.

Conflicts of Interest

The authors declared no potential conflicts of interest with respect to the research, authorship, and/or publication of this article.

Acknowledgments

This work was supported by The National Natural Science Foundation of China (41602154) and Projects of Talents Recruitment of GDUPT (2018rc01).

References

[1] Y. Chen, Z. Lin, Z. Xing, G. Wang, and Y. Gu, "Deep learning-based classification of hyperspectral data," *IEEE Journal of Selected Topics in Applied Earth Observations & Remote Sensing*, vol. 7, no. 6, pp. 2094–2107, 2014.

[2] L. Xue, Z. Ning, and X. Xing, "Reservoir characteristics and three-dimensional architectural structure of a complex fault-block reservoir, beach area, China," *Journal of Petroleum Exploration and Production Technology*, vol. 8, no. 4, pp. 1535–1545, 2018.

[3] X. Tan, Y. Liu, X. Zhou, L. I. U. Jiandang, R. Zheng, and J. I. A. Chao, "Multi-parameter quantitative assessment of 3D geological models for complex fault-block oil reservoirs," *Shiyou*

Kantan Yu Kaifa/Petroleum Exploration and Development, vol. 46, no. 1, pp. 194–204, 2019.

[4] H. Cui, Y. Guan, H. Chen, and W. Deng, "A novel advancing signal processing method based on coupled multi-stable stochastic resonance for fault detection," *Applied Sciences*, vol. 11, no. 12, p. 5385, 2021.

[5] Z. H. Zhang, F. Min, G. S. Chen, S. P. Shen, Z. C. Wen, and X. B. Zhou, "Tri-partition state alphabet-based sequential pattern for multivariate time series," *Cognitive Computation*, pp. 1–19, 2021.

[6] W. Mahmood, A. S. Mohammed, P. Sihag, P. G. Asteris, and H. Ahmed, "Interpreting the experimental results of compressive strength of hand-mixed cement-grouted sands using various mathematical approaches," *Archives of Civil and Mechanical Engineering*, vol. 22, no. 1, pp. 1–25, 2022.

[7] S. Firebaugh, "Manipulation of microrobots using Chladni plates and multimode membrane resonators," *Engineering Proceedings*, vol. 4, 2021.

[8] G. Litjens, T. Kooi, B. E. Bejnordi et al., "A survey on deep learning in medical image analysis," *Medical Image Analysis*, vol. 42, no. 9, pp. 60–88, 2017.

[9] J. Lee, "Integration of Digital Twin and Deep Learning in Cyber-Physical Systems: Towards Smart Manufacturing," *IEEE Transactions on Semiconductor Manufacturing*, vol. 38, no. 8, pp. 901–910, 2020.

[10] L. June-Goo, J. Sanghoon, C. Young-Won et al., "Deep learning in medical imaging: general overview," *Korean Journal of Radiology*, vol. 18, no. 4, pp. 570–584, 2017.

[11] D. Ravi, C. Wong, F. Deligianni et al., "Deep learning for health informatics," *IEEE Journal of Biomedical & Health Informatics*, vol. 21, no. 1, pp. 4–21, 2017.

[12] Y. Zhang, H. Huang, L. X. Yang, Y. Xiang, and M. Li, "Serious challenges and potential solutions for the industrial internet of things with edge intelligence," *IEEE Network*, vol. 33, no. 5, pp. 41–45, 2019.

[13] H. Ye, G. Y. Li, and B. Juang, "Power of Deep Learning for Channel Estimation and Signal Detection in OFDM Systems," *IEEE Wireless Communication Letters*, vol. 7, no. 1, pp. 114–117, 2017.

[14] D. L. Wang and J. Chen, "Supervised Speech Separation Based on Deep Learning: An Overview," in *IEEE/ACM Transactions on Audio, Speech, and Language Processing*no. 99, p. 1, 2017.

[15] X. X. Zhu, D. Tuia, L. Mou et al., "Deep learning in remote sensing: a comprehensive review and list of resources," *IEEE Geoscience & Remote Sensing Magazine*, vol. 5, no. 4, pp. 8–36, 2017.

[16] W. Hou, X. Gao, D. Tao, and X. Li, "blind image quality assessment via deep learning," *IEEE Transactions on Neural Networks and Learning Systems*, vol. 26, no. 6, pp. 1275–1286, 2015.

[17] Y. Tom, H. Devamanyu, P. Soujanya, and E. Cambria, "Recent trends in deep learning based natural language processing," *IEEE Computational Intelligence Magazine*, vol. 13, no. 3, pp. 55–75, 2018.

[18] P. Shan, X. Lai, and X. Liu, "Correlational analytical characterization of energy dissipation-liberation and acoustic emission during coal and rock fracture inducing by underground coal excavation," *Energies*, vol. 12, no. 12, p. 2382, 2019.

[19] H. Fazlollahtabar and S. Niaki, "Integration of fault tree analysis, reliability block diagram and Hazard decision tree for industrial robot reliability evaluation," *Industrial Robot*, vol. 44, no. 6, pp. 754–764, 2017.

[20] M. A. Alatorre-Zamora, J. O. Campos-Enríquez, E. Fregoso-Becerra, L. Quintanar-Robles, R. Toscano-Fletes, and J. Rosas-Elguera, "Gravity evidence for shaping of the crustal structure of the Ameca graben (Jalisco block northern limit). Western Mexico," *Journal of South American Earth Sciences*, vol. 82, 2018.

[21] S. Li, S. Zeng, X. Deng, L. Wang, T. Wang, and L. U. Xinwei, "Large-scale fracturing technology for Fushan complex fault block oil and gas reservoir," *Well Testing*, vol. 28, no. 1, pp. 60–66, 2019.

[22] X. Li, T. Tong, and T. Lu, "Reservoir characteristics and three-dimensional architectural structure of a complex fault-block reservoir, beach Area, China," *China. The Open Petroleum Engineering Journal*, vol. 10, no. 1, pp. 276–286, 2017.

[23] L. Yin, X. Li, L. Gao, C. Lu, and Z. Zhang, "A novel mathematical model and multi-objective method for the low-carbon flexible job shop scheduling problem," *Sustainable Computing: Informatics and Systems*, vol. 13, no. 3, pp. 15–30, 2017.

[24] J. Liu, W. Ding, J. Dai, Z. Wu, and H. Yang, "Quantitative prediction of lower order faults based on the finite element method: a case study of the M35 fault block in the Western Hanliu fault zone in the Gaoyou Sag, East China," *Tectonics*, vol. 37, no. 10, pp. 3479–3499, 2018.

[25] J. Han, Z. Su, Y. Liu, C. Zhang, and L. Huang, "Reservoir controlling mechanism and hydrocarbon exploration potential of buried-hill belt in Yaha fault block, Tarim Basin," *Shiyou Xuebao/Acta Petrolei Sinica*, vol. 39, no. 10, pp. 1081–1091, 2018.

[26] J. Choo and W. C. Sun, "Coupled phase-field and plasticity modeling of geological materials: From brittle fracture to ductile flow," *Computer Methods in Applied Mechanics & Engineering*, vol. 330, pp. 1–32, 2018.

[27] H. Wang, X. Zhang, L. Zhou, X. Lu, and C. Wang, "Intersection Detection Algorithm Based on Hybrid Bounding Box for Geological Modeling With Faults," *IEEE Access*, vol. 8, pp. 29538–29546, 2020.

[28] J. Zheng, W. Pan, A. Shen et al., "Reservoir geological modeling and significance of Cambrian Xiaoerblak Formation in Keping outcrop area, Tarim Basin, NW China," *Petroleum Exploration and Development*, vol. 47, no. 3, pp. 536–547, 2020.

[29] I. Hassen, C. Fauchard, R. Antoine et al., "3D geological modelling of a coastal area: case study of the Vaches Noires cliffs, Normandy, France," *Bulletin of Engineering Geology and the Environment*, vol. 80, no. 2, pp. 1375–1388, 2021.

[30] F. Grassmann, J. Mengelkamp, C. Brandl et al., "A deep learning algorithm for prediction of age-related eye disease study severity scale for age-related macular degeneration from color fundus photography," *Ophthalmology*, vol. 125, no. 9, pp. 1410–1420, 2018.

[31] K. Grm, V. Štruc, A. Artiges, M. Caron, and H. K. Ekenel, "strengths and weaknesses of deep learning models for face recognition against image degradations," *IET Biometrics*, vol. 7, no. 1, pp. 81–89, 2018.

[32] R. Ranjan, S. Sankaranarayanan, A. Bansal et al., "Deep learning for understanding faces: machines may be just as good, or better, than humans," *IEEE Signal Processing Magazine*, vol. 35, no. 1, pp. 66–83, 2018.

Hindawi
Wireless Communications and Mobile Computing
Volume 2022, Article ID 8134290, 12 pages
https://doi.org/10.1155/2022/8134290

Research Article

5G Embedded Sensor Network System for Sports Information Service Hotspot Recommendation

Zhong Wu[1] **and Chuan Zhou**[2]

[1]*Physical Education School, Wuhan Business University, Wuhan, 430056 Hubei, China*
[2]*Institute of Mechanical Engineering, Wuhan Institute of Shipbuilding Technology, Wuhan, 430062 Hubei, China*

Correspondence should be addressed to Chuan Zhou; 20150459@wbu.edu.cn

Received 29 November 2021; Revised 18 January 2022; Accepted 11 February 2022; Published 4 March 2022

Academic Editor: Mohamed Elhoseny

How to rationally allocate and integrate existing resources has become the top priority of the development of sports public information services in the transition period, but it is also a weak link in the construction of current social information resources. This article is aimed at studying how to develop sports information service hotspots based on 5G embedded sensor network systems. Methods such as the network structure based on 5G embedded sensors, the Kriging algorithm based on global optimization, and sensor distance measurement are proposed and also conducted experiments on the application of 5G embedded sensor network system in sports information service hotspot recommendation. The results show that people are satisfied with the sports information service of the wireless sensor network, with a maximum score of 9.8, which is suitable for the information provision of sports information services. The development of the times has met the needs of most people.

1. Introduction

With the rapid iteration of information flow in the era of big data and the professional development of the sports industry market, the information value of the sports industry has exploded, and the sports information industry has emerged as the times require. With the development of the socialist market economy, the social structure has undergone tremendous changes, and the sports management system has also undergone a fundamental change to some extent. The wave of reform and opening up and the process of economic system transformation have shaken the foundation of the original sports management system and to a large extent led its epoch-making pace. As one of the important areas of the Internet, sensor networks play an important supporting role. The sensor network is responsible for the collection and transmission of data. The sensor network is composed of multiple sensor nodes, which send the acquired data to users. Through wireless multihop communication, the acquired data is transmitted to the user terminal.

In the era of "Internet +", with more and more forms of nationwide fitness information services, based on Internet technology, the speed of software and hardware upgrades should also be accelerated, and many information service platforms with strong practical value have been established. It provides users with various services such as physical guidance, health consultation, and classes, which greatly promotes users' sports and fitness activities. This plays a very important role in promoting the healthy development of the people.

With the continuous acceleration of the development of social network informatization, sports services are becoming more and more informatized. Xu et al. believes that the urban sports energy-saving information service network has not yet formed. The rapid flow of information and sharing features has not yet been released. According to the characteristics and laws of urban sports development, the integrated functions of urban sports information network services are manifested in the aspects of universal value, cooperative organization, and diversified benefits. It is also necessary to implement the content, characteristics, and regional innovation and development strategies of sports information network services, using the reform of the

student union portal as a driving force to strengthen the integrity and regional characteristics of urban sports information, establishing an information exchange and sharing operation platform supported by network technology, and strengthening the exchange of cooperation among various social forces. In order to explore the relationship between value balance and realization, it is possible to conduct a comprehensive investigation of the internal components of the service in combination with the new ideas developed in the era of the "smart city" service information platform, to promote the development of service information platform and design ideas and direction information platform. It can fully characterize the intelligent and humane ecological development and design concepts [1]. The purpose of Howard MS's experiment is to determine whether athletes are interested in information services and to determine whether pharmacists popularize and promote knowledge of athletes. He conducted an experimental survey of local sports athletes and collected the age, gender, and the degree of understanding of the information services of the sports athletes, including where they live. The statistical information of the sports athletes collected by his survey includes information services Interest, desire for knowledge, and obstacles to learning. The results show that their understanding of information services is not high [2]. Cain et al. has conducted research on two sports universities to understand the value of information services provided by the society and the needs of sports personnel for information services. The results show that the methods used by the two sports universities to apply sports information services depend on the needs of sports athletes. The results provide a method for the development of sports information services and help predict the changing information needs of a wider range of sports players [3]. With the popularization and development of the Internet, information has changed people's lives and production extensively and deeply, and information construction has become the main direction of sports information services in the future. In the era of rapid development of information technology, it is of great significance to study the combination of the sports industry and the information industry and evaluate the capabilities of smart sports information services. The purpose of this research is to explore a methodological approach. Evaluation of sports information services provides insights for the theoretical research and practical development. First, determine the objects and key evaluation items of intelligent sports information services through factor analysis. Secondly, the application of analytic hierarchy process takes the evaluation of sports university as an example to verify the authenticity and operability of the index system and proposes corresponding measures. The research results show that only by improving the public sports database, big data can analyze the establishment of the system and its various forms of application [4]. Gope and Hwang found that the emergence of the Internet of things is due to the continuous development of information technology. In modern sports, the use of Internet of things technology can bring convenience to sports lovers, and they are also used in various sports. Sensor network technology is one of the important factors in the development of sports information service. In this article, he found that the security function of the sports system can be met by the sports information service of the Internet of things [5]. Abraham and Li found that the indoor air quality information system helps to improve indoor air quality. In this paper, he proposed a low-cost and high-quality wireless sensor network system for indoor air quality monitoring. He also found that sensor calibration and measurement data conversion can be solved by methods based on linear least squares estimation. In this article, he introduces the theoretical knowledge and practical methods of wireless sensor nodes. Through the analysis of results and experiments, the importance of wireless sensor networks is proved [6]. Hammoudeh et al. analyze that national security is affected by external border monitoring. Wireless sensor networks can reduce costs and give solutions based on intelligent technology to effectively monitor complex areas. In this article, he uses an appropriate index to measure the quality of transmission detection. He also proposed a method to calculate the number of sensor nodes and then found a new crosslayer routing protocol, hierarchical partition graph, which is specially used to solve the communication requirements of topological linear applications [7]. Zhang et al. studied the energy-saving distributed filtering in sensor networks and found that the switching system method can achieve this goal. The first mock exam is to switch the system, and he put forward a unified model to capture the problems of low speed and poor signal. The system has obtained a sufficient condition for the exponential stability of the filtering error system in the mean square sense, and the performance of the system is qualified. All experimental studies have proved that the new design technology he proposed is very reliable [8]. Through the experiments and research of scholars, it can be known that the application of sensor networks in real life is becoming more and more extensive. The development of sports information services based on the 5G embedded sensor network system is a major trend today. How to use the sensor network system is a difficult problem for sports information services today.

The innovations of this article are as follows: (1) investigation and research of modern sports enthusiasts' sports information services based on wireless sensor networks through investigation and research methods, researching and analyzing the actual effects of sports applications on sports enthusiasts and then discussing how to use sports information services healthily, and (2) adopting the Kriging algorithm based on global optimization and developing sports information services based on wireless sensor networks to promote the popularization of the importance of sports information services.

2. Kriging Algorithm Based on Global Optimization

2.1. The Network Structure of the Sensor. Kriging is a regression algorithm for spatial modeling and prediction of stochastic processes based on covariance functions. In certain stochastic processes, such as inherently stationary processes, Kriging can give optimal linear unbiased estimates, so it is also called spatially optimal unbiased estimator in

geostatistics. The wireless sensor network integrating sensor technology, embedded computing technology, distributed information processing technology, wireless communication technology, and the latest microelectronic technology are a new information acquisition and information processing network technology [9, 10]. They have a wide range of application prospects and are suitable for all aspects of human activities such as national security, military, environmental monitoring, health care, and smart homes. The wireless sensor network is composed of three parts, mainly sensor nodes, base station nodes, and background user management interfaces in the field of network monitoring, as shown in Figure 1.

As shown in Figure 1, the sensor network node not only completes the collection of surrounding environmental parameters but also maintains the network topology and routing information. This is a microembedded system that can complete the fusion processing of the collected data and the data sent by other nodes [11, 12]. Routing algorithms, also known as routing algorithms, can be differentiated by a number of characteristics. The goal of the algorithm is to find a "good" path from the source router to the destination router. At the same time, it cooperates with other nodes to complete specific tasks such as target tracking. The base station node has completed the overall network data fusion processing and conversion based on the Internet communication protocol, and its communication capabilities, processing capabilities, and storage capabilities are relatively strong [13]. User management completes tasks such as task start, data analysis, network management, and other functions.

Currently, wireless sensor networks generally adopt topological structures, and the mesh structure topology is shown in Figure 2.

As shown in Figure 2, the mesh structure is a peer-to-peer structure. The nodes of all structures are sensor nodes and synchronization nodes. Nodes in the network can communicate directly when they are within the communication range. In addition, the nodes within the communication range [14] can be used as transition nodes. The characteristic of this structure is the robustness and reliability of the network, but this kind of network structure is complex and requires higher additional overhead [15].

In different applications, the composition of sensor network nodes is not the same [16, 17]. But generally, it is composed of data acquisition unit, data processing unit, data storage unit, data transmission unit, power supply, and embedded operating system, as shown in Figure 3.

As shown in Figure 3, as a complete microcomputer system, the performance of its components must be coordinated and efficient. The choice of each module's implementation technology needs to be weighed and selected according to the actual application system requirements. The remote wireless upgrade of the wireless sensor network is a process of distributing the new code image to each node through the network to complete the replacement of the old and new codes, thereby realizing the upgrade process. It mainly includes two processes: the distribution of new application code images and the replacement of new and old codes [18].

2.2. Kriging Algorithm Based on Global Optimization. The Kriging method is based on a series of known observation points $Z_i = Z(a_i), i = 1, \cdots, n$ in a random area $Z(a)$ and interpolating the function value $Z(a)$ of a_0 at the unknown point. The Kriging method is based on space, relying on observation points to quantify the variance change $\gamma(a, b)$ or expectation $\mu(a)$ and the covariance function $C(a)$ of the random model, and calculates $Z(a)$ the optimal linear unbiased estimate $Z(a_0)$ as formula (1):

$$Z(a_0) = \sum_{i=1}^{n} \omega_i(a_0) Z(a_i). \tag{1}$$

This type of task is usually issued by the sink node, and the sensor node collects the data that meets the requirements and reports it to the sink node [19]. The error obtained in the Kriging model is as formula (2):

$$a_K^2(a_0) = Var[Z(a_0) - Z(b_0)]. \tag{2}$$

The routing algorithm should be easy to implement and low in computational complexity. In the case of nodes with limited computing $Z(b_0)$ power in wireless sensor networks, it is necessary to avoid the use of complex optimization methods [20, 21]. Although multiobjective optimization algorithms exist, more single-metric optimization algorithms are used. According to the unbiased condition, formula (3),

$$E[Z(a) - Z(b)] = \sum_{i=1}^{n} \omega_i(a_0)\mu(a_i) - \mu(a_0) = 0. \tag{3}$$

First assume that the response value at point A to be evaluated $b(a)$ is Equation (4):

$$b(a) = C^T(a)B, C^T(a) \in R^n. \tag{4}$$

Under this condition, the predicted mean square error $\psi(a)$ is formula (5):

$$\psi(a) = E\left[b(a) - b(a)^2\right] = E\left[C^T Z - Z\right] \tag{5}$$

2.3. Correlation Function Algorithm. For stochastic processes, as described in formulas (4) and (5) above, the main research object is correlation function $R(\theta, \omega, a)$. The basic form of the correlation function model used in this article is formula (6);

$$R(\theta, \omega, a) = \prod_{i=1}^{n} R(\theta_i, \omega_i, a_i). \tag{6}$$

The "variance" θ_i is a measure used in probability theory to measure the degree of deviation between a random variable ω_i and its estimated value a_i.

The Gaussian function is named after the great mathematician Johann Karl Friedrich Gauss. The Gaussian function has a wide range of applications and can be seen in

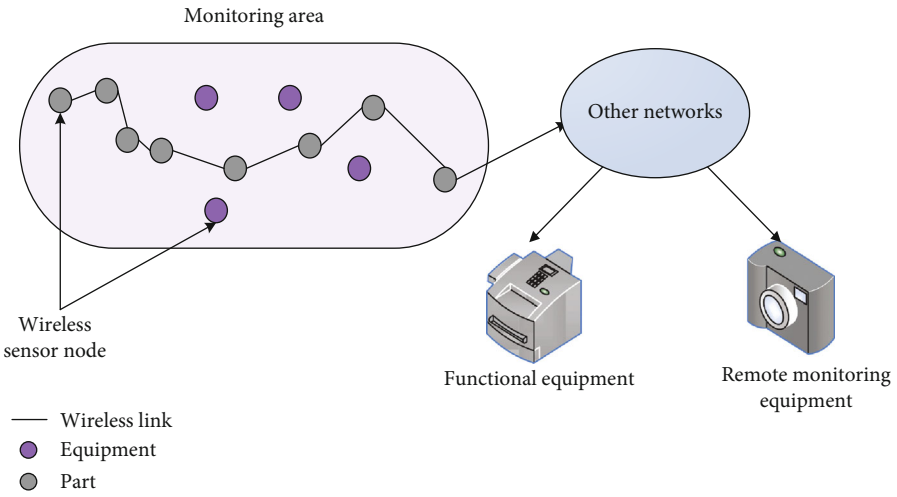

Figure 1: Node diagram of sensor network.

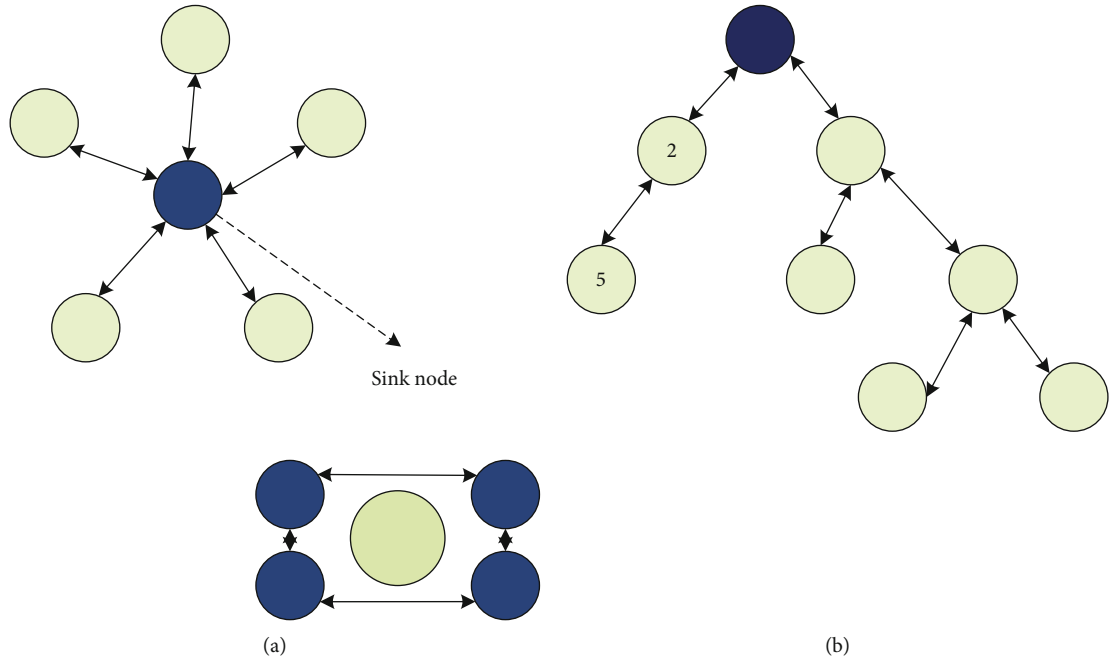

Figure 2: Topology diagram of mesh structure.

the natural sciences, social sciences, mathematics, and engineering. The following lists 8 different forms of correlation functions as shown in Table 1:

As shown in Table 1, the selection of correlation functions should be based on actual physical phenomena. If the phenomenon under study is continuously differentiable, then the correlation function is likely to show a parabolic linear state near the origin. That means Gaussian function, cubic function, and curve function should be selected [22]. In addition, linear functions, cubic functions, spherical functions, and curvilinear functions are compact functions. For distances greater than the support radius, its value is 0, while other functions are global functions and tend to be asymptotically to 0 (18).

Assuming that the correlation function is a Gaussian process $\psi(\theta)$, the optimal coefficients of the correlation function can be solved, and the equation is as Equation (7):

$$\min\left\{\psi(\theta) = \frac{1}{m}\sigma^2\right\}. \tag{7}$$

The typical trend of the expression function in Table 1 is shown in Figure 4.

As shown in Figure 4, the expression function decreases with the increase of the number of experiments, from 0.4 to 0.2.

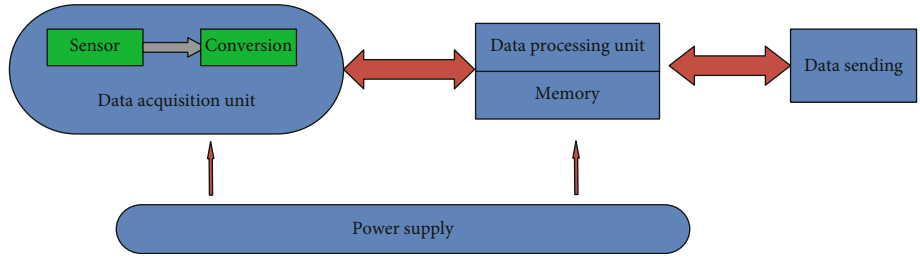

Figure 3: The basic composition diagram of the node.

Table 1: Forms of 8 different correlation functions.

Name	$R(\theta, \omega, a)$
EXP model	$b(a) = C^T(a)B, C^T(a) \in R^n$
EXP model A	$b(a) = C^T(a)B, C^T(a) \in R^n$
EXP model B	$a_K^2(a_0) = Var[Z(a_0) - Z(b_0)]$
Linear model	$Z(a_0) = \sum_{i=1}^{n} \omega_i(a_0) Z(a_i)$
Gaussian model	$Z_i = Z(a_i), i = 1, \cdots, n$
Spline model	$\gamma(a, b)$
Ball model	$R(\theta, \omega, a) = \prod_{i=1}^{n} R(\theta_i, \omega_i, a_i)$

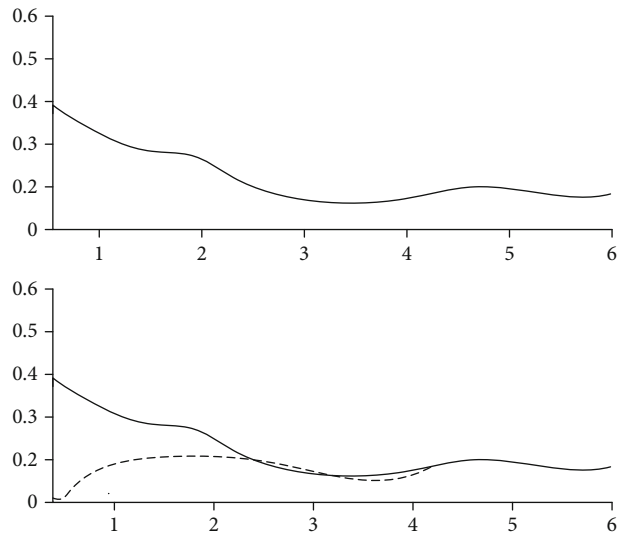

Figure 4: Typical trend chart.

2.4. Distance Measurement Method. There is an important concept in greedy embedding—distance. The distance is a function defined in the metric space. In general distance space, the distance between two points is usually measured by the norm of a vector composed of two points. In daily life, the most general distance is the distance in Euclidean space as the quadratic norm [23]. In graph theory, distance is the number of edges that pass the shortest path between two nodes. In analytic geometry, distance is a first-order norm. In the n-dimensional Euclidean space, there are three commonly used distance measurement methods [24].

(1) Manhattan distance (L1 distance): it is a geometric term used in Euclidean geometric metric space to indicate the sum of absolute wheelbases of two points in a standard n-dimensional coordinate system. The Manhattan distance of two points a_i, a_j in N-dimensional Euclidean space is formula (8):

$$d_{ij} = \sum_{k=1}^{n} |a_{ik} - a_{jk}|. \tag{8}$$

(2) Euclidean distance (L2 distance): the most commonly used distance measurement method is also the default distance measurement method in reality. The Euclidean distance of two points a_i, a_j in N -dimensional Euclidean space is formula (9):

$$d_{ij} = \sqrt{\sum_{k=1}^{n} |a_{ik} - a_{jk}|}. \tag{9}$$

(3) Chebyshev distance (L distance) is also called the maximum distance. It is used to indicate the maximum absolute wheelbase of two points in the standard n-dimensional coordinate system. The Chebyshev distance of two points a_i, a_j in N -dimensional Euclidean space is formula (10):

$$d_{ij} = \max \sum_{k=1}^{n} |a_{ik} - a_{jk}|. \tag{10}$$

Distance measurement is required in work such as triangulation, traverse, topographic, and engineering surveys. The accuracy of distance measurement is expressed as relative error. It can be seen from formula (10) that in order to realize the concise and greedy embedding of a graph $\sum_{k=1}^{n} |a_{ik} - a_{jk}|$, it is necessary to consider factors such as the measurement space, the distance measurement method, and the coordinate representation method. These factors provide directions for subsequent research [25], as shown in Figure 5.

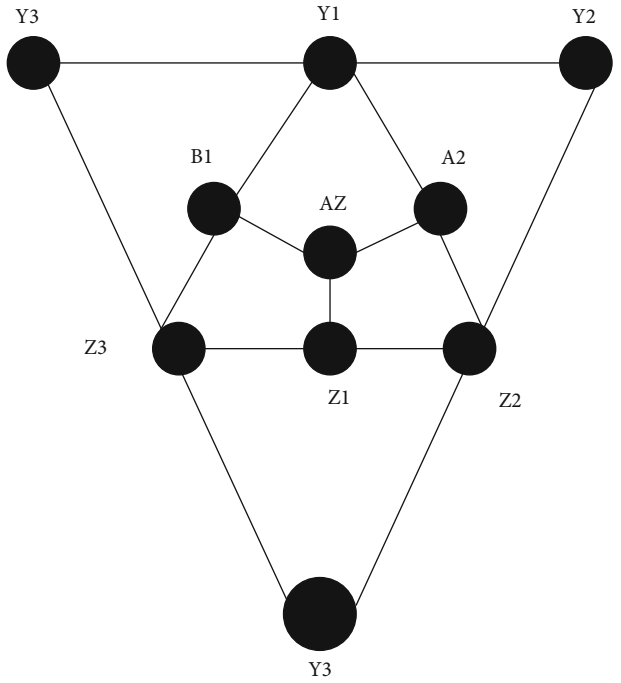

Figure 5: Recursive planar graph not greedy embedded.

As shown in Figure 5, in order to use graph theory to study wireless sensor networks, it must first determine the connectivity of the network. Through simulation experiments, the relationship between the average connectivity of the network formed by several random throws and the number of nodes in the network and the communication radius of the nodes is given [26–28].

2.5. Kriging Algorithm Implementation. For the convenience of explanation, this section uses the function y to represent the above functions and constructs a Kriging model [29]. Obtaining the pressure value of a set of pressure measurement points from the sample $P_1, P_2, P_3, \cdots P_N$, its estimated value is as shown in formula (11):

$$Y(P) = \mu(P) + Z(P). \tag{11}$$

Among them, μ is an unknown constant, Z is a Gaussian random process, the expected value is zero, and the variance value is σ^2. The value of μ can be calculated by the least square method using the previous input data, which is formula (12):

$$\mu = \frac{1^T(\varphi + \lambda I)^{-1}b}{1^T(\varphi + \lambda I)^{-1}1}. \tag{12}$$

Introduced by the basic principles of the Kriging algorithm in the previous section $(\varphi + \lambda I)^{-1}b$, the Kriging model can be transformed into formula (13):

$$\phi_{ij} = \mu + \varphi^t(b + 1). \tag{13}$$

Among them, φ is the covariance vector, which can be expressed as formula (14):

Table 2: List of node energy consumption.

Classification	State	Symbol	Typical energy consumption
CPU	Start up	ECPU	5.4 mA
CPU	Energy saving	ECPU	0.542 mA
RF transceiver	Send	ETRX	21 mA
RF transceiver	Take over	ETRX	54 mA
RF transceiver	Idle	ETRX	1.8 mA
RF transceiver	Dormant	ETRX	0.07 mA

$$\varphi_{ij} = \exp\left(-\sum_{k=1}^{d}\theta\left|\rho_{ik} - \rho_{jk}\right|^{ik}\right). \tag{14}$$

Among them, the value of hyperparameter θ can be used to adjust the width of the function model, and the hyperparameter can be used to adjust the smoothness of the function. The entire covariance matrix is Equation (15):

$$\varphi_{ij} + \delta_{ij}\lambda = \exp\left(\sum_{k=1}^{d}\theta_k\right)^2. \tag{15}$$

The above is the Kriging model established for atmospheric data $\delta_{ij}\lambda$, but the hyperparameters need to be obtained by the maximum likelihood estimation method to facilitate calculation [30]. The maximum likelihood function of B is Equation (16):

$$L = -\frac{1}{2}n\left(\partial^2\right)^2. \tag{16}$$

At this point, the angle of attack and the angle of sideslip can be directly calculated through the known pressure values of each pressure measurement point $(\partial^2)^2$. And through software calculations and wind tunnel experiments, a large amount of data was obtained, and the covariance matrix was established [31].

2.6. Node Energy Consumption Analysis. The energy consumption of sensor nodes is mainly divided into two parts, namely, the energy consumption of the on-board microprocessor and the energy consumption of the radio frequency transceiver. Typical energy consumption data of sensor nodes is shown in Table 2.

As shown in Table 2, for any time slot, according to the previous assumptions, each node must be in one of the following three states: packet sending, vacancy including back-off, and interframe idle. The probabilities are, respectively, formula (17):

$$\rho^7 = \rho r = \text{Lpsenspcca}. \tag{17}$$

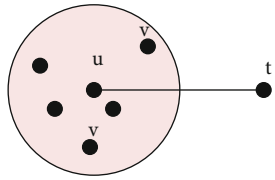

Figure 6: The closest rule to the destination.

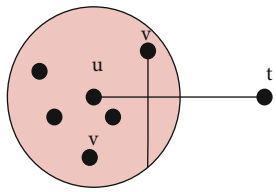

Figure 7: Maximum forward rule within a circle.

Sensor nodes are usually small embedded systems with weak processing, storage, and communication functions, and their energy is supplied by limited batteries. From the point of view of network function, each sensor node considers the dual functions of the terminal and router of the previous network node. In addition to collecting local information and processing data, it is also necessary to save, manage, and merge the transmitted data, according to other nodes cooperate with other nodes to complete several specific tasks.

The rule of closest to the destination is as follows: the current node chooses the node closest to the destination node among the neighbor nodes as the next hop node, as shown in Figure 6.

As shown in Figure 6, only the nodes closer to the destination node t than the node u are candidate nodes. Otherwise, it will not be able to move forward, and the algorithm will fail at this time. The line segment from u to this neighboring node has the longest projection length on the line segment ut, as shown in Figure 7.

As shown in Figure 7, the nearest forward rule, a node selects the nearest neighbor node with a forward progress component as the next hop node. Node u chooses node v as the next hop node.

The tracking algorithm is based on the target's motion model. If the sensor node sends measurement data to the central node control node in the form of a nonfixed period, this increases the complexity of the central node's current position estimation and future position prediction algorithms for the target, which is not conducive to effective tracking. Considering the following dynamic objects, including a discrete event dynamic subsystem $a_i[K+1]$ as Equation (18),

$$a_i[K+1] = A_i[k] + \omega_i[k]. \tag{18}$$

Corresponding to each subsystem $\omega_i[k]$, a sensor node is deployed in a reasonable location to measure the status of each subsystem separately. The sensor measurement value $b_i[k]$ is Equation (19):

$$b_i[k] = C_i[k]b[k] + u_i[k]. \tag{19}$$

Therefore, in practical applications, the selection of the above parameters should be determined according to the network scale, protocol, environmental interference, controller calculation performance, and algorithm complexity. The centralized method has poor scalability and is not applicable when the network scale is large. With the development of hardware and emerging application requirements, control systems for large-scale networks have gradually become a trend; so, scalability has become particularly important. For this reason, the control tasks are concentrated into decentralized and fully utilized resources. The tasks of the centralized controller are decomposed and shared by some nodes, such as distributed controllers or algorithm agents, to reduce the workload of a single point, thereby improving scalability.

With the accelerated pace of work and increased life pressure in modern society, the popularization of sports and fitness information services on the Internet undoubtedly provides people with a good way to solve health problems. However, there are a series of problems such as complex network environment, explosive sports fitness information, and uneven network fitness guidance team. This brings many challenges to the sports and fitness safety of ordinary people.

3. Experiment and Analysis Based on Sensor Network and Questionnaire

With the development of social economy, the physical fitness of the masses has also been steadily improved. The main task of the development of information services is to promote sports culture and promote the all-round development of people. The national level attaches great importance to the physical exercise of the masses, and the masses should also actively participate in physical exercises. At present, national fitness has become an upsurge, and people's fitness awareness is slowly being awakened. Therefore, the masses' demand for sports information service information is increasing.

Information exchange and processing on the Internet prepare for the organization and arrangement of actual physical activities. Through the Internet or community service information systems, residents can enjoy online sports and fitness information services provided by the community, and realize online competition to open the time and place of sports games and activities, and information such as operating platforms provided by local residents. This article investigates the degree of satisfaction of sports fans with information services, as shown in Table 3:

As shown in Table 3, sports enthusiasts are generally satisfied with sports information services accounted for a larger proportion, very satisfied at the least, accounting for only 5.6%, dissatisfied and relatively dissatisfied accounted for 16.5%. It shows that the masses are very dissatisfied with the current sports information services, and there is a problem of information lag in sports information services. This

Table 3: Satisfaction of sports enthusiasts with information services.

	Frequency	Percentage	Effective percentage	Cumulative percentage
Very satisfied	26	5.6	5.6	5.6
Quite satisfied	76	21.6	21.6	30
Generally	154	52.5	52.5	89
Relatively dissatisfied	34	6.7	6.7	76
Dissatisfied	20	7.8	7.8	78

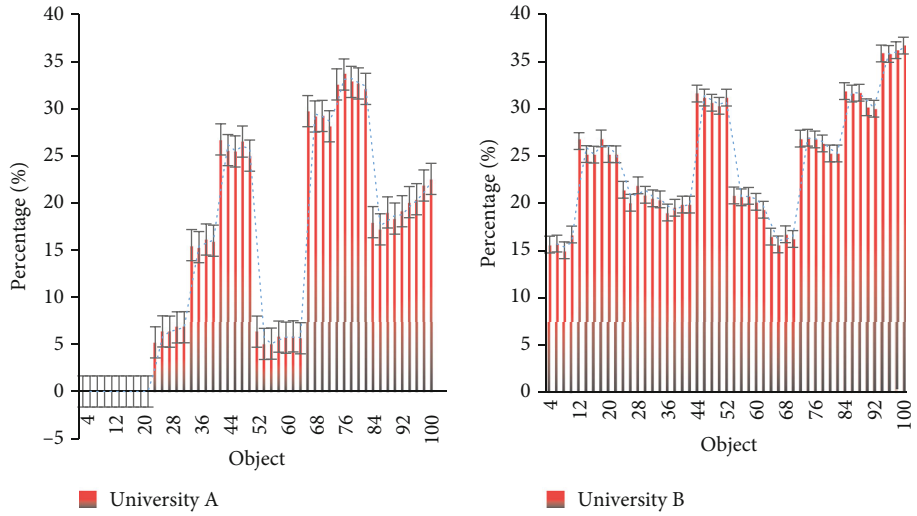

Figure 8: Information service efficiency map based on traditional methods in two sports universities.

Table 4: Questionnaire on hot spots of sports information services conducted by 10 sports enthusiasts.

Survey object	Use sensor networks	No sensor network used	Score A	Score B
1	Yes	No	6.7	2.1
2	Yes	No	7.8	1.8
3	Yes	No	8.6	0
4	Yes	No	8.5	0
5	Yes	No	7.8	2.1
6	Yes	No	8.5	1.5
7	No	Yes	6.4	1.7
8	Yes	No	9.8	1.4
9	No	Yes	7.5	2.6
10	Yes	No	5.5	3.1

article summarizes the status quo and development problems of sports public information service industry during the social transition period by consulting a large number of sports and related interdisciplinary literature materials and serves as the theoretical basis for the research content. Next, this article investigates the efficiency of information services based on traditional methods in two sports universities, as shown in Figure 8.

As shown in Figure 8, university A's information service efficiency based on traditional methods is the highest around 33%, and the lowest is around 5%; university B's information service efficiency based on traditional methods is the highest around 35%, and the lowest is around 15%; although, universities are less efficient than universities; in general, the information services of the two schools lag behind. This article conducts a survey of 10 sports enthusiasts on the hot spots of sports information services. The survey results are shown in Table 4.

As shown in Table 4, among the 10 sports enthusiasts, 8 enthusiasts are using sports information services based on wireless sensor networks. They feel that the information on this basis is comprehensive and reliable; there are 2 sports enthusiasts who did not use the sports information service based on the wireless sensor network, but they also want to try. So, it can be known that sports information services based on wireless sensor networks should be widely used. Next, it will investigate the efficiency of information services based on the sensor network system in the other two schools, as shown in Figure 9.

As shown in Figure 9, the use of sports information services by University C and University D in 2016 is very unstable, and the highest rate will not exceed 20%. In 2020, the use of sports information services by University C and University D will gradually stabilize, and the utilization rate will be higher and higher, with a maximum of 69% and a minimum of 35%. It can be seen that sports information services based on wireless sensor networks are becoming more and more popular with the public. Multiple linear regression analysis can explain the quantitative relationship of dependent changes between one or more independent variables

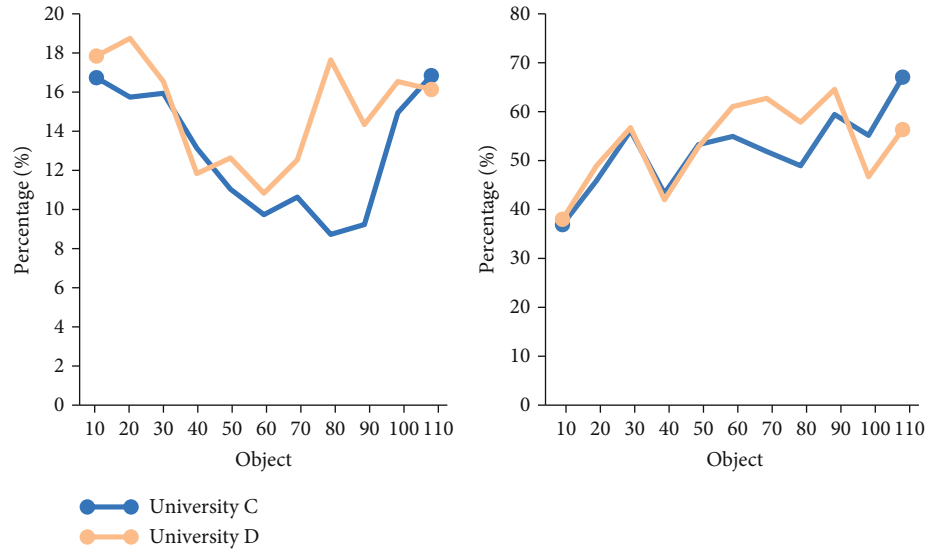

Figure 9: The efficiency map of two schools' information services based on the sensor network system in 2016 and 2020.

Table 5: Regression coefficients of the characteristics of public sports information services on the overall public satisfaction.

Model	Standardization factor Beta	t value	p value
(constant)	232	2.321	0.12
Accuracy	56	2.764	0.14
Content reliability	231	1.321	0
Timeliness	56	1.564	0
Openness and transparency	76	3.543	0
Accessibility	143	3.567	0
Patency of feed channel	212	3.875	0
Effectiveness of monitoring methods	167	3.543	0

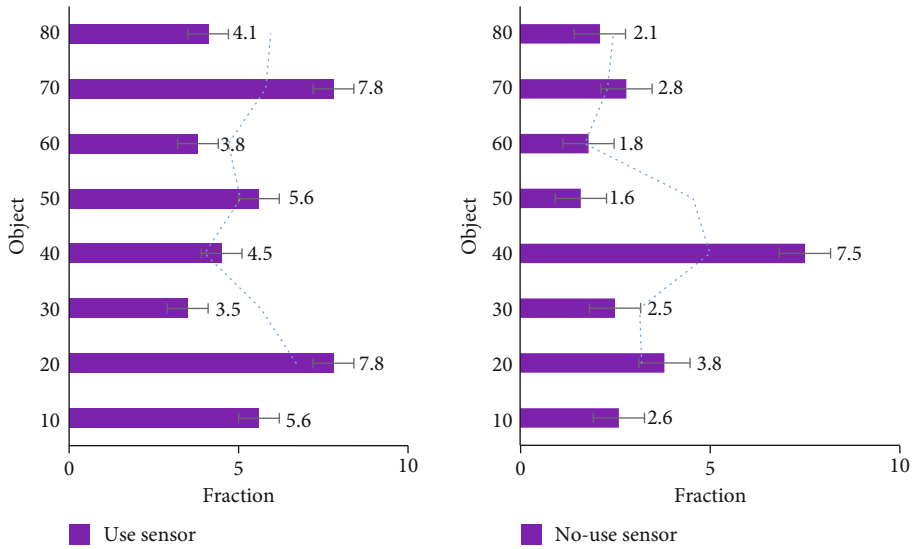

Figure 10: Comparison chart of the scores of whether to use wireless sensor network sports services.

and the same dependent variable. Usually multiple linear regression is used to explore whether the eight independent variables will have a significant impact on the overall satisfaction of public sports information services. The results show that regression analysis is significant. It shows that the 8 independent variables are closely related to the

dependent variable; that is, the regression line fits the sample data points to a higher degree. The summary results of regression coefficients are shown in Table 5.

As shown in Table 5, the reliability of information content, the transparency of information, the convenience of information acquisition, the smoothness of information feedback channels, and the effectiveness of information supervision methods are significantly related to the overall satisfaction of public sports information services. The effect of the accuracy of information presentation and the timeliness of information release on the overall satisfaction of information services are not significant. The reliability of information content, the transparency of information, the convenience of information acquisition, the smoothness of information feedback channels, and the effectiveness of information supervision methods can effectively predict the overall satisfaction of the public. Under the current public service system, improve the reliability of information content, the transparency of information, the convenience of information acquisition, and the smoothness of information feedback channels. And the effectiveness of information supervision methods may improve the public's satisfaction with public sports information services to a certain extent. This article analyzes the scores of sports information services that use wireless sensor networks and the scores of sports services that do not use wireless sensor networks, as shown in Figure 10.

As shown in Figure 10, it can be known that the lowest score for sports services without the wireless sensor network is 1.6 points, and the highest score is 7.5 points. The average score is around 3.5, which is very low overall; the lowest score for sports services using the wireless sensor network is 3.5 points, the highest is 7.8 points, and the average is around 5 points. The overall score is very high. Therefore, it can be known that information using wireless sensor network sports services is more popular.

The number of sports fitness information services provided is rapidly increasing. If the scope of information release cannot be expanded within time, it will be difficult to achieve sustained and effective development. Facing this huge crisis, fitness information service providers must master effective methods to expand communication and popularization and effectively promote their position in the market. Therefore, sports and fitness information service providers need to continuously improve information coverage, attract more users' attention, and realize their own development.

The experimental significance of this paper is to analyze the 5G embedded sensor network system, so as to obtain the role it plays in the sports information service. Through the experiment, we can know that the sports information service plays a huge role in the sports industry, and it is also convenient Sports fans get sports information.

4. Discussion

This article analyzes the development of sports information services based on the 5G embedded sensor network system, and elaborates the related concepts of the 5G embedded sensor network system and sports information services. The related theories based on 5G embedded sensor network system are studied,, and the design methods of sports information service hot spots are explored, through the questionnaire survey method case to discuss the importance of sports information services to contemporary society. Finally, take the 5G embedded sensor network system integrated into the sports information service as an example to discuss the correlation between the two.

This paper also makes reasonable use of the Kriging algorithm based on the 5G embedded sensor network system. As the Kriging algorithm has become more widely used, its importance has gradually become more prominent. Many scholars have begun to match the Kriging algorithm theory with real application scenarios and propose feasible algorithms. Kriging algorithm is a mathematical operation, and according to this operation, it is known that strengthening sports information services through the Internet is an indispensable part of life.

The advantages of Kriging algorithm are linear, unbiased, small variance, and suitable for spatial analysis. So, it is very suitable for geology, meteorology, geography, cartography, etc. relative to other interpolation methods. The main disadvantage is that the response speed is very slow because he has to consider the calculation influence range, consider whether the anisotropy is not, select the variogram model, and calculate the variogram value.

Through the questionnaire survey method, this article knows that the information using wireless sensor network sports services is more popular. Therefore, combining the characteristics of the "Internet +" era and finding a new communication method to enable people to receive relevant sports information services correctly and comprehensively is the key to promoting the development of sports information services.

With the rapid development of my country's economic construction, the people have gradually realized the importance of physical exercise, and sports have become a way of life for modern people. Social subjects are an important force in the construction of my country's public sports system. The public sports services provided by social subjects are not utilitarian and adhere to the principles of voluntary and semivoluntary.

5. Conclusions

This article mainly starts from theoretical knowledge based on 5G embedded sensor network system and sports information service and discusses how to establish a more reliable sports information service system based on sensor network system and 5G. Based on the global optimization of Kriging algorithm and sensor network structure, it can be seen that the global optimization of Kriging algorithm is applied in the process of sports information service, which can obtain better evaluation results and provide a new idea for sports information service. Moreover, the process is faster and more accurate, which has certain guiding significance for how to develop sports information services. Based on the 5G embedded sensor network system, the related scientific

fields involved are relatively extensive; so, the concept of sports information service has always been disputed. It can be seen from the experiments that the 5G embedded sensor network system can effectively promote the development of sports information services. The author's knowledge has not yet reached the perfect position, the author's academic theory and professional ability are relatively weak, and there are still many deficiencies. But at the same time, the author is constantly discovering and solving problems, striving to be the best.

Data Availability

No data were used to support this study.

Conflicts of Interest

The authors declare that there is no conflict of interest with any financial organizations regarding the material reported in this manuscript.

Acknowledgments

This work was supported by the School-level Academic Team Project of Wuhan Business University (2018TD011), the Wuhan University of Business Doctoral Fund projects (2021KB002), and the Application Foundation Frontier Project (2020010601012294).

References

[1] X. F. Xu, P. Sun, L. Wang et al., "Study of urban sport energy conservation information network service system," *Energy Education Science and Technology*, vol. 34, no. 4, pp. 343–350, 2016.

[2] M. S. Howard, K. L. DiDonato, D. L. Janovick et al., "Perspectives of athletes and pharmacists on pharmacist-provided sports supplement counseling: an exploratory study," *Journal of the American Pharmacists Association*, vol. 58, no. 4, pp. S30–S36.e2, 2018.

[3] T. J. Cain, F. M. Cheek, J. Kupsco, L. J. Hartel, and A. Getselman, "Health sciences libraries forecasting information service trends for researchers: models applicable to all academic libraries," *College & Research Libraries*, vol. 77, no. 5, pp. 595–613, 2016.

[4] Q. Guo, L. Jian-Xia, and W. Yu-Ming, "Evaluation of intelligent tourism information service capabilities: a case study of Hanzhong City," *Ecological Economy*, vol. 1, pp. 2–13, 2021.

[5] P. Gope and T. Hwang, "BSN-care: a secure IoT-based modern healthcare system using body sensor network," *IEEE Sensors Journal*, vol. 16, no. 5, pp. 1368–1376, 2016.

[6] S. Abraham and X. Li, "Design of a low-cost wireless indoor air quality sensor network system," *International Journal of Wireless Information Networks*, vol. 23, no. 1, pp. 57–65, 2016.

[7] M. Hammoudeh, F. Al-Fayez, H. Lloyd et al., "A wireless sensor network border monitoring system: deployment issues and routing protocols," *IEEE Sensors Journal*, vol. 17, no. 8, pp. 2572–2582, 2017.

[8] D. Zhang, P. Shi, W. A. Zhang, and L. Yu, "Energy-efficient distributed filtering in sensor networks: a unified switched system approach," *IEEE Transactions on Cybernetics*, vol. 47, no. 7, pp. 1–12, 2016.

[9] L. Dong, W. Shu, X. Li, G. Han, and W. Zou, "Three dimensional comprehensive analytical solutions for locating sources of sensor networks in unknown velocity mining system," *IEEE Access*, vol. 5, no. 99, pp. 11337–11351, 2017.

[10] I. Butun, P. Österberg, and H. Song, "Security of the Internet of Things: vulnerabilities, attacks, and countermeasures," *IEEE Communications Surveys & Tutorials*, vol. 22, no. 1, pp. 616–644, 2020.

[11] A. Mukherjee, D. K. Jain, P. Goswami, Q. Xin, L. Yang, and J. J. P. C. Rodrigues, "Back propagation neural network based cluster head identification in MIMO sensor networks for intelligent transportation systems," *IEEE Access*, vol. 8, no. 1, pp. 28524–28532, 2020.

[12] L. Wu, Q. Zhang, C. H. Chen, K. Guo, and D. Wang, "Deep learning techniques for community detection in social networks," *IEEE Access*, vol. 8, pp. 96016–96026, 2020.

[13] P. Giri, K. Ng, and W. Phillips, "Wireless sensor network system for landslide monitoring and Warning," *IEEE Transactions on Instrumentation and Measurement*, vol. 68, no. 4, pp. 1210–1220, 2019.

[14] N. Alsaedi, F. Hashim, A. Sali, and F. Z. Rokhani, "Detecting sybil attacks in clustered wireless sensor networks based on energy trust system (ETS)," *Computer Communications*, vol. 110, no. 15, pp. 75–82, 2017.

[15] W. Gao, S. Emaminejad, H. Nyein et al., "Fully integrated wearable sensor arrays for multiplexed _in situ_ perspiration analysis," *Nature*, vol. 529, no. 7587, pp. 509–514, 2016.

[16] M. Adil, H. Song, J. Ali et al., "Enhanced AODV: A Robust Three Phase Priority-based Traffic Load Balancing Scheme for Internet of Things," *IEEE Internet of Things Journal*, 2021.

[17] G. M. Abdulsahib and O. I. Khalaf, "Accurate and effective data collection with minimum energy path selection in wireless sensor networks using mobile sinks," *Journal of Information Technology Management*, vol. 13, no. 2, pp. 139–153, 2021.

[18] W. Sun, "Research on the construction of smart tourism system based on wireless sensor network," *Mathematical Problems in Engineering*, vol. 2021, no. 18, pp. 1–8, 2021.

[19] B. M. Todorović and D. Samardžija, "Road lighting energy-saving system based on wireless sensor network," *Energy Efficiency*, vol. 10, no. 1, pp. 239–247, 2017.

[20] S. Hong, "Design of air quality information service based upon geographic context information model in ISO19154," *Spatial Information Research*, vol. 25, no. 1, pp. 39–47, 2017.

[21] B. Han, J. Li, J. Su, and J. Cao, "Self-supported cooperative networking for emergency services in multi-hop wireless networks," *IEEE Journal on Selected Areas in Communications*, vol. 30, no. 2, pp. 450–457, 2012.

[22] Y. C. Kaplan, B. Karadaş, G. Küçüksolak et al., "Counselling pregnant women at the crossroads of Europe and Asia: effect of teratology information service in Turkey," *International Journal of Clinical Pharmacy*, vol. 39, no. 4, pp. 783–790, 2017.

[23] S. Xue, L. Xiong, S. Yang, and L. Zhao, "A self-adaptive multi-view framework for multi-source information service in cloud ITS," *Journal of Ambient Intelligence & Humanized Computing*, vol. 7, no. 2, pp. 205–220, 2016.

[24] T. Oh, H. Sung, and K. D. Kwon, "Effect of the stadium occupancy rate on perceived game quality and visit intention," *International Journal of Sports Marketing and Sponsorship*, vol. 18, no. 2, pp. 166–179, 2017.

[25] H.-W. Park and S.-H. Kim, "Analysis of factors influencing the self-perceived health status of elderly people," *Korean Journal of Sports Science*, vol. 26, no. 2, pp. 1213–1225, 2017.

[26] C. K. Harrison, S. Bukstein, G. M. Botts, and S. M. Lawrence, "Female spectators as customers at National Football League games," *International Journal of Sports Marketing and Sponsorship*, vol. 17, no. 2, pp. 172–200, 2016.

[27] A. I. Rynarzewska, "Virtual reality: a new channel in sport consumption," *Journal of Research in Interactive Marketing*, vol. 12, no. 4, pp. 472–488, 2018.

[28] O. I. Khalaf, G. M. Abdulsahib, and B. M. Sabbar, "Optimization of wireless sensor network coverage using the bee algorithm," *Journal of Information Science and Engineering*, vol. 36, no. 2, pp. 377–386, 2020.

[29] G. Dartmann, H. Song, and A. Schmeink, *Big data analytics for cyber-physical systems: machine learning for the Internet of Things*, Elsevier, 2019.

[30] E. Strumbelj, "A comment on the bias of probabilities derived from betting odds and their use in measuring outcome uncertainty," *Journal of Sports Economics*, vol. 17, no. 1, pp. 12–26, 2016.

[31] R. Biscaia, A. Correia, M. Yoshida, A. Rosado, and J. Marôco, "The role of service quality and ticket pricing on satisfaction and behavioural intention within professional football," *International Journal of Sports Marketing & Sponsorship*, vol. 14, no. 4, pp. 301–325, 2016.

Hindawi
Wireless Communications and Mobile Computing
Volume 2022, Article ID 9689272, 11 pages
https://doi.org/10.1155/2022/9689272

Research Article

Interactive Cultural Communication Effect in VR Space of Intelligent Mobile Communication Network

Xiaoxia Li,[1] Xi Deng,[1] and Hongfei Xu[2]

[1]*School of Fine Arts and Design, Hainan University, Haikou, 570228 Hainan, China*
[2]*School of Creative Design, Zhejiang College of Security Technology, Wenzhou, 325016 Zhejiang, China*

Correspondence should be addressed to Hongfei Xu; 15076043@zjcst.edu.cn

Received 2 December 2021; Revised 24 January 2022; Accepted 12 February 2022; Published 25 February 2022

Academic Editor: Mohammed Hammoudeh

Virtual reality technology can provide more display techniques to realize the interactive design of multiexhibition area of red humanities and natural resources. First of all, through the three-dimensional interactive display of cultural relics and scene reproduction of historical events, visitors can enjoy the unrestrained and immersive appreciation, make up for people's lack of understanding of history, and let tourists personally feel the difficulties and hardships in the development of Chinese revolutionary history. Second, the digital method also provides for the pavilion and the scenic spot design personnel more creative method; dynamic scene reappearance interaction design based on virtual reality technology to promote education, protection of cultural relic collection and utilization, academic research, and the industrial development and multidimensional public welfare publicity results is blended in among them, through the panoramic, immersive, and interactive display technique, such as multilevel multiway spread red brigade culture. Virtual reality constantly imitates the real-life environment, and the application of perception sensing equipment has perception. This new technology requires us to continue to explore and research it. Virtual reality technology is a very cutting-edge subject and research field, which is very challenging. The communication form of culture has also been constantly evolving. Virtual reality technology (VR) has changed the way of traditional culture appreciation through the transmission of visual information, bringing people a new aesthetic enjoyment. Mainstream media is used to mobilize the red cultural heritage protection and scholars at home and abroad, to explore the application of virtual reality in the red culture tourist attraction planning, and to explore virtual reality applications in red open spot virtual roaming: exploration of virtual reality in the application of historical and cultural sites to red tourism management and exploration of virtual reality in the brand historical and cultural sites in the application of the travel marketing, to build an intelligent mobile communication network communication platform and broaden the new path of inheritance and protection. On the basis of studying the communication effect of traditional culture, this paper studies the possible communication effect of symphony orchestra under the new technology format under the framework of communication studies. It also analyzes and explores various factors such as the practical value, difficulty, civilized prestige, adaptability, and resistance to adversity of the culture in cultural communication and compares the methods of cultural communication. By developing a virtual instrument placed in the sphere of virtual reality space, the traditional symphony orchestra can be transformed into an interactive culture communication in virtual reality space. In this communication design, users can define their own instruments to play interactive culture communication, change the position of the instrument on the sphere interactively, and even change the sound effect of the symphony interactively by rotating or adjusting the size of the sphere, so as to achieve the best communication effect of the symphony.

1. Introduction

Under the new intelligent mobile communication network, the forms of media memory have more diversified expressions. The thinking logic of mass media digitizes, imagines, and stories the way of memory, breaking through the time limit of material carrier inheritance. The media memory of red culture can strengthen the strength of

social collective memory through multiple forms of memory. We should pay attention to the preservation and repair of material carrier; on the other hand, we should also open up new media forms of red culture memory, so that the red culture can remain in the collective memory of the public. Virtual reality has three characteristics, namely, perception, VR should have all the perceptions that humans have; existence, VR should have an immersive experience for the experiencer; and interactivity, VR should have the function of interactive experience between humans and machines. What virtual reality technology emphasizes is "immersion," which makes people seem to be in the scene. The times are constantly changing, and VR plays a very important role in the research of digital space art. With the widespread popularization of computer, smart phone, and network, human beings have entered a high information age. In the past, people lacked the means of communication, interaction, dissemination, and sharing of traditional historical and cultural knowledge such as culture and painting, and the problems of abstract characters and incomprehensible semantics in traditional propaganda methods were urgently needed to be solved in the process of dissemination and promotion. Nowadays, the form of culture communication has been continuously developed and evolved. The addition of visual information has changed the traditional way of culture appreciation and brought people a new aesthetic enjoyment. Culture communication and promotion based on the interactive experience of Unity3D space can build the cultural resources of symphonic culture into an interactive three-dimensional scene to realize the visualization of symphonic culture scene. By using simple mobile devices, people can interact with objects in the virtual environment, making users feel as if they were in the real symphony environment, which can not only satisfy the perception but also have interaction, which is also more conducive to stimulating the interest of the new generation in the learning of symphony culture. Interactive experience is mainly an experience between the experiencer and the space. It expresses a kind of "immersion." The so-called "immersion" expresses the experience of the experiencer in the space. For experiencers, a good interactive experience can bring them sensory enjoyment and endless fun. The monotonous life, through the connection of virtual reality technology, adds a new understanding of space. Although the space art and the experiencer are not the same subject of expression, they are connected and integrated into a whole through the operation of virtual technology and even realize the dialogue function of human-computer interaction.

The rich connotations and historical deposits of red culture always constitute the value system and spiritual style of the Chinese nation. Therefore, in the communication environment of the new era, it is an important issue for us to think about how red culture fits into the contemporary context of intelligent media communication and how to create a communication mode integrating red gene and new media. The virtual reality technology of interactive experience is characterized by immersion, interaction, and imagination. Based on computer technology, it creates a three-dimensional and all-round environment by simulating the real world and human vision, hearing, and touch [1]. Culture communication and promotion based on the interactive experience of Unity3D space can build cultural resources into an interactive three-dimensional (3D) scene to realize the visualization of cultural transmission resource interpretation [2]. As a typical romantic country, France is one of the most successful countries in integrating aesthetic concepts with modern technology and is also the country with the earliest and most extensive research on virtual technology in the world [3]. Due to the huge benefits achieved in the application of virtual reality technology in some special fields, more developed countries have invested large research resources in this field [4]. In China, the research on virtual reality started late and there is a gap between it and foreign research results, but it has attracted great attention from relevant government departments [5]. Especially in recent years, in the field of civil use, its research results have begun to focus on various complex sensory operations of the human body [6]. On the whole, while keeping up with the international new technology, the research is paying more and more attention to the application of virtual laboratory, virtual leisure experience, virtual art appreciation, and other aspects [7].

The light field is used as the input source of the VR device. Since the light field can provide visual information of moving parallax, binocular parallax, and selective focus at the same time, the imaging result is improved from the traditional 2D plane image to the 4D light field image; eliminating the dizziness of the VR experience greatly improves the sense of immersion and fidelity and blurs the boundary between reality and vitality. It can be said that VR equipment is currently the best device for stereoscopic display of light field, and light field is also the most suitable application of VR equipment. Interactive cultural transmission equipment has its own unique properties and plays its functions in different types of works and also forms unique rules and principles [8]. In order to make the communication effect of interactive cultural transmission equipment, this study puts forward a new design idea to fully reflect its universality and interactivity. The research content is still focused on the interactive virtual cultural transmission based on VR space, which makes the communication site more authentic through basic interactive design. The research will focus on analyzing and summarizing the types and characteristics of symphonic cultural transmission, so as to fully grasp the interactive relationship between image and modern cultural transmission, which both promote and restrict each other. During the development of the system, the key technologies involved and the principles and functions of these technologies are studied and analyzed, including the selection of the platform and the integration of the implementation technology into the virtual experiment of computer assembly. The research also combines the recent survey of the audience of symphony popular concert to study the communication effect of concert in the framework of communication studies. These interactive settings of the components of the

multimedia information are used to maximize the reusability of the virtual exhibition hall.

2. Research Overview and Technical Plan

2.1. Connotation of Cultural Dissemination Communication. Break the space-time concept of narrative scene, and reconstruct the "immersive" experience scene. Due to the limited communication capacity, people's communication activities mostly take place in fixed space and time places. The emergence of intelligent media technology breaks the limitation of communication frame and makes information interaction more three-dimensional. The media connect the receivers and receivers and place them in the same virtual space. The information transmission and feedback activities in this space construct a variety of narrative scenes, which become one of the main features of intelligent media communication. The application of online virtual space constructs a broader and free space for the dissemination of red culture. Red historical stories are the most vivid carrier of red culture. Real and vivid stories are permeated with the nobleness and sacredness of red culture, which can make the people clarify the drama, reject vulgarity, and worship heroes. For example, the red memorial hall without walls and virtual simulation "immersion" experience hall are built to realize the organic combination of online virtual space and offline real experience, so as to improve the communication efficiency of red culture and enhance its identification. At the same time, efforts should be made in "interaction" and "service" to set up friendly interactive interfaces and participation links, such as cultural knowledge question-and-answer, one-click costume change and virtual scene online experience, to enhance the fun and immersion of cultural products.

The essence of culture communication is the behavioral process in which people produce culture information, disseminate culture information, and receive culture information. Cultural transmission refers to the interaction of culture from one society to another, from one area to another, and from one group to another. In this dynamic process, both parties interact and influence each other and achieve a kind of communication and resonance in the spiritual level [9–11]. The development of red tourism brings more visitors but also increases the difficulty of protecting the material resources of red culture. In addition, museums and red tours are open to the public free of charge according to the relevant policies of the state and Hainan Province. Real-time interaction means people can like the real world and the virtual world for real-time interaction and diversified simulation using each kind of sensor information interaction, and people with special equipment and all interact in virtual reality, just like in the real-world experience in virtual environment and real environment as well as the corresponding response. For example, if you grasp an object in the virtual world with your hand, you will feel as if you are grasping something. The captured virtual object will react in real time as if it is in your hand. This is the real-time interaction of virtual reality. Nowadays, the forms of cultural communication tend to be diversified and popular, and various forms of communication emerge endlessly. The medium of cultural transmission is mainly the migration and flow of people, especially the migration of people which is more important. Important means of cultural transmission are immigration, war, invasion, and occupation. In addition, tourism and the flow of other people are also important media for the dissemination of culture. In this context, to attract the public's attention, the media of red culture communication strives for innovation, so as to better spread the spirit of red culture. In addition, the rapid development of digitalization, the combination of virtual reality and cultural industry, and the performance design based on virtual reality are a communication medium for red culture to conform to the development of digital era and a new form of red culture communication. The dissemination of red culture is the cultural dissemination of red culture as the main content, which means that the communicator conveys the content of red culture consciously and purposefully through various communication carriers and media and through various communication methods. The red spirit is given to the communicator, and the behavior and value orientation of the communicator are influenced by the red culture. The dissemination of red culture is an important way to inherit red culture. Promote the spirit of red culture, show the deeds of revolutionary history, and arouse the resonance of the red spirit. In order to make red culture spread, let the red culture get better civilization inheritance [12]. Cultural dissemination communication can be divided into two forms: natural communication and technical communication. These two forms of communication are divided by the different media and channels of communication, so there are some differences in the effect of communication. The technical communication of culture is closely related to the development of science and technology, which means that the intervention of other media besides air makes the channels of communication diversified, the clarity of communication effect, and the unprecedented expansion of communication scope and speed [13]. Natural culture communication refers to the face-to-face communication of music information between receivers and receivers using air as the transmission medium, which results in the transparency of the relationship between transmission and reception and enhances the sense of reality of communication effect [14, 15]. In terms of technical communication means, for the first time, recording was used to complete the storage of sound, which broke the limitation of time and space, and the range and speed of communication were expanded unprecedentically, resulting in the unprecedented development of culture communication [16]. In the natural route of transmission, the first performer performs to stimulate the audience's emotions and to strengthen the presence of the audience, the audience watching the show of emotion, and instant feedback to the performers, thus stimulating the mood of performers and mobilize their enthusiasm; the audience can see more wonderful performances [17, 18]. The face-to-face communication of music information between

performers and viewers results in transparency of the relationship between transmission and reception, which enhances the sense of reality of communication effect [19].

2.2. Symphony Communication Integrates Virtual Reality and Audio. For the development of the platform, users can feel the speed of time and no longer have to travel far away; as long as they pick up mobile phones and other devices, they can feel the convenience of digital technology in people's lives. And for creators with dreams, young people can be actively encouraged to create and develop platform exchanges, which can drive the trend of the times and lead the development of the society's related industries of virtual reality technology, thereby driving the direction of new media technology and promoting the new media era. VR technology has played an undoubtedly key role in interactive applications in the digital space. With the arrival of the information age, electronic technology develops at a high speed, and culture communication forms are constantly developing and evolving; from natural cultural transmission, these two forms of culture communication not only inherit in time sequence but also show mutual integration at the spatial level [20, 21]. Virtual reality (VR) and other immersive technologies play an important role in the immersive experience of video games and movies [22]. Virtual reality technology includes technologies that blur the boundaries between the real world (reality) and the digital world (analog reality) [23]. According to our vision, hearing, and touch, virtual reality allows users to have immersive experiences with different contents [24]. Because of this, each category has its own special device, which users must wear or use in order to experience different types of immersive content [25]. Unlike virtual reality, "augmented reality"-based technologies can also experience environments or events that do not use a monitor, as it is often implemented in applications and projected into the real world. In other words, augmented reality (AR) can supplement the user's current visual sense with any simulator [26]. But when these simulated objects are superposed into a virtual object, people can interact with them in the real world, which becomes a hybrid reality and seamlessly merges the real-world objects with the virtual analog objects into the digital world, so that they can coexist and interact together.

The emergence of these modern communication media broadens the scope and audience area of culture communication and enriches the styles of music art. However, traditional culture communication methods will not disappear, but will be shown to us in new forms. With the intervention of modern technology, we can enjoy more mysterious scene of the live concert, romantic or popular bar music, a variety of street art, etc. Together with modern music media, they create a three-dimensional space for people to enjoy music together. More importantly, this experience is an immersive spherical video, and users can also control the position of their perspective in the video in all directions, making elegant music and folk music more widely available.

VR (virtual reality) is to completely separate reality, so that you are fully integrated into the real world. AR (augmented reality) overlays the real world with electronic content [27]. MR (mixed reality) is a mix of the real world and the virtual world; you can feel the electronic content exists in your real world.

2.3. Construction of Interaction Scheme. In the construction of interactive cultural transmission system, the system realization needs to obtain the body movement of the performer through the camera and interact with the system accordingly. The design principle of this interactive scheme is to require participants to always be in automatic browsing mode. Although participants are in a state of touring, apart from the adjustment of the picture by the system itself according to the perspective of participants, participants can control the rhythm of touring and obtain some detailed information through body movements. The avoidance of participants wearing other sensor devices not only makes the use of the system more convenient and the cost of the system lower but more importantly enables participants to interact with the system more naturally. When participants visit in the automatic tour mode, they can control the automatic tour mode to stop the tour and introduce the relevant words and sounds according to the content of the picture, so that participants can have a further understanding and understanding of the relevant browse content.

CAVE is a virtual reality system, which organically combines high-resolution stereoprojection technology, three-dimensional computer graphics technology, and sound technology to produce a completely immersive virtual environment. Interactive cultural transmission system is based on CAVE's real scene information display and interactive tour of virtual environment. In the virtual environment system, the panoramic camera and sensor devices allow to get a panoramic view of the stage in video images and other sensory information and the transmission of information to the Unity3D engine; thus, the panoramic video and other sensory information are shown in the CAVE system and access to a user action information is through it, which is transmitted to the Unity and translated into control instruction in 3D, by the Arduino, to control the movement of panoramic camera and sensor devices in the environment. The schematic diagram of interactive cultural transmission system is shown in Figure 1.

In the self-guided tour mode, participants should not only adjust the content of the picture according to the point of view but also control and select the tour route and movement state through their own body movements. Therefore, participants are required to make specific actions for interaction and control. In the CAVE system, the movement of the platform can be controlled by sending control instructions to the Arduino through the program after recognizing the body movements of participants. Video footage from the panoramic camera is also transmitted in real time to the CAVE system, where it is displayed.

2.4. Fine Optimization Modeling. About the definition of virtual reality technology, there are no unified standard, comprehensive, and multiple claims that can be summarized as follows: virtual reality technology is a kind of modern high-tech means, with computer technology as the core,

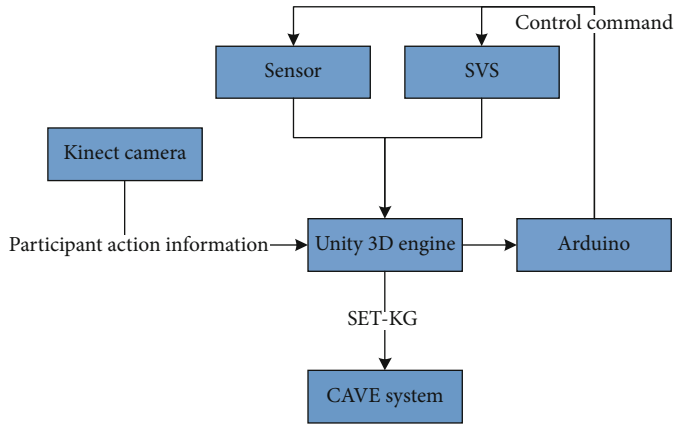

Figure 1: Schematic diagram of interactive cultural transmission system.

can build a break time and space constraints, and have a realistic vision, hearing, touch, smell, and taste, such as the integration of virtual environment; users with special helmet input/output devices, such as gloves and glasses, can interact with objects in the virtual world through gestures such as hand movement, head rotation, and body walking, so as to get real-time three-dimensional feedback and create an immersive experience.

The rapid development of virtual reality technology has been integrated into every aspect of social life, which can be called the creation with the most development potential in the 21st century. It has important application value in the protection and dissemination of red culture. Through the application of virtual reality technology, it can promote the protection and dissemination of the rural red cultural, promote the red cultural relics to "shine" and red resources to "live," and carry forward the red culture. Through the application of virtual reality technology, it can expand the radiation side and educational side of the red culture, enhance the attraction of the red culture, inspire more people to have the feelings of patriotism, love the party, love the hometown, and have far-reaching educational value. Through the application of virtual reality technology, it can inject new vitality into local red culture tourism, promote cultural exchanges, accelerate the development of local economy to a certain extent, and help rural revitalization. Red culture is the condensation and accumulation of the traditional culture and humanistic spirit of the Chinese nation. It contains profound historical and cultural connotations and is an important carrier and resource for propaganda and education in the new era. Red cultural heritage has attracted more and more attention in today's society; the use of modern means of virtual reality technology to protect the red culture and propaganda is very necessary and can firmly show cultural self-confidence, show the distinctive glamour of red cultural, and effectively play a positive education significance and practical application value.

Therefore, based on the working principle of VRML and considering the network transmission efficiency and user experience, the size of VRML files should be minimized so that the display speed can be guaranteed, display delay can be avoided, and its advantages can be realized to give users a better experience, as shown in Figure 2.

VRML to realize the virtual laboratory is a blend of network technology and can be accessed via a browser; the working principle of the VRML is by establishing a file containing description node in virtual reality, with the aid of the client browser to explain, but it must install a plugin to browse; only the corresponding plug-in installed on the client is used to establish virtual environment and the display of real-time rendering.

2.5. The Effect of Cultural Communication. The rapid development of virtual reality technology has been integrated into every aspect of social life, which can be called the creation with the most development potential in the 21st century. It has important application value in the protection and dissemination of red culture. Virtual reality technology truly restores the red historical events, providing students with an immersive learning experience that is not restricted by the venue and rich in content, so that the red curriculum can be organically combined with the base. Using high-tech means such as virtual reality improves the way of simply explaining and visiting research institutions and research bases, supports the better inheritance of red-themed research, and makes red research a spiritual inheritance that touches the soul. The application of virtual reality technology can promote the protection and dissemination of red cultural heritage, can promote the red cultural relics as "bright" and red resources "alive", and will carry forward the red culture. Through the application of virtual reality technology, the radiation and education of red culture can be expanded, the attraction of red culture can be enhanced, and more people can be inspired to love their country, the party, and their hometown, which has far-reaching educational value. Through the application of virtual reality technology, it can inject new vitality into local red culture tourism, promote cultural exchanges, and accelerate the development of local economy to a certain extent. Red culture is the condensation and accumulation of the traditional culture and humanistic spirit of the Chinese nation. It contains profound historical and cultural connotations and is

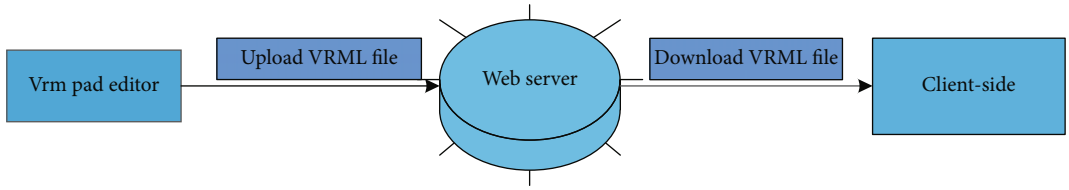

Figure 2: VRML transmission flow chart.

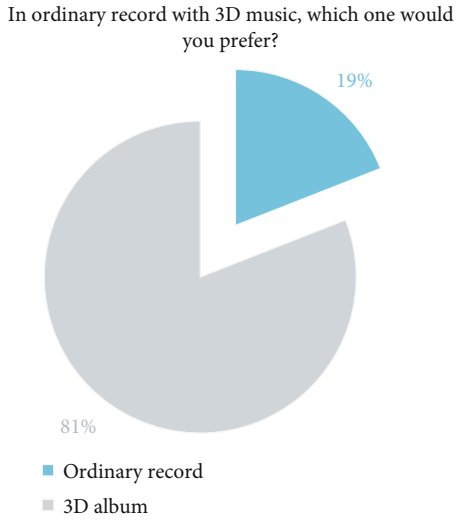

Figure 3: Which of the survey results do you prefer between CDS and 3D music.

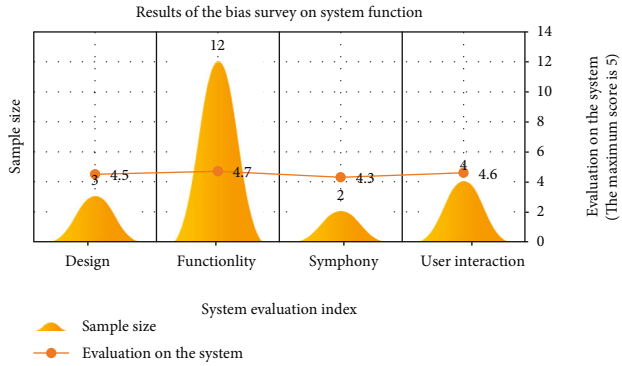

Figure 4: Survey results on system functional orientation.

Table 1: Feedback and suggestion results of users to the system.

Criteria	Number of times suggested
Improved design	2
More red culture	3
Add more features	2

an important carrier and resource for propaganda and education in the new era. In today's society where more and more attention is paid to the red cultural heritage, it is very necessary to use modern virtual reality technology to protect and publicize the red culture, which can strengthen cultural confidence, show the unique charm of red culture, and effectively play a positive educational significance and practical application value.

The intelligent communication network is based on the original communication network and provides new telecommunication services. The core of the intelligent communication network is how to efficiently provide users with various new services. The development cycle of new services is shorter than that of traditional services. This means that the development and funding services can be opened to users in advance and will be recovered early. A large amount of fund improves the utilization rate of the network and enhances the intelligence of the network; this is the source of the rapid development of the intelligent communication network. This will bring huge economic benefits and convenience to the telecommunication door and users. The basic idea of the intelligent communication network is to separate switching and intelligence in the network and implement centralized business control. This is achieved by setting up some network functional components.

Cultural exchange is also called cultural diffusion, which refers to the process of expanding human culture from the source of culture to the outside or from a social group to another social group that can be divided into direct sending and indirect sending. The former usually includes people who directly spread the culture of specific spiritual or material cultural content through convoys, military, etc., including new agricultural technologies and inventions. The latter shows more complex cultural diffusion. It mainly refers to borrowing from specific social groups. The principle of foreign cultural characteristics is to implement a kind of stimulating popularization of civilization creation activities.

The process of cultural dissemination depends on many factors such as the actual value of the culture, its difficulty, the prestige of civilization, the adaptability of the times, and the resistance to adversity. In fact, the characteristics and identity of the communication media often determine the characteristics of the communication culture. For example, in the 17th century, Italian missionaries played a role in stimulating communication to a certain extent on Chinese garden architecture and religious features, the culture of the time.

Due to the complexity of the origin of culture, the method and path of cultural transmission, and the factors that affect diffusion, investigating the origin of specific cultural characteristics is a difficult point in cultural geography.

Generally, because a certain region has a high similarity to other regions in terms of cultural characteristics, it can be inferred that the popularity of foreign culture is greater

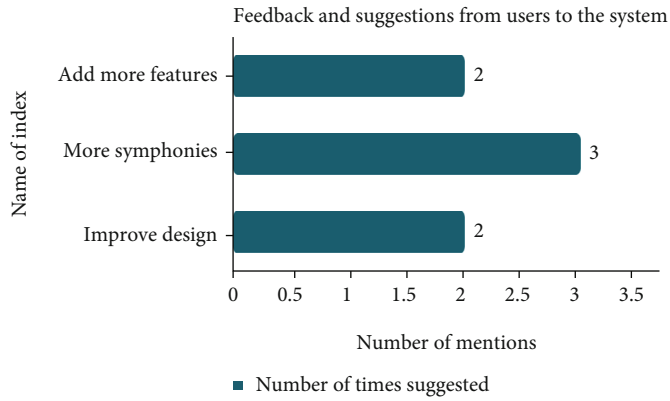

Figure 5: Feedback and suggestion result of users to the system.

than the creativity of local culture. In recent years, some cultural geographers have adopted the model of induction. The probability and law of cultural diffusion provide a new research method for in-depth understanding of cultural exchange phenomena.

There are two ways to popularize culture and media. The first is direct borrowing, directly accepting foreign cultural factors or cultural clusters. The other is indirect communication. In other words, cultural factors or cultural clusters are introduced into the region, allowing people present to think, thereby giving the people who introduce it an opportunity to create a new culture. This phenomenon is called "stimulus transmission."

The media for cultural exchange are mainly people's immigration and flow, especially people's immigration which is more important. Immigration, war, aggression, and occupation are important channels for cultural dissemination. Immigrants bring foreign cultures, and victorious countries always impose their own culture on failed countries. In addition, the movement of people such as trade and sightseeing is also an important medium for spreading culture. In modern times, with the development of transportation and communication technology, the media for cultural exchanges are increasing, and cultural communication does not necessarily depend on the movement and flow of people. The spread of culture in the world through various channels at an unprecedented scale and speed will inevitably improve the uniformity of world culture. The popularization of culture is one of the important reasons for social change. Critically borrowing and absorbing foreign culture are a necessary condition for implementing social reforms and promoting social progress.

To sum up, the application of VR technology can better play the lofty spirit and core value of red culture, create fresh historical scenes through virtual technology, and strengthen the contemporary expression of red culture in the flow and immersion scene of red spirit.

3. Interactive System Design

3.1. System Demand Analysis. According to the theme and activity planning of red tourism scenic spots, virtual reality technology is used to realize online and offline dynamic display, to create intelligent mobile communication network position of red culture and tourism, and to broaden the communication platform of intelligent mobile communication network. Mainstream media is used to mobilize the red cultural heritage protection and scholars at home and abroad, to explore the application of virtual reality in the red culture tourist attractions planning, and explore virtual reality applications in red open spots virtual roaming: exploration of virtual reality in the application of historical and cultural sites to red tourism management and exploration of virtual reality in the brand historical and cultural sites in the application of the travel marketing to build an intelligent mobile communication network communication platform and broaden the new path of inheritance and protection: first, to organize the pilot project of intelligent mobile communication network brand of red culture and tourism resources and to carry out commercial, public welfare, and educational publicity projects of sustainable development and utilization of red culture and tourism. Second, the government shall make overall planning and management, issue relevant promotion policies, coordinate functional departments at all levels, and formulate construction plans for intelligent mobile communication network platforms. Third, adhere to the policy of "protection first, rational use, strengthen management"; strengthen the red culture and tourism development, census, and registration; and expand the collection of intelligent mobile communication network. Fourth, make use of smart mobile communication network platform, in line with the trend of economic transformation; introduce capital investment through multiple channels; seize the opportunity of 5G era; and guide all kinds of enterprises and social organizations to participate in development, operation, and construction.

Interactive communication system is required to break the traditional mode of communication participation and provide participants with a virtual environment free from time, space, and place restrictions. The transmission system and interactive design technology can produce the same feeling and realistic environment, through the external devices that can operate in the scene modeling; modeling of object is based on the principle of the real scene to the participants to make corresponding feedback that enables participants to achieve immersive experience.

The design of the system should make a comprehensive and in-depth breakthrough from the following aspects: first, provide participants with a diagram of the individual modeling in the scene, promote participants' better understanding and understanding of interactive devices through three-dimensional modeling tools, provide guidance for participants to enjoy music successfully, and satisfy participants' desire for appreciation. Second, provide participants with a realistic appreciation of the environment; improve the effectiveness of participants' interest and participation, through vivid modeling and interactive design to create a sense of reality very strong appreciation of the environment; and make the participants not only observe performance animation but also participate in the scene of operations, to provide participation and promote the participant music ability enhancement. Thirdly, it provides a free communication environment for participants.

3.2. Functional Design. The system can be divided into two main parts: virtual exhibition hall configuration generation part and virtual exhibition hall operation part. With the development of the Internet of technological innovation and the different needs and feelings of public viewers, the design of online virtual exhibition halls and exhibition halls emerges from time to time [28]. For professional exhibition hall design and production companies, it is necessary to have the ability to complete the specific and virtual display work of the exhibition hall design. The specific system structure hierarchy module analysis is as follows:

(1) High-level module

Users configure the running parameters and exhibition content of the exhibition hall through the UI and generate configuration files. The actual loading data and operation process of the whole application are determined by the configuration files. The parameter violation detection includes whether the input parameter is within the valid range and whether the loaded model meets the requirements of the system.

(2) Middle-level module

The violation detection module includes the violation detection and parameter. The module and configuration file are read, and the configuration file is parsed and read to achieve the final simulation effect that meets the actual needs of consumers. Run-time violation detection includes problems such as not roaming according to the prescribed route and walking beyond the scope of the scene. The interface logic control module includes the management of UI controls such as buttons and menus and the construction of the UI control logic framework of the program.

(3) Underlying module

The underlying module includes the control of the system and the UI input control of interface interaction. The crossplatform sound API of Delta3D OpenAL free software is used for audio playback, and the video is developed by the video dynamic link library. The keyboard and mouse input control adopts the function module of Delta3D. Delta3D contains the OSG scene management engine, which is used to manage and render the state of the entire 3D model of the scene. Layer modules should not depend on low-level modules, both should depend on abstraction, abstraction should not depend on implementation, and implementation should depend on abstraction.

3.3. Interactive Interface Design. Good user interface design is the overall design of beautiful interface style, human-computer interaction, and operation logic. It can make the system more easy to use and reasonable. It is an important part of product design. In this system, in order to increase interaction and conduct behavior guidance for participants, a row of buttons is set on the upper right of the system interface. Users can click the call button. Click the music button to play the soft song. In the design features, the main color is gray; gray is a very elastic color; it represents calm, introverted, and low-key. In the upper right corner of the system interface, it conforms to the daily operation habits of most users and does not affect the viewing of users when the system is running. When playing music, the center of the system interface will scroll some live photos to increase the amount of information and guide the audience's soul resonance. Participants can break the constraints of time and space, break the constraints of hardware devices, and freely enjoy the experiment according to their own schedule. They can also exchange experimental experiences with different participants and gain experience in cultural transmission.

4. Results and Analysis

4.1. Test and Analysis of System Propagation Effect. Through the above research, we have implemented an interactive cultural transmission system in VR space, where users can interact with instruments in virtual reality. A survey of these people is performed to take the online mode; the researchers will provide questionnaires, uploaded to the cloud server system program; the participants download and install the client for audiovisual experience actively and submit the feedback form data which is passed to the experimenter; among them, the answer to question 1 results is shown in Figure 3, and the answer to question 2 results is shown in Figure 4. The first experiment had 15 participants, and the second experiment had 6 participants. So, these results are based on 21 participants.

In our survey, participants were also asked about suggestions for system improvement, and 7 effective feedbacks were obtained. The feedback results are shown in Table 1 and Figure 5. Based on the recommendations made, we have proposed three criteria relating to the number of mentions. When calculating the results, the number of times each stimulus variable caused a certain response must be obtained, and the threshold value should be determined according to the number of occurrences, and the threshold value should be obtained by linear interpolation. Of the suggestions made by the participants, "improved design" was suggested twice. It is suggested to "add red culture" 3 times and "add

features" 2 times. The results tell us that users want to see more substantial improvements.

4.2. Relevant Discussions. By digital way of virtual reality technology, the introduction of healthy and orderly development of the tourism pattern, red in these areas as historical sites, and cultural relic information detailed records is through virtual means according to the historical evolution and the nature of red cultural heritage resources, shape, size, distribution characteristics of red databases, and data repair at the same time, to lay the foundation protection, using data. Database integration to introduce public welfare, commercial and artistic development projects, and innovative means of expression increases the experience and participation of the project. Take advantage of modern aesthetic concept and tourists' consumption orientation, close to market demand; clear management of red resources in scattered and economically backward and remote areas; and overcome disadvantages such as geographical remoteness and imperfect regional supporting facilities. Optimize the configuration, standardize the management process, strengthen regional information sharing, and share the red revolution information of these regions with people from all over the country and even the world in an interactive way through the intelligent wireless communication network, so as to show the inheritance of historical and cultural development and the uniqueness of regional culture.

In this era of rapid development of information transmission technology and digital technology, virtual reality technology is gradually integrated into daily life, and people begin to pay more attention to virtual reality technology and deepen their understanding of it. Virtual reality technology through continuous development gradually tends to mature, continues to spread to all areas, and is used in all aspects of society. Moreover, in the past two years, virtual reality has ushered in a period of explosion; virtual reality headsets have been put into the commercial market and used by consumers. At this point, virtual reality began to tend to life and popularity. The development and popularization of virtual reality technology have not only enriched people's life but also produced inestimable influence in the field of design and art. Due to the continuous development and progress of science and technology, virtual and surreal performance can now be displayed, designers using virtual technology can create the world of virtualization, virtual reality draw a kind of artistic life experience, and most of these experiences are personalized, and the knowledge system and the objective reality of now have a very big gap. As the form of exhibition is gradually digitized, the application of virtual reality technology in exhibition design becomes possible. Exhibition design based on virtual reality technology has a new form in the communication of design content. Through the design and construction of virtual objects and virtual space, the audience can be immersed in the virtual world created, so that the exhibition of design content becomes more direct and more efficient. Virtual reality technology enables human beings to cross time and space to experience events that have already occurred or have not yet occurred in the world; it can enable human beings to break through physiological limitations and enter the macro or micro world for research and exploration; it can also simulate conditions due to restrictions, etc., tasks that are difficult to achieve due to reasons.

Performance of virtual reality technology of red culture is the fusion of red cultural tourism development of digital technology in an integral form; it is not only the development of tourist economy, and the important content of construction of Chinese characteristic tourism is a more political significance of the red culture education, patriotism education, and ideological and moral construction of strategic project or show times important way. The application of virtual reality technology in the digital exhibition of red culture in this paper is the development trend of the digital experience of red culture exhibition and the exploration of the form of communication in the inheritance and development of red culture, which can provide practical reference and theoretical guidance for future related research.

5. Conclusion

With the vigorous development of Internet mode, the development mode of cultural and tourism industry has been unprecedentedly impacted. In the dissemination and protection of red cultural tourism, the public's requirements for new aesthetics, new functions, and new qualities of inheritance approaches and expression forms make the protection and inheritance of red cultural tourism and virtual reality technology have more converging points. At present, the three contradictions of mobile communication network, user perception demand, and network monitoring strength exist, and they are not in a state of mutual promotion and harmonious development. In short, there are the following problems: users have higher and higher requirements for the quality of network operations, especially the higher and higher requirements for the perceived quality of using different business processes; traditional network monitoring index systems are increasingly unable to truly reflect the user's perception of the situation, and the development of monitoring technology has not caught up with the development of mobile communication networks. These scenes are all derived from the reflection of real life, and the purpose is to get closer to reality and let the experiencer experience the scenes immersively. Experiencers are no longer boring to watch two-dimensional pictures like in the past. Through the communication and interaction between humans and machines, what it shows is incomparable with the past technology. Interactive cultures have their own unique properties and play their functions in different types of culture works, as well as form unique rules and principles. However, the communication effect of VR interactive cultural communication based on the intelligent mobile communication network is different under different communication methods, and the way of communication is also quite different. Although we are still in the early stages of implementing the system, we believe these problems can be solved in the future. We hope that future researchers will consider our recommendations and put them into practice, conducting more tests and studies. In recent years, the research and

application of virtual reality technology in various industries have brought more convenience and experience mode to people's life, and the application of virtual reality technology in red literature travel has a certain era and inevitability. The immersive experience mode brought by digitization and informatization through visual, auditory, and touch perceptual behaviors brings new opportunities and challenges to the protection of red culture and tourism development. In the digital wave, we need to seize the opportunity to create red tourism pilot, realize the transformation and upgrading of red tourism, and spread the spirit of the red revolution further.

Data Availability

No data were used to support this study.

Conflicts of Interest

There are no potential competing interests in our paper.

Authors' Contributions

All authors have seen the manuscript and approved to submit to your journal.

Acknowledgments

This work was supported by the Hainan Province Philosophy and Social Sciences 2021 Planning Project "Research on the Innovative Communication of Hainan's Red Culture Based on Virtual Reality" (Number: HNSK(ZC)21-157).

References

[1] V. A. de Jesus Oliveira, L. Brayda, L. Nedel, and A. Maciel, "Designing a vibrotactile head-mounted display for spatial awareness in 3D spaces," *IEEE Transactions on Visualization and Computer Graphics*, vol. 23, no. 4, pp. 1409–1417, 2017.

[2] L. Yin, "Virtual design method of indoor space environment based on VR technology," *Paper Asia*, vol. 34, no. 5, pp. 39–43, 2018.

[3] N. Du, X. Wang, J. Guo, and M. Xu, "Attraction propagation: a user-friendly interactive approach for polyp segmentation in colonoscopy images," *PLoS One*, vol. 11, no. 5, article e0155371, 2016.

[4] J. Yi and Tensing, "A method of visualizing 3D sound effect based on web VR," *Software Engineering*, vol. 22, no. 8, pp. 14–16, 2019.

[5] Y. Yao, Y. Li, X. Xiong, Y. Wu, H. Lin, and S. Ju, "An interactive propagation model of multiple information in complex networks," *Physica A: Statistical Mechanics and its Applications*, vol. 537, no. 1, article 122764, 2019.

[6] M. R. Caanen, N. E. Schouten, E. A. Kuijper et al., "Effects of long-term exogenous testosterone administration on ovarian morphology, determined by transvaginal (3D) ultrasound in female-to-male transsexuals," *Human Reproduction*, vol. 17, no. 7, p. 1457, 2017.

[7] J. M. Cho, Y. D. Kim, S. H. Jung, H. Shin, and T. Kim, "78-4: screen door effect mitigation and its quantitative evaluation in VR display," *SID Symposium Digest of Technical Papers*, vol. 48, no. 1, pp. 1154–1156, 2017.

[8] M. S. Solovieva, A. A. Rozhnoi, V. Fedun, and K. Schwingenschuh, "Effect of the total solar eclipse of March 20, 2015, on VLF/LF propagation," *Geomagnetism and Aeronomy*, vol. 56, no. 3, pp. 323–330, 2016.

[9] V. Ciric, I. Milentijevic, and A. Cvetkovic, "The significant bits propagation model in fault-tolerant system design," *Romanian Journal of Information ence and Technology*, vol. 20, no. 2, pp. 161–176, 2017.

[10] Y. Bouanan, G. Zacharewicz, J. Ribault, and B. Vallespir, "Discrete event system specification-based framework for modeling and simulation of propagation phenomena in social networks: application to the information spreading in a multi-layer social network," *SIMULATION*, vol. 95, no. 5, pp. 411–427, 2019.

[11] D. Vladislavic, D. Huljenic, and J. Ozegovic, "Virtual network resource optimization model for network function virtualization," *Wireless Communications and Mobile Computing*, vol. 2021, Article ID 9928210, 21 pages, 2021.

[12] Z. Chiba, N. Abghour, K. Moussaid, A. el Omri, and M. Rida, "A novel architecture combined with optimal parameters for back propagation neural networks applied to anomaly network intrusion detection," *Computers & Security*, vol. 75, pp. 36–58, 2018.

[13] P. Zhang and M. Zhou, "Security and trust in blockchains: architecture, key technologies, and open issues," *IEEE Transactions on Computational Social Systems*, vol. 7, no. 3, pp. 790–801, 2020.

[14] X. Zhang, G. Yin, and N. Qi, "Research on high-resolution improved projection 3D localization algorithm and precision assembly of parts based on virtual reality," *Neural Computing and Applications*, vol. 31, pp. 103–111, 2019.

[15] D. Wanxing, "The exploratory research of the effect communication model and effect improving strategy of interactive advertising," *International Journal of Multimedia & Its Applications*, vol. 8, no. 1, pp. 19–34, 2016.

[16] K. Namkoong, S. Nah, R. A. Record, and S. K. van Stee, "Communication, reasoning, and planned behaviors: unveiling the effect of interactive communication in an anti-smoking social media campaign," *Health Communication*, vol. 32, no. 1, pp. 41–50, 2017.

[17] H. Andrea, W. Michael, and A. K. Jain, "The WISHED trial: implementation of an interactive health communication application for patients with chronic kidney disease," *Canadian Journal of Kidney Health and Disease*, vol. 3, no. 1, p. 29, 2016.

[18] S. Akritidou, G. R. Husted, K. Kazakos, and K. Olesen, "The effect of using interactive communication tools in adults with Type-2 diabetes," *Nursing Reports*, vol. 7, no. 1, p. 1, 2017.

[19] T. Boris and V. Neven, "Exploring the effect of design asymmetry in vehicular communication using visible light communication technology," *Transactions on Emerging Telecommunications Technologies*, vol. 1, no. 1, p. e 3485, 2018.

[20] J. Du, Y. Shi, Z. Zou, and Z. D. CoVR, "CoVR: cloud-based multiuser virtual reality headset system for project communication of remote users," *Journal of Construction Engineering and Management*, vol. 144, no. 2, pp. 1–19, 2018.

[21] R. Liesa, S. Aline, and L. Gerrit, "VR-based gamification of communication training and oral examination in a second language," *International Journal of Game-Based Learning*, vol. 6, no. 2, pp. 46–61, 2016.

[22] S. Lian, J. Xu, G. Zuo, X. Wei, and H. Zhou, "A novel time-incremental end-to-end shared neural network with attention-based feature fusion for multiclass motor imagery recognition," *Computational Intelligence and Neuroscience*, vol. 2021, Article ID 6613105, 2021.

[23] G. D. Dracoulis, B. Fabricius, T. Kibedi et al., "Spectroscopy of 175Ir and 177Ir and deformation effects in odd iridium nuclei," *Nuclear Physics A*, vol. 534, no. 1, pp. 173–203, 2016.

[24] E. Panadero, G. T. L. Brown, and J. Strijbos, "The future of student self-assessment: a review of known unknowns and potential directions," *Educational Psychology Review*, vol. 28, no. 4, pp. 1–28, 2016.

[25] V. R. Montequín, S. C. Fernández, F. O. Fernández, and J. V. Balsera, "Analysis of the success factors and failure causes in projects: comparison of the Spanish Information and Communication Technology (ICT) sector," *International Journal of Information Technology Project Management*, vol. 7, no. 1, pp. 18–31, 2016.

[26] P. Rosedale, "Virtual reality: the next disruptor: a new kind of worldwide communication," *IEEE Consumer Electronics Magazine*, vol. 6, no. 1, pp. 48–50, 2017.

[27] S. Kim, H. Ko, J. Y. Hong, and H. Choi, "A study on experience contents of Baekje Muryeong royal tomb using virtual reality," *Journal of Ambient Intelligence and Humanized Computing*, vol. 4, 2019.

[28] S. Sun, M. Kadoch, L. Gong, and B. Rong, "Integrating network function virtualization with SDR and SDN for 4G/5G networks," *IEEE Network*, vol. 29, no. 3, pp. 54–59, 2015.

Hindawi
Wireless Communications and Mobile Computing
Volume 2022, Article ID 5667012, 11 pages
https://doi.org/10.1155/2022/5667012

Research Article

SFDWA: Secure and Fault-Tolerant Aware Delay Optimal Workload Assignment Schemes in Edge Computing for Internet of Drone Things Applications

Abdullah Lakhan,[1] **Mohamed Elhoseny**,[2,3] **Mazin Abed Mohammed**,[4] **and Mustafa Musa Jaber**[5,6]

[1]*College of Computer Science and Artificial Intelligence, Wenzhou University, Wenzhou 325035, China*
[2]*College of Computing and Informatics, University of Sharjah, UAE*
[3]*Faculty of Computers and Information, Mansoura University, Egypt*
[4]*College of Computer Science and Information Technology, University of Anbar, Anbar 31001, Iraq*
[5]*Department of Computer Science, Dijlah University College, Baghdad, Iraq*
[6]*Department of Medical Instruments Engineering Techniques, Al-Farahidi University, Baghdad 10021, Iraq*

Correspondence should be addressed to Mazin Abed Mohammed; mazinalshujeary@uoanbar.edu.iq

Received 11 November 2021; Accepted 28 January 2022; Published 25 February 2022

Academic Editor: SK Hafizul Islam

The number of automobiles has rapidly increased in recent years. To broaden inhabitant's travel options, push transportation infrastructures to their limitations. With the rapid expansion of vehicles, traffic congestion and car accidents are all common occurrences in the city. The Internet of drone vehicle things (IoDV) has developed a new paradigm for improving traffic situations in urban areas. However, edge computing has the following issues such as fault-tolerant and security-enabled delay optimal workload assignment. The study formulates the workload assignment problem for IoV applications based on linear integer programming. The study devises the fault-tolerant and security delay optimal workload assignment (SFDWA) schemes that determine optimal workload assignment in edge computing. The goal is to minimize average response time, which combines network, computation, security, and fault-tolerant delay. Simulation results show that the proposed schemes gain 15% optimal workload assignment for IoV application compared to existing studies.

1. Introduction

The usage of vehicle transport in the workload has been growing for different purposes [1]. There are different types of carriers used to achieve other goals, such as cars, trucks, buses, railways, and drones [2]. But for the last decade, the usage of drone technologies has been increasing for different tasks day by day [3]. Drones are aircraft machines that fly in the sky to achieve various tasks. There are two significant types of drone aircraft, semiautonomous and full autonomous [4]. In the semiautonomous, the drone is handled by the remote control, which is operated by the ground-level human [5]. At the same time, self-autonomous is a fully automated machine that can handle the device itself without the interaction of any human being or remote from the ground level [6].

Recently, with the emerging development in cloud computing, different cloud models are introduced to handle the Internet of drone vehicle things by the servers [7]. For instance, ground-level services are integrated at other base stations along with fog nodes and edge nodes. The fog and edge nodes are cloud models which brought remote cloud services at the edge of base stations. The goal is to handle the Internet of drone vehicles (IoDV) from servers with their mechanism instead of the human being from ground level [8]. The edge and fog clouds have different categories for IoDV vehicles; for instance, IoDV can use many cloud applications to achieve other practice objectives and daily life

objectives. The main advantage of edge computing and fog computing is to provide a scalable environment without caring about the resources for the data process and store during the execution of IoDV applications in the network [9].

The fundamental challenge of IoDV in edge computing is to schedule workloads with the minimum delay requirements. Whereas each workload has a specific deadline and delay requirements, their executions at edge computing are critical tasks for IoDV applications. Many efforts were done in different research approaches to minimize the delay of drone applications in edge computing. These studies [2, 5, 6, 8] presented the network delay optimal solutions for drone applications in edge computing and proposed their schemes in work. The mobility and migration delay is considered in the network delay during offloading and processing of workload in the edge-enabled network, which is placed at the different locations. The computational delay for drone applications was also investigated in [1–3, 7] to achieve the workload execution in edge computing. The offloading of data from resource-constraint drone devices allows running applications to the available edge computing for the processing in the network. However, many other research challenges exist in the literature work due to offloading [9–11].

However, many research challenges exist in the existing delay optimal workload assignment strategies for drone applications. The existing studies only focused on drone applications' communication delay and computations delay. These delays did not handle any security and failure issues of applications in the edge computing network. Due to heavy workloads, the untrusted network has big security and failure due to malware attacks and scarcity of the resources at edge computing. Each workload has the particular deadline; the computational delay and network delay are sufficient to optimize but need to consider more delay types of drone applications in the edge computing.

In the paper, the study has the motivation to consider more delays, ensuring the security and failure of drone applications at heterogeneous edge computing. The study solves the following research questions. (i) The study optimizes the four types of delays in the proposed work: network delay, computational delay, security delay, and failure delay in the problem. (ii) The study optimizes the resource efficiency and meets the deadline of all workloads in edge computing. (iii) The study will design the simulation in which all proposed solutions can easily cooperate with edge computing.

The paper makes the following contribution to the work.

(i) The study drives the security and failure delay aware workload assignment (SFDWA) greedy metaheuristic in which the problem is to be solved with the different heuristics. That is called the dynamic divided and conquer programming model. The goal is to minimize all delay types of drone applications in edge computing and execute them under their deadlines

(ii) The work designs the architecture in which the process of the applications can show in terms of beginning and execution under different components as shown in Figure 1

(iii) In this work, there is design of the delay optimal mathematical model for the drone application in edge computing with the applications and node constraints

The manuscript consists of different sections from beginning to end. Section 2 shows all existing methods' strengths and research efforts for the delay-enabled applications. Section 3 defines the proposed architecture and mathematical models of drone applications in edge computing. Section 4 shows the processing model of the SFDWA metaheuristic for the considered problem. Sections 5 and 6 show the simulation process and conclusion part of the study.

2. Related Delay Optimal IoDV Schemes

Many promising solutions suggested metaheuristic-enabled methods to solve the workload assignment problem of drone applications in the homogeneous and heterogeneous edge cloud network. However, the Internet of drone vehicle things (IoDV) requires a challenging environment that consists of different drone sensors, wireless technologies, and edge cloud computing. For the simple transport applications, VANET and MANET are the famous platform to achieve the optimal workload assignment and have different dynamic heuristics that meet the deadline of applications. However, MANET and VANET cannot meet the requirements of IoDV applications in edge computing. Therefore, this session only discusses the closely related studies which solve the workload assignment problem of IoDV applications in edge computing as shown in Table 1.

In these studies [1–4], the authors suggested the genetic algorithm-based solutions for the drone applications considering both semiautonomous and fully autonomous case studies in the adaptive environment. These studies integrated the machine learning-enabled local search inside the genetic algorithm and minimized the studies' communication delay and computation delay. The study [5] suggested the IoDV application enabled a secure scheme where tasks are encrypted and decrypted at the edge cloud. The RSA-based encryption and decryption enabled IoDV-enabled method in mobility edge computing suggested in the network [2]. The computational delay optimal [6] schemes are suggested for IoV application in the edge cloud network. The goal is to reduce the processing delay of applications in edge computing. The network delay enabled IoV applications aware schemes suggested in [7, 8]. The goal is to minimize end to end network delay of applications. The RSA-based authentication and authorization for IoV application in distributed edge computing are devised in [9, 11–16].

As shown in Table 1, the existing studies focused on delay during workload assignment in edge computing. Table 1 demonstrates the difference between existing and the proposed work in edge computing during workload assignment problems. However, delay due to security and fault tolerant with network and computational delays is widely ignored in the literature's state as mentioned earlier of art. The work-study solves the workload assignment problem of IoV applications by considering the security and

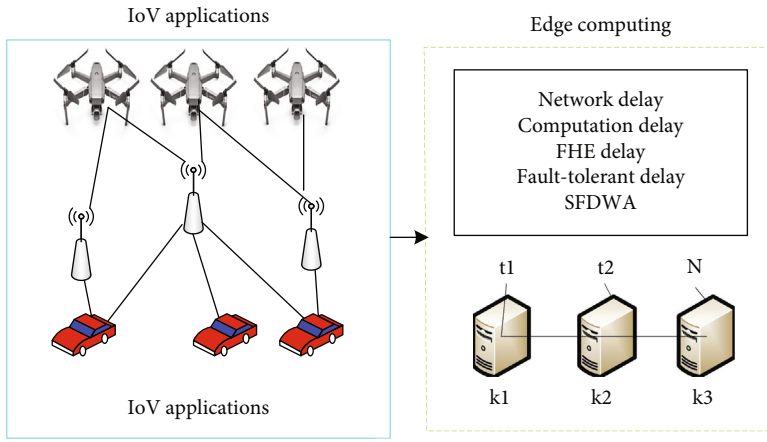

Figure 1: IoV architecture based on SFDWA schemes.

Table 1: Existing delay optimal workload assignment schemes for IoDV.

Research	IoV application	Security delay	Fault-tolerant delay	Network delay	Computation delay	Method
[1]	Traffic guidance	No	No	Yes	Yes	ILP greedy
[2]	Safe navigation	No	No	Yes	Yes	MILP greedy
[3]	Signal control	No	No	Yes	Yes	Knapsack greedy
[4]	Crash prevention	No	No	Yes	Yes	Iterative greedy
[5]	Toll collection	No	No	Yes	Yes	GA
[6, 7]	Traffic monitoring	No	No	Yes	Yes	PSO
[8, 9, 11]	Map route	No	No	Yes	Yes	Ant colony
[12, 13]	Location finding	No	No	Yes	Yes	MILP greedy
[14–16]	Fire ticketing	No	No	Yes	Yes	Partitioning greedy
[10, 17, 18]	Vehicle searching	No	No	Yes	Yes	Dynamic greedy
[19, 20]	Radar finding	No	No	Yes	Yes	Knapsack
[12, 21–25]	Radar safety	No	No	Yes	Yes	PSO greedy
Proposed	Package delivery	No	No	Yes	Yes	Iterative greedy

fault-tolerant delays, including computation delay and network delay for IoDV applications in edge computing. This work is totally different from closely related existing studies [17–25].

With the best of the authors' knowledge, the existing only considered the communication delay and computational delay of IoDV applications in the homogeneous edge networks. In the paper, the study has the motivation to consider more delays, ensuring the security and failure of drone applications at heterogeneous edge computing. The study solves the following research questions. (i) The study optimizes the four types of delays in the proposed work: network delay, computational delay, security delay, and failure delay in the problem. (ii) The study optimizes the resource efficiency and meets the deadline of all workloads in edge computing. (iii) The study will design the simulation in which all proposed solutions can easily cooperate with edge computing.

3. Problem Statement and Proposed System

The study formulates the delay optimal workload assignment at edge computing. There are different types of workload delays considered in the study. For instance, network delay, computation delay, security delay, and fault-tolerant delay are considered in this work in the edge computing for the workload. However, existing studies [1, 5, 8, 12] only felt the network delay and computational delay, which cannot be obtained from the security and failure of workload in their models. The study devises the SFDWA scheme-enabled system, which consists of different components as shown in Figure 1. The Internet of vehicle applications consists of fine-grained tasks with additional delay requirements such as network delay, security, computational delay, and fault-tolerant delay. All the jobs (e.g., tasks), e.g., $t = 1 \in N$, are independent, and each task has a deadline. On the other hand, edge computing consists of heterogeneous edge servers such as $k = 1, \in K$. The study devises the secure failure delay optimal workload assignment (SFDWA), consisting of different of network, computational, FHE (fully homomorphic encryption) delay schemes to execute workload in the heterogeneous edge nodes.

3.1. Problem Formulation. The study considered the T different types of IoDV applications in the considered problem. From T, each workload t has particular workload w_t and

execution deadline deadline_t. The study assumes the K heterogeneous edge nodes geographically distributed in 10 kilometers with the fixed environment. From K heterogeneous nodes, the edge node k has CPU speed ζ_k and resource limitation ε_k. All the applications connect to the edge nodes via B number of fixed base stations, where b from B only supports a fixed number of t workload requests from IoDV in the heterogeneous edge networks. The study describes the delay optimal as the partitioned combinatorial convex optimization problem as the PT. At the same time, the PT divides into four subproblems: security delay, network delay, computational delay, and failure delay.

3.1.1. Security Fully Homomorphic Delay. The study suggests a lightweight security scheme based on fully homomorphic additive encryption to minimize the security delay. It is an application requirement that all workloads encrypt and decrypt at the local devices and share cipher data to the edge nodes for computation and storage. Therefore, the study assumes that a D number of drones can encrypt and decrypt data locally inside applications T. The drone d has CPU processing capability p_d and determines the encryption and decryption in the following way, whereas $x_{k,t}$ and $y_{b,t}$ are the binary assignment to the base stations and edge nodes

$$\text{Encryption}_{tw} = \frac{w_t}{p_d} \times \text{Public} - \text{Key} \times \text{mod} \times x_{t,k}, y_{b,t}. \quad (1)$$

Equation (1) determines the encryption of workload w_t of application t with drone d based on 256-bit primary key with the additive module. The workload can decrypt on the same drone after execution in the following way

$$\text{Decryption}_{tw} = \text{Encryption}_{tw} \times \text{Private} - \text{Key} \times \text{mod}. \quad (2)$$

Equation (2) determines the decryption of workload w_t based on private key at the drone d. Therefore, the total security delay of all applications T on all drones D is determined in the following way:

$$\text{Security} - \text{Delay} = \sum_{t=1}^{T} \sum_{d=1}^{D} \text{Encryption}_{tw} + \text{Decryption}_{tw}. \quad (3)$$

Equation (3) determines the total security delay in the problem.

3.1.2. Drone Offloading Network Delay. All workloads are initially locally encrypted, and then, an offloader inside the drone offloads applications to the available base stations. The drone cannot directly offload all workloads to the edge nodes because all edge nodes are implemented at the base stations. Therefore, drone offload workloads to the base station and network delay are determined in the following way:

$$N\text{Delay} = \sum_{b=1}^{B} \sum_{t=1}^{T} \frac{(S/N) + \left(\text{Encryption}_{tw}/B_{\text{up}}\right)}{R} \times \text{status} = \text{ON} \times y_{b,t}. \quad (4)$$

In equation (4), $y_{b,t}$ is the binary assignment where $y_{b,t} = 1$ means the status of network is good; otherwise, it becomes 0, and S/N is the inference S and noise N with the error R and upload bandwidth up with the encrypted workloads from T to t_w. Equation (4) determines the network delay, if the network status becomes on and availability of base stations is optimal inside networks.

3.1.3. Heterogeneous Computational Delay. The workload assignment is to be done on the heterogeneous edge nodes in the following way.

$$C\text{Delay} = \sum_{k=1}^{K} \sum_{t=1}^{T} \frac{\text{Encryption}_{tw}}{\zeta_k} \times x_{k,t} \times \text{status} = \text{ON}. \quad (5)$$

Equation (5) determines allocation of encrypted workload to the optimal edge node k when it has binary assignment $x_{k,t} = 1$; otherwise, it becomes 0.

3.1.4. Failure of IoDV and Edge Delay. The failure can be identified by the status of work when process status becomes off, and then, scheduler will search another node within the deadline of workload in the edge node network.

$$\text{Failure} = \sum_{k=1}^{K} \sum_{t=1}^{T} \sum_{b=1}^{B} RT \times y_{b,t} \longleftarrow \text{status} = \text{OFF} \& x_{k,t} \longleftarrow \text{status} = \text{OFF}. \quad (6)$$

Equation (6) determines the failure status when it becomes OFF and recover time RT determined in the following way.

$$\text{RT} = \sum_{k=1}^{K} \sum_{t=1}^{T} \sum_{b=1}^{B} \text{RT} \longleftarrow \text{encryption}_{tw} \longleftarrow \text{status} = \text{ON} \leq \text{deadline}_t. \quad (7)$$

Equation (7) determines recovery time of the workload when it becomes ON in the network.

The problem PT is mathematically optimized in the following way.

$$\begin{aligned} \min\text{PT} = {} & \text{Security} - \text{Delay} + N\text{Delay} + C\text{Delay} \\ & + \text{Failure}, \quad \forall t = 1, \cdots, T. \end{aligned} \quad (8)$$

Equation (8) shows the objective function of the all workloads in the edge nodes network, subject to

$$\sum_{k=1}^{K} \sum_{t=1}^{T} \sum_{b=1}^{B} w_t \leq \varepsilon_k. \quad (9)$$

Equation (9) determines that all the workloads can execute under the available resources in the edge networks.

$$\sum_{k=1}^{K}\sum_{t=1}^{T}\sum_{b=1}^{B}\frac{w_t}{\zeta_k} \leq \text{deadline}_t. \tag{10}$$

Equation (10) determines that all the workloads execute under their deadlines in the edge networks.

$$\sum_{t=1}^{T} y_{b,t} = 1,\forall,b = 1, \cdots, B. \tag{11}$$

Equation (11) determines that each base station can offload one workload at a time.

$$\sum_{t=1}^{T} y_{k,t} = 1,\forall,k = 1, \cdots, K. \tag{12}$$

Equation (12) determines that each edge node can execute one workload at a time.

4. Proposed Algorithm SFDWA

The study solves the combinatorial convex optimization problem PT into partitioned subproblems called dynamic programming problems for IoDV applications in heterogeneous edge nodes. The study devises the secure failure delay workload assignment (SFDWA) metaheuristic; it has the following subheuristics: solving the subproblems into optimal solutions. The SFDWA is a complete metaheuristic consisting of different components for each IoDV application in the edge node networks. Each part is a heuristic independent of another element, which means the optimization of each element is calculated individually in the metaheuristic. In this way, we can control the application deadline performances with each component in the problem PT. Algorithm 1 is a metaheuristic which consists of different processes in the algorithm.

4.1. Security Delay-Enabled Component. Algorithm 2 takes the input of all applications in terms of their workloads and encrypts them on the local drone machine before offloading to the base station. The study allows drones to encrypt and decrypt the data, and base station and edge nodes can process data computation only on the cipher data. This work is totally different from existing studies; in this work, the cipher data process on the base station and edge node without decrypting them in the network. The data encrypted based on 256-bit primary key generated based on advanced standard encryption scheme in work. The two random large integers are exploited in public and private keys at the drone device, where data is encrypted and decrypted with both public and private keys. All the encrypted are offloaded to the base station for further processing.

4.2. Network Delay-Enabled Component. Algorithm 3 takes the encrypted data of all applications in terms of their workloads if the status of all base stations is equal to 1 not zero. The status ON and OFF shows that the availability of base stations is sufficient and bandwidth can offload workload to the edge nodes for the processing.

4.3. Computational Processing Delay. The study devises the combinatorial convex-enabled dynamic scheduling scheme where objective function PT optimizes the heterogeneous edge nodes. At the same time, the deadline and resource limitations are the convex set in the problem. The scheduler sorts all encrypted workloads into their deadline order to minimize the computational delay. The minor deadline enabled workloads to get high priority in the scheduling queue. The scheduler has two phases: topological

Input: $b = 1, \cdots, B, k = 1, \cdots, K,$
$t = 1, \cdots, T$, minPT.
1 B**egin**
2 Status = 0, 1 = ON or OFF;
3. Component 1 secure mechanism;
4. Component 2 offloading networking delay scheme;
5. Component 3 computing delay scheme;
6. Component 4 failure recovery mechanism;
7. Optimize status PT* ⟵ = 1, b, k, t;
8. End main;

Algorithm 1: SFDWA metaheuristic algorithm.

Input: $t = 1, \cdots, T, d = 1, \cdots, D, k = 1, \cdots, K$
1 B**egin**
2 PK ⟵ PrimaryKey;
3 PV ⟵ PrivateKey;
4 Encryption process;
5 **for each** (tw ⟵ $t1$)
6 Determined encryption time based on equation (1);
7 Generate large random number p, q;
8 mod ⟵ PK ⟵ 256 *bits*;
9 Encryption_{tw} ⟵ t_w ⟵ $t1 \times d1 + p \times q \times \text{mod}$;
10 Decryption process;
11 **for each** (Encryption_{tw} ⟵ t_w ⟵ $t1 \times k1$) **do**
12 $\text{Decryption}_{tw}[t1, T]$ ⟵
Encryption_{tw} ⟵ PV;
13 End main;

Algorithm 2: Fully homomorphic encryption scheme.

Input: $\text{Encryption}_{tw}[t, T], b \in B$
1 B**egin**
2 (b ⟵ Status = 1) **then**
3 b ⟵ status = ON:
4 Determined the available B_{UP}:
5 Determined the network delay based on equation (4);
6 Make the initial assignment based on $y_{b,\text{encryption}_{tw},t} = 1$;
7 Offload $\text{Encryption}_{tw}[t1, T]$;
8 End main;

Algorithm 3: Network delay component.

Input: MQW$[t, T]$, RQ$[k, K]$
1 **Begin**
2 **for each** (MQW$[t, T]$ & RQ$[k, K]$) **do**
3 Determined the computational delay based on equation (5);
4 Make the initial assignment based on equations (11) and (12);
5 Determined the deadline and resources based on (10) and (9);
6 **if** (Encryption$_{tw} \longleftarrow t \longleftarrow k \leq$ deadline$_t$) **then**
7 PT $\longleftarrow x_{k,t}$;
8 PT = Security − Delay + NDelay + CDelay + Failure;
9 Schedule $x_{k1,t1} \in T \longleftarrow$ Status == ON based on equation (8)
10 Optimize PT;
11 **if** ($x_{k,t} \longleftarrow$ Status == 0) **then**
12 Schedule $x_{k,t} \longleftarrow$ Status == OFF based on equation (8);
13 Apply local search;
14 **if** (PT $\longleftarrow k1 \leq$ PT $\longleftarrow k2$) **then**
15 replace $f(\text{PT}^*) \longleftarrow f(\text{PT})$;
16 Call checkpointing;
17 Reschedule schedule $x_{k2,t1} \in T \longleftarrow$ Status == ON based on equation (8);
18 End main;

Algorithm 4: Computational processing delay component.

prioritizing and sharing parallel execution of workloads in edge nodes. Initially, all the workloads arrived randomly in the M/M/1-PS sharing edge nodes queue where there is no waiting delay. The M/M/1-PS Queue-Workload (MQW) [14] sorts all workloads based on their deadlines. For instance,

$$\text{MQW}[t, T] = \text{Sorting}\left(\sum_{t=1}^{T} \text{Encryption}_{tw,t,T} \longleftarrow \text{deadline}_t\right). \tag{13}$$

Equation (13) sorts all the workloads into their deadline before being executed to the edge nodes. All the edge nodes sort according to their availability of the resources and high speed in the resource queue (RQ) as determined in

$$\text{RQ}[k, K] = \text{Sorting}\left(\sum_{k=1}^{K} \varepsilon_k \& \zeta_k\right). \tag{14}$$

High-speed nodes have less delay and should have sufficient resources to run the scheduled workload in the edge networks.

Algorithm 4 is a greedy algorithm that schedules all encrypted workloads based on their deadlines and available resources of edge nodes. Each encrypted workload must be executed its deadline and within available resources with status == 1 and status == ON. If the failure occurs in a particular edge node $k1$, then the status becomes status == 0 and status == OFF. The checkpointing enabled delay optimal policy call and search another edge node with the optimal objective function $f(\text{PT}^*) \longleftarrow k2 \longleftarrow f(\text{PT}) \longleftarrow k1$ which replaces the failure objective function to another node objective function in the network. This way, we can optimize all workload execution in terms of the objective function in the network.

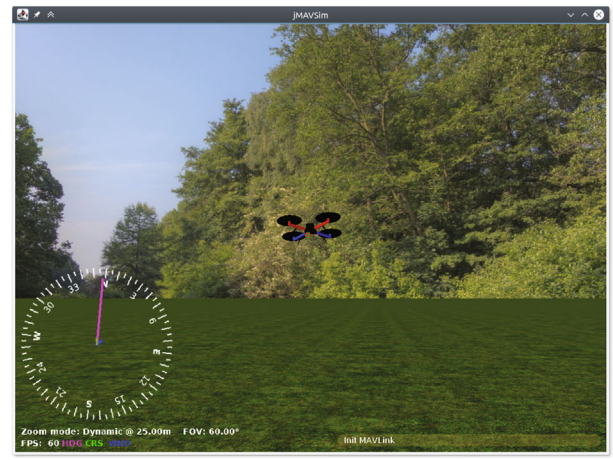

Figure 2: jMAVSim simulation tool enabled IoDV experimental environment.

5. Performance Evaluation

In the evaluation part, the study implemented SFDWA algorithm framework, and baseline 1 and baseline 2 approaches in available jMAVSim simulation tool enabled IoDV experimental environment.

The study designed the simulation environment on the available tool jMAVSim on the link "https://github.com/PX4/jMAVSim." Figure 2 shows the jMAVSim simulation environment with the IoV task application in the distributed system. This simulation environment is already implemented in our previous manuscript [16] and is widely deployed in the simulation environment with the blockchain and scheduling techniques.

Table 2: IoDV package delivery application dataset and sensors.

N	w_t (MB)	deadline$_t$ (seconds)	B	K (core)	ε_k (GB)	b_{bw} (MBPS)	$D \longleftarrow$ Mavic IoDV drone sensors
$t1$	10	300	500	1	High core	10	Drone
$t2$	10	300	500	1	High core	10	Drone
$t30$	10	300	500	1	High core	10	Drone
$t100$	10	300	500	1	High core	10	Car
$t200$	10	300	500	1	High core	10	Car
$t250$	10	300	500	1	High core	10	Car
$t300$	10	300	500	1	High core	10	Drone

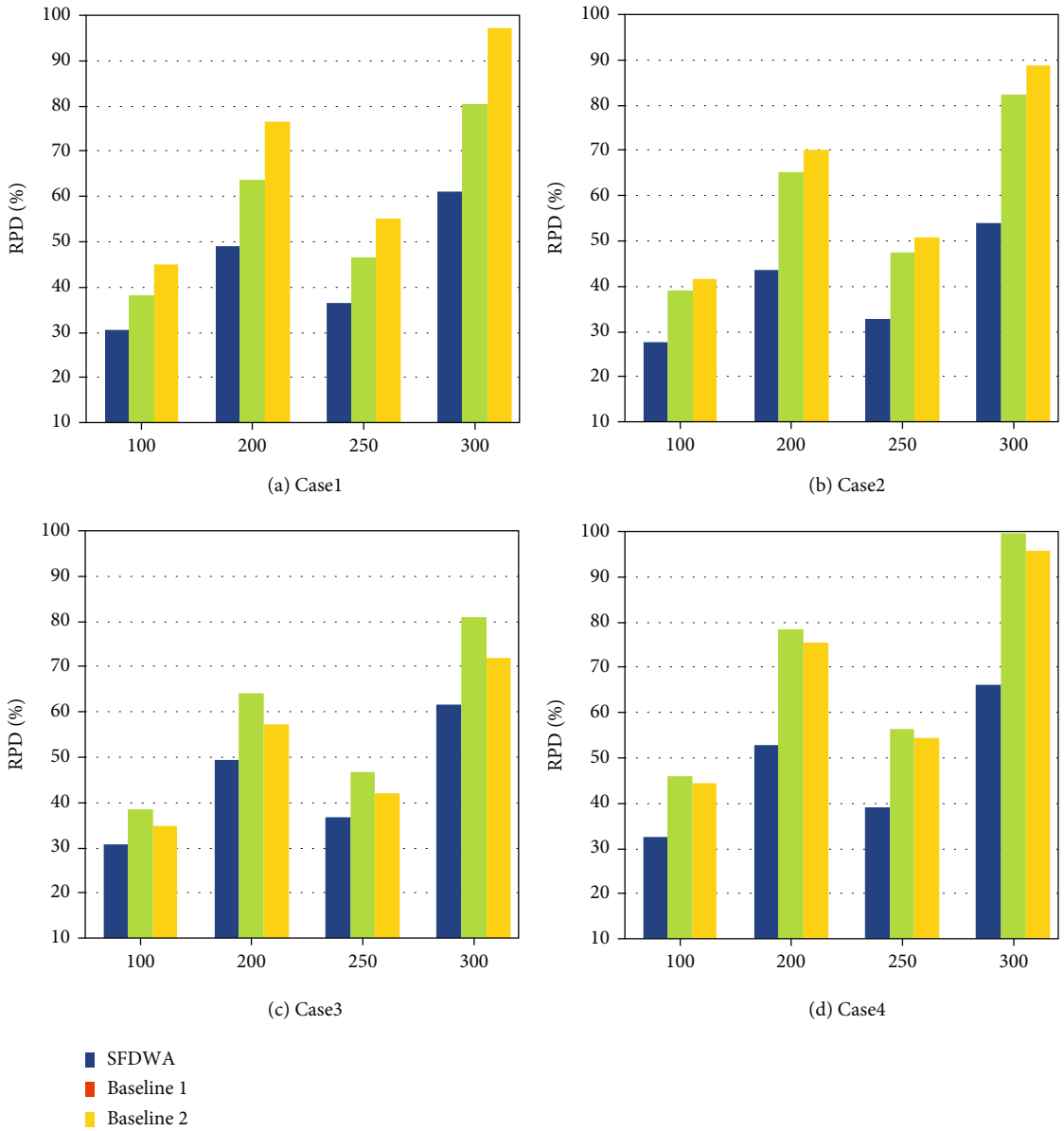

Figure 3: Network delay in different cases.

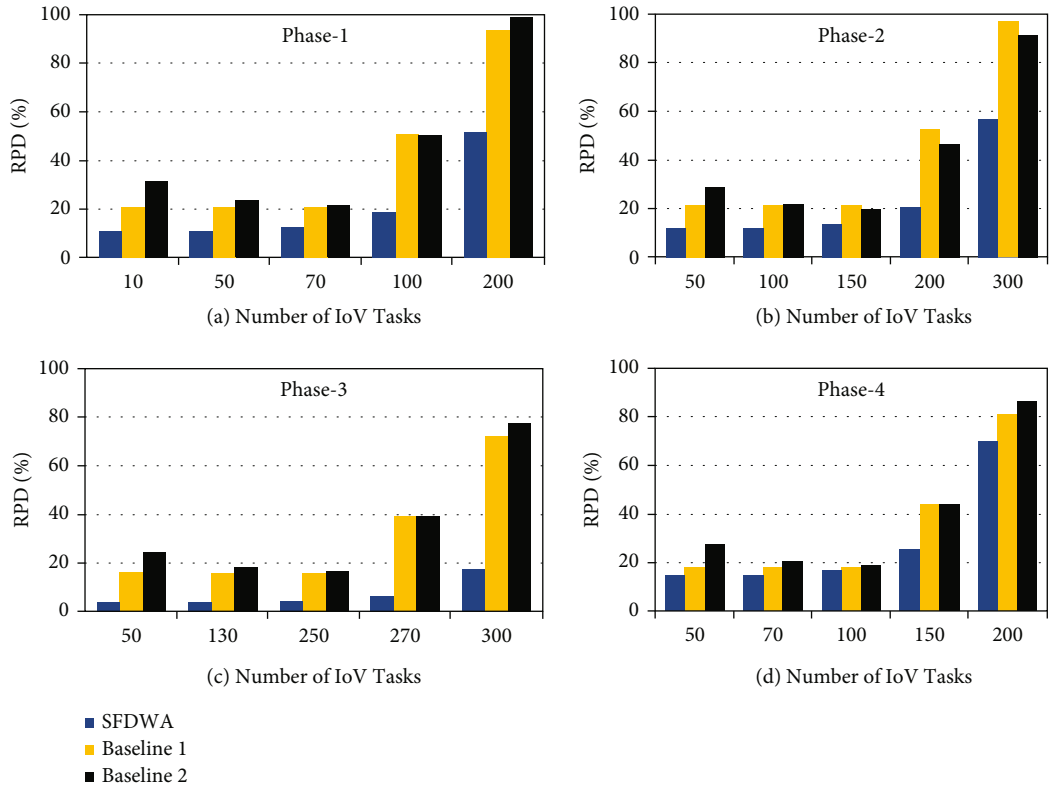

Figure 4: Workload assignment performances in all phases.

5.1. IoDV Application Dataset. The dataset parameters of the IoDV applications are shown in Table 2 implemented in the simulation. The dataset detail is available in [16] study. The study exploited the real dataset for the experiment, which is obtained and detailed in [16] site.

5.2. Closely Related Baseline Approaches. The study is going to make an experimental comparison of the proposed solution with other similar works, whereas baseline 1 [3, 5, 7, 9, 16] widely implemented delay optimal drone applications in the edge computing network. These studies considered network delay and computational delay for workload assigning edge computing, whereas baseline 2 is widely deployed in [1, 4, 6, 11, 13] studies. These studies tried to minimize end to end delay of applications with minimum consumption of latency for IoDV applications.

5.3. Performance Metrics. The study exploits statistics to evaluate the results of the proposed schemes with relative percentage deviation (RPD) as follows.

$$\mathrm{RPD}(\%) = \frac{\mathrm{PT}^* - \mathrm{PT}}{\mathrm{PT}^*} \times 100\%. \tag{15}$$

Z^* displays the optimal workload assignment of IoV applications.

5.4. Result Discussion. This section discusses the obtained results of the methods for the considered problem with different metrics as follows in different subsections.

5.5. Network Delay in Different Cases. The study considered the different cases for the network delay in the simulation part based on the objective function. If S is 20 dB, b_{bw} is 4 kHz for the network delay. Then, we discussed it with different cases and evaluated the performances in the simulation. Case 1: bandwidth = 15000 $N(1 + S = 200) = 4000$ $R(101) = 36.63$ kbit/s. Case 2: bandwidth = 7000 $S(1 + 100)$ $= N = 7000$ $R(101) = 46.63$ kbit/s. Case 3: bandwidth = 2000 $S(1 + 100) = N = 2000$ $R(101) = 16.63$ kbit/s. Case 4: bandwidth $S(1 + 100) = N = 4000$ $R(101) = 26.63$ kbit/s. These different values are implemented in the simulation config file for the simulation.

Figure 3 shows that, with different IoV tasks, the network delay with different cases could be changed in RPD%. Therefore, in Figures 3(a)–3(d), the proposed SFDWA outperformed all existing baseline approaches in terms of network delay in RPD%.

5.6. Comparison of Workload Assignment Algorithms. Figure 4 shows the performances of all phases with the proposed scheme and baseline approaches. The RPD% of all existing baseline approaches is shown in the evaluation result. Figure 4(a) shows the RPD% of the network delay for IoV applications with a random number of tasks in edge computing. Figure 4(a) shows the RPD% of the proposed SFDWA outperformed all existing schemes due to many reasons. The first reason is that all existing only focused on network delay without considering the availability of edge computing resources. These baseline 1 and baseline 2 only assumed the network delay resource and ignored the

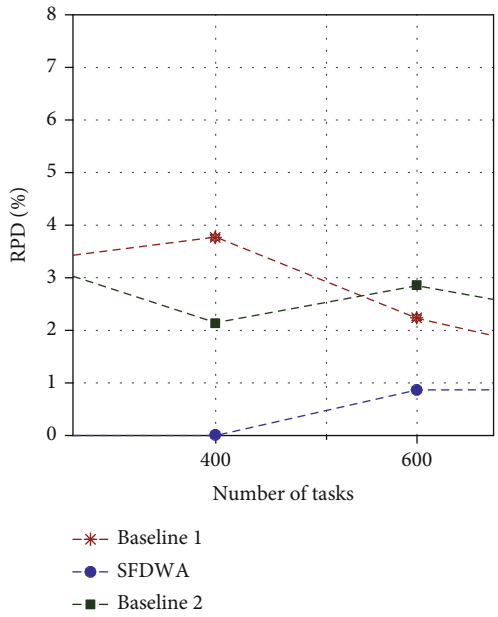

Figure 5: RPD% performances of IoDV tasks with network delay.

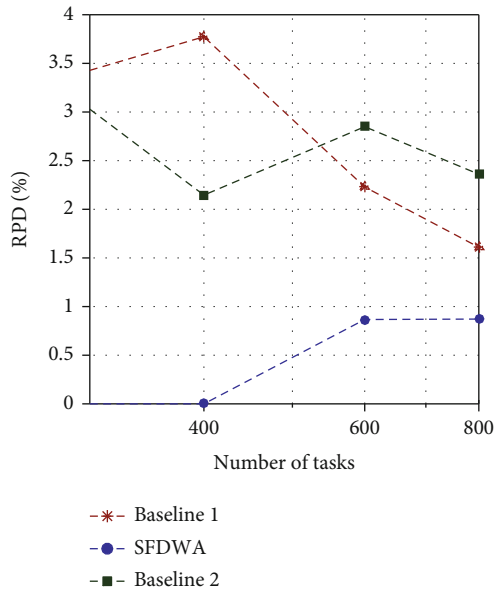

Figure 6: RPD% performances of network delay and computational delay for IoDV workloads.

schemes' security and fault-tolerant edge computing delay. Figure 4(b) shows the computational delay and RPD% could be improved whenever the network and computational delay are jointly optimized simultaneously in the edge computing node. Another reason is that we determined the resources of computing nodes in advance by implementing resource profiling technologies at the compile time. Figures 4(c) and 4(d) show the SFDWA outperformed all existing baseline approaches. The main reason is that all current studies in phase 1, phase 2, phase 3, and phase 4 only considered the network delay and computational delay without considering the security delay and fault tolerant in the edge computing network. Another reason is that all existing schemes did not consider the deadline of application tasks; therefore, minimizing the delay for IOV applications without deadline constraint is ineffective in edge computing. The resource leakage could be possible if the number of requests exceeds the resource limits and be incurred with longer end to end delay. Therefore, the proposed scheme SFDWA has a control from offloading to execution with both security and deadline constraints and improved the overall RPD% of different phases in edge computing.

Figure 5 shows the RPD% performances of the computational delay for IoV tasks by applying the proposed method and baseline approaches. The study only considers case 1 in this experimental part, where the computational delay was determined before offloading to edge computing with the related base stations. Still, SFDWA outperforms computational delay compared to existing baseline approaches because existing works only considered the case 1 situation where network availability is only considered and other parameters are widely ignored, as we discussed in different cases, the performance of network delay. Therefore, network delay is also a vital aspect of offloading workloads to edge computing.

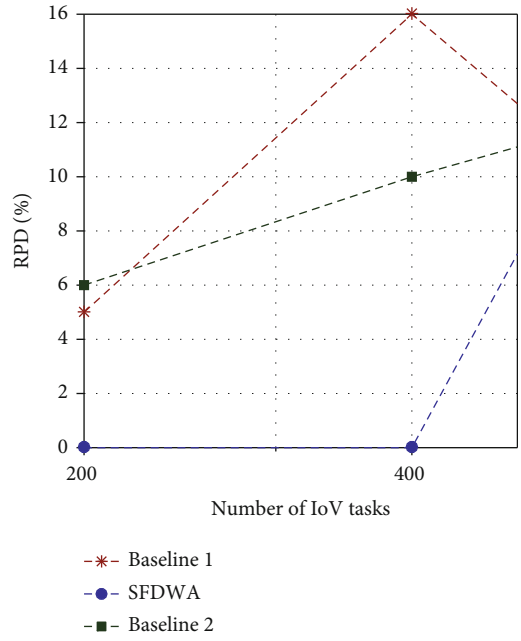

Figure 7: RPD% performances of IoDV workload with network delay.

Figure 6 shows the RPD% performances of computational delay and communication delay for IoV tasks in edge computing. The delay increases when both computational and communication delays are calculated in edge computing. However, the study exploited different cases and not allowed offload tasks to the weak signal networks and overloading edge nodes; in this way, low priority tasks can offload later and minimizes the computational delay and communication delay in the edge computing network. Therefore, SFDWA outperformed all existing baseline approaches in terms of computational delay and communication delay.

Figure 7 is the total delay including network delay, computational delay, security delay, and fault-tolerant delay and the impact of uncertainty delays can be analyzed in Figure 7. The ratio of delay with both baselines approaches growth compared to SFDWA. The main reason is that all existing baseline approaches only considered the computational delay and network delay in their schemes for IoV tasks in edge computing. Therefore, the proposed idea and SFDWA are optimal and effective in edge computing to control the different types of delay for IoDV workloads.

In Figure 7, there is a lot of impact of different delays according to requirements. For instance, security is the demand in the recent developed system, and fault tolerant is the backbone; therefore, these delays cannot be ignored in the edge computing for IoV applications. If we leave them, only considering the communication delay and computational delay, Figure 7 shows the impact of delays for IoDV workloads in the edge computing.

6. Conclusion

The study formulates the workload assignment problem for IoV applications based on linear integer programming. The study devised the fault-tolerant and security delay optimal workload assignment (SFDWA) schemes that determined optimal workload assignment in edge computing. The goal is to minimize average response time, which combines network, computation, security, and fault-tolerant delay. Simulation results show the proposed schemes gain 15% optimal workload assignment for IoV application in edge computing compared to existing studies.

In the future work, the study will discuss the mobility delay and migration delay in the current architecture to improve the mobility performance of the IoV applications.

Data Availability

All the experimental data are generated at the local institution servers. Therefore, it cannot be made publicly available for other researchers.

Conflicts of Interest

The authors declare that there is no conflict of interest.

References

[1] A. Salama, A. M. Mostafa, S. Gunasekaran et al., "An agent architecture for autonomous uav flight control in object classification and recognition missions," *Soft Computing*, vol. 3, pp. 1–14, 2021.

[2] S. A. Mostafa, M. S. Ahmad, A. Mustapha, and M. A. Mohammed, "Formulating layered adjustable autonomy for unmanned aerial vehicles," *International Journal of Intelligent Computing and Cybernetics*, vol. 10, no. 4, pp. 430–450, 2017.

[3] Q. Fan and N. Ansari, "Workload allocation in hierarchical cloudlet networks," *IEEE Communications Letters*, vol. 22, no. 4, pp. 820–823, 2018.

[4] M. A. R. Dantas, P. E. Bogoni, and P. Jos'e De Freitas Filho, "An application study case tradeoff between throughput and latency on fog-cloud cooperation," *International Journal of Networking and Virtual Organisations*, vol. 23, no. 3, pp. 247–260, 2020.

[5] V. Chamola, C. K. Tham, S. Gurunarayanan, and N. Ansari, "An optimal delay aware task assignment scheme for wireless sdn networked edge cloudlets," *Future Generation Computer Systems*, vol. 102, pp. 862–875, 2020.

[6] A. Lakhan, M. A. Mohammed, A. N. Rashid et al., "Smart-contract aware ethereum and client-fog-cloud healthcare system," *Sensors*, vol. 21, no. 12, p. 4093, 2021.

[7] R. Deng, L. Rongxing, C. Lai, T. H. Luan, and H. Liang, "Optimal workload allocation in fog-cloud computing towards balanced delay and power consumption," *IEEE Internet of Things Journal*, vol. 3, no. 6, pp. 1171–1181, 2016.

[8] S.-C. Wang, S.-C. Tseng, K.-Q. Yan, and Y.-T. Tsai, "Reaching agreement in an integrated fog cloud iot," *IEEE Access*, vol. 6, pp. 64515–64524, 2018.

[9] W. Zhang, Z. Zhang, S. Zeadally, H.-C. Chao, and V. C. M. Leung, "Masm: a multiple-algorithm service model for energy-delay optimization in edge artificial intelligence," *IEEE Transactions on Industrial Informatics*, vol. 15, no. 7, pp. 4216–4224, 2019.

[10] A. Lakhan, M. A. Dootio, A. H. Sodhro et al., "Cost-efficient service selection and execution and blockchain-enabled serverless network for Internet of medical things," *Mathematical Biosciences and Engineering*, vol. 18, no. 6, pp. 7344–7362, 2021.

[11] C. Martín, D. Garrido, L. Llopis, B. Rubio, and M. Díaz, "Facilitating the monitoring and management of structural health in civil infrastructures with an edge/fog/cloud architecture," *Computer Standards & Interfaces*, vol. 81, article 103600, 2022.

[12] X. Guo, R. Singh, T. Zhao, and Z. Niu, "An index based task assignment policy for achieving optimal power-delay tradeoff in edge cloud systems," in *2016 IEEE International Conference on Communications (ICC)*, pp. 1–7, Kuala Lumpur, Malaysia, 2016.

[13] H. Chegini, R. K. Naha, A. Mahanti, and P. Thulasiraman, "Process automation in an iot–fog–cloud ecosystem: a survey and taxonomy," *IoT*, vol. 2, no. 1, pp. 92–118, 2021.

[14] H. Cao and M. Wachowicz, "An edge-fog-cloud architecture of streaming analytics for Internet of things applications," *Sensors*, vol. 19, no. 16, p. 3594, 2019.

[15] F. Al-Turjman, M. Z. Hasan, and H. Al-Rizzo, "Task scheduling in cloud-based survivability applications using swarm optimization in Iot," *Transactions on Emerging Telecommunications Technologies*, vol. 30, no. 8, article e3539, 2019.

[16] R. O. Aburukba, M. AliKarrar, T. Landolsi, and K. El-Fakih, "Scheduling Internet of Things requests to minimize latency in hybrid fog- cloud computing," *Future Generation Computer Systems*, vol. 111, pp. 539–551, 2020.

[17] A. Lakhan, M. A. Mohammed, O. I. Obaid, C. Chakraborty, K. H. Abdulkareem, and S. Kadry, "Efficient deepreinforcement learning aware resource allocation in SDN-enabled fog paradigm," *Automated Software Engineering*, vol. 29, no. 1, pp. 1–25, 2022.

[18] Y. Deng, Z. Chen, D. Zhang, and M. Zhao, "Workload scheduling toward worst-case delay and optimal utility for single-hop fog-iot architecture," *IET Communications*, vol. 12, no. 17, pp. 2164–2173, 2018.

[19] H. Mora, F. J. Mora Gimeno, M. T. Signes-Pont, and B. Volckaert, "Multilayer architecture model for mobile cloud computing paradigm," *Complexity*, vol. 2019, Article ID 3951495, 13 pages, 2019.

[20] X. Wang, W. Guo, W. Zhang, M. K. Khan, and K. Alghathbar, "Cryptanalysis and improvement on a parallel keyed hash function based on chaotic neural network," *Telecommunication Systems*, vol. 52, no. 2, pp. 515–524, 2013.

[21] A. Lakhan, M. A. Mohammed, S. Kadry, K. H. Abdulkareem, F. T. Al-Dhief, and C.-H. Hsu, "Federated learning enables intelligent reflecting surface in fog-cloud enabled cellular network," *Peer J Computer Science*, vol. 7, article e758, 2021.

[22] A. H. Sodhro, Z. Luo, A. K. Sangaiah, and S. W. Baik, "Mobile edge computing based qos optimization in medical healthcare applications," *International Journal of Information Management*, vol. 45, pp. 308–318, 2019.

[23] A. H. Sodhro, S. Pirbhulal, and V. H. C. De Albuquerque, "Artificial intelligence-driven mechanism for edge computing-based industrial applications," *IEEE Transactions on Industrial Informatics*, vol. 15, no. 7, pp. 4235–4243, 2019.

[24] A. H. Sodhro, S. Pirbhulal, Z. Luo, and V. H. C. de Albuquerque, "Towards an optimal resource management for iot based green and sustainable smart cities," *Journal of Cleaner Production*, vol. 220, pp. 1167–1179, 2019.

[25] S. A. Hassan and Y. Li, "Medical quality-ofservice optimization in wireless telemedicine system using optimal smoothing algorithm," *E-Health Telecommunication Systems and Networks*, vol. 2, no. 1, pp. 1–8, 2013.

Hindawi
Wireless Communications and Mobile Computing
Volume 2022, Article ID 2141194, 9 pages
https://doi.org/10.1155/2022/2141194

Research Article

Research on Intelligent Estimation Method of Human Moving Target Pose Based on Adaptive Attention Mechanism

Meishuang Ding[1] **and Jing Zhao**[2]

[1]*Employment and Entrepreneurship Guidance Center, Hefei Gongda Vocational and Technical College, Hefei, China*
[2]*School of Innovation and Entrepreneurship, Anhui Vocational and Technical College of Mechatronics, Wuhu, China*

Correspondence should be addressed to Meishuang Ding; 617541131@qq.com

Received 4 November 2021; Revised 19 January 2022; Accepted 2 February 2022; Published 23 February 2022

Academic Editor: Xiaohui Yuan

In daily physical education, posture performance is an important basis for making excellent results. This paper explores an intelligent method to estimate the target pose based on adaptive attention mechanism. First, the regional attention is iteratively generated from a global level to a local level based on the attention mechanism. Human decision-making patterns are imitated to evaluate the effectiveness of regional attention in real time. The level of attention mechanism is adaptively adjusted and focused layer by layer to achieve precise target detection and tracking. Second, with the target frame obtained from each frame, the pose estimation algorithm finds the key points of human body, enabling the human body pose optimization strategy to solve the crossover problem of the key points. Results of experiments on sports video images show that the proposed method has a higher accuracy in pose estimation than other algorithms and can help sportsmen adjust their training methods scientifically.

1. Introduction

Nowadays, sports results account for an increasing proportion of a student's total academic results. In daily physical education, posture performance is an important basis for giving excellent results. As physical teachers have always acquired the information about pose of students via field observation, there are many problems such as one-sidedness of information extraction and low teaching efficiency. With the development of the video technology, it is likely to intelligently analyze the pose using deep learning, which provides technical support for daily physical education.

Pose analysis includes target tracking and pose estimation, between which the former, as the prerequisite for analyzing and detecting the region of interest in the video, has been widely applied to a variety of scenarios. Target tracking algorithms can be roughly divided into the following two: (1) the algorithms that glean the information about target position, size, etc., by predicting the score map of the candidate area, but cannot perceive the aspect ratio of the target [1, 2]; (2) the algorithms that position the target accurately by carrying out bounding box regression, and making use of deep learning to predict the aspect ratio and adjust the predictive box [3, 4]. Among those deep learning-based target tracking methods, MDNet [5] is a masterpiece of early CNN-based tracking algorithms, which uses multidomain network branches to fit different target objects and then calculates the final result by external frame regression. SiamRPN [6] constructs a Region Proposal Network (RPN) structure based on twin network, where the template image and the search region use the exact same convolutional network to extract the feature map, the classification and regression are carried out through two independent network branches to determine the target location and size, and then the external frames are optimized by regression results. On the other hand, Fully Convolutional Network (FCN) [7] is the classical network structure in semantic segmentation, where all network layers use convolutional layers, and the original image size is recovered by upsampling layers, so that the output segmented image size is exactly the same as the input image size. Those target tracking algorithms are still restricted by appearance deformation, light fluctuation, fast

motion, and other problems. According to findings of neuroscience researches, human brain cannot receive all image information visually input. It responds to special areas and ignores the remainder until the response is completed. Such rapid response mechanism is called the attention mechanism [8, 9], which is completely identical to target tracking in essence. The attention mechanism has become an important part of deep web designing and has been widely applied to speech recognition, language translation, and target tracking.

Accurate pose estimation is a prerequisite for detection of target behaviors in video images. In the early pose estimation algorithms, complex structured prediction was performed, and global and local features were fused to predict the pose in a globally uniform manner [10–12]. With the advent of deep learning, recent algorithms for pose estimation generally use ConvNets as the main module to predict the key points of human pose either from the top down or from the bottom up [13–16]. Top-down approaches usually use advanced human detectors to first detect all people from the image and then scale the image block containing a single person to a fixed size to send to a single person pose estimator for prediction. Bottom-up approaches, on the other hand, do not rely on human detectors and directly infer the location information of all human key points in the image and group the key points to obtain the pose of all people [17–19].

At present, artificial intelligence, represented by deep learning, has widespread applications [20]. Multilevel higher-order abstract features of the target object can be obtained from shallow to deep via operations of convolutional and pooling layers, which is consistent with the human perception mode running from globally to locally. However, the trial-and-error pattern of the target tracking network structure leads to a shortage of universal samples in invariant eigenspace and classification criteria generated by fixed architecture network. Faced with similar and dissimilar samples with different scales, the reliability of the target detection results of the fixed-scale learning model deteriorates. The traditional deep learning-based target tracking system can be boiled down to an open-loop system with uncertain image inputs and unassured target outputs [21–23]. Due to invariant eigenspace and the posterior statistics of the target tracking results, coupled with the absence of adaptive attention mechanisms, this system greatly differs from the human decision-making pattern that can adaptively adjust the multilevel eigenspace and validate the reliability of the target tracking results in real time.

Therefore, in order to solve the problems of the traditional target tracking network construction model and imitate the human cognitive model, this paper explores an intelligent target pose estimation method based on the adaptive attention mechanism. First, the regional attention is iteratively generated from a global level to a local level based on the attention mechanism. Human decision-making patterns are imitated to evaluate the effectiveness of regional attention in real time, and the level of attention mechanism is adaptively adjusted and focused layer by layer to achieve precise target detection and tracking. Second, combined with the target frame obtained from each frame, the pose estimation algorithm finds the key points of human body, enabling the human body pose optimization strategy to solve the crossover problem of the key points. Results of experiments on sports video images show that the proposed method has a higher accuracy in pose estimation than other algorithms and can help sportsmen adjust their training methods scientifically.

The innovations of this paper can be summarized as follows: (1) an iterative generation mechanism of regional attention from global to local is proposed; (2) a real-time evaluation method of regional attention effectiveness is constructed; (3) an adaptive adjustment mechanism of regional attention is established.

2. Target Detection Model Based on Adaptive Attention Mechanism

This paper proposes a target detection method based on the adaptive attention mechanism, which is composed of convolutional layers, target positioning network, target position feature evaluation and cropping module, etc. See Figure 1 for its structure and functions.

First, the target detection model completes the first round of reliability test, by sending the input image to the deep neural network M_0 for training and getting the deep feature map F_1. According to the entropy theory, a target evaluation function can be established to validate the reliability of F_1. If the threshold is satisfied, positioning of the target to be detected in the background image is considered reliable, and the trained deep network is stored as the first model into the detection model set of the attention mechanism; otherwise, the order of attention is adaptively adjusted to provide heuristic information for the positioning network. F_1 is then input into the positioning network weighted by the level of adaptive attention, and the target area is clipped according to the positioning characteristics of the output target. Adjust the clipped image to the size consistent with that of the input image, and start the second round of test; enter the deep neural network M_1 again to extract the deep feature map; repeat the above process to establish the second attention mechanism detection model, or generate a new image to be detected to initiate the next round of test until the test requirement is met or the number of focusing reaches the threshold. Finally, the image of the target precisely positioned is obtained.

2.1. Reliability Test of Target Detection Results and Adjustment Mechanism of Attention. Facing uncertain detection/recognition results, people will adaptively adjust their cognitive strategies to further perceive micro-information and get more reliable results. For the feature maps extracted by the Resnet-18 deep neural network, a reliability test is required to provide a quantitative basis for generation of the attention detection model and construction of the focus relocation model.

Define the train set as U, and let $U = \{U_1, U_2, \ldots, U_h\}$. Using Resnet-18 model M_0, U_j is given the fully connected

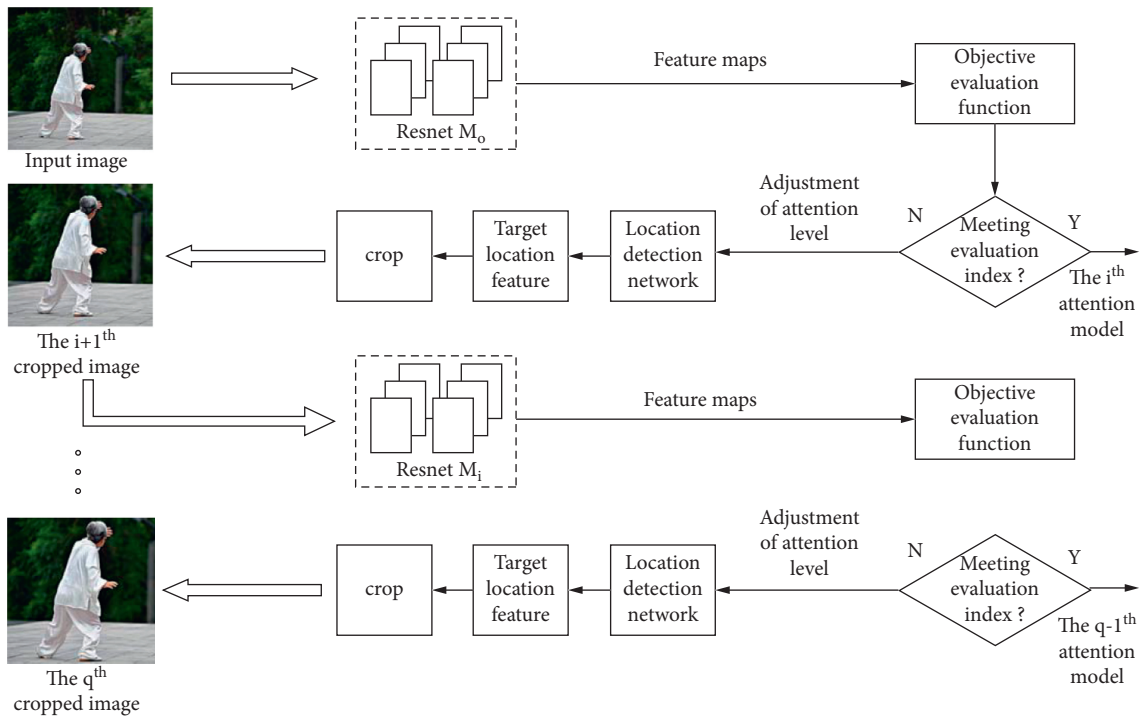

Figure 1: Target detection model based on adaptive attention mechanism.

feature vector $\mathbf{F}_j = [f_{j1}, f_{j2}, \ldots, f_{jd}]$ of the feature map, where d is the feature dimension. Take the fully connected feature vector set, given to U's real target area via the pretrained Resnet-18 model N, as $\mathbf{Y} = [\mathbf{y}_1, \mathbf{y}_2, \ldots, \mathbf{y}_h]$, where $\mathbf{y}_j = [y_{j1}, y_{j2}, \ldots, y_{jd}]$, and define the target detection error entropy of U_j as

$$A_j = -\frac{\left\|1_{h\times 1} \times \mathbf{F}_j - \mathbf{Y}\right\|_2}{\sum_{j=1}^{h}\left\|1_{h\times 1} \times \mathbf{F}_j - \mathbf{Y}\right\|_2} \ln \frac{\left\|1_{h\times 1} \times \mathbf{F}_j - \mathbf{Y}\right\|_2}{\sum_{j=1}^{h}\left\|1_{h\times 1} \times \mathbf{F}_j - \mathbf{Y}\right\|_2}. \quad (1)$$

Larger entropy values v indicate less reliability of the feature information about the positioning area of the sample in the current deep network model. When the reliability threshold $\varrho = \lambda(\sum_{i=1}^{h} A_i)/h$ is exceeded, it is necessary to further focus and relocate the sample to perceive detailed information and save the current deep network model M_0 into the attention detection model set. Otherwise, the samples with smaller entropy values are deleted, and the train set is thus updated.

Let the proposed attention adjustment mechanism be $q \leftarrow q + \Delta q, 1 \le q \le q_{\max}, 1 \le \Delta q \le q_{\max}$, where Δq represents the increment to levels of attention adjusted according to feedback, and $q_{\max}$ represents the maximum level of attention.

2.2. Position Detection Network Model. The feature map generated by the deep neural network is used as the input of the position detection network. Under the constraint of the heuristic information of adaptive attention, the deep neural network is evolved synergistically with the position detection network through Alternating Training to get better detection results. Since the input item is the extracted deep feature map, it is possible to construct the position detection network with two fully connected layers without the need for carrying out complicated operations such as convolution, pooling, and activation.

Define the deep features of the input image U, which is extracted by the deep neural network, as $W_c * U$, where $*$ represents convolution, activation, pooling, and other operations, and W_c represents all parameters of the deep neural network. The position detection network model will more accurately deliver a target prediction area, expressed as follows:

$$\left[\frac{t_x, t_y, t_l}{\Delta q}\right] = g(W_c * U), \quad (2)$$

where t_x and t_y respectively represent the center coordinates of the square target prediction area, t_l half of the side length of the area, and $g()$ the position detection network. By analyzing the mechanism of human cognition, we can see that the granularity of cognitive information is changed in a nonuniform manner from macroscopically to microscopically. Therefore, in order to accomplish the nonuniform adjustment of the target prediction area, the transformation function is established for cognitive information granularity with decline characteristics, and the heuristic information of the increment to level of attention is used to weight the target prediction area.

In order to guarantee that an effective area is selected during the forward propagation, and the network can be optimized during the backward propagation, a two-dimensional rectangular function is proposed as a basis to perform the approximate clipping operation. Assuming that the upper left corner of the original image is the origin of

coordinates, the coordinates of the upper left and lower right corners of the target area are

$$t_{x1} = t_x - \frac{t_l}{\Delta q},\ t_{y1} = t_y - \frac{t_l}{\Delta q},$$
$$t_{x2} = t_x + \frac{t_l}{\Delta q},\ t_{y2} = t_y + \frac{t_l}{\Delta q}. \tag{3}$$

To clip, the original image and the coordinates are masked. In order to prevent images from discontinuity caused by the traditional masking method based on 0/1 dot product, this paper adopts the logistic regression function $\sigma(x) = 1/1 + e^{-kx}$ to construct a similar step function and uses a step that is about zero to produce an effect similar to 0/1 masking effect. When k is large enough, $x \geq 0, \sigma(x) \approx 1$; $x < 0, \sigma(x) \approx 0$. At this point, $\sigma(x)$ approximates a first-order function. If $x_0 < x_1$, $\sigma(x - x_0) - \sigma(x - x_1)$ is a smooth step function; if $x < x_0$ or $x > x_1$, $\sigma(x - x_0) - \sigma(x - x_1) \approx 0$; if $x_0 < x < x_1$, $\sigma(x - x_0) - \sigma(x - x_1) \approx 1$. Therefore, the following function is constructed:

$$U^{at} = U \odot M\left(t_x, t_y, \frac{t_l}{\Delta q}\right), \tag{4}$$

where U^{at} represents the image area that is worthy of attention, and $M()$ the calculated masking results of coordinates, as shown in the following:

$$M\left(t_x, t_y, \frac{t_l}{\Delta q}\right) = \left[\sigma(x - t_{x1}) - \sigma(x - t_{x2})\right] \cdot \left[\sigma\left(y - t_{y1}\right) - \sigma\left(y - t_{y2}\right)\right]. \tag{5}$$

After the original image is clipped, the useless information is deleted. As the features extracted from the localized image are weakened due to the reduced resolution, the bilinear interpolation method is adopted to enlarge the clipped target image to the size that the original image has so as to extract finer target features.

2.3. Backpropagation Process of the Target Detection Network. The output values t_x, t_y and t_l of the position detection network should be backpropagated for iterative optimization. Since these three coordinate parameters are the same in location, their backpropagation process is the same. Here, take t_x as an example, and calculate its derivatives by the chain rule:

$$L'_{rank}(t_x) = \frac{\partial L_{rank}}{\partial t_x} \propto D_{top} \odot \frac{\partial M\left(t_x, t_y, t_l/\Delta q\right)}{\partial t_x}, \tag{6}$$

where $\odot$ represents element-Wise product, and D_{top} represents the derivative propagated by the previous network. If $L'_{rank}(t_x) < 0$, t_x increases, or it decreases. Further, calculate $-\|L_{rank}(t_x)\|_2^2$ to determine the parameter optimization direction. $M'(t_x)$ represents the derivative of the mask function to t_x, which can be defined by the following piecewise function:

$$M'(t_x) = \begin{cases} < 0, & t_x \longrightarrow t_{x1}, \\ > 0, & t_x \longrightarrow t_{x2}, \\ = 0, & \text{otherwise}. \end{cases} \tag{7}$$

$M'(t_y)$ can be deduced in the same way. Since $M'(t_l/\Delta q)$ is positive on both sides of the boundary and negative inside the boundary, it can be defined as follows:

$$M'\left(\frac{t_l}{\Delta q}\right) = \begin{cases} > 0, & t_x \longrightarrow t_{x1} \text{ or } t_x \longrightarrow t_{x2}, \\ t_y \longrightarrow t_{y1} \text{ or } t_y \longrightarrow t_{y2}, & \\ < 0, & \text{otherwise}. \end{cases} \tag{8}$$

In summary, since the interval of negative values in the derivative is consistent with *that of* $M'(t_x)$, it is easy to conclude that $L'_{rank}(t_x)$ is positive. Similarly, $L'_{rank}(t_y)$ and $L'_{rank}(t_l/\Delta q)$ are also positive. Therefore, t_x, t_y, t_l will all decrease in the next iteration, indicating focused areas of attention. This is consistent with the human perception model.

2.4. Multimode Selection Method for Target Detection. The target detection model based on the adaptive attention mechanism can establish an attention detection model set, in which models are similar in structure but different in parameters. When the sample set is tested against the multi-attention detection model and since a model cannot give full play to its advantages in the premise of averagely weighted outputs, the decision-making attention mechanism is used according to the defined target detection error entropy to detect the outputs of the model set.

To obtain the output feature map and the focused images that have been clipped, the test set images are, respectively, input to each attention detection model in the model set.

According to formula (1), the target detection error entropy $A_q, 1 \le q \le q_{max}$ of q_{max} models with respect to the input image is calculated. When $A_{q_1} \le A_{q_2} \le \cdots \le A_{q_m}, q_1, q_2, \ldots, q_m \in [1, q_{\max}]$, select the model M_{q_1} corresponding to A_{q_1} as the best model, of which the output image is the final adaptive positioning image.

3. Pose Estimation Model Based on Deep Learning

3.1. Pose Estimation Model Based on Hourglass Network. DeepPose utilizes deep learning to transform the problem of pose estimation into the one related to joint point regression and performs estimated regression of the entire image to position each human joint point. Another type of method integrates multiscale features to generate a heatmap of the key points of the human body. Based on the above two methods, the hourglass network adopts the convolutional layer architecture of upsampling first and then downsampling. It integrates multiscale features at the bottom layer and the top layer of the network, improving the prediction accuracy of key points. The structure and the parameters of each module of the hourglass network are shown in Figure 2. The image resolution of the network input in Figure 2 is 256×256, Max pool in the figure stands for Down Sample, Up Sample stands for Up Sample, and Res stands for Residual Module, as shown in Figure 3.

During specific pose estimation, the stacked hourglass network is repeatedly upsampled and downsampled to generate the heatmap. The point with the highest heatmap score is taken as the key prediction point for each corresponding joint, and the key points are then converged to obtain the distribution diagram of key points of the human body. In addition, the symmetrical topology of the hourglass network helps predict the pose in both forward and backward directions, which improves the accuracy of pose estimation.

3.2. Evaluation Criteria for Human Pose Estimation. After the key points of the human body are predicted, it is necessary to evaluate the similarity with the ground truth (GT). The common Object Keypoint Similarity (OKS) index is defined as follows:

$$OKS_p = \frac{\sum_i \exp\left\{-d_{pi}^2 / 2S_p^2 \sigma_i^2\right\} \delta\left(v_{pi} = 1\right)}{\sum_i \delta\left(v_{pi} = 1\right)}, \tag{9}$$

where p represents the ID number of the target in the GT, i the number of the key points of the human body, d_{pi} the Euclidean distance between the key points of each person in the GT and the predicted result, S_p the scale factor of the p-th target, σ_i the i-th normalization factor of the key point, v_{pi} the visibility of the i-th key point of the p-th target, and δ the function deduced by selecting the visible key point.

From formula (9), the similarity between two key points of the human body can be deduced. If there are M persons in an image among whom N persons are predicted, an $M \times N$ OKS matrix should be constructed, of which the maximum value of each row is used as the OKS value of the i-th person. For several images in the test set, the Average Precision (AP) is used to measure the human pose estimation. The calculation is as follows: if OKS is greater than the threshold t, detection of the key points succeeds; otherwise, it fails. Count the number of OKS values that are greater than t, and calculate the ratio to the total number of OKS values.

3.3. PoseFix-Based Pose Estimation Optimization Strategy. Incorrect pose estimation may usually be caused by jitter, switching, and loss. Learning from DeepPose and facing most of the key points with good pose input or small deviations, the PoseFix model [24] focuses on the trusted key points and corrects the postprediction results. It can effectively solve the crossover problem. Its structure is shown in Figure 4.

PoseFix uses Gaussian distribution to represent the input poses in the form of heatmap, which are then spliced with the input image and sent to PoseFix. Such practice is not only suitable for convolution operations, but helps estimate key points by making use of the information around the features. Another advantage of PoseFix is that it has no connection with the method of generating the key points of the pose. Thus, it can be used as a postprocessing optimization strategy for any pose estimation method.

4. Experimental Results and Analysis

4.1. Experimental Data. In order to verify the feasibility and effectiveness of the proposed method, solo sports videos such as long jump, high jump, and 100-metre sprint are selected. Each video is about 30 minutes in length.

The video is converted and clipped by OpenCV into images with $1080 * 1080$ resolution, among which 70% are sampled randomly to construct the train set, and the remaining 30% make up for the test set. In this experiment, the maximum attention level of the target detection model is $q_{\max} = 6$, and the training epoch is set as 2000. In order to guarantee smoothness of the human detection/recognition process, let $\Delta q = 1$ to construct a compact set model for attention detection. Extract similar training sample sets with different qualities to multilevelly position the features. All experiments run under the environment of CPU i7-8700, 32G memory, and GTX1080Ti.

4.2. Experimental Results and Analysis. Figure 5 displays the target positioning results of the method proposed in this paper. Take the three-level attention as an example.

We can see from the figure that, in the busy background of the training field, the direct target detection method may damage detection accuracy and comprehensiveness, because possible crowds and light changes may have an impact on extraction of the main target features. The adaptive attention mechanism, however, allows the input image to be continuously positioned and focused and avoids the interference from useless areas, which helps represent and detect the features.

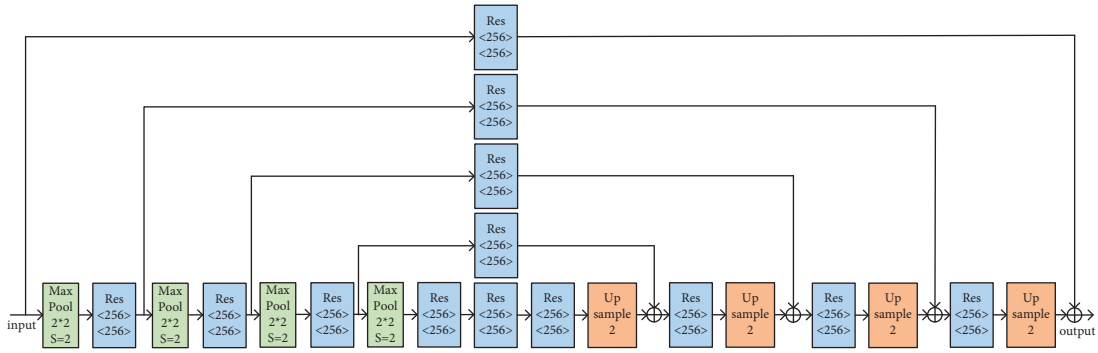

Figure 2: Hourglass network structure.

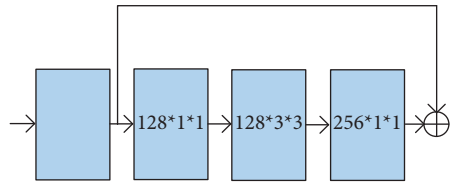

Figure 3: Residual module.

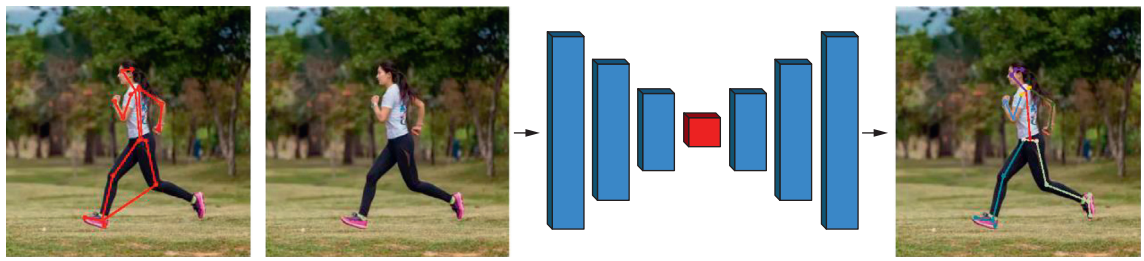

Figure 4: PoseFix structure.

Figure 6 shows the changing curve of target detection error entropy of the multilevel attention detection model under the condition of different maximum levels of attention q_{max}. Here, $q_{\max} = \{2, 3, 6\}$, where the Y- coordinate is the detection error entropy, and the X-coordinate is the number of iterations.

It can be seen from the figure that, with a decline in levels of attention focusing, the training efficiency of the model is increased. As the iteration process continues, the target detection error entropy of the model shows a rapid decline at $q_{\max} = 2$. When the number of iterations reaches 1000, the model presents the most reliable target detection results but works not stably. After the number of iterations exceeds 1000, the error entropy fluctuates, indicating that the attention mechanism malfunctions at $q_{\max} = 2$, and the target cannot be accurately positioned if some samples are focused only twice. Because of the lack of the ability in sample characterization, the feature extraction network should be further optimized. Similar problems occur at $q_{\max} = 3$. When the upper limit is raised ($q_{\max} = 6$), the training efficiency of the model decreases, because the model is no longer limited by the levels of attention and spends more time in seeking a more suitable focusing stage and extracting the marked features of the detected target. The reliability of target detection can be improved, as the iteration process goes on.

The precision and success rate of the proposed method with other target tracking algorithms are given in Table 1, where precision is defined as the distance between the predicted target position and the real target position $\text{dist} = \sqrt{(G_x - P_x)^2 + (G_y - P_y)^2}$. Tracking of this image is considered accurate if the distance is less than a threshold value. The success rate is calculated from the IoU score. If the IoU value is greater than a threshold, the tracking of this image is considered successful. Here, the precision threshold is set to 20 pixels, and the success rate threshold is set to 0.5.

As shown in Table 1, the proposed method is compared with seven mainstream tracking algorithms, including MDNet, SiamRPN, FCN, TADT, C-RPN, DAT, and SPM. It can be seen that the proposed method outperforms other

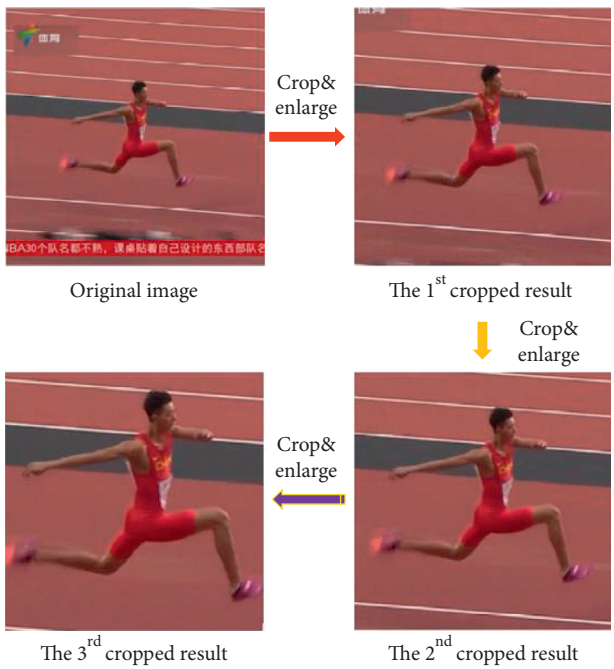

Figure 5: Schematic diagram of three-level attention focusing.

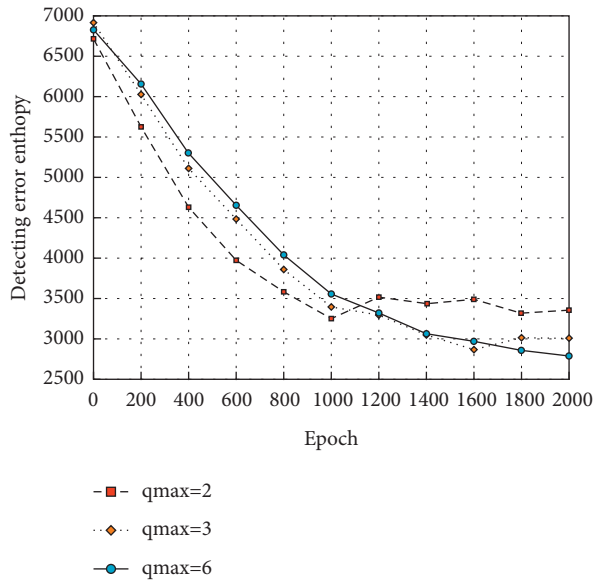

Figure 6: The changing curve of target detection error entropy under the condition of different levels of attention.

Table 1: Evaluation results of various trackers.

Recognition method	Precision	Success rate
Our method	0.910	0.685
MDNet [5]	0.861	0.641
SiamRPN [6]	0.891	0.666
FCN [7]	0.901	0.68
TADT	0.865	0.67
C-RPN	0.876	0.675
DAT	0.902	0.672
SPM	0.899	0.667

Table 2: Comparison in pose estimation between different methods.

Recognition method	AP	Posture estimation time (s)
Our method	76.2	0.27
Tompson et al. [25]	74.3	0.012
Feng et al. [26]	74.1	0.073
Cao et al. [27]	72.8	0.028
CPN [28]	75.8	0.18
Hourglass [29]	75.3	0.14

target tracking algorithms in terms of both precision and success rate of tracking, which is due to its imitation of human decision patterns, real-time evaluation of regional attention effectiveness, and iterative generation of regional attention from global to local to focus on samples at different scales. The above characteristics improve its tracking robustness in complex environments.

In addition, the algorithm proposed is also compared with other human pose estimation algorithms, such as Tompson et al. [25], Fang et al. [26], Cao et al. [27], CPN [28], and Hourglass [29]. Taking AP as an evaluation index, Table 2 gives the estimation results of the test sample set, and the average time consumed for pose estimation.

It can be seen from Table 1 that the proposed method performs better in pose estimating than other methods, because the multilevel focusing mechanism of the adaptive attention mechanism can get rid of the interference from useless areas in the complex image, which provides more accurate target areas for subsequent estimation. By integrating multiscale features at both the bottom level and the top level, the PoseFix pose optimization strategy enhances the pose feature representation effect. In addition, the pose estimation time allows to evaluate the overall complexity of the algorithm. Although the method proposed in this paper is inferior to other methods in time consumed, it in fact makes no difference with CPN and Hourglass under the same order of magnitudes. The long estimation time is due to the good real-time tracking and pose estimation performance as the model is exploring more suitable focus levels to obtain accurate target detection results.

5. Conclusions

Higher accuracy in pose estimation is a prerequisite for excellent sports results. In order to solve the problem related to low efficiency of labor-based physical education, this paper explores an intelligent method of estimating target posture based on adaptive attention mechanism, which provides technical support for daily physical education. First, according to the human decision-making model, regional attention is gradually focused and iteratively generated. By evaluating the performance of target features in real time, and adaptively adjusting levels of the attention, precise positioning of the detected target is achieved. Second, the PoseFix pose optimization strategy is adopted to solve the crossover problem of the key points of the human body posture estimated by the hourglass network. Experiments on

sports video images demonstrate the feasibility and effectiveness of this method.

Data Availability

The data used to support the findings of this study are available from the corresponding author upon request.

Conflicts of Interest

The authors declare that they have no conflicts of interest.

Acknowledgments

This research was supported in part by the Key Humanities and Social Science Research Project in Anhui Province (SK2020A0955) and Anhui School-Enterprise Cooperation Practice Education Base Project (2020sjjd102).

References

[1] K. He, X. Zhang, S. Ren, and J. Sun, "Spatial pyramid pooling in deep convolutional networks for visual recognition," *IEEE Transactions on Pattern Analysis and Machine Intelligence*, vol. 37, no. 9, pp. 1904–1916, 2015.

[2] S. Ren, K. He, and R. Girshick, "Faster R-CNN: towards real-time object detection with region proposal networks," *IEEE Transactions on Pattern Analysis and Machine Intelligence*, vol. 39, no. 6, pp. 1137–1149, 2016.

[3] A. Bochkovskiy, C. Y. Wang, and H. Y. M. Liao, "YOLOv4: optimal speed and accuracy of object detection," 2020, https://arxiv.org/abs/2004.10934.

[4] C. Y. Wang, H. Y. M. Liao, and Y. H. Wu, "CSPNet: a new backbone that can enhance learning capability of CNN," in *Proceedings of the 2020 IEEE Conference on Computer Vision and Pattern Recognition*, pp. 1571–1580, Seattle, WA, United States, June 2020.

[5] H. Nam and B. Han, "Learning multi-domain convolutional neural networks for visual tracking," in *Proceedings of the IEEE Conference on Computer Vision and Pattern Recognition (CVPR)*, pp. 4293–4302, Las Vegas, NV, USA, June 2016.

[6] B. Li, J. Yan, and W. Wu, "High performance visual tracking with siamese region proposal network," in *Proceedings of the IEEE Conference on Computer Vision and Pattern Recognition (CVPR)*, pp. 8971–8980, Salt Lake City, UT, USA, June 2018.

[7] J. Long, E. Shelhamer, and T. Darrell, "Fully convolutional networks for semantic segmentation," in *Proceedings of the IEEE Conference on Computer Vision and Pattern Recognition (CVPR)*, pp. 3431–3440, Boston, MA, USA, June 2015.

[8] N. Chen, J. Zhu, J. Chen, and T. Chen, "Dropout training for SVMs with data augmentation," *Frontiers of Computer Science*, vol. 12, no. 4, pp. 694–713, 2018.

[9] J. Redmon, S. Divvala, and R. Girshick, "You Only Look Once: unified, real-time object detection," in *Proceedings of the IEEE Conference on Computer Vision and Pattern Recognition*, pp. 779–788, Las Vegas, NV, United States, June 2016.

[10] W. Ouyang, X. Chu, and X. Wang, "Multi-source deep learning for human pose estimation," in *Proceedings of the IEEE Conference on Computer Vision and Pattern Recognition*, pp. 2337–2344, Columbus, OH, United States, June 2014.

[11] Q. Li, H. Tang, Z. Liu, J. Li, X. Xu, and W. Sun, "Optimal resource allocation of 5G machine-type communications for situation awareness in active distribution networks," *IEEE Systems Journal*, pp. 1–11, 2021.

[12] Q. Y. Li, T. Cao, and W. Sun, "An optimal uplink scheduling in heterogeneous PLC and LTE communication for delay-aware smart grid applications," *Mobile Networks and Applications*, vol. 26, no. 4, pp. 1–14, 2021.

[13] G. Hidalgo, Y. Raaj, and H. Idrees, "Single-network whole-body pose estimation," in *Proceedings of the IEEE International Conference on Computer Vision*, pp. 6982–6991, Seoul, South Korea, June 2019.

[14] S. Kreiss, L. Bertoni, and A. A. Pifpaf, "Composite fields for human pose estimation," in *Proceedings of the IEEE Conference on Computer Vision and Pattern Recognition*, pp. 11977–11986, Seoul, South Korea, June 2019.

[15] W. Sun, Q. Li, C. Zhao, and S.-K. Nguang, "Mode-dependent dynamic output feedback H∞ control of networked systems with Markovian jump delay via generalized integral inequalities," *Information Sciences*, vol. 520, pp. 105–116, 2020.

[16] W. Sun, L. Huang, Z. Liu, Q. Li, C. Zhao, and D. Mu, "Distributed controller design and stability criterion for microgrids with time-varying delay and rapid switching communication topology," *Sustainable Energy, Grids and Networks*, vol. 29, p. 100566, 2022.

[17] A. Maharjan, X. Yuan, Q. Lu, Y. Fan, and T. Chen, "Non-rigid registration of point clouds using landmarks and stochastic neighbor embedding," *Journal of Electronic Imaging*, vol. 30, no. 3, p. 031202, 2021.

[18] A. Maharjan and X. Yuan, "Registration of human point set using automatic key point detection and region-aware features," in *Proceedings of the IEEE winter conference on applications of computer vision (WACV)*, pp. 4–8, Waikoloa, HI, USA, June 2022.

[19] L. Kong, X. Yuan, and A. M. Maharjan, "A hybrid framework for automatic joint detection of human poses in depth frames," *Pattern Recognition*, vol. 77, pp. 216–225, 2018.

[20] M. M. Bronstein, J. Bruna, Y. LeCun, A. Szlam, and P. Vandergheynst, "Geometric deep learning: going beyond euclidean data," *IEEE Signal Processing Magazine*, vol. 34, no. 4, pp. 18–42, 2017.

[21] W. T. Li, D. Jiao, and Q. Zhang, "Research on intelligent cognition method of self-exploding state of glass insulator based on deep migration learning," *Proceedings of the CSEE*, vol. 40, no. 11, pp. 3710–3720, 2020.

[22] Q. Zhang, W. Li, H. Li, and J. Wang, "Self-blast state detection of glass insulators based on stochastic configuration networks and a feedback transfer learning mechanism," *Information Sciences*, vol. 522, pp. 259–274, 2020.

[23] W. Li, H. Tao, H. Li, K. Chen, and J. Wang, "Greengage grading using stochastic configuration networks and a semi-supervised feedback mechanism," *Information Sciences*, vol. 488, pp. 1–12, 2019.

[24] M. R. Ronchi and P. Perona, "Benchmarking and error diagnosis in multi-instance pose estimation," in *Proceedings of the IEEE International Conference on Computer Vision*, pp. 369–378, Venice, Italy, June 2017.

[25] J. Tompson, A. Jain, and Y. LeCun, "Joint training of a convolutional network and a graphical model for human pose estimation," in *Proceedings of the Conference and Workshop on Neural Information Processing Systems*, pp. 1799–1807, Montreal, Canada, December 2014.

[26] H. S. Fang, S. Xie, and Y. W. Tai, "RMPE: regional multi-person pose estimation," in *Proceedings of the IEEE International Conference on Computer Vision*, pp. 2353–2362, Venice, Italy, October 2017.

[27] Z. Cao, T. Simon, and Y. Sheikh, "Realtime multi-person 2D pose estimation using part affinity fields," in *Proceedings of the International Conference on Computer Vision and Pattern Recognition*, pp. 1302–1310, Honolulu, HI, USA, July 2017.

[28] Y. Chen, Z. Wang, and Y. Peng, "Cascaded pyramid network for multi-person pose estimation," in *Proceedings of the IEEE Conference on Computer Vision and Pattern Recognition*, pp. 7103–7112, Salt Lake City, USA, June 2018.

[29] A. Newell, K. Yang, and J. Deng, "Stacked hourglass networks for human pose estimation," in *Proceedings of the European Conference on Computer Vision*, pp. 483–499, Amsterdam, Netherlands, October 2016.

Hindawi
Wireless Communications and Mobile Computing
Volume 2022, Article ID 1304951, 16 pages
https://doi.org/10.1155/2022/1304951

Research Article

Clustering Optimization Algorithm for Data Mining Based on Artificial Intelligence Neural Network

Shuyue Zhang and Chao Duan

Engineering College, Guangzhou College of Technology and Business, Guangzhou 510850, Guangdong, China

Correspondence should be addressed to Shuyue Zhang; zhangshuyue666@163.com

Received 10 November 2021; Revised 7 December 2021; Accepted 21 January 2022; Published 17 February 2022

Academic Editor: Mohamed Elhoseny

Social production and life have become increasingly prominent. Cluster analysis is the basis for further processing of the data. The concept of data mining and the application of neural networks in data mining are introduced. According to the related technology of data mining, this article introduces in detail the two-layer perceptron, backpropagation (BP) neural network, RBF radial basis function network for processing classification problems, and self-organizing map (SOM) self-organizing neural network for unsupervised clustering problems. According to the characteristics of self-adaptive and self-organizing capabilities of these algorithms, we learn and design and implement data mining clustering optimization algorithms. In this paper, the neural network-based data mining process consists of three stages: data preparation, rule extraction, and rule evaluation. This paper studies the teaching-type and decomposition-type rule extraction algorithms. After analyzing the BP decomposition-type algorithm, the correlation method is used to calculate the correlation of the input and output neurons. After sorting by the degree of correlation, the RBF neural network is used for node selection. This can greatly reduce the number of input nodes of the neural network, simplify the network structure, reduce the number of recursive splits of the subnet, and improve calculation efficiency. Taking the model as an example, the training error is calculated through data mining technology and clustering algorithm. Data mining clustering optimization algorithm mainly improves the popular neural network from two aspects: finer model design and model pruning, and simulates model complexity, computational complexity, and errors through simulation experiments. The rate is measured, and finally, the simulation experiment is performed. The results show that the proposed algorithm for differential distributed data mining has higher accuracy and stronger convergence ability and overcomes the shortcomings and shortcomings of several original genetic algorithm optimization neural network data mining models; it can effectively improve the searchability and search accuracy of the algorithm and improve the efficiency of data mining. Accuracy and accuracy have a wide range of applications.

1. Introduction

The amount of data on the Internet is exploding, and the impact of data on many areas of social production and life is becoming more and more prominent, using traditional data analysis methods. Based on this, data mining techniques and clustering optimization algorithms are generated. Firstly, we determine the mining task and then select the corresponding mining algorithm to implement the data mining operation. The mining process is a process of human-computer interaction and repeated many times. It mainly includes defining problems, establishing data mining libraries, analyzing data, preparing data, establishing models, evaluating models, and implementing them. The whole process of data mining is inseparable from professional knowledge in the application field, database, data warehouse, or other information repositories.

Its research goal is to divide the collection of limited data objects in a database or data warehouse into a group of clusters. Theoretical analysis shows that the data mining clustering algorithm is very suitable for using neural computing. A cluster composed of clusters is a collection of a set of data objects, which are similar to objects in the same cluster and different from objects in other clusters. The

analysis results can not only reveal the internal connections and differences between the data but also provide an important basis for further data analysis and knowledge discovery. After the global analysis of the similarity between data objects, the similarity will be high. Data objects are grouped together in the same class while data objects with low similarity are grouped into different classes. Commonly used techniques include probability analysis and correlation analysis. The learning and training of sets result in the required patterns or parameters. Since various methods have their own functional characteristics and applicable fields, the choice of data mining technology will affect the quality and effect of the final results. In the actual application process, multiple technologies are usually combined to form complementary advantages.

Jorge observed that most of the calculations are essentially invalid. Jorge's observations inspired CN volatile (CNV), which eliminated most of these invalid operations, improved performance and energy, and had no precision loss compared with the most advanced accelerator [1]. Han proposed an energy-efficient inference engine (EIE) [2]. After learning and extracting microwave data, Wang uses a neural network model in the microwave design process through a process called training to provide instant answers for the learned tasks. Appropriate neural network structure and training algorithm are two main problems in developing neural network model of microwave application [3]. Tapas designed a classifier based on syntax bee colony and applied it to medical data mining [4, 5]. Tapas applied this method to 10 medical datasets and compared it with the Levenberg Marquardt algorithm trained multilayer perceptron classifier [6, 7]. Sadiq takes the students in the affiliated colleges of the University of Diburgarh as the research object [8]. Chauhan studies different text mining techniques to extract relevant information as needed [9, 10]. Under the Map Reduce paradigm, Sudhakar implements three variants of Apriori algorithm [11], namely, trie and hash technology, by using three data structures: hash tree, trie, and hash table trie. Sudhakar focuses on the significance of these three data structures to Apriori algorithm on Hadoop cluster [12]. Xingyi proposed an evolutionary algorithm [13]. T ü Lin studies the spatial clustering problem without prior information [14]. The clustering method proposed by t ü Lin solves several challenges of clustering [15]. Pham proposed an automatic image in FCPFS [16].

The innovation of this paper is to optimize the data mining clustering algorithm based on artificial intelligence neural network and propose the K-means clustering algorithm to optimize the data mining algorithm, using the scalability and uniformly distributed data types of the K-means algorithm. Data mining can be better. And combined with the actual application, the algorithm is selected to ensure the real-time performance of the algorithm. Main research contents and some useful results are obtained. In this paper, theoretical research is the main part, supplemented by some simulation experiments, and the standard data and real data of UCI data warehouse, such as power load sequence, verify the simulation experiments.

2. Proposed Method

2.1. Neural Network. It is an algorithmic mathematical model that imitates the behavioral characteristics of animal neural networks and performs distributed and parallel information processing. This kind of network relies on the complexity of the system and achieves the purpose of processing information by adjusting the interconnection between large numbers of internal nodes. A machine learning method learns from samples. The purpose of neural characteristics (expressed in the form of conditional distribution $P(t|x)$) of the laws produces samples. It is mainly composed of three basic components:

(1) Random sample generator, which is used to extract random sample x independently from a fixed but unknown distribution $P(x)$. Generally, sample x is a multidimensional vector, and distribution $P(x)$ is a multidimensional random distribution.

(2) System internal mapping: according to the mapping, input a random vector x and return output y with a certain probability. Input vector x and output vector y obey a fixed but unknown conditional distribution $P(y|x)$. The definition of this mapping considers the influence of noise, and it is actually a kind of random mapping.

(3) Learning machine (or algorithm), which can realize a certain kind of function $f(x, a)$ to approximate the internal mapping of the system.

A common BP neural network model is usually composed of an input layer, hidden layer, and output layer, as shown in Figure 1.

Each layer contains an unequal number of neuron nodes, where W_{ij} represents the connection weight between neurons. Each node neuron has multiple inputs and one output, which can be expressed as

$$T_i = f\left(net_i\right), \tag{1}$$

where T_i represents the output value of node i on a layer.

$$\begin{aligned} Net_i &= \sum W_{ij} \cdot x_i - \theta_j, \\ R &= \alpha Q y + \beta_1 B - W\beta_2 N + \gamma, \\ Z &= \left(1 - \frac{|M| - |P|}{|P|}\right)\phi, \\ \mathrm{L}_P &= B_0 + B_1\, \mathrm{d}u \times \mathrm{d}t + \sum_{i=1}^{N} B_j XG + \kappa_u. \end{aligned} \tag{2}$$

Input a training sample P from the input layer. Through system analysis, the single sample training error of the BP neural network can be defined as

$$E_p = \frac{1}{2}\sum\left(d_{pj} - O_{pj}\right)^2. \tag{3}$$

In the formula, the expected output value is

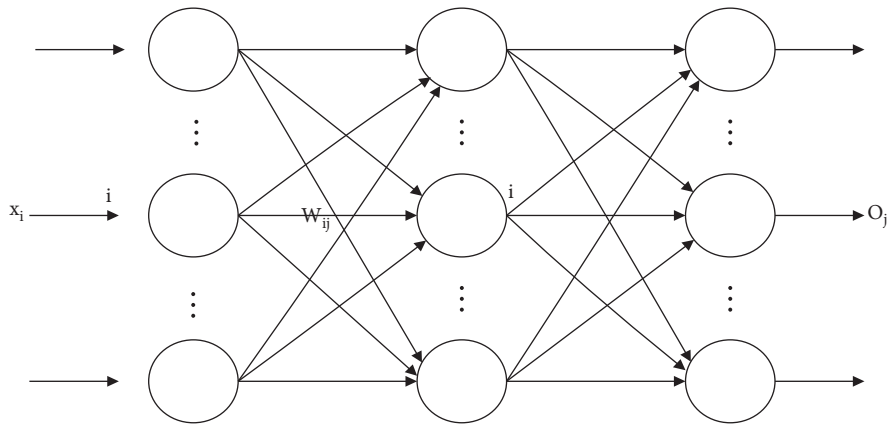

Figure 1: BP neural network model.

$$E = \frac{1}{p'} \sum_{p=1}^{p'} E_p. \tag{4}$$

With the deepening of research, more and more researchers tend to use evolutionary programming to study evolutionary neural networks and think that it is more appropriate to use evolutionary programming to study evolutionary neural networks. Therefore, the combination of evolutionary programming and the neural network model is a more effective model. The combination of evolutionary programming and neural network model can better imitate and evolve learning behavior. Based on this analysis, a typical EPNet evolutionary neural network model has been proposed, which has strong representativeness and pertinence. As a relatively mature neural network evolution system, EPNet has the following characteristics: first, EPNet emphasizes the plan of ANN behavior and uses some technologies, such as local training after each structural variation and node splitting, to maintain the behavior relationship between the parent and its offspring, while some previous EP systems have little emphasis on this behavior relationship. The usual way of structural variation is to randomly add or delete a hidden layer neuron or connection. Obviously, this method tends to destroy the behavior that the parents have learned and weaken the behavior relationship between the parents and the children. Secondly, EPNet uses different mutation operations according to a certain priority level and gives higher priority to mutation operations that can generate a simplified network structure. Take structural variation as an example. Before adding nodes, always try to delete nodes or connections first. If the deletion can increase the fitness of individuals, the subsequent mutation operation will not be used. Compared with the existing methods, which limit the network scale by adding the penalty term of network complexity in the fitness function, this method can avoid the laborious attempt to find the parameter of the penalty term. Finally, in order to eliminate the influence of permutation problems, the EP algorithm without a crossover operator is used in the EPNet system. The basic flow of the EPNet model is shown in Figure 2.

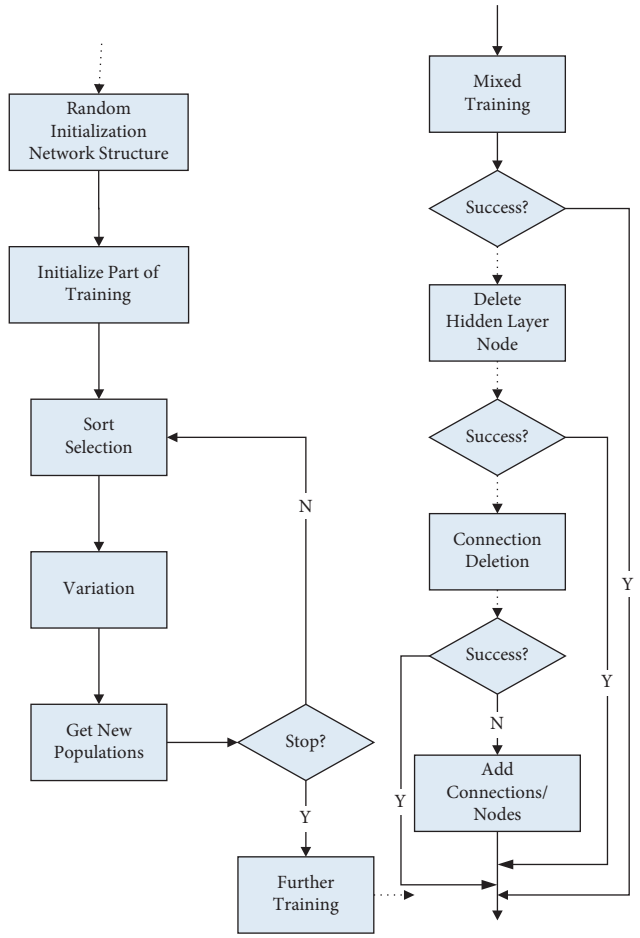

Figure 2: EPNet model structure diagram.

2.2. Data Mining. In order to realize the differential distribution, calculate the global kernel function and the hybrid kernel function, adopt the hybrid particle swarm optimization method, use the differential distributed data of limited samples for training, and pass a nonlinear mapping:

$$\begin{aligned}
&\Phi\colon x \in R^n \longrightarrow F,\\
&F(S_1 \| S_2) = \frac{1}{2}F\left(S_1 \middle\| \frac{S_1+S_2}{2}\right) + \frac{1}{2}F\left(P_2 \middle\| \frac{S_1+S_2}{2}\right),\\
&(\mathrm{In}(S-\alpha R))M = (\mathrm{In}-\alpha S)XM + \gamma,\\
&M\left(X_i, w_j\right) = N(X_i)P\left(R_j X\right);\\
&P\left(w_j \mid T_i\right) = \sum_{k=1}^{K} P\left(w_j \mid C_k\right)P(C_k \mid T_i).
\end{aligned} \tag{5}$$

Each particle in the particle swarm represents a possible solution to a problem. The intelligence of problem-solving is realized through the simple behavior of individual particles and the information interaction within the swarm. Due to its simple operation and fast convergence speed, PSO has been widely used in many fields such as function optimization, image processing, and geodesy.

The nonlinear time series of differential distributed data is projected to high-dimensional space f by the global call method of inertia weight, assuming that the training sample set of differential distributed data, $x_i \in R^n$, is the input vector for mining control of differentiated distributed data, and $y_i \in R^{\mathrm{n}}$ is the target value of particle swarm optimization. Thus, the total standard value of load balance of differential distributed data output in big data information base is obtained as follows:

$$\begin{aligned}
s(t) &= \sum_{k=1}^{N} p_k \sin\left(\omega_k n + \Phi_k\right) + \zeta(n),\\
H_G^*(x) &= \sum \frac{W_{\mathrm{data}}(x)}{W_{\mathrm{data}}(x) + W_g(x)},\\
E &= \log \frac{T_R(X)}{(1/2)\left[T(X) + T_g(X)\right]},\\
KL\left(V_1 \| V_2\right) &= E \log \frac{J_1}{J_2}.
\end{aligned} \tag{6}$$

Among them, $\zeta(n)$ is the modulation error of data mining, Φk is the data fusion degree, and ωk is the characteristic scale of distributed data. The data mining clustering in this study is shown in Figure 3.

The main data mining algorithms are as follows. (1) Association analysis: in nature, there are many related relationships among events, some of which are often known, and some of which are not easy to be found. For example, in the shopping basket, bread and milk are well-known collocations. When they are put together to promote sales, they can promote each other's sales. Without data analysis, people do not know the relationship between beer and diapers. Putting them together can also promote sales. In short, association analysis is the mining of association rules. For example, website designers can discover the relationship between visitors' habits and website pages according to visitors' logs; e-commerce can analyze customers' preferences according to customers' browsing records and stay time, so as to make targeted recommendations. Association analysis is the basis of other data mining research and has achieved good results in practical application. (2) Sequential pattern mining: the core of sequential pattern association analysis is to find out the pre- and postrelevance of the development of things, so as to dig out the laws with certain causal properties. Association analysis generally only considers simple association relations, while sequential pattern mining should consider time, space, and other factors. For example, after buying a new mobile phone, we will generally consider buying accessories such as film, which is the sequence relationship. Generally, we will not buy accessories before buying a mobile phone! This kind of sequence relation is very obvious, which is a typical sequence relation. The main algorithms are the Apriori algorithm and pattern growth framework. (3) Classification algorithm: the classification algorithm is a very important mining algorithm. Its main idea is to establish a classification model, then input data, and then use the classification model to predict its category. Classification mining is usually represented by a predicate. The typical applications of classification algorithms include credit rating, curative effect diagnosis, and customer rating. The main algorithms are k-nearest neighbor classification, decision tree classification, Bayesian classification, and so on. (4) Clustering algorithm: the clustering algorithm is also called group analysis. In classification, the class of samples is predictable. There are much other text mining, web mining, and so on. The design of each module of data mining is shown in Figure 4.

Data mining process is as follows:

(1) Data preprocessing: generally, the data is incomplete and polluted, and sometimes, there are inconsistencies in the data, such as code or name differences. The quality of data will determine the quality of mining. Generally speaking, low-quality data will produce poor quality data mining results. Therefore, before data mining, data preprocessing is generally needed to improve the quality of mining data.

(2) Mining process: after data preprocessing, select the appropriate data mining algorithm according to the mining purpose and task. There are also many data mining algorithms. Different mining algorithms have different characteristics, and the scope of application is different. The mining results are different. No one mining algorithm is suitable for all types of mining, and different mining algorithms will produce different mining results.

(3) Pattern evaluation: generally, the mining algorithm should remove useless output, provide the mining results to users in a way that users are interested in and easy to understand, and store the mining results effectively. That is, by setting a reasonable threshold of user interest to select the mode of user interest, it can effectively prevent the useful mode from drowning in the mode of many users not interested.

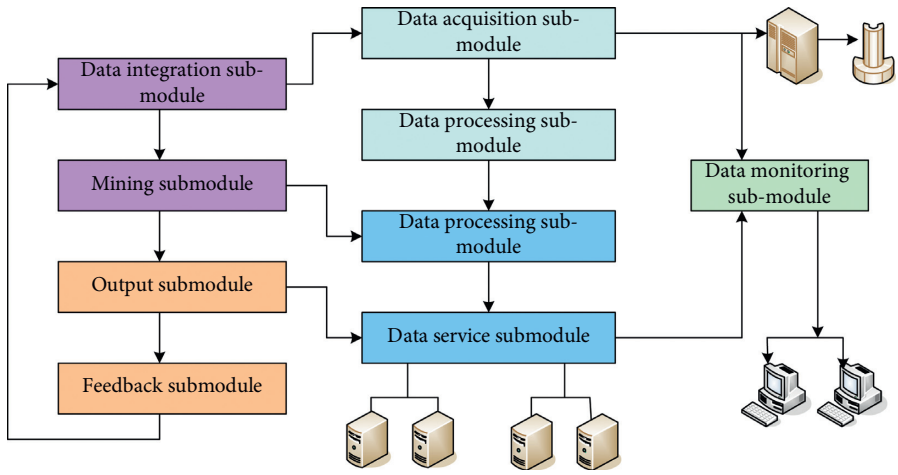

Figure 3: The data mining clustering in this study.

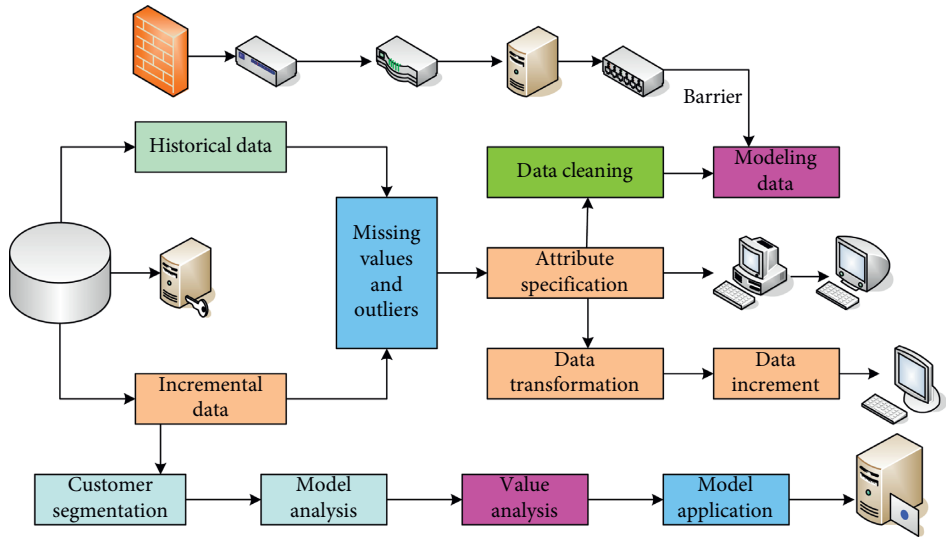

Figure 4: The design of each module of data mining.

Finally, data mining will output knowledge. Generally, this knowledge cannot be found by our intuition. Some knowledge even goes against our intuition, which is unexpected. But the more such knowledge, the more valuable it may be. The detailed process of data mining is shown in Figure 5.

2.3. Cluster Optimization. We call the process of segmentation a clustering process and the method of segmentation a clustering algorithm. In clustering analysis, data are divided according to certain rules. The result of its function is to divide the data into classes so that the similarity between classes is small and the similarity within classes is large. At present, although there are many kinds of clustering algorithms, they all have their own characteristics and applicability. Taking the definition forms of five basic clustering

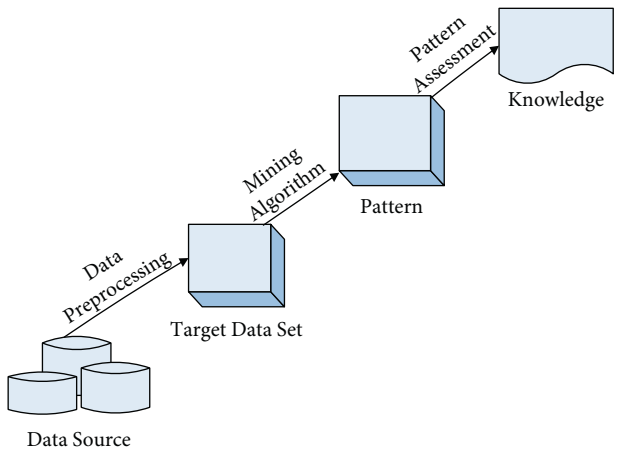

Figure 5: Basic process of data mining.

algorithms as examples, this paper makes the following explanation:

(1) Partition method: this method can find the spherical mutually exclusive clusters, and the center of clusters is represented by mean value or center point. This algorithm is suitable for those clustering problems with a fixed number of clusters and a small data set. Among these methods, K-means and K-median are the most classical ones.

(2) Hierarchical method: this method is based on the idea of hierarchical decomposition clustering. The disadvantage of this method is that it cannot be corrected, such as the error of merging or splitting, and this kind of method can carry out multilevel clustering at different granularity. That is to say, if you want to process very complex data, you have to know how to summarize and count these data in a systematic and purposeful way.

(3) Density-based method: the cluster density described in this clustering method refers to the minimum number of samples in a single sample space. This algorithm can find clusters with different regular shapes without forcing the shape of clustering. It is suitable for clustering with an irregular number and random shape and has the advantage of reducing or even eliminating noise.

(4) Which can analyze the validity of the data model, such as data fitting? It is suitable for data distribution that has been classified.

(5) Grid-based method: the algorithm clusters the quantitative grid space, speed, and a strong computing advantage.

The boundary between different types of clustering algorithms is usually not very clear. Taking mean shift algorithm as an example, its basic idea is to move sample points from areas with low density to areas with high density: from the perspective of density estimation and density gradient estimation, it can be regarded as a density clustering algorithm; however, some K-means algorithms can be regarded as mean shift using special kernel function At the same time, the maximum entropy clustering algorithm based on physical model can also be regarded as mean shift algorithm with a special kernel function. Five clustering methods are introduced as follows.

2.3.1. Segmentation and Clustering. K-means and K-means are two typical segmentation and clustering methods, which usually need the number of clusters input by users. Through continuous iterative optimization, the minimum distance within the cluster is the maximum distance between the clusters. Randomly select k clustering centers: $\mu 1$, $\mu 2$, and μk; repeat the following steps to convergence; for each sample, calculate its class:

$$
\begin{aligned}
c_i &= \arg\min_j \left\| x^{(i)} - \mu_j \right\|^2, \\
V(M,N) &= E_{x\sim p\text{data}(x)}[\log M(x)] \\
&\quad + R_{z\sim pz(z)}[\log(L - N(G(K)))], \\
Y(B,D) &= R[\log C(X \mid Y)] + M[\log(V - G(M(L \mid K)))], \\
D_H^*(x) &= \frac{Q_D(x)}{Q_D(x) + Q_D(x)}.
\end{aligned}
\tag{7}
$$

The K-means algorithm is more efficient for small-scale data sets, while the K-Medoids algorithm has better performance for large-scale data, but it has poor scalability. In addition, the K-means algorithm has two main defects: second, the clustering results are affected by the initial cluster center. There are many researches on the improvement of K-means in the scientific community. K-means++ is a representative one. And the difference lies in the selection strategy of the clustering center: the clustering center of K-means is located at the average of coordinates of all points in the cluster, while the clustering center of K-means must be a sample point in the cluster, and the cluster distance of all points in the cluster with it as the center is the smallest. Compared with K-means, the complexity of the segmentation clustering algorithm is low, and it is suitable to deal with large-scale data. CLARANS algorithm is a representative algorithm. It makes large-scale data clustering have high efficiency and good scalability through random search strategy. The segmentation clustering algorithm is usually easy to parallelize, and it is active in big data processing platforms in recent years.

2.3.2. Hierarchical Clustering Algorithm. According to the similarity between data points, the hierarchical clustering algorithm decomposes hierarchically and creates a nested clustering tree with a hierarchical structure. The bottom-up hierarchical decomposition corresponds to the agglomerative method and the top-down hierarchical decomposition corresponds to the splitting method. The basic flow of aggregation method and splitting method is shown in Figure 6. For example, in the first step, {a, b, c, d, e} is a cluster, in the first step, B and C elements which are both quadrilateral are clustered into a cluster, in the second step, D and e elements which are both circular are clustered into a cluster, in the third step, polygon elements are clustered into a cluster, and in the fourth step, all elements are clustered into a cluster. According to the different distance measurement methods between clusters, SL hierarchical clustering has a single linkage), CL hierarchical clustering has complete linkage), and Al hierarchical clustering has an average linkage). The typical hierarchical clustering algorithms are birch, cure, and chameleon. In recent years, some improved algorithms improve their efficiency and robustness.

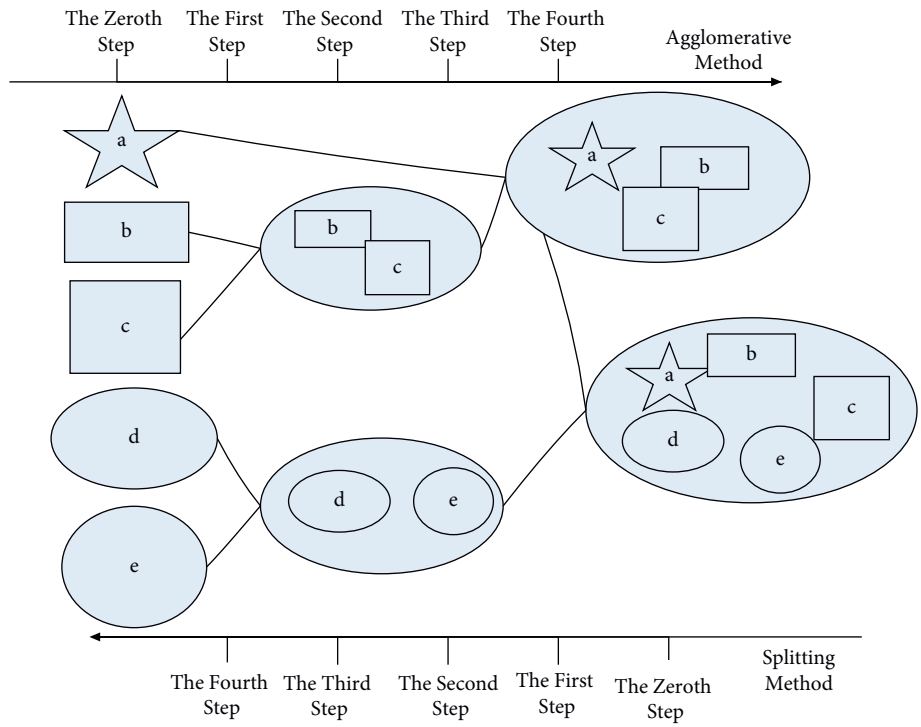

Figure 6: The basic flow of cohesion method and splitting method.

2.3.3. Density Clustering. The earliest idea of clustering based on density may come from the DBSCAN algorithm: the algorithm divides the regions with sufficient density into clusters and finds clusters of arbitrary shapes in the noisy spatial database. It defines the clusters as the largest collection of points with connected density, according to the local density of sample points; it can be divided into core points. DBSCAN is very sensitive to parameters, and slight changes of parameters may lead to abrupt changes in clustering results, which seems to be caused by the sensitivity of core points and boundary points to local density thresholds. Nonspherical clusters, GDBSCAN, ENDBSCAN, options, cancel, clusters, and other density clustering algorithms can identify clusters of any shape, besides DBSCAN like clustering algorithm, mean shift clustering algorithm, and density peak.

2.3.4. Grid Clustering. The grid clustering method divides the space into several grids and analyzes the data on the grid. The complexity of the clustering process is usually related to the number of grids and the number of sample points, so it is more efficient in processing some data. Common grid clustering methods include sting, wave cluster, clique, optigrid, and enclus. Sting algorithm is a multiresolution clustering method, the data space is divided into several rectangular cells, and each high-level rectangular cell is nested with many fine-grained rectangular cells. Generally speaking, the grid clustering method should consider how to divide the cells, how to choose the appropriate cell size, and how to store the updated cell information. If the grid cells are not refined enough, the accuracy will be lost, and if the grid cells are too refined, the computation cost will be increased. The scalability of the grid clustering method depends on the strategy of storing and updating grid cells to a great extent. Because the boundary of grid cells is horizontal or vertical, the grid clustering method can only find grid-like clusters, not inclined boundaries.

2.3.5. Model Clustering. The model clustering algorithm assumes that the data is mixed according to a specific probability distribution, which is dedicated to finding the best fit between the data and the given model: statistical learning/machine learning methods (such as cobweb) and artificial neural network methods (such as SOM). Taking the SOM algorithm as an example, it is a neural network composed of the input layer and competition layer, as shown in Figure 7.

In the process of clustering, each node first initializes its own parameters randomly, then matches the best node for each input data, then updates the adjacent nodes according to the activated nodes, and finally updates the node parameters according to the gradient descent method, and then repeats the iterative updating until convergence. In the process of the development of model clustering, many researchers put forward the improved algorithm, which is applied to text data.

3. Experiments

3.1. Subjects. Three classic data sets Iris, wine, and zoo are for experimental verification. The accuracy and convergence are analyzed and verified. The characteristics of the test data set are described in Table 1.

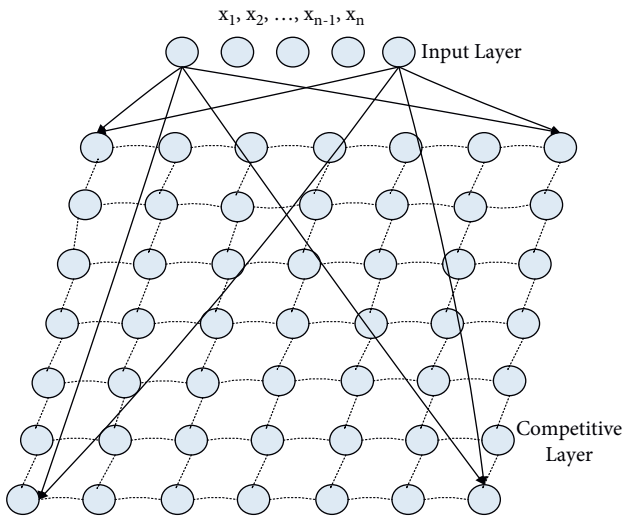

Figure 7: Kohonen network structure.

The main parameters are set, learning factor cmax = 2.5, and the minimum value cmin = 0.5. Other parameters can be set flexibly according to the experimental situation.

3.2. Experimental Setup. At present, most clustering effect analysis often uses F-measure, which includes recall and precision. Recall and precision, respectively, examine the completeness and accuracy of experimental analysis. The definitions are as follows.

$$\text{Recall}(i, j) = \frac{N_{ij}}{N_j},$$
$$\text{Precision}(i, j) = \frac{N_{ij}}{N_i}, \tag{8}$$

where i is the known category; see the following formula:

$$F(i) = \frac{2 * \text{Precision}(i, j) * \text{Recall}(i, j)}{\text{Precision}(i, j) + \text{Recall}(i, j)}. \tag{9}$$

The commonly used measurement method of cluster analysis is the weighted average value of category i:

$$F - \text{measure} = \frac{\sum_{i \in n} |i| * F(i)}{\sum_{i \in n} |i|}. \tag{10}$$

The average value is the final F-measure measurement value, as shown in Table 2.

It can be seen from Table 2 that the ADPSO-k-mean algorithm has higher accuracy than the traditional k-mean algorithm and the PSO-k-mean algorithm and has relatively large optimization effect; especially in the Iris data set, the experimental accuracy has increased by 19.5% and 7%, respectively, with the most obvious effect.

4. Discussion

4.1. Test of Each Fitness Value When Each Algorithm Converges Stably. Also, Iris, wine, and zoo are used to test the stability of the algorithm. The fitness values ($f_{\min}$, $f_{\max}$, and f_{ave}) of each algorithm are recorded when the algorithm converges stably, and the $f(x)$ on three kinds of data sets are, respectively, in the following formula:

Table 1: Test data set.

Test data set	Number of data	Cluster number
Iris	151	4
Wine	177	2
Zoo	100	8

$$f(x) = \frac{\zeta}{\sum_{j=1}^{k} \sum_{X_i \in C_j} d\left(X_i, C_j\right)},$$
$$M = \frac{|S_1 \cap S_2|}{KL}. \tag{11}$$

From 103, 105, and 102, ζ is the constant $d(X_i, C_j)$, which represents the Euclidean metric distance from sample X_i to the corresponding cluster center C_j. Tested many times, the average value of all similar test data is taken as the final value (for example, by all tests, it is taken as the maximum fitness value). The test records are shown in Table 3.

According to the analysis of test results in Table 3: on the whole, the improved ADPSO-IKM algorithm has a relatively small $f(x)$ fluctuation range in these three types of data sets. The PSO-k algorithm and ADPSO-IKM algorithm improve 9.95%, 12.44%, and 20.85%, respectively, in three data sets. And the improvement of the center K-means algorithm itself ensures the effective search and better convergence performance of the algorithm. In order to further illustrate the convergence of ADPSO-IKM algorithms and the fitness value of each algorithm with the increase of iterations, the convergence graphs on three datasets are drawn. The format design of the training sample of the digit recognizer is shown in Table 4.

After training the network, we test the function approximation ability of the network with the test sample set of an unknown result. The output of the test sample set in the network model is shown in Figure 8.

It can be seen from the final test results that the network model can reach an accuracy rate of approximately 78.5%.

The drug is used as a classification attribute, and there are 5 categories in total; others are used as input attributes. All nominal attributes must be processed numerically; for example, BP is converted to 0: high; 1: low; and 2: normal. We design an RBF network so that it can correctly reflect the drug classification of the sample data after training. The training sample data is shown in Table 5.

We take the drug as the classification attribute, a total of 5 categories, and others as input attributes. All nominal attributes must be processed numerically; for example, BP is converted to 0: high, 1: low, and 2: normal. We design an RBF network so that it can correctly reflect the drug classification of the sample data after training. The training sample data is shown in Table 6.

The attributes of these animals are mapped to the two-dimensional output plane of SOM, and the self-organizing

Table 2: Experimental results of *F*-measure.

Algorithm	Data Set		
	Iris	Wine	Zoo
K- mean value	0.706	0.622	0.555
PSO-K-mean value	0.830	0.700	0.602
ADPSO-k-mean value	0.875	0.711	0.620
KHM-CPSO	0.884	0.720	0.673
ADPSO-IKM	0.900	0.728	0.696

Table 3: Results of algorithm fitness value.

Data set	$f(x)$	K- mean value	PSO-K-mean value	ADPSO-k-mean value	ADPSO-IKM
Iris	$f_{\min}$	8.2424	10.2494	10.2716	10.2980
	$f_{\max}$	10.2495	10.3833	10.4043	10.4540
	f_{ave}	9.5843	10.3019	10.3785	10.4011
Wine	$f_{\min}$	5.3290	5.8155	5.8791	5.8914
	$f_{\max}$	5.8966	5.9026	5.9130	5.9779
	f_{ave}	5.5981	5.8290	5.9011	5.9533
Zoo	$f_{\min}$	6.0471	6.4329	6.5706	6.5910
	$f_{\max}$	6.3126	6.5872	6.6015	6.6305
	f_{ave}	6.2156	6.4138	6.5881	6.6222

Table 4: The format design of the training sample of the digit recognizer.

Number	$X0$	$X1$	$X2$	$X3$
0	0	0	1	1
1	1	0	1	0
2	0	0	1	0
3	1	1	0	0
4	1	1	1	0
5	1	1	1	1
6	1	1	0	0
7	1	1	1	0
9	1	1	0	1

clustering process is used to test the rule that the attributes of samples between adjacent clusters are similar. There are 13 kinds of animals in the training set, and each animal is represented by a 9-dimensional vector. The training samples are shown in Table 7.

After 10,000 times of network training, the SOM network maps the pattern features of the high-dimensional space input data to the two-dimensional output plane in an orderly manner. The training results show that 15 neurons arranged in a $5 * 3$ rectangular (Gridtop) structure finally form 9 effective clusters. The clustering results are shown in Table 8.

The learning error change of the BP network combined with the genetic algorithm for the approximation of the sine function is shown in Figure 9. Because the genetic algorithm has a global search property, the optimized initial weight generated iteratively is compared with the real solution space in the direction of the optimal solution is closer; this makes the error of the BP network training process based on the gradient descent method tend to drop quickly at the beginning.

The change of the learning error of the pure BP algorithm is shown in Figure 10. The error convergence effect of BP network learning combined with the genetic algorithm is still better than the pure BP algorithm.

We reduced the network training times by 2 K/time, and the training results are shown in Table 9.

The attribute field includes the content of certain chemical substances in the DFM sample, the average daily alcohol consumption, etc. Take 180 of the data set samples as the training sample set and 50 as the test sample set. Part of the data is shown in Table 10.

Display the clustering results in the form of statistical histograms: this is mainly done by using the open-source chart drawing toolkit JfreeChart. The visual display of its clustering statistical histogram is shown in Figure 11.

In the system's BP neural network parameter settings, set the target error to 0.001, the number of training times to be 1,000, and the learning rate to be 0.01, respectively. The "weight" method reads the initial connection weight selected before and then starts the formal network training. After system operation analysis, the output error curves are shown in Figure 12.

4.2. Performance Comparison of Different Algorithms

4.2.1. Convergence of Each Algorithm on Iris. In the Iris data set, from the iterative trend line within 20 times of PSO-K-means algorithm, it can be seen that the ADPSO algorithm can significantly expand the overall optimization space of the algorithm between 20 and 30 times of iteration and avoid falling into the local extreme situation, and the iteration to 30 times has become stable convergence state. The convergence on Iris is shown in Figure 13.

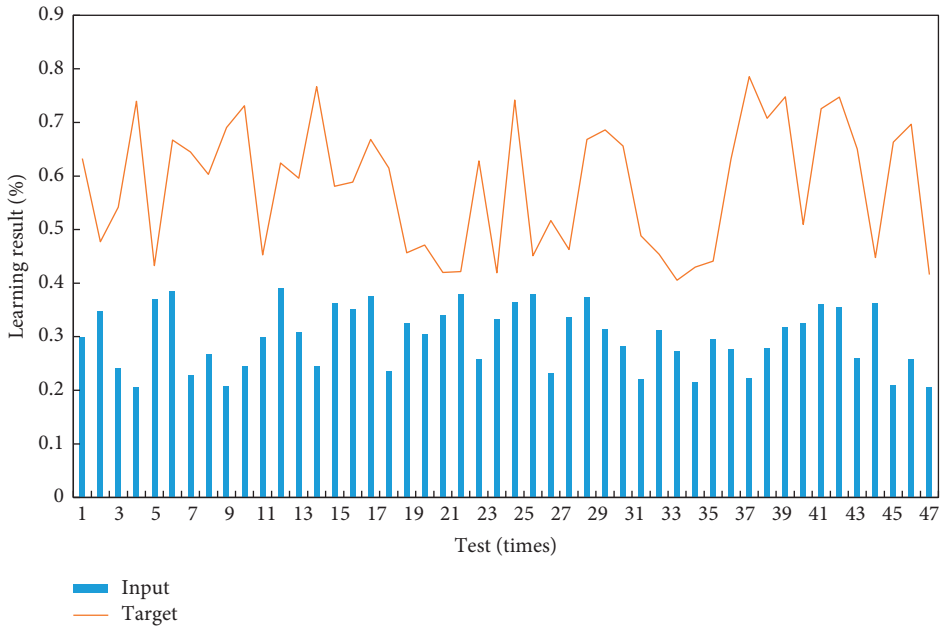

Figure 8: The output of the test sample set in the network model.

Table 5: The training sample data.

Number	$X0$	$X1$	$X2$	$X3$
0	0	0	1	1
1	1	0	1	0
2	0	0	1	0
3	1	1	0	0
4	1	1	1	0
5	1	1	1	1
6	1	1	0	0
7	1	1	1	0
9	1	1	0	1

Table 6: The training sample data.

Age	Sex	BP	Na/K
23	F	High	25.35
47	M	Low	13.09
47	F	Low	10.11
28	F	Normal	7.80
61	F	Low	18.04
22	F	Normal	8.61
49	M	Normal	16.28
41	F	Low	11.04
60	M	Normal	15.17

Table 7: The training samples.

Animal	Body type	Number of limbs	Mane
A	Small	2	0
B	Small	2	0
C	Small	2	0
D	Small	4	0
E	Small	4	0
F	Middle	2	0
G	Middle	2	0
H	Middle	2	1
I	Small	2	0

Table 8: The clustering results.

Animal	Body type	Water	Body type	Number of limbs
Clustering0	Small	0	Small	2
	Small	0	Small	2
	Small	0	Small	2
Clustering2	Small	0	Small	4
	Small	1	Small	4
Clustering4	Middle	0	Middle	2
	Middle	0	Middle	2
	Middle	0	Middle	2
Clustering6	Small	0	Small	2

4.2.2. Convergence of Each Algorithm on Wine. The high latitude wind data set, from the overall trend chart of the algorithm, has the same convergence trend, and compared with the k-mean algorithm, the convergence effect is obvious. ADPSO-IKM algorithm iterates 40 times to reach a stable convergence state. The convergence on wine is shown in Figure 14.

4.2.3. Convergence of Each Algorithm on Zoo. In the data set zoo, the ADPSO-IKM algorithm approximately iterates 30 times and converges to the best situation. The introduction of the IKM algorithm can obviously accelerate the clustering speed of iterations between 25 and 35 times and also can quickly find excellent solutions. The convergence on wine is shown in Figure 15.

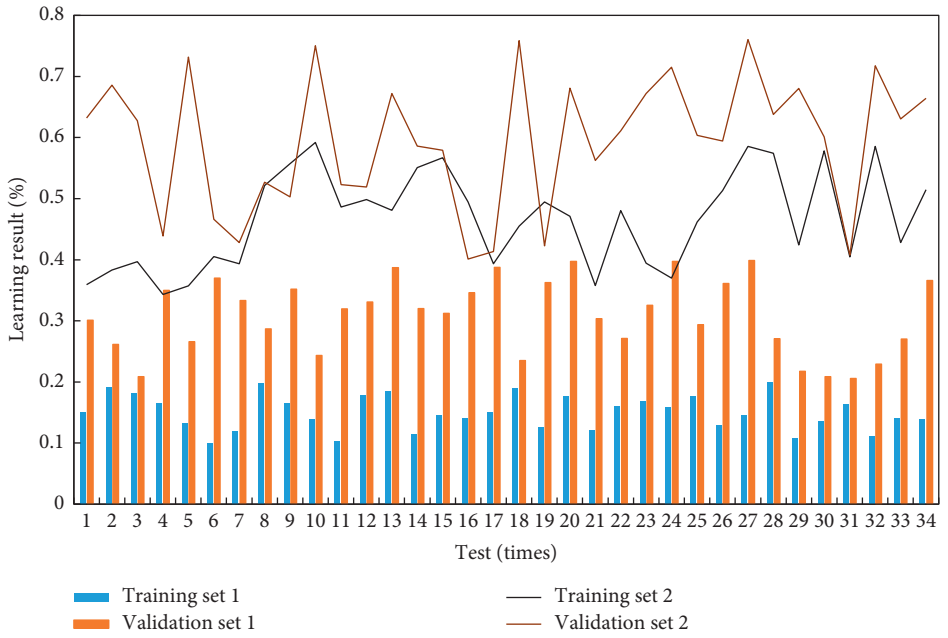

Figure 9: The learning error change of the BP network combined with the genetic algorithm for the approximation of the sine function.

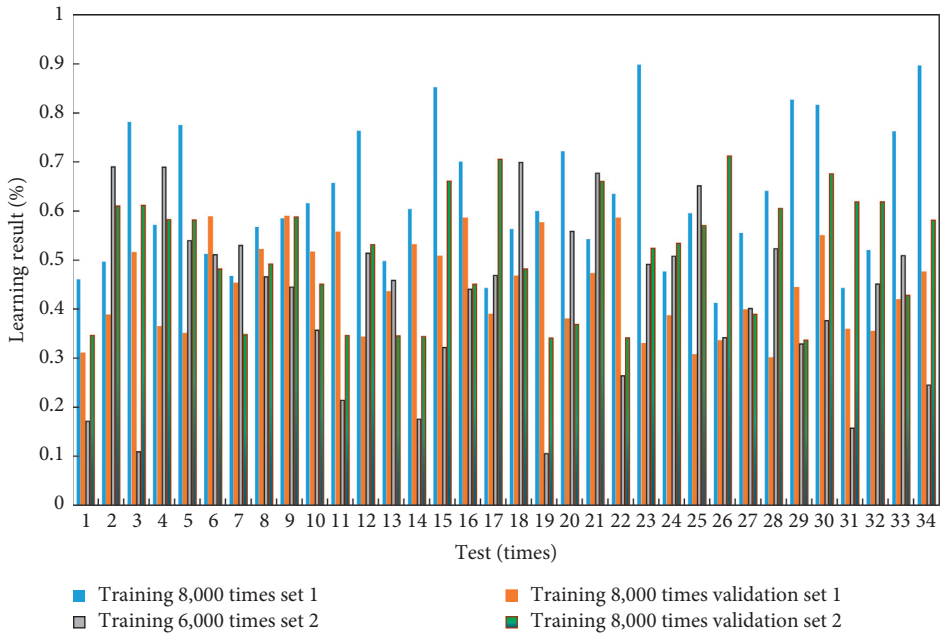

Figure 10: The change of the learning error of the pure BP algorithm.

Table 9: The training results.

Training times	Water	Error of BP network learning combined with genetic algorithm	Pure BP algorithm learning error
8000	0.001	Error of BP network learning combined with genetic algorithm	0.002
6000	0.001	Error of BP network learning combined with genetic algorithm	0.007
4000	0.002	Error of BP network learning combined with genetic algorithm	0.029

Table 10: Part of the data.

A1	A2	A	A4	A5
37	78	20	24	86
98	70	21	28	10
88	55	25	11	7
88	62	13	20	1

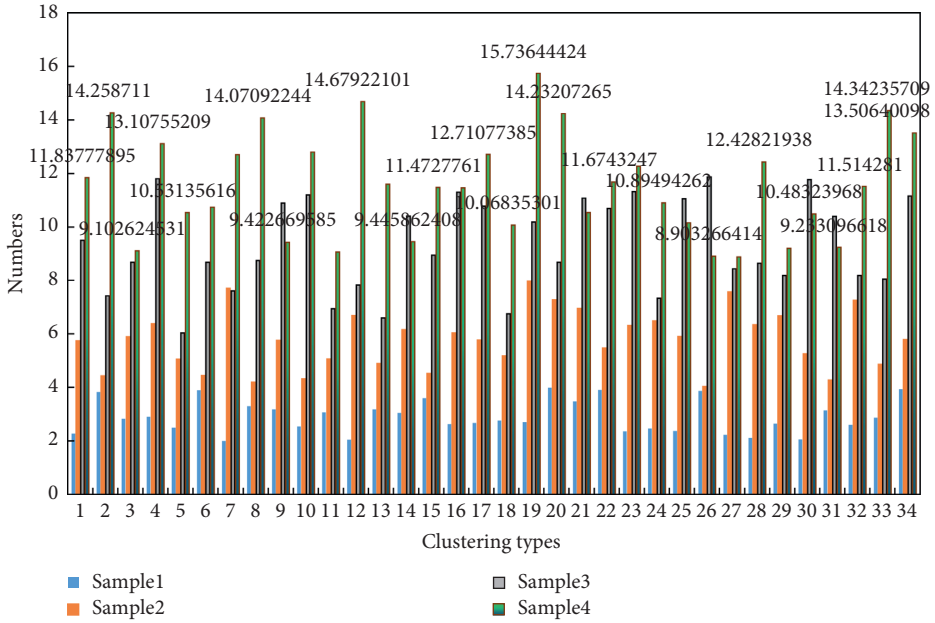

Figure 11: The visual display of its clustering statistical histogram.

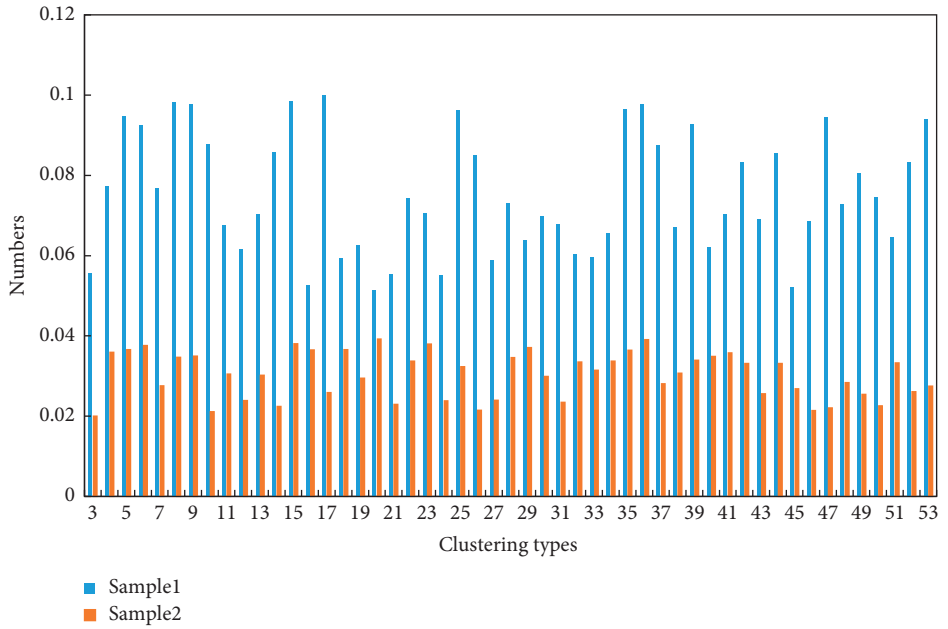

Figure 12: The output error curves.

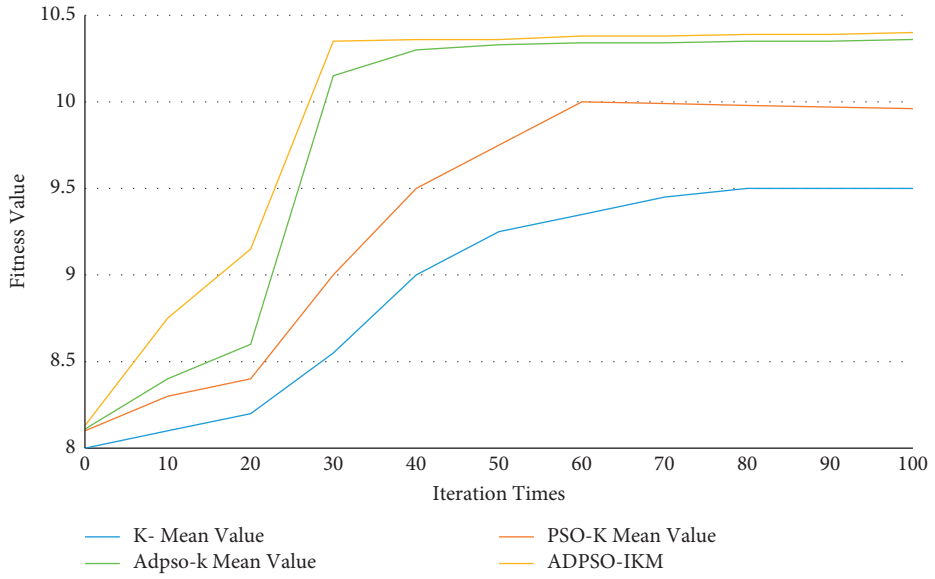

Figure 13: Convergence of each algorithm on Iris.

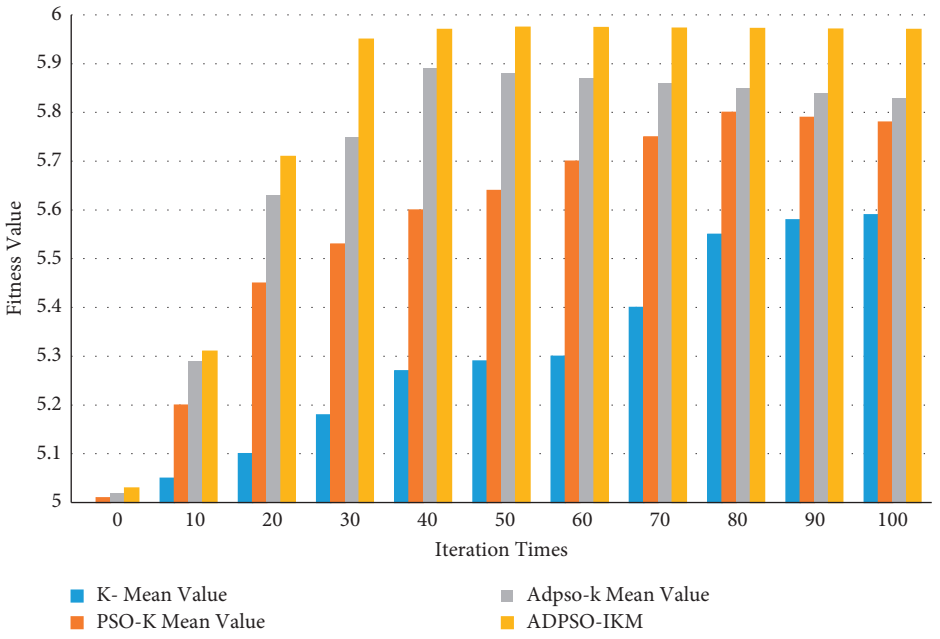

Figure 14: Convergence of each algorithm on wine.

On the whole, the algorithm iterates on the dataset and tends to be stable and convergent. Compared with other algorithms, the ADPSO-IKM algorithm has better convergence performance and can reduce the influence of initial cluster center selection on the volatility of the K-means algorithm. Moreover, the improved neighborhood fusion idea can make the algorithm extend to the effective search area. In a small iteration range, it can get a good clustering

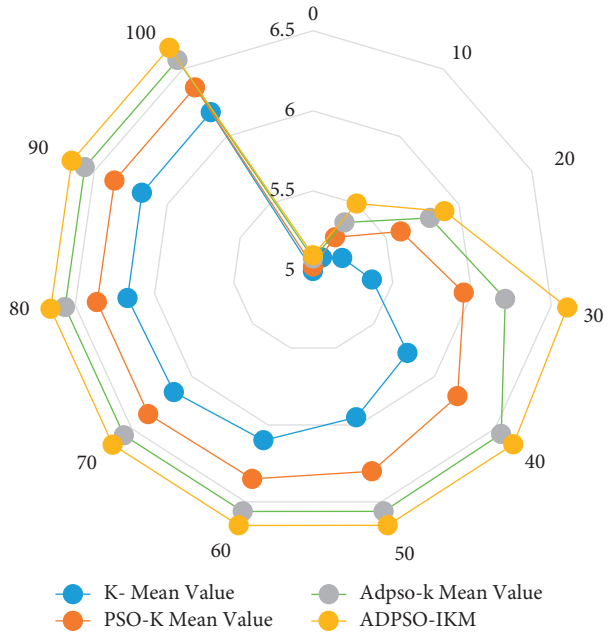

Figure 15: Convergence of each algorithm on the zoo.

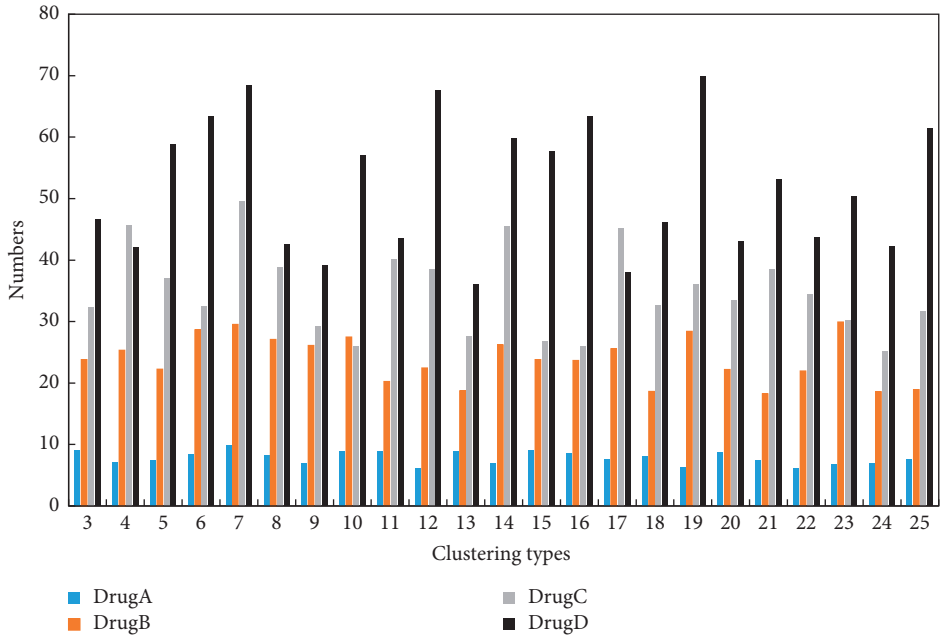

Figure 16: The new data classification result of the drug classification problem.

convergence effect. According to the overall trend chart of the three data sets, the ADPSO-IKM algorithm has good optimization performance and can quickly converge to the clustering effect of a fixed value. In the ADPSO-k average algorithm and the introduction of the IKM algorithm, the overall clustering optimization effect of the algorithm has not been significantly improved, and the research in this area needs to be improved. The new data classification result of the drug classification problem is shown in Figure 16.

The prediction result based on the improved algorithm is shown in Figure 17.

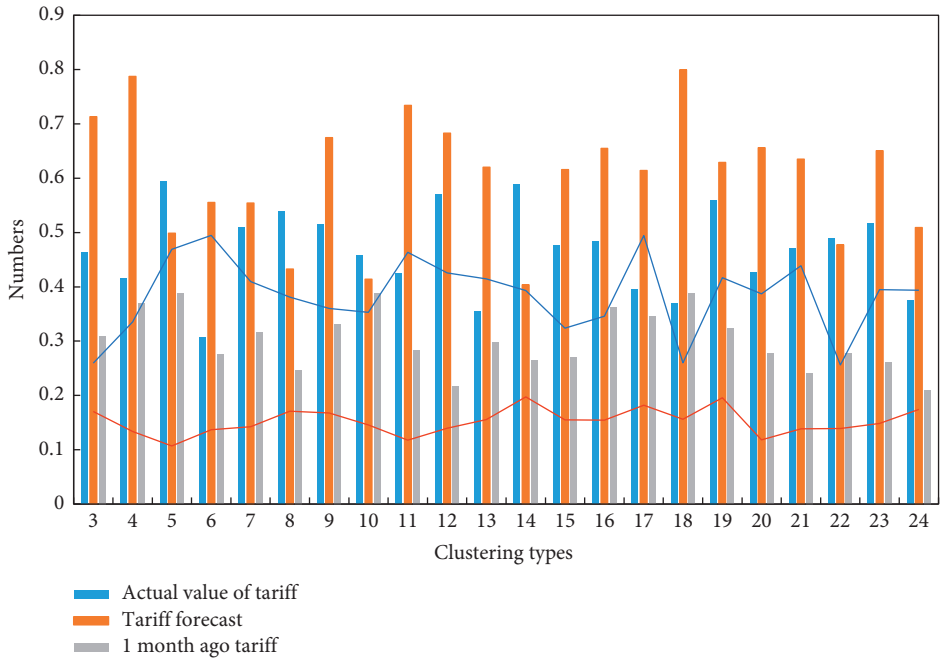

Figure 17: The prediction result based on the improved algorithm.

5. Conclusions

In this era of massive data, data mining is extremely important, its application is more and more extensive, and its importance is more and more obvious. As long as an enterprise has a data warehouse or database with analysis value and demand, it carries out purposeful data mining. Data mining will mean a new wave of productivity growth and the arrival of the consumer surplus wave. In the data mining project, if a reasonable network model can not be determined in advance when dealing with some complex problems with the BP model, used for global optimal search, this algorithm is very effective for improving the accuracy and accuracy of data mining in CRM and obtaining a lot of valuable data.

The traditional clustering algorithm is difficult to deal with data with multidimensional and uncorrelated characteristics. The selection of clustering methods directly determines the quality of data mining. In order to improve the quality of clustering, people continue to explore and explore better clustering analysis methods. The group intelligence, self-adaptability, and robustness are shown by the group intelligence optimization algorithm; combined with the group intelligence optimization, cluster analysis develops rapidly.

The generalization ability of particle swarm learning is used to calculate the clustering center of data mining, to realize data mining optimization. The clustering algorithm of neural network data mining proposed in this paper can realize the clustering completed by the K-means method. At the same time, the improved neural network algorithm can automatically merge the clustering results with smaller granularity according to the preset warning value, thus effectively preventing the occurrence of unreasonable clustering results caused by too many specified clustering numbers. Because the artificial neural network has the characteristics of highly nonlinear to noisy data, BP neural network is more popular. Because the artificial neural network has the characteristics of highly nonlinear learning ability and fault tolerance to noisy data, the artificial neural network and BP neural network are more popular. The ability of artificial neural networks to extract rule knowledge needs to be further strengthened. The artificial neural network uses the "black box" model to process data and mine knowledge. In some data mining applications, people often expect the system to express deep-level knowledge of laws in an intuitive way similar to "if-then." Therefore, we need to know how to break this black box and explicitly present the useful knowledge hidden.

Data Availability

No data were used to support this study.

Conflicts of Interest

The authors declare that they have no conflicts of interest.

Acknowledgments

This work was supported by the Young Innovative Talents Project in Guangdong Province in 2020 (no. 2020KQNCX109).

References

[1] J. Albericio, P. Judd, T. Hetherington, T. Aamodt, N. E. Jerger, and A. Moshovos, "Cnvlutin," *ACM SIGARCH - Computer Architecture News*, vol. 44, no. 3, pp. 1–13, 2016.

[2] S. Han, X. Liu, H. Mao et al., "Eie," *ACM SIGARCH - Computer Architecture News*, vol. 44, no. 3, pp. 243–254, 2016.
[3] F. Wang, V. K. Devabhaktuni, and C. Xi, "Neural network structures and training algorithms for RF and microwave applications," *International Journal of RF and Microwave Computer-Aided Engineering*, vol. 9, no. 3, pp. 216–240, 2015.
[4] L. Qiao, Y. Li, D. Chen, S. Serikawa, M. Guizani, and Z. Lv, "A survey on 5G/6G, AI, and robotics," *Computers & Electrical Engineering*, vol. 95, Article ID 107372, 2021.
[5] T. Si and S. Sujauddin, "A comparison of grammatical bee colony and neural networks in medical data mining," *International Journal of Computer Application*, vol. 134, no. 6, pp. 1–4, 2016.
[6] S. Hussain, J. Hazarika, and P. Buragohain, "Educational data mining on performance of under graduate students of dibrugarh university using R," *International Journal of Computer Application*, vol. 114, no. 11, pp. 975–8887, 2015.
[7] X. Zhou, X. Liang, X. Du, and J. Zhao, "Structure based user identification across social networks," *IEEE Transactions on Knowledge and Data Engineering*, vol. 30, no. 6, pp. 1178–1191, 2018.
[8] S. R. Chauhan and A. Desai, "A review on knowledge discovery using text classification techniques in text mining," *International Journal of Computer Application*, vol. 111, no. 6, pp. 12–15, 2015.
[9] H. Chen, Y. Shang, and K. Sun, "Multiple fault condition recognition of gearbox with sequential hypothesis test," *Mechanical Systems and Signal Processing*, vol. 40, no. 2, pp. 469–482, 2013.
[10] S. Singh, R. Garg, and P. K. Mishra, "Performance analysis of Apriori algorithm with different data structures on Hadoop cluster," *International Journal of Computer Application*, vol. 128, no. 9, pp. 975–8887, 2015.
[11] X. Zhang, Y. Tian, and R. Cheng, "A decision variable clustering-based evolutionary algorithm for large-scale many-objective optimization," *IEEE Transactions on Evolutionary Computation*, vol. 99, 2016.
[12] Z. Lv, Y. Han, A. K. Singh et al., "Trustworthiness in industrial IoT systems based on artificial intelligence," *IEEE Transactions on Industrial Informatics*, vol. 99, p. 1, 2020.
[13] A. Zl, A. Dc, A. Rl, and B. Aa, "Artificial intelligence for securing industrial-based cyber–physical systems," *Future Generation Computer Systems*, vol. 117, pp. 291–298, 2021.
[14] T. . İnkaya, S. Kayalıgil, and N. E. Özdemirel, "Ant Colony Optimization based clustering methodology," *Applied Soft Computing*, vol. 28, pp. 301–311, 2015.
[15] X. Xu, D. Cao, Y. Zhou, and J. Gao, "Application of neural network algorithm in fault diagnosis of mechanical intelligence," *Mechanical Systems and Signal Processing*, vol. 141, Article ID 106625, 2020.
[16] P. H. Thong and L. H. Son, "A novel automatic picture fuzzy clustering method based on particle swarm optimization and picture composite cardinality," *Knowledge-Based Systems*, vol. 109, pp. 48–60, 2016.

Hindawi
Wireless Communications and Mobile Computing
Volume 2022, Article ID 1863568, 8 pages
https://doi.org/10.1155/2022/1863568

Research Article

Retweet Prediction Based on Multidimensional Features

Xiaomeng Fu, Suyan Cheng, Li Zhao, and Jiaguo Lv

College of Medical Information and Engineering, Jining Medical University, Rizhao 276826, Shandong, China

Correspondence should be addressed to Jiaguo Lv; jglv2018@mail.jnmc.edu.cn

Received 10 November 2021; Revised 7 December 2021; Accepted 21 January 2022; Published 16 February 2022

Academic Editor: Mohamed Elhoseny

With the wide use of artificial intelligence-driven mobile devices, more and more Chinese people take part in the Twitter-like social sites, which makes Weibo an excellent communication platform. In view of the wide application of information diffusion in various fields, Weibo has become one of the most important research issues in mobile social computing. In Weibo, the retweet statuses of tweets of other users are considered to be the key mechanism for spreading information. How to predict whether a tweet will be retweeted by a user has received increasing attention in recent years. Research shows that the users' retweet behavior is driven by their interest and personality. However, most previous works ignore the roles of users' personality in their retweet behavior. To this end, a prediction model MDF-RP (multidimensional feature-based retweeting prediction) including personality feature is proposed. The prediction model integrates the features from three dimensions, such as author, tweet, and user. And the personality score is obtained based on the well-known Big Five personality trait model. The experimental results under different classifiers show that the performances of MDF-RP features outperform the basic features. And the experiments of cross-validation also demonstrate the stability of MDF-RP features.

1. Introduction

In recent years, along with the extensive use of artificial intelligence-driven mobile devices, various mobile applications become more and more popular and profoundly change people's life. Due to the thousands of millions of users' participation, the mobile social network has been the most popular one. As the most popular online social media in China, Weibo has become an import platform for people to get and share information. In the Twitter-like social media sites, a user may share his or her life, works, and opinions with other users in the form of short message. A user may follow another user without his consent, and information can spread belong the following relationship among users, which forms an information diffusion network. Some characteristics of Weibo, such as the usage of "@, #, . . ." and weak friendship of users, make it different from other social media in terms of universality and immediacy of user participation, information diffusion mode, and speed. When users find interesting tweets and want to share them with their followers, they can retweet them using a button or other mechanisms to copy and post these tweets. The retweet function provided by this platform is usually considered to be the key mechanism for spreading information among users. To capture the dynamics of information diffusion occurring in social networks, it is necessary to model and predict user's retweet behaviors. Retweet prediction can predict whether a tweet can be retweeted by an individual and predict the diffusion scale of a given tweet. With the help of retweet prediction, some tweets that may trigger a large-scale outbreak will be found as soon as possible. Retweet prediction plays an important role in hot-topic detection [1], personalized tweet recommendation [2, 3], and information propagation prediction [4–6].

The rest of this article is organized as follows. The related work is described in Section 2. In Section 3, the prediction problem is formally defined. In Section 4, the MDF-RP method is introduced. Section 5 shows the experimental setup and evaluation results. Finally, the work is concluded in Section 6.

2. Related Work

Due to the enormous usefulness of prediction, a variety of studies have been conducted on the retweet prediction problem. The studies are carried out in two ways: one is

author-centered, and the other is user-centered. For a given tweet, the former is employed to predict the scale of its retweet volume, and the latter is to predict whether a given user will retweet it or not. The author-centered work usually gets the influential factors via the statistics of the author, Twitter content, and post time. For example, those tweets with hashtag, URL, and other information are more likely to be retweeted. The more authoritative the author is, the more likely his tweet will be retweeted. Although the author-centered work has achieved good performance, it ignores the individual difference of each user. Therefore, researchers turned to the user-centered work. Different from the author-centered work, in the user-centered prediction, besides the tweet and author features, user features should be taken into account. Under the MRF (Markov random field) energy optimization framework, Wang et al. [7] analyzed the effects caused by user attributes, tweet content, the constraints between users' retweet behavior, and the group retweet priors. Then, they constructed the corresponding energy function on the basis of the LR (logistic regression) model to predict users' retweet behaviors globally, which improved the accuracy of the proposed method. Taking into account the effects of tweet emotional difference on retweet prediction, Tang et al. [8] extended the semantic features of tweet text by Wikipedia knowledge base to mine users' interest and verified the effectiveness of the method with experiments. Analyzing the effects of users' interest, tweet contents, and others on retweet prediction, based on the factor graph model, Yang et al. [9] proposed a semisupervised framework to predict users' retweet behavior and found that the proposed method performed better than other existing methods. From the perspectives of users' dynamic interest, social relationship, and retweet behavior, the authors [10] proposed a prediction method combining multiple retweet features and found that social relationship had the greatest promotion on prediction accuracy. Wang et al. [11] extracted features from user profiles, user history, target tweet, and user network by a deep learning method to address the retweet prediction problem, which can effectively predict the retweet behavior of users in the experiments.

The existing author-centered work predicated users' retweet behaviors with their interest, which was mined from their historical tweets [9, 10, 12–16]. In psychology, psychologists attributed individuals' different reactions in the same environment to their personality. Personality is a stable mode of thoughts, emotion, and behaviors across time and situation [15]. Research showed that people's behavior in the social network was highly consistent with that in reality. Users' retweet behavior in Weibo was an explicit reflection of their personality. Tweet content was reflective of the author's personality. In the personality theory, Big Five personality [17] is the most effective one in evaluating individual differences. Big Five personality describes an individual's personality traits from five dimensions: extroversion (EXT), neuroticism (NEU), agreeableness (AGR), conscientiousness (CON), and openness (OPN). Therefore, the personality trait score obtained from a user's tweets will be selected as an import feature for retweet prediction problem.

In conclusion, taking the user as the center, considering the factors affecting a user's retweet behavior from three dimensions of author, tweet text, and user, the multidimensional features for retweet prediction were obtained. These features were fused together in a classic decision tree algorithm, which improved the prediction performance greatly.

3. Problem Definition

Weibo network can be modeled as a weighted directed graph $G(V, E, W)$, where V, E, and W denote the node set, edge set, and edge weight set, respectively. In G, u and v are two users in the Weibo network. If u is a follower of v, then there is an edge $e(u, v)$ in graph, and $w(u, v)$ is the weight of edge $e(u, v)$. In fact, $w(u, v)$ is usually estimated by the interaction behaviors between node u and v.

Let m be a tweet posted by v, and $H(u, v, m) = (f_1, f_2, f_3, \ldots)$ is a vector composed of features that can influence the retweet behavior of u. $p(r = 1|H(u, v, m))$ represents the probability that u retweets m, where r is a binary variable indicating whether u retweets m. Given u, v, and m, the retweet prediction problem is how to determine the vector $H(u, v, m)$ and then estimate the retweet probability $p(r = 1|H(u, v, m))$.

This work focuses on the analysis of the factors influencing users' retweet behavior. The author-centered work usually obtains the prediction features from the statistics of the hot tweets. However, the features of hot tweets only reflect the overall trend of all users' retweet behavior and ignore the individual difference of each user. So, the user features are taken into account in this work.

The working procedure of algorithm MDF-RP is shown in Figure 1. As can be seen from Figure 1, the algorithm first extracts the features of the author, tweet, and user from the original dataset and then integrates these features with some classifier to predict whether the tweet will be retweeted by the user.

4. Proposed Method

The selection of retweet features is crucial to the performance of the prediction method. In this work, the prediction features are extracted from the information, which comes from user u, author v, tweet m, and the historical tweet sets of u and v.

4.1. Author Features. On the basis of the previous work, some author features, such as the number of fans, whether the author is authenticated, average number of tweets posted by the author every day and the popularity are chosen to predicate the retweet behavior.

4.1.1. Number of Fans. The number of fans is very important to evaluate the influence of a tweet author. The feature reflects the size of the author's audience. The statistics on the real dataset show that the number of fans of a tweet author is

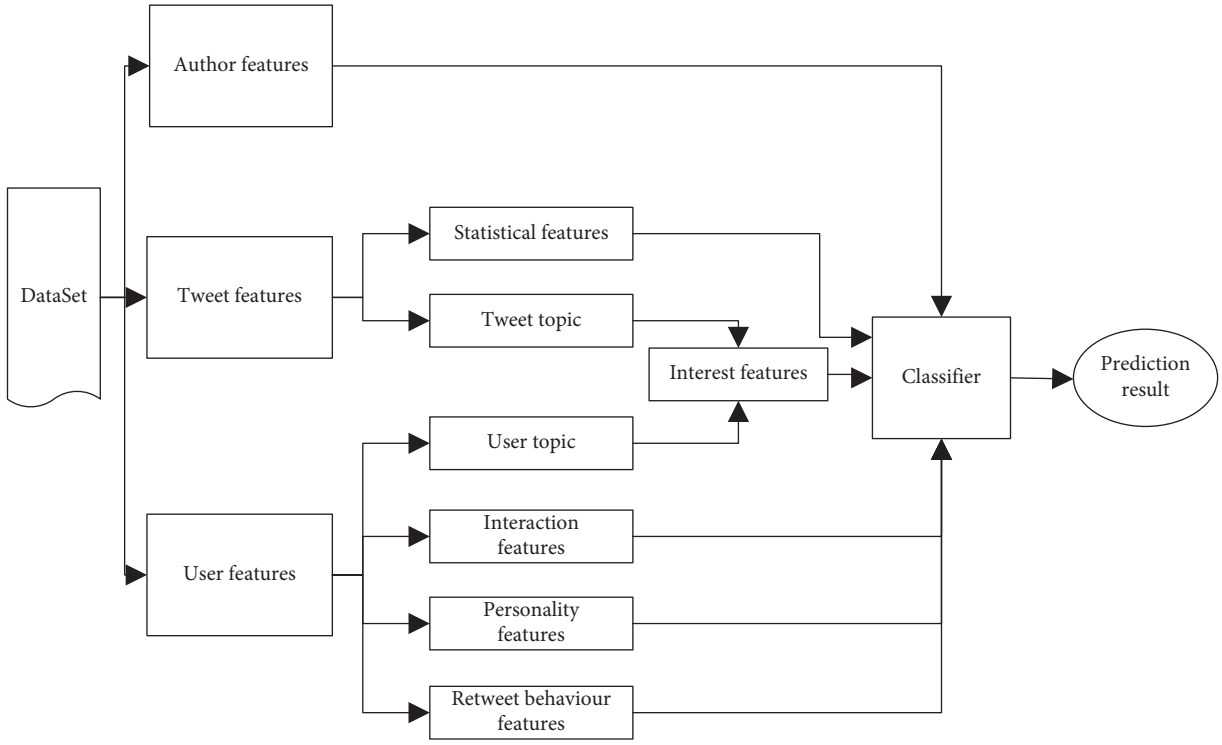

Figure 1: Working procedure of algorithm MDF-RP.

positively correlated with the number of times his tweets are retweeted.

4.1.2. Authenticated or Not. Authenticated user is the user whose profile has been authenticated by the Weibo platform. It is obvious that an authenticated user has higher credibility than an ordinary one. The statistics on the real dataset also show that the number of retweets posted by authenticated users is 3.2 times that of unauthenticated users.

4.1.3. Average Number of Tweets Posted Daily. The number of tweets posted daily means the activity of the author. A tweet author needs to post more tweets to maintain and increase his fans. Generally speaking, for a tweet author, the more fans he has, the more likely his post is to be retweeted. The average number of tweets daily of v is calculated as follows:

$$\text{daily}(v) = \frac{\text{posts}(v,t)}{\text{days}(t)}, \tag{1}$$

where posts (v, t) and days (t) refer to the number of tweets posted by v and the number of days during time t.

4.1.4. Popularity. To a certain extent, popularity reflects the approval degree of an author's posts. Suppose n (m) denotes the retweet number of post m. Given a threshold ζ, if n (m) is greater than ζ, m is popular. As for a tweet author, popularity refers to the proportion of the popular posts among all his posts. For a tweet author v, the popularity is calculated as follows:

$$\text{popularity}(v) = \frac{|\text{hotposts}(v)|}{|\text{posts}(v)|}, \tag{2}$$

where hotposts(v) is the tweet set of popular posts of v, and posts(v) refers to the tweet set of v.

4.2. Tweet Features. Tweet features refer to whether the tweet contains some special information found in popular tweets, such as Hashtag, URL, @, picture, video, and whether it is original. Statics show that when a tweet contains this special information, it is more likely to be retweeted. Tweet features employed in this work will be described in detail in part 5.

4.3. User Features. Four kinds of user features, including retweet behavior preference, interest, personality, and social interactions, are taken into account to predict the retweet behavior.

4.3.1. Retweet Preference. In the Weibo platform, the user has a variety of interaction behaviors, such as retweet, comment, and like. Retweet preference features are used to describe whether a user tends to retweet a tweet. They are described in two ways: retweet behavior preference and retweet activity.

As for a Weibo user, retweet behavior preference is the tendency of his retweet behavior by comparison with other interaction behaviors. Statistics of the Weibo platform show that users tend to spend their limited time in their favorite interaction behaviors. Compared to other users, those with

high retweet behavior preferences are more likely to retweet a post. The retweet behavior preference of a user is evaluated as follows:

$$\mathrm{pre}(u) = \frac{w_r N_r(u)}{w_r N_r(u) + w_c N_c(u) + w_l N_l(u)}, \quad (3)$$

where $N_r(u)$, $N_c(u)$, and $N_l(u)$ are the times of retweet, comment, and like of u; w_r, w_c, and w_l are the weights of these three actions, and $w_r + w_c + w_l = 1$. Generally speaking, retweet action requires more emotion, followed by comment and like actions. In experiments, the weight values are obtained empirically according to the average number of these three behaviors in our dataset. Suppose nr, nc, and nl are the average times of retweet, comment, and like in the dataset, w_r: w_c: $w_l = 1/n_r$: $1/n_c$: $1/n_l$. Finally, w_r, w_c, and w_l are set to 0.6, 0.3, and 0.1, respectively.

Retweet activity reflects a user's activity in retweet action. Statistics show that only a few users have high retweet times, and the distribution of users' retweet times obeys long-tail distribution approximately. To avoid the impact of long-tail distribution on data standardization, grade classification is employed to estimate the retweet activity. First, all users are sorted by their retweet times ascending, and then, they are divided into n levels. The number of users in each level is $[|v|/N]$. Let $N_r(v)$ represent the retweet times of user v and k is the maximum retweet times in level $k(\eta_0 = 0)$. If $N_r(v)$ is in $(\eta_{k-1}, \eta_k]$, then v is in level k. The retweet activity act (v) is calculated as follows:

$$\mathrm{act}(v) = \frac{k-1}{n} + \frac{N_r(v)}{n * \eta_k}. \quad (4)$$

4.3.2. Retweet Interest Features. Psychological research shows that one's interest will not change in a short time. Users' retweet behavior in Weibo is driven by their interests. In Weibo, users' interest can be mined from those tweets posted or retweeted by themselves. Due to the diversity of users' interest, the tweet content can be divided into different topics with algorithm LDA, and then, interest feature will be extracted from those topics.

Let $D(u)$ denote all tweets of user u. Firstly, the tweets of $D(u)$ are clustered by algorithm LDA to obtain n topics. Let $D(u,k)$ denote all tweets in $D(u)$ of the kth topic. For each topic of $D(u)$, top 10 words with the highest TF-IDF are taken as the feature words. With these feature words, the feature vector $i(u,k)$ $(k \in \{1, 2, 3, ..., n\})$ will be obtained, which is used to represent the kth interest of user u. The importance of $i(u,k)$ is calculated as follows:

$$i(u,k)_{\mathrm{weight}} = \frac{M(D(u,k))}{M(D(u))}, \quad (5)$$

where $M(D(u))$ and $M(D(u,k))$ denote the tweet number of $D(u)$ and $D(u,k)$, respectively. With the same method, the feature vector $j(m)$ of tweet m can be obtained. As for user u, its retweet interest feature fac(u, m) for tweet m is calculated as follows:

$$\mathrm{fac}(u,m) = \sum_{k=1}^{n} i(u,k)_{\mathrm{weight}} * \mathrm{sim}(i(u,k), j(m)), \quad (6)$$

where sim $(i(u, k), j(m))$ represents the similarity of vector $i(u, k)$ and $j(m)$. In this work, the similarity is calculated with cosine similarity, which is described as follows:

$$\mathrm{sim}(i(u,k), j(m)) = \frac{i(u,k) * j(m)}{\|i(u,k)\| \times \|j(m)\|}. \quad (7)$$

4.3.3. Interaction Features. In social network, users' behavior is usually influenced by their friends. The influence is estimated by the number of retweets, comments, and likes of u on author v in a period of time (one month is selected in the experiments). Let $N_r(v, u)$, $N_c(v, u)$, and $N_l(v, u)$ denote the number of retweets, comments, and likes of u on v, and then, the influence inf(v, u) is calculated as follows:

$$\mathrm{inf}(v,u) = w_r N_r(v,u) + w_c N_c(v,u) + w_l N_l(v,u), \quad (8)$$

where w_r, w_c, and w_l denote the weight of retweet, comment, and like actions.

4.3.4. Personality Features. There are two kinds of methods to obtain users' personality from their text information: one is based on machine learning, and the other is based on psychological dictionary. As for the method based on machine learning, it is difficult to obtain the training set containing users' real personality. The acquisition of users' personality is generally carried out by questionnaire survey in psychology, which will consume a lot of human and material resources. The method based on psychological dictionary needs the quantitative relationship between the function of words and personality traits.

LIWC (Linguistic Inquiry and Word Count) [18] was released by Pennebaker et al., which discovered the relationship between personality traits and language habits by calculating the frequency of specific words. LIWC focuses on the analysis of English text. In order to facilitate the personality analysis of Chinese texts, with the official authorization of LIWC, Huang et al. [19] transformed it into C-LIWC and SC-LIWC, which are suitable for the analysis of traditional Chinese text and Simplified Chinese text, respectively.

In this work, SC-LIWC dictionary is employed to analyze the personality of tweet users, and the Big Five personality model is used as the psychological theory to study the personality of users, and the personality traits of users reflected in tweet texts are analyzed. When conducting personality analysis based on SC-LIWC, emotion words and degree adverbs are also necessary to be considered. Emotional words reflect the user's attitude and feelings towards the relevant object, which can be divided into a positive one and a negative one. Degree adverb expresses the degree of emotion. The UTNSD-Simplified Chinese Emotion Polarity Dictionary published by National Taiwan University divides 11086 emotion words into 2810 positive words and 8276 negative words.

HowNet is a common sense knowledge base developed by the Chinese Academy of Sciences. A dictionary for sentiment analysis (beta) was released by HowNet in

October 2007. On the basis of the dictionary of LIWC2007 and C-LIWC, a Chinese language psychological analysis system TextMind was developed by the Institute of Psychology, Chinese Academy of Sciences. In this system, the relationship between 71 function words in SC-LIWC and each dimension of the Big Five personality was statistically quantified. In SC-LIWC, a word may have multiple functions. TextMind provides the corresponding table between function words and personality trait score. Based on this, the personality trait score of the tweet user can be calculated.

Definition 1 Tweet personality. In the Big Five model [17], personality is composed of five traits. The different proportion of these five traits in personality forms different personality performance. Personality is defined as follows:

$$\text{Personality} = (S\_\text{open}, S\_\text{cons}, S\_\text{extr}, S\_\text{agree}, S\_\text{neur}), \quad (9)$$

where S_open, S_cons, S_extr, S_agree, S_ Neur indicate the scores of personality trait in openness, conscientiousness, extroversion, agreeableness, and neuroticism, respectively.

Definition 2 BFM. BFM denotes the importance of word w in the ith dimension of the Big Five personality. It is calculated as follows:

$$\text{BFM}(w, i) = \frac{\sum_{j=1}^{n} p(j, i)}{n}, \quad (10)$$

where n is the number of function words of word w, and p (j, i) denotes the relationship between the jth function word and the ith personality factor. In formula (10), p (j, i) is obtained from TextMind.

BFM takes into account the relationship between the function words and the personality traits. However, the personality trait score is also related to the importance of the word in the tweet. In this work, TF-IDF is employed to denote the importance of word w in tweet m. PTS (m, w, i) denotes the ith personality trait score of word w in tweet m, and it is estimated as follows:

$$\text{PTS}(m, w, i) = \text{BFM}(w, i) * tf - \text{idf}(w, m), \quad (11)$$

where tf-idf(w, m) denotes the tf-idf value of word w in tweet m.

When calculating the tweet personality score of tweet m, not only the personality score and word frequency of each word w in m, but also the emotional words and degree adverbs in front of w should be taken into account. The calculation algorithm of the tweet personality score is described in Algorithm 1.

5. Experiments

5.1. Datasets. In order to evaluate the method in this work, we crawled data from Weibo, which is a social network in China like Twitter. We randomly selected 80 users as the seed users from 8 fields such as technology, entertainment, and tourism and then crawled 44273 tweets posted or retweeted by these users from June 1, 2018 to July 31, 2018. Then, we obtained the followed list of these seed users including 3,352 users and got 316,829 tweets published by these users. The data in June are used as the historical data, and the rest data are employed as experimental data. The historical data are used to mine retweet habits, and the experimental data are used to train and test the prediction model.

In order to improve the credibility of the experiment, cross-validation is employed to test the performance of the retweet prediction method. In experiments, 4-fold cross-validation is used. Two groups of experiments are designed to verify the effectiveness and stability of the proposed method. One is used to verify the contribution of the proposed features to improve the performance of retweet prediction, and the other is to verify the stability of the proposed features on different classifiers and training sets.

5.2. Evaluation. In order to measure the performance of the retweet prediction method, precision, recall, and F1-score are used in this work. These measures are defined as follows:

$$\text{precision} = \frac{\#\text{correctly classified as retweet}}{\#\text{classified as retweet}},$$

$$\text{recall} = \frac{\#\text{correctly classified as retweet}}{\#\text{true retweet}}, \quad (12)$$

$$F1 - \text{score} = \frac{2 * \text{precision} * \text{recall}}{\text{precision} + \text{recall}}.$$

5.3. Experimental Results. The experiment environment of this work is as follows:

Hardware: CPU: Intel(R) Xeon(R) CPU E5-2696 v2 @ 2.50 GHz; Memory: 48G

OS: CentOS 7

On the basis of the features of the author, tweet, and user, classic classifiers including decision tree C4.5 and LR are employed to predict the individual retweet behavior.

5.3.1. Experimental Results. All the features employed in method MDF-RP are shown in Table 1.

In order to verify the effectiveness of the proposed method, author features and tweet features (features 1–9) are selected as benchmarks. The benchmark features and author features are employed in algorithm C4.5, and the experimental results are shown in Table 2.

As shown in Table 2, after user features are added, F1-score is increased by 6.519%. Comparing the basic features, user features fully consider the key factors such as users' retweet behavior preference, activity, interest in tweet, personality trait scores, and the influence from the tweet author, which effectively improves the performance of algorithm MDF-RP.

In order to obtain the contribution of each user feature to the performance improvement, comparative experiments on the prediction performance of each user feature are

```
Input: tweet m, personality trait dictionary pt_dict, degree adverb dictionary c_dict, positive emotional dictionary s_p_dict and
negative emotional dictionary s_n_dict
Output: personality vector of tweet m
initialize the tweet personality vector, personality = (0, 0, 0, 0, 0)
for sent in m.sents{ //m.sents denotes the sentence set of tweet m
  initialize the temporary personality vector, tmpPersonality = (0, 0, 0, 0, 0).
  cnt = sent.wordNum //cnt denotes the number of words in sent.
  for idx = 0 to cnt{
    word = sent[idx]
    For trait = 1 to 5{
      If word in pt_dictionary {
        res = PTS (m, word, trait)
        if idx > 0 {
        preWord = sent[idx-1]
        if preWord in c_dictionary{
          res = c_dictionary (preword, trait) * res }//if
        }
      If word in s_p_dictionary{
      res+ = res * s_dictionary (word)
          } else if word in s_n_dictionary{
          res- = res * s_n_dictionary (word)
          } //if
        tmpPersonality[trait] + = res
      } //for trait
    } //for idx
  } //for sent
```

Algorithm 1: get_tweet_personality_score.

Table 1: Summary of features in MDF-RP.

Category	Feature	Description
Author features	f_a_follows	Number of follows of the author
	f_a_if_aut	Whether the author is authenticated
	f_a_daily	The average number of tweets posted by the author daily
	f_a_popularity	A feature denotes the popularity of an author's tweets
Tweet features	f_m_if_hashtag	Whether the tweet contains hashtag #
	f_m_if_url	Whether the tweet contains hyperlink
	f_m_if_@	Whether the tweet contains @
	f_m_if_multimedia	Whether the tweet contains some multimedia materials
	f_m_if_org	Whether the tweet is original
User features	f_u_ret_pre	The retweet behavior preference of the user
	f_u_act	The retweet activity of the user
	f_u_int	The interest similarity of the user and the given tweet
	F_u_inf	The influence of the author on the user
	f_u_personality	The personality trait vector of the user

Table 2: Performance of retweet prediction with benchmark methods and MDF-RP.

Feature	Precision	Recall	F1-score	F_promotion_rate (%)
Basic_Features	0.793	0.742	0.767	—
MDF-RP	0.851	0.785	0.817	6.519

conducted, and the experimental results are shown in Table 3.

It can be seen from Table 3 that the performance promotion of f_u_personality is the highest, reaching 6.519%, and the promotion of f_u_ret_pre is the lowest, reaching 0.780%.

5.3.2. Performances of Different Classifiers. In order to verify the performance of MDF-RP features, experiments of basic features and MDF-RP features under different classifiers are conducted. To verify the stability of these features, cross-validation is employed. K-Fold cross-validation divides the dataset into k parts. It takes $k-1$ parts as the training set and the remaining part as the test set in turn. It estimates the prediction performance of the algorithm by the mean of k experimental results. The experimental results of basic features and MDF-RP features under different classifiers are shown in Figures 2–4.

It can be seen from Figures 2–4 that under different algorithms F1-score of MDF-RP features is higher than that of the basic features. The MDF-RP features of all algorithms

Table 3: Contribution of user features to retweet prediction.

Feature	Precision	Recall	F1-score	F_promotion_rate (%)
Basic_Features	0.793	0.742	0.767	—
Basic_Features + f_u_ret_pre	0.801	0.747	0.773	0.780
Basic_Features + f_u_act	0.820	0.760	0.789	2.876
Basic_Features + f_u_int	0.824	0.762	0.792	3.234
Basic_Features + F_u_inf	0.824	0.748	0.784	2.252
Basic_Features + f_u_personality	0.828	0.765	0.795	3.699
MDF-RP	0.851	0.785	0.817	6.519

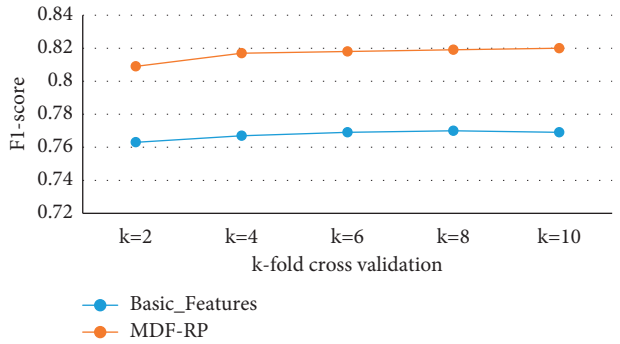

Figure 2: Prediction performance of algorithm C4.5.

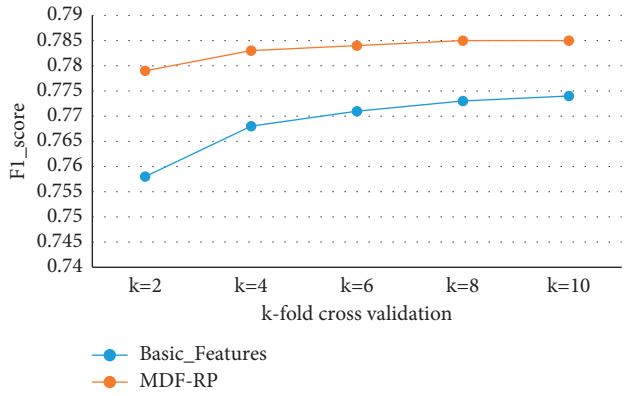

Figure 3: Prediction performance of algorithm logistic regression.

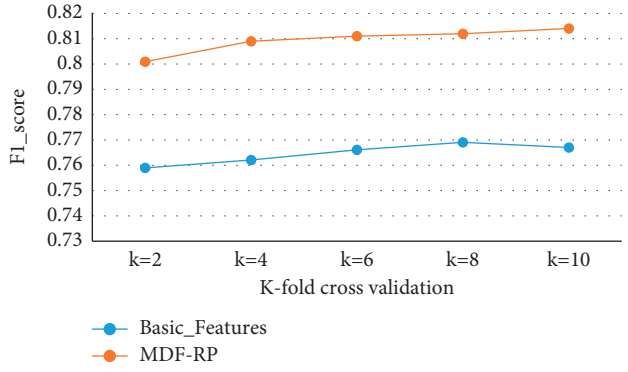

Figure 4: Prediction performance of algorithm SVM.

can obtain a high F1-score in the case of a small training set. In addition, F1-score of MDF-RP can be gradually improved with the rise of the training data size.

In algorithm C4.5, under 2-fold and 10-fold cross-validation, compared with the basic features, F1-scores of MDF-RP features are increased by 6.03% and 6.63%, respectively. Under 2-fold cross-validation, the F1-score of MDF-RP features is 0.809. From 2-fold to 10-fold cross-validation, F1-scores of MDF-RP features increase by 1.36%. However, the F1-score of basic features decreases under the 10-fold cross-validation.

In algorithm LR, under 2-fold and 10-fold cross-validation, compared with the basic features, F1-scores of MDF-RP features are increased by 2.77% and 1.42%, respectively. Under 2-fold cross-validation, the F1-score of MDF-RP features is 0.779. From 2-fold to 10-fold, the F1-score of MDF-RP is improved by 0.77%, whereas the F1-score of basic features is improved by 2.11%.

In algorithm SVM, under 2-fold and 10-fold cross-validation, compared with the basic features, F1-scores of MDF-RP features are increased by 5.24% and 5.77%, respectively. Under 2-fold cross-validation, the F1-score of MDF-RP features is 0.801. From 2-fold to 10-fold, the F1-score of MDF-RP is improved by 1.04%, whereas the F1-score of basic features is improved by 1.59%.

The experimental results under different classifiers show that, compared with the basic features, the user features can effectively predict the user's retweet behavior for a given tweet. In experiments, the classifier with MDF-RP features can obtain high performance on a smaller training set. Moreover, with the increase in the size of the training data, the performance improves steadily. This is because the MDF-RP features contain the information of tweet content, user interests, user personality, user interaction, and others, which can describe the features of user's retweet behavior. So, the classifier with these features trained on a small dataset can obtain better and more stable performance.

6. Conclusion

With regard to the retweet prediction problem of a given user, from the dimensions of the author, tweet content, and user, a prediction method based on multidimensional features is proposed in this work.

(1) In the dimension of the tweet author, from the perspectives of the influence, credibility, activity, and the quality of his tweets, four features are designed, including number of fans, authenticated user or not, number of tweets posted daily, and popularity, which effectively measure the influence of the tweet author on whether the tweet will be retweeted

(2) In the dimension of the tweet content, according to the common features of those hot posts, five features are designed, including whether the tweet contains topic tags, hyperlinks, @, multimedia materials, and whether it is original, which measure the impact of the tweet's statistical feature effectively

(3) In the dimension of the tweet user, five features based on his personality, retweet behavior preference, retweet activity, interest in the tweet content, and the influence from the tweet author are chosen to effectively measure the impact on the retweet prediction problem

Based on these multidimensional features, a tweet prediction method is proposed. The effects of these multidimensional features on different classification methods are verified in the real datasets. The experiments show that these features effectively improve the prediction performance. The prediction performance of algorithm C4.5 is the highest, and it can achieve the best prediction effect on a smaller training set. In fact, users usually play different roles in the dissemination of tweets with different themes. As future work, we plan to extend this work by incorporating user's role in tweet propagation to further improve the performance of retweet prediction.

Data Availability

The data that support the findings of this study are available from the corresponding author upon reasonable request.

Conflicts of Interest

The authors declare no potential conflicts of interest with respect to the research, authorship, and/or publication of this article.

Acknowledgments

This work was partially supported by the National Innovation Training Foundation for college students (Grant no. 201910443011) and Supporting Fund for Teachers' Research of Jining Medical University (Grant no. JYFC2019KJ038).

References

[1] Y. Wang, Z. Zhang, C. Chang, and M. A. Zia, "Identifying and tracking topic-level influencers in the microblog streams," *Machine Learning*, vol. 107, no. 3, pp. 551–578, 2018.

[2] C. De Maio, G. Fenza, M. Gallo, V. Loia, and M. Parente, "Time-aware adaptive tweets ranking through deep learning," *Future Generation Computer Systems*, vol. 93, no. 924–932, 2019.

[3] J.-H. Zhao, D.-L. Zeng, J.-T. Qin, H.-M. Si, and X.-F. Liu, "Simulation and modeling of microblog-based spread of public opinions on emergencies," *Neural Computing and Applications*, vol. 33, no. 2, pp. 547–564, 2021.

[4] Z.-Y. Han, L.-L. Kong, and H.-L. Qi, "Time segment language model for microblog retrieval," *Neural Computing and Applications*, vol. 33, no. 10, pp. 4763–4777, 2021.

[5] W. Liu, M. He, L. H. Wang, Y. Liu, H. W. Shen, and X. Q. Cheng, "Research on microblog retweeting prediction based on user behavior features," *Chinese Journal of Computers*, vol. 39, no. 10, pp. 1992–2006, 2016.

[6] B. Jiang, J. Liang, Y. Sha, and L. H. Wang, "Message clustering based matrix factorization model for retweeting behavior prediction," in *Proceedings of the 24th ACM International on Conference on Information and Knowledge Management*, pp. 1843–1846, Melbourne, Australia, 2015.

[7] W. Wang, X. W. Zhang, G. H. Ren, D. X. Qin, and L. L. Liu, "Predicting microblog user retweet behaviors on energy optimization," *Acta Electtronica Sinica*, vol. 45, no. 12, pp. 2987–2996, 2017.

[8] X. B. Tang and Y. L. Luo, "Integrating emotional divergence and user interests into the prediction of microblog retweeting," *Library and Information Service*, vol. 61, no. 9, pp. 102–110, 2017.

[9] Z. Yang, J. Guo, K. Cai, J. Tang, J. Z. Li, and L. Zhang, "Understanding retweeting behaviors in social networks," in *Proceedings of the 19th ACM International Conference on Information and Know Ledge M Anagement*, pp. 1633–1636, ACM, Toronto, Canada, 2010.

[10] B. Bi and J. Cho, "Modeling a retweet network via an adaptive Bayesian approach," in *Proceedings of the 25th International Conference on World Wide Web*, pp. 459–469, Montreal, Canada, 2016.

[11] C. Wang, Y. Fan, Y. Du, and Z. Sun, "Predict individual retweet behavior based on multi-feature," *IOP Conference Series: Materials Science and Engineering*, vol. 790, no. 1, Article ID 012046, 2020.

[12] S. N. Firdaus, C. Ding, and A. Sadeghian, "Retweet prediction considering user's difference as an author and retweeter," in *Proceedings of the 2016 IEEE/ACM International Conference on Advances in Social Networks Analysis and Mining (ASONAM)*, pp. 852–859, IEEE, San Francisco, CA, USA, 2016.

[13] Q. Zhang, Y. Gong, Y. Guo, and X. J. Huang, "Retweet behavior prediction using hierarchical dirichlet process," *Proceedings of the AAAI Conference on Artificial Intelligence*, vol. 29, no. 1, 2015.

[14] Q. Zhang, Y. Gong, and J. Wu, "Retweet prediction with attention-based deep neural network," in *Proceedings of the 25th ACM International on Conference on Information and Knowledge Management*, pp. 75–84, Indianapolis, IN, USA, 2016.

[15] D. C. Funder, "On the accuracy of personality judgment: a realistic approach," *Psychological Review*, vol. 102, no. 4, pp. 652–670, 1995.

[16] Z. M. Xu, D. Li, T. Liu, S. Li, G. Wang, and S. L. Yuan, "Measuring similarity between microblog users and its application," *Chinese Journal of Computers*, vol. 37, no. 1, pp. 207–218, 2014.

[17] L. R. Goldberg, J. A. Johnson, H. W. Eber et al., "The international personality item pool and the future of public-domain personality measures," *Journal of Research in Personality*, vol. 40, no. 1, pp. 84–96, 2006.

[18] J. W. Pennebaker, "Linguistic styles: language use as an individual difference," *Journal of Personality & Social Psychology*, vol. 77, no. 6, 1999.

[19] C. L. Huang, C. K. Chung, and N. Hui, "The development of the Chinese linguistic inquiry and word count dictionary," *Chinese Journal of Psychology*, vol. 54, no. 2, pp. 185–201, 2012.

Hindawi
Wireless Communications and Mobile Computing
Volume 2022, Article ID 6243347, 12 pages
https://doi.org/10.1155/2022/6243347

Research Article

Multimodal Sentiment Analysis Based on Interactive Transformer and Soft Mapping

Zuhe Li,[1,2] **Qingbing Guo**,[1] **Chengyao Feng**,[3] **Lujuan Deng**,[1] **Qiuwen Zhang**,[1] **Jianwei Zhang**,[2] **Fengqin Wang**,[1] **and Qian Sun**[1]

[1]*School of Computer and Communication Engineering, Zhengzhou University of Light Industry, Zhengzhou 450002, China*
[2]*Henan Key Laboratory of Food Safety Data Intelligence, Zhengzhou University of Light Industry, Zhengzhou 450002, China*
[3]*Brandeis High School, San Antonio, TX 78249, USA*

Correspondence should be addressed to Qian Sun; 331907020384@zzuli.edu.cn

Received 27 November 2021; Revised 23 December 2021; Accepted 15 January 2022; Published 3 February 2022

Academic Editor: Mohamed Elhoseny

Multimodal sentiment analysis aims to harvest people's opinions or attitudes from multimedia data through fusion techniques. However, existing fusion methods cannot take advantage of the correlation between multimodal data but introduce interference factors. In this paper, we propose an Interactive Transformer and Soft Mapping based method for multimodal sentiment analysis. In the Interactive Transformer layer, an Interactive Multihead Guided-Attention structure composed of a pair of Multihead Attention modules is first utilized to find the mapping relationship between multimodalities. Then, the obtained results are fed into a Feedforward Neural Network. The Soft Mapping layer consisting of stacking Soft Attention module is finally used to map the results to a higher dimension to realize the fusion of multimodal information. The proposed model can fully consider the relationship between multiple modal pieces of information and provides a new solution to the problem of data interaction in multimodal sentiment analysis. Our model was evaluated on benchmark datasets CMU-MOSEI and MELD, and the accuracy is improved by 5.57% compared with the baseline standard.

1. Introduction

Sentiment analysis aims to detect affective states or subjective information from data. It is often used to understand or judge people's attitudes, opinions, and sentiment. Traditional sentiment analysis mainly focuses on text data, using statistical knowledge combined with natural language processing and machine learning techniques to study and analyze the sentiment polarity of sentences or documents [1]. In reality, human sentiment is expressed not only through language, but also through acoustic information (e.g., speakers' tone of voice) and visual information (e.g., speakers' facial expressions and body movements). For example, social media users are no longer satisfied with sharing feelings and emotions in the form of text but tend to use multimedia forms such as pictures or videos when sending blog posts. In this way, they can express their attitudes more abundantly. The multimodal information at different granularity levels is spread out by people, and traditional sentiment analysis methods cannot handle this problem well. On the basis of text information, multimodal sentiment analysis can use multimodal representation learning, multimodal alignment, and multimodal fusion technologies to combine acoustic and visual information to eliminate ambiguity caused by a single modality.

At present, the research of multimodal sentiment analysis can be divided into two categories according to the number of talkers: multimodal narrative sentiment analysis and multimodal conversational sentiment analysis [2]. Multimodal narrative sentiment analysis usually transmits the author's personal attitude with narrative information. The expression of information is relatively independent and does not involve the interaction between multiple speakers. For example, in the analysis of public opinion, multimodal narrative sentiment analysis is used to analyze the information in social media platforms such as microblog and

twitter to obtain users' attitude towards a hot event. In contrast, there is more than one speaker in multimodal conversational sentiment analysis. The sentiment or attitude of each talker is transmitted in the form of dialogue or communication. In the process of interaction, the sentiment state of speakers is mutually influencing, jumping, and unstable. For example, in customer sentiment analysis, multimodal conversational sentiment analysis is used to obtain interaction clues among multiple customers and to predict sentiment evolution trend in the interaction process.

The research of multimodal sentiment analysis is not mature, and there are still some unsolved problems. Among them, the establishment of multimodal information fusion mechanism has become the main bottleneck restricting the development of this field. Multimodal information fusion aims to fuse the representations of different modalities and retain the key information in each modality during the fusion process. To solve this problem, there are several ideas: feature-level fusion, decision-level fusion, and hybrid fusion [3, 4], as shown in Figure 1. The yellow part in Figure 1 shows the feature-level fusion mechanism, which extracts feature vectors from multimodal data, respectively, and fuses them into a multimodal feature vector. The fused vector is used to judge sentiment [5, 6]. This fusion method can obtain the association among various modalities, but the features need to be mapped to a shared space for fusion because the semantic spaces of different modalities are different from each other. The blue section in Figure 1 shows the decision-level fusion mechanism, which first conducts single modality sentiment analysis independently and then fuses the results to obtain the final decision [7, 8]. This fusion method can design a feature extraction method for the semantic space of each modality to obtain the optimal single modality decision, but independent learning will cause the overall time cost to be too large. The green area in Figure 1 shows the hybrid fusion mechanism, which comprehensively uses the feature-level fusion and decision-level fusion methods to reduce the time cost on the basis of fully learning the associated information of each modality.

In addition, multimodal interaction is also a hot topic. Multimodal interaction aims to supplement the information of different modalities. When the information of one modality information is missing, the data of another modality is used to make up the missing part. This kind of interaction is concealed, complex, and dynamic. It makes multiple modalities related to each other and affects the final sentiment judgment. How to accurately and comprehensively model the complex interaction in multimodal data is still troublesome in this field. Multimodal interaction mainly includes two situations: the interaction between features and the interaction between decisions. For the interaction between features, multimodal features in a shared space need to be aligned through semantic space barriers across different domains to achieve semantic fusion. Several methods such as feature concatenation [9, 10] and attention mechanisms [11] have been developed to solve this problem. For the interaction between decisions, it is necessary to understand the correlation between multimodal data, and this is a comprehensive cognitive decision-making process. The voting method and linear weighting method are proposed to solve this problem.

In view of the above two problems, it can be seen that, in the process of multimodal information fusion, making full use of the correlation among different modalities to make each modality learn from each other is the key to multimodal sentiment analysis. Based on the Transformer-Encoder framework [12], we propose a model to learn the information of different modalities. In this process, we utilize the Guided-Attention mechanism [13] to introduce the information of other modalities. Then, the unimodal results are mapped to higher dimensions for fusion, and the final decision is made according to the fusion results. The main contributions of this work can be summarized as follows:

(i) We propose a multimodal sentiment analysis model based on Interactive Transformer and Soft Mapping. This model can achieve the optimal decision of each modality and fully consider the correlation information between different modalities.

(ii) We propose the Interactive Transformer (IT) structure, which can mine the interactive information between modalities.

(iii) We propose the Soft Mapping (SM) structure, which projects each modality representations to a new space for fusion.

(iv) The experimental results on two benchmark datasets show that the proposed method can achieve better accuracy than those existing methods only using linguistic and acoustic information.

The remaining sections of this paper are arranged as follows. In Section 2, we will review the related work on CMU-MOSEI dataset and MELD dataset. In Section 3, we will describe our method and the core content of the model structure in detail. In Section 4, we will describe the datasets and the method of data preprocessing. In Section 5, we will provide experimental results and analysis. In Section 6, we will summarize the paper and discuss the potential future work.

2. Related Work

In the early studies, researchers focused on the problem of multimodal fusion, and they tried to solve the problem of multimodal sentiment analysis by improving the fusion method. For example, some models fuse each modality representations according to different granularities.

Amir Zadeh et al. proposed the Memory Fusion Network (MFN) [14] to solve the problem of multimodal sequence modeling. The interaction problem is divided into view-specific interactions and cross-view interactions, which is implemented in three steps. Firstly, they use LSTM to learn view-specific interactions individually. Then, they learn the cross-view interactions by Delta-memory Attention Network (DMAN). Finally, they summarized it through time with a Multiview Gated Memory. MFN takes the interaction between modalities as a breakthrough point, which ensures the performance without sacrificing the time complexity and

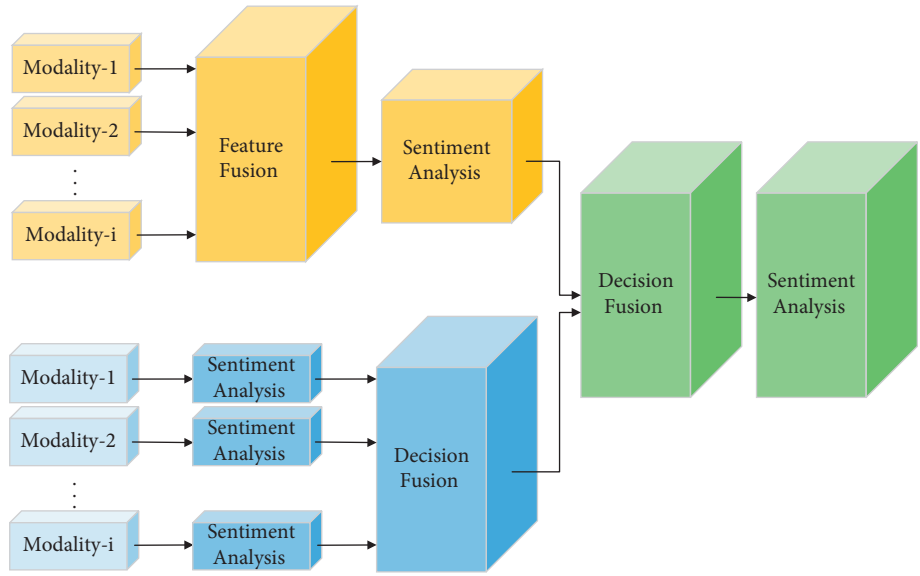

Figure 1: Multimodal fusion mechanisms.

space complexity of the model. Amir Zadeh et al. proposed Graph Memory Fusion Network (Graph-MFN) [15]to improve the Memory Fusion Network (MFN). In this way, they use a new fusion model called the Dynamic Fusion Graph (DFG) to build the n-modal interactions and replace the original fusion component in MFN. This improvement enables the method to dynamically select the appropriate fusion graph according to its importance in the process of multimodal information fusion.

The above methods provide ideas for the research in the field of multimodal sentiment analysis, but they all ignore the interaction between modality representations, such as supplementing by one modality when the information of another modality is scarce. This defect makes these methods unstable. With the development of deep learning, researchers begin to pay attention to the interaction between modalities. Some researchers try to use LSTM model to obtain the contextual information around each discourse from the perspective of time. Some researchers use gating mechanism or attention mechanism to couple features. These ideas promote the development of multimodal sentiment analysis research.

Kumar et al. proposed a gating mechanism, named learnable gates [16]. This mechanism considers that each modality is not of equal importance and needs to be dynamically adjusted according to the linguistic information, tone of the speaker, and facial expressions of utterance. This method explains how multiple modalities contribute to sentient, selectively learning cross fusion vectors to solve the noise problem in the process of multimodal information fusion. Sahay et al. proposed Relational Tensor Network architecture [17]. Tensor fusion is applied to the modality features of each video clip, and LSTM network is used to model the sequence between clips. In this method, the interaction between modalities is refined to a single time segment from the time level, and the operation can be performed frame by frame. Shenoy and Sardana proposed an end-to-end RNN architecture [18], named Multilogue-Net. They assume that the sentiment or emotion governing a particular utterance predominantly depends on 4 factors: interlocutor state, interlocutor intent, the preceding and future emotions, and the context of the conversation. Firstly, the model represents the speaker's state by learning multiple state vectors of a given utterance and then uses pairwise attention mechanism to obtain the relationship among all modalities. This method starts with the emotional states of both sides of the conversation and fully obtains the relevance and context information between modalities to assist multimodal emotion recognition.

Transformer draws the global dependency between input and output completely based on the attention mechanism without recurrence and convolutions [12]. It utilizes the Multihead Attention to replace the recurrent layers and achieves excellent results in translation tasks. At present, researchers have tried to apply it to multimodal sentiment analysis, providing new research directions for solving problems in this field. Delbrouck et al. describe a Transformer-based joint-encoding (TBJE) architecture for the task of Emotion Recognition and Sentiment Analysis [19]. The model uses Transformer-Encoder framework for emotion recognition, and the proposed joint-coding framework can fuse any kind of modality information.

In summary, we believe that it is necessary to grasp the implicit correlation between modalities. For example, in the issue of sentiment ambiguity, because of the difference in intonation and context, the true meaning of the language can be very different. Implicit correlation is used to analyze the language environment. At the same time, acoustic information and visual information are used to analyze intonation and body language. After comprehensive analysis, we can get the real sentiment and emotion contained in the information. Finally, we choose to use the Transformer-Encoder framework to draw the internal dependence of a single modality, which is doped with residual transformation

and layer normalization to enhance the adaptability of the model. The Multihead Attention module in the coding framework is improved by the idea of Guided-Attention mechanism, so that the information of a certain position can notice the representation information in other modalities.

3. The Proposed Method

This section mainly introduces the framework structure of the model. Interactive Transformer layer is based on the Transformer model, which uses the coding framework to learn the representation information of different modalities. It only needs to rely on the attention mechanism combined with feedforward neural network to achieve the effects of other network models. In fact, the model can obtain the global dependency between input and output without involving the recursive structure of sequence coding. In this process, the Interactive Multihead Guided-Attention (IMHGA) structure proposed by us can introduce the information of other modalities to complete interaction. IMHGA structure is a combination of two improved Multihead Attention (MHA) modules; we will elaborate its principle in Section 3.2. Finally, Soft Mapping is used to map the local results of each modality to higher dimensions for fusion, and the final decision is based on the fusion results.

3.1. Overall Architecture. As shown in Figure 2, in addition to the data preprocessing part, the model consists of two parts: Interactive Transformer (IT) layer and Soft Mapping (SM) layer. The Interactive Transformer layer is composed of N blocks stacked side by side; each block is composed of IMHGA structure and Feedforward Neural Networks (FNN). The Soft Mapping layer consists of stacking Soft Attention (SA) module and the output of SA module. After preprocessing, the data is transferred to Interactive Transformer layer, in which the representation information of each modality is learned. Because the information of other modalities is introduced, it can superimpose the information from different representation subspaces in the learning of a single modality representation information. Then, the result is passed into the FNN layer which is composed of full connection layer and nonlinear activation function. In each block, the two sublayers are finally subjected to a residual transformation and layer normalization (A & L), as shown in the following formula:

$$\text{LayerNorm}\,(x + \text{Sublayer}\,(x)). \tag{1}$$

Through our experiments, it is found that the best result can be obtained when $N = 4$ and all blocks' parameters are independent. The output of the previous block is used as the input of the next block. Finally, the output of coding module is input into Soft Mapping layer. They will be mapped to a higher dimensional space for fusion in order to obtain the final result.

3.2. Interactive Multihead-Guided Attention. The Interactive Multihead Guided-Attention (IMHGA) structure is composed of a pair of improved Multihead Attention (MHA) modules, which we call Guided-Attention (GA). The core idea of it is to use attention mechanism to determine the corresponding relationship between two languages, and there is no dependency during forward propagation. Therefore, attention mechanism can execute operations in parallel and speed up the training of the model to reduce the time cost. We apply this idea to multimodal problems, hoping to find the mapping relationship between two-modality information. On this basis, with the help of Multihead Attention mechanism, we use the other modality information as a guide when learning one modality information.

The query (Q), key (K), and value (V) in IMHGA structure come from multiple modality data. It is not like traditional MHA module, which comes from the same modality data. As shown in Figure 3, GA-x and GA-y learn modality-x and modality-y, respectively, where the vectors K and V come from the currently learning modality and the vector Q comes from another modality. Taking GA-x's learning of modality-x as an example, all vectors are subjected to a linear transformation. Then, the query (Q_y) from the modality-y and the key (K_x) from the modality-x are used to calculate the similarity weight by the dot product function, and results are normalized by Softmax function. Finally, the weight is used to perform a weighted summation of the value (V_x) from modality-x. The calculation method in this step is the result of Guided-Attention module. The specific process is shown in the following formula.

$$\text{Guided} - \text{Attention}\left(Q_y, K_x, V_x\right) = \text{soft}\max\left(\frac{\left(Q_y K_x^T\right)}{\sqrt{d}}\right)V_x. \tag{2}$$

The above operations are performed for a total of h times, and each time is regarded as a head module. The result of IMHGA structure can be obtained by splicing and linear changing the results of h times. Note that, in order to make the dot product not too large, the calculated similarity weight is usually divided by the dimension of K and the parameter W of linear transformation in each head is different. The specific process is shown in the following formulas:

$$\text{head}_i = \text{Guided} - \text{Attention}\left(Q_y W_i^Q, K_x W_i^k, V_x W_i^V\right), \tag{3}$$

$$\text{IMHGA}\left(Q_y, K_x, V_x\right) = \text{Concat}\left(\text{head}_1, \ldots, \text{head}_h\right)W^O. \tag{4}$$

Through a large number of experiments, we found that the model can play the best effect when using the language and acoustic data. In this paper, we mainly use the fusion of two-modality data. Generally speaking, the language modality is used as main information, and the acoustic modality is used as auxiliary information. However, some important information may be ignored, such as mood and intonation in acoustic modality. They can help us identify such special situations as polysemy and irony in the language modality. Therefore, we regard the status of the two as equal and make them modulate each other. This is the meaning of Interactive in IMHGA structure. After IMHGA structure, the two generated matrices are output to the next Soft Mapping layer in parallel through FNN for fusion.

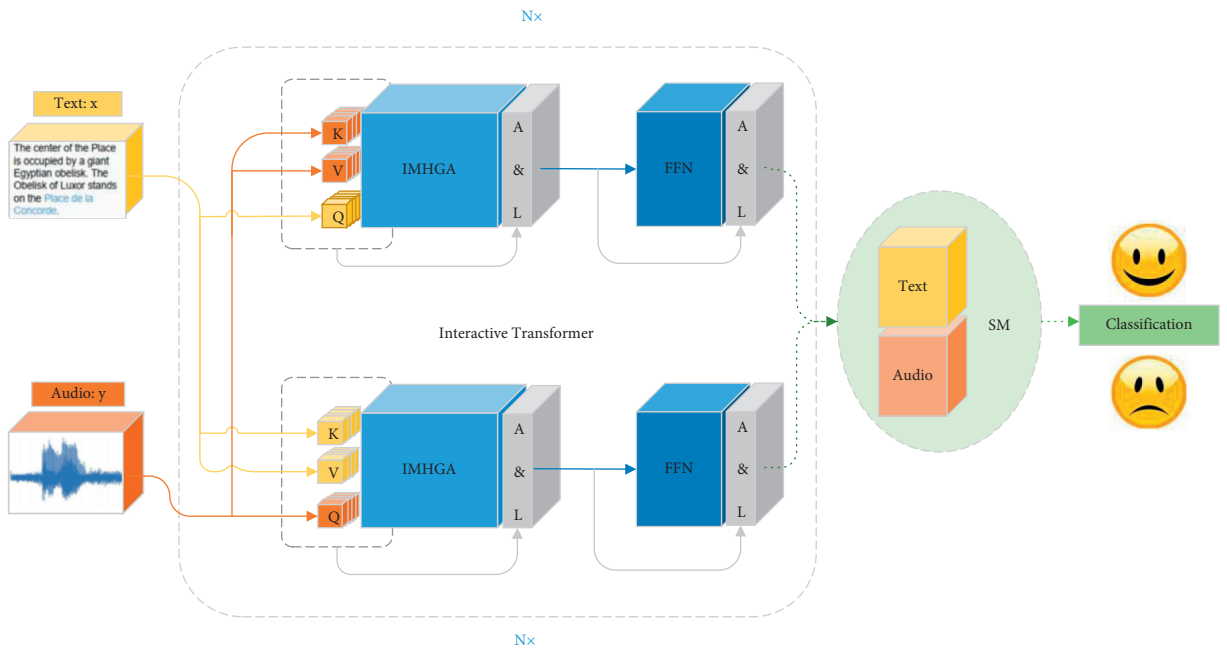

Figure 2: Overview of the proposed framework.

3.3. Soft Mapping. So far, the model has learned the interaction information between the modalities. Before sentiment classification, the learning results of each modality need to be projected into a new performance space in SM for fusion, as shown in Figure 4. Specifically, we map vectors $f_{\text{text}}, f_{\text{audio}}$ from each FNN to a higher dimension, as shown in the following formula:

$$E_i = w_i f_i^T, \quad \{i \in \text{text}, \text{audio}\}, \tag{5}$$

where w_i is a $2k \times 1$ transformation matrix and the vector f_i is embedded into a higher dimension $2k \times k$. Then, we use the set $\{v_j\}$ of vector size $1 \times 2k$ to do Soft Attention for matrix in the high dimensional space. After the results are weighted and summed, they are integrated into the vector m_i of size k. The calculation process is shown in the following formulas:

$$a_{ij} = \text{Soft max}(v_j E_i), \quad j \in [1, N], \tag{6}$$

$$\text{SoftAttention}(E_i) = m_i = \sum_{j=1}^{N} (a_{ij} E_j), \tag{7}$$

where m_i is the calculation result on a single node on the sequence. Therefore, we need to stack the results of all nodes in the whole sequence to get the Soft Mapping feature. As is shown in the following formula, we have

$$s = \text{Stacking}\left(\sum_{j=0}^{N} (m_j)\right). \tag{8}$$

Note that a residual transformation and layer normalization are carried out to ensure that the input of the next round contains the result of the previous round, at the end of this process. It is shown in the following formula:

$$E = \text{LayerNorm}(E + s). \tag{9}$$

The vector s is the result of each modality. On this basis, the vectors obtained from the two modalities are summed according to the element order, and the sum results are classified and predicted according to the following formula:

$$y \sim p = W_a(\text{LayerNorm}(s_{\text{text}} + s_{\text{audio}})). \tag{10}$$

4. Data Preparation

4.1. CMU-MOSEI Dataset and MELD Dataset. We use CMU-MOSEI dataset [15] to verify our model. It is mainly composed of personal monologue video, including 250 different themes and thousands of different speakers. The dataset decomposes the video into video, audio, and text forms and contains a variety of tags. The first is sentiment, which is divided into seven levels [−3, 3], including the following: [−3: highly negative, −2 negative, 1 weakly negative, 0 neutral, +1 weakly positive, +2 positive, and +3 highly positive]. The other is based on Ekman emotions; Ekman emotions of the following: {happiness, sadness, anger, fear, disgust, and surprise} are annotated on a [0, 3] Likert scale for presence of emotion x: [0: no evidence of x, 1: weakly x, 2: x, 3: highly x]. The label distribution of CMU-MOSEI dataset is shown in Figure 5.

In addition, we use MELD dataset [20] to evaluate the model. It selects the multiperson dialogue scene in the TV series Friends as its material, which also contains linguistic, acoustic, and visual information. Its label is also multi-category, which divides emotions into anger, trouble, fear, joy, neutral, sadness, and surprise. In order to adapt to different needs, the above classification is divided into rougher negative, positive, and neutral sentiments. The label distribution of MELD dataset is shown in Figure 6.

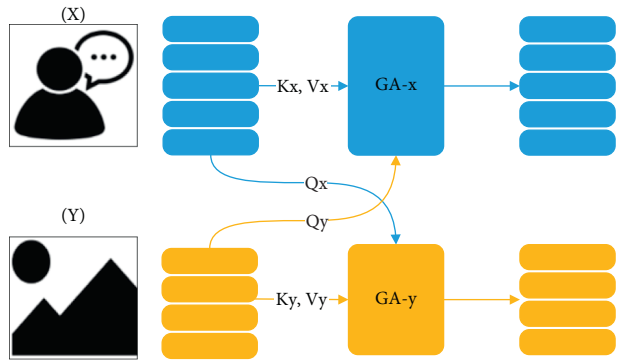

Figure 3: The structure of interactive Multihead Guided-Attention.

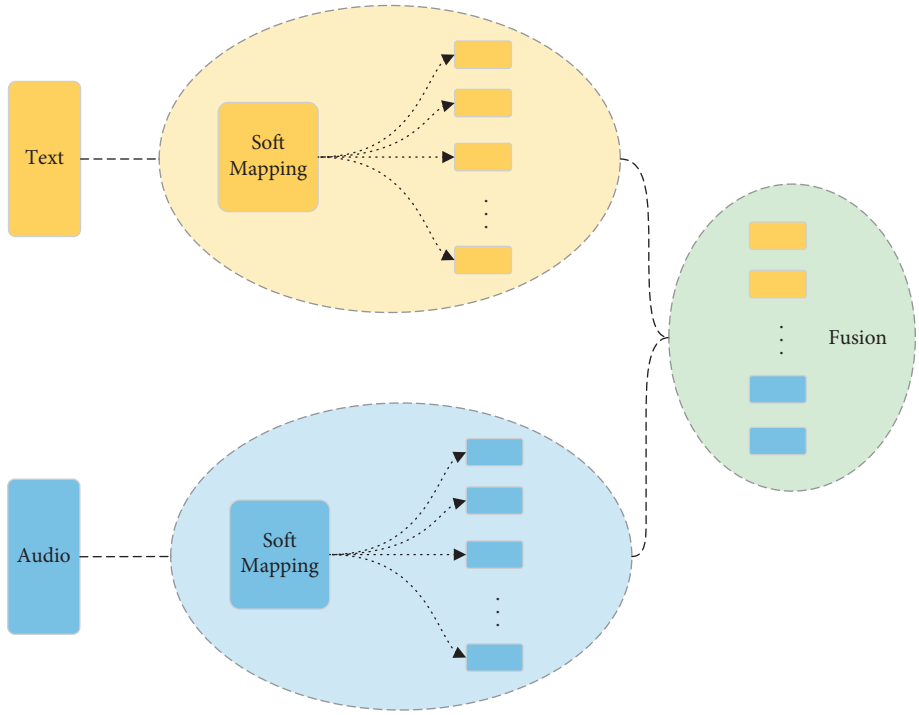

Figure 4: The structure of Soft Mapping.

4.2. Feature Extraction. Next, the preprocessing process of modality data is introduced, and different methods are selected to extract features according to their respective characteristics.

4.2.1. Linguistic Feature. Sentiment analysis has a long history of development in linguistics. It has its own characteristics from semantic-based sentiment dictionary methods to machine learning-based sentiment classification methods. In this study, in order to enable the fusion of multimodal data, the above methods will no longer be applicable and should be processed from a more abstract point of view. For linguistic data, we need to transform it into a vector containing semantic and grammatical information to represent it. Firstly, the original linguistic data is analyzed to construct a cooccurrence matrix for words. Then, based on the distributed representation of the matrix, the cooccurrence matrix is decomposed by using the association between words to obtain the representation vector of words. Specifically, we process the text data to obtain valid words and then count the frequency of word occurrences and record them in the cooccurrence matrix X. The element of X is $x_{(i,j)}$, which indicates the number of times word-i and word-j appear in the same window. Because there are 14176 independent words, we create a cooccurrence matrix X with dimension 14176×14176. We use GloVe [21] to embed the matrix X, and each word is embedded into a vector of 300 dimensions.

4.2.2. Acoustic Feature. Audio is a way for human beings to express their emotions. Intuitively speaking, acoustic information is another form of linguistic information, and the emotion at this time is consistent with the expression of linguistic information. However, acoustic data is more

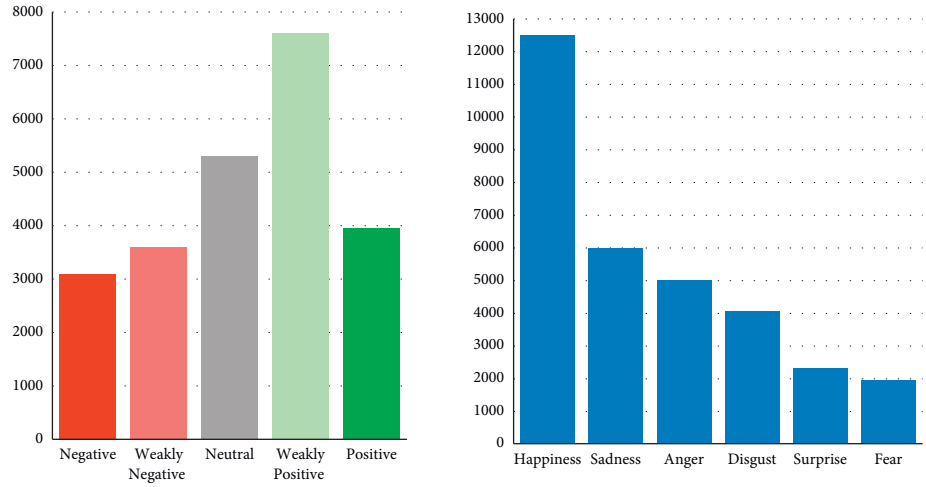

Figure 5: Motion histogram of CMU-MOSEI dataset [15].

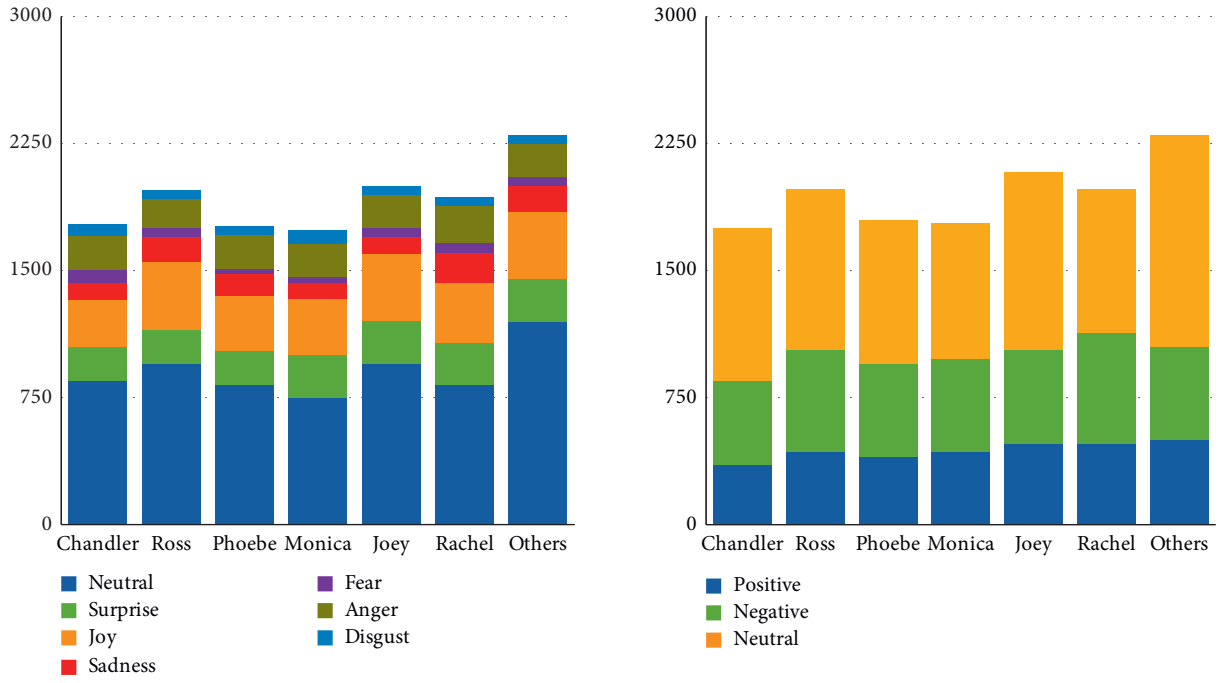

Figure 6: Character distribution across MELD [20].

complex than linguistic data and also contains a large part of unique acoustic information, such as laughter, sighs, high intonation, and low intonation. These are the key tasks of acoustic data in multimodal emotion recognition. The most abundant emotions in acoustic data are contained in human voice. When extracting speech features, it is necessary to remove irrelevant noise and focus on the human voice. Mel scale can be used to divide the sensitivity of human ear to frequency, so in this study Mel-Frequency Cepstral Coefficients (MFCC) [22] are used to extract acoustic features. Specifically, the 40 ms time scale is used to synthesize multiple sampling points of continuous audio signal within the time scale, which is called "frame." Then, the signal is preenhanced through a high-pass filter to compensate for the high frequency part of the speech signal, and Fourier transform is used to transform it from the time domain to the frequency domain to observe the state of energy part. Next, the frequency spectrum obtained by each frame is filtered by Mel filter to remove the frequency information that cannot be distinguished by human ear. After extracting the logarithmic energy on each Mel scale, the inverse discrete Fourier transform is performed. Finally, we can get acoustic features; the vector for it contains 80 dimensions.

4.2.3. Visual Feature. Video contains a lot of extremely abstract visual information, such as human facial expressions, human body movements, and even the color of the

entire video picture. They can play a certain role in emotion recognition. In this study, we use pretrained CNN to extract visual features [23], which uses a two-dimensional convolution kernel to extract spatial information and a one-dimensional convolution kernel to extract temporal information. Because the introduction of visual information brings more noise, we will not show the content of visual information in the follow-up experiments.

4.3. Baselines

4.3.1. Graph-MFN. This method uses a new fusion model called the Dynamic Fusion Graph (DFG) to build the n-modal interactions and replace the original fusion component in MFN [15].

4.3.2. B2 + B4 W/Multimodal Fusion. It utilizes self-attention to capture long term context and gating mechanism to selectively learn cross attended features [16].

4.3.3. Multilogue-Net. The model focuses on effectively capturing the context of a conversation and treats each modality independently, taking into account the information a particular modality is capable of holding [18].

4.3.4. TBJE. The approach relies on a modular coattention and a glimpse layer to jointly encode one or more modalities [19].

4.3.5. Text-CNN. The method achieves excellent results by a simple CNN with little hyperparameter tuning and static vectors [24].

4.3.6. BcLSTM. The model designed based on LSTM can capture the contextual information in the conversation [8].

4.3.7. DialogueRNN. The method is based on recurrent neural networks that keeps track of the individual party states throughout the conversation and uses this information for emotion classification [25].

5. Experiments

In this section, we will report the result on CMU-MOSEI dataset and MELD dataset. It is worth mentioning that the model can achieve good results in the case of only using linguistic feature and acoustic feature.

5.1. Implementation Details. In order to ensure the training speed and training results at the same time, the SWATS optimization method proposed by Keskar and Socher [26] was used in the experiment. Using Adam optimizer in the early stage can bring the advantage of fast convergence. Using SGD optimizer in the later stage can help the model find the optimal solution in a small range. Specifically, when using Adam optimizer, calculate the learning rate of SGD optimizer after each iteration. If it is found that the learning rate basically remains unchanged, it means that the bottleneck has been reached and you can switch at this time. At this time, the orthogonal projection of SGD optimizer on the descending direction of Adam optimizer should be exactly equal to the descending direction of Adam optimizer. It is shown in the following formula:

$$\mathrm{proj}_{\eta t}^{\mathrm{SGD}} = \eta_t^{\mathrm{Adam}}. \tag{11}$$

Therefore, the initial learning rate of SGD optimizer is shown in the following formula:

$$\alpha_t^{\mathrm{SGD}} = \frac{\left(\left(\eta_t^{\mathrm{Adam}}\right)^T \eta_t^{\mathrm{Adam}}\right)}{\left(\left(\eta_t^{\mathrm{Adam}}\right)^T\right) g_t}. \tag{12}$$

Then, we found that the number of blocks in interactive transformer directly affects the final result. Considering that the change of structure will bring some influence, we find the best setting of value by comparing the change of 2-class sentient accuracy under different N values. The specific results are shown in Figure 7. The results use five times average value and finally use $n = 4$ to ensure the best performance of the model, and the hidden layer size of each coding block is 512. In addition, we set the Interactive Multihead Guided-Attention structure to 4-head modules and the hidden layer size of Feedforward Neural Networks to 1024. In order to prevent the overfitting phenomenon, we set dropout of 0.1 on the output of each FNN and of 0.5 on the input of classification.

5.2. The Result of CMU-MOSEI Dataset. We compare the evaluation results of the model on CMU-MOSEI dataset with Graph-MFN [14], B2 + B4 w/multimodal fusion [16], Multilogue-Net [18], and TBJE [19]. The results of 2-class-sentiment are shown in Table 1. It should be noted that our model does not use visual information and integrating it into the noise makes the results unsatisfactory, which is also the direction of our next efforts. In general, only using linguistic feature and acoustic feature has been able to make our model achieve good results, which has been improved compared to other methods.

The results of 7-class-sentiment and 6-class-emotion are shown in Table 2. We show the average value of the classification results and only compare with the model using the same calculation method. It can be seen that the effect of the model on emotion multiclassification task is only slightly improved compared with other methods, which will be the direction of our future work. In addition, the performance of 7-class-sentiment classifications is not as good as that of 6-class-emotion classifications, which is in line with the expectation. It is also a common fault of all methods, because 7-class-sentiment deals with more fine-grained classification, with only very subtle differences between each category.

We randomly selected 4662 samples from the test set to verify 2-class-sentiment results and calculated True Positive Rate (TPR) and False Positive Rate (FPR) by using the

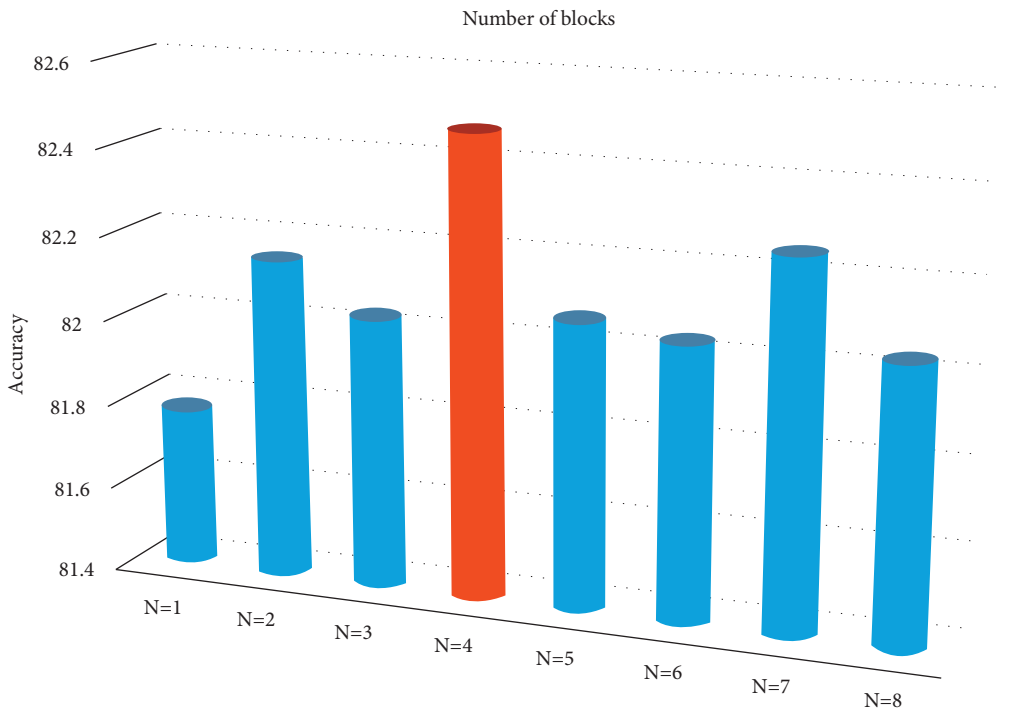

	N=1	N=2	N=3	N=4	N=5	N=6	N=7	N=8
Accuracy	81.774	82.148	82.033	82.472	82.067	82.039	82.255	82.042

Figure 7: 2-class-sentiment accuracy according to the number of blocks per Interactive Transformer.

Table 1: 2-class-sentiment of CMU-MOSEI dataset.

Model	2-class-sentiment	
	Accuracy (%)	F1-score (%)
Graph-MFN (T + A + V) [14]	76.90	77.00
B2 + B4 w/multimodal fusion (T + A + V) [16]	81.14	78.53
Multilogue-Net (T + A) [18]	80.18	79.88
Multilogue-Net (T + A + V) [18]	82.10	80.01
TBJE (T + A) [19]	82.30	/
TBJE (T + A + V) [19]	81.50	/
The proposed approach (T + A)	82.47	81.23

Table 2: 7-class-sentiment and 6-class-emotion of CMU-MOSEI dataset.

Model	7-class-sentiment		6-class-emotion	
	Accuracy (%)	F1-score (%)	Accuracy (%)	F1-score (%)
Graph-MFN (T + A + V) [14]	45.00	/	/	/
TBJE (T + A) [19]	45.36	/	81.48	/
TBJE (T + A + V) [19]	44.40	/	80.68	/
The proposed approach(T + A)	45.58	42.93	81.57	81.16

prediction results of the model and the real labels of the samples, so as to approximate the continuous Receiver Operating Characteristic (ROC) curve. As shown in Figure 8, we can see that our model has excellent performance.

5.3. The Result of MELD Dataset. We compare the evaluation results of the model on MELD dataset with text-CNN [24], bcLSTM [8], DialogueRNN [25], and the weighted F-score shown in Table 3. Neither text-CNN model nor our model uses context information, so the results are not very different. But bcLSTM model and DialogueRNN model using context information have better performance. Horizontal comparison shows that the performance of the model on the two datasets is different. The reason may be that the content of CMU-MOSEI dataset is different from MELD dataset. The CMU-MOSEI dataset is mainly composed of individual monologue scenes. The data of each modality is only related

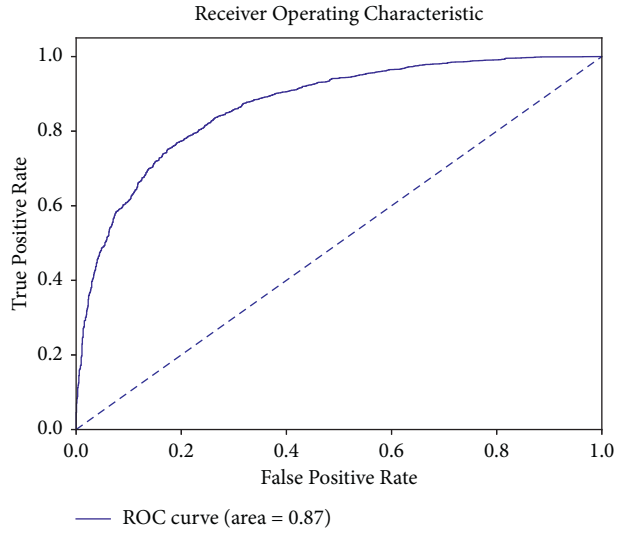

Figure 8: Receiver Operating Characteristic curve of CMU-MOSEI dataset.

Table 3: The result of MELD dataset.

Model	F1-score (%)	
	3 sentiments	7 emotions
Text-CNN (T) [24]	64.25	55.02
BcLSTM (T + A) [8]	66.68	59.25
DialogueRNN (T + A) [25]	67.56	60.25
The proposed approach(T + A)	64.67	55.23

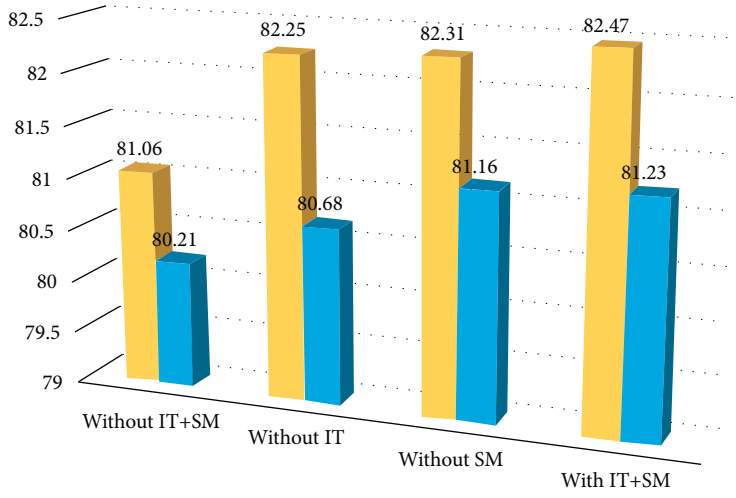

	Without IT+SM	Without IT	Without SM	With IT+SM
Accuracy	81.06	82.25	82.31	82.47
F1-score	80.21	80.68	81.16	81.23

Figure 9: Ablation experiment on CMU-MOSEI dataset.

to the emotion of a single person, and there are no other interference factors. The MELD dataset is mainly composed of multiperson dialogue scenes. Taking acoustic modality data as an example, there may be multiple people talking at the same time, which will cause interference to sentiment analysis. And the emotional state of multiple people will affect each other. When analyzing a person's emotional state, it is necessary to consider the influence of other people. Our model has not been improved for the multiperson dialogue scene, which is the direction of our next work.

5.4. Ablation Study. In this study, we propose two structures: Interactive Transformer (IT) and Soft Mapping (SM). The Interactive Transformer layer interacts with each other when learning a modality to improve the learning effect, while the Soft Mapping layer fuses the learning results of each modality to better classify emotions. In order to verify the effectiveness of these two structures, we have carried out the ablation experiment. The experiment was divided into four situations: the first is completely not using Interactive Transformer layer and Soft Mapping layer, only Interactive Transformer layer is removed, only Soft Mapping layer is removed, and Interactive Transformer layer and Soft Mapping layer are used at the same time.

When we do not use Interactive Transformer, we choose traditional Transformer to replace it, which means that we lose the ability of interaction between modalities. When SM is not used, we directly perform weighted average calculation on the learning results of each modality and then perform sentiment classification. The results are shown in Figure 9. It can be seen that the improvement is obvious when using IT or SM alone, but the improvement is very limited when using both at the same time. The reason may be that the roles of IT and SM are duplicated, and they are both designed for modal interaction. So, when they are used alone, the information between modalities can be complementary, and the results are similar. When using them at the same time, the supplementary information that they mined is repeated, so the improvement is not obvious. In the follow-up, we will try to dig out related information in different directions in a targeted manner to make the division of labor between IT and SM clearer.

6. Conclusions and Future Work

In this paper, we propose an Interactive Transformer and Soft Mapping based method for multimodal sentiment analysis. The proposed model can fully consider the relationship between multiple modality pieces of information, which is helpful for sentiment analysis after data fusion. Although our model has achieved competitive results on the CMU-MOSEI dataset, there are still some shortcomings. Our model does not make full use of the visual modality information, and it only uses data from linguistic modalities and acoustic modalities. Trying to add data from visual modalities makes the results unsatisfactory. In the next step, we will continue to look for the method of integrating visual data, because expression and body movements of characters in the visual data also contain rich and delicate emotions, which can be of great help to emotion recognition. In addition, the evaluation results of MELD dataset also reflect some problems. Our model ignores that people's emotions affect each other in multiperson dialogue scenarios. For example, when a person expresses negative emotions externally, the emotional state of other people will also shift negatively. In the future, we will focus on the emotional analysis of multiperson dialogue from four aspects: role of context, interspeaker influence, emotion shifts, and contextual distance.

Data Availability

The data that support the findings of this study are available from the corresponding author upon reasonable request.

Ethical Approval

This paper does not contain any studies with animals performed by any of the authors.

Conflicts of Interest

The author(s) declare that there are no conflicts of interest with respect to the research, authorship, and/or publication of this paper.

Acknowledgments

This paper was supported by the National Natural Science Foundation of China under Grants 61702462, 62072416, 61873246, and 61771432, the Scientific and Technological Project of Henan Province under Grants 222102210010, 192102210108, 202102210137, 202102210517, and 192102210109, and the Research and Practice Project of Higher Education Teaching Reform in Henan Province under Grants 2019SJGLX320 and 2019SJGLX020.

References

[1] S. Poria, E. Cambria, R. Bajpai, and A. Hussain, "A review of affective computing: from unimodal analysis to multimodal fusion," *Information Fusion*, vol. 37, pp. 98–125, 2017.

[2] Y. Zhang, L. Rong, D. Song, and Z. Peng, "A survey on multimodal sentiment analysis," *Pattern Recognition and Artificial Intelligence*, vol. 33, no. 5, pp. 426–438, 2020.

[3] S. Verma, C. Wang, L. Zhu, and W. Liu, "DeepCU: integrating both common and unique latent information for multimodal sentiment analysis," in *Proceedings of the 28th International Joint Conference on Artificial Intelligence*, pp. 3627–3634, Macao, China, August 2019.

[4] P. K. Atrey, M. A. Hossain, A. El Saddik, and M. S. Kankanhalli, "Multimodal fusion for multimedia analysis: a survey," *Multimedia Systems*, vol. 16, no. 6, pp. 345–379, 2010.

[5] A. Zadeh, M. Chen, S. Poria, E. Cambria, and L. P. Morency, "Tensor fusion network for multimodal sentiment analysis," in *Proceedings of the 2017 Conference on Empirical Methods in Natural Language Processing*, pp. 1103–1114, Copenhagen, Denmark, January 2017.

[6] Z. Sun, P. K. Sarma, W. Sethares, and E. Bucy, "Multi-modal sentiment analysis using deep canonical correlation analysis," in *Proceedings of the 20th Annual Conference of the International Speech Communication Association*, pp. 1323–1327, Graz, Austria, July 2019.

[7] M. Wöllmer, F. Weninger, T. Knaup, and B. Schuller, "YouTube movie reviews: in, cross, and open-domain sentiment analysis in an audiovisual context," *IEEE Intelligent Systems*, vol. 28, no. 3, pp. 46–53, 2013.

[8] S. Poria, E. Cambria, D. Hazarika, N. Majumder, A. Zadeh, and L.-P. Morency, "Context-Dependent sentiment analysis in user-generated videos," in *Proceedings of the 55th Annual Meeting of the Association for Computational Linguistics*, pp. 873–883, Vancouver, BC, Canada, June 2017.

[9] V. Pérez-Rosas, R. Mihalcea, and L. P. Morency, "Utterance-level multimodal sentiment analysis," in *Proceedings of the 51st Annual Meeting of the Association for Computational Linguistics*, pp. 973–982, Sofia, Bulgaria, August 2013.

[10] S. Poria, E. Cambria, and A. Gelbukh, "Deep convolutional neural network textual features and multiple kernel learning for utterance-level multimodal sentiment analysis," in *Proceedings of the 2015 Conference on Empirical Methods in Natural Language Processing*, pp. 2539–2544, Lisbon, Portugal, July 2015.

[11] J. Wagner, E. Andre, F. Lingenfelser, and J. Kim, "Exploring fusion methods for multimodal emotion recognition with missing data," *IEEE Transactions on Affective Computing*, vol. 2, no. 4, pp. 206–218, 2011.

[12] A. Vaswani, N. Shazeer, N. Parmar et al., "Attention is all you need," in *Proceedings of the 31st Annual Conference on Neural Information Processing Systems*, pp. 5999–6009, Long Beach, CA, USA, December 2017.

[13] Z. Yu, J. Yu, Y. Cui, D. Tao, and Q. Tian, "Deep modular co-attention networks for visual question answering," in *Proceedings of the 2019 IEEE Conference on Computer Vision and Pattern Recognition*, pp. 6281–6290, Long Beach, CA, USA, June 2019.

[14] P. Amir Zadeh, P. Liang, N. Mazumder, S. Poria, E. Cambria, and L.-P. Morency, "Memory fusion network for multi-view sequential learning," in *Proceedings of the 32nd AAAI Conference on Artificial Intelligence*, pp. 5634–5641, New Orleans, Lousiana, USA, February 2018.

[15] A. A. Zadeh, P. P. Liang, S. Poria, E. Cambria, and L.-P. Morency, "Multimodal language analysis in the wild: CMU-MOSEI dataset and interpretable dynamic fusion graph," in *Proceedings of the 56th Annual Meeting of the Association for Computational Linguistics*, pp. 2236–2246, Melbourne, Australia, January 2018.

[16] A. Kumar and J. Vepa, "Gated mechanism for attention based multi modal sentiment analysis," in *Proceedings of the 2020 IEEE International Conference on Acoustics, Speech and Signal Processing*, pp. 4477–4481, Barcelona, Spain, May 2020.

[17] S. Sahay, S. H. Kumar, R. Xia, and J. Huang, "Multimodal relational tensor network for sentiment and emotion classification," in *Proceedings of the 1st Grand Challenge and Workshop on Human Multimodal Language*, pp. 20–27, Melbourne, Australia, January 2018.

[18] A. Shenoy and A. Sardana, "Multilogue-net: a context aware RNN for multi-modal emotion detection and sentiment analysis in conversation," in *Proceedings of the 58th Annual Meeting of the Association for Computational Linguistics*, pp. 19–28, Stroudsburg, PA, USA, February 2020.

[19] J.-B. Delbrouck, N. Tits, M. Brousmiche, and S. Dupont, "A transformer-based joint-encoding for emotion recognition and sentiment analysis," in *Proceedings of the 2nd Grand Challenge and Workshop on Multimodal Language*, pp. 1–7, Seattle, WA, USA, June 2020.

[20] S. Poria, D. Hazarika, N. Majumder, G. Naik, E. Cambria, and R. Mihalcea, "MELD: a multimodal multi-party dataset for emotion recognition in conversations," in *Proceedings of the 57th Annual Meeting of the Association for Computational Linguistics*, pp. 527–536, Florence, Italy, January 2018.

[21] J. Pennington, R. Socher, and C. Manning, "Glove: global vectors for word representation," in *Proceedings of the 2014 Conference on Empirical Methods in Natural Language Processing*, pp. 1532–1543, Doha, Qatar, January 2014.

[22] B. Mcfee, C. Raffel, D. Liang et al., "Librosa: audio and music signal analysis in Python," in *Proceedings of the 14th Python in Science Conference*, pp. 18–24, San Jose, CA, USA, August 2015.

[23] D. Tran, H. Wang, L. Torresani, J. Ray, Y. LeCun, and M. Paluri, "A closer look at spatiotemporal convolutions for action recognition," in *Proceedings of the 2018 IEEE Conference on Computer Vision and Pattern Recognition*, pp. 6450–6459, Salt Lake City, UT, USA, June 2018.

[24] K. Yoon, "Convolutional neural networks for sentence classification," in *Proceedings of the 2014 Conference on Empirical Methods in Natural Language Processing*, pp. 1746–1751, Doha, Qatar, August 2014.

[25] N. Majumder, S. Poria, D. Hazarika, R. Mihalcea, A. Gelbukh, and E. Cambria, "DialogueRNN: an attentive RNN for emotion detection in conversations," *Proceedings of the AAAI Conference on Artificial Intelligence*, vol. 33, pp. 6818–6825, 2019.

[26] N. S. Keskar and R. Socher, "Improving generalization performance by switching from Adam to SGD," in *Proceedings of the 6th International Conference on Learning Representations*, Vancouver, Canada, December 2018.